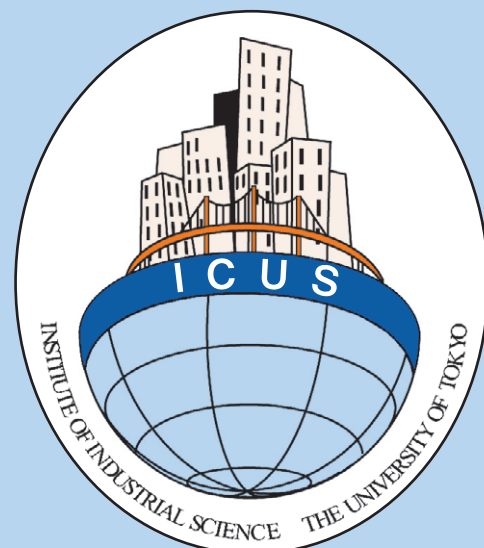


ICUS REPORT 2008-03



***INTERNATIONAL CENTER FOR
URBAN SAFETY ENGINEERING***

***INSTITUTE OF INDUSTRIAL SCIENCE
THE UNIVERSITY OF TOKYO***

2008
**NEW TECHNOLOGIES FOR
URBAN SAFETY OF MEGA CITIES IN ASIA**

Edited by

**Kawin Worakanchana
ICUS, IIS, The University of Tokyo, Japan**

New Technologies for Urban Safety of Mega Cities in Asia

*21-22 October 2008
Beijing, China*

Edited by

Kawin Worakanchana

Co-Organized by

*Center for Public Safety Research,
Tsinghua University, China*

∫

*International Center for Urban Safety Engineering (ICUS)
Institute of Industrial Science
The University of Tokyo, Japan*

NEW TECHNOLOGIES FOR URBAN SAFETY OF MEGA CITIES IN ASIA

KIMIRO MEGURO

Director and Professor of International Center for Urban Safety Engineering
Institute of Industrial Science, The University of Tokyo, Japan

ICUS Report No 31, February, 2009

Preface

Over half of the world's population is concentrated in urban areas covering just four percent of the world land area. It is estimated that by 2015, more than 50% of the megacities with a population of more than 10 million and with high population density, will be in Asia. Also, in this part of the world, rapid economic development is fast accelerating the pace of urbanization. Unfortunately, the rapid expansion of infrastructure for urbanization is not adequately balanced with appropriate measures for their maintenance and management, and resulted in urban disasters.

In 2007 and 2008, there were big disasters in Asia, such as killer cyclones Sidr in Bangladesh (2007) and Nargis in Myanmar (2008), and the devastating Sichuan earthquake in China (2008). The number of fatalities and missing reported due to these disasters was well over 240,000 human lives. These unprecedented events are typical examples that show us the importance of urban safety.

International Center for Urban Safety Engineering (ICUS) was established in 2001 at the Institute of Industrial Science (IIS), the University of Tokyo, in response to the need of a center to focus on urban safety engineering including, but not limited to, design, construction, and maintenance of urban infrastructure, forecasting of likely disasters, disaster management and urban risk management through active international collaboration. Based on the research output and capability accumulated at IIS till now, ICUS has been carrying out research and implementing them towards the realization of safer cities in the 21st century.

To bring together the research communities in Asia and the world in order to fully realize our vision of safer cities in Asia, ICUS has been annually co-organizing the International Symposium on New Technologies for Urban Safety of Megacities in Asia (USMCA) with its partners in Asian region. Modern technologies such as Geographic Information System, Global Positioning System, remote sensing and satellite image analysis, computer simulation, non-destructive testing method, and non traditional construction materials as well as innovative solutions combining existing and/or conventional technologies can be very useful for realization of safer cities. Here, the phrase "new technology" within the name of the symposium, does not only mean advanced and/or sophisticated technology. Even lower-level technologies, which are not well-known or cutting-edge, but are useful for improving urban safety through innovative ways of deployment, are termed

here as new technologies. When I went through this volume of the proceedings, there are several papers which fit very well to this category. I believe that this type of technology is also very important and essential part of this symposium.

The primary objective of the symposium is to bring together decision makers, practitioners and researchers involved in the field of urban safety to share their expertise, knowledge and experience in tackling the critical issues for safer cities in Asia. It has also provided an environment to create and reinforce collaboration networks among experts in the fields relevant to urban safety. Previous USMCAs have been successfully held in Bangkok, Thailand (2002), Tokyo, Japan (2003), Agra, India (2004), Singapore (2005), Phuket, Thailand (2006), and Dhaka, Bangladesh (2007).

In year 2007, the Center for Public Safety Research (CPSR), Tsinghua University, China and ICUS, which have a long collaborative relationship, signed up a Memorandum of Understanding (MOU). As a result of this MOU, ICUS co-organized the 7th USMCA in Beijing together with CPSR, Tsinghua University.

I hope that the present volume, which contains the papers presented during the symposium, provides valuable reference material in the fields of urban safety. Finally, I would like to gratefully acknowledge the sincere efforts of the Steering Committee, Technical Committee, and the Organizing Committee of USMCA2008 for their hard work, valuable suggestions, efficient coordination and praisable initiatives to make this symposium a success. Also, I would like to thank all the participants who actively attended the Symposium, and the sponsors listed below, who financially contributed to this great event.

Sponsors

National Natural Science Foundation of China,
China

Illinois Fire Service Institute,
University of Illinois at Urbana-Champaign, USA

Homeland Security Research Center, Illinois, USA

Beijing Global Safety Technology Co. Ltd., China

The Foundation for Promotion of Industrial Science,
Japan (SEIKEN SYMPOSIUM 53)

Global Center of Excellence (GCOE) for
Sustainable Urban Regeneration,
The University of Tokyo, Japan

China National Institute of Standardization, China

TOKYO GAS Co. Ltd., Japan

Table of Contents

| | <i>Page</i> |
|---|-------------|
| Opening Session | |
| SECTION 1 Keynote Lectures | |
| Research on Public Safety <i>(Keynote Lecture)</i> <i>Fan Weicheng, Liu Yi, Weng Wenguo</i> | 1 |
| Lessons from Recent Storm Surge Disasters --Katrina, Sidr and Nargis <i>(Keynote Lecture)</i> <i>Shibayama Tomoya</i> | 11 |
| Industrial Safety in the 21st Century and Role of Safety Engineering <i>(Keynote Lecture)</i> <i>Tamura Masamitsu</i> | 19 |
| Monitoring of Urban Sustainability by Use of Remote Sensing <i>(Keynote Lecture)</i> <i>Yasuoka Yoshifumi</i> | 31 |
| The Restoration Plan of Dujiangyan After the Great Sichuan Earthquake Disaster in 2008 <i>(Keynote Lecture)</i> <i>Ishikawa Mikiko</i> | 39 |
| Comprehensive Disaster Management and Response <i>(Keynote Lecture)</i> <i>Jaehne Richard L</i> | 49 |
| Importance of Maintenance Technologies to Keep Existing Structures Safe to the Public <i>(Keynote Lecture)</i> <i>Uomoto Taketo</i> | 57 |
| Disaster Mitigation for Inhabitants of Mega Cities <i>(Keynote Lecture)</i> <i>Sakata Toshibumi</i> | 69 |
| Strategy for Efficient Use of Earthquake Early Warning System for Earthquake Disaster Reduction <i>(Keynote Lecture)</i> <i>Meguro Kimiro</i> | 73 |
| Technical Sessions | |
| SECTION 2 Rehabilitation and Retrofitting of Urban Structures against Disasters and Impact Loads | |
| Damage to Buildings Due to 2008 MAY 12 WenChuan Earthquake and Cooperative Activities for Damage Restoration by Japanese Experts <i>Nakano Yoshiaki</i> | 85 |

| | |
|--|-----|
| Flexural Behavior of Corroded RC Members with Patch Repair <i>Kato Yoshitaka, Sahamitmongkol Raktipong</i> | 95 |
| Shaking Table Test of Timber Masonry House Models Retrofitted by PP-band Meshes <i>Sathiparan Navaratnarajah, Mayorca Paola, Meguro Kimiro</i> | 105 |
| Relation between Strength Reduction and Ductility Demand for PP-Band Mesh Retrofitted Houses <i>Mayorca Paola, Meguro Kimiro</i> | 115 |
| Strength and Durability Consideration of Brick Aggregate Concrete Containing Fly Ash <i>Noor M. A., Kaoser A. R</i> | 123 |
| Mechanical Behavior of Concrete Member Subjected to Repeated Impulsive Force <i>Yokota Hiroshi, Iwanami M., Takahashi S., Matsubashi T</i> | 135 |
| Review of Emergency Technologies to Support Urban Resilience and Disaster Recovery <i>Feniosky Peña-Mora, Zeeshan Aziz, Mani Golparvar-Fard, Chen Alberty, Plans Albert P., Mehta Saumil J</i> | 145 |

SECTION 3 Advanced Technologies for Monitoring, Assessment and Management of Urban Safety 1

| | |
|---|-----|
| Prior Disaster Review System for Disaster Assessment in Korea <i>Yi Waon-ho, Shim Jae-hyun, Chung Jae-hak</i> | 155 |
| Management of Urban Disaster with Special Emphasis on Fresh Water Scarcity and Surface Water Pollution in Dhaka City <i>Ahmed Murshed</i> | 165 |
| Investigating the Performance of Alos Prism to Estimate Building Heights for Urban Risk Management <i>Takeuchi Wataru, Worakanchana Kawin, Tadono Takeo, Warnitchai Pennung</i> | 183 |
| Analytical Cost Model in Protective Design Methodology <i>Liu Chunlin, John Crawford RA, Fang Yea Saen</i> | 189 |
| Introduction to Enhanced Architectural Protective Systems <i>Liu Chunlin, Palermo David</i> | 201 |
| Identification of Pollutant Sources in Urban Area Using Inverse CFD Modeling <i>Huang Hong, Kato Shinsuke, Bady Mahmoud</i> | 215 |
| Research and Test Appliance for Protective Garment and Equipment-Thermal Manikin System <i>Pan Jin, Tang Xiaoyu</i> | 223 |

SECTION 4 Risk Assessment, Prediction and Early-warning of Urban Disasters 1

- Role of Logistics during Cyclone SIDR** 233
Ansary Mehedi Ahmed, Das Rubel, Afifa Imtiaz Bnus
- Seismic Microzonation Based on Site Amplification Study of Cox's Bazar in Bangladesh** 239
Afifa Imtiaz A.B., Ansary Mehedi Ahmed, Dhar Ashutosh Sutra
- The Wildfire Early-warning and Early-detection System in Japan** 251
Sawada Haruo, Sawada Yoshito, Nagatani Izumi
- Landslide Induced Lake-Tsunami at Aratosawa Dam due to the Iwate Miyagi Nairiku Earthquake 2008** 259
Johansson Jörgen, Tajima Yoshimitsu, Fujita Tomohiro, Konagai Kazuo
- Integrated Information System for Landslide Disaster Management** 269
Meguro Kimiro, Kawasaki Akiyuki, Torres Tatiana
- Defense Against Intentional Attacks: Framework for Modeling and Simulation** 279
Zhang Jing, Shen Shifei, Yang Rui

SECTION 5 Environmental Impact Assessment due to Rapid Urbanization

- A Holistic Approach for Analysing Impacts of Climatic changes on Coastal Zone Systems** 287
Dutta Dushmanta, Wright Wendy, Adeloju Samuel
- Researches and Applications of Land Use Planning Based on Risk Analysis** 297
Zheng Cao, Mao Liu, Qingshui Li, Qing Mu
- Numerical Simulation of Relationship between Climatic Factors and Ground Ozone Concentration in Summer over the Kanto Area Using the MM5/CMAQ Model** 317
Ooka Ryoza, Khiem M.V., Huang Hong, Hayami Hiroshi
- Considering the Impact of Climate and Land Cover Change on a Local Hydrological Flow: The Case Study of Srepok River Basin in Viet Nam and Cambodia** 335
Kawasaki Akiyuki, Rogers Peter, Herath Srikantha, Meguro Kimiro
- Study on Relaxation Measures for Outdoor Thermal Environment on Present Urban Blocks in Tokyo Using Coupled Simulation of Convection, Radiation and Conduction** 345
Chen Hong, Ooka Ryoza, Huang Hong, Tsuchiya Takashi
- Development of E-learning Contents for Increasing Emergency Response Capacity of Doctors and Nurses in Key Disaster Hospitals** 355
Ohara Miho Y., Kitsuta Yoichi, Yahagi Naoki, Koyama Fujio, Miyazaki Sanae, Meguro Kimiro

SECTION 6 Evacuation Management for Urban Safety

- Dynamic Behaviour of Jamuna Multipurpose Bridge due to Vehicular Loading** 365
Ansary Mehedi Ahmed, Rahman Syed Zillur, Ahsan Raquib

| | |
|---|-----|
| Risk Analysis of Crowd Evacuation using the Monte Carlo method | 377 |
| <i>Li Jianfeng, Yao Xiaohui, Liu Xiaoqing, Wang Yutian, Zhang Bin</i> | |
| Study on Risk Assessment of Crowd Evacuation in Venue Area | 393 |
| <i>Li Pan, Weng Wenguo, Ji Xuwei</i> | |
| Flood Simulation with an Improved SPH Model | 405 |
| <i>Bao Kai, Zhang Hui, Zheng Lili, Wu Enhua</i> | |
| Agent-based Simulation and Modeling of Emergency Response on Repast Platform | 415 |
| <i>Wu Jianhong, Weng Wenguo</i> | |
| Network Based Pedestrian Simulator | 421 |
| <i>Soeda Shunsuke, Yamashita Tomohisa, Noda Itsuki</i> | |

SECTION 7 Emergency Management for Urban Disasters 1

| | |
|--|-----|
| Research on the Architecture of Emergency Intelligent Decision Support System | 427 |
| <i>Shao Quan, Weng Wenguo, Yuan Hongyong</i> | |
| Analysis of the Emergency Derivation Chain Characteristics Caused by Snow Disaster | 435 |
| <i>Chen Changkun, Sun Yunfeng, Li Zhi</i> | |
| Urban Fire Risk Mapping Using GIS: A Case Study of a Part of Kunshan City, China | 439 |
| <i>Gai Chengcheng, Weng Wenguo, Yuan Hongyong</i> | |
| Application of Fuzzy Comprehensive Assessment Method to Evaluate Full-Scale Emergency Exercise Plan | 449 |
| <i>Du Ligang, Shen Shifei, Qin Tingxin</i> | |
| Application of NSGA II in Emergency Point Layout Optimization of Industrial Zone | 457 |
| <i>Li Dongxue, Liu Mao</i> | |
| Network Public Opinion Caused by Public Safety Incidents | 467 |
| <i>Zheng Kui, Shu Xueming</i> | |

SECTION 8 Advanced Technologies for Monitoring, Assessment and Management of Urban Safety 2

| | |
|--|-----|
| A New Kriging-based Finite Element Method for Highly Accurate Dynamic Analysis | 475 |
| <i>Worsak Kanok-Nukulchai, Citra Wicaksana, Bui Thanh Tam</i> | |
| Analyzing the Socio-Economic and Demographic Determinants of Crime in China | 487 |
| <i>Yan Jun, Shu Xueming, Yuan Hongyong</i> | |
| The Comparison and Selection of the Risk Analysis Methodologies on the Whole Process of Dangerous Chemical Accident | 495 |
| <i>Zhang Chao, Cai Dongshan, Liu Yi</i> | |

Reducibility of Seismic and Post-earthquake Urban Fire Hazard in Densely Inhabited Districts by Simultaneous Seismic & Fire-resistive Reinforcement of Low-rise Wooden Buildings 505
Kawagoe Yuko, Hasemi Yuji, Murakami M., Kawai N., Yamada M

A Study for Promoting Communication between Research Institutes and General Society 517
Abe Mariko, Meguro Kimiro

Study on Epidemic Spreading on Alternate Social Networks 527
Ni Shunjiang, Weng Wenguo

SECTION 9 Emergency Management for Urban Disasters 2

Application of Social Theory to The Development Process of an Emergency Retrofitting Method 539
Henry Michael, Kato Yoshitaka

Role of Fire Forces in Rescue and its Development Trends in the Future 549
Yang Jianfeng, Chen Yingchun

Development of Emergency Retrofitting Method Using Fiber Sheets Containing Hydraulic Resin 555
Suzuki Masamitsu, Suzuki Ryo, Ito Masanori, Kato Yoshitaka

Assessment of Emergency Response Policy Based on Markov Process 565
Zhou Yafei, Liu Mao

Emergency Response of Radiological Attacks Happened in the City 575
Zheng Qiyuan, Zhang Lijun, Huang Weiqi

Research on Universal Mode of Describing and Organizing Emergency Cases Based on Case-based Reasoning 581
Zhong Qiuyan, Zhang Yingju, Ye Xin, Qiu Jiangnan

Comparison of Estimated and Observed Seismic Intensity Map of Selected Earthquakes 591
Noor M. A., Kumagai H.

SECTION 10 Safety Assessment of Existing Infrastructure

Collector Comparison of Air-borne Salt Attack for Marine Infrastructures in Taiwan 603
Hsu Kai-Lin, Chang Chao-Shun

An Evaluation of Potential Community Hill Slope Instability around Metropolitan Area in Taiwan 613
Tseng Kuo-Hung

Influence of Initial Curing on Chloride Penetrating Characteristics in Concrete Exposed to Different Marine Environment 621
Xue Wen, Dai Jianguo, Yokota Hiroshi, Jin Weiling

| | |
|--|-----|
| Seismic Performance of Wooden Buildings in Japan <i>Koshihara Mikio</i> | 631 |
| Trial Test on The Evaluation of Soil Cementation Generated by The Function of Microorganism <i>Sugimoto Daisuke, Kuwano Reiko</i> | 641 |
| Development of Hazard Prediction System for Intentional Attacks in Urban Areas <i>Ohba Ryohji, Yamashita Tomohisa, Ukai Osamu, Kato Shinsuke</i> | 647 |
| Earthquake Evacuation Plan for Old Dhaka, Bangladesh <i>Jahan Israt, Yousuf Reja M.D., Ansary Mehedi Ahmed</i> | 657 |
| Remote Sensing and GIS for Tsunami Damage Assessment - A Case Study <i>Premadasa Wuditha Nuwan, Dmdok Dissanayake</i> | 671 |
| A Method on Improving the Adaptability of Time Series Models and its Application in the Analysis of Public Security <i>Wang Wei</i> | 679 |

SECTION 11 Risk Assessment, Prediction and Early-warning of Urban Disasters 2

| | |
|---|-----|
| Risk Assessment of Global-Scale Natural Disaster <i>Chang Taiping</i> | 689 |
| Model Tests on the Behavior of Flexible Buried Pipe in Sandy Backfill with Insufficient Compaction <i>Kuwano Reiko, Ko Dong Hee</i> | 699 |
| Experimental Study on the Evaluation of Loosening Surrounding a Cavity in Soil <i>Sato Mari, Kuwano Reiko</i> | 709 |
| A Study on Estimation of Crown Projection Area for Wind Pressure Analysis Using Lidar Data <i>Endo Takahiro, Taguchi Hitoshi, Baruah P.J., Sawada Haruo</i> | 715 |
| Green Buildings: Current Status and Prospects <i>Baruah Pranab J., Sumi Akimasa, Endo Takahiro</i> | 723 |
| Cyclone Disaster Risk of Bangladesh <i>Noor M. A., Ahmed N</i> | 735 |
| Traffic Flow Analysis for an Appropriate Evaluation of Lost Time in Signal Control <i>Tanaka Shinji, Ono Takeshi, Kuwahara Masao</i> | 745 |
| Safety Assessment of Structural Concrete with Defects and Damages <i>Maekawa Koichi, Naga Koheii</i> | 753 |
| Oil Supply Chain Security Evaluation and Countermeasures <i>Xu Guangyong, Yong Qidong</i> | 763 |

Photograph



USMCA2008 Group Photo



Symposium hall



Exhibition Panels



Opening ceremony



Opening ceremony

(All participants joined silent mourning for victims in the 2008 Sechuan earthquake.)



*Prof. Weicheng Fan
(Chairperson, 7th USMCA organizing committee
and Director, Center for Public Safety Research)*



*Prof. Meguro Kimiro
(Director, ICUS)*



*Prof. Hu Dongcheng
(Vice president, Tsinghua University)*



*Prof. Richard L. Jaehne
(Keynote speaker)*



*Prof. Shibayama Tomoya
(Keynote speaker)*



*Prof. Tamura Masamitsu
(Keynote speaker)*



*Prof. Sakata Toshibumi
(Keynote speaker)*



*Prof. Uomoto Takeo
(Keynote speaker)*



*Prof. Yasuoka Yoshifumi
(Keynote speaker)*



*Prof. Waon-Ho Yi
(Invited speaker)*



*Prof. Worsak Kanok-Nukulchai
(Invited speaker)*



*Dr. Dushmanta Dutta
(Invited speaker)*



*Prof. Yokota Hiroshi
(ICUS)*



*Dr. Ansary Mehedi Ahmed
(Invited speaker)*



*Dr. Kai-Lin Hsu
(Invited speaker)*



*Prof. Tai-Ping Chang
(Invited speaker)*



*Prof. Sawada Haruo
(ICUS)*



*Dr. Koshihara Mikio
(ICUS)*



Dr. Kuwano Reiko
(ICUS)



Dr. Kato Yoshitaka
(ICUS)



Dr. Hong Huang
(ICUS)



Dr. Ohara Miho
(ICUS)



Dr. Ooka Ryoza
(IIS)



Dr. Tanaka Shinji
(ICUS)



Dr. Takeuchi Wataru
(IIS)



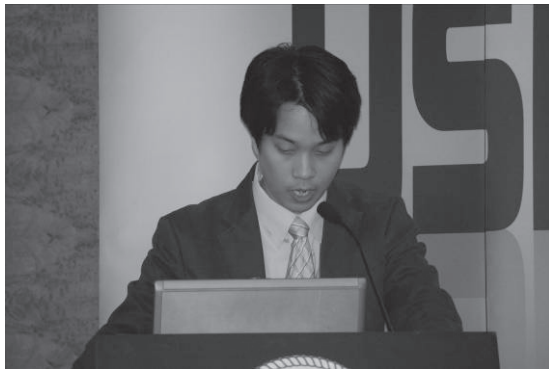
Dr. Endo Takahiro
(ICUS)



*Dr. Mayorca Paola
(ICUS)*



*Dr. Baruah Pranab J.
(ICUS)*



*Dr. Kawin Worakanchana
(ICUS)*



Banquet



*Prof. Meguro handed souvenir to
Prof. Ishikawa Mikiko. (Keynote speaker)*



*Prof. Meguro handed souvenir to
Prof. Nakano Yashiaki. (Invited speaker)*



*Announcement for USMCA 2009
by Prof. Waon-Ho Yi*



Young-researcher-award awardees



*Group photo
at Beijing National Olympic Stadium*



*Group photo
at Great wall of China*



*Prof. Sawada gave speech
at symposium welcome party*



Symposium farewell party

Opening Session

RESEARCH ON PUBLIC SAFETY

WEICHENG FAN^{1,2}, YI LIU¹ and WENGUOWENG¹

¹ Center for Public Safety Research,
Tsinghua University, Beijing, 100084, P.R. China
wfan@tsinghua.edu.cn

² State Key Laboratory of Fire Science,
University of Science and Technology of China,
Hefei, 230026, P.R. China

ABSTRACT

The framework and methodology of public safety research are presented in this paper, from the study on catastrophe cases study. The emergency, acceptor, and response and management linked by hazard elements constitute the framework of public safety research. The methodology comprises the deterministic methods, stochastic methods, sensor-based methods, complex system approach, and the combination of them. Examples are provided to show the methodology.

1. INTRODUCTION

In these years, China's economy has maintained a good growth, which comes from the national policy of deepen reform and opening-up. Unfortunately some unstable and uncertain factors are on rise. One of the most important problems is public safety (Premier Wen, 2006). The Chinese government is convinced that public safety is a lion in the way during the process of constructing a well-off society. And so it attaches much importance to public safety. The clout of public safety is that all of the related work is human-oriented, which means the human lives are most important in dealing emergency management.

In fact, many governments all over the world attaches much importance to emergency management due to many existing public emergency incidents, e.g. Indian Ocean Earthquake and Tsunami, Double benzene plant explosion at Jilin Petrochemical Company in China, SARS rampant in China, Hurricane Katrina in USA, 911 incident in USA, and the recent Wenchuan Earthquake in China, etc. One of the reasons for that is the current society is more and more weak. The highly developed technology gives us the convenient living, but at the same time, provides more and more probability of the occurrence of public emergency incidents. The public safety needs supports of science and technology, and public safety also provides challenges for scientific researchers. However, it is somehow still difficult to provide a general view of public safety research due to its complexity. It is a multi-subsystem, multi-level, multi-function system, and the systems and factors involved are very often uncertain, non-linear, dynamic and open. There always exist two questions: what is the connotation and extension for public safety research? What is the

methodology that fit the research requirement of public safety? In these paper, section 1 discusses what we can learn from the catastrophe case study, section 3 and 4 give the framework and methodology of public safety research, respectively, followed by concluding remarks.

2. CATASTROPHE CASE STUDY

There are many catastrophe cases that call for thinking.

Earthquake and tsunami in India Ocean occurred on December 26, 2004. It was propagated from India's Sumatra to Sri Lanka taking about 2 hours, with Tsunami's propagation speed of 200 m/s, the head height of 4-6m, the peak height of 8-10m, and the water impact of 300kg/m^2 , the peak impact of $1000\text{-}2000\text{kg/m}^2$. The sequel was terrible. The dead persons were more than 200,000, and the missing ones reached 50,000. The displaced persons were more than 500,000 (Homepage 1). Twenty countries were involved with the earthquake and tsunami. Indonesia's Aceh Province reached 4.5 billion U.S. dollars of damage, which was about 97% of GDP. The direct loss in Sri Lanka was about one billion U.S. dollars. And the tourism industry damage equivalent was about 300 million U.S. dollars. It provides us two scientific thinking. The first is the study of disasters feature information access and analysis at its early stage. Sri Lanka was struck 2 hours later of the initial tsunami. The casualties could be greatly reduced if the tsunami early warning signs were obtained and the organized evacuation preparations were made. The second is the mechanism study and science-based forecast. Various disasters and accidents will develop following its own law, it is important to study the cause and evolution of disasters and pre-warning methods so as to enhance our ability to response and cope with unexpected events.

At Jilin Petrochemical Company in China, aniline devices T-102 tower was block due to improper handling causing explosion on November 13, 2005, which resulted in about 100 tons of benzene pollutants entered the Songhua River, polluted water was flowed over the length of 1000km along its pathway in the River, and large-scale disruption of water supply affected the normal production and life (Homepage 2). The catastrophe gives us three scientific thinking. The first is to study derivatives, secondary and coupling disaster. Coupling of leak, water pollution and diplomatic problems was the typical secondary disasters. Mechanisms and rules, and multi-factor risk assessment theory and methods were among the key scientific problems in the area of unexpected event management. The second is to study coordinated multi-agencies response mechanism. An incident often involved multiple governmental administrations, such as safety monitoring and control, agriculture, water conservancy, environmental protection, foreign affairs and other government departments. Establishing a mechanism to communicate, coordinate and cooperate among various departments is crucial in emergency management. The third is to study multi-stage multi-objective decision-making contingency theory. Emergency response is the contingency for multiple goals and decision-making and response optimization at different stages of events such as quick

report for the incident, cleanup and disposal, pollution monitoring, information dissemination and other policy.

On April 3, 2003, 16 countries reported 2,270 cases of severe acute respiratory syndrome (SARS), among which 79 Chinese died (Homepage 3). The infected areas (referring to a secondary local transmission), included Toronto (Canada), Singapore, Hanoi (Vietnam), Beijing, Guangdong, Shanxi, Hong Kong and Taiwan (China). And as of April 12, 21 countries or regions reported 2,960 SARS cases and 119 deaths. This also gives us thinking. One is to study the mechanism for information sharing. Multi-channel, rapid and accurate information transmission and dissemination mechanisms among all levels of government, and public announcement were needed in dealing catastrophe like SARS. Another is to study the cognitive psychology and behavior. Psychological impacted by the incident and the extent of the uncertainty, emergency measures, and the transmission mechanism of social panic should be considered.

Hurricane Katrina in USA killed 1,000s people, and caused 500,000 become homeless, and affected 5 million (Homepage 4). The economic loss reached 100 billion U.S. dollars (risk management company statistics: economic losses amounted to 1 trillion U.S. dollars). The low efficiency in providing basic security and a stable social environment is oppugned. In emergency, only notice of danger for public was issued, but no timed evacuation plan and slow relief supplies. The main shelter in New Orleans (superball stadium) – a safe place for hurricane refugee became a man-made disaster site, where there was no proper facilities, disordered management, and some riots happened in this place. Two scientific thinking is induced from this catastrophe. The first is the impact of emergency decision shortcomings on the stability of society, i.e. study of disaster psychology, mass evacuation strategies, emergency response and the allocation of resources. The second is the effect of information dissemination mechanism on rescue, e.g. study on the emergency information gathering mechanism, and the optimal scheduling and distributing rescue forces.

On September 11, 2001, terrorists hijacked airplanes to hit the World Trade Center, causing the collapse of buildings. "9.11" incident left 3,200 people dead or missing, and economic losses running into hundreds of billions of dollars (Homepage 5). It was evidenced that this was an incident related to fire caused large buildings collapse. It was related to fire dynamics, safe evacuation, structural security and integrity, ad emergency response technology. Fire dynamics showed the formation of favorable building fire environment subject to complex thermal boundary conditions in a major building fires and its impact on heat transfer characteristics of building structure. Safe evacuation included the human behavior and evacuation model under a major building fire disaster. Structural security and integrity were involved with the conditions and modes of building structure failure and damage when subject to large change of heat settings, and thermo-mechanical coupling. Emergency response technology included decision-making and rescue under no early warning of emergency.

On May 12, 2008, 8 level earthquake occurred in Wenchuan. It caused 69226 death, 17923 missing, and direct economy loss was 8451 hundred million RMB (Homepage 6). In dealing with the earthquake, it had some problems. The first one is the knowledge of the mechanism of secondary

and derived disaster, i.e. what are the critical conditions. The second one is the traffic guarantee, i.e. how to design the traffic network for the robustness. The third one is the communication restoring, e.g. how to construct communication backup system. And the last one is the succor equipment, i.e. how to develop effective succor equipment for earthquake.

It should be noted that these catastrophe cases give us not only experiences, but also lessons. What can we learn from these catastrophe cases? It firstly states complicated scientific issues in public safety, which has the characteristics of multi-disaster, multi-factor, multi-scale, and variability. And there are key scientific questions in emergency management, e.g. risk assessment, monitoring and control, forecasting and early warning, command and decision-making, rescue and reconstruction, etc. This relies on public safety research.

3. FRAMEWORK OF PUBLIC SAFETY RESEARCH

Looking into the whole process of the emergency and its response, one can identify three key topics: the emergencies, the acceptors, and the response and management. What links the topics is the so-called “hazard elements”. Based on such ideas, a framework of public safety research is symbolized as a Triangle shown in Figure 1. The emergency is to study its occurrence, development, evolution laws to know the type, intension and time-and-space distribution characteristics for acceptors. The acceptor is to study destroy mechanism and mode from emergency, and know the incident chain effect. And the response and management is to study the type, time, strength of mankind’s interventions for both of emergency and acceptor.

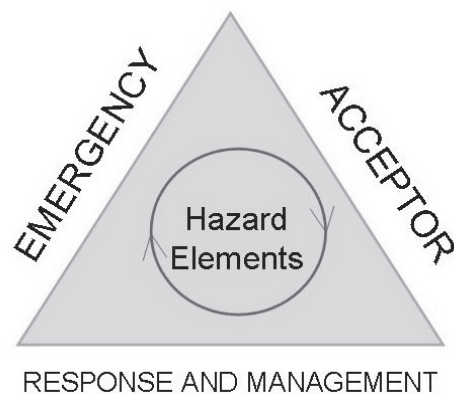


Figure 1: Triangle of public safety research

Hazard elements have forms of the matter, the energy, and the information. The way hazards elements induce emergency is to reach a critical value or meet with some activators. For example, the earthquake’s hazard element is crustal motion with the form of energy. Earthquake occurs when the crustal motion reaches a certain intension, i.e. energy reaches a critical value. The hazard element of a hazard materials leakage accident is the hazardous materials with the form of matter. When the hazardous materials mass exceeds the capacity of tank (critical value), or there are

some cracks causing explosion (activator), the hazardous materials leakage accident will take place. One of the society panic's hazard elements is the rumor with the form of information. If the information mass reaches a critical volume, or some inducing factors happen, the society panic may occur.

Emergency refers to those disasters or events that will bring damages to human beings, physical objects, and the social and natural environment. The evolution of emergency obeys some certain laws, and study of emergency is normally to find the temporal and spatial distribution of emergency effect and the affection manner with the form of energy, matter, and information.

Acceptor means the objects which receive the actions produced or released or carried by the emergencies. It is represented as human beings, substances (such as buildings, facilities, life-lines, etc), and operational social and economical systems. Acceptors' failure has two forms: body destruction or function failure. Failures of acceptors may cause unexpected release or activation of "hazard elements", which may induce secondary disasters forming the incident chain effects. We can think about the acceptors of earthquake as an example. The acceptors of earthquake include human beings, substance of buildings and lifeline system, etc. and system of environment and society, etc. Body destruction and function failure of the human beings are death and injured, and behavior ability, respectively. For substance, the body destruction is building collapse and tube crack, and the function failure is no residency and no water, etc. The function failure of systems takes the form of ecosystem destruction and society function loss, etc. Fire is the often occurred secondary incidents due to gas tube crack from earthquake. It is evidenced that gas tube is the acceptor of earthquake and behaves as the hazard element of fire.

The response and management refers to all the mankind's interventions aiming to disaster prevention and mitigation. It includes evaluation, preparedness, response and recovery etc. It is performed to the emergencies or to the acceptors, so as to reduce emergencies' actions or strengthen acceptors or break down the incident chain effect.

Studies of public safety are normally to find the evolution laws of hazard elements and to know the type, the intensity, and the temporal and spatial variation of the emergency's actions on the acceptors, to understand the states variation, the failure criterion, the vulnerability and reliability, and strengthen method for acceptors, and to find suitable manner, strength, time and scale to perform response and management. In summary, the core of the researches is to study the behaviors of hazard elements. That is, how the hazard elements convert to emergencies, how the hazard elements act on acceptors by emergencies, and how the failed acceptors cause domino effect via the hazard elements. Thereby one knows how to perform well-timed emergency managements appropriately.

4. METHODOLOGY OF PUBLIC SAFETY RESEARCH

The Methodologies of the above studies include five aspects of deterministic, stochastic, sensor-based methods, complex system approach, and combined methods.

The usual deterministic methods include experiments and simulations. Laboratory gravity currents are frequently used to model the dynamics of avalanches, accidental dense gas releases, and fire propagation (Hallworth et al. 1993). 3-d fluid dynamical model are used to simulate hazardous gas leakage (Chen, et al. 2007). Firstly grids of landform and city zone are built. Secondly number computation is carried out to get the hazardous gas distribution, and then the results are embedded into GIS. Figure 2 shows sulfureted hydrogen gas blowout simulation results. The flow rate is $200,000\text{m}^3/\text{h}$, and the concentration of mouth of well: 0.12 kg/m^3 .

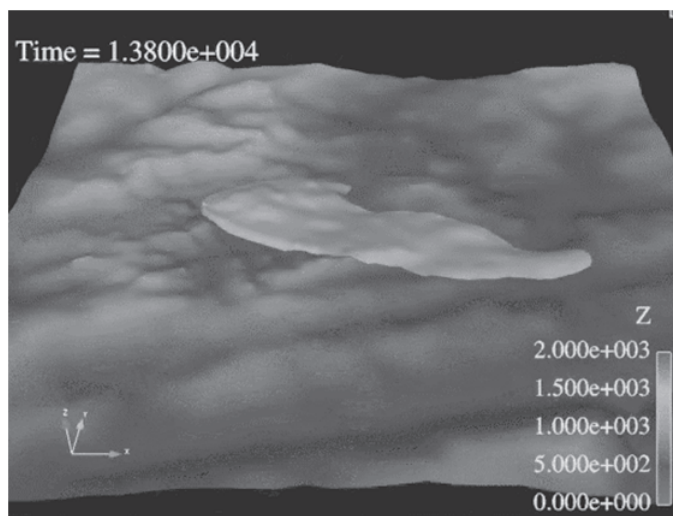


Figure 2: Sulfureted hydrogen gas blowout simulation results

Unfortunately, the deterministic method is not practicable for all kinds of emergencies, and some have to recur to stochastic models. Crime forecasting is a new research field of public safety. It is difficult to forecast crime with deterministic method due to its complexity. With 110 CAD crime data, time series model can be designed and short-term forecasting of property crime can be made. Two steps are designed to build the models. The first step is model recognition, and the next is to determine the model order and parameters. Based on the actual crime data, we can use Moving Average (MA) with the order of 1. Figure 3 gives the forecasting trend is consistent with the actual ones by week.

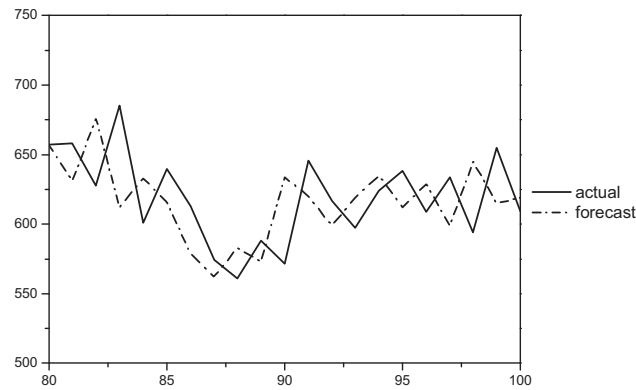


Figure 3: Property crime and its forecasting trend (by week)

Sensor-based methods are also important tools for public safety research. Information captured by detection apparatuses and analyzed is used to understand the temporal and spatial variation of disaster. The relationship between logged forest fire and droughts caused by El Niño are studied using coarse- and high-resolution optical and radar satellite imagery (Siegert, et al. 2001). When the materials accidentally release in a densely populated urban center, it is important to predict the transport characteristics of the plume to effectively manage emergency response and mitigate consequences. So it is necessary to develop an approach to determine the source location and its strength by an array of independent sensors distributed in the urban areas, combined with environment conditions, e.g. wind direction, wind velocity. A method of Markov Chain Monte Carlo sampling based on Bayesian inference is developed to determine the hazardous materials source using sensor data. Figure 4 shows the joint distributions of the source location on the plane with this method.

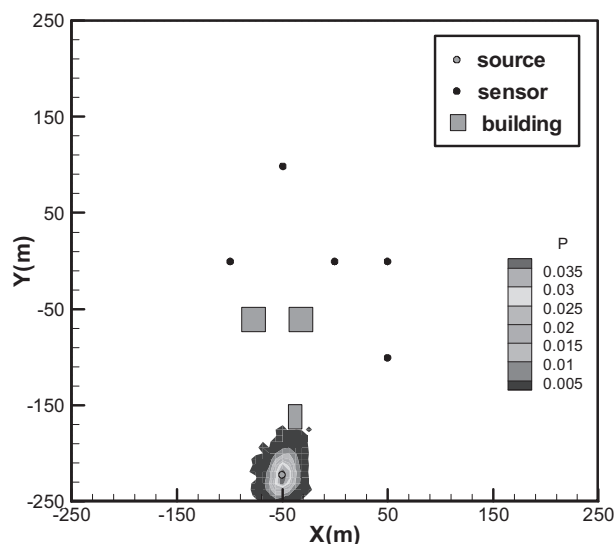


Figure 4: The joint distributions of the source location on the plane

Complexity in public safety results in more applications of complex system approach. Complex network theory is one of the most useful methods to study disease outbreak (Riley, 2007) and rumor spread in groups (Moreno, et al. 2004). It is also frequently used to study the robustness and resilience of life-line systems with the existing form of network (Albert, et al. 2000). The human travel has scaling law and the social group has evolution self-optimization characteristics (Brockmann, et al. 2006, Palla et al. 2007). Forest fire is an example of self-organized critical behavior (Malamud, et al. 1998). Decision-making is the key problem of emergency response and management, and the complex system approach, e.g. game theory and neural network, etc. is usually used to understand the decision-making task (Sanfey, 2007). To explore the effects of human travel patterns on the spatio-temporal dynamics of large scale epidemics, heterogeneous spatial metapopulation networks is constructed with the scaling laws of human travel, i.e. $p(r) \sim r^{-(1+b)}$ and $p(t_w) \sim t_w^{-(1+a)}$. Figure 5 gives the example time series of newly infected cases. The simulation results show that the occurrence probability of global outbreaks or the survival probability is significantly dependent on the characteristic travel distance, the characteristic waiting time and the memory effects of human travel.

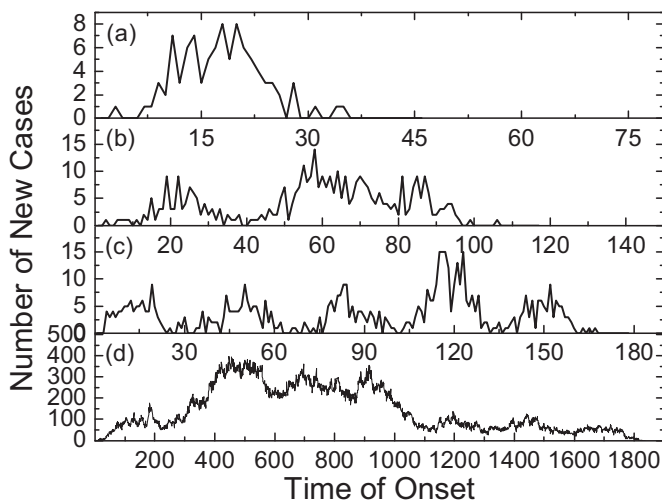


Figure 5: Example time series of newly infected cases

It is not easy to solve a public safety problem using only one of the above four methods due to its complexity. It has frequently a case that a main method performs with some other methods as supplements, i.e. combined methods. Information from sensor-based method is usually used for determination of some parameters for deterministic method, and modification of the data for stochastic method (Malamud, et al. 1998). Node or link dynamics using the deterministic model is useful to understand the whole network mechanism with the complex system approach (Albert, et al. 2000). Some models in the complex system approach are usually built by embedding the deterministic, stochastic and sensor-based methods (Batty, 2005). Integrated risk analysis is a typical case with the combined method. The occurrence probability of emergency is based on stochastic methods, and the evolution sequel of emergency is from deterministic methods.

Failure effects of acceptor are frequently based on deterministic methods. And the consideration of response and management are possibly based on sensor-based methods and complex system approach, etc.

5. CONCLUDING REMARKS

This paper presents some scientific thinking from catastrophe cases such as Indian Ocean Earthquake and Tsunami, Double benzene plant explosion at Jilin Petrochemical Company in China, SARS rampant in China, Hurricane Katrina in USA, the “911” incident in USA, and the recent Wenchuan Earthquake in China. Based on the case study, framework and methodology of public safety research are given. The emergency, acceptor, and response and management linked by hazard elements constitute the Triangle of public safety research. The methodology includes the deterministic, stochastic, sensor-based methods, complex system approach, and combined methods.

It should be noted that natural disasters and man-activity related incidents are common enemy of human being, and public safety is a general problem all over the world. Public safety research is complex in the framework and methodology, and has extensive problems to be solved. International cooperation and exchange among the countries should be enhanced, so as to jointly cope with calamity with more efficiency. Center for Public Safety Research, as a member of the community, will make further efforts in public safety research and education, and hopefully contributes to a better and safer environment for human life.

REFERENCES

- Albert R, Jeong H and Barabási AL., 2000. Error and attack tolerance of complex networks. *Nature*, 406: 378-382.
- Brockmann D, Hufnagel L and Geisel T., 2006. The scaling laws of human travel, *Nature*, 439: 462-465.
- Chen JG, et al. 2007. Numerical prediction and transportation study of poisonous gas transportation on complex terrain. *Journal of Tsinghua University*, 47: 381-384. (In Chinese)
- China State Council, 2006. *National Emergency Response Plan*. (In Chinese)
- Hallworth MA, Phillips JC, Huppert HE and Sparks RSJ., 1993. Entrainment in turbulent gravity currents, *Nature*, 362: 829-831.
- Homepage 1, <http://news.sina.com.cn/w/2005-02-04/17055047882s.shtml>.
- Homepage 2, <http://env.people.com.cn/GB/1073/3887374.html>.
- Homepage 3, <http://web.haoyisheng.com/html/hysh/sp-topic/sars/others/taolun02.htm>.
- Homepage 4, http://news.xinhuanet.com/world/2005-08/31/content_3424479.htm.
- Homepage 5, <http://dip.sinoth.com/Doc/article/2008/9/11/server/1000024157.htm>.
- Homepage 6, http://www.china.com.cn/news/txt/2008-08/21/content_16294134.htm.
- Malamud BD, Morein G and Turcotte DL., 1998. Forest fires: an example of self-organized critical behavior, *Science*, 281: 1840-1842.
- Moreno Y, Nekovee M and Pacheco AF., 2004. Dynamics of rumor spreading in complex networks, *Physical Review E*, 69: 066130: 1-7.

- Palla G, Barabási AL and Vicsek T., 2007. Quantifying social group evolution, *Nature*, 446: 664-667.
- Riley S., 2007. Large-scale spatial-transmission models of infectious disease, *Science*, 316: 1298-1302.
- Sanfey AG., 2007. Social decision-making: insights from game theory and neuroscience, *Science*, 318: 598-602.
- Siegert F, Ruecker G, Hinrichs A and Hoffmann AA., 2001. Increased damage from fires in logged forests during droughts caused by El Niño, *Nature*, 414: 437-440.
- Wen, J.B., 2006. *Government work report*. (In Chinese)

LESSONS FROM RECENT STORM SURGE DISASTERS -KATRINA, SIDR AND NARGIS

TOMOYA SHIBAYAMA
Yokohama National University, Yokohama, Japan
tomo@ynu.ac.jp

ABSTRACT

The present paper is a summary of the field surveys of storm surge disasters caused by the recent three major cyclones or hurricanes. Hurricane Katrina landed in Louisiana State, USA in August 29, 2005 and it gave strong impacts to the coastal area. In November 15, 2007, Cyclone Sidr passed southern part of Bangladesh. For this case, cyclone shelters that were constructed after the serious damage of 2001 cyclone were very effective to save lives. In May 2, 2008, cyclone Nargis attacked the south part of Myanmar that are the river basins of Irrawaddy and Yangon. Since there were few experience of cyclone attacks to river delta area, there were severe damages in the river basins.

1. INTRODUCTION

Coastal environments are vulnerable to three possible natural disasters, namely, tsunami, storm surge, and high wave attack due to storms. Since a storm surge is also caused by a Typhoon or a Cyclone, there is a considerable probability that the second and the third types of disaster can arrive to the same area at the same time.

In the history of human beings, many people have lost their lives, houses, properties, etc. due to coastal disasters. For example, in Nagoya city, Japan, 4,697 people were killed in 1957 due to the effects of a storm surge. In Netherlands, a similar disaster occurred in 1953. Recently, in 1991, a strong storm surge came to Bangladesh and in 2005 Hurricane Katrina came to the U.S. south coast. Hence, the Japanese experience became a strong motivation for the Japanese government to construct storm surge barriers along coastlines of concentrated urban coastal areas. Nonetheless, designing structures towards the protection against storm surges is a very important research topic in Coastal Engineering. Figure 1 shows a typical research flow for disaster mitigation. At the first stage of the flow, it is necessary to perform field survey to know the reality of disaster mechanisms.

In these three years, we have frequent attacks of storm surges. They are as follows.

- 1) Hurricane Katrina, south part of USA, August 29, 2005
- 2) Cyclone Sidr, south part of Bangladesh, November 15, 2007
- 3) Cyclone Nargis, south part of Myanmar, May 2, 2008.

For these three disasters, the author was the leader of disaster survey teams (Shibayama et al., 2006, Shibayama et al., 2008-1, Shibayama et al., 2008-2). In the following part, the survey results are briefly explained.

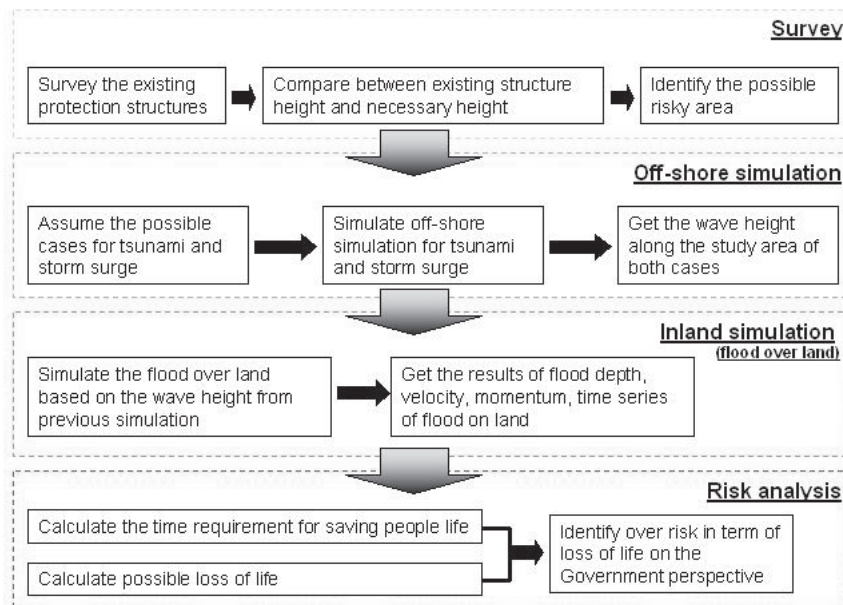


Figure 1: Flow of risk management for coastal disasters.

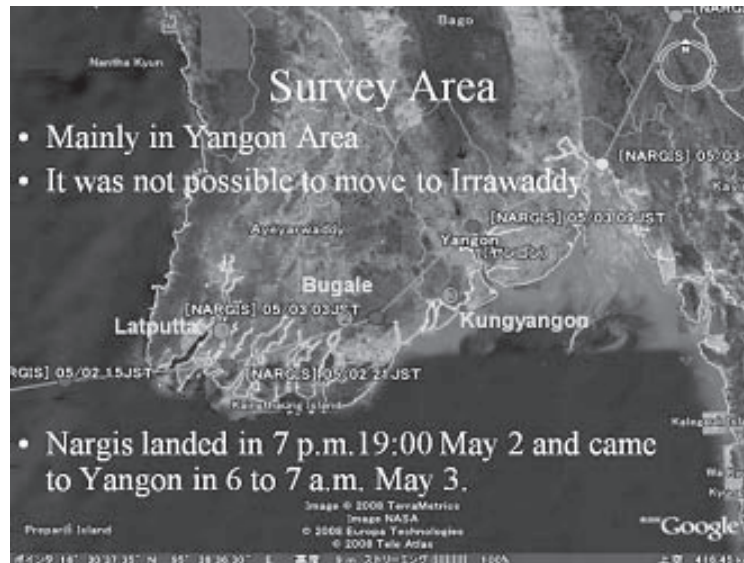
2. SURVEYS

2.1 Cyclone Nargis (Shibayama et al., 2008b)

Figure 2 shows the route of Nargis. It crosses the south part of Myanmar. Figure 3 shows our survey points along Yangon river. Significant storm surge occur in all survey points. Surge level changes from place to place and the maximum height in Yangon district was more than 3 m. Wave height over water level was also high up to more than 2 m. In rainy season under flood, the water level becomes almost equivalent to the ones in Nargis cyclone. Therefore people knew where to evacuate. Even for the cases that surge level was 0.3 to 0.4 m, houses were destroyed due to wind waves. Figure 4 shows one example of measurements. Due to strong restriction by the army, the survey area was limited.

The major findings are as follows.

- 1) The storm surge level was over 3 m in Yangon river basin and 4 m in Irrawadi river basin.
- 2) Storm surge traveled trough major rivers, branch rivers and irrigation channels, and flooded over land.
- 3) Residents are accustomed to floods in rainy season but not to storm surges.
- 4) It is worth while to compare with cases of Hurricane Katrina, Cyclone Sidr, and Indian Ocean Tsunami.



(Shibayama et al., 2008b)

H'. Thilewaa Port (old port)

N16 39'35.13", E96 15'28.49"
(27km from the river mouth)

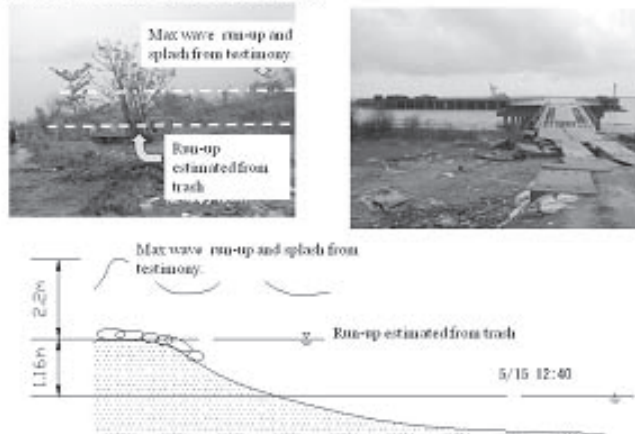


Figure 4: Result in Thilewaa Port (Shibayama et al., 2008b)

(Shibayama et al., 2008b)



Figure 5: Survey route and measured results after Sidr (Shibayama et al., 2008a)

2.2 Cyclone Sidr (Shibayama et. al, 2008a)

Field surveys were performed in the southwest of Bangladesh to learn lessons out of severe disasters due to Cyclone Sidr. Spatial distributions of inundation heights were measured around the most damaged area. Figure 5 shows survey route and measured heights. Inundation heights along the Baleshwar river and the Burishwar river were relatively high compared to those observed on the coast of Kuakata although these sites are far from the coast. Detailed surveys were thus performed in these three areas and there found several residents who witnessed bore-like waves hitting on the damaged area. Embankments along the river had been eroded before the storm while dikes on the coast significantly functioned to reduce the damages of the coastal area behind. Figure 6 shows one example of measurements in Sombonia.

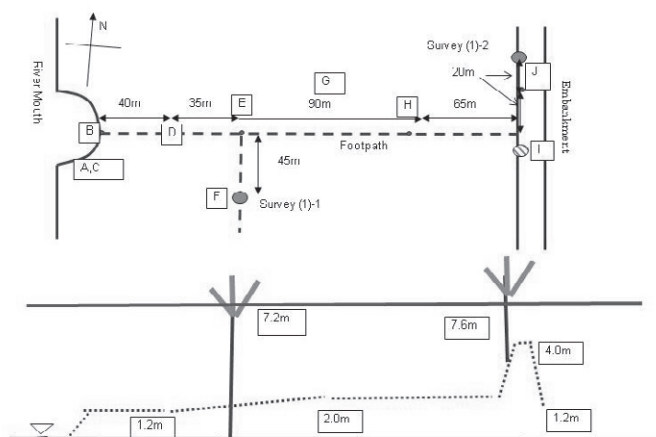


Figure 6: Results in Somboniya (Shibayama et al., 2008a)

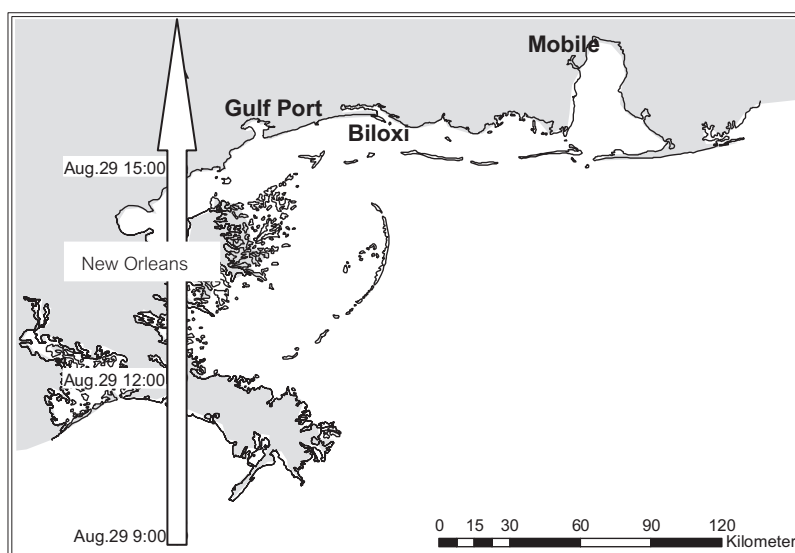


Figure 7: Route of Katrina (Shibayama et al., 2006)

2.3 Hurricane Katrina (Shibayama et al., 2006)

Figure 7 shows the route of Katrina and she hit the New Orleans and coast of Louisiana. Figure 8 shows measured result of Gulf Port and Figure 9 shows the result of Waveland. In Waveland, information from the real time video record was obtained. They are as follows.

- 1) Storm surge came to the city of Waveland at around 9:40 in the morning.
- 2) Almost in 20 minutes water level raised very rapidly and come to the level of roof of the 1st floor at 10:00.
- 3) At 13:30, water level became less than 1m inside of the house.

Wave effect on the damage characteristics

- Houses are totally collapsed in the area of about 250m from the coastline, and it is considered that damage by wave attack was remarkable in this area.

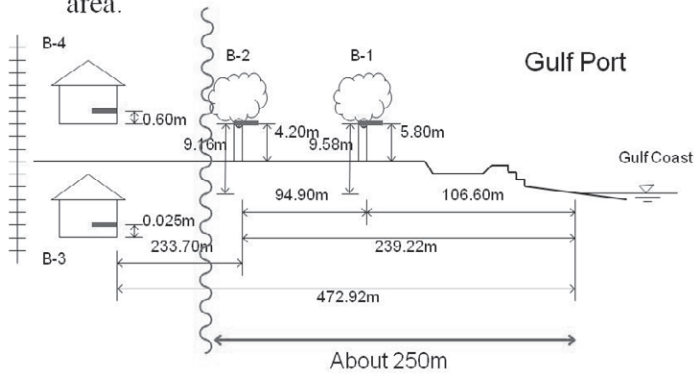


Figure 8: Results in Gulf Port
(Shibayama et al., 2006)

- Activity of storm surge is like flood and small waves with height less than 10cm were accompanied.
- Disaster mainly depended on flow level and flow velocity and wave effect looks minor from the video in this area.

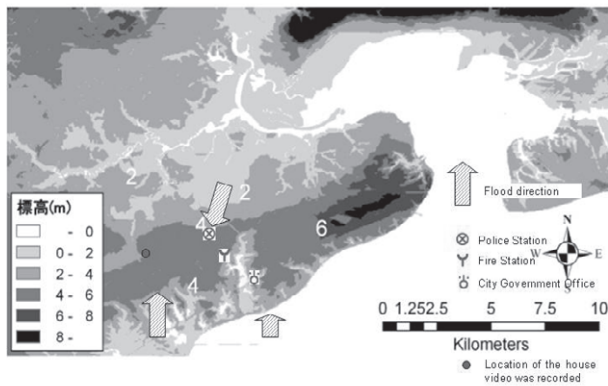


Figure 9: Results in Waveland
(Shibayama et al., 2006)

- 4) At 15:15, there were no water inside the house but in the street, water level was still half of the level of car doors.
- 5) At 16:00, water already went out from the street.

The storm surge stayed in the city for almost 5-6 hours but major disaster occurred during the first 3 hours.

As results of the survey we obtained the following conclusions.

- 1) Activity of storm surge is like flood and small waves with height less than 10cm were accompanied.
- 2) Disaster mainly depended on water level and flow velocity and wave effect looks minor from the video in this area.

- 3) The view of disaster site after storm surge looks like those of south Sri Lanka or Banda Ache of Indonesia which we observed in our tsunami survey work in those areas.
- 4) Water with high momentum suddenly came and washed away houses and destroyed them.
- 5) It was found that the wave force is more effective on the damage than the inundation only.
- 6) The major difference from Japanese concept comes out from land use and density of population in coastal area and also the policy of central or local government.

3. CONCLUSIONS

From the field surveys, it appeared that the number of lives lost depended on the geographical and social conditions of local area. For the retreat and recovery process, we should consider the local condition of the topography and the social conditions of the area. In order to establish a reliable disaster prevention system, we should design appropriate protection structures and also should design evacuation plan for residents in the area.

REFERENCES

- Shibayama T., Tajima, Y., Kakinuma, T., Nobuoka, H., Yasuda, T., Ahsan, R., Rahman, M. M., Islam, S., 2008a, Storm Surge due to Cyclone Sydr in Bangladesh, *Annual Journal of Coastal Engineering*, 52(2) (in Japanese)
- Shibayama, T., Takagi, H. and Hgun Hnu, 2008b, Survey of storm surge by cyclone Nargis, *JSCE Magazine 'Civil Engineering'*, Vol. 93, No. 7, 41-43, (in Japanese).
- Shibayama, T., Yasuda, T., Kojima, H., Tajima, Y., Kato, H., Nobuoka, H., Yasuda T., and Tamagawa, T., 2006, Survey of Disaster Damages by Hurricane Katrina, *Annual Journal of Coastal Engineering*, 50(2), 401-405 (in Japanese).

INDUSTRIAL SAFETY IN THE 21ST CENTURY AND ROLE OF SAFETY ENGINEERING

MASAMITSU TAMURA
Professor, Yokohama National University
Emeritus Professor, The University of Tokyo
Japan
m-tamura@ynu.ac.jp

ABSTRACT

In order to highlight recent industrial safety problems, we cite a few chemical accidents that recently occurred in Japan and discuss their background factors from the viewpoints of a change in human perspective and social situations and changes in the industrial structure.

Accordingly, we put forth a proposal for industrial safety in the 21st century. It is as follows: every product must be harmonized with individuals, society, and the environment at every stage of its life cycle—from production to consumption to disposal—and safety should be one of the most important considerations for industrial activities.

In order to ensure industrial safety in the 21st century, we classify a few influential factors on the recent industrial safety problems and introduce and discuss a concept of “safety power”.

Safety power indicates the safety level of plants and is composed of potential safety basis and safety culture. For the promotion of self-controlled safety, the concepts of safety power, potential safety basis, and safety culture and their evaluation indicators must be discussed so that they can be established, and a system for evaluating and intensifying safety power must be developed.

In order to promote industrial safety, safety engineering should be developed and established; the systemization of safety engineering and the development of the basis of safety engineering should be discussed.

It is expected that safety engineering will help the improvement of not only industrial safety but also social safety.

1. INTRODUCTION

Today, chemical substances have become indispensable for living a comfortable life. For one, they play a vital role as sources of energy; fine chemicals such as drugs and agricultural products, materials, etc—in

essence, all applications that have resulted in making our lives more comfortable.

Their several advantages notwithstanding, chemical substances may potentially cause energy hazards, health hazards, and environmental hazards. Improper handling of chemicals with potential hazards without adequate knowledge may result in fires or explosions, health problems, and environmental problems.

In this report, we cite a few chemical accidents that occurred in the recent past in Japan in order to highlight recent industrial safety problems, and we discuss their background factors from the viewpoint of changes in human perspective and social situations and changes in the industrial structure. We can easily relate influential background factors on the recent industrial safety problems in other industries to those associated with the chemical industry.

In this work, we put forth a proposal for industrial safety in the 21st century. It is as follows: in this, the 21st century, every product must be harmonized with individuals, society, and the environment during every stage of its life cycle—from production to consumption and then, finally, to disposal—and safety should be one of the most important considerations as far as industrial activity is concerned.

In order to ensure industrial safety in the 21st century, influential factors on the recent industrial safety problems have been classified and a concept of “safety power” has been suggested and discussed. Safety power indicates the safety level of a plant and is composed of two parameters—potential safety basis and safety culture. In order to promote self-controlled safety, each concept of safety power, potential safety basis, and safety culture should be discussed, their evaluation indicators should be determined, and a system should be developed for evaluating and intensifying safety power.

In addition, safety engineering should be developed and established so that it can contribute to the promotion of industrial safety. In this paper, we discuss the systemization of safety engineering and the development of the basis of safety engineering.

2. RECENT SAFETY PROBLEMS AND THEIR BACKGROUND

2.1 Recent safety problems involving chemical substances

Several accidents and problems involving chemical substances have recently occurred in Japan; for example, an explosion accident during the transport of hydrogen peroxide in 1999, an explosion accident of hydroxylamine during preparation in 2000, an explosion accident of fireworks, a fire and explosion accident of RDF during storage, a fire accident in petroleum tanks during an earthquake, an explosion accident of a gas holder during storage and a fire accident in a rubber plant during preparation in 2003, a fire accident in a petroleum tank during storage, and some fire accidents in a hydrogenation process, an accessory equipment of a topper, and the hydrogen preparation process at petroleum plants in 2006. All these accidents occurred could be attributed to factors such as a lack of

safety awareness; insufficient safety knowledge; shortcomings in safety management such as deterioration of equipments, investment cuts, and personnel reduction due to outsourcing and increased utilization of subcontractors; and insufficient budget allocation, personnel affairs, etc.

2.2 Background of safety problems

The recent economic development and an improvement in people's lifestyle have drastically altered human perspective and social situations and have changed industrial structure remarkably by way of rapid advancement, multiplicity, complexity, and internationalization of industries. This has brought about drastic changes in all spheres of social life: education programs have changed, families now include a smaller number of children, the basic family unit is witnessing a shift from an extended setup to a nuclear setup, and internationalization is taking place. However, these changes lead to various problems. For example, the younger generation may have a low sensitivity to hazards, a different sense of values, and a low social awareness due to the protected and restricted environment they are exposed to and their limited experience of hazards during their childhood.

In addition, the existing game generation believes that any action can be approached like a game and, therefore, can be performed without deep consideration.

We must bear in mind that due to rapid advancement, multiplicity, complexity, internationalization, and extreme situation of industries, the potential hazards of materials and processes increase. Secondly, due to differentiation, specialization, and computerization of jobs, engineers and workers have some difficulties in comprehending the overall picture as well as the individual processes. Thirdly, due to rationalization and restructuring, there remain only a few experienced workers capable of understanding the contents of the processes. These features may lead to difficulties in technical transfer on process safety from experienced workers to young workers.

3. INDUSTRIAL SAFETY IN THE 21ST CENTURY

Society in the 21st century is expected to be harmonized with safety and the environment. Therefore, in addition to focusing on their quality and productivity targets, industries must also endeavor to harmonize technology with safety and the environment.

Therefore, it is imperative that every product must be harmonized with individuals, society, and the environment during every stage of its life cycle—from production to consumption to disposal—and safety should be one of the most important considerations with regard to industrial activities.

In order to ensure industrial safety in the 21st century, it is important to classify the influential factors on the recent industrial safety problems, and efforts must be made to intensify self-controlled safety by (1) promoting the concept of safety power and (2) by improving international competitive power.

Figure 1 shows the classification of influential factors on recent industrial safety problems.

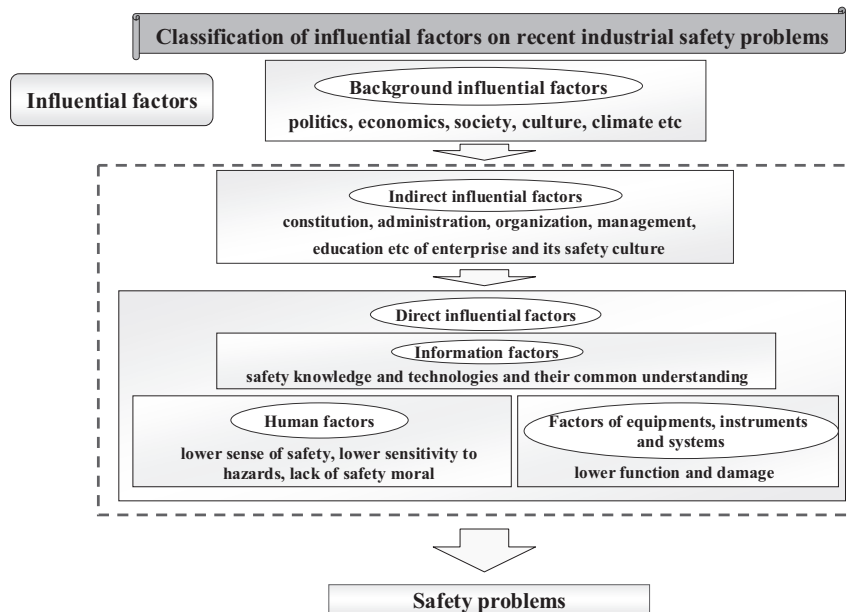


Figure 1: Classification of influential factors on recent industrial safety problems

Accidents such as an explosion or fire at a plant involve direct influential factors such as human factors (low sense of safety, low sensitivity, lack of safety morals, etc.); factors concerning equipment, instruments, and systems; and information factors (safety knowledge and technology and their common ownership). However, in many cases, in addition to the direct influential factors, certain indirect influential factors such as constitution, administration, organization, management, education, and safety culture of plants may be involved. In such a scenario, it becomes essential to consider that a solution to essential problems may not be found only by solving problems due to direct influential factors. Furthermore, some background influential factors such as regulations, economics, society, culture, climate, etc. may also exist, in which case it may not be possible to solve the problems existing at the plant by our efforts.

Then, in order to increase awareness of self-controlled safety, we introduce and discuss a concept described as “safety power”.

Safety power indicates the safety level of plants and is composed of (1) potential safety basis and (2) safety culture, to support potential safety basis.

Figure.2 shows the two components of safety power.

In the production process, products are manufactured from raw materials using equipment, instruments, and systems. Safety can be ensured by adequate safety management, operation management, and equipment management. Potential safety basis would imply the use of some adequate technologies, organizations, and management to carry out production from the viewpoints of quality, efficiency, and safety.

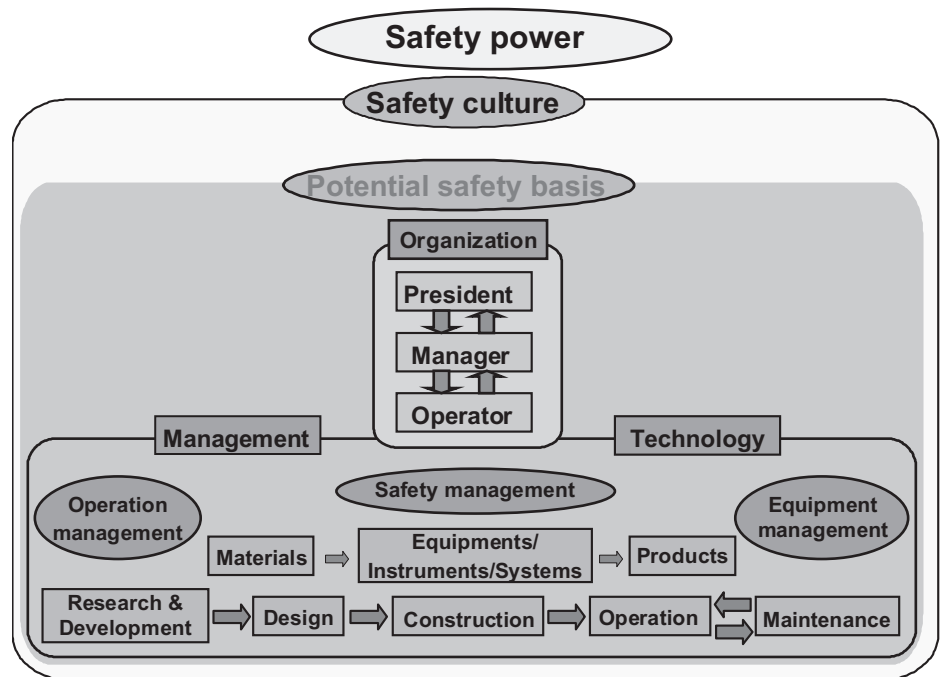


Figure 2: An idea for safety power composed of potential safety basis and safety culture

Figure 3 shows a change in risk with the introduction of safety systems. Risk could be reduced by introducing equipments and instruments for the prevention of accidents and perfecting manuals and guidelines at the first stage and, furthermore, by introducing a risk management system at the second stage. Then, the task ahead is to think about the introduction of safety culture for additional risk reduction at the third stage.

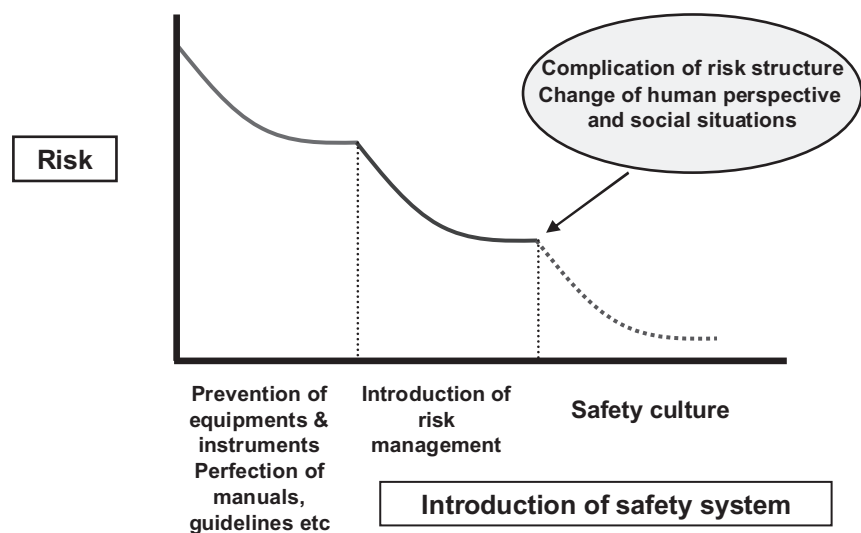


Figure 3: Introduction of safety systems and risk

Figure 4 shows an idea for systemization of safety culture. It comprises eight elements, namely, top governance and commitment as top management; source management and work management as management; awareness, motivation, and learning as a potential ability of individuals and the organization; and communication in the internal organization and with the external organization.

It then becomes necessary to discuss each concept of safety power, potential safety basis, and safety culture in order to establish them and determine their evaluation indicators.

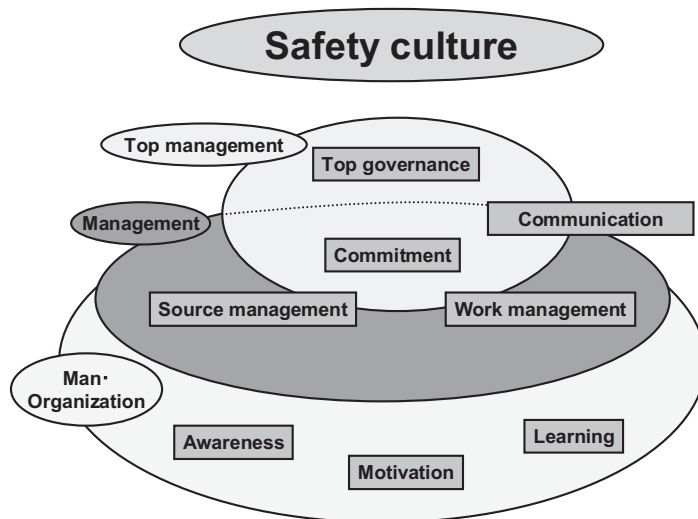


Figure 4: An idea for systemization of safety culture

Figure 5 shows a system for evaluating and intensifying safety power. We can establish an evaluation method for safety power by developing a process safety management program and a safety culture program, following which we can intensify safety power by using the established evaluation methods. In such a case, the evaluation of safety power should be conducted first by self-evaluation and then by a third-party evaluation for the purpose of objectivity and the intensification of safety power should be carried out not only by self-intensification but also by the support of a third party. In addition, supporting systems can be used for evaluating and intensifying safety power.

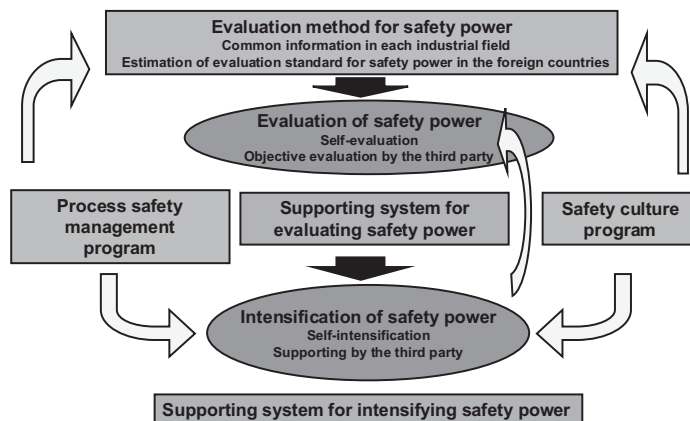


Figure 5: System for evaluating and intensifying safety power

4. ROLE OF SAFETY ENGINEERING AND ITS DEVELOPMENT

In this section, we describe the systemization of safety engineering, the development of the basis of safety engineering, and the social contributions of safety engineering.

4.1 Systemization of safety engineering

First, we discuss the concepts of risk and safety and then discuss the systemization of safety knowledge. We are faced with many risks indicating frequency and effect of incidents and accidents in our daily life and society; due to food, clothing, shelter, sports, leisure, travel, hobby, etc. As shown in Figure 6, safety would imply a situation in which the level of risk decreases below a predecided social allowance level due to efforts of individuals, organization, and society. In this case, a social allowance risk level implies an allowance risk level decided by society after considering both benefit and risk.

To clarify the concept of systemization of safety engineering, we first consider the systemization of safety knowledge.

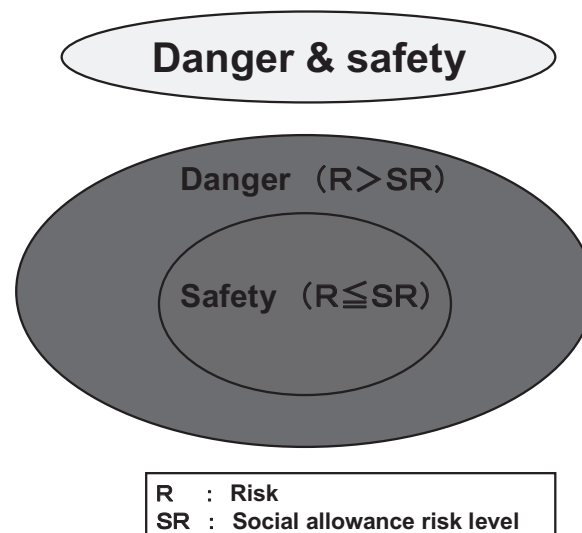


Figure 6: An idea for danger and safety

Figure 7 shows a system of safety knowledge. In order to ensure safety, it is necessary to carry out hazard identification first, followed by risk evaluation and, finally, risk management from the viewpoints of benefit and risk. Further, it would be necessary to develop a system comprising the organization, management, education, regulations, etc. so that individuals and the organization could ensure safety by using safety knowledge basis on common knowledge in all fields and specific knowledge in each field.

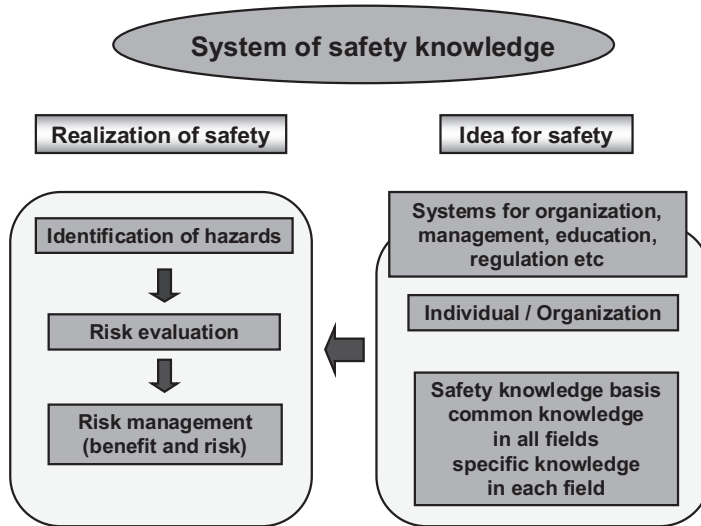


Figure 7: System of safety knowledge

Figure 8 shows the utilization fields of safety.

Enterprises should operate by taking into consideration not only safety administration (finance, credit, etc.), production safety such as material safety and process safety, and product safety, but also regulation, internationalization, and the private and social lives.

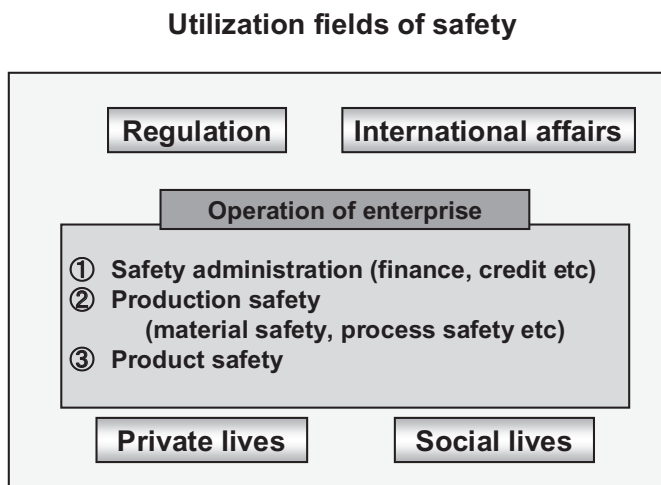


Figure 8: Utilization fields of safety

Figure 9 shows the systemization of safety engineering fields. As shown in the figure, safety engineering broadly comprises common fields and specific fields. Figure 10 shows the systemization of safety knowledge in the chemical industry as an example; in this case, safety knowledge encompasses common knowledge as well as specific knowledge.

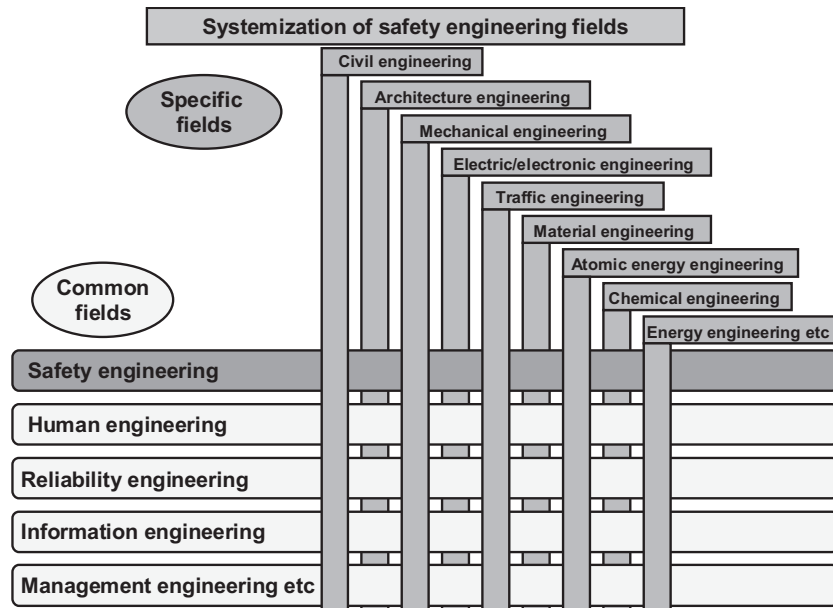


Figure 9: Systemization of safety engineering fields

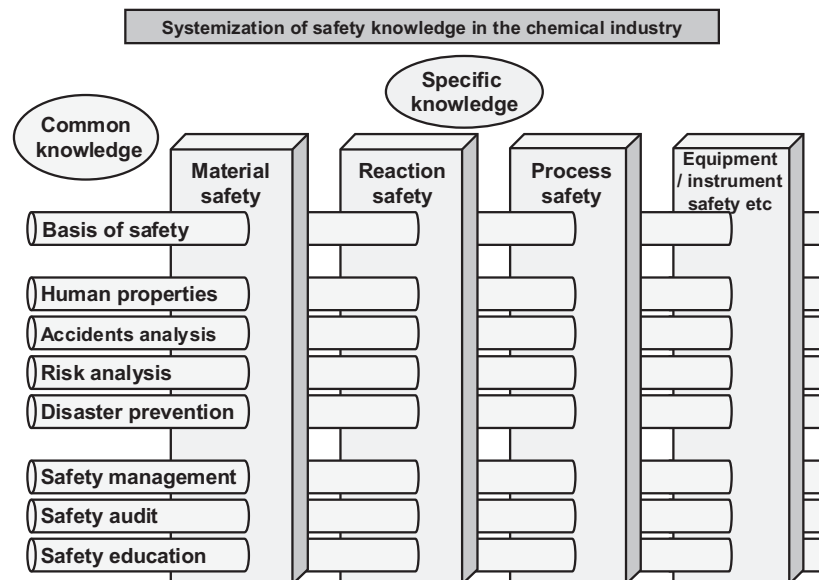


Figure 10: Systemization of safety knowledge in the chemical industry

4.2 Development of the basis of safety engineering

Figure 11 shows the concept of industrial safety that also takes into consideration social safety. Henceforth, when dealing with industrial safety, we must consider not only production safety in industry but also product safety in society

Figure 12 shows the development of a forcing engine for safety engineering for contribution to society. To develop a forcing engine for safety engineering, we should make up safety specialists data base (DB) and their training method in the general and specific fields, develop a safety knowledge basis in the common and specific fields, and develop safety engineering methods such as hazard prevention methods, safety evaluation

methods, risk prevention methods, and accident analysis methods in the common and specific fields.



Figure 11: A concept of industrial safety considering social safety

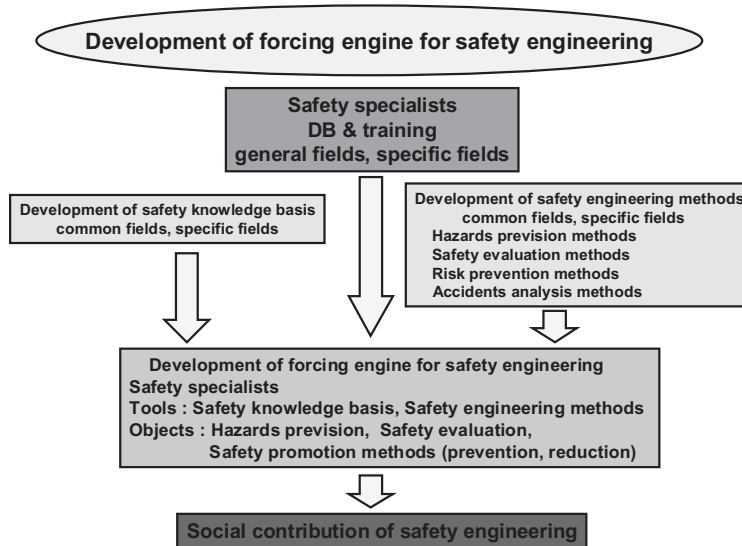


Figure 12: Development of forcing engine for safety engineering

4.3 Social contribution of safety engineering

Figure 13 shows the social contribution of safety engineering. Imparting safety education and training as general education for safety basis and as education for safety specialist would contribute not only to industrial safety but also to social safety. In our study, safety education and training comprise an understanding of safety basis and development of safety culture (safety ethics, sensitivity to hazards, scientific discussion and decisions based on benefit and risk), training imparted to citizens, and training safety specialists to provide them with high safety knowledge, high safety technologies and risk management abilities.

Imparting special knowledge on safety and safety engineering methods would contribute mainly to industrial safety and the suggestion of a

safety policy would benefit administration. Safety support would contribute to industrial safety, social safety, as well as administration.

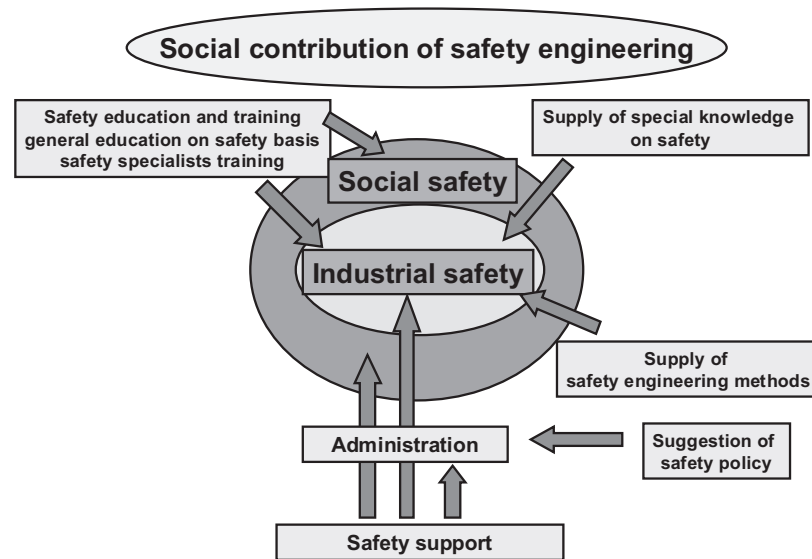


Figure 13: Social contribution of safety engineering

5. SUMMARY

In this paper titled “Industrial Safety in the 21st Century and Role of Safety Engineering,” some recent industrial safety problems have been cited and some background has been provided from the viewpoints of change in human perspective and social situations and a change in the industrial structure.

Accordingly, a proposal for industrial safety in the 21st century has been put forth.

In order to ensure industrial safety in the 21st century, influential factors on the recent industrial safety problems have been listed and a concept of safety power—which indicates the safety level of plants and is composed of potential safety basis and safety culture—has been introduced and discussed. In order to promote self-controlled safety, each concept of safety power, potential safety basis, and safety culture and their evaluation indicators should be discussed so that these concepts can be established, and a system for evaluating and intensifying safety power must be constructed.

In addition, it has also been shown that safety engineering should be developed and established so that it can promote industrial safety; further, the systemization of safety engineering and the construction of the basis of safety engineering should be discussed.

It is expected that safety engineering would help the improvement of not only industrial safety but also social safety.

MONITORING OF URBAN SUSTAINABILITY BY USE OF REMOTE SENSING

YOSHIFUMI YASUOKA

National Institute for Environmental Studies
16-2 Onogawa, Tsukuba, Ibaraki 305-8506 Japan

+81-29-850-2301

yasuoka@nies.go.jp

ABSTRACT

Monitoring of urban infrastructure and environment is the first step in the proper management of urban system. However, it requires the measurement of a wide variety of parameters covering physical, chemical, biological, and geographical aspects. Furthermore, it needs to consider extensive parameters encompassing the local to regional scale, or sometimes to global scale within short- to long-term periods. It is, therefore, not easy to monitor these varied parameters and to establish a database system for urban safety and sustainability using conventional ground survey methods alone. Remote sensing from space is expected to provide a new tool for regularly observing a wide range of variables over extensive areas.

Development of remote sensing technology has been very rapid, and today various types of remotely sensed data are available, ranging from high spatial resolution data for local monitoring to coarser wide coverage data for regional/global surveillance. Information from remote sensing, however, has not necessarily been fully utilized yet. In this paper, new technologies in remote sensing are surveyed, and their applications are introduced, with emphasis on the assessment of urban infrastructure and environment.

1. INTRODUCTION

Sustainable urban system requires sound infrastructure and sound environment. Degradation of infrastructure and environment, however, has become a critical social problem in most cities of the Asian countries during the past decade. On a local scale, we have experienced building collapse or dangerous concrete block falls in railway tunnels or under highway bridges due to concrete disintegration. Also on a regional scale we have been suffering from air pollution, water quality degradation or heat island phenomena. Furthermore nowadays global warming or global scale climate change may cause new types of urban risks threatening people living in cities.

Assessment of urban infrastructure and environment is an essential component in realizing urban sustainability. However, it requires the

measurement of a wide variety of parameters covering physical, chemical, biological, social and geographical aspects. Furthermore, it needs to consider extensive parameters encompassing the local to regional scale, or to global scale.

Remote sensing is an observation tool to identify objects, measure or analyze their characteristics without directly contacting them. By using aircraft or satellite as an observation platform it enables us to measure various parameters over extensive areas at a regular interval. It is expected that a wide variety of urban parameters may be measured spatially and regularly over extensive areas by remote sensing.

This paper introduces new technologies in remote sensing, and their applications with emphasis on the monitoring urban infrastructure and environment.

2. REMOTE SENSING

2.1 SPECTRAL CHARACTERISTICS

Remote sensing utilizes electromagnetic radiation as a medium for the measurement. The measurement principle in remote sensing is based on the fact that all matter reflects, absorbs, transmits, and emits electromagnetic radiation in a unique way with respect to wavelength. These unique properties in matter with respect to electromagnetic radiation are called its "spectral characteristics (spectral signatures)", and objects are identified, measured, and analyzed based on their different spectral signatures.

2.2 REMOTE SENSOR

In remote sensing, the reflected or emitted electromagnetic radiation from a target is detected by a device called a "remote sensor". Cameras or scanners are typical examples of these. A vehicle to carry the sensor is called a "platform", and aircraft or satellites are usually used. Human eyes can only detect a specific range of electromagnetic radiation called the "visible range". However, remote sensing can utilize a wide variety of wavelengths covering the visible, near-infrared, and infrared to microwave ranges with various types of sensors. Utilization of different wavelengths enables the monitoring of various types of environmental parameters. For example, vegetation is characterized primarily in the near-infrared range, whereas thermal characteristics are distinguished in the thermal infrared wavelength band.

The performance of a remote sensor is determined by various specifications including spectral range, spectral resolution, spatial resolution, observation width (swath), or observation frequency. Different types of remote sensor have been developed with respect to these specifications. Table 1 summarizes the properties of typical remote sensors used for environmental and disaster monitoring. High spatial resolution sensors such as LANDSAT TM, SPOT HRV, or IKONOS are used for local or regional observation, whereas low spatial resolution, but wide coverage

and high observation frequency sensors such as NOAA/AVHRR, ADEOS/OCTS, and TERRA/MODIS are used for continental or global scale vision.

Table 1 Specifications of typical remote sensors.

| Satellite | Sensor | Wavelength (μ m or GHz) | No. of bands | Spatial Res. (m) | Swath (km) | Cycle (day) |
|-----------|---------|---------------------------------|--------------|---------------------|---------------|----------------|
| LANDSAT | TM | 0.45-12.5 | 7 | 30 | 180 | 17 |
| SPOT | HRV | 0.50-0.89 | 4 | 10-20 | 60 | 26 |
| ERS-1 | SAR | 5.3 GHz | 1 | 20 | 100 | 35 |
| JERS-1 | OPS | 0.52-0.86 | 4 | 18 | 75 | 44 |
| " | SAR | 1.275 GHz | 1 | 18 | 75 | " |
| NOAA | AVHRR | 0.58-12.5 | 5 | 1000 | 2700 | 0.5 |
| ADEOS | AVNIR | 0.40-0.92 | 4 | 8 - 16 | 80 | 41 |
| " | OCTS | 0.40-12.5 | 12 | 700 | 1400 | " |
| TERRA | ASTER | 0.52-11.3 | 14 | 15 - 90 | 60 | 16 |
| " | MODIS | 0.66-14.2 | 36 | 250-1000 | 2330 | " |
| IKONOS | Pan/MSS | Vis./Near-infrared | 1/4 | 1-4 | 11 | 11 |
| ALOS | AVNIR-2 | 0.42-0.89 | 4 | 10 | 70 | 46 |
| | PRISM | 0.52-0.77 | 1 | 2.5 | 70/35 | " |

2.3 PARAMETERS BY REMOTE SENSING

Urban parameters expected to be measured by remote sensing are ranging from physical, chemical, biological to socio/economic variables. They are also from practical/operational level to research level. Examples of parameters are summarized as follows.

Practical level

Land: land surface temperature, topography (DEM), 3-dimensional structures of buildings and vegetations, land cover classification, vegetation classification, vegetation index (NDVI, etc.), soil index, human habitats

Water: surface temperature, water quality including suspended sediment and chlorophyll, surface wind-vector, sea-ice

Atmosphere: temperature, water vapor, cloud

Others: precipitation

Research level

Land: detail land cover classification, detail vegetation classification, soil type classification, soil moisture, LAI (Leaf Area Index), biomass, tree height, canopy structures, NPP (Net Primary Productivity), CO₂ flux (NEP: Net Ecosystem Exchange), chlorophyll/lignin/cellulose in tree canopy

Water: chlorophyll (high accuracy), algae, pCO₂

Atmosphere: CO₂, CH₄, water vapor, CLO, NO_x, SO_x, O₃, aerosols

It should be noted that remote sensing may provide spatial distribution of these parameters from a local scale to a regional or a global scale with various sensors shown in Table1. Conventional ground-based observation methods may provide only point-based information.

3. NEW TECHNOLOGY DEVELOPMENT IN REMOTE SENSING

(1) High-Spatial Resolution Observation

Spatial resolution is one of the most important observation performance factors in remote sensing. It has been dramatically improved in the last 20 years, and, today, one-meter spatial resolution is realized in satellite sensors. From these images, for example, individual buildings or tree canopies can be identified from space. High spatial resolution observation enables us to retrieve more detailed information on human settlements, land surface characteristics, or topography from remotely sensed data.

(2) Hyper-Spectral Observation

The number of spectral channels in conventional remote sensors has been limited to 10 or at most to several tens in satellite and airborne systems. New hyper-spectral sensor systems have the capability of observing the land surface using a couple of hundred channels. For example, the Hyperion on EO-1 has 256 channels. Airborne sensor systems such as CASI and AVIRIS also have more than 200 channels and their spectral resolution is as narrow as nanometers in wavelength. Data from such hyper-spectral sensors have indicated the possibility of observing new urban parameters, including vegetation water stress or detailed vegetation categories that could not be observed by conventional sensors. Recently, new observation methods using the hyper-spectral remote sensors have been developed to detect concrete degradation.

(3) Microwave Range Observation

With optical remote sensing we cannot observe the ground through cloud or dense haze. Microwave remote sensing has an advantage in all weather observations due to its longer wavelength. This observation capability enables us to monitor land surface conditions regularly, even in heavily clouded regions, including tropical or high latitude regions. A synthetic aperture radar (SAR) is a typical microwave sensor that enables high spatial resolution observation. Microwave remote sensing also has the capability of monitoring precipitation and soil moisture.

(4) Three-Dimensional Observation

Three-dimensional (3-D) structure in urban area is one of the essential information for the assessment of the environment and the extent of disaster. The information derived may be used for base data in wind simulation, run-off modeling, or landscape analysis. Since urban infrastructure is complicated by buildings, roads, or trees, it is not easy to extract 3-D information using conventional observation or survey methods alone. New remote sensing technologies may provide details of 3-D structures with a high spatial resolution. Laser ranging observation, for example, enables us to produce height distribution maps of buildings or trees.

4. APPLICATIONS OF REMOTE SENSING TO URBAN SUSTAINABILITY MONITORING

4.1 Local Scale Applications

(1) Monitoring Of Concrete Degradation

Concrete degradation has become serious problems in Asian urban areas. Recent years, for example in Japan, railway trains were damaged by the fallen concrete blocks in tunnels. These were proved to be due to concrete degradation. Spectral signatures observed by hyper-spectral remote sensing may provide key information on concrete degradation. Figure 1-2 shows the examples of spectrum for the degraded concretes due to carbonation. Normal concretes (Figure 1) contain 25% of calcium hydroxide. Concretes damaged by carbon dioxide (Figure 2) generates calcium dioxide in its process. Absorption peak observed around 1450nm in normal concrete is hardly observed in degraded concretes. These characteristics indicate that the spectrum of concretes damaged by carbon dioxide is strongly affected by the spectrum of calcium dioxide that is generated in its degradation process.

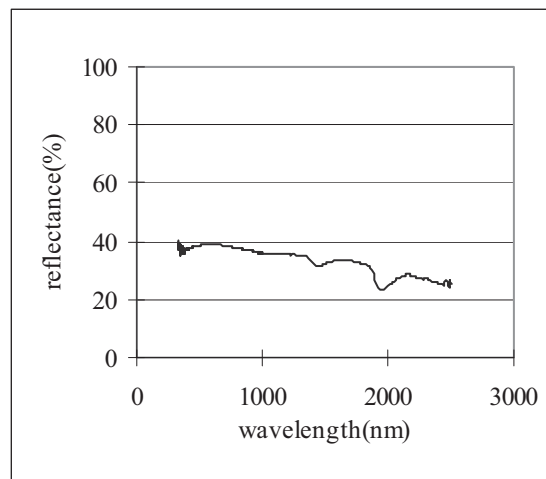


Figure 1: Spectrum of normal concrete

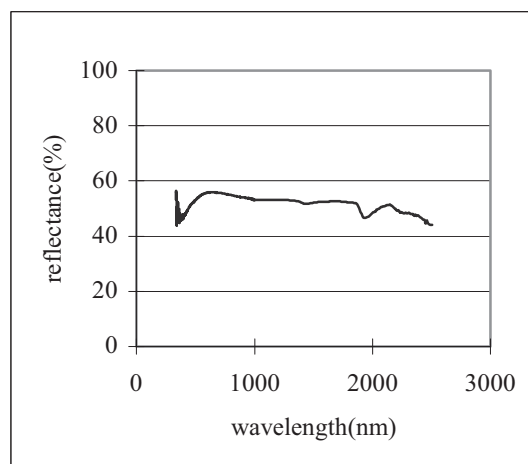


Figure 2: Spectrum of degraded concrete by CO₂

(2) Urban Landscape Simulation

Urban 3-D structure is one of the most essential factors that define the characteristics of urban sustainability. Distribution of buildings and vegetation play a key role in microclimate simulation, traffic navigation, or landscape planning. Figure 3 demonstrates an example of an urban 3-D image with buildings and trees in the Shinjuku area of Tokyo. In this application, an urban 3-D model is produced from the ALS data combined with high spatial resolution satellite data (IKONOS). Heights are extracted from the ALS data, and land-cover information including buildings and trees is extracted from IKONOS data (Guo, 2003). The trees in Figure 3 are simulated by a growth model after identifying their position, canopy size, and species from both the IKONOS image and the ALS data. This model enables us to simulate tree growth and conditions for the different seasons. Here, the 3-D tree model is generated using Nat-FX and 3-D modeling software. Nat-FX is a 3-D tree growth model developed based on the Atelier of Modeling of Architecture and Plants (AMAP) (Yasuoka, 2003).



Figure 3: Urban 3-D model produced from IKONOS satellite image and airborne laser scanner (ALS) data. Trees are simulated using a growth model after identifying tree positions and species from remotely sensed data.

4.2 REGIONAL SCALE APPLICATIONS

(1) Urban Heat Island

The heat island effect is a typical phenomenon in urban areas associated with an increase of population and human activity. It may have negative impacts on the physical environment and social infrastructure in most mega-cities in the near future. Monitoring and prediction of a heat island, however, is not easy since the thermal conditions of urban areas are not visible. Remote sensing has provided an observation tool to monitor land surface temperature (LST) and to assess heat island conditions in cities using infrared wavelengths. Figure 4 illustrates heat island conditions in Asian cities observed from MODIS data. Statistical analysis indicated that there is a strong correlation between land surface temperature and land cover types (Hung, 2005).

(2) Monitoring Of Forest Fire

Forest fire gives serious impact to local and regional society. It affects surrounding environment and human health. Establishing forest fire monitoring and forecasting system is crucial to decrease damages by fire events and to decrease environmental and disaster risks in urban area.

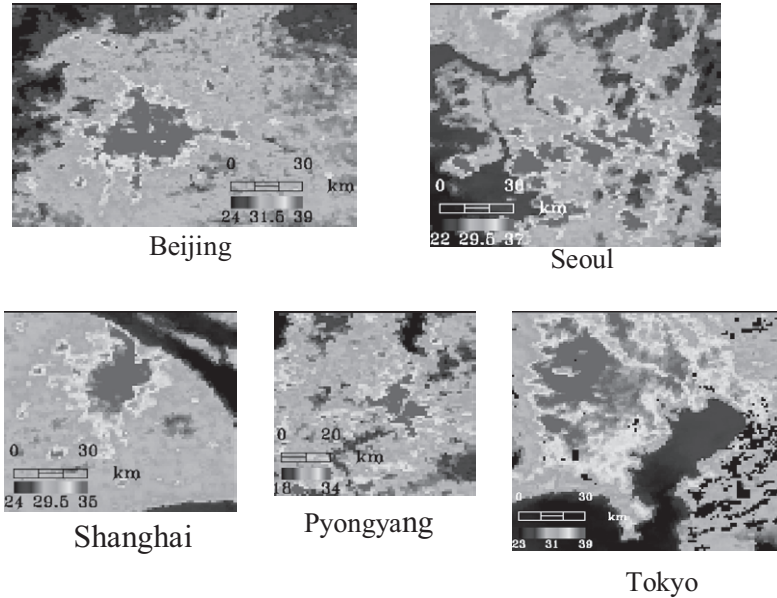


Figure 4: Land surface temperature maps over Asian cities observed from MODIS data.

It is, however, not easy to develop practical forest fire monitoring system since it requires near-real time observation over extensive areas. The Institute of Industrial Science (IIS), the University of Tokyo (UT) has developed and implemented forest fires monitoring system from MODIS data (<http://webmodis.iis.u-tokyo.ac.jp>). Figure 5 illustrates an example of forest fire map over East Asian region derived from MODIS data. The map is revised everyday and is open on the above website.

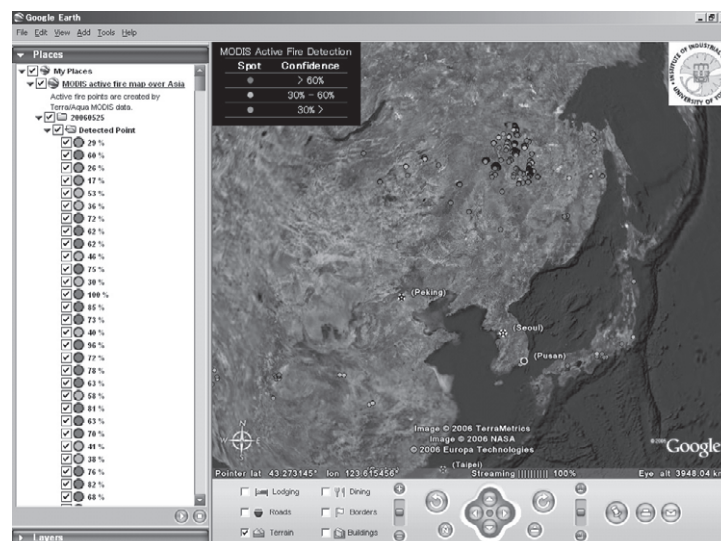


Figure 5: An example of forest fire maps observed from MODIS data (<http://webmodis.iis.u-tokyo.ac.jp>)

5. CONCLUSIONS

According to the United Nations forecast, in the middle of this century, the percentage of population in urban areas will be more than 60%, and the total number of mega-cities in the world will exceed 22. Sustainability will be a critical factor in urban management and the monitoring of urban sustainability is a first step towards managing urban systems. It is not easy, however, to collect adequate information and survey data over extensive areas periodically and regularly. [

Remote sensing has potential advantages in urban monitoring that are summarized as follows:

- # it does not disturb the object in measurement
- # it can cover extensive areas in a short time
- # it can measure parameters in the same spatial and temporal scales
- # it can cover land, ocean, and atmosphere where sometimes we

cannot make direct observations

Development of remote sensing technology has been very rapid, and today various types of remotely sensed data are available, ranging from high spatial resolution data for local monitoring to wide coverage data for regional/global monitoring. It is still difficult to realize operational and practical monitoring only with remote sensing or only with ground observation. It is expected to realize a practical monitoring system for urban sustainability.

REFERENCES

- Guo, T., Y. Yasuoka, Y. (2003): Reconstruction of Buildings from Satellite Image and LIDAR Data, the 24th Asian Conference on Remote Sensing and International Symposium on Remote Sensing (CD-ROM).
- Hung T., Y. Uchihama, Y. Yasuoka (2006): Assessment with satellite data of the urban heat island effects in asian mega cities, *International Journal of Applied Earth Observations and Geoinformation* 8, pp.34-48.
- Hirano, Y., Y. Yasuoka, T. Ichinose (2004): Urban climate simulation by incorporating satellite-derived vegetation cover distribution into a mesoscale meteorological model, *Theoretical and Applied Climatology*, 79, pp175-184.
- Yasuoka, Y., Y. Yamagishi, T. Guo, T. Endo (2003): Extraction and 3D Visualization of trees in Urban Environment, Proc. of the Third USMCA Symposium, India.

THE RESTORATION PLAN OF DUJIANGYAN AFTER THE GREAT SICHUAN EARTHQUAKE DISASTER IN 2008

MIKIKO ISHIKAWA

The University of Tokyo, Department of Urban Engineering
ishikawa@epd.t.u-tokyo.ac.jp

ABSTRACT

On May 12, 2008, Sichuan Earthquake had occurred, and 87,000 people died. On May 30, 2008, Chinese government announced to call for the restoration plan for the city of Dujangyang, which was designated as World Heritage City. 47 teams from all over the world expressed their will to propose the plan, and ten teams were nominated. This paper shows the outline of the reconstruction plan for Dujangyang, proposed by the team consisted of Tokyo University (Center for Sustainable Urban Regeneration), Keio University and West-South University in China.

First of all, we carried out the extensive survey on the damage, we took a field survey, also by utilizing IKONOS data, tried to clarify the overall damage from community level to regional level. Second step was the evaluation of the present Master plan of Dujangyang. We studied the vision of historical city, and recalculated the population forecast.

Based on above review, we concluded that the existing trend of rapid growth scenario was not adequate. We propose the three fundamental concept for the restoration. ① Immediate Strategies for securing suffered people, ② Change the growth formation of the future city from the spread city to the compact city, ③ Create the ecological city, by designating biotope unit and connecting those units by green and water corridor.

Then, we proposed the actual plan, especially focusing, historical district, heavy damaged district, agricultural village, and new natural symbiosis city. Finally, we focused the restoration of community and proposed the process planning until 2015.

1. PURPOSE AND BACKGROUND

On May 12, 2008, Sichuan Earthquake had occurred, and 87,000 people died. Chinese government announced to call for the restoration plan for the city of Dujangyan. 47 teams from all over the world expressed their will to propose the plan, and ten teams were nominated. This paper shows the restoration plan for Dujangyan, proposed by the team consisted of Tokyo

University (Center for Sustainable Urban Regeneration), Keio University and West-South Transportation University in China.

On June, 2008, our team had carried out the extensive survey of Dujiangyan, including the status of damaged architecture and open spaces, the place of refuges, transportation, and the present conditions and will of refugees. Since the city office itself had been severely damaged, it was impossible to have data from the municipality. Therefore, we used IKONOS picture which was taken before the earthquake (1m, accuracy). By comparing ALOS picture after the earthquake (2.5m, accuracy), we identified the damaged buildings, and calculated the story of buildings and estimated the number of people who had lived there (Figure 1 and 2). By accumulating this process one by one, we estimated the number of damaged buildings and people. Also, we checked all the open spaces, including parks, river side, woods, plaza, agricultural lands, and vacant spaces and made the extensive data base. Open spaces in emergency were very important, since they became immediate refuges and it will become the fundamental structure for establishing the safe city in future.



Figure 1 (Left): Dujiangyan before the 2008 Sichuan Earthquake
Figure 2 (Right): Dujiangyan after 2008 Sichuan Earthquake

2. EVALUATION OF EXISTING MASTER PLAN

The next step which we carried out was the evaluation of existing master plan in Dujiangyan, which was proposed in Feb. 2008, just before the earthquake and had not authorized yet. The population in 2008 was 680,000 and in this master plan, it was estimated that the population in 2050 would become 1,200,000, almost double compared with the present population. The new required urban areas would be 153 km², since the national standard of urban space per person was 120 m².

In order to verify this estimation, our team analyzed the population forecast model. Checking the population data in recent 10 years, it became clear that natural growth of population in Dujiangyan was stable, and the future growth was highly dependent on incoming population. The major source of this flow would be the commuting time between Dujiangyan and Chéngdū. It was planned that the commuting train would be constructed in

2008, and it would be opened in 2012. Considering this fundamental changes, we estimated that the population in 2012 would be 710,000, and in 2020, it would be 800,000. Therefore, the population growth between 2008 and 2020 would be 200,000. Based on the Chinese government standards for the restoration of the earthquake, the necessary space per person is 90 m². Using the above standard, we calculated that the required new urban spaces in 2020 would be 18 km².

Figure 3 shows the existing condition of Dujiangyan, and Figure 4 is the expanding pattern of the master plan. The most precious characteristics of Dujiangyan are the relation between forest, city and agricultural land, which have succeeded over 2000 years' history. They are consisted from numerous water and canal system, utilizing the delicate differences of landforms. If the city adopted this expanding master plan, it would eventually destroy the structure of Double World Heritage City.

Therefore, we concluded that the restoration plan should not be the expanding plan, but the city should choose the way toward the compact and sustainable city, which would also relieve the energy consumption. Figure 5 is the basic strategy of our restoration plan. We allocated the required increase of 200,000 people and 18km² urban areas, to three portions, namely, the new town near Jyugen area, Seijyo mountain area, and the existing city and agricultural villages.



Figure 3 (Upper left): Existing Condition of Dujiangyan

Figure 4 (Lower left): Master Plan in Feb.2008

Figure 5 (Right): The proposal of the Restoration Plan

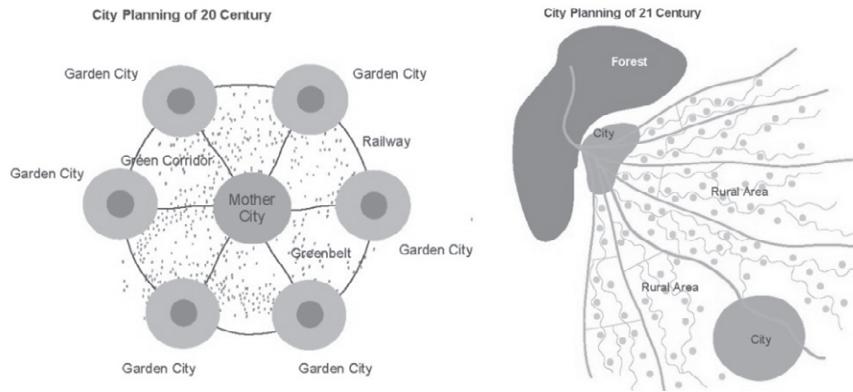


Figure 6 (Left): Garden cities (Ebenezer Howard, 1898)

Figure 7 (Right): Ecological City in the Restoration Plan (2008)

3. CONCEPT OF RESTORATION PLAN

We set up three main concepts for the restoration. The process of the restoration would take the long difficult way, therefore, it is essential to share the common goal in the very starting point.

Concept 1: The restoration plan should be encourage refugees and provide hopes for their future.

Concept 2: To seek the compact city in order to sustain the 2000 years' assets of Double World Heritage City

Concept 3: To create the Ecological City as the ideal of the 21st Century

The 20th century was the era of the expansion of cities. Figure 6 is the modification of the famous model of "Garden Cities", proposed by Sir. Ebenezer Howard in 1898. The model was consisted from major city and surrounding garden cities and it was said, thus, created the region. However, since there exist no evident rules between city and country, the policy of green belt which would support the regional structure did not work effectively in many countries. Figure 7 shows the proposal of new relation between city and country. As we have investigated that in Dujiangyan, there exists the historical structure of water system which had supported this region for 2000 years. We thought the future structure of city and country in the restoration plan should be based on this structure. We call it "Ecological City". Figure 8 shows the principals of the restoration plan, green, water and culture.

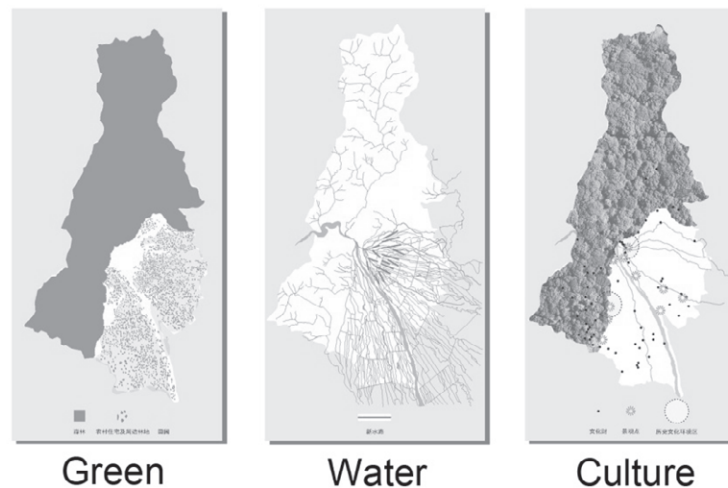


Figure 8: The principals of restoration plan

4. RESTORATION PLAN

The restoration plan is made from the following four points. The first is the overall plan of the city of Dujiangyan as “Ecological City”. The second is the restoration of the central area where the historical heritage exists. The third is the agricultural village where new policies have been expected before the earthquake. The fourth is the community planning for actualizing the above plans.

4.1 Ecological City

Considering the restoration process in Japan, after 1923 Kanto earthquake and 1995 Hanshin-Awaji earthquake, open space planning is essential for securing the safe city for future generation. In emergency, it was the open space where people evacuated and spent the temporary, sometimes long stay before they found the way for ordinal life. If the city would built up disorderly, it becomes impossible to change the urban structure. Therefore, in the beginning of the restoration, the proper open space planning should be introduced.

As I mentioned in data analysis, we carried out the extensive survey on existing open spaces in Dujiangyan. Figure 9 shows the result of our analysis. Figure 10 is the map of damaged areas. We combined those maps and identified the priority for open space planning, then proposed the overall open space system. We call it “Park System of Dujiangyan” (Figure 11).

We also analyze the quality of natural environment and estimate 37 different bio-tope units. Since in the west of city, there exist huge forests which are designated as Natural World Heritage. It is important to establish ecological corridor from forest to city. For enriching bio-diversities, the consideration of the function is not enough. Figure 12 shows the basic map of bio-diversities which will become the guideline for “Ecological City”.



Figure 9 (Left): Analysis of Existing Open Space
 Figure 10 (Right): Damaged Area by 2008 Sichuan Earthquake

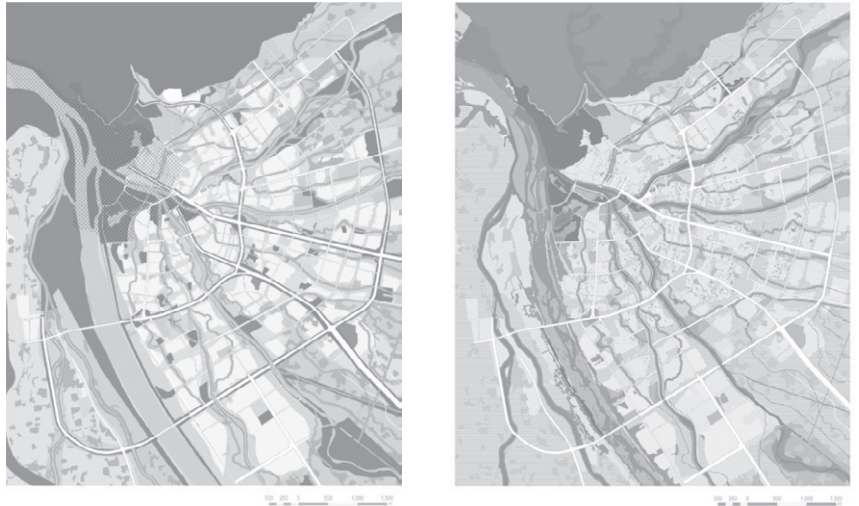


Figure 11 (Left): Proposed Park System
 Figure 12 (Right): Biotope Map for Ecological City

4.2 Restoration of Historic Heritage

It is the urgent issue that how to restore the historic heritage, since it is the major resources of economic incomes. Dujiangyan was established as the origin of canal system which has been providing water to Sichuan Flats over 2000 years. Figure 13 shows the structure of the original city. It was surrounded by the wall, but few of them remained. Most of the buildings received damages, but careful restoration policies should be introduced since the number of historic assets was very limited.

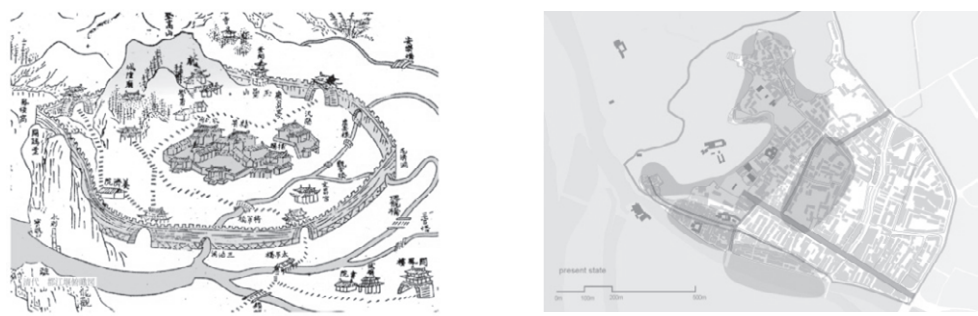


Figure 13: Analysis of Historic District

Our proposal is the restoration plan should be combine the existing three separate historic sites altogether, and create new World Heritage Park. By introducing new public transportation system, the old city and present lower park will become the real core of the city. Also, providing the safe pedestrian networks to the upper park, it will produce another attractiveness to the city (Figure 14).



Figure 14: Proposed Site Plan of Historic District and World Heritage Park

4.3 Agricultural Village Restoration

How to renovate the agricultural village is another difficult issue. It was the basic theme in this region before the earthquake. We carried out the investigation on the agricultural village, and clarified the structure of the scattered village pattern, consisted from canal system, rice fields, forests and small villages. Along the main street, we introduced the civic facilities, such as schools, new agricultural industries and new housing. Surrounding this civic center, the new program of agricultural-tourism is proposed. In addition to this, we proposed low-cost sewer system using new technology, and circulate waste materials to the resources of the bio fertilizer (Figure 15)

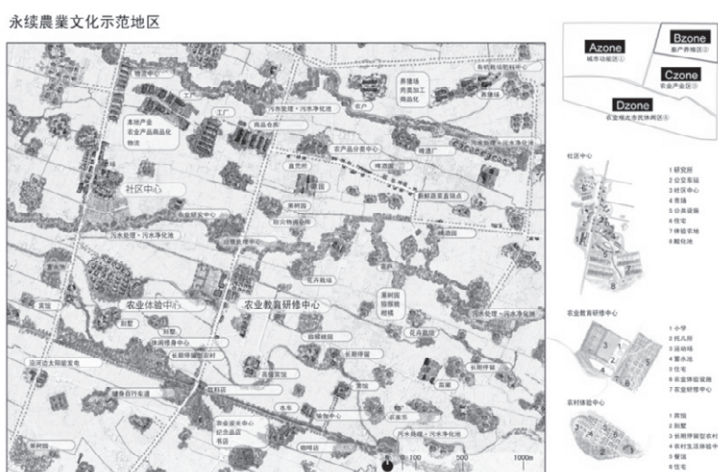


Figure 15: The restoration plan of agricultural villages

4.4 Community Planning

We proposed the new concept of “Water City Community Unit” as the basic component of the restoration. It is a community which is enclosed by canals, having 8,000—15,000 people. The size and structure of this community unit is proposed, reflecting the actual formation of urban features in Dujiangyan (Figure 16, Table.1). In the center of this community unit, the existing narrow canal will become the central, linear common space, and many activities will be gathered into this space (Figure 17). It is a new model of Neighborhood Unit. Each community units will be connected with public transportation.

We also proposed the process planning of the restoration. According to the hearing of refugees which we carried on June 2008, many people wanted to return to the same community where they lived. “On site, and Continuous Living in the Same Place” (OCLS) is our principal for the restoration. Since in Japan, we had hard experiences that many elder people died lonely in the isolated temporary house, even though they had survived from the disaster of earthquake. We proposed to build the temporary housing within the same community where people lived, and developed the program which would be enable the gradual transition from temporary to permanent houses. This program would provide hopes for the future, which are the most important goals of the restoration.



灾前人口与住宅受灾比率 ⇒ 规划人口

| 社区编号 | 推断人口(人) | 住宅受灾比率 | 住宅受灾人数(人) | 社区编号 | 计划人口(人) | 增减人口 |
|------|---------|--------|-----------|------|---------|-------|
| A1 | 10,000 | 20% | 2,000 | A1 | 8,000 | -20% |
| A2 | 7,000 | 70% | 4,900 | A2 | 0 | -100% |
| B1 | 5,000 | 55% | 2,750 | B1 | 8,000 | 60% |
| B2 | 8,000 | 50% | 4,000 | B2 | 8,000 | 13% |
| B3 | 9,000 | 35% | 3,150 | B3 | 10,000 | 11% |
| B4 | 11,000 | 25% | 2,750 | B4 | 12,000 | 9% |
| B5 | 8,000 | 20% | 1,600 | B5 | 10,000 | 25% |
| B6 | 1,000 | 10% | 100 | B6 | 10,000 | 900% |
| C1 | 8,000 | 50% | 4,000 | C1 | 8,000 | 13% |
| C2 | 13,000 | 5% | 650 | C2 | 13,000 | 0% |
| C3 | 1,000 | 0% | 0 | C3 | 10,000 | 900% |
| C4 | 1,000 | 0% | 0 | C4 | 11,000 | 1000% |
| C5 | 4,000 | 10% | 400 | C5 | 8,000 | 100% |
| D1 | 4,000 | 0% | 0 | D1 | 8,000 | 100% |
| D2 | 5,000 | 0% | 0 | D2 | 8,000 | 60% |
| D3 | 4,000 | 0% | 0 | D3 | 8,000 | 100% |
| E1 | 11,000 | 40% | 4,400 | E1 | 12,000 | 9% |
| E2 | 7,000 | 10% | 700 | E2 | 8,000 | 14% |
| E3 | 8,000 | 0% | 0 | E3 | 8,000 | 0% |
| E4 | 15,000 | 0% | 0 | E4 | 15,000 | 0% |
| E5 | 7,000 | 5% | 350 | E5 | 10,000 | 43% |
| E6 | 3,000 | 0% | 0 | E6 | 10,000 | 100% |
| F1 | 12,000 | 30% | 3,600 | F1 | 13,000 | 8% |
| F2 | 7,000 | 0% | 0 | F2 | 8,000 | 14% |
| F3 | 3,000 | 0% | 0 | F3 | 10,000 | 233% |
| G1 | 8,000 | 45% | 2,700 | G1 | 8,000 | 33% |
| G2 | 8,000 | 0% | 0 | G2 | 8,000 | 33% |
| G3 | 8,000 | 30% | 1,800 | G3 | 8,000 | 33% |
| G4 | 5,000 | 5% | 250 | G4 | 10,000 | 100% |
| G5 | 3,000 | 15% | 450 | G5 | 10,000 | 233% |
| 合计 | 200,000 | 20% | 40,550 | 合计 | 280,000 | 40% |

Figure 16 (Left): Water City Community Unit
 Table 1 (Right): Population of Water City Community Unit



Figure 17: Image of Water City Community

5. PROCESS OF RESTORATION

Figure 18 shows the process of the restoration. In order to proceed the restoration project, it is necessary to establish the corporative community association, supported by municipality, firms and professional planners. They will collect the demand of refugees and propose the actual restoration plan altogether. In a process of the Great Hanshin-Awaji Earthquake Disaster in 1995, a number of similar associations were set up, and it became the real engine of the accomplishment of the restoration.

Finally, in this paper, the author discussed the fundamental structure of future, safe city. At this point, our team from Center for Sustainable Urban Regeneration in Tokyo University is continuing to work on the identification of damaged buildings, the way of restoration, the existing conditions of temporary housings, and the creation of park system.

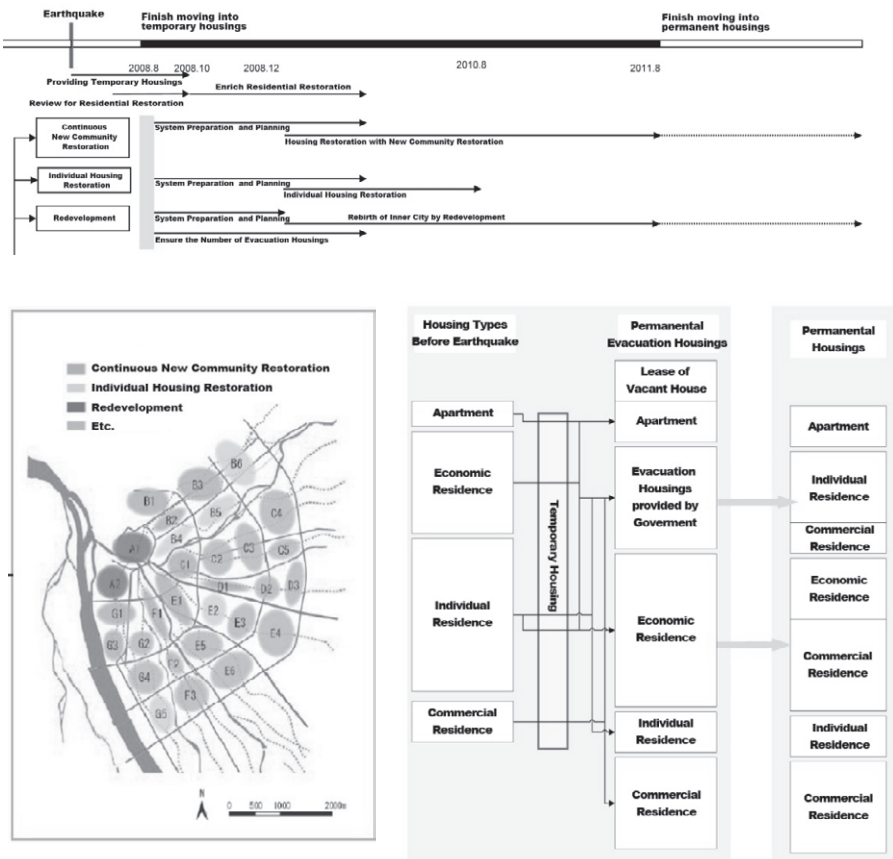


Figure 18: Process of Restoration

REFERENCES

The Center for Sustainable Urban Regeneration in Tokyo University, Keio University, Graduate School of Media and Governance, The Architectural Dept. of West-South Transportation University in China, July 2008. *The Restoration Plan of Dujianyan after the Great Sichuan Earthquake Disaster in 2008*

COMPREHENSIVE DISASTER MANAGEMENT AND RESPONSE

RICHARD JAEHNE

Illinois Fire Service Institute, University of Illinois at Urbana-Champaign
11 Gerty Dr., Champaign, IL 61820, USA
Jaehne@fsi.uiuc.edu

ABSTRACT

This paper describes a list of core competencies that have been identified for effective disaster response and the management and response procedures of a type 3 incident in USA, taking 2008 flood in Illinois as an instance. Based on the concept of National Incident Management System (NIMS) and Incident Command System (ICS), Incident Management Teams (IMTs) were trained and established in Illinois. They were deployed into various positions to assist the governmental organizations at different levels in planning, commanding, decision making, etc.

1. INTRODUCTION

During the past century, societies and nations have struggled to define and implement effective, comprehensive policies, programs and actual capabilities to respond to both natural and man-made disasters. This paper presents an overview of some of the key disaster management response challenges that must be addressed and a short case study on how a newly developed and implemented national incident system provided for an integrated and effective national, state, regional and local response to major flooding in the United States Midwest this year.

Many factors have added to the complexity and potential impacts of disasters, including the growth of: populations and urban densities, interconnectivity of global economies, demand for robust power and communications infrastructure, effects of climate change on the occurrence and intensity of natural disaster such as floods, hurricanes/typhoons/cyclones, and earthquakes; as well as the seemingly endless human carnage from conflict and crime.

A century ago, disaster response was routinely left to those most affected to “take care of themselves” for weeks until aid and assistance could arrive. Ongoing wars and conflict led to the organization of civil defense teams of local citizens, backed up by military forces often days or weeks after the disaster occurred. Today, citizens around the globe learn of disasters as they are happening. They expect and demand immediate, comprehensive response; yet governments still struggle to “catch up” to the disaster, prioritize requirements and coordinate response.

In the United States following events of 9/11/2001 and Hurricane Katrina (2004), a national effort has been undertaken to create a single National Incident Management System (NIMS) that connects community

leaders, responders and citizens locally to state, interstate and federal assistance before, during and after a disaster. The system demands that planning, mitigation, response and recovery be integrated within that system, rather than operating as four separate, often disconnected systems. Recent Hurricanes in the Gulf of Mexico are a testimony to the effectiveness of this effort and the challenges that remain.

2. COMMON UNDERSTANDING ON DISASTER

Disasters can be divided into different categories based upon their source; however, there are several key factors to human survival and the reduction of human loss of life, which are common to all disaster management efforts:

- The amount of warning time available for evacuation and staging of response.
- When disaster strikes without warning, the ability of citizens and responders in the immediate area to act to save lives before outside assistance arrives.
- Prevention of disease following disasters.
- Timely identification and response to secondary threats such as hazardous materials release, damaged transportation infrastructure critical to evacuation and response, landslides and related flooding.
- Coordination of massive, diverse relief assistance that descends on a disaster area from around the globe.

The reality of disaster response is that most lives are saved by one of four things:

- 1) The effective mitigation of known threats to human safety from past disasters, including both the development and implementation of building and infrastructure standards and robust evacuation planning and response.
- 2) The ability of citizens and responders in the immediate vicinity of the disaster impact area to act before, during and immediately after a disaster strikes. In reality, 9 out of 10 lives at risk in the first days of a disaster are saved by them.
- 3) The ability federal, state and regional governments have to define, prioritize and coordinate the deployment of critically needed capabilities from both public and private sources to meet the immediate and secondary threats to human safety and to facilitate recovery and rebuilding. This includes robust all-hazard, all-source intelligence / information fusion to identify and predict threats.
- 4) The ability to prevent disaster-related disease through proactive preventative medical efforts, provision of safe water and food, temporary shelter, and evacuation, as required. For every one who dies in the initial disaster at least 10 can be saved through effective preventative medical programs.

3. 2008 FLOOD DISASTER RESPONSE

Illinois is a river state. Lying between the Great Lakes, the Mississippi and Ohio Rivers, Illinois is surrounded and crisscrossed by major bodies of water, which carry the annual rain and snow-melt runoff of nearly half of America's land mass. The 2008 spring rains and winter runoff inundated these rivers generating a flood that migrated down the rivers throughout the Mississippi and Ohio River basins. A similarly "perfect storm" of conditions occurred in the spring and summer of 1993 resulting in some \$18 billion in damage and ranking as the worst flood disaster in United States history.



Figure 1: Sketch map of Illinois in US

The 2008 flood response built upon the lessons learned in 1993 and from the Illinois Terrorism Task Force (ITTF) created in 2000 to integrate planning, mitigation, response and recovery efforts. As a result, critical groups worked together before and during the flood, to reduce loss of life and property. These included: (1) local public and private community leaders, (2) first responders representing emergency management, fire, law enforcement, emergency medical, and public works each operating within a robust "mutual aid" response system, (3) Illinois State government led by the Illinois Emergency Agency (IEMA), which encompassed all state agencies in a coordinated planning and response system, (4) federal government agencies coordinated through the Federal Emergency Management Agency (FEMA) region and a single Federal Coordinating Officer appointed by the President, (5) private sector and non-government organizations such as the Red Cross integrated with government response. While the 2008 flood did not have the duration or level of damage of the 1993 flood, the integrated emergency planning and direction of all critical actions reduced the actual and potential impacts. Prior to the flood, FEMA and IEMA worked together to conduct a critical needs and gap analysis of the most critically required and requested assistance. Levee augmentation, at risk critical infrastructure and evacuation modeling were conducted. Essential equipment and supplies were moved into safe staging areas near the potential flood impact areas in order to be available on short notice.

Self-contained and self-sufficient mobile command, control and communications assets that had been designed and developed by the ITTF were quickly deployed into the flood area to provide uninterrupted incident command infrastructure and continuous connectivity from local through regional, state and federal commanders. The state established an Area Command Center in the flood area that provided a base for all levels of command to coordinate their activities with local leaders and responders.

3.1 Response under NIMS

Under the National Incident Management System (NIMS), command and control of a disaster is established and maintained at the local level whenever possible, while state and federal authorities establish command authority to direct state and federal assets to support local response. While this ensures that locally elected officials retain the authority vested in them by citizens, it can overwhelm the ability of these officials in a disaster. NIMS establishes both the process and structure for intra-state, inter-state and federal government assistance. A weak link is often the ability of local officials to coordinate and direct the extraordinary amount of required assistance provided to them and to coordinate with neighboring officials in nearby communities. In 1993, the ability of local communities to establish a unified command approach to disaster planning and response had been identified as an area of concern.

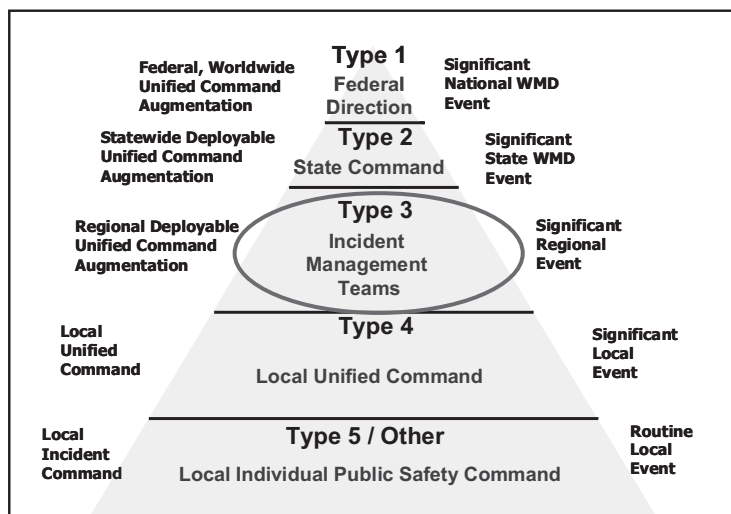


Figure 2: Triangle of response in NIMS

The statewide Illinois Terrorism Task Force worked with local, state and federal partners to identify individual first response officers from emergency management, fire, law enforcement, and emergency medical disciplines in local communities who were capable of deploying to a disaster to help establish and operate a unified command system with local officials. These individuals would be formed into Incident Management Teams (IMT), trained to use the structured NIMS planning process for disaster management and available for immediate deployment whenever disaster struck. Since their organization, IMT's have been activated and deployed in support of tornado, flood and school shooting incidents.

To assist in the development of the Incident Management Teams (IMT's), the Illinois Fire Service Institute hosted national training and developed a series of courses that brought together the disaster response leaders of whole communities to develop a unified planning response based upon the new National Incident Management System (NIMS). Importantly, this training placed students into the roles of the IMT staff and presented them with several different disaster scenarios. Building upon these local efforts, IMT's were formed from a group of individuals hand-picked by their communities and response disciplines to help fill the planning and coordination gap between local and state emergency management. IMT members were trained to use an all-hazards incident planning system that would assist and augment local incident management teams, rather than to replace them.

Each IMT was organized around 8 key positions and used a structured planning process to plan for and direct all agencies operating in a specific area during a specific operational period. Each IMT had an Incident Commander, who provided policy direction and connectivity to local and state leaders. A core staff was formed around the key leadership positions of Operations, Planning, Logistics and Finance who used pre-established forms and a standardized planning process to plan and direct all response activities. Special staff were also provided to focus on Public Information, Safety and Liaison with outside organizations. The IMT structure and planning process has been used to coordinate wildland firefighting activities over vast areas for decades. Now this same structure was being applied to all hazards.

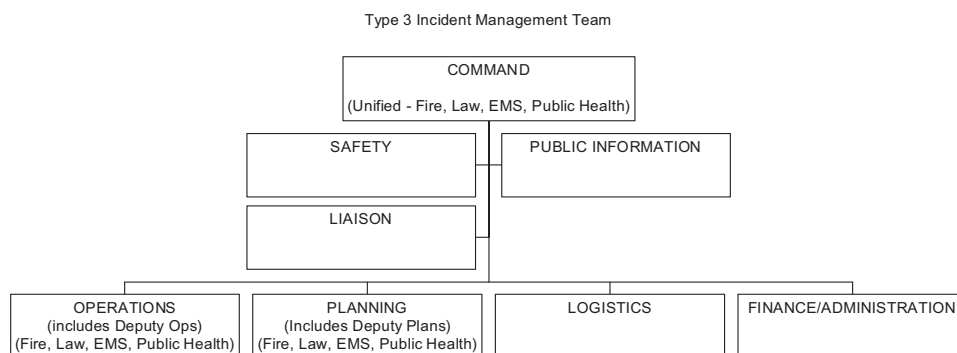


Figure 3: Component of IMT

3.2 Deployment of IMT

During the 2008 flood response these teams were deployed in three distinct ways. One IMT was activated to provide a long-range planning cell for IEMA. They were part of the State Emergency Operations Center that was designated to coordinate statewide response efforts. This IMT focused on looking at the gaps that might be developing between current operations and evolving threats and capabilities beyond the immediate operational period. In essence, this team was to focus their lens at the “maturation point” of current decisions, taking into account the time delay between decision and response and the ongoing dynamics of the flood and related

secondary threats. Road, rail and navigable transportation infrastructure, economic damage loss forecasting and flood footprint for evacuation decisions were examples of areas where the IMT was able to dedicate a current planning effort on a future-critical-point.

A second set of IMTs were deployed into the flood disaster area to assist the two State Area Command Teams established in the disaster area with day-to-day planning and response coordination with communities throughout the flood impact area. The individual IMT members were already trained to augment the Operations, Plans and Logistics staffs and to use the NIMS planning process to generate an integrated single set of daily orders to direct the activities of all response activities. This included the development and implementation of a comprehensive safety plan for all those working to reinforce the levees, planning for emergency levee-related evacuation contingencies, rerouting and repair of the transportation network, and contingency planning to restore river-based potable water service.

A third set of IMT's were deployed into the areas directly impacted by the flood, to assist and augment the local incident command organizations. A founding principle of the IMT was that it was to integrate into and assist rather than replace local command structures. Based upon this, the IMT members were rapidly accepted by local commanders and integrated into their command structures. During the development of the training courses for the IMT's, IFSI had designed and procured 3 sets of laptop computer-based "command and staff" suites that were pre-loaded with all of the NIMS forms and planning documents. These were quickly deployed to support the IMT staff and augment local command. Using these tools and the standardized NIMS planning process IMT staff were able in hours to develop and have ready to execute contingency plans for local evacuation and debris removal.

On lesser and greater-scale disasters Incident Management Teams are only one example of how comprehensive emergency planning and response has evolved in the United States. The value of organizing, training and equipping a key set of first responders from local communities to deploy in support of other local communities in a disaster is proving to be an invaluable and important addition to comprehensive emergency planning and response.

4. GAP ANALYSIS

In October 2008, Illinois hosted the first national meeting of Incident Management Teams with the intent to share best practices and to help provide a key component of the National Incident Management System. Importantly, the meeting was sponsored by Northern Illinois University in DeKalb, Illinois who received IMT support for a campus shooting and mass casualty incident in 2008. The meeting was also supported by both FEMA and the Illinois Terrorism Task Force as an opportunity to expand the IMT concept nationwide.

In a broader sense, FEMA and the United States government are embracing the requirement for robust collaboration and coordination with state and locals in all phases of disaster management. At a recent

conference of all emergency managers in Illinois, the FEMA Region V Director stated that all levels of emergency response must work together to develop “core competencies” in planning, mitigation, response and recovery from disasters. The near-term list of core competencies that require concerted effort include:

- Incident Management
- Operational Planning
- Disaster Logistics
- Emergency Communications
- Service to disaster victims
- Continuity Programs
- Public Disaster Communications
- Integrated Preparedness
- Hazard Mitigation

Each item on the list will require local and state collaboration. Each must be translated into practical plans and operations. The Incident Management Team will play an important part in translating core competencies into effective disaster response.

IMPORTANCE OF MAINTENANCE TECHNOLOGIES TO KEEP EXISTING STRUCTURES SAFE TO THE PUBLIC

TAKETO UOMOTO

Professor Emeritus, University of Tokyo
Professor, Shibaura Institute of Technology
3-7-5 Toyosu, Koto-ku, Tokyo 135-8548, Japan
uomoto@sic.shibaura-it.ac.jp

ABSTRACT

Tremendous amount of structures have been built in recent years throughout the world. These structures are important properties to the people as far as they are used by the people. Looking at the situation now in our country, although the amount of the structures is tremendous, these structures are not always being maintained well by the public. Especially in Japan, due to natural hazards, such as earthquakes, typhoons, floods, etc., and the change of the economy and politics, it is difficult to maintain all the structures in convenient state. This paper explains how we have been looking at the problem and maintains the existing structures especially reinforced concrete structures. The technologies related to maintenance are also explained in the paper.

1. INTRODUCTION

Up till now in Japan, the economic growth was rapid in the period of 1960 ~ 1980. More than 100million cubic meters of concrete were used to construct the structures such as buildings, bridges, tunnels, dams, etc. to support the activities of Japanese people. As a result, these infrastructures rapidly reached 50 years in service, and due to deterioration of the structures, maintenance of these structures has become a major interest among the owners and the civil engineers.

On the other hands, population of Japan will reduce from now on because of fewer babies in a family approximately 1.2 children per one family. Although high technologies have been developed in recent years, it is sure that fewer engineers have to take care of the huge amount of structures from now on, which has never experienced in the past. Due to reduction in the economical growth, the budget for both construction and maintenance will be reduced in the future. The maintenance of existing structures must be done with the following conditions: 1) rapid increasing of the amount of existing structures reaching to the age of 50 years, 2) less amount of engineers to maintain the structures, 3) less amount of budget can be used to maintain the structures.

Although there are many hazards in each country, concrete structures are expected to be safe for long period of time. Main hazards for the structures in Japan are as follows:

1. Earthquake and volcanic action
2. Landslide and flood
3. Typhoons and strong wind
4. Fire and Thunder
5. Accidents
6. Terrorism

If the structure is deteriorated before the hazards, the structure may easily collapse and difficult to maintain the safety of the people. The Figure 1 shows an example of a collapsed pier during Hanshin Awaji Great Earthquake. As shown in the photo, the pier was deteriorated to large extent due to alkali aggregate reaction. Concrete is cracked severely and is just like a bundle of concrete blocks.



Figure 1: Collapsed reinforced concrete pier affected by alkali aggregate reaction

In order to keep the safety of urban area, it is important to study and investigate not only on hazards but also on durability aspects of existing structures. Even a small amount of concrete spalling may cause traffic accidents to large extent as we experienced in Sanyo-Shinkansen in 1999.

Considering these situations now, this paper explains what is happening now in Japan and how we are dealing with the problems through researches and engineering.

2. GENERAL MAINTENANCE METHODS BEING USED UP TILL NOW

The maintenance of concrete structures has been done mostly by the owners of the structures. In case of public structures, the ministries, etc. maintain the structure after the structures are completed. For the time being, the methods for the maintenance differ according to the owners of the structures. Although there are some differences, the main concept of the maintenance can be summarized as follows (Uomoto and Misra, 2001):

1. Periodic inspection and evaluation of deterioration degree
2. Detailed inspection and decision making
3. Repairing and strengthening of deteriorated structures

For periodic inspections, the inspectors inspect the structures visually, sometimes with the help of binoculars and hammers, once a year or once in several years according to the importance and time after the structure is completed. The inspectors are mostly trained engineers with experiences. The detailed inspection is done when the estimated degree of deterioration exceeds certain limit, or when some new phenomenon is found during the periodic inspection. The detailed inspection is done by visual inspections with the aid of non-destructive tests or taking core samples out from the inspected structure. The purpose of the inspection is to decide the cause of the deterioration and also to evaluate whether repair and/or strengthening is needed or not.

To repair or strengthen the existing structures, it is important to design and select sufficient methods and materials. The most popular repair method for corrosion of steel bars due to carbonation is to eliminate the carbonated concrete and replace it by new concrete and apply coatings with and without FRP sheets. But in case of steel corrosion due to chlorides from the surrounding environment, the highly chloride concentrated portion of concrete are taken out, anti-corrosive treatment is applied to the surface of the bar, and polymer cement mortar is generally used to repair the concrete before coating the concrete surface.

3. NEW STANDARD SPECIFICATIONS OF JSCE

After the investigations of many deteriorated concrete structures, the importance of durability was fully recognized by the civil engineers. To deal with the problem not only JSCE, AIJ, and JCI recommending methods to deal with the problems but also the Ministries, and other authorities started to propose practical counter measures to cope with the situation. As a result, a large amount of researches has been done related to the durability of concrete structures including non-destructive inspection methods.

Among these authorities, the Concrete Committee of JSCE, the leading committee in the field of concrete in Japan, has published the translated version of “Standard Specifications for Concrete Structures-2002” in English to deal with the problems of durability. A new version of the Standard Specification was published in the year 2007 in Japanese (JSCE, 2007a, 2007b and 2007c). The concept written in the specifications will surely be adopted by other institutions.

The main proposals of the “Standard Specifications 2007” are the following two items:

- 1) Propose a new method to design and construct new concrete structures that can be used for specified lifetime without large amount of maintenance cost.
- 2) Propose an effective and economical system to maintain existing concrete structures with small number of engineers and workers.

The concepts of the new Standard Specifications are briefly explained in the following chapters.

3.1 Durability design of concrete structures for new structures

Performance-based durability design was introduced to “Standard Specification of Concrete Structures” by the Concrete Committee of JSCE in the year 2000 and be translated to English version in 2005 (JSCE, 2005c). Although durability of concrete structures was considered important in the previous specifications, performance-based design method was not used. The previous specifications described the importance of durability by proposing that the concrete structures are durable for a long time when specified materials, mixes, covers, etc. are used. But these specifications did not mention about the duration of service time, etc.

The proposed performance-based new durability design can be summarized as follows:

1. The concrete structure must be quantitatively checked whether the structure possesses required performance within the designed period.
2. The degree of deterioration of the structure in service on specified cause must be specified.
3. To maintain the structure above the specified degree of deterioration, the required performance must be specified.

To examine the performance on durability, a kind of limit state design scheme was introduced for the durability of concrete structures. The equation can be written as shown in Equation (1):

$$\gamma_i \cdot A_d / A_{\text{lim}} \leq 1.0 \quad (1)$$

where, A_d is designed performance of the structure at specified time considering the specified deterioration cause, A_{lim} is limit of the performance of the structure, and γ_i is coefficient of the structure considering the importance, etc.

Generally, performance of concrete has to be verified to satisfy the required performance. Not only resistances against deterioration but also mechanism properties of concrete have to be verified as shown below.

1. Compressive strength
2. Carbonation rate
3. Diffusion coefficient of chloride ions in concrete
4. Dynamic modulus of elasticity
5. Resistance to chemical attack
6. Resistance to alkali aggregate reaction
7. Coefficient of water permeability of concrete
8. Fire resistance
9. Adiabatic temperature rise
10. Drying shrinkage characteristics
11. Setting characteristic

The Figure 2 shows an example of the calculated result for minimum cover thickness to prevent carbonation induced corrosion at different years of service for OPC concrete and BFSC concrete. As shown in the figure,

the cover thickness required changes according to the type of cement to be used, water-cement ratio of concrete, years of service and exposed condition (wet or dry) of the structure to be constructed. When the structure is designed for long period of time, the cover thickness may become too large, and it is recommended to use other countermeasures such as Epoxy-coated bars.

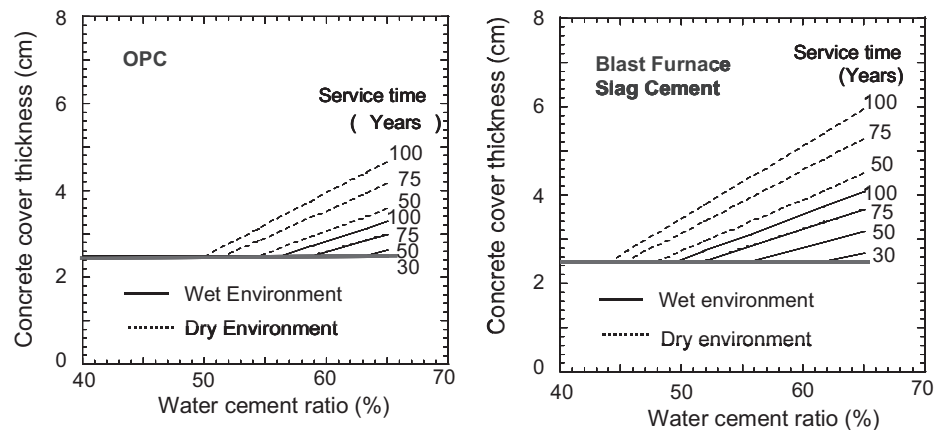


Figure 2: Calculated results of concrete cover according to JSCE Standard Specification

3.2 Methods of maintenance newly proposed by JSCE

The methods used in the new Standard Specification are basically the same as the conventional method. The differences are that the new method requires maintaining the structure within their required performances throughout their service life. Firstly, the listed below issues have to be clearly specified.

1. To maintain a structure, performances required for the structure must be clearly defined.
2. The performances required for general structures are “safety”, “serviceability”, “hazards to the public”, “aesthetics and landscape” and “durability”.

And the basic principles of maintenance works are as follows:

1. Structures must be maintained according to a designated maintenance category by formulating a maintenance program to retain the performance within the specified tolerances throughout their service life. And maintenance system includes adequate “initial inspection”, “deterioration prediction”, “inspection”, “assessment/judgment”, “remedial action”, and “record”.
2. To maintain a structure, in addition to the assessment and evaluation at the time of inspection, assessment and evaluation must be made throughout the service life of the structure based on prediction of deterioration.
3. To predict the deterioration, required performances of the structure must be clearly defined, and also the design service life must be made clear.
4. The records on design, construction, initial inspection, deterioration prediction, periodical inspection, assessment and/or

evaluation, and remedial actions must be kept throughout the service life.

Standards for maintenance of concrete structure deteriorated by different mechanisms are also discussed. The lists below are the standard maintenance method published in this standard:

1. Standard maintenance method for carbonation induced deterioration
2. Standard maintenance method for chloride induced deterioration
3. Standard maintenance method for frost attack
4. Standard maintenance method for chemical attack
5. Standard maintenance method for alkali aggregate reaction
6. Standard maintenance method for fatigue of RC slab of road bridge
7. Standard maintenance method for fatigue of RC beam of railway bridge

In detail for an example, the standard method for chloride induced deterioration recommends the model to predict chloride ion diffusion, progress of steel corrosion, and correction of the prediction. Also the methods of initial inspection, routine inspection, periodic inspection, and detailed inspection as well evaluation and judgment method are also discussed. Finally, recommendation of selection of remedial measurement both of repair or strengthening is given also the information has to be recorded.

One of the difficulties is how to predict the degree of deterioration at the end of their service life. There are several researches being done to predict the deterioration in numerical manner. In the published Standards, several numerical prediction methods are introduced as references for structures suffering cyclic fatigue loads, carbonation induced corrosion and chloride induced corrosion. In case of cyclic fatigue, S-N curves are used to predict the service life. In case of carbonation induced and chloride induced corrosion of steel bars, diffusion equations for carbon dioxide and chloride are used to predict the degree of corrosion. Using these prediction methods, deterioration degree can be estimated to certain degree. (See Figure 3) But for other deterioration problems, which has not been studied numerically, a quantitative model has not been proposed yet. To deal with the problem, a qualitative method “Grading method” is introduced in the Standard.

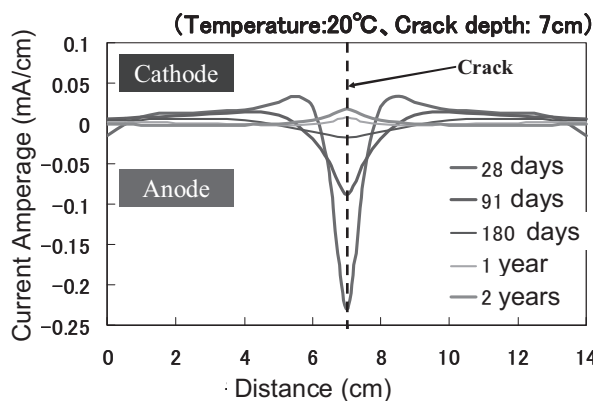


Figure 3: Quantitative prediction of corrosion in marine environment with cracks (Tsukahara et al., 2000)

4. PROBLEMS IN ACTUAL EXISTING STRUCTURES

When a civil engineer is asked by the owner to check the safety of an old existing structure, one of the largest problems is that there are neither drawings nor construction records of the structure available. No problem may occur in case of important facilities, which is maintained with great care. But in case of normal structures, the owners do not know the importance of these documents.

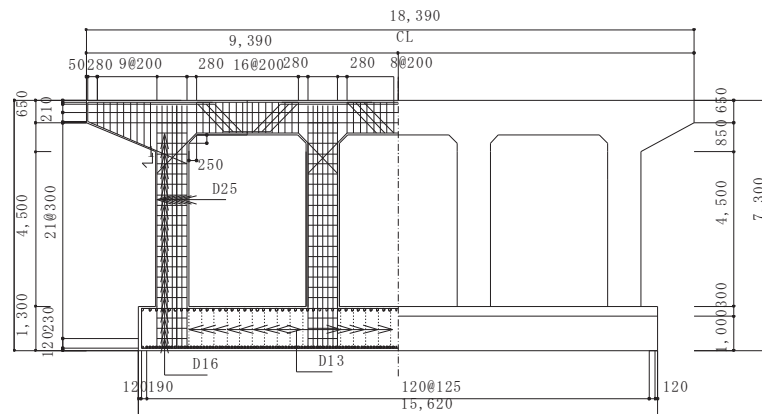


Figure 4: Re-designed reinforced concrete pier of a bridge (Okazaki, 2005)

To deal with the problem, NDI is not enough. Fortunately, our structures are not too old, and they are mostly designed and constructed by the method specified by JSCE, AIJ or other associations. Considering these, the only way is to re-design the structure again using the methodologies used at the time of construction. Figure 4 shows an example of re-designed bridge pier constructed about 35 years ago. From the figure, it is much easier for a civil engineer to check the safety of the structure under several hazards. It will become more important for the owners and engineers to keep these documents throughout the service life of a structure.

6. NON-DESTRUCTIVE INSPECTIONS

New Technologies for NDT are also developed. Among all I would like to introduce some technologies developed by us.

6.1 Appearance and surface deterioration of concrete structures

When inspection of existing concrete is performed, the most essential method is to inspect the structure visually. If the inspector is well trained, visual inspection is the most simple and economical method especially in case of periodic inspection. The problem is that visual inspection offers no objective document, which can be compared in the next inspection by

different inspector. To deal with the problem, sketches and photographs have been used to record the inspected results.

Recently, digital still camera has been used for recording the inspected results, such as distribution of cracks and honeycombs that can be seen by visual inspection. The photographs taken by the digital still camera can be easily mounted on a computer, the distorted portion can be modified, especially the corners of the photograph. Also, the results of other inspected data can easily mounted on the photograph.

Table 1: Application of NDI for existing concrete structures

| Time | Items | Measurement | Methods | Comments |
|------------------------------|------------------------------------|---------------------------|--|---|
| Just after construction | Dimension | Cross sectional dimension | Measure, Transit, Laser | When the structure is in the open air |
| | | | Ultra-sonic, Impact echo, Radar | When a part of the structure is embedded |
| | Arrangement of steel reinforcement | Concrete cover | Radar, Electro-magnetic, X-ray | Surface bars only |
| | | Bar spacing | Radar, Electro-magnetic, X-ray | Surface bars only |
| | | Bar diameter | Electro-magnetic method | Surface bars only |
| | Structure | Overall stiffness | Oscillation test | Amplitude, frequency |
| After several years of usage | Appearance | Deterioration | Visual inspection, Photograph | Stain, cracks, |
| | | Defects (Surface) | Digital still camera, Thermograph | Including honeycomb, cold joints |
| | | Defects (Inside) | Sonic, Thermograph, Radar U-sonic, X-ray, Impact echo | Voids inside and at the back of the structure |
| | Stress & Strain | Deformation(Macro) | Measure, Transit, Laser | |
| | | Deformation(Micro) | Dial gauge, Strain gauge | |
| | | Vibration | Acceleration Sensor, LVDT Laser deformation measurement | |
| | | Stress | Mold gauge, Optical sensor | |
| | Strength & Stiffness | Concrete strength | Core sample test | General method |
| | | | Rebound hammer, Pull-out test | Problem of accuracy |
| | | Modulus of Elasticity | Core sample test Ultra-sonic velocity | |
| | Cracks & Spalling | Distribution | Digital still camera, Thermograph | |
| | | Crack width | Digital still camera, Thermograph | Direct measurement possible |
| | | Crack depth | Ultra Sonic | Effect of bars |

| Time | Items | Measurement | Methods | Comments |
|------|-----------------|------------------|--|---------------------------------|
| | | Cracking | Acoustic Emission | Continuous measurement required |
| | Diffusion Depth | Carbonation | Core sample test | Analysis by core samples |
| | | Chlorides | Core sample test | |
| | | Acids | Core sample test | |
| | | Other substances | Multi-spectrum method | Limited to concrete surface |
| | Permeability | Permeability | On-site permeability test | |
| | Steel Corrosion | Location | Natural potential | Location at that time |
| | | Corrosion degree | Natural potential, Electric current analysis | periodic measurement required |

Note: indicates application of NDI.

Thermograph is another valuable tool. When any void exist close to the surface of concrete structure, they can easily detected by using thermograph. The tool looks the same with digital still camera but the information we can obtain is different. When a void with certain size exists close to the surface, due to sun light, etc., surface temperature of concrete becomes slightly higher (less than 1 degree in most cases) than the surroundings. As a result, the voids in concrete can be easily detected as shown in Figure 5.



Detected void by thermograph

Figure 5: Thermograph of concrete wall with void underneath

6.2 Detection of voids and reinforcing steel bars

In case of old concrete structures, it is quite difficult to obtain detailed drawing of reinforcements. Both electro-magnetic method and radar systems are often used to clarify the arrangement and location of reinforcing steel bars within concrete structure or to measure the cover to the bars.

Radar system is often used to measure the cover thickness of the reinforcing bars and location of voids. The microwave transmitted from radar reflects at the surface of concrete, steel bars or voids. The time difference is used to measure the depth of the target.

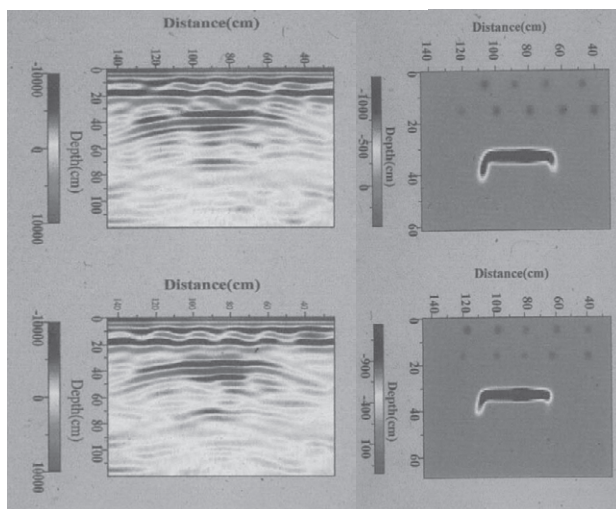


Figure 6: Inspection of void in concrete under steel reinforcements

An example of Radar inspection apparatus, available now in Japan, give the result as shown on the left side of Figure 6. But it is difficult to find out the inspected results by normal engineers. In our laboratory, a new method is developed to display the results as shown in the right side of the figure 3. These developments are required to utilize NDT for evaluation.

3.3 Detailed inspection of concrete

X-ray is used to detect voids, defects and bar arrangements in concrete. The results can easily be understood by civil engineers. When more than 2 photographs are taken at different locations, three-dimensional information can be obtained. If high energy X-rays can be used, a detailed inspection can be done as shown in Figure 7. The only problem is that x-rays are harmful for human beings, animals, plants, etc., and it is difficult to use high-energy X-rays at field. Normally, with compact apparatus, the thickness of concrete is limited to less than 30cm in order to obtain good quality measurements.

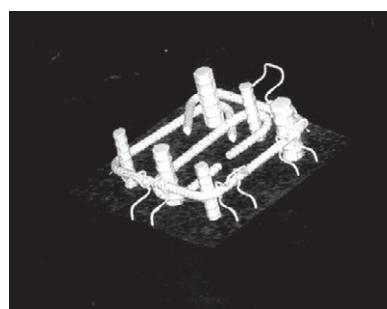


Figure 7: Detection of steel bar arrangement in concrete using High energy X-ray CT/DR

3.4 Multi-Spectral Inspection of concrete

Near-infrared spectral imaging system was introduced in order to detect distribution or concentration of deterioration factors remotely. This system consists of near-infrared irradiation equipment, imaging spectroscopy and near-infrared CCD camera. This system consists of near-infrared irradiation equipment, imaging spectroscopy and near-infrared CCD camera. Dispersed near-infrared rays through the spectroscopy can be received in each wavelength by light-sensitive element on CCD camera.

Detection of chloride penetration was also attempted using the system. Figure 8 shows spectral image of 2266nm and result of EPMA analysis (Target: Cl). Cement paste specimen was soaked in salt water, so chloride was penetrated from its surface. Chloride containing cement paste absorbs near-infrared light of 2266nm, so high chloride concentration area appears dark.

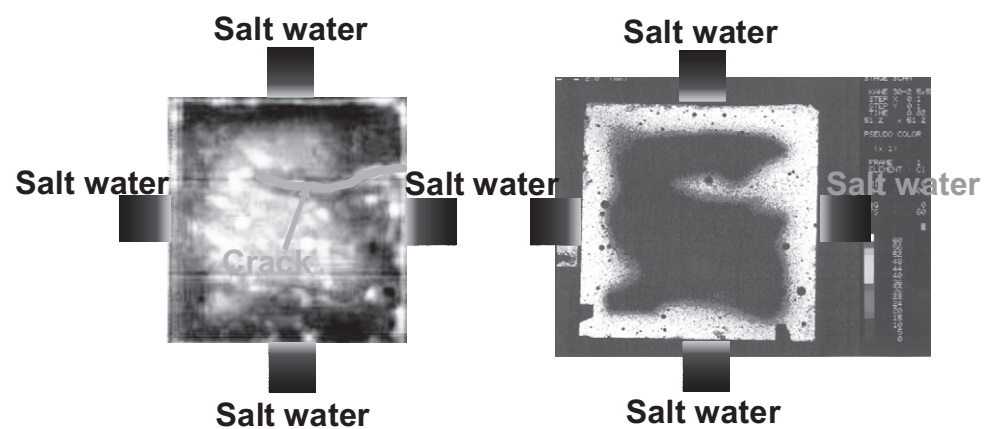


Figure 8: Spectral image (Left) and result of EPMA analysis (Right)
(by Dr. H. Kanada)

6. CONCLUDING REMARKS

Engineering is not always complete, and further research works are needed. To sustain existing structures, durability of the structure is important. One good method is to construct durable structures, but for the existing structures maintenance is the only way to deal with the problem. Although concrete committee of JSCE has set up a good system for maintenance of existing concrete structures, there are still many things to be done: not only researches but also education to the students and engineers about durability and maintenance. I hope this paper may become a help to the concrete engineers of the world who are trying to design, construct and maintain concrete structures.

REFERENCES

- Concrete Committee of JSCE, *Standard Specifications for Concrete Structures-2007 "Design"*. JSCE, Tokyo.
Concrete Committee of JSCE, *Standard Specifications for Concrete*

- Structures-2007 "Materials and Construction"*. JSCE, Tokyo.
Concrete Committee of JSCE, *Standard Specifications for Concrete Structures-2007 "Maintenance"*. JSCE, Tokyo.
- Okazaki, S., 2005. *Development of monitoring system for RC bridge based on restoration design method*. Thesis submitted to the University of Tokyo for Master of Engineering degree.
- Tsukahara, E., Koyama, R., Hoshino, T., and Uomoto T., 2000. Estimation Method of Corroded Portion of Reinforcing Steel Bar by Natural Potential Measurement. *Non-destructive Testing in Civil Engineering 2000*, Elsevier.
- Uomoto, T., and Misra S., 2001. Role of Engineers to Improve Quality of Concrete Structures. *Proceedings of EASEC-8*, Singapore.
- Park S.K. et al: Estimation of the Volume of Three-Dimensional Subsurface Voids by Microwave Polarization Method, pp.13-24, *JSCE No.592/V-39, 1998.5*
- Izumi S. et al: Application of High Energy X-ray CT/DR to Non-Destructive Testing of Thick Concrete Structure, *3rd Non-destructive Symposium using X-rays, 1999 .11*

DISASTER MITIGATION FOR INHABITANTS OF MEGA CITIES

TOSHIBUMI SAKATA

Research and Information Center, Tokai University, and
Advanced Earth Science and Technology Organization, Japan
sakata@aesto.or.jp

ABSTRACT

This paper proposes mitigation measures for the potential disasters faced by mega cities. A growing number of cities throughout the world have populations in excess of 10 million people. These cities are varied and complex in structure, and are likely to encounter enormous challenges in the event of a disaster. The proposal focuses on the residents of these mega cities, and discusses the importance of mutual cooperation through sharing of information with everyday acquaintances.

1. INTRODUCTION

Natural and man-made disasters are an issue of growing concern for large cities the world over. As cities modernize and transport and communication networks expand over wide areas, worldwide the number of mega cities in particular continues to grow. In addition to their huge populations, these mega cities contain zones of industrial, financial and commercial activity, residential areas and administrative bodies, and their influence is therefore felt globally, from the foundations of everyday social life to high-level economic activity. This global issue transcends any particular region or city, and the question of how to respond to and mitigate large-scale disasters has attracted great interest, even those disasters unlikely to lead to change in social structure, global economic collapse, and so on. At the same time, the impact of large-scale disasters on social structures and socioeconomic systems is a subject of importance for all countries to consider at the national, industrial and academic level. In the fields of science and technology, much effort has been placed on reducing the level of damage caused by major disasters; however, these issues also need to be studied from new perspectives provided by the social sciences and humanities.

2. THE NATURE OF DISASTERS

The world we inhabit is constantly undergoing change as a result of both natural phenomena and human activity. Natural phenomena change the planet's topography and environment, which in turn brings about changes in the plant and animal worlds. As a part of the animal world, the human world experiences both benefit and harm from natural changes, and we call this harmful aspect disaster. The many different forms of natural disaster include

earthquakes, volcanic eruptions, typhoons, hurricanes, tornadoes, tsunami, landslides, land deformation, rise and fall in sea level, climate change, heat waves and cold waves, warming and cooling. Fire damage to grassland and forest is often the result of natural disaster, but is also increasingly caused by human activity. In contrast to natural disaster, the harmful results of human activity are labeled as accidents, and these too can cause large-scale damage. Every year, an increasing number of accidents occur involving plants such as petroleum, chemicals, energy and steel plants, transportation such as airplanes, trains and shipping, structures such as bridges and buildings, and so on. Given this situation, disaster prevention and damage limitation need to be tackled as an issue for all human beings. Well-known historical examples of disasters striking cities include the natural disasters of the volcanic eruption that engulfed Pompeii and the earthquakes that destroyed San Francisco, Tokyo and Kobe, and the disaster of the Great Fire of London resulting from human action.

3. CITIZENS OF MEGA CITIES

Disaster strategies in large cities are complex, having various different elements. It is human beings themselves who must respond to disaster, and those same people rely on the functioning of the city for many aspects of their daily lives, yet when disasters or accidents occur the power of the individual is of little use. The convenience provided by a functioning city is one of the benefits of living in large groups, and it is perhaps this goal which has attracted people to cities. Historically, the convenience of everything from trade to shared defense drew people to the city, while its inhabitants strove to achieve those goals. Permanent inhabitants of the city and temporary residents therefore perhaps have a different consciousness of the city as its citizens. At times of disaster, the transition from protecting ones neighborhood to evacuation is likely to differ between mere residents of the city and people whose awareness of the city stretches from its history to the atmosphere of its streets, buildings, urban areas and local neighborhoods. There is perhaps not so much difference between the ordinary citizen and the inhabitant of a small village or town, comfortable in the familiarity of the place where they live and provided with opportunities for social interaction. With this in mind, I wish to consider what kind of behavior is necessary for minimizing the impact of disaster on inhabitants of mega cities such as Tokyo and Beijing.

4. ISSUES FOR CITIES DURING DISASTER

Areas known globally as earthquake zones, volcanic regions and coastlines prone to tsunami have been identified and analyzed on the basis of historical data. Monitoring is also carried out by meteorological stations and monitoring stations around the world, and by artificial satellites. Weather conditions are now monitored 24 hours a day at ground level and from space, enabling short-term and long-term forecasts to be made. Global warming presents a stark warning for the future of mankind, and attention is turning

to the environmental problems of mega cities in particular as a window on this warming trend. The issue of disaster is not just one of rapid change, but must also be considered in terms of gradual change, as exemplified by the urban heat island phenomena. By capturing infra-red energy given off by cities, nighttime images from satellites around the globe reveal the bright glow of mega cities. This brightness is, of course, an indicator of population as well a representation of electricity consumption, and as such it implies other activities occurring alongside energy use, since human populations also require a supply of food and water. Disaster not only brings physical destruction and loss, but also leads to the breakdown of these systems. Most cities are of course well aware of this and have strategies for dealing with such problems.

5. FOCUSING ON DISASTER MITIGATION

Most cities are equipped with various systems, organizational structures, equipment and facilities for dealing with disasters. Naturally, the necessary buildings, structures and communication systems are in place before disaster occurs; however, being mostly for emergency use rather than daily use, their performance during a disaster is not guaranteed. After a disaster, evacuation is the biggest problem to be faced. Strategies for damage by wind and flood will differ from those for unpredictable disasters such as earthquakes, and will also differ between local administrative bodies. The various conditions described above have generated different methods and strategies for responding to disaster, but a human-centered perspective on the problem seems to have been lacking until now. In the midst of damage caused by disaster, most important are human life, information and cooperation. In a disaster, the number one priority is human life – ones own life. I identify four forms of help: self-help refers to helping oneself, mutual help refers to helping people in close proximity, cooperative help is help between friends and colleagues, groups, and within and between companies, and lastly, public help is help provided by public organizations and systems. In the event of a disaster, the first priorities are self-help and mutual help, which are fundamentally based on the individual. These forms of help depend on one's everyday acquaintances and the possibility of information sharing and cooperation, yet for inhabitants of mega cities, such cooperation and information sharing, while being the most important aspect in disaster mitigation, are lacking. Cooperative help involves mutual help on a wide scale between acquaintances, regions, workplaces and businesses. The DiMS Disaster Mitigation Strategy Forum set up in 2006 has discussed aspects of these problems as part of activities focused on disaster mitigation. This forum's members include people from the worlds of academia, business and also those with experience in public administration.

STRATEGY FOR EFFICIENT USE OF EARTHQUAKE EARLY WARNING SYSTEM FOR EARTHQUAKE DISASTER REDUCTION

KIMIRO MEGURO

International Center for Urban Safety Engineering
Institute of Industrial Science, The University of Tokyo, Japan
meguro@iis.u-tokyo.ac.jp

ABSTRACT

On October 1st 2007, the Japan Meteorological Agency (JMA) has started disclosing Earthquake Early Warning (EEW) information to the general public. Although this information can be very useful to reduce damage in coming earthquakes, if used inappropriately, it could, in the worst case scenario, be more damaging than no information at all. In order to avoid this situation, it is important that the general public understands the meaning and limitations of the information that is being provided therefore avoiding false expectations.

The EEW system uses the difference of wave velocity between Primary wave (P-wave) and Secondary wave (S-wave), to disclose the seismic intensity and arrival time with considerable accuracy before the strong ground motion is felt. As many seismometers have been installed in Japan, when an earthquake occurs, the nearest location seismometer can detect P-wave and this information will be immediately be sent to the JMA. Using the information, JMA can calculate the location and magnitude of the earthquake from which the observed P-wave is generated within 4 seconds since the P-wave detection time. With occurrence time, location and magnitude of the earthquake, seismic intensity and arrival time of the expected ground motion can be estimated and informed to the persons who are located at some distance from the earthquake source.

The EEW system has six steps: a) P-wave detection by the nearest location seismometer, b) data transmission to JMA, c) calculation of location, magnitude and occurrence time of the event by JMA, d) delivery of the information to dissemination and disaster-related organizations by JMA, e) delivery of the information by these organizations to users, f) use of the information for disaster reduction by the users. In this paper, issues with the current EEW system will be classified following to these steps and discussed. Then, their solutions will be introduced for proper use of EEW system.

1. INTRODUCTION

The Japan Meteorological Agency (JMA) started disclosing Earthquake Early Warning (EEW) information to the general public on the 1st October

1st 2007) almost one year after the advanced system, intended for special users, was launched. Since the start of the service, there have been some troubles and as a result EEW information was not delivered to the affected sites before strong ground motion arrived as expected. Many mass media repeated the limitation and negative aspect of the system and sometimes they reported that EEW system have no meaning.

Different from the advanced system, in case of ordinary EEW system, the general public, who are not trained well and do not understand well the meaning and the limitations of EEW information and how to use the information, are the potential users. There are many issues for proper use of ordinary EEW system. In this paper, I will summarize the issues and introduce their solutions for properly use of EEW information provided by ordinary EEW system. Issues will be classified into six following the six steps of EEW system. Also, I will explain the effects of EEW information and point out the importance of indirect effects of EEW system.

2. FUNDAMENTAL KNOWLEDGE ON EARTHQUAKE EARLY WARNING INFORMATION

2.1 Basic knowledge and terminology for EEW system

Earthquake is generated by the rupture of the underground seismic fault. As shown in Figure 1, fault rupture is spatial and temporal behavior and the rupture starting point is called hypocenter and its right above ground surface point is called epicenter. During the rupture of the fault, stress wave is generated and propagated. This wave vibrates ground and is called seismic wave. There are two kinds of seismic waves, one is body wave and the other is surface wave (Figure 1). Body wave, traveling directly from the fault to the observation point, is composed of two type of the waves, primary wave (P-wave) and Secondary wave (S-wave). P-wave is longitudinal wave and its component is along the propagation direction. It is usually felt as an up-down movement. While S-wave is shear and transverse wave, its component is perpendicular to the propagation direction. It is usually felt as horizontal movement and is major cause of earthquake damage. Surface wave, traveling to the surface and then propagate along to surface to the observation point, is composed of two types of waves, Rayleigh and Love waves. It affects large tanks and bridge, and high rise buildings.

Although there are some varieties due to stress condition and asperity characteristics on the fault plane, definition of the magnitude, which explain the energy of the earthquake, can be generally discussed by the final rupture area of the fault. However, at the beginning and/or progress stage of the rupture, it is physically impossible to determine accurately the final magnitude of the event. There is a trade off the between available time and accuracy.

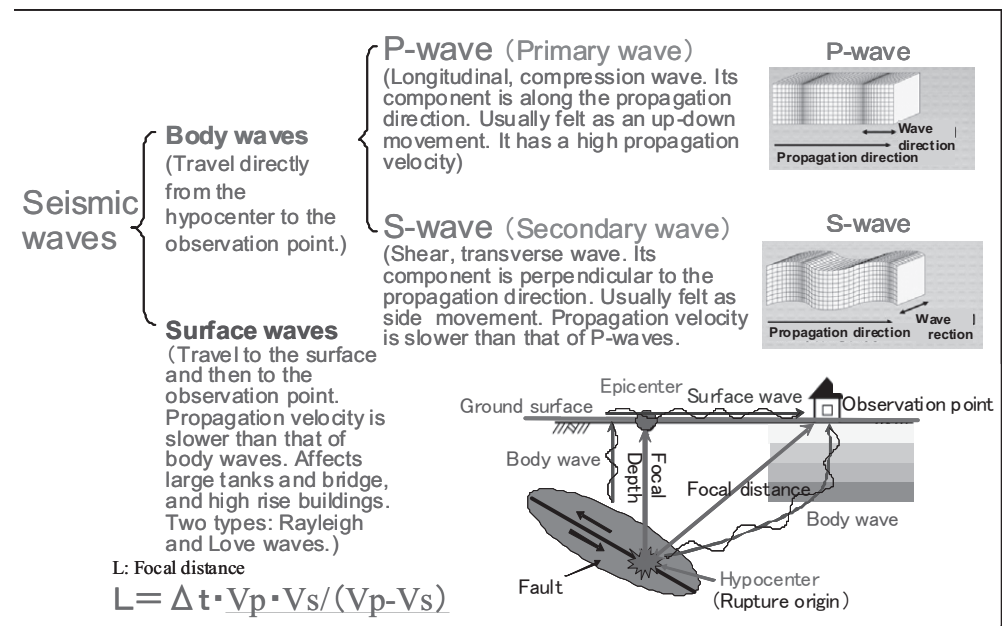


Figure 1: Types and characteristics of seismic waves

When we measure the ground motion by seismometer, waves such as shown in Figure 2 are recorded. From the records, we can understand that the order of the wave propagation velocity and predominant frequency is P-wave, S-wave and surface wave and that of the predominant period from longer one is opposite.

EEW system is that using the difference of wave velocity between P-wave and S-wave, before strong ground motion attacks the observation point, seismic intensity and arrival time is informed with considerable accuracy. As we have installed many seismometers in Japan, when an earthquake occurred, nearest location seismometer can detect P-wave and this information will be immediately sent to the JMA. Using the information, JMA can calculate the location and magnitude of the earthquake from which the observed P-wave is generated by around 4 seconds since the time of the P-wave detection. With occurrence time, location and magnitude of the earthquake, seismic intensity and arrival time of the expected ground motion can be estimated and informed to the person who is located a little far from the earthquake. This is EEW system.

Distance from the observation point to earthquake can be calculated by the Equation (1).

$$L = \Delta t \cdot V_p \cdot V_s / (V_p - V_s) \quad (1)$$

where Δt is P-S arrival time difference, V_p and V_s are P-wave and S-wave velocity, respectively.

As the underline part of the Equation (1) is normally 7 to 8 km/s, considering four seconds required for calculation, distance, L becomes around 30 km. Therefore, even if seismometer is located at the site of the earthquake, it is impossible to deliver the warning before strong ground motion arrives within 30 km focal distance.

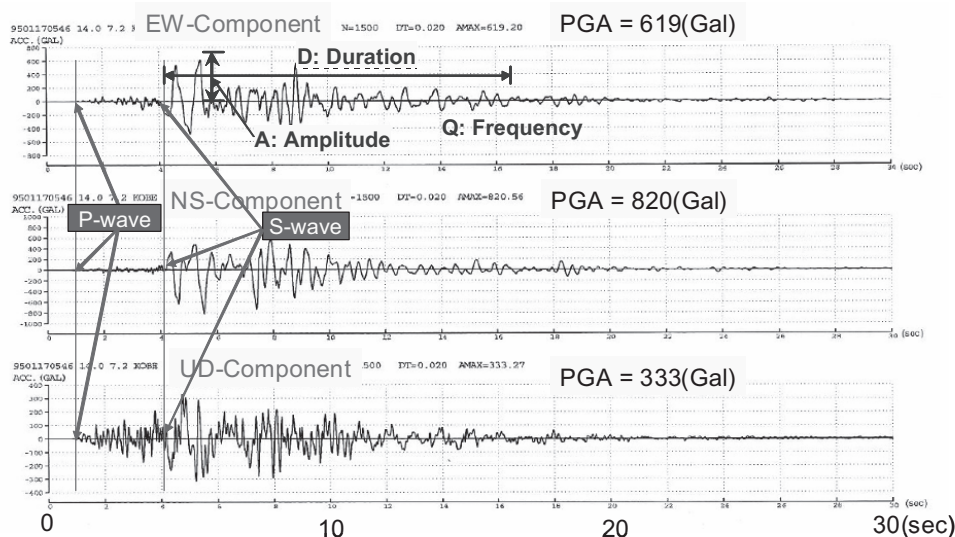


Figure 2: Three important characteristics of ground motion causing damage (1995 Kobe ground motion observed at Kobe Marine Meteorological Observatory)

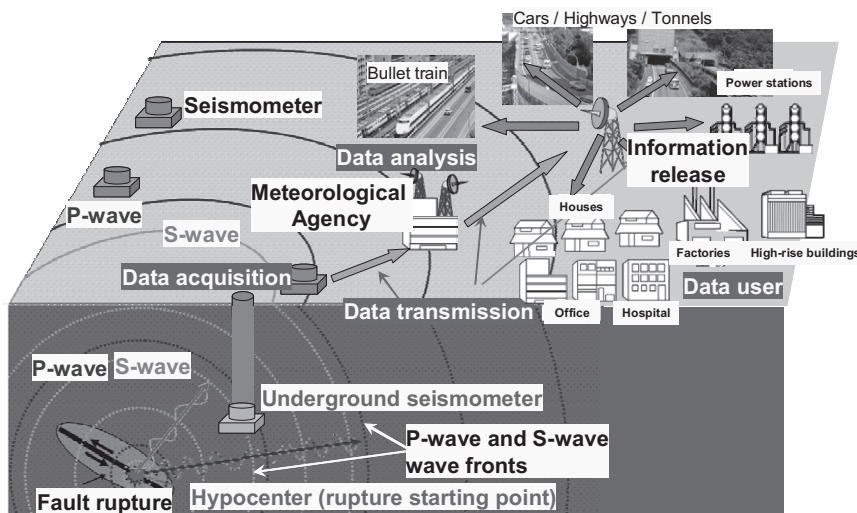


Figure 3: Earthquake early warning system (Processes and tasks)

2.2 Relation among earthquake damage and ground motion characteristics

Figure 2 shows the 1995 Kobe earthquake ground motion recorded at JMA Kobe marine observatory station. Effects of ground motion on earthquake damage can be discussed by three major parameters, such as A: maximum amplitude, D: duration and Q: frequency characteristics of the strong ground motion. Damage becomes severer when the maximum amplitude is larger, duration is longer, and frequency characteristics are close to those of target system and structure as resonance may occur. JMA seismic intensity, the most popular index to discuss the effect of ground motion in Japan is also defined by basically these three parameters.

There are also three major parameters that strongly affect above mentioned three parameters of ground motion. These are ‘source

characteristics’, ‘wave propagation path from source to the observation point’, and ‘site effect of observation point.’ Each of them can be discussed by mainly, magnitude of the earthquake, focal distance, and surface soil condition of the site, respectively. Table 1 describes relations among these three by three parameters. Understanding these relations is the key to use well of EEW system.

When you discuss the effects of magnitude on ground motion, the other two, i.e. focal distance and surface soil condition should be fixed. When a magnitude is larger, maximum amplitude becomes bigger, and duration does longer and relatively lower frequency component, which affects strongly structural damage, does predominant. About the effects of focal distance, when it is longer, maximum amplitude becomes smaller, and duration does longer but its effect is less as amplitude becomes smaller, and relatively lower frequency component does predominant as high frequency components attenuate. About the surface soil condition at the observation site, when the ground is softer and thicker, maximum amplitude becomes larger, and duration does longer, and predominant frequency does lower.

2.3 Relation between ground motion parameters and EEW system

Based on characteristics discussed above, the relation between ground motion parameters and the EEW system may be found as summarized in Table 2. For instance, when an earthquake with large magnitude occurred close to the observation site, it is difficult to deliver EEW information to the site before ground motion attacks the site. Good condition earthquake with high efficiency of EEW system is large magnitude one but focal distance is some long. As distance is long, available time is longer but because of large magnitude, damage may occur.

The effect of site condition on the ground motion characteristics is also very strong, for accurate ground motion information delivery and efficient response based on it, it is important to consider the user’s location and his/her site condition beforehand. Even the same magnitude of the event same focal distance, when the soil condition is different, ground motion become different, even soil condition is also the same, shaking that the user will feel is quite different at under ground, ground surface, and upper floor of high rise building. The motion that a car driver will feel on elevated high way bridge, is driver’s seat response due to response of driving car due to amplified structural response of bridge due to strong ground motion. The characteristics on the motion, that a person working at the building construction site will feel, is changing everyday based on the progress of construction of the building.

Table 1: How do ground motion characteristics affect damage?

| Representative parameters | Source characteristics | | Propagation path and distance | | Local site effect | |
|---------------------------|-----------------------------------|------------------------------------|--|------------------|------------------------------|--|
| | Magnitude (M) (Source effect) | | Focal distance (Between observation point and fault) | | Ground conditions Topography | |
| | Larger | Smaller | Longer (Further) | Shorter (Closer) | Hard soil | Soft soil |
| A: Maximum amplitude | Becomes larger | Becomes smaller | Becomes smaller (Attenuated) | No change | No change | Amplification (However, if soil liquefies, the shaking becomes less intense) |
| D: Strong motion duration | Becomes longer | Becomes shorter | Becomes longer (However, amplitude becomes smaller, then damage decreases) | No change | No change | Becomes longer |
| Q: Frequency content | Low frequency component increases | High frequency component increases | Low frequency content increases (Because high frequency component attenuates faster) | No change | No change | Low frequency content increases (Predominant period becomes longer, low frequency waves amplify) |

Table 2: Relation between ground motion parameters and earthquake early warning

| | Source characteristics | Propagation distance and path | Observation point topography, soil conditions, others |
|---|--|---|---|
| Relation to earthquake early warning | There is a trade off between accuracy and time. Earthquake is an spatial and temporal event and its magnitude becomes bigger as the fault plane area becomes larger. In case of a large earthquake, it takes time for the rupture to take place. As a result, it takes time to identify it and issue the warning, leaving shorter time for action. If the warning is issued sooner – with less certainty – more time for action is available but also a larger chance of an inaccurate evaluation. | The time between the warning and the shaking is shorter if the focal distance is shorter. The warning system is not so effective for locations close to the epicenter of large earthquakes. This areas are expected to have the largest damage. The system is most effective for locations not so close to the epicenter of a large earthquake. | Even for the same magnitude and focal distance, the shaking amplitude, frequency content and duration can be very different depending on the observation location. Even in the same building, the shake at the basement or at higher up floors is very different. In a car, on a viaduct or a bridge, the shake is affected by the dynamic response of the viaduct/ bridge. At a building construction site, the response changes with the changing characteristics of the structure being built. |

3. ISUSES FOR WELL USE OF EARTHQUAKE EARLY WARNING SYSTEM

3.1 Issues in general

There are two levels of use of EEW system. One is an advanced system and the other is general public use system. Ideal use of EEW information is advanced one and is that first, ground motion intensity and arrival time are calculated accurately considering the user’ condition, secondly, the information is delivered immediately and surely to the user, thirdly user uses them well based on pre-event good preparation and training and reduce the damage as much as possible. However, in case of ordinary system different from an advanced system, the general public, who are not trained well and don’t understand well the meaning and the limitation of this information and how to use it, are potential users. Therefore, it is very

difficult to deliver the information considering user's location, expecting seismic intensity, and available time before arrival of strong ground motion attack. Then in case of ordinary EEW system, JMA consider the conditions below for information delivery to avoid troubles. a) the number of information delivery of one event is one in principle, b) information is delivered only when strong ground motion is expected, c) prevent false information delivery by mistake, d) deliver the information as soon as possible, e) proper description which can consider estimation error is adopted, f) confine areas with some accuracy where countermeasures such as evacuation is needed, g) include information that is necessary for information delivery by TV broadcast. Namely, JMA decided to deliver EEW information to the areas where JMA seismic intensity is expected 4 or more when at least two stations detect ground motion with JMA seismic intensity 5– or more. National land is divided into 200 parts and each part is used for area unit for information delivery. Concrete value of seismic intensity and available time are not informed.

It is understandable that JMA decided to serve ordinary EEW system in the above mentioned manner. However, I think that in future even the system for the general public had better aim to be advanced system. Therefore, in this session, I will summarize the issues towards future advanced system and introduce solutions for them. Figure 3 shows the total processes of EEW system. As shown in the figure, there are six steps from P-wave detection to use of EEW information by users. a) P-wave detection by the nearest location seismometer, b) send this information to JMA, c) JMA calculate location, magnitude and occurrence time of the event, d) JMA deliver them to information dissemination organizations and disaster-related organizations, e) information dissemination and disaster-related organizations deliver them to users, f) users use them for disaster reduction. All the issues on each step will be classified into two, i.e. information dissemination and receiving sides, and discussed.

3.2 Issues for information dissemination organizations to deliver information quickly and correctly

Among the six steps of EEW system, five ones from a) to e) are issues for information dissemination side issues. However, step e) has both aspects as the organization receives the information from JMA. Information dissemination organizations are required to detect P-wave as soon as possible after earthquake, calculate the location, magnitude and occurrence time of the event accurately and immediately as much as possible, and deliver them to users as soon as possible. I will explain briefly about relations between these missions and all five steps from a) to e).

P-wave detection by the nearest seismometer of above a) is for quick monitoring of ground motion, therefore, it is important to install seismometer at the site close to event. To implement this situation, installation of dense seismometer array network, deep bore hole seismometers, ocean bed seismometers, are important. In case that target seismic fault is recognized, seismometer network near to the fault is effective. Sending P-wave information to JMA of b), Analyzed data delivery by JMA to information dissemination organizations and disaster-

related organizations of d), and EEW information delivery by information dissemination and disaster-related organizations to users of e), etc. are all issues related with quick information transfer and its reliability. On the calculation of location, magnitude and occurrence time of the event by JMA of c), improvement of method and system is a key issue. About EEW information delivery to users by information dissemination and disaster-related organizations of e), consideration of users' situation and purpose of EEW is key as contents and accuracy of EEW information are different. About the use of EEW information by users for disaster reduction of f), disaster imagination of user is the key issue.

3.3 Issues for information receivers to use EEW information smoothly and correctly

For information receivers to use EEW information smoothly and correctly, disaster imagination is a key issue as well as understanding the meaning and limitation of EEW information. It is impossible for people to respond well for unimaginable situation. To improve disaster imagination capability, I have developed some tools, such as Meguro-method²⁾ and Meguro-maki²⁾ which is simplified version of Meguro-method. With the Meguro-method, table as shown in Figure 4 is used. Vertical axis shows the typical daily life pattern and horizontal axis shows the time since the occurrence of the earthquake. When the daily life patterns are prepared, seismic capacity of the house, furniture layout, environment around your home and your working company, location and actions of other family members depending on time, etc. are also checked. Moreover considering the case that transportation system cannot be functional, check the time needed for walking.

Then, assuming season, weather, day of the week, with the condition that earthquake occurred at each time of your action, imagine what will happen around you as time passes, and consider what you should do in such each situation. Many people cannot write anything as they can imagine nothing. This means that they cannot perform well in case earthquake occurs.

Strong points of Meguro-methods are; a) people can understand fully that earthquake is their own problem, b) People can understand that ordinary, abled person is considered as temporally disabled person, c) people can understand multiple tasks that individual person has, and d) people can consider the story after they died in disaster. By these points, people can improve their disaster imagination capability.

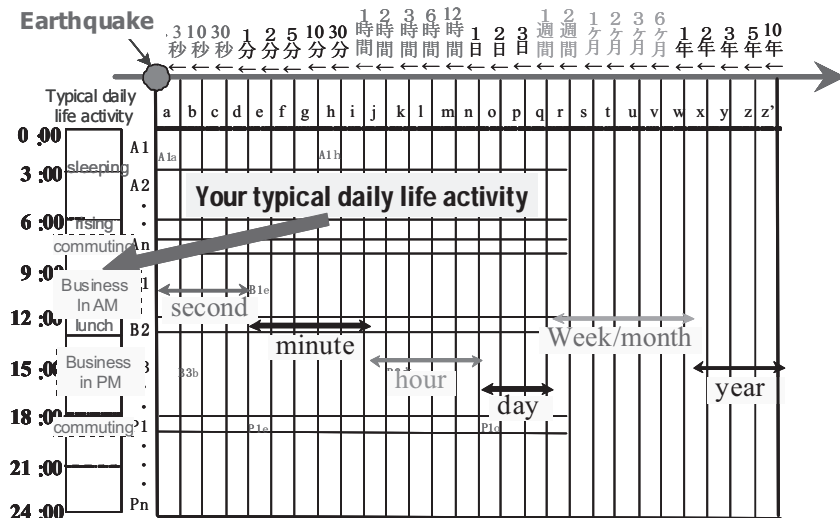


Figure 4: What will happen around you when you feel strong ground motion?

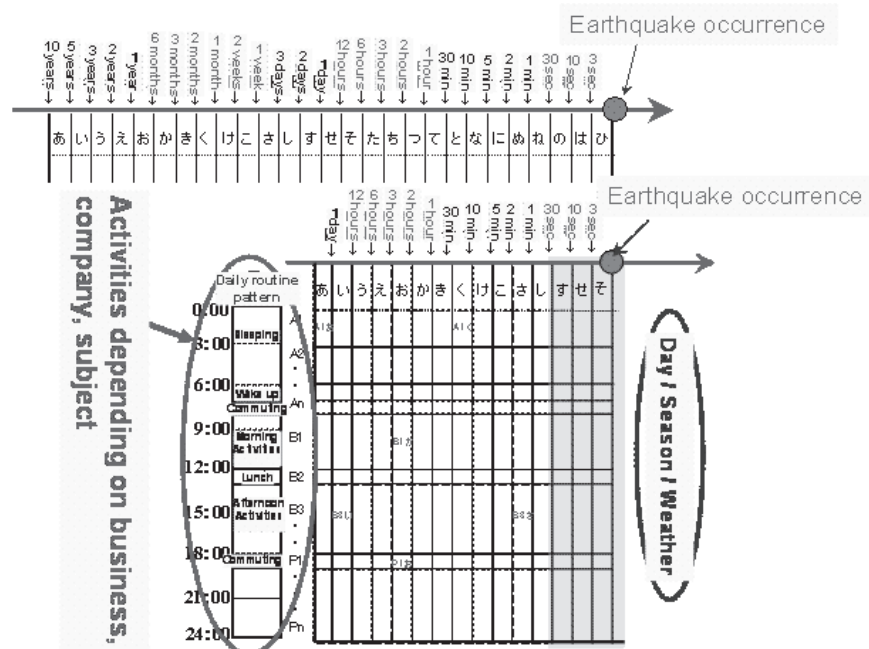


Figure 5: What can you do before an earthquake occurs ?

As the next step of the method, different table as shown in Figure 5 which shows the time up to the future earthquake is used. Once disaster imagination capability is improved, people can understand their own current problems and they start thinking seriously about solution of the problem and can use the time before earthquake comes to solve these problems. Then, their disaster resiliency can be increased before an earthquake and damage due to future earthquake can be reduced. While conventional style of disaster training such as ‘Do A, do B, don’t do C’ may stop the people thinking disaster seriously and has less education effect. What we should do from now as disaster education is to increase the number of the people who can really imagine what happens around them and what they should do in disaster as time goes since it happens considering the conditions, such as, time of occurrence, season, weather, location, and their roles at the time, etc. When the available time becomes less than tens of seconds, this is a time

range for EEW system as shown in the bottom table in Figure 5. To use efficiently this limited time, detailed information of user's situation is essential. People recognize the importance of pre-event preparation.

4. DIRECT AND INDIRECT PLUS AND MINUS EFFECTS THAT EEW SYSTEM HAS

The effects that EEW system has can be classified direct and indirect, and each plus and minus. So far, direct effects have been focused as major discussion points. However, I believe that indirect effects are the more important and we should pay much more attention to indirect effects. I will introduce direct and indirect effects, and their each plus and minus aspects.

*Table 3: Effects of early earthquake warning
(Direct effects are usually discussed. However, indirect effects are also very important, often overlooked, and should be discussed.)*

| | Direct effect | Indirect effect |
|------------------------|--|---|
| Positive impact | Early earthquake warning can reduce damage | Opportunity to promote disaster countermeasures before the event |
| Negative impact | Improper use of the disclosed information may lead to more damage. | -Unreal sense of safety hampering disaster countermeasure implementation -Influence on stock market etc. |

Direct plus effects are that many people expect. With better understanding of meaning and limitation of EEW information and preparation for efficient use of EEW information, EEW information can be used for disaster mitigation. Typical examples are human casualty reduction by proper evacuation guidance based on EEW information, structural damage reduction by vibration control based on EEW information, Machine trouble prevention such as elevator and industrial machines by automatic stop system based on EEW information, fire problem reduction by automatic stop system of gas and electric heater by EEW system, damage protection by over turning protection devices automatically controlled by EEW system, Start of action and preparation of emergency operation of fire fighting offices and of hospitals, traffic accident prevention of train and cars by EEW system.

Direct minus effects are also well known. In case that people don't know well about meaning of EEW system and how to use it, EEW information may give some trouble to the people and they cannot use it well for reduction of damage, they may increase damage, especially in the case that they become panic. This situation should be avoided and a key is education and training beforehand. Improvement of disaster imagination capability is essential issue for education and training as explained before.

On indirect plus, which was not so far used widely, but only limitedly used for education, however, I think that for ordinary EEW system, this indirect plus effects should be considered the most important. EEW information dissemination is an initial opportunity for the general public to promote real disaster mitigation countermeasures. With the start of EEW service, people start thinking how to use EEW information. If we have two seconds, five seconds before strong ground motion attacks us at living room, what we can do for save us and disaster mitigation. How about sleeping time? If the house is collapsed, furniture is over turned, we cannot evacuate. When the people's imagination capability is high enough through such as Meguro-method and/or Meguro-maki, they can recognize the importance of pre-event preparation and countermeasures, and understand that there are many damages that cannot be prevented only by EEW system. Finally, people conclude that pre-event countermeasures such as installation of furniture over turning protection device and retrofit of structure, creation of disaster resilient city are very important and these countermeasures are promoted. Then, in both cases that EEW system can and cannot give time before strong ground motion arrival, damage can be reduced by pre-event countermeasures.

About indirect minus effects, I think that this should be absolutely avoided. The effects are that EEW information reassures the general public about earthquake risks without any valid evidence. This hinders the general public from promoting pre-event countermeasures. As the result, future earthquake damage increases. Also, the effect on the stock market is considered a kind of indirect minus effect. Besides the earthquake damage, big negative economical impact can be given to the affected area and the country by EEW system. To make EEW system popular in the world for earthquake disaster mitigation in the world, we should prevent such a situation. A new stock market regulation should be established from international viewpoint.

5. CONCLUSIONS

In this paper, I summarized the issues and introduced their solutions for properly use of EEW information provided by ordinary EEW system. Issues are classified into six, following six steps of EEW system from P-wave detection by seismometer to end user's EEW information use, and discussed. Also, I explained the effects of EEW information and pointed out the importance of indirect effects.

Different from an advanced system, in case of ordinary EEW system, the general public, who are not trained well and do not understand well the meaning and the limitations of EEW information and how to use the information, are potential users. JMA's current principle on EEW information service is understandable. However, for better use of it, we had better pay much attention to indirect effects that EEW information has. Efforts for increase indirect plus and decrease indirect minus lead the general public to increase direct plus and decrease direct minus. For implementation of this environment, disaster imagination is also a key issue as well as understanding the meaning and limitations of EEW information. It is impossible for people to respond well for unimaginable situation. To improve disaster imagination capability, I recommended using the tools, such as Meguro-method and Meguro-maki. With these tools, when they

improve their capability, they can understand their current problems and can use the time available before an earthquake to solve their problems.

Also, when they try to find the good way to use EEW information considering their own situation, they can recognize that there are many damages which cannot be reduced or prevented by only EEW system, and can realize that they should take actions long before an earthquake occurs. The most important and effective actions should be taken much earlier. The public should recognize that EEW information alone cannot reduce much of the damage unless there is good preparation before the event. We should never face a situation in which we visit an elementary school after an earthquake and realize that the well prepared and warned students protected themselves under their desks just to be killed by the collapsed structure. Only if structural measures are taken before the earthquake, it will be possible to take fully advantage of any EEW information. The launching of this type of system is offering a unique opportunity to discuss disaster countermeasures and to increase disaster awareness among the general public.

I believe that the ideal use of the EEW information is that dissemination of this information becomes a good opportunity for the general public to consider more seriously about earthquake problem and improve disaster imagination capability. As a result, EEW information becomes a driving force to promote disaster mitigation countermeasures, such as retrofitting of low earthquake resistant structures, and to increase our society resilience. We should not have false expectations that EEW information alone will reduce earthquake damage.

REFERENCES

Japan Meteorological Agency (JMA) Website,

<http://www.jma.go.jp/jma/indexe.html>

Kimiro MEGURO: Towards proper use of earthquake early warning system in Japan, Proceeding of the 6th workshop on national land safety networking, 2007.2 (in Japanese).

Technical Sessions

DAMAGE TO BUILDINGS DUE TO 2008 MAY 12 WENCHUAN EARTHQUAKE AND COOPERATIVE ACTIVITIES FOR DAMAGE RESTORATION BY JAPANESE EXPERTS

YOSHIAKI NAKANO

Institute of Industrial Science, The University of Tokyo, Tokyo, Japan
iisnak@iis.u-tokyo.ac.jp

ABSTRACT

A destructive earthquake occurred on May 12, 2008, and caused extensive damage to Sichuan Province in China. Immediately after the event, Japanese scientific/engineering societies that had experiences and know-how on damage restoration of structures in the past major earthquakes jointly formed a council to technically support the restoration of the hardest hit areas through their mutual cooperation and sharing information. Since then, the council has been actively cooperating with Chinese experts from academic and engineering fields through damage investigations and extensive discussions on technical and practical issues for damage restoration. This paper briefly overviews damage to buildings and some relevant activities for their restoration mainly made under the cooperation of Southwest Jiaotong University in Chengdu, Sichuan Province.

1. INTRODUCTION

The Wenchuan Earthquake of magnitude 7.9 (USGS) jolted major cities in Sichuan Province, Central China at 14:28 local time on May 12, 2008. The damage is widespread and devastating, and more than 80,000 people are reportedly killed mainly due to collapse of buildings. Immediately after the event, the following seven Japanese scientific/engineering societies (initially the first five societies listed below) jointly set up a Technical Supports Council for Damage Restoration after Sichuan (Wenchuan) Earthquake (Council Chair: Dr. M. Hamada, Professor of Waseda University).

* Council member societies

1. JSCE (Japan Society of Civil Engineers)
2. AIJ (Architectural Institute of Japan)
3. JGS (The Japanese Geotechnical Society)
4. JAEE (Japan Association for Earthquake Engineering)
5. SSJ (Seismological Society of Japan)
6. CPIJ (The City Planning Institute of Japan)
7. AJG (The Association of Japanese Geographers)

The major purpose of the Council's activity is to form a technical support team under a close cooperation of seven societies that are well experienced in post-earthquake activities and to help researchers, engineers, and practitioners in the affected area restore damaged structures and

communities through sharing knowledge and experiences of recent damaging earthquakes such as 1995 Kobe and 2004 Chuetsu earthquakes.

After the earthquake, the Council dispatched technical support teams during May 28 through June 1 and June 20 through 25, and organized a Special Lectures on Engineering Seismology and Earthquake Engineering in September. In this paper, damage observation of building structures and technical supports activities for their restoration made during the second visit in June are briefly described.

2. BUILDING DAMAGE OBSERVATIONS

Damage surveys were primarily made in Dujiangyan city and Hanwang town of Mianzhu city. The surveys were organized by the Southwest Jiaotong University in Chengdu city, which was the Chinese counterpart for the technical support activities. Figure 1 shows the surveyed areas. During surveys, two major structural types, brick structures and RC frames with URM (unreinforced masonry) walls, are found. In the subsequent sections, major damage patterns found during surveys in May and June are briefly described for each structural type.

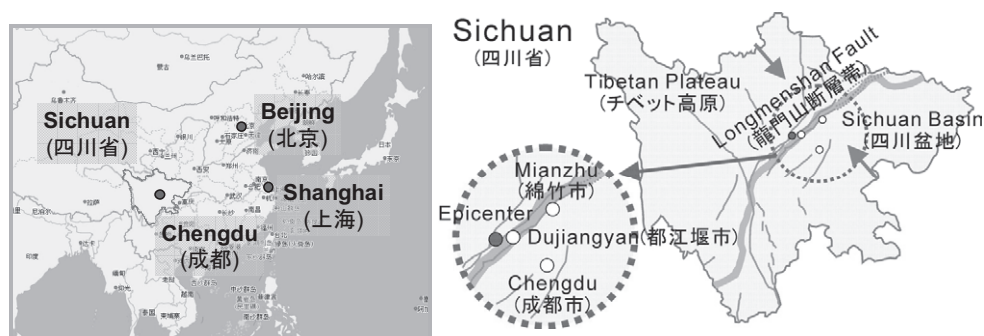


Figure 1: Surveyed areas

2.1 Brick buildings

Brick buildings are most seriously damaged and they often sustain partial or total collapse. They have UR brick walls having RC ring beams and precast hollow-core slabs on the walls. The major cause of the fatal damage is attributed to the low resistance and brittleness of URM walls and poorly detailed joints between precast members and RC beams. Photos 1 and 2 show typical damage to brick buildings.

2.2 RC buildings

In RC buildings, several damage patterns are found. They include damage to UR brick walls, shear failure in columns, flexural compression failure at column top and/or bottom, beam-column joint failure, and structural damage resulting from soil/ground failure underneath.

2.2.1 Damage to UR brick walls

Reinforced concrete shear walls are much less frequently provided in RC buildings than UR brick walls. Lightly reinforced small-sized columns are often placed later between UR brick walls so that the walls should serve as the form in casting RC columns. During the surveys, shear cracks and failure of brick walls are found in many buildings as shown in Photo 3. It should be noted, however, that lath-mortar finishing on the exterior surface of UR walls is found to help avoid their out-of-plane failure, although they are heavily cracked. Such efforts therefore should be encouraged to minimize falling hazard to residents and users during and after major quakes.

2.2.2 Shear failure in RC column

Shear failures in RC columns shortened by partial height brick walls are found in several buildings, as have been found elsewhere in the past damaging earthquakes. Photo 4 shows a typical shear failure in the first story of a building in Dujiangyan city. Photo 5 shows another failure, where the column is shortened and failed in shear leaving vertical cracks along the interface between the column and brick wall. The damage is attributed to the presence of partial height brick walls, which are generally neglected in the structural design but significantly affect the building's behavior during strong shaking.



Photo 1: Seriously damaged brick buildings



Photo 2: Partially collapsed brick buildings with hollow-core slabs



Photo 3: Shear failure in brick wall (left) and survived wall (right)



Photo 4: Typical shear failure in RC short columns



Photo 5: Shear failure in RC column shortened by partial height brick wall

2.2.3 Flexural compression failure at the top and bottom of RC column

Seriously damaged RC buildings often show flexural compression failure at the top and the bottom of their columns. Photos 6 and 7 show the damage to columns in the first story of a six story apartment building in Dujiangyan city. Hooks of lateral reinforcement are pulled out of crushed

concrete core. Main rebars buckles and fractures as shown in the photos. As will be found later, the building is employed for a sample building to investigate possible restoration schemes and to discuss their feasibility.



Photo 6: General view of six story RC apartment house



Photo 7: Flexural compression failure at the top and bottom of columns

2.2.4 Damage to RC beam-column joints

Damage to beam-column joints are less frequently found than other failure patterns such as shear failure in columns, flexural compression failure at the top of columns. Photo 8 shows the damage to the beam-column joint of RC apartment buildings, which were under construction at the time of the earthquake.

2.2.5 Structural damage due to soil failure

Structural damage due to soil failure underneath a building and resulting differential settlement is found in some buildings located at the foot of a mountain slope in Dujiangyan city. Photo 9 shows damage to a retaining wall, causing soil outflow and differential settlement of superstructures.



Photo 8: Failure in beam-column joint



Photo 9: Structural damage due to soil failure

3. SINO-JAPAN SEMINAR ON RESTORATION OF DAMAGED BUILDINGS

Along with the aim of the Council's activities, AIJ dispatched an expert team on building damage assessment and restoration led by the author during the period of June 20 through 25 following the first preliminary surveys in May. After two-day surveys of affected areas in Dujiangyan city and Hanwang town of Mianzhu city, the Sino-Japan Seminar on Techniques for Rehabilitation and Reconstruction after the Sichuan (Wenchuan) Earthquake was held on June 24 at Southwest Jiaotong University (SJU).

3.1 Outline of the seminar

The purpose of the seminar is primarily to present concrete strategies for damage restoration and to discuss their feasibility and applicability with seminar participants in detail. To this end, an example building is selected from those inspected during the field surveys considering Chinese side requests and then restoration schemes for the building are investigated and proposed by the Japanese side in the seminar.

In the seminar, summaries of damage surveys and basic ideas widely applied in Japan for restoring earthquake damaged buildings are first

presented. Then restoration scheme candidates for buildings damaged due to Wenchuan Earthquake are proposed by the Japanese side and their applicability, problems to be solved from the practical design and construction point of view in China are discussed in detail.

3.2 Example building

The example building is a six story RC apartment building in Dujiangyan city which appeared earlier in Photos 6 and 7 of 2.2.3. The structure was already completed at the time of the earthquake. The first story designed for a parking garage has no walls, while the upper stories have dwelling units with brick walls as shown in Photo 10 and Figure 2.

Almost all columns in the first story form plastic hinges both at their top and bottom, causing concrete crushing and rebar buckling (Photos 6 and 7) resulting in the soft-first story mechanism with a residual lateral drift of approximately 10% of the story height. No major damage is, however, found in the upper stories.

The observed damage is rated [unsafe] based on the Japanese quick inspection manual and [heavy damage] based on the Japanese post-earthquake damage evaluation guidelines (JBDPA 2001). The building therefore is identified to be evacuated and shored to avoid life-threatening risk and damage progress due to aftershocks.

3.3 Restoration strategies

To understand the fundamental seismic performance of the building, the Japanese seismic evaluation procedure (JBDPA 2001) is applied and the seismic capacity index I_s of the first story is evaluated. Table 1 summarizes the result. The building is found ductile with F index of 2.6, which is consistent with observed damage with a large lateral residual displacement.

Table 1: Seismic capacity index of example building prior to damage

| C | F | E_o | I_s |
|------|------|-------|-------|
| 0.14 | 2.60 | 0.67 | 0.67 |
| 0.12 | 2.99 | | |

Note: $I_s = E_o \times S_D \times T$

$$E_o = (0.14 + 0.12) \times 2.6 = 0.67$$

E_o : basic structural capacity index defined by $C \times F$

C : strength index defined in terms of shear coefficient

F : ductility index (ranging from 1.0 to 3.2) defined mainly by shear-to-flexure strength ratio, yielding displacement, etc.

S_D and T : reduction factors for E_o to allow for irregularity and deterioration of building (both assumed 1.0 herein)



Photo 10: Example six story RC apartment building

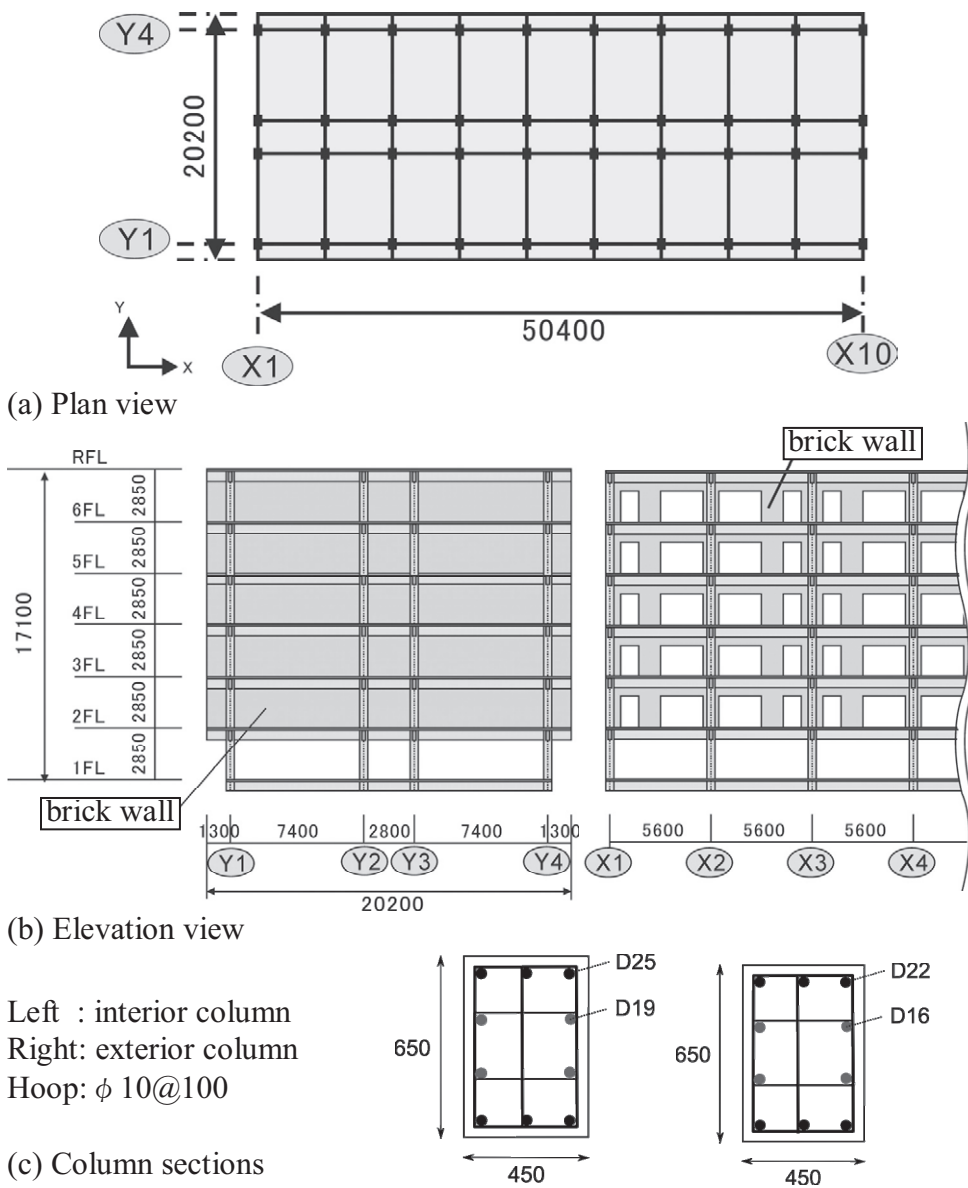


Figure 2: Structural configuration and column size of example RC building

To restore the damage, the following six schemes are proposed in the seminar. Table 2 summarizes and illustrates the basic ideas of the schemes.

3.4 Discussions in the seminar

More than ninety participants including researchers, engineers, and SJU students attended the seminar, and the applicability of the proposed restoration schemes are discussed as well as other general issues related to restoration techniques.

Table 2: Restoration scheme candidates

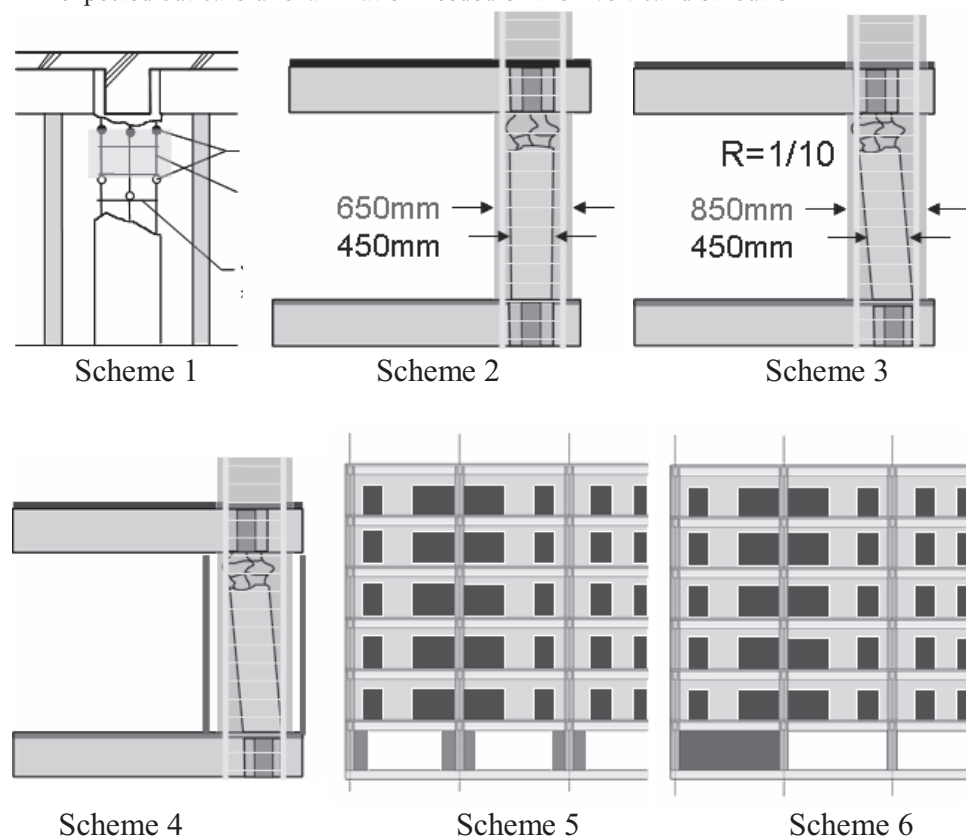
| Scheme (F-: flexural / S-: shear) | General description | Expected* difficulties | Expected# performance |
|--|--|---------------------------|--------------------------|
| 1. Repair | Repair to initial configuration after re-centering | (1) | (a) |
| 2. F-strengthening | RC jacketing after re-centering | (1) (2) | (b) |
| 3. F-strengthening | RC jacketing w/o re-centering | (2) | (b) |
| 4. F- and S-strengthening | Scheme 3 & steel jacketing | (2) | (b) |
| 5. Repair & strengthening w/ new wing-walls | Scheme 1 & wing walls | (1) | (b) |
| 6. Repair & strengthening w/ new shear walls | Scheme 1 & shear walls | (1) | (b) |

* Expected difficulties and necessary construction works

(1) Jack-up and re-centering of building; (2) Anchorage of longitudinal rebars for jacketing and arrangement of shear reinforcement in beam-column joints

Expected post-restoration performance

(a) Damage expected under future major earthquake; (b) Higher resistance and stiffness expected but careful examination needed on their vertical distribution



In the seminar, the Japanese side emphasized that the continuous distribution of strength and stiffness, smooth transfer of actions through structural members and their interface under seismic excitations, anchorage of new reinforcement in existing RC frame etc. were of highest priority in re-designing the damaged buildings, although the restoration proposals were made only in the first story for simplified discussions. It was also pointed out that the buckling of column reinforcing bars associated with flexural compression failure could be observed in areas close to their interface between upper beams rather than in their mid-span, and confinement of beam-column joints using additional lateral reinforcement should be provided to effectively eliminate further damage.

After long and enthusiastic discussions, the Chinese participants concluded that schemes 2 and 3 were most realistic and practical. It was also very interesting for Japanese participants to learn that schemes 5 and 6 were much less acceptable by the Chinese participants although they might be most likely to be accepted in Japan. This is mainly because the mixture of different structural types (i.e., RC frames with shear walls in the first story and RC moment resisting frames in the upper stories) is not specified in the structural design code while it may be accepted in Japan if its effects by the change in stiffness and strength distribution along building height on structural behavior are carefully taken into account.

4. CONCLUDING REMARKS

Typical damage to buildings due to Wenchuan Earthquake and activities by the Japanese experts under close cooperation with Southwest Jiaotong University are briefly presented. In especial, damage in Hanwang, where the fault runs across the edge of the town, is extensive, and many buildings are found totally collapsed. The Chinese side has high level background on seismic design and restoration techniques, but there still remain various types of difficulties even on the technical aspects as has been usually found in the earthquake aftermath elsewhere since such a devastating disaster and its aftermath are the first experience even for researchers and engineers in the most affected areas. The author therefore sincerely and deeply wishes that continued cooperative efforts, sharing information and experiences such as those having been done by the Council would effectively help restore damaged structures and communities.

REFERENCES

- JBDPA / The Japan Building Disaster Prevention Association, 1977, 1990, 2001 (English version in 2005). *Standard for Seismic Evaluation of Existing Reinforced Concrete Buildings*.
- JBDPA / The Japan Building Disaster Prevention Association, 1991, 2001. *Guidelines for Post-earthquake Damage Evaluation of RC Buildings*.

FLEXURAL BEHAVIOR OF CORRODED RC MEMBERS WITH PATCH REPAIR

YOSHITAKA KATO¹ and RAKTIPONG SAHAMITMONGKOL²

¹International Center for Urban Safety Engineering, IIS,
University of Tokyo, Japan
katoyosh@iis.u-tokyo.ac.jp

²Construction & Maintenance Technology Research Center, SIIT
sahamit@siit.tu.ac.th

ABSTRACT

Structural performance of RC repaired by patching method was experimentally investigated and compared with non-corroded as well as corroded RC. Two repair materials; namely, polymer-modified mortar and epoxy based repair material was applied for the repair work. The mechanical properties as well as the bonding characteristics of these two repair materials are different. It was found that the polymer-modified mortar can partially restore the structural performance while the more ductile epoxy based repair material strengthen corroded RC structure so that its ultimate load carrying capacity is beyond that of non-corroded RC.

1. INTRODUCTION

Deterioration of concrete structure is a serious problem which may drastically degrade both load-carrying capacity as well as serviceability of the structure. The corrosion reduces cross sectional area of reinforcing bar as well as induces corrosion cracking which destroys the bonding between concrete and reinforcing bar. It was reported that, when degree of corrosion increases, the ultimate strength of steel bars as well as the corresponding elongation of the bar before failures decreases (Almusallam 2001). The corrosion can also severely degrade ultimate load carrying capacity as well as ductility of RC (Uomoto and Misra 1984). Toongernthong and Maekawa (2005) studied structural performance of corroded RC under shear load and reported that the loss of bond caused by corrosion crack may change failure mode of RC and capacity of anchorage performance as well as the strength in shear span. The brittle failure by buckling of compression reinforcement may also be induced if the corrosion of compression reinforcement takes place (Uomoto and Misra 1984). Remedial action is necessary not only to maintain safety and serviceability of the deteriorated structure but also to extend its service-life. The patching repair method is recommended as an appropriate method for the RC members which are in the corrosion acceleration period as well as the deterioration stage (JSCE, 2001). There have been some researches on the performance of RC in both structural as well as durability aspects (Shash 2005; Nounu et al 1999). It is generally accepted that the response of the repair system to the changes exerted by the repair must be understood for design and construction of durable concrete

repair (Emmons and Vaysburd 1995). Satisfactory compatibility of repairing materials to base concrete structure in both structural performance and durability aspect must be ensured. There are several factors affecting the performance of RC structure repaired by patching method. Effect of rebar cleanliness, surface preparation of based concrete, and mechanical properties of repair materials and patching area have been experimentally investigated (Al-Dulaijan 2002). However, there is still no general methodology to analyze the structural behavior after repair precisely.

This study is therefore an attempt to investigate the structural performance of RC repaired by patching method. The repair procedure is controlled to be as similar to the practical operation as possible. Two different repair materials were selected for the study since these two materials are commercially available and possess different mechanical properties.

2. EXPERIMENTAL PROCEDURE

2.1 Specimen Preparation and Reinforcement Arrangement

All specimens prepared for flexural test have same dimensions. The width, height, and length are 150 mm, 200 mm, and 1700 mm, respectively. The drawing of specimens is shown in Figure 1. The deformed steel bars with 16-mm diameter and one with 12-mm diameter were used as tensile reinforcement and compression reinforcement, respectively. The shear reinforcement was 6-mm diameter round bar. Cover thickness is 25 mm. Both longitudinal reinforcement and shear reinforcement were prepared according to Figure 1. 5-mm holes were drilled at the free end of hooks and electrical wires were connected to the tensile reinforcement by 5-mm nut. The electrical wires were used to supply direct current into the tensile reinforcement. Since the objective of this study is to investigate the degradation of structural performance caused by the corrosion of tensile reinforcement only, the electrical insulators were installed at the connection between tensile reinforcement and stirrups in order to limit the corrosion to be in tensile reinforcement only. Table 1 shows a list of flexural RC specimens. The specimens can be broadly categorized into 3 types; non-corroded, corroded, and repaired specimens. Lengths of corrosion zone or repair area were varied as 300 mm, 1000 mm, and full length (1700 mm). Two types of repair materials were applied in this study.

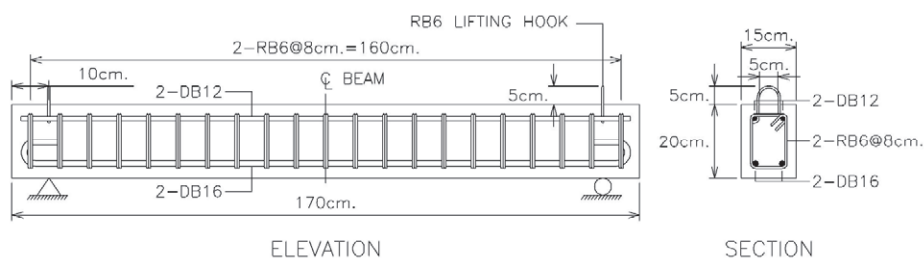


Figure 1: Drawings of specimen & Arrangement of Reinforcement

Table 1: List of flexural RC specimens.

| ID | Categories | Corroded/Repair Length | Repair Materials |
|---------|--------------|------------------------|-------------------------|
| NCB - 1 | Non-corroded | - | - |
| NCB - 2 | | - | - |
| FCBNR-I | Corroded | 300 mm | - |
| FCBNR-O | | 1000 mm | - |
| FCBNR-F | | 1700 mm | - |
| FCB1R-I | Repaired | 300 mm | Polymer Modified Mortar |
| FCB1R-O | | 1000 mm | |
| FCB1R-F | | 1700 mm | |
| FCB2R-I | | 300 mm | Epoxy Based Material |
| FCB2R-O | | 1000 mm | |
| FCB2R-F | | 1700 mm | |

2.2 Materials

Ordinary Portland cement-only concrete with water to cement ratio of 0.49 was used. The longitudinal reinforcement and shear reinforcement are deformed bar (Grade SD40) and round bar (Grade SR24), respectively. Two types of repair materials – polymer modified mortar and epoxy based repair material were used for patching repair. Polymer modified mortar contains cement and silica powder as important ingredients. Its behavior is therefore similar to cement paste with high early strength. The mix proportion of polymer modified powder to water was 4:7 by weight. The epoxy based repair material provides outstanding bonding capacity and lower modulus. It is therefore generally recommended as an adhesive to bond most surfaces in general structure. The epoxy based repair material has the ratio between epoxy and sand of 4:3 by weight.

2.3 Corrosion Acceleration of Flexural Member

In order to induce the corrosion of the RC member, cracking was initially introduced into specimen by slow loading. The location of cracks was ensured to be in the predetermined location. Three points loading was applied to induce crack in the specimen to have shortest repair region (FCBNR-I, FCB1R-I, and FCB2R-I) and four-point loadings with constant moment span of 350 mm and 500 mm was applied to the specimen to have a repair region of 1000 mm (FCBNR-O, FCB1R-O, and FCB1R-O) and full length (FCBNR-F, FCB1R-F, FCB2R-F), respectively. All induced cracks had a specified depth of 50 to 60 mm from bottom surface. Examples of flexural cracks induced by pre-cracking process are shown in Figure 2. The cracked specimens were connected to the direct current supply and the corrosion was accelerated.

In order to confirm the level of corrosion, the actual corrosion level of corroded RC specimen was measured after the loading. The corroded tensile reinforcements were taken out by cutting out of corroded reinforcement with specific lengths. Actual weight losses of the taken corroded reinforcement samples were then calculated based on original weight of reinforcement with same length. The actual weight losses of reinforcement of all specimens were from 0.3 to 0.4 g/cm²/cm. The patterns of induced

corrosion cracks are also shown in Figure 3. Corrosion cracks were observable on the sides as well as at the bottom of specimens.

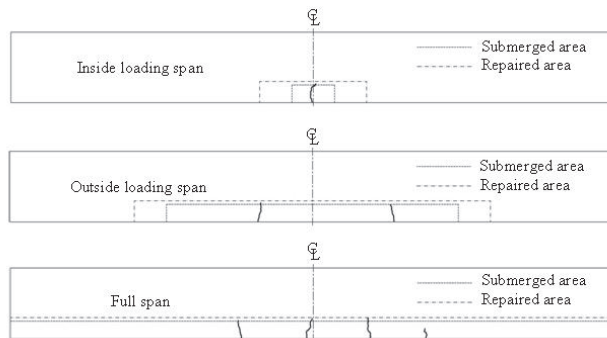


Figure 2: Examples of Pre-cracked Specimens

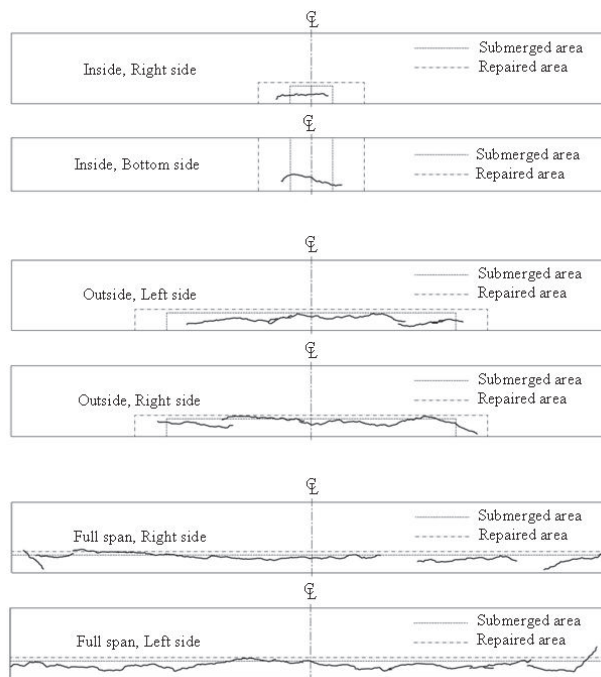


Figure 3: Examples of corrosion cracking patterns of FCBNR series

2.4 Patching Repair Procedure

Six corroded specimens (FCB1R series and FCB2R series) were repaired by patching repair method. The patching regions were 300 mm, 1000 mm and 1700 mm (full span) for specimens with 120 mm, 820 mm, and full span corrosion acceleration, respectively. Initially, the damage portions of concrete were removed by a portable demolisher powered by high pressure pump. The reinforcements were then polished carefully by the electrical polishing tools equipped with steel brush. Chisel steel rods were then used to trim the area to be repaired into rectangular shape with uniformly rough surface. The patching areas were then cleaned by high pressured air activated by air pump. The specimens were flipped so that the patching area is on the top during patching in order to fill the repairing materials in to the patching area efficiently as well as to ensure a quality of

compaction. After patching, the patched portions were wrapped by the plastic sheets in order to prevent the early lost of water from the repair materials.

2.5 Flexural Loading Test

The non-repaired RC flexural members (NCB series) were loaded at the age of 28 days. The corroded RC members (FCBNR series) were loaded at 7 days after galvanic corrosion acceleration was completed. And, the repaired RC members were loaded at 14 days after repair work. All specimens were loaded under 4-points loading with a total clear span of 1500 mm. The distance between two loading points and shear span were 500 mm. Displacement transducers were installed at the middle of the specimens, at the location of loading points, and at the supports in order to measure the deflection of the specimen during the loading. Monotonic loading was slowly applied to specimen. The loading continued until the specimens failed.

3. EXPERIMENTAL RESULTS

3.1 Non-corroded Flexural RC Specimens (NCB-1 and NCB-2)

Cracking loads were between 15-20 kN. Flexural cracks form initially in the constant moment span followed by the formation of shear cracks. Both NCB-1 and NCB-2 collapsed by flexural-compression failure. The loading capacity of NCB-1 and NCB-2 were 145.97 kN and 144.99 kN, respectively. The final crack pattern of NCB-2 is shown in Figure 4.

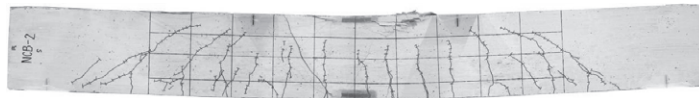


Figure 4: Final crack pattern of non-corroded flexural RC member (NCB-2)

3.2 Corroded Flexural RC Specimens

Three corroded RC specimens with different corrosion lengths were tested under flexure. Slight reductions of ultimate loading capacity were observed in all corroded RC specimens. The ultimate load of FCBNR-I, FCBNR-O, and FCBNR-F were 137.34 kN, 138.52 kN, and 139.4 kN, respectively. The load-deflection relationship of NCB-1, FCBNR-I, FCBNR-O, and FCBNR-F is given in Figure 5. The reduction in ultimate loading capacity is approximately 4.5% to 6% when compared with non-corroded RC specimens. The loss of cross sectional area of tensile reinforcement is a main reason of the lower ultimate loading capacity. It could be observed that the stiffness of all corroded specimen is significantly degraded mainly because bonding between tensile reinforcement and concrete was destroyed. However, final crack patterns of FCBNR-I was very similar to the final crack pattern of non-corroded specimen. In the case

of FCBNR-O specimen, less flexural cracks was observed. The propagation of flexural cracks was also interrupted by the existing longitudinal corrosion cracks (Figure 6b). The final crack pattern was drastically changed in the case of FCBNR-F. Propagation of shear cracks was disturbed by the corrosion crack. As the result, no traditional shear cracks were observable in this case. The shear crack which started from support was trapped by corrosion crack. (Figure 6c); however, this mechanism did not have any significant effect on load carrying capacity of the beam. The absence of shear crack may be the reason why the deflection of FCBNR-F is smaller than that of FCBNR-O at the same load.

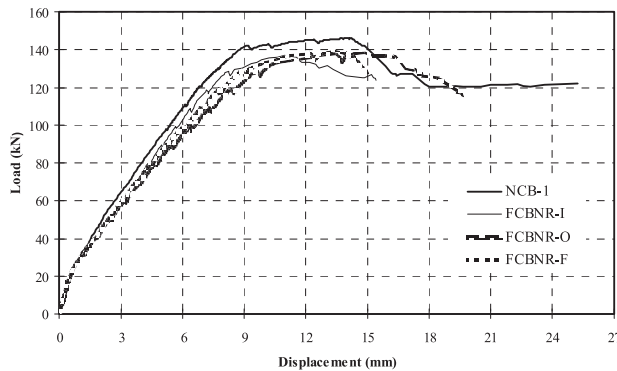


Figure 5: Load – deflection relationship of FCBNR series

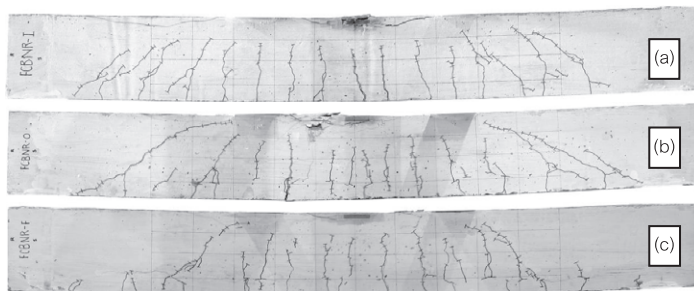


Figure 6: Final crack patterns of FCBNR series; (a) -I, (b) -O, (c) -F

3.3 Specimens Repaired with Polymer Modified Mortar

Figure 7 shows the comparison between the load-deflection relationships of flexural RC specimens repaired with polymer modified mortar and that of non-corroded RC specimen (NCB-1). The specimen with shortest patching area shows very similar structural behavior to the control RC specimen regardless of lower cracking load. The ultimate loading capacity of FCB1R-I, FCB1R-O, and FCB1R-F were 143.42 kN, 143.23 kN, and 139.40 kN, respectively. The stiffness of FCB1R-I is almost same with non-corroded RC specimen (NCB-1). This indicates that the loss of cross sectional area may not significantly affect the drop of stiffness if the bonding is restored by the repairing material. However, the stiffness of FCB1R-O and FCB1R-F was decreasing when load increased, especially beyond 100 kN. This loss of stiffness is caused by the shear cracks as well as the interface failure in shear span.

Figure 8a shows the final crack pattern of FCB1R-I. It was found that the first flexural crack was formed at the interface between polymer modified mortar and base concrete. One additional crack was formed at the middle of repair material. These cracks propagated vertically toward neural axis of the section without any horizontal cracks observable at the interface between repair material and based concrete. The shear crack formation of FCB1R-I is similar to non-corroded RC specimen. In the case of FCB1R-O of which the patching area is 1000 mm, the first flexural cracking took place at the vertical interface between polymer-modified mortar and base concrete although the flexural bending moment is smaller than the middle of the span (Figure 8b). The subsequent crackings within the patching area were observed. When the loading continued, the cracks in the patching show larger crack growth. Discontinuity of the vertical bending cracks at the horizontal interface was observable. The shear crack was subsequently developed in the shear span and there was a clear interface failure caused by the excessive shear force in the interface (Figure 8b). The interface cracks was connected with flexural cracks in repair material and propagated along the vertical interface at the end of patching area subsequently. Later on, additional shear crack (outermost) formed when the load increased and followed by the crushing of concrete in compression zone. The similar interface failure was also observed in FCB1R-F. It was found that the number of shear cracks in shear span increased in this case and there was no formation of larger shear crack at all. This is because the repair interface was extended to the end of the specimen. Final crack pattern of FCB1R-F is shown in Figure 8c.

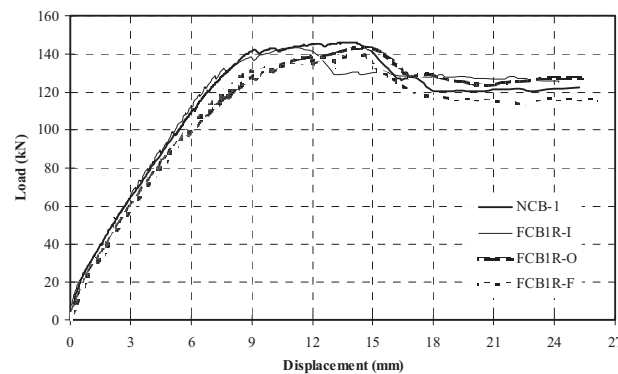


Figure 7: Load – deflection relationship of FCB1R series

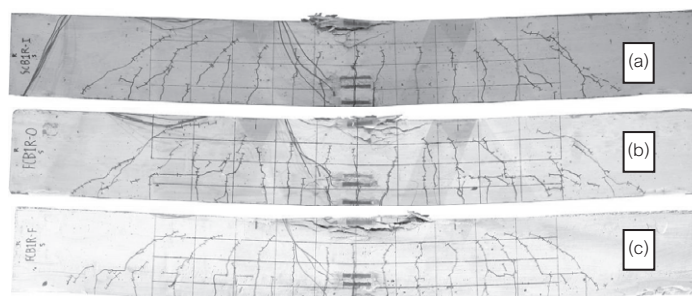


Figure 8: Final cracks pattern of FCB1R series; (a) -I, (b) -O, (c) -F

3.4 Specimens Repaired with Epoxy Based Repair Material

Figure 9 shows the final crack patterns of the specimens repaired with epoxy-based repair material and their load-deflection relationships are given in Figure 10. It should be noted that, before the first cracking, the deflections of NCB and FCB2R-I were smaller than those of FCB2R-O and FCB2R-F under the same load because of the smaller modulus of elasticity of epoxy-based repairing material. The structural behavior of FCB2R-I is very similar with the control RC specimen because the patching area is shorter than the loading span (300 mm). The failure of FCB2R-I was governed by the compression failure of the concrete inside the constant moment span but outside the patching area. Since epoxy-based repairing material applied in this study is very ductile and strong in both tension and bonding. In FCB2R-O and FCB2R-F, the flexural cracks were formed in the base concrete without flexural cracks in the epoxy-based repair material (see Figure 9b and 9c). A good cracking resistance of epoxy-based repair materials contributed to the stiffness of the member. The deflections of NCB and FCB2R-I therefore became larger than the deflections of FCB2R-O and FCB2R-F after flexural cracking. When the load increased, distributed damage at the horizontal interface between epoxy-based repair material and base concrete could be observed in both FCB2R-O and FCB2R-F; however, it was observable that there is still some stress transfer across the interface. The bonding was not completely vanished by these small distributed cracks. At approximately 90 kN, large shear cracks formed in FCB2R-O (Figure 9b) and hence the deflection of FCB2R-O was consequently increased. On the other hand, the formation of a shear crack in FCB2R-F was prevented by the interface between concrete and repair material. As a result, several shear cracks were formed instead of a single large shear crack (Figure 9c). The FCB2R-O failed by crushing of concrete after the shear crack fully propagated while the failure of FCB2R-F was caused by a sudden rupture of epoxy-based material. The maximum loading capacity of FCB2R-I, FCB2R-O, and FCB2R-F were 154.12 kN, 171.77 kN, and 184.53 kN, respectively.

Figure 11 shows the comparison among different RC specimens in the study. All corroded beams show a lower load carrying capacity when compared with non-corroded RC of which the load carrying capacity was approximately 145 kN. Patching repair with polymer-modified mortar was able to slightly improve the load carrying capacity of corroded RC; however, the load carrying capacity after repair is still less than the original capacity of RC. The loss of load carrying capacity is caused mainly by the loss of cross-sectional area of reinforcement. It should be also noted that the load carrying capacity of the RC repaired with polymer-modified mortar reduced when the patching length increased in this study. This may be due to a larger effect of debonding between repairing material and base concrete in specimens with longer patching areas. The most interesting experimental result in this study is that the patching repair with epoxy-based modified mortar can restore or even strengthen the flexural capacity of RC. The flexural capacity was increased up to 27% in the case of full-span patching although there is no replacement of reinforcement. In addition, the ultimate capacity increased when the patching length was longer. By comparing FCB2R-O and FCB2R-F which have the same cross-section in the loading span,

it can be concluded that the ultimate load carrying capacity of RC repaired with epoxy-based repair material is not controlled by the cross section at the maximum moment. The structural behavior of RC is influenced by the stress transfer in the shear span especially in the case that repair material is very ductile.

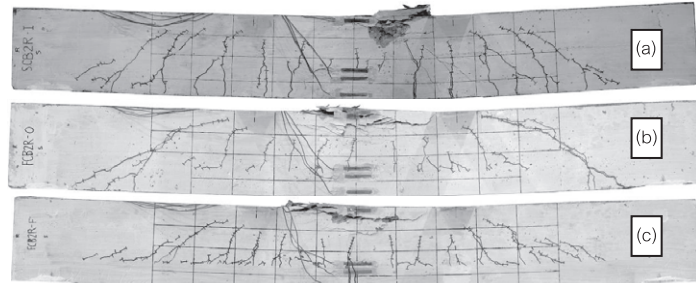


Figure 9: Final cracks pattern of FCB2R series; (a) -I, (b) -O, (c) -F

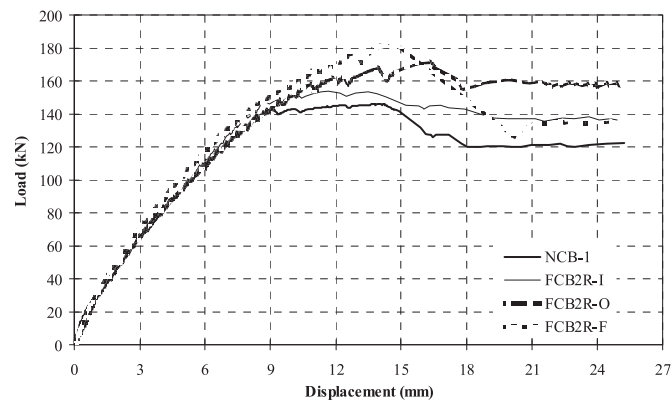


Figure 10: Load – deflection relationship of FCB2R series

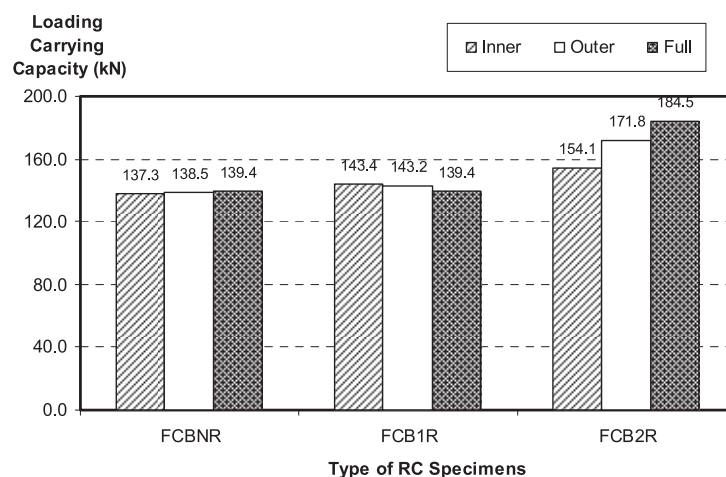


Figure 11: Comparison of Load Carrying Capacity

4. CONCLUSION

Based on experimental observations repaired RC member, major findings can be concluded as follows:

1. The structural behaviors of corroded RC specimens repaired by patching method are different based on both mechanical properties of repairing materials and patching area. However, in all cases, the repairing improves the structural behaviors when compared with corroded RC without repair.
2. When polymer modified mortar is used as a repairing material, the failure of interface between repair materials is very likely to take place in the shear span. The interface failure disturbs the stress distribution in shear span as well as reduces overall stiffness of the repaired RC.
3. Since the epoxy-based repair material is very ductile under tension, the flexural cracking was not observable in the patching area experimentally. The interface failure could also be successfully prevented by a better bonding characteristic which change brittle interface failure into distributed tiny cracks around the interface.
4. The load carrying capacity of RC repaired by epoxy-based repair materials is higher than that of non-corroded RC. And the improvement of load carrying capacity is greater for the longer patching area.

REFERENCES

- Al-Dulaijan, S.U. et al. (2002). "Effect of rebar cleanliness and repair materials on reinforcement corrosion and flexural strength of repaired concrete beams." *Cement & Concrete Composites*, 24, 139-149.
- Almusallam, A.A. (2001). "Effect of degree of corrosion on the properties of reinforcing steel bars." *Construction of Building Materials*, 15, 361-368.
- The International Federation for Structural Concrete (1990). "CEB-FIP Model Code 1990"
- Emmons, P.H. and Vaysburd, A.M. (1996). "System concept in design and construction of durable concrete repairs." *Construction and Building Materials*, 10(1), 69-75.
- JSCE, (2001), "Standard specifications for concrete structures – maintenance." Japan Society of Civil Engineers.
- Nounu, G. and Chaudhary, Z. (1999) "Reinforced concrete repairs in beams." *Construction and Building Materials*, 13, 195-212.
- Shash, A.A. (2005) "Repair of concrete beams – a case study." *Construction and Building Materials*, 19, 75-79.
- Toongoenthong, K. and Maekawa, K. (2005). "Multi-mechanical approach to structural performance assessment of corroded RC members in shear." *Journal of Advanced Concrete Technology*, 3(1), 107-122.
- Uomoto, T. and Misra, S. (1984). "Behavior of concrete beams and columns in marine environment when corrosion of reinforcing bars takes place." *ACI Special publication SP-109*, 127-146

SHAKING TABLE TEST OF TIMBER MASONRY HOUSE MODELS RETROFITTED BY PP-BAND MESHES

NAVARATNARAJAH SATHIPARAN¹, PAOLA MA YORCA²
and KIMIRO MEGURO³

¹The University of Tokyo, Japan

² ICUS, Institute of Industrial Science,
The University of Tokyo, Japan

³ICUS, Institute of Industrial Science,
The University of Tokyo, Japan
sakthi@risk-mg.iis.u-tokyo.ac.jp

ABSTRACT

Unreinforced masonry is one of the most popular construction materials in the world. It is also unfortunately, the most vulnerable against earthquakes. Damage to unreinforced masonry buildings has caused huge number of human casualties historically and during recent earthquakes in developing countries. Therefore, retrofitting of low earthquake-resistant masonry structures is the key issue for earthquake disaster mitigation in developing countries to reduce the casualties significantly. When we propose the retrofitting in developing countries, retrofitting method should respond to the structural demand on strength and/or deformability as well as to availability of material with low cost including manufacturing and delivery, practicability of construction method and durability in each region. Considering these issues of developing appropriate seismic retrofitting techniques for masonry buildings to reduce the possible number of casualties due to future earthquakes in developing countries, a technically feasible and economically affordable PP-band (polypropylene bands) retrofitting technique has been developed and many different aspects have been studied by Meguro Laboratory, Institute of Industrial Science, The University of Tokyo. PP-band is commonly used for packing.

In order to understand the dynamic response of masonry houses with and without PP-band mesh retrofitting, crack patterns, failure behavior, and overall effectiveness of the retrofitting technique, shaking table tests were carried out. In this experimental program, 1/4 scale single box shape room structure with wooden roof models were used. Addition to that, effect of surface plaster on PP-band retrofitted house model also studied.

From the experimental results, it was found that a scaled dwelling model with PP-band mesh retrofitting was able to withstand larger and more repeatable shaking than that without PP band retrofitting, which all verified to reconfirm high earthquake resistant performance. When surface finishing applied above house model, due to improve bond connection between PP-band and brick wall, surface plaster kept well with wall.

1. INTRODUCTION

A real scale model test makes possible to obtain data similar to real structures. However, it requires large size testing facilities and large amount research funds, so it is difficult to execute parametric tests by using full scaled models. Recently, structural tests of scaled models become larger and larger as the overall behavior of the system can be understood from scaled model also. In this experimental program $\frac{1}{4}$ scale models were used to investigate the seismic behavior of masonry houses and effectiveness of PP-band retrofitting technique.

2. EXPERIMENTAL PROGRAM

2.1 Description of the specimens

For shaking table experiment, four models were built in the reduced scale of 1:4 using the unburnt bricks as masonry units and cement, lime and sand (1:2.8:8.5) mixture as mortar with cement/water ratio of 33%. Attention was paid to make the models as true replica of adobe masonry buildings in developing countries in terms of masonry strength even though the construction materials used were those available in Japan.

All the building models dimensions were 933mmx933mmx720mm with 50mm thick walls. The sizes of door and window in opposite walls were 243x485mm² and 325x245mm² respectively.

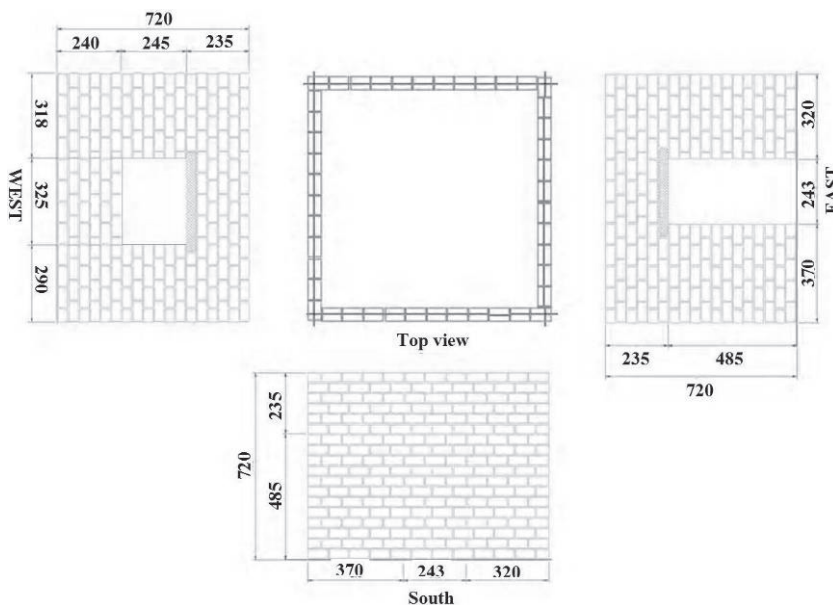


Figure 1: Model dimension (mm)

All specimens consisted of 18 rows of 44 bricks in each layer except openings. Construction process takes place in two days, first 11 rows in first day and remaining rows construct in following day. The geometry, construction materials and mix proportion, construction process and technique and other conditions that may affect the strength of the building

models were kept identical for better comparison. The cross-section of the band used was 6mm×0.32mm and the pitch of the mesh was 40mm.

All four models were represented one-storey box-like building including two models without surface finishing and other two models with surface finishing. This simple geometry and boundary conditions were considered as the data generated will be used for numerical modeling in future.

The specimens were named according to the following convention:

B-R-P-S in which;

B is masonry unit,

A: unburned brick;

R is roof connection type,

4: roof connected to all four walls;

P is retrofitted condition,

NR: non retrofitted

RE: retrofitted;

S is condition of surface finishing applied above masonry house,

X: no surface finishing applied

P: 7.5 mm surface finishing applied;

For surface finishing material mixing ratio as follows; Water: Cement: Sand: Lime = 1.00: 0.14: 2.80: 1.11. Totally two models were retrofitted with PP-band mesh after construction.

Table 1: Mechanical property of masonry specimens

| Specimen | Diagonal shear strength (MPa) | Compression strength (MPa) | Shear strength (MPa) | Bond Strength (MPa) |
|----------|-------------------------------|----------------------------|----------------------|---------------------|
| A-4-NR-X | 0.041 | 4.28 | 0.0057 | 0.0046 |
| A-4-RE-X | 0.045 | 4.36 | 0.0068 | 0.0046 |
| A-4-NR-P | 0.048 | 4.29 | 0.0061 | 0.0050 |
| A-4-RE-P | 0.050 | 4.35 | 0.0056 | 0.0048 |

2.2 Retrofitting Procedure

The procedure presented below is illustrated with photos taken during the experimental program.

- PP-bands arranged in mesh fashion was prepared (because of original purpose of the PP-bands is to serve as packing material, so far PP-band meshes are not produced. we would like to gratefully acknowledge SEKISUI JUSHI CORPORATION for providing the PP-band meshes used in the reported experimental program).
- PP-band mesh was cut in convenient size according to the dimension of the house.
- Straw, which placed in holes are removed (in this experiment, during construction of model house, we placed the straw in where we required a holes. Straw are placed at approximately 200mm pitch. In real case holes can be prepared by drilling through the wall) and the model house walls are cleaned.

- The meshes are installed on both sides of the wall and wrapped around the corner wall edges. An overlapping length of approximately 300mm is recommendable.
- Wire is passed through the holes and used to connect the meshes on the both wall sides. In order to prevent the wires cutting the PP-bands, aluminum plates (20mm×20mm) were placed between the band and the wire. Initially, fixing the meshes with connectors along the wall and at the foundation is recommendable.
- Connecting inner and outer meshes by wires and aluminum plates except around the openings.
- Fixed connectors around the openings after the mesh was cut and overlapped on the other side.

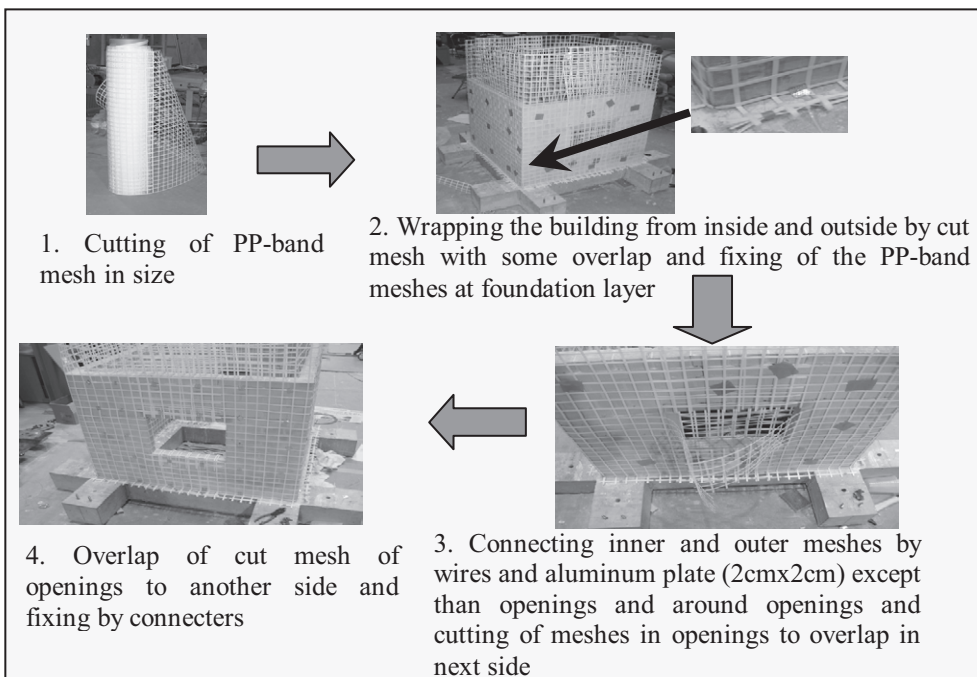


Figure 2: Retrofitting process by PP-band

2.3 Input motion

Simple easy-to-use sinusoidal motions of frequencies ranging from 2Hz to 35 Hz and amplitudes ranging from 0.05g to 1.4g were applied to obtain the dynamic response of both retrofitted and non-retrofitted structures. This simple input motion was applied because of its adequacy for later use in the numerical modeling. Figure 3 shows the typical shape of the applied sinusoidal wave.

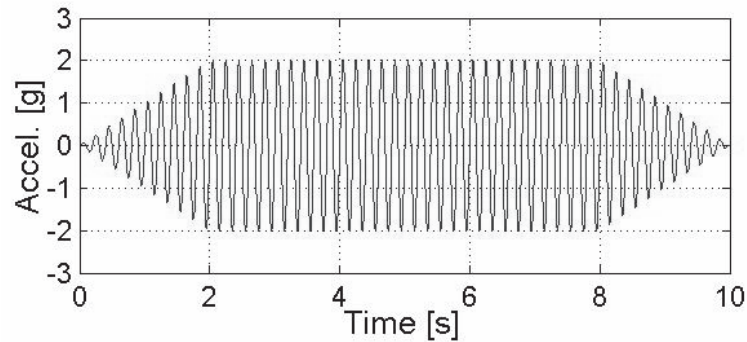


Figure 3: Typical Shape of Input Sinusoidal Motion

Loading was started with a sweep motion of amplitude 0.05g with all frequencies of 2Hz to 35Hz for identifying the dynamic properties of the models. The numbers in table 2 indicate the run numbers. General trend of loading was from high frequency to low frequency and from lower amplitude to higher amplitude. Higher frequencies motions were skipped towards the end of the runs.

Table 2: Loading Sequence

| Amplitude | Frequency | | | | | | | |
|-----------|-----------|-----|------|------|------|------|------|------|
| | 2Hz | 5Hz | 10Hz | 15Hz | 20Hz | 25Hz | 30Hz | 35Hz |
| 1.4g | | 50 | | | | | | |
| 1.2g | 54 | 49 | | | | | | |
| 1.0g | | 48 | | | | | | |
| 0.8g | 53 | 47 | 43 | 40 | 37 | 34 | 31 | 28 |
| 0.6g | 52 | 45 | 42 | 39 | 36 | 33 | 30 | 27 |
| 0.4g | 51 | 44 | 41 | 38 | 35 | 32 | 29 | 26 |
| 0.2g | 46 | 25 | 24 | 23 | 22 | 21 | 20 | 19 |
| 0.1g | 18 | 17 | 16 | 15 | 14 | 13 | 12 | 11 |
| 0.05g | 10 | 09 | 08 | 07 | 06 | 05 | 04 | 03 |
| sweep | 01,02 | | | | | | | |

3. CRACK PATTERN AND FAILURE BEHAVIOR

3.1 Models A-4-NR-X & A-4-RE-X

In both specimens, due to shrinkage, some minor cracks were observed before the test. These cracks mainly appear closer to opening in horizontal direction.

For non-retrofitted specimen (A-4-NR-X) up to Run 21, no major crack was observed. Major cracks were observed closer to openings from Run 23. At run 28, crack was observed at one of the top corner of the door opening and it propagates up to top layer of the wall. After that, cracks widened with each successive run. At run 44, there were large amount cracks observed in walls in the direction of shaking. Exciting cracks widened and connection between adjacent walls was become weak. In case of walls perpendicular to shaking direction, top part of the east wall (part, above the door opening) was totally separated from the specimen. It was

removed from specimen before next test run proceed. At run 45, all top part of the wall with opening was totally separated from the specimen. It was fallen from specimen. Now the roof only supported by two walls, which were in the direction of shaking. Therefore, due to walls subjected to out-of-plane load; they were bursts outwards in shaking direction. This finally led to the structure collapse.

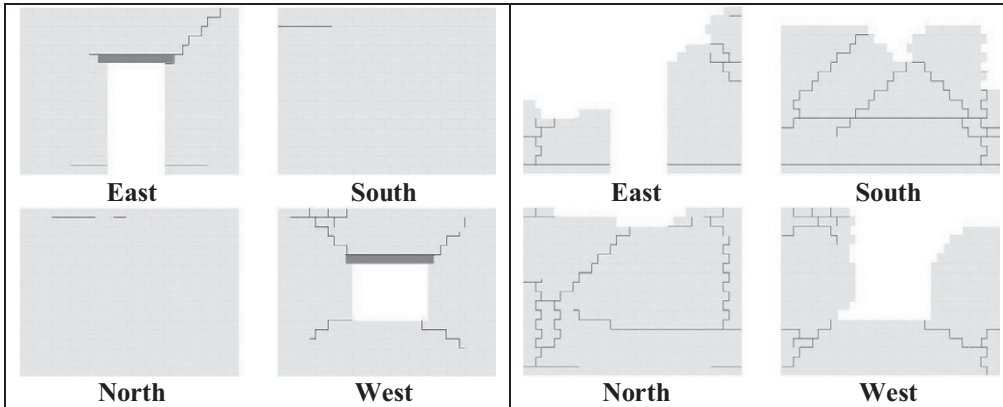


Figure 4: Crack pattern after Run 28 (left) and after run 45(right) for specimen A-4-NR-X

For retrofitted specimen (A-4-RE-X) up to run 21, no major crack was observed in this model. Major cracks were observed closer to openings from Run 25. After those new cracks appear in each run and cracks widened with each successive run, thus, extensive cracking was observed. Although the PP-band mesh kept the structure integral during the shaking, it allowed the sliding of the bricks along these cracks to some extent. In later stages, there was significant permanent deformation of the structure. At the final stage of the test, run 52, with 37.3mm base displacement, 6 times more than the input displacement applied in run 45 and 2.5 times more velocity, virtually all the brick joints were cracked and the building had substantial permanent deformations. However, building did not loose the overall integrity as well as stability and collapse was prevented in such a high intensity of shaking.

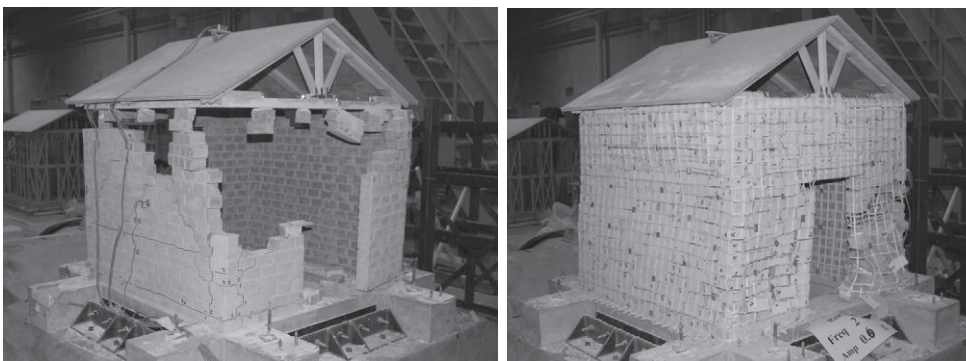


Figure 5: Specimen A-4-NR-X after run 45 (left)
Specimen A-4-RE-X after run 52 (right)

3.2 Models A-4-NR-X & A-4-RE-X

For specimen A-4-NR-P, at run 26, major cracks were observed close to connection between roof and south wall. At run 43, lot of damage observed in the modal. Separation between east wall and its adjacent walls was observed. Also lot of surface finishing separated from the walls. At run 44, Top corner of the east wall and its adjacent walls was totally separated from specimen. At run 45, all the top part of the north and south walls was totally separated from specimen. Now roof only supported by two walls, which are in the perpendicular direction of shaking. This finally led to the structure collapse at run 47 (Figure 6).



Figure 6: Specimen A-4-NR-P after run 47

In case of the retrofitted model A-4-RE-P, similar cracks as non-retrofitted building started from top corner of the south wall in the run 33. After that, the process of widening of the cracks occurred and propagation of new cracks continues until the run 50. Although at the end of 50th run almost cracks observed in entire walls, the specimen did not lose stability. Some bricks from bottom part of east wall were spilled out from PP-band mesh. Therefore some looseness was observed in bottom part of the wall. Even this very high input motion, most of the surface finishing still attached with walls.

At the final stage of the test, run 54, with 74.6 mm base displacement, 9 times more than the input displacement applied in run 47 and 3.7 times more velocity, virtually all the brick joints were cracked and the building had substantial permanent deformations. However, building did not lose the overall integrity as well as stability and collapse was prevented in such a high intensity of shaking. Thus, PP-band retrofitting technique maintained the integrity of the structural elements. Further, the retrofitted model showed the better energy dissipation mechanism as many new cracks were propagated without losing the overall integrity and stability of the structure.

When we applied the surface finishing to house model, due to improve bond connection between PP-band and brick wall, surface plaster kept well with wall. This is not observed in non-retrofitted model. Because of this,

brick unit confined effect inside the PP-band mesh is improved and it improves the overall earthquake resistant performance.

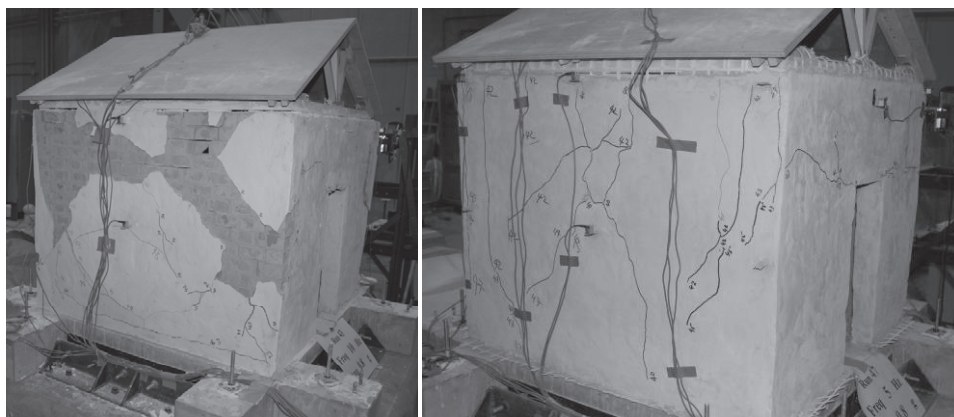


Figure 7: Specimen A-4-NR-P after run 43 (left)
Specimen A-4-RE-P after run 48 (right)

4. PERFORMANCE EVALUATION

The performances of the models were assessed based on the damage level of the buildings at different levels of shaking. Performances were evaluated in reference to five levels of performances: light structural damage, moderate structural damage, heavy structural damage, partially collapse, and collapse.

Table 3: Damage categories

| Category | Damage extension |
|--------------------------------|--|
| D0: No damage | No damage to structure |
| D1: Light structural damage | Hair line cracks in very few walls. The structure resistance capacity has not been reduce noticeably. |
| D2: Moderate structural damage | Small cracks in masonry walls, falling of plaster block. The structure resistance capacity is partially reduced. |
| D3: Heavy structural damage | Large and deep cracks in masonry walls. Some bricks are fall down. Failure in connection between two walls. |
| D4: Partially collapse | Serious failure of walls. Partial structural failure of roofs. The building is in dangerous condition |
| D5: Collapse | Total or near collapse |

The Japan Meteorological Agency seismic intensity scale (JMA) is a measure used in Japan to indicate the strength of earthquakes. Unlike the Richter magnitude scale (which measures the total magnitude of the earthquake, and represents the size of the earthquake with a single number) the JMA scale describes the degree of shaking at a point on the Earth's surface.

The JMA scale was colored according to the following convention:

| | | | | | | |
|-------|--------|--------|--------|--------|--------|-------|
| Index | JMA ~4 | JMA 5- | JMA 5+ | JMA 6- | JMA 6+ | JMA 7 |
|-------|--------|--------|--------|--------|--------|-------|

Table 4 shows the performances of non retrofitted model A-4-NR-X and retrofitted model A-4-RE-X with different JMA intensities. Partial collapse of the non-retrofitted building was occurred at the 44th run at intensity JMA 5-. The retrofitted building performed moderate structural

damage level at 45th run at which the non-retrofitted building was partially collapsed. Moreover, moderate structural damage level of performance was maintained until 50th run, leading to intensity JMA 6-. As the model was already considerably deformed beyond the limit of measurement system, test was stopped after the 52nd run. It should be noted again that this model survived 7 more shakings in which many runs were with higher intensities than JMA 5- at which the non-retrofitted building was collapsed before reaching to the final stage at the 52nd run.

Table 4: Performance of A-4-NR-X and A-4-RE-X

| Performance of A-4-NR-X model | | | | | | | | | Performance of A-4-RE-X model | | | | | | | | |
|-------------------------------|----------------|---|----|----|----|----|----|----|-------------------------------|----------------|----|----|----|----|----|----|----|
| Acceleration (g) | Frequency (Hz) | | | | | | | | Acceleration (g) | Frequency (Hz) | | | | | | | |
| | 2 | 5 | 10 | 15 | 20 | 25 | 30 | 35 | | 2 | 5 | 10 | 15 | 20 | 25 | 30 | 35 |
| 1.4 | | | | | | | | | 1.4 | | D2 | | | | | | |
| 1.2 | | | | | | | | | 1.2 | | D2 | | | | | | |
| 1.0 | | | | | | | | | 1.0 | | D2 | | | | | | |
| 0.8 | | | | D3 | D2 | D2 | D2 | D2 | 0.8 | | D2 | D2 | D2 | D2 | D2 | D1 | D1 |
| 0.6 | | | D4 | D3 | D2 | D2 | D2 | D2 | 0.6 | | D4 | D2 | D2 | D2 | D2 | D1 | D1 |
| 0.4 | | | D4 | D3 | D2 | D2 | D2 | D2 | 0.4 | | D3 | D2 | D2 | D2 | D2 | D1 | D1 |
| 0.2 | | | D3 | D1 | D1 | D1 | D1 | D0 | 0.2 | | D2 | D1 | D1 | D1 | D1 | D1 | D1 |
| 0.1 | | | D0 | D0 | D0 | D0 | D0 | D0 | 0.1 | | D1 | D1 | D1 | D1 | D0 | D0 | D0 |
| 0.05 | | | D0 | D0 | D0 | D0 | D0 | D0 | 0.05 | | D0 |

Table 5 shows the performances of non retrofitted model A-4-NR-P and retrofitted model A-4-RE-P with different JMA intensities. Total collapse of the non-retrofitted building was occurred at the 47th run at intensity JMA 5+. The retrofitted building performed moderate structural damage level at 47th run at which the non-retrofitted building was partially collapsed. Moreover, moderate structural damage level of performance was maintained until 48th run, leading to intensity JMA 6-. It should be noted again that this model survived 7 more shakings in which many runs were with higher intensities than JMA 5+ at which the non-retrofitted building was collapsed before reaching to the final stage at the 54th run.

Table 5: Performance of A-4-NR-P and A-4-RE-P

| Performance of A-4-NR-P model | | | | | | | | | Performance of A-4-RE-P model | | | | | | | | |
|-------------------------------|----------------|---|----|----|----|----|----|----|-------------------------------|----------------|----|----|----|----|----|----|----|
| Acceleration (g) | Frequency (Hz) | | | | | | | | Acceleration (g) | Frequency (Hz) | | | | | | | |
| | 2 | 5 | 10 | 15 | 20 | 25 | 30 | 35 | | 2 | 5 | 10 | 15 | 20 | 25 | 30 | 35 |
| 1.4 | | | | | | | | | 1.4 | | D3 | | | | | | |
| 1.2 | | | | | | | | | 1.2 | | D4 | D3 | | | | | |
| 1.0 | | | | | | | | | 1.0 | | D2 | | | | | | |
| 0.8 | | | D5 | D3 | D3 | D2 | D2 | D1 | 0.8 | | D4 | D2 | D2 | D2 | D1 | D1 | D0 |
| 0.6 | | | D5 | D3 | D2 | D2 | D2 | D1 | 0.6 | | D3 | D2 | D2 | D1 | D1 | D0 | D0 |
| 0.4 | | | D4 | D3 | D2 | D2 | D1 | D1 | 0.4 | | D3 | D2 | D2 | D1 | D1 | D0 | D0 |
| 0.2 | | | D5 | D0 | D0 | D0 | D0 | D0 | 0.2 | | D2 | D0 | D0 | D0 | D0 | D0 | D0 |
| 0.1 | | | D0 | D0 | D0 | D0 | D0 | D0 | 0.1 | | D0 |
| 0.05 | | | D0 | D0 | D0 | D0 | D0 | D0 | 0.05 | | D0 |

6. CONCLUSION

Four adobe masonry building models, identical in terms of masonry strength and geometry were constructed and two models were retrofitted with an easy-to-install and economic retrofitting technique. Models were tested on shaking table by applying similar input motions. Dynamic behaviors of the models were studied. Cracks patterns were analyzed and failure behavior and performances were evaluated.

- Shaking table test showed that; a scaled dwelling model with PP-band mesh retrofitting is able to withstand larger and more repeatable shaking than that without PP band retrofitting, which all verified to reconfirm high earthquake resistant performance.
- When we applied the surface finishing to house model, due to improve bond connection between PP-band and brick wall, surface plaster kept well with wall. This is not observed in non-retrofitted model. Because of this, brick unit confined effect inside the PP-band mesh is improved and it improves the overall earthquake resistant performance.

From the experimental results, it was found that this retrofitting technique can enhance safety of both existing and new masonry buildings even in worst case scenario of earthquake ground motion like JMA 7 intensity. Therefore proposed method can be one of the optimum solutions for promoting safer building construction in developing countries and can contribute earthquake disaster in future.

REFERENCE

- Sathiparan, N., 2008. *Experimental Study on PP-Band Mesh Seismic Retrofitting for Low Earthquake Resistant Masonry Houses*, Ph.D. Dissertation, The University of Tokyo, Japan.
- Mayorca, P., 2003. *Strengthening of Unreinforced Masonry Structures in Earthquake Prone Regions*, Ph.D. Dissertation, The University of Tokyo, Japan.
- T.Okada, F.Kumazawa, S.Horiuchi, M.Yamamoto, A.Fujioka, K.Shinozaki, Y.Nakano, *Shaking Table Tests of Reinforced Concrete Small Scaled Model Structures*, Bull. ERS, No.22 (1989).
- Roko Zarnic, Samo Gostic, Adam J. Crewe and Colin A.Taylor, *Shaking Table Tests of 1:4 Reduced Scale Models of Masonry Infilled Reinforced Concrete Frame Buildings*, Earthquake Engineering and Structural Dynamics. 2001, Vol.30, 819-834.
- Alidad Hahemi and Khalid M.Mosalam, *Shake-table Experiment on Reinforced Concrete Structure Containing Masonry Infill Wall*, Earthquake Engineering and Structural Dynamics. 2006, Vol 35, 1827-1852.

RELATION BETWEEN STRENGTH REDUCTION AND DUCTILITY DEMAND FOR PP-BAND MESH RETROFITTED HOUSES

PAOLA MAYORCA and KIMIRO MEGURO
International Center for Urban Safety Engineering
Institute of Industrial Science, the University of Tokyo
paola@iis.u-tokyo.ac.jp

ABSTRACT

Most earthquake related fatalities in developing countries are due to the collapse of seismically weak adobe/masonry structures. It is, thus, urgent to improve their seismic performance in order to reduce future casualties and to protect the existing housing stock. Inexpensive and easy to implement technical solutions, such as retrofitting by PP-band meshes, are desirable to promote the strengthening of weak houses. These bands, commonly used for packing, are resistant, inexpensive, durable and worldwide available.

Experiments and advanced numerical simulations have shown that PP-band meshes can dramatically increase the seismic capacity of adobe/masonry houses. Although a simple design method has been outlined, there are still some points to be clarified in order to apply it. One of this is the relation between strength reduction factor and ductility demand. Generally, the structures targeted for PP-band retrofitting are very weak and therefore, strength reduction is high. Although retrofitting by PP-band can provide large ductility reserve, too large deformations may result in second order effects which could trigger the structure instability and collapse.

In this paper, the relation between strength reduction factor and ductility demand of PP-band mesh retrofitted houses is discussed.

1. INTRODUCTION

Collapse of weak adobe/masonry houses is responsible for most of the fatalities due to earthquakes in developing countries. Furthermore, the consequent property losses are a threat to the sustainable development of these regions. The only way to change this situation is to increase the seismic resistance of the existing housing stock. Because people living in this type of structures have limited resources, inexpensive and easy to implement solutions are necessary. Retrofitting by polypropylene band (PP-band) meshes satisfies these requirements. These bands commonly used for packing are resistant, inexpensive, durable and worldwide available.

PP-band meshes are wrapped on both sides of the walls and attached with wire connectors. After meshes are installed the wall is plastered with either mud, in case of adobe houses, or mortar, in case of brick structures. This cover protects the meshes from the ultraviolet radiation and other external agents, fills any gaps that may be left between the mesh and the wall after its installation, improves the bond between mesh, mortar, and wall, and gives a good appearance to the retrofitted structure.

Experiments and numerical simulations have shown that PP-band meshes improve the seismic performance of otherwise poor earthquake resistant adobe/masonry houses. This is mainly achieved by increasing the structure ductility and energy dissipation capacities. Under moderate ground motions, PP-band meshes provide enough seismic resistance to guaranty limited and controlled cracking of the retrofitted structures. Under extremely strong ground motions, they are expected to prevent or delay the collapse, thus, increasing the survival ratio.

Although a simple design method has been outlined, there are still some points to be clarified in order to apply it. One of this is the relation between strength reduction factor, R_d , and ductility demand, μ_{dem} . In this paper, the proposed design method is briefly introduced and then the R_d - μ_{dem} relation discussed. Issues requiring further study are also pointed out.

2. PROPOSED DESIGN METHODOLOGY

The scope of the design methodology proposed hereinafter is 1-story adobe/masonry houses with flat roofs. Structures with vault/dome roofs are not considered. Figure 1 shows the flowchart of the proposed retrofitting design. The process can be summarized as follows:

1. Determine the original structure strength, V_c , and natural period, T .
2. Calculate the elastic base shear, V , according to the regional seismic code.
3. From the relation between V and V_c , estimate the strength reduction factor, R_d .
4. Choose a certain PP-band mesh density, D , and determine the ductility demand, μ_{dem} , from the μ_{dem} versus R_d graph, and also the maximum displacement, $\Delta_{max} = \mu_{dem} \times$ first cracking displacement.
5. Assess Δ_{max} .
If Δ_{max} is acceptable, proceed with out-of-plane verification.
If Δ_{max} is unacceptable, reduce the μ_{dem} . Repeat the calculation.
6. Verify that out-of-plane deformations do not cause instability

Determining the properties of existing structures is not easy especially for adobe/masonry houses due to their low quality and great variability. Because these structures are stiff compared to the PP-band stiffness, their initial natural period does not change after retrofitting. Furthermore, experiments have shown that PP-band meshes do not increase the structure strength before cracking. Therefore, it can be assumed that the retrofitted structure will have the same V_c and T as the original, unreinforced, house.

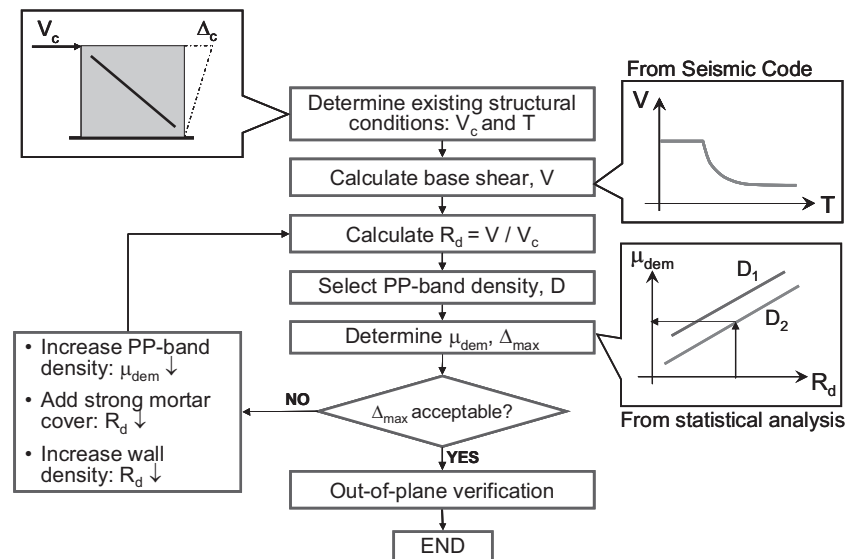


Figure 1: Flowchart of the proposed design methodology

The expected R_d will be fairly high due to the relatively low resistance of the adobe/masonry houses. The higher the reduction factor, the larger the ductility demand will be, as shown schematically in Figure 1. Intuitively the larger the PP-band mesh density, the less μ_{dem} for the same R_d .

Large deformations and controlled damage are anticipated in PP-band mesh retrofitted structures. Therefore, the most important points to check in the design are maximum displacements at the corners (maximum acceptable displacement associated with in-plane actions) and the wall body (out-of-plane verification). Secondary order effects should be avoided. Excessive out-of-plane wall deformations will reduce their in-plane resistance capacity.

If displacements due to in-plane actions are unacceptable, μ_{dem} should be reduced. This can be achieved by increasing the PP-band density. Another solution is to reduce R_d by adding a strong mortar cover, i.e. increasing V_c , or providing additional walls so that the demand on each of them is lower. The latter, however, is more expensive and probably difficult to accept by the house owner. In either case, there will be an increase in mass and as a result V needs to be recalculated.

3. STRENGTH REDUCTION VERSUS DUCTILITY DEMAND

As mentioned in the previous section, the relation between R_d and μ_{dem} for different PP-band mesh densities is needed to estimate the maximum displacement that the structure will experience. In order to develop a simple relation between these two parameters, non-linear time history analyses of several structures subjected to various strong ground motions were carried out.

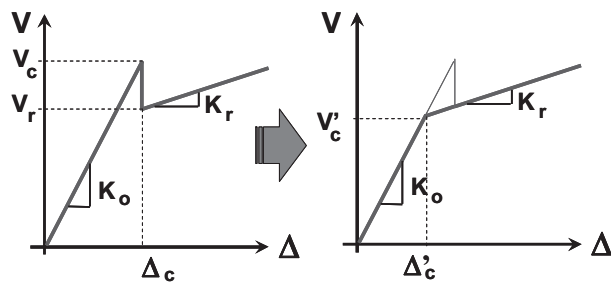


Figure 2: Idealization of shear force versus lateral deformation for a wall retrofitted with PP-band mesh

3.1 Parametric study conditions

Static monotonic tests have shown that the shear force – lateral deformation curve of a PP-band retrofitted walls can be roughly idealized as shown in the left curve of Figure 2. V_c and Δ_c correspond to the shear strength and cracking deformation of the original wall whereas V_r and K_r correspond to the residual strength and stiffness after the wall cracking. The first two parameters are mainly dependent on the masonry itself, V_r depends on both masonry and PP-band mesh and K_r depends mostly on PP-band. Under cyclic loading, the skeleton curve resembles the monotonic one with a gradually decreasing unloading stiffness.

To model the retrofitted adobe/masonry structures, the skeleton curve was further idealized as shown on the right side graph of Figure 2. Additionally, the hysteresis was represented with a Modified Clough model with unloading degrading stiffness. Two additional parameters to control the later decay are necessary. In total, the model is completely defined with five parameters. The comparison between the force deformation curve obtained with experiments and the proposed model is discussed elsewhere (Mayorca and Meguro, 2008)

A total of 144 strong ground motion records were considered. All of them were recorded at sites with average shear wave velocities higher than 180 m/s in the upper 30 m of the soil profile. In all the cases, the peak ground acceleration (PGA) was larger than 0.1g and they were recorded on free field or the first floor of low-rise buildings. All the records have high frequency contents below 0.4s. The natural period of 1-story adobe/masonry structures fall in this range.

Four structures with mechanical properties representing single story adobe/masonry houses and three different weight roofs as detailed in Table 1 were considered. The parameters were chosen so as to represent one of the two main walls of a 3m-high, 3m-long, 1-story adobe/brick house. In all the cases, V_r/V_o was considered equal to 0.75, a value which experiments have shown is relatively easy to achieve by tightly attaching an adequate volume of PP-band mesh.

Table 1: Structures considered for the study

| Structure type | V_c [kN] | K_o [kN/mm] | K_r/K_o | Mass [$\times 10^3$ kg] |
|----------------|------------|---------------|-------------|--------------------------|
| Adobe | 35 | 10 | 0.00, -0.02 | 8.70, 12.75, 17.25 |
| Brick | 100 | 50 | 0.00, -0.02 | 8.70, 12.75, 17.25 |

3.2 Results and discussion

Figure 3 show the force-deformation curves of two groups of structures, with different roofs, subjected to the same strong ground motion record. Because the adobe structure has lower strength, the ductility demand is larger. Structures with heavier roofs experience larger inertial forces and therefore larger ductility demands.

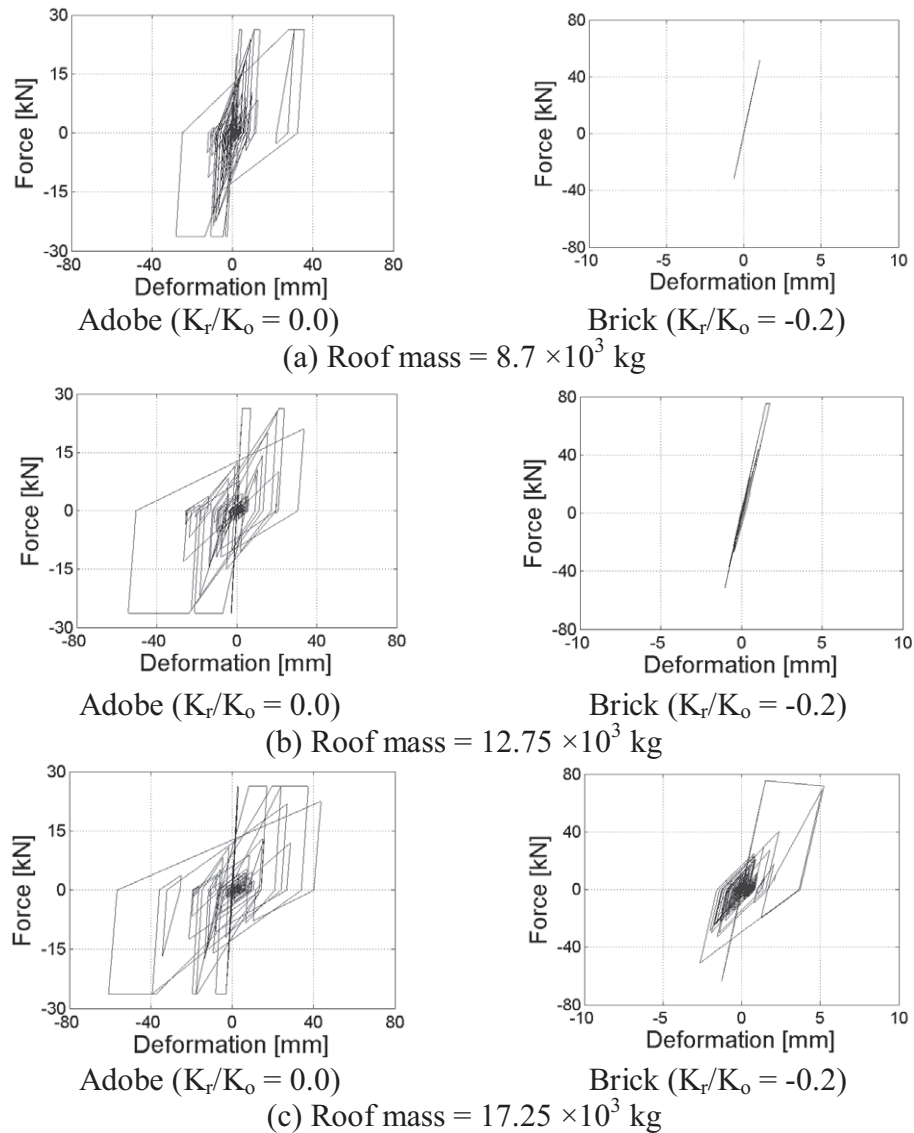


Figure 3: Results of the nonlinear analysis, input motion: Northridge Eq., Station USGSVA 637

For all the records and structures analyzed, μ_{dem} and R_d were determined and plotted as shown in Figures 4 and 5. Maximum R_d for adobe and masonry structures were 10.9 and 3.4, respectively. The values of μ_{dem} were 41.5 and 23.6 in the same cases. Regression functions were determined for each group as shown in Table 2 and are shown in thick lines in Figures 4 and 5. In general, the results are scattered, especially for adobe structures. For instance, for R_d equal to 3, μ_{dem} ranges from 2 to 35, if $K_r/K_o=0$, and from 2 to 20, if $K_r/K_o=-0.2$.

Table 2: Regression functions obtained for each of the group structures considered in the study

| Structure type | K_r/K_o | Regression function | R^2 |
|----------------|-----------|--|-------|
| Adobe | 0.00 | $\mu_{dem} = 1.0018 \times R_d^{1.4539}$ | 0.620 |
| | -0.02 | $\mu_{dem} = 1.0121 \times R_d^{1.4873}$ | 0.630 |
| Brick | 0.00 | $\mu_{dem} = 1.0247 \times R_d^{1.5359}$ | 0.66 |
| | -0.02 | $\mu_{dem} = 0.9905 \times R_d^{1.6512}$ | 0.71 |

The large scatter does not seem to be caused by the post-peak softening behavior of the structure. Groups with different values of K_r/K_o give similar scattered results. Nor does it seem to be caused by the used strong ground motion records, which have similar characteristics. Additional evaluation of the model used is necessary to grasp the causes of the dispersed results.

Even though the results require further evaluation, a few conclusions may be drawn. For instance, it seems that the factor K_r/K_o does not affect considerably the maximum displacements experienced by the structure. Initial and residual strengths (V_o, V_r) are more important as suggested in previous studies. Also, for R_d values lower than 9, μ_{dem} may be considered at most 9 for adobe structures. For masonry, a μ_{dem} of at most 5, may be expected for R_d up to 4.

A more comprehensive statistical analysis, considering more strong ground motion records and structures with larger R_d is required to reach to a final expression of μ_{dem} as a function of R_d .

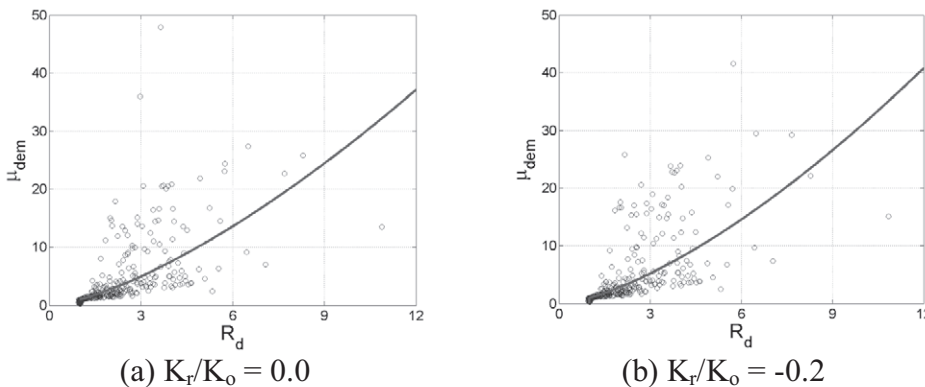


Figure 4: Strength reduction versus ductility demand for adobe structures

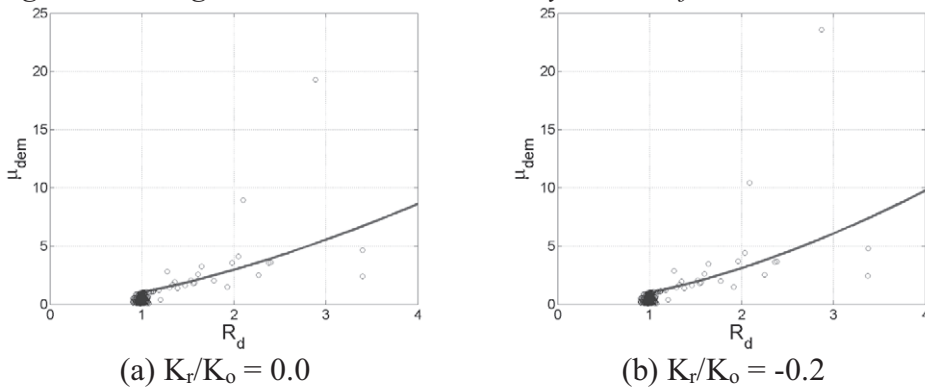


Figure 5: Strength reduction versus ductility demand for masonry structure

4. MAXIMUM ACCEPTABLE DISPLACEMENT AND OUT-OF-PLANE VERIFICATION

A maximum acceptable displacement or drift should be defined to guaranty the structure stability. Material tests have shown that PP-band retrofitted walls under in-plane loads can tolerate very large drifts, in the order of 10% or more, without losing their in-plane resistance capacity. However, such large deformations along the plane of certain walls will cause excessive out-of-plane deformations on the walls perpendicular to them. If a structural wall is excessively damaged by out-of-plane actions, its ability to resist in-plane forces will be reduced.

There are two ways to take into account the interaction of the in-plane and out-of-plane actions on the wall in the design. One is to reduce the in-plane resistance with a penalty factor which should be a function of the maximum out-of-plane displacement. Although presently this point is under study, so far there is no model to determine what factor would be appropriate. Another way is to limit the maximum acceptable displacement to a conservative low value. Although more analyses and calculations are required to determine the most appropriate value, at this point, it is recommended to set it as a half of the wall thickness so that the resultant of vertical loads on the wall (under out-of-plane actions) always falls within the limits of the wall base.

The maximum acceptable displacement discussed in the previous paragraphs corresponds to the drift of the walls under in-plane actions or in other words, to the displacement of the walls subjected to out-of-plane actions at their side borders. If the unsupported length of the walls under out-of-plane actions is too long, the center of the walls may be subjected to considerable larger displacements perpendicular to their plane. Presently, a model to determine the displacements due to out-of-plane seismic actions for PP-band retrofitted walls is being developed.

Experiments have shown that attaching the PP-band mesh so that it is wrapped around the roof frame can greatly contribute to control out-of-plane displacements. Whenever possible, it is recommended to install the mesh in this way. Another solution to limit out-of-plane displacements in walls with large length/height ratio is to provide intermediate supports by means of pilasters well attached to the wall with PP-band meshes.

5. CONCLUSIONS

A methodology to design 1-story, flat roof, adobe/masonry houses with PP-band meshes was briefly introduced and the $R_d-\mu_{dem}$ relation, necessary for it, discussed. Although a final formulation for this relation is not proposed yet, some conclusions were drawn from the statistical non-linear time history analysis. Maximum lateral drift and out-of-plane deformations were also discussed and remaining issues to be addressed pointed out. It is important to keep in mind that the outlined design procedure is just one step towards the development of a simple set of rules of thumb than can be used in the field for determining the most appropriate PP-band mesh arrangement for each particular situation.

Permanent displacements are expected when PP-band mesh retrofitted structures are subjected to strong ground motions. If these are too large, the remaining structure may be either unusable or too expensive to repair. This information is very important to assess the suitability of PP-band mesh retrofitting, taking into account initial investment and eventual reparation costs. A procedure to evaluate permanent displacements of PP-band mesh retrofitted structures will be investigated in the future.

REFERENCES

- Guragain, R., Mayorca P., Kawin W., and Meguro K. 2006. *Simulation of brick masonry wall behavior under in-plane cyclic loading using applied element method*, Proc. of the 8th International Summer Symposium of JSCE, pp. 55-58.
- Mayorca, P., Sathiparan, N., Guragain, R., Nesheli, N., and Meguro, K. 2006. *Seismic Behavior of Masonry Houses Retrofitted with PP-Band Meshes Evaluated through Shaking Table Tests*, Proc. of the 1st European Conference on Earthquake Engineering and Seismology, Geneva, Switzerland, CD-ROM.
- Mayorca, P. and Meguro, K. 2008. *A Step Towards the Formulation of a Simple Method to Design PP-Band Mesh Retrofitting for Adobe/Masonry Houses*, Proc. of the 14th World Conference on Earthquake Engineering, Beijing, China.
- Miranda, E. 2000. *Inelastic displacement ratios for structures on firm sites*, Journal of Structural Engineering, Vol. 126, No. 10.
- Sathiparan, N., Mayorca, P., Nesheli, N., Guragain, R., and Meguro, K. 2005. *In-plane and Out-of-plane behavior of PP-band retrofitted masonry wallettes*. Proc. of the 4th International Symposium on New Technologies for Urban Safety of Megacities in Asia, Singapore.
- Pacific Earthquake Engineering Research (PEER) Center Strong Ground Motion Database, peer.berkeley.edu/smcat/

STRENGTH AND DURABILITY CONSIDERATION OF BRICK AGGREGATE CONCRETE CONTAINING FLY ASH

M. A. NOOR and A. R. KAOSER
Bangladesh University of Engineering and Technology, Dhaka 1000,
Bangladesh
mnoor@ce.buet.ac.bd

ABSTRACT

The result of a study on the properties of concrete made of burnt clay aggregate instead of crushed stone aggregate containing fly ash is presented herein. In subcontinent this burnt clay aggregate concrete, popularly known as brick aggregate concrete, is very popular in the concrete construction industry due to economic reasons. Mainly hardened properties are reported. Concrete were made by weight using both CEM I cement and CEM I with different percentage of fly ash in it. Locally available natural river sand popularly known as Sylhet sand was used. Mixtures were proportioned to have similar slump and constant powder content. Fly ash content ranging from 0 to 30 percent by weights of CEM I was used. Water to powder ratio ranging from 0.4 to 0.5 by weight was used. Comparison was also made with the concrete made of natural crushed stone aggregate. It is shown that concrete containing fly ash is more durable. It is also shown that brick aggregate concrete is less durable than crushed stone concrete. Laboratory specimens tested for compressive strength, sulfuric acid degradation, chloride penetration, are presented.

1. INTRODUCTION

The use of fly ash as a component in concrete is now extremely common in Bangladesh and elsewhere. Fly ash used in concrete for reasons including economics, improvements and reduction in temperature rise in fresh concrete, workability and contribution to durability and strength in hardened concrete. Fly ash makes efficient use of the products of the hydration of Portland cement. Solution of calcium and alkali-hydroxide, which exist in the pore structure of the cement paste and the heat, generated by hydration of Portland cement, an important factor in initiating the reaction of the fly ash. It is well known that the properties of concrete are closely related to its microstructure and products of hydration (Jiang, 1998; Ramachandran et. el., 1981; Ben-Bassat et. el., 1990). The microstructure and products of hydration of concrete depend on its reaction and progress of hydration. It is important to know about the characteristics of hydration in fly ash concrete binder.

Chloride diffusion is largely concerned when durability is considered. The chloride-induced corrosion can cause significant deterioration of

reinforced concrete structures, resulting in costly repair (Berke et. el., 1988). The water powder ratio is an important control parameter in concrete mix proportioning. The properties controlled by w/p ratio in conventional concrete, are workability and durability. Soluble sulfates which exist in soils, ground waters and sewage waste corrode and eventually destroy Portland cement concrete unless it is designated with fly ash to maximize sulfate resistance. In recent years, it has become evident that some fly ashes increase the sulfate resistance of concrete while other fly ashes encourage the deterioration of concrete in a sulfate environment. Current ACI recommendation (ACI 226, 3R-92) for selecting fly ash to be used in sulfate-resistant concrete are based on research performed at the United States Bureau of Reclamation (Dikeou, 1975; Dunstan, 1980).

In developed countries, many experiments have been done on the properties of fly ash concrete. In those experiments fly ash with stone chips as coarse aggregate are generally used. Recently in Bangladesh many contractors have used fly ash, with brick aggregate, as cementitious material. This paper deals with locally available materials such as brick aggregate, coarse sand and fly ash available in Bangladesh (Indian fly ash). The experimental research program outlined here is carefully designed to investigate the strength and durability properties of brick aggregate concrete. Compressive strength of concrete at different w/c ratio will be studied using different percentage of fly ash. The study will also include the investigation of chloride and sulfate resistance of concrete at different percentages of fly ash with constant w/p ratio.

2. RESEARCH SIGNIFICANCE

In the subcontinent brick aggregate is very popular due to economic reason. It is important to ascertain the durability of this type of concrete against chlorine and sulphate attack. It is also important to know the behavior of fly ash with brick aggregate concrete. This research is conducted to evaluate the effect of fly ash on compressive strength and durability (mainly chloride and sulfate resistance) of concrete made of brick aggregate.

3. TEST PROCEDURES

The physical properties of brick and fine aggregate and both physical and chemical properties of cement and fly ash have been evaluated. ASTM standard testing procedure was followed.

Physical properties

Different physical properties of both fine and coarse aggregate have been evaluated following different ASTM codes. Fineness modulus, unit weight and specific gravity of coarse aggregate have been performed according to ASTM C117-95, ASTM C29-97 and ASTM C127-88, respectively. Physical properties like fineness, setting time and compressive strength of both cement and fly ash have been tested according to ASTM C115-96, ASTM C191-99 and ASTM C150-00, respectively. The chemical compositions of OPC and fly ash have been tested according to ASTM

C618-00. Compressive strength of concrete has been tested as per ASTM C39-01. Chloride resisting test of fly ash brick aggregate concrete has been performed according to BS 812: Part 117: 1988. A non-standard test has been performed for determining the deterioration rate of sulfate-ion on concrete. Physical properties of aggregate and cement are given in Table 1 and 2. Gradation curve for fine aggregate and brick aggregate used for the study are shown in Figure 1 and 2.

Table 1: Physical properties of aggregate

| | Fine Aggregate | Brick Aggregate |
|------------------|----------------|-----------------|
| Specific gravity | 2.64 | 1.87 |
| Fineness modulus | 2.47 | 7.62 |
| Absorption (%) | 1 | 9.7 |

Table 2: Physical properties of cement

| Physical properties of cement | |
|-------------------------------|-----|
| Fineness, m ² /kg | 348 |
| Initial setting time, min | 85 |
| Final setting time, min | 250 |

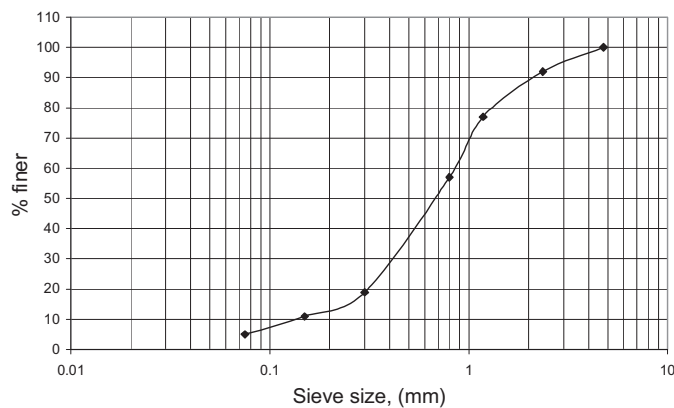


Figure 1: Gradation of fine aggregate

Chemical properties

Chemical properties of cement and fly ash are done following ASTM standards mentioned earlier and given in Table 3.

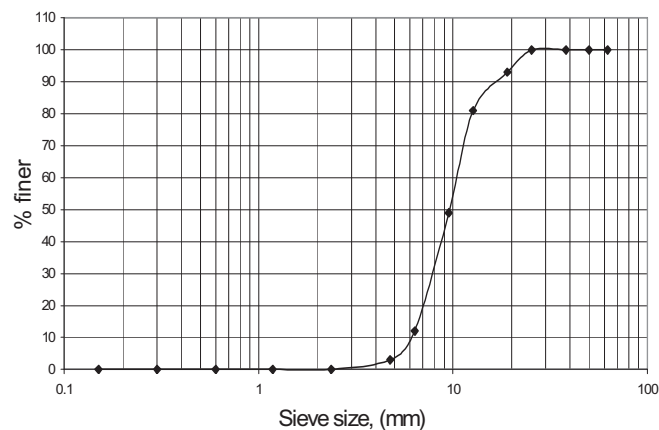


Figure 2: Gradation of brick aggregate

Table 3: Chemical properties of cement and fly ash

| | Fly ash (%) | OPC (%) |
|--|-------------|---------|
| Silicon dioxide, SiO ₂ | 53 | 21.5 |
| Aluminum oxide, Al ₂ O ₃ | 27.6 | 5.3 |
| Ferric oxide, Fe ₂ O ₃ | 6.2 | 2.5 |
| Ammonium hydroxide group | 33.8 | 7.8 |
| Sulfur trioxide, SO ₃ | 2.6 | 2.7 |
| Calcium oxide, CaO | 5.0 | 64.5 |
| Magnesium oxide, MgO | 3.0 | 1.2 |
| Loss on ignition | 0.8 | 1 |
| Others | -- | 1.3 |

4. PARAMETER USED

Water to powder ratio used in the study is in the range of 0.4 to 0.5. Variation of fly ash used in the current study is in the range of 0 to 30 percent (Table 4). Mix design were prepared using these above ranges and given in Table 5. After mixing and cured for 1 day samples were kept under water having different chloride concentration and sulphuric acid strength for durability test. Variation of chloride concentration and sulphuric acid strength used in the present study are given in Table 4. After submerging the samples for 14, 28 and 90 days under respective solutions samples were tested for penetration depth. Chloride ion and sulphur ion penetration depth in the samples were calculated. Compressive strengths are also performed in the respective days to observe the reduction of concrete strength from the control mix.

Table 4: Variation of parameters taken for study

| w/p | Chloride Concentration (mol/L) | Sulphuric acid strength (mol/L)[pH] | Fly ash replacement (%) |
|----------------|--------------------------------|-------------------------------------|-------------------------|
| 0.4, 0.45, 0.5 | 0.1, 0.35, 0.7 | 0.01 [2], 0.1[1], 0.5[0.3] | 0, 15, 30 |

Table 5: Mix proportions used for the present study

| w/p ratio | Fly ash (%) | Water (kg/m ³) | Cement (kg/m ³) | Fly ash (kg/m ³) | Fine aggregate (kg/m ³) | Coarse aggregate (kg/m ³) | Slump (mm) |
|-----------|-------------|----------------------------|-----------------------------|------------------------------|-------------------------------------|---------------------------------------|------------|
| 0.5 | 0 | 185 | 370 | - | 630 | 1170 | 36 |
| 0.5 | 15 | 185 | 314.5 | 55.5 | 630 | 1170 | 33 |
| 0.5 | 30 | 185 | 259 | 111 | 630 | 1170 | 35 |
| 0.45 | 0 | 172 | 383 | - | 630 | 1170 | 32 |
| 0.45 | 15 | 172 | 325.55 | 57.45 | 630 | 1170 | 33 |
| 0.45 | 30 | 172 | 268 | 115 | 630 | 1170 | 30 |
| 0.4 | 0 | 158.5 | 396.5 | - | 630 | 1170 | 30 |
| 0.4 | 15 | 158.5 | 337 | 59.5 | 630 | 1170 | 31 |
| 0.4 | 30 | 158.5 | 277.5 | 119 | 630 | 1170 | 31 |

5. RESULTS AND DISCUSSIONS

5.1 Compressive strength

Compressive strength test of the concrete samples is performed for different w/p ratio and different fly ash replacement. For a constant w/p ratio and at a particular age concrete strength decreases with the increase of fly ash replacement (Figure 3). This observation is expected and also valid for brick aggregate concrete. Compressive strength of concrete also depends on the physical properties of aggregates. It should also be noted that brick aggregate concrete always gives lower strength than stone aggregate concrete at particular age and w/p ratio, which is shown in Figure 4.

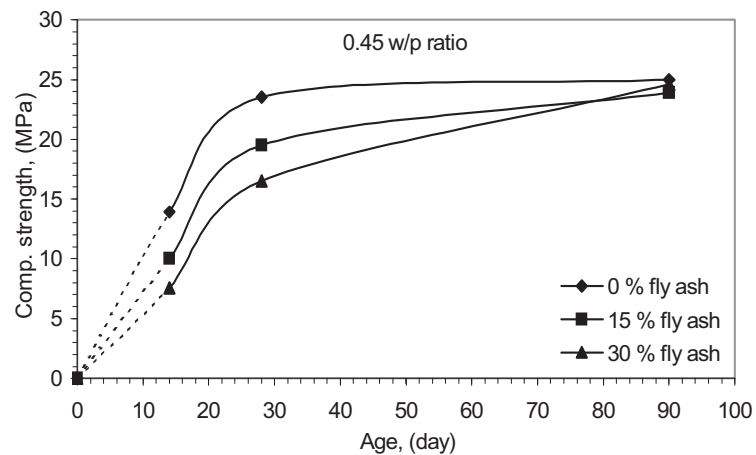


Figure 3: Variation of compressive strength with age

Interesting to note that strength is independent of fly ash replacement at 90 days (Figure 3 and Figure 5). For a constant powder content irrespective of fly ash replacement should give same strength at or after 90 days. This can reduce the cost of concrete if 90 days concrete compressive strength can be used during the design.

5.2 Chloride ion penetration depth

Concrete samples were kept under solution of different concentration of chloride ion. Samples were tested for chloride ion penetration depth at 14, 28 and 90 days of submersion. Penetration depth increases with age for a particular chloride concentration. Here only control curve (no fly ash) is shown (Figure 6). Similar results are obtained for other fly ash replacements. Fly ash replacement has a profound effect on depth of penetration. Depth of penetration decreases with the increases of fly ash replacement (Figure 7).

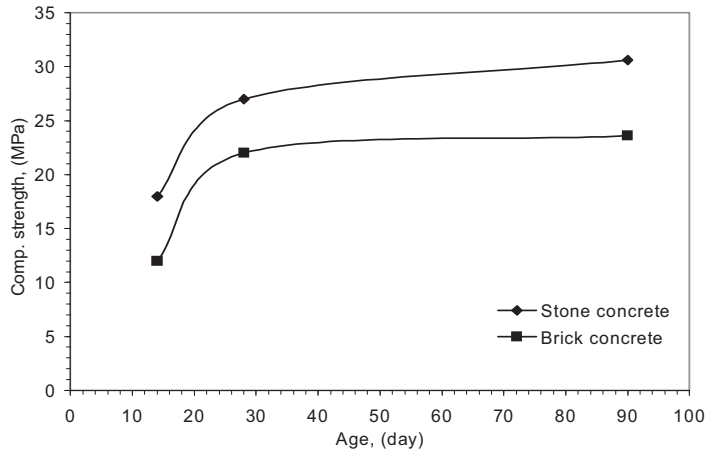


Figure 4: Comparison of strength between brick and stone aggregate concrete

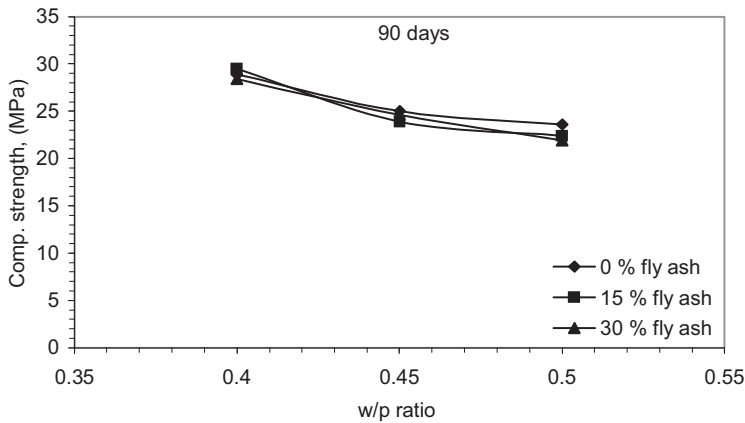


Figure 5: Compressive strength at 90 days

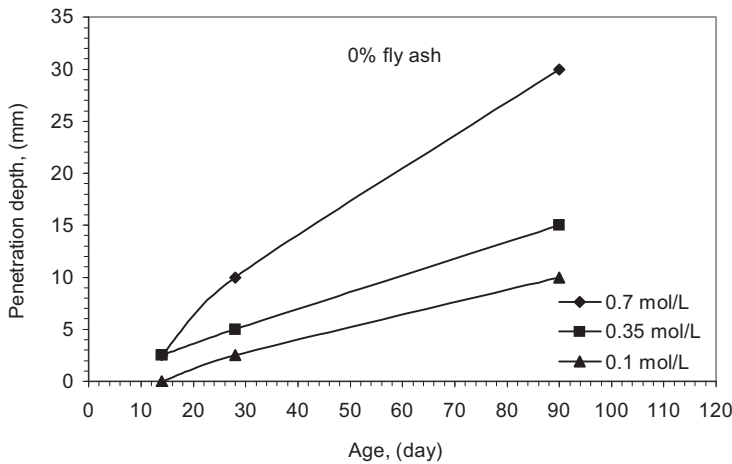


Figure 6: Variation of penetration depth with age

Present study also calculates the percentage of chloride ion at a particular depth for chloride ion concentration and fly ash replacement. Here, only the results for fly ash are shown (Figure 8). Later average percentage of chloride ion is calculated and reported here. Average chloride ion percentage increases with the age of submersion. Fly ash help reduces the ion percentage at a particular concentration. Brick aggregate concrete is

porous concrete than stone aggregate concrete. Percentage of chloride ion at particular depth, for a particular concentration and age of submersion, is more in brick aggregate concrete than stone aggregate concrete, which is shown in Figure 9.

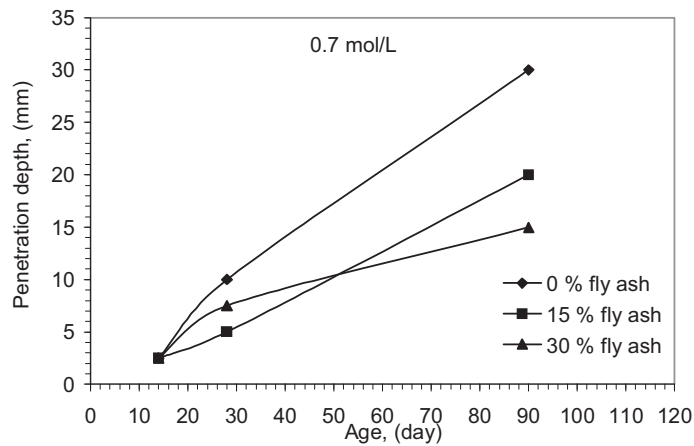


Figure 7: Variation of penetration depth with age

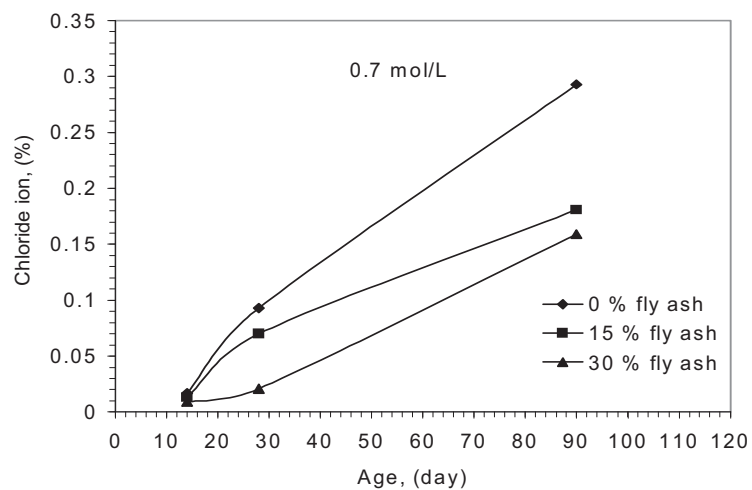


Figure 8: Variation of chloride ion percentage with age

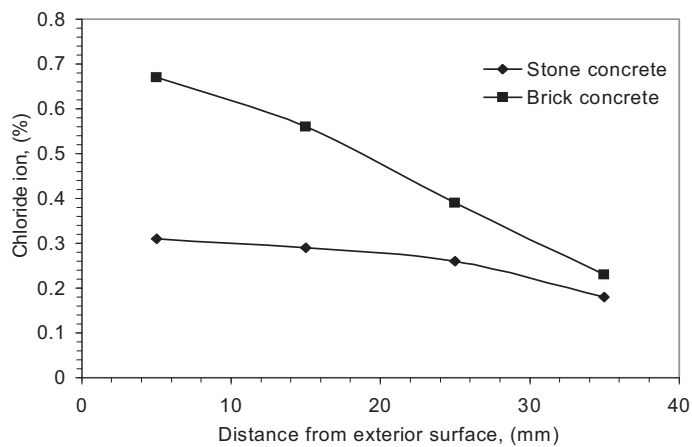


Figure 9: Comparison of chlorine ion percentage with aggregate type

Compressive strength of the concrete also decreases with the penetration of chloride ion and depth of penetration. Figure 10 gives an indication of strength reduction for 90 day submersion and solution of 0.7 mol/L. For control concrete reduction is higher with the age but for concrete with 30 percent fly ash reduction decreases with age. This is a very important finding because permeability of fly ash decreases with age thus reducing the chloride ion percentage as well as depth of penetration. Thus, decreases the compressive strength reduction of concrete.

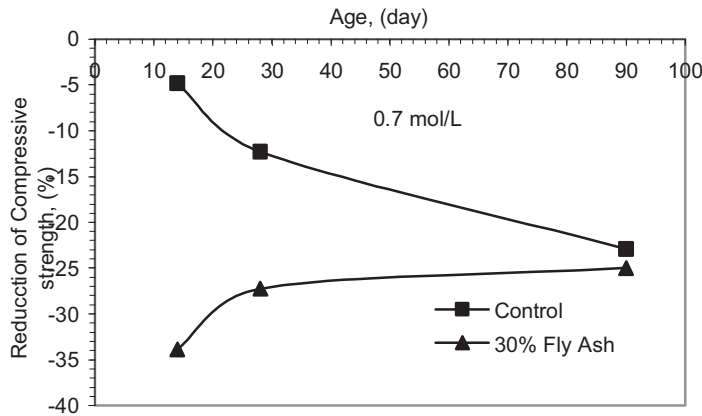


Figure 10: Reduction of compressive strength with age

5.3 Sulphuric acid degradation

Concrete samples were kept under solution of different concentration of sulphuric for durability test. Samples were tested for degradation depth at 14, 28 and 90 days of submersion. Degradation depth increases with age for a different acid concentration for a particular fly ash replacement (Figure 11). Similar results are obtained for other fly ash replacements. Fly ash replacement has a profound effect on depth of degradation. Depth of degradation decreases with the increases of fly ash replacement (Figure 12).

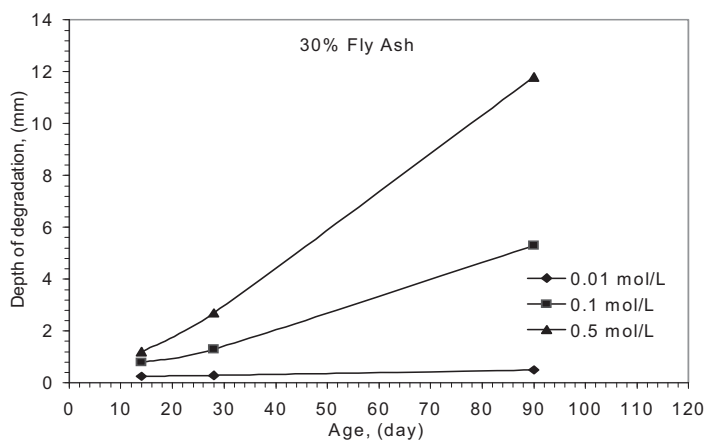


Figure 11: Variation of degradation depth with age

Fly ash help reduces the ion percentage at a particular concentration. Brick aggregate concrete is porous concrete than stone aggregate concrete. degradation for a particular acid concentration and age of submersion, is

more in brick aggregate concrete than stone aggregate concrete, which is shown in Figure 13.

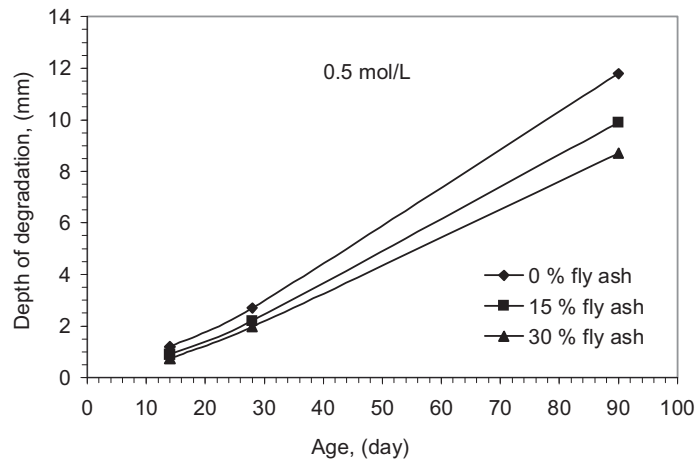


Figure 12: Variation of degradation depth with age

Compressive strength of the concrete also decreases with the penetration of sulphuric ion and depth of penetration. Figure 14 gives an indication of strength reduction for 90 day submersion and solution of 0.5 mol/L. For control concrete reduction is higher with the age but for concrete with 30 percent fly ash reduction decreases with age. This is a very important as permeability of fly ash decreases with age thus reducing the chloride ion percentage as well as depth of degradation. Thus, decreases the compressive strength reduction of concrete.

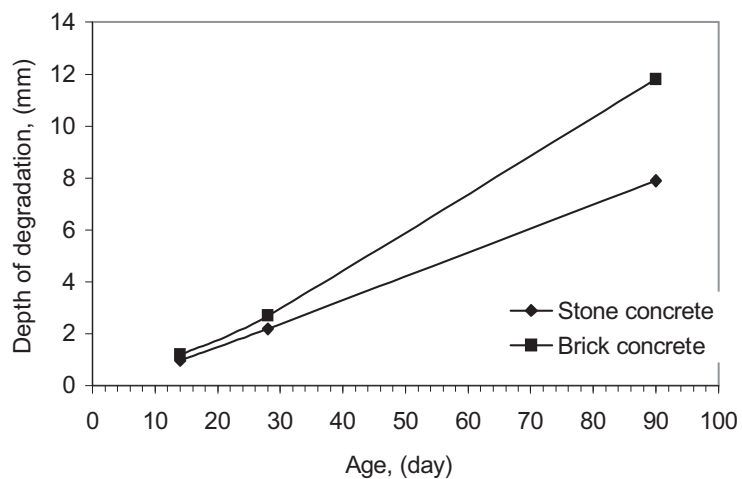


Figure 13: Comparison of degradation depth for with aggregate type

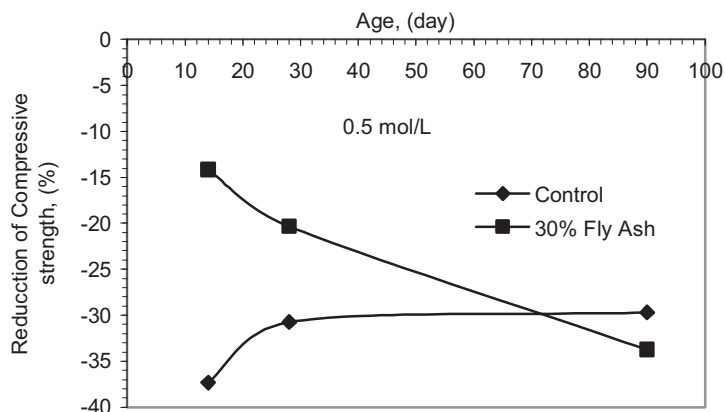


Figure 14: Reduction of compressive strength with age

6. CONCLUSIONS

The compressive strength of cement-replaced fly ash concrete is lower than that of concrete and mortar without fly ash at the early age (14 and 28 days), since the pozzolanic reaction proceeds slowly. But due to continued pozzolanic reaction, cement-replaced fly ash concrete develops greater strength at later age (90 days), almost equal to the strength of concrete without fly ash. Moreover, strength of concrete depends on aggregate physical properties. From the experiment it is found that strength of stone aggregate concrete is higher than that of brick aggregate concrete.

The chloride-ion penetration resistance suggests that cement-replaced fly ash concrete perform better than that of concrete without fly ash. Rate of chloride-ion penetration for fly ash concrete is lower than that of concrete without fly ash. This suggests that where durability of reinforced concrete (against chloride ingress) is the primary requirement fly ash can be used as an admixture to produce dense concrete. Chloride ion penetration in concrete also depends on aggregate physical properties. From the experiment it is found that chloride ion penetration in brick aggregate concrete is higher than stone aggregate concrete.

It has been also found that pozzolanic material like fly ash reduces the sulfate attack. The pozzolanic material like fly ash is responsible for impermeability of concrete. Fly ash makes concrete dense to ingress sulfate-ion in it. Thus, cement-replaced fly ash concrete reduces sulfate-ion deterioration rate. Degradation of concrete due to sulfuric acid attack also depends on aggregate physical properties. From the experiment it is found that degradation of brick aggregate concrete is higher than stone aggregate concrete.

REFERENCES

- ASTM C39/C39M-01 (2001) Standard Test Method for Compressive Strength of Cylindrical Concrete Specimens, ASTM International, West Conshohocken, PA, www.astm.org.

- ASTM Standard C29-97 (2003) Standard Test Methods for bulk density and Voids in aggregate, ASTM International, West Conshohocken, PA, www.astm.org.
- ASTM Standard C115-96a (1999) Standard Test Method for Fineness of Portland Cement by the Turbidimeter, ASTM International, West Conshohocken, PA, www.astm.org.
- ASTM Standard C117-95 (2005) Standard Test Method for Materials Finer than 75- μ m (No. 200) Sieve in Mineral Aggregates by Washing, ASTM International, West Conshohocken, PA, www.astm.org.
- ASTM Standard C127-88 (1999) Standard Test Method for Specific Gravity and Absorption of Coarse Aggregate, ASTM International, West Conshohocken, PA, www.astm.org.
- ASTM Standard C128-97 (1999) Standard Test Method for Specific Gravity and Absorption of Fine Aggregate, ASTM International, West Conshohocken, PA, www.astm.org.
- ASTM Standard C150-00 (2001) Standard Specification for Portland Cement, ASTM International, West Conshohocken, PA, www.astm.org.
- ASTM Standard C191-99 (1999) Standard Test Method for Time of Setting of Hydraulic Cement by Vicat Needle, ASTM International, West Conshohocken, PA, www.astm.org.
- ASTM Standard C618-00 (2001) Standard Specification for Coal Fly Ash and Raw or Calcined Natural Pozzolan for Use as a Mineral Admixture in Concrete, ASTM International, West Conshohocken, PA, www.astm.org.
- Ben-Bassat, M., Nixon, P. J. and Hard Castle, J., (1990), "The Effect of Differences in Composition of Portland Cement on Properties of Hardened Concrete," Magazine of Concrete Research, V.42, No.151, PP:59-66.
- Berke, N. S.; Pfeifer, D. W. and Weil, T. G., (1988), Protection Against Chloride-Induced Corrosion, Concrete International, V.10, No.12, PP.45-55.
- Dikeou, J. T., (1985), "Effect of Fly Ash on Concrete," Research Report No. 23, USBR, Denver.
- Dunstan, E. R. Jr. (1980), "Possible Method for Identifying Fly Ashes That Will Improve Sulfate Resistance", Cement, Concrete and Aggregates, CCAGDP, V.2, No.1, PP.20-30.
- Jiang, L. H. (1998), "Studies on Hydration, Microstructure, and Mechanism of High Volume Fly Ash Concrete," Ph.D. thesis, Hohai University, Nanjing, China.
- Ramachandan, V. S., Feldman, R. F. and Beaudoin, J. J., (1981), "Concrete Science, Heyden and Son Ltd., London.

MECHANICAL BEHAVIOR OF CONCRETE MEMBER SUBJECTED TO REPEATED IMPULSIVE FORCE

HIROSHI YOKOTA¹, M. IWANAMI², S. TAKAHASHI²
and T. MATSUBASHI²

¹ICUS, IIS, The University of Tokyo, Japan

²Port and Airport Research Institute, Japan

hyokota@iis.u-tokyo.ac.jp

ABSTRACT

This paper deals with impulsive forces acting on marine concrete structures due to wave breaking and structural response against these forces. At first, the characteristics of impulsive forces generated by wave breaking were investigated by hydraulic experimental tests. The dynamic response of reinforced concrete beams was also investigated by applying these forces repeatedly. Then, structural behavior of reinforced concrete beams was examined by falling weight impact loading tests. Furthermore, to enhance structural capacity, the applicability of PVA short fiber was discussed. It was found that the number of repetitions of impact force applications at the ultimate state is greatly affected by the impact velocity. Also, it was made clear that the impact resistance of reinforced concrete members will be improved when mixing PVA short fiber with concrete.

1. INTRODUCTION

Repeated impulsive forces due to waves often apply to marine structural members during storms, which may bring catastrophic effects. In fact, many examples of collapse due to repeated impulsive forces by wave breaking have been collected in reinforced concrete (RC) walls of breakwater caissons (Takahashi, et al., 1998a). In the present design of such concrete structures, the impulsive wave force, which has large variations with regard to time and space, is converted into equivalent distributed static loads in order to compare to the load carrying capacity of structures in static conditions. Therefore, it is one of the problems that scatters of impulsive wave forces and dynamic behavior of concrete structures are not taken into account.

Many studies have been undertaken experimentally and analytically to make clear the structural performance of RC members against impulsive forces. Most of them are for impulsive forces caused by falling of rocks, collision of cars/vessels, etc. Few studies, however, have been carried out against impulsive forces caused by ocean waves. The major differences between impulsive forces due to ocean waves and those due to falling or collision are the number and duration of the forces applied. The impulsive force by wave breaking is characterized that it applies to structures a few

thousand times during one storm and each impulse lasts for only about 60ms for breakwater caisson walls (Takahashi, et al., 1995 and 1998b).

The characteristics of impulsive forces generated by waves were investigated experimentally in this study. Hydraulic tests were carried out in an experimental wave flume in which waves were repeatedly applied to RC beams. Moreover, mechanical behavior of RC beams subjected to repeated impulsive forces was discussed and the process to the ultimate state was made clear. In addition, it is necessary to examine how to improve structural performance of marine concrete structures against repeated impact loads. In the previous study carried out by Ito et al. (2005), for example, it was revealed that structural performance of RC members may be improved in static conditions by mixing PVA short fiber into concrete. Based on this, it is expected that impact resistance of concrete members are improved by PVA short fiber. Therefore, in this study, to investigate the applicability of PVA short fiber to improve impact resistance of marine concrete structures, mechanical behavior of concrete beams reinforced with PVA short fiber under repeated impact loads was examined by conducting falling-weight impact loading tests.

2. IMPULSIVE WAVE FORCE AND ITS EFFECT ON STRUCTURAL BEHAVIOR OF RC BEAM

Hydraulic experimental tests were carried out to understand the dynamic response and the failure process of RC beams due to repeated impulsive forces (Yokota, et al., 2001). The experimental test was done in the wave flume of 105m long and 3m wide. The tested beam was horizontally supported just in front of a reflection wall with the clearance, s , from the still water surface. Regular standing waves were generated by a wave generator with wave height, H , of 100 to 600mm, period, T , of 2, 3, 4s, and wave length of 5.6 to 13.49m. The clearance was either 0 or 300mm. The water depth at the reflection wall was 1.3m.

Two experimental test programs were undertaken. At first, RC beams with 100, 200 or 300mm thick, 400mm wide, and 2400mm in span length were prepared for measuring the wave force resultant and dynamic response under wave impulsive forces. The other experimental program was to understand the failure process of RC beams with 50 or 80mm thick, 1000mm wide, and 2400mm in span length. Measurement was made for water elevation by wave gauges, local wave pressures by wave pressure gauges attached on the bottom surface of the beam and wave force resultant by load cell at the supports of the beam. A total of 20 wave pressure gauges were installed in 4 lines along the longitudinal axis of the beam; (1) refers to those in the most reflection wall side and (4) in the most wave generator side. Acceleration of the tested beam and strains in rebar and in concrete were monitored throughout the test. Concrete strength at the time of the test was ranged from 30.3-38.9MPa and yield strength of rebars was ranged from 337-357MPa. The ultimate static load-carrying capacities in terms of uniformly distributed load converted from the concentrated load were 36.8kPa for the 100mm thick beam and 22.1kPa for 50mm thick beam.

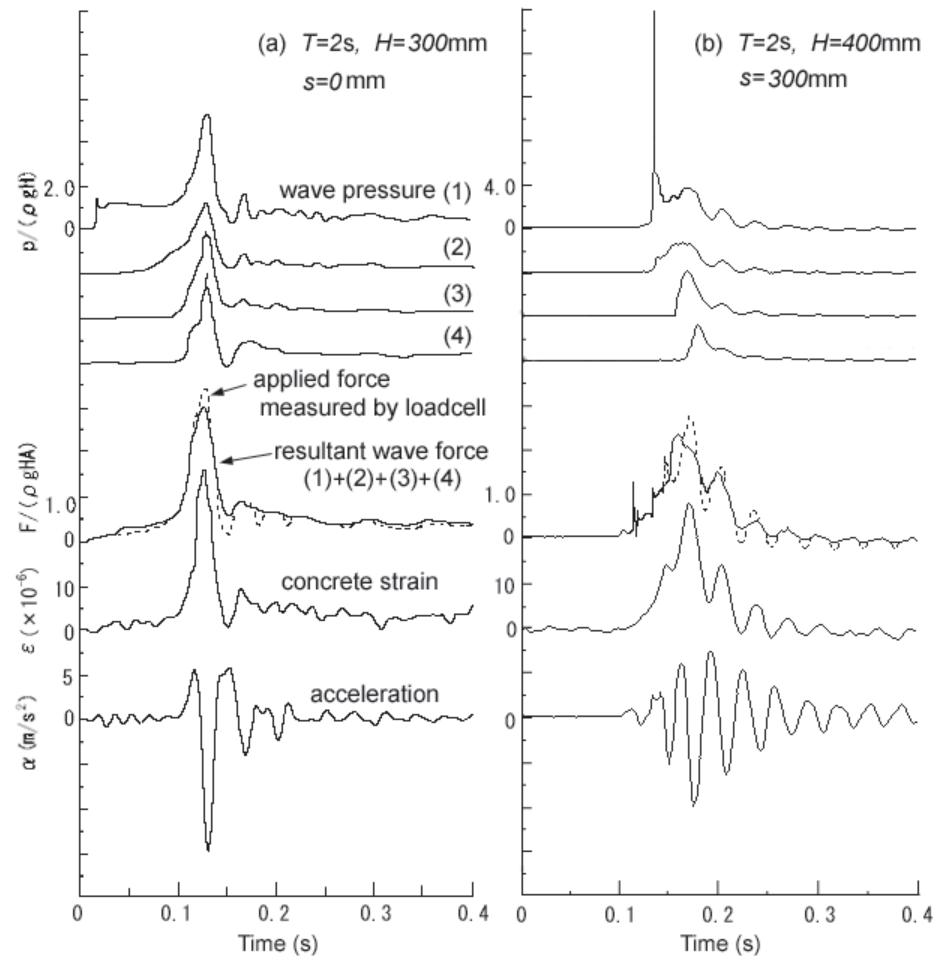
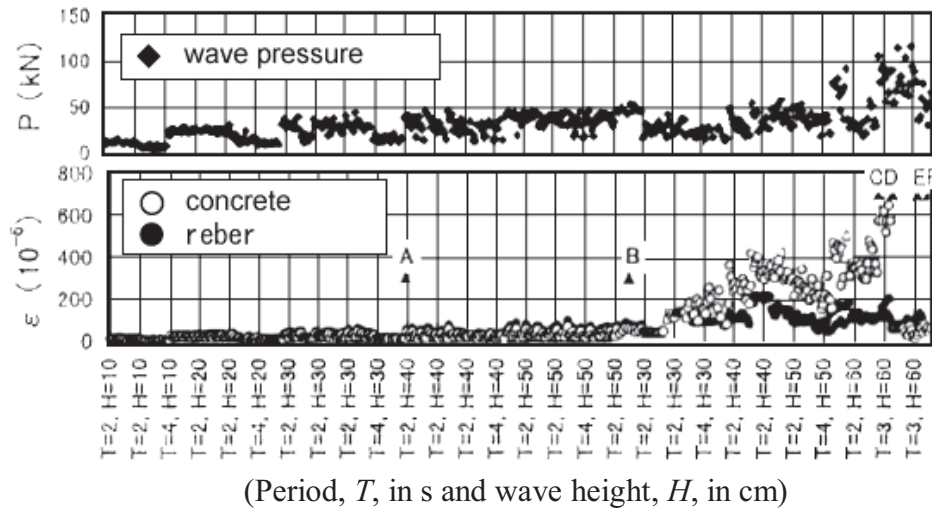


Figure 1: Response of RC beam subjected to impulsive wave force

Figure 1 shows dynamic responses of RC beams of 100mm thick and 400mm wide in which wave pressure, p , acceleration, α , and concrete strain, ε , resultant wave force, F , are plotted. In case of (a), the Bagnold type impulsive force occurred because air was trapped between the surface of wave and the beam. The duration of impulsive force was about 34ms. Wave pressure measured at line (1) was 26kPa and about 19kPa at the other lines. Wave force resultant measured by the load cell was almost the same as that of the sum of local wave pressures measured by wave pressure gauges as about 15.7kN. The measured acceleration was more than 10m/s^2 with the period of about 25ms.

In case (b), the Wagner type impulsive wave pressure was recognized where waves touched at the beam from the reflection wall side running towards the wave generator side without trapping air. The peak value of the wave pressure reached 97kPa and its duration was only 3ms. However, the wave force resultant was not so large; 9.9kPa and the duration was 75ms. The time history of concrete strain was in accordance with that of resultant forces due to waves.



(Period, T , in s and wave height, H , in cm)
 Figure 2: Failure process and strain accumulation

Figure 2 shows the failure process of the tested beam of 80mm thick in terms of resultant wave forces and concrete and rebar strains. Repeated waves with increasing height from 100 to 600mm were applied as shown in the figure. The total number of waves applied was about 2000. At first, a crack was initiated at the fixed end of the beam, indicated as A in Figure 2, and then three cracks occurred at the other end and the midspan of the beam (B). Due to further application of waves, concrete was crushed at the both ends of the beam to reach the ultimate state (C). Action by waves formed plastic hinges at the both ends and plenty of cracks and falling of cover concrete were observed (D). Finally, concrete was completely removed at some parts (E), and some rebars were broken (F). Before the initiation of the first crack, induced strain of concrete was rather small even if large impulsive forces were applied. However, once a crack was formed, local failure was rapidly progressed, resulting in entire collapse of the beam by repeated waves as roughly equivalent to those during only one storm. Compared with the static loading test, locations of cracks were almost the same. Rebars were broken in the repeated impulsive loading test, but not broken in the static loading test. It seemed that the test beam has high ductility after rebar yields but can easily be broken due to repeated impulsive forces.

3. EXPERIMENTAL PROCEDURE FOR STRUCTURAL BEHAVIOR INVESTIGATION

Two kinds of RC beams were prepared: normal concrete beams (N-beams) and fiber reinforced concrete beams (F-beams). Beams in both series are 250mm wide, 250mm high, and 3300mm long, as shown in Figure 3.

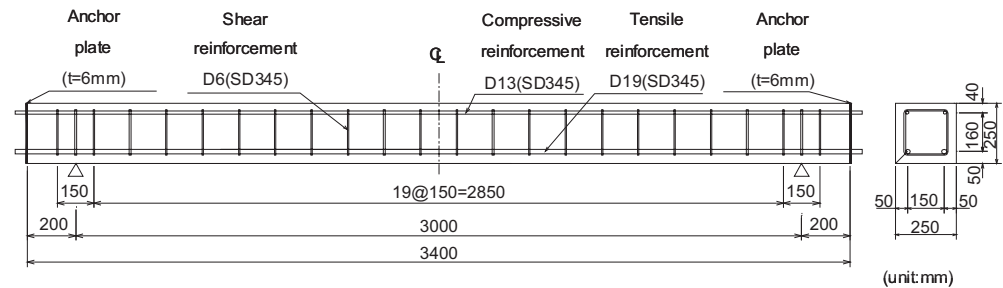


Figure 3: Beam for loading test

PVA (Polyvinyl alcohol) short fiber was used to improve mechanical properties of concrete. PVA short fiber has high tensile strength and high resistance against corrosion compared with other types of synthetic fiber. Also, it is expected that PVA short fiber can adhere chemically to cement matrix, causing excellent bond properties between the fiber and the matrix. The dimensions of PVA short fiber used in this experiment were 0.66mm in diameter and 30mm long. Its tensile strength and Young's modulus were 880MPa and 29.4GPa, respectively. The fiber reinforced concrete contained PVA short fiber in 1.5 vol%.

Since fiber reinforced concrete was produced by adding PVA short fiber into normal concrete, the bulk properties of fiber reinforced concrete were the same as that of the normal concrete. The compressive strength of concrete at the test was ranged from 30.8-33.0MPa.

Table 1 summarizes the test cases. The loading tests were conducted by static loading and repeated impact loading with the constant impact velocity. The impact velocity was set at 2.0, 2.5, 3.0 and 4.0m/s, considering velocities of impulsive wave forces observed in an actual marine structure. For repeated impact loading, an impact loading testing machine was used. A steel weight is lifted to the predetermined height by a small crane and then it freely falls by releasing a hook. The weight was dropped onto the top surface of a test beam at the midspan. The mass of the weight is 400kg, and the impact face of the weight has a spherical shape with a diameter of 565mm. To prevent the beam from bouncing out, the beam is held with steel bars at its two supports. To reduce scatters of impact response caused by damage of the top surface of the beam, a rubber sheet of 10mm in thickness is placed at the impact position of the beam. The ultimate state of the beam was defined as the cumulative residual midspan displacement reached 2.0% of the span length (JSCE, 2004), that is 60mm. The impact loads were applied repeatedly until the ultimate state.

The impact force developed between the weight and the beam was measured using a load cell mounted to the falling weight. The reaction forces at supporting points were measured using load cells set at the supports. The midspan displacement of the beam was measured using a laser-type displacement sensor. Also, cracks of the beam were observed periodically.

Table 1: Test case

| Type | Designation | Loading method | Impact velocity (m/s) |
|------|-------------|-----------------|-----------------------|
| N | N-S | Static | - |
| | N-V2 | Repeated impact | 2.0 |
| | N-V2.5 | | 2.5 |
| | N-V3 | | 3.0 |
| | N-V4 | | 4.0 |
| F | F-S | Static | - |
| | F-V2 | Repeated impact | 2.0 |
| | F-V2.5 | | 2.5 |
| | F-V3 | | 3.0 |
| | F-V4 | | 4.0 |

4. EXPERIMENTAL RESULTS

4.1 Effect of impact velocity on displacement

By static loading tests, it was made clear that the tensile rebar yields when the midspan displacement reaches about 12mm. Also, crushing of top concrete occurred when the midspan displacement reached about 30mm. Figure 4 shows the relationships between the impact velocity and midspan displacement at the first impact load. The maximum midspan displacement of N-beams was 13.3, 18.4, 25.0 and 38.2mm for the impact velocities of 2.0, 2.5, 3.0 and 4.0m/s, respectively. Similarly, the maximum midspan displacements of F-beams were 12.7, 16.4, 22.0 and 34.6mm. It was found that the maximum displacement of N-beams becomes slightly larger than those of F-beams. Here, it is supposed that the dependence of strain rate on mechanical properties of concrete and steel bars was ignored and that structural behavior due to impact loading was similar to that of static loading. Comparing with the load-displacement curves of the beam under static loading, it could be regarded that the impact load with the impact velocity of 2.0m/s was equivalent to static load not to make tensile rebars yield. Similarly, the impact loads with the impact velocity of 2.5m/s and 3.0m/s were equivalent to static load to make tensile rebars yield but not to cause crushing of top concrete, and the impact load with the impact velocity of 4.0m/s was equivalent to static load to cause both yielding of tensile rebars and crushing of top concrete.

4.2 Number of repetitions at failure

Table 2 summarizes the result of repeated impact loading tests in terms of the number of repetitions of impact loading at the ultimate state. From this table, even comparatively small impact could make the beam fail in bending because the impact loads were applied to the beams repeatedly. For example, in case of the impact velocity of 2.0m/s, the beam reached the

ultimate state after 590 impacts for N-V2 and 105 impacts for F-V2. The beams reached the ultimate state after less number of repetitions when impact velocities were larger. The difference in the number of repetitions of impact loading until the ultimate state became remarkable in the range between 2.0 and 2.5m/s in impact velocity.

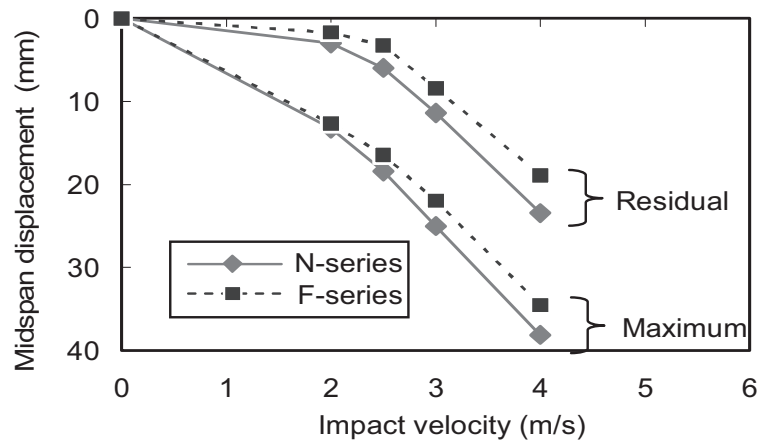


Figure 4: Impact velocity vs midspan displacement

Comparing F-beams with N-beams, the number of repetitions for F-beams was 5.6 times more than that for N-beams in case of 2.0m/s. Similarly, the number of repetitions for F-beams was 1.7 times more in case of 2.5m/s, and 1.8 times more in case of 3.0m/s. Therefore, it was found that impact resistance of RC beams may be improved by mixing PVA short fiber into concrete and the effect of PVA short fiber became significant when impact velocity was small. However, in case of 4.0m/s, the beams with or without PVA short fiber failed at the third impact, showing no improvement of impact resistance by PVA short fiber mixing.

4.3 Relationship between the number of repetitions and displacement

Figure 5 shows the relationships between midspan displacement of the beam and the number of repetitions of impact loading. In case of 2.0m/s in the impact velocity, the midspan displacement of the beam progressed remarkably at the small number of repetitions. Then, after a slow progress, midspan displacement again increased acceleratedly. The whole tendency drew an S-shaped curve. On the other hand, in the other cases, the progress of midspan displacement was almost linear with increase in the number of repetitions, which was considerably different from the case of 2.0m/s. The reason for this difference was considered why the impact load with the impact velocity of 2.0m/s is equivalent to static load not to make tensile rebars yield so that the failure process was similar to that of RC beams showing fatigue failure. Also, it was why the number of repetitions of impact loading until ultimate state changed drastically in the range between 2.0 and 2.5m/s in impact velocity.

Table 2: Number of repetitions of impact loading at failure

| | Impact velocity (m/s) | | | |
|----------------------|-----------------------|--------|------|------|
| | 2.0 | 2.5 | 3.0 | 4.0 |
| Designation | N-V2 | N-V2.5 | N-V3 | N-V4 |
| Number of repetition | 105 | 15 | 5 | 3 |
| Designation | F-V2 | F-V2.5 | F-V3 | F-V4 |
| Number of repetition | 590 | 25 | 9 | 3 |

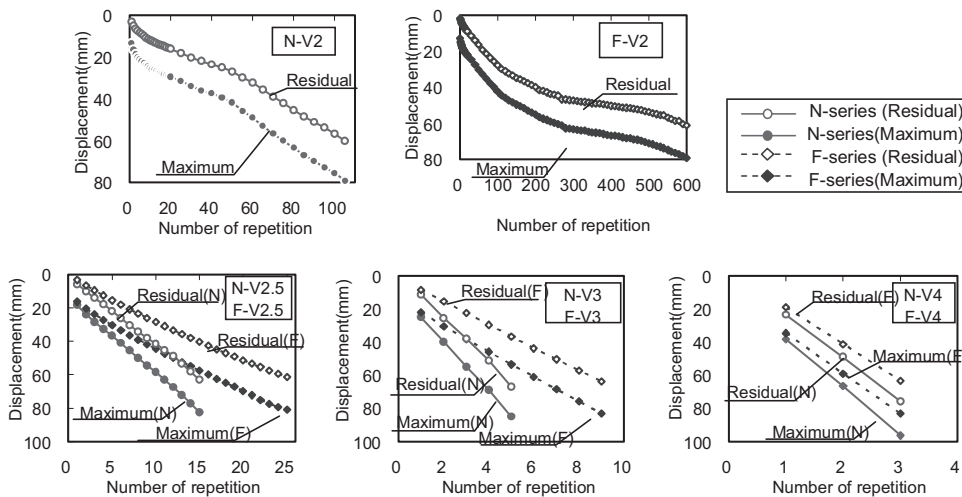


Figure 5: Number of repetitions vs midspan displacement

In addition, as shown in Figure 5, the progress of cumulative residual displacement of N-V2 was accelerated since the number of repetitions reached 50 (maximum and residual displacements were 42mm and 27mm, respectively). This number of repetitions coincided with the stage when crushing area of top concrete was spread greatly. On the other hand, the cumulative residual displacement of F-V2 increased acceleratedly since the number of repetitions reached 470 (maximum: 69mm and residual: 52mm). In this case, crushing of top concrete and spalling of concrete cover was not remarkable, and the increment of cumulative residual displacement for one impact was relatively small. For these facts, it was considered that PVA short fiber transferred tensile stress in cracked concrete together with reinforcing bars and prevented concrete cover from spalling off, improving impact resistance of the beam. It was confirmed that PVA short fiber reduces the damage of RC beams subjected to repeated impact loads, resulting in improvement of impact resistance of concrete structures.

5. CONCLUSIONS

The following conclusions were drawn in this study:

- 1) The hydraulic experiment made clear the characteristics of wave impulsive force acting on a marine RC structural member.
- 2) Once a crack was initiated in a concrete member, failure of the member rapidly progressed to entire collapse under repeated wave impulsive forces.

3) Under the experimental condition in this study, it was found that the number of repetitions of impact loading until the ultimate state is greatly affected by the impact velocity, and the number of repetitions at failure is considerably changed between 2.0 and 2.5m/s of impact velocity.

4) The number of repetitions of impact loading until the ultimate state increased in case of reinforced concrete beams with PVA short fiber. Therefore, the impact loading resistance of marine RC structures will be improved by mixing PVA short fiber into concrete.

REFERENCES

- Ito, H., Iwanami, M. and Yokota, H., 2005. Experimental Study on Shear Capacity of Reinforced Concrete Beams with PVA Short Fiber. *Proceedings of the 6th International Congress on Global Construction*, Dundee, UK, 551-560.
- Japan Society of Civil Engineers, 2004. *Practical Methods for Impact Test and Analysis*. Structural Engineering Series 6 (in Japanese).
- Takahashi, S., Suzuki, K. and Aburatani, S., 1995. Experimental Study on Soil Pressure and Strain Observed in a Caisson Wall Subjected to Impulsive Breaking Waves. *Proceedings of Coastal Engineering*, JSCE, Vol.42, 906-910 (in Japanese).
- Takahashi, S., Tsuda, M., Suzuki, K., Shimosako, K., 1998a. Experimental and FEM Simulation of the Dynamic Response of a Caisson Wall against Breaking Wave Impulsive Pressures. *Coastal Engineering*, 1986-1999.
- Takahashi, S., Tsuda, M., Shimosako, K., Yokota, H. and Kiyomiya, O., 1998b. Numerical Calculations on Dynamic Response of Caisson Wall due to Impulsive Breaking Wave. *Proceedings of Coastal Engineering*, JSCE, Vol.45, 751-755 (in Japanese).
- Yokota, H., Takahashi, S., Yamada, M. and Tsuda, M., 2001. Mechanical Behavior of RC Members Subjected to Repeated Impulsive Forces due to Waves. *Proceedings of the 1st fib Congress*, Osaka, Japan, CD-ROM.

REVIEW OF EMERGENCY TECHNOLOGIES TO SUPPORT URBAN RESILIENCE AND DISASTER RECOVERY

PENA-MORA FENIOSKY, AZIZ ZEESHAN,
GOLPARVAR-FARD MANI,
ALBERTY CHEN, ALBERT P. PLANS and SAUMIL J. MEHTA
University of Illinois at Urbana-Champaign, USA
feniosky@illinois.edu

ABSTRACT

This paper presents an inclusive state-of-the-art review of various emerging technologies to support urban disaster response and recovery. This review was undertaken as a part of the CP2R project (Collaboration Framework for Preparedness against, Respond to and Recovery from eXtreme Events (XEs) involving critical physical infrastructure) which has focused on improving the collaboration among key actors that should be involved in different steps of preparedness against (i.e., before disaster), response (i.e. during disaster) and recovery (i.e., after disasters). A realistic disaster response scenario emphasizing on the crucial need for development of CP2R system as well as supporting technologies are presented. Technologies reviewed include application of Radio Frequency Identification (RFID) based techniques for structural assessment, a Segway-based information provisioning platform for field-responder's mobility and disaster site data collection, Geospatial Information System (GIS) for optimal resource optimization, Computer Vision and Image Processing technologies for scene reconstruction using real-time visual data (images and/or video stream) from disaster site, and Augmented Reality technology for visualization of disaster damages and accessibility to various locations, application of Building Information Modelling for knowledge extraction for pre-disaster status and also as a baseline for visualization of structural discrepancies as well as building black-box for in-building data storage. The paper concludes that emerging ICTs (Information and Communication technologies) can play a pivotal role in disaster preparedness, response and recovery processes. The need for further exploitation of convergence and synergy between various technologies and their application to support existing disaster response processes is also discussed.

1. INTRODUCTION

Modern large or mega cities are complex and inter-dependent systems including a mix of utilities, transportation, communication and power infrastructure, home and office buildings. Recent disasters have shown that

this complexity and inter-dependency increases the potential impact of disasters in urban areas. It has long been recognized that Information Technologies can play a critical role in addressing short-comings of existing disaster response operations. Recent advancements in technologies, such as those in hardware (e.g. miniaturization, increased processing power), transmission systems (e.g. high bandwidth wireless technologies) and real-time location tracking and data collection systems, have enabled new possibilities for effectively meeting challenges imposed by man-made and natural disasters. To address challenges imposed by disasters in modern cities and to exploit possibilities emerging as a result of recent technological advances, CP2R project (Collaboration Framework for Preparedness against, Respond to and Recovery from eXtreme Events (XEs) involving critical physical infrastructure) was initiated at University of Illinois at Urbana-Champaign. A key objective of the CP2R project is to enhance the role of civil engineers in disaster response and mitigation. Existing role of civil engineers during disasters is mostly limited to monitoring and securing the structural stability of the built environment for the search and rescue operations (Aldunate et al. 2005). CP2R research efforts are focused on augmenting the role of civil engineers by further enhancing traditional structural engineering functions (e.g. temporary shoring and structural stability monitoring) as well as incorporating their knowledge on issues like decision making related to Critical Physical Infrastructure (CPI), task resource allocation (e.g. managing response machinery and personnel) and construction management (e.g. temporary re-constructability of damaged areas and management of rescue construction machinery). Also, participation of engineers and contractors involved in original design and construction of the CPI may bring critical insights for the disaster response and recovery operation.

This paper reviews various emerging technologies that can be used to augment civil engineer's role in urban disaster response and recovery operations. Rest of the paper is organized as follows. Section 2 describes a scenario that has guided further technological development in the CP2R project. Section 3 reviews various emerging technologies with a focus on their application in disaster response and recovery operations. Section 4 discusses key issues that need to be addressed to facilitate the uptake of these technologies.

2. DISASTER SCENARIO

This Section describes a scenario that highlights the efficiency of the CP2R system during urban search and rescue. Consider a major urban city being struck by a magnitude 7 earthquake on the Richter scale. Initial damage estimated by running an earthquake simulator based on U.S. Geological based on given soil conditions and demographic distribution suggests that over 10,000 buildings in the city could be partially or completely collapsed while others may have sustained structural damage. Other components of CPI including elements of micro (e.g. power and water distribution networks, gas pipelines as well as sewerage) and macro infrastructure (e.g. bridges, rail lines, airports) suffered severe disruptions and damages.

Immediately after the disaster struck, “Building Black-Box Systems” (Section 3.1) located in various locations in critical infrastructures responded by taking real-time decisions related to building including alerting occupants. Also, relevant information about the building (e.g. structural stability information as well as Building Information Model) is transmitted in real-time to city disaster management command centre and relevant agencies. Local emergency responders including Emergency Medical Services (EMS), policemen and fire-fighters immediately arrive at the disaster site. A mobile coordination centre is used to provide necessary collaboration and communication support for field operatives. It serves as a central hub for information collected from different sources including that collected from field responders (e.g. rescue team or access blockage locations, engineer’s report on damage/infrastructure assessment, resources required), Geospatial Information Systems (e.g., site and various infrastructure maps), pre-disaster conditions (BIM model), as well as physical and visual sensors (e.g. during disaster or post-disaster conditions). This information will feed into information processing, data analysis systems and will result in a better coordination and response and will support strategic level decision making.

In this scenario, a collaborative system of autonomous unmanned wireless antennas, acting similar to an ants’ colony communication model (Aldunate et al., 2005), is deployed in the affected area. High reliability and speed of messages spread, based on epidemic multicast protocols allows the system to trigger an early response process. This help to reducing the time gap until federal agencies could arrive to manage the disaster relief operations. First response engineering teams undertake damage reconnaissance operation to size-up current situation and collect information from multiple perspectives to facilitate decision making. These teams first perform an initial triage assessment of the damaged area to prioritize the order of the response operations. Once the first response engineering teams have completed their operations, engineering teams come into the affected zone and perform a rapid building assessment. Aerial Reconnaissance techniques and Satellite imagery is also used to provide an initial assessment of the situation. As time is of essence during initial search and rescue operations, a Segway-based mobility platform is used to enable responders to traverse a large area in a relatively short period of time for the initial triage assessment. Mobility platform is augmented with image/video capturing devices and captured data is transmitted in real-time to on-site command post using mobile ad-hoc networks. Such real-time communications is crucial in order to ensure rescuers’ safety and expedite and support the decision making process by developing high levels of Situation Awareness in early stages of the disaster. The information gathered also serves as a basis for spatially prioritizing the search and rescue operation and assigning roles to all responders.

At the onset of the disaster, a rapid assessment by engineering teams is undertaken is to consider feasibility of performing search and rescue operations within affected buildings. These assessments are undertaken by structural specialists and are based on ATC-20 (Applied Technology Council Rapid Evaluation Safety Assessment) specifications. Civil Engineers can also access Building Information Model (BIM) and other pre-

disaster related data from building black-boxes. Meanwhile during-disaster or post-disaster collected data (through visual and physical sensors) will provide the pre and post-disaster status of the building. The discrepancies between these two datasets will be measured and reported back to engineers. Based on their prior experiences and knowledge, engineers will be able to conduct a better assessment on the impact of the disaster on built environment. Such information is critical to support search and rescue operations.

3. TECHNOLOGY REVIEW

Section 2 described a chaotic, inhospitable, stressful, and life-threatening scenario. This Section elaborates on how early collaborative preparedness, response and recovery processes, as facilitated by the CP2R-based technological solutions could play a critical role in reducing the disaster consequences and improving coordination, collaboration as well as communication among first responders during response and recovery operations.

3.1. Geospatial Information Systems (GIS) for Disaster Response

Geospatial Information Systems (GISs) plays a critical role in spatial analysis to help develop high levels of situation awareness and facilitate critical decision making. GIS can be used during all four phases of disasters including preparedness, response, recovery, and mitigation. During the preparedness phase, spatial data and geospatial analysis services are to be prepared and deployed. Real-time data collection, integration, and analysis can be performed based on GIS during the response phase, while during the recovery phase large scale spatial planning and progress monitoring for repair of infrastructure and housing can be executed. During the mitigation phase, simulation models and cost analysis can be studied through visualization and comparison in GIS to have alternative disaster mitigation plans for future disasters.

A resource allocation optimization application has been developed under the CP2R project. Prior to disasters, resources, facility locations, and road network data are geo-coded into geospatial databases. After the disaster, the application takes destinations and traffic conditions as inputs, and analyzes the updated road network data for optimal allocation routes and resource distribution decisions. The application is automated for easy and efficient use under stressful and complex conditions. Moreover, different optimization models can be plugged into the system for different scenarios for resource allocation. Figure 1 illustrates GIS applications for supporting decision making during disasters. Firstly, spatial data critical to disaster response is prepared prior disasters. During disasters, graphical representation of collected spatial information, traffic conditions and disaster sites, is done using GIS. Also, GIS facilitates critical decision making and emergency response planning through services such as facility location selection and emergency route finding for optimal resource allocation.

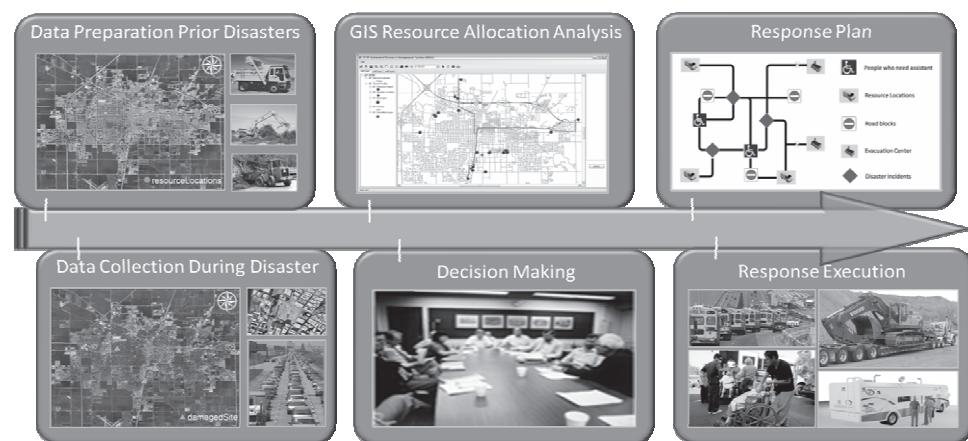


Figure 1: Applications of GIS in Urban Disaster Response and Recovery

3.2. RFID/Mobile Ad-hoc Networks for building assessment

Building assessment is one of the key tasks undertaken by the engineering workforce during Urban Search and Rescue operations (US&R) during disaster response and recovery operations (McGuigan, 2002). As part of the CP2R research, next generation disaster resilient Radio Frequency Identification (RFID) technology was employed to support assessment of building conditions and status of rescue operations.

The rationale of tracking building conditions during Urban Search and Rescue operations is twofold. Firstly, responders, entering buildings need to know which parts of building are structurally safe and without hazardous materials. Secondly, identifying buildings that are safe for re-occupancy can reduce overall chaos and allow staging areas for people dispersed from their houses. Apart from the structural assessment markings, building assessments also include information like potential victim location and number of victims rescued. In the existing practice, building assessment information is posted on buildings with the help of spray paints. Recording assessment information using spray paints has many limitations including poor visibility in foggy/smoky conditions. Also, this information is not recorded in computers resulting in lack of overall situation awareness about the search and rescue process. Forms containing critical building assessment information are submitted only towards end of an operation cycle causing delays in communication. However, for optimal resource allocation, it is imperative that decision makers are made aware of site conditions as quickly as possible. During disasters such real-time access is often made difficult because of the failure of pre-existing infrastructures such as telecommunication networks. As part of the CP2R project, a Building Assessment System is developed using Mobile Ad-hoc Networks (MANETs) as a data based communication system. The system uses long range Ultra High Frequency RFID tags to store information and MANETs to broadcast the captured information. Data can be stored and retrieved from RFID tags by computing devices such as laptops, PDAs, blackberries, etc. These devices share information about building conditions and rescue

progress to create greater awareness. The Building Assessment System displays building assessment information on a geographically referenced map of the area (Figure 2). Making such information ubiquitously available among responders will lead to proactive decision making and better coordination.

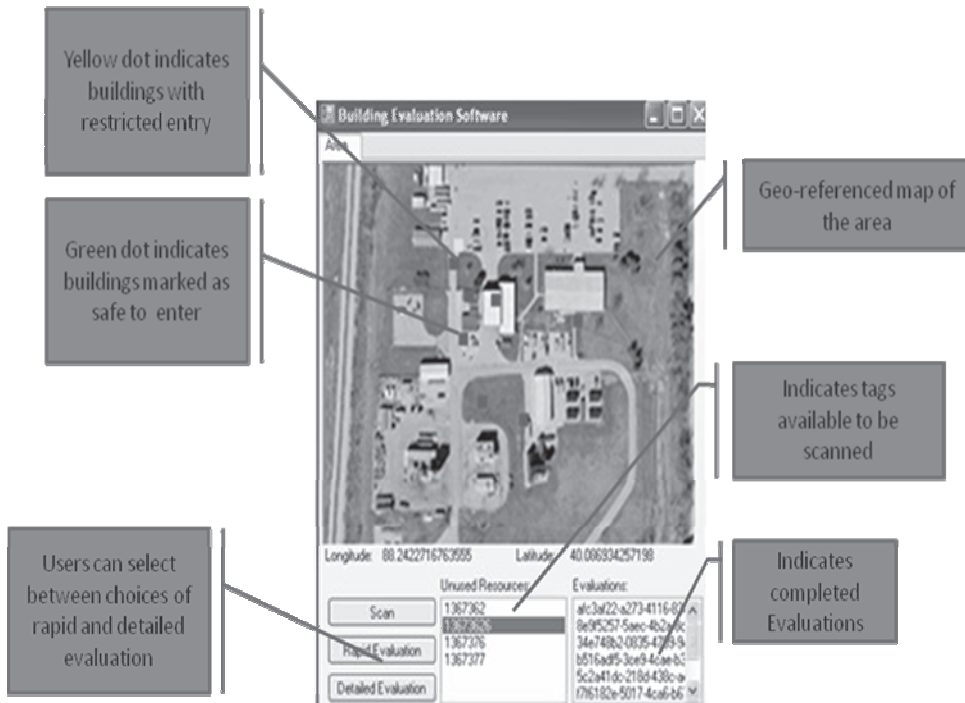


Figure 2: Monitoring Building Assessments using Building Evaluation Software

3.3. Building Black Box

Building black-boxes are ruggedized and disaster resistant information storage hubs which are embedded in buildings to support building assessment during disaster response operations. Building black boxes serve to achieve two pronged objectives: Firstly, to store static building information such as building information model, building drawings, historical maintenance and operations data. Secondly, to provide dynamic building information through disaster resilient sensors such as temperature, humidity, stress/strain in structural elements as well as visual sensors locating personnel/victim locations inside a building. System testing was done to meet disaster resilience, secure communications and resilience requirements. Regular backups of information stored in building black boxes was done at secure data mirroring centers and emergency offices in order to ensure building information availability during incident response. In cases where regular communication infrastructure is not available after disaster events, engineers can access information stored in the black box using a mobile ad hoc networks or through a satellite up-link.

3.4. Reconstruction of the during or post disaster built environment using real-time images or video stream data from disaster site

Visualization of built environment using photographs and videos allow first responders and decision makers - regardless of their level of knowledge and expertise- understand spatial constraints of the disaster site and explore rescue and recovery operation alternatives. In addition, during disaster response and recovery operation, there is a very limited time for assessing the stability of the disaster site. Therefore, reconstruction of the scene based on images could become a good source for during and post disaster *site stability assessment* and act as good *communication* tool among first responders.

Knowing camera pose (location, orientation, and field of view) allows disaster site photographs be placed into common 3D coordinates and consequently disaster responders will be able to virtually explore the scene by moving in 3D scene from an image to another while the special configuration of the images within the 3D scene are preserved. The camera pose information could be retrieved either by GIS or wireless location tracking techniques (Behzadan et al. 2008) or could be recovered by Image-based Modelling (IBM) techniques wherein three dimensional models are reconstructed from a collection of input images based on Structure from motion (SfM) techniques (Pollefeys et al. 2004; Hartley and Zisserman 2004). This visual dataset allows photographs and video stream images of the post-disaster scene to be posed in locations where images were taken.

On the other hand, the BIM model retrieved from the Black box (Section 3.3) allows the pre-disaster situation to be known. Superimposing the reconstructed scene on the pre-disaster virtual model environment, allows the photographs and video snapshots to be registered within the virtual environment. Within such registered environment, images could be analyzed using image processing techniques such as (Brilakis et al. 2006; Varma and Zisserman 2005) and the severity of disaster incident could be assessed. Also within the registered environment, the structural deviations between pre-disaster and post-disaster conditions could be measured and reported to disaster responders.

3.5. Augmented Reality techniques for Disaster Visualization

Once the camera pose is known for each image, the video stream or each photograph would be registered with the 3D model. This in turn creates an Augmented Reality environment wherein the pre-disaster virtual model is superimposed with post-disaster images. Using an Augmented Reality model (Golparvar-Fard et al. 2008) with US Homeland Security Advisory System color coding scheme (2008), different structural or hazardous conditions are visualized. The augmented photographs provide a consistent platform for representing pre-disaster, post-disaster and structural discrepancies information and facilitate communication and reporting processes among first responders.

3.6. 3D laser scanning

During urban search and rescue operations there is little time for a rigorous structural analysis and a limited time to decide the remaining stability of the building and/or the temporally shoring measures required (McGuigan, 2002). The large variety in structural typologies and different levels of damage make it difficult to model simple patterns for building behaviour. LIDAR (Light Detection and Ranging) techniques could provide a quick way to gather building data from the disaster scenario and tools to improve building assessment. Laser technologies serve as a valuable tool to gather real-time information in the response phase of an extreme event.

3.7. Robust Wireless Communication Networks

Need to improve collaboration and coordination in disaster response effort has been highlighted in various studies. Also various pitfalls related to collaboration, such as lack of trust, information sharing, communication and coordination, have been well documented. In the hours and even days following a major disaster, communication is often limited because existing infrastructure may be destroyed or the event may have occurred in an area without infrastructure. Voice service may be severely restricted.

Challenges imposed by disasters emphasize that the collaboration medium provide attributes such as high availability, improved transmission capability, and appropriate information dissemination. To achieve these goals, a reliable and transparent Mobile Ad-hoc Space for Collaboration (MASC) was developed to support collaboration among first response organizations and leverage civil engineers' role during disaster response and recovery operations (Aldunate et al., 2005). MASC was tested through software simulations in a search and rescue exercise at the Illinois Fire Service Institute. The results obtained showed that it is possible to build a system for traditional teams of first responders exhibiting 98% of availability in square areas where the side length is about three times the wireless communication range. Furthermore, the search and rescue exercise allowed the research to confirm results found through simulation runs about availability and to demonstrate that MASC is also portable among different devices, transparent to first responders, and able to adequately manage and disseminate information in disaster scenarios. Such results demonstrate appropriateness of Mobile Ad-hoc Space for Collaboration. Currently we are exploring ways to scale up MASC for large set of response teams, with tools such as Mobile Communication Bridges [Peña-Mora et al, 2004] that would allow responders to communicate reliably and securely.

4. DISCUSSION AND CONCLUSIONS

The paper has highlighted critical and evolving role of emerging technologies in effective disaster management. Application of these technologies to address collaboration, coordination as well as communication and information delivery to field personnel during preparedness, response and recovery is discussed.

Advanced information and communication technologies offer a way to address complex communication, collaboration and decision making problems faced during disaster response and recovery operations. However, design and implementation of these technologies without proper understanding of user requirements/situation may result in poor alignment with end user requirements, which could possibly result in serious consequences.

Another critical issue to ensure effective disaster response is the response of the individual disaster responders on the ground which will ultimately determine how effectively disasters can be dealt with. ICT applications such as those discussed in this paper are required to provide suitable information access and communication capabilities. However effective use of various technological solutions such as those discussed in this paper is highly dependent on individual context disaster responders find themselves in, and this is highly dynamic and situation dependent. Factors that can effect individuals' level of Situation Awareness include location (pose and elevation) of people, places, objects and resources; the activity or status of the individual; and aspects of time, including temporal relationships. It is imperative that ICT solutions are designed keeping in perspective responders' context of use and to enhance individual, organizational and inter-organizational levels of situation awareness. Without such an emphasis on meeting end user requirements full potential of ICT solutions can not be realised. It is also imperative to develop a deep understanding of different types of information required by specific roles at different times to effectively perform their functions during disaster response and recovery operations. A "Socio-behavioral-technical" approach to analysis will provide a much needed perspective to align emerging technological possibilities with requirements of disaster response and recovery operations. Such a comprehensive approach is important because of the phenomenal growth in ICTs which often outpace the rate at which organizations and individuals are adapting to technology.

REFERENCES

- W Aldunate, R., F. Peña-Mora and G. Robinson, *Collaborative Distributed Decision Making for Large Scale Disaster Relief Operations: Drawing Analogies from Robust Natural Systems*, Complexity, Wiley, Hoboken, NJ, Vol. 11, No. 2, December 2005, pp. 28-38.
- McGuigan, D. M. (2002) *Urban Search and Rescue and the role of the engineer*. M.S. thesis, University of Canterbury, New Zealand
- Midkiff, S.F and Bostian, C.W. (2004) *Rapidly-Deployable Broadband Wireless Networks for Disaster and Emergency Response*”,
- Behzadan A. H., Aziz Z., Anumba C., and Kamat V. R. (2008), *Ubiquitous Location Tracking for Context Specific Information Delivery on Construction Sites*, *Automation in Construction*, 17(6), Elsevier Science, New York, NY, 737-748.
- Pollefeys, M., Van Gool, L., Vergauwen, M., Verbiest, F., Cornelis, K., Tops, J., and Koch, R. (2004). *Visual modeling with a hand-held camer*. *Int. J. of Computer Vision*, 59 (3), pp.207-232.

- Hartley, R. I., and Zisserman, A. (2004). *Multiple View Geometry*. Cambridge University Press, Cambridge, UK.
- Brilakis, I., Soibelman, L., and Shinagawa, Y. (2006) *Construction Site Image Retrieval Based on Material Cluster Recognition*, Journal of Advanced Engineering Informatics, Elsevier Science, Volume 20, Issue 4, October 2006, Pages 443 – 452
- Varma M. and Zisserman A. (2005). *A statistical approach to texture classification from single images*. International Journal of Computer Vision: Special Issue on Texture Analysis and Synthesis, 62(1--2):61-81, April 2005.
- Homeland Security Advisory System (2008) *Color coding for different threat condition*
<http://www.whitehouse.gov/news/releases/2002/03/20020312-5.html> (last accessed Aug 12, 2008)
- Golparvar-Fard, M., Peña-Mora, F., Arboleda C. and Lee, S.H. (2008) *Visualization Of Construction Progress Monitoring With 4D Simulation Model Overlaid On Time-Lapsed Photographs*, ASCE Journal of Computing in Civil Engineering, Graphical 3D Visualization in Architecture, Engineering, and Construction Special Issue (Under Publication)

PRIOR DISASTER REVIEW SYSTEM FOR DISASTER ASSESSMENT IN KOREA

WAON-HO YI, JAE-HYUN SHIM and JAE-HAK CHUNG
National Institute for Disaster Prevention, Korea
whyi1208@nema.go.kr

ABSTRACT

Korea has been involved risk due to frequent typhoon and heavy rain. Specially, urbanization and industrialization has increasing hazard vulnerability. In other words, due to the natural and man-made causes, disasters occur frequently every year. Therefore it is necessary that we should establish the countermeasures to save the lives and properties. And also, to reduce the disaster damage from initial period in development process, we have to execute the Prior Disaster Review System (PDRS).

Based on the Natural Disaster Countermeasures Law, the PDRS program as a regulation for prevention of disaster has enacted. Major items which the PDRS treats are risk factors topographically and impacts of near areas or facilities due to development. Through this system, developers have to construct flood mitigation facilities to reduce increased damages of flooding due to development project. For example, The PDRS program prevents the facilities which population could be concentrated from being planned and enforces to establish adequate countermeasures such as a pumping station, a detention facility, a drainage way.

In this paper, we are to introduce the definition and progresses of PDRS program. Also, we will explain the future activities for effective operation. This program will contribute to management the flood disasters and to reduce flood damage in urbanized watershed.

1. INTRODUCTION

In the "Natural Disaster Countermeasures Law" in Korea, the natural disasters classified as typhoon, flood, torrential rain, wind storm, drought, blizzard, and earthquake etc. But over 95% of damages are caused by floods with typhoons & torrential rains. The average annual economic damage of natural disasters was 2 billion dollars, and 119 persons were dead (Table 1).

Especially, in 2002, the largest scale of flood damage was caused by flash floods with typhoon Rusa. Total amount of damages were over 7 billion dollars and the government had to expend 9 billion dollars for recovery.

Table 1: Annual Damage of Natural Disasters during last 10 years

| Year | Death (person) | Evacuee (person) | Inundation (ha) | Public Facilities (million US \$) | Damages (million US \$) |
|---------|-------------------|---------------------|--------------------|--|-------------------------------|
| 1997 | 38 | 6,296 | 45,773 | 184 | 240 |
| 1998 | 384 | 30,308 | 91,629 | 1,378 | 1,777 |
| 1999 | 89 | 26,656 | 76,128 | 1,084 | 1,398 |
| 2000 | 49 | 3,665 | 53,092 | 596 | 725 |
| 2001 | 82 | 4,165 | 20,012 | 432 | 1,419 |
| 2002 | 270 | 71,204 | 61,579 | 5,575 | 6,929 |
| 2003 | 148 | 63,133 | 51,412 | 3,434 | 4,886 |
| 2004 | 14 | 8,814 | 56,903 | 539 | 1,285 |
| 2005 | 52 | 9,914 | 26,782 | 456 | 1,073 |
| 2006 | 63 | 2,883 | 34,759 | 1,692 | 1,942 |
| Average | 118.9 | 22,703.8 | 51,806.9 | 1,537 | 2,167.4 |

cf) currencies are based on 2006

2. CLASSIFICATION OF FLOOD DAMAGE CAUSES

The causes of flood damage in Korea can be divided into two categories, natural and human induced factors. The natural factors also have two categories, meteorological and geomorphologic factor. Due to the seasonal concentration of rainfall, two thirds of the annual rainfall is concentrated in summer, on the other hands, drought occurs frequently in other seasons. In the geomorphologic aspects, about 70% of the mountainous area covers the total area of Korean peninsula. When it rains; the flood discharges are concentrated at the downstream area rapidly. From such natural factors, the flash flood event, small or large scale, occur frequently every year. The effects of development projects on hydrologic systems have aggravated the vulnerabilities of flood disaster. Highly condensed developments in Korea took economic growth effectively, but, nowadays as the shadow of welfare, it also took lots of disaster causes.

Urbanization, the development for business and residential purposes, has affected the land uses. In the process of urbanizing a basin, man converts natural pervious areas to impervious surfaces. These area cause an increased volume of runoff, the surface is usually smoother thereby allowing more rapid drainage, and depression storage is reduced. The other cause of flood event is the climate changes and global warming originated from combustion of fossil fuels and deforestation. Due to the climate change, flash flood occurs frequently and historical record of rainfall phenomena is renewed every year. The Table 2 show the rapid changes of historical rainfall records, and some of the marked (*) records below are not officially recognized.

Table 2: Rapid changes of historical rainfall events in Korea

| Classification | Historical Records |
|-------------------------|--|
| Maximum Hourly Rainfall | Up to 1998 : 118.6 mm/hr (Seoul, 1942) 1998 : 145 mm/hr (Suncheon, JiRi Mountains) 1999 : 116*mm/hr (Buyeo, Chungnam) 2008 : 106*mm/hr (Busan, Kim-Hae) |
| Annual Rainfall | In 1970 : 1,159 mm In 1980 : 1,274 mm In 1990 : over 1,360*mm |

3. SIMULATION ON RUNOFF DUE TO DEVELOPMENT

ILLUDAS (Illinois Urban Drainage Area Simulator) model is applied to estimate the hydrological changes due to landuse variations for urbanization at Seoul and two small basins, Yongsan, Seongnae. The frequencies of design rainfall are 10, 30, 50 years and Huff's quartile method and instantaneous method (I.I.M.) are used to distribute design rainfall. To check the characteristics of runoff variation, the basins are classified into upper, middle, and lower sub-basins. The Figure 1 explains the hydrographs of each basin, and it is obvious that Seongnae basin already has potential of flooding at the 10 year rainfall.

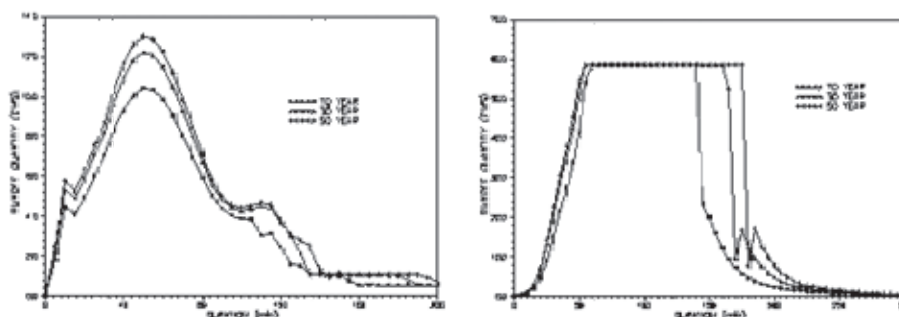


Figure 1: Hydrograph of Yongsan(left) and Seongnae(Right) basin

To estimate the runoff increment due to urbanization, the present status and future land use planning of each basin are investigated. The Table 3 and 4 show the total increments of runoff for each basin. In the table, the unit of land use is percentage of impervious area and total runoff is tonnage.

The difference of total runoff between two basins is obvious from its dependence on drainage area and basin morphology. To identify the damage potential by urbanization, total runoff is converted into unit increment of runoff (see Table 5). Table 5 shows the net total runoff increment by urbanization at 30year rainfall event and its unit is tonnage per hectare.

Table 3: The runoff increment due to urbanization (Yongsan basin)
(unit : tons)

| Return Period | | 10 year | | 30 year | | 50 year | |
|---------------------------------------|---------------|---------|--------|---------|--------|---------|--------|
| Time Distribution Land Use Changes | | Huff | I.I.M. | Huff | I.I.M. | Huff | I.I.M. |
| Upper basin | Present(70%) | 58,390 | 58,266 | 71,418 | 71,349 | 77,363 | 77,264 |
| | Land Use(80%) | 58,654 | 58,546 | 71,682 | 71,628 | 77,627 | 77,545 |
| | Land Use(90%) | 58,918 | 58,826 | 71,945 | 71,909 | 77,891 | 77,825 |
| | Land Use(95%) | 59,050 | 58,967 | 72,076 | 72,049 | 78,023 | 77,964 |
| Middle Basin | Present(85%) | 58,390 | 58,266 | 71,418 | 71,349 | 77,363 | 77,264 |
| | Land Use(90%) | 58,415 | 58,292 | 71,443 | 71,374 | 77,387 | 77,289 |
| | Land Use(95%) | 58,439 | 58,317 | 71,467 | 71,399 | 77,412 | 77,315 |
| | Land Use(97%) | 58,449 | 58,345 | 71,477 | 71,410 | 77,421 | 77,325 |
| Lower Basin | Present(85%) | 58,390 | 58,266 | 71,418 | 71,349 | 77,363 | 77,264 |
| | Land Use(90%) | 58,410 | 58,287 | 71,438 | 71,369 | 77,383 | 77,285 |
| | Land Use(95%) | 58,430 | 58,308 | 71,467 | 71,390 | 77,403 | 77,306 |
| | Land Use(97%) | 58,436 | 58,317 | 71,477 | 71,399 | 77,411 | 77,314 |

Table 4: The runoff increment due to urbanization (Seongnae basin)
(unit : tons)

| Return Period | | 10 year | | 30 year | | 50 year | |
|---------------------------------------|---------------|---------|---------|---------|---------|---------|---------|
| Time Distribution Land Use Changes | | Huff | I.I.M. | Huff | I.I.M. | Huff | I.I.M. |
| Upper basin | Present(60%) | 401,392 | 400,741 | 492,454 | 492,077 | 534,458 | 533,187 |
| | Land Use(70%) | 402,234 | 401,615 | 493,295 | 492,956 | 535,378 | 534,067 |
| | Land Use(80%) | 403,078 | 402,493 | 494,136 | 493,834 | 536,289 | 534,950 |
| | Land Use(90%) | 403,922 | 403,372 | 494,978 | 494,713 | 537,136 | 535,832 |
| Middle Basin | Present(70%) | 401,392 | 400,741 | 492,454 | 492,077 | 534,458 | 533,187 |
| | Land Use(80%) | 404,793 | 403,990 | 495,577 | 495,369 | 537,751 | 536,474 |
| | Land Use(90%) | 408,496 | 407,287 | 499,248 | 498,662 | 540,884 | 539,762 |
| | Land Use(95%) | 410,210 | 408,937 | 501,053 | 500,309 | 542,448 | 541,406 |
| Lower Basin | Present(75%) | 401,392 | 400,741 | 492,454 | 492,077 | 534,458 | 533,187 |
| | Land Use(80%) | 401,488 | 400,834 | 492,548 | 492,177 | 534,576 | 533,287 |
| | Land Use(85%) | 401,584 | 400,928 | 492,643 | 492,277 | 534,695 | 533,386 |
| | Land Use(90%) | 401,679 | 401,022 | 492,737 | 492,377 | 534,813 | 533,486 |

Table 5: The Total Runoff Increment due to Urbanization (30year event)
(unit : tons/ha)

| Classification | Upper Basin | | Middle Basin | | Lower Basin | |
|----------------|-------------|--------|--------------|--------|-------------|--------|
| | Huff | I.I.M. | Huff | I.I.M. | Huff | I.I.M. |
| Yongsan | 125.71 | 133.33 | 125.64 | 132.77 | 125.00 | 131.25 |
| Seongnae | 122.03 | 126.67 | 130.81 | 126.81 | 120.00 | 116.88 |

4. INTRODUCTION OF PDRS

4.1 BACKGROUNDS

In Korea, besides the natural vulnerabilities of flood caused by the meteorological and geo-morphological factors, the condensed development has aggravated flood risks. The development certainly induced the land use changes and the urbanization transfers green land to impervious areas such as roads and buildings inevitably. In the hydrological aspects, the development reduced the infiltration, interception, and evapotranspiration, so the direct runoff increased and time of concentration is shortened (Figure 2). And, in the economic point of view, land owner have a right to develop for one's own wealth, but the hazards caused by the development can affect on other persons who live in the lower part of development sites.

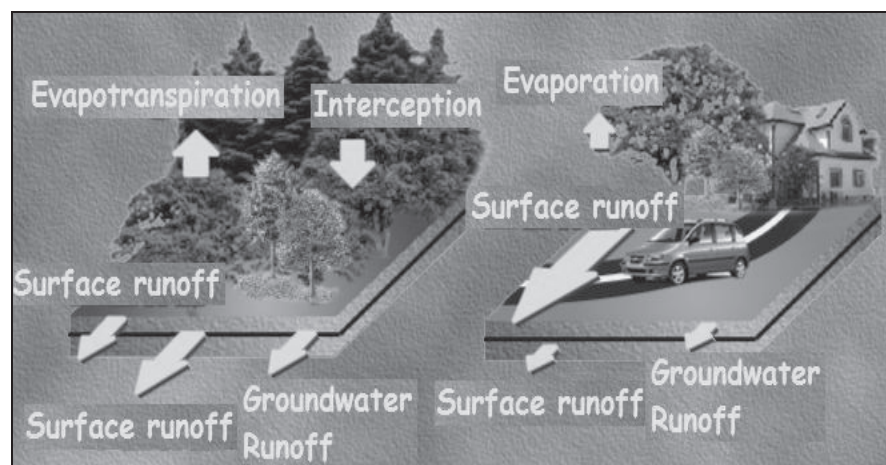


Figure 2: The changes of runoff phenomena due to development

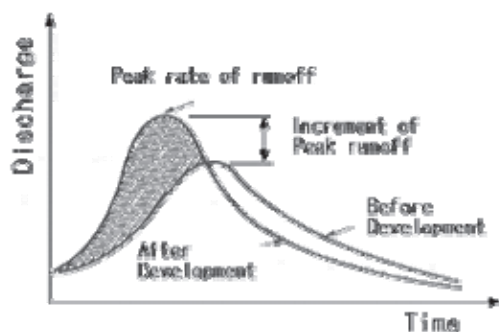


Figure 3: The changes of hydrograph due to development

4.2 DEFINITION

Korea has executed a DIA (Disaster Impact Assessment) program since 1996. The DIA program is defined as a regulation which is to minimize the vulnerabilities of flood due to development through the preliminary comprehensive assessment.

This program is applied to specified development projects larger than 30,000m². Therefore the DIA can't be applied at the initial stage of developing process. Also, it can't assess various projects such as road, railway etc. In addition, the DIA is only applied for implemental developing projects when all the administrative process is finished. So, DIA could assess only for implemental design process for limited developing area.

Because of above-mentioned limited states, Korea has executed a PDRS program since 2005. The PDRS program reduces the disaster damage from initial period in development process. Based on the Natural Disaster Countermeasures Law, the PDRS program as a regulation for prevention of disaster has enacted.

Many disaster prone areas in Korea would not be damaged seriously if there were reconsiderations of disaster impacts when they were planned.

4.3 PROCEDURE OF PDRS

The procedure of PDRS starts with submitting the plan of development. This plan is delivered to director of National/Local Headquarters and assessed by Council for PDRS and Related Organizations. Council for PDRS is comprises 76 members drawn from professor, engineer, researcher, etc.

The main items of assess are as follows;

- 1) Disaster risk factors by surrounding circumstances
- 2) Disaster impacts to near areas or facilities due to development
- 3) Disaster mitigation countermeasures proposed by developer

Finally, developer should notify of an assessment result and complete the final report. Details of procedure are informed at Figure 5.

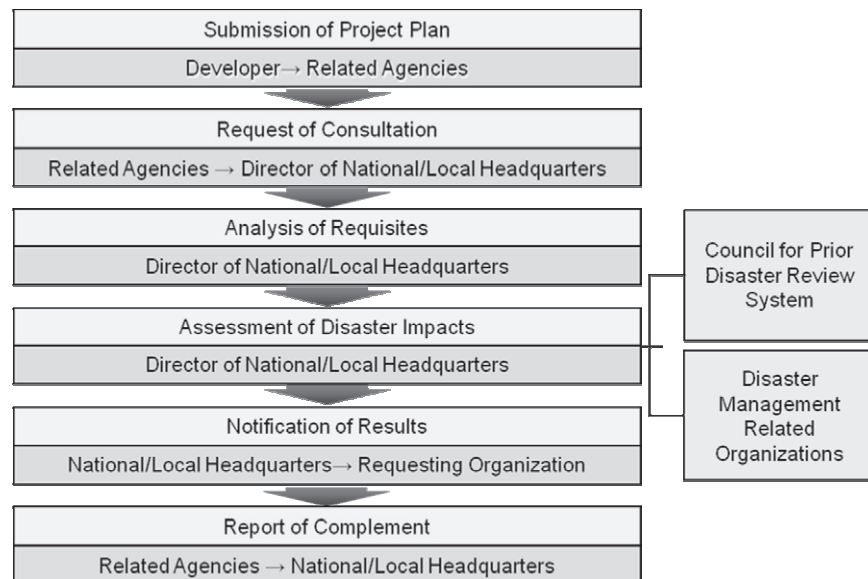


Figure 5: Procedure to execute PDRS

4.4 Items of PDRS

In this chapter, we suggest important key points for disaster assessment by landuse type.

4.4.1 Urban Areas

Urban development projects have to be assessed about disaster vulnerability. Urban areas involve a lot of risk. The typical items are low-lying areas of densely populated districts and low land of the neighborhood river.

Therefore, we are ready for disaster response by PDRS. For example, we will construct pumping stations, detention facilities and drainage channels to prevent inundation.



Figure 6: Flood at urban area

4.4.2 Coast Areas

We check the response plan for frequent storm surge to ensure that the residents are safe from disasters. Particularly, we analyze the sea level rising in reclaimed land.

As mentioned above analysis, we construct multi-purpose detention, park and sports facilities in storm surge prone areas. And we consider how to cope with the erosion of seashore.



Figure 7: Surge storm at coast area

4.4.3 Mountainous Areas

In the geomorphologic aspects, the mountainous area covers about 70% of the total area of Korea peninsula. So, many development plans lie in mountainous areas. Therefore it is very important that we assess the vulnerability of disaster. For example, we takes measures against landslide, soil yield and sediment runoff.

Based on PDRS program, we restrict the form of large-scale cut slopes and suggest the plan of countermeasures to minimize the impact of mountainous development.



Figure 8: landslide at mountainous area

5. CONCLUSIONS

Development changes natural land into impermeable areas such as asphalt or concrete. Hence, it brings decrease of infiltration amount of rainfall. As a result, amount of direct runoff is increased. Peak rate of runoff is drastically increased and its concentration time is shortened rather than before development. This may cause flooding damage. In addition to that, land

slide is affected by amount, intensity, frequency of rain and soil condition, vegetation and inclination of slope.

Accordingly, forecast and analysis of causes of disaster due to development should precede business to establish adequate reducing method. In order to accomplish this, we have enforced PDRS program.

Henceforth, as an aspect of advanced preventing, it will be necessary for comprehensive and systematic evaluation.

REFERENCES

- Akan, A. O., 1993. *Urban Stormwater Hydrology -A Guide to Engineering Calculations-*. Technomic Publishing Co. Inc.
- Chen, C. N. and Wong, T. S. W., 1994. Critical Rainfall Duration for Maximum Discharge from Overland Plane: Closure. *Jour. of Hydraulic Eng., ASCE*, Vol. 120, No. 12, 1484-1486.
- Debo, T. N. and Reese, A. J., 1995. *Municipal Storm Water Management*. CRC Press, Inc.
- Huff, F. A., 1967. Time Distribution of Rainfall in Heavy Storms. *Water Resources Research*, Vol.3, No.4, 1007-1019.
- Keifer, C. J. and Chu, H. H., 1957. Synthetic Storm Pattern for Drainage Design. *Jour. Hyd. Div., ASCE*, Vol.83, No.4, 1-25.
- Lee, J. T., Yun, S.E., and Lee, J. J., 1993. Critical Duration of Design Rainfall for Detention Pond with Pump Station. *Sixth International Conference on Urban Storm Drainage*, Niagara Falls, Ontario, Canada, pp.312-317, Sep. 12-17, IAWPRC and IAHR.
- Lee, J. J. et. al., 1996, A Study on the Hydrologic Design of Detention Storage Ponds in Urbanized Area. *Korean Journal of Hydrosciences*, Vol.7, 21-35.
- Shim, J. H., 1994. The Evaluation of Runoff variation due to Urban Development (with Korean). *The Korea Local Administration Review*, Vol. 8, No. 4, 147-165.
- Shim, J. H. and Lee, J. S., 2000. *Development of Guidelines on DIA Report*(with Korean). National Institute for Disaster Prevention.

MANAGEMENT OF URBAN DISASTER WITH SPECIAL EMPHASIS ON FRESH WATER SCARCITY AND SURFACE WATER POLLUTION IN DHAKA CITY

MURSHED AHMED

Director, Directorate of Project Evaluation
Bangladesh Water Development Board, Bangladesh
mahmed_3ch@yahoo.com

ABSTRACT

Dhaka, the capital of Bangladesh, is a Mega-City accompanied by a compelling problem of accommodating more people in a limited piece of land and thereby creating excessive demand for dwelling houses and industries which result in construction of high-rise buildings and growing slum areas simultaneously. These give rise to environmental hazards along with paucity of fresh water for household and industrial use. Like many other cities in Asian developing countries, Dhaka is exposed to serious threats of versatile urban disasters viz. seismic, flood, cyclone, fire and the like. Now, environmental hazard in particular has become a community concern in Dhaka Metropolitan City. Non-use of water gives environmental benefits to city population which is awfully absent or decreasing in Dhaka. The environment within and around urban areas are worsening day by day due to unplanned and improper use of water and land. Ensuring safe and reliable water supply has been one of the major urban challenges. The main sources of surface water of Dhaka city are the river Buriganga and other peripheral rivers namely, Shitalyakra, Turag and Balu which are extremely polluted by discharge of more than 1.3 million cubic meters of untreated effluents and 0.5 million cubic meters of sewage daily. Most of these waters are unusable for human and other living organism. These polluted waters can no longer be considered suitable for chemical treatment. On the other hand, the riverbanks and beds are encroached by the illegal occupants. The scarcity of surface water, therefore, results in increasing pressure on ground water abstraction. Groundwater level of Dhaka city is alarmingly lowering down by 2 to 3 meter every year because of groundwater mining which may result in land subsidence. In such a situation if water of surrounding rivers is not improved both in quality and quantity, the capital city will not remain environmentally fit for human habitation. The situation may improve through co-ordination and integration of different institutions engaged in urban development activities under the umbrella of an apex body for emergency mitigation of disaster. The present paper attempts to discuss major essential aspects of human-induced urban disasters with special emphasis on fresh water scarcity and surface water pollution, highlighting measures for mitigating them through appropriate Environmental Management Plans (EMPs) including awareness building,

active community participation, institutional development and strict enforcement of regulatory and legislative measures. Recommendations are prescribed for judicious use of land and water with proper planning and management of water resources using advanced technologies.

1. INTRODUCTION

Mankind is suffering from various kinds of disasters caused by flood, tropical cyclone, storm surge, tornado, river erosion, draught, earthquake, arsenic and environmental pollution. The environment within and around urban areas like Dhaka city are deteriorating day by day due to over abstraction of ground water and pollution of surface water of the nearby rivers and unplanned use of land. Dhaka is already over-crowded by the dwelling houses, government offices and installations and infrastructures. The socio-economic conditions of people of the entire country depend greatly on Dhaka for various reasons. Dhaka is one of the mega-cities of the world which has already been rated as the environmentally most polluted one. City dwellers have been facing acute scarcity of safe drinking water for shortage of supply against demand. In the backdrop of rising demand for water in domestic, industrial and high-rise buildings and commercial centres, a new paradigm shifts is required in the light of globalization. So, it will be a great challenge for the concern citizen to save the city from the threat of environmental degradation. This paper focuses on and responds to major urban disasters regarding water related issues. Rapid growth of population in a given area is the main reason for the multiple problems in our city. Groundwater level of Dhaka city is now alarmingly lowering down by 2 to 3 meter every year (IWM, 2006) resulting from mining and disaster threats of land subsidence which has become alarming for the urban planners. Time may come when the city will fail to bear the burden of the increasing population with severe impact of environmental imbalance that will lead a special type of disaster herein termed as human-induced disaster. How this type of disasters can be managed with efficient and emergency response system is the main focus of the paper.

2. THEME OF THE STUDY

Access to fresh water resources is a global concern since the beginning of human civilization as urban centres started growing and technology advanced the issue got more importance in course of time. In this paper, water refers to surface fresh water from such places as rivers, lakes and wetlands as well as underground water sources. For the last few decades secured, safe, reliable and stable supply of water has been one of the leading economic and social challenges faced by the Asian developing countries as their population, economy, urban areas and mega-cities grow geometrically. Water quality problems are becoming increasingly serious day by day. All surface water bodies within and around the urban industrial centres are now highly polluted. Surface and ground water is also becoming increasingly contaminated within and around growth centres of population and industrial

areas. The major factors are human activities and interventions which include encroachment on the river bank, flood plains and low lying areas, sewage and solid waste disposal, insufficient water supply and sanitation, industrial waste disposal, upstream diversions and abstractions (Ahmed, 2004). Waste assimilation capacity of the rivers is decreasing day by day and micro-organism is being destroyed due to increasing water quality deterioration. Now Dhaka has also a large slum population that will create problems for getting safe drinking water, inadequate sanitation and water shortages. The urban poor have become the worst sufferer of unplanned and irrational urbanization. The main objectives of the study are to highlight mechanism for mitigating fresh water scarcity and polluted surface water through good governance by coordinated and integrated approach of different agencies and institutions, and Participatory City Management (PCM) to improve the social, economic, physical and biological environment significantly.

3. HISTORICAL BACKGROUND

Bangladesh is historically a riverine country with important ecological zones. A riverine environment shapes the life-style of its societies along its river banks. From time immemorial nations, societies, cities as well as civilization have grown near rivers. The city of Dhaka was established by the Mughals on the bank of the river Buriganga in the early 17th century considering its immense potentiality of growth and development. Since then this Buriganga river has been serving the people of Dhaka city with its entire resources with a flourishing river port. Undoubtedly Dhaka, the capital of Bangladesh- has an exciting history and a rich culture. Historically known as the city of mosques and muslims, it started attracting travellers from far and near from time immemorial. According to history, it was founded in 1608 AD as the seat of imperial Mughal Victory of Bengal. It became a trade centre for the British, the French and the Dutch before coming under British rule in 1757. It was again named the capital of East Bengal in 1905 and became the capital of East Pakistan after the partition of the Indian subcontinent in 1947. As the capital of Bangladesh since 1971, Dhaka has now grown into a dynamic city offering opportunity for millions of migrants with an area of about 256 square kilometre (GOB, 2003) excluding peripheral towns and slum dwelling places. Dhaka's population is currently around 12 million and is projected to grow to 20 million in 2020, making it the worlds third largest city (World Bank, 2007). Possessing a blend of old and new architectural trends, Dhaka is developing fast as a modern metropolitan city. Dhaka is surrounded by Buriganga, Turag and Sitalakhya rivers and inter-connected canals which used to form a life-line for city residents in the past. During the last twenty years, a convergence of unregulated industrial units, rapid rural to urban migration, encroachment of the rivers and channels, disposal of untreated pollutants to the rivers, unplanned road network and non-compliance of environmental regulations have all degraded surface water quality. Developers of lands and buildings have made many of the canals non-existent damaging the drainage system and created water logging. The surface water of the rivers surrounding the

Dhaka city is meagre and polluted during the dry season. Most of the surface waters are environmentally unfit for any human use and living organism. The city authorities could not prepare and implement any effective urban planning to keep the rivers free from water pollution and encroachment of the perennial water bodies and channels even till recent days.

4. NEED FOR THE STUDY

A pollution-free environment is vital for a decent standard of living. Availability of fresh water and healthy environment is a fundamental right of the city dwellers. Unfortunately, with rapid urbanization and industrialization, urban governance, the provision of adequate safe water, land and housing remained below the standard. Poverty has further been aggravated the situation with increasing number of slums and squatters in metropolitan cities. Given the magnitude of the problems, the present study emphasizes the need for strategies for accessing safe water towards socio economic enhancement. Emphasis has also been given on planned development of urban areas by strengthening environmental governance through involvement of all the stakeholders for achieving environmental sustainability.

5. RISK PARAMETERS AND FACTORS

- Overpopulation and extreme poverty
- Unabated urbanization and industrialization
- Non-judicious use of natural resources
- Water and air pollution
- Groundwater depletion
- Inadequate utility services
- Untreated industrial waste and improper treatment of sewage/garbage
- Contamination of surface water and groundwater
- Illegal encroachments on public land and rivers
- Absence of good governance
- Immoral political and bureaucratic involvement
- Lack of appropriate legal action
- Lack of proper zoning and landscape design
- Lack of application of the state-of-art technologies

5.1 Conditions and Challenges

Massive and unprecedented urbanization in Dhaka has produced new types of water and wastewater related problems and challenges. The immediate needs in terms of management of demand for and supply of fresh water for the city for environment friendly conditions are as follows:

- Augmentation of fresh water supplies from outside Dhaka city from both surface and ground water sources to arrest continuing falling of groundwater level and increase water supply. Water treatment plants and well fields outside Dhaka will be required.
- All waste water needs to be treated before disposal of the nearby river. All residential houses, commercial places and industrial units within Dhaka need to be connected with sewerage disposal system.
- Proper land utilization planning keeping provision for open area for recreation and water bodies need to be provided.
- Proper land use planning and implementation of plan need to be controlled by participation of city dwellers and public organization through a strong corporate body.
- The city area must be extended wherever possible.

Other continuing works are:

- Compliance of environmental legislation
- Improving aesthetics and opportunities for recreation
- Rationale use of natural resources
- Maintaining the riverine eco-system
- Political will and consensus
- Promoting institutional co-ordination
- Improving legal and regulatory framework

The present and future challenges faced by the Dhaka city are multifaceted that need to be managed efficiently for reducing risks and vulnerability. These challenges are posing threat for optimisation and sustainable management of water resources and poverty reduction strategies. The dynamics of water for growth are extremely complex and highly dependent on driving forces like physical, technological, cultural, political, social and economic priorities.

6. SOCIO-ECONOMIC IMPACTS OF WATER POLLUTION

Dhaka suffers from water pollution, scarcity of pure drinking water, sewage management, water logging etc. which are posing a serious threat to public health, ecosystems and socio-economic life of the people. Pollution of the rivers and the change in the environment has seriously influenced the livelihood and living pattern of the city dwellers of Dhaka. Dhaka has not been able to keep pace with the needs of the rapidly transforming social and economic demands of the growing population. Most migrants come from rural areas and their contribution to economic growth is significant, as they provide essential services to garments factory, housing, manufacturing services etc. Dhaka has emerged as a mega city in the new millennium (World Bank, 2007). Dhaka, being a very large and dynamic city, has drawn substantial industrial investments, particularly in the Ready Made Garment industry, which has created demand for workers and services. This migration, however, also adds tremendous strain on an already crowded city with limited inhabitable land and a low level of public services. The socio-

economic characteristics of the city now include excessively high land prices, a large slum population, poor quality housing, traffic congestion, water shortage, poor sanitation and drainage, irregular electric supply, increasing air pollution and poor governance. There is no urban planning to protect peripheral rivers and channels which would accommodate the drainage water and to assimilate the waste discharges. Various studies and reports reveal that the impact of river pollution is now at an alarming level. Industry alone is responsible for discharge of more than 1.3 million cubic meters of effluents into the rivers everyday compared to the daily discharge of 0.5 million cubic meter household waste water (Daily Star, 2008). As a result, natural resources and social life are severely endangered. Due to bad smell and unhygienic physical environment, people in large number, are migrating from river side to other places. Inhabitants have become socially isolated from their relatives and friends. People are less interested to build relationship with the people living along river sides.

Three major types of diseases: skin diseases, diarrhoea and dysentery are spreading sporadically with industrial water pollution. Moreover, 20 types of illness due to industrial pollution have been increasing in the last ten years. Evidence of ground and surface water contamination has been found in areas near the polluted river Buriganga particularly in Hazaribag area. High values of *E. coli* form have been observed in these areas (RPMC, 2008). Even people living in the vicinity of Buriganga are likely to be attacked by cancer for their contact with chemical wastes dumping into the water. The number of fish species has severely declined from water pollution in the rivers. A recent study conducted by the Water Resources Department of Bangladesh University of Engineering and Technology (BUET) reveals the oxygen level of the Buriganga and Turag is less than 1 mg/L. All species of local fish need 4-6 mg/L oxygen to survive. Many of the fishermen and boatmen dependent on the rivers for livelihood have shifted to other professions as the rivers have been polluted and dried up. Most of the the industrial effluents are dumped directly into the rivers Buriganga, Balu and Sitalakhya. Pollution from tanneries in Hazaribagh is responsible for increasing in the health-related expenditure 125 US dollar per capita of people living in the vicinity of the tanneries (GOB, 2005). These pollutants are causing serious damage to freshwater and healthy ecosystems as well. The unabated dumping of industrial wastes and sewage has polluted the waters to such a magnitude that it is no longer economically viable for chemical treatment. These kinds of pollution have a strong human health impact particularly among the poor communities who are exposed to water-borne diseases.

7. EFFECTS OF URBANIZATION ON WATER RESOURCES

Safe, affordable and stable water supply, proper sanitation facilities are vital requirement for human development and ecosystem survival. Without adequate quantity and quality of water, it will not be possible to ensure food, energy, health and environmental security (ADB, 2007). But as a result of rapid urbanisation and population boom, Dhaka city is facing serious

environmental problems. Industrial expansion, rural to city migration and encroachment of the rivers/canals/water bodies and lack of strict enforcement of environmental regulations with climatic change have significantly been contributing towards increased intensity of disasters. Consequently access to freshwater now has become a serious concern for city population and mankind as a whole. Unplanned urbanization and unregulated industrial expansion produce adverse impact on:

- Drainage situation
- Water quality
- Recharge of ground water
- Wetland ecology
- Water retention

Dhaka-Narayanganj-Demra (DND) project covering an area of 56.79 sqkm was ranked as one of the most successful projects of Bangladesh Water Development Board (BWDB), but it has now become a burning example where extreme environmental degradation has occurred due to unplanned urbanization and population increase, growth of illegal fish farms and encroachment of canals/ borrowpits by the filling stations without proper drainage facilities. The continual growth of fish farms in the project area is responsible for water logging. These fish farms block free flow of water into the canals to maintain their ponds leading to water logging. Another problematic factor is the encroachment of the canals those are being filled up by the filling stations (CNG/petrol pump) in the project area. Highway borrowpits/canals which were 100 feet wide have been narrowed down at points to only 12 feet. Most of the canals in the DND area have been filled up due to industrial waste and garbage dumping causing severe water logging during the monsoon because the project area is beyond the jurisdiction of municipal authority to dispose up the garbages. About 1.5 million people (2005) of the DND project area live with the risk as the authorities concerned failed to take long term measures to improve the situation. Two national highways such as Dhaka-Chittagong road and Dhaka-Narayanganj link road have bifurcated the DND project into three parts without adequate drainage facilities which cause obstruction of natural flow of water. Unplanned road network also causes flood hazards, drainage congestion and disruption in urban utility services. So, to improve the existing drainage situation, re-excavation of drainage canal, rehabilitation of pump station and construction of road crossing bridge and culverts need to restore the normal livelihood for the dwellers in the project area adjacent to Dhaka mega-city with socio-economic and environmental upgradation (BWDB, 2008). Hence the urban planning should depend on comprehensive and integrated approach towards mitigation of such adverse impacts.

7.1 Water Quality

Surface water of Dhaka is in very poor condition, especially in the dry season. Consequently, dilution of contaminants is drastically reduced in the dry season (World Bank, 2006). The water quality of the rivers has been seriously affected. Water and air pollution has already become a serious concern. The surface water in Dhaka is polluted severely through dumping

of municipal solid wastes, indiscriminate discharge of untreated waste water and industrial effluents, oil and lube spillage from the operation of river ports and ship wreckage. The serious surface water pollution is found in Buriganga river due to tannery wastes and industrial discharges and domestic sewage (Islam, et.al, 2003). It has been reported in recent surveys that around 60% of pollutants are generated from industrial sources and the rest 40% are mainly from domestic sources and to a lesser extent from untreated dispersal of lube and burnt oils from river transport/vessels. It is reported that more than 60,000 Cubic meter/day of toxic waste from industries enters the Dhaka canal and river system. Both industrial effluent and domestic waste water are being disposed mostly untreated into the wetlands and natural streams in and around Dhaka city causing pollution of river water and affecting ground water quality. Every year ground water level is receding fast due to over extraction. River encroachment is narrowing the river width and reducing the water flow. Large scale sedimentation in river beds is causing reduction of normal depth of river (RPMC, 2008). Because of human activities like encroachment of rivers, floodplains and low lying areas, disposal of sewage and solid waste, industrial waste disposal and high rate of migration of the poor people in the slum areas of Dhaka city, the peripheral rivers are being polluted seriously. Apart from industrial sources, surface water in Dhaka is also extensively polluted by human faeces as sanitation is inadequate.

8. ENVIRONMENTAL CONCERNS

Dhaka city is under threat due to rapid urbanization, population pressure and extensive resource use, conversion of wetlands and channels into housing settlement and other various human interventions. Interrelationships of different factors of disasters and their possible impacts are shown diagrammatically in figure - 1. Human interference on nature has limited the biodiversity and aquatic habitats. Bio-diversity preservation is an urgent need of time to save the civilisation and face the challenges of the 21st century. Quality of water and soil has been deteriorated due to unplanned land use, undesirable encroachment for settlements, indiscriminate disposal of hazardous industrial and sewage wastes. The serious problem in the urban areas is mushroom growth of real estate business which accelerate filling of low lying areas, natural channels and ponds for construction of high-rise residential and commercial buildings.

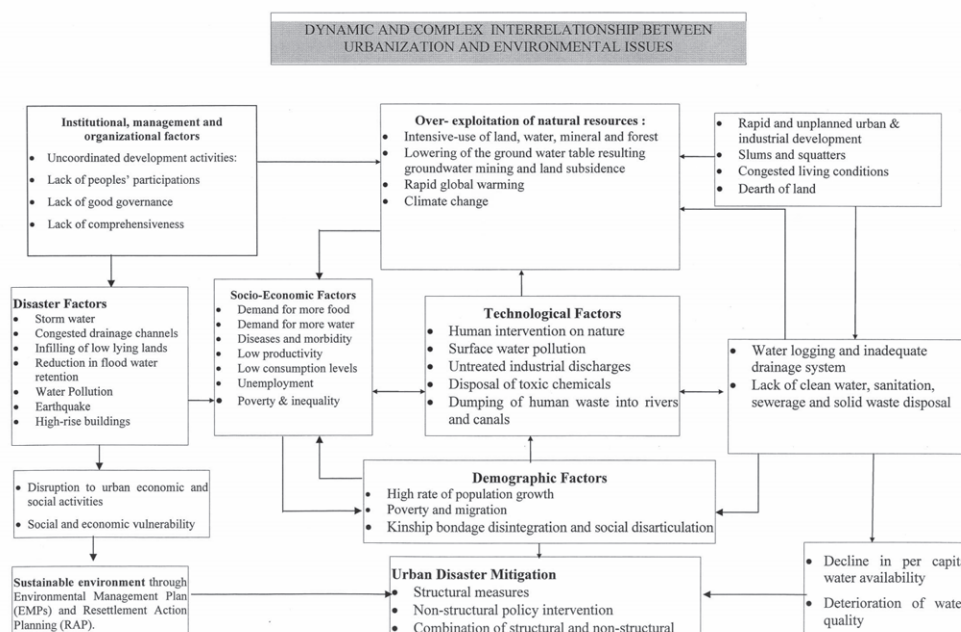


Figure 1: Linkages between causes of Disaster and Impact on natural resource Base

This is causing reduction in the floodwater retention areas and thereby causing water logging and drainage problems in the city area. Illegal occupation and constructions in the surrounding rivers drastically reduced the drainage potentialities of the city which enhanced degraded environmental condition. Smooth navigation and fisheries are also adversely affected by such kind of encroachments (BWDB, 2007).

9. ROLE OF GOVERNMENT IN COMBATING SURFACE WATER POLLUTION

The pollution of both surface and ground water around various industrial centres by untreated effluent discharge into water bodies is a critical water management issue (NWPo, 1999). The National Water Policy on industrial pollution states that the policy (1999) of government in this regard is:

- Zoning regulations will be established for location of new industries for fresh and safe water availability and effluent discharge possibilities
- Effluent disposal will be monitored by relevant government agencies to prevent water pollution
- Standards of effluent disposal into common watercourses will be set by Water Resources Planning Organization (WARPO) in consultation with Department of Environment (DoE)
- Industrial polluters will be under law to pay for the cleanup of water-body polluted by them

The departmental agencies and their functions involved in combating surface water pollution are as follows.

Table 1: Responsibilities of Government Institutions regarding water quality of Dhaka

| Agency | Services |
|---|---|
| Department of Environment (DoE) | Enforcement of environmental rules, administration of the Open Space and Wetland Conservation Act, 2000 and Urban Water Body Protection Law, 2001. |
| Dhaka City Corporation (DCC) | Responsible for handling and disposal of solid waste; management of public green spaces; surface drainage maintenance of some lakes, operation of health facilities. |
| Rajdhani Unnayan Kartipakha (RAJUK) | Detailed Area Plan (DAP) for a planned townships ensuring environmental upgradation. |
| Dhaka Water and Sewerage Authority (DWASA) | Responsible for ensuring supply of pure, safe, and dependable water to city dwellers and regular disposal of sewage. |
| Bangladesh Water Development Board (BWDB) | Implementation and Maintenance of water resources projects for flood control, drainage and environmental improvement. |
| Ministry of Land (MoL) | Control and administration of government owned land including land reclassification and settlement of land reclaimed and accreted. |
| Bangladesh Inland Water transport Authority (BIWTA) | Responsible for inland water transport and maintaining navigable waterways; dredging, shipping terminal maintenance |
| Ministry of Industry | Overall policy direction for industrial development; a role in development of industry in specified zones in compliance with pollution control regulations in factory design. |

Encroachment and pollution of the rivers surrounding Dhaka continue despite the existence of good number of government agencies involved in the management of the rivers and water bodies. It has worsened due to lack of co-ordination among different service agencies like DCC, Roads and Highways Department (RHD), RAJUK, BWDB, DWASA and DoE. There is a serious problem of overlapping of jurisdictions among many government agencies which leads to inaction. The roles of DCC, the planning authority RAJUK and the line ministries in urban management are not clear and co-ordination among them is very limited. All relevant government agencies need to come forward for a comprehensive management of environment in land and water in and around Dhaka city. The existing laws and regulations need to be updated including restructuring and re-organization of the different development agencies and their co-ordination for effective and balanced development of the mega-city in the present context of socio-political and structural realities. It is important to establish an apex body with administrative, financial and enforcement power for co-ordination of their activities effectively as well as for cost-effective mitigation measures to build support for better management. Environmental concerns are multi-sectoral issues for which institutional arrangements are critical to the success and failure of all initiatives.

9.1 Promoting Compliance

Industrial discharges into rivers, canals and ground water must be controlled if water quality is to be improved. This will require strict enforcement of environmental clearance condition and effluents standards. There has been no strict enforcement of environmental regulations to date. To reduce the pollution of surface water bodies, both on-site and centralised treatment plants for industrial effluents are required. Each industrial unit should have an effluent treatment plant according to the Environment Conservation Act-1995. To reduce the pollution of ground water bodies, a reduction of pollutants leached to the aquifer can be achieved by on-site treatment in combination with improved conveyance of effluents to a centralised treatment facility. Strict control on new industrial set up around the city must be applied through more effective use of the Environmental Impact Assessment (EIA) and Social Impact Assessment (SIA). It is highly appreciating that Government of Bangladesh (GOB) has already taken decision to remove the Hazaribagh tannery in the industrial complex at Savar with a provision of treatment plants of the effluents. Similar action should be taken for Dholai Khal outfall containing sewage wastes.

9.2 Priority Projects Under BWDB

Dhaka Integrated Flood Protection Project was implemented covering the most densely populated western part of about 136 sq. km. with a view to providing the city dwellers a living condition free from flood, drainage and environmental hazards (BWDB, 1992). Environment of city improved as polluted water does not stay within the city area and trees have been planted on the sides of the embankment. Living standard of the city dwellers have improved due to this project. Yet a vast area of about 124 sq.km. of Eastern part remains unprotected for which Dhaka Integrated Flood Control Embankment cum Eastern Bypass Road Multipurpose Project is under process of approval of GoB (BWDB, 2008) to protect the eastern part of Dhaka city from flood, drainage and environmental hazards. Realistic remedial measures are also being undertaken to augment the flow of Buriganga for ensuring proper management of water resources for environmental conservation (BWDB, 2006). Besides, some steps need to be undertaken for protecting the existing flood control works, preventing illegal use of land and illegal occupants including construction of illegal structures which create the problem of water logging by narrowing the drainage canals. Treatment of all industrial waste needs to be ensured to protect environmental degradation. It is also equally important to recover areas occupied up by land grabbers in absence of Rajuk Detailed Area Plan (DAP) for accumulating waste water for pumping and protecting the overall environment.

9.3 Further Actions to be Taken

Government should have a dynamic role to mark the areas of rivers and canals which were illegally encroached to bring back their original shapes and sizes which includes following effective steps.

- Land reclassification for industries, commercial and residential areas
- Strengthening water quality monitoring for participatory EMP/ETP
- Strict enforcement of the Environment Conservation Act-1995 & Rules for maintaining a habitable environment
- Establishment of standards of effluent disposal into common watercourses
- Providing fiscal and other financial incentives for retrofitting or for reduction of effluents from industries
- Devising effective water quality management technology
- Applying polluters pay principle to make the polluters land to rectify them

10. PARTICIPATORY CITY MANAGEMENT (PCM)

Administrative structure of service delivery in Dhaka city by government institutions is complex. Services are delivered by different agencies with poor governance and lack of co-ordination. The main causes are the limited role and authority of the DCC that plays in urban management. It has limited role in city planning and management and highly dependent on central government. Urban planning still lies on top down planning approach without consultation of the local. The approach should be bottom up wherein the local will be involved and participate in urban planning and management. The Government alone can never solve the problems and disasters properly without people's participation with its limited resources and manpower. For this reason peoples' participation is essentially required. DoE has the responsibility of controlling environmental regulation as these affect land and housing development. Under the circumstances without public awareness, consciousness development and structured planning procedures, it is impossible to achieve better institutional framework. It is experienced that government failed to solve and mitigate the different problems faced by city dwellers. What is still lacking is structured planning, development and management procedure with enhanced peoples' participation in city management. In case of Dhaka being a mega-city with a population of about 12 million, government alone cannot face the different types of urban disasters. For successful management and mitigation of water-related disaster, awareness building amongst peoples' participation is essential. So, participatory approach of city management has been given emphasis to cope effectively with complex issues of current trends of urbanization. Government alone is not enough to manage, mitigate and to rescue operation during the onset of disaster. A strong apex body should be formed to promote cross-sectoral coordination and minimize jurisdictional conflicts. An important element of the strategic framework will be adequate to monitor environmental pollution in compliance with public information, aimed at raising awareness of the causes and impacts of environmental degradation and at disseminating information about related intervention. Such initiatives are essential to build civil society and private sector support, both for the necessary investment and for strengthening enforcement of

environmental regulations. The participatory approach of management has been proved to be pragmatic in different sectors e.g. water sector, community self help programs etc. The PCM will work in other areas of city management including disaster. An organizational framework of PCM may be conceived as follows (chart 1):

A suggested organizational framework for Integrated Environmental Management (IEM) in Dhaka city

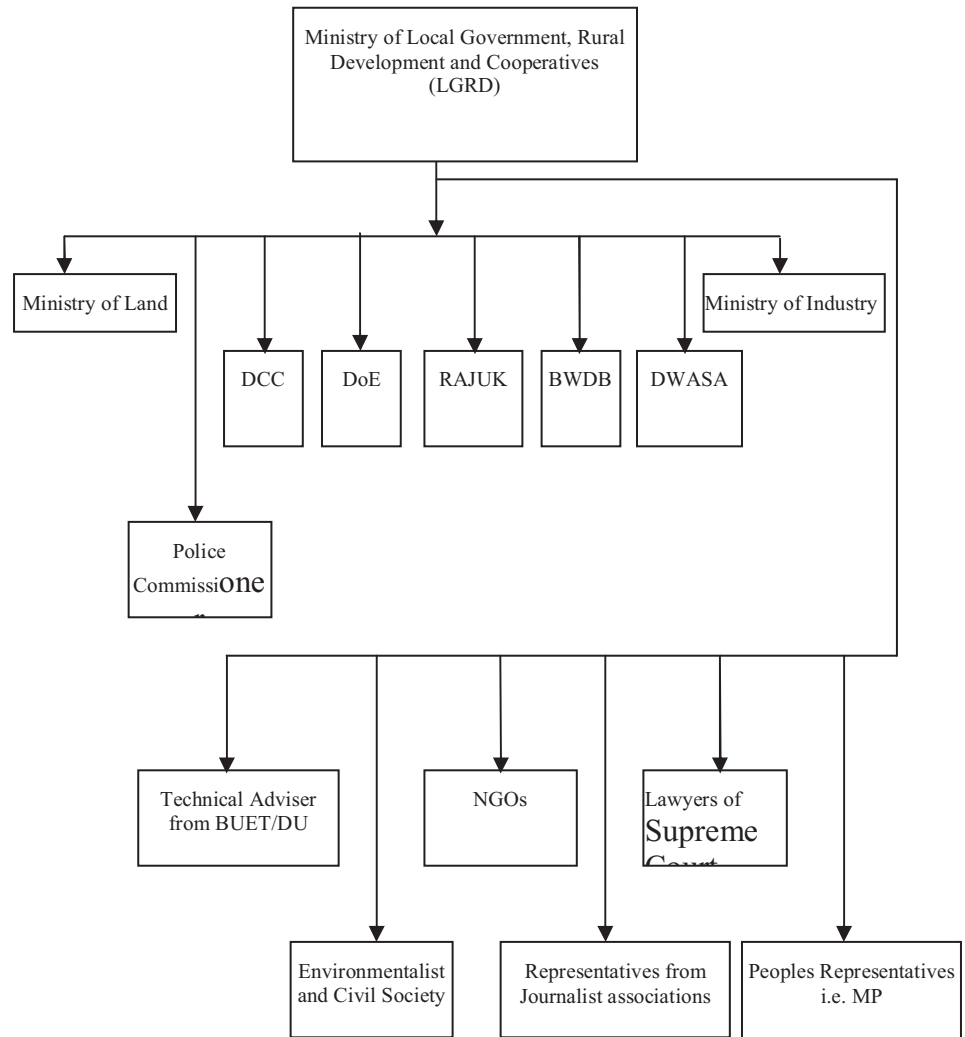


Chart 1: Organizational framework for IEM in Dhaka city

PCM will bring opportunities for local people participation to achieve compactness in townships to maximum level of economy, convenience and beauty. Both government and people should come forward for sustainable service delivery. By ensuring good governance PCM will determine the preparation and implementation of city master plan to a great extent. PCM is one in which people can work and perform their tasks easily, conveniently and economically. The purpose of PCM is to make the city functionally efficient for all the residents and users making the city environmentally healthy and sustainable. Nevertheless, PCM will secure a proper relationship of man, society, activity to attain social, economic, biological and physical environment in balance.

11. MITIGATION MEASURES OF URBAN DISASTERS

Urban disaster management in Dhaka is not only limited to technical aspects but it encompasses also social, economic, cultural and environmental needs. The mitigation measures will include integrated strategies for structural and non-structural interventions, institutional participation, infrastructural security, enhanced community safety and resilience. In a nutshell, integrated disaster risk management, effective monitoring and evaluation, active community participation and networking are the key factors for successful mitigation of urban disaster. It recommends appropriate method of mitigation, preparedness and emergency response, proper education, information, effective forecasting and early warning.

Recommendations are made for implementation method of land use planning and legislation, housing and settlement, landscape design, urban conservation and the management of the water resources up to the optimal level. More attention should be given while implementing projects for flood protection and road network. Any solution to be permanent and sustainable for mitigation of disaster calls for broad political and social consensus for the comprehensive plan. The present system as experienced cannot be the solution and it must be changed. What is needed is to think strategically for a properly planned city to promote PCM to enforce regulatory measures to protect environment and combat surface water pollution. There should be PCM to deal with public health, education, water supply and sanitation problems necessary for healthy growth and socio-economic development. It is essential for participatory approach of city management for overall improvement of economic, social and environmental condition. It is urgently needed to establish an apex body which will co-ordinate the activities of DWASA, RAJUK, DCC, BWDB and other agencies to save Dhaka city from any disaster. Citizen should be sensitized and motivated through awareness building by DCC and through community participation. DCC should provide adequate service to urban people and formulate an appropriate slum development policy with the participation of slum dwellers.

The mitigation measures can be phased into three stages for prioritized implementation

Immediate measures

- Strengthening the performance and promoting co-ordination of the government and non-government institutions.
- Restoring illegally occupied lands in canals and rivers of Dhaka city and to finalize the Detailed Area Plan by Rajuk, which would be removed with the help of local administration
- Building awareness amongst the citizens and ensuring participatory management.
- Ensuring sustainability of water supply and monitoring of water quality by DWASA.
- Compelling the polluters to install Effluent Treatment Plants (ETP) for all industries mandatory.
- Shifting of Hazaribag Tannery and treatment of Dholai outfall containing sewage

- Establishing sewage treatment plants.
- Water quality monitoring by applying polluters penalty system.

Mid-term Measures

- Opening silted up river and channels by dredging for improving the drainage water flow systems and navigations.
- Shifting of dockyards from Buriganga river banks to further downstream for making proper environmental management.
- Establishment of phase wise Central Effluent Treatment Plants (CETP) in industrial areas.
- Increasing DWASA's sewage coverage from present 30% to 75% of the city area.
- Bringing industrialists under a broader commitment for overall pollution control.

Long term Measures

- Augmentation of the Buriganga flow by restoring silted up links with Jamuna by BWDB.
- Maintaining navigability of the Buriganga and improvement of water quality of the surrounding rivers.
- Ensuring full sewage coverage by DWASA.
- Bringing all industrial units under full CETP coverage within 2015.
- Using state-of-art technologies and a wide range of alternative materials
- Decentralising Dhaka and spreading out the economic activities outside Dhaka
- Motivating industrialists to introduce cleaner production technology to minimize pollution load at industries.
- Implementation of Dhaka Integrated Flood Control Embankment cum Eastern Bypass Road Multipurpose Project to protect the eastern part of the city from floods, to remove water logging and to upgrade overall environmental condition by BWDB.
- Development of master plan for protecting floods and proper drainage of the city area and implement through PCM approach.
- Need-based research and development on monitoring and evaluation of water resources in Dhaka city.

12. CONCLUSION

Among the disasters happened, human-induced disasters are not less important. Both natural disasters and human-induced disasters are equally important. Pollution of both surface and ground water caused by human activities and interventions may create a havoc making the city uninhabitable. Hence, natural disasters and human-induced disasters should be concomitantly addressed. Water use efficiency and pollution control of both surface and ground water in the future should be taken within the framework of emerging technology, social goals, national and international rules and regulations, environmental concerns and socio-economic realities. Needless to say, surface water treatment would be cost effective if the

pollution level of surface water can be reduced substantially through effective preventive measures in cognizance with acceptable water quality standards. Existing pollution of surface water should be treated and protected from further pollution by untreated domestic and industrial waste water. Many opine that the urban environment is going to face impending crises if the surrounding rivers and water bodies are not appropriately protected to make a pollution free healthy environment. Improved performance and coordination among the Governments and NGOs are crucial with greater involvement of participation of the commons. GoB alone will not be able to face all of these problems. As an approach to solve the problems, PCM may be considered as a possible strategy by involving all the stakeholders of a city to address such a complex issue. In fine, management of water-related disaster in an over-overtly populated mega city like Dhaka needs an intensive and comprehensive study. People of Dhaka city would discover a “new sun” shining overhead when such anthropocentric vision would ultimately be achieved. Indeed, this leads utmost help to humanity in the long run.

ACKNOWLEDGEMENTS

The author gratefully acknowledges the contribution of following institutions for providing valuable information that has proved extremely useful in producing this paper: Bangladesh Water Development Board (BWDB), Institute of Water Modelling (IWM), Centre for Environmental and Geographic Information Services (CEGIS) and South Asian Disaster Management Centre (SADMC) of International University of Business Agriculture and Technology (IUBAT), Dhaka, Bangladesh University of Engineering and Technology (BUET)

REFERENCES

- ADB, 2007, *Asian Water Development Outlook 2007*, Asian Development Bank, P.3
- ADB, 2003, *The Water Policy of the Asian Development Bank*, Published by ADB, June2003, P.17
- Ahmed, Murshed (2004), *Development and management Challenges of Integrated Planning for Sustainable Productivity of Water Resources*, Bangladesh Journal of Political Economy (BJPE), Bangladesh Economic Association, Volume 21, No. 2, December 2004, P.123
- BWDB, 2006, *Development Project Proposal for Augmentation of Buriganga flow by Restoring Silted up links with Jamuna*, DPP January-2006, P. 52
- BWDB, 1992, *Development Project Proposal for Dhaka Integrated Flood Protection Project (BWDB Component: Flood Protection and Project Implementation Assistance)*, DPP 1992, P.15
- BWDB, 2008, *Development Project Proposal for Dhaka Integrated Flood Control Embankment Cum Eastern Bypass Road Multipurpose Project*, DPP Jan-2008, P. 17.

- BWDB, 2008, *Revised Development Project Proforma/Proposal (RDPP) for Drainage Improvement of Dhaka-Narayangonj-Demra (DND) Project (Revised)*, Jun-2008, P. 5.
- Daily Star, 2008, *The Daily Star, A national daily newspaper of Bangladesh*. May 1, 2008
- GoB, 2003, *Bangladesh At a Glance*, Published by Department of Films and Publications, 2003 edition, Ministry of Information, Govt. of the People's Republic of Bangladesh, P.127
- GoB, 2005, *National Strategy for Accelerated Poverty Reduction*, General Economics Division, Planning Commission, Government of the People's Republic of Bangladesh, October 2005. P.178
- NWPo, 2009, *National Water Policy*, Ministry of Water Resources, Government of the People's Republic of Bangladesh, P.12, Section 4.8
- Islam, Sirajul and Miah, Sajahan, 2003, *Banglapedia, National Encyclopaedia of Bangladesh (ed.)*, Volume 10, Asiatic Society of Bangladesh, March 2003 P. 362
- IWM, 2006, *Resource Assessment and Monitoring of Water Supply Sources for Dhaka City DWASA - 2006*, Institute of Water Modelling, Volume - I Main Report, July 2006, P. 2-52
- RPMC, 2008, *Report on Mitigation of River Pollution of Buriganga and linked rivers – Turag, Tongi Khal, Balu, Sitalakhya and Dhaleswari*; River Pollution Mitigation Committee, May 2008, P. 5.
- The World Bank, 2007, *Dhaka: Improving Living Conditions for the Urban Poor, Bangladesh Development Series*, Paper No. 17, June 2007, P. xiii, 33
- The World Bank, 2006, *Bangladesh Country Environmental Analysis, Bangladesh Development Series*, Paper No. 12, September 2006, P. 28

INVESTIGATING THE PERFORMANCE OF ALOS PRISM TO ESTIMATE BUILDING HEIGHTS FOR URBAN RISK MANAGEMENT

WATARU TAKEUCHI^{1,2}, KAWIN WORAKANCHANA^{1,2},
TAKEO TADONO³ and PENNUNG WARNITCHAI⁴

¹IIS, University of Tokyo, Japan

²RNUS, Asian Institute of Technology, Thailand

³EORC, Japan Aerospace Exploration Agency, Japan

⁴SET, Asian Institute of Technology, Thailand

wataru@iis.u-tokyo.ac.jp

ABSTRACT

This research is investigating the performance of ALOS PRISM to estimate building height for urban risk management. Firstly, triplet ALOS PRISM images acquired on October 30, 2007 are collected including three independent optical systems; nadir (UN), forward (UF) and backward (UB) looking, respectively. Secondly digital surface model (DSM) are mapped using three types of stereo pairs; (1) UN and UF, (2) UN and UB, and (3) UF and UB to evaluate DSMs estimated with different base-height ratios. Finally satellite derived DSMs are compared with a point based building height database it was found that root mean square errors are 2.71-13.54 m with respect to sensor view model combinations. It is concluded that PRISM has reasonably moderate vertical resolution for building heights estimation on urban risk management purposes.

1. INTRODUCTION

Needs for better information

Earthquakes affecting urban areas can lead to catastrophic situations and hazard mitigation requires preparatory measures at all levels. Structural assessment is the diagnosis of the seismic health of buildings (Wasti *et. al*, 2006). Assessment is the prelude to decisions about rehabilitation or even demolition. The scale of the problem in dense urban settings brings about a need for macro seismic appraisal procedures because large numbers of existing buildings do not conform to the increased requirements of new earthquake codes and specifications or have other deficiencies.

Our project is designed for the purpose of “Earthquake Risk and Disaster Management” for Bangkok in Thailand and has two segments according to risk assessment for before the known scenario earthquakes and quick loss estimation based on damage detection just after the crisis (even after days and weeks following the event) that potentially includes the effects of earthquakes caused by unknown faults. The risk assessment part includes the evaluation and the implementation of different vulnerability

and risk algorithms using extensive database created and developed for Bangkok in addition to satellite remote sensing.

Satellite based monitoring of urban area

Advanced Land Observing Satellite (ALOS) is one of the most promising satellite mission to achieve this goal. ALOS has three sensors including two optical sensors (AVNIR and PRISM) and one SAR sensor (PALSAR). PRISM panchromatic instrument has been designed mainly for mapping purpose with a specific aim towards digital surface model (DSM) extraction. Indeed, PRISM is capable of simultaneous stereoscopic acquisition of the observed landscape which should easier the automatic processing of such data for DSM extraction (JAXA, 2007).

However few studies have already been done concerning the qualitative validation of PRISM (Tadono, 2004) stereoscopic acquisition with respect to DSM extraction. One reason may be the recent commercial availability of PRISM data along with geometric information provided as rational polynomial coefficients (RPC) models. Another reason may be the short list of available digital processing solutions to generate high quality DSM from PRISM stereoscopic acquisition. Geometric information about the ALOS platform is available in addition to RAW images in order to rigorously model the sensor geometry and to achieve high accuracy measurements from these instruments.

Objective of this study

The objective of this study is investigating the performance of ALOS PRISM to estimate building height for urban risk management. Three types of satellite derived DSMs are compared with a point based building height database to evaluate if they have enough vertical resolution for building heights estimation on urban risk management purposes.

2. METHODOLOGY

2.1 PRISM sensor model

PRISM sensor is characterized by each viewing angle one particular camera with a number of Linear Array CCD chips in the focal plane. Three PRISM images per scene are acquired almost simultaneously in forward, nadir and backward modes in along-track direction as shown Figure 1. The nominal viewing angles are (-23.8, 0, 23.8) degrees respectively.

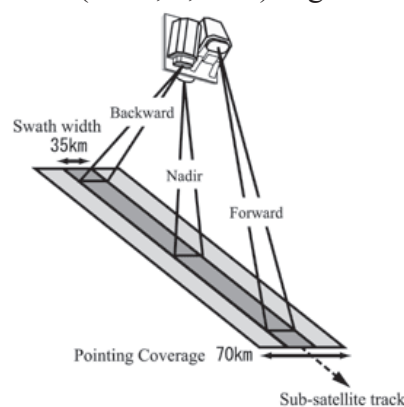


Figure 1: Observation geometry of the ALOS PRISM sensor

2.2 RPC as a camera replacement model

A set of rational polynomial coefficients (RPC) are used as a camera replacement model. They are provided by the image distributors and are known to have a significant bias. This bias can be removed with at least one well-defined GCP (Fraser et al., 2006). The transformation relating the 2D image coordinates of a point with its object coordinates is given as follows;

$$x + B_0 + B_1 \cdot y + B_2 \cdot x = \frac{Num_x(\varphi, \lambda, h)}{Den_x(\varphi, \lambda, h)}$$

$$y + A_0 + A_1 \cdot y + A_2 \cdot x = \frac{Num_y(\varphi, \lambda, h)}{Den_y(\varphi, \lambda, h)}$$

where

| | |
|-------------------------|--|
| φ, λ, h : | latitude, longitude, and ellipsoidal height |
| x, y : | image coordinates |
| Num_x, Den_x : | cubic polynomial functions of object coordinates for x |
| Num_y, Den_y : | cubic polynomial functions of object coordinates for y |
| A_i, B_i : | affine parameters of offset correction. |

In this study, we have collected 10 GCPs based on ground surveyry supplemented by a visual interpretation of Google Earth. It resulted in the full affine bias correction model which guarantee the best geometric performance (Willneff, 2008).

2.3 Digital surface model from PRISM

Figure 2 shows the flowchart of this research to estimate building height from PRISM. Firstly, triplet ALOS PRISM images acquired on October 30, 2007 are collected including three independent optical systems; nadir (UN), forward (UF) and backward (UB) looking, respectively. This allows for production of a panchromatic stereoscopic image in 2.5 m horizontal resolution along a satellite's track. Secondly digital surface model (DSM) are mapped using three types of stereo pairs; (1) UN and UF, (2) UN and UB, and (3) UF and UB to evaluate DSMs estimated with different base-height ratios. Traditional aero-triangulation processing is carried out supplemented by ground control points (GCP). Finally satellite derived DSMs are compared with a point based building height database from LiDAR to evaluate if they have enough vertical resolution for building heights estimation on urban risk management purposes. A bunch of DSM processing has been implemented on IDL code (ITT, 2008).

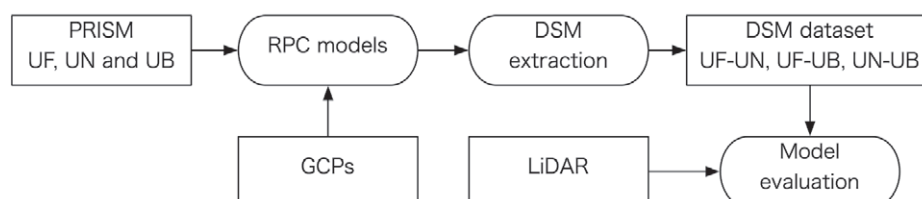


Figure 2: A flowchart to derive digital surface model (DSM) from PRISM.

3. RESULTS AND DISCUSSIONS

By computing individual digital surface model between all pairs of images (backward, nadir and forward) and analyzing them, it was possible to highlight some repeating undulations in the resulting elevation images as illustrated by the following figure. Figure 3 shows DSMs derived from three geometries including forward, nadir and backward modes with ALOS PRISM, respectively. A profile of LiDAR flight measurement path is shown in Figure 3-(d) in east-west (cross-track) direction.

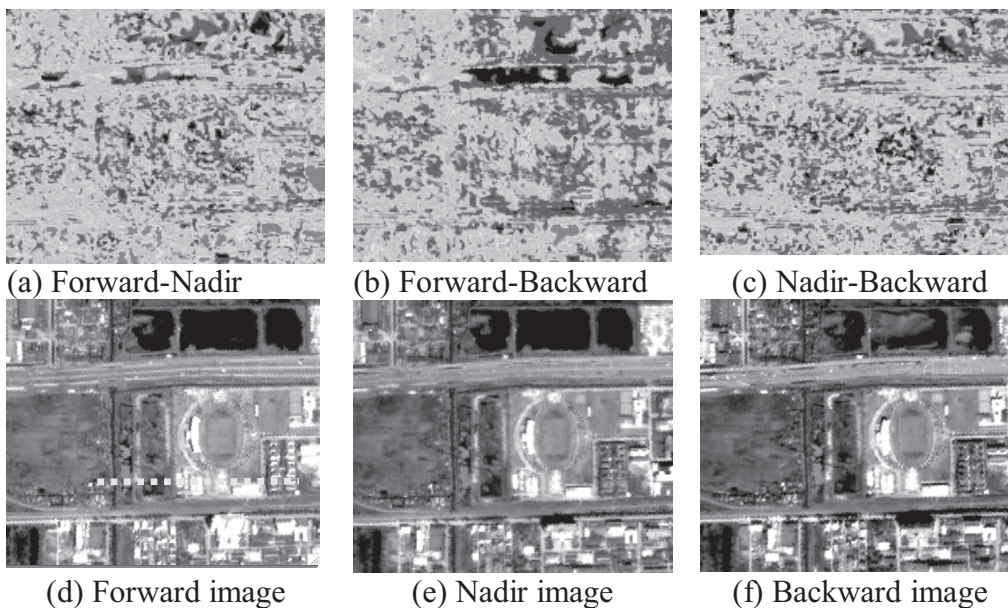


Figure 3: Digital surface models derived from three geometries including forward, nadir and backward modes along with ALOS PRISM images. Dotted line in figure (d) shows a profile of LiDAR measurement path.

Figure 4 shows a comparison of PRISM derived DSMs and LiDAR data respectively. The flight path includes mainly three higher buildings: (A) 110 in pixel number, 17.2 m height, 3-story and 10 m width, (B) 160 in pixel number, 10.0 m height, 2-story and 50m width, and (C) 170 in pixel number, 16.8 m height, 3-story and 30m width, respectively. The number of building story is supplemented by ground level survey.

(A)-building is the most accurately estimated by UF-UN image followed by UB and NB. (B)-building height estimations are carried out the most accurately by UF-UB, UF-UN and UN-UB. (C)-building heights and width are estimated relatively accurately by UF-UN, followed by UN-UB and poorly by UF-UB. A flat area (play ground) from pixel number 0 to 100 is well represented by LiDAR measurement, however, no DSMs from PRISM shows flat area correctly with 1-10 m vertical errors. They are originated from the on-board image compression into JPEG format and this artifact can have a bad influence on the stereo-matching algorithm as it will introduce some false patterns that may confuse the matching process, especially in lower elevations than PRISM pixel size (2.5m).

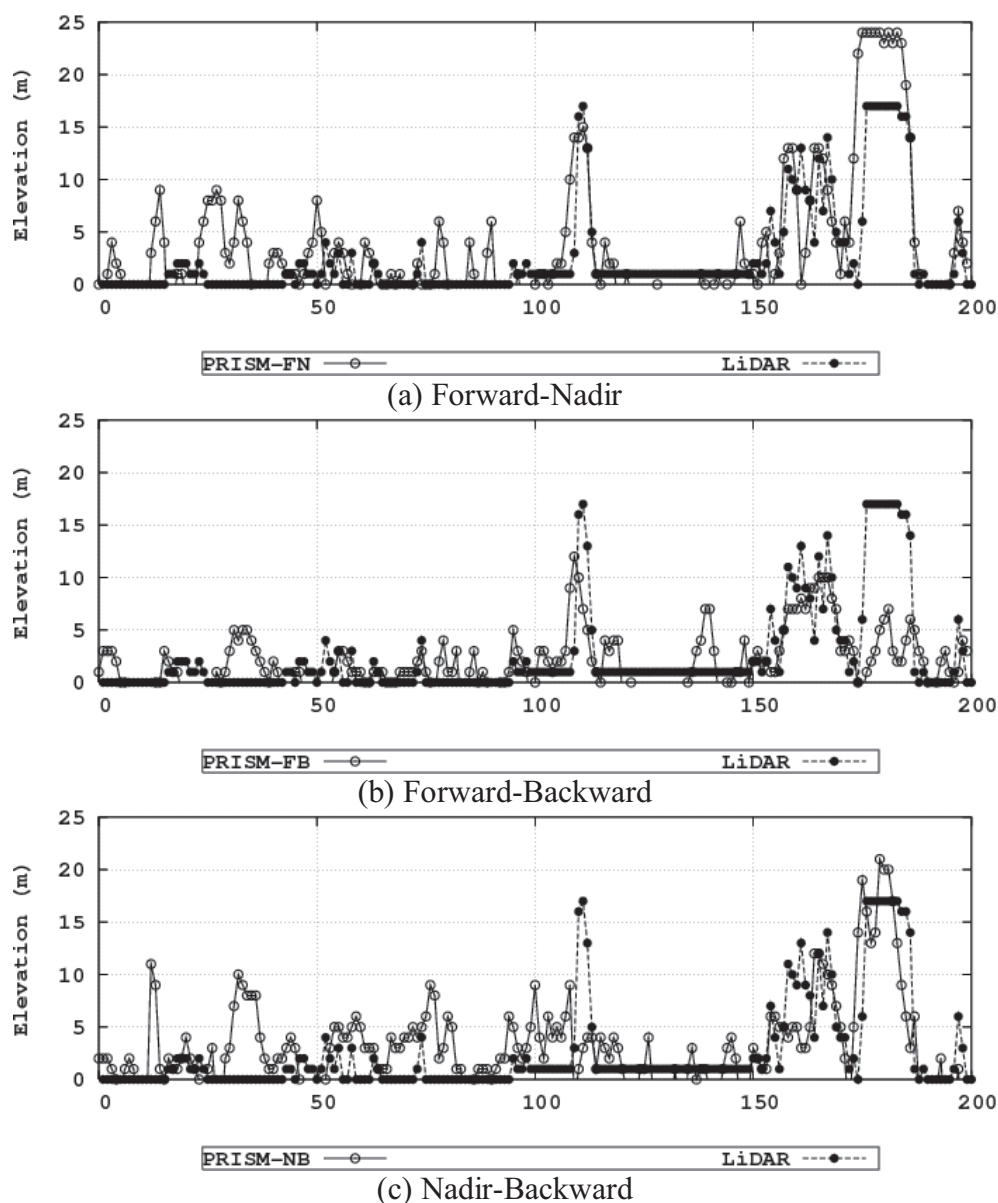


Figure 4: Comparison of PRISM derived DSMs and LiDAR.

Table 1. Standard deviations of DSMs compared with LiDAR in meters.

| | UF-UN | UF-UB | UN-UB |
|-------------------|-------|-------|-------|
| 0-5 m (0-story) | 3.86 | 2.71 | 3.76 |
| 5-10 m (1-story) | 6.97 | 3.67 | 5.79 |
| 10-15 m (2-story) | 2.91 | 6.23 | 6.74 |
| 15-20 m (3-story) | 6.69 | 13.54 | 7.98 |

Table 1 shows a statistical analysis of ALOS DSMs with a standard deviation. When partitioning this statistical analysis along with building story every 5 meters height, we end-up with standard deviation around 2.71-3.86 m for 0-story, 3.67-6.97 for 1-story, 2.91-6.74 for 2-story and 6.69-13.54 for 3-story respectively. Those results are consistent with other reports (Wolff *et. al.*, 2007) available in the scientific literature about PRISM derived DSM.

4. CONCLUDING REMARKS

We have investigated the performance of ALOS PRISM to estimate building height for urban risk management. Triplet ALOS PRISM images with three independent optical systems are used to map DSMs UN-UF, UN and UB, and (3) UF and UB to evaluate DSMs estimated with different base-height ratios. Finally satellite derived DSMs are compared with a point based building height database it was found that RMSE are 3.4m, 2.1m and 2.9m respectively. It is concluded that PRISM has reasonably moderate vertical resolution for building heights estimation on urban risk management purposes.

Addition to that, problems still exists in the interior orientation. Comparison of PRISM DSM and reference LiDAR show a constant offset in flight direction, while across flight direction, the differences vary in a huge range. This effect can also be detected when regarding the co-registration of nadir and backward view: The residual size and direction vary across flight direction, whereas they remain nearly constant in flight direction.

REFERENCES

- Wasti, S. Tanvir; Ozcebe, Guney (Eds.), 2006. Advances in Earthquake Engineering for Urban Risk Reduction. *Series: NATO Science Series: IV: Earth and Environmental Sciences*, Vol. 66, XXI, 551 ISBN: 978-1-4020-4569-1.
- Tadono T., Shimada M., Watanabe M., Hashimoto T., Iwata T., 2004. Calibration and Validation of PRISM Onboard ALOS. *International Archives of Photogrammetry and Remote Sensing*, Vol. XXXV part B1, 13-18., Istanbul, Turkey.
- Bignone, F. and Umakawa, H., 2008. Assessment of ALOS PRISM digital surface model extraction over Japan. *International Archives of Photogrammetry and Remote Sensing*, Vol. XXXVII part B1, 1135-1138, Beijing, China
- Willneff, J., Wester, T., Rottensteiner, F. and Fraser, C. S., 2008. Precise georeferencing of CARTOSAT imagery via different orientation models. *International Archives of Photogrammetry and Remote Sensing*, Vol. XXXVII part B1, 1287-1294, Beijing, China.
- ITT Visual Information Solutions, Image Processing & Data Analysis. <http://www.ittvis.com/> (Accessed on 20 Sep. 2008)

ANALYTICAL COST MODEL IN PROTECTIVE DESIGN METHODOLOGY

CHUNLIN LIU^{1,2}, RA JOHN CRAWFORD¹ and YEA SAEN FANG¹

¹K&C Protective Technologies Pte Ltd(KCPT), 159361, Singapore

²School of Civil Engineering, Tsinghua University, 100084, Beijing
P.R., China

liu.chun.lin@kcpt.com.sg

ABSTRACT

The 911 event has prompted governments and corporations to take risk management actions to provide greater protection for their operations, businesses, assets and personnel against man-made hazards, particularly improvised explosive devices (IEDs) like vehicle-borne IEDs (VBIEDs) and personnel-borne IEDs (PBIEDs).

However many have found that when they commenced on a physical security upgrade, they were up against many factors which made the process complex. Some may not realize this complexity or the interests of the various stakeholders as it is a relatively new topic.

However over a period of time, with greater experience, shared knowledge and various public guidelines and standards, stakeholders are increasingly more confident in implementing mitigation and protective measures.

One of the requirements of a physical security upgrade exercise is that it should address as many of the key concerns as possible beside security and protection, e.g. aesthetics, image, workflow efficiency, user convenience, value-for-money.

A systematic and multi-factor approach is hence essential to satisfy the requirements of various stakeholders. A holistic protective design methodology is needed which can consider a panoply of relevant factors, even if it is outside of one's area of expertise, and weigh their respective and combined cost-effectiveness to produce a successful balanced outcome.

A key requirement is funding for without a budget, protective measures will not be implemented even if their importance is recognized. Hence convincing stakeholders with cost figures and cost effectiveness is an important part of the process.

The analytical cost model described in this paper provides a tool that embodies an essential component of the holistic protective design methodology. In other words, without an effective cost model, it would be unlikely that the resources available for security at a given site will be wisely spent or protected.

A simple cost model is shown in the paper to illustrate the process. Although a limited number of parameters have been included to demonstrate the model, inclusion of other relevant factors can be done without violating the basic concept.

1. INTRODUCTION

The 911 event has seen many governments and businesses take a risk management approach to protect their operations, businesses, image, assets and personnel against the potential man-made hazards, particularly improvised explosive devices (IEDs). Vehicle-borne IEDs (VBIEDs) and personnel-borne IEDs (PBIEDs) are of particular concern.

Initially the process employed to address these risks was tentative and inconsistent, but with increasing experience and sharing of knowledge, including publishing of homeland security guidelines, stakeholders have become more confident.

With security and protective design solutions being added to agendas of many corporations, businesses have endeavored to establish a systematic approach to identifying the steps and quantifying the resources needed, and to defining the outcomes desired and estimating the likelihood of achieving them.

This paper attempts to advance the process by arguing for a systematic approach to be used in creating a protective design methodology, and that such a methodology be holistic (i.e., able to address the many relevant factors, both individually and as a whole), and incorporate an analytic cost model to determine cost-effectiveness and facilitate decision-making.

Technology solutions for buildings and infrastructure to protect against man-made IED threats include features like blast and anti-ram walls and bollards at the perimeter to mitigate blast effects and stop potential VBIEDs; structural protections like column carbon-fibre wraps and steel jacketing; and fabric catcher and cable catcher systems for windows and clear protective films and panels for glazing to prevent their debris entering the building.

These technologies are commonly used where a serious risk has been established (i.e., where the most protection value can be obtained). The magnitude of risk is commonly recognized as a function of the type of threat, and its probability and consequence. Evaluating the risks related to man-made threats is further complicated (i.e., in contrast to natural or accidental hazards) by the inability to use past events to reliably predict future ones.

For a holistic methodology, a wide range of measures would need to be evaluated to obtain a final group of them, which achieves an optimal result. To be able to do this, a cost needs to be given to each mitigation or protection measure and to the losses that might transpire without these

measures (e.g., cost of repairing broken windows, lost time), so that tradeoff studies can be performed for the purposes of achieving an optimal outcome.

This paper presents an example involving the provision of protection against an IED to illustrate the protective design methodology and analytical cost model described.

2. ELEMENTS OF THE ANALYTICAL COST MODEL

2.1 Overall Framework – the Protective Design Methodology

The protective design methodology envisioned herein offers a panoply of features, including aspects which may require expertise outside of protective design. Figures 1 and 2 depict some of these features influencing the protection needed and provided for a facility. In the holistic methodology, other factors including policing and national law enforcement effectiveness are considered in relation to the protection for one's own facility.

There are roughly four stages to protective engineering services, which are described in Figure 3. The first stage is the risk analysis, which is the focal point of this paper. Other stages include design, implementation, and research and development.

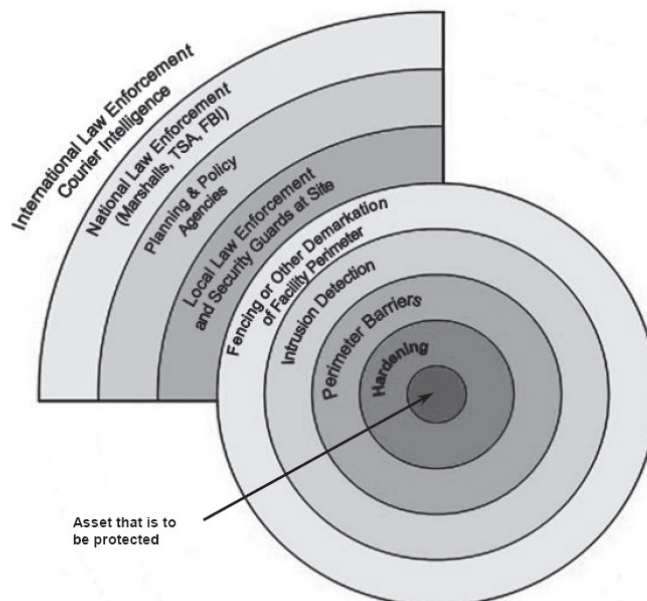


Figure 1: Illustration of the holistic nature of protection design of the engineering (red) and policing/planning (blue) aspects of providing protective technologies; this figure implies that a close working relationship between planning, policing, and engineering aspects of protective design is needed.

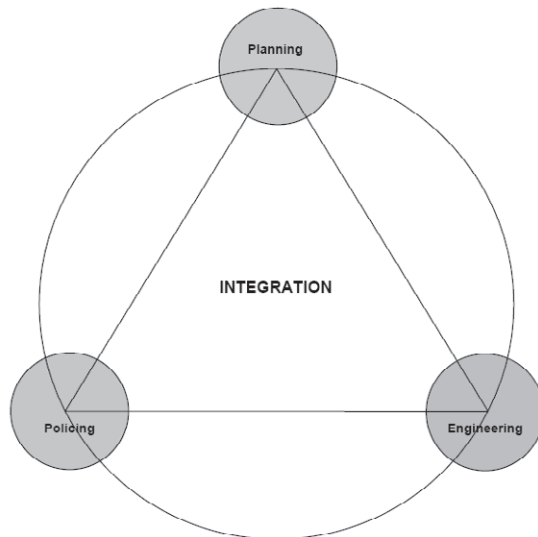


Figure 2: Depiction of the three key aspects of protective design and the need to seamlessly integrate the different disciplines involved in planning, policing, and engineering, to ensure no gaps and maximum effectiveness of the protection provided.

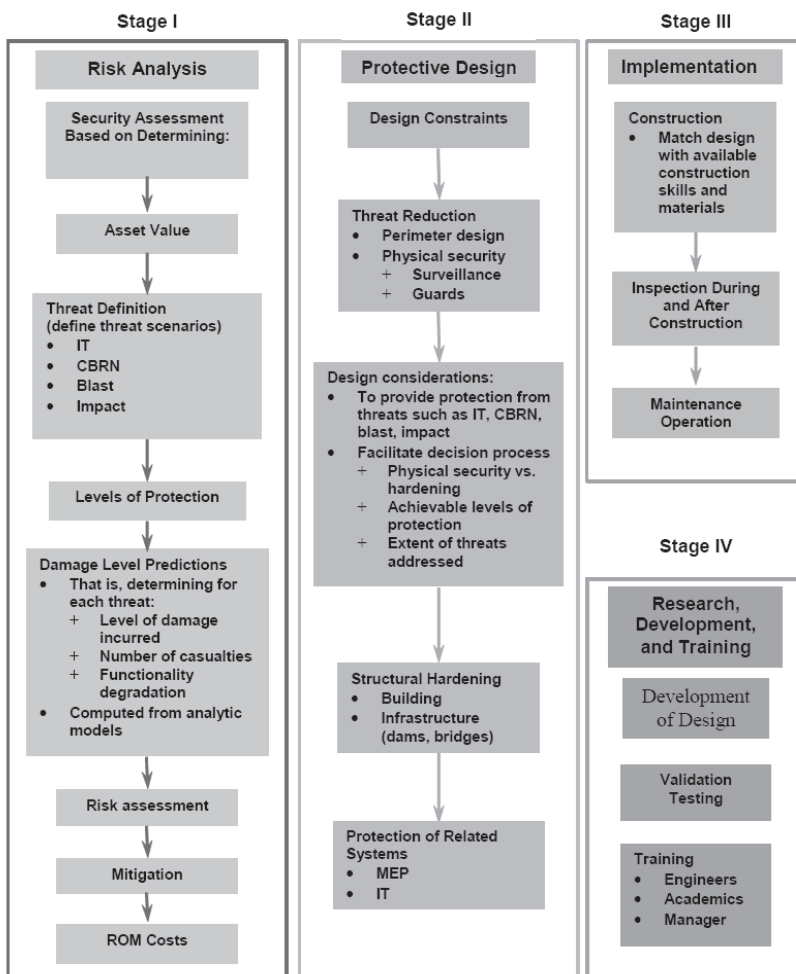


Figure 3: Protection engineering services may be divided into four stages; all are important to achieve secure facilities.

2.2 Determining Greatest Protection Value through Risk Assessment

Risk is commonly defined as a function of probability and consequences, (i.e. a high risk is when the threat is likely and its consequences severe). Hence for protective design to be relevant, the risk assessment must be good so that resources are committed to provide protective design to a credible risk. The next two tables show the process of identifying threats, aggressors’ tactics, assessing likelihood and consequences.

Table 1: Malevolent threats representative of security concerns pertaining to terrorists, vandals, disgruntled employees, criminals, and saboteurs.

| Threat Class | | Typical Threat | | Description |
|-------------------|-------------------------------------|----------------|-------------------|--|
| Type | Mechanism | Likelihood | Consequences | |
| WMD | CBRN | Very low | High to very high | Chemical (C), biological(B), radiation (N), and nuclear(N) threats represent a rare but high consequence class of threats |
| Physical security | Blast effects | Low | Low to high | Blast effects include those from HE detonations, vapor cloud explosions (VCE),and other forms of detonations and rapid deflagrations that may cause transient airblasts and high gas pressures, water and ground shocks, or high velocity fragments. Typical threats in this class include: <ul style="list-style-type: none"> • Satchel charge • Vehicle bomb • Very large, nearby vehicle bomb • Natural gas explosion |
| | Forced entry (FE), ballistic impact | Very high | Low to medium | Impact threats range from the relatively small scale associated with FE/BR windows (i.e., forced entry, ballistic resistant glazing) to rocket-propelled shape charges like RPGs and armor piercing rounds. Typical threats in this class include those from: <ul style="list-style-type: none"> • Hand tools(e.g., sledge hammers) for forced entry • Small arms fire |
| | Impact | High | Very low to high | Impact threats range from low-speed impacts by automobiles to high-speed impacts by large aircraft. Most typical of this class are the impact threats associated with the design of perimeter devices intended to prevent vehicle entry. Typical threats in this class include impacts from: <ul style="list-style-type: none"> • Vehicle • Barge • Airplane |
| | Shock | Low | Low | Shock loadings (from impact or blast) can damage equipment and cause electronic systems to fail. |

| | | | | |
|---|--|------|------------------|--|
| Electronic infrastructure, information technology(IT) | Disruption, degradation, compromise, and loss of information | High | Very low to high | <p>The electronic network provides an ever increasing facility for performing transactions, operating systems, using computer resources, and communication that if compromised can seriously threaten the commerce and lives of those effected. Because of the long time menace of the computer vandal, many steps have been taken to protect IT systems. Typical threats include:</p> <ul style="list-style-type: none"> • Hackers, virus purveyors, • spammers(i.e., computer vandals) • Criminals • State sponsored • Disgruntled/unscrupulous employees(perhaps worst case because of inside knowledge) |
|---|--|------|------------------|--|

Table 2: Security assessment methodology.

| Category | Criteria Element | Step No. | Function | |
|---------------------|---------------------------|---|---|--|
| Attack scenario | Assets | 1 | Identify and categorize assets | |
| | | 2 | Assess asset value | |
| | Threats | | 3 | Identify the aggressors likely to target the asset and assess the likelihood of their attempting to compromise the asset |
| | | | 4 | Identify the likely tactics and their associated severity levels for each aggressor relative to each asset |
| | | | 5 | Consolidate tactics from all applicable aggressors for each asset into a design basis threat |
| Level of Protection | 6 | Determine the level of protection for each applicable tactic for each asset | | |
| Consequence | Determining Damage Levels | 7 | Damage levels range from negligible, through various degradation levels, to catastrophic destruction. Damage levels are typically computed analytically, often using various software tools | |
| | Risk Assessment | 8 | For a particular site or facility, the predicted damage levels to components for the threat scenarios considered and other factors (e.g., whether damage to an asset has a consequence for other assets- for example, the loss of a power station may cause many other facilities to cease functioning) provide the basis for assessing the risks associated with a particular class (Table 1) of malevolent threats. | |
| Remediation | Constraints | 9 | Identify design constraints pertinent to the design of the protective system | |
| | Mitigation | 10 | Identify mitigation concepts and strategies and their ROM costs | |
| | Costs | 11 | Identify long and short term costs and costs related to lost/damaged personnel, equipment, and functionality. | |

2.3 Analytical Cost Model for Protective Design for IED threat

Stakeholders (primarily owners) typically will want to minimize their risks at a minimum cost. They will also want to prioritize their risks so that the maximum ones, which correspond to a threat assessed to have high probability and high consequences (top right quadrant in Figure 4), are the ones addressed first.

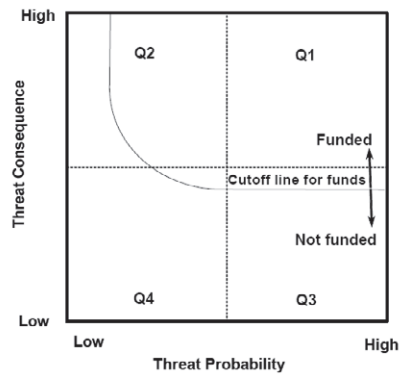


Figure 4: Decisions concerning protection design are likely to be driven by the relationship of threat consequence (i.e., police judgment)-one of the ways that the engineering and policing functions combine in the protective design process.

Once a risk has been identified for action, the risk management process goes on to see what kind of measures should be taken to achieve cost-effective results.

2.3.1 Blast Pressure and Distance

Traditionally, standoff has been the number one measure for protection against bomb blast and is likely to be a big cost driver (Figure 6). As is well known, the blast pressure decreases inversely proportionately to the distance from the source of the blast (Figure 5). Blast pressure (and impulse) rapidly declines with distance. However in many cities, land is at a premium and increased standoff spells ‘sterilised’ land which cannot be effectively used. One can argue its conversion to a landscaped area is a good idea, but to enforce this all the time will result in an inflexible and costly guide to use of the site.

Hence the conventional wisdom is to use some relatively limited amount of standoff combined with protective measures. What this paper attempts to answer is how much protection should be afforded by standoff as compared to the amount of protective measures installed.

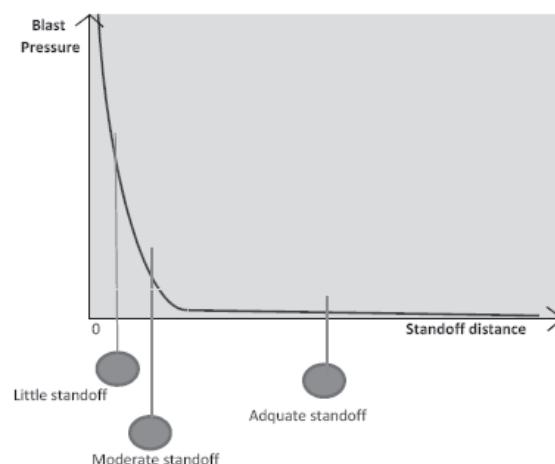


Figure 5: Blast pressure vs. standoff.

2.3.2 Evaluating Standoff Costs

Where increased standoff distance is used as a sole means of protection, a distance of 30m is commonly cited. This distance may be reasonable for a rural or suburban sites, where land is less expensive and an increased standoff is possible, or for a government agency where land is allocated from the state. However in a city or urban context where site plot sizes are often limited, and for a developer purchasing and developing a property, there is a strong desire to limit the amount of standoff as the developer would want to maximize use of the land.

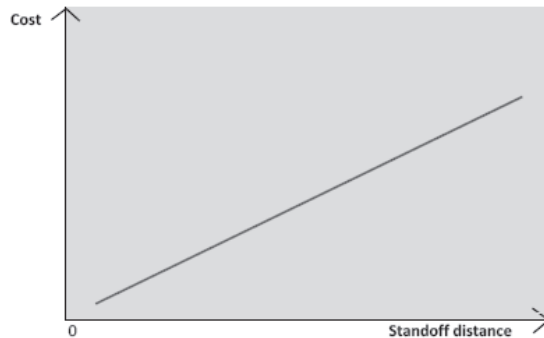


Figure 6: Cost of land used as standoff protection

Land cost in major cities is high, and can vary for different cities and at different points in time. For example, in Singapore land costs can go up to US\$700 per square metre. Costs would obviously be highest in the Central Business District (CBD) and decline when one moves to the suburbs.

The cost of one metre less standoff (i.e., based on the US\$700 per square metre cost) can be compared with the cost of enhancing the protective measures needed to achieve the same level of protection as before the reduction of standoff. This would be approached by considering the cost differential over a one-metre strip of the façade (including the structural system), as indicated in Figure 7.

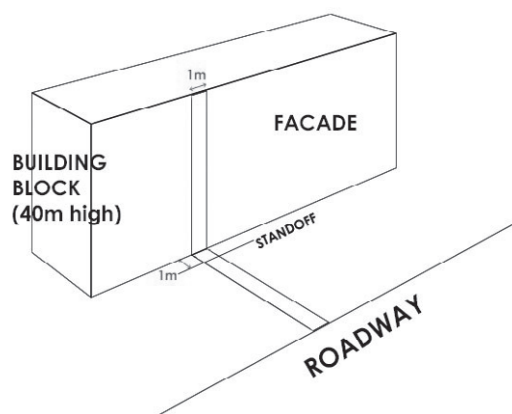


Figure 7: Cost of one metre less standoff can be allocated to protecting equivalent 1-m strip of façade and structure

2.3.3 Corresponding Cost of Mitigation and Protective Measures at Different Standoff

In Figure 5, three standoff scenarios were shown, more could be drawn up. Corresponding to each is a set of protective measures for which a cost can be computed.

- Little standoff: blast pressure high, and protective measures could include:
 - Blast shield wall and building façade will have to incorporate blast shield element.
 - Structural protection required
 - Perimeter protection to enforce standoff
- Moderate standoff: moderate blast pressure, protective measures include:
 - Protection to wall and window system
 - Protection to structural element like columns to prevent progressive collapse
 - Perimeter protection
- Adequate standoff: blast pressure low; protective measures include:
 - Anti-shatter protection to glazing
 - Perimeter protection to enforce standoff – likely to be greater as the site is bigger

The cost of the protective measures corresponding to the standoff distance can be plotted onto a graph as shown in Figure 8.

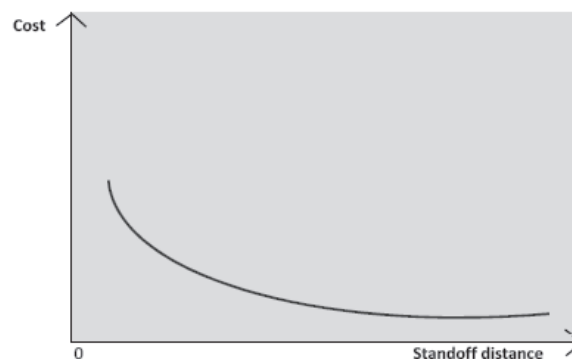


Figure 8: Cost of protective measures vs. standoff distance

2.3.4 Minimum Protection Costs

For a specific level of protection, combining the costs into a single factor (e.g., costs for the land used as standoff protection and for protective measures), one gets a third curve. Moreover, there is an optimal zone as shown in Figure 9, where the combined cost of land and protective measures is lowest for the same level of protection.

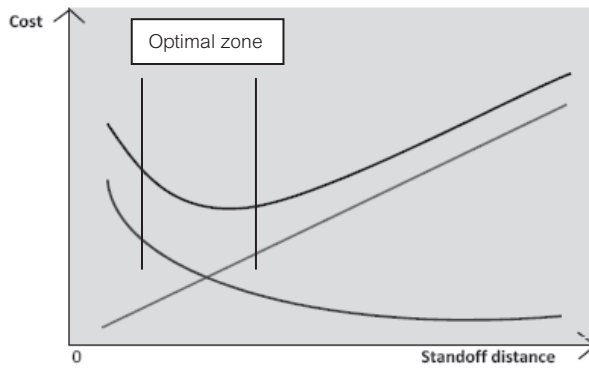


Figure 9: Combined cost (top curve) of land used to obtain standoff protection and of protective measures, as a function of standoff distance

3. EXTENSION OF THIS MODEL

The analytical cost model has been illustrated with reference to protection against an IED threat. It can be enlarged to include other threats and other relevant factors. For example, other factors might include life-cycle costing with respect to maintenance.

A client should also apply it in the periodic security review when protective measures need to be updated to correspond to current threats.

A client should also use a qualified protective design consultant, with relevant experience, access to specialized blast engineering software and test validation data, who can capitalize on the protective design methodology and the analytical cost model when embarking on a physical security upgrade project.

4. CONCLUSION

The holistic protective design methodology, which embodies a multi-factor approach, is scalable to include multi-hazards, e.g. other man-made or natural hazards, as the solution to each hazard individually is likely to overlap with each. For example some aspects of seismic design overlap with blast design. There is, hence, the opportunity for synergy and where contradictions occur, they may be ironed out early so that the final outcome can achieve the optimum performance expected of the multi-facet and multi-hazard approach described herein.

This is an ambitious challenge. However where stakeholders are happy to handle a limited set of factors or hazards, the approach described in this paper is still applicable and can deliver an optimal and balanced outcome.

REFERENCES

- Betts, Curt P., 2005. *Guidance for Security Engineering*. ASCE 2005, US Department of Defense.
 Building and Construction Authority, Singapore, January 2005. *Enhancing*

Building Security.

Department of Defense, 8 October 2003. *UFC 4-010-01, DoD Minimum Antiterrorism Standards for Buildings.*

Department of the Army Headquarters, Washington DC, January 2001. *FM 3-19.30 Physical Security.*

FEMA, Dec 2003. *FEMA 427 - Primer for Design of Commercial Buildings to Mitigate Terrorist Attacks.*

J. E. Crawford, C.L.Liu., "Minimization of Blasts Effects Damage on Critical Buildings," Prepared for Global Security Asia 2007 Conference, March 2007, Singapore.

Karagozian & Case website. *How to select a blast consultant.*

National Security Coordination Centre (Singapore), 2004. *The Fight Against Terror – Singapore's National Security Strategy.*

Standards Australia. HB 167:2006, Security Risk Management.

Standards Australia. AS/NZS 4360:2004 Risk Management.

Crawford, John E., Liu Chunlin, Lan Shengrui. *Protective Technology Services.*

LIU Chunlin. CEO, K&C Protective Technologies Pte Ltd , 19 Jalan Kilang Barat, Acetech Centre, #04-07, Singapore 159361; Vice President, Karagozian & Case, 2550 North Hollywood Way, Suite 500, Burbank, CA 91505-5026; Department of Construction Management, School of Civil Engineering, Tsinghua University, Beijing, 10084

liu.chun.lin@kcpt.com.sg

INTRODUCTION TO ENHANCED ARCHITECTURAL PROTECTIVE SYSTEMS

CHUNLIN LIU¹ and DAVID PALERMO²

¹K&C Protective Technologies Pte Ltd (KCPT), 159361, Singapore
School of Civil Engineering, Tsinghua University, 100084,
Beijing, P.R., China

²Sherwin-Williams Company, South Holland, IL 60473, USA
liu.chun.lin@kcpt.com.sg

ABSTRACT

An explosive blast mitigation technology that has become a validated alternative for architectural elements of structures is the installation of “catcher” systems. These systems “catch” or repel the failure of the in-fill wall, whether masonry, EIFS, windows, doors, or curtain walls, protecting life and property from ballistic shards or fragments. They can be designed to be stand-alone in new construction and structural retrofits or used to augment structural hardening techniques. Cables, fabrics, and thin gauge sheet steel are examples of catcher systems used in the past. A new and proven category of catcher systems are based on polymeric materials that can be used for wall, window, and door upgrades. These products are a thoroughly tested blast mitigation concept to protect against real world threat levels. The blast engineering design capability of K&C Protective Technologies Pte Ltd (KCPT) together with polymeric material engineering of Life Shield Engineered Systems, LLC (LSES) a subsidiary of The Sherwin-Williams Company (SW) creates total engineered systems for even greater in-use performance.

1. INTRODUCTION

The protection of lives from an explosive event is a responsibility not taken lightly by any organization or company. The research, development, and testing of technologies that are used to reduce the loss of life and damage to assets in a blast event have led to the creation and wide spread use of live blast test protocols, instrumentation and modeling [1-2]. Based on this testing, the typical protection concepts used are structural hardening or increasing the standoff against the threat. An explosive blast mitigation alternative has been to increase the safety of structures by use of “catcher” systems.

These systems “catch” or repel the failure of the materials of construction that exist between structural elements such as columns and slabs. This infill area can consist of masonry, EIFS, windows, doors, or curtain wall construction. All these materials are a source ballistic shards or fragments when impacted by the energy of an explosion. Since this infill area is architectural in nature, catcher systems can be designed to be stand-

alone in new construction and in retrofits, with attention paid to aesthetics as well as protection. Cables, fabrics, and thin gauge sheet steel are examples of catcher systems used in the past.

A new and proven category of catcher systems is based on polymeric materials that can be used for architectural infill wall upgrades. These products have been thoroughly tested and validated as a blast mitigation concept. These are recognized as an Enhanced Protective Film System for windows, Enhanced Protective Panel System for walls, and under development, Enhanced Protective Door System. The blast engineering design capability of K&C Protective Technologies Pte Ltd (KCPT) together with polymeric material engineering of Life Shield Engineered Systems, LLC (LSES) creates total engineered systems for even greater in-use performance.

2. METHODS TO REDUCE BLAST HAZARDS

Explosive safety first began in manufacturing facilities where energetic materials could impose an explosive hazard to the workers. As the state of the world is changing today, terrorist activity has spread these concerns to other areas beyond those of manufacturing and storage blast hazards. This new requirement for blast mitigation has opened the door for the research and development of new blast mitigation technologies, allowing the field to transition from traditional mass based systems of steel and concrete reinforcement or thick glass laminates to more compact, efficient, aesthetically sensitive alternatives.

Structural protection concepts started with the physical hardening of a structure or increasing the stand-off distance against the threat. Later through the experimentation of materials, polymer based elastomers were found to be an effective architectural hardening alternative for blast mitigation. Polymeric materials absorb large amounts of energy from blast events due to their elastomeric material properties. These materials have also become part of “catcher” systems for the retrofit of architectural elements. The use of polymeric materials for blast protection is expanding to address the need for the protection of existing buildings that require a retrofit to improve its blast resistance. With proper international cooperation, polymeric materials for architectural protection can enhance mitigation design solutions.

Physically hardening existing structures uses anti-shatter window film, glass laminates, or concrete and steel reinforced materials throughout a structure. These materials work well in new construction applications and in retrofits where aesthetics are not an issue. Although physical hardening is effective and a low cost alternative for blast mitigation technologies, it is not the correct option for all situations. In structures with smaller rooms, a concrete retrofit may not be viable due to size constraints. Also, in commercial, corporate, or historic buildings, physical hardening may not be an option due to the visually undesirable aesthetics and business disruption of the retrofit. This need for alternative blast mitigation technologies with similar or greater effectiveness, cleaner aesthetics, and less mass created an opportunity for the use of polymeric materials for structural protection.

The primary characteristic of the polymeric material is the ability to absorb a blast event's energy throughout a polymeric network. This allows for a large displacement of force that can be seen visually. The elastomer bends, stretches and flexes as the initial impulse of a blast event comes in contact with the polymer panel. On a molecular level, the polymer chains realign throughout the panel while it is stretched allowing the polymer to withstand large pressure loads. These attractive material properties make elastomeric materials an effective solution for the blast mitigation. The amount of deflection of course, is a function of blast load and anchor design.

Although the use of polymeric materials for blast mitigation may sound very specialized, there are a variety of options for this type of technology. Polymeric materials can be used in new construction as an integrated catcher system. This system is built into the wall of a building while it is erected and is concealed within the structure. However, many buildings that require blast protection require a retrofit installation. These structures can also utilize a polymeric catcher system that is installed on the interior of an existing wall. These retrofits are similar to an integrated system during new construction but require engineering and contractor expertise to install the retrofit onto a wall appropriately.

Catcher systems are a unique technology in the blast mitigation field because they do not attempt to protect from a blast with shear mass. The technology is used to absorb a blast's energy rather than block it. This prevents blast pressure and the outer wall or window fragments of a structure from penetrating into the interior of a building. This is achieved by installing a polymeric catcher system on the interior surface and anchoring it to the infrastructure, whether that is the floor and ceiling slabs or the columns. In a blast event the outer wall, window, or door will fracture and take on the form of smaller projectiles moving at a high velocity towards the interior of a structure. It is this debris that has been demonstrated to cause the greatest harm to people and property on the interior of the building. Polymeric catcher systems prevent outer wall and window debris from entering into the structure by absorbing and deflecting the blast. Their unique material properties allow the system to deflect and flex under the initial load of the blast minimizing the load to the anchorage fastener points, and therefore, into the structure. This is an important property of catcher systems because if a large amount of energy is observed at the anchorage points the panel can rip out of its attachment system or the capacity of a load bearing member in a structure could be compromised.

3. ENHANCED PROTECTIVE FILM SYSTEM

The anchorage system of a polymeric panel to a structure is a significant aspect of the blast mitigation process. Earlier work on engineered fabric systems showed a large amount of energy directed at the fasteners that anchor the polymer to the structure. This energy then adds to accumulated effect that leads to the initiation of progressive collapse. Attachment systems must be engineered to find a balance of strength and elasticity allowing for the polymeric panel to deflect and flex but not tear away from the anchor point in the structure. Furthermore, the anchorage system is

unique to each installation as every building is different. Due to the assortment of options for types of polymeric blast mitigation and the variety of anchorage options it is important to classify each system with specific performance parameters in order to define the appropriate and cost effective use.

To implement the use of catcher systems, K&C Protective Technologies of Singapore collaborated with Life Shield Engineered Systems of the United States to create an Enhanced Protective Film System (Figure.1-5). This system combines material properties with attachment design to create a system that can readily withstand realistic explosive blast loads greater than 300psi-msec even close to the 400psi-msec level. It consists of a clear composite material of good clarity for windows. This clear composite offers a large blast resistance capacity with anchoring systems that can be modified based on the size of the threat. These products are provided under the brand name Life Shield®. The clear panels can be attached independent of the glazing allowing for enhanced anchoring designs. Even though the polymeric material has proven to withstand very large blast loads anchor design to the threat load now becomes the critical factor. It has been shown that flexible attachment systems outperform ones that are hard mounted as in typical in most blast window attachment systems.

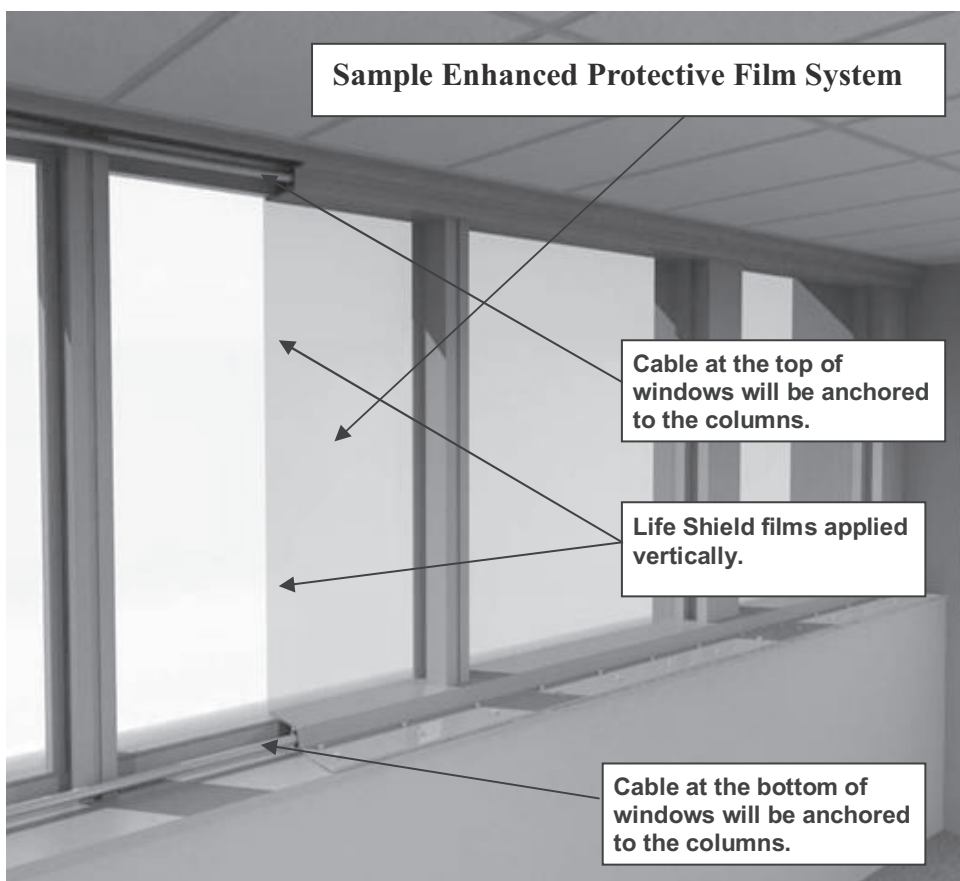


Figure 1: Sample Enhanced Protective Film System (a)

Another enhanced protective feature of the clear panels is that they can be utilized in window constructions of many different types. (Figure. 2)

With such a variety of designs, architectural aesthetics are easily incorporated.

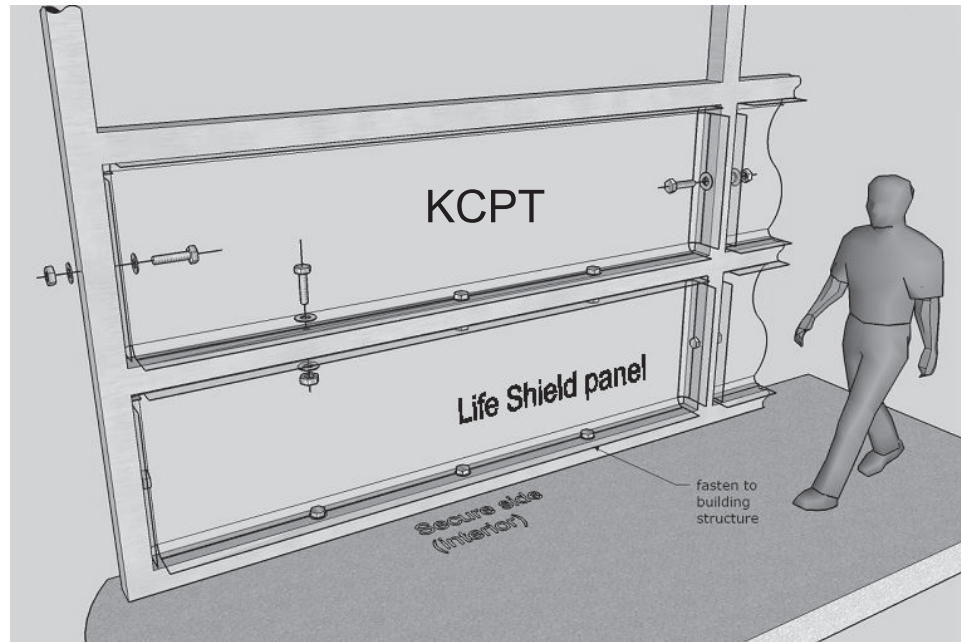


Figure 2: Sample Enhanced Protective Film System (b)

In order to testify the quality of Enhanced Protective Film System, K&C Protective Technologies and Security Coating Systems team cooperate to do the site blast test.



Figure 3: Test Site Installation: Notice Clarity of Retrofit



(a) Outside view of Test Specimen



(b) At the Beginning of Blast



(c) ASF Protected Windows Begins to Fail



(d) EPFS Repelling Entire Window Mass Including Shards



(e) Blast Pressure Pulverizes ASF Glazing



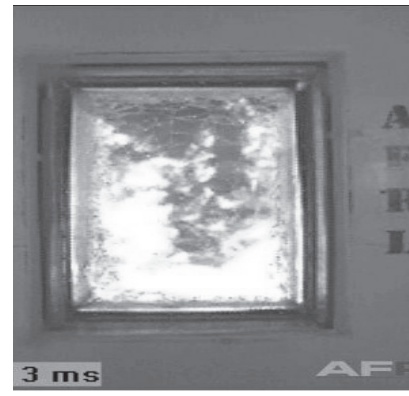
(f) Entire Window Mass and Shards Kept out of Building Interior

Figure 4: Blast Test for Enhanced Protective Film System

Exterior View: Four 4ftx6ft windows with 7mil PET Anti-shatter film applied to the glazing. Retrofitted with Life Shield LSC-150 EPFS. Blast pressure is over 20 times GSA standard for anti-shatter window film requirements and over 8 times blast window requirements.



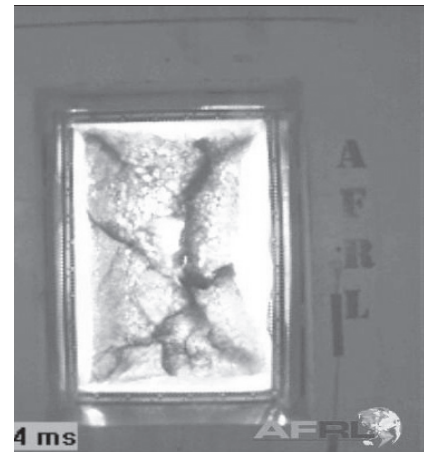
(a) 0ms (At the Beginning of Test)



(b) 3 ms



(c) 12ms EPFS engages and begins to deflect as ASF glazing fails



(d) 14 ms ASF glazing obviously fails



(e) 31ms ASF glazing rejected by EPFS



(f) 116ms EASF glazing pulverized no fragments or shards inside structure.

Figure 5: Result of Blast Test for Enhanced Protective Film System

From the test example shown in the Figure 3, Figure 4 and Figure 5, it can be seen that the Enhanced Protective Film System can successfully resist the blast loading which is over 20 times GSA standard and over 8 times blast window requirements.

4. ENHANCED PROTECTIVE PANEL SYSTEM

The system for walls (Figure 6) performs in a very similar fashion as the Life Shield clear composite panels in that they are anchored to the infrastructure element and catching the load, debris and fragments. Testing for wall only polymeric solutions has been ongoing for a number of years.

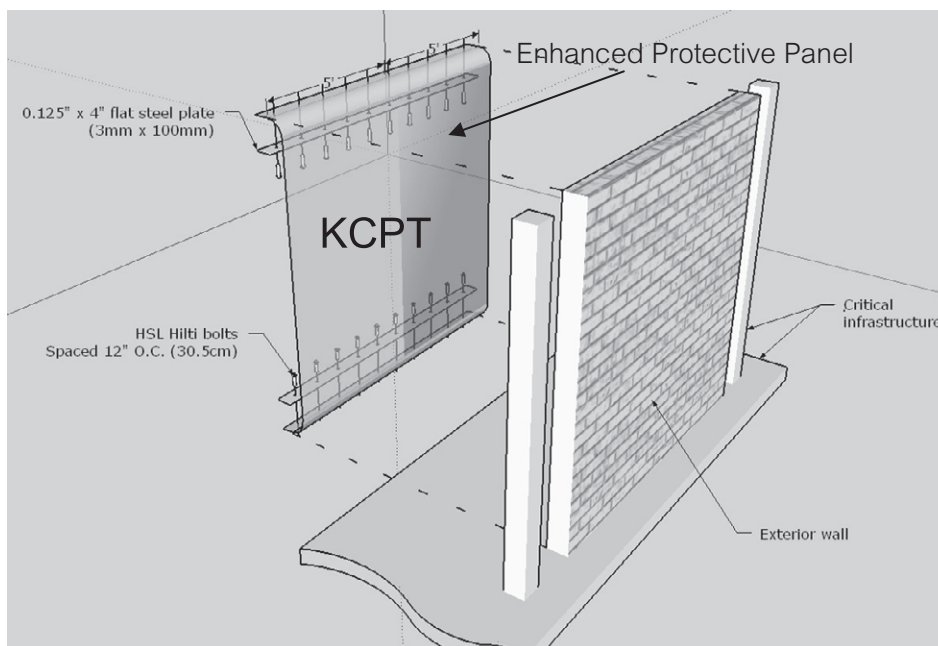


Figure 6: Concept drawing for Enhanced Protective Panel System For protecting the architectural infill element between the slabs and columns

However, the vast majority of product development for blast protection has been centered on stand alone structural or architectural elements. This has shown to be a disconnect from the reality of current construction techniques. It is obvious that windows fail first in a blast event as proven in numerous tests and real world events. Testing the protection of windows alone as the sole target is valid for low pressure testing criteria such as is widely used in the North America. These tests are used to validate anti-shatter window films and window laminates for the 4psi/28psi-msec and 10psi/89psi-msec criteria.

The reality is that most exterior architectural elements have window glazing and wall sections to take into consideration. The collaboration between KCPT and LSES has created the first ever total protection system. (Figure 7) These combinations have been thoroughly tested utilizing flexible anchoring designs. (Figure8)

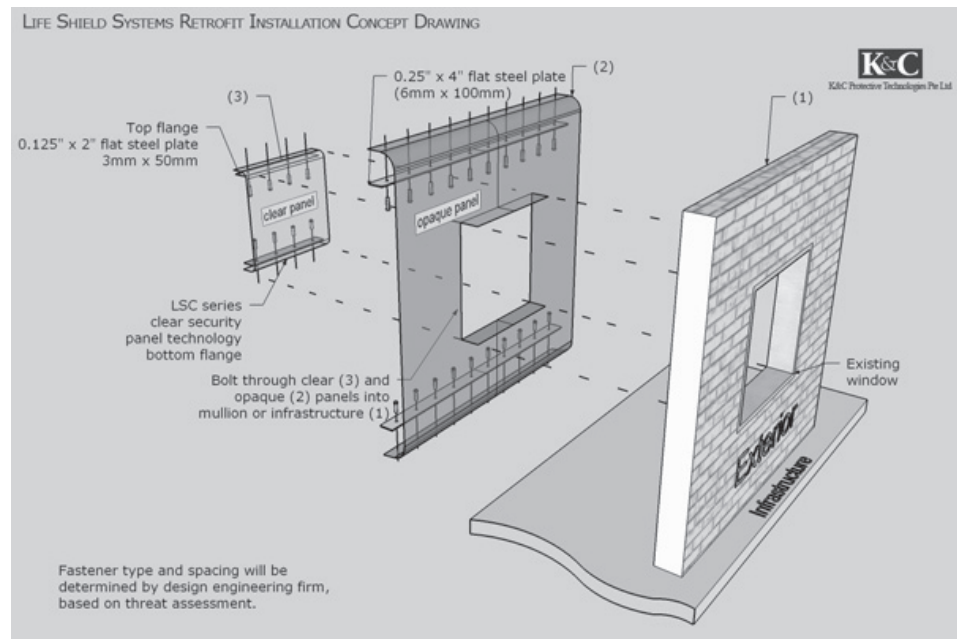


Figure 7: Concept drawing for Enhanced Protective Window and Panel System Combination. For protecting the architectural infill element between the slabs and columns.



Figure 8: Testing of Enhanced Protective Window and Panel System Combination For protecting the architectural infill element between the slabs and columns



Figure 9: Shield Wall Panels installed 33 feet from detonation on ungrouted masonry infill wall

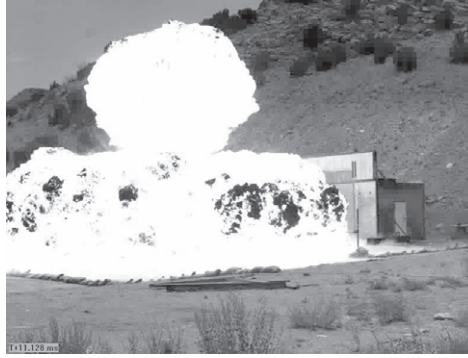


Figure 10: Pressure wave and fire ball travel towards infill wall



Figure 11: Life Shield Wall Panels intact on the left side, control fails catastrophically on right side



Figure 12: Series of Life Shield Wall Panel tests against 4 kilograms of TNT at 50, 70, and 120 centimeters in fragmentation casing



Figure 13: Interior side of structure pre-detonation.



Figure 14: Post detonation pictures of threat side and building interior side. No debris on interior side and no evidence of anchor loading



Figure 15: Post-detonation picture of threat side and structure interior side. No evidence of anchor loading.



Figure 16: Post-detonation picture of threat side and structure interior side. Slight anchor loading due to placement of charge 50cm off the corner

5. ENHANCED PROTECTIVE DOOR SYSTEM

To complete the total systems approach for protecting all architectural elements KCPT has designed a door concept. The focus is on reducing the weight of the door while integrating it into the Life Shield wall protection retrofit. (Figure 17) Included in the design is ballistic protection which has currently exceeded NIJ IIIA levels.

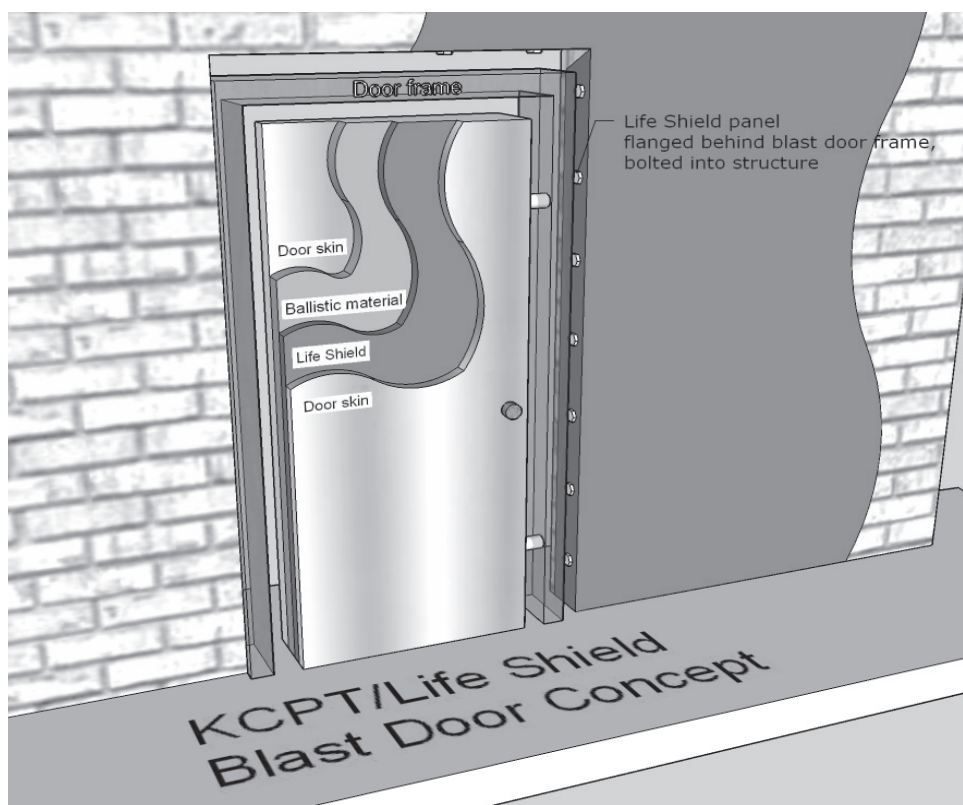


Figure 17: Testing of Enhanced Protective Panel and Door System Combination

6. CONCLUSION

The creation and testing of materials other than concrete, steel, anti-shatter window film, and laminated glass for blast mitigation has been completed, documented, and live blast test proven. Coupling material design with engineering analysis to create a total systems protective film solution for wall and windows is a natural evolution to broaden the use of this technology around the world. Catcher systems cannot be any stronger than the structure itself. The advantage of the catcher system is the ability to be designed into the strongest attributes of the structure, be it the slabs or the columns. Additionally, the use of flexible anchorage systems such as exist in the total systems protective film solution allow the mitigation system to perform at higher blast loads by managing the deflection.

ACKNOWLEDGEMENTS

The authors would like to acknowledge the K&C Protective Technologies and Life Shield Engineered Systems team in their work pertaining to the research, design, manufacturing, and installation of preformed polymeric panels used for blast protection.

REFERENCES

- D. Bogosian, H. Der Avanessian. *To film or not to Film: Effects of Anti-Shatter Film on Blunt Trauma Lethality from Tempered Glass*. Proceedings of the 17th International Symposium on the Military Aspects of Blast and Shock[C], Jun2 2002, Las Vegas, Nevada
- D. Bogosian, H. Der Avanessian, et al. *Assessment of Human Injury Data from Cubicle Experiments*[R]. Karagozian & Case and Biodynamics Engineering, Inc., TR-03-9, July 2003
- LIU Chunlin. CEO, K&C Protective Technologies Pte Ltd , 19 Jalan Kilang Barat, Acetech Centre, #04-07, Singapore 159361; Vice President, Karagozian & Case, 2550 North Hollywood Way, Suite 500, Burbank, CA 91505-5026; Department of Construction Management, School of Civil Engineering, Tsinghua University, Beijing, 10084
liu.chun.lin@kcpt.com.sg

IDENTIFICATION OF POLLUTANT SOURCES IN URBAN AREA USING INVERSE CFD MODELING

HONG HUANG¹, SHINSUKE KATO² and MAHMOUD BADY³

¹Institute of Industrial Science, The University of Tokyo, Japan
hhong@iis.u-tokyo.ac.jp

²Institute of Industrial Science, The University of Tokyo, Japan
kato@iis.u-tokyo.ac.jp

³Graduate School of Engineering, The University of Tokyo, Japan
mbady@iis.u-tokyo.ac.jp

ABSTRACT

The present research introduces a technique to determine pollution source locations in urban areas -when the pollutant concentration field is known- through the use of reversed time marching method (RTMM). The method depends primarily on the solution of the scalar transport equation with time integration in the negative direction. This leads to reversing the velocity field and also the diffusion term. The study demonstrates how to use the inverse CFD model with the reversed time marching method to identify pollution sources in urban areas. An example was given in order to examine the accuracy of RTMM in identifying pollutant sources in urban areas, in which the wind flow around a single building was investigated for two different source locations. Steady state numerical simulations were carried out at first in order to estimate the wind flow fields. With the steady-state airflow patterns, direct CFD modeling (forward-time simulation) was used to calculate pollutant concentration distributions for step-function sources. In the last stage, the scalar transport equation was solved again but with the reversed flow field and the negative diffusion term. By using peak concentration, one could identify the pollution source location. Results of the study demonstrated that the RTMM can identify pollution sources locations in urban areas with a satisfied accuracy.

1. INTRODUCTION

Nowadays, reverse modeling seems to be one of the promising topics to be considered in the urban safety research. The importance of reverse modeling arises from the increased levels of pollution sources due to continuing expansion of industries coupled with population growth, especially in large cities. In addition, the terrorist attacks are becoming frequent and deadlier such as sarin gas attack on Tokyo subway 1995, which resulted in 12 dead and 6000 injured (Yokoyama, 2007; Okumura, et al., 1996]. Moreover, the ability to predict pollution source locations, source strength, and release time is required to get complete image about the air quality conditions within release domain. Accordingly, the identification of pollution (or

release) source location immediately after release became an urgent matter to be investigated in order to ensure people safety. Reverse modeling represents an efficient and promising tool in this matter.

In recent years, some researchers have studied reverse modeling techniques in identifying pollution sources locations either in air or in groundwater. Chen et al. (Zhang and Chen, 2007) studied the contaminant source identification in a 2-D aircraft cabin and in a 3-D office by applying inverse CFD modeling. They used the quasi-reversibility equation instead of the contaminant transport equation since it is numerically stable when time is reversed. According to the study results, they concluded that the inverse CFD model could identify the contaminant source locations but not very accurate contaminant strength because of the dispersive property of the quasi-reversibility equation. Gomez-Gesteira et al. (Gomez-Gesteira, et al., 1999) used the particle tracking method to investigate contaminant dispersion process in two different sites located along the North West coast of Spain under summer conditions. Bagtzoglou et al. (Bagtzoglou, et al, 1992) applied the particle tracking method to identify the sources of contamination in the groundwater systems by reversing the velocity field and leaving the diffusion/dispersion unchanged. Wilson et al. (Wilson, et al, 1994) studied the particle tracking method to determine groundwater pollution sources through the solution of stochastic differential equations backwards in time for 1-D and 2-D. Their method results in time (or space) dependent probability maps for the water in the study well, which they called it: travel time probability map and location probability map.

It is clear from the previous studies that the diffusion term represents a problem when dealing with the reversed scalar equation due to the instability caused by such term. Accordingly, the purpose of this paper is to develop and also to verify the method for backward problems that accounts for the diffusion as well as the convection through the use of reversed time marching method (RTMM). The method depends primarily on the solution of the scalar transport equation with time integration in the negative direction. This leads to reversing the velocity field and also the diffusion term. The method is applied to two simple examples of a flow in an open boundary layer and of a flow around a single building. Direct CFD simulations were carried out at first to calculate both flow and concentration fields. The reversed time marching method is then conducted to find the pollution source location.

2. REVERSED TIME MARCHING METHOD

Pollutant concentrations are predicted based on the convection-diffusion equation including meteorological data, transport diffusion, and the relevant emissions. It can be written as:

$$\frac{\partial(\phi)}{\partial t} + \frac{\partial(u_i \phi)}{\partial x_i} = \frac{\partial}{\partial x_i} \left(\frac{K}{\rho} \frac{\partial \phi}{\partial x_i} \right) + \frac{S}{\rho} \quad \text{where } t \rightarrow \infty \quad (1)$$

where ϕ denotes the concentration (kg/kg), t is the time (s), u_i is the Cartesian components of the velocity (m/s), x_i is the Cartesian coordinates

(m), ρ is the air density (kg/m^3), S is the pollutant source strength ($\text{kg/m}^3/\text{s}$), and K is the diffusivity coefficient for the concentration ($\text{kg/m}^2/\text{s}$).

By reversing time direction in Equation (1), the sign of the unsteady terms becomes negative. Thus, the above equation with the absence of the source becomes:

$$-\frac{\partial(\varphi)}{\partial t} + \frac{\partial(u_i \varphi)}{\partial x_i} = \frac{\partial}{\partial x_i} \left(\frac{K}{\rho} \frac{\partial \varphi}{\partial x_i} \right) \quad \text{where } t \rightarrow \infty \quad (2)$$

Rearranging this equation, then:

$$\frac{\partial(\varphi)}{\partial t} + \frac{\partial[(-u_i)\varphi]}{\partial x_i} = -\frac{\partial}{\partial x_i} \left(\frac{K}{\rho} \frac{\partial \varphi}{\partial x_i} \right) \quad \text{where } t \rightarrow \infty \quad (3)$$

It is obvious from Equation (3), that the reversed time marching method is very easy to be implemented and can be used to evaluate pollution sources. However, there are two important problems arising from this equation. The first is that; neglecting the diffusion can be a problem when the convection is weak. The second problem is that, if the transport equation is solved (as shown in Equation (3)); the solution is numerically unstable due to the negative sign of the diffusion term. In order to make the governing equation solvable with numerical stability, this study proposes the use of a filter to deal with negative concentration gradients in order to avoid unrealistic solutions. Indeed, the presence of such filter affects the solution accuracy and decreases the method effectiveness in identifying the exact locations of pollution sources. However, the effect of adding a filter to the reversed scalar equation (i.e. Equation (3)) will be evaluated in the present paper according to the obtained results.

In order to determine the source location within a domain through the use of inverse modeling, concentration distributions are needed. In the daily life, the concentrations should come from data measured by concentration sensors. Since this paper is to explain the method of inverse modeling, a direct CFD simulation was conducted at first to solve the flow field and then the calculated flow field is used to estimate the concentration field, which is used as initial condition when carrying out the inverse modeling.

3. EXAMPLE OF APPLYING THE RTMM IN IDENTIFYING SOURCES LOCATIONS

3.1 Wind flow around a single building

The example for identifying pollution source location in urban areas using RTMM is shown in Fig. 1, in which wind flows around a single building. The building dimensions are 10 (x) \times 10 (y) \times 30 (z) m and the dimensions of the computational domain are 300 (x) \times 110 (y) \times 70 (z) m with a mesh size of 444,800 cells.

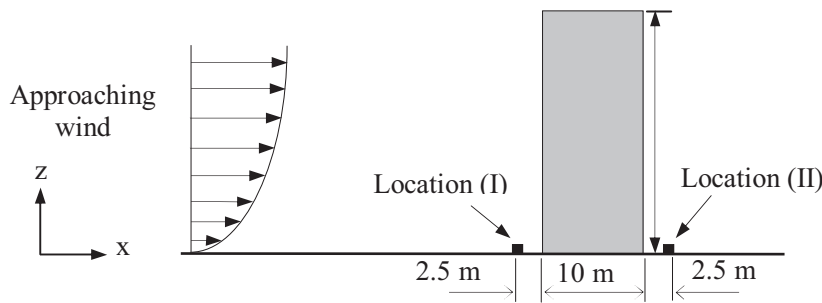


Figure 1: Geometry of flow around a block and pollution source locations (I) and (II)

Two different locations for the source were considered in order to examine the effect of pollutant source location on the prediction accuracy of the RTMM: location (I) which is 2.5 m upwind the building and location (II) which is 2.5 m downwind the building. In both cases, the source strength was set to 0.01 kg/m³/s and its dimensions were 0.5 m × 0.5 m × 0.6 m.

3.2 Numerical simulation

Numerical simulations were carried out through the CFD code Star-CD, based on a finite-volume discretization method. During forward simulation, steady state analysis was adopted for the flow field and Monotone Advection and Reconstruction Scheme (MARS) (STAR-CD, 2004) was applied to the spatial difference. The standard k-ε model was used to simulate the turbulence effects and the pressure / velocity linkage is solved via the SIMPLE algorithm.

At the inflow boundary, a constant flux layer was assumed for the turbulent energy k, and turbulent intensity was assumed to be 10 % of the inflow wind velocity at a representative height (Z₀) of 74.6 m. A 1/4 inflow wind profile is used. Free slip condition was applied on the top and the sides' boundaries. The generalized logarithmic law with the parameter E = 9 was applied to building walls and ground surface as smooth walls.

Once the flow field is solved, it is considered as steady flow field and then the concentration fields in both direct and reverse simulations are solved in time. The wind flow distribution together with the pollutant concentrations of the direct simulation are used as initial conditions for the reverse simulation. A time step of 0.1 s was used with the implicit scheme.

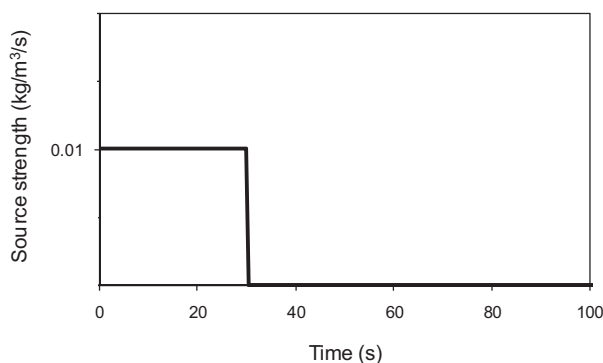


Figure 2: Pollutant source strength as a function in time

In direct simulation (forward-time simulation), a pollutant source of strength $0.01 \text{ kg/m}^3/\text{s}$ was released in the period from $t = 0$ to $t = 30 \text{ s}$. Then, the solution of the transport equation is continued with the absence of the source until $t = 200 \text{ s}$. Fig. 2 shows the release source as a function in time.

In reverse simulation, the flow field calculated by direct simulation is reversed at first and the source term is set to zero. Then the transport equation is solved from the moment of $t = 200 \text{ s}$ in reverse time direction. The time at which the reversed simulation is stopped is not known in reality. In other words; starting from the moment of solving the transport equation in the reverse time direction, the time $t = 0$ at which the calculations has to be stopped is not known in advance. Since the present examples are introduced just to explain the idea of reverse simulation using RTMM, the end time is known.

4. RESULTS AND DISSCUSTIONS

Figure 3 shows the computed airflow pattern around a single building under steady state. The subplot (a) shows the flow field calculated by the direct simulation and the subplot (b) shows the reversed flow field which was used to carry out the reverse simulation. In subplot (a), a symmetrical flow field is shown around the building, where two identical circulation regions are formed around the building.

It is expected that the effectiveness of RTMM in identifying the pollution source location is affected with the source location. So, as mentioned before, two locations for the pollutant source were examined here; location (I) and location (II). The first location is upwind the building and the second location is in the wake region downwind the building.

4.1 Source location (I)

The concentration fields around the building obtained for the source location (I) are shown in Fig. 4. In subplot (a), at $t = 1 \text{ s}$, the plume starts to

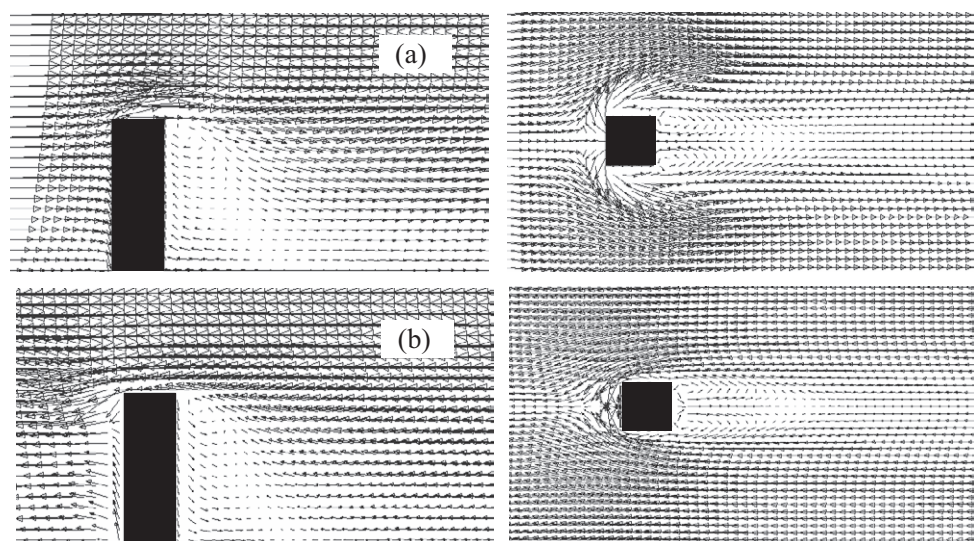


Figure 3: Wind flow field around a building; (a) direct flow, (b)

diffuse where the concentration field touches the upwind face of the building. The plume is then travels with the wind downwind the building. The pollutant is continued to be released until the moment $t = 30$ s. At this time, the emission source was stopped and the scalar transport equation was solved in time using direct simulation without the source. At $t = 200$ s, two identical regions were formed far from the building. The conditions at such time were used as the initial conditions for the inverse modeling. Fig. 4 (c) shows the concentration field obtained by the inverse modeling. In such figure, the concentration field area is wider than that of the direct simulation. By detecting the location of maximum pollutant concentration over all locations, the source location is clearly determined. It is located downwind the building along the domain centerline. However, the maximum concentration occupies a wide area in front of the block. This shows that the estimation of the source location will not be 100 % accurate.

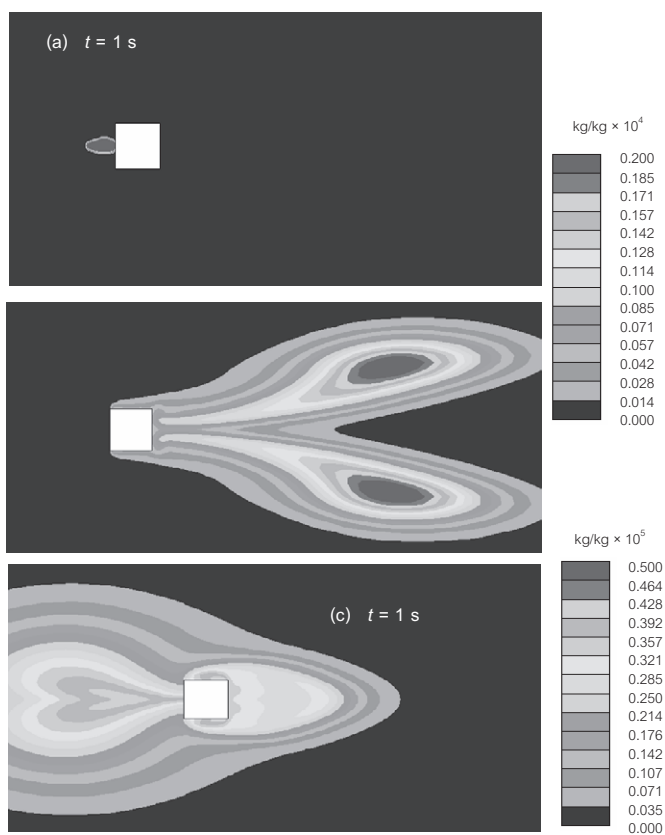


Figure 4: Concentration fields when the source is in location (I), (a) at $t = 1$ s obtained by direct simulation, (b) at $t = 200$ s obtained by direct simulation. (c) at $t = 1$ s obtained by reverse simulation field

Compared with the peak concentration obtained with the direct CFD modeling as shown in Fig. 4(b), the source strength identified by the inverse CFD modeling of Fig. 4(c) is more dispersive. The reason is that the transport equation is not exactly the same as the governing transport equation for the pollution concentration due to the presence of a filter. Indeed, the filtration process affects the accuracy of the RTMM and this appears clearly in the wide area of high concentrations, which give a wide range of possibilities for the pollution source location. This is not the ideal distribution when the determination of gas release position is needed.

4.2 Source location (II)

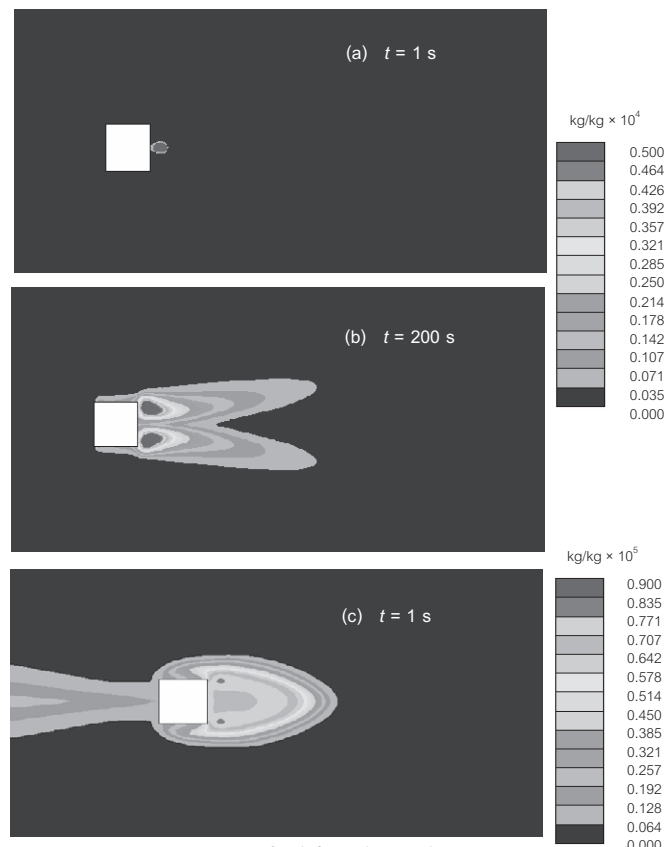


Figure 5: Concentration fields when the source is in location (II), (a) at $t = 1$ s obtained by direct simulation, (b) at $t = 200$ s obtained by direct simulation, (c) at $t = 1$ s obtained by reverse simulation.

Figure 5 shows the concentration fields around the building when the pollutant source is in location (II). The subplot (a) shows the source location which is 2.5 m downwind the building rear surface. Similar to the case of location (I), the pollutant is emitted in the period from $t = 0$ to $t = 30$ s and then the scalar transport equation was solved with the absence of the source term until the moment $t = 200$ s. In subplot (b), two high concentration regions are formed behind the building. The diffusion of the pollutant in such case is limited to a narrow region compared with the case of location (I).

Figure 5(c) shows the concentration field obtained using inverse modeling. The figure shows that the peak concentration region occupies narrow region compared with the case of location (I). This can be attributed to the presence of the source in the wake region where low wind velocity exists and the convection is weak. In such case, the location of pollution source estimated by the reverse simulation is not clear. In Fig. 5(c), there are two peak concentration regions near the edges of the block. So, the identification of the source location in such case is not easy.

5. CONCLUSIONS

The present research introduces a technique to determine pollution source locations in urban areas -when the pollutant concentration field is known- through the use of reversed time marching method (RTMM). The method depends primarily on the solution of the transport equation of the contaminant with time integration in the negative direction. In order to examine the accuracy of RTMM in identifying pollution sources in urban areas, an example was given in which the wind flow around a single building was investigated for two different source locations. The study results demonstrated that the RTMM can be applied to identify pollution source locations in urban areas. However, the prediction accuracy decreases in case of weak convection.

REFERENCES

- Bagtzoglou, A. C., Dougherty, D. E. and Tompson, A. F. B., 1992. Application of particle methods to reliable identification of groundwater pollution sources. *Water Resources Management*, 6, 15–23.
- Gomez-Gesteira, M., Montero, P., et al., 1999, A two-dimensional particle tracking model for pollution dispersion in A Coruna and Vigo Rias (NW Spain), *Oceanologica Acta*, 22, 167-177.
- Okumura, T., Takasu, N., et al., 1996. Report on 640 victims of the Tokyo subway sarin attack. *Ann Emerg Med*, 28, 129–135.
- STAR-CD, Methodology, Version 3.22, 2004. Computational Dynamics Limited.
- Wilson, J. L. and Liu, J., 1994. Backward tracking to find the source of pollution. *Water Management and Risk Remediation*, 1, 181-199.
- Yokoyama, K., 2007. Our recent experiences with sarin poisoning cases in Japan and pesticide users with references to some selected chemicals, *Neurotoxicology*, 28. 364-373.
- Zhang, T. and Chen Q., 2007. Identification of contaminant sources in enclosed environments by inverse CFD modeling, *Indoor Air*, 17, 167-177.

RESEARCH AND TESTING OF PROTECTIVE GARMENTS AND EQUIPMENT USING A THERMAL MANIKIN SYSTEM

JIN PAN and XIAOYU TANG
TEST International Group, China
cicitang@test-tech.com.cn

ABSTRACT

Thermal manikins are a valuable and accurate research tool for evaluating the safety of personal protective garments and equipment, while also providing data useful for improving their comfort and performance. Over the long history of thermal manikin development, including thermal manikins with specialized functions, users can now safely research and test special protective garments and equipments. Thermal manikins placed into various disaster environments can help simulate human metabolic response in a disaster. Through the testing of personal protective garments and equipments, we can analyze and predict more accurately their true level of protection in a disaster situation.

Key Words: *protective garments and equipments, thermal, manikin, comfort*

1. INTRODUCTION

To better prepare for disasters, such as the recent "Wenchuan Earthquake", emergency teams including army, police and firemen must have the tools to continue their rescue work, regardless of the situation. We need to improve the efficiency of automotive and airplane air conditioning units, protect rescue workers from hazardous environments with protective garments and equipments, and keep them in top form at all times. To ensure top performance, rescue workers need to be safe and comfortable – any time, any place. Using thermal manikin systems as precision instruments for measuring and evaluating the thermal comfort of protective garments and equipments in hazardous environments can help improve their safety, comfort, and performance.

2. MANIKIN HISTORY

The original application for thermal manikin testing was an American Army garments test. Prior to 1941, there was no method available to accurately assess thermal heat transfer through protective clothing ensembles. The development of the clo unit in 1941 by Gagge, Burton, and Bazett was an important advancement in clothing science. This concept of insulation was

the first to establish a relationship between man, his clothing and the environment.

2.1 Early Thermal Manikin History

The building of the first working thermal manikin for the U.S. military is attributed to Dr. Harwood Belding in 1941. During the World War II, they investigated reports of inadequacies in protective clothing capabilities from various battlefronts, and suggested possible improvement. In 1945, Belding and his thermal manikin joined the U.S. Army Quartermaster General's new Climatic Research Laboratory. In September 1945, along with detailed data from an anthropometric study of nearly 3000 Army Air Force cadets they constructed another electroplated copper shell manikin based on the average physical dimensions of a young U.S. military recruit. Gagge and his associates used this new manikin to completely redesign most Army Air Force aviators clothing away from the use of natural materials to newly developed artificial materials, and worked on improving environmental protection for U.S. military personnel.

2.2 Thermal Manikin Research: 1950's

By the early 1950's, clothing researchers had successfully used thermal manikins to measure the resistance to sensible, dry, heat transfer of a wide range of protective garments from all the military services. In the process, military footwear, handwear, sleeping bags, and combat clothing ensembles were further improved for comfort, durability, and environmental protection.

Thermal manikin research during this decade also revealed that the highly curved surfaces of the human body created a complex and dynamic microclimate between the clothing and skin surface. Unlike the heat transfer characteristics of textiles established from earlier guarded ring flat plate work, thermal manikins showed that actual clothing, when draped over the human figure, can have localized variations in thermal conductivity as well as in the ensemble's convective and radioactive properties.

2.3 Thermal Manikin Research: 1960's

In 1961, most military thermal manikin work was centered at the new U.S. Army Research Institute of Environmental Medicine (also known as "USARIEM"). One area of new research was focused on the resistance by protective clothing to the transport of water vapor and its impact on soldier performance. This moisture permeability index (im) characterized the permeability of garments materials to the transfer of water vapor. "Sweating" manikins outfitted with tight fitting cotton skins that could be saturated with water to simulate a sweat wetted skin surface, could now measure the maximum evaporative heat transfer allowed to an individual wearing a given protective ensemble.

2.4 Thermal Manikin Research: 1970's

Comparisons made between thermal manikin data and controlled human volunteer studies indicated that the movement of air within and immediately adjacent to a multilayered clothing system could have a dramatic impact on the evaporative cooling potential of the protective ensemble. Givoni and Goldman used thermal and water vapor resistances from thermal manikins along with the derived pumping coefficient to develop a series of equations that predicted rectal temperature when wearing military clothing in a range of cool to very hot environments. Thermal manikin data are used to assess the impact of the level of dehydration and effects of acclimatization on wearers of protective garments.

2.5 Thermal Manikin Research: 1980's To Present

In the early 1980's, the U.S. Army began a complete redesign of major clothing systems for air, ground, and vehicle based personnel utilizing a variety of novel technologies and materials. On an increasing basis, the military has evaluated and then adopted numerous commercial textile developments (i.e., Gore-Tex, Thinsulate, Primaloft) for use in these new protective garments, footwear, handwear, and sleeping systems. Many textile manufacturers used manikins for novel developments and test results. Thermal manikin could simulate the bodily movements involved in walking and running. The manikin is housed in a climatic chamber with precise control over the air velocity directed at the manikin.

3. MODERN MANIKINS

Thermal manikins have evolved in U.S. as a direct result of the need to provide better personal protective garment and equipment in an increasing variety of environmental zones of operation. Thermal manikin data has been instrumental in improving both the comfort and functional performance of a multitude of protective garment and equipment as well as providing input to develop practical human performance predictive models.

As the development of modern technology moves forward, manikin manufactures have developed new carbon-epoxy shells and porous metal sweating skin surfaces to replace heavy copper or aluminum forms, and have greatly improved manikin responsiveness and accuracy. For example, the carbon-epoxy "NEWTON" thermal manikin and advanced porous metal skinned "ADAM" thermal manikin apply for different requirements.

3.1 Thermal Manikin "NEWTON"

The "Newton" thermal manikin consists of a carbon-epoxy shell with internal heater elements, temperature sensors, and an optional integrated fluid supply system to simulate metabolic heat and perspiration levels. A dedicated Dell Pentium computer running ThermDAC software controls the manikin temperature and internal systems while automatically logging data.

Manikin size: 50th percentile Western or Asian Male, Weight ~ 30 kg

Standard zones: 20, 26, or 34 independently controlled thermal regions

The “NEWTON” manikin is articulated at the shoulders, elbows, hips, knees and ankles (Table 1).

Table 1: Ranges of motion for the joints

| Joint | Rotary motion | Lateral motion |
|-----------|---------------------|----------------|
| shoulders | - 45 to 180 degrees | none |
| elbows | 0 to 90 degrees | +/- 8 degrees |
| hips | - 30 to 90 degrees | none |
| knees | 0 to 90 degrees | +/- 8 degrees |
| ankles | +/- 30 degrees | +/- 8 degrees |

3.1.1 Heating Zones

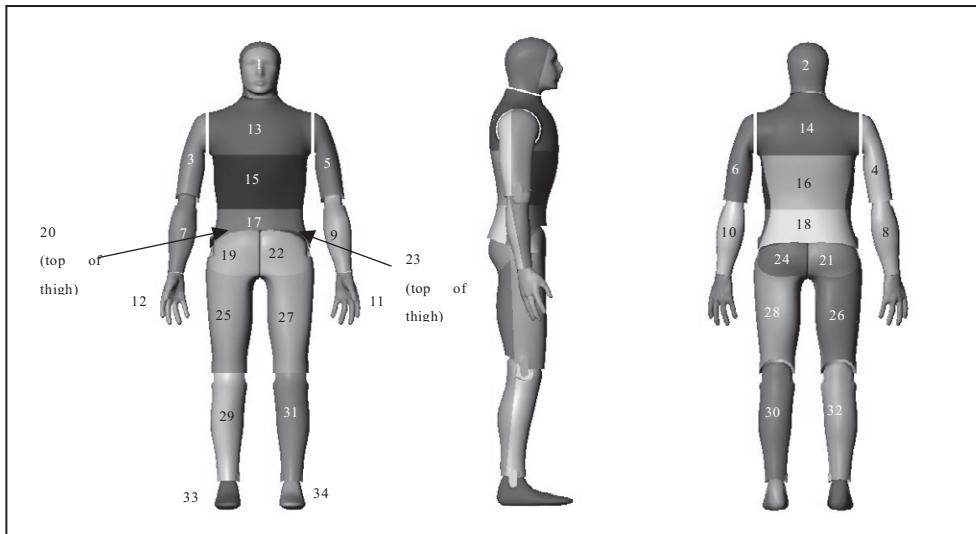


Figure 1: Zone segmentation and identification for 34-zone manikin

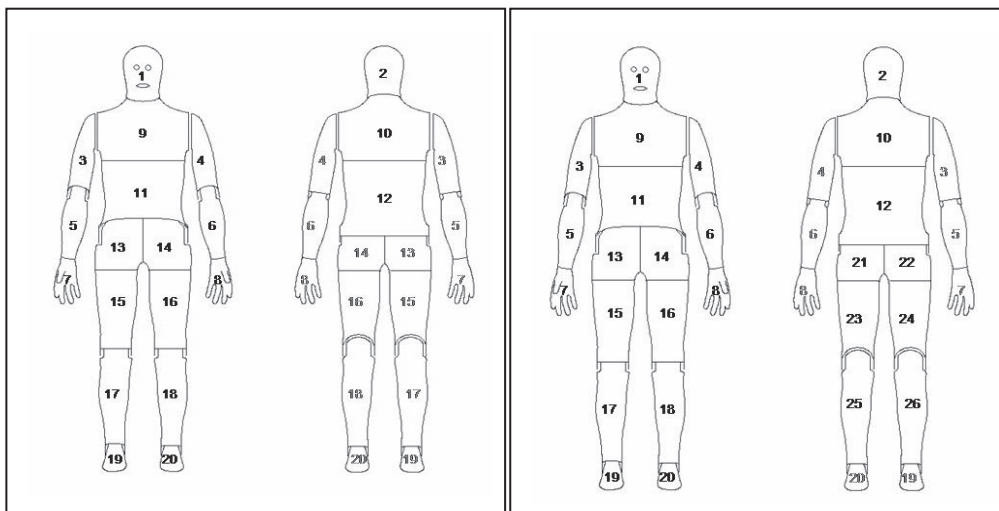


Figure 2: 20 Zone manikin

Figure 2: 26 Zone manikin

3.1.2 Sweating Skin Layer

The sweating skin system provides volumetric flowrate control by manikin region. It is based on a matrix of pores over the active surface of the manikin with a removable fabric outer shell to distribute water over the manikin surface. Each zone controller within the manikin modulates the fluid volume passing through its on-board flow control valve. The fabric skin layer consists of a tightly fitting, elastic suit, including hands, feet, and hood. Using the ThermDAC software interface, each manikin zone can be controlled to a specific flowrate setpoint.

3.1.3 Control modes

Four control modes are available:

- Temperature control mode (= skin temperature fixed / heat flux variable): measurement is the heating power required for maintaining skin temperature at a fixed setpoint.
- Heat flux mode (= heat flux constant / skin temperature variable): the heating power is set a fixed value, representative of the metabolic production of the human being (for instance 70 W/m²). The resulting skin temperature of the manikin is measured.
- Comfort mode: this mode follows the Madsen comfort model, with power output dynamically adjusted to the local temperature to reproduce – to a certain extent – real human skin temperature (lower on segments exposed to cold). User-adjustable gains allow use of alternative numerical models.
- Programmable control mode: In this operating method, the manikin setpoints are obtained from a time-sequential text file. This provides the ability to simulate different activity levels or work cycles on a precise time schedule.

3.1.4 Walking and Motion Stand (Option)

This roll-around walking stand replicates the walking motions required for ENV342 garment testing, while also supporting the manikin and making it easy to move and dress by a single technician.

- Stand includes motor and actuators for generating the walking motion
- Speed variable from 0 to 55 double steps per minute (~ 70 meters/min)

3.2 Thermal Manikin “ADAM”

The advanced 126-zone "ADAM" thermal manikin with porous metal sweating skin is used for the detailed evaluation of transient environmental conditions. The manikin consists of a carbon-epoxy skeleton and individual porous metal skin segments that contain heater elements, temperature sensors, and fluid distribution system. The manikin mimics human responses such as sweating and breathing with incredible accuracy, and its high spatial resolution and rapid response to environmental changes allow it to respond realistically to transient, non-uniform inputs. A dedicated Dell

Pentium computer running ThermDAC software controls the manikin temperature and all internal systems while automatically logging data.

3.2.1 “ADAM” Specifications

Manikin size: 50th percentile Male: Height 175cm, Weight ~ 60 kg
Standard zones: 126 independently controlled thermal regions

3.2.2 Heating zones

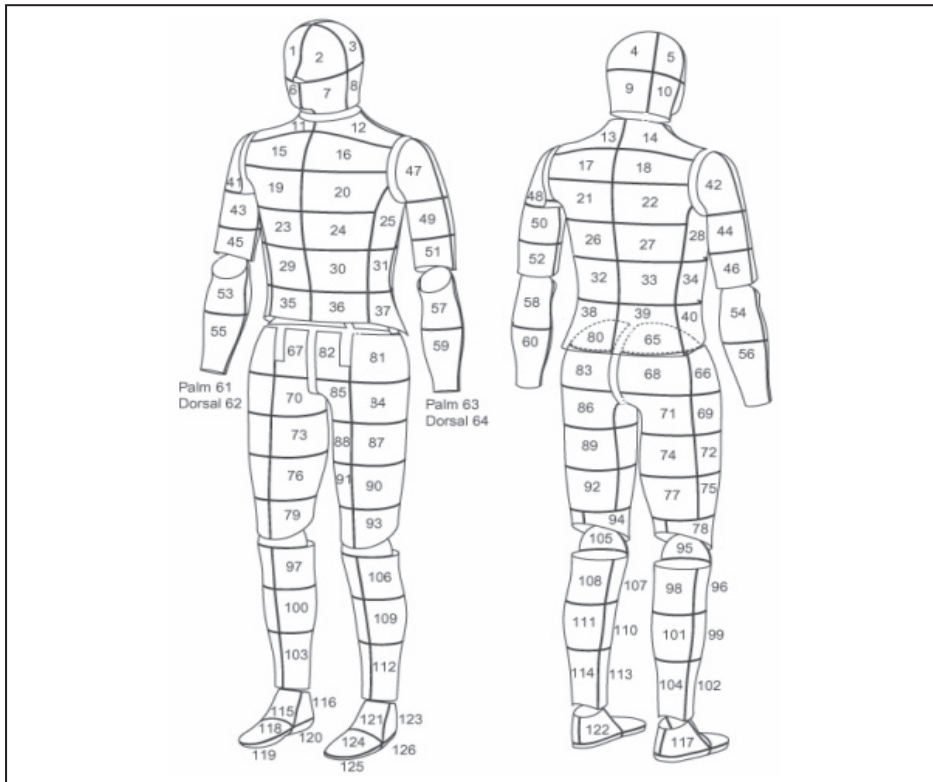


Figure 4: Zone segmentation and identification for 126 zone manikin

3.2.3 ADAM Sweating Skin System

ADAM’s sweating system is integrated into the manikin skin surface, and is based on a computer controlled fluid delivery system that provides volumetric flowrate control by manikin region. Fluid supply for this system utilizes a single constant pressure pump external to the manikin. This is connected through a quick-disconnect coupling to the manikin’s internal fluid distribution tubing. Each zone controller within the manikin modulates the fluid volume passing through its on-board flow control valve. This metered volume is distributed to the manikin’s porous metal skin layer, where it spreads evenly within the zones inner layers and then migrates to the skin surface for evaporation. Using the ThermDAC software interface, each manikin zone can be controlled to a specific flowrate setpoint.

3.2.4 ADAM Options

“ADAM” thermal manikin can be manufactured with internal wireless transmitter & receiver for communication with computer, heated humidifier for warm moist breath in the nose and mouth, internal or external breathing pump for inflow/outflow, and internal battery charging and power

management controller with 36 Volt battery pack for at least two hours of manikin use.

4. MANIKIN APPLICATIONS

As thermal manikin research studies become more advanced, manufacturers have developed manikin technologies for different test environments: flame environments, submerged environments, and contaminated environments.

4.1 Flame Test Thermal Manikin

The advanced flame test manikin with integrated heat sensors and computational burn model is designed to meet the ASTM F1930 testing standard, and consists of a high-temperature carbon-epoxy shell with 115 integrated heat sensors (excluding hands and feet), and a dedicated Dell Pentium computer running “Burn Model” software to automatically log sensor data and, based on test results, automatically calculate the degree and total area of predicted burn injury. The system allows the operator to characterize the performance of single layer garments or protective clothing ensembles in a simulated flash fire environment having controlled heat flux, flame distribution, and duration. An optional burn chamber can also be added to obtain a comprehensive flame testing solution.

4.1.1 Manikin Sensors

115 evenly distributed and integrated heat sensors can measure the incident heat flux over a range from 0.0 to 4.0 cal/cm²·s (167 kW/m²), with each sensor output value automatically polled once every 0.5 seconds during the test period. Minimum response time: ≤ 0.1 second.

4.1.2 Manikin Software

“Burn Model” software automatically receives and data logs the output of all sensors, calculates the heat flux, predicts the burn injury level at each sensor, and the total predicted burn injury area as a result of the thermal exposure. The time predicted to cause second-degree and third-degree burn injury for each sensor is also calculated. For burn injury assessment, the sum of the areas represented by sensors that received sufficient heat to result in a calculated second-degree burn shall be the second-degree percentage burn area assessment. The sum of the area represented by the sensors that received sufficient heat to result in a calculated third-degree burn shall be the third-degree percentage burn area assessment. The sum of these two areas shall be the total percentage burn injury assessment resulting from exposure to the flash fire condition.

4.1.3 Modular Burn Chamber

A fully ventilated, fire-resistant burn enclosure with viewing windows and access door can be provided to house the manikin and burner apparatus. The chamber will be sized to meet the F1930 standard’s minimum dimensions of 2.1 x 2.1 x 2.4 meters, to provide a uniform flame exposure and sufficient space for safe movement around the manikin for dressing

without accidentally jarring and displacing the burners. A properly sized forced air exhaust system will permit rapid removal of combustion gas products and aid in cooling after the data acquisition period. A system of propane gas piping, pressure regulators, valves, and pressure sensors shall be provided to safely deliver gaseous fuel to the ignition system and exposure torches. This delivery system shall be sufficient to provide a uniform heat flux of at least $2.0 \text{ cal/cm}^2\cdot\text{s}$ (84 kW/m^2) for an exposure time of at least 5 seconds.

The burner system shall consist of a safety pilot flame, one ignition pilot flame for each exposure burner, and sufficient burners to provide the required range of heat fluxes with flame distribution uniformity to meet the requirements of ASTM F1930. The flame exposure burners will be large, induced combustion air, industrial style propane burners positioned around the manikin to produce a uniform laboratory simulation of a flash fire. A minimum of eight burners shall be used and positioned to yield the required exposure level and uniformity. A system for recording a visual image of the manikin before, during, and after the flame exposure shall be provided. In addition, the exposure chamber shall be equipped with approved fire suppression systems.

4.2 Waterproof Thermal Manikin

The “NEMO” true-weight Waterproof Thermal Manikin consists of a sealed aluminum shell with internal heater elements, temperature sensors, and an (optional) integrated fluid supply system to simulate metabolic heat and perspiration levels. Its aluminum body form with waterproof joints and 21 independently controlled thermal zones can be fully submerged up to 3 meters and support maximum heat flux rates to 1100 W/m^2 .

4.3 Breathing Thermal Manikin

The Breathing Thermal Manikin is used to study how and at what rate contamination particles moving in an airflow might enter the human body by aspiration during breathing. The manikin is capable of regulated breathing through the mouth and/or nose. A custom airflow manifold with aerosol collection filter was designed and mounted inside the manikin head, and an external breathing machine was developed to generate the necessary respiration features.

The manikin features a split mouth and split nose, with a special airflow manifold that connected to an external breathing system via four hoses - two for inhalation and two for exhalation. This manifold was designed to allow for breathing through the nose or mouth in any of the following combinations:

- Mouth inhalation/Mouth exhalation (top/bottom split)
- Nose inhalation/Nose exhalation (left/right split)
- Mouth inhalation/Nose exhalation
- Nose inhalation/Mouth exhalation

The external breathing system consists of pneumatic cylinders that are cycled in and out by a servo linear actuator to replicate the cycle, frequency, and volume of human breathing. Three user-adjustable variables allow

control of tidal volume, breathing rate, and Inhale: Exhale (I: E) ratio. The ThermDAC control system automatically monitors user-set inputs and adjusts the motion of the air cylinders accordingly. The tidal volume depends on the distance that the pistons are moved in the cylinder, and the breathing rate is determined by the speed that the piston moves. The piston speed can be different on the inhale and exhale cycles giving an I:E ratio matching the user input.

4.4 Specialty Thermal Manikin

Evaluating the thermal comfort and moisture management of automobile seating, gloves, footwear, or any other product requiring an anatomical testing form requires a specialty thermal manikin: Thermal Hand System, Thermal Foot System, ST-2 Comfort Test System, Seat Test Automotive Manikin, and other customized specialty systems. Independently controlled thermal regions with temperature sensors, porous metal sweating sections, and fluid supply simulate metabolic heating and perspiration levels with high repeatability. User-friendly ThermDAC software controls fluid systems and temperature while logging data.

5. CONCLUDING REMARKS

Thermal Manikin Systems together with a disaster simulation environment chamber are a superior research and test appliance for evaluating the safety and comfort of various protective garments. Many famous universities and research labs in the world are using thermal manikins to research and test protective garments and disaster environments, e.g. Tsinghua University has a 20 zone thermal sweating manikin with breathing and walking systems, which includes the most comprehensive functions of thermal manikins. As the standards and requirements for safety and protective garments continue to increase, thermal manikin systems will become even more important as protective garment quality inspection instruments.

REFERENCES

- Thomas L. Endrusick, B.Sc., Leander A. Stroschein, B.Sc. and Richard R. Gonzalez, Ph.D. *United States Military Use of Thermal Manikins In Protective Clothing Research*
- U.S. Army Research Institute of Environmental Medicine. *Biophysics and Biomedical Modeling Division*. Kansas Street, Natick, MA 01760-5007 Mosley.
- Measurement Technology Northwest. *Thermal Products Descriptions and Proposals*. 4211 24th Avenue West, Seattle WA 98199, USA.

ROLE OF LOGISTICS DURING CYCLONE SIDR

MEHEDI AHMED ANSARY, RUBEL DAS and AFIFA IMTLAZ BNUS
BUET, Bangladesh
ansary@ce.buet.ac.bd

ABSTRACT

A huge economical and live loss occurs every year in Bangladesh due to natural and man made disaster. It will be a daydream to prevent the natural disaster. But the loss can be mitigated by pragmatic planning. Logistics management is a key point to tackle disaster successfully. The roles of logistics during and after a disaster are discussed in this paper. Cyclone SIDR has been taken as a case study. The limitations of resources relating logistics are pointed out and studied how these affect the disaster management. The problems faced by the authorities have been identified to distribute relief and evacuate people to safe and sound place after SIDR. It has been tried to solve this problem and suggest some point such as Decentralization of Control and Command Centre, Upgrading Private Sector etc. It is hoped that if the suggestions are implemented, Bangladesh will be able to overcome the affect of a disaster and minimize the loss.

1. INTRODUCTION

Bangladesh faces a lot of economical and live loss every year due to natural and manmade disaster. As natural disaster is not preventable it is rational to enrich resources and coping capacity to face it. Is Bangladesh ready to tackle any disaster? After any disaster, relief activities are hampered due to various reasons. One of them is Logistics management. Before going to focus on logistic management, the present condition of transportation are given below.

There are four modes in Bangladesh such as Railway, Roadway, Waterway and Airway. According to 2005 Bangladesh govt report, the total length of Railroad is 2706 km of that 923 km are broad gauge (1.67 meter) tracks (mostly in the western region) while the remaining 1822 km are meter gauge tracks (mostly in the central and eastern region).

There is no railway track in southern part of Bangladesh. Bangladesh has eleven airports but due to socio economic condition airways play a trivial role in internal transport. Bangladesh had 8430 km of Navigable waterways. There are seasonal difficulties in the navigability of rivers and canals for the traditional country boats. (1988). In 1997, the total length of paved road under the Roads and Highways Department stood at more than 20000 kilometer. It is estimated that mechanized road transport carry about 70% of the country's total passenger and cargo.

The transportation in southern part of Bangladesh is not improved yet. The movement of people is dependent on Ferry service. According to Roads

and Highway Department seven Ferry have to be used to go from Barisal to Kuakata and five ferry to go from Barisal to Barguna (see Figure 1). It takes a larger time to pass a short distance.

It is clear that the transportation condition of Bangladesh is not sufficient. During in disaster period the condition becomes critical. The scarcity was seen clearly after SIDR. The shortage is more in southern part of Bangladesh where SIDR hit at 15th November, 2007.

During any disaster, evacuation of people to a safe and sound place becomes the foremost activity. Cleaning of debris after any disaster is another concern. Except effective logistics plan it is impossible to do herein uninterrupted way. So it is the urging demand for introducing disaster logistics in disaster prone zone.



Figure 1: Position of ferry service in Bangladesh

2. OBJECTIVE OF THE STUDY

According to Stephenson (1993) “The Emergency or Relief Logistics is the basic task of a logistics system: to deliver the appropriate supplies, in good condition, in the quantities required, and at the places and the time they are needed. Relief Logistics encompass the relocation of disaster affected people, transfer of casualties, and the movement of relief workers.” Bangladesh has no plan for Emergency or Relief Logistics. .

A Bangladesh Network Office for Urban Safety (BNUS) team has visited the SIDR affected areas from 4th may to 11th may 2008. They have met different professionals from Govt. and NGO sectors and some affected population. The main objectives of this study are as follows:

- To create awareness that logistics is the vital element to face any disaster
- To realize that the effectiveness of disaster logistics depends on the investment

- To identify the predicament faced by the authorities during evacuation of people and distribution of relief

3. LOSSES IN THE DISTRICTS

The super cyclone SIDR passed through Khulna and Barisal divisional coastal districts, huge damages took place in those districts. The worst and badly affected 13 districts were Barguna, Bagerhat, Pirojpur, Patuakhali, Jhalokathi, Bhola, Barisal, Madaripur, Sariatpur, Gopalganj, Khulna and Satkhira.

Huge loss of life, damages to houses, livestock, crops, educational institutions, roads and embankments have been reported from 1811 unions of 200 upazilas of 31 districts. Official sources admitted about 3500 deaths. Total or partial destruction of more than 80% thatched houses, took place 70% of the almost harvestable paddy, 60 to 70% of fisheries and huge number of live stocks. Severity of damages in different districts is shown in Figure 2. Different economists are assessing the economic loss using diverse techniques, but most have found the damage to be USD 1.6 Billion (World Bank, 2008).



Figure 2: SIDR affected area (color density represents the severity of damages)

4. LIMITATION OF RESOURCES

The devastation of super cyclone SIDR was catastrophic. To maintain other activities in parallel to relief activities, the authority faced some limitation which is described below:

- *Shortage of Logistics Support:* There was sufficient stock of relief to distribute among affected people. But the authorities face a problem of shortage of logistics. Even the fare of this logistics was excessive. One District commissioner told that he had no fund to meet this expense. Even he had no account to transfer the relief to the affected people.
- *Shortage of fuel and Spare parts:* Another problem after SIDR there was lack of fuel and spare parts. It was one of the hindrances on distribution of relief. When the vehicle was out of order in the road, it creates a huge problem.

- *Storage problem:* Bangladesh got ample amount of aid after SIDR. But there was problem of storage of this aid. As proper storage was not designed, a huge amount of truck was in queue for unloading.
- *Shortage of Helicopter landing:* There are a few helicopter landing. After disaster all roads were disrupted. So airway is the inimitable way to carry the relief to the affected people efficiently.
- *Falling of trees:* The little amount of roads remained were blocked by the fallen trees. There were huge amount of fallen trees on the road. So the road was not accessible.

5. PROBLEMS AFTER SIDR

Most of the people living in the southern part of Bangladesh have not seen such devastating and destructive cyclone like SIDR. The authority has to face difficult situation to tackle the effect of SIDR. The logistics dependent problems are discussed below:

- *Duplication:* Many SIDR affected people in some areas did not receive any relief even after several days after SIDR. The reason was not lack of relief. The main reason was inaccessibility of those areas. During that period, Bangladesh got huge amount of domestic and foreign aids. NGOs and other Groups distribute their aid to places which are accessible. Duplication of relief activities in some places could not be avoided.
- *Long queue of Trucks:* There was shortage of storage, so trucks have to wait for a long time for unloading. Security of relief is considerable issue after SIDR disaster.
- *Collapse of Bridge:* After 10 days of SIDR a bridge at Patuakhali was collapsed due to overload. Four people died and many were injured in this accident. It happened due to lacking of co-ordination distributing authorities. Figure 3 shows a collapsed bridge during the distribution of relief goods.
- *Dropping of Relief:* The army has dropped the relief to the affected people from the helicopter hanging in air. Many people were injured during collection of relief.
- *Inaccessibility of Road:* after SIDR some days were lost to clear road as a huge amount of trees were fallen on the road. The evacuation of affected people was delayed due to inaccessibility of road.



Figure 3: The collapsed bridge during relief distribution

7. SOLUTION MEASURES

To mitigate the problem after disaster following suggestion are provided.

- *Decentralization of Control and Command Centre*: Initially only in Dhaka later on Regional Centre was opened at Barisal which was headed by an advisor.
- *Supply Speed Boat*: Only Water Development Board has two speed boats in whole patuakhali district. Other department has no water craft. As there are no road connection in some island, to save this people from those islands the only way to serve is use of speed boat.
- *Plowing Deep Rooted trees*: Plowing trees beside trees is a common practice in Bangladesh. It is required to increase the forestation. The trees that fell on the road were shallow rooted. SIDR could not uproot the deep rooted trees. So it is advisable to plow deep rooted trees beside the road.
- *Upgrading Private Sector*: It is necessary to upgrade private sector to distribute the relief efficiently. Government can not handle any disaster alone. Except NGOs and other private sector, it is impossible to tackle disastrous loss.
- *Application of GIS*: GIS can be used as a decision making tool during disaster. Using GIS the deficiency can be identified and proper steps can be taken.
- *Helipads*: During disaster it is impossible to carry relief aid to disaster affected area on road. The easiest and quickest way to carry the relief is the using of airways. So by making proper plan helipad must have build up in disaster prone area.
- *Improving communication technique*: Recently whole Bangladesh has come under the mobile network coverage. According to local people the mobile network coverage collapsed at 15th November, 2007 at 8.00 pm.

Communication Networks involving radio, radio-telex, and satellite links like satellite phones should be adopted to update real time information for recovery operations in disaster affected areas (Hanaoka and Qadir, 2005). Recently BUET has started an experimental set-up of early warning system in Cox'sbazar. BUET has set up 20 instruments in different local administration in Cox'sbazar and higher authorities in Dhaka. It is a satellite based warning system. It can run almost eight days without any electricity or power.

8. CONCLUSIONS

Bangladesh is a disaster prone country. Planned logistics is required to evacuate people during disaster. Coordination is mandatory for managing pre and post disaster situation. Government unknowingly has taken some logistic management initiatives. With proper planning pre-disaster and post disaster situation can be better managed.

REFERENCES

- Stephenson, R. S., 1993. Logistics; Disaster Management Training Programme (1st ed.). *UN Development Programme (UNDP) & UN Department of Humanitarian Affairs (DHA)*, pp.9.
- Hanaoka, S. and Qadir, F. M., 2005. *Logistics problems in recovery assistance of indian ocean earthquake and tsunami disaster*, Regional symposium, AIT, Thailand
- World Bank Report, 2008. *Cyclone SIDR in Bangladesh*, April, 2008.

SEISMIC MICROZONATION BASED ON SITE AMPLIFICATION STUDY OF COX'S BAZAR IN BANGLADESH

A. B. AFIFA IMTIAZ¹, MEHEDI AHMED ANSARY²
and ASHUTOSH SUTRA DHAR³
Dept. of Civil Engineering, BUET, Bangladesh
affaimt@gmail.com
ansary@ce.buet.ac.bd
ashutoshdhar@ce.buet.ac.bd

ABSTRACT

Earthquake hazard zonation for urban areas, mostly referred to as seismic microzonation, is the first and most important step towards a seismic risk analysis and mitigation strategy in densely populated regions, since damage due to an earthquake may vary even within a few meters due to variation in local site conditions. Site Amplification is an important basis of microzonation. The basic intention of amplification assessment is to estimate the effect of local site conditions through the site response analysis. This factor is highly dependent on the local soil conditions and on the expected earthquakes. Cox's Bazar and the nearby area fall in the Zone of frequent seismic activities. The area is also characterized by a significant amount of sediment and landfill, which may greatly amplify seismic waves and is another issue of concern for studying the site effects. Historic and recent records reveal that motion from nearby and more distant larger earthquakes has been felt widely in and around Cox's Bazar over the past few hundred years with magnitude between 6 and 7. There has been also a rapid urbanization of Cox's Bazar in the last few decades including construction of significant number of buildings and other structures. It is essential to develop seismic microzonations of the area based on site characterizations.

In this study, subsurface investigation conducted at 30 locations across the district has been used for site amplification analysis. The necessary geotechnical parameters and boring log information have been assembled into a Geographic Information Systems (GIS) database and Microzonation Map has been developed. The computer program SHAKE has been used to compute the response subjected to vertically travelling shear waves, by incorporating the geotechnical parameters from the subsurface investigation.

1. INTRODUCTION

Bangladesh is located close to the boundary of two active plates: the Indian plate in the west and the Eurasian plate in the east and north. As a result of such a geographical location, the country is always under a potential threat

of earthquake. The frequent shakes in and around the country, particularly Chittagong and Cox's Bazar regions, point toward the potential of much high intensity earthquakes than that projected. Cox's Bazar, located in the southeastern part of Bangladesh, is a strategically and economically important city of the country. The district is exposed to most devastating natural disasters of the country where earthquake has recently appeared as additional threat to this region. Therefore, it is essential to develop an earthquake preparedness program for the region in order to reduce the potential losses expected from the disaster. In order to achieve this goal, earthquake vulnerability of Cox's Bazar District has been assessed on the basis of Site Amplification. This paper deals with the development of a microzonation map based on the spatial variation of site amplification for the District.

2. SITE AMPLIFICATION

The basic principle behind the microzonation technique is to explore the local subsurface conditions and to evaluate ground shaking effects. During earthquakes, the ground motion parameters such as amplitude of motion, frequency content and duration of the ground motion change as the seismic waves propagate through overlying soil and reach the ground surface. The phenomenon, wherein the local soils act as a filter and modify the ground motion characteristics, is known as 'soil amplification problem'. Physically the problem is to predict the characteristics of the seismic motions that can be expected at the free surface (or at any depth) of a soil stratum. Mathematically the problem is one of wave propagation in a continuous medium. If the medium is linearly elastic and the geometry is relatively simple, analytical solutions can be obtained for any kind of waves. In practice, since the wave content of a potential earthquake is hard to predict, solutions are often limited to the simple case of shear wave propagating vertically.

3. SEISMIC MICROZONATION BASED ON SITE AMPLIFICATION

To locate and quantify earthquake hazards estimation of the site-specific dynamic response of a layered soil deposit, soil amplification study is required. In seismic microzonation the variation in seismic response of the subsurface is displayed and subsequently where the soil is being amplified to a level that may damage existing buildings or other structures at that location is determined. The spatial variation of the estimated amplification and frequency is then plotted in the GIS on the site map. This analysis is generally the preliminary step for most aseismic studies. This study enables to calculate site natural periods, assess ground motion amplification and response spectra, the parameters which are important for design and safety evaluation of structures. From microzonation maps it will be possible to outline the hazardous areas for buildings. Again certain building types are more vulnerable to different frequencies of ground motion vibration than

others. Since seismic micro zoning can show the frequency content of vibration due to different local ground condition, it can be used to ensure that a match does not occur between buildings vulnerable to certain frequencies of vibration and ground conditions that are likely to vibrate in that frequency range. Thus avoiding building being damaged by ‘resonance effect’ in zones where the ground is likely to vibrate in certain frequency ranges.

4. COX’S BAZAR: THE STUDY AREA

4.1 Vulnerability of the Area

Historical study suggests that Bangladesh is susceptible to earthquakes of moderate to high magnitude. Mild tremors continue to occur in the southern parts of the country without any significant casualties or life loss, so far. Figure 1 shows epicenters of the historical earthquake data in and around Cox's Bazar district over the last fifty years (Ansary, 2006). Data reveals that a 6.5 magnitude earthquake occurred in this zone in 1955 and there is a possibility of occurrence of high magnitude earthquake in the upcoming years in and around Cox's Bazar district.

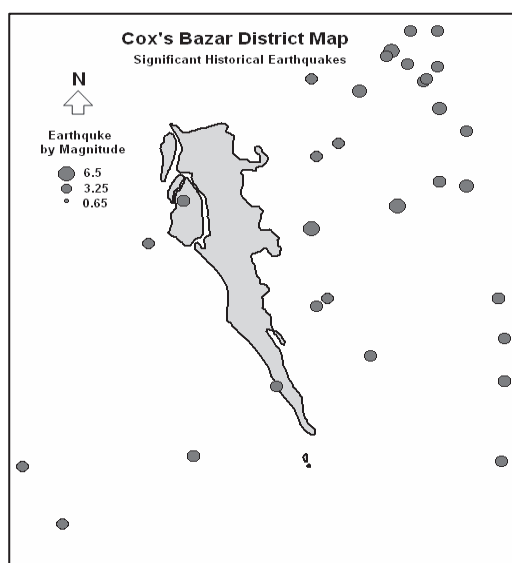


Figure 1: Historical earthquakes around Cox’s Bazar

4.2 Geological Condition of Cox’s Bazar

The district of Cox's Bazar is bound on the west and south by the Bay of Bengal, on the east by the hill ranges of elevation around 100-200 m. Basin of Matamuhuri River and Bakkhali river form the morphological pattern on the North of the district. The continent of the district of Cox's Bazar includes two distinct geological settings namely Tertiary folded belt and coastal deposits. The tertiary folded belt extends north-south as part of the Indo-Burmese mobile belt, that is characterized by long narrow folds (Alam et al 1990). Coastal deposits overlies the Tertiary formation, resulting in different surfacial forms. The present day morphology of the area are

believed to be influenced by the Holocene sea level rise, tidal and fluvial discharges and very special type of physical set up of the plain around Tertiary Hills (Huq and Ahmed, 1997). Figure 7 shows the geological structures in Cox's Bazar area after Alam et al (1990). Figure 7 reveals that the area around the city of Cox's Bazar predominantly composed of Dihing Formation and Dupi Tila formation of pliocene-pleistocene age. The Formations are characterized by fine to medium grained poorly consolidated sandstone and clayey sandstone of variable colors ranging from yellow, brown to grey. To the south of Dihing and Dupi Tila formation is the Girujan clay of Pleistocene and Neogene age followed by Tipam sandstone of Neogene age. The formations covers Ukhia Upazila on the South, part of Ramu Upazila on north and north east and a thin zone to the east of Cox's Bazar. The Girujan clay is grey to greenish grey, red mottled silty shale, shale and clay stone inter bedded with subordinate thin bedded silt stone and cross bedded sand stone. The Tipam sandstone is fine to medium grained sandstone, siltstone on shale, massive to thin bedded, locally cross bedded and current bedded. The south of Giruan and Tipam formation is the Bokabil formation of Neogene age and Bhuban formations of Miocene age. The area includes Teknaf Upazila on south and eastern part of Cox's Bazar city. The formations are characterized as massive to thin bedded shale, siltstone and sandstone. Figure 2 shows the geological structure of Cox's Bazar District from the Geological Map of Bangladesh published by Geological Survey of Bangladesh in 1990.

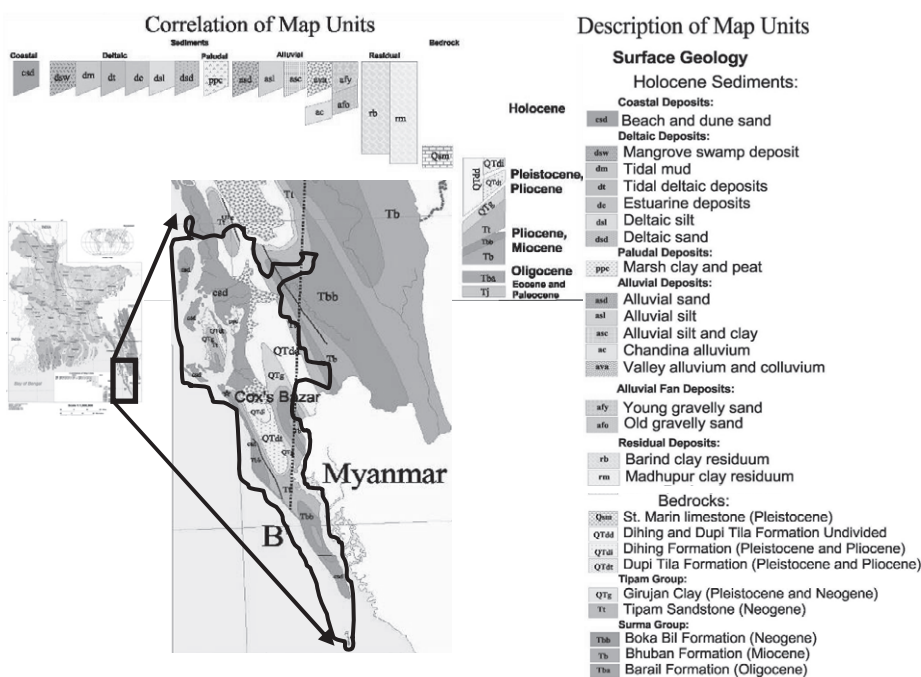


Figure 2: Geological Structures (after Alam et. al., 1990)

5. ASSESSMENT OF SITE AMPLIFICATION

5.1 Methodology Review

Several methods for evaluating the effect of local soil conditions on ground response during earthquake are presently available. Most of these methods are based on the assumptions that the main response in a soil deposit are caused by the upward propagation of shear waves from the underlying rock formation. Analytical procedures based on this concept incorporating non-linear soil behavior, have been shown to give results in good agreement with field observations in a number of cases. Accordingly they are found in increasing use in earthquake engineering for predicting responses within soil deposits and the characteristics of ground surface motions. The analytical procedure generally involves the following steps:

- Determination of the characteristics of the motions likely to develop in the rock formation underlying the site
- Determination of the dynamic properties of the soil Deposit
- Computation of the response of the soil deposit to the base rock motion

Excitation of a compliant medium (e.g. a soil deposit) takes time for the effects of the excitation to be felt at distant/different points. The effects are felt in the form of waves that travel through the medium. The manner in which these waves travel is a function of the stiffness and attenuation characteristics of the medium and will control the effects they produce. Usually, the geological materials are treated as continua and the dynamic response of these materials to dynamic/transient loading such as earthquakes are evaluated in the context of one or two or three-dimensional wave propagations depending on the geometry and loading conditions.

5.2 One-dimensional Wave Propagation Analysis

One-dimensional ground response analyses are widely used for ‘soil amplification studies’. These types of analyses are believed to provide conservative results and are time tested. Most design projects in the past designed using this methodology survived the earthquakes. Moreover, a large number of commercial programs with different soil models based on this principle are also available for use on personal computers. The assumptions considered in one-dimensional ground response analysis are

- All boundaries are horizontal and soil layers and bedrock are assumed to extend infinitely in the horizontal direction (half-sphere)
- The ground surface is level
- The incident earthquake motions are spatially-uniform, horizontally-polarized shear waves, and propagate vertically, that is, inclined incoming seismic rays are reflected to a near-vertical direction, because of decrease in velocities of surface deposits

In the areas of strong earthquake motion, the stress waves, from the earthquake focus propagate nearly vertically when they arrive at the earth’s surface. Wave velocity generally decreases from the earth’s interior towards

the surface, and hence stress waves from the focus are bent by successive refractions into a nearly vertical path. Even if the waves within the firm ground propagate in a shallow inclined direction, the waves set up within the soil by refraction at the interface between the firm ground and soil propagate nearly vertically. Soil properties generally vary more rapidly in the vertical direction than in the horizontal direction. A complete ground response analysis should consider the major factors such as site characteristics, rock motions as well as the additional factors such as rupture mechanism at the source of earthquake, propagation of seismic waves through the crust to the top of bedrock. However, these factors are difficult to quantify and hence the whole procedure becomes highly complicated. Therefore, one-dimensional ground response analyses are used extensively due to their simplicity.

5.3 Analysis Method for Soil Amplification

A number of techniques (linear, equivalent linear or nonlinear) are available for 'ground response analysis'. In this research the Equivalent Linear Analysis (Schnabel et al. 1972) has been used. This addresses nonlinear hysteretic stress-strain properties of sand by using an equivalent linear method of analysis. The method was originally based on the lumped mass model of sand deposits resting on rigid base to which the seismic motions were applied. Later, this method was generalized to wave propagation model with an energy-transmitting boundary. The seismic excitation could be applied at any level in the new model.

5.4 Estimation of Site Effects

Wave propagation is particularly affected by the local geology and the geotechnical ground conditions. Large amplification of the seismic signals generally occurs in areas where layers of low seismic velocity overlie material with high seismic velocity, i.e. where soft sediments cover bedrock or more stiff soils. In this research the effect of local soil conditions on ground response has been evaluated using widely used computer program SHAKE, capable of computing the responses for a known motion given anywhere in a system. The rock motion is assumed not to vary within a region. The program incorporates non-linear soil behavior, the effect of the elasticity of the base rock and systems with variable damping.

5.4.1 Description of the Program SHAKE

The earliest software written that uses the principle of one-dimensional analyses is called: SHAKE. The computer program SHAKE was written in 1970-71 by Dr. Per Schnabel and Prof. John Lysmer (Schnabel et al., 1972). This has been by far the most widely used program for computing seismic response of horizontally layered soil deposits. The response of the soil deposit is considered here to be caused by shear waves propagating vertically from the underlying bedrock. The program is based on the continuous solution to the wave-equation adapted for use with transient motions through the fast Fourier transform algorithm. A so-called Transfer Function is used as a technique for 1D ground response analysis.

Here the time history of the bedrock (input) motion is in the frequency domain represented as a Fourier series using Fourier transform. Each term in the Fourier series is subsequently multiplied by the Transfer Function. The surface (output) motion is then expressed in the time domain using the inverse Fourier transform. The nonlinearity of the shear modulus and damping is accounted for by the use of equivalent linear soil properties using an iterative procedure to obtain values for modulus and damping compatible with the effective strains in each layer.

5.5 Use of SPT-value for Shear Wave Velocity

The Standard Penetration Test (SPT) has been widely used to investigate soil deposit for identifying subsurface soil profiles. There are several empirical relations correlating the SPT-N value and Shear Wave Velocity (V_s) as Shown in Table 1.

Table 1: Empirical Relations Correlating SPT-N value and Shear Wave Velocity (After TC4, 1993)

| Researchers | Equation |
|----------------------------|--|
| Imai and Yoshimura (1970) | $V_s = 76 N^{0.33}$ |
| Ohba and Toriumi (1970) | $V_s = 84 N^{0.31}$ |
| Ohta and Goto (1978) | $V_s = 69 N^{0.17} D^{0.2} F_1 F_2$ Where $F_1 = 1.0$ (H); $F_2 = 1.00$ (clay) $= 1.3$ (P); $= 1.09$ (f. sand) $= 1.07$ (m. sand) $= 1.14$ (c. sand) $= 1.15$ (g. sand) $= 1.45$ (gravel) |
| Imai (1977) | $V_s = a N^b$ Where $a = 102$; $b = 0.29$ (H. clay) $= 81$; $= 0.33$ (H. sand) $= 114$ $= 0.29$ (P. clay) $= 97$ $= 0.32$ (P. sand) |
| Okamoto et al. (1989) | $V_s = 125 N^{0.3}$ (P. clay) |
| Tamura and Yamazaki (2002) | $V_s = 105 N^{0.187} D^{0.179}$ |

Here,

V_s = Shear Wave Velocity (m/s); N = Corrected SPT blow count

D = Depth (m); H = Holocene; P = Pleistocene

f = Fine; m = Medium; c = Coarse; g = Gravelly

6. ASSESSMENT OF SITE AMPLIFICATION IN COX'S BAZAR

6.1 Site Soil Condition and Data Collection

The procedure employed to assess the site amplification is based on Standard Penetration Test (SPT) blow counts in soil bore logs. A total of 30 soil boring logs with SPT have been used for site amplification study of Cox's Bazar District. Most of the soil data were collected from the depths

up to 30 meters. Almost all the boring data include SPT N-value measured at 1.5 m (5ft) interval. The soil borehole locations used in this study are shown in Figure 5. Figure 6 shows a typical soil profile of the District for a Borehole from Kutubdia, Cox’s Bazar.

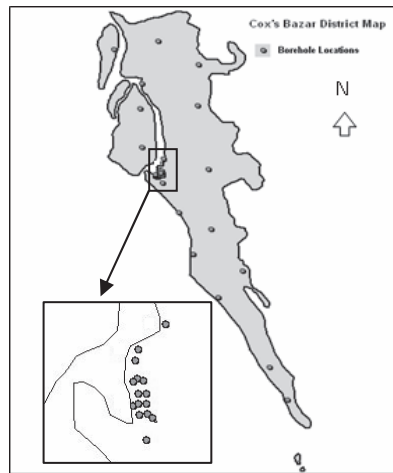


Figure 5: Cox’s Bazar District Map Showing Boring Locations

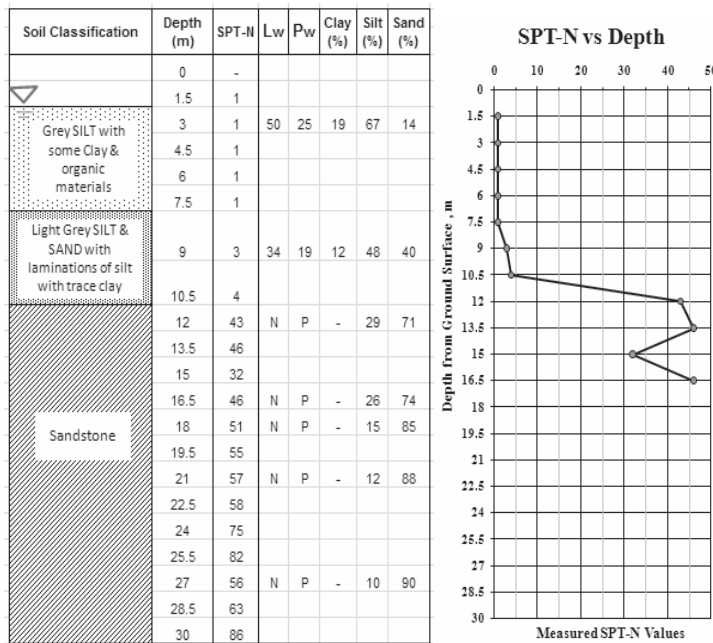


Figure 6: Typical soil profile from Kutubdia, Cox’s Bazar

The geotechnical investigation through the boreholes reveals that the subsoil of the Cox’s Bazar district is predominantly sand. The data reveal that top layers of soil of the area has mostly loose sand to medium stiff clay and middle layers are medium dense while underlying soil is medium dense to dense sand. The very dense sand with SPT-N values over 50 is assumed to be sandstone. The depth of the Sandstone appears to increase from North to South.

6.2 Estimation of Site Amplification

In the present study local site conditions have been used for microzonation of Cox's Bazar District. At the Borehole points shear wave velocities were estimated by using SPT test results. A soil database of 30 boreholes was developed in MS-EXCEL. Empirical correlations between shear wave velocity (V_s) and number of blows from Standard Penetration Test (SPT-N) were used for the estimation of amplification factors. Site amplification was assessed using estimated values of V_s and one dimensional site response numerical modeling program SHAKE. From the Table 1, the equations of Ohta and Goto (1978) and Tamura and Yamamzaki (2002) have been selected as best suited for the analysis as both of them combine both depth and SPT-N value with soil conditions and are expected to compute the most hazardous condition. Using both the relationships Shear Wave Velocities (V_s) at different depths for all the boreholes were computed. Since the correlation proposed by Tamura and Yamamzaki (2002) based on 7677 soil data collected from 1000 Japanese K-NET strong motion accelerometer locations, produced higher values of V_s , it was used as the basis of further analysis, taking the worst conditions in the account. Using the soil configurations transfer functions were calculated for different points of the district employing SHAKE numerical code. The computation was made in the frequency range of 0 to 20 Hz, at frequencies every 0.05 Hz interval. The loss of energy of seismic waves in the soil layers was also considered. In this study, the engineering bedrock was assumed to be the layer at which the shear wave velocity (V_s) exceeds 400 m/s, which exist almost 30 m deep from the surface of the study area. An estimation of the fundamental frequency and the maximum value of the amplification were obtained for each site (Table 2).

Table 2: Amplification Factor and Corresponding Predominant Frequency

| Sl No. | Borehole Location | Easting | Northing | Predominant Frequency (Hz) | Amplification |
|--------|-----------------------------------|---------|----------|----------------------------|---------------|
| 1 | Press Club | 91.99 | 21.47 | 5.15 | 2.87 |
| 2 | Central Govt Primary School | 91.99 | 21.45 | 10.10 | 1.99 |
| 3 | Peshkarpara Govt. Primary School | 91.99 | 21.46 | 7.55 | 3.23 |
| 4 | Kustura Ghat Govt. Primary School | 91.98 | 21.45 | 8.40 | 2.45 |
| 5 | Kolatoli World Vision | 91.99 | 21.42 | 8.25 | 2.39 |
| 6 | Shahporir Dwip Govt PS | 92.33 | 20.77 | 5.00 | 1.58 |
| 7 | Pallanpara Govt PS | 92.28 | 20.87 | 14.35 | 2.64 |
| 8 | Ukhia Model Govt PS | 92.12 | 21.28 | 6.27 | 1.67 |
| 9 | Bat Tali Moshjid | 92.21 | 21.15 | 10.00 | 3.22 |
| 10 | Md. Shair Bil Govt PS | 92.05 | 21.21 | 14.90 | 2.08 |
| 11 | Pancha Dwip Govt PS | 92.04 | 21.33 | 12.50 | 2.61 |
| 12 | Noniachara-World Vision | 91.98 | 21.47 | 5.93 | 1.70 |

Table 2 (contd.): Amplification Factor and Corresponding Predominant Frequency

| Sl No. | Borehole Location | Easting | Northing | Predominant Frequency (Hz) | Amplification |
|--------|--------------------------------------|---------|----------|----------------------------|---------------|
| 13 | Pachar Ghona-Khurushkul | 91.99 | 21.49 | 7.85 | 1.93 |
| 14 | Shamlapur Govt PS-Teknaf | 92.14 | 21.07 | 10.30 | 1.81 |
| 15 | Mondalpara Govt PS-Ramu | 92.12 | 21.46 | 4.83 | 2.21 |
| 16 | Baitus Salat | 91.98 | 21.44 | 9.95 | 1.97 |
| 17 | Bgd Red Crecent | 91.97 | 21.44 | 9.85 | 2.07 |
| 18 | Bgd Water Development Board | 91.98 | 21.44 | 6.45 | 1.80 |
| 19 | Tekpara Govt PS | 91.99 | 21.45 | 4.20 | 3.72 |
| 20 | Ghonapara (near Kaderia Govt PS) | 91.98 | 21.44 | 8.20 | 2.21 |
| 21 | Mosjid, ICE Factory | 91.99 | 21.45 | 3.95 | 2.70 |
| 22 | Ramkrishna Sheba Shram | 91.99 | 21.44 | 5.30 | 2.56 |
| 23 | Khutakhali Govt PS | 92.09 | 21.65 | 6.10 | 3.03 |
| 24 | Chakaria Model Govt PS | 92.09 | 21.77 | 4.20 | 2.91 |
| 25 | Eunuskhali Govt PS | 91.94 | 21.71 | 5.75 | 1.65 |
| 26 | Time Bazar Govt PS | 91.93 | 21.64 | 4.35 | 1.60 |
| 27 | Charpaa (Leadership Varsity) | 91.94 | 21.52 | 5.30 | 1.91 |
| 28 | Pekua Govt PS | 91.98 | 21.84 | 2.05 | 1.99 |
| 29 | Kutubdia Govt PS | 91.86 | 21.82 | 3.70 | 3.02 |
| 30 | Primary Education Officer's Compound | 91.99 | 21.44 | 11.90 | 2.29 |

The vibration characteristics of each site such as frequency and amplification were found, through plotting the results of the analysis. Typical graphic representation of frequency versus amplitude is shown in Figure 7. From the plotted data the first peak has been considered for microzonation since the largest amplification of the soil will occur at the lowest natural frequency or its fundamental frequency (Equation 1). The period of vibration corresponding to the fundamental frequency is called the characteristic site period (Equation 2).

$$\omega_0 = \frac{\pi V_s}{2H} \tag{1}$$

Here,

ω_0 = fundamental frequency, V_s = Shear wave velocity, H = Soil thickness

$$T_s = \frac{2\pi}{\omega_0} = \frac{4H}{V_s} \tag{2}$$

Here, T_s = Characteristic site period

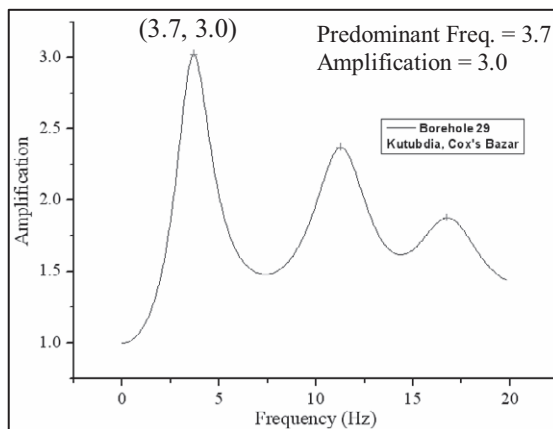


Figure 7: Amplification Factor and Corresponding Predominant Frequency

The characteristic site period, which only depends on the soil thickness and shear wave velocity of the soil, provides indication of the period of vibration at which the most significant amplification can be expected. By incorporating the variation in soil thickness and the average shear wave velocity, the spatial variation in the characteristic site period was modelled in a raster-based GIS approach.

7. GENERATION OF MICROZONATION MAP

Seismic hazards due to soil amplification can be estimated by combining the available soil parameters with the current hazard models. In current research GIS (Geographical Information System) technology has been utilized for seismic microzonation of Cox's Bazar District. The computed results from the site amplification potential analysis have been exported to a GIS environment for further processing and visualization. They have been classified into different classes according to the extent of amplification factors and plotted on the district map. From the findings, microzonation maps based on Site Amplification (times) (Figure 8) and Frequencies (hz) (Figure 9) have been plotted using spatial interpolation (Inverse Distance Weighting) among the borehole locations and converting the vectorial point features into continuous raster map through grid generation.

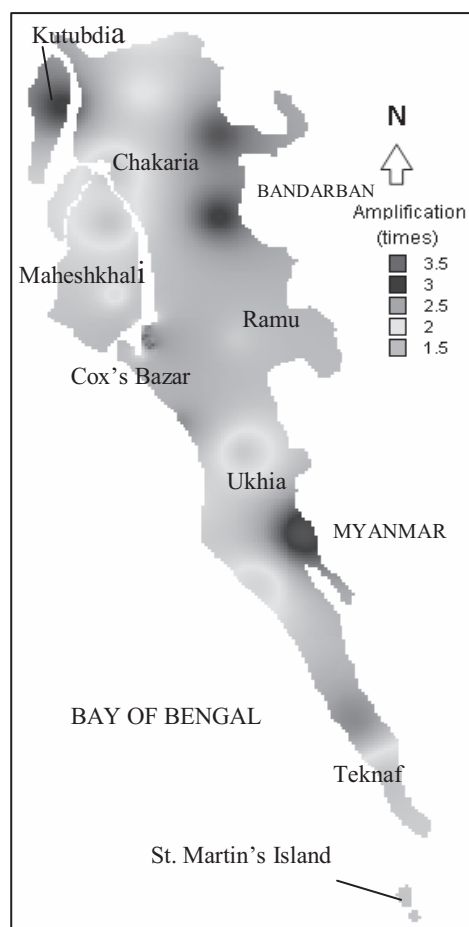


Figure 8: Microzonation Map based on Amplification

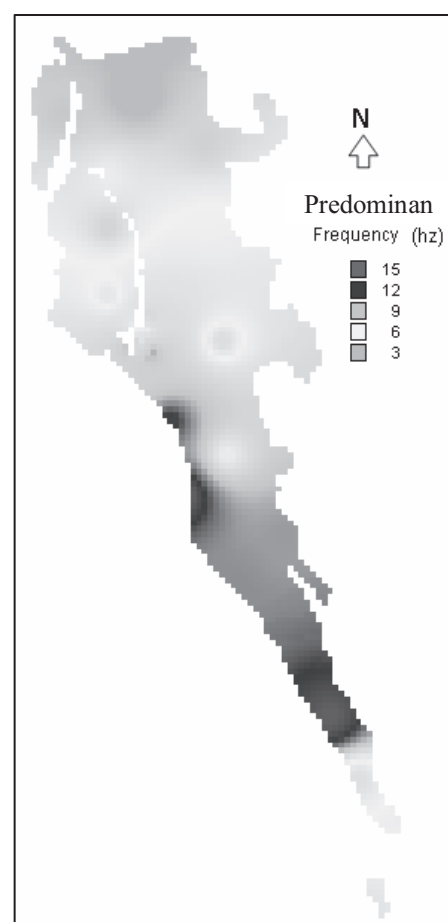


Figure 9: Amplification Map based on Fundamental Frequencies

The generated microzonation maps can be used as a guideline for General and Effective Land Use planning, Zoning Ordinances, Capital Invest Planning, Ground-failure Susceptibility Estimation, Post Disaster Planning Disaster Mitigation Planning etc. From this map, it was found that most of the areas of the district are affected by the 2.5 times amplification and few areas are subjected to 2 or 3 times amplification.

8. CONCLUSIONS

The purpose of this research was to develop a microzonation map using GIS technology to quantify the seismic risk in terms of the spatial variation of site Amplification. Seismic Hazard maps provide important guidance when earthquake hazard assessment for particular site might not be feasible. They play very significant roles in seismic design of structures by identifying different level of hazard potential for a site. Thus hazard mapping can be a very suitable tool for developing country like Bangladesh where it is worthy to incorporate safety and economic considerations at a time in seismic design of structures and planning of sites. The findings of this study is expected to be of advantage for engineers, planners, emergency personnel, and anyone who may be concerned with the potential consequences of seismic activity in Cox's Bazar district. The frequency map can be used to impose restrictions on the types of building structures that may have similar frequency. The map can act as a guide for the authorities at the national and regional levels in land use management, revision and enforcement of appropriate building codes and formulation of plans for mitigating measures against earthquake risk affecting the region considered.

REFERENCES

- Alam M.K., Hasan A.K.M. and Khan M.R., (1990). *Geological Map of Bangladesh*. Geological Survey of Bangladesh, Govt. of the People's Republic of Bangladesh
- Ansary M.A. (2006), Personal Communication, Department of Civil Engineering, BUET, Dhaka, Bangladesh
- Huq N.E and Ahmed N.K. (1997). Geomorphology of the Lower Matamuhuri Basin, Cox's Bazar, Southeast Bangladesh. *Bangladesh Journal of Geology Vol 16 p31-42*
- Schnabel, P.B., J. Lysmer and H.B. Seed (1972). SHAKE: a computer program for earthquake response analysis of horizontally layered sites, *Report no. EERC 72-12*. Earthquake Engineering Research Center, Berkeley, California, 1972
- Tamura, I. And F. Yamazaki (2002). Estimation of S-wave velocity based on geological survey data for K-NET and Yokohama seismometer network. *Journal of Structural Mechanics and Earthquake Engineering No. 696, Vol. I-58, 237-248 (in Japanese)*
- TC4 (1993). Manual for zonation on seismic geotechnical hazards. *Published by ISSMFE*

The wildfire early-warning and early-detection system in Japan

HARUO SAWADA

ICUS, Institute of Industrial Science, the University of Tokyo, Japan
sawada@iis.u-tokyo.ac.jp

YOSHITO SAWADA

System Hi-dent Co. Ltd., Japan
yoshitos@hi-dent.jp

IZUMI NAGATANI

Agriculture, Forestry and Fisheries Research Information Center, Japan
nagatani@affrc.go.jp

ABSTRACT

Abnormal weather phenomena are becoming one of big issues and large wild fires are sometimes reported because of severe drought in the world. In Japan, more than 2000 wild fires occur every year and the amount of damages is estimated about US\$ 9 million. To tackle with this problem, we developed the wild fire early-warning and early-detection system using satellite remote sensing data.

Every NOAA, TERRA and AQUA satellite data (in daytime and night time) are used to detect fires and it makes us possible to observe wild fires more than ten times a day in Japan. Because these satellite data sometimes detect heat power stations and other hot factories as "fire (hot spot)", GIS are used to collecting the knowledge on those permanent hot spots. The process time is less than 10 minutes for each image and the location data of fires are directly sent to the fire station and forest administration of related prefectures through the automatic mailing system. After the fire, high resolution satellite with infrared and middle-infrared data is sometimes used to classify the severity of the fire damages for rehabilitation of the land.

Early-warning is also very important for wild fire management and we introduced a dryness index derived from MODIS data. The dryness index is created every week and the time-series filtering (LMF-KF) is applied for modeling seasonal change of each pixel. The dryness index of the following week is predicted by the model parameters of LMF-KF and used as information for early-warning of wild fire. This information is useful to control the access and activities in the field. The information on fire and early-warning are uploaded on the web site as images of kml-format, which allows one to check them on the "Google Earth".

1. INTRODUCTION

More than 2,000 wild fires occur and around 1,500 ha of forests are burned out every year in Japan. The amount of damage is estimated about US\$ 9 million. Although the total number of fire in a year is around 2,000, there is seasonality and we have to suppress more than 700 fires in April (Fig.1). As for the each damaged area, 133 ha of forest were destroyed by the fire in Ehime in 2005. To tackle with this problem, we developed the wild fire early-warning and early-detection system using satellite remote sensing data.

Authors developed the forest fire early-warning and early-detection system for South East Asia in 1999 in one of the JST research projects, entitled the “Asia-Pacific Network for Disaster mitigation using Earth observation satellite (ANDES)”. In the ANDES project (Sawada, 2001), we detected hot-spots in the night time by satellite data and informed them to related countries by e-mail. Therefore the system was rather simple and we could use enough time for processing.

For the new system in Japan, however, it is required to detect forest fires in much earlier stage than ANDES project because people in Japan inform about fires to fire control offices soon after they notice wild-fire. It is normally difficult for satellite information to compete with these people in the speed. However, because number of people is increasing to enjoy the outdoors using fire in camping as their recreation and it is becoming difficult to find out the forest fires caused by carelessness of these people within appropriate time. Therefore, satellite observation systems for early warning to control fire use and early detection to suppress fire are expected also in Japan in forest fire management.

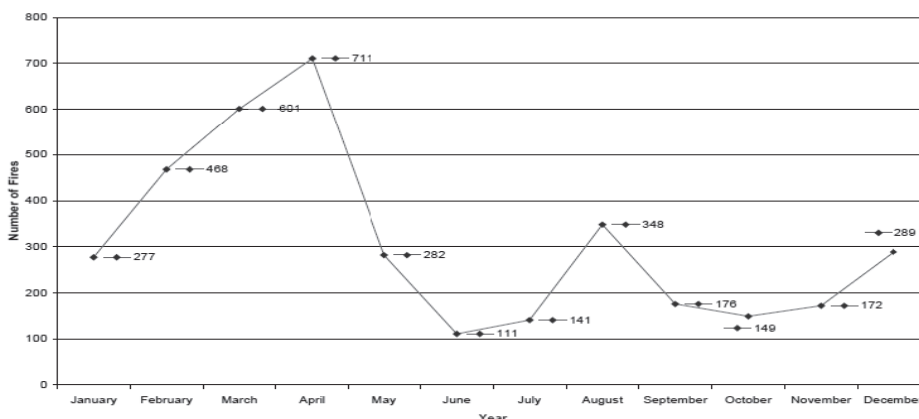


Figure 1. Seasonality of forest fire occurrence in Japan

2. WILD FIRE EARLY-WARNING SYSTEM

2.1 Dryness Index

NDVI and NDII data of MODIS data were used to develop the dryness index. The distribution map was created using the combination on NDVI and NDII when the NDVI has the largest value of a year in each pixel (Fig 2.). The recurrence line seems a good indicator which delineates dry area and wet area. The snow index (S3) is also clearly shown of its usefulness on the figure which identifies snow covers.

The dryness index (DNI) is defines as;

$$\text{DNI} = [\text{Observed NDII}] - [\text{Estimated NDII from NDVI}] \quad (1)$$

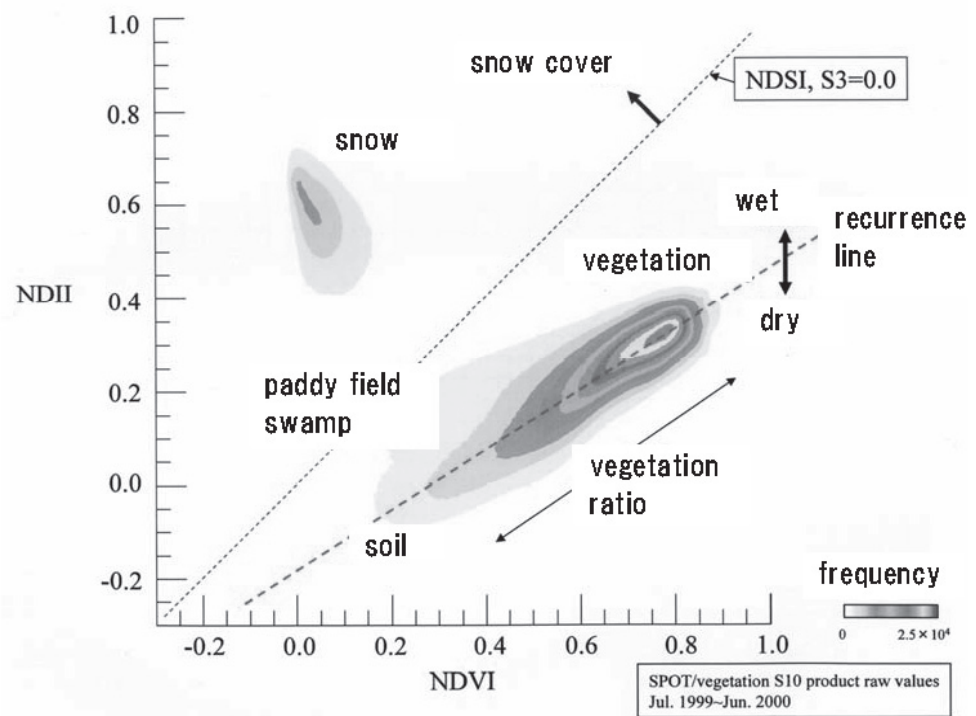


Figure 2. Distribution map of NDVI and NDII at the highest NDVI of a year

2.2 Evaluation of the Dryness Index

We experienced severe dry summer in 2005 in Shikoku and the water level of a dam site became zero. The big forest fire in Ehime occurred during that time and damaged 133 ha in one night. We created the dryness index map of every eight days in that year and checked them. The MODIS has possibility to classify the dryness every pixel, which allows forester to control forest fire risk intensively. We check the compatibility of the dryness index with the effective humidity which is normally used for fire control in Japan. The

relation between satellite dryness index and the probability when the effective humidity becomes less than 50% fit the logistic regression (Fig. 3). It indicates that the satellite dryness index might be also useful for forest fire control activities.

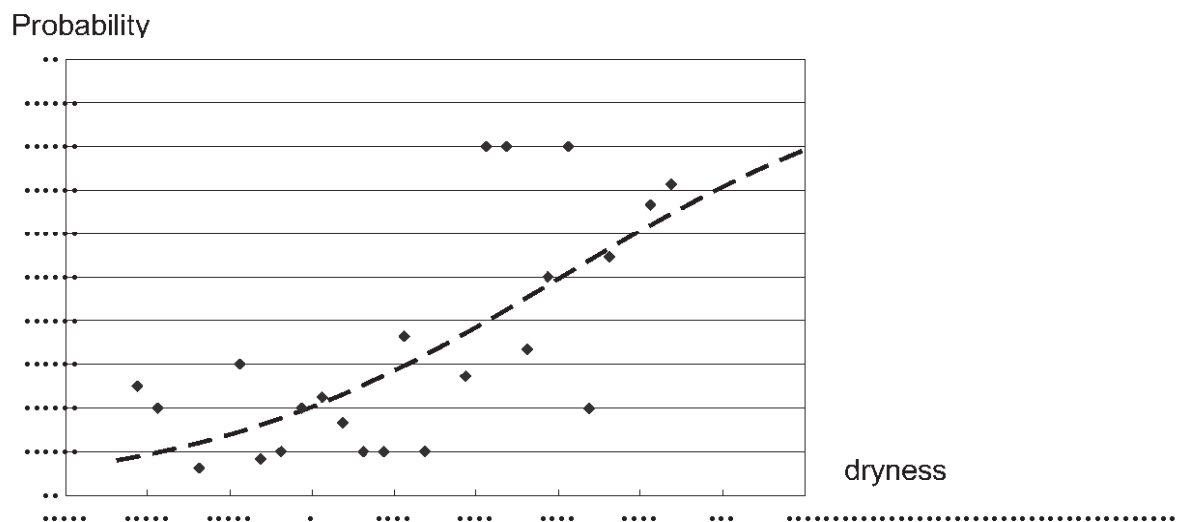


Figure 3. Relation between satellite dryness index and the probability when the effective humidity becomes less than 50%

3. WILD FIRE EARLY-DETECTION SYSTEM

To detect forest fire in early stage, we decided to use every satellite available to monitor forest fire. NOAA (12.15.17.18), TERRA and AQUA have such possibilities because of their observation capabilities on thermal band as well as daily observation. Each satellite can observe the Earth in day and night using thermal band. There is possibility to observe more than 10 times a day if we can use all these data regularly. We tried to set up a system which processes satellite data to detect hot-spots and inform them to related prefectural organizations within 10 minutes.

3.1 Detection of Hotspot

NOAA has AVHRR sensor and TERRA and AQUA have MODIS sensor. Because both sensors have different characteristics of themselves and of the satellites, it was required to develop the processing system for both systems.

3.1.1 Detection of Hotspot by NOAA

It is necessary to apply geographic correction to the observed data because of a large geographic distortion on the image data caused by the position of satellite and the rotation of the Earth. The channel 3 and 4 of NOAA are used for detecting temperature. The temperature, however, saturated rather low temperature and that makes it difficult to exactly

identify fires. For example, factories with high temperature, ex. power plant, are identified as hot-spot. Therefore, we introduced vegetation cover map which has created by the MODIS data to make clear the target land covers.

3.1.2 Detection of Hotspot by TERRA and AQUA

By the same reason with NOAA satellite, the geographic correction is required to MODIS. Because the parameters for geographic correction for MODIS are delivered after a few hours of observation, we can get rather good results in geographic correction. However, we can not wait for a few hours for the forest fire early-detection and we introduced the “gbad” system to get the geographic parameters of the satellites to process geographic corrections to MODIS data immediately after the observation.

3.2 Identification of Prefectures to be informed

It is necessary to identify the prefectures related to the fire events for informing the locations by automatic e-mail system. The GIS data was introduced to get the prefecture names within 10 km from the hotspots. At the same time the forest cover ratio map is also checked to be sent together with hotspot locations as the hotspot information.

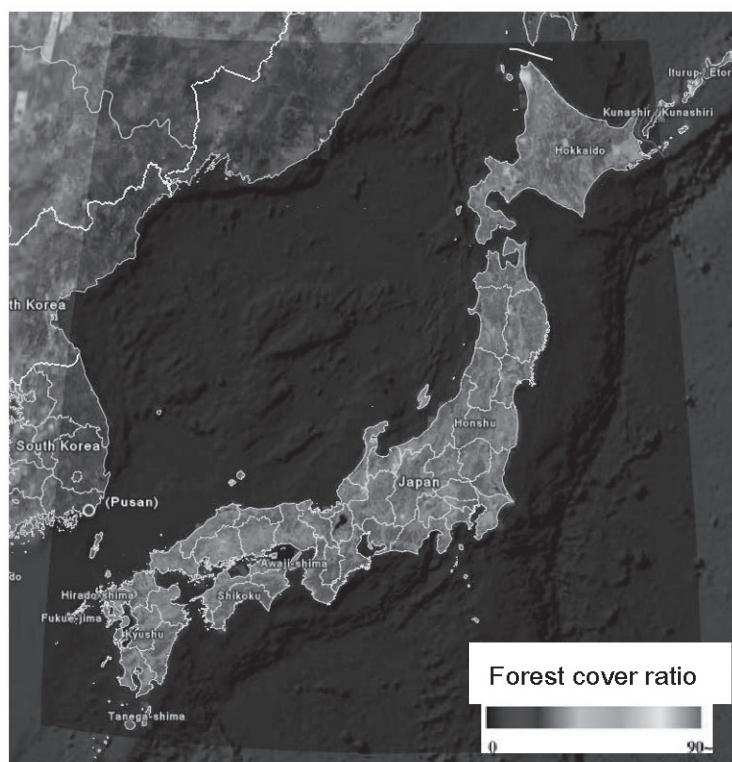


Figure 4. Forest cover ratio of Japan derived from MODIS

4. FIRE DAMAGE MAPPING

The fire damages map is essential to identify the damage levels and make plans for recovering the forest. Aerial photography is sometimes used for that purpose and interpreters create the fire damage maps by photo interpretation. High resolution satellite image with multiple bands is also useful to develop the fire damage map.

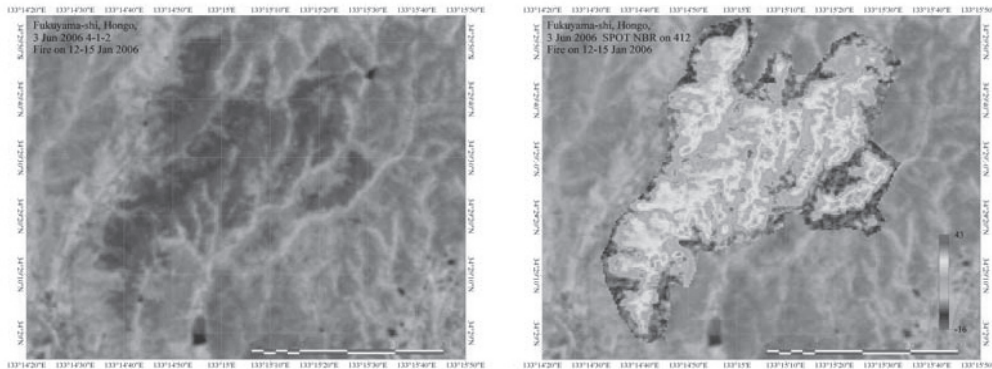


Figure 5. Color composite image of SPOT-HRG (left) and forest fire damage level map (right) in 2006

5. RESULTS

5.1 Early-Warning System

The dryness index is predicted by applying the LMF-Kalman filters (Sawada, 2005) to MODIS data every 8 days and the results are uploaded to the website:
<http://hinomiyagura.dc.affrc.go.jp/dryness/>

The ground resolution is 500m and the dryness levers are classified into 3 levels. This image includes not only forested area but also agriculture land. The kml format file is also served to be used as an image on the Google Earth.



Figure 6. The early-warning system

5.2 Early-Detection System

The location and forest cover data at the hotspot (Fig.7) is sent to related institute, such as prefectural fire stations and department of forestry as soon as the processing finished. The throughput for processing the hotspot is less than 10 minutes.



Figure 7. Hotspot information (<http://hinomiyagura.dc.affrc.go.jp/gmap/>)

The capability of the algorithms to detect fire is checked several times and we could find the possibilities as observed in Fig 8. and Fig 9.

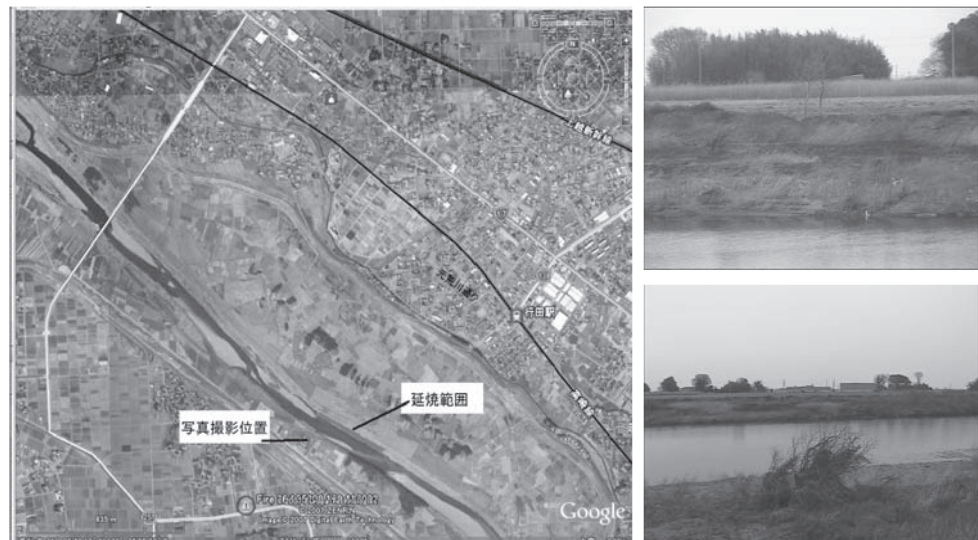


Figure 8, Fire along the bank detected as hotspot by MODIS



Figure 9. An example of open burning detected as hotspot

6. DISCUSSIONS

The average area of fire damaged forest in Japan is only 0.75 ha but sometime big forest fire occurs during March to May according to the weather condition. Therefore automatic system has some advantage to keep watching all day long. This is the first operational system which monitors forest fire by using multiple satellites in one system. It must be necessary to acquire experiences of the operational use of the system for further development.

There are many factors which influence wildfire, such as fuels on the ground (types, amount and dryness), meteorological factors (wind direction, wind speed, humidity and sunshine), and terrain condition. It must be necessary to introduce these factors into the system to enhance accuracies. For example, USA and Canada use normal passenger plane for collecting necessary parameters and predict the possibilities of forest fire.

REFERENCES

- Sawada, H., G. Saito, Y. Takayama, M. Kodama, Y. Saito, T. Shinmura, X. Song and I. Nagatani, Asia-Pacific Network for Disaster Mitigation Using Earth Observation Satellite (ANDES), *Proc. International Workshop on Next Generation Internet and its Applications Proc. Internet Workshop 2001*, 2:75-80, 2001.
- Sawada., H., Ais Pacific Network for Disaster Mitigation Using Earth Observation Satellite (ANDES) International Sawada, Y., H. Saito and H. Sawada, 2005, Development of a Time-series Model Filter for High Revisit Satellite••Data, *Proceedings of the 2nd International VEGETATION Users Conference*, Office for Official Publication of the European Communities, 83-89

LANDSLIDE INDUCED LAKE-TSUNAMI AT ARATOSAWA DAM DUE TO THE IWATE MIYAGI NAIRIKU EARTHQUAKE 2008

JORGEN JOHANSSON, TAJIMA YOSHIMITSU,
FUJITA TOMOHIRO and KAZUO KONAGAI
University of Tokyo, Japan
jorgen@iis.u-tokyo.ac.jp

ABSTRACT

In the Iwate Miyagi Nairiku earthquake June 14 2008 a large landslide of some 50 million cubic meters caused a lake-tsunami of several meters when some 1.5 million cubic meters soil flowed into the Aratosawa dam lake. The landslide mass covers an area some 1200x800m and has average thickness approximately 50m. The landslide occurred in a soil deposit of volcanic origin in the mountainous area on the border between Iwate and Miyagi, south-east of the Kurikoma volcano. Assumingly a deep layer of very porous saturated fine grained volcanic soil liquefied and created a base for the overlying soil to slide on. Even though the base slope was very gentle the soil masses moved some 200 to 500 meters and causing a tsunami, which flowed over into the spill way, but did not flow over the dam crest. No major damage to the dam infrastructure due to the tsunami itself has been reported. However one person fishing from a small boat on the lake allegedly drowned. Estimating by back-calculation the landslide characteristics such as impact velocity its relation to relation to the resulting seiche height could allow for proper discussion of possible threat to downstream population and facilities at similar dams, and possibly to come up with appropriate remedial measures. Therefore we have documented tsunami high water marks around lake, which serve as input data for a tsunami-simulation code.

1. INTRODUCTION

In the Iwate Miyagi Nairiku earthquake June 14 2008 some 25 km to the West of Ichinoseki a 50 million m³ large landslide ((marked by a green arrow in Figure 1; see Figure 2 and *Figure 3* for an aerial photos.) caused a seiche of up 8 meters when some 1.5 million cubic meters of soil slid into the dam lake. The seiche flowed into the spill way but did not flow over the dam crest.



Figure 1: Location of the Aratozawa dam site in Kurikomabunji, Kurihara city, Miyagi Prefecture (宮城県栗原市栗駒文字). The red line is approximate location of fault surface rupture observations.

With the purpose of back calculating a possible sliding velocity with the help of a tsunami simulation tool, we have recorded high water marks around the dam lake. Topography before and after the earthquake and bathymetry data is also being collected to use as input data.

2. DESCRIPTION OF THE LANDSLIDE

Figure 2 shows aerial photo of the largest landslide with Kurikoma Volcano rising behind. The terrain here suggests that similar landslides have been reactivated. A wide-spread and almost horizontal laminar structure of loose volcanic sands and ashes is being exposed on the escarpment. Comparing two aerial photos (Figure 3) taken before and after the earthquake, one can grasp the size of the landslide, which is approximately 1200 meters long, 800 meters wide, and has an average thickness of some 50 meters. It is also

seen in the *Figure 3* that the lake is brown colored due to a large amount of fine soil sediment suspended in the water.



Figure 2: Landslide at Aratosawa dam: Aerial photo of the largest landslide with Kurikoma Volcano rising behind. The terrain here is suggestive that similar landslides have been reactivated.

A height colored the digital elevation model with road location before and after the sliding is shown in Figure 5. The arrows show that Points P1 P2 and P3 have respectively moved about 200m, 300m and 500m SSE towards the dam lake. Even though the slope was very gentle (The cross-section A-A' Figure 5b) shows a gradient of about 3-4 degrees) the landslide moved between 200 to 500 meters towards and into the dam lake. Between June 15 and July 19 deformation was still going on and a new large crack appeared behind point A in *Figure 5a*).

Walking around at the lower part of the landslide several different volcanic soil types were found, ranging from weathered conglomerates to sandy and silty fine grained soils. In some locations evidence of liquefaction was found, in such as areas one would easily sink down to the knees in very soft sandy soils with high water content. Water was also seeping out in many locations. The part of the landslide that actually entered in to the lake, seems to have been more like a debris flow then a coherent soil mass. Tree trunks and road guard rails were found mixed into the soil mass. A traffic sign found on the soil mass that entered into the lake indicate the long travelling distance.

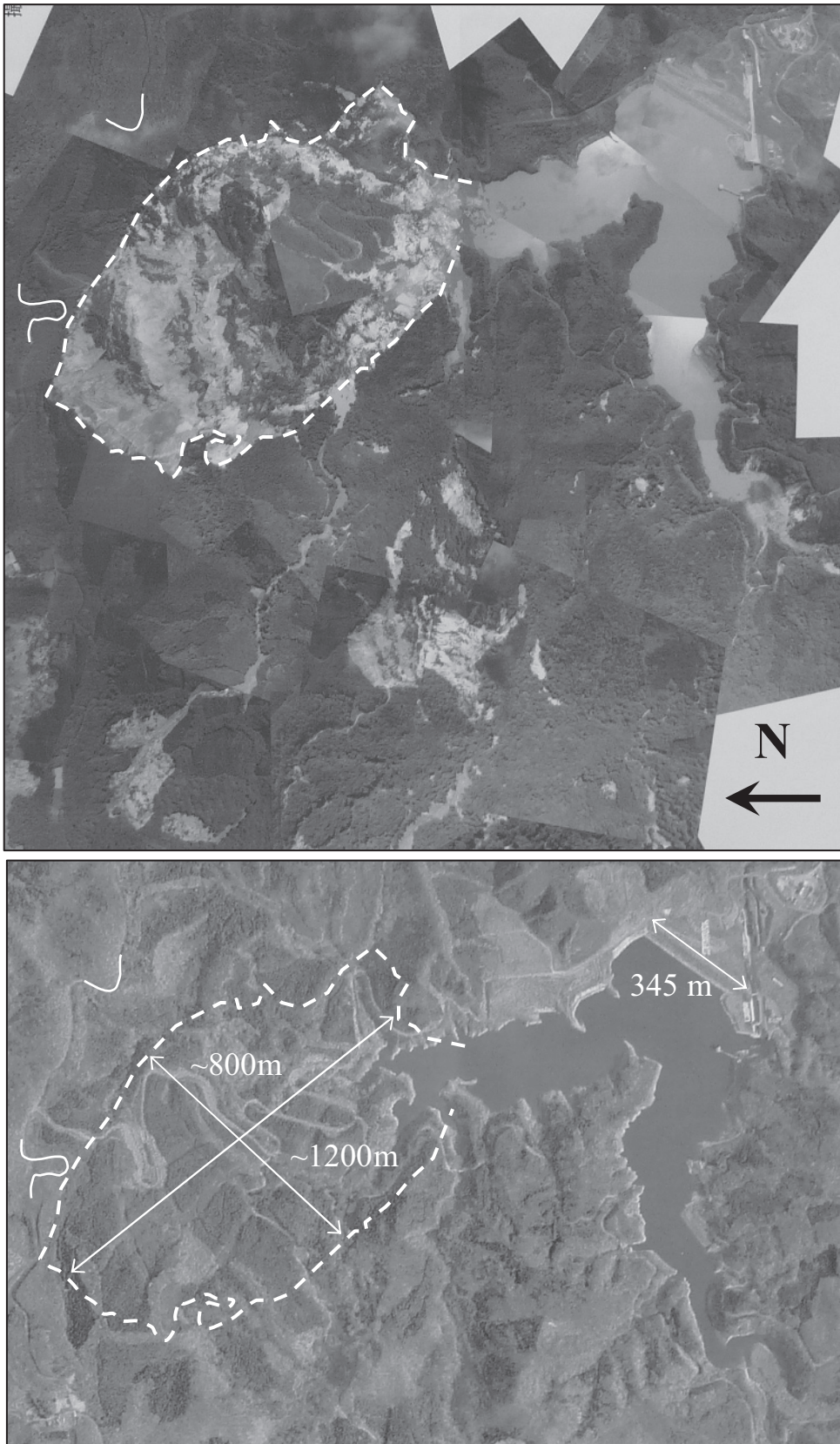


Figure 3: Aratasawa dam landslide escarpment outlined with dashed line after (upper) and before (below) the earthquake. The solid lines to the left shows some road sections for easier correlation of the photos.

Some pieces of light-gray rock fragments (see

Figure 4) were sampled at the toe of the landslide, at point Ps (38.8942N, 140.8545E) shown in *Figure 5*. The specific gravity immediately after the sampling (2008/06/16, 18:00) was 1.78 g/cm³, and after drying one day at 105 degrees C in oven it was 1.18 g/cm³. After soaking the sample in water for three hours it increased to 1.69 g/cm³. It is remarkable that the specific gravity of the dried sample is quite small, indicating the presence of large volume of voids. When soaked up with water, the sample smells hydrogen sulfide, an evidence of the volcanic origin of the soil. It is likely that such a porous soil did liquefy during the earthquake, and thereby played an important roll in triggering the slide.

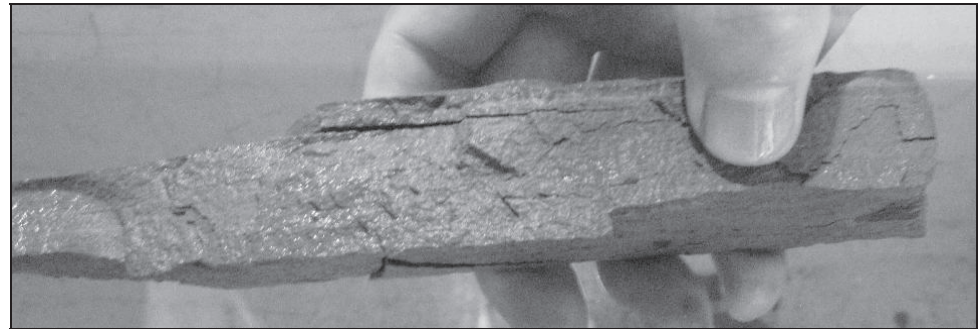


Figure 4: Rock sample smelling strong hydrogen sulfide taken from Point Ps in Figure 5.

Not only shaking may have been the cause of the slide, but tectonic deformation accompanying the earthquake may have played a roll. An investigation team of the Active Fault Research Center (AFRC, 2008) have documented surface fault features at several locations (marked approximately by the red line in the upper part of *Figure 1*.) An AFRC team found a surface fault segment some 500 meter long with right lateral slip of up to 7 meters and vertical off-sets of 2-3 meters (see *Figure 6*) to the east of the landslide scarp. It is possible that this surface fault have contributed to the triggering of the landslide.

The shaking also caused compaction and settlements of the ground around lake. E.g. near the parking lot on the eastern side of the lake a vertical pvc pipe used for measurement cables was sticking out of ground some 10-15 cm indicating that the surrounding soil had settled a lot. It was also reported (Kayen et. el., 2008) that the dam body had also settled some 40 cm and moved a few centimeters towards north.

3. TSUNAMI TRACES

When the landslide entered into the lake it casued a seiche travelling at some 10 to 15 m/s towards main dam body, reaching it after minute and half or so after that the landslide entered into the lake. The seiche travel velocity, v , was roughly estimated with formula, $v = \sqrt{gh}$, where g is the gravitational acceleration and assuming the depth h is some 10 to 20 m. The seiche flowed over into the spill way, but did not flow over the dam crest.

No major damage to the dam infrastructure due to the tsunami itself has been reported. However one person fishing from a small boat on the lake allegedly drowned.

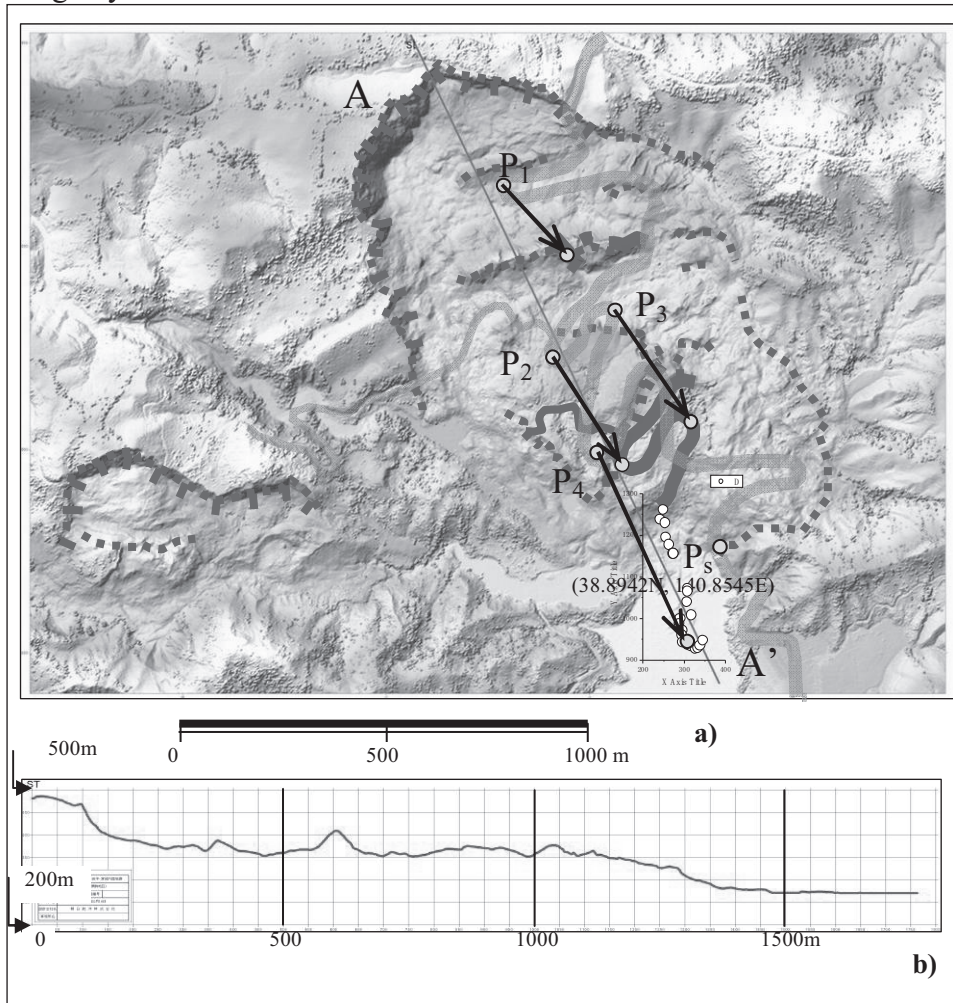


Figure 5: Landslide at Aratosawa dam. The road locations after and before (gray) the earthquake. Even though the base slope was very gentle the soil masses have moved some 200 to 500 meters. (Aero Asahi Co. provided the digital elevation model).

With idea of back calculating possible sliding characteristics such as soil volume entering into the lake and its impact/sliding velocity, we measured seiche high water marks on July 13 and 25. We used a for the locations of the high water marks and a handheld laser ranger was used to measure the height above the lake elevation. Since the lake was being emptied slowly we corrected the height for the difference between lake elevations on the days of measurements and the time of the earthquake. Table 1 gives lake water elevations as measured by dam management office. The water level was lowered with some 15 to 20 cm/day and as of this writing the lake is completely empty (water elevation 237 m) as to allow for inspection of the basin. Table 2 gives coordinates and corrected seiche heights in meters with respect to the lake elevation before the earthquake (268.5m.)

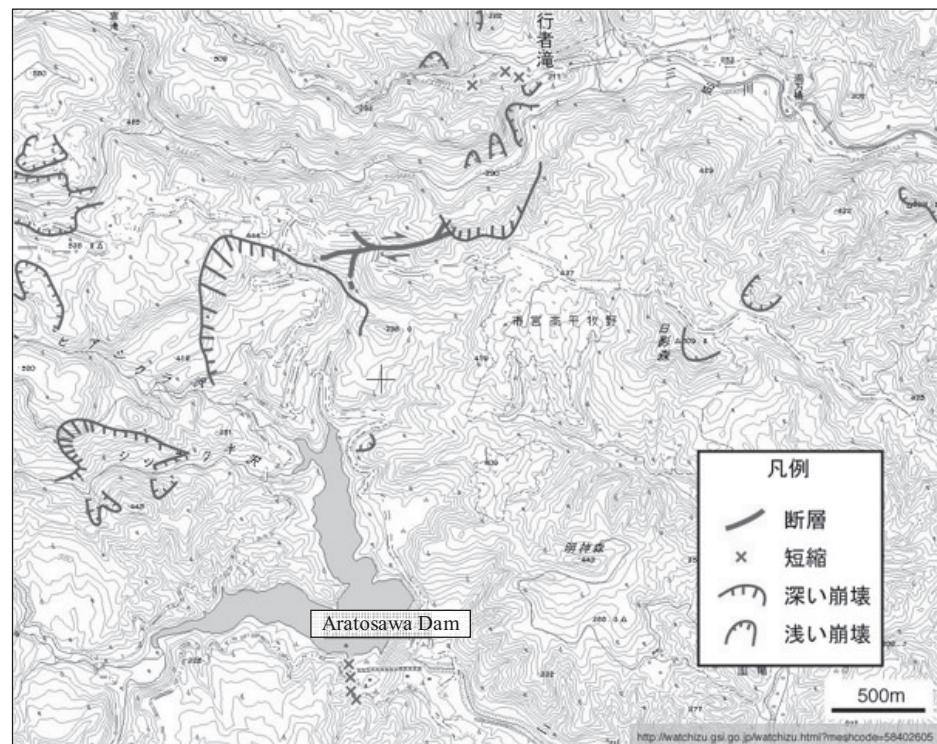


Figure 6: Map with landslide escarpment in purple and surface fault in red (after Active Fault Research Center).

As can be seen in Table 1 the lake elevation increased from 268.5 m before the earthquake to 270.9 m after the earthquake. The difference in lake elevation before and after the earthquake is due to that a part of the landslide mass entered into the lake and possibly also due to some tectonic deformation accompanying the earthquake. Assuming the lake elevation increase was only due to the landslide, it is estimated that out of the 50 million cubic meter large landslide some 1.5 million cubic meters entered into the lake.

Table 1: Dam Lake elevations measured by Dam Management Office

| Date | Elevation [m] | Remark |
|--------------|---------------|---|
| June 14 2008 | 268.5 | Before Earthquake |
| June 14 2008 | 270.9 | After Earthquake, water level increased due to landsliding and possibly due to tectonic deformation |
| July 13 2008 | 261.2 | Reference elevation for measurements on July 13 (Lake is being emptied slowly) |
| July 25 2008 | 259.1 | Reference elevation for measurements on July 25 |

Table 2. GPS data and high water marks with respect to the lake elevation before earthquake for July 13 and July 25.

| Point Id | Latitude | Longitude | Height above lake elevation before earthquake [m] | Time |
|----------|--------------|---------------|---|--------------|
| 3 | 38 53 28.9 N | 140 51 18.7 E | 8.7 | July 13 2008 |
| 4 | 38 53 28.4 N | 140 51 17.0 E | 4.2 | July 13 2008 |
| 6 | 38 53 24.3 N | 140 51 20.1 E | 8.5 | July 13 2008 |
| 8 | 38 53 35.2 N | 140 51 16.1 E | 4.1 | July 13 2008 |
| 9 | 38 53 34.2 N | 140 51 16.1 E | 5.5 | July 13 2008 |
| 10 | 38 53 33.4 N | 140 51 16.1 E | 6.1 | July 13 2008 |
| 11 | 38 53 1.6 N | 140 50 25.6 E | 4.5 | July 13 2008 |
| 12 | 38 53 4.7 N | 140 50 28.7 E | 3.7 | July 13 2008 |
| 13 | 38 53 7.9 N | 140 50 31.3 E | 7.7 | July 13 2008 |
| 14 | 38 53 4.8 N | 140 50 32.4 E | 3.2 | July 13 2008 |
| 15 | 38 53 10.6 N | 140 50 51.4 E | 4.2 | July 13 2008 |
| 16 | 38 53 10.6 N | 140 50 52.8 E | 4.5 | July 13 2008 |
| 194 | 38 53 36.4 N | 140 51 06.5 E | 9.35 | July 25 2008 |
| 196 | 38 53 33.4 N | 140 51 04.0 E | 7.25 | July 25 2008 |
| 197 | 38 53 32.1 N | 140 51 03.9 E | 7.35 | July 25 2008 |
| 198 | 38 53 31.1 N | 140 51 04.8 E | 5.95 | July 25 2008 |
| 199 | 38 53 30.7 N | 140 51 05.1 E | 6.55 | July 25 2008 |
| 200 | 38 53 29.5 N | 140 51 06.4 E | 4.15 | July 25 2008 |
| 201 | 38 53 28.9 N | 140 51 05.8 E | 6.35 | July 25 2008 |
| 202 | 38 53 27.0 N | 140 51 04.6 E | 7.75 | July 25 2008 |
| 203 | 38 53 26.8 N | 140 51 05.0 E | 6.75 | July 25 2008 |
| 204 | 38 53 26.8 N | 140 51 07.2 E | 5.15 | July 25 2008 |
| 205 | 38 53 26.3 N | 140 51 06.8 E | 5.75 | July 25 2008 |
| 206 | 38 53 25.7 N | 140 51 07.1 E | 6.85 | July 25 2008 |
| 207 | 38 53 25.0 N | 140 51 06.9 E | 5.85 | July 25 2008 |
| 208 | 38 53 23.4 N | 140 51 06.9 E | 5.25 | July 25 2008 |
| 209 | 38 53 22.8 N | 140 51 07.6 E | 6.45 | July 25 2008 |
| 210 | 38 53 22.4 N | 140 51 07.9 E | 7.25 | July 25 2008 |
| 211 | 38 53 21.0 N | 140 51 09.2 E | 5.45 | July 25 2008 |
| 212 | 38 53 20.1 N | 140 51 09.8 E | 6.25 | July 25 2008 |
| 213 | 38 53 18.9 N | 140 51 09.8 E | 7.45 | July 25 2008 |
| 214 | 38 53 19.0 N | 140 51 10.4 E | 7.75 | July 25 2008 |
| 215 | 38 53 18.5 N | 140 51 10.9 E | 8.05 | July 25 2008 |
| 216 | 38 53 18.0 N | 140 51 11.8 E | 6.35 | July 25 2008 |
| 217 | 38 53 17.3 N | 140 51 13.8 E | 4.95 | July 25 2008 |

The high water marks (from

Table 2) are plotted in Figure 7. We can see that on the right side in the Figure 7 (East side) the elevation increases from 4.1 meters to 8.7. On the Western side there is a zig-zag patterns of heights, whether this may be

due to the topographical features of the lake border and/or due to error in our measurements. One can often not be sure of having identified the highest high-water-mark in the field. At the far end, points 11, 12, 14 in *Figure 7*, heights are lower, likely since here the seiche can spread and run up long distances. However at point 13 which is close to a fairly steep location the seiche height reached 7.7m.

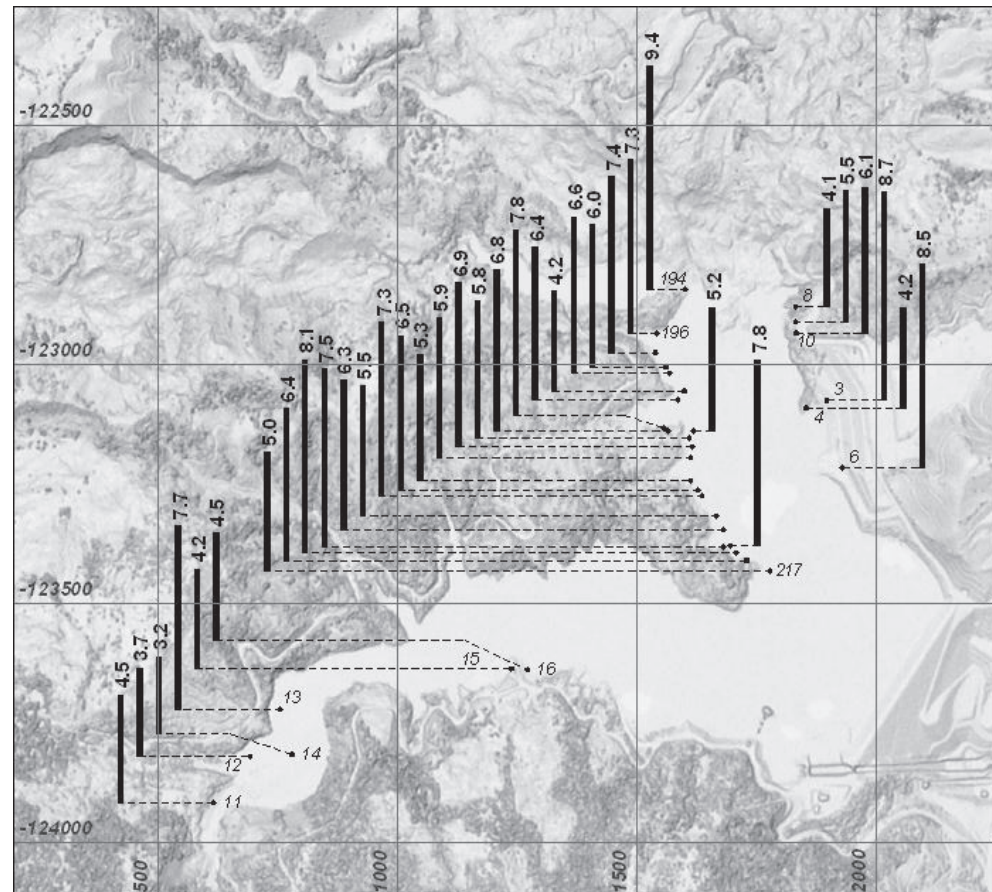


Figure 7: Seiche heights, with respect to lake elevation before the earthquake, as measured in the field on July 13 and July 25.

The high water marks together with topography (digital elevation models) of the area before and after the earthquake, are now used as inputs to a shallow water wave propagation code, with which we hope to perform a parametric study to back calculate the possible landslide characteristics such as sliding velocity. The velocity of the landslide in combination with the geometry of how the landslide enters into a body of water would be useful when considering different remedial measures for similar dams. It is important e.g. to evaluate the landslide velocity needed for the water to flow over the dam crest and thereby possibly causing damage to the dam infrastructure and/or becoming a threat to the people living below the dam.

4. SUMMARY

A 50 million m³ large earthquake induced landslide at Aratosawa dam caused a tsunami when entering to the lake and flowed over into the spillway, but not over the crest. While one person is believed to have died due to the tsunami no damage to dam infrastructure or to down stream occurred. However lessons from this tsunami may be very useful when dealing with the possibility of future events. There we have documented high water marks around the lake with the future objective of back calculating and evaluating important parameters, characterizing the interaction between the landslide mass and water in the lake, such as impact velocity and geometry.

ACKNOWLEDGEMENTS

We thank Prof Suzuki Takasuke for explaining the local geology, Toshihiko Katagiri and Date Masaki for helping during the field reconnaissance and Edwin Leon for plotting the tsunami heights.

REFERENCES

- Active Fault Research Center, Quick Report on the 2008 Iwate Miyagi Nairiku Earthquake”, (in Japanese), 2008, Web site last accessed August 5,
2008,年岩手 宮城内陸地震速報.
http://unit.aist.go.jp/actfault/katsudo/jishin/iwate_miyagi/report/080709/index.html
- Robert Kayen, Brady Cox, Jorgen Johansson, Clint Steele, Paul Sommerville, Kazuo Konagai, Yu Zhao, Hajime Tanaka, Geoenvironmental and Seismological Aspects of the Iwate Miyagi-Nairiku, Japan Earthquake of June 14, 2008, GEER Web Report 2008.2 v.1, 2008.
http://research.eerc.berkeley.edu/projects/GEER/GEER_Post%20EQ%20Reports/Japan_2008/Cover_Japan2008.html

INTEGRATED INFORMATION SYSTEM FOR LANDSLIDE DISASTER MANAGEMENT

KIMIRO MEGURO, AKIYUKI KAWASAKI and TATIANA TORRES
International Center for Urban Safety Engineering, Institute of Industrial
Science, The University of Tokyo
meguro@iis.u-tokyo.ac.jp,

ABSTRACT

Specialized publications available on the field of landslide assessment indicate that significant developments have taken place in the last decades. However, there is a gap between the information provided by scientific and technological advances and the tools that really find their way into practice. A systematic approach to incorporate these developments within the landslide management practice is presented herein.

This paper presents a new decision support tool to enhance the use of landslide information in landslide management practice and to assist decision makers in planning an efficient and systematic landslide assessment. The proposed system integrates landslide management actions with type of assessment, method, data, and scale, in order to assist users to get hold of relevant information for their purpose. The prototype system was developed as a web-based computer application, which combines a relational database and updating strategies that guarantees a sustainable and affordable system for landslide management.

1. INTRODUCTION

Landslides might not be as impressive as other natural disasters; however they are the most widespread geohazard on the earth. According to Varnes (1984), landslides cause more life and property losses than any other geological hazard. Moreover, a significant part of the damages and casualties associated to other natural disasters such as earthquakes or intense storms are due to landslides triggered during or after these events.

These losses are expected to rise with the increase in demands for living spaces. Countermeasures have to be taken as long as overpopulation and the uncontrolled growth of urban areas increase the exposure of people to natural threats. Landslide management strategies to avoid or mitigate the adverse effects of these disasters are required to tackle with this problem.

Clear final targets have to be highlighted in order to produce valuable information. A dearth of guidelines or strategies to match landslide assessment with user requirements and constraints is regarded as the critical issue to take advantage of developments in landslide assessment.

This paper presents a new decision support tool called Integrated Landslide Management System –ILMS- to help decision makers, managers and other users involved in landslide management to effectively carry out landslide assessments aimed at producing useful information. ILMS guides the user through the complex choices involved in landslide assessment to meet user’s specific needs. A prototype of this tool is implemented as an internet based application linked to a relational database.

2. INFORMATION IN LANDSLIDE DISASTER MANAGEMENT

Landslide management is the set of actions or strategies taken in order to reduce the occurrence of landslides or to minimize their effects. These actions often deal with cost and time constraints, and sometimes adverse social, economical and environmental consequences. In order to overcome this complex condition, decision makers are called to make effective use of information and tools for enhancing the effectiveness of the actions and to avoid the waste of resources and undesired effects. Unfortunately the gap between decision maker requirements and available information hinders decision makers from using proper information.

The importance of information in landslide management; as pointed by Wold (1989), lies on the fact that landslide losses that have occurred might have been prevented or avoided if relevant landslide information has been available and used.

The role of information in landslide management can be understood based on the decision making cycle (See Figure 1). This scheme portrays the flow of information along the execution of actions. The process engages the use of information for each stage. In this scheme, information represents the support necessary to examine feasibility, cost-effectiveness and the likely impacts of actions. In brief, information is the base needed to support actions. As Kim (2007) states “having the right and timely information represents a higher probability of making a right decision”.

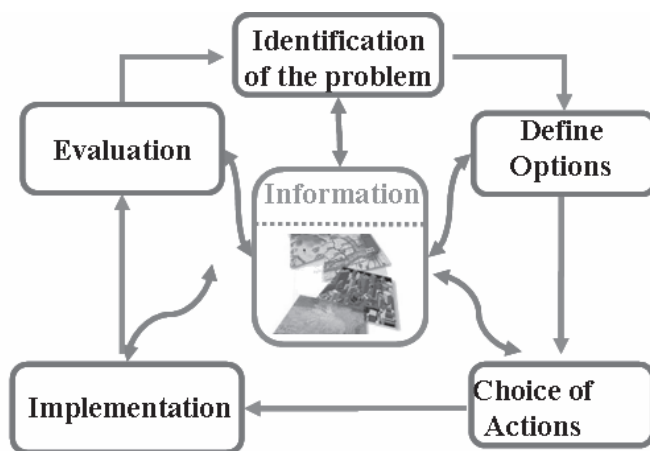


Figure 1: Decision making cycle

However in most of the cases; decisions are based on values, preferences, intuitions, prejudices and social situations of the organizations and individual who make them. Therefore, a significant challenge in landslide management might be using the appropriate information at the appropriate place and time from a practical point of view.

It is important to keep in mind that information deals with different scales and contents. Therefore, decision makers who will act on the findings of the assessment should help to frame the issues that will be assessed in order to produce useful information. As MA (2005) asserts, even if an assessment is technically credible and focused on relevant issues, the intended users of an assessment may not use the findings if they do not participate in the definition process. In fact, Aleoti (1999) states that less than 25% of the landslide assessment has been fully utilized from a practical point of view.

It might be stated that existing landslide assessments do not make practical use of the information. Moreover, keeping in mind that the cost of acquiring information is significant and there is a tradeoff between the cost and the value of information; a strategy for linking assessment and the information needs for supporting actions is in fact required.

3. INTEGRATED INFORMATION SYSTEM

Integrated Landslide Management System ILMS is a decision support tool for decision makers, manager and others who use landslide assessment for taking their actions. It guides the user through the complex choices involved in landslide assessment to meet his needs.

The main target of ILMS is to provide a guide to maximize benefits of available landslide assessment and technologies in order to produce relevant information for taking an action. In addition, the proposed system may be regarded as a mean to find better landslide assessments and to prioritize the required improvements in terms of data in order to achieve more detailed studies.

3.1 Conceptual Framework

The conceptual framework of the system is shown in Figure 2. It is suggested that the planning of landslide assessment process should start from fixing the action and based on that, identifying what is the purpose or scope of the intended information. This evaluation will help to establish the content and scale characteristics. These two issues play a key role to reach relevant information; they define what should be done. In the context of the proposed system, the explicit definition of these elements makes a rational link between landslide assessment and its use.

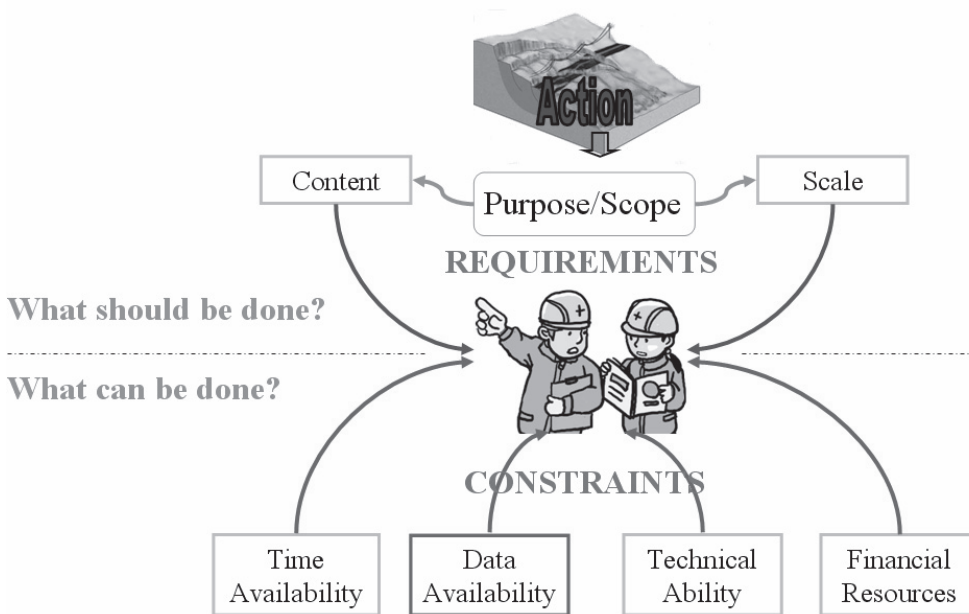


Figure 2: ILMS conceptual framework

However, due to restrictions in time, funds, data, and technology; the intended information is inevitably constrained. Therefore, a second question arises: what can be done. It is important to mention that if constraints are the main driver in assessment planning, there is a possibility that the results become useless and a waste of time, money and resources. ILMS prototype includes data availability as a controlling constraint; further improvements should be done in order to take into account other constraints.

The system's features and its relations are shown in Figure 3. First, an action determines the required information; then the required information controls the selection of method and data. Finally, the constraints define the applicable method and control the produced information.

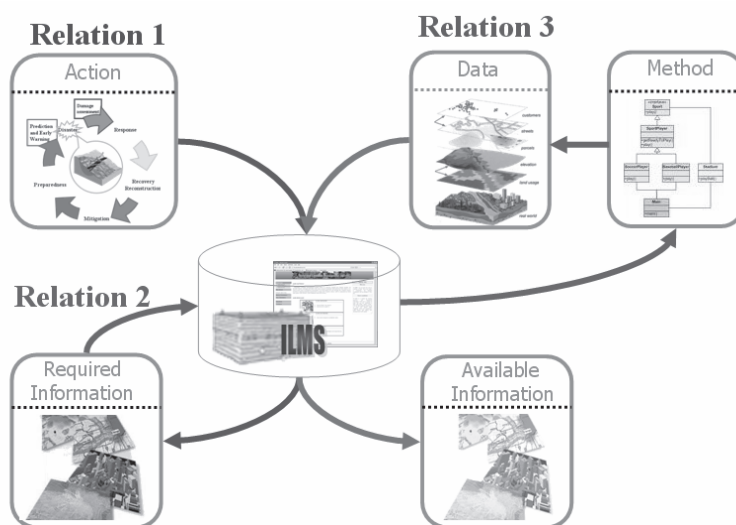


Figure 3: Relationships among key features of ILMS.

3.2 System Development

The ILMS development strategy is illustrated in Figure 4. The prototype system was made by collating, evaluating, summarizing, and interpreting the scientific and practical knowledge in the landslide assessment field. The scientific knowledge is based on technical reports, papers, books, and the practical knowledge is elicited from experts involved in landslide management. The knowledge collected was interpreted and encoded in a structured knowledge database that contains the rules, methods, and data, arranged in a useful form in order to support an efficient information management. An extensive integration and harmonization process in non-standardized data structures was required in the development of ILMS.

Once the structured knowledge data was consolidated, a web based application was developed in order to create a platform to interact with the database. The application is composed of two elements; the inference engine and the user interface. The inference engine contains the code at the core of the system while the user interface allows the dialog between the user and the system through consults and feedback.

Apache was used as web server software, MySQL as database management software and php as scripting language. Basically, when a user makes a consult, the web server passes the consult to the engine, then the engine calls the knowledge stored in the database management system. It is made through a runtime compiled code that also allows returning the response to the user interface.

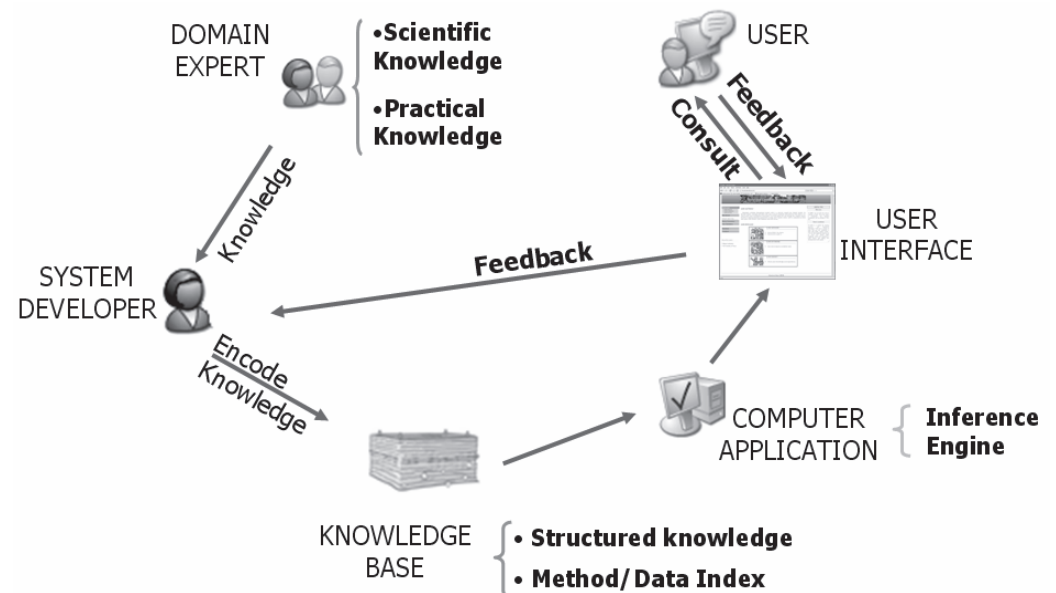


Figure 4: ILMS development process

The user interface layout of ILMS is shown in Figure 5. The layout is composed of 6 sections; the head, navigation menu, explanation, links, main frame and navigation control. The head, navigation menu, and link frame are common for all the modules included in the system, whereas the main, explanation and navigation frames change depending on the module. The

navigation menu is a driven-menu and it allows users to navigate among all modules part of ILMS. The main frame contains the interactive core, in which users are asked for inputs and the system provides an output report. The explanations frame provides guidelines about the use of the system.

3.3 System Components and Functionalities

The main components are ILMS survey, ILMS update, ILMS data base, and ILMS advisor (See Figure 5).

ILMS advisor provides recommendations about the assessment's characteristics for meeting the user's specific needs. It also suggests methods and data appropriate for accomplishing a specific assessment. Finally, it provides advices for finding methods that match user constraints. ILMS advisor helps the user to examine both requirements and constraints.

ILMS database represents the structured knowledge discussed in Section 3.2. It is a database of relations, methods, and data involved in landslide assessment that can be expanded. It was designed to provide a rapid mechanism for comparison among landslide assessment methods. It includes relevant features of assessment methods, such as limitations and scope among others, from which it is possible to rationally select a suitable method.

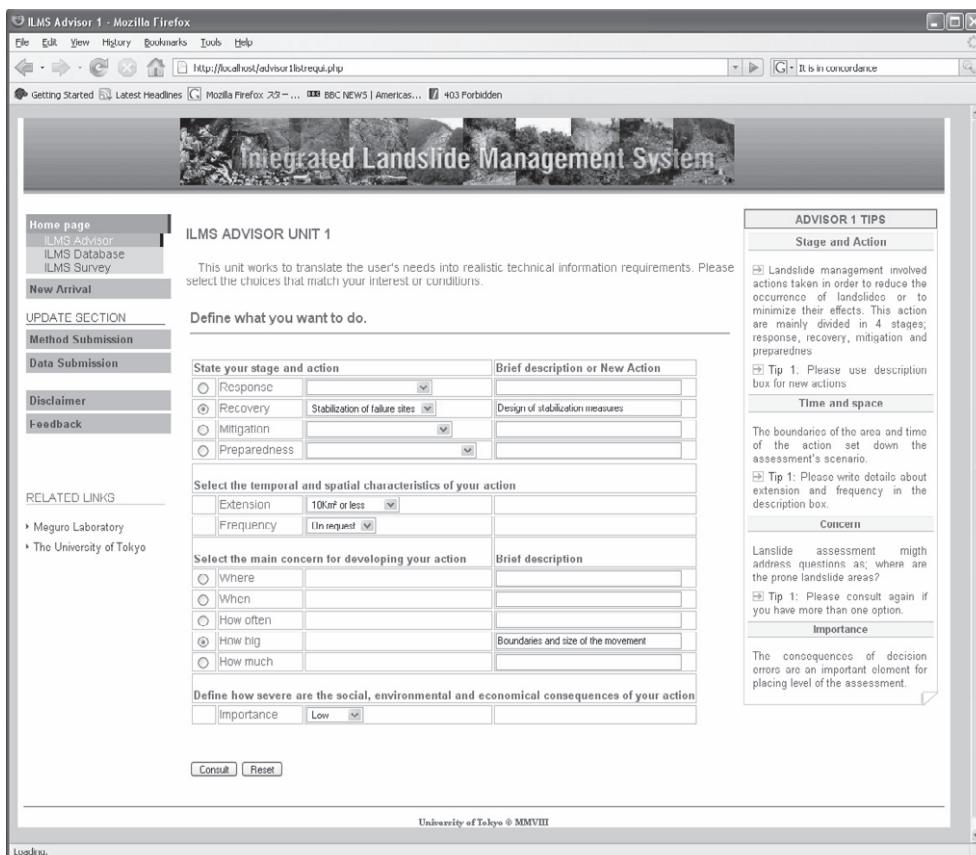


Figure 5: ILMS user interface

ILMS survey is focused on summarizing the opinions of different people whose activities are related to landslide disaster management. The

designed questionnaire allows the incorporation of practical knowledge to improve continuously the knowledge database.

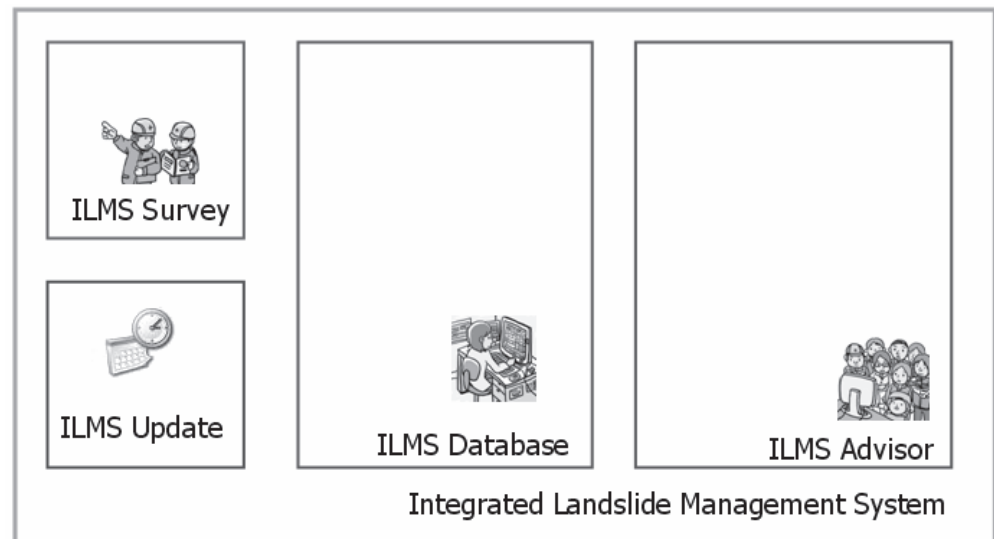


Figure 6: ILMS functions and components

3.4 System accessibility and update strategies

ILMS can be accessed through internet by using any web browser so that it offers public accessibility; one of the desired features for having a sustainable and affordable system.

Three specific modules were designed; ILMS survey, ILMS feedback and ILMS update. As mentioned before, ILMS survey gathers opinions from experts in order to enrich the relations included in ILMS database. ILMS feedback focuses on gathering suggestions and advices to make the system better. Missing elements in the system can be reported through this module.

ILMS update is the access to enrich the data and methods database, it makes possible to incorporate new developments into the database. This module asks the user for the characteristics of the method following the structure established for the database.

4. USING THE SYSTEM ADVISOR

ILMS advisor helps user to analyze feasible assessment in the light of the action to be taken and existing constraints. ILMS advisor is composed of three subunits, Unit 1 and Unit 2 focus on what should be done. And Unit 3 focuses on what can be done. The units can be used independently or sequentially. The process sequence is illustrated in Figure 7.

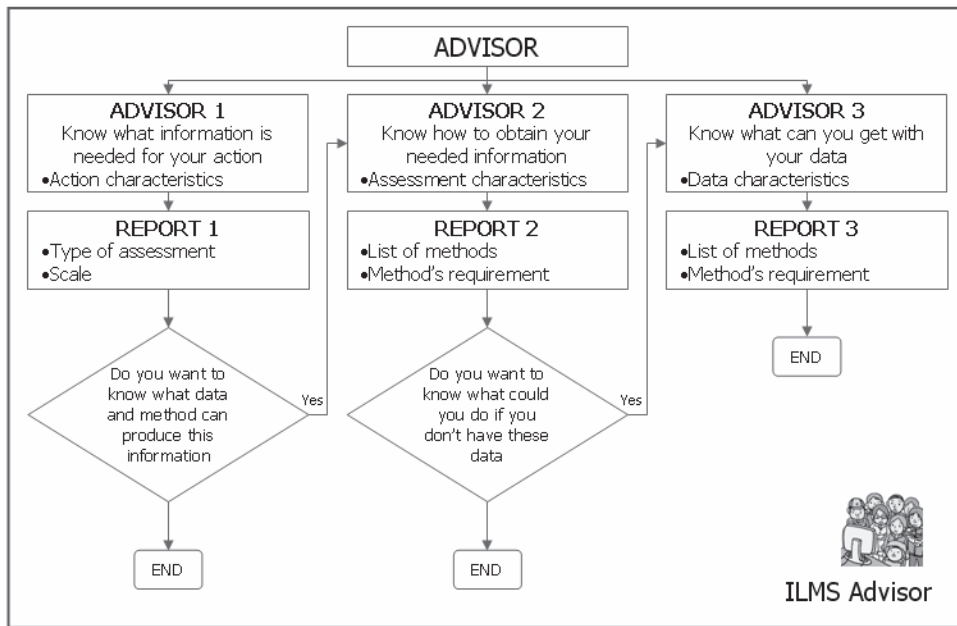


Figure 7: ILMS functions and components

This first unit translates the user needs into realistic technical information. Advisor Unit 1 asks for information about the landslide management action and then provides the required information for that specific condition. Users are asked to select among options in order to match their interests or conditions in terms of the intended action. After defining the characteristics that matches the action, an advising report is displayed. It suggests the type of assessment, spatial and temporal scale, and category of analysis according to the relations stored in ILMS knowledge database.

The second unit assists the users to determine which method and data is required to reach the information needs. Advisor 2 asks for information about the type of assessment, scale, category and type of landslide. The output report contains a list of methods that matches the selected options.

The third unit helps finding what information can be achieved taking into account user constraints. ILMS prototype includes data availability as a constraint. Therefore, Advisor 3 asks for information about the available data and its characteristics in terms of scale and quantity. Through Advisor 3 users are able to establish what methods match with their data and what methods might be used if the quality and amount of data are improved.

5. CONCLUSIONS

The landslide assessment process is complex, time consuming and costly; in order to avoid wasting of resources in useless information a systematic approach for planning landslide assessment is required. The key element to achieve this goal is a clear link between user requirements and existing approaches in such a way that developments in modeling techniques are kept up to date so that strategies for landslide management are defined more rationally.

The proposed Integrated Landslide Management System –ILMS– provides the tool to link actions, methods and data and to encourage the use of scientific information in landslide management. ILMS prototype might be considered as a platform for a systematic information management. It is also starting point to manage and share experiences, and developments so that it might help users to make informed-based decisions.

The system's backbone, built around ILMS, is ready to accept new the data, models, users and actions in such a way that it can be easily extended to take into account new developments and the dynamics of requirements.

This prototype provides a framework to be customized for others fields related to information management.

REFERENCES

- Aleotti P. and Chowdhury.R. 1999. Landslide hazard assessment: summary review and new perspectives. *Bull Eng Geol Env*, 58:167_184.
- Kim, J. 2007. Efficiency of critical incident management systems: Instrument development and validation. *Decision Support System*, 44:235-250.
- MA. 2005. Global assessment reports. Scenarios assessment. millennium ecosystem assessment. Technical Report 2, Millennium Ecosystem Assessment Scenarios Working Group.
- Mussi, S. 2002. Sequential decision-theoretic models and expert systems. *Expert System*, 19(2).
- Varnes, D. 1984. Landslide hazard zonation: a review of principle and practice. United Nations Educational, Scientific and Cultural Organization.
- Wold R. and Jochim C. 1989. Landslide Loss Reduction: A guide for state and local government planning. Number Earthquake hazards reduction series 52. Federal Emergency Management Agency.

DEFENSE AGAINST INTENTIONAL ATTACKS: FRAMEWORK FOR MODELING AND SIMULATION

JING ZHANG, SHIFEI SHEN, RUI YANG and JIANHONG WU
Department of Engineering Physics,
Center for Public Safety Research,
Tsinghua University, China
jing-zhang05@mails.tsinghua.edu.cn

ABSTRACT

Intentional attacks by human have been a worldwide catastrophe risk and threaten public safety. As a typical case of this disaster, terrorism events not only cause casualties and economic damage, but also change the national security and the way governments function. Different from natural disasters and accidents caused by human error, intentional attacks are rational behaviors of people. The existence of dynamic interactions between defenders and attackers corresponds to the strategic risk. This paper studies the characteristics of decision-making in strategic risk and allocation the limited resources optimally for mitigating the strategic risk. A framework for studying the defense and response against intentional attacks is presented. Game-theoretic resource allocation modeling and agent-based simulation are described. Different types of target relationship are also discussed. The research results could provide decision-making support for the counter-terrorism defense, emergency rescue operation and hazard mitigation.

Keywords: *man-made emergency; resource allocation; strategic risk; decision-making modeling; agent-based simulation*

1. INTRODUCTION

Intentional attacks, especially terrorism events, aiming at against the public for political, religious, or ideological reasons, probably cause great loss of property and lots of victims. Recent terrorist attacks like the 9.11 attack and the 3.11 Madrid bombing had made the public and the government quite aware of the risk of man-made emergencies. More attention has been put on how to defense and response against the attacks with limited resources.

One basic feature of intentional attacks is the conflict between the attackers and defenders. The two adversaries, as players of defense game,

have to estimate the opponent's strategy and choose own advantaged actions against this strategy. The attackers rationally choose the most unguarded one among lots of potential buildings or dense population as the target; correspondingly, the defenders will allocate the limited security resources based on the available information about the possible attacks. The result of the interactive decision-making depends on the decisions of both sides.

Terrorism risk represents as a function of the expected consequences of attacks, taking into account the likelihood that attacks occur and that they are successful is attempted (Willis, 2007). Because of the rational behavior of attacker, intentional attack risk is a kind of strategic risk that the likelihood of attack against a specific target depends on the consequence of the attack and the security vulnerability of all the potential targets. This kind risk is considered dynamic during the interactions of the attackers and defenders. To effectively allocate limited resources among potential targets to reduce the total strategic risk, it's useful to model the interactive decision-making between attacker and defender, and the relationship between targets should also be discussed.

The effort to allocate resources based on terrorism risk has been limit until recently. Several progresses have been made on the research of terrorism insurance and risk management. Garrick et al (2004) developed a methodology for terrorism risk assessment. The process includes the threat understanding, vulnerability understanding and risk analysis and mitigation. McGill et al (2007) set up a framework for critical asset assessment, which includes five phases: scenario identification, consequence and criticality assessment, security vulnerability assessment, threat likelihood assessment, and benefit-cost analysis. Another methodology for regional terrorism risk assessment was developed by Willis and LaTourrette (2008), using the probabilistic terrorism risk model to estimate the overall risk from terrorist attacks in the U.S. and providing advices for counter-terrorism fund. Researches up to now most focus on a critical asset or cities which considered independent, usually estimating risk in a probabilistic way, ignoring the interactive decision-making process of the attacker and defender.

In this paper, a framework for studying the defense and response against intentional attacks is presented. Game-theoretic defense modeling is described in section 2. To better understand the interactions of different kinds, different types of relationship among potential targets are discussed in section 3, which can help the defender to distribute security resources among these targets. The need for incorporating agent-based modeling and simulation is described in section 4. Conclusions of this work are presented in section 5.

2. FRAMEWORK FOR DEFENSE MODELING

The process of defense against intentional attack like terrorism can be studied in 3 phases as follows:

- Depending on the game between the attackers and defenders, a proactive allocation of the limited defensive resources (for example, guard and equipment) among all the potential targets should be performed;
- When attack occurs, defender distributes the emergency resources such as first responders (police, fire and ambulance) to the affected targets;
- During the emergency response, the remained resources should be relocated to cover all the potential targets have not been attacked yet to mitigate attack cascade risk.

A framework for modeling the defense against intentional attacks is shown in Figure 1. The core issue is that the defender should distribute limited defensive and emergency resources among or covering all the potential targets for preventing and responding to the possible attacks.

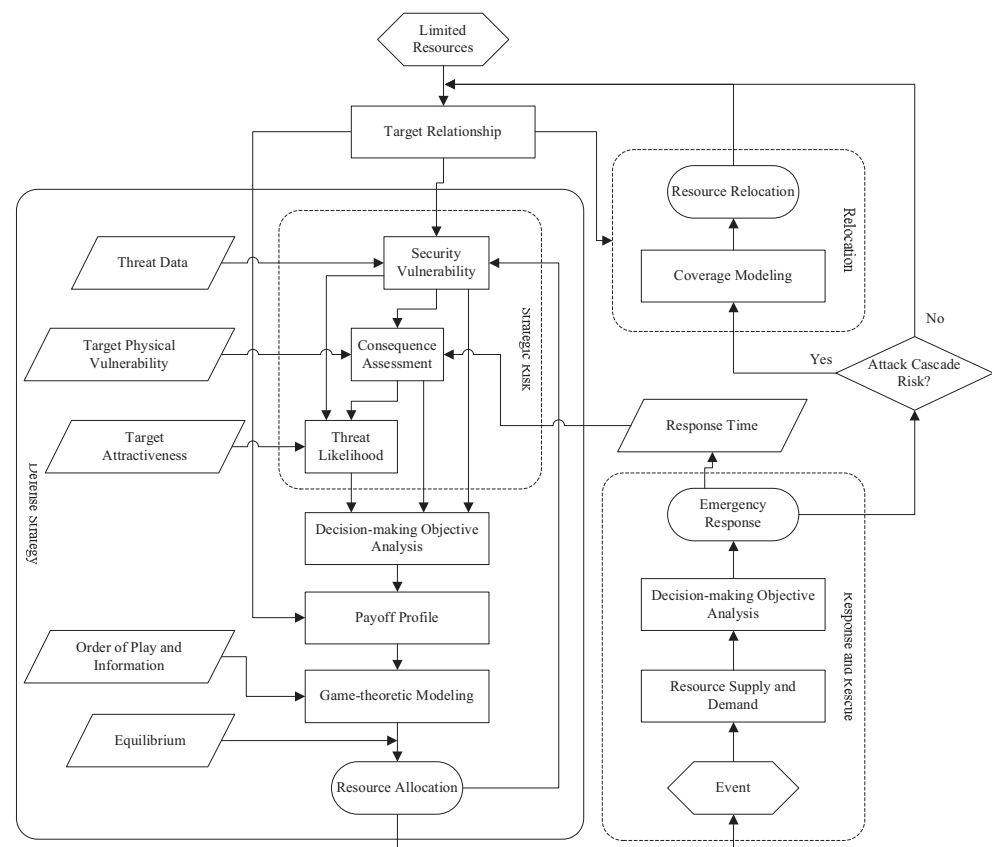


Figure 1: The framework of defense modeling

2.1 Game-theoretic Modeling for Allocating Defensive Resources

A proactive defensive allocation aims to reduce the total risk of all the potential targets. As mentioned above, the intention attack risk is a strategic and dynamic risk depending on the two players' decisions. For a specific target, this strategic risk is a function of threat (possibility of being attacked), security vulnerability (probability of adversary success for a given attack) and consequence (the result of damage). The consequence depends on the physical vulnerability of the target, which represents the damage may be caused by attack so differs from the security vulnerability. The **Threat** likelihood is determined by both the security vulnerability and consequence.

Traditional methodologies such as deterministic and probabilistic decision-making theories are not adequate for the strategic risk mitigation in intentional attacks because they are unable to handle the interaction between the two players of the game. Instead, game theory provides a nature way to address this problem. Game theory studies how a rational player choosing his actions, while the strategic interactions exists among the players (Osborne, 2005). In this problem, attacker and defender play games with opposing objects like loss of lives and economy, social effect, etc. Attacker chooses target and decides the strength of the attack, while defender makes a proactive distribution of defensive resources to minimize the loss. The interaction of the two players' decisions determines the **Security Vulnerability** of target so affecting the consequence of a given attack.

Several game-theoretic models for allocating defensive resources have been developed. Major (2002) developed a complete information zero-sum game model for the situation that attacker and defender make decision at the same time. Kardes and Hall (2005) discussed repeated game between attacker and defender. Bier (2007) discussed the situation that attackers may be able to observe the defenses and revise their attack strategies accordingly. Powell (2007) developed a signaling game because defenders are likely to have private information about the vulnerability of the targets they are trying to protect.

2.2 Emergency Resources Location and Relocation

Once the attack occurs, it's important to decide how to distribute the emergency resources to different affected targets for a best relief of the disaster. In some cases, there may be the shortage of emergency resources at the beginning of response so that the affected targets have to compete for the limited resources. In this situation, a game will be played among these targets. Meanwhile, there are multiple decision-making objectives should be achieved in a tradeoff way for resource distribution. It requires us to model the emergency resource distribution problem combining game theory with multi-objective optimization. In addition, there may be multiple supplies in

different locations, so the transportation and accessibility under disaster among the supplies and demands should also be considered. The shortage of resources and transportation delay may weaken the relief efficiency so increase the **Consequence** of the attack, thus increasing the strategic risk.

Some works discussed the game among targets. Heal and Kunreuther (2007) discussed the defense against terrorism as a game among defense agents.

Since the emergency resources has been located and distributed to the attacked targets, there may be some potential target left uncovered. It's necessary to relocate the spare resources to cover the most demands.

3. RELATIONSHIP OF TARGETS

Since the connection of targets and potential competition for scarce resources, the strategic risk of each target is not independent with others. Three basic types of relations are defined here: Exclusive, Sharing and Related. The exclusive relation means that if we strengthen the defense of one target, the risk of the other one will increase. Buildings compete for guards are of this type. The sharing relation means that if the defense of one target is strengthened, the risk of the other will also be reduced. One example is railway stations that are connected by railways. The related type is a weaker relationship of interdependence. Targets are related in manners that are neither fully in exclusive nor fully in sharing. By these types of relations, multiple targets can form a network of risk transfer or interdependence. In this framework, different target relationships will leads to different defensive resource allocation plans.

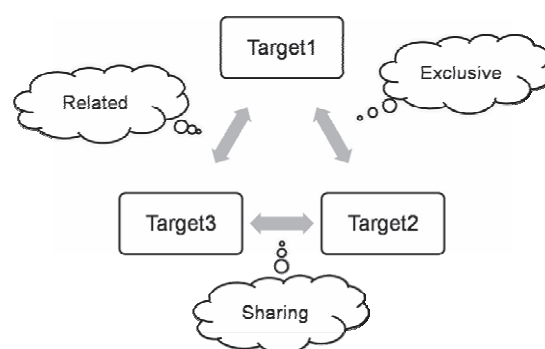


Figure 2: Relationship of targets leading to risk interdependence

4. AGENT-BASED SIMULATION

Agent-based modeling is a powerful technique to simulate autonomous agents capable to make decisions interacting with each other. It's helpful to incorporating this technique to better understand the strategic interactions between the attacker and defender. Agent-based modeling can not only provide a way to verify the game-theoretic models developed above, but also helps to solve the mathematical models in a distributed way that can be easily performed by computer.

To develop a gaming agent model, there are two steps: defining the roles of attack agents and defense agents and modeling different types of agents by set their objectives and rules for interaction. The development can be done on common agent-model development toolkits.

The game in the framework could be modeled in 3 types:

- Static game
- By simulating the static game between attacker and defender, “what-if” scenarios are provided to test what is the best defense resource allocation before attacks.
- Dynamic game
- The strategic risk determines the strategies of resource allocation by defender. However, strategic adversaries probably move sequentially so the attacker's awareness of defensive resource allocation plans and the possible delay of emergency response will affect the strategic risk as a feedback. By simulating the dynamic game, the effect of this feedback can be discussed.
- Evolutionary game

Attacker and defender are considered as two individuals with bounded rationality who only knows limited information about the other as in the real world. They can adjust their strategies by learning through repeated games to finally reach or approach the best solution.

5. CONCLUSIONS

As mentioned above, traditional risk analysis is not likely to be sufficient to analyze the intentional attack risk, since it doesn't take into account rational attacker's response to the defense strategies that defenders will take. This paper presents a framework for studying the defense and response of intentional attacks based on game-theoretic models and multi-objective optimization, to capture the strategic interactions between attacker and defender and the competition for scarce resources among targets. Different types of relationship of targets are defined and discussed. In the future, agent-based modeling and simulation should be incorporated to better understand these interactions, and provide a platform to perform the analysis

more easily and extensible by computer.

ACKNOWLEDGEMENT

This research is supported by “11th Five-Year Plan” National Scientific and Technological Supporting Project-“Key Technical Standards Project” (2006BAK04A08)

REFERENCE

- Bier V. M., 2007. Choosing what to protect: Strategic Defensive Allocation against an Unknown Attacker. *Risk Analysis*, 27(3), 607-620.
- Garrick B. J., Hall J. E., Kilger M., McDonald J. C., O’Toole T., Probst P. S., Parker E. R., Rosenthal R., Trivelpiece A. W., Van Arsdale L. A., Zebroski E. L., 2004. Confronting the risks of terrorism: making the right decisions. *Reliability Engineering & System Safety*, 86(2), 129-176.
- Heal G., Kunreuther H., 2007. Modeling Interdependent Risks. *Risk Analysis*, 27(3), 621-634.
- Kardes E., Hall R., 2005. Survey of Literature on Strategic Decision Making in the Presence of Adversaries. Report of Center for Risk and Economic Analysis of Terrorism Events, University of Southern California.
- Major J. A., 2002. Advanced Techniques for Modeling Terrorism Risk. *The Journal of Risk Finance*, 4(1), 15-24.
- McGill W. L., Ayyub B. M., Kaminskiy M., 2007. Risk Analysis for Critical Asset Protection. *Risk Analysis*, 27(5), 1265-1281.
- Osborne M. J., 2005. *An introduction to game theory*. Shanghai University of Finance & Economics Press.
- Powell R., 2007. Allocating Defensive Resources with Private Information about Vulnerability. *American Political Science Review*, 101(4), 799-809.
- Willis H. H., 2007. Guiding Resource Allocations Based on Terrorism Risk. *Risk Analysis*, 27(3), 597-606.
- Willis H. H., LaTourrette T., 2008. Using Probabilistic Terrorism Risk Modeling for Regulatory Benefit-Cost Analysis: Application to the Western Hemisphere Travel Initiative in the Land Environment. *Risk Analysis*, 28(2), 325-339.

A HOLISTIC APPROACH FOR ANALYSING IMPACTS OF CLIMATIC CHANGES ON COASTAL ZONE SYSTEMS

DUSHMANTA DUTTA, WENDY WRIGHT and SAMUEL ADELOJU
School of Applied Sciences and Engineering,
Monash University, Australia
dushmanta.dutta@sci.monash.edu.au

ABSTRACT

In recent years, there has been an increasing concern, particularly with the growing population, rapid urbanization and industrial developments in coastal areas of Asia Pacific region that the current management practices adopted in most of these countries are unsustainable (Hong et al., 2002). It has been realized that the rapid developments, extraction or manipulation of resources cannot exceed the sustainable limits without compromising the ecological integrity of the coastal ecosystems. This has now led to a growing concern that if the current trend of growth and exploitation continues, it would result in adverse effects on social, economic and environmental well-being in coastal zones. An holistic approach (that combines physical modelling, vulnerability assessment with triple bottom line and life cycle analysis principles and multi-criteria decision making (MCDM) tools) to coastal zone management is needed to resolve the conflicting demands of society for products and services, taking into account both current and future interests.

The paper presents an overview of an innovative integrated tool developed as a part of an on-going project for accurately capturing changes in hydro-biogeochemical processes in coastal zone systems in the context of climate change and anthropogenic forcing for identifying sound metrics for assessment of impacts of these changes and for examining long-term adaptation and mitigation measures for sustainable management. The tool comprises three major components: integrated hydro-biogeochemical model, Impact Assessment and MCDM tools. The tool has been applied in six case study areas in six countries of the Asia-Pacific region for climate change impact analysis.

1. INTRODUCTION

Many studies have predicted a strong impact of the global warming on mean sea level (MSL) and its adverse effects on coastal zones around the world (Jones, 2001; Jansson, et al., 2003; McInnes et al., 2003; Cacamise *et al.*, 2005; Carton *et al.*, 2005). The Third Assessment Report (TAR) of the Intergovernmental Panel on Climate Change (IPCC) predicted that the global MSL may rise as much as 88 cm by the end of the 21st century (IPCC,

2001) (Figure 1). According to the Fourth Assessment Report (AR4) of IPCC, Global MSL rise in the second half of the 20th century was estimated as $1.8 \pm 0.3 \text{ mm yr}^{-1}$, which is consistent with the TAR's estimate of $1.5 \pm 0.5 \text{ mm yr}^{-1}$ for the 20th century (IPCC, 2007). Moreover, because of the thermal inertia of the oceans, the global mean temperature will probably increase beyond 2100 and sea level will continue to rise at a similar rate in the future centuries, even if greenhouse gas concentration were stabilized by then (Nicholls, 2002; Burroughs, 2003; Antonov *et al.*, 2005). Approximately 20% of the global population lives within 30 km of coastal areas and the number is expected to become double by 2025 (Cohen *et al.*, 1997; Hinrichsen, 1998). The sea level rise will have wide ranging effects on coastal population and ecosystem, such as saline water intrusion, erosion of shorelines, amplified intensity and frequency of coastal flood inundation, etc. (Srivastava, 1998; Reeve, 1998; Sherif & Singh, 1999; van der Meji & Minnema, 1999; Kim *et al.*, 2005). It is estimated that a sea-level rise of one meter could displace some 70 million people in both Bangladesh and China (Burroughs, 2003).

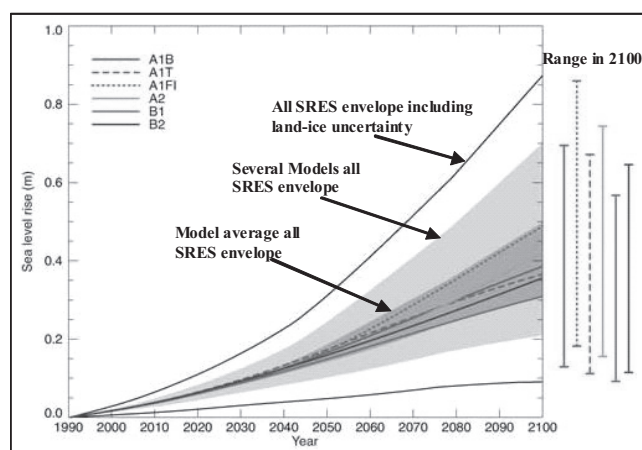


Figure 1: Global average sea level rise (1990-2100) (Church *et al.*, 2001)

In recent years, there has been an increasing concern, particularly with the growing population, rapid urbanization and industrial developments in coastal areas of Asia Pacific region that the current management practices adopted in most of these countries are unsustainable (Hong *et al.*, 2002). It has been realized that the rapid developments, extraction or manipulation of resources cannot exceed the sustainable limits without compromising the ecological integrity of the coastal ecosystems. This has now led to a growing concern that if the current trend of growth and exploitation continues, it would result in adverse effects on social, economic and environmental well-being in coastal zones. The extents of these consequences are further exacerbated by the adverse impacts being incurred from global climate change including extreme climatic events and sea level rises (IPCC CZMS, 1992; Titus, 1998; IPCC, 2001; Mitchell *et al.*, 2000; Dutta *et al.*, 2005).

For comprehensive understanding the changes in the physical processes due to combined effects of climate and human-induced changes, a spatially distributed process-based integrated approach, is essential, which

models the different inter-connected processes at appropriate spatio-temporal resolutions (Gordon *et al.*, 1996; Hong *et al.*, 2002; Nakayama *et al.*, 2004). An holistic approach (that combines physical modelling, vulnerability assessment with TBL and LCA principles and MCDM tools) to coastal zone management is needed to resolve the conflicting demands of society for products and services, taking into account both current and future interests (Post & Lundin, 1996; Neumann and Livesay, 2001; Walsh, 2004; APN, 2005; Dutta *et al.*, 2005). Agenda 21 and in particular its Chapter 17 'Protection of The Oceans' reaffirmed this need. Given these scenarios, the real challenge in achieving optimal sustainable management strategy in coastal zones relies on the ability to design, develop and implement an integrated management program that not only maximizes benefit to society and economy based on accurate understanding of the impacts of changes in physical processes, but that also ensures that the ecosystems are adequately protected or preserved.

In response to the need for sustainable management practices, several developed countries have developed and/or implemented sustainable coastal zone management strategies (Kay and Adler, 1999; Thom, 2002; Walsh, 2004). The developing countries in the Asia-Pacific region, lacking behind in this front, have revealed some knowledge and approach gaps, thus presenting the opportunity to break new ground on subsequent strategies. The strategies should be the vehicle in facilitating Integrated Coastal Zone Management (ICZM) principles, but how this can be done is still unclear and yet to be demonstrated (Clark, 1992; Post and Lundin, 1996; Walsh, 2004).

The paper presents the overview of an on-going research project designed to develop an innovative integrated tool for accurately capturing changes in hydro-biogeochemical processes in coastal zone systems in the context of climate change and anthropogenic forcing, for identifying sound metrics for assessment of impacts of these changes and for examining long-term adaptation and mitigation measures for sustainable management. The main objective of the project, sponsored by the Asia Pacific Network for Global Change Research, is to develop a more holistic approach and tool to apply Life Cycle Analysis (LCA) principles to the coastal zone systems in cross-cutting issues in the Asia Pacific region. In doing so, this project has intended to overcome the limitations of the existing fragmental approaches for evaluating more complex and interrelated biogeochemical and physical processes in coastal zones that include nutrient flux, salinity, floods, erosion and sedimentation and their impacts on society, economy and environment. To achieve these goals, the project has focused on selected coastal zones that have all of these attributes in six countries of the Asia Pacific region. A major expected outcome of the project is to develop multi-criteria decision-making and fuzzy preference models that will support broad stakeholders' engagement in regional coastal zone sustainable management strategy.

2. PROJECT FRAMEWORK

A comprehensive framework, as shown Figure 2, has been devised to implement the project including the development of the integrated tool and

its applications in the selected coastal areas. The project has taken a systematic approach for developing the integrated assessment tool and its implementation to achieve its objectives. The project has been carried out in five phases as follows:

- *Phase 1: Planning*
- *Phase 2: Data and Information Collation*
- *Phase 3: Development of Integrated Assessment Tool*
- *Phase 4: Scenario analysis*
- *Phase 5: Recommendations report, awareness campaign and capacity building*

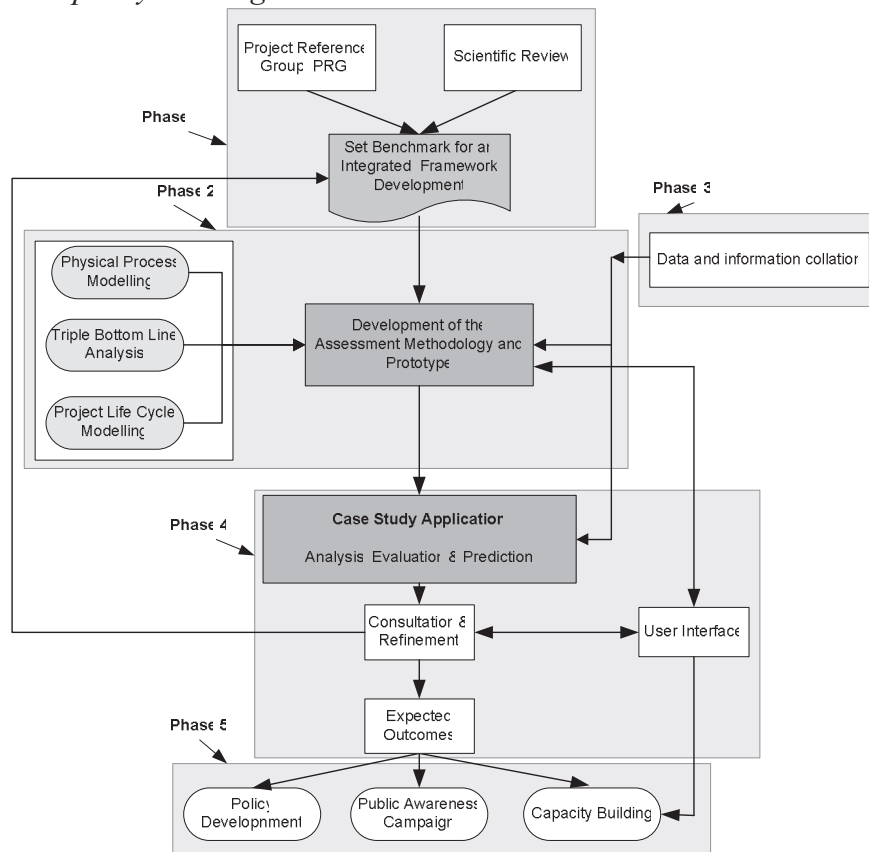


Figure 2: Project Framework

Six countries of the Asia-Pacific regions have been involved in this project, namely: Australia, Bangladesh, Japan, Sri Lanka, Thailand and Vietnam, with at least one collaborating researcher from each country as a core member in the project team. After conducting a series of consultations with the stakeholders of each of the member countries through the Project Reference Groups, which was established at the very beginning of the project, the following coastal areas have been identified as the case study areas for application of the integrated tool.

1. Gippsland Lakes Area (Australia)
2. Gorai River Basin (Bangladesh)
3. Kushiro Wetland Area (Japan)
4. Colombo (Sri Lanka)
5. Bangkok and Chao Phraya Delta (Thailand)

6. Nam Dinh Coast (Vietnam)

The holistic tool includes three major components: i) *Process model (PM)*, ii) *Impact Assessment Tool (IAT)*, and iii) a *Multi-Criteria Decision Making and Support System (MCDMSS)*. The Process model is used to simulate hydro-biogeochemical processes in coastal zone systems in the context of climate change and anthropogenic forcing. The impact analysis model, which included a series of response functions, is used for assessment of impacts of these changes to economy, society and environment. The concept of the integrated tool is shown in Figure 3.

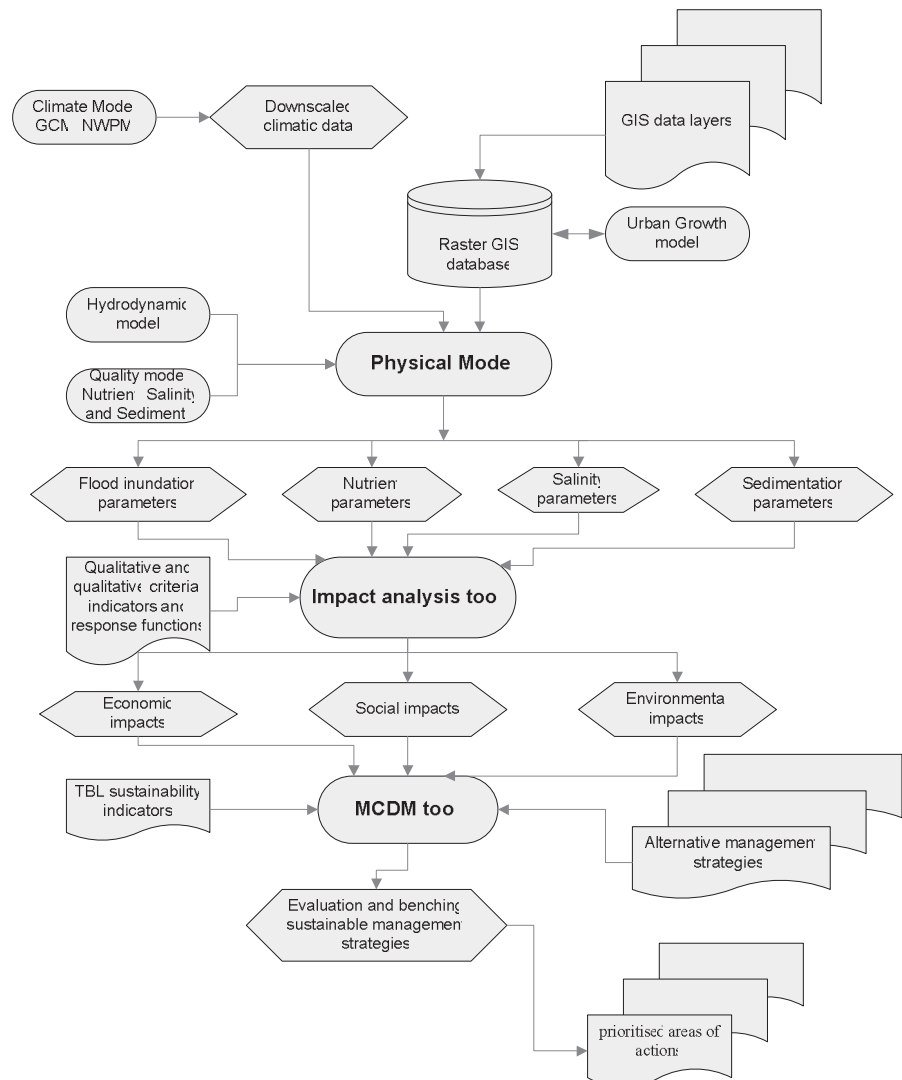


Figure 3: Project Methodology

i) Process model (PM):

An integrated process model has been built on existing and new scientific knowledge of different physical processes in coastal zone systems including hydrological and biogeochemical processes and their exchange through water and soil and pathways in the river catchment and coastal sea interactions for scientific understanding of changes in these processes due to combined effects of global climate change and anthropogenic developments

(Gordon *et al.*, 1996, Hong *et al.*, 2002; Nakayama *et al.*, 2004; Garnier *et al.*, 2005; Bhattarai and Dutta, 2005; Nakayama, K., 2005; Dutta *et al.*, 2007). An example of the flood inundation modelling by the integrated model under sea level rise conditions (rise of sea level) in Chao Phraya delta including Bangkok is shown in Figure 4.

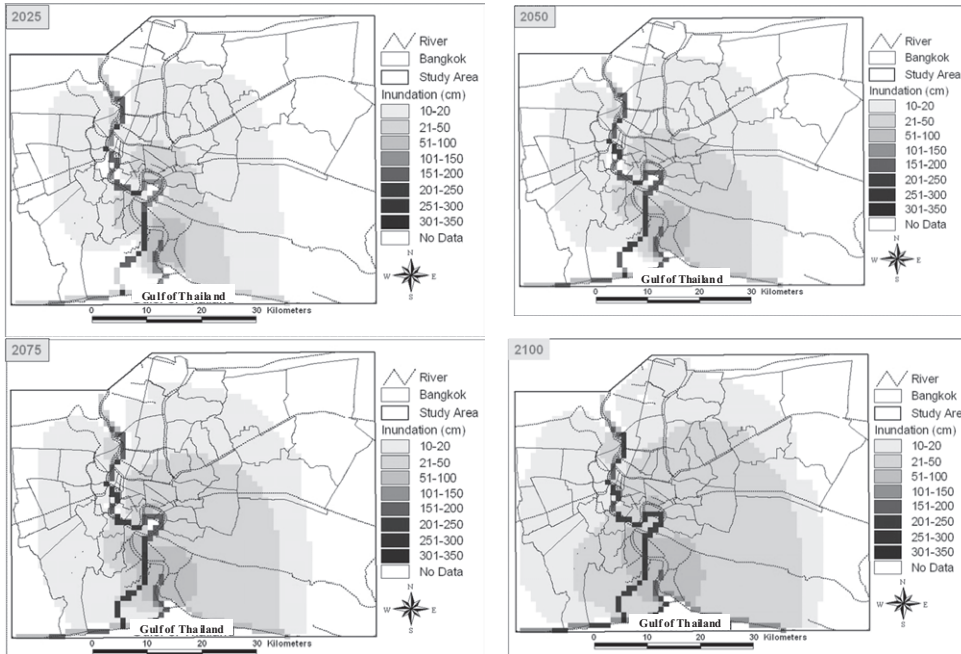


Figure 4: Simulated flood inundation maps due to sea level rise by 14 cm (2025), 32 cm (2050), 58cm (2075), and 88 cm (2100)

ii) Impact Assessment Tool (IAT):

A brainstorming workshop was held last year among the project members of the six countries to identify the most important water quantity and quality parameters associated with coastal zone flooding and can be simulated by the process-based model and the social, economic and environmental (TBL) sectors/issues that could be impacted by these parameters for developing a set of criteria, indicators and appropriate response functions relating to the changes in the simulated parameters due to climatic and anthropogenic changes in the selected coastal areas (Belfiore, 2003). Table 1 shows the modelling parameters and Table 2 shows the sectors identified for impact analysis.

A set of questions has been designed to obtain feedback from experts and stakeholders to develop a series of response functions to assess the impacts of changes in hydro-biogeochemical processes in coastal zone systems in the context of climate change and anthropogenic forcing on various social, economic and environmental issues (TBL issues) in coastal areas. The main purposes of the questionnaire survey were:

- To assist with development of response functions
- Essentially, a survey of stakeholders to find
 - which issues (assets) they are most concerned about
 - Whether intensity of flood parameters affects which issues they are most concerned about

Table 1: Water quantity and quality parameters to be modelled by process-based model under climatic change conditions

| Water Quantity (Flood) | Water Quality |
|--------------------------------------|--|
| Depth, Duration, Velocity, Frequency | Nutrients (TN, NO2, NO3, TP, PO4), Salinity, Turbidity |

Table 2: Sectors/issues in Coastal areas identified for climate change impact analysis

| | |
|---------------------------|--|
| Infrastructure | Drainage |
| | Roads |
| | Railways |
| | Ports & Harbours |
| | Dykes |
| | Coast protection structure |
| | Landuse planning |
| Buildings | Residential |
| | Non-residential |
| Potable water | |
| Water quality | |
| Erosion | |
| Tourism | |
| Population | Short-term displacement |
| | Long-term resettlement |
| Agriculture | |
| Fishery | |
| Fish habitat/distribution | |
| Wetland health | Extent |
| | Flora biodiversity (no. of veg. species) |
| | Fauna biodiversity (no. of bird species) |
| Mangroves | |

iii) Multi-Criteria Decision Making and Support System (MCDMSS):

A set of criteria and indicators have been developed representing social, economic and environmental sustainability of coastal zone systems. Fuzzy Preference modelling with multi-objective optimisation approach is used to model the stakeholders’ preferences and expectations in the decision appraisal process (Doloi and Jaafari, 2002; Manivong *et al.*, 2004). Using these criteria and indicators, a multi-criteria decision making system has been established for strategic planning, policy development and enhancement and pathways for sustainable management of coastal zones.

3. CONCLUDING REMARKS

The paper has introduced an innovative and integrated tool with LCA and TBL principles to the coastal zone systems in cross-cutting issues for sustainable management under climatic and anthropogenic changes. The tool has been developed by integrating existing and new scientific knowledge on hydro-biogeochemical process modelling, triple bottom line (TBL) analysis, multi-criteria decision making and fuzzy preference modeling. The tool is currently being applied in six case study areas from six different countries in the Asia-Pacific region. It is expected that the tool will help decision makers to apply Life Cycle Analysis and TBL principles to develop pathways and potential coping mechanisms for sustainable management of coastal zone systems in the Asia Pacific region.

ACKNOWLEDGEMENT

The authors gratefully acknowledge the financial support provided by the Asia Pacific Network for Global Change Research (APN) for this project.

REFERENCE

- Antonov J.I., S. Levitus, and T. P. Boyer (2005). Thermohaline sea level rise, 1955–2003, *Geophysical Research Letters*, Vol. 32, L12602, 2005.
- APN (2005). APN Strategic Plan (2005-2010), Asia-Pacific Network for Global Change Research, Kobe, Japan, 20pages.
- Belfiore, S. (2003). The growth of integrated coastal management and the role of indicators in integrated coastal management: introduction to the special issue. *Ocean and Coastal Management* 46, 225-234.
- Bhattacharai, R. and D. Dutta (2005). Analysis of Soil Erosion and Sediment Yield using Empirical and Process Based Models, *Proceedings of the MTERM International Conference, AIT*, 215-226.
- Burroughs, W. (2003)(ed). *Climate into the 21st Century*, World Meteorological Organization, Cambridge University Press, 240p.
- Caccamise, D.J., M.A. Merrifield, M. Bevis, J. Foster, Y.L. Firing, M. S. Schenewerk, F. W. Taylor, and D. A. Thomas (2005). Sea level rise at Honolulu and Hilo, Hawaii: GPS estimates of differential land motion, *Geophysical Research Letters*, Vol. 32, L03607, 2005.
- Carton, J.A., B. S. Giese and S. A. Grodsky (2005). Sea level rise and the warming of the oceans in the Simple Ocean Data Assimilation (SODA) ocean reanalysis, *Journal of Geophysical Research*, Vol. 110, C09006, 2005.
- Clark, J.R. (1992). *Integrated Management of Coastal Zones*. FAO, Rome, FAO Fisheries Technical Paper No. 327.
- Doloi, H. and Jaafari, A. (2002) "Towards a Dynamic Simulation Model for Strategic Decision Making in Life Cycle Project Management" *Project Management Journal*, Vol. 33 (4), December 2002, 23-38.
- Dutta, D., M.S. Babel and A. Das Gupta (2005). *An Assessment of the Socio-Economic Impacts of Floods in Large Coastal Areas*, Final

- Report for APN CAPaBLE Project: 2004-CB01NSY-Dutta, Asian Institute of Technology, ISBN 974-93908-0-6, 205 pages.
- Dutta, D., J. Alam, K. Umeda, M. Hayashi and S. Hironaka (2007). A two dimensional hydrodynamic model for flood inundation simulation: a case study in the Lower Mekong River basin, *Hydrological Processes*, 21:1223-1237.
- Garnier, J., J. Nemery, G. Billen and S. Thery (2005). Nutrient dynamics and control of eutrophication in the Marne River system, *Journal of Hydrology* 304, 397-412.
- Gordon, D.C. Jr., P.R. Boudreau, K.H. Mann, J.-E. Ong, W.L. Silvert, S.V. Smith, G. Wattayakorn, F. Wulff, and T. Yanagi. (1996). LOICZ Biogeochemical Modelling Guidelines, LOICZ Reports & Studies No. 5. Second Edition, vi +96 pp. LOICZ, Texel, The Netherlands.
- Hong, G.H., H.H. Kremer, J. Pacyna, Chen-Tung Arthur Chen, H. Behrendt, W. Salomons and J.I. Marshall Crossland (2002). LOICZ Global Assessment and Synthesis of River Catchment-Coastal Sea Interaction and Human Dimensions. East Asia Basins, LOICZ Reports & Studies No. 26, ii + 262 pages, LOICZ IPO, Texel, The Netherlands
- IPCC (2007). Climate Change 2007, 4th Assessment Report (AR4) of the Intergovernmental Panel on Climate Change (AR4), United Nations.
- IPCC (2001). Climate Change 2001: The Scientific Basis. Houghton, J.T., Ding, Y., Griggs, D.J., Noguer, M., Van der Linden, P.J., and Xiaoasu, D. (eds.), Cambridge and New York: Cambridge University Press, 881 pages.
- IPCC CZMS (1992). A common methodology for assessing vulnerability to sea level rise, 2nd revision. In: *Global Climate Change and the Rising Challenge of the Sea*. Report of the Coastal Zone Management Subgroup, Response Strategies Working Group of the Intergovernmental Panel on Climate Change, Ministry of Transport, Public Works and Water Management, The Hague, Appendix C.
- Jones, R.N. (2001). An Environmental Risk Assessment/Management Framework for Climate Change Impact Assessments, *Natural Hazards*, 23: 197-230.
- Kay, R., and J. Adler (1999). *Coastal Planning and Management*. Routledge, 375 pages.
- Kim, J-H, L. Dupont, H. Behling and G. J. M. Versteegh (2005). Impacts of rapid sea-level rise on mangrove deposit erosion: application of taraxerol and Rhizophora records, *Journal of Quaternary Science*, 20(3): 221–225.
- Manivong, K. Jaafari, A., Gunaratnam, D., and Doloi, H. (2004). Architecture of an Intelligent Project Management Information System for Optimistic Capital Projects, *Proceedings of the World IT Conference for Design and Construction, INCITE 2004*, Langkawi, Malaysia, 18-21 Feb., pp 515-522.
- McInnes, K.L., K.J.E. Walsh, G.D. Hubbert and T. Beer (2003). Impact of Sea-level Rise and Storm Surges on a Coastal Community, *Natural Hazards*, 30: 187–207.
- Mitchell, W., Chittleborough, J., Ronai, B., and Lennon, G.W. (2000). Sea level rise in Australia and the Pacific, In: *The South Pacific Sea Level and Climate Change Newsletter*, 5(1), January 2000.

- Nakayama, K., D. Dutta, G. Tanaka and T. Okada (2004). Integration of Hydrological Model and Estuary Model, *Journal of Japan Society of Hydrology and Water Resources*, 18(4), 390-400.
- Nakayama, K. (2005). Modeling the effect of stratification on sediment deposition, *River, Estuary and Coastal Morphodynamics*, Vol. 4, pp.1027-1034, 2005.
- Nicholls, R.J. (2002). Analysis of global impacts of sea-level rise: a case study of flooding, *Physics and Chemistry of Earth*, 27: 1455-1466.
- Neumann, J.E. and N.D. Livesay (2001). Coastal structures, dynamic economic modeling. In: Mendelsohn, R. (ed.), *Global warming and the American economy , a regional assessment of climate change impacts*. Cheltenham, U.K.: Edward Elgar, 132-148.
- Post, J. C and C. G Lundin (1996), *Guidelines to Integrated Coastal Zone Management*, World Bank, Washington DC.
- Sherif, M.M. and V. P. Singh (1999). Effect of climate change on sea water intrusion in coastal aquifers, *Hydrological Process*, 13:1277-1287.
- Srivastava, G.S. (1998). Impact of Sea Level Rise on Seawater Intrusion into Coastal Aquifer, *Journal of Hydrologic Engineering*, January 1998, 74-78.
- Titus, J.G., 1998. Rising seas, coastal erosion, and the takings clause: how to save wetlands and beaches without hurting property owners. *Maryland Law Review* 57, 1279-1399.
- Thom, B.G. (2002) CZM in NSW: The Good, the Bad and the Ugly. In: *Coast to Coast 2002*, proceedings, 468-470.
- van der Meij, J.L., B. Minnema (1999). Modelling of the effect of a sea-level rise and land subsidence on the evolution of the groundwater density in the subsoil of the northern part of the Netherlands, *Journal of Hydrology*, 226:152–166.
- Walsh, K. (2004). *Climate Change and Coastal Response*, A theme report from the Coast to Coast 2002 National Conference, Gold Coast, November 2002, Melbourne University, Australia, 34p.

RESEARCHES AND APPLICATIONS OF LAND USE PLANNING BASED ON RISK ANALYSIS

CAO ZHENG, LIU MAO and LI QINGSHUI, MU QING
Research Center of Urban Public Safety, Nankai University, China
nkcz5208@mail.nankai.edu.cn

ABSTRACT

The establishments that produce, store and use kinds of inflammable, explosive or toxic materials may induce accidents, such as fire, explosion or poisonous gas dispersion etc. Once these accidents occur, the impacts often go beyond establishments' borders, causing a number of casualties and severe property losses. If accident occurred in urban area or the area where population is large, the consequences will be more serious.

Therefore, based on risk analysis in the vicinity of these establishments, there is a need to (i) locate these establishments appropriately and (ii) conduct land use planning. For example which district can be residential area and which district of population density should be restricted etc, thus these measures can balance the utility of land use and risk. On one hand, there is the attempt to exploit the land in the best possible way, on the other to avoid major urban public safety risk.

Consulting advanced experience that obtained from land use planning in European countries, this paper studies on:

- (i) hazardous establishment location based on risk index;*
- (ii) land use planning based on consequence-probability; and*
- (iii) land use planning based on individual risk.*

Above three approaches' frameworks and procedures were determined and applied to a proposed LNG station.

Firstly, the authors confirm risk index (RI) for site selection, and find that the risk is too high if it does not change the current situation of surrounding land use. Therefore, corresponding adjustments must be made to alter the status.

Secondly, adjusting schemes for land use are made by applying individual risk-based and accident consequences-based methods. Based on the consequences-based method, we use death probability that corresponding to 1% and irreversible health effects probability that corresponding to 50%, and risk zones are divided according to thresholds

of these two probabilities. On the basis of individual risk-based method and according to different individual risk, that is 10^{-5} , 10^{-6} and 3×10^{-7} , we divide risk zones. The two methods show the same outcomes: two settlements and one plant around the LNG reserve need relocate.

The three methods are feasible when we consider major projects' location and their surrounding buildings or establishments' layout.

1. INTRODUCTION

The establishments that produce, store and use kinds of inflammable, explosive and poisonous chemicals may cause severe fire, explosion and toxic gas diffusion, as a result of contrived, installation, management and environment factors by intriguing leakage. Once such accidents happen, it always beyond the establishments' border and lead to casualty and property loss. We can take Mexico oil company's liquefied petroleum storages (or transportation stations) explosion incident as an example. Fireball's diameter was up to 360 meters, 4 round and 44 horizontal storage tanks were all destroyed, the equipment in the tank/transfer station were almost completely destroyed either. It affected the buildings about 1200 meters around the plant, causing the historic tragedy of 650 residents' death, 60,001 be injured and nearly 31,000 people become homeless. To prevent the occurrence of such major casualties, we need conduct reasonable dangerous facilities' locations and surrounding land use planning (LUP), including i) reasonable location of dangerous establishments, and ii) which part of district can be the residential area, which part can be the commercial area and where the population density should be restricted etc. Thus we can balance the relationship between land effectiveness and risk. In that mean, land can be applied in the maximal degree and will not lead to a major urban public safety risk.

At present, according to the SEVESO-II Directive's requirement, several countries in Europe introduce risk analysis into LUP. U.K, Netherlands, France and Germany have set up mature process of LUP. South Europe such as Italy, Greece, Spain and Portugal follow their steps, while other countries such as Denmark will set up process and standard of LUP.

Based on their advanced experience, there are three methods: i) location estimate method based on risk index (RI), ii) LUP method based on consequence's happening probability, and iii) LUP method based on individual risk can be used for LUP which involves dangerous establishments.

2. LOCATION ESTIMATE METHOD BASED ON RISK INDEX (RI)

Location estimate method based on risk index (RI) simply quantifies location's risk, which was proposed by Health& Safety Executive. This method defines a new risk index (RI). If we can get F/N curve, the RI can be calculated exactly; if not, it also can be calculated approximately. According to risk acceptable standards of HSE's ALARP guidelines, if the RI is lower than the standards, then the risk is reasonable and the location of dangerous facilities too. On the contrary, the dangerous facilities need appropriate adjustments or re-location. General steps are shown in Figure 1.

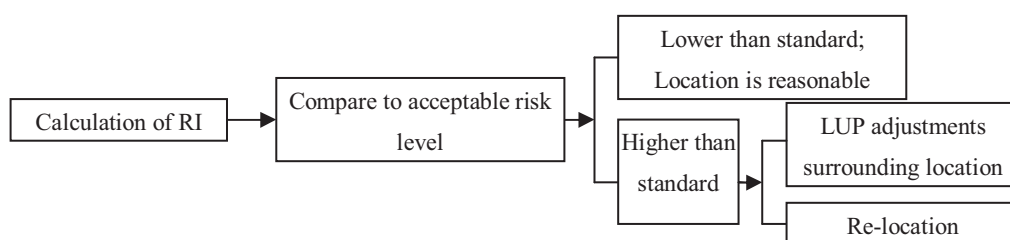


Figure 1: General steps of location estimate method based on risk RI

2.1 Calculation of RI

When dangerous facilities' F/N curve is known, HSE's definition of risk integral parameters is:

$$RI = \sum_{N=1}^{N_{max}} f(N)N^a \quad (1)$$

Here N is the number of casualties; f(N) is the frequency of casualties (chances per million per year, cpm /a); a demonstrates the degree of aversion to risk, which is a constant between 1 and 3. The degree of aversion to risk increases with the value of a.

However, when F/N curve is difficult to get as a result of unknown operation of equipment and security measures, we need estimate RI. We assume that dangerous facilities happen the most serious incidents. That is to say, these accidents cause the largest number of victims. Based on the assumption, we calculate RI approximately and denoted as ARI (Approximate RI).

Considering two kinds of cases while calculating ARI:

1) The most serious accident influence several directions, such as fireballs, the explosion of a steam cloud, the ARI can be expressed as:

$$ARI = f(N_{max})N_{max} \left[\sum_{N=1}^{N_{max}-1} \frac{N^{a-1}}{N+1} + N_{max}^{a-1} \right] \quad (2)$$

Here, N_{max} is the maximum number of people affected by the most serious accident; $f(N_{max})$ (cpm·a⁻¹) is the frequency of the accident that

corresponding to N_{max} .

2) The most serious accident influence single direction, which is a particular direction, such as poisonous gas dispersion.

$$ARI = f(N_{max})N_{max}^2 \sum_{N=1}^{N_{max}} N^{a-2} \quad (3)$$

Here, N_{max} and $f(N_{max})$ are same as above.

The calculation steps of ARI are as follows:

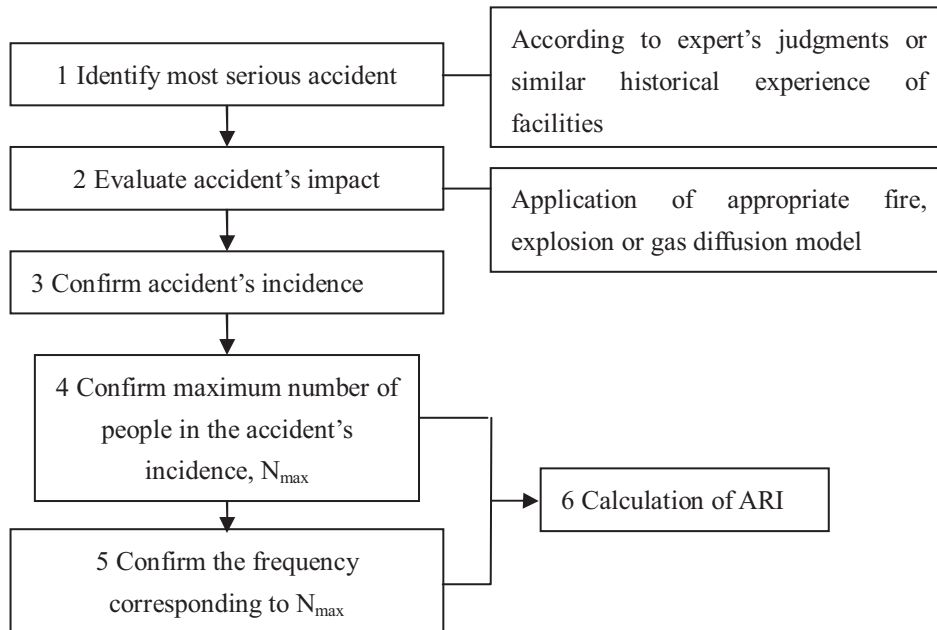


Figure 2: Calculation steps of ARI

Following two points need be paid attention to when calculating ARI:

1) Determine accident's incidence, the heat flux or overpressure threshold at the affected areas border, or toxic concentration corresponding to LD₅₀ doses, which can cause the death of the 50 percent personnel.

2)When the most serious accident influence single direction, the frequency of accident is the product of failure frequency of facilities, probability of conditional clouds, combination probability of weather and wind speed, deviation parameters of wind rose map and population distribution parameters.

Here:

i) $POCC = \frac{2 \arctg\left(\frac{MVOCS}{DTMVOCS}\right)}{360^\circ}$, POCC (Probability of Conditional

Clouds), MVOCS (Maximum value of Cloud's Semi-wide), DTMVOCS (Distance to MOCS).

ii) Combination probability of weather and wind speed is combination of atmosphere stability and wind speed that can induce probability of most serious accident.

iii) Wind rose map is a tool for fire supervision department carry out construction and examination work in accordance with national fire protection technical specifications. It always be provided by local meteorological department. If the wind rose map is consistent, then value of deviation parameters is 1; if not, the wind cause the probability of wind flows in the direction of most serious accident may large or small, then its value is larger or less than 1 correspondingly. For example, its value is 0.8, saying that the probability of wind flows in the direction of most serious accident is 80% of the situation of no deviation.

iv) Population distribution parameters reflect whether a small deviation in the direction of most serious accident causes significant change on the number of affected people. If there will be no significant change, then its value is equal to 1; if the number of people has significant changes in a local area that far from affected region, then its value should be equal to 0.2. In most cases, the value of the distribution population parameters should be through visual observation, and their value is equal to 0.5 under normal circumstances.

2.2 Acceptable risk level

British Health and Safety Executive Board applies ALARP guidelines and establishes ARI acceptable standard. As China has not yet establishes our own. So we use it as a reference, as shown below.

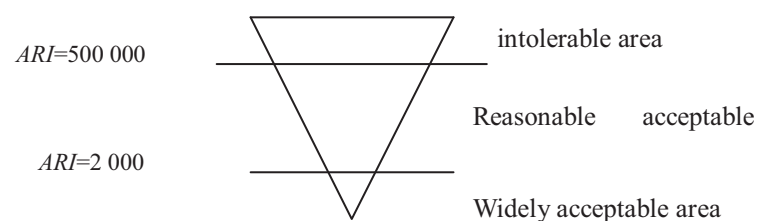


Figure 3: Acceptable risk level confirmed by ARI

As shown in Figure 3, ARI = 2,000 and 500,000 are dividing line of widely acceptable and reasonable area, acceptable and intolerable area. If ARI less than 2,000, risk is acceptable, then the location is reasonable; if ARI larger than 500,000, no matter what measures to be taken, risk are unacceptable, and the dangerous facilities should be re-located or proper adjustments need be made on the surrounding land use. If ARI is between 2,000 and 500,000, the risk is acceptable and location of this facility is reasonable, but some adjustments need to be made on the surrounding land use.

3. LUP BASED ON RISK-CONSEQUENCES' PROBABILITY

The method based on risk-consequences' probability bases on abundant accident scenes. Evaluating the most serious accident scene, we divide risk region according to the distance corresponding to 1% mortality rate and the distance corresponding to irreversible health effects with a probability of 50%. Finally, land use planning and layout adjustments are made in accordance with different risk regions' functions.

3.1 The general process of risk-consequences-based land use planning

LUP based on risk-consequences' probability is composed of four modules:

Module 1: Identify the referenced accident scene;

Module 2: The calculation of R_1 and R_2 , where R_1 is the distance corresponding to 1% mortality rate under the condition of the occurrence of accident; R_2 is the distance corresponding to irreversible health effects (for example, severe burned, moderate injured etc.) with a probability of 50%.

Module 3: The division of risk region. We compare R_1 and R_2 under accident scene, and identify R_{1max} and R_{2max} . Based on R_{1max} and R_{2max} , we divide the risk region; and

Module 4: Land use planning and layout adjustments.

The general process of this method can be seen in Figure 4.

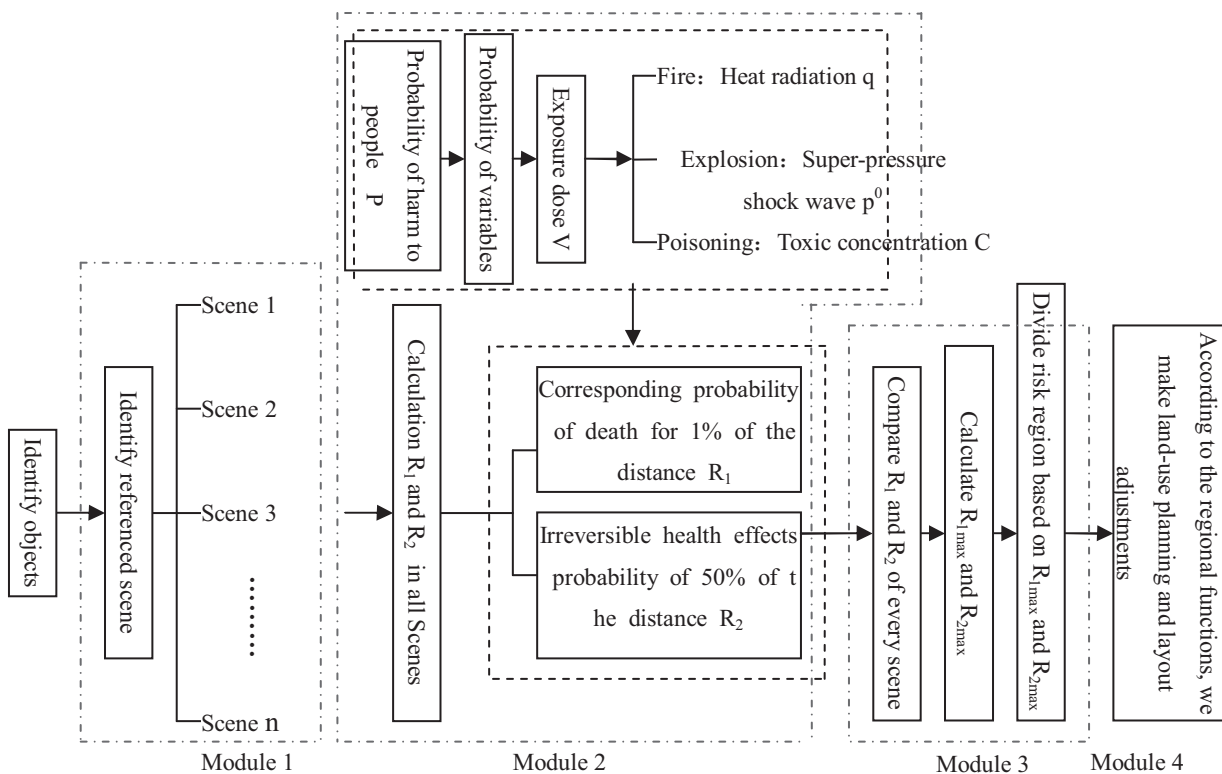


Figure 4: General process of land use planning based on risk consequences' probability

3.2 Identify the referenced accident scene

The identification of referenced accident scene is mainly based on past accidents and possible incidents' analysis. Under general circumstances, for the various risk facilities, we consider the following six major accident scenes:

Table 1: Summarization of referenced accident scene

| Referenced accident scene | Facilities' type |
|--|--|
| Boiling liquid expanding vapor explosion (BLEVE) | Liquefied combustible gas facilities are involved |
| Unconfined vapor cloud explosion(UVCE) | Liquefied combustible gas facilities are involved |
| Instant big rupture of container | Liquefied/ unliquefied poisonous gas containers |
| Instant rupture of pipeline of big diameter | Poisonous facilities(Wall is used to resist external and internal material damage to the reaction) |
| Large storage tanks catch fire; fixed roof storage tank of gas explosions; fireball and jet caused by the combustion due to splash | Inflammable liquid's big storage tanks |
| A huge amount of explosives explosion or explosion caused by reaction | Facilities for storing or using explosives |

3.3 The calculation of R₁ and R₂

After the accident scenes being identified, we should calculate R₁ and R₂ for risk region division.

Here we adopt 1% probability of death which corresponds to distance R₁ and its purpose is to prevent major accidents and limit the consequences of accident; Irreversible health effects' probability is 50% which corresponds to distance R₂, and it is used to separate dangerous sources and regions that sensitive, fragile groups appear (such as schools and hospitals) or dense population region.

The steps for calculation of R₁ and R₂ are shown in Figure 5.

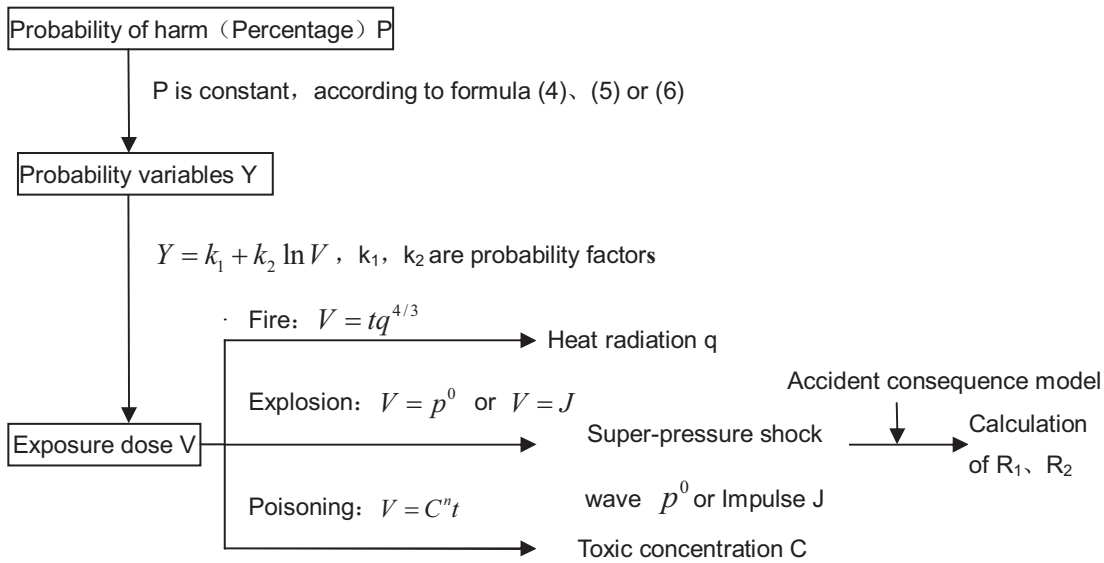


Figure 5: Steps for calculation of R1 and R2

In figure 5, t is exposure time(s); q is heat radiation intensity (W/m^2); p^0 is maximum super-pressure shock wave (N/m^2); J is impulse ($N\cdot s/m^2$); C is toxic concentration (ppm); n is constant, which depends on different substance.

The relationship between probability (or percentage) P and probability of variables Y is expressed in formula (1):

$$P = \frac{1}{\sqrt{2\pi}} \int_{-\infty}^{Y-5} \exp\left(-\frac{u^2}{2}\right) du \quad (4)$$

We use formula (2) to transform probability (or percentage) P and probability of variables Y in practice.

$$P = 50 \left[1 + \frac{Y-5}{|Y-5|} \operatorname{erf}\left(\frac{|Y-5|}{\sqrt{2}}\right) \right] \quad (5)$$

Here **erf** is the error function, which is the Gaussian distribution integral, and subjects to the following relations:

$$\operatorname{erf}(x) = \int_0^x e^{-t^2} dt \quad (6)$$

When calculate R_1 and R_2 , as long as probable accident scenes may happen, we should calculate 6 scenes that mentioned above.

3.4 Confirm R_{1max} and R_{2max}

After calculating R_1 and R_2 in probable happening accident scenes, we compare every R_1 and R_2 , and then we get R_{1max} and R_{2max} . It is shown in

Figure 6.

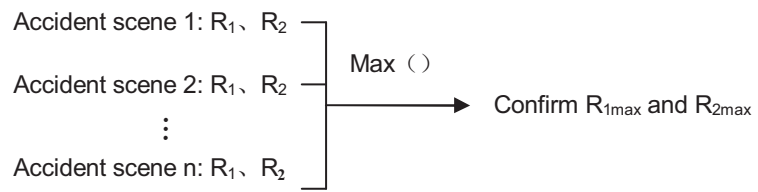


Figure 6: Confirm $R1_{max}$ and $R2_{max}$

3.5 Division of risk region

We consider fire and explosion’s impact area is circle, and it does not affected by weather condition. On the contrary, toxic substance’s spill or diffuse is well depended on weather condition. Owing to the uncertainty of wind direction, we consider its impact area is circle, either. Thereafter, we assume accident site as the center of the circle, R_{1max} and R_{2max} as radius, and we define 3 risk regions: Z_1 , Z_2 and Z_3 . This is shown in Figure 7.

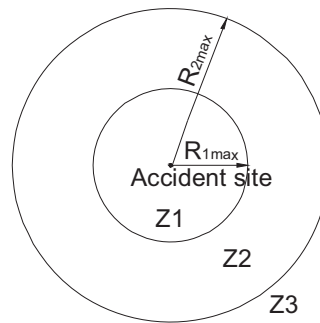


Figure 7: Division of risk regions

3.6 Land use in every risk region

In this step we consider land use planning in three risk region. From HSE’s experience, we get Table 2.

Table 2: Land use planning in every risk region

| Risk Region | Land use type |
|-------------|---|
| Z_1 | Not allowed to build homes, public buildings and industrial plants |
| Z_2 | Allow smaller population density, other public buildings except high-rise building construction and outside buildings with more staff; when it meets certain basic conditions, construction of industrial facilities are allowed. These basic conditions are: ① A small amount of emergency personnel; ② Industrial activities are compatible; ③ Workers can carry out emergency training |
| Z_3 | There is no restrictions |

4. LUP BASED ON INDIVIDUAL RISK

The objective of this method is to prevent serious casualties and reduce accident's impact by using LUP. According to quantitative analysis of individual risk, we divide risk regions, which base on distances corresponding to individual risk of 10^{-5} , 10^{-6} and 3×10^{-7} . Then layout and adjustments of land use are made in accordance with functions of every risk region.

4.1 General steps of LUP based on individual risk

LUP based on individual risk is composed of 3 modules, as shown in Figure 8.

- Module 1: Quantitative analysis of individual risk;
- Module 2: Division of risk regions;
- Module 3: Layout and adjustments of LUP.

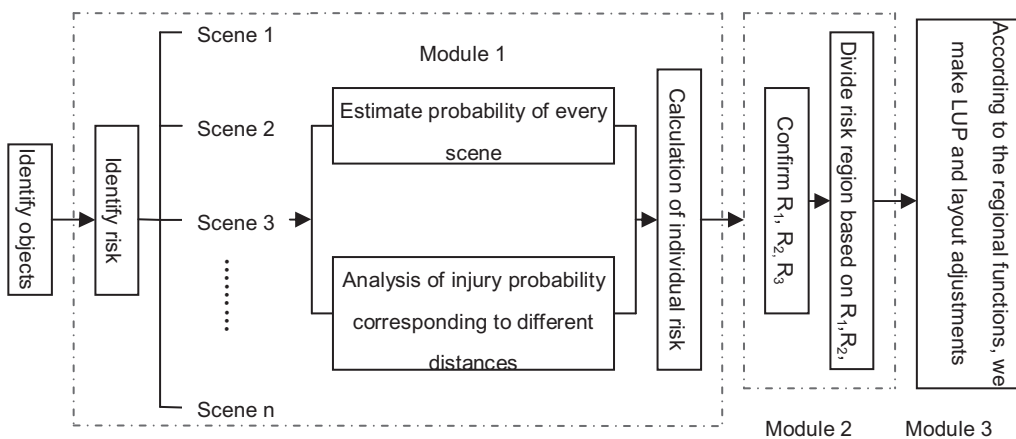


Figure 8: General steps of LUP based on individual risk

4.2 Quantitative analysis of individual risk

Individual risk (IR) refers to possibility of one non-protective person permanently stays in a particular place owing to injury being caused by accident. Individual risk is relative to the distance from the risk source. The nearer one is from the risk source, the greater of its individual risk, and vice versa. Individual risk is usually used in the form of risk contour on the map intuitively, Figure 9 is a typical dangerous facilities' individual risk contour map.

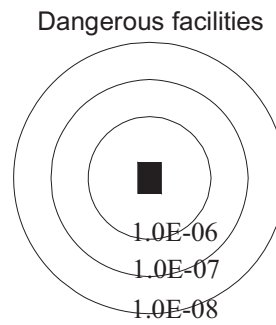


Figure 9: Individual risk contours of dangerous facilities

Quantitative analysis of individual risk in LUP includes 4 phases^[3]:

- 1) Identification of risk;
- 2) Analysis of accident's probability;
- 3) Analysis of injury probability corresponding to different distances
- 4) Calculation of individual risk.

The calculation of individual risk usually uses the formula below^[3]:

$$IR = P_f \cdot P_{d/f} \tag{7}$$

Here, P_f is probability of accident; $P_{d/f}$ is injury probability of being caused by accident.

4.3 Division of risk regions

Division of risk regions depends on individual risk. We use risk contour to divide Z_1 , Z_2 , and Z_3 around dangerous facilities. There are two kinds of division of risk regions: 1) dangerous facilities can be seen as the type of point or polygon; and 2) dangerous facilities are the type of lines, as shown in Figure 10 and 11.

The value of individual risk decreases as three regions. The risk contours from dangerous facilities' critical distances are confirmed by the calculation of quantitative analysis of individual risk.

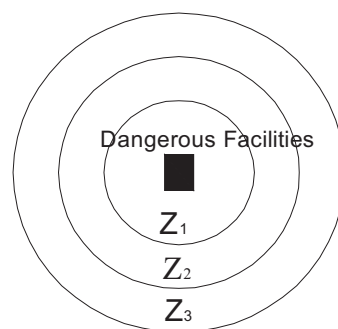


Figure 10: The type of point or polygon

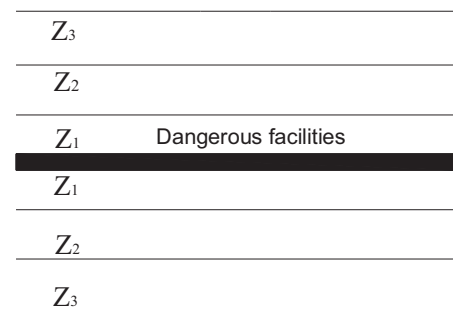


Figure 11: The type of lines

As a result China has yet not establishes LUP from the view of risk and the standard of risk regions division are inconsistent, this paper according to HSE’s LUP experience. Table 3 shows individual risk standard of different risk regions in LUP.

Table 3: Individual risk standards of risk regions based on HSE

| | Region Z ₁ | Region Z ₂ | Region Z ₃ |
|--------------------------------|-----------------------|-----------------------|-----------------------|
| <i>IR of different regions</i> | $> 10^{-5}$ | $> 10^{-6}$ | $> 3 \times 10^{-7}$ |

4.4 LUP in every risk region

After dividing risk regions and according to three regions’ functions, layouts of LUP are made. Table 4 are HSE’s LUP types of every risk region.

Table 4: LUP types of every risk region

| LUP types | Region Z ₁ ($IR > 10^{-5}$) | Region Z ₂ ($IR > 10^{-6}$) | Region Z ₃ ($IR > 3 \times 10^{-7}$) |
|--|---|---|--|
| Sensitive or big public (school, hospital, coliseum) | Not allowed | No more than 25 | Need detailed estimate |
| Habitation area (houses, hotels, resort villages) | No more than | No more than 75 | Allowed |
| Public gathering places (large-scale retail stores, community and leisure venues) | No more than 100 | No more than 300 | Allowed |
| Low population density of small factories, open playground | Allowed | Allowed | Allowed |

5. LUP OF PROPOSED LNG STORAGE RESERVE

We plan a proposed LNG storage, which locates in the site A with a capacity of 100,000 cubic meters that is composed of two 50,000 cubic meters of LNG storage tanks. According to the providing documents, the storage site A is from the settlements B 230 meters in the east, from the industrial plant 180 meters in the south-east, from the settlements C 600 meters in the south with mountain barrier in the middle, from the golf course 700 meters in the west with mountain barrier in the middle, from settlements D 400 meters in the north-west. There are 300 people in area B, 100 workers in C, and 400 habitants in D. It is shown in Figure 12.

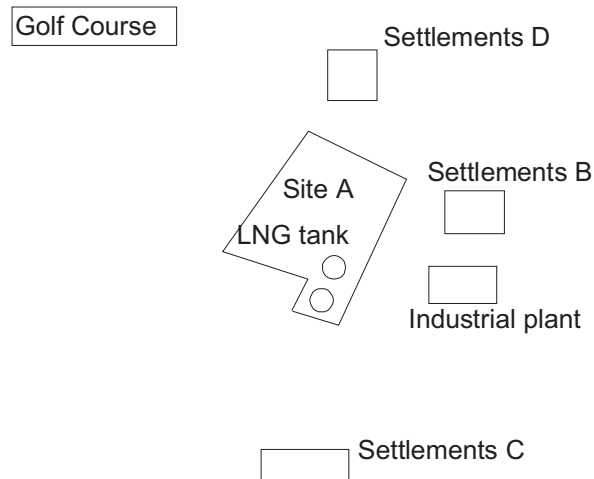


Figure 12: The location of LNG reserve and its surrounding layout

5.1 Analysis of possible accident scenes

The possible accident scenes of LNG storage reserve are analyzed by event tree, as shown below:

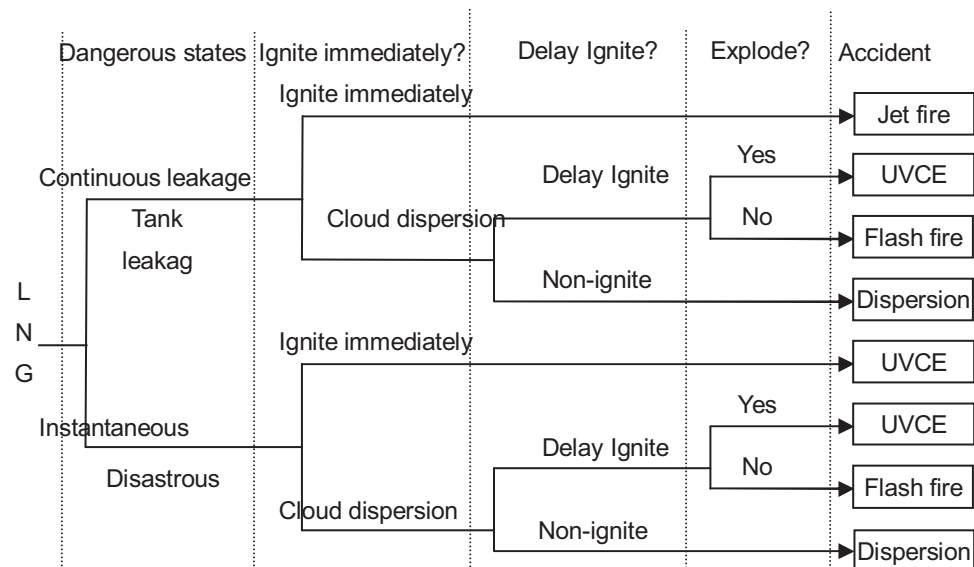


Figure 13: Possible accident scenes of LNG tank's leakage
(Notes: UVCE refers to Unconfined Vapor Cloud Explosion)

As can be seen from the analysis of Figure 13, LNG storage reserve's fire or explosive accidents include jet fire, flash fire, cloud explosion and BLEVE. Because of enormous storage capacity of LNG reserves, if the tank ruptures and leads to LNG storage's instantaneous leakage, then the fire, explosion will be much more serious and much greater than continuous leakage. In addition, flash fire is a non-explosive combustion process, and often concealed by the vapor cloud explosion. So we select the case of LNG

storage tank's overall rupture, which leads to BLEVE and vapor cloud explosion and causes the most serious consequence.

5.2 RI Calculation of LNG storage reserve

The extreme case is LNG tank's overall rupture and all leaked LNG causes the formation of BLEVE fireball. As for BLEVE, the main harm is heat radiation. For a normal adult, heat radiation's impact is:

$$Y = -36.38 + 2.56 \ln(tq^{4/3}) \tag{8}$$

Here, Y is probability variable; q is heat radiation flux taken over by one's body (W/m^2); t is exposure time in the heat radiation (s). In this case, fireball's duration time is 14.72s. Here, we define Y as 5 and its corresponding death probability is 50%, exposure time in heat radiation equals to fireball's duration time (t). Heat flux threshold corresponding to death probability of 50% is $23786W/m^2$ (q). The corresponding distance is 344.5m that is calculated by the BLEVE's solid flame model.

Main harm of vapor cloud explosion is the over-pressure while exploding. The over-pressure often causes bleeding of lung and even death. It is calculated by the formula below.

$$Y = -77.91 + 6.91 \ln P^0 \tag{9}$$

Here, Y is probability variable; P^0 is over-pressure (Pa). We define Y as 5 and its over-pressure threshold is $P^0=161251Pa$ that corresponds to 50% death probability. The corresponding distance based on vapor cloud explosion is 45m that is calculated by the TNT equal model.

As can be seen from the distances of two accidents, BLEVE is much more serious than vapor cloud explosion. Therefore, the most serious accident's incidence is the circle with the radius of 344.5 meters, as shown in Figure 14.

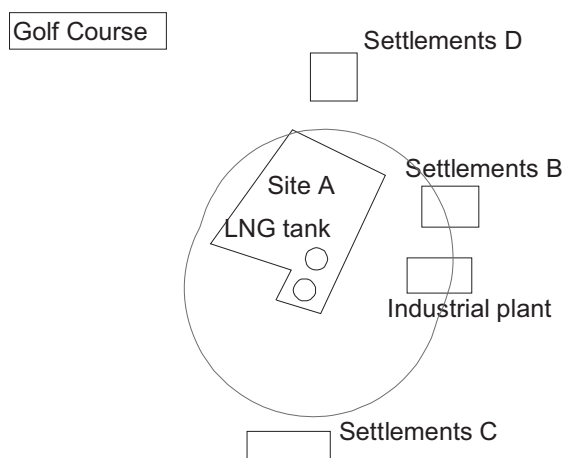


Figure 14: Incidence of BLEVE

The settlements B and industrial plant are both influenced by the BLEVE, and the number of affected people is 400. That is to say N_{max} equals to 400. The frequency of BLEVE caused by LNG storage reserve is 10 cpm/a, and thus $f(N_{max})$ equals to 10 cpm/a.

As BLEVE influences several directions, then ARI is 139869 according to formula (1). Comparing to risk acceptable standard shown in Figure 3 of section 2.2, RI is acceptable. Thereafter, LNG reserve can be located in site A. But some proper adjustments should be made on its surrounding land use, and to reduce risk as much as possible.

5.3 Calculation based on R_1 and R_2 in planning

Based on the consequences calculated by BLEVE and vapor cloud explosion, BLEVE is much more serious. Considering extreme cases, we assume a storage tank's overall rupture and it results in all LNG leakage and causes BLEVE.

5.3.1 Calculation of R_1 and R_2 under the scene of BLEVE

We suppose spilled LNG all involved in the formation of BLEVE fireball. LNG density $\rho = 0.7 \text{ kg / m}^3$. Irreversible health effects were set as first-degree burn.

(1) Calculation of R_1 , see Table 5.

Table 5: Steps for calculating R_1

| | |
|---|-------------------------------|
| Probability of death (percentage) P (%) | 1 |
| Probability variables Y | 2.67 |
| Relationship between Y and V | $Y = -36.38 + 2.56 \ln V$ |
| Relationship between V and q | $V = tq^{4/3}$ [7] |
| Corresponding heat radiation intensity q (kW/m^2) | 12.27 |
| Accident consequences model | Three dimensional flame model |
| Corresponding distance R_1 | 493.3 m |

(2) Calculation of R_2 , see Table 6.

Table 6: Steps for calculating R_2

| | |
|---|-----------------------------|
| first-degree burn probability (percentage) P (%) | 50 |
| Probability variables Y | 5 |
| Relationship between Y and V | $Y = -39.83 + 3.0186 \ln V$ |
| Relationship between V and q | $V = tq^{4/3}$ |
| Corresponding heat radiation | 9.067 |

| intensity q (kW/m^2) | |
|-----------------------------------|-------------------------------|
| Accident consequences model | Three dimensional flame model |
| Corresponding distance R_2 | 578 m |

5.3.2 Division of risk region Z_1 , Z_2 and Z_3

We supposed storage site as the center of circle, $R_{1\max}=493.3\text{m}$ and $R_{2\max}=578\text{m}$ as radius respectively, then we confirmed 3 risk region: Z_1 , Z_2 and Z_3 , see Figure 15.

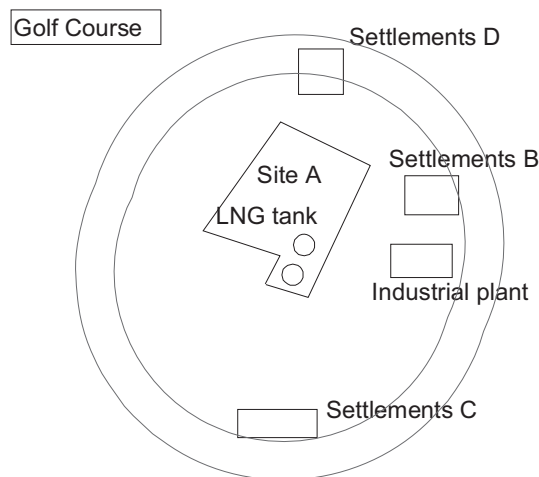


Figure 15: Risk region Z_1 , Z_2 and Z_3

5.3.3 Land use planning and layout adjustments in every risk region

According to Table 3 in section 2.5, suggestions on the planning and adjustments in risk region Z_1 , Z_2 and Z_3 are as follows:

(1) In the region Z_1 ($R < 493.3\text{m}$), it is not allowed to build homes, public buildings and industrial plants, thus from LNG reserves 230 m of the settlements A in the east, 400 m of the settlements D in the north-west and 180 m of industrial plant in south-east must be relocated.

(2) In the region Z_2 ($493.3 \text{ m} < R < 578\text{m}$), it allowing a smaller population density, other buildings except high-rise building construction public buildings with a large number of people presentation (such as stadiums, shopping), but it does not allow as schools, hospitals, Jingleo Yuan, which are sensitive, vulnerable places; when it meets the following conditions ① a small amount of emergency personnel; ② industrial activities are compatible; ③ workers to carry out emergency training, it allows building corresponding industrial facilities.

(3) In the region Z_3 ($R > 578\text{m}$), there is no restrictions. The storage tanks do not affect settlements C and golf course. Also there are mountain barrier between settlements C or golf course and storage tank. So they do not need relocate.

5.4 The method based on individual risk (IR)

5.4.1 Quantitative analysis of IR

(1) Relationship between death probability and distance

In the case of one tank's overall rupture, all leaked LNG causes BLEVE or vapor cloud explosion.

i) The scene of BLEVE

The relationship between death probability and the distance to LNG storage tank is shown in Figure 16, which is calculated by solid flame model.

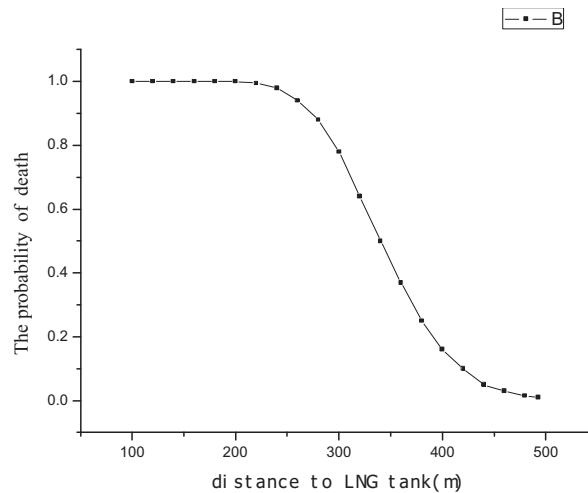


Figure 16: The relationship between death probability and the distance to LNG storage tank

ii) The scene of vapor cloud explosion

The relationship between death probability and the distance to LNG storage tank is shown in Figure 17, which is calculated by TNT equal model.

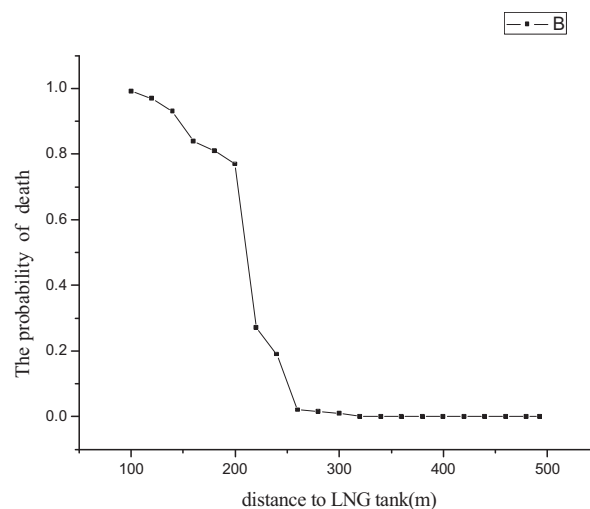


Figure 17: The relationship between death probability and the distance to LNG storage tank

(2) Calculation of IR

Here, the frequency of BLEVE and vapor cloud explosion is 10^{-5} per year. According to formula (3), IRs corresponding to different distances is shown below.

120 meters: $IR = \sum_1^2 P_{fi} P_{d/fi} = 10^{-5} \times 1 + 10^{-5} \times 0.97 = 1.97 \times 10^{-5}$

240 meters: $IR = \sum_1^2 P_{fi} P_{d/fi} = 10^{-5} \times 0.98 + 10^{-5} \times 0.19 = 1.17 \times 10^{-5}$

280 meters: $IR = \sum_1^2 P_{fi} P_{d/fi} = 10^{-5} \times 0.88 + 10^{-5} \times 0.015 = 8.95 \times 10^{-6}$

Alikely, IR corresponding to other distances are shown in Figure 18.

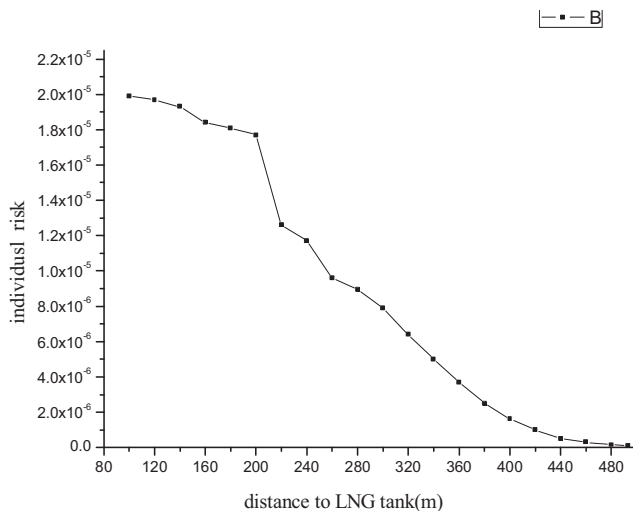


Figure 18: Relationship between IR and distance

5.4.2 Division of risk regions

As can be seen from Figure 18, the critical distances from LNG storage tank are 250m, 420m and 460m that correspond to IR of 10^{-5} , 10^{-6} and 3×10^{-7} respectively. Then we use LNG tank as the center of the circle, and 250m, 420m and 460m as radius respectively. Therefore, three different risk regions are defined, see Figure 19.

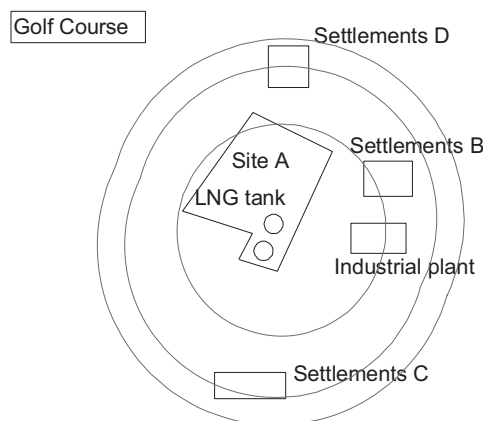


Figure 19: Division of risk regions

5.4.3 Layout and adjustments of LUP in every risk region

According to the regulation of Table 4, layout and adjustments in regions Z_1 , Z_2 and Z_3 are as follows.

(1) In the region Z_1 ($R < 250\text{m}$, $IR > 10^{-5}$), as the number of residents is 300, which is much larger than allowed number (25), so settlements B in the east of LNG storage reserve need move away. So does industrial plant.

(2) In the region Z_2 ($250\text{ m} < R < 420\text{m}$, $10^{-5} > IR > 10^{-6}$), as the number of residents is 80, which is much larger than allowed number (75), so settlements B in the north-west of LNG storage reserve needs move away.

(3) In the region Z_3 ($420\text{m} < R < 460\text{m}$, $10^{-6} > IR > 3 \times 10^{-7}$), there is not any objects need relocate. Some layouts can be made based on Table 4, such as residential area or small industrial plant can be located here.

6 CONCLUSIONS

(1) As can be seen from the planning of LNG storage reserve, three methods above introduce risk analysis into land use planning. They are feasible for major projects' locations and their surrounding layout.

(2) Basis of the three methods is different. Location estimate method based on risk index goes on the most serious accident that causes the maximum number of affected people. RI is confirmed based on it. By the means of comparing with risk acceptable level, we estimate the reasonability of location and make some reasonable adjustments. Risk-consequences-based method adopts two distance thresholds, which corresponding to 1% of death probability and 50% of irreversible health effects respectively. Based on these, we divide three risk regions. While the method based on IR of 10^{-5} , 10^{-6} and 3×10^{-7} and their corresponding distance thresholds. Some layout and adjustments are made according to risk regions that are divided by these thresholds, and their functions.

(3) The three methods above not only apply to LNG storage reserve's planning, but also any major projects' locations and their surrounding land use that involve public safety and sensitive attentions.

REFERENCES

- Lin Yong-zhang, Ge Wei-zhong, Xu Qi-ming. Recalling series of major disasters (6) — Study on explosion of liquefied petroleum gas tank in Mexico Pemex . Chemical industry. 2001, 48(2): 107-123.
- Michalis D. Christou, Aniello Amendola, Maria Smeder. The control of major accident hazards: The land-use planning issue. Journal of Hazardous Materials (65) 1999. 151-178
- HIRSTI L, CARTER D A. A "worst case" methodology for obtaining a rough but rapid indication of the societal risk from a major accident

- hazard installation[J]. *Journal of Hazardous Materials*, 2002, A92: 223–235.
- Guidance on ‘as low as reasonably practicable’ (ALARP) decisions in control of major accident hazards (COMAH). <http://www.hse.gov.uk/comah/circular/perm12.htm>.
- Secretary of State to the French Prime Minister for the Environment and the Prevention of major technological and nature risks, Control of Urban Development around High-Risk Industrial Sites, October 1990.
- Risk analysis Theory and approach for accident. Lecture of Center for Urban Public Safety Research in Nankai University
- Papazoglou. I.A., Nivolianitou. Z.S, Bonanos. G.S. Land use planning policies stemming from the implementation of the SEVESO-II Directive in the EU. *Journal of Hazardous Materials* 61(199).345–348.
- JONKMAN S N, VAN G P, VRIJLING J K. An overview of quantitative risk measures for loss of life and economic damage[J]. *Journal of Hazardous Materials*, 2003, A99: 1–15
- Health and Safety Executive., Risk criteria for land use planning in the vicinity of major industrial hazards, Health and Safety Executive, UK, 1989.
- VAN DEN BOSCH C J H. Methods for the determination of possible damage to people and objects resulting from releases of hazardous materials[M]. The Hague :The Netherlands Organisation of Applied Scientific Research (TNO).1992: 60–87.
- Center for Chemical Process Safety Guidelines for evaluating the characteristics of vapor cloud explosion, flash fires, and BLEVEs. New York: The American Institute of Chemical Engineers, 1994: 157–242.

NUMERICAL SIMULATION OF RELATIONSHIP BETWEEN CLIMATIC FACTORS AND GROUND OZONE CONCENTRATION IN SUMMER OVER THE KANTO AREA USING THE MM5/CMAQ MODEL

R.OOKA¹, M.V.KHIEM² and H.HUANG³

Institute of Industrial Science, University of Tokyo,
4-6-1 Komaba Meguro-ku, Tokyo Japan.

¹ ooka@iis.u-tokyo.ac.jp

² khiem@iis.u-tokyo.ac.jp

³ hhong@iis.u-tokyo.ac.jp

H. ayami,

Central Research Institute of Electric Power Industry,
1646 Abiko, Abiko-shi, Chiba-ken 270-1194, Japan.

haya@criepi.denken.or.jp

ABSTRACT

In recent years, the urban atmospheric pollution is still an important environmental problem due to the rapid urbanization and industrial development. It is found that atmospheric pollutant concentration can be strongly affected by some local climatic factors (e.g., temperature, humidity, wind, radiation, etc.). In this study, we use the MM5/CMAQ model to examine relationship between these climatic factors and ground ozone (O_3) concentration over Kanto (Japan) area. The nested grid system which cover a region of Kanto with grid resolutions of 9 km, 3 km, and 1 km respectively have been employed to this study. The relationship between the simulated O_3 concentration with temperature, solar radiation, relative humidity, and urban heat island were analyzed over the August 2005, representing typical summer climate. The numerical simulation shows O_3 concentration as function of temperature, solar radiation, and relative humidity. The positive correlation was found between O_3 concentration with temperature and solar radiation, while the negative correlation was found between O_3 concentration and relative humidity. The result of this study suggests that O_3 concentration has a close relationship with climatic factors over Kanto area.

1. INTRODUCTION

Kanto area is the largest inland and the most highly developed, urbanized, and industrialized part of Japan. This area encompasses seven prefectures which overlap the Greater Tokyo Area: Gunma, Tochigi, Ibaraki, Saitama, Tokyo, Chiba, and Kanagawa, as shown in Figure 1. Its area extends about

100 km in the E-W direction and 200 km in the N-S direction. With the increasing trend of city-growth and urbanization, Kanto area also has to face air pollution problem. According to the Tokyo Metropolitan Government Environmental White Paper 2006, the concentration of most of air pollutants are decreasing in Tokyo Metropolitan area due to the application of smoke control regulations to factories and industrial complex, and introduction of regulations to control diesel emissions from automobiles. However, the concentration of photochemical oxidant (O_3) has not achieved the Environmental Quality Standards (one-hour value of 0.06 ppm or less) and the number of the days which high concentration of O_3 is recorded has been increasing. It is well known that O_3 is formed as a result of complex non-linear interaction of chemistry and climatic factors. Therefore, besides chemical mechanics, to understand how high O_3 produce in Kanto area, the influence of climate condition needs to be investigated. Many studies on the relationship between climate condition and air pollution over Kanto area have been reported; for example Wakamatsu et al. (1983, 1990), Uno et al. (1984), Kurita et al. (1985, 1986), Fujibe et al. (1985), Yoshikado et al. (1994, 1996)... These studies showed that air pollution is strongly affected by climate condition.

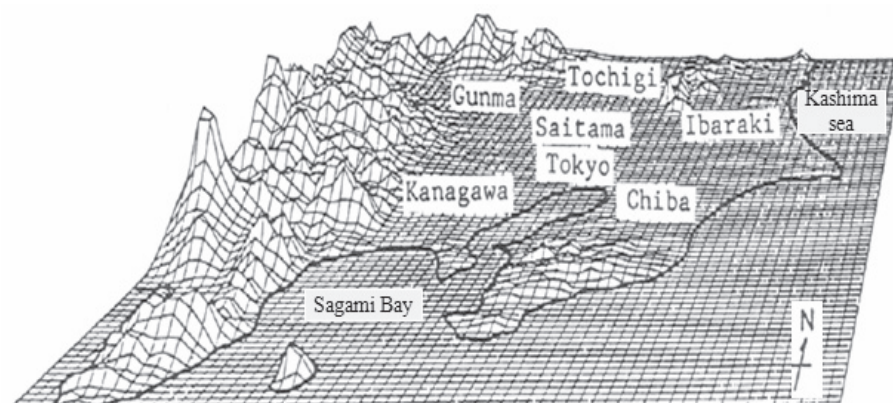


Figure 1: Topography of the Kanto area viewed from the south-east direction

In summer, the air pollution is mainly influenced by local wind circulation, especially land-sea breeze. Using aircraft measured data Wakamatsu et al. (1983) found that O_3 concentration strongly depend on the land-sea breeze. In the morning, the O_3 concentration is near the shore of Tokyo Bay where there exist the Keihin and Keiyo Industrial Complex. This O_3 concentration mass was then moved to inland by the penetration of sea breezes. In some cases, in the early morning Kanto area was dominated by the land breeze with northerly and northeasterly directions. In this situation, the last nighttime radiation inversion which persists into the early morning prevents the dispersion of primary pollutants emitted from the big coastal industrial zones around Tokyo Bay. Uno et al. (1984) showed that these pollutants are then transported by land breeze to the Sagami Bay area where acts as storage tank. Conversion of such pollutants results in a high O_3 air mass inland with the penetration of sea breeze in daytime. Generally, the transportation of air pollution mass from these sources to inland strongly

depends on the complicated interaction among sea breezes (southeasterly direction from Tokyo Bay, southerly direction from Sagami Bay, and easterly direction from Kashima Bay) as well as the mountain/valley circulations and thermal condition. Tsuruma (1983) summarized three main trajectories of high air pollution mass are frequently transported from the source area, these are; course A to north; course B to the northwest; and course C to the west. Kurita et al. (1985, 1986), and Fujibe et al. (1985) demonstrated that the transport of air pollution mass with course B due to sea land breezes, mountain/valley circulations, the generation of a strong thermal low in the inland mountain region, a steady onshore wind driven by the diurnal-mean land-sea temperature difference, and subsidence inversion under a synoptic high pressure system. This transport mechanism usually occurs on clear days associated with weak wind, it results in night smog in the mountain area far from pollution source.

In contrast, in winter the distribution of high pollutants concentration over Kanto Plain usually accompanied with two main weather patterns: (1) occurring a local stationary front across Tokyo Bay due to merging between northwesterly air flow and southwesterly air flow; (2) the calm and stable condition associated with 'cold air lake' in central Kanto. This pattern is result of merging northwesterly or northerly cold air mass in lower atmosphere and southwesterly warmer air mass in upper air (Yoshikado et al. 1994). The interaction between urban heat island (UHI) and sea breeze also affect air pollution over Kanto area. Yoshikado et al. (1996) showed that in early winter the temperature contrast between land and sea is quite small to induce sea breeze, at the same time an urban heat island circulation (HIC) is generated by the thermal contrast associated with the heat island. This circulation tends to reinforce the sea breeze in the shore area and prevents the penetration of sea breeze inland. In this case the air pollution often concentrates over the urban area for a long time. Therefore air pollution will become very high in urban area.

Besides above observational study and analysis, the numerical simulations have been studied and reported. Numerical applications are able to solve some problem such as lack of measured data over complex area as well as upper air layer. Although these numerical models used some simple assumptions, it showed good results. For example, the role of local wind circulation for the transportation of air pollution over Kanto Plain is studied numerically in Kimura et al. (1983, 1985, and 1989) and Chang et al. (1989). From previous studies, it can be concluded that:

- There is a close relationship between air pollution and local climatic conditions and the land/sea breeze play an important role in the transport of high air pollution concentrations over Kanto area.
- Urban Heat Island and its interaction with sea breeze has great effects on air pollution concentrations
- The air pollution mass was mainly transported toward west, northwest, and north during summer days with high air pollution.
- A few detailed numerical study mentioned on a combination of climatic factors, i.e., temperature, humidity, solar radiation, synoptic meteorology pattern, especially the effect of urban heat island and its interaction with land/sea breeze circulation during high O₃ concentration episode in summer.

In this paper, the authors investigate the relationship between climatic factors and ground ozone concentration over Kanto area using the coupled MM5/CMAQ model. The main purpose is to find the role of climatic factors such as temperature, humidity, solar radiation, local circulations as well as synoptic weather patterns during high O₃ concentration episode in summer. This study may help to better understand the climatic factors which control O₃ concentration over Kanto area.

2. MODEL DESCRIPTION

2.1 Meteorology model

The Fifth-Generation NCAR / Penn State Mesoscale Model (MM5) version 3.7, a limited-area, non-hydrostatic, terrain-following sigma-coordinate model (Dudhia, et al, 2005), is used in this research to provide spatial and temporal distribution of meteorological fields to the air quality model. It has some characteristics such as: (i) a multiple-nest capability, (ii) non-hydrostatic dynamics, which allows the model to be used at a few-kilometer scale, (iii) multitasking capability on shared- and distributed-memory machines, (iv) a four-dimensional data-assimilation capability (FDDA), and (v) more physics options.

2.2 Air Quality modeling

The Community Multi-scale Air Quality (CMAQ) modeling system version 4.6 developed by Environmental Protection Agency (USA), which was released in 2006, was used in this study. It is a multiple scale and multiple pollutant chemistry-transport model that includes all the critical science processes such as atmospheric transport, deposition, cloud mixing, emissions, gas- and aqueous-phase chemical transformation processes, and aerosol dynamics and chemistry. The CMAQ system can simulate concentrations of troposphere ozone, acid deposition, visibility, fine particulate and other air pollutants in the context of “one atmospheric” perspective involving complex atmospheric pollutant interactions on regional and urban scales.

3. ANALYSIS OUTLINE

3.1 Analysis domain

In this study, the MM5 simulation was performed with three nested domains (Figure 2). Detailed configuration of the domains is summarized in Table 1. The nested grid system with 3 domains which with grid resolutions of 9 km, 3 km, and 1 km, respectively is employed. The second domain size is 73x88 grid points and the third domain is 100x121 grid point. All of the domains have 23 vertical sigma levels from the surface to the 100-hPa level.

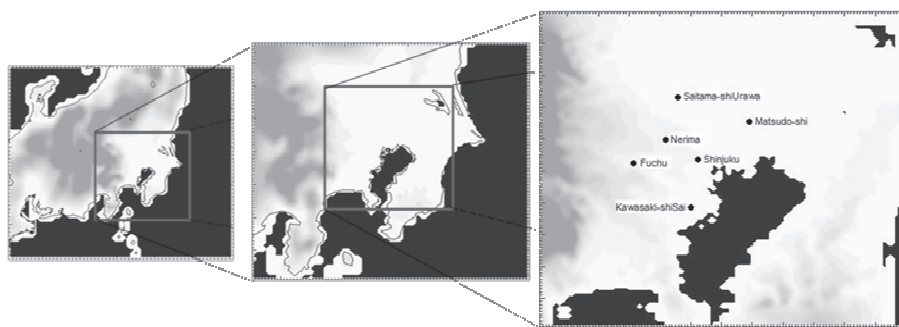


Figure 2: Analysis domain and monitoring stations for CMAQ validation

Table 1: Analysis size domains and grid resolution

| | Computation domain (X[km] x Y[km]) | Grid number | Horizontal resolution (km) |
|----|---------------------------------------|-------------|----------------------------------|
| D1 | 450x540 | 51x61x23 | 9 |
| D2 | 216x261 | 73x88x23 | 3 |
| D3 | 99x120 | 100x121x23 | 1 |

3.2 Model configuration

For this study, the physical options in the MM5 simulation are as follows: Grell cumulus parameterization scheme(Grell et al., 1994); MRF planetary boundary layer scheme(Hong et al., 1996); explicit simple ice microphysics(Hsie et al., 1984); cloud-radiation scheme(Dudhia, 1989) and FDDA. The cumulus parameterization scheme is not used for the 3 and 1-km domains. The CMAQ was configured with the following options: (1) CB-IV speciation with aerosol and aqueous chemistry; (2) the Piecewise Parabolic Method for both horizontal and vertical advection; (3) eddy vertical diffusion; (4) photolysis; (5) no Plume-in-Grid; (6) the EBI chemistry solver configured for CB05; (7) use of the 3rd-generation aerosol model; (8) use of the 2nd-generation aerosol deposition model; (9) use of RADM cloud model; (10) 14 vertical layers. More detailed description of the scientific mechanisms and implementations of CMAQ can be found in Byun and Ching (1999).

3.3 Study period and simulation condition

The August 2005 was selected for MM5/CMAQ simulation. Meteorological conditions with weak surface wind and high temperature in this month are favorable for high photochemical production of ozone. All days observed O₃ concentration exceeds the Japan environmental quality standard (60 ppb), especially during from 4th to 8th and 14th, 15th, O₃ becomes very high, there are some monitoring stations which observed O₃ concentration exceeds 120 ppb as seen in Figure 3. Global meteorological data (FNL) from NCAR with horizontal resolution of 1°x1° was used to provide initial and boundary conditions for MM5 model and FDDA process. Hourly emission data used here are the horizontal 3km x 3km emission estimated by Hayami et al., (2004) (Figure 4). After MM5 simulation, CMAQ model was performed in domain 2 with the initial and boundary condition were derived from climatologic profile of atmospheric pollutants

as described in Byun and Ching (1999) and the observation report of Japan Clean Air Program (Table 2). Finally, output of CMAQ model in domain 2 used to produce initial and boundary condition for CMAQ model in domain 3. Result of CMAQ and MM5 simulation in domain 3 are used to analysis relationship between climatic factors and O₃ concentration.

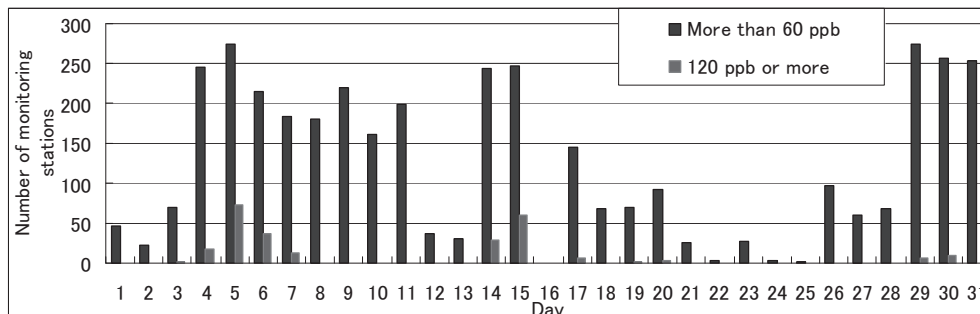


Figure 3: Changes in the number of monitoring station by O₃ level in August over Kanto area

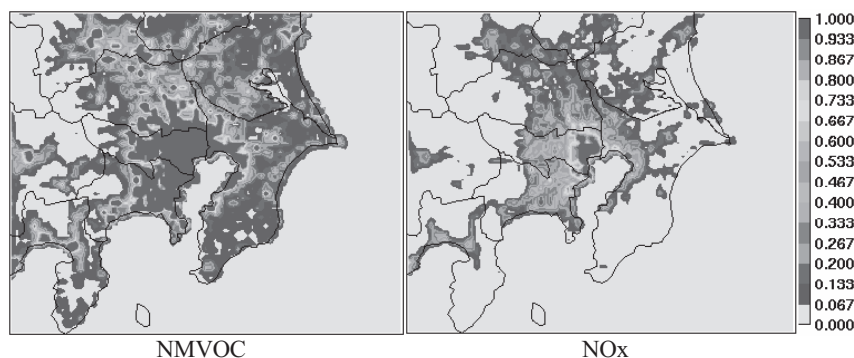


Figure 4: Hour emission data for CMAQ at 14 JST August 6 (mole/s/grid)

Table 2: Initial and boundary condition (ppb) for CMAQ model (JCAP, 1999)

| Species | O ₃ | NO | NO ₂ | ALD | FORM | ETH | OLE | TOL | XYL | ISO | PAR | |
|---------|----------------|---------|-----------------|-----|------|-----|-----|------|------|-----|------|------|
| ICs | 28 | 2.0 | 4.0 | 1.8 | 2.2 | 1.4 | 1.6 | 14.4 | 0.6 | 0.5 | 74.3 | |
| BCS | N | 28 | 2.0 | 4.0 | 1.8 | 2.2 | 1.4 | 1.6 | 14.4 | 0.6 | 0.5 | 74.3 |
| | E | 25 | 2.0 | 4.0 | 1.8 | 2.2 | 1.4 | 1.6 | 14.4 | 0.6 | 0.5 | 74.3 |
| | W | 30 | 2.0 | 4.0 | 0.9 | 1.1 | 1.3 | 0.4 | 6.0 | 0.7 | 0.5 | 37.8 |
| | S | Default | | | | | | | | | | |

4. RESULT AND DISCUSSION

4.1. Comparison of simulation and observation

In this study, the results from the CMAQ model in domain 3 were compared to measured data from air quality monitoring stations located within Kanto area; Shinjuku, Nerima, Fuchu, Saitama-shiUrawa, Matsudo-shi, and Kawasaki-shiSai, which are shown in Figure 2. The ozone time series comparison between the CMAQ simulation and observation at the 6 monitoring stations are shown in Figure 5. Generally speaking, the

model simulation shows different results depend on the location of monitoring station. It can be said that there is a good agreement between simulated O₃ concentration tendency and observation. However, for the days with low ozone concentration, the simulated O₃ concentration tends to overestimate, this may relate to calculating of the vertical diffusion coefficient in the MM5 model, initial and boundary conditions of CMAQ model.

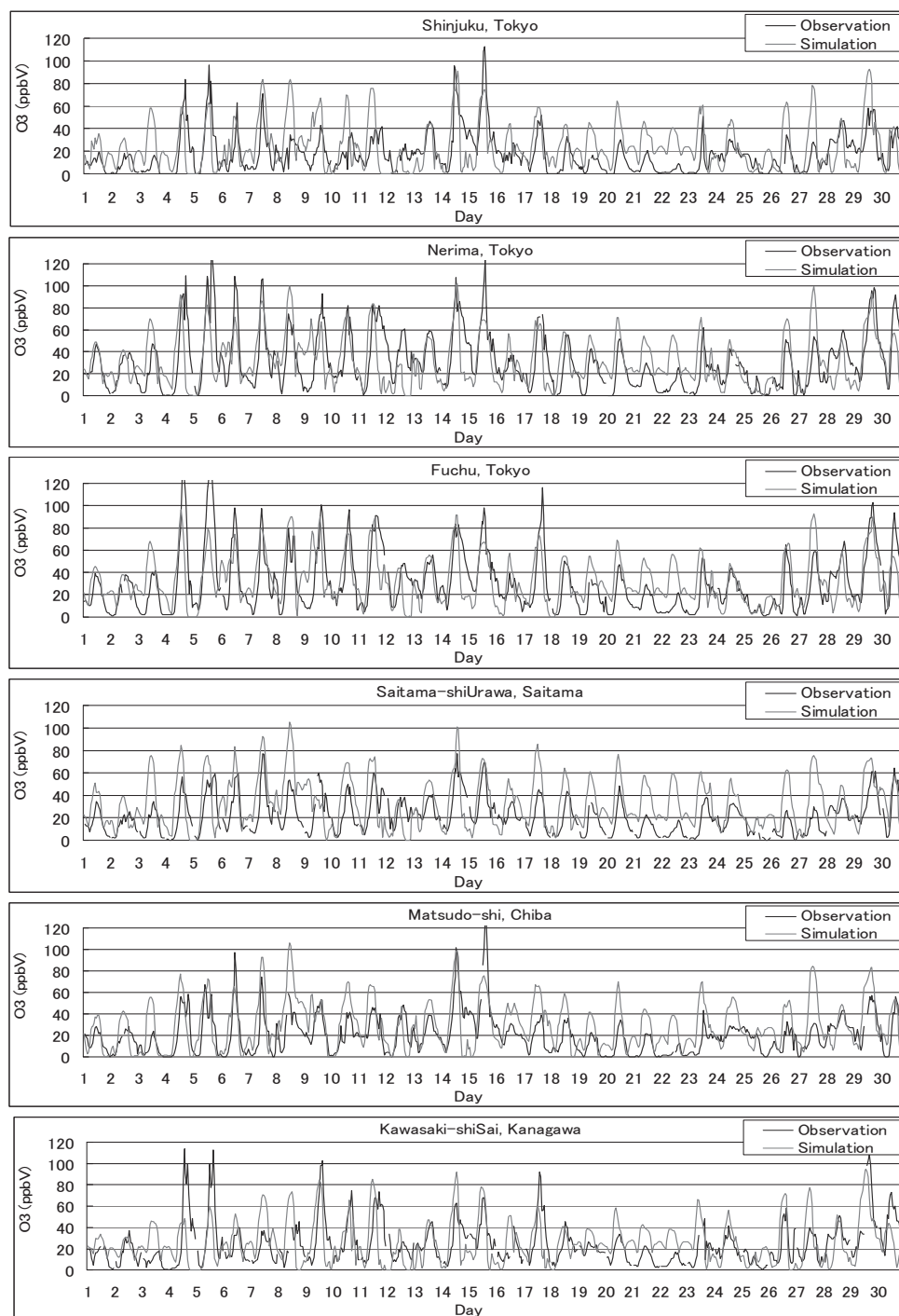


Figure 5: Hour ozone concentration time series variation of observation and simulation at some stations during August 2005

4.2. Relation between simulated ozone concentration and climatic factors

4.2.1 Synoptic circulation

There are many spatial scales in urban climate, from macroscale to mesoscale and microscale. Their interaction and effect on air pollution are very complex. In order to detect the synoptic circulation condition accompanying high ozone days in Kanto area, we carefully analyzed synoptic patterns based on large scale pressure distribution. The result showed five main types of synoptic patterns cause high ozone concentration over Kanto area as shown in Figure 6. These are described as follows:

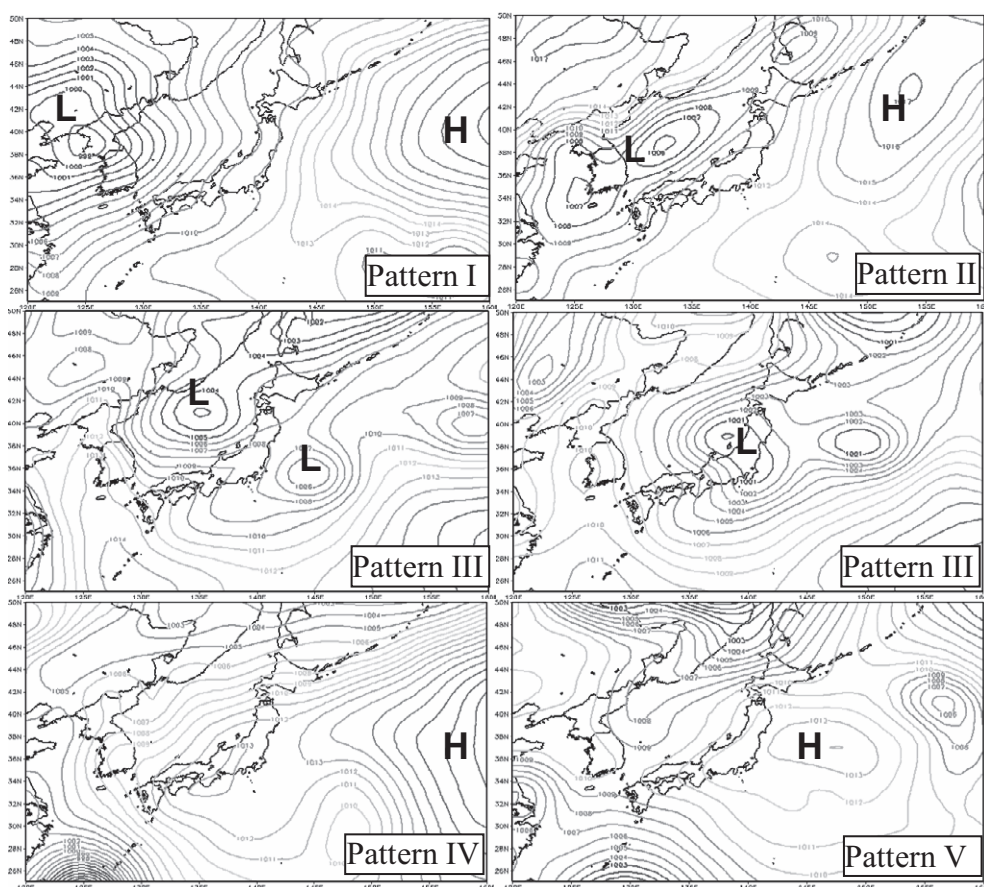


Figure 6: The synoptic patterns are favorable for high O_3 formation over Kanto

- (I) Kanto area is under control of low pressure system in western and high pressure system in eastern. In this case, the isobars line parcel to north-south direction and cause strong southerly gradient wind. On these days with this pattern, O_3 is often low.
- (II) Kanto area is under control of the belt of high and low pressure system. In this case, the isobars line parcel to southwest-northeast direction and cause strong southwesterly gradient wind. On these days, because of the SW gradient wind, it is not favorable for developing sea breeze and the high O_3 often appears in northwestern part of Kanto.

- (III) Under the control of a low pressure system. There are two abilities in this case. Firstly, Kanto area is between two low pressure systems, one is western and the other is eastern part of Kanto. Two systems create ridge with high pressure cover Kanto area. Secondly, Kanto area is under a low pressure system, the westerly gradient wind will be blocked by high mountain barrier in western and split into two currents which pass around the central Kanto area. In both situations, the weather is characterized by high temperature, high solar radiation, low humidity and the mostly calm wind. Therefore, surface O₃ becomes very high in Tokyo city and around Tokyo Bay.
- (IV) Under the control of Pacific Subtropical high pressure ridge, this pattern was mentioned by some researches, on these days with this pattern the weather is clear, high temperature and very weak wind speed. Especially the Urban Heat Island (UHI) develops and affects O₃ formation very strongly. The O₃ of these days is very high.
- (V) Under the control of local high pressure system. In this case, Kanto area was cover local pressure, the climatic condition is favorable for O₃ formation, but it is not as high as pattern IV.

4.2.1 Temperature

The relationship between ozone concentration and temperature is indicated in Figure 7. It is well known that the high temperature can raise the rate of chemical reaction between nitrogen oxides (NO_x) and Volatile Organic Compounds (VOCs), this leads to significantly increase surface ozone concentrations in city areas. In order to investigate the effect of temperature on ozone concentration, the scatter plot is used to describe ozone concentration – climate relation. In Figure 7 we can see ozone concentration at all monitoring stations in Kanto area as a function of temperature. Ozone concentration is small at low temperature (below 27°C), but it significantly increases with increasing temperature. The linear correlation coefficient between simulated ozone and temperature at all station are shown in Table 3. It is found that there is a strong relationship between simulated ozone and temperature in August. The maximum correlation coefficient is found as 0.74 at Saitama-shiUrawa and the minimum correlation coefficient is found as 0.50 at Kawasaki-shiSai. This result also shows that the temperature above 28°C is one of the factors which cause the exceedance of ozone concentration (>60ppb).

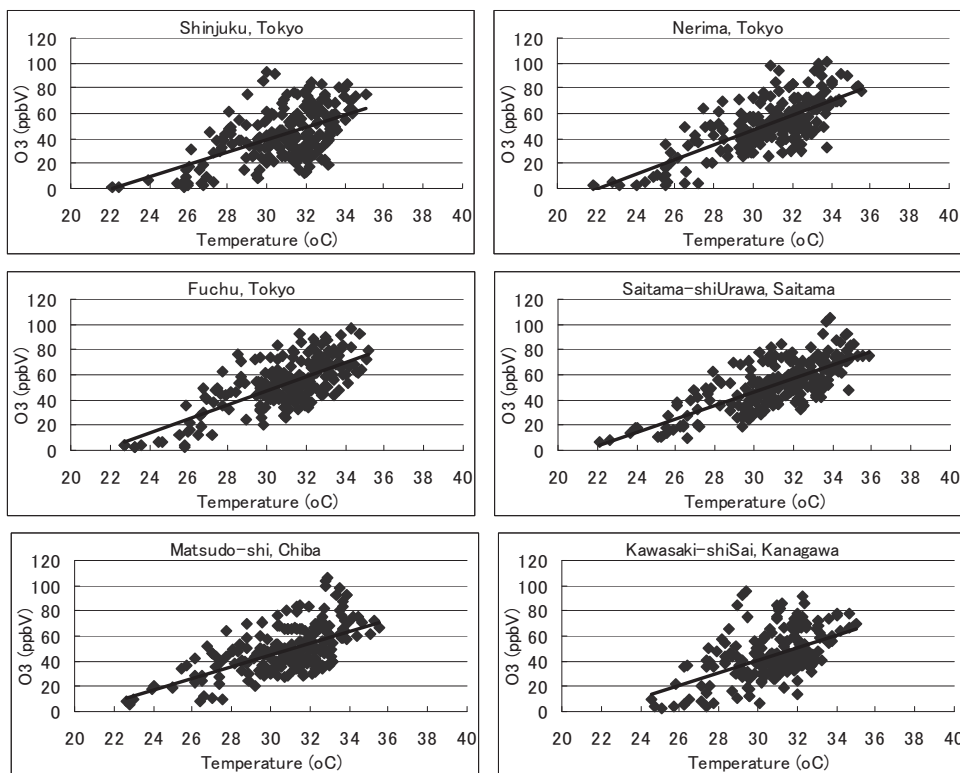
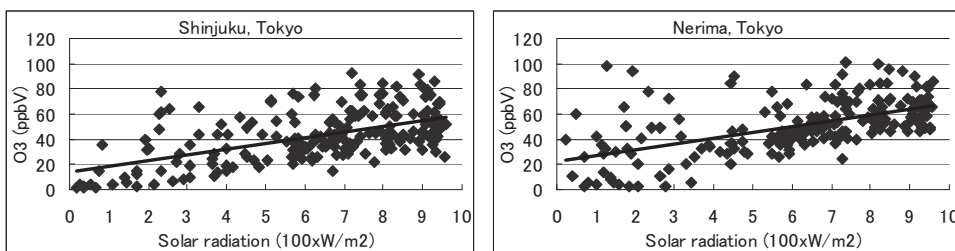


Figure 7: Relationship between O_3 and temperature at every hour from 8:00 to 14:00h in August 2005 base on MM5/CMAQ simulation

Table 3: Correlation coefficients between simulated ozone and climatic factors at some monitoring stations base on MM5/CMAQ simulation

| Station Variables | Shinjuku | Nerima | Fuchu | Saitama- shiUrawa | Matsudo- shi | Kawasaki- shiSai |
|----------------------|----------|--------|-------|----------------------|-----------------|---------------------|
| Temperature | 0.56 | 0.73 | 0.71 | 0.74 | 0.59 | 0.50 |
| Solar radiation | 0.56 | 0.57 | 0.57 | 0.70 | 0.50 | 0.52 |
| Relative humidity | -0.75 | -0.82 | -0.80 | -0.82 | -0.73 | -0.75 |



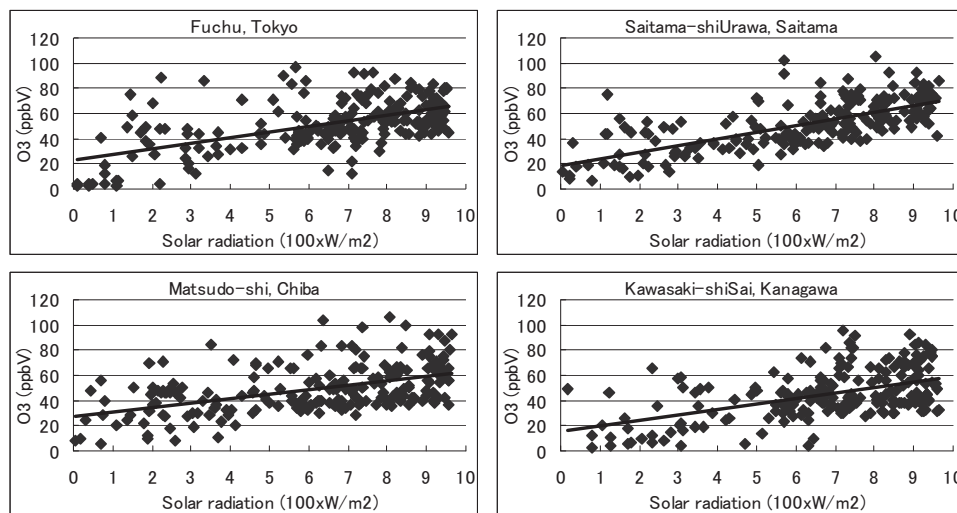
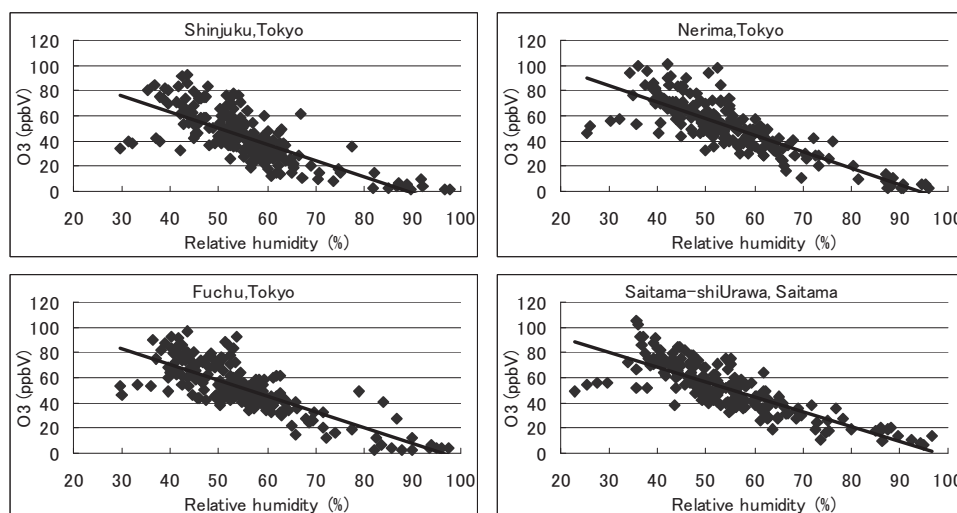


Figure 8: Relationship between O₃ and solar radiation at every hour from 08:00 to 14:00h in August 2005 base on MM5/CMAQ simulation

4.2.2 Solar radiation

It is well known that the rate of photochemical reaction depends on the intensity of solar radiation, therefore solar radiation is an important factor in the formation of ground ozone concentration. Figure 8 shows ozone concentration at monitoring stations in Kanto area as a function of the intensity of solar radiation. It is clear that increasing the intensity of solar radiation tends to increase the ground ozone concentration. When the intensity of solar radiation is low, the high ozone concentration depends on other factors such as temperature, humidity, wind, etc. The positive correlation is found at all monitoring stations as seen in Table 3. Comparing to temperature, the solar radiation has not much effect, the correlation coefficient varies from 0.5 at Matsudo-shi to 0.7 at Saitama-shiUrawa.



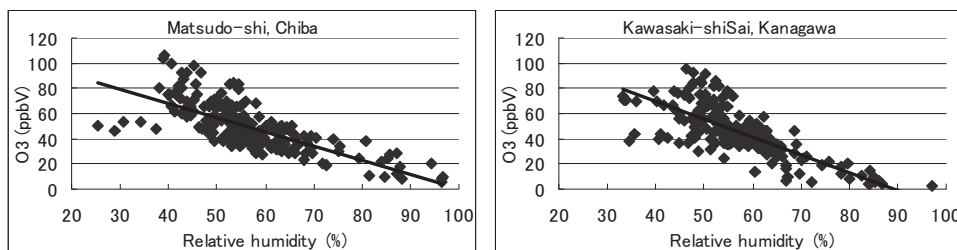


Figure 9: Relationship between O₃ and relative humidity at every hour from 08:00 to 14:00h, in August 2005 base on MM5/CMAQ simulation

4.2.3 Relative humidity

Water vapor plays an important role in O₃ chemical and photochemical processes; it can absorb the substances in the atmosphere. On other hand, hydrogen and hydroxyl radicals can be formed from water vapor and, consequently, cause reactions that destroy ozone molecules. Figure 9 shows ozone concentration at monitoring stations in Kanto area as a function of relative humidity. The ozone concentration is decreasing with increasing relative humidity. The ozone concentration does not exceed environmental quality standards with the relative humidity above 60 %. The negative correlation is found at all monitoring stations as seen as in Table 3. The result analysis shows the simulated ozone concentration is influenced by relative humidity as much as temperature and solar radiation. The linear correlation coefficient is very high at all monitoring station with the maximum is -0.82 at Saitama-shiUrawa and Nerima. Because the relative humidity is dependent variable, it depends on temperature, pressure, etc. Therefore, it is necessary to fix related variables. For example, in order to minimize effect of temperature we sort relative humidity into 5 categories base on temperature in degrees Celsius: Rh1 with T1= (28, 30]; Rh2 with T2= (30, 31]; Rh3 with T3= (31, 32]; Rh4 with T4= (32, 33]; and Rh5 with T5= (33,]. The result in Table 4 show the effect of humidity strongly depends on temperature, it is very complex and non-linear. This result suggested that O₃ concentration not only depends on separate climatic factor, but it depends on relation of climatic factors. Therefore, relationship between O₃ and climatic factor need to be considered in relation of another climatic factor.

Table 4: Correlation coefficients between simulated ozone and various relative humidity categories at some monitoring stations base on MM5/CMAQ simulation, the value in brackets indicates sample number.

| Station Variables | Shinjuku | Nerima | Fuchu | Saitama-shiUrawa | Matsudo-shi | Kawasaki-shiSai |
|-------------------|------------|------------|------------|------------------|-------------|-----------------|
| Rh1 | -0.49 (31) | -0.59 (38) | -0.52 (33) | -0.66 (33) | -0.64 (34) | -0.61 (37) |
| Rh2 | -0.53 (34) | -0.58 (29) | -0.66 (32) | -0.49 (35) | -0.48 (31) | -0.83 (40) |
| Rh3 | -0.70 (43) | -0.50 (36) | -0.57 (45) | -0.51 (32) | -0.48 (41) | -0.71 (52) |
| Rh4 | -0.79 (40) | -0.73 (41) | -0.69 (34) | -0.79 (31) | -0.78 (48) | -0.41 (42) |
| Rh5 | -0.71 (36) | -0.67 (36) | -0.49 (35) | -0.88 (50) | -0.52 (29) | -0.55 (17) |

4.2.4 The relationship between Urban Heat Island and ozone concentration

Observational analysis of Yoshikado (1996) suggested that during winter the temperature contrast between land and sea is quite small to induce sea breeze (about 2°C). This sea breeze interacts with UHI causing high air pollution over the city. Therefore, how is the influence of UHI when the temperature contrast is large in summer? In order to understand this problem, we select simulation result on August 4, 2005 which associated with daytime UHI event over Tokyo area for analysis. This day, the Pacific Subtropical High expands to the west (Figure 10), the Kanto area was covered by its ridge and the weather was fine. Figure 11a shows the spatial distribution of the surface temperature and 10m wind from MM5 simulation in domain 3. We can see the region of temperature higher than 37°C over Tokyo metropolitan at 12 JST and the horizontal wind speed is a little weak. The high temperature associated with UHI causes pressure deficiency over city and creates a circular pressure gradient pattern around the city as shown in Figure 11b. In this situation, the sea breeze from Tokyo Bay (S-SE), Sagami (SW-S) and Kashima (E) merged and combine with flow from suburban. This system remained without moving for some hours and cause high O₃ concentration over city (Figure 12). Although the difference of temperature between land and sea is very high, the sea breeze cannot pass through city due to of persistence of UHI. Interaction between UHI and sea breeze also is very important in high O₃ formation over Kanto area. This interaction can be described by vertical cross of circulation vector from shore to suburban AA' (Figure 13). On this day, there is no land breeze because the land surface remains hotter than sea surface from last night. During the early morning the Tokyo Metropolitan area is calm, the sea breeze can be recognized near shore and begins to penetrate inland. Until mild morning, when surface was heated by sun, it appears an area with high temperature over Tokyo city. The contrast of temperature between urban and suburban area creates urban heat island circulation (HIC). At surface, the flow from suburban meets sea breeze at city and goes up. This updraft of HIC acts like 'block' preventing the penetration of sea breeze inland, therefore high O₃ concentration results over city area. Moreover, because Kanto area is under control of high pressure system, it is generated subsidence inversion from 9 to 15 JST near 850 mb level as seen in Figure 14. Under this inversion, the air pollution cannot be mixed well within the atmospheric and high O₃ concentration can be understood.

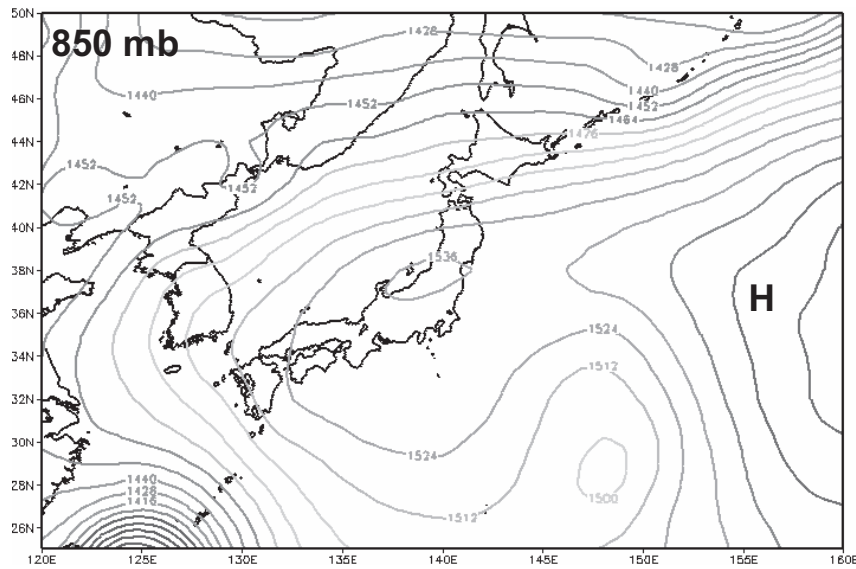


Figure 10: Geopotential height [gpm] at 9 JST August 4

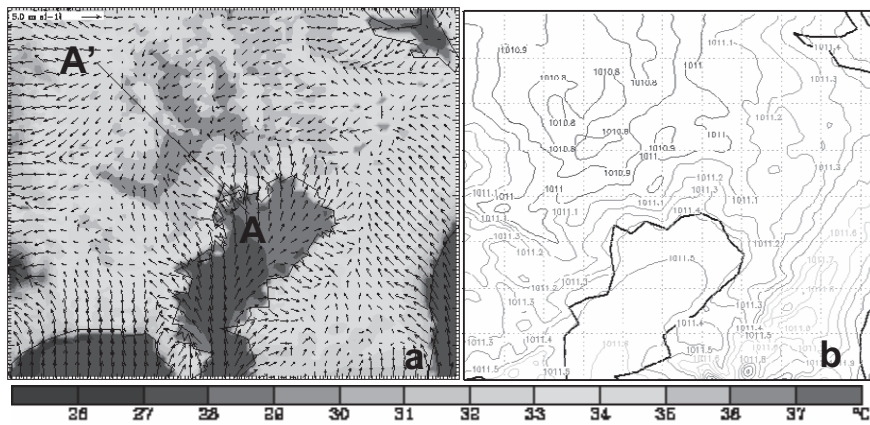


Figure 11: The simulation result from MM5 model at 12 JST August 4; (a) simulated surface temperature ($^{\circ}\text{C}$), 10m-wind; (b) surface pressure (mb)

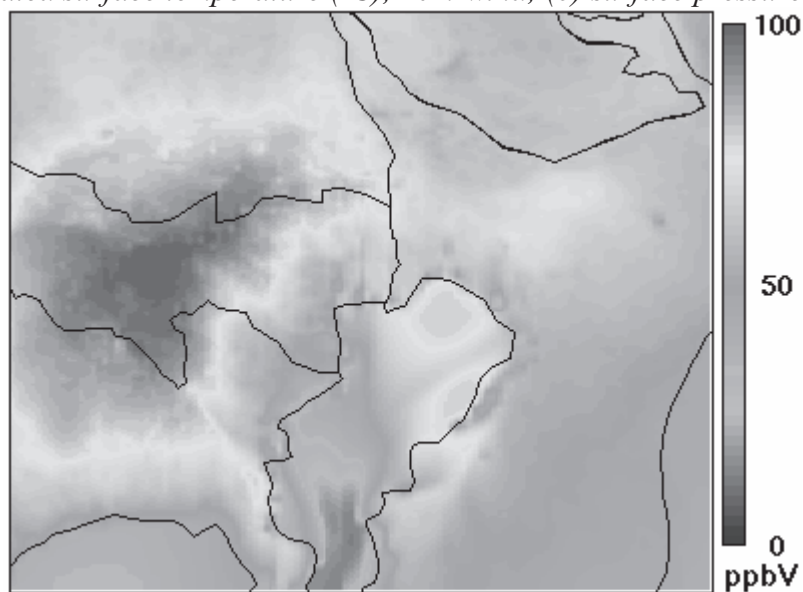


Figure 12: The CMAQ simulated O_3 (ppbV) in D3 at 14 JST August 4

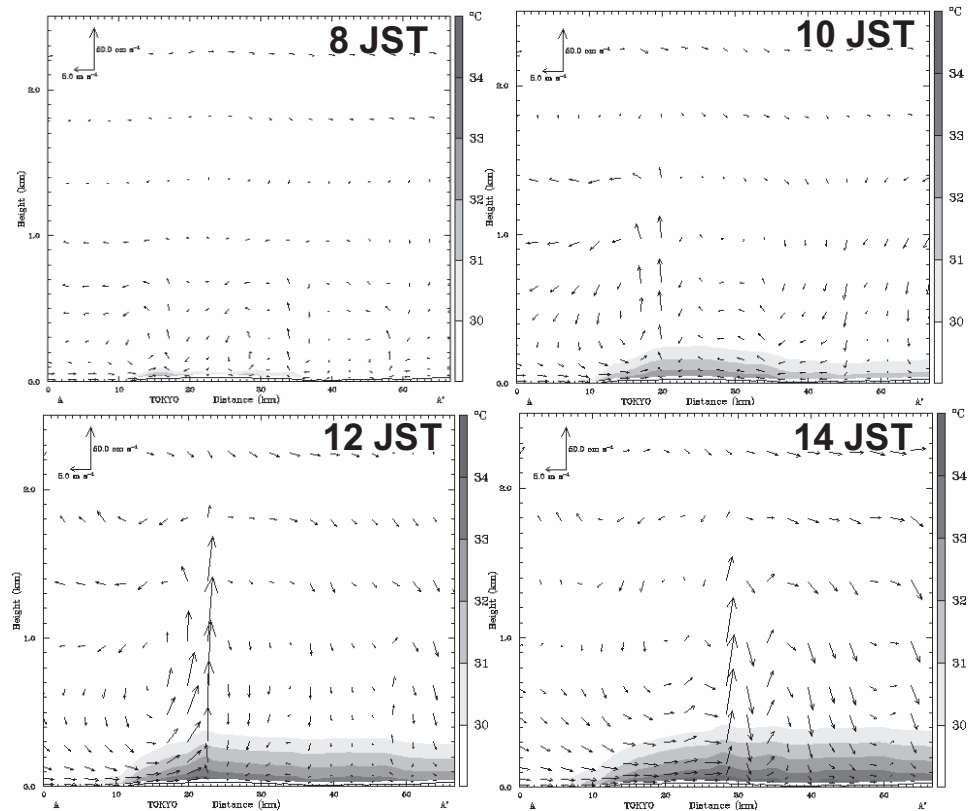


Figure 13: Circulation vector in the plain of the cross section A'A for August 4

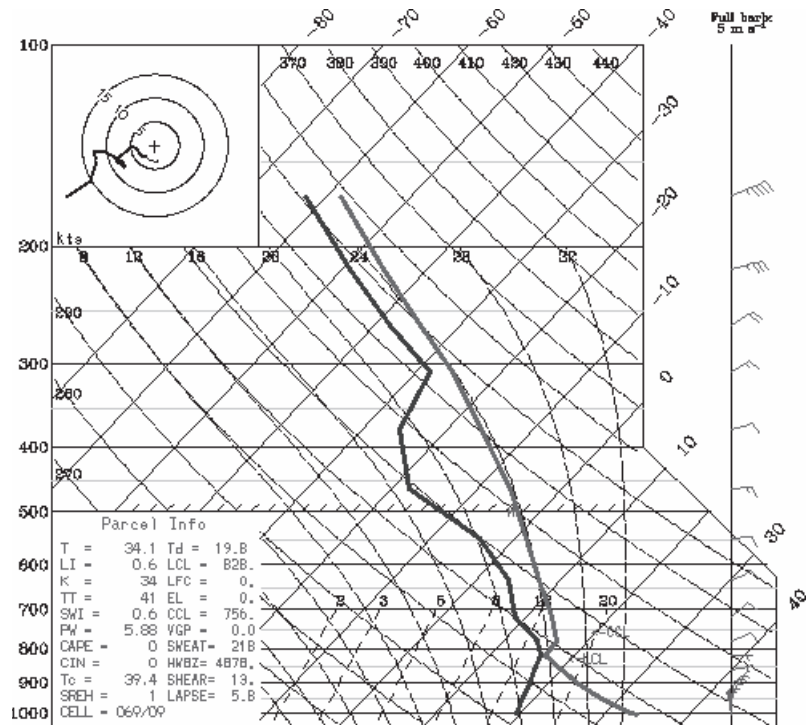


Figure 14: The Skew-T diagram at 14 JST August 4 at Nerima

5. CONCLUSIONS

A coupled MM5/CMAQ model is first used to investigate the relationship between ground ozone concentration and climatic factors over Kanto area. The analysis results showed that there is a close relationship between climatic factors and ground ozone concentration in Kanto area. O₃ strongly depends on the synoptic pattern. Of the 5 major patterns that are identified, pattern III and IV cause significantly high O₃ concentration. Simulation analysis gives the ground ozone concentration as function of temperature, solar radiation, and relative humidity. The increase in temperature, solar radiation and the decrease in humidity lead to increase ozone concentration. The relative humidity has the most important effect. This analysis also showed that the extreme of O₃ concentration appears on the day which Kanto area is controlled by Pacific subtropical high pressure system. These days seem to have all favorable climate conditions for high O₃ formation, high temperature and solar radiation, low humidity and mostly calm wind. Especially urban heat island and its interaction with sea breeze have strong effect on O₃ concentration over Kanto area. Although the difference of temperature between land and sea is favorable for developing sea breeze, the sea breeze cannot pass city due to persistence of UHI. Moreover the subsidence inversion on these days also is one of the factors cause significantly high O₃ concentration in this area. This study suggested that the coupled MM5/CMAQ model can be useful tool for urban environment and climate analysis. However, to get more detailed information it is necessary to combine the MM5/CMAQ model with finer model such as urban canopy, wind tunnel, and roadside model. That is our research interests in future work.

REFERENCES

- Byun, D.W., Ching, J.K.S. (Eds.), 1999. Science Algorithms of the EPA Models-3 Community Multi-scale Air Quality (CMAQ) Modeling System. NERL, Research Triangle Park, NC.
- Chang, Y.S., Carmichael, G.R., Kurita, H., Ueda, H., 1989. The transport and formation of photochemical oxidants in central Japan. *Atmospheric Environment*, Volume 23, Issue 2, Pages 363-393
- Dudhia, J., 1989. Numerical study of convection observed during the winter monsoon experiment using a mesoscale two-dimensional model. *Journal of Atmospheric Science* 46, 3077–3107.
- Dudhia, J. Gill, D. Yong-Run Guo. and Manning K., 2005. PSU/NCAR Mesoscale Modeling System. Tutorial Class Notes and User's Guide: MM5 Modeling System Version 3
- Fujibe, F., 1985. Air pollution in the surface layer accompanying a local front at the onset of the land breeze. *Journal of Meteorology Society of Japan*, 63, pp.226-237,
- Grell, G.A., Dudhia, J., Stauffer, D.R., 1994. A description of the fifth-generation Penn State/NCAR mesoscale model (MM5). NCAR Technical Note NCAR/TN-398+STR, 117pp.

- Hayami, H., and Kobayashi, S., 2004. Modeling of Concentration of Atmospheric Secondary Aerosol, CRIEPI Report T03037, 17.(in Japanese)
- Hong, S.Y., Pan, H.L., 1996. Nonlocal boundary layer vertical diffusion in a medium-range forecast model. *Monthly Weather Review* 124, 2322–2339.
- Hsie, E.Y., Anthes, R.A., 1984. Simulations of frontogenesis in a moist atmosphere using alternative parameterizations of condensation and precipitation. *Journal of Atmospheric Science* 41, 2701–2716.
- JCAP., 1999. Air Modeling (4), Observation results of Kanto area in summer, Technical Report of Japan Clean Air Program. (in Japanese)
- Kurita, H., Sasaki, K., Muroga, H., Ueda, H., Wakamatsu, S., 1985. Long-range transport of air pollution under light gradient wind conditions. *Journal of Climate and Applied Meteorology*. 24, pp. 425–434.
- Kurita, H., Ueda, H., 1986. Meteorological conditions for long-range transport under light gradient winds. *Atmospheric Environment* 20, pp. 687–694
- Kimura, F., 1983. A numerical simulation of local winds and photochemical air pollution (I) : Two- dimensional land and sea breeze. *Journal of Meteorological Society of Japan*, 61, 862-873.
- Kimura, F., 1985. A numerical simulation of local winds and photochemical air pollution (II) : Application to the Kanto Plain. *Journal of Meteorological Society of Japan*, 63, 923-936.
- Kimura, F., 1989. A simulation of wind and air pollution over complex terrain using a hydrostatic numerical model. *Atmospheric Environment*, 23, 723-730
- Tsuruta, H., 1983. Report of Special Research Project on Environmental Science, Grants in Aid for Scientific Research, B180-5702, 94-114, (in Japanese).
- Uno, I., Wakamatsu, S., Ogawa, Y., Murano, K., 1984. Three-dimensional behaviour of photochemical pollutants covering the Tokyo metropolitan area. *Atmospheric Environment*, Volume 18, Issue 4, 1984, Pages 751-761
- Wakamatsu, S., Ogawa, Y., Murano, K., Goi, K., Aburamoto, Y., 1983. Aircraft survey of the secondary photochemical pollutants covering the Tokyo metropolitan area. *Atmospheric Environment*, Volume 17, Issue 4, Pages 827-835
- Wakamatsu, S., Uno, I., Suzuki, M., 1990. A field study of photochemical smog formation under stagnant meteorological conditions. *Atmospheric Environment*. Part A. General Topics, Volume 24, Issue 5, Pages 1037-1050
- Yoshikado, H., Tsuchida, M., 1996. High Levels of Winter Air Pollution under the Influence of the Urban Heat Island Along the Shore of Tokyo Bay . *Journal of Applied Meteorol.*, 35, pp.1804-1813,
- Yoshikado, H., Mizuno, T., Shimogata, S., 1994. Terrain-induced air stagnation over the southern Kanto plain in early winter. *Boundary-Layer Meteor.*, 68, pp.159-172,

CONSIDERING THE IMPACT OF CLIMATE AND LAND COVER CHANGE ON A LOCAL HYDROLOGICAL FLOW: THE CASE STUDY OF SREPOK RIVER BASIN IN VIET NAM AND CAMBODIA

AKIYUKI KAWASAKI¹, PETER ROGERS²
SRIKANTHA HERATH³ and KIMIRO MEGURO¹

¹ IIS, The University of Tokyo, Japan

² Harvard University, USA

³ United Nations University, Japan
akiyuki@iis.u-tokyo.ac.jp

ABSTRACT

The impact of climate change on the quantity, variability, and spatial distribution of water resources is increasingly cited as a possible brake to economic and social development in underdeveloped countries. This study investigated the potential impact of climate and land-cover change on a local hydrological flow, by creating a simple analysis method by integrating current data, models and technologies into common GIS environment. The level of uncertainty in predicting the outcome of hydrological simulations using existing methods and data will be discussed. Suitable adaptations for a given area will be proposed in light of these uncertainties, and the options of local decision makers and stakeholders will be explored. The Srepok River basin, the main tributary of the Lower Mekong, was selected as a study area.

These results suggest that population increases and land development, and therefore growth in human water demand, has a far greater effect than precipitation change will in the next 50 years. However, these results are based on several assumptions in simplifications. A more thorough study might address a non-uniform change in precipitation and climate and more severe or other land cover change scenarios.

1. INTRODUCTION

In the 21 century, water is proving to be at the heart of serious environmental, political and economic issues around the globe. The impact of climate change on the quantity, variability, and spatial distribution of water resources is increasingly cited as a possible hindrance to economic and social development in underdeveloped countries. This is exacerbated by the fact that many of the large river basins of the world are shared among several nations (Rogers, 1993; Beach *et al.*, 2000).

The contributions of climate change, human development and their combination to the future state of global water resources were reported by Vorosmarty *et al.* (2000) and Oki and Kanae (2006). The IPCC's regional analysis indicates freshwater availability in South-East Asia, particularly in large river basins, is projected to decrease by the 2050s (Cruz *et al.*, 2007). Recently, the impacts of climate change on future hydrology in the entire large river basin level were investigated in the Nile and the Mekong River basin (Beyene *et al.*, unpublished; Kiem *et al.*, 2008). The IPCC (2007) has promoted "adaptation" as the best means for responding to climate change. To study water resource adaptation, attention to local scale is essential because the structure of the solution is different for each scale and set of local characteristics. Concrete adaptations based on practical analysis are often lacking, particularly on local and regional scales.

As yet, a reliable framework and tools needed to support climate adaptation in river basins remain unavailable. However, recent developments in modeling and data acquisition and processing have made integrated approaches to sustainable water resource management more feasible. The purpose of this study is to investigate the potential impact of climate and land-cover changes on local stream flow in the next several decades. The level of uncertainty in predicting the outcome of hydrological simulations using existing methods and data will be discussed.

Developing analysis process of the climate and land-cover impact on local stream flow should not only contribute to decision support for a given area, but also in many locations with different situations. We plan to develop such an approach using the IPCC and other hydrological scenarios. The significance of this project is developing a systematic approach for integrating a wide range of data models, data formats, and research methodologies into common GIS computing environments for conducting hydrological simulations in local level.

2. STUDY AREA AND DATA

2.1 Study area

The Mekong River is the largest international river in Asia, which rises in the Tibetan Plateau and empties into the South China Sea after travelling 4,000 km and flowing through six countries: China, Myanmar, Thailand, Lao PDR, Cambodia and Vietnam. Srepok River Basin, the main tributary of the Lower Mekong, was selected as a study area (Figure 1). The total length of Srepok River is 315km and the catchment area is 30,100km². Population growth and agricultural-land expansion, especially in upstream of Viet Nam side, are of increasing concern (CarlBro Intelligent Solutions, 2005). To realize a fair water use in both upstream and downstream, exploitation and the use of water resources in the basin should be taken into consideration for the benefit of the whole region.

Rainy season begins in May and ends in October in the upper Srepok River basin. Dry season is from December to March. The stream flow in dry season in the upper Srepok River basin is less than 30% of annual flow (Ty, 2008). Basic meteorology data in Srepok River basin is shown as follows

(CarlBro Intelligent Solutions, 2005): The average annual temperature: 23 °C; annual humidity: 78-83%; annual evaporation: 1,300 mm; and average rainfall: 1750 mm.

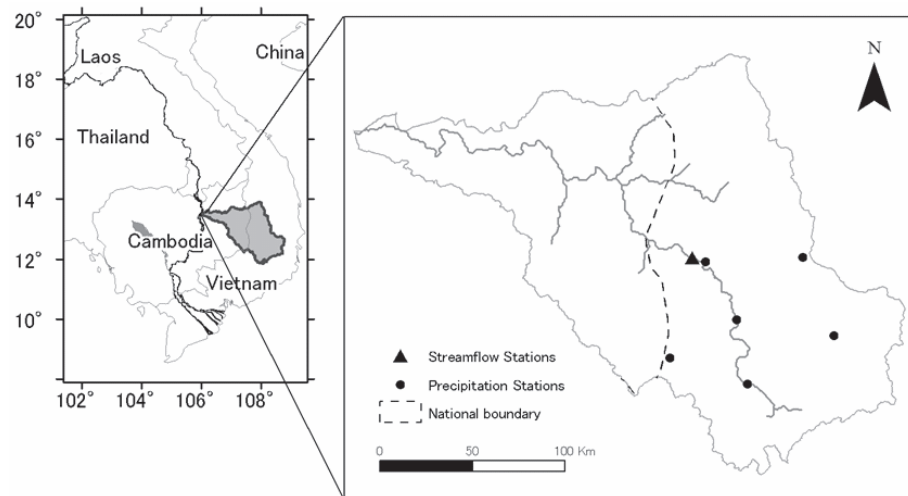


Figure 1: Srepok River basin and the hydro-meteorological stations.

2.2 Data

Contemporary GIS data such as land-cover, soil, and digital elevation models was obtained from the Mekong River Commission Secretariat, Lao PDR. Daily precipitation data of four locations (Ban Don, Duc Xuyen, Cau 14, Krongbuk) and daily stream flow data at Ban Don were obtained by the Hydro-Meteorological Data Center (HyMetData), Viet Nam. Table 1 shows the data list of this study.

Table 1: Data list.

| Theme | File name | Year | Data type, Scale | Data Source |
|---------------|--|-----------|---|--|
| Land Cover | Forest and Land Cover Types | 1997 | Polygon, 1:50,000 | Mekong River Commission |
| Soil | Soil Map of the Lower Mekong Basin | 2002 | Polygon, 1:50,000 (Viet Nam) 1:100,000 (Cambodia) | Mekong River Commission |
| Terrain | Digital Terrain Model (DTM) for the Lower Mekong Basin | 2005 | Raster data, 50 m resolution | Mekong River Commission |
| Population | Gridded Population of the World: Future Estimates | 2000 | Raster data, 2.5 arc-minutes resolution | CIESIN, Columbia University (2008) |
| Precipitation | Monthly (daily) precipitation | 1978–2006 | Table, 4 locations | Hydro-Meteorological Data Center (HyMetData), Viet Nam |
| Stream flow | Monthly (daily) stream flow | 1978–2006 | Table, 1 location | Hydro-Meteorological Data Center (HyMetData), Viet Nam |

3. METHODOLOGY

The overall structure of this project involved integration of two software programs – a hydrological simulation tool (Hydrologic Modeling System; HEC-HMS) and a GIS environment (ArcGIS). HEC-HMS is designed to simulate the precipitation-runoff processes of dendritic watershed systems (US Army Corps of Engineers, 2008). The integration better reflects effects of changing climate and land cover over time on a localized scale. Specifically, Arc Hydro Tools (Maidment, 2002) and Hec-GeoHMS (US Army Corps of Engineers, 2008), two ArcGIS-based system applications

were used to process climate and rainfall data into one integrated model of the hydrological processes in the SrePok Basin.

3.1 Creating the Basin Model

ArcGIS was used to create a spatially relevant basin model that integrated rainfall data and land characteristics. To analyze the effects of streamflow at a more localized level, terrain processing tools in the ArcHydro Tools application were used to delineate a main river and subbasins from a DEM (Digital Elevation Model) of the SrePok River Basin. Subbasin slope and area were also calculated from the terrain processing procedure using the ArcHydro Tools application. Rainfall time series data were mapped from four rainfall observation sites (Ban Don, Duc Xuyen, Cau 14, Krong Buk) to individual subbasins using Thiessen’s Polygon method. Since all the rainfall observation sites were located in Vietnam (as no such data was readily available from Cambodia), there is significant simplification in this rainfall distribution model as all subbasins downstream of BanDon are assumed have the same rainfall.

The land cover characteristics used in this study was based on the U.S. Soil Conservation Service (SCS) curve number (CN) system (McCuen, 1982; Soil Conservation Service, 1986) – which determines a runoff coefficient from a simple land cover and soil drainage type table (Table 2). Using available Land cover and Soil Type maps for the region and a modified CN Lookup Table (to match key land cover types of interest in this study), curve numbers and curve number based lag times were calculated aggregated for each individual subbasin. The lag time, time between peak rainfall and peak streamflow, was also calculated based on SCS formulas (below). These calculations were all excuted in the ArcGIS environment using HecGeo-HMS Tools application. SCS Curve Numbers were generated from modified curve number lookup table and averaged over the entirety of the subbasin (US Army Corps of Engineers, 2000).

Table 2: Modified Curve Number Lookup Table.

| Land Cover Category | Soil Type | | | |
|---------------------|-----------|-----|-----|-----|
| | A | B | C | D |
| Thick cover forest | 30 | 55 | 70 | 77 |
| thin cover forest | 43 | 65 | 76 | 82 |
| Mosaic | 43 | 65 | 76 | 82 |
| Open land | 39 | 61 | 74 | 80 |
| cloud | 50 | 50 | 50 | 50 |
| Agriculture | 67 | 77 | 83 | 87 |
| Glass land | 30 | 58 | 71 | 78 |
| Urban | 89 | 92 | 94 | 95 |
| Water | 100 | 100 | 100 | 100 |

Soil Type ranges from A (absorbent) to D (not absorbent). For Antecedent Moisture Conditions II (regular conditions, see below) :

$$\text{CN-based Lag Method: } t_{lag} = \frac{2.587 \cdot L^{0.8} \left(\frac{1000}{CN} - 9 \right)^{0.7}}{1900 \cdot H^{0.5}}$$

where L = longest flow path in subbasin (m), H = basin slope (%) and t_{lag} = lag time (hr)

3.2 Simulation and Calibration

The local basin model was then integrated into HEC-HMS software environment for simulating streamflow from precipitation at a daily level for the year 2001, so that the results could be calibrated to observed daily streamflow data from 2001. In addition to the curve number and lag times imported from ArcGIS with the Basin model, the SCS formula was used to calculate initial abstraction, which includes all losses before runoff begins such as water retained in surface depressions, water taken up by vegetation, evaporation, and infiltration (US Army Corps of Engineers, 2000).

$$\text{Initial abstraction (mm)} = 0.2 \left(\frac{1000}{\text{CN}} - 10 \right)$$

The Muskingum Routing method was chosen to model stream routing since it required fewest assumptions about unknown data. Assumptions include a Muskingum X value of 0.1 (indicating a small, natural stream), a subreach value of 2, and a streamflow speed of 2 miles/hr was used to calculate Muskingum K value (length of time to travel a stream reach) (US Army Corps of Engineers, 2000). Simulation results were then compared to observed streamflow at BanDon station in 2001. The initial simulation from the model reflected too high a sensitivity in the streamflow to precipitation. This disparity with observed data resulted largely from not accounting for the human control of flow through hydropower dams and reservoirs in the area. However, data about policies of flow control in the dam was not available. To account for human streamflow control, the effects of precipitation from all subbasins upstream of the BanDon hydropower site were replaced with a constant monthly baseflow adjusted to match observed streamflow. Also to smooth out the curve and reduce the volatility of the streamflow, the lag time was increased in all subbasins by a factor of 4.

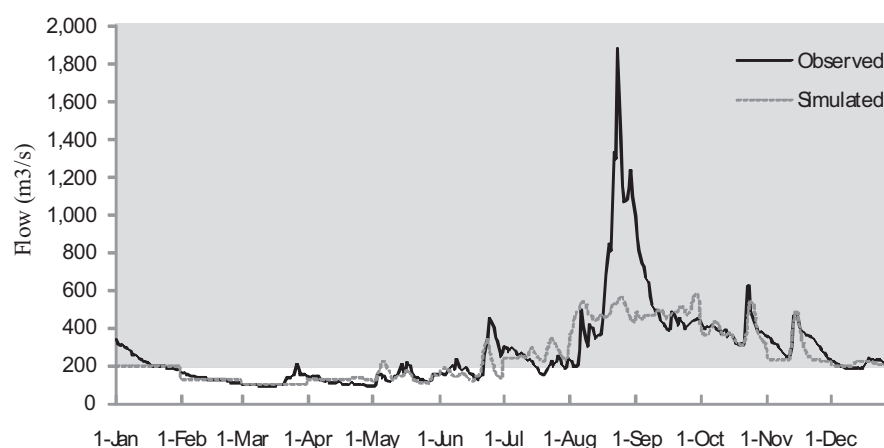


Figure 2: Hydrograph at BanDon Streamflow station.

While this method achieved adequate fitness with respect to observed data for this level of the study, it does create difficulties later on in the study

as all future changes rainfall activity and land cover characteristics of subbasins upstream of Ban Don will not be accounted for in this adjusted basin model. Ideally, more available data on flow levels and the spatial distribution of local reservoirs and dams and future plans for reservoir and dam activity would provide a more comprehensive study.

Also after generating initial results, it was also clear that the vast differences in climate conditions between the wet and dry season in the country necessitated different treatment of the model for the two seasons. Specifically, SCS curve number calculations vary significantly depending on climate conditions, or Antecedent Moisture Conditions (AMC). Dry season conditions match the conditions of AMC I, where as wet season conditions match those of AMC III. The current CN (II) conditions were converted using CN equivalence formulas (Chow *et al.*, 1988):

$$\begin{array}{ll} \text{Dry season: January – April} & \text{Wet season: May – October} \\ \text{CN (I)} = \frac{4.2 \text{ CN (II)}}{10 - 0.058 \text{ CN (II)}} & \text{CN (III)} = \frac{23 \text{ CN (II)}}{10 + 0.013 \text{ CN (II)}} \end{array}$$

3.3 Creating Future Land Cover Scenarios

Land cover information was used to determine two key factors in the streamflow model - runoff and water demand. Future land cover scenarios were needed to determine future impact of land development. Given that data was not available about future land cover policy decisions, population density data was used to predict future land cover (CIESIN, 2008). The two future scenarios focused on urban and agricultural development in 2025 and 2050. A per annum population growth rate of 1.95% (Carl Bro Intelligent Solutions, 2005) was uniformly applied across population density grids to generate population density grids for 2025 and 2050. Comparing population in 2000 with the available land cover data from 1997, threshold values were set for what population densities were in various land cover types. These same threshold values were then reapplied to the new population density grids for 2025 and 2050 to determine future land cover. Currently undeveloped land (i.e. forest) could become more developed, but not vice versa. Curve numbers, lag times, and initial abstraction values were recalculated based on these two new land cover scenarios for their respective future simulations.

Land cover change, specifically urban and agricultural development, also heavily affects human water demand. Annual water demand (measured in million cubic meters) was used to calculate factors of water demand per area for agricultural and urban land types. These factors were then multiplied by their respective agricultural and urban areas in each subbasin, creating a new water demand per subbasin based on future land cover scenarios. Seasonality was also accounted for as annual water demand was split into dry and wet season demand, where a historically accurate ratio of 1:2 was assumed (Carl Bro Intelligent Solutions, 2005). To incorporate water demand changes into the streamflow model, the difference in future water demand and current water demand was directly subtracted from all subbasins' respective baseflows.

Table 3: Water Demand Data for Vietnamese SrePok.

| | Water Demand (MCM) | Area (km ²) | Demand/Area (m ³ /m ²) |
|-----------------|--------------------|-------------------------|---|
| Agriculture | 1,618.0 | 5,996.6 | 0.3 |
| Urban | 51.8 | 6.7 | 7.6 |
| (Industry) | 30.5 | - | - |
| (City Domestic) | 21.3 | - | - |

Table 4: Future Land Cover and related Water Demand in Whole SrePok.

| Year | Agricultural Area (km ²) | Urban Area(km ²) | Total Annual Water Demand (MCM) |
|------|--------------------------------------|------------------------------|---------------------------------|
| 1997 | 6,368.8 | 6.7 | 1,770.3 |
| 2025 | 9,260.6 | 195.3 | 3,995.1 |
| 2050 | 11,453.1 | 842.4 | 9,546.1 |

3.4 Creating Future Precipitation Scenarios

Several options were considered for creating a simple future precipitation scenario, given that there is so much variability in current models. Initially, various General Circulation Models (GCMs) available from the IPCC were considered. GCMs are generally reliable for temperature predictions relative to precipitation, wind, humidity or air pressure predictions. As Christofides *et al.* (2008) suggested, these large scale models were unsuitable for predicting regional precipitation change. A stochastic model was also briefly explored that was based on more reliable temperature change – however given that the goal of the project was not to accurately predict future rainfall, but to create a framework for integrating tools – a uniform 5% increase in 50 years was assumed instead. This simplification allowed for work on the greater goals of developing a framework for approaching this type of analysis, while remaining within suggested implications from the IPCC. Since most estimates for changes in global precipitation vary between no change and 5% increase in 50 years (Meehl *et al.*, 2007), a separate simulation was also run with no precipitation change.

4. RESULTS AND DISCUSSION

Results were studied both at the BanDon streamflow station in Vietnam and at the Outlet of the SrePok in Cambodia. In general, the simulated streamflow for 2025 and 2050 were similar to 2001, as a uniform transformation in precipitation was used to predict future rainfall. At both BanDon and the Outlet, flow decreased by about 20 m/s in 2025 and by about 50 m/s in 2050 in the dry season, and decreased variably in the wet season as well. These decreases were comparable both at Ban Don and at the Outlet, despite that the most development occurred around and upstream of Ban Don. In Figure 3, Min stands for No Change in Precipitation and represents simulations that were conducted using unmodified precipitation data from 2001, representing the lower end of the range of expected overall

change in precipitation over the next 50 years. Max simulations were generated with a future precipitation prediction of 2.5% uniform increase in 2025 and 5% in 2050.

The greatest factor in reducing future streamflow seems to be human water demand, which was accounted for directly in reducing baseflow. In dry seasons, with no precipitation, decreased flow was virtually a direct effect of increased human water demand in the future. In the wet season, if anything, increase precipitation ameliorated the decrease in baseflow from increased human water demand. Changing curve numbers and relevant calculated values (lag time and initial abstraction) had a relatively insignificant effect. This is not surprising since runoff is more important for smaller time scales (singular events, storms) than year long simulations.

As for precipitation change, the simulations ran with no change in precipitation resulted in decreased flow compared with simulations with the maximum expected increase of 5% by 2050 – but the decrease in flow was less than 10 m/s. If anything, the most extreme expected climate change (5% increase in precipitation) would ameliorate reduced streamflow from increased water demand.

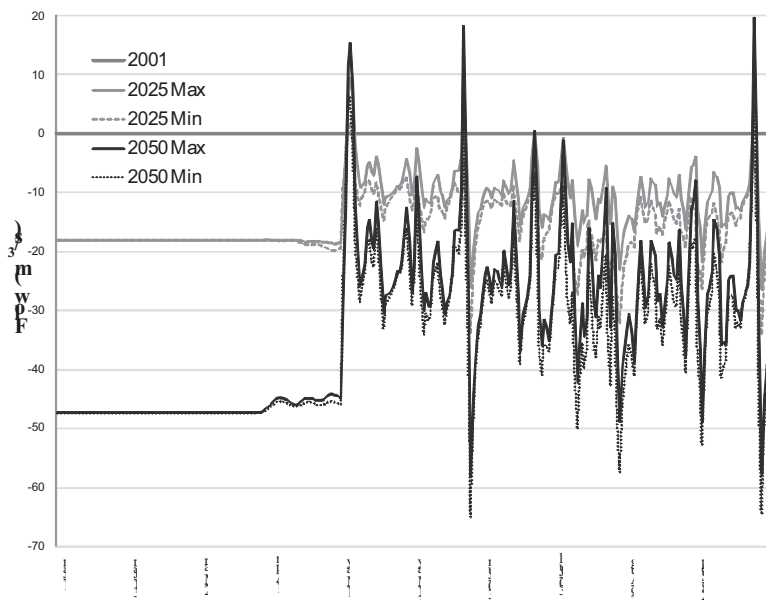


Figure 3: Difference Graphs for Streamflow at BanDon

These results suggest that population increases and land development, and therefore growth in human water demand, has a far greater effect than precipitation change will in the next 50 years. The results suggest that an adaptation strategy should focus on maintaining steady water supply in the dry season for human use as water demand increases. This may involve a readjustment in policy in land development – but this is unlikely given economic incentives and tendencies in the area to expand agricultural land. More likely, these results call for more reservoirs and dams to control flow and better ensure the availability of water in surplus in the wet season during the dry seasons, where higher demand will strain the already reduced supply of water in future years.

5. SUMMARY

This study investigated the potential impact of climate and land-cover change on a local hydrological flow, by creating a simple analysis method by integrating current data, models and technologies into common GIS environment. However, these results are based on several assumptions in simplifications. A more thorough study might address a non-uniform change in precipitation and climate and more severe or other land cover change scenarios.

ACKNOWLEDGEMENT

We are grateful to Ms. Janet He, an undergraduate student of Harvard University, for her dedicated work to conduct the simulations in this study. Also, we appreciate Mr. Tran Van Ty, a former graduate student of the Asian Institute of Technology, for his valuable support of data collection in Viet Nam. This study was supported financially by Research Fellowships of the Japan Society for the Promotion of Science for Young Scientists.

REFERENCES

- Beach, H.L., Hamner, J., Hewitt, J.J., Kaufman, E., Kurki, A., Oppenheimer, J.A., Wolf, A.T. (2000) *Transboundary Freshwater Dispute Resolution: Theory, Practice, and Annotated References*. Tokyo, New York, Paris: United Nations University Press.
- Beyene, T., D.P. Lettenmaier, and Kabat ,P (2007) Hydrologic impacts of climate change on the Nile River basin: Implications of the 2007 IPCC climate scenarios, *Climatic Change* (in review)
- CarlBro Intelligent Solutions (2005) *Sre Pok River Basin Profile*, Report No. T-203-1.
- Center for International Earth Science Information Network (CIESIN) at Columbia University (2008) Population, Land Use, and Emissions (PLUE). Available at: <http://sedac.ciesin.columbia.edu/plue/>.
- Chow, V.T., Maidment, D.R., Mays, L.W.(1988) *Applied Hydrology*. McGraw-Hill Series in Water Resources and Environmental Engineering. McGraw-Hill.
- Christofides, A., Koutsoyiannis, D., Efstratiadis A., N. Mammassis (2008) On the credibility of Climate Predictions. *Hydrological Sciences*. IAHS Press. 671-684.
- Cruz, R.V., H. Harasawa, M. Lal, S. Wu, Y. Anokhin, B. Punsalmaa, Y. Honda, M. Jafari, C. Li and N. Huu Ninh, (2007) Asia. *Climate Change 2007: Impacts, Adaptation and Vulnerability*. Contribution of Working Group II to the Fourth Assessment Report of the Intergovernmental Panel on Climate Change, M.L. Parry, O.F. Canziani, J.P. Palutikof, P.J. van der Linden and C.E. Hanson, Eds., Cambridge University Press, Cambridge, UK, 469-506.

- Intergovernmental Panel on Climate Change (IPCC) (2007) *Fourth Assessment Report: Climate Change 2007 Synthesis Report*. Available at: <http://www.ipcc.ch/ipccreports/ar4-syr.htm>.
- Kiem, A.S., Ishidaira, H., Hapuarachchi, H.P., Zhou, M.C., Hirabayashi, Y., Takeuchi, K. (2008) *Hydrol. Process.* 22, 1382–1394.
- Kundzewicz, Z.W., L.J. Mata, N.W. Arnell, P. Döll, P. Kabat, B. Jiménez, K.A. Miller, T. Oki, Z. Sen and I.A. Shiklomanov (2007) Freshwater resources and their management. *Climate Change 2007: Impacts, Adaptation and Vulnerability*. Contribution of Working Group II to the Fourth Assessment Report of the Intergovernmental Panel on Climate Change, M.L. Parry, O.F. Canziani, J.P. Palutikof, P.J. van der Linden and C.E. Hanson, Eds., Cambridge University Press, Cambridge, UK, 173-210.
- Maidment, D.R. (2002) *Arc Hydro: GIS for Water Resources*, Redlands, USA: ESRI Press.
- McCuen, R.H. (1982) *A Guide to Hydrologic Analysis Using SCS Methods*, Prentice Hall, Inc. Englewood Cliffs, New Jersey.
- Meehl, G.A., T.F. Stocker, W.D. Collins, P. Friedlingstein, A.T. Gaye, J.M. Gregory, A. Kitoh, R. Knutti, J.M. Murphy, A. Noda, S.C.B. Raper, I.G. Watterson, A.J. Weaver and Z.-C. Zhao (2007) Global Climate Projections. In: *Climate Change 2007: The Physical Science Basis*. Contribution of Working Group I to the Fourth Assessment Report of the Intergovernmental Panel on Climate Change [Solomon, S., D. Qin, M. Manning, Z. Chen, M. Marquis, K.B. Averyt, M. Tignor and H.L. Miller (eds.)]. Cambridge University Press, Cambridge, United Kingdom and New York, NY, USA. 763.
- Oki, T., Kanae, S. (2006) Global Hydrologic Cycle and World Water Resources, *Science*, Vol. 313. no. 5790, 1068-1072.
- Rogers, P. (1993), The Value of Cooperation in Resolving International River Basin Disputes, *Natural Resources Forum*, Vol. 17, No. 2, pp. 117-131.
- Soil Conservation Service (1986) *Urban Hydrology for Small Watersheds*, Technical Release 55 (TR-55).
- US Army Corps of Engineers (2000) *HEC-HMS Technical Reference Manual*.
- US Army Corps of Engineers (2008) Hydrologic Engineering Center HEC-HMS. Available at: <http://www.hec.usace.army.mil/software/>
- Ty, T.V. (2008) *GIS application on water infrastructure inventory and accessibility of water resources in the upper Srepok basin, Vietnam*. Master's course thesis of the Asian Institute of Technology, Thailand.
- Vörösmarty, C.J, Green, P., Salisbury, J., Lammers, R.B, (2000) Global Water Resources: Vulnerability from Climate Change and Population Growth, *Science*, Vol. 289. no. 5477, 284 – 288.

STUDY ON RELAXATION MEASURES FOR OUTDOOR THERMAL ENVIRONMENT ON PRESENT URBAN BLOCKS IN TOKYO USING COUPLED SIMULATION OF CONVECTION, RADIATION AND CONDUCTION

HONG CHEN,¹ RYOZO OOKA,² HONG HUANG,²
and TAKASHI TSUCHIYA,²

¹ School of Architecture and Urban Planning,
Huazhong University of Science & Technology, Wuhan, China

² Institute of Industrial Science, The University of Tokyo, Tokyo, Japan
chenhong.hust@gmail.com

ABSTRACT

The heat island phenomenon and degradation of the urban thermal environmental have become serious problems in Japan. In order to improve the outdoor thermal environment, it is necessary to understand quantitatively the effects of various measures. In this paper, the authors have performed coupled simulations of convection, radiation and conduction to evaluate the outdoor thermal environment over different present urban blocks: Ōtemachi as representative of a high-rise area and Kyobashi as a mid-rise area in Tokyo, Japan, to compare the effects of measures such as the heat-release point and means of air-conditioning, greening, high surface albedo, and traffic volume. The results showed that the effectiveness of moderation measures differed according to the configuration of the urban blocks.

1. INTRODUCTION

The heat island phenomenon has become considerably worse, and causes various other problems, such as an increase in the number of heat disorders or tropical nights. The underlying reasons behind the heat island phenomenon are considered to be the release of artificial heat, change in surface coverage due to urbanization, and a reduction in green space. Various measures to moderate the heat island phenomenon have been proposed and researched, and their effectiveness evaluated using numerical simulations. Although these effects are highly dependent on the property of each city block, insufficient comparison has been made of these effects between different city blocks. Therefore, the authors undertook coupled simulations of convection, radiation and conduction to evaluate the outdoor thermal environment over two different present urban blocks in Tokyo: Ōtemachi, as a high-rise business district, and Kyobashi, which is typified by mid-rise business district. The cases are set to compare the effects of

measures such as the heat-release point and means of air-conditioning, as well as greening, high surface albedo, and traffic volume.

2. ANALYSIS

2.1 Analysis outline

In this study, the numerical method of coupled simulations of convection, radiation, and conduction developed by the authors (H. Chen et al. 2004) (S. Yoshida et al. 2000) was used. Figure 1 shows an analysis outline. Using input data concerning the place, weather, urban configuration, material and surface, the ground and wall surface temperatures are calculated using radiation simulation. After that, the surface temperature is used as a boundary condition for computational fluid dynamics (CFD) simulations, which are then performed.

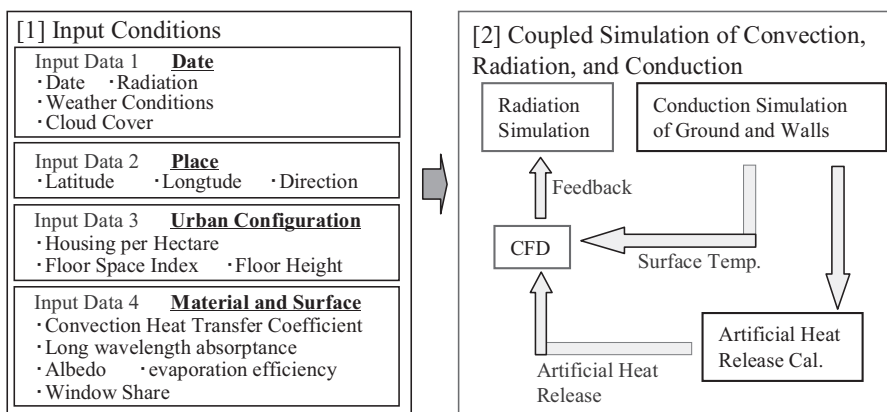


Figure 1: Analysis Outline

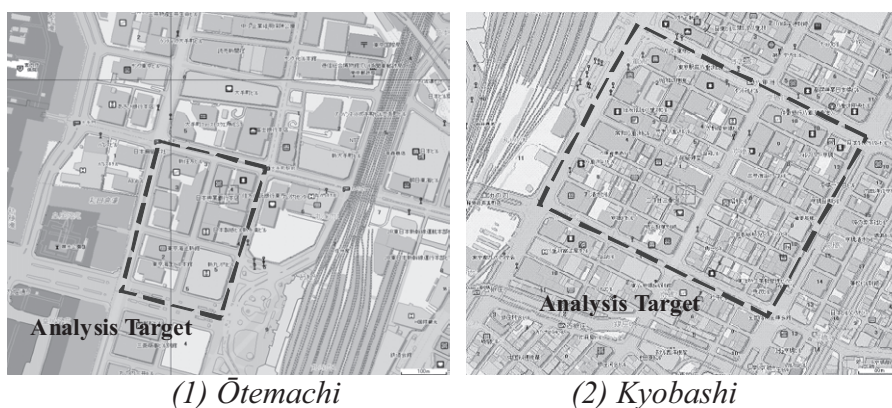
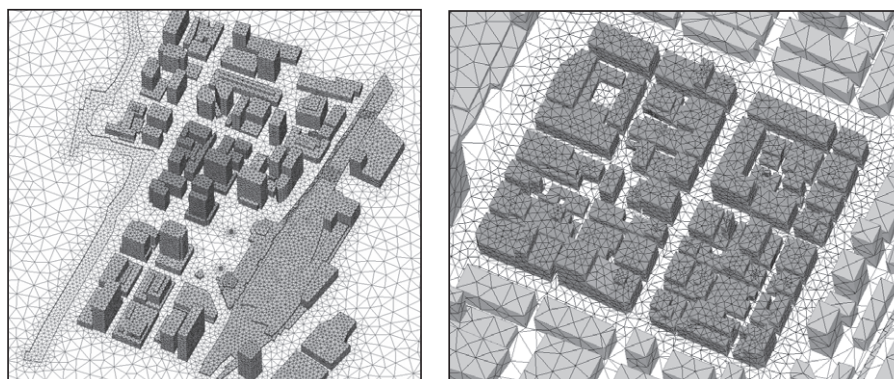


Figure 2: Analysis Targets



(1) Ōtemachi (2) Kyobashi

Figure 3: Analysis Models

Table 1: Urban Configuration of Simulation Models

| | Ōtemachi | Kyobashi |
|------------------------------|---------------|-----------|
| Mean Gross Building Coverage | 75.8% | 86.9% |
| Mean Net Building Coverage | 62.9% | 71.2% |
| Legal Floor Space Index | 900% or 1300% | 600%~800% |
| Mean Floor Space Index | 1179.0% | 664.3% |
| Mean Building Height | 67.4m | 28.6m |

2.2 Analysis target and model

Figure 2 shows the analysis targets. Ōtemachi represents a typical high-rise business district, while Kyobashi is a typical mid-rise business district in Tokyo. Ōtemachi and Kyobashi are located to the west and east of Tokyo station respectively. Table 1 illustrates the urban configuration of each domain, as calculated using simulation models. While Ōtemachi has wider spaces between its buildings, those in Kyobashi are crowded.

Figure 3 shows the simulation analysis models based on GIS data. They incorporate an unstructured grid system. The model for Ōtemachi is 1,930 m (W) \times 2,720 m (L) \times 600 m (H), with 379,706 grids. The Kyobashi model is 2,460 m (W) \times 3,630 m (L) \times 600 m (H), with 372,000 grids. The analysis targets are set on some blocks near the center.

2.3 Analysis cases

Tables 2 and 3 show the analysis cases in Ōtemachi and Kyobashi respectively. Ten cases are adopted for Ōtemachi, and nine for Kyobashi. Cases 1-1 and 2-1 are basic cases. Cases 1-0 and 2-0 are without any artificial heat release. Cases 1-3, 1-4, 2-3 and 2-4 involve the buildings' roofs in the target area being changed to high-albedo or greening surfaces. Cases 1-5, 1-6, 1-7, 1-8 and 2-4, 2-5, 2-6 involve high-albedo, greening or water retention of the road and ground surface in the target area. Cases 1-9 and 2-8 concern the release of heat from traffic.

Table 2: Analysis Cases (Ōtemachi)

| Case | Road | | | Ground | Building Roof | | Heat Release | | Release Point | Search Points |
|----------|-----------------|-------------|----------------------|---------------|---------------|-------------|---------------|-------------|---------------|---|
| | Water Retention | High Albedo | Traffic Heat Release | Rate of green | Greening | High Albedo | Sensible Heat | Latent Heat | | |
| Case 1-0 | 0% | 0% | No | 0% | 0% | 0% | 0% | 0% | — | No heat release |
| Case 1-1 | 0% | 0% | No | 0% | 0% | 0% | 30% | 70% | Roof | Basic Case |
| Case 1-2 | 0% | 0% | No | 0% | 0% | 0% | 100% | 0% | Roof | AC Heat: Sensible |
| Case 1-3 | 0% | 0% | No | 0% | 100% | 0% | 30% | 70% | Roof | Roof: Greening |
| Case 1-4 | 0% | 0% | No | 0% | 0% | 100% | 30% | 70% | Roof | Roof: High Albedo |
| Case 1-5 | 100% | 0% | No | 100% | 0% | 0% | 30% | 70% | Roof | Road: Water Retention Ground: Greening |
| Case 1-6 | 0% | 0% | No | 100% | 100% | 0% | 30% | 70% | Roof | Ground: Greening |
| Case 1-7 | 0% | 100% | No | 0% | 0% | 0% | 30% | 70% | Roof | Road: High Albedo |
| Case 1-8 | 0% | 100% | No | 100% | 0% | 0% | 30% | 70% | Roof | Road: High Albedo Ground: Greening |
| Case 1-9 | 0% | 0% | Yes | 0% | 100% | 0% | 30% | 70% | Roof | Traffic Heat |

Table 3: Analysis Cases (Kyobashi)

| Case | Road | | | Ground | Building Roof | | Heat Release | | Release Point | Search Points |
|----------|-----------------|-------------|----------------------|---------------|---------------|-------------|---------------|-------------|------------------------|---|
| | Water Retention | High Albedo | Traffic Heat Release | Rate of green | Greening | High-Albedo | Sensible Heat | Latent Heat | | |
| Case 2-0 | 0% | 0% | No | 0% | 0% | 0% | 0% | 0% | — | No heat release |
| Case 2-1 | 0% | 0% | No | 0% | 0% | 0% | 100% | 0% | Roof: 50% Side: 50% | Basic case |
| Case 2-2 | 0% | 0% | No | 0% | 0% | 0% | 10% | 90% | Roof: 100% | All Heat from Roof AC Heat: Latent 90% |
| Case 2-3 | 0% | 0% | No | 0% | 0% | 0% | 100% | 0% | Roof: 100% | All Heat from Roof |
| Case 2-4 | 0% | 0% | No | 0% | 100% | 0% | 100% | 0% | Roof: 50% Side: 50% | Roof: Greening |
| Case 2-5 | 0% | 0% | No | 0% | 0% | 100% | 100% | 0% | Roof: 50% Side: 50% | Roof: High Albedo |
| Case 2-6 | 100% | 0% | No | 100% | 0% | 0% | 100% | 0% | Roof: 50% Side: 50% | Road: Water Retention Ground: Greening |
| Case 2-7 | 0% | 100% | No | 0% | 0% | 0% | 100% | 0% | Roof: 50% Side: 50% | Road: High Albedo |
| Case 2-8 | 0% | 0% | Yes | 0% | 0% | 0% | 100% | 0% | Roof: 50% Side: 50% | Traffic Heat |

2.4 Analysis conditions

15:00 on July 23rd – a fine day weather-wise – was set for the analysis. The sun was at an attitude of 45.1°, the wind was southerly at a velocity of 3.0 m/s at a height of 74.6 m. The inflow wind velocity is set at 1/4th power profile. The air temperature was 31.6°C, with a relative humidity of 58%. Table 4 shows the building and ground conditions. The temperature inside the building was fixed at 26°C, and the buildings are considered to be made from concrete. The albedo and long wavelength emissivity of concrete were set to 0.2 and 0.9, respectively. Indoor convection heat transfer coefficient was 4.64 [W/m²K].

The ground temperature was fixed at 26.0°C under 0.5 m, and the ground surface was covered with asphalt. The albedo and long wavelength emissivity of asphalt were set to 0.1 and 0.95, respectively. The Discrete Transfer Method (DTM) was used for the radiation simulation. In the CFD simulation, the turbulence model adopted was the standard k-ε model. The side and upper boundary was free slip. At the wall boundary, the wind velocity followed the generalized log law.

Table 4: Building and Ground Conditions

| | | |
|----------|---|---------------------------|
| Building | Wall | Concrete |
| | Albedo | 0.2 |
| | Thickness | 0.2m |
| | Indoor Convection Heat Transfer Coefficient | 4.64 [W/m ² K] |
| | Indoor Air Temperature | 26°C |
| | Long Wavelength Emissivity | 0.9 |
| Ground | Ground | Asphalt |
| | Albedo | 0.1 |
| | Thickness | 0.5m |
| | Long Wavelength Emissivity | 0.95 |
| | Ground Temp. | 26°C (under 0.5 m) |

2.5 Setting of artificial heat release

The buildings' internal heat load was assumed using the product of the total floor area and the unit heat load intensity (Research and Exploratory Committee 2003). While all air-conditioning heat was assumed to be released from the roof in the Ōtemachi area, half of the air-conditioning heat was assumed to be released from the roof with the rest from the sides of the buildings in the Kyobashi area because the Ōtemachi urban block is composed of large buildings which have cooling towers, whereas many small buildings in the Kyobashi area have installed single-room air-conditioners.

3. ANALYSIS RESULTS

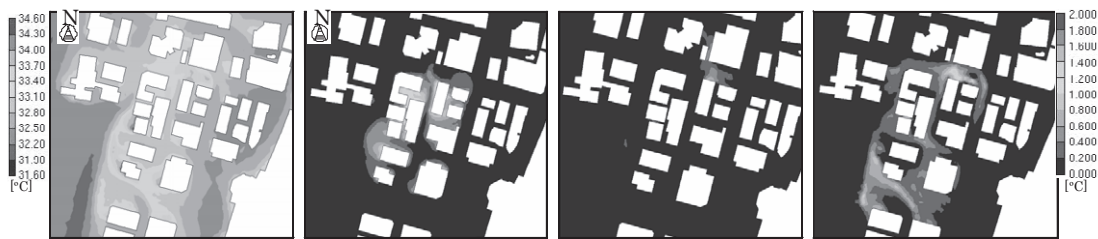
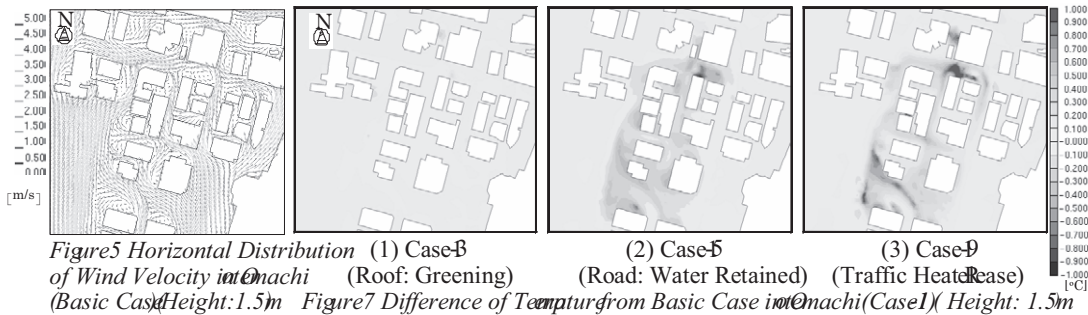
3.1 Ōtemachi area

Horizontal distribution of wind velocity and air temperature: Figure 4 shows the horizontal distribution of the wind velocity at a height of 1.5 m throughout Ōtemachi in order to evaluate the pedestrian area. Figure 5 illustrates the horizontal distribution of the air temperature in Case 1-1. There is a relationship in so far as that the air temperature is higher where the wind is weaker. In particular, the wind is weakened and the air temperature rises on the leeward side of the buildings.

Figure 6 shows the differences in air temperature from the basic case (Case 1-1) at a height of 1.5 m. Image (1) shows the result for Case 1-3, in which the roof surface is greened. In Case 1-3, there is not a large difference. Changing the roof material hardly affects the air temperature in the pedestrian area. Image (2) presents Case 1-5, in which the ground surface is changed into a water-retaining material. The air temperature broadly falls. This decrease is particularly noteworthy on the leeward side of the buildings. Image (3) presents Case 1-9, in which heat is released from traffic. The same trend as in Case 1-5 is exhibited, and the maximum increase in air temperature is more than 1°C.

Horizontal Distribution of Impact Index: In order to compare the influence of surface temperature, air-conditioning heat release and traffic heat release, the impact index, as presented by the author ^[Note 1] (Chen H. et al. 2007) was calculated. Figure 8 shows the Horizontal Distribution of

Impact Index at 1.5 m height. Image (1) shows the affect of a surface temperature rise of 1°C. The surface temperature of the buildings has a substantial effect on the air temperature. Specifically, it affects the small canopy space and areas next to the buildings remarkably. Image (2) presents the air-conditioning heat release. This has no discernible effect on the air temperature in the pedestrian area. Image (3) is of the traffic heat release. Compared to the building surfaces, this affects a larger area.

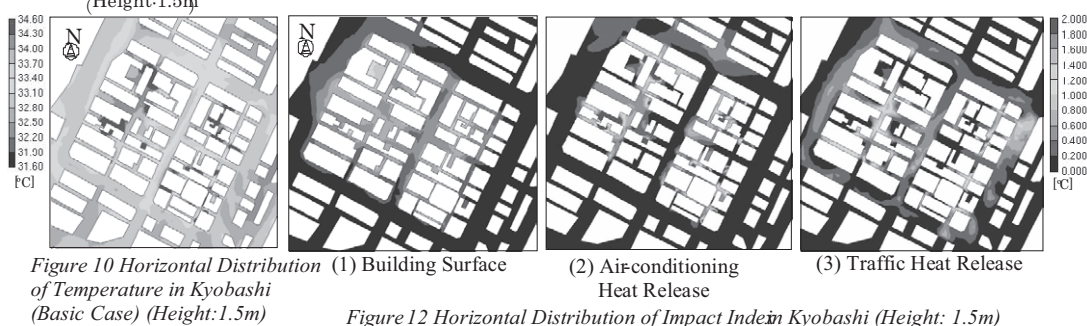
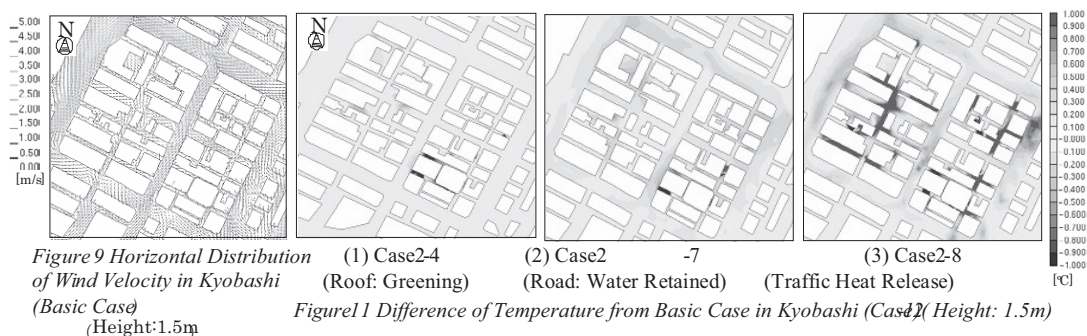


3.2 Kyobashi area

Horizontal distribution of Wind velocity and air temperature: Figure 8 shows the horizontal distribution of wind velocity at a height of 1.5 m in Kyobashi to evaluate the pedestrian area. Figure 9 shows the horizontal distribution of air temperature. As in Otomachi, there is a relationship between the wind and air temperature. However, compared to Otomachi, the maximum air temperature is much higher because the buildings are crowded together and the wind has limited opportunity to exhaust the heat from the small canopies in Kyobashi.

Figure 10 shows the differences in air temperature compared to the basic case (Case 2-1) at a height of 1.5 m. Image (1) is of Case 2-4, in which the roof is greened. Image (2) shows Case 2-7, in which the ground and roads are greened or changed to water-retaining materials. While changing the roof material only cuts the air temperature a little, changing the road and ground materials sharply curtails the air temperature. As in Otomachi, the air temperature falls in small canopies and where the wind is weak. Image (3) concerns Case 2-9, which is of traffic heat release. The air temperature increases locally. Compared with on the road, in the small canopies, it increases considerably. The maximum increase exceeds 1°C. There are several locations where the air temperature decreases. The reason is assumed to be that the flow field has been significantly affected by the large traffic heat release.

Horizontal Distribution of Impact Index: Figure 11 illustrates horizontal distribution of the impact index. Image (1) shows the effects of the building surfaces. These have a broad effect on the target area. The impact is especially pronounced near to the buildings and in small canopies where the wind is weak. Image (2) shows the difference from air-conditioning heat release compared to the basic case (Case 2-1). Because half of the air-conditioning heat release is from the sides of buildings in the Kyobashi area, its impact is massive and has a strong local effect. Near to any sideways release of heat generates an air temperature increase in excess of 2°C. Image (3) concerns traffic heat release. Compared with air-conditioning heat release, its effect is primarily along the road, but it also has a local effect, such as in small canopies.



4. COMPARISON BETWEEN ŌTEMACHI AND KYOBASHI AREAS

In order to compare the effect of urban block configurations, the mean velocity, mean air temperature, and mean impact index at 1.5 m were calculated. Table 5 shows the mean air temperature and wind velocity in the target area. In both areas, Cases 1-0 and 2-0, in which there is no heat released, the mean wind velocity decreases. Furthermore, the release of traffic heat increases the air temperature by more than 0.2°C in both areas. In addition, the wind velocity clearly increases in Cases 1-9 and 2-8.

Table 6 shows the mean impact index. In Ōtemachi, because the buildings are high, the release of air-conditioning heat from roofs hardly has any effect. For the same reason, the roofs do not have any tangible effect although their surface temperature is high. In Kyobashi, the roofs and south-facing walls have a pronounced effect because the buildings are mid-rise types and the surface temperature of south-facing walls and roofs are higher than the other surfaces. Furthermore, the release of air-conditioning heat has a notable effect too.

Table 5: Mean Air Temperature and Wind Velocity

| Ōtemachi | | | Kyobashi | | |
|----------|---------------------------|--------------------------|----------|---------------------------|--------------------------|
| Case | Mean Air Temperature [°C] | Mean Wind Velocity [m/s] | Case | Mean Air Temperature [°C] | Mean Wind Velocity [m/s] |
| 1-0 | 32.96 | 1.47 | 2-0 | 32.99 | 0.90 |
| 1-1 | 32.96 | 1.51 | 2-1 | 33.19 | 1.19 |
| 1-2 | 32.96 | 1.49 | 2-2 | 32.97 | 1.10 |
| 1-3 | 32.96 | 1.49 | 2-3 | 33.07 | 1.26 |
| 1-4 | 32.96 | 1.49 | 2-4 | 33.20 | 1.16 |
| 1-5 | 32.82 | 1.45 | 2-5 | 33.18 | 1.15 |
| 1-6 | 32.93 | 1.48 | 2-6 | 33.05 | 1.17 |
| 1-7 | 32.86 | 1.49 | 2-7 | 33.07 | 1.25 |
| 1-8 | 32.82 | 1.48 | 2-8 | 33.57 | 1.28 |
| 1-9 | 33.16 | 1.58 | | | |

Table 6: Mean Impact Index [°C]

| | Ōtemachi | Kyobashi |
|------------------|--------------|--------------|
| East | 0.052 | 0.005 |
| West | 0.042 | 0.052 |
| South | 0.060 | 0.117 |
| North | 0.037 | 0.020 |
| Roof | 0.004 | 0.108 |
| All Surfaces | 0.195 | 0.303 |
| Air-conditioning | 0.019 | 0.205 |
| Traffic | 0.232 | 0.381 |

5. CONCLUSIONS

(1) In the high-rise Ōtemachi and mid-rise Kyobashi business districts, coupled simulations of conduction, radiation and convection have been performed. With cases showing changes to the heat release point and means of air-conditioning, as well as greening, high surface albedo, and traffic volume, various measures for moderating the thermal environment are quantitatively compared.

(2) In both of the Ōtemachi and Kyobashi areas, artificial heat release from traffic increases the air temperature in the overall target area at a height of 1.5 m; in particular, the leeward sides of the buildings are strongly affected. By the same token, the relaxation measures concerning the ground and road surfaces affect both areas.

(3) While the heat released from the air-conditioning systems does not increase the air temperature at a height of 1.5 m in Ōtemachi, it increases the air temperature locally; and in narrow streets with low wind velocity, the air temperature increase is especially notable. It was shown that the effectiveness of the relaxation measures differs depending on the configuration of the urban blocks.

NOTE

The impact index for outdoor thermal environment focuses on sensible heat to evaluate the influence on air temperature increases of open

spaces from heat flux from building walls and the ground, and artificial heat release.

a) Impact index of sensible heat from building surface to outdoor thermal environment [$^{\circ}\text{C}$]

$$imp_{jw} = \left(\frac{\Delta T_{airj}}{\Delta T_{walli}} \right) \times (T_i - T_{ai})$$

b) Impact index of heat release from building equipment to outdoor thermal environment [$^{\circ}\text{C}$]

$$imp_{jb} = (T_{jb} - T_j)$$

c) Impact index of traffic heat release to outdoor thermal environment [$^{\circ}\text{C}$]

$$imp_{jr} = (T_{jr} - T_j)$$

Abbreviations:

imp_{jw} : Impact index of building surface at cell j

imp_{jb} : Impact index of heat release from building equipment at cell j

imp_{jr} : Impact index of traffic heat release at cell j

ΔT_{airj} : Air temperature rise at cell j (case of high wall temperature – basic case)

ΔT_{walli} : Surface temperature rise at wall i (i : north, south, east, and west)

T_i : Surface temperature of wall i

T_{ai} : Mean air temperature of cell attached to wall

T_{jb} : Air temperature of cell j considering air-conditioning heat release

T_j : Air temperature of cell j in basic case

T_{jr} : Air temperature of cell j considering traffic heat release

REFERENCES

- Chen Hong et al., 2007, Study on the Impact of Buildings on the Outdoor Thermal Environment Based on a Coupled Simulation of Convection, Radiation, and Conduction, ASHRAE Transactions, Volume 113, Part 2.
- Chen Hong et al., 2004, Study on outdoor thermal environment of apartment block in Shenzhen, China with coupled simulation of convection, radiation and conduction, Energy and Buildings, Volume 36, 1247~1258
- Research and Exploratory Committee for Artificial Heat of the Heat Island Phenomenon, 2003, Report of the Heat Island Relaxation Measures by Depressed Artificial Heat in Urban Areas in 2003. (In Japanese) <http://www.env.go.jp/air/report/h16-05/>
- Yoshida Shinji et al., 2000, CFD Prediction of Thermal Comfort in Microscale Wind Climate, Computational Wind Engineering 2000, 27~30

DEVELOPMENT OF E-LEARNING CONTENTS FOR INCREASING EMERGENCY RESPONSE CAPACITY OF DOCTORS AND NURSES IN KEY DISASTER HOSPITALS

MIHO Y. OHARA¹, YOICHI KITSUTA², NAOKI YAHAGI²,
FUJIO KOYAMA³ SANAE MIYAZAKI and KIMIRO MEGURO⁴

¹Center for Integrated Disaster Information Research,
Interfaculty Initiative in Information Studies,
The University of Tokyo, Japan

²The University of Tokyo Hospital, Japan

³Division for Environment, Health and Safety,
The University of Tokyo, Japan

⁴International Center for Urban Safety Engineering,
Institute of Industrial Science, The University of Tokyo, Japan

ohara@iis.u-tokyo.ac.jp

ABSTRACT

Hospitals should accommodate a lot of seriously-injured victims in case of a big earthquake. The best way to increase hospital's emergency response capacity is to increase the number of the doctors, nurses and other staffs who can imagine the disaster situations realistically so that they can take proper actions before a future event. In this paper, an e-learning system to train doctors and nurses on emergency medical responses is presented. The-learning program consisted of three parts. The first part aimed at understanding the priorities of emergency medical response through decision-making simulation and learning detailed procedures on hospital disaster manual. The second part aimed at learning how to quickly triage many patients. The third part aimed at acquiring practical techniques for triage and treatment through decision-making simulations. In decision-making simulations, a learner could experience typical confusing situations that may occur after an earthquake and imagine his/her reactions in each case. About 250 doctors and 800 nurses finished learning in September, 2007. Questionnaires were done before and after the-learning in order to assess the effect of the e-learning. More than 80% of the learners answered that they could imagine the disaster situation by e-learning. The authors think that e-learning is a very effective tool to share the common images of disaster situations among staffs and simultaneously familiarize them with the emergency medical response manual.

1. INTRODUCTION

Recently, Japan is at risk of being hit by several huge earthquakes such as Tokyo Inland Earthquake, Tokai Earthquake, Tonankai Earthquake and

Nankai Earthquake. Hospitals should accommodate a lot of seriously-injured victims in case such big earthquakes occur in the future. The best way to increase hospital's emergency response capacity is to increase the number of doctors, nurses and other staffs who can imagine the disaster situations realistically so that they can take proper actions before a future event. In Japan, key disaster hospitals must have disaster training every year. However, the number of the staffs who join it is very limited because hospitals cannot stop their daily routine of caring for patients. As a result, it is very difficult for hospital staff to get familiar with the emergency medical response manual, even if informative manuals are published.

In this paper, an e-learning system to train doctors and nurses on emergency medical responses is presented. This system was developed and operated at the University of Tokyo Hospital, one of the key disaster hospitals in Tokyo, Japan. About 250 doctors and 800 nurses finished learning in September, 2007. Questionnaires were done before and after the learning and answers were analyzed in order to survey the effect of e-learning.

2. OUTLINE OF E-LEARNING SYSTEM

2.1 Benefits of e-learning system

After the 1995 Kobe Earthquake, key disaster hospitals were assigned to accommodate seriously-injured disaster victims. Large scale hospitals with earthquake resistant facilities are usually selected as key disaster hospitals. A key disaster hospital must have more than 200 beds. The average number of beds of key disaster hospitals in Tokyo is about 600. Large hospitals have many staffs and it is difficult to build the common understanding of emergency medical responses among them. Especially, nurses work two or three shifts and it is impossible to give seminars to all of them at the same time. In large hospitals, staffs are usually doing their daily works via intranet system and they are familiar with using PC. In this situation, e-learning system may be useful because all the staffs can study the common material at their most convenient time.

2.2 Objectives of e-learning

The purpose of disaster medicine is "to provide appropriate medical treatment at the right place and at the right time." In order to achieve this purpose, the Advanced Life Support Group in the U.K. proposed seven priorities of emergency medical responses in its education program named "Major Incident Medical Management and Support (MIMMS)". These priorities are called as "CSCATTT" taking initials of each step. The first step of emergency medical response is to recognize their roles. The second step is to establish their safety by wearing gloves, masks and helmets. The third step is to prepare equipments for communication and the fourth is to assess whether there are victims and building damage. After that, triage and treatment will start. Patients will be transported if necessary. This time, e-

learning system was developed to study what to be done in each stage of "CSCATTT".

C: Command
 S: Safety
 C: Communication
 A: Assessment
 T: Triage
 T: Treatment
 T: Transport

2.3 Methodology to develop e-learning system

e-learning system was developed by using the software published by Sharp System Product Corporation. This consists of software for creating educational materials and managing education on the web. Learners can access the system through the intranet/internet at any time. Only a web browser is necessary on the user side and new capital investment is not required for them. Answers to the questions are recorded on the server and the e-learning manager can check the understanding level of each learner.

2.4 Contents of e-learning

The-learning program consisted of three parts. The contents of each part and the number of web page are listed in the Table 1. The first part aimed at understanding the priorities of emergency medical response through the decision-making simulation and learning detailed procedures on the hospital disaster manual. Figure 1 is an example of a page of the decision-making simulation. In the simulation, a learner could experience typical confusing situations after an earthquake occurred and imagine his/her proper reaction in each case. In the simulation, the best response is to return to the staff station as soon as possible and get instructions on his/her role from the leader because C:Command is the first priority among all. When he/she does not choose the right answer, he/she has to do the simulation again following the advice. The second part aimed at learning how to quickly triage many patients. It contained movies instructing how to triage patients and several triage exercises. The third part aimed at acquiring practical techniques for triage and treatment through decision-making simulations.

Photos and video images taken during past disasters and disaster drills were used for comprehensive explanation of the hospital disaster manual.

Table 1 Contents of each part of the e-learning

| No. | Classification | Contents | CSCATTT | Pages |
|-----|---|--|---------|-------|
| 1 | First action at the time of a big earthquake | | | |
| | Knowledge | The possibility of a big inland earthquake in the capital area | | 2 |
| | Explanation | The aim of this e-learning | | 1 |
| | Simulation and Questions | What should be done just after a big inland earthquake in a hospital ward? | Command | 8-19 |
| | | What should be done when going back to a staff station? | Safety | 3 |

| No. | Classification | Contents | CSCATTT | Pages |
|----------|--|---|---------------|-------|
| | | What should be done at a staff station? | Command | 2 |
| | Answers and a Commentary | A priority at the time of disaster | | 1 |
| | | Staff role allotment | Command | 1 |
| | | How to communicate between a ward and the hospital control center | Communication | 1 |
| | | Checklist of each room and ward | Assessment | 1 |
| 2 | Medical response at the time of a big earthquake 1: Basic triage method | | | |
| | Explanation | Review of No.1 | | 1 |
| | Simulation and Questions | What should be done at a staff station? | Command | 2 |
| | | The role of a leader of doctors / nurses | Command | 2 |
| | | What is needed when going to a catchment area? | | 2 |
| | Explanation | What is triage? | Triage | 1 |
| | | Study how to triage according to START method through video | Triage | 6 |
| | Questions and Answers | Triage exercise (4 cases) | Triage | 4 |
| 3 | Medical response at the time of a big earthquake 2: Triage simulation | | | |
| | Explanation | Review of No.2 | | 1 |
| | Simulation and Questions | How to perform the triage in a real ward | Triage | 10 |
| | Explanation | What is treatment at the time of disaster? | Treatment | 4 |
| | Questions and Answers | What is needed for treatment at the time of disaster? | Treatment | 2 |

2. 地震時の初動対応シミュレーション

状況: 大地震発生!!



平日の午後2時です。点滴の差し替えが必要になり、あなたはその患者の病室への廊下を歩いています。途中で、お見舞いに来た70歳代の女性に、病室を尋ねられました。

ちょうどその時、激しい揺れが起こり、あなたは立っていることができません。大地震が発生したようです。

気がつくと、廊下にあった点滴スタンドの幾つかが横倒しになっているのが見えました。70歳代の女性も倒れており、“うっ”と弱々しく唸っています。

Q1: あなたはこの時どうしますか？

文頭のボタンを一つ選んでクリックしてから、「次へ」のボタンを押してください。

「誰か来て下さい」と助けを呼ぶ

倒れた見舞い客の反応を確認した後、呼吸を数える

まずナースコールのあった部屋へ向かう

Figure 1: Decision-making simulation in the first part of the e-learning



Figure 2: Explanation of response manual in the first part of the e-learning

3. EFFECT OF E-LEARNING SYSTEM

Login ID, password, and URL were sent to doctors and nurses of the University of Tokyo Hospital on August 21, 2007 and they were requested to carry out the e-learning before the disaster drill on September 4, 2007. Questionnaires were done before and immediately after the e-learning to measure its effectiveness. As of October 1, all the data was summarized and the trends of the answers were analyzed.

3.1. Characteristics of learners

The numbers of doctors who learned the first, second, and third parts were 310, 275 and 256, respectively. The number of learners amounted to 15% of the total number of doctors in the hospital. 20% The numbers of nurses who learned the first, second and third parts were 844, 786 and 795, respectively. The number of learners amounted to 70% of the total number of nurses in the hospital. The number of doctors and nurses who finished e-learning was 10 times the number of the participants of the annually held hospital disaster drill. Through the e-learning, many staffs could have a common understanding of a disaster situation.

Figure 3 shows when doctors and nurses learned each part. Most of the doctors learned during daytime. On the other hand, learning time of the nurses had three peaks at 4-6 p.m., 9 a.m. and midnight. It was verified that e-learning system has the advantage that learners can study at their most convenient time.

3.2. Disaster awareness before-learning

Before e-learning, a questionnaire about disaster awareness was done. Q1 was a question asking if the respondent thought that a big earthquake would occur in the near future. About 80% of doctors and nurses answered

that they thought it would occur. Q2 was a question asking if they felt uneasy when they imagined what to do in case of a big earthquake. 94% of the nurses and 77% of the doctors felt uneasy as shown in Figure 4. More nurses had anxieties than doctors. There was no difference of answers according to ages and leading positions of the learners.

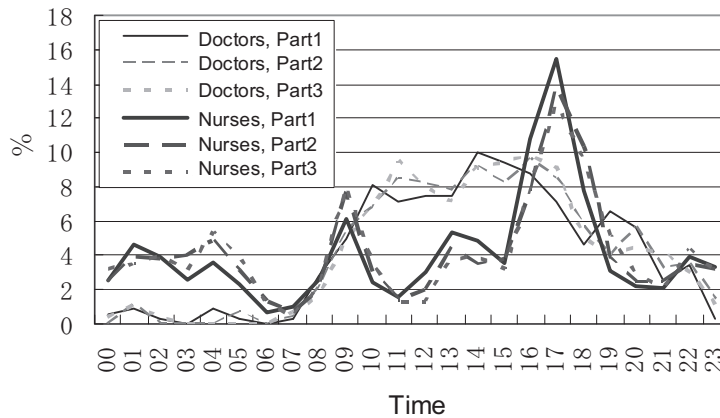


Figure 3: Learning time of doctors and nurses

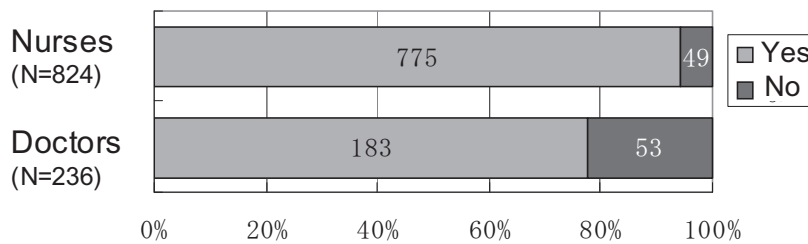


Figure 4: Learners' anxiety to a big earthquake

3.3. Effect of decision-making simulation in the first learning

The decision-making simulation in the first part of the-learning aimed at making learners imagine how severe a disaster situation was. After the-learning, a questionnaire was done in order to survey if the decision-making simulation could give them a real disaster image. Figure 5 shows the learners' feelings after the simulation. 80% of the doctors and 90% of the nurses were able to image the disaster situation, but only 30% of the doctors and 15% of the nurses were confident that they would respond well in case of an earthquake. 50% of the doctors and 75% of the nurses felt uneasy even after finishing the-learning. It was verified that the decision-making simulation by e-learning succeeded in giving disaster image to learners but additional training was necessary for giving them confidence on their appropriate medical response.

Figure 6 shows the feelings of leader nurses and other nurses after the decision-making simulation. Leader nurses are those with positions such as chief nurses or sub-chief nurses. The ratio of leader nurses who had confidence on a proper response in case of an earthquake was twice the ratio of other nurses. The decision-making simulation in the e-learning was especially effective for leader nurses.

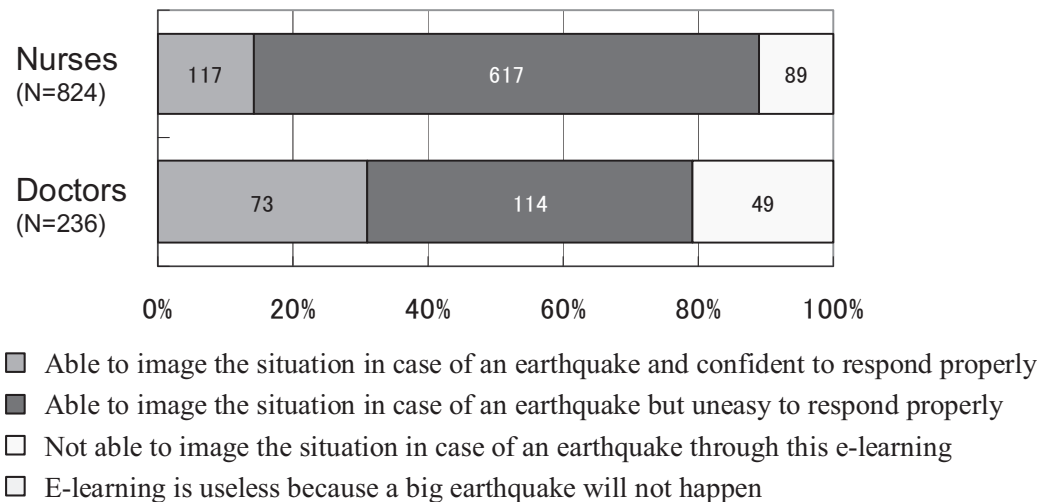


Figure 5: Feelings after the decision-making simulation

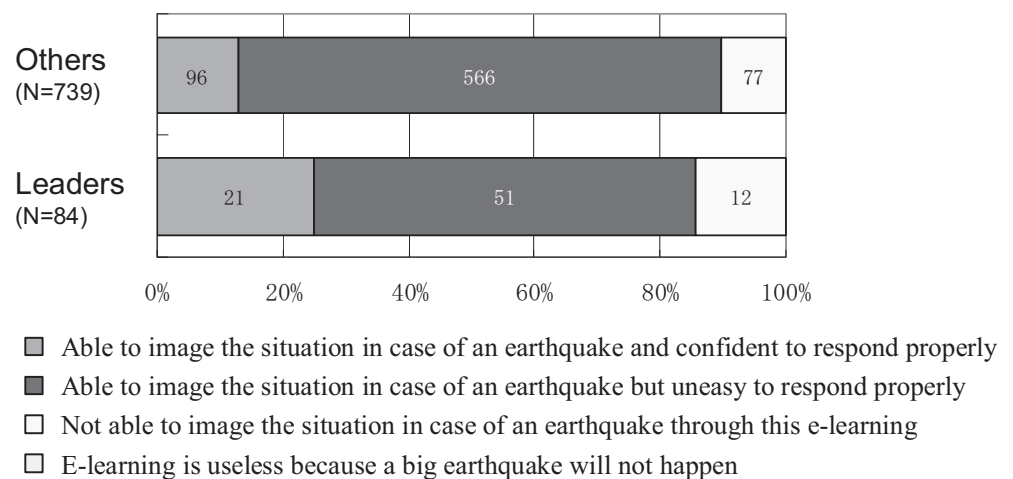


Figure 6: Nurses' Feelings after the decision-making simulation

3.4. Effect of all the-learning

Figure 7 shows the feelings of doctors and nurses after finishing all the-learning. About 70% of the doctors and nurses wanted to learn about other disaster responses such as fire or manmade disasters because they felt an e-learning was useful. 23% of the doctors and 43% of the nurses felt necessary to have physical training because e-learning was only training on website. The ratio of the nurses who felt necessary to have physical training was almost twice the ratio of doctors. 10% of the doctors and nurses felt that the amount of e-learning was too much because it consisted of three parts. The learners who felt that e-learning was meaningless were very few.

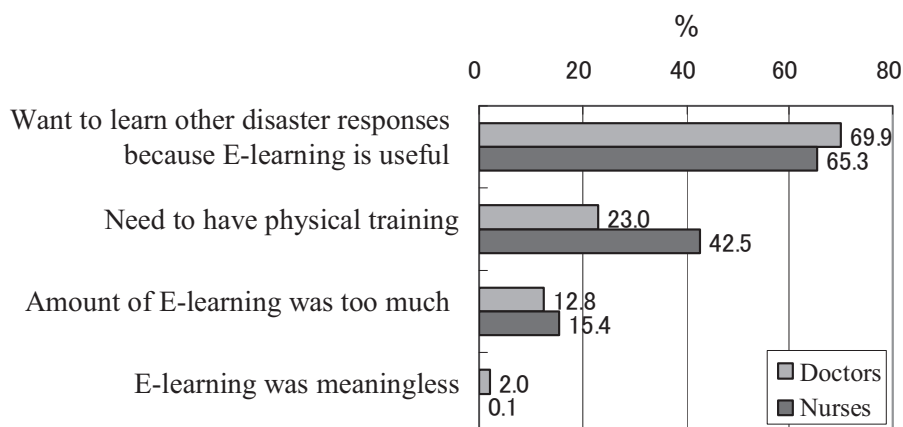


Figure 7: Feelings after all the e-learning

4. CONCLUSIONS

In this paper, an e-learning system to train doctors and nurses on emergency medical responses was presented. The contents were developed and operated at the University of Tokyo Hospital, one of the key disaster hospitals in Tokyo, Japan. It was developed using software and only a web browser was necessary on the learners' side. About 250 doctors and 800 nurses finished learning in September and October, 2007. The number of learners amounted to 15% of the total number of doctors and 70% of the total number of nurses in the hospital.

The-learning program consisted of three parts. The first part aimed at understanding the priorities of emergency medical response through decision-making simulation and learning detailed procedures on the hospital disaster manual. 80% of the doctors and 90% of the nurses were able to image the disaster situation. It was verified that the decision-making simulation succeeded in giving disaster image to learners but additional training was necessary to give them confidence of their emergency medical response. Compared with the effect for leader nurses and other nurses, the decision-making simulation was especially effective for leader nurses.

The second part aimed at learning how to triage numerous patients quickly. The third part aimed at acquiring practical techniques for triage and treatment through decision-making simulation. After all the-learning, about 70% of the doctors and nurses wanted to learn other disaster responses because they felt e-learning was useful. 23% of the doctors and 43% of the nurses felt necessary to have physical training.

Based on this study, the authors think that e-learning is very effective tool to share the common images of disaster situations among hospital staffs and familiarize them with the emergency medical response manual. It could also motivate learners to train more against other disasters. It will be more effective if both e-learning and physical training are provided. The authors are now developing other e-learning programs and training courses combining e-learning and physical training.

ACKNOWLEDGEMENT

The authors would also like to express our gratitude to Mr, H. Tsukada, Mr. K. Akatsuka, Dr. K. Harada in the University of Tokyo Hospital for their invaluable comments to the e-learning contents.

REFERENCES

- Tokyo Prefecture, 2003. *Guideline of installation and operation of key disaster hospitals*, Japan.
- Advanced Life Support Group, 2005. *MIMMS: Major Incident Medical Management and Support*, 2nd Edition.

DYNAMIC BEHAVIOUR OF JAMUNA MULTIPURPOSE BRIDGE DUE TO VEHICULAR LOADING

MEHEDI AHMED ANSARY, SYED ZILLUR RAHMAN and RAQUIB AHSAN
Department of Civil Engineering, BUET, Bangladesh
ansary@ce.buet.ac.bd

ABSTRACT

The Jamuna Multipurpose Bridge is the longest and most important bridge in Bangladesh which has established the long cherished road link between the East and West of Bangladesh. The bridge is located in a seismically active region. Seismic pintles have been used for seismic protection of the bridge. The bridge was instrumented with accelerometers in order to monitor the performance of the seismic devices as well as overall dynamic behavior. Weight and speed of a vehicle are major concern for the bridge. Study has been conducted to observe the behavior of the bridge due to vehicular movement in different weight and speed limit.

Train induces a lot of vibrations in the bridge when it is in higher speed. Response of the bridge due to heavily loaded truck with high speed is greater than that of the low speed train. When these kinds of trucks frequently move on the bridge their response will be a major concern for this bridge. Two weight groups of vehicle can be noticed. One group weighs between 11 to 15 tons, which are buses and other group of vehicles 19 to 22 tones, which are trucks. From the response between two weight groups less overlapping in acceleration is found in the longitudinal direction and less overlapping in velocity is found in the transverse direction. Thus acceleration data of the longitudinal direction and velocity data of the transverse direction may be used for detection of overweight vehicles from the bridge response. If the response of the bridge exceeds 0.70 cm/sec^2 in longitudinal direction then the vehicle may exceed the weight limit of 20 tons or the speed limit of 40 km/h or the both. Then the vehicle can be identified. Previously train used to move at higher speed, therefore response of bridge was higher. Later the train is restricted to run in a lower speed. Response due to two broad gauge rails is also studied. They both have a speed of 17 km/h. But the response of presently recorded data due to train movement is larger than the previously recorded data. This may be due to the recently occurred cracks in the bridge.

1. INTRODUCTION

The Jamuna Multipurpose Bridge is instrumented with accelerometers in order to monitor overall dynamic behavior. The accelerometers are also used for different types of vehicular and train data acquisition by keyboard

triggering. Weight and speed of vehicle as well as speed of train is the major concern for the bridge. An analysis has been done to observe the behavior of the bridge due to vehicular movement under different speed and weight limit. Train induces a lot of vibrations in the bridge when it is in higher speed.

2. COLLECTION OF DATA

Ambient data, Traffic data, Train data are recorded by the seismic instrumentation system. Sensors collect input data (earthquake excitation or noise) and record them. Data is triggered by giving an impulse in the sensors. This is done by keyboard trigger using Altus QuickTalk (ATLUS QuickTalk, 1996-2000) and QuickLook (ATLUS QuickLook, 1994-2000) software. After collecting data, it is necessary to process this data by software. In this analysis, Microcal Origin (Origin, 1991-2000) is used to obtain corrected acceleration time history and Fast Fourier Transform of noise data from various stations. Time history plots of 13 bridge sensors can be produced simultaneously by the system installed in the bridge. Various ambient, train, truck and bus data are collected by this installed system. Data for individual train can be collected by these accelerometers with the help of GPS. The data of individual vehicle and also in a group are collected with respect to the GMT time. After collection of these data, the individual data is separated according to the time of recording. Speed limit of vehicles on the Jamuna Bridge is 40 km/h. It can be observed that trucks and buses are frequently exceeding the speed limit. Speed of a vehicle is measured with the help of a speed gun and weight of a vehicle is measured by the weighing machines installed at both sides of the bridge.

3. RESPONSE OF THE BRIDGE IN DIFFERENT LOADING

The data were collected from the instrument in raw format. This data were corrected with the help of the SMA and Microcal Origin. Time histories of earthquake events or vehicular response values are obtained after corrections. Time history data on deck (BR5) of trains, trucks and buses are recorded in different time. This time domain data are converted to frequency domain data with the help of Fourier Transform. Following the Caltech format, Fourier spectrum is evaluated with the software Origin 5.0. For this analysis 45 Hz of cut off frequency is used. Then it is smoothen with 15-point Adjacent-Averaging technique. This smoothen technique is perform to get smooth curves and clear peaks. Fourier spectrum of amplitude vs. frequency is plotted with this smoothened data. Peaks of lower frequencies of the Fourier Spectrum are important for a bridge from earthquake consideration.

Train and truck excite the bridge with comparatively greater load. Due to huge input energy bridge excites close to its predominant frequency which is described earlier. Moreover other vehicles like bus, motorcycle, zip etc. have lower energy input. Therefore, peaks are not clear in the Fourier Spectrum. BR 1, BR 5 and BR 11 are the sensors in transverse direction.

These sensors show predominant frequency of 1 Hz and 3 Hz in the Figures 1, 5 and 10 respectively for different train, truck and bus data recorded in different times. BR 2, BR 6 and BR 10 are the sensors in longitudinal direction. These sensors show a predominant frequency of 2 Hz in Figures 2, 6 and 9 respectively. BR3, BR4, BR7 and BR9 are the sensors in the vertical direction. These sensors show a predominant frequency of 2.5 Hz in Figure 3, 4, 7 and 8 respectively.

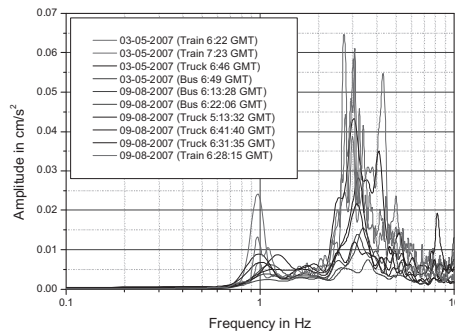


Figure 1: Fourier Spectrum of BR1X for various traffic loads.

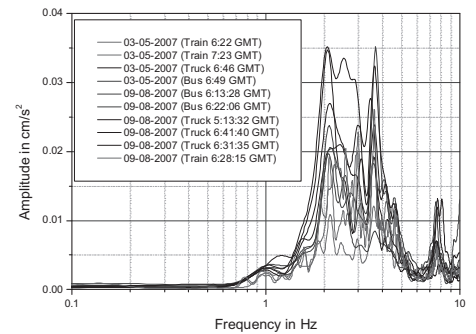


Figure 2: Fourier Spectrum of BR2Y for various traffic loads.

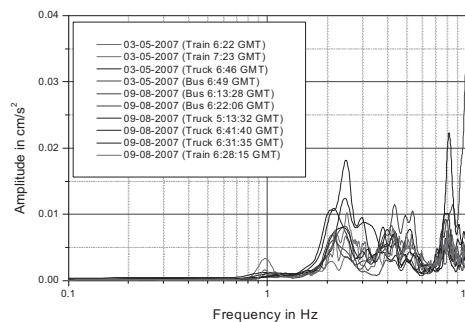


Figure 3: Fourier Spectrum of BR3Z for various traffic loads.

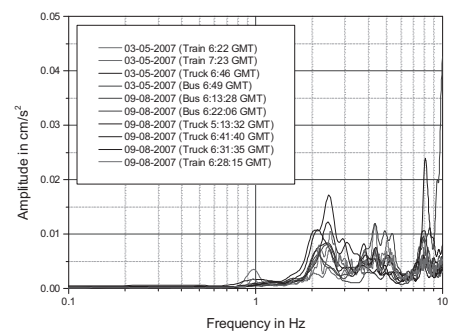


Figure 4: Fourier Spectrum of BR4Z for various traffic loads.

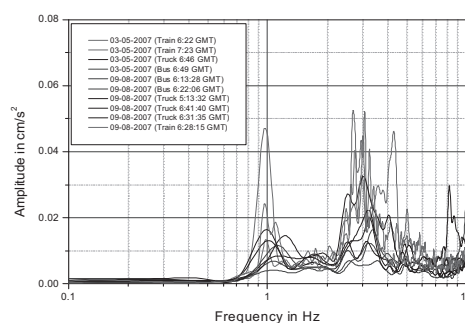


Figure 5: Fourier Spectrum of BR5X for various traffic loads.

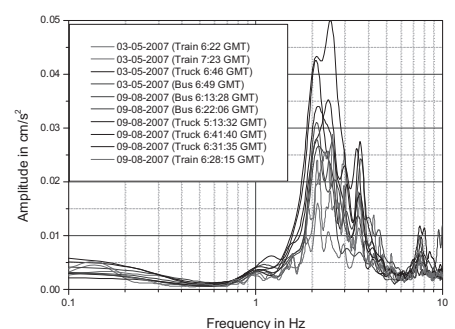


Figure 6: Fourier Spectrum of BR6Y for various traffic loads.

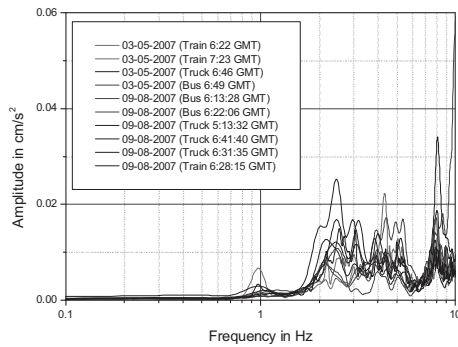


Figure 7: Fourier Spectrum of BR7Z for various traffic loads.

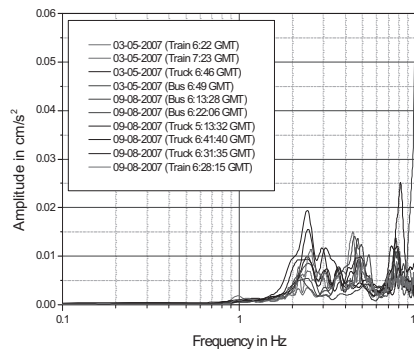


Figure 8: Fourier Spectrum of BR9Z for various traffic loads.

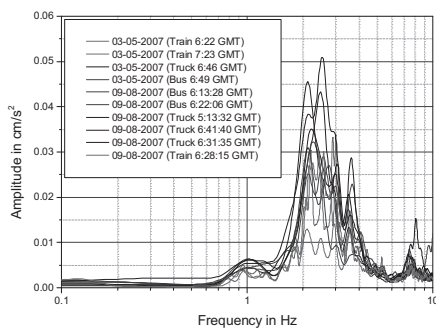


Figure 9: Fourier Spectrum of BR10Y for various traffic loads.

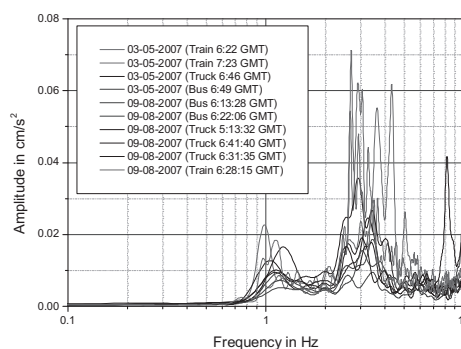


Figure 10: Fourier Spectrum of BR11X for various traffic loads.

The dynamic response of a bridge due to passing a vehicle depends on the weight and velocity of the vehicle. Jamuna Multipurpose Bridge is a busy transport facility. So, superposition occurs between responses of successive passing vehicles. Moreover, wind, wave and stream of river water cause ambient vibration, which also have effect on the response. If a heavy vehicle (e.g. train) passes, then other vehicles have unrecognizable effect on the response of the bridge. For a very small weight vehicle (e.g. motorcycle) no visible impact on the response of the bridge occurs. Maximum acceleration of the train data is the smallest for a train without any simultaneous traffic. Such data were recorded on a hartal day. Lower frequency peaks of the Fourier Spectrum of the recorded data are important for bridges from seismic point of view.

4. RESPONSE OF THE BRIDGE TO DIFFERENT VEHICLE WEIGHT

For the present study traffic data and ambient data were collected at different times. It is observed that the trucks and buses that passed through the bridge are in the range of 10 tons to 22 tons of weight. It is obvious that as the weight of traffic increases the acceleration, velocity and displacement of bridge structure also increase. In the transverse and longitudinal direction of the bridge deck, the acceleration increases with the increase of weight of

vehicle. Figures 11 to 12 describe the above findings. The velocity and displacement also increase with increase of weight. Figures 13 to 16 describe the above findings.

In-fact, two weight groups of vehicle can be noticed from the graphs. One group weighs between 11 to 15 tons, which are buses and other group of vehicles weighting between 19 to 22 tones, which are trucks. From Figure 11, it is clearly seen that the two groups produce different response of the bridge. Buses cause acceleration of 1.3 to 2.1 gals in transverse direction and 0.8 to 1.1 gals in longitudinal direction. These vehicles caused velocity of 0.02 to 0.04 cm/sec in transverse direction and 0.037 to 0.057 cm/sec in longitudinal direction. Displacement in the range of 0.045 mm to 0.076 mm in transverse direction and 0.058 mm to 0.2 mm in longitudinal direction was observed for the same vehicles.

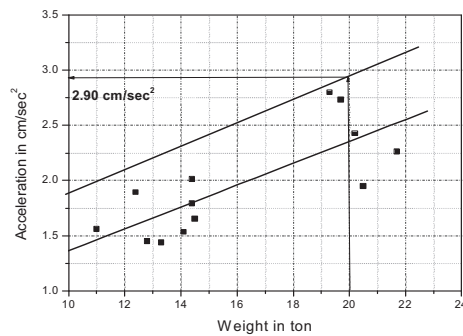


Figure 11: Acceleration of bridge deck (BR5) in transverse direction

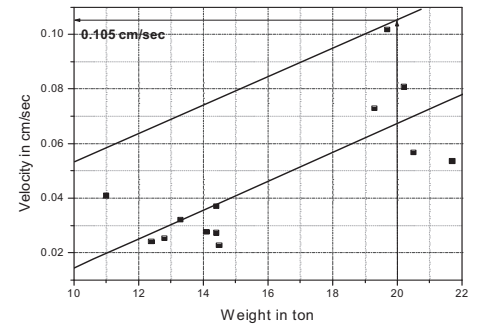


Figure 12: Acceleration of bridge deck (BR6) in longitudinal direction

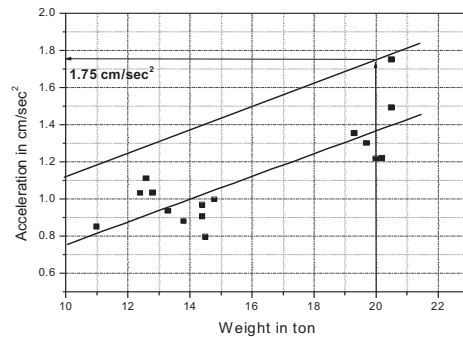


Figure 13: Velocity of bridge deck (BR5) in transverse direction

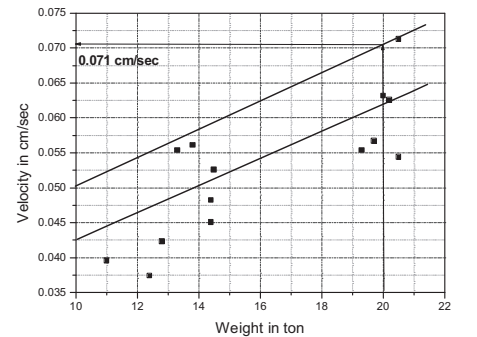


Figure 14: Velocity of bridge deck (BR6) in longitudinal direction

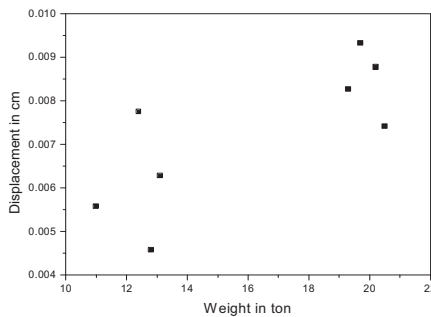


Figure 15: Displacement of bridge deck (BR5) in transverse direction

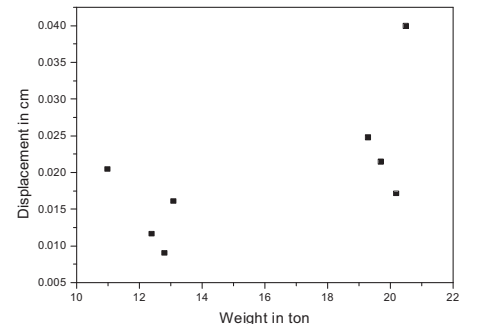


Figure 16: Displacement of bridge deck (BR6) in longitudinal direction

Trucks cause acceleration of 2.0 to 2.8 gals in transverse direction and 1.25 to 1.8 gals in longitudinal direction. These vehicles caused velocity of 0.055 to 0.10 cm/sec in transverse direction and 0.055 to 0.064 cm/sec in longitudinal direction. Displacement in the range of 0.075 mm to 0.094 mm in transverse direction and 0.17 mm to 0.4 mm in longitudinal direction was observed for the same vehicles. From the response between two weight groups less overlapping in acceleration is found in the longitudinal direction and less overlapping in velocity is found in the transverse direction. Thus acceleration data of longitudinal direction and velocity data of transverse direction may be used for detection of overweight vehicles from the bridge response. Figures 11, 13 and 15 describe acceleration, velocity and displacement in transverse direction for vehicles passing from east to west direction. Figures 12, 14 and 16 describe acceleration, velocity and displacement in longitudinal directions for vehicles coming from east. From the maximum limit of weight and maximum limit of speed, maximum limit of vibration data that is acceleration, velocity and deformation can be determined.

Figure 11 shows the best fitted line which shows the acceleration in different weight limits. A line parallel to the best fitted line is then plotted. This is the line of maximum acceleration with respect to different weight in the transverse direction of bridge on deck (BR5). If the busses and trucks are restricted not to carry over 20 tons, then for 20 tons the response of bridge in acceleration can be measured from the parallel line of the best fitted line. From that figure the acceleration is found 2.90 cm/sec^2 . So if the response of the bridge goes over 2.90 cm/sec^2 the vehicle can be identified. If the busses and trucks are restricted not to carry over 20 tons, similar exercise can be carried out for velocity in the transverse direction. If the response of the bridge goes over 0.105 cm/sec (Figure 12) the vehicle can be identified. Similarly in the longitudinal direction, if the response of the bridge goes over 1.75 cm/sec^2 in acceleration or 0.071 cm/sec in velocity, the vehicle can be identified. The acceleration and velocity graph is shown in Figures 13 and 14 respectively.

5. RESPONSE OF THE BRIDGE TO DIFFERENT VEHICLE SPEED

The speed is also another important factor. The range of speed is from 35 km/h to 85 km/h. Buses have relatively higher speed than trucks. It can also be observed that as the speed of vehicles increases the response of the bridge increases. The bus has a weight range of 11 to 15 tons where the truck has a weight range of 19 to 22 tons. In Figure 17 it is observed that the acceleration increases with respect to increase of speed. A 14.1 ton bus which has a speed of 37 km/h gives a lower response (1.138 cm/sec^2). On the other hand, a 12.6 ton bus with a speed of 68 km/h has higher response (2.235 cm/sec^2). Figure 18 shows the same finding for the bridge in transverse direction for the weight of 19 to 22 tons of truck.

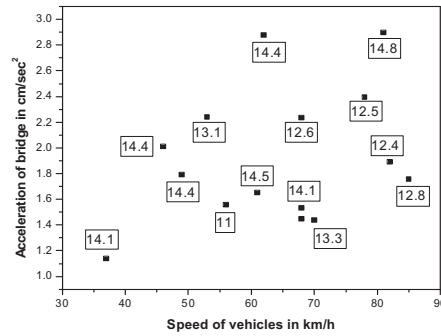


Figure 17: Response of bridge deck in form of acceleration in transverse direction with respect to speed for vehicles weighing 11 to 15 tons.

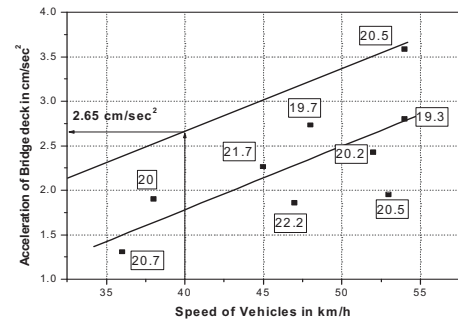


Figure 18: Response of bridge deck in form of acceleration in transverse direction with respect to speed for vehicles weighing 19 to 22 tons.

The response of bridge deck in transverse direction (BR5) for the vehicles weighing in the range of 19 to 22 tons is described with respect to speed in Figure 19. For this data a best fitted line is drawn for finding the response of the bridge in different speed limit. A line parallel to the best fitted line is also drawn for finding the maximum response of the bridge in acceleration. Now if the vehicles are restricted not to pass over speed limit of 40 km/h, then the response from the plot will be 2.65 cm/sec². If the vehicle crosses this acceleration, then the vehicle can be identified as crossing the speed limit. Here the vehicle weight is in the range of 19 to 22 tons. So this is possible to find out the maximum response a vehicle weighing 20 tons with a speed 40 km/h from Figure 19.

From the Figure 19 a line can be drawn parallel to the best fitted line and through the point of response for vehicle weighing 20 tons. From that figure the response is found 2.08 cm/sec². From this value it can be concluded that if the response of the bridge exceeds 2.05 cm/sec² then the vehicle may exceed the weight limit of 20 tons or the speed limit of 40 km/h or the both. Then the vehicle can be identified.

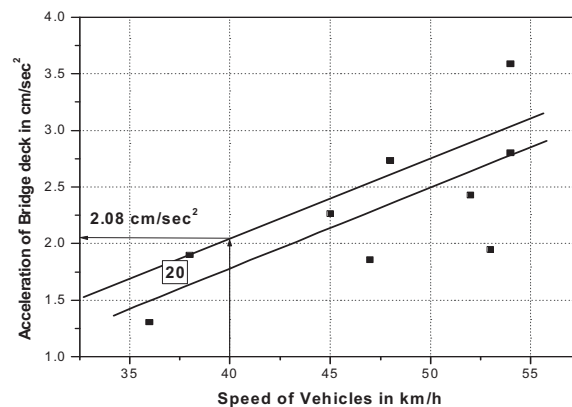


Figure 19: Response of bridge deck in form of acceleration in transverse direction (BR5) with respect to speed for vehicles weighing of 20 tons.

Figure 20 and 21 show the acceleration on deck of the bridge in longitudinal direction. The first figure shows for the bus vibration and second one for the vibration of truck. It is noticed that two buses weighing 14.4 tons both have greater responses than the 11 and 13.8 ton bus in Figure 20. So the response of bus weighing 14.4 tons with a speed of 46 km/h has a little bit higher than the bus weighing 11 tons with a speed of 56 km/h. So, the weight governs here. For the truck the speed is very important cause of vibration on deck of bridge. For trains speed is the most important factor of bridge vibration because of their heavy load. In Figure 21 a best fitted line is drawn for the response in terms of acceleration on deck in longitudinal direction. Then a parallel line is drawn for the maximum response. The maximum response is found to be 0.98 cm/sec². For the vehicle of 20 tons of weight the response is found to be 0.70 cm/sec². From this value it can be concluded that if the response of the bridge exceeds 0.70 cm/sec² in longitudinal direction then the vehicle may exceed the weight limit of 20 tons or the speed limit of 40 km/h or the both. Then the vehicle can be identified.

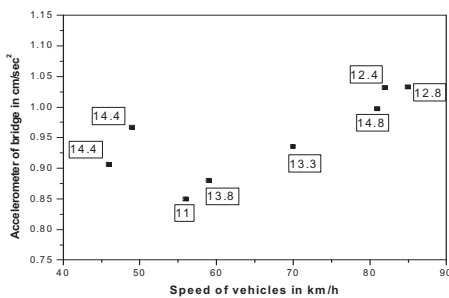


Figure 20: response of bridge deck in acceleration in longitudinal direction in respect of the speed of vehicles in weight of 11 to 15 tons.

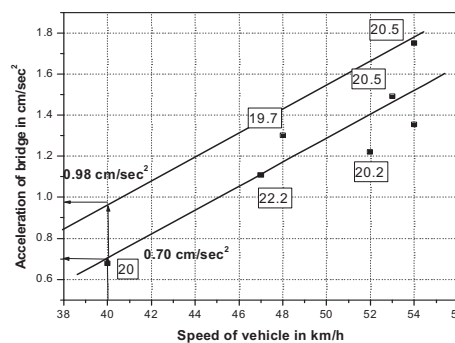


Figure 21: Response of bridge deck in acceleration in longitudinal direction in respect of the speed of vehicles in weight of 19 to 22 tons.

It can be observed clearly that when the weight increases the acceleration increases and when the speed increases the acceleration also increases in a regular pattern. But some values give a little bit anomalous results. This is because of the superposition of the response of other vehicles. The study cannot be done stopping all the vehicles passing on the bridge and by collecting data just for only a single vehicle. Another thing is that there are two lanes on each side. The vehicles do not pass in the same lane always. Sometimes they pass in first lane, sometimes in the second lane and sometimes in the middle of the two lanes.

6. COMPARISONS AMONG DIFFERENT TRAIN DATA

Response of the bridge for different train data (from 2003 to 2008) is presented in Figure 22. Previously trains used to move at higher speed and therefore response of the bridge was higher. Recently the train is restricted

to run in a lower speed. So, the response of the bridge is lower than the previous response. Thus the train speed is a very important factor for the bridge vibration. Response of bridge is the lowest for train without any other traffic. This seems natural because superposition of traffic is absent.

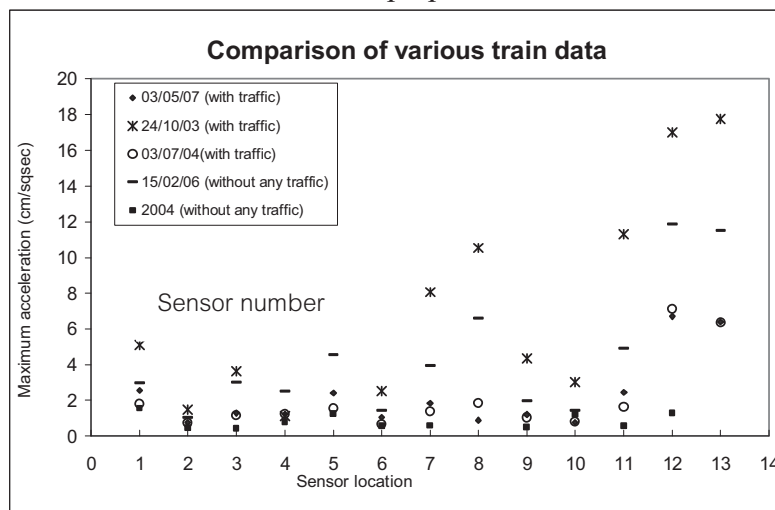


Figure 22: Comparison of response of thirteen bridge sensors for different train data.

From Figure 22, it is observed that for the train with traffic on 24/10/03 when the speed of the train was higher, the response of the bridge is higher than that of any present day low speed trains.

Weight and speed of trains are governing factors for bridge response. When a train passes over the bridge with empty 25 oil bogies, the response is lower than the same train passing with full oil bogies. All the sensors of the bridge have greater response when oil bogies are full than when they are empty. The train with empty bogies has a speed of 17 km/h and the train with full oil bogies run at speed of 15 km/h. If their speed remains same then the difference will be more. Among all the data oil train with full oil gives the highest response for the bridge.

Response of the bridge due to two broad gauge trains is compared. The first train has an engine and 6 bogies. The speed of the train was 17 km/h. This data was collected on 20/05/08. On the other hand, second train has an engine and 7 bogies. The speed of the train was 18 km/h. This data is recorded on 21/05/08. From these two series of data it is observed that, the second data have higher value than the first one. The response on bridge deck increases about 22% adding of one bogie. The study indicates the increase in bridge response due to addition of bogies. The 12 and 13 number sensors have always higher value. This is because of the sensors are in the middle of span, that means they are far from the support. So the vibration is higher in middle of the span.

The train, truck and bus vibration data are collected several times for the analysis to find out the response. Data recorded in the past show a pattern of similarity. When the weight of the bus and truck increases the response also increases. When the speed increases remaining the weight same the response also increases. For the train when the speed decreases the response decreases. However among the previously recorded data and

recently recorded data there is difference. For the same type of train previous response was lower than the recently recorded response.

In Table 1, it is clearly observed that the response of the bridge is greater in presently recorded data. The train data of 03/05/07 was for a Broad Gauge train. And the train data of 20/05/08 is also for a Broad Gauge Train and it has 6 bogies with an engine. The speed of the two trains was same (17 km/h). However the response of presently recorded data due to train movement is larger than the previously recorded data. This may be due to the recently occurred cracks in the bridge.

Table 1: The comparison of acceleration in cm/sec^2 due to train movement recorded on bridge deck in transverse direction.

| Sensor No | BR 1 | BR 2 | BR 3 | BR 4 | BR 5 | BR 6 | BR 7 | BR 8 | BR 9 | BR 10 | BR 11 | BR 12 | BR 13 |
|---------------|------|------|------|------|------|------|------|------|------|-------|-------|-------|-------|
| On 3/5/07 | 2.54 | 0.76 | 1.27 | 1.23 | 2.42 | 1.05 | 1.82 | 0.90 | 1.21 | 0.77 | 2.44 | 6.69 | 6.41 |
| On 20/5/08 | 3.87 | 1.51 | 2.23 | 2.66 | 6.58 | 2.57 | 7.71 | 3.33 | 3.43 | 2.37 | 6.59 | 16.8 | 13.7 |
| Increase in % | 52 | 99 | 75 | 116 | 172 | 145 | 324 | 270 | 183 | 208 | 170 | 151 | 114 |

7. CONCLUSIONS

Train and truck excite the bridge with their comparatively greater load. Due to huge input energy bridge excites close to its predominant frequency. However other vehicles like bus, motorcycle, zip etc. has lower energy input. BR1, BR5 and BR11 which are in transverse direction show predominant frequency of 1 Hz and 3 Hz for different train, truck and bus data recorded in different times. BR 2, BR 6 and BR 10 are the sensors in longitudinal direction. These sensors show predominant frequency of 2 Hz. Two weight groups of vehicle can be noticed. One group weighs between 11 to 15 tons, which are buses and the other group of vehicles are 19 to 22 tones, which are trucks. Weight and speed of a vehicle are major concern for the bridge. If the response of the bridge in transverse direction exceeds 2.05 cm/sec^2 then the vehicle may exceed the weight limit of 20 tons or the speed limit of 40 km/h or the both. Then the vehicle can be identified. On the other hand, if the response of the bridge in longitudinal direction exceeds 0.70 cm/sec^2 then the vehicle may exceed the weight limit of 20 tons or the speed limit of 40 km/h or the both.

Previously trains used to move at higher speed; therefore response of the bridge was higher. Recently the train is restricted to run in a lower speed. So, the response of the bridge is lower than the previous response.

REFERENCES

- ALTUS QuickLook for windows Ver.2.89(12/18) 14 dec, 2000 Copyright 1994-2000, Kinematics, Inc. 222, Vista Avenue, Pasadena, California, USA 91107.
- ALTUS QuickTalk for windows Ver. 2.16 Copyright 1996-2000, Kinematics, Inc. 222, Vista Avenue, Pasadena, California, USA 91107
- Origin 6.1 v6.1052 (B232), Copyright 1991-2000, OriginLab Corporation, One Roundhouse Plaza, Northampton, MA 01060, USA

RISK ANALYSIS OF CROWD EVACUATION USING THE MONTE CARLO METHOD

JIAN-FENG LI ^{1,2}, XIAOHUI YAO, XIAOQING LIU,
YUTIAN WANG and BIN ZHANG

1 Beijing Municipal Institute of Labor Protection, Beijing, 100054,
P.R.China

2 Urban Public Safety Research Center, Nankai University, Tianjin, 300071
P.R.China

ABSTRACT

Available safe egress time (ASET) is an important indicator in measuring the safety of public venues. In order to evaluate the safety evacuation performance from the perspective of quantitative risk analysis, the Monte Carlo simulation approach has been employed. First, Xiaobailou Metro station in Tianjin has been selected as the research object. Second, the limit state equation has been established to describe the available safe egress time (ASET) in the metro. Third, through using the software @risk, the Monte Carlo simulation was accomplished, and obtained the fatality rates corresponding to the different scenarios. Finally, to integrate the fatality rates and the probabilities of occurrence of different scenarios, it estimates the final fatality rate of the passengers under the condition of fire in Xiaobailou Metro station. The result indicates that the Monte Carlo simulation approach is a powerful tool to describe complex problems characterized by parameter uncertainty as well as model uncertainty.

1. INTRODUCTION

Available safe egress time (ASET) is an important indicator to quantify the safety level of public venues. The ASET could be defined by the time period from accident happen to safe egress from the dangerous zone that is equivalent to reach the safe position. Figure 1 described the accidents development chain and the different time span used in evacuation. In order to evaluate the safety evacuation performance from the standpoint of quantitative risk analysis, the Monte Carlo simulation has been employed in Tianjin city Xiaobailou Metro station that is selected as the case study ^[1].

A Metro system is an important part in urban transportation network that is made up of by many equipments and facilities. Also, it is a typical crowd massing public venues that is vulnerable to be subject to fire, explosion, earthquakes, flood, equipment breakdown, etc., which not only cause human casualties and material loss but also induce society shock. The configuration in Metro system has its characteristics. Being subject to the limited space and number of exits, once the accidents happened, the difficulty of passenger interior escaped from disaster is comparatively great; moreover, exterior rescue action is hard to carry out. For one thing, passenger flux is high that is difficult to control. Escaping conditions and

circumstance is bad (tremendous vertical depth, little escaping route, long escaping distance). Many barriers cumber the pass engages' safe egress that made available safe egress time is short. For another, once the fire in metro occurs, the accident is paroxysmal with multiversity and complexity, so effective salvation is untoward. Furthermore, in emergency, poisonous gas, traffic jam in escaping routes, poor communications and inappropriate wrecking equipments result in balking at salvation.

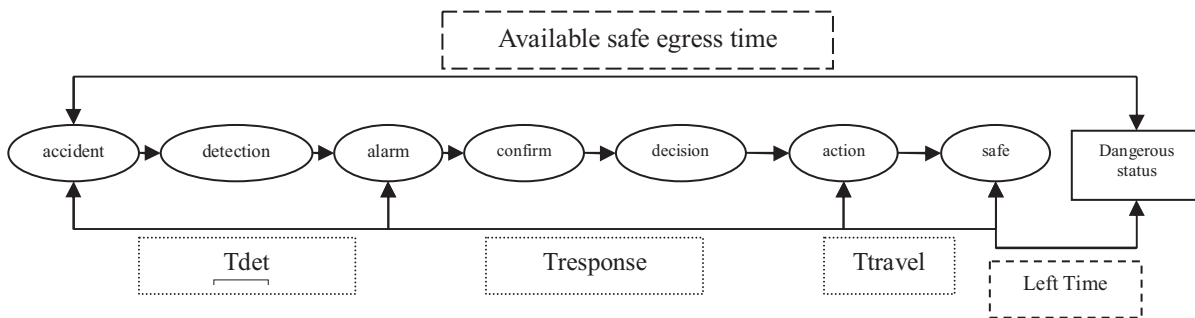


Figure 1: Composition of Available safe egress time

2. DESCRIPTION OF METRO SYSTEM

A Metro system is a complex system In general, based on its function, user requirements and different position, Metro system is divided into three sections: subway station, interzone section, and vehicle section.

Subway station is an important part in Metro system, which benefits for passengers, at the same time, centralizes a large part of technological fixing and management system. Interzone section connects two stations, which directly relates to the circulation, which influences the coziness feeling of passengers and train velocity. Vehicle section is used to park the train and perform ordinary maintenance together with personnel training. These paper emphases on the subway station. It makes up of station (platform, hall, living and working locales), passageway, route way, ventilation passage, ground intake, etc.

In order to make the following chapters somewhat less abstract we already here introduce our basic calculation example. The building type is defined as a subway station and the analysis is the available safe egress time (ASET) margin for a fire in the station itself. The scenario event tree is shown by Figure 2, outlining the various outcome cases for functioning/non-functioning fire alarms, sprinklers and emergency doors. The event tree indicates the routes by which the initial event (including evacuation) can develop. At each branch, a question is posed related to the development of the event and branch probabilities are assigned, based on statistical data. Each path through the event tree defines a scenario, and accordingly the event tree in Figure 1 defines eight scenarios 1-8. The possible scenarios are shown in Figure 2.

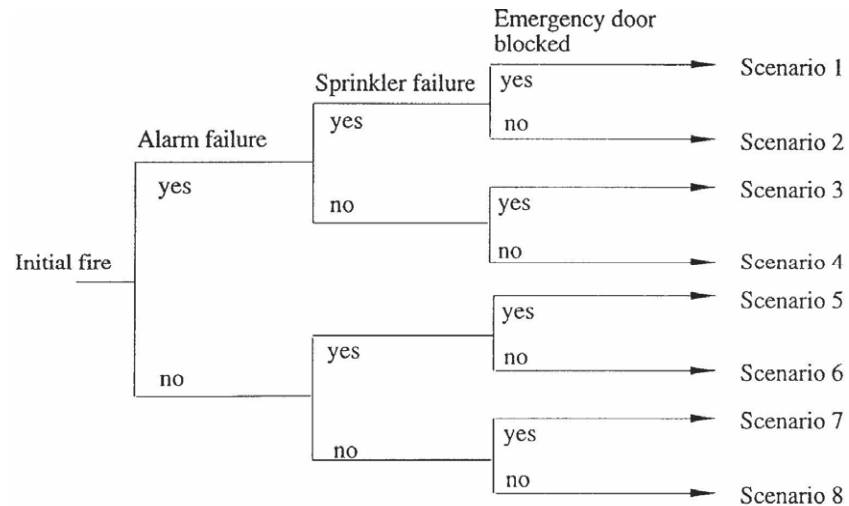


Figure 2: Event tree describing the eight scenarios

3. THE LIMIT STATE EQUATION OF THE ASET OF MONTE CARLO

3.1 Basic Limit State Equation of the ASET

The limit state equation of the available safe egress time (ASET) for a fire in an indoor space can be formulated as:

$$G = S - D - R - E \geq 0 \tag{1}$$

Where : G is the available safe egress time margin;

S is the time for smoke filling to 1.5m above floor level;

D is the detection time;

R is the response and behavior time prior to evacuation;

E is the movement time to exit;

In equation (1) all parameters are considered stochastic. This paper assumes that smoke-filling to 1.6 m that is the breath surface of human being is a criterion of the SAFE-NOT SAFE boundary. It ignores the variability of smoke effects on the occupants before the smoke reaches 1.5 m.

The parameters S , D and E should be obtained by computer simulation or empirical formula, so they contains uncertainties, we induce three uncertainty parameters to rectify the models as following:

$$G = M_S S - M_D D - R - M_E E \tag{2}$$



Figure 3: Setting of the computational grid

3.2 Construction of the Limit State Equation

The essence of this part is derivation of regression equations and knowledge uncertainty. To carry out the analytical and numerical calculation of safety level, well-established response surface equations for smoke filling time S , detection time D are necessary.

The derivation of regression equations can be divided into two stages. The first one is to obtain sufficient number of output values of prediction models to cover the whole range of variation of stochastic parameters. Then the regression analysis will be carried out to fit an appropriate equation to the output values. The errors of the prediction made by regression equation should be quantified as well. They can be included in the knowledge uncertain parameters described in equation 2.

3.2.1 Evolution model of fire growth - critical time S

The process of fire growth is unstable essentially and will endure non-linearity stage at first, then reach the stable burning. An empirical equation is suggested in NFPA92B for the smoke layer height during the t^2 -fires ($Q = \alpha t^2$ [kW]). The equation is^[3]:

$$\frac{z}{H} = 0.91 \left[t H^{-4/5} \left(\frac{1000}{\alpha} \right)^{-1/5} \left(\frac{Area}{H^2} \right)^{-3/5} \right]^{-1.45} \quad (3)$$

Solving for t , we get,

$$t = 3.74 \alpha^{-0.2} H^{0.3} Area^{0.6} z^{-0.69} \quad (4)$$

Where, z is the height of smoke layer above fire [m], $Area$ is the floor area [m^2], H is the ceiling height [m], t is the time [s], α is the fire growth rate [kW/s^2]. As for the Xiaobailou subway station, H and $Area$ are constants. So, the critical time S that is equivalent to the time span that the smoke layer reach to the breath surface can be formulated to be exponential function with the parameter α .

Now, critical time can be formulated as: $S = C\alpha^n$.

The parameters C and n will be determined through computer simulation under the real scenario of Xiaobailou subway station.

Large Eddy Simulation (LES) in FDS code will be used to simulate the process of fire growth and spread^[4]. According to the fire scenarios defined above, the input file in FDS code can be determined. Considering the simulation precision and computational capacity, we defined the grid to be $0.67m \times 0.53m \times 0.5m$, so totally 97200 units in the whole.

First, we consider the scenario that mechanical ventilation system is down. NFPA92B (2000) puts forward four kinds of typical fire growth patterns. The corresponding fire growth rate α and the maximum time to reach fire power 10MW have been listed in table 1.

Table 1: Typical fire growth patterns

| Fire growth patterns | α (kW/s ²) | Time (s) |
|----------------------|-------------------------------|----------|
| Slow | 0.002931 | 1847 |
| Medium | 0.01111 | 949 |
| Fast | 0.04689 | 462 |
| Very fast | 0.1878 | 231 |

Separately, the simulation of the fire development process that defers to four kinds of typical fires growth patterns can produce calculation results of temperature in any grid point and at any time. To take the profile that connects the platform with passenger train for example, the distribution of temperature at specific time have been displayed in Figure 4.

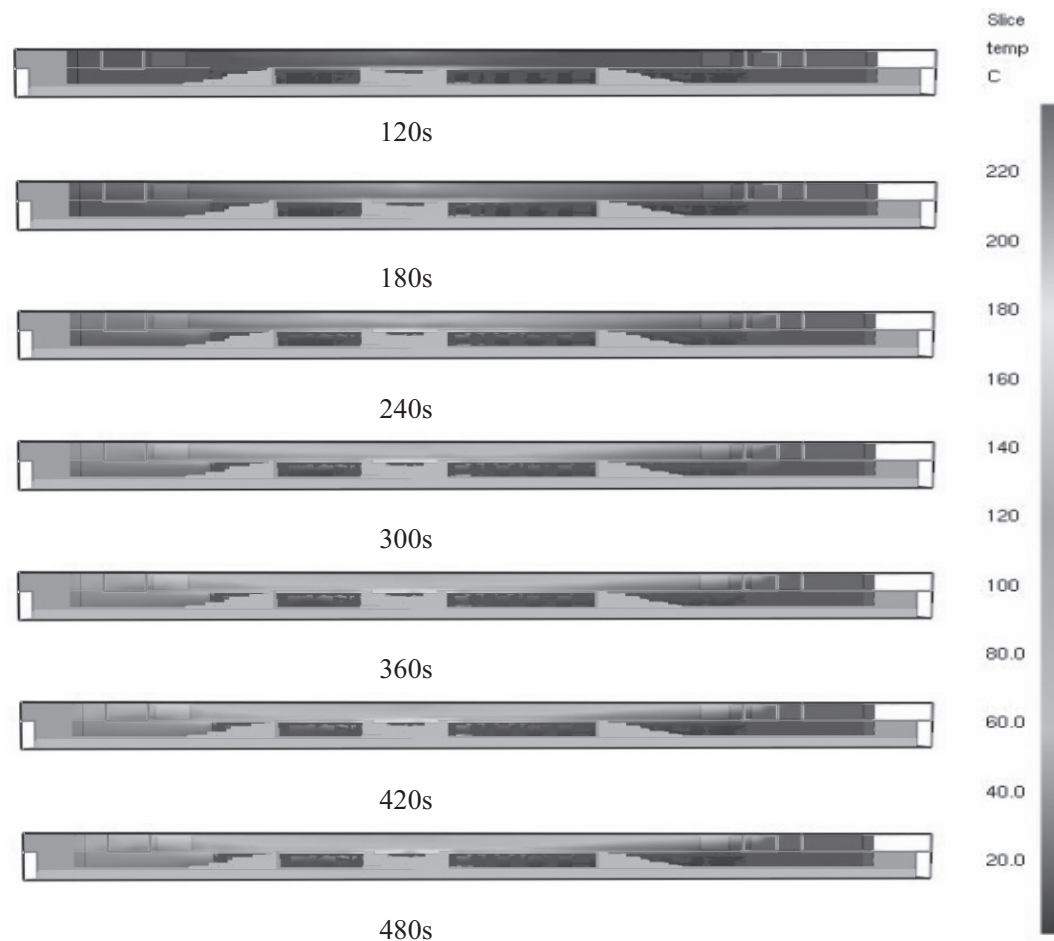


Figure 4: Profiles of the temperature distribution

More to the point, when the passengers evacuate from the platform to station hall, the crowded status could occur in the egress passage such as staircase and escalator. Thus, the passenger would be detained for a longer time in the neighborhood of the entrance to safe zone. Therefore the profiles of the entrance to safe zone should be paid much attention to check for its smoke layer altitude and temperature distribution.

In terms of the safety requirements, the most dangerous point, namely the position mostly approaching to the fired train, can be taken out as the representative to reflect the situation of entire section. See Figure 5. According to the FDS simulation result, various curves describing smoke layer altitude and temperature in the entrance to staircases and escalators could be obtained at different time ^[5].

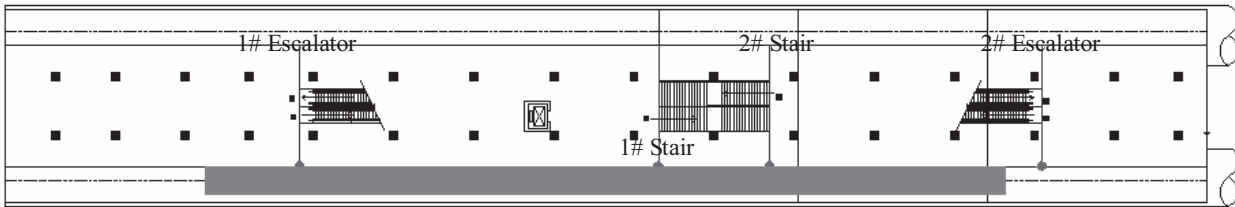
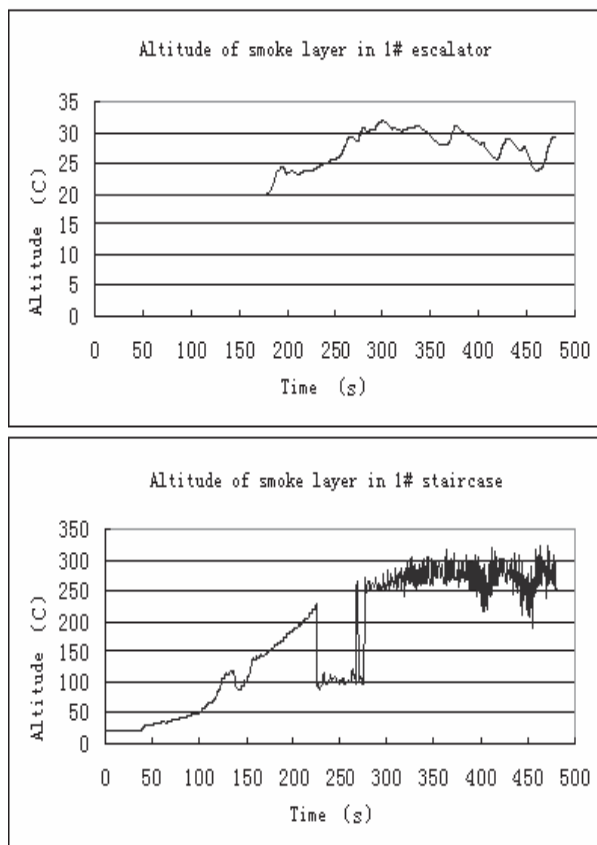


Figure 5: Entrance profiles to different egress passage and the most dangerous points

- Notes: (1) blue lines represent the position of entrance profiles
- (2) red points represent the most dangerous points

To take the “very fast” fire as example, various curves describing smoke layer altitude and temperature in the entrance to staircases and escalators have been showed in Figure 6 and Figure 7.



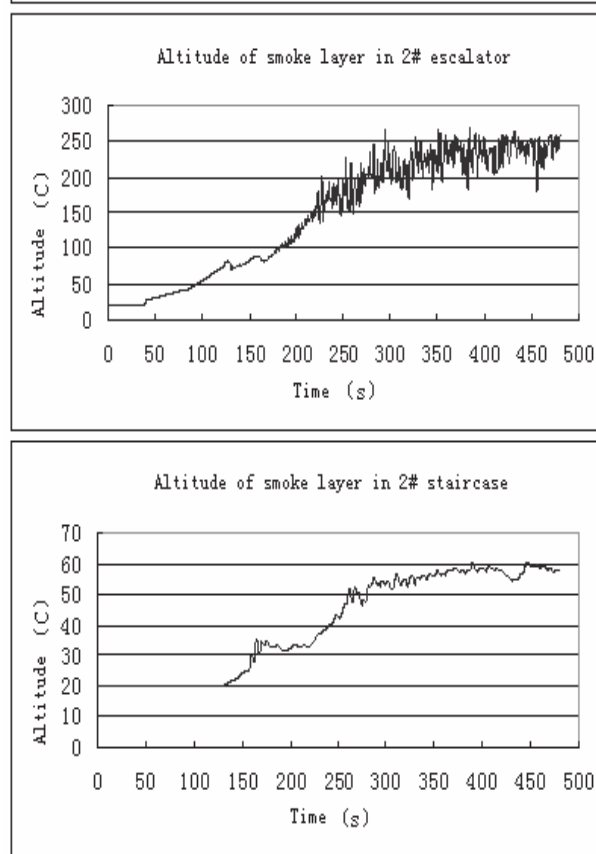
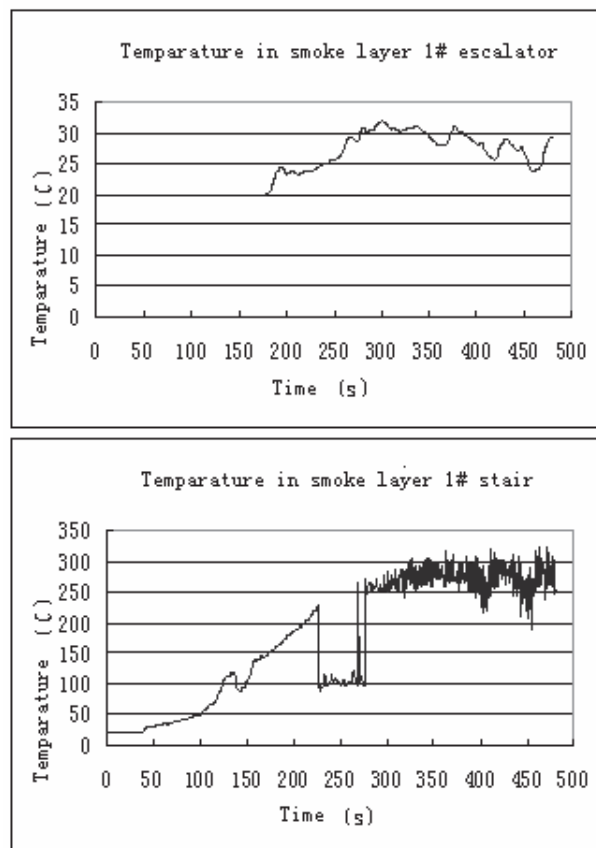


Figure 6: Altitude of smoke layer



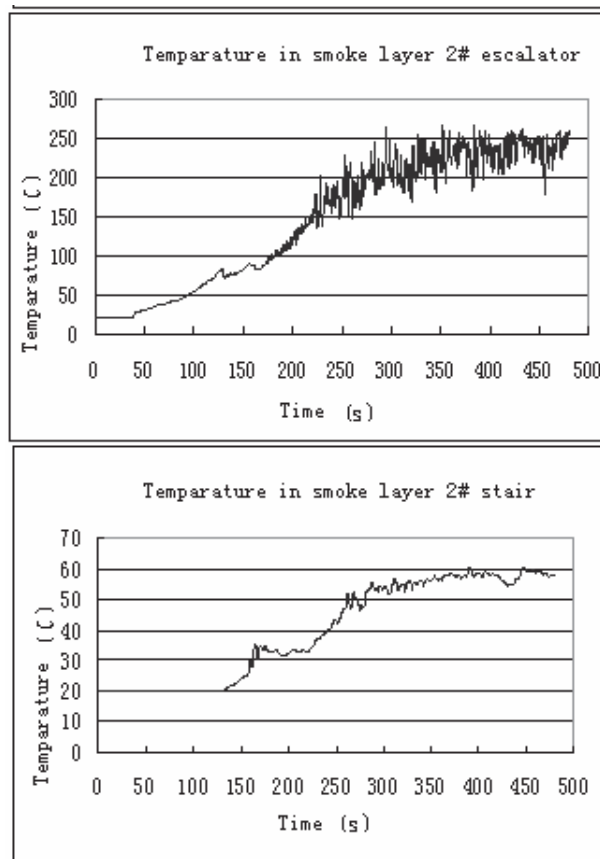


Figure 7: Temperature in smoke layer

Notes: the data above is the simulation result when mechanical ventilation system is down.

From these figures, we can see:

(1)As for the two escalators left and right, excluding several short-term periods that smoke layer drop down below to 1.5m, smoke layer always keeps up to 3.5m. Moreover, the temperature has not up to 60 , even if the smoke is dropping down below to 1.5m, it will not pose the threat to passengers.

(2)As for the two staires in the middle, although the smoke layer always keeps up to 1.5m, the temperature quickly exceeds 180 . For instance, in 196 second, the temperature in 1# stair reaches to 180 that satisfied the first judgment criterion that reflects the fatal injury caused by fire. Thus, when mechanical ventilation system is down, the “very fast” fire determined the critical time S is 196 second.

Similarly, when mechanical ventilation system is down, we can acquire the critical time corresponding to four typical fire growth patterns, see table 2.

Table 2: Simulation results of the critical time corresponding to four typical fire growth patterns

| Fire growth patterns | α (kW/s ²) | Time (s) |
|----------------------|-------------------------------|----------|
| Slow | 0.002931 | 1317 |
| Medium | 0.01111 | 718 |
| Fast | 0.04689 | 377 |
| Very fast | 0.1878 | 196 |

Based on the data in table 2, we used the statistical software 1stOpt to make the regression, and then obtain the parameter C and n in $S=C\alpha^n$. The final results are listed as following:

- Optimal value of C : 93.1;
- Optimal value of n : -0.45;
- Standard deviation: 1%;
- $S=93.1\alpha^{-0.45}$; (11)

By the same way, when mechanical ventilation system works, evolution model of fire growth will be changed to $S=83.8\alpha^{-0.48}$. (2)

3.2.2 Awareness time - detection time D

DETECT-T2 is a program for calculating the actuation time of thermal devices below unconfined ceilings. It can be used to predict the actuation time of fixed temperature and rate of rise heat detectors, and sprinkler heads subject to a user specified fire which grows as the square of time. DETECT-T2 assumes that the thermal device is located in a relatively large area that is only the fire ceiling flow heats the device and there is no heating from the accumulated hot gases in the room. The required program inputs are the ambient temperature, the response time index (RTI) for the device, the activation and rate of rise temperatures of the device, height of the ceiling above the fuel, the device spacing and the fire growth rate. The program outputs are the time to device activation and the heat release rate at activation^[6].

Its mathematical model is:

$$\frac{dT_{\text{tank}}}{dt} = \frac{\sqrt{U_g} (T_g - T_{\text{tank}})}{RTI} \tag{13}$$

Here,

- T_{tank} : detection temperature;
- T_g : temperature of fire ceiling flow;
- U_g : velocity of fire ceiling flow;
- RTI : response time index.

In Metro system, we define $T_{\text{tank}}=57$, $RTI=32$.

Table 3: Detection time in different fire patterns

| Fire growth patterns | α (kW/s ²) | Detection time D (s) |
|----------------------|-------------------------------|----------------------|
| Slow | 0.002931 | 268 |
| Medium | 0.01111 | 169 |
| Fast | 0.04689 | 104 |
| Very fast | 0.1878 | 67 |

Based on the data in table 3, we used the statistical software 1stOpt to make the regression, and then obtain the parameter C and n in $D=C\alpha^n$. The final results are listed as following: $D=37.1\alpha^{0.37}$.

3.2.3 Movement time - E

The evacuation time or more precisely the movement time is simply calculated by looking at the time it takes for a crowd to pass through the egress passage. The movement time is composed of the time it takes to walk to the door and the time consumed having a crowd passing a door. But as the passing time usually is much larger than the walking time to reach the door the latter is omitted. The movement time is dependant on the number of available exits, their width and the number of persons in the room. The number of persons in a room is dependant on the type of assembly room and the floor area. In some rooms the number of persons is fixed by the number of seats but in others the number could vary depending on the type of occupancy in the room^[7].

One of the other branches in the event tree is whether or not one emergency door is blocked. This blockage could be caused by either the fire or by the locking of the door. For example, if the fire occurs close to an emergency exit that exit will not be used and people tend to use other exits. Locked emergency doors are not very frequent but a door could be blocked by other reasons. Goods could be stored in front of a door preventing it from being used. An emergency exit could also be unused because of reasons not tied to a physical blockage of the door. If people are not familiar with the building layout and the fire exits, these exits will not be used to any large extent. This will result in consequences, as if the door was blocked. In places of assembly this is almost always the case i.e. people tend to use the same ways out as they entered the building through. It is however possible to some extent guide people to different exits with the use of exit signs and evacuation alarms with verbal messages. Using the latter a quicker evacuation is to be expected. In conclusion emergency doors are not used if:

- a) The fire is close to the door;
- b) The door is locked or blocked or the door is unfamiliar to the people.

The time people used to pass through egress passage (escalator and stair) from the platform to station hall, can be calculated as following:

$$E = \frac{N \cdot Area}{\sum_{i=1}^n F_i W_i} \quad (14)$$

Here,

F_i : the capability of the i th passage;

W_i : the width of the i th passage;

N : crowd density.

According to «Code for the design of metro (GB 50157—2003)», the traveling capability of the staircases are 1.03 person/(s-m), the capability of the escalators are 2.25 person/ (s-m)^[8].

The width of staircase and escalator in Xiaobailou subway station is 2.5m and 2m respectively. So,

$$\sum_{i=1}^n F_i W_i = 2 \times 1.03 \times 2.5 + 2 \times 2.25 \times 2 = 14.15 \text{ person/s.} \quad (15)$$

The total area of Xiaobailou subway station is 1440m². [5]

Thus, the movement time E = 101.8N.

The egress passage has some possibility to be blocked by the discarded baggage or passengers themselves. Then, supposed the blocked emergency exit is 1# escalator, we can get:

$$\sum_{i=1}^n F_i W_i = 2 \times 1.03 \times 2.5 + 1 \times 2.25 \times 2 = 9.65 \text{ person/s.} \quad (16)$$

The movement time when one passage was blocked is E = 149.2N.

3.2.4 Fire growth rate - α

London Fire Brigade’s real fire library is a database of information collected from real fire incidents by specialist teams of experienced fire investigators operating in the Greater London Area. A sample of this data collected over a five-year period has been used to characterize the distributions of fire sizes, fire growth rates and times between events that occur in building fires in a form suitable for use with probabilistic risk assessment.

Table.4 Log-normal parameters characterizing the distribution of fire growth parameters for each occupancy group^[9]

| Occupancy group | μ_α | σ_α | $E(\alpha) (kW/s^2)$ | $\alpha_{95} (kW/s^2)$ |
|--------------------------|--------------|-----------------|----------------------|------------------------|
| Care homes | -7.7 | 1.1 | 0.001 | 0.003 |
| Higher/further education | -7.2 | 0.8 | 0.001 | 0.003 |
| Hospitals | -7.1 | 1.3 | 0.002 | 0.007 |
| Hotels | -7.7 | 2.1 | 0.004 | 0.014 |
| Offices | -7.1 | 1.8 | 0.004 | 0.016 |
| Public buildings | -6.2 | 1.9 | 0.012 | 0.045 |
| Licensed premises | -6.6 | 2.2 | 0.016 | 0.053 |
| Retail | -5.4 | 1.9 | 0.027 | 0.101 |
| Factories | -5.9 | 2.2 | 0.030 | 0.100 |
| Warehouse | -4.0 | 1.9 | 0.107 | 0.405 |

Here, the log-normal distribution parameters ($\mu_\alpha ; \sigma_\alpha$) estimated for fires occurring in metro system are -6.2 and 1.9.

3.2.5 Response time - R

Empirically, when fire alarm is on, the crowd will not take action right now. Only through the “confirm” and “decision” stage, the crowd will take action. On the process of “confirm”, people just realized the accidents’ occurrence together with doubts. On the stage of “action”, people will interrupt their usual activities and prepare for the evacuation that include gathering the accessories, summoning children, exploring the dangerous situation around them, seeking possible exit and sending out alarm. Response time includes both of them.

D.A. Purser has analyzed the data obtained from the exercise in

different type of assembly and achieved the conclusion that before the movement, the response time approximately defers to the lognormal distribution^[10].

H. Frantzich has drawn the conclusion that response time R defers to the log-normal distribution with the parameters (130,120) when the alarm is on. Besides, when the alarm is down, some passengers will detect the fire first by naked eye and send out alarm to others. So, the total response time will be:

$$R = \text{Lognormal}(10, 5) + \text{Lognormal}(300, 300) \text{.}^{[11]}$$

3.2.6 Crowd density - N

According to "Tianjin Subway Line No.1 Feasibility Report", the early peak capacity of passenger in Xiaobailou subway station is^[5]:

Boarding southward, 1768 people per hour;

Boarding northward, 7375 people per hour.

If we suppose one train every two minutes, then the population in the platform waiting for a train is: $(1768 + 7375) / 30 = 305$ people. Further, the train is composed by 4 compartments, 2 compartments with power plus 2 trailers without power that contains 275 and 252 person respectively (1054). Thus the total number of people need to escape is 1359.

The total area of the Xiaobailou subway station is 1440m^2 . So, in the station, greatest density of the crowd is 0.94 person of $/\text{m}^2$. Therefore, the crowd density can be supposed to defer to triangle distribution with the parameter (0.1, 0.75, and 0.94).^[12]

3.2.7 Uncertainty analysis of the model

Equation (11) and (12) are obtained from regression of simulation result of FDS code. The equation contains uncertainty from two sides:

- (1) The difference between simulation results in FDS code and the data from field experiments (1# error);
- (2) The difference between regression model and simulation results in FDS code (2# error).

Correspondingly, the regression model needs to be rectified as following:

- (1) Based on the field experiments in tunnel conducted by L.H. Hu, the temperature obtained from FDS code is somewhat greater than the data from field experiments. See Figure 8.

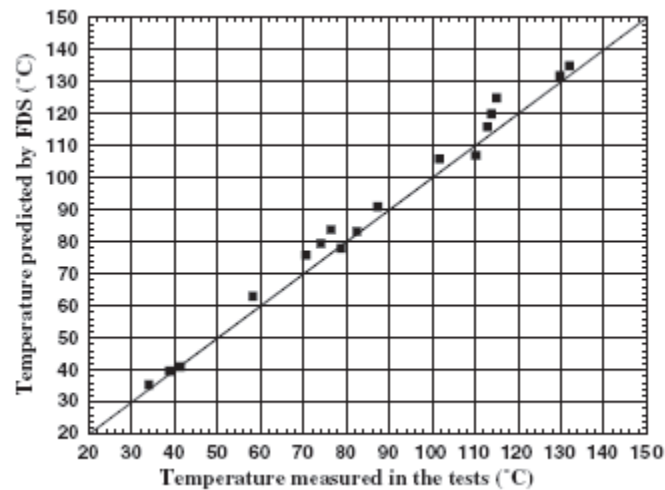


Figure 8: Comparison of the data from FDS simulation and field experiments

In terms of the empirical model presented by Alert, we can estimate the function between temperature and fire growth time^[13]. The optimal rectification coefficient is 0.973, standard deviation 0.026, i.e., the 1# error defers to normal distribution with the parameters (0.973, 0.026) .

(2) When it comes to 2# error, we can acquire the error distribution from 1stOpt code. The average value of the relative error is 0.002, standard deviation is 1%, i.e., the 2# error defers to normal distribution with the parameters (1.002, 0.01) .

In summary, the uncertainty parameter M_s includes both two parts above, and then we get:

When mechanical ventilation system is down,

$$M_s = Normal(0.973 \times 1.002; \sqrt{0.026^2 + 0.01^2}) = Normal(0.975, 0.028) .$$

When mechanical ventilation system works,

$$M_s = Normal(0.973 \times 0.99; \sqrt{0.026^2 + 0.023^2}) = Normal(0.963, 0.035) .$$

The uncertainty parameters M_D and M_E have not been determined now. According to the opinion of Sven Erik Magnusson, he put forward the probability distribution of M_D and M_E subjectively^[2]:

$$M_D = Normal(1.0, 0.2) , M_E = Normal(1.0, 0.3) .$$

4. MONTE CARLO SIMULATION OF EIGHT SCENARIOS

4.1 Simulation results

The sampling type is Latin Hypercube and the number of iterations are 1000. The summary quick report is shown in table 5. To take scenario 1 for example, the histogram for output together with its descending cumulative line are displayed in Figure 9. Then, the probability of (ASET - RSET) = P(G<0)=7.76%, i.e. the death probability in scenario 1 is 7.76%.

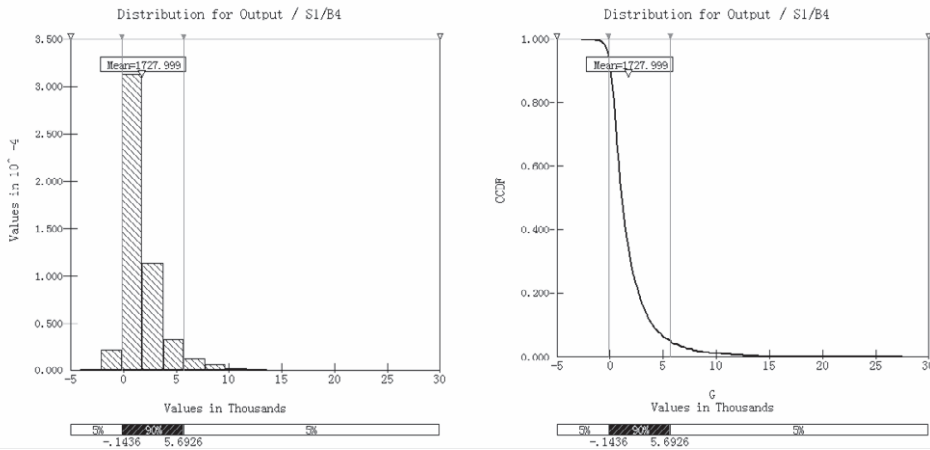


Figure 9: The histogram and descending cumulative line of scenario 1

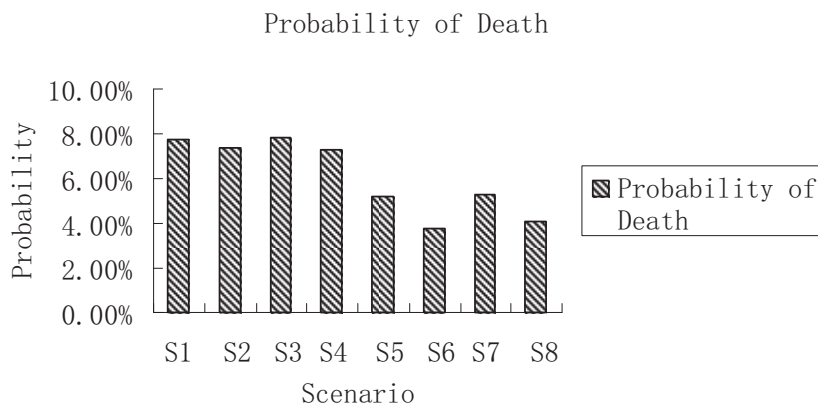


Figure 10: The distribution of probabilities of death totally

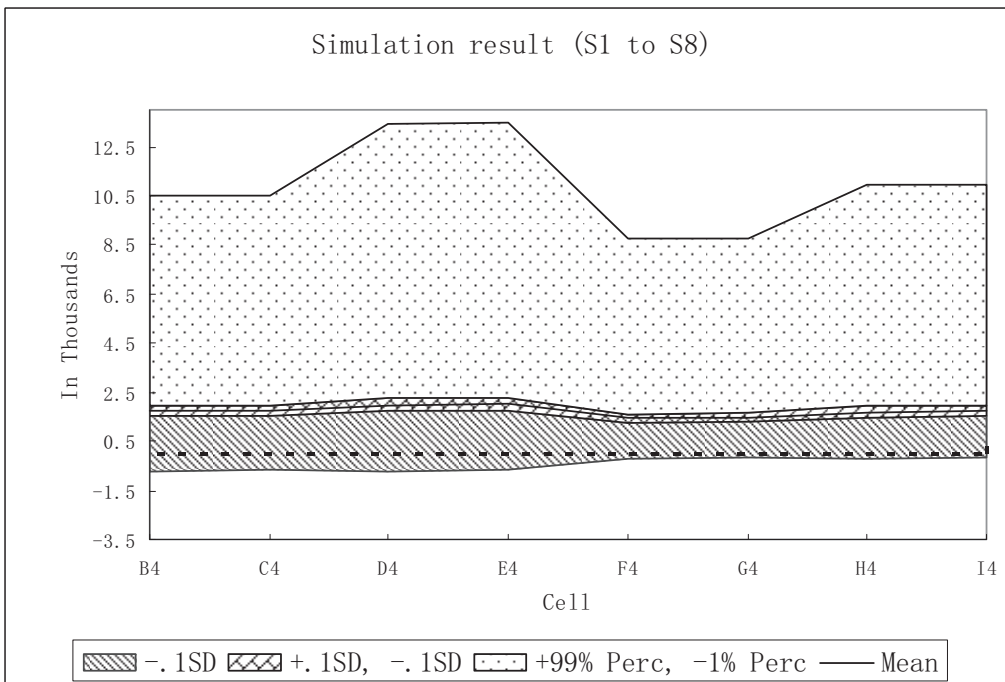


Figure 11: Summary graph of the simulation results

4.2 Probability of death in Xiaobaolou metro station under fire

Probability of death in Xiaobaolou metro station under fire can be obtained by integrating the death probability in scenario 1~ 8 as following:

$$F_{death} = \sum_{i=1}^8 p_i F_i = 4.62\%$$

p_i : The probability of the occurrence of the i th scenario, see table 5. Here, the probabilities are determined by experts' opinion.

Table 5.1: Summary quick report in@risk

| Input | | Statistics | | | | | | |
|---------------|------|--------------|-------------|-------------|-------------|----|-------------|-----|
| Name | Cell | Minimum | Mean | Maximum | x1 | p1 | x2 | p2 |
| Value / alpha | B2 | 3.48013E-06 | 0.0118915 | 0.989627361 | 8.84828E-05 | 5% | 0.045850936 | 95% |
| Value / R1 | C2 | 1.811091661 | 10.00660966 | 51.87601089 | 4.099381924 | 5% | 19.38884354 | 95% |
| Value / R1 | C2 | 14.98388195 | 301.0678725 | 4636.603516 | 53.65330505 | 5% | 833.5031738 | 95% |
| Value / R2 | D2 | 8.430717468 | 130.1674075 | 1552.313477 | 26.0709095 | 5% | 346.3157654 | 95% |
| Value / N | E2 | 0.11213474 | 0.596670507 | 0.93107152 | 0.263985306 | 5% | 0.850209355 | 95% |
| Value / MS1 | F2 | 0.87811178 | 0.97499993 | 1.067834854 | 0.928701282 | 5% | 1.020802498 | 95% |
| Value / MS2 | G2 | 0.825978875 | 0.962976038 | 1.080174446 | 0.905105829 | 5% | 1.0204494 | 95% |
| Value / MD | H2 | 0.370083809 | 0.99998917 | 1.618977904 | 0.669680834 | 5% | 1.32721591 | 95% |
| Value / ME | I2 | -0.192221791 | 0.999862821 | 2.017042398 | 0.50521332 | 5% | 1.490677118 | 95% |

| Output | | Statistics | | | | | | |
|-------------|------|--------------|-------------|-------------|----|-----------|-------------|-----|
| Name | Cell | Minimum | Mean | Maximum | x1 | p1 | x2 | p2 |
| Output / S1 | B4 | -4126.612305 | 1727.9994 | 27503.04883 | 0 | 7.763347% | 5692.55127 | 95% |
| Output / S2 | C4 | -4088.635254 | 1756.297421 | 27519.93359 | 0 | 7.334278% | 5727.445801 | 95% |
| Output / S3 | D4 | -4057.251465 | 1995.367361 | 33280.5625 | 0 | 7.850174% | 6809.61084 | 95% |
| Output / S4 | E4 | -4019.27417 | 2023.665379 | 33297.44531 | 0 | 7.316536% | 6859.499512 | 95% |
| Output / S5 | F4 | -396.4351501 | 1435.684563 | 24520.70898 | 0 | 5.18946% | 4659.746094 | 95% |
| Output / S6 | G4 | -365.9989929 | 1463.982588 | 24537.59375 | 0 | 3.761901% | 4682.128418 | 95% |
| Output / S7 | H4 | -403.9936218 | 1703.052522 | 30298.22266 | 0 | 5.262702% | 5744.608398 | 95% |
| Output / S8 | I4 | -359.959198 | 1731.350545 | 30315.10742 | 0 | 4.084711% | 5773.994141 | 95% |

Table 5.2: Limit state equation of the eight scenarios with its parameters

| | p_i | Limit State Equation | α | R | N | M_s | M_D | M_E |
|------------|-------|--|----------------------|--------------------------------------|----------------------------|----------------------|------------------|------------------|
| Scenario 1 | 0.1% | $G = 93.1\alpha^{-0.45} \cdot M_s - R - 149.2N \cdot M_E$ | Lognormal (-6.2,1.9) | Lognormal(10,5) + Lognormal(300,300) | Triangular (0.1,0.75,0.94) | Normal (0.975,0.028) | Normal (1.0,0.2) | Normal (1.0,0.3) |
| Scenario 2 | 0.4% | $G = 93.1\alpha^{-0.45} \cdot M_s - R - 101.8N \cdot M_E$ | Lognormal (-6.2,1.9) | Lognormal(10,5) + Lognormal(300,300) | Triangular (0.1,0.75,0.94) | Normal (0.975,0.028) | Normal (1.0,0.2) | Normal (1.0,0.3) |
| Scenario 3 | 1.9% | $G = 83.8\alpha^{-0.45} \cdot M_s - R - 149.2N \cdot M_E$ | Lognormal (-6.2,1.9) | Lognormal(10,5) + Lognormal(300,300) | Triangular (0.1,0.75,0.94) | Normal (0.963,0.035) | Normal (1.0,0.2) | Normal (1.0,0.3) |
| Scenario 4 | 7.6% | $G = 83.8\alpha^{-0.45} \cdot M_s - R - 101.8N \cdot M_E$ | Lognormal (-6.2,1.9) | Lognormal(10,5) + Lognormal(300,300) | Triangular (0.1,0.75,0.94) | Normal (0.963,0.035) | Normal (1.0,0.2) | Normal (1.0,0.3) |
| Scenario 5 | 0.9% | $G = 93.1\alpha^{-0.45} \cdot M_s - 37.1\alpha^{-0.37} \cdot M_D - R - 149.2N \cdot M_E$ | Lognormal (-6.2,1.9) | Lognormal(130,120) | Triangular (0.1,0.75,0.94) | Normal (0.975,0.028) | Normal (1.0,0.2) | Normal (1.0,0.3) |
| Scenario 6 | 3.6% | $G = 93.1\alpha^{-0.45} \cdot M_s - 37.1\alpha^{-0.37} \cdot M_D - R - 101.8N \cdot M_E$ | Lognormal (-6.2,1.9) | Lognormal(130,120) | Triangular (0.1,0.75,0.94) | Normal (0.975,0.028) | Normal (1.0,0.2) | Normal (1.0,0.3) |
| Scenario 7 | 17.1% | $G = 83.8\alpha^{-0.45} \cdot M_s - 37.1\alpha^{-0.37} \cdot M_D - R - 149.2N \cdot M_E$ | Lognormal (-6.2,1.9) | Lognormal(130,120) | Triangular (0.1,0.75,0.94) | Normal (0.963,0.035) | Normal (1.0,0.2) | Normal (1.0,0.3) |
| Scenario 8 | 68.4% | $G = 83.8\alpha^{-0.45} \cdot M_s - 37.1\alpha^{-0.37} \cdot M_D - R - 101.8N \cdot M_E$ | Lognormal (-6.2,1.9) | Lognormal(130,120) | Triangular (0.1,0.75,0.94) | Normal (0.963,0.035) | Normal (1.0,0.2) | Normal (1.0,0.3) |

5. CONCLUSIONS

In the field of risk analysis, the actual experiments can seldom be done due to the limitation in real world. This limitation necessitates the use of approximate numerical methods, with Monte Carlo simulation being one of the most general and easily applied methods. From the research of the ASET simulation of crowd in metro, we see the Monte Carlo approach is

efficacious. The method involves computing the output of the risk model for many sets of combinations of inputs. The combinations of the input values are obtained by random sampling from the distributions assigned to the input variables. Dependencies among the input variables can be accounted for by specifying the covariance between pairs of such variables. The resulting distribution of outputs is then interpreted as an approximation of the desired probability distribution.

REFERENCE:

- Hakan Frantzich. Risk analysis and fire safety engineering. *Fire Safety Journal* 31(1998)313-329.
- Sven Erik Magnusson, Hakan Frantzich, Kazunori Harada, Fire safety design based on calculations: Uncertainty analysis and safety verification, *Fire Safety Journal* 27(1996) 305-334.
- NFPA 92 B. Recommended Practices for Smoke Management in Atria Malls NFPA Quincy, MA 1991.
- Kevin McGrattan, Glenn Forney. Fire Dynamics Simulator (Version 4) User's Guide. NIST Special Publication 1019, 2005.
- Tianjin Subway Line No.1 Feasibility Report.
- User information for DETACT-QS and DETACT-T2 programs.
- MAGNUSSON S E, FRANTZICH H, HARADA K. Fire safety design based on calculations [R]. Sweden: Department of Fire Safety Engineering, Lund University, 1995.
- Code for the design of metro (GB 50157—2003) .
- Holborn, P, G., Nolan, P. F. & Golt, J., An analysis of fire sizes, fire growth rates and times between events using data from fire investigations, *Fire Safety Journal* 39 (2004) 481–524.
- D.A. Purser, M. Bensilum. Quantification of behaviour for engineering design standards and escape time calculations. *Safety Science* 38 (2001):157~182.
- Frantzich H.. Reaction times prior to evacuation for shops, restaurants and public dance-halls. Estimates done by fire officers, LUTVDG/TVBB 3071 SE, Department of Fire Safety Engineering, Lund University, Lund 1993.
- QUINCY. NFPA 92B: Guide for Smoke Management Systems in Malls, Atria, and Large Areas, 2000 Edition [M]. MA: National Fire Protection Association, 2000.
- L.H. Hu, R. Huo. On the maximum smoke temperature under the ceiling in tunnel fires. *Tunnelling and Underground Space Technology* 21 (2006): 650~655.

STUDY ON RISK ASSESSMENT OF CROWD EVACUATION IN VENUE AREA

P. LI, W.G. and WENG, X.W. JI
Center for Public Safety Research,
Department of Engineering Physics,
Tsinghua University, Beijing, 100084, P.R. China
lipan07@mails.tsinghua.edu.cn

ABSTRACT

There are many situations in which a large number of pedestrians evacuate in a short period of time after a large-scale activity in venue area. If some emergencies happen, it will be more likely to cause crowd disaster, e.g. trampling and crushing, etc. Therefore it is necessary to study an appropriate quantitative assessment method to determine the risk of crowd evacuation in venue area. In this paper, a systematic procedure for the quantitative risk assessment caused by crowd evacuation is developed. A subsequent case study considering the crowd evacuation in normal scenario and accidental scenario is applied to use the quantitative risk assessment procedure. It is evidenced this method can identify the high risk areas quantitatively. In addition, the method can be used to contrast the difference between normal and accidental scenarios in order to provide scientific warrant for crowd evacuation risk management.

1. INTRODUCTION

Many crowd related tragedies happened over the past decade. Annually, numerous events of large pedestrian crowds that have ended in tragedy took approximately 2000 lives per year on average [1]. For instance, a severe crowd disaster occurred in Miyun, northern suburb of the Chinese capital, has caused 37 tourists died and 24 hurt. Crowd incidents involve large numbers of casualties and hence generally have a greater impact on the community than less sensational incidents that occur more frequently [2]. Especially we should pay particular attention to crowd disaster in venue area in large cities since after large-scale activities high population densities often cause potential risk for crowd crush which normally results into injury or casualty. In sum, crowd evacuation risk after large-scale activities in venue area is an important but largely neglected issue of science and engineering.

Up to now, some studies about trampling and crushing in crowd have been developed. Hughes and Lee have explained the development of crowd crushing using a continuum theory for crowd motion at both high and very high densities of pedestrians [3], and studied strategy for minimizing the risks of trampling in a crowd [4]. Helbing proposed a force model of pedestrian behavior to investigate the mechanisms of panic and jamming and suggested practical ways to prevent dangerous crowd pressures [5]. Zhen Xiaoping summarized systematically crowd evacuation models based on seven methodological approaches [6]. Smith and Dickie considered simple physical engineering of crowd safety in terms of the performance and life of structures to look at how structures fit the behavior of people and how the structure can promote people's safety [7]. Yet risk of crowd evacuation in venues area is not frequently considered. In this paper, the systematic procedure for risk assessment of crowd evacuation (RACE) is presented, and then a case study applying this procedure is discussed, followed by the conclusion.

2. PROCEDURE FOR RACE IN VENUE AREA

Generally there are two most disastrous forms of collective human behavior: crowd trampling and pedestrian crushing. These two kinds of crowd behavior in venue area could be triggered in life-threatening situations such as fires, terrorism, rainstorm and so forth. Therefore, to assess the risk of crowd evacuation in a particular venue area, the first step should be "identification of possible accidental scenario" which induces crowd trampling or crushing. Considering the actual situation of the venue area, credible accidental scenario could be chosen. Next step is to select critical parameters (or indexes) for risk assessment. Then models or software should be seriously chosen to acquire these results of parameters (or indexes). Conclusion of preliminary risk assessment could be reached based on these parameters or index obtained and relative criteria. Judging whether the preliminary conclusion are accord with actuality of this venue area, we go straight ahead if it is "Yes", or go back to alter these parameters (or indexes) selected in the third step if it is "No". Considering existing measures, conclusion of practical risk assessment could be attained. Lastly, based on these results, scientific advices could be presented to reduce the possibility of crowd trampling and pedestrian crushing in this venue area. Fig. 1 summarizes the main steps of the methodology. Generally, the first and second steps (marked by red frame) belong to the phase of background materials collection; the third and fourth steps (marked by yellow frame) is the process of quantitative risk parameters calculation; the fifth to ninth steps (marked by dark blue frame) belong to the final phase of drawing conclusion which include risk assessment and improvement.

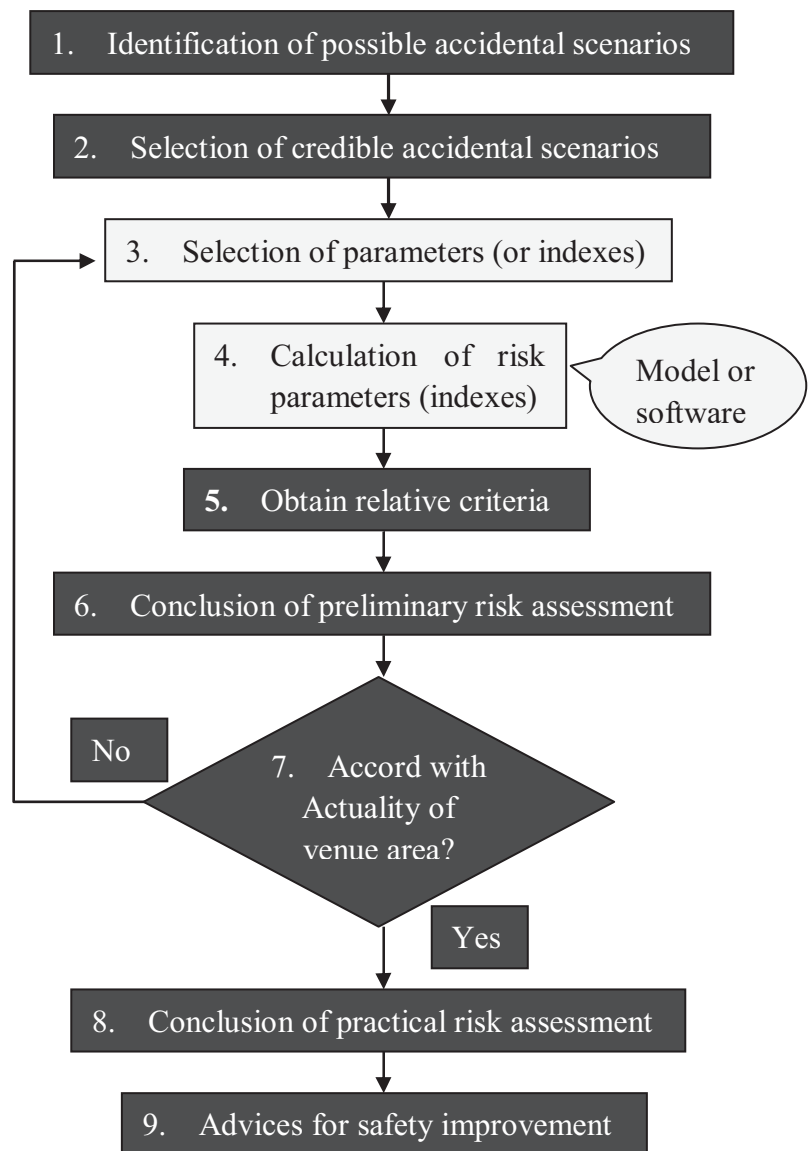


Figure 1: Flow diagram of the procedure used for the quantitative assessment of crowd evacuation risk in venues area

2.1 Accidental Scenario

Data required to apply the procedure in Fig. 1 are discussed in detail in the following:

- All possible accidental scenarios that may trigger or aggravate crowd trampling or pedestrian crushing are determined. History data could be referenced on these crowd disasters happened in the discussed venue area or in other public areas.
- Geography information of the discussed venue area, which may include: pavements, area exits, barriers, venue pedestrian stay, weather condition, surrounding condition around discussed venue area, and so forth, is got.
- Population information of the discussed venue area, which may

include the total number of evacuating pedestrian, and proportion of evacuating crowd is got.

This present study summarize some crowd related accidents occurred before (table 1) which could be referenced when identify possible accidental scenarios in the first steps.

Table 1: Examples of crowd related accidents

| Year | Place | Event | Cause of Disaster | Deaths | Injuries |
|------|--------------------------|--------------------|--|--------|----------|
| 1985 | Mexico City | Football match | Trampling happened when fans tried to force into a stadium | 10 | 29 |
| 1986 | Sheffield, UK | Football match | Tragedy occurred when police open gates to alleviate | 96 | 400 |
| 1992 | South Korea | Pop concert | Fans rushed to the stage during a pop band's concert which was packed with about 16,000 fans | 1 | 50 |
| 1993 | Lan Kwai Fong, Hong Kong | Street party | Trampling occurred during the dispersion of a New Year's eve street party | 21 | 67 |
| 2000 | Denmark | Pock concert | Crowds slipped and fell in mud at front of stage | 9 | 26 |
| 2000 | Indonesia | Pop concert | Five teenagers were crushed to death during an oversold performance of Shelia | 5 | — |
| 2001 | Sydney | Rock concert | A teenage girl was killed in a festival crowd crush | 1 | — |
| 2001 | Glasgow, Scotland | Rock concert | Crowd surge forward to the front of the stage at rock concert | 0 | 45 |
| 2003 | Benin, West Africa | Pop concert | 15 concertgoers were killed in a crowd crush near the front of stage | 15 | — |
| 2005 | Wai, India | Religious festival | 258 Hindu pilgrims were trampled to death during a stampede at an annual religious festival | 258 | 200 |

Based on these data above, credible accidental scenarios of the discussed venue area should be selected from all the possible accidental scenarios. It is also necessary to aware that even though no trigger accident will happen, crowd trampling and (or) pedestrian crushing are still possible to happen if the evacuation process of the discussed venue area is highly populous, or geographical condition of this venue area is not convenient for evacuating. That is why geographical information and population information are both needed in this procedure.

2.2 Selection and calculation of risk parameters

Generally collective movement is quantitatively described by three fundamental characteristics: density, speed, and flow, all of which are expressed as rates. Therefore to specify the risk of crowd disaster, these three fundamental characteristics could be examined. Here we use definitions in Handbook of Fire Protection Engineering, which specified density, speed, and flow as follow [9]:

- Density – the number of persons in a unit area of walkway. And this characteristic could be referred by using the inverse of density, that is, the area per person or pedestrian module.
- Speed – the distance covered by a moving person in a unit of time.
- Flow – is specifically the number of people that pass some reference point in a unit of time.

It is necessary to aware that these three characteristics are related. Speed is dependent on density. The closer people result in the more constrained movement. Aside from constraint of moving speed, high-density situations are also uncomfortable depending on social culture and the relationship to others nearby. In general, pedestrian could move at an average unrestricted speed (about 1.25m/s) when the crowd density is less than 0.5 persons/m²; moving speed could decreases to reach a standstill when the crowd density is about 4 to 5 persons/m². While at low density, speed is mainly determined by occupants' characteristics such as age, gender, psychology and grouping. And when speed and density are available, flow could be obtained as[9]:

$$\text{Flow} = \text{speed} \times \text{density} \times \text{width} \quad (1)$$

In a word, to assess the risk of crowd disaster in venue area, one or all of these three characteristics could be employed depending on the necessity and data available in practical condition. However, lots of other judging indexes could also be referred under different situation.

After choosing the assessing parameters, next step is “calculation of selected parameters”, which could be achieved by appropriate models or software. According to scale, there are two types of models: micro-simulation models and macro-simulation models. The former type, including cellular automata models, lattice gas models, social force models, agent-based models, game theoretic models, focus on each pedestrian including the velocity and interaction. The latter type, including fluid-dynamic models which describe how density and velocity change over time with the use of partial differential equations, overlook the difference of each pedestrian and focus on integral indexes, such as velocity, density, and flow [10]. Obviously, macro-simulation models are appropriate to assess risk of crowd disaster in venue area. To aid readers to select appropriate models for specific project, the present study describe three mainly fluid-dynamic models below.

Table 2: Three main macro-simulation models

| Source | Situation | content |
|---|---|--|
| Hughes' continuum theory for the flow of pedestrians [11] | In particular large crowds under normal situation | Derived the equations of motion governing the two-dimensional flow of pedestrians for flows of both single and multiple pedestrian types. |
| Hughes' the flow of human crowds [12] | Normal | Developed a continuum modeling of crowds as "thinking fluid" based on well-defined hypotheses. |
| pedestrian flows and non-classical shocks [13] | Emergency | Presented a model for the flow of pedestrians which are typical of this flow, such as the fall due to panic in the outflow of people through a door. |

Aside from evacuating models, evacuating software also could be referred to calculate selected parameters. The present study lists frequently used walking evacuating simulation software below.

Table 3: Frequently used evacuating simulation software at home and abroad [14]

| NAME | Country | Research Group | Principle |
|-----------|-----------|---|---------------------------------------|
| EVACNET | USA | University of Florida | No code of conduct |
| SIMULEX | Britain | — | Complex conduct |
| SGEM | China | City University of Hong Kong & Wuhan University | No code of conduct or complex conduct |
| HAZARD | USA | — | — |
| EGRESSPRO | Australia | — | Artificial intelligence |
| EXIT | USA | National Fire Protection Association | Code of conduct |
| STEPS | Britain | Mott MacDonald. | No code of conduct or complex conduct |

2.3 Risk analysis and improvement

When we obtain the results of selected evaluating parameters, the next step is to compare these data with current criteria or standards required and reach the conclusion of preliminary risk assessment. If this result is accord with actuality in administrators' judgments, go straight to the next step to reach conclusion of practical risk assessment considering measure that have been taken. If not, go back to the third step to rectify selected parameters and repeat these steps above. Generally speaking, this section is flexible in standards according to different need.

3. CASE STUDY

This section will present a case to apply the above procedure. After a large-scale activity 5000 persons will evacuate from a venue (the area marked by pink lines) to three gates (short lines marked by green) in a large area as showed below. Blue closed rectangles are buildings or other barriers to pedestrians.

3.1 Identification and selection of accidental scenarios

According to historical materials and current local condition, terrorism are likely to happen which need to evacuate people in the venue out of this area quickly. This emergency situation may induce crowd disaster. Besides, rainstorms often attack the city where this area locates in summer. Therefore, two kinds of accidental scenarios are identified as terrorism and rainstorms. However, the risk assessment is carried out in winter. Thus rainstorms are not the accidental scenario required to consider by administrators at that time. The credible accidental scenario hence could be selected as terrorism. Besides even though no emergency happens, after a large-scale activity it is crowded for 5000 people evacuate out of this venue area simultaneously. Thereby crowd disaster risk under normal situation and terrorism are both needed to be evaluated here.

3.2 Selection and calculation of risk parameters

Here we choose crowd density as the assess index of the crowd evacuation risk. Firstly, the crowd density is the most important index to judge the risk for both crowd trampling and crowd crushing. Besides, software simulation proves that crowd density in this situation are not so high as to cause crushing, in which internal pressure in a crowd is an important criterion determining the likelihood of crushing [3]. To obtain the data of crowd density during the simulated evacuation, software STEP are employed. In the screenshots, there are five primary evacuating paths and six turning areas that are crowded on observation. Thus crowd densities in these six turning areas are examined and simulation output densities of these areas. 80% of 5000 people are adults (denoted by blue) and 20% of 5000 people are children (denoted by yellow). Under the emergent situation, pedestrians evacuate faster than those under normal condition.

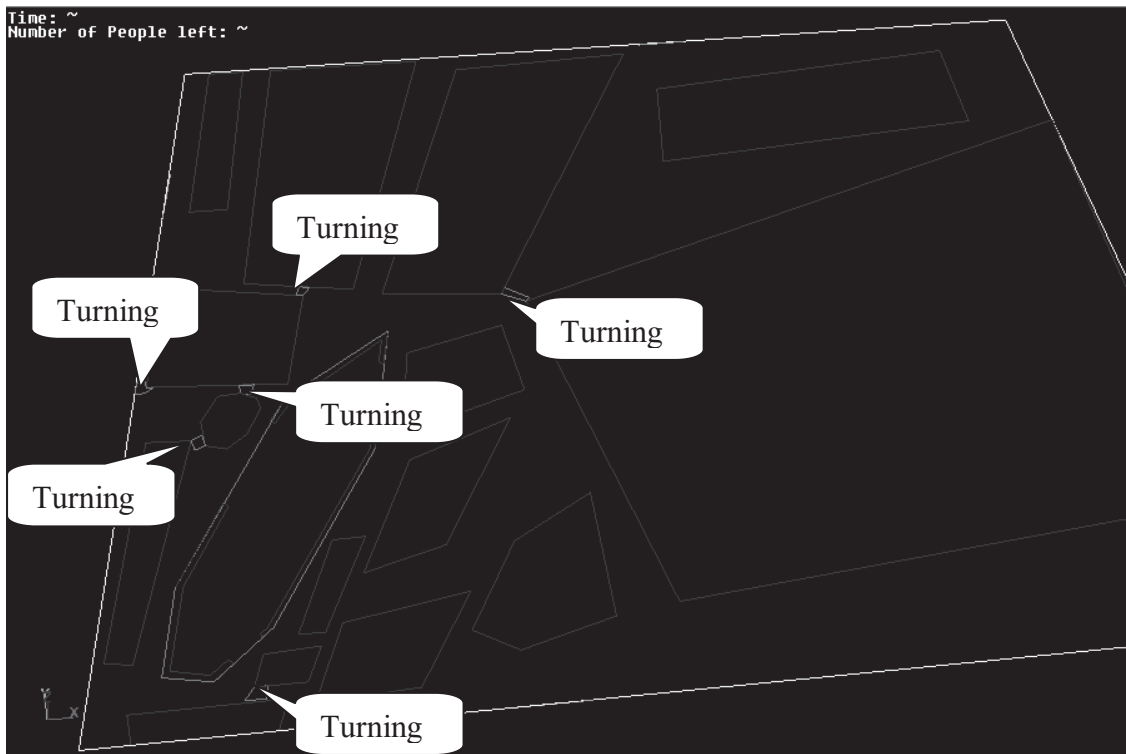


Figure 2: The selected venue area

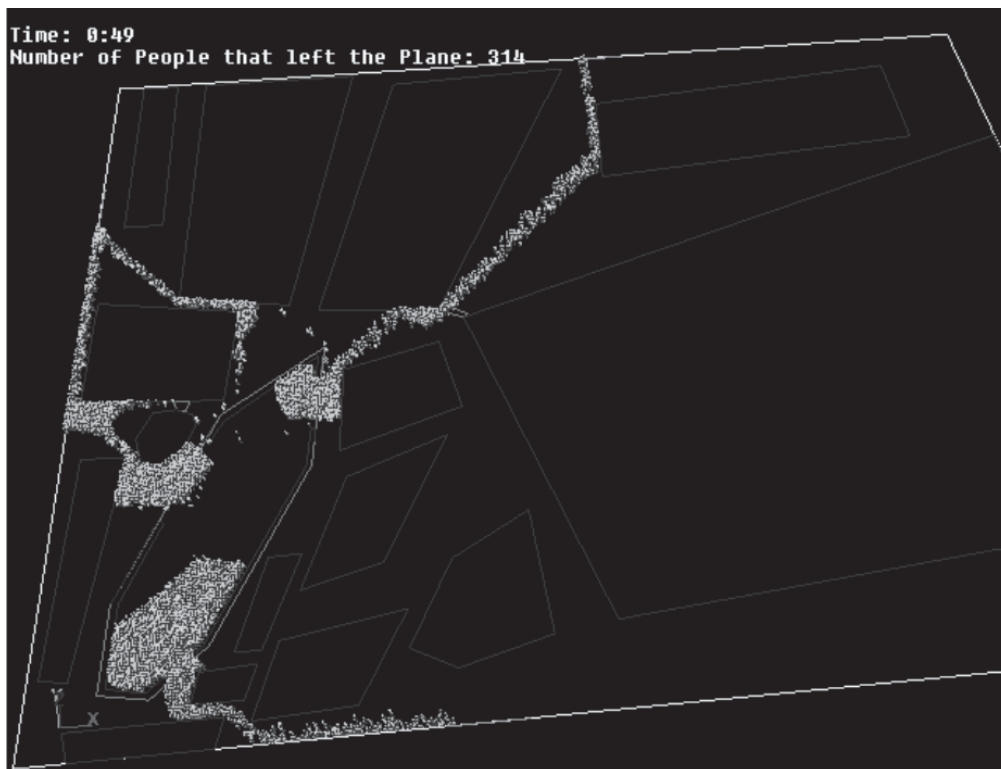
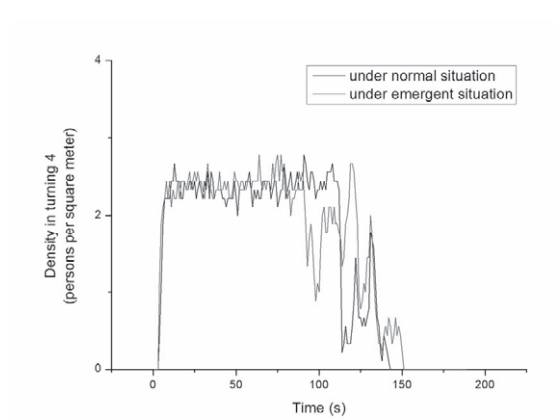
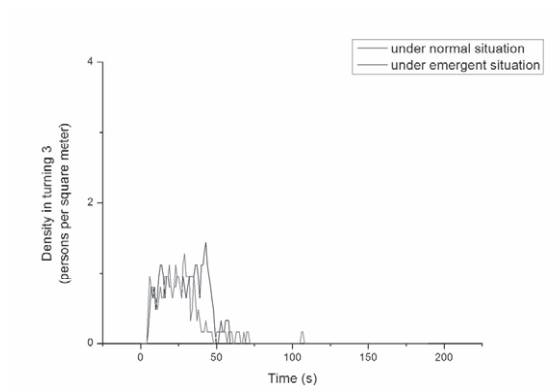
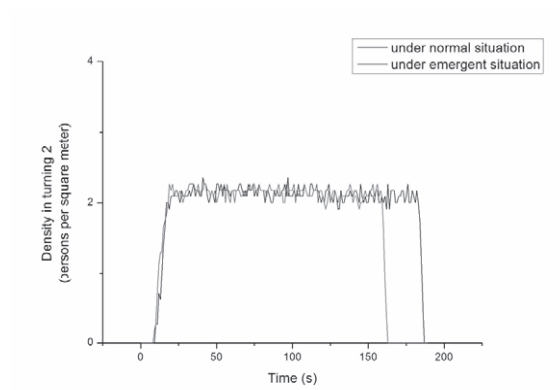
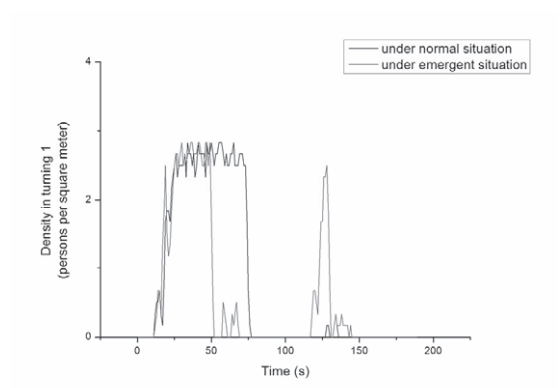


Figure 3: Simulation of 5000 people evacuating out of a selected venue area

Total evacuation time under normal situation is 3:34, and total evacuation time under emergent situation is 3:09. Crowd densities in six turning areas under both situations are showed below in Figure 4.



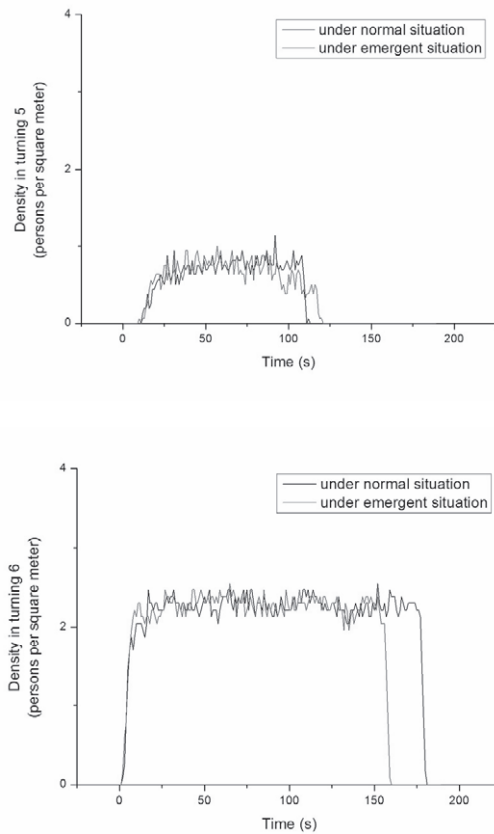


Figure 4: Crowd densities in 6 turning areas under normal situation and emergent situation

3.3 Obtain relative criteria

The critical density for an accident involving trampling is approximate 5 persons/m² and for crushing is larger at about 10 persons/m² which may occur nearly static crowds.

3.4 Risk analysis and improvement

The highest crowd density in this case does not exceed 3 persons/m². Therefore crowd trampling is comparatively less likely to happen except some areas are needed to be noticed at some time. From these data it is clear to see which rounding areas and at what time in the process of evacuation comparatively high level of crowd density is reached, which could be quantitatively referred by administrators in the risk management of the venue area. These rounding areas should be attend are listed in Table 3 and 4.

Table 4: Rounding areas should be attend under normal situation

| | TIME | AREA | CROWD DENSITY |
|---|-----------|-----------|---|
| 1 | 0:23-1:13 | Turning 1 | About 2.6 persons/m ² on average |
| 2 | 0:11-1:52 | Turning 4 | About 2.3 persons/m ² on average |

Table 5: Rounding areas should be attend under emergent situation

| | TIME | AREA | CROWD DENSITY |
|---|-----------|-----------|---|
| 1 | 0:25-0:49 | Turning 1 | About 2.7 persons/m ² on average |
| 2 | 2:06-2:08 | Turning 1 | About 2.4 persons/m ² on average |
| 3 | 0:49-1:19 | Turning 4 | About 2.3 persons/m ² on average |
| 4 | 0:22-0:40 | Turning 4 | About 2.4 persons/m ² on average |

In addition, evacuation time under emergency should also be sent to administrators to judge whether 3:09 is accord with their requirement. Measures to avoid crowd disaster in evacuating after large-scale activities are seldom and this simulation process is accord with practical situation; therefore practical conclusion of risk assessment could be reached and warrant for crowd disaster risk management could be drawn scientifically.

4. CONCLUSIONS

The present study has developed a flow diagram of the procedure used for the quantitative risk assessment of crowd evacuation in venues area. Nine steps of this procedure are discussed in detail, and a subsequent case study considering the crowd evacuation in normal scenario and accidental scenario is applied to use the presented procedure. And It is evidenced that this procedure could identify high risk areas during the evacuation process quantitatively.

ACKNOWLEDGMENT

The authors would like to acknowledge the supports provided by the Fund of National Eleven Five-Year Great Scientific and Technical Support Plans (2006BAK06B02) and Beijing Municipal Science & Technology Commission (D08050600380801).

REFERENCES

Hughes, R.L., 2003. *The flow of human crowds*. Annu. Rev. Fluid Mech. 35,169–182.

- Qingsong Zhang, Mao Liu, Caihong Wu, Guomin Zhao. *A stranded-crowd model (SCM) for performance-based design of stadium egress*. Building and Environment 2007: 2630–2636.
- R.S.C. Lee, R.L. Hughes. *Exploring trampling and crushing in crowds*. J. Trans. Eng. 131 (8) (2005) 576–582.
- Ris S.C. Lee, Roger L. Hughes. *Minimisation of the risk of trampling in a crowd*. Mathematics and Computers in Simulation 2007: 29–37
- Dirk Helbing, Illes Farkas & Tamas Vicsek. *Simulating dynamical features of escape panic*. NATURE, VOL 407, 28 SEPTEMBER 2000
- Xiaoping Z, Tingkuan Z, Mengting L. *Modeling crowd evacuation of a building based on seven methodological approaches*. Building and Environment (2008), doi:10.1016/j.buildenv.2008.04.002
- R.A. Smith and J.F. Dickie (eds.). *Engineering for Crowd Safety [M]*. Elsevier, Amsterdam, 1993
- Ris S.C. Lee, Roger L. Hughes. *Prediction of human crowd pressures*. Accident Analysis and Prevention 38 (2006) 712–722
- Philip J. DiNenno, Dougal Drysdale, Craig L. Beyler, W. Douglas Walton, Richard L. P. Custer, John R. Hall, Jr., John M. Watts, Jr.. *Handbook of Fire Protection Engineering (Third Edition)*.
- LU Chunxia. *Analysis of Compressed Force in Crowds*. J Transpn Sys Eng & IT, 2007, 7(2), 98–103.
- Hughes RL. *A continuum theory for the flow of pedestrians*. Transportation Research Part B 2002;36:507-35.
- Hughes RL. *The flow of human crowds*. Annual Review of Fluid Mechanics 2003;35:169-82.
- Colombo RM, Rosini MD. *Pedestrian flows and non-classical shocks*. Mathematical Methods in the Applied Sciences 2005;28:1553-67.
- M, L. Jin. *Mixed Traffic Flow Evacuation in City Emergency: [dissertation]*. Beijing: Tsinghua University, 2008.

FLOOD SIMULATION WITH AN IMPROVED SPH MODEL

KAI BAO¹, HUI ZHANG², LILI ZHENG³ and ENHUA WU⁴

^{1,4}State Key Laboratory of Computer Science,
Institute of Software, Chinese Academy of Sciences, Beijing, China
Graduate University of Chinese Academy of Sciences, Beijing, China
baokai@ios.ac.cn

²Department of Engineering Physics, Tsinghua University, Beijing, China
ehwu@umac.mo
zhhui@tsinghua.edu.cn

³School of Aerospace, Tsinghua University, Beijing, China
zhenglili@tsinghua.edu.cn

ABSTRACT

Smoothed Particle Hydrodynamics (SPH), as one of the meshless Lagrangian methods, has been widely used in simulating free surface problems. In the paper, several improvements, including pressure-correction scheme, signed distance field based boundary treatment and SPS turbulence model are implemented to the basic SPH to simulate flooding flow. The improved SPH model is used to investigate the flow over staircase and the tsunami impacting on coastline. The results demonstrate that the current SPH model can be used as a powerful tool to study flooding phenomena with violent water fragmentation and complex topography.

1. INTRODUCTION

Numerous modern numerical techniques can be used to simulate the free surface flow problems. Most of them are based on meshed methods in which the surface tracking or capturing schemes are usually required in order to obtain the position and speed of the flow surface, such as the volume of fluid, level set method or front tracking. Recently, the Smoothed Particle Hydrodynamics (SPH) method, one of the meshless Lagrangian methods, was applied to various applications, including free surface simulation.

In the SPH method, the continuum is represented by a set of particles each with a given mass and velocity, and the macroscopic values are evaluated through particle interpolation. As it requires no computational grids, SPH offers some advantages over grid methods. For example, the free surface can be easily tracked, mass conservation is coherently guaranteed, and large deformation and violent fragmentation can be handled straightforwardly. A fairly extensive review of SPH method has been provided by Monaghan (2005).

In this paper, several improvements are developed to the basic SPH model for simulating the free surface flow. In the improved SPH model, a pressure correction scheme is proposed to make the local pressure propagate

to the neighboring areas so as to overcome tensile instability. A signed distance field based solid boundary treatment is also used for handling complex topography. The SPH model, together with an SPS model for taking into account of turbulence effects, is used to study the phenomena related to water pouring into underground building and tsunami impacting on coastline with complex topography.

2. METHODOLOGY

2.1 Basic SPH Formulations

In the SPH model, the Lagrangian form of the Navier-Sokes equations is used:

$$\frac{D\rho}{Dt} + \rho \nabla \cdot \mathbf{v} = 0 \quad (1)$$

$$\frac{D\mathbf{v}}{Dt} = -\frac{1}{\rho} \nabla p + \nu \nabla^2 \mathbf{v} + \mathbf{g} \quad (2)$$

where \mathbf{v} is velocity vector, p is pressure, ρ is fluid density, \mathbf{g} is gravitational acceleration vector, and ν is the kinetic viscosity. As a meshless Lagrangian particle method, the fluid is discretized with the Lagrangian particles instead of computational grids. To find the value of a particular quantity f at an arbitrary position \mathbf{x} , an interpolation is applied with the neighboring particles, i.e. particle approximation:

$$f(\mathbf{x}) = \sum_{j=1}^N f_j W(\mathbf{x} - \mathbf{x}_j) V_j \quad (3)$$

where f_j is the value of f at the position of particle j , which locates at \mathbf{x}_j , $W(\mathbf{x} - \mathbf{x}_j)$ is the smoothing function and V_j is the volume of particle j , determined with the particle mass m_j divided by the particle density ρ_j .

If f is taken as the fluid density, ρ , the density of particle i , locating at \mathbf{x} , can be evaluated by:

$$\rho_i(\mathbf{x}) = \sum_{j=1}^N m_j W(\mathbf{x} - \mathbf{x}_j) \quad (4)$$

By applying the SPH particle approximation to the Lagrangian form of the Navier-Stokes equations, the momentum equation in the SPH form can be obtained as follows:

$$\frac{d\mathbf{v}_i}{dt} = -\sum_{j=1}^N m_j \left(\frac{p_i}{\rho_i^2} + \frac{p_j}{\rho_j^2} \right) \nabla_i W_{ij} + \nu \sum_{j=1}^N \frac{m_j}{\rho_j} (\mathbf{v}_j - \mathbf{v}_i) \nabla^2 W_{ij} + \mathbf{g} \quad (5)$$

where \mathbf{v}_i is the velocity of particle i , p_i is the pressure of particle i .

In order to solve Eq. (6), it is necessary to use the equation of state to evaluate the fluid pressure, even for an incompressible flow. Based on the fact that a theoretically incompressible flow is practically compressible, Morris et al. (1997) introduced the artificial compressibility equation:

$$p = c^2 \rho \quad (6)$$

where c is the sound speed. The sound speed is generally chosen according to the following rules:

$$c^2 = \max\left(\frac{V_o}{\delta}, \frac{\nu V_o}{\delta L_0}, \frac{FL_0}{\delta}\right) \quad (7)$$

where $\delta = \Delta\rho / \rho_0$, V_o and L_0 are the reference velocity and length, respectively. Since the pressure force is generally related to the gradient of the pressure, the following form of the equation of state can be used to increase the stability of simulation,

$$p = c^2(\rho - \rho_0). \quad (8)$$

This form provides good density targeting property, while some artificial surface tension could be introduced near the free surface. With the equation of state, the time-consuming Poisson equation solving is avoided, thus simulations can be performed much faster. However, this may cause the pressure field accumulated locally, resulting in numerical instability.

2.2 Pressure Correction Scheme

Due to the artificial compressibility in Eq.(6) and (8), the incompressibility or volume conservation of the flow is not well satisfied. The density deviation can cause pressure disturbance, which may introduce numerical instability. Some researchers enforced strict incompressible simulation by solving the pressure Poisson equation (Lo and Shao, 2002), thus the computation is increased dramatically. In the following, a flexible pressure-correction equation is introduced so as to increase the stability of the simulation as well as the efficiency of the SPH model.

We first substitute Eq. (7) into the continuity equation, i.e. Eq. (1) to yield:

$$\frac{Dp}{Dt} + \rho c^2 \nabla \cdot \mathbf{v} = 0 \quad (9)$$

The SPH formulation of Eq. (9) is written by

$$\frac{P_i^{n+1} - P_i^n}{c^2 \delta t} + \sum_{j=1}^N m_j (\mathbf{v}_j^{n+1} - \mathbf{v}_i^{n+1}) \nabla_i W_{ij}^n = 0 \quad (10)$$

where n denotes the current time step. It is noted that the RHS of Eq. (10) should be zero if computation is convergent. It, however, is not satisfied usually. Let us set

$$S = \frac{P_i^{n+1} - P_i^n}{c^2 \delta t} + \sum_{j=1}^N m_j (\mathbf{v}_j^{n+1} - \mathbf{v}_i^{n+1}) \nabla_i W_{ij}^n \quad (11)$$

According to the Newton's method, a pressure-correction equation can be obtained:

$$\begin{aligned}
 \delta p_i^{n+1} &= -\frac{S}{(\partial S / \partial P)} \\
 &= -\left(\frac{1}{c^2 \delta t}\right)^{-1} \left[\frac{p_i^{n+1} - p_i^n}{c^2 \delta t} + \sum_{j=1}^N m_j (\mathbf{v}_j^{n+1} - \mathbf{v}_i^{n+1}) \nabla_i W_{ij}^n \right] \\
 &= -\left[p_i^{n+1} - p_i^n + c^2 \delta t \sum_{j=1}^N m_j (\mathbf{v}_j^{n+1} - \mathbf{v}_i^{n+1}) \nabla_i W_{ij}^n \right]
 \end{aligned} \tag{12}$$

The pressure of new time step can be corrected by:

$$p_i^{n+1} = p_i^{n+1} + \omega \delta p_i^{n+1} \tag{13}$$

where ω is the relaxation factor with a value of 0.8~1.0.

The velocity correction term can be obtained from the momentum equation,

$$\frac{D\mathbf{v}}{dt} = \nabla \cdot (\nu \nabla \mathbf{v}) - \frac{\nabla p}{\rho} + \mathbf{f} \tag{14}$$

where ν is the kinetic viscosity. Then the velocity correction can be obtained by:

$$\frac{\delta \mathbf{v}_i^{n+1}}{\delta t} = -\frac{\delta p_i^{n+1}}{\delta x_i \rho_i} \tag{15}$$

and the velocity is updated with

$$\mathbf{v}_i^{n+1} = \mathbf{v}_i^{n+1} - \Omega \frac{\delta t}{\rho_i} \frac{\delta p_i^{n+1}}{\delta x_i} \tag{16}$$

where Ω is the relaxation factor.

In each given time step, Eqs. (13) and (16) are used iteratively until Eq.(11) is satisfied. During the iteration, pressure disturbance will propagate to a large neighboring area and it finally diminished.

2.3 Solid Boundary Conditions

In this paper, a signed distance field based solid boundary treatment is used to enforce the solid boundary condition, with which the usual generation of extra virtual boundary particles or ghost particles is avoided. Signed distance fields are widely used in the collision detection in the field of computer graphics, and some researchers used it to enforce the solid boundary conditions in the particle method.

For the solid boundary, a signed distance field is generated and stored in a trilinear grid as a part of preprocessing. For each particle i , which locates at \mathbf{x}_i , the signed distance value $\phi(\mathbf{x}_i)$ can be evaluated by a trilinear interpolation from the eight neighboring grid nodes. A penetration is detected when $\phi(\mathbf{x}_i) \leq 0$, and the contact normal \mathbf{n}_i is evaluated by normalizing the gradient of the distance field. To resolve the penetration, the penetrating particles are mirror reflected back into the computation domain in the normal direction. The velocity of the penetrating particle i is separated into normal and tangential components:

$$\mathbf{v}_i^n = (\mathbf{v}_i \cdot \mathbf{n}_i) \mathbf{n}_i \tag{17}$$

$$\mathbf{v}_i^r = \mathbf{v}_i - \mathbf{v}_i^n \quad (18)$$

Then the velocity is updated as follows:

$$\mathbf{v}_i^n = -(1 - \mu)\mathbf{v}_i^n \quad (19)$$

$$\mathbf{v}_i^r = (1 - \omega)\mathbf{v}_i^r \quad (20)$$

where μ and ω are parameters to enforce different solid boundary conditions. The free-slip and non-slip boundary conditions are enforced by $\omega = 0$ and $\omega = 1$ respectively.

2.4 SPS Model

In order to handle the turbulence effects in the flow, a Sub-Particle Scale (SPS) turbulence model is used. The SPS approach to modeling turbulence was first described by Gotoh et al. (2001) to represent the effects of turbulence in their MPS model, so did Lo and Shao (2002) in their incompressible SPH scheme. Dalrymple and Rogers (2006) firstly introduced SPS model to weakly compressible SPH scheme. The SPS model used here follows Dalrymple and Rogers' work.

A flat-top spatial filter is applied to the governing equations:

$$\frac{D\tilde{\mathbf{v}}}{Dt} = -\frac{1}{\tilde{\rho}}\nabla\tilde{p} + \nu\nabla^2\tilde{\mathbf{v}} + \mathbf{g} + \frac{1}{\tilde{\rho}}\nabla\cdot\tau^* \quad (21)$$

where τ^* represents the SPS stress tensor and

$$\frac{1}{\tilde{\rho}}\tau_{ij}^* = 2\nu_t S_{ij} - \frac{2}{3}\kappa\delta_{ij} - \frac{2}{3}C_I\Delta^2\delta_{ij}|S_{ij}|^2 \quad (22)$$

C_I is taken to be 0.0066, S_{ij} is the strain tensor, κ is the SPS turbulence kinetic energy, C_s is the Smagorinsky constant and used to evaluate the eddy viscosity:

$$\nu_t = (C_s\Delta)^2|S| \quad (23)$$

where $C_s = 0.12$, Δ is the initial particle spacing and the local strain rate is given by $|S| = (2S_{ij}S_{ij})^{1/2}$.

With a symmetric formulation of Lo and Shao (2002), the SPS stresses can be evaluated with:

$$\frac{1}{\tilde{\rho}}\nabla\cdot\tau^* \Big|_i = \sum_{j=1}^N m_j \left(\frac{\tau_i^*}{\rho_i^2} + \frac{\tau_j^*}{\rho_j^2} \right) \cdot \nabla_i W_{ij} \quad (24)$$

For more information on the SPS model used here, the readers are referred to Dalrymple and Rogers (2006).

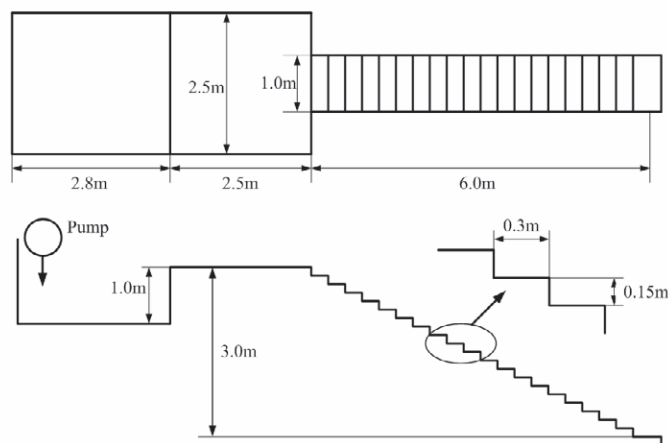


Figure 1: Configuration of the staircase model

3. EXAMPLES

3.1 Water Flowing into Underground Building

Many floods were caused by heavy rainstorm and bank burst, and many of them occurred in fully urbanized areas. On July 18th, 2007, a three-hour heavy rainfall inundate the underground shopping mall in the Square Quancheng in the city of Jinan City, China, and human lives were seriously threatened in the event. Usually, a refuge from the underground space needs to pass staircase, which is also the route of flood invasion. Therefore, it is necessary to model and analyze the flow characteristics over the staircases.

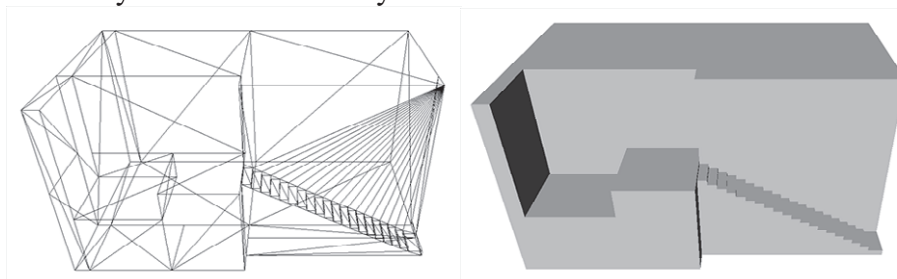


Figure 2: The cutaway view of the model used in the simulation (left: wireframe, right: 3D rendering)

To evaluate the flow characteristics accurately, experiments were conducted. Ishigaki et al. (2005) conducted experiments with real size model of staircase and doors to study the evacuation from underground building. In addition, Gotoh et al. (2005) performed numerical simulation on water stream over staircase used a 3D MPS scheme. However, due to the expensive solving of the Poisson equation, their computation was really time-consuming.

In this paper, following the real scale model used in Ishigaki et al. (2006), water flow over staircase is simulated. Figure 1 shows the configuration, which is almost the same as the one used in the experiment

(Ishigaki et al., 2006), except that a smaller water reservoir is used for saving computation. Figure 2 shows a cutaway view of the mesh of solid boundary used in the simulation, with which, a distance field is generated to represent the solid boundary. The free-slip solid boundary condition is enforced here.

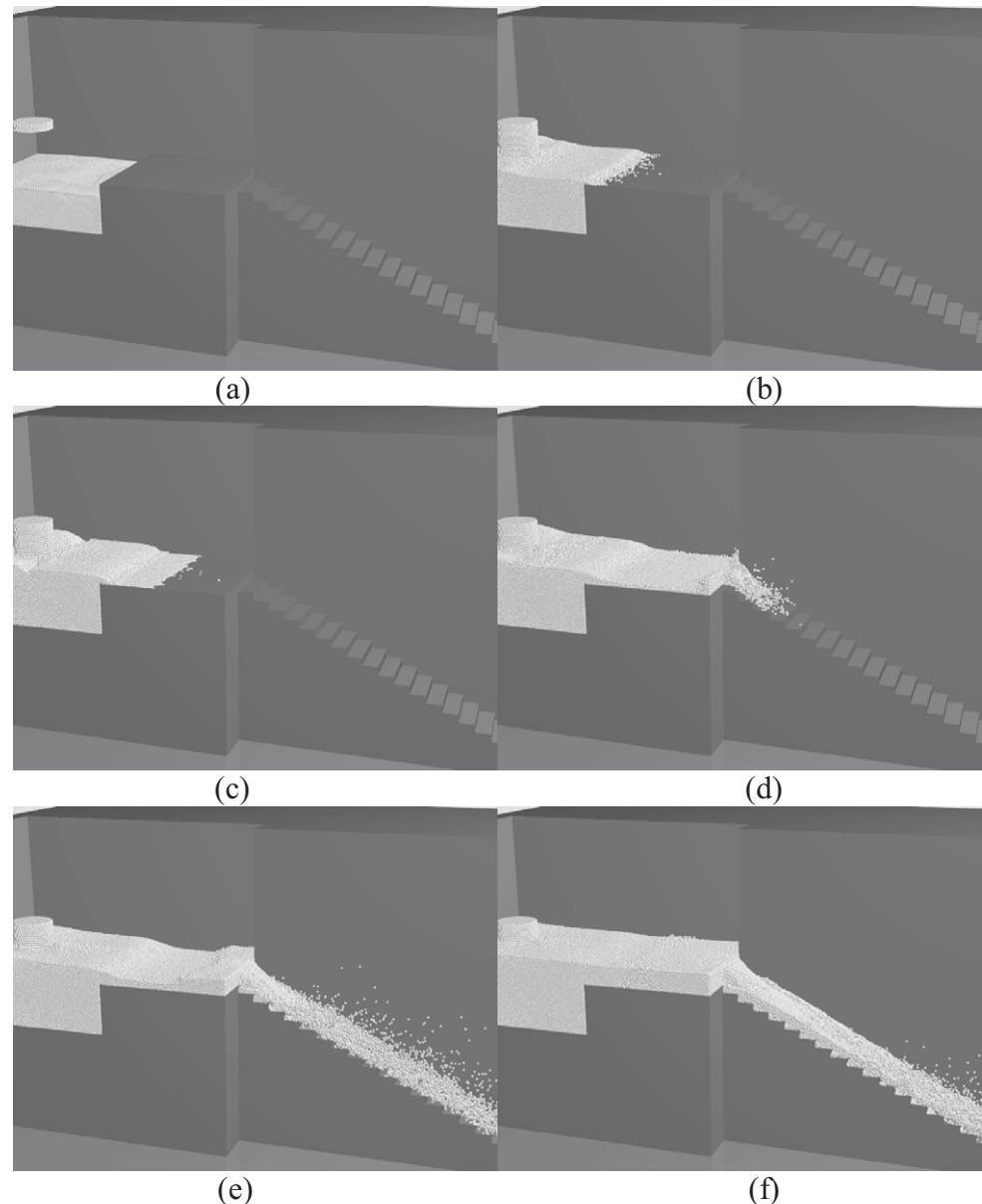


Figure 3: The results of the staircase simulation at (a) $t=0s$, (b) $t=2.3ms$, (c) $t=3.1s$, (d) $t=4.65s$, (e) $6.15s$, (f) $10.15s$

Numerical results at six different time of the simulation are shown in Figure 3. At the initial time (Figure 3a), water is injected from pump at the rate of $0.7m^2/s$ to the water reservoir (with some water initially in the reservoir to save computation time). After the reservoir has been filled up, water begins to flow out the reservoir towards the staircase. When the water reaches the staircase, it flows downwards following the path of the staircase. Violent splash and fragmentation are produced. During simulation, the fluid particles are simply deleted at the bottom of the staircase to enforce a simple outflow boundary condition. At the time 10.15s (Figure 3f), a stable state is

reached, which agrees well with the experimental case of $0.7\text{m}^2/\text{s}$ in (Ishigaki et al., 2006) with the water depth of near 0.5m. Turbulent structure is also well reproduced in the simulation.

The number of particles at the stable state is about 450,000, and the entire simulation takes about 30 hours with a single CPU thread. Compared with the simulation taken in Gotoh et al.(2005), which took about 296 hours for 10s simulation with about 200,000 particles, the numerical technique taken in this paper is more efficient since it avoids the time-consuming solution of the Poisson equation. The results here are rendered with an open-source ray-tracer POV-Ray.

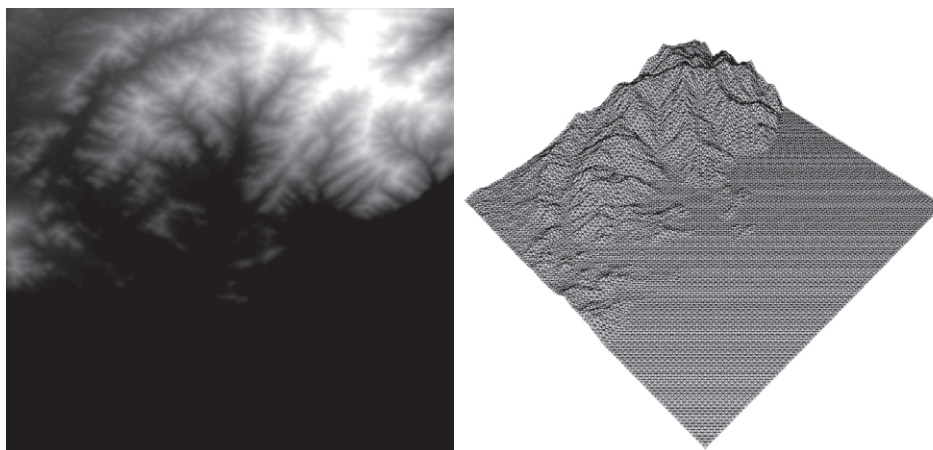


Figure 4: The DEM data (left) and the terrain surface mesh (right) used in the simulation

3.2 Tsunami simulation

Flood caused from tsunami or typhoons is also attacking many Chinese cities. Simulation on flow over a complicated topography is carried out to test the performance of our SPH model on handling complicated topography. In the simulation, digital elevation model (DEM) data is used to generate the terrain surface mesh. DEM is a digital representation of the topography. The DEM data used in the simulation is SRTM 90m DEM data of the city of Tsingdao, which locates at 120:19E, 36:04N and by East China Sea, and is provided by CGIAR-CSI (<http://srtm.csi.cgiar.org>). The DEM data used is shown in Figure 4(a). The gray level represents the ground height of the corresponding position. The terrain surface mesh generated is shown in Figure 4(b). Same with the staircase simulation, a distance field is created with the mesh to handle the solid boundary condition. And also, free-slip solid boundary condition is used here.

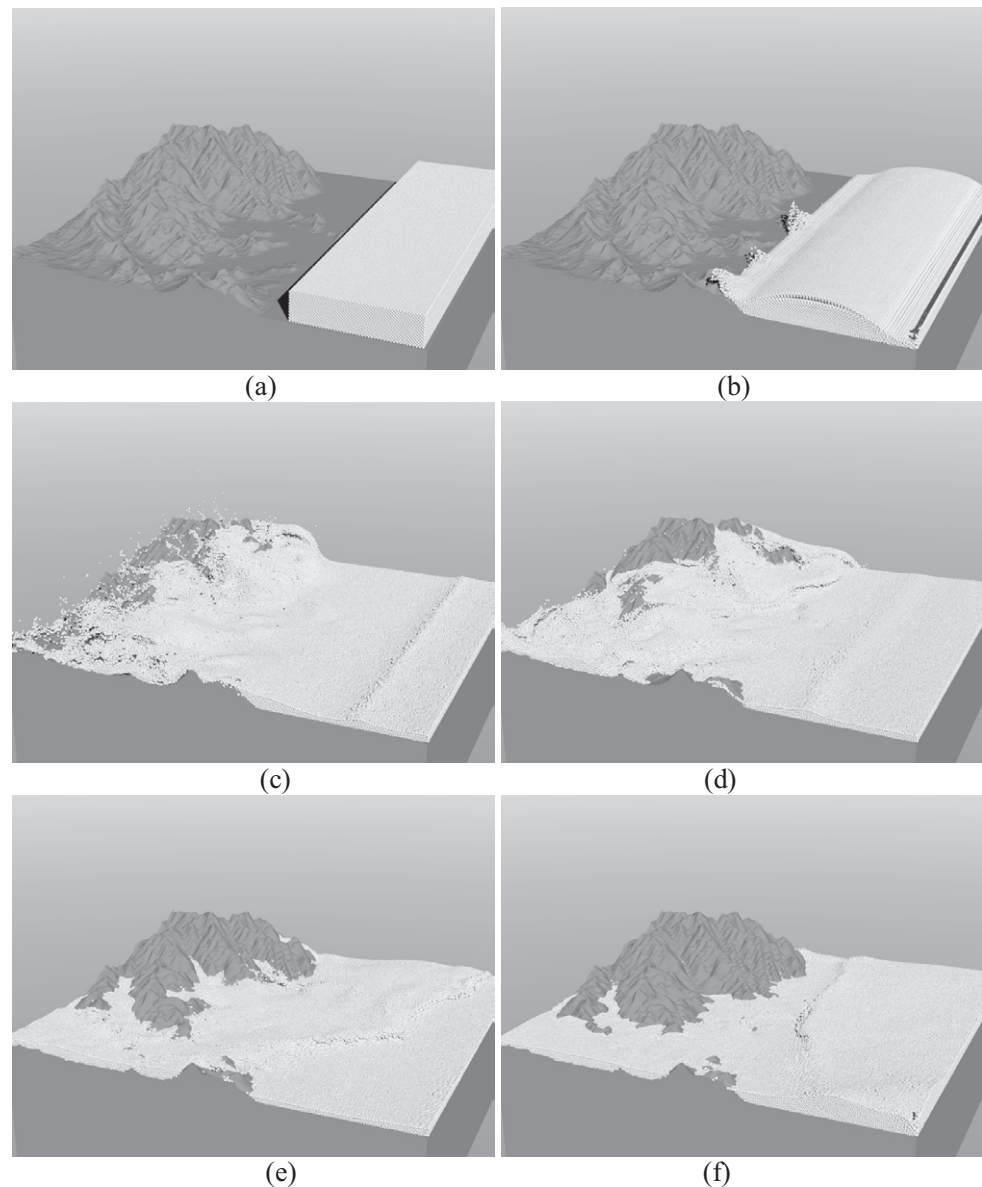


Figure 5: The results of the simulation of flows over terrain at (a) $t=0s$, (b) $t=0.35s$, (c) $t=1.8s$, (d) $t=2.5s$, (e) $t=4.2s$, (f) $t=7.35s$

A small-scale simulation is performed. The size of computation domain is 10m in both horizontal directions and the initial velocity of water body is 2m/s as shown in Figure 5(a). When water interacts with terrain surface, violent breakage and fragmentation occur. Wave propagation and reflection is well produced. With the complicated topography, the present SPH model performs well. The number of the particles used in the simulation is about 310,000. For 8 second simulation, it takes about 24 hours.

4. CONCLUSIONS

The SPH method offers advantages on the simulation of free surface problems. Several improvements to the basic SPH model, such as pressure-correction scheme and the treatment of solid boundary conditions, are

developed in this paper. The improved SPH model has been used in the simulation of flow over staircase and complex topography. The capability of the current SPH model in handling violent free surface and complicated topography have been demonstrated.

However, the improved SPH model is still an ongoing work and the results are preliminary, requiring further analysis and improvement. More comparison with other numerical methods and experimental data will be conducted. Also the current SPH model in the practical applications needs to be validated in the future.

ACKNOWLEDGEMENT

The research work is supported by Changjiang Scholar plan for the second author and by NSFC (60773030), the Grant of University of Macau (RG-UL/07-08S/Y1/WEH/FST) and the National Fundamental Research 973 Project (2002CB312102) for the first and fourth authors.

REFERENCES

- Dalrymple, R.A., and Rogers, B.D., 2006. Numerical modeling of water waves with the SPH method. *Coast. Eng.*, 53, 141–147.
- Gotoh, H., Shibahara, T., and Sakai, T., 2001. Sub-particle-scale turbulence model for the MPS method-Lagrangian flow model for hydraulic engineering. *Computational Fluid Dynamics Journal*, 9(4), 339-347.
- Gotoh, H., Ikari, H., and Sakai, T., 2005. Numerical simulation of stream over staircase by 3D particle method, *Proc MPMD-2005*, Kyoto, Japan, pp. 185–190.
- Ishigaki, T., Toda, K., Baba, Y., Inoue, K. Nakagawa, H., Yoshida, Y., and Tagawa, H., 2005. Experimental study on evacuation from underground space by using real size models. *Annuals of Disas. Prev. Res. Inst., Kyoto Unvi.*, No. 48B (in Japanese)
- Lo, E., and Shao, S., 2002. Simulation of near-shore solitary wave mechanics by an incompressible SPH method. *Applied Ocean Research* 24, 275-286.
- Monaghan, J. J., 2005. Smoothed particle hydrodynamics. *Rep. Prog. Phys.* 68,703-1759.
- Morris, J.P., Fox, P.J., and Zhu, Y., 1997. Modeling low Reynolds number incompressible flows using SPH. *J. Comput. Phys.* 136, 214–226.

AGENT-BASED SIMULATION AND MODELING OF EMERGENCY RESPONSE ON REPAST PLATFORM

JIANHONG WU, WENGUO WENG and JING ZHANG

Department of Engineering Physics,
Center for Public Safety Research,
Tsinghua University, China
jh-wu05@mails.tsinghua.edu.cn

ABSTRACT

Agent based simulation has been accepted in disaster management to model the complex interactions among a mass of independent agents. In this paper, an agent-based model was developed to capture human interactions during emergency response in an urban area. It provides a reality simulation environment for testing different population evacuation strategies and rescue strategies. Emergency response activities are simulated by modeling each group involved as an agent. Customized agents play deferent roles in the simulation and can perform different tasks. The model is developed based on the Java version of Repast 3.1, and the framework of the simulation is presented. An evacuation case is studied as an illustration on the map of Huangshi city.

Keywords: *Agent-based simulation and modeling, Complex adaptive system, emergency response, evacuation, Repast*

1. INTRODUCTION

Large scale disasters happen in cities, ranging from natural disasters such as Asian Tsunami and earthquake in Sichuan of China, to man-made disasters such as subway sarin gas attack in Tokyo and 9/11 attacks in New York, can do great damage and cause lots of deaths and injuries. Responding in a timely and effective way can save the most lives. The inherent complexity of emergency response poses great challenges for policy-makers to make the right decision for disaster mitigation. As so, many efforts have been made by governments to develop emergency response plans for different scenarios in advance and strengthen the training and drill system. However, there exist no practical way to evaluate the possible consequences of these pre-defined strategies, such as evacuation plan and resource allocation, in a specific scenario.

Simulation based on desktop can help to solve this problem by providing a realistic and flexible environment to analyze the system dynamic of different emergency scenarios and find a best response strategy. A city is a complex environment for emergency response that a large number of population and different kinds of resources interacting with each other. Agent based modeling and simulation (ABMS) has been proved to be a powerful technique to analyze such complex systems. The essential idea of ABMS is that many phenomena, even very complex ones, can best be understood as systems of autonomous agents that are simple and follow relatively simple and follow relatively simple rules for interaction [1]. ABMS provides a framework for developing experimental platform that detailed assumptions about the behaviors and interactions of agents can be varied and the overall dynamics of the whole system will emerge. For emergency response simulation, the alternative strategies can be defined as the control rules of agents, and the effectiveness can be evaluated based on the results of simulations.

Emergency response simulation using ABMS has attracted more and more attention through recent years. In the field of AI, several multi-agent models have been developed to simulate the cooperation and coordination of heterogeneous rescue agent in the adverse environment to find out informatics solutions for rescue activities. One example of such efforts is within Robocup-Rescue Simulation Project. Other simulation frameworks for disaster rescue include the I-RESCUE and DEFACTO project. Besides these, some models have been developed to analyze the overall dynamics of emergency response dynamics. DrillSim is an example of evacuation model to simulate the evacuation plans of a limited number of agents restricted to a floor of a building. PLANC project of NYC is a platform for urban disaster simulation and emergency planning features a variety of reality-based agents interacting on a realistic city map and can simulate the complex dynamics of emergency responses in different large mass casualty incident scenarios. Policy for hospital operation can be test and explored.

In this paper, a project of urban disaster simulations based on the java version of Repast 3.1, a popular software toolkit for ABMS development, is described. The rest of this paper is organized as follows. A total description of the system is presented in section 2. Section 3 describes the agent models and in section 4, a case of evacuation conducted in the city map of Huangshi is illustrated. Future work is concluded in section 5.

2. FRAMEWORK of THE SIMULATION

The system is an agent-based model of the urban emergency response dynamics for different natural disasters or chemical, radiological and other hazardous scenarios. It provides a test bed to simulate and analyze the

possible consequence of the disaster and evaluating the effectiveness of different response plans. The robust multi-agent system can simulate the interactions of the city residents and rescue resources such as polices, fire brigades and ambulances, and capture the complexity inherent. By integrating theories and algorithms, it aims to help the government to improve their preparedness of catastrophes and develop optimal strategies of evacuation and resource allocation.

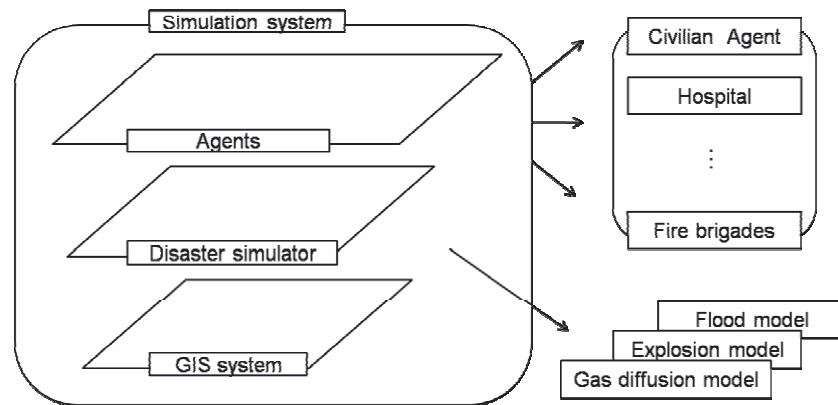


Figure 1: System Architecture

The software architecture of the system is shown in figure 1. The system is a plug-and-play system consisting of 3 layers. The GIS system provides the real geographic space information, such as roads and buildings, as the environment of the emergency scenarios. The disaster simulator is a simulation program of a type of disaster like flood, explosion or toxic gas diffusion, that can provide the disaster spreading data over time and describes the effect on affected population. The multi-agent system is the core of the system. Numbers of different kinds of agents are deployed in the simulation environment to simulate the human behaviors and interactions, testing the strength of different emergency response plans. The disaster simulator and the multi-agent system run at each simulation time step and the results are displayed respectively in the GIS system as two overlays. The system is flexible and new disaster simulators and agent models can be plugged in, and the disaster dynamics and agent behaviors in different scenarios can be observed.

The system is developed on the top of the java version of Repast 3.1, which is one of the most widely used open source toolkits [1]. Repast provides a friendly, flexible and powerful library that users can easily build up and run a simulation model and find lots of tools for analysis, statistics and charts. GIS is also supported by Repast, GIS data can be read and displayed by OpenMap or ESRI ArcGIS. Recent release of Repast has extended it to handle large-scale agent simulation application development.

3. TOPOLOGY AND REPRESENTATION OF THE GIS MAP

The simulations are carried out on a GIS environment, especially the road network of a city. The GIS road map used in the system is a shapefile data. After network analysis in ArcGIS, the junctions of the roads are extracted and so the map can be converted into a simple graph with a number of nodes. Each node represents an intersection of two roads, and each edge represents a road connecting two nodes. The edges are of different types with different capacity and all assumed to be bidirectional. All the person and vehicle agents are restricted to move only along the edges. All the locations like buildings, hospitals and shelters are all approximated to the nearest node on the graph. The topology of the roads is exported to a txt file and then read by the Repast project for route planning. The visualization of the map is performed by Repast. The shapefile data is read and displayed by Openmap, a free GIS toolkit.

4. AGENT MODEL

The city population and rescue resources are modeled as different kinds of agents. An agent is an autonomous component that can sense the world and make decision of its own to take actions interacting with the environment and other agents. Every agent in this paper has the same four-component architecture shown in figure 2. Every agent has the following components: communication, state, knowledge and action.

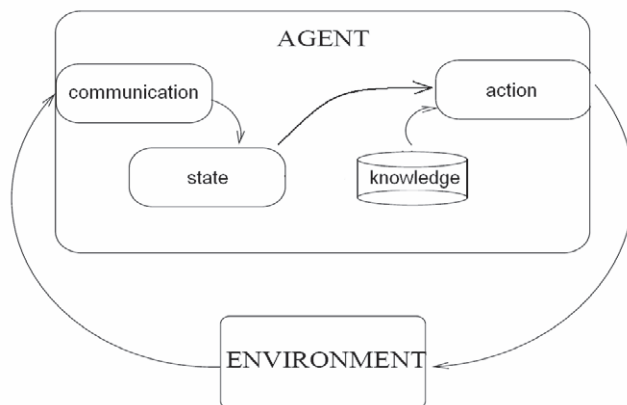


Figure 2: Agent Model Architecture

Communication is the interface for an agent to receive data about the environment and exchange information with other agents. For instance, a person in evacuation can see the traffic condition of different roads or find guidance. He can also talk to other people. This component defines what information an agent can get and what message it can send to other agents.

Knowledge is some rules and intelligent algorithms stored in the agent. It contains all the knowledge for making decisions, like the triage of hospitals and route finding algorithm for persons. These rules or algorithms can be updated through the simulation by training or learning.

State is the properties collection of an agent, including information about the status of the agent, like current location, degree of health or rescue capacities, and all the information an agent knows about the world, like road network, traffic information, the location and current capacities of known hospitals. It also contains the decisions the agent has taken, and the plans to be achieved.

Action is what an agent can do according to its role, like move along the roads or rescue people. These actions will be performed during the simulations time steps.

The agent model runs as follows in each time step, shown in Figure 2:

- The agent gets the necessary information about the environment or other agents through **Communication**.
- This information can be formed and stored into the **State**.
- After the **State** is updated, the agent starts the process of decision making, generating a plan to achieve its goal using the rules and algorithms stored in the **Knowledge** based on the known information of the agent and the world stored in the **State**.
- The Agent executed the **Actions** according to the plan.

5. CONCLUSIONS AND FUTURE WORK

The complexity inherent for emergency response brings lots of challenge for decision making. An effective test bed for analyzing the dynamics of emergency response for different scenarios and evaluating the strength of rescue strategies is crucial for improving disaster planning and preparedness. Simulation provides an effective and low-cost approach to address this problem.

This paper presents a framework for agent based simulation and modeling for urban emergency response. By incorporating GIS data, the model provides a reality environment for analyzing emergency evacuation and resource allocation in a city. The plug-in architecture makes it easy to define new agent models or edit behavior rules.

FUTURE WORK

Base on the simulation system, more efforts should be focus on the evaluation and optimization of evacuation plans and resource allocation models for emergency response. New agent model for residents should be defined and tested to capture the evacuation phenomenon on the scale of city. Personalities of people and emergency guidance could be taken into account.

Rescue activities could be modeled according to the rescue activities in the real world, and resource allocation Algorithms in the AI can be used. Finally, the system is able to predict what an output can be reached providing a response plan as input. Incorporating with optimization mythologies like operations research or evolution algorithms, we can explore different plans and get a simulation-based optimized solution for decision-makers.

ACKNOWLEDGMENT

The authors would like to acknowledge the supports provided by Beijing Municipal Science & Technology Commission (D08050600380801).

REFERENCE

- Wooldridge M., 2002. *An Introduction to Multi-agent Systems*. John Wiley & Sons, UK.
- Samuelson D., and Charles M., 2006. Agent-based Simulation Comes of Age, *OR/MS Today*, Vol. 33, Number 4, pp. 34-38, Lionheart Publishing.
- Hiroaki Kitano, Satoshi Tadokoro. RobCup rescue: A grand challenge for multiagent and intelligent systems. *AI Magazine*, Spring 2001, 22(1): 39-52
- Schurr N., Marecki J., Tambe M., Scerri P., Kasinadhuni N., and J.P. Lewis, The Future of Disaster Response: Humans Working with Multiagent Teams using DEFACTO. *AAAI Spring Symposium on Homeland Security*.
- Siebra C., and Tate A., I-RESCUE: A Coalition Based System to Support Disaster Relief Operations, *the Third International Association of Science and Technology for Development (IASTED)*, 2003
- Massaguer D., Balasubramanian V., Mehrotra S., and Venkatasubramanian. N., 2006. Multi-agent simulation of disaster response, *First International Workshop on Agent Technology for Disaster Management*, pp. 124-130.
- Narzisi G., Mysore V., Nelson L., Rekow D., Triola M., Halcomb L., Portelli I., and Mishra B., Complexities, Catastrophes and Cities: Unraveling Emergency Dynamics. *International Conference on Complex Systems (ICCS 2006)*, Boston, MA, USA June 25-30, 2006.
- Mysore V., Narzisi G., Nelson L., Rekow D., Triola M., Shapiro A., Coleman C., Gill O., Daruwala R. S. and Mishra B. Agent Modeling of a Sarin Attack in Manhattan. *The First International Workshop on Agent Technology for Disaster Management (ATDM)*, Future University, Hakodate, Japan, 8th May 2006

NETWORK BASED PEDESTRIAN SIMULATOR

SHUNSUKE SODEA, TOMOHISA YAMASHITA and ITSUKI NODA
National Institute of Advanced Industrial Science and Technology, Japan
shunsuke.soeda@aist.go.jp

ABSTRACT

We propose a network based pedestrian simulator, for evacuation simulation from disasters caused by CBR terrorism. There is a recent rise in the need for systems that could cope with disasters caused by CBR terrorism - terrorism by Chemical, Biological and Radiological weapons. These disasters, which are likely to be caused in urban areas, have many characteristics different from natural disasters. These disasters are caused intentionally, which means we must prepare for the worst; there are still few cases that CBR terrorism were actually conducted, which means we still know little about what damage will be caused by such terrorism; unlike natural disasters, these disasters are not always harmful to some of the urban infrastructure, which means that they could be utilized for more efficient evacuation. We built a network-based pedestrian simulator, to be used to estimate the damage done by CBR terrorism. Compared to previous grid based and space based simulators which took days to conduct simulations with less than thousands of evacuees, our simulator are designed to conduct simulations much faster, taking less than ten minutes for simulation with ten thousands of evacuees. Our simulator can also utilize infrastructure available. Currently, we implemented elevators for evacuations from buildings, showing that they could speed up evacuation from high story buildings if used properly. Our simulator is designed to be used with air-flow simulator, which calculates how harmful gases spread. These results could be used to make and evaluate plans against CBR terrorism.

1. INTRODUCTION

CBR terrorisms – terrorism caused by Chemical, Biological, and Radiological means – are attacks by terrorists against crowds using hazardous materials. These hazardous materials include toxic gases, bacteria, viruses, and radioactive substance, and they might be sprinkled, vaporized, or spread with an explosion. As these attacks are targeted against crowds, they would naturally be conducted in the urban areas.

Although there are fears against such attacks, there are still few cases that CBR terrorism that was actually conducted. This means that we do not have much experience that we could rely on when we plan our response for CBR terrorism. This problem could be solved by using tools to estimate and illustrate the damage done by CBR terrorism.

In this paper, we show a network based pedestrian simulator that could be used to simulate people evacuating from CBR terrorism. This simulator could be used together with gas diffusion simulators currently being developed by The University of Tokyo, Mitsubishi Heavy Industries, and Advancesoft to estimate the damage done by CBR terrorism. The simulator handles both indoor evacuations (evacuation from buildings to outside) and outdoor evacuation. Our simulator has two key features, both from the characteristics of CBR terrorism.

The first feature is that our simulator is much faster than previous pedestrian simulators. As we do not know much about CBR terrorism, we must consider various scenarios and evacuation plans, in order to find a likely-to-happen attack and a good evacuation plan to cope with it. For example, if a toxic gas was spread out-doors, we do not know either we should have the people inside the buildings to evacuate from the building or to stay inside. Our simulator models evacuation paths as links connecting nodes. It could simulate several phenomena seen in disaster evacuation, while being able to conduct the simulation up to 5 times the speed of real time.

The second feature is that our simulator can simulate evacuation using transportation infrastructure. As CBR terrorism is not an attack directly to infrastructures, there are chances to utilize such infrastructure for evacuation. These infrastructure ranges from public transportation such as buses and trains, to building infrastructures such as elevators.

In section 2, we show how we designed the network based pedestrian simulator. In section 3, we show elevators incorporated in our simulator, as an example of an infrastructure in our simulation. In section 4, we make concluding remarks.

2. NETWORK BASED PEDESTRIAN SIMULATOR

Various kinds of pedestrian simulators have been developed for various purposes. Pan roughly classifies them into three categories (2006); fluid and particle systems, matrix-based systems, and emergent systems. However, all of these systems are two dimensional systems, which allow evacuating people to move around two dimensionally.

Unlike other pedestrian simulators, our simulator simplifies the evacuation path by representing it with a graph model – a model with links and nodes (Fig. 1). The paths where the evacuating people move around are represented as links, and these links are connected at nodes. As the evacuating people could move only along the links, our model is more one dimensional than two dimensional.

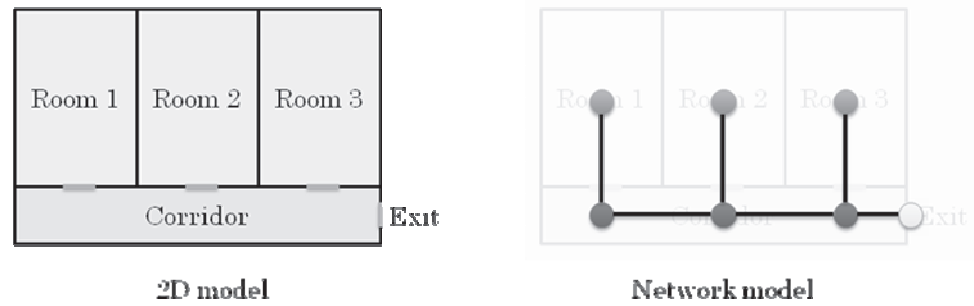


Figure 1: 2D model and Network model

This approach has often been used in traffic simulators (Burmeister, 2002), but not for pedestrian simulator. We chose the network model for our simulator, as we concentrated on the macroscopic side of evacuation. Our simulator cannot, for example, simulate people evacuating large space, but could be used to reveal bottlenecks in the evacuation as well as to compare evacuation plans.

2.1 The Speed of Evacuating Person

The speed of an evacuating person is calculated from the density of the crowd on the link. Each link has a width and a length, which is used to calculate the area of the link. Then, the density of the crowd on the link could be calculated from the number of people on the link.

The speed of a person is calculated from the following formula, where v_0 represent the speed of the person when not in a crowd, and d represents the density of the crowd:

$$v = \begin{cases} v_0 & (d < 1) \\ d^{-0.7945} v_0 & (1 \leq d \leq 4) \\ 0 & (d > 4) \end{cases} \quad (1)$$

Figure 2: shows the coefficient to the speed

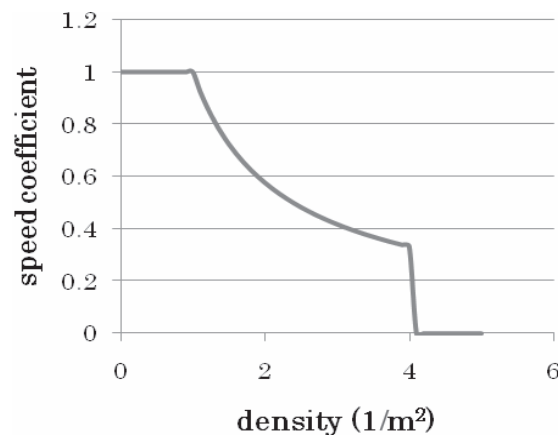


Figure 2: The coefficient of the speed and the density of the crowd

The exception to this formula is the person on the head of a crowd on the link. For this person, the speed v_0 is used regardless of how the link is crowded. Note that when the density of a link exceeds 4people/m^2 , all the people on the link cannot move except for the one who is on the head of the crowd.

2.2 Confluence

Confluences – where two or more paths meet together – slow down the evacuation. To illustrate slow-down by confluence, we used a simple model of limiting the number of people who could enter a link.

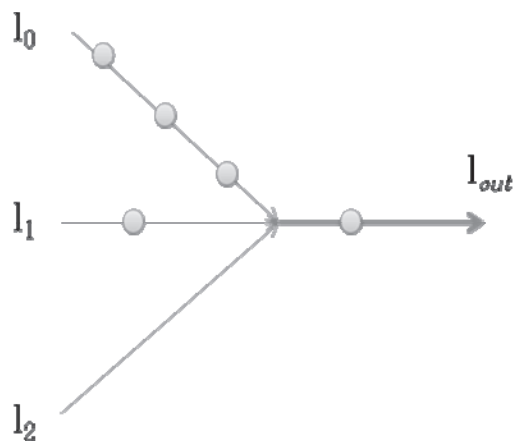


Figure 3: Modeling confluence

The maximum number of people entering link l_{out} is determined from the width of the link. When there are people on l_{out} already, the number of people that could enter l_{out} is decreased at some ratio. When there are more than two links where people are trying to enter l_{out} , this number is divided among the links depending on the number of people trying to enter l_{out} . Also, in this case, the total number of people able to enter l_{out} is also reduced.

3. UTILIZING TRANSPORTATION INFRASTRUCTURE

Evacuation using infrastructures such as buses and elevators are usually not considered in evacuation from disasters, as these infrastructures are usually damaged by the disaster and are not usable. However, attacks by CBR terrorism do not necessarily damage such infrastructures, and thus might be used for evacuation.

Planning how to use resources such as transportation is itself a challenging problem. Therefore, we first started by implementing a simple elevator for indoor evacuation.

3.1 Elevators

The elevators are implemented as special type of links, which people could move through only at specific conditions; when they are on a carriage. The carriage runs under simple rules:

- When the carriage is empty, it goes to the topmost floor where there are people waiting for the elevator.
- The carriage fills itself up to the capacity, and then goes straight to the floor closest to the exit, ignoring intermediate floors.

People who use the elevators are pre-defined; that is, a person who uses elevators goes straight to the elevator hall if it is ever available, and never uses stairs unless they are on floors that do not have elevators taking them closer to the exit.

3.2 Experiments

We conducted an experiment to see if elevators are any effective in evacuating from buildings. Two 37-floored building with 6 sets of elevators and 2 sets of stairs was used for the experiment. The buildings are connected to an underground mall, which have exits away from the buildings. The elevators have the capacity of 20 people, and moves at 1m/s.

Each building had 7,500 people evenly distributed among the building, making a total of 15,000 people evacuating. The speed of the evacuators varies, but averages to 1.3m/s on flat floor, and their speed drop to 0.7 times of this on stairs. The evacuators head for exits through the underground mall. They try to take the shortest path to the closest exit.

We increased the number of evacuators using elevators from 0 to 2,500, and recorded how long it will take for all the evacuators to evacuate to the exits. The results are shown in fig. 4.

As seen from the results, the time to evacuate all people in the building slightly decreases up to around 1,000 people using the elevator. However, when more than 1,000 people use the elevator, the total evacuation time increases. This is caused by people who wait for the elevator even when the stairs are not crowded.

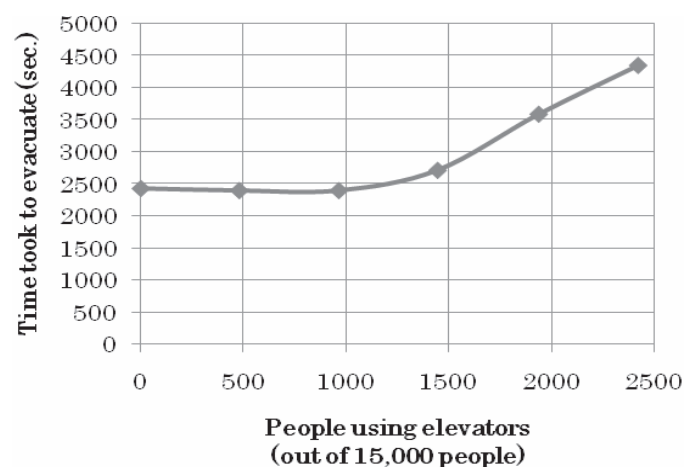


Figure 4: The time to evacuate using elevators

4. CONCLUSION AND FUTURE WORK

We proposed a network based pedestrian simulator, which could be used to simulate evacuation from CBR terrorism attacks. The simulator could be run 5 times faster than real time, enabling simulation of various scenarios and various evacuation plans. Elevators are also implemented in the simulator, as an example of evacuation using infrastructures. We showed that using elevators could speed up evacuation if used properly.

The following future work are suggested:

- The combination with other pedestrian simulators; the network based pedestrian simulator is not good at simulating open areas. The combination with other types of simulator could improve this.
- Transportation infrastructures; other kind of infrastructures each have their difficulties, e.g. buses share the road with pedestrians.

ACKNOWLEDGEMENT

This work was supported by the Science and Technology for Safe and Secure Society Project by the Ministry of Education, Culture, Sports, Science and Technology of Japan.

REFERENCES

- Burmeister, B., Haddadi, A., Matylis, G. 2002, Application of Multi-Agent Systems in Traffic and Transportation. *Software Engineering*, Vol. 144, Issue 1, 51-60.
- Pan, X., 2006. *Computational Modelling of Human and Social Behaviours for Emergency Egress Analysis*. Ph.D. Dissertation, Department of Civil and Environmental Engineering, Stanford University.

RESEARCH ON THE ARCHITECTURE OF EMERGENCY INTELLIGENT DECISION SUPPORT SYSTEM

QUAN SHAO, WENGUO WENG and HONGYONG YUAN
Center for Public Safety Research, Department of Engineering Physics,
Tsinghua University, Beijing, 100084, P. R. China
shaoq06@mails.tsinghua.edu.cn

ABSTRACT

Nowadays, due to increasing congestion in industrial complexes and increasing density of human population around such complexes, decision-making of emergency become more and more difficult. The architecture of emergency intelligent decision support system (EIDSS) is presented, which consists of an information system, a model base, a knowledge base, and a case base. The EIDSS is mainly based on the emergency model base. GIS technology was used to integrate geographic data and emergency related data. The decision-making processes included emergency simulations, risk assessment, emergency response, loss evaluation and emergency material allocation. An illustrative case is used to show how to use the EIDSS to help emergency decision-making. The EIDSS provides a good emergency solution and dynamic model combination according to different decision-making environment and objects. Quantitative physical model and the method of comprehensive evaluation based on analytic hierarchy process can be used to quantify some decisions. The results are useful to help managers make scientific preparedness plan during emergency response

1. INTRODUCTION

Nowadays, due to increasing congestion in industrial complexes and increasing density of human population around such complexes, decision-making of emergency become more and more difficult. One of the principal problems of emergency intelligent decision support system (EIDSS) in technical domains is to bridge the gap between the information system, the model base, the knowledge base, the case base and the geographically distributed resources. Another problem is how to bridge the gap between emergency simulations, risk assessment, emergency response, loss evaluation and emergency material allocation.

Decision Support System (DSS) design is an inter-disciplinary research topic that spans many disciplines such as industrial engineering, computer science, and psychology (Nan, 2002). DSS in the military, medical, financial and other aspects have been successfully applied. But the DSS application in disasters and emergencies management and handling is still in its early stage. Risk assessment and management is the main function of some disasters and emergencies decision support system. To represent the

underlying processes, such as, for example, chemical spills, atmospheric dispersion, fire, and explosion, scientifically based analysis requires complex dynamic and three-dimensional stochastic models (e.g., Fedra, 1995, 1998). The use of such complex analytical tools is difficult and demanding. To use them in a real-time decision-making situation, and, in particular, under the stress of an incident management scenario, is nearly impossible. The same is true for the domain of technical training, where the inherent complexity of the underlying tools is supposed to support the training by providing a more realistic problem representation and analytical capabilities, rather than to distract from the core message of a lecture unit.

One approach to a solution is the integration of expert system technology with model-based decision support systems. The role of expert systems as pre- and post-processors for environmental simulation models is well documented (e.g., Hushon, 1990; Liebowitz, 1997; Fedra, 2000). Here the expert system can perform the role of the overall logical framework, the domain expert or tutor that selects, configures, runs, and interprets the analytical tools depending on the evolving context of an application such as the control of an emergency situation. The primary function is to provide a well-structured simplified access to the complexity of the underlying analytical tools. But the sequence of model operation is a rigid or a rule-based framework is predefined in many expert systems. So many expert systems can't improve their intelligence by learning from the process of using the systems.

By combining the paradigms of forward chaining systems that easily can be adapted to a dynamic, protocol-based but context-sensitive and time-aware action sequence and a backward chaining strategy that can be used to compile and classify information required for the analytical tools and to interpret their results, a new hybrid expert system strategy has been developed (Fedra, 2002). In combination with a powerful heterarchical object data structure describing the elements of an application such as the control of an emergency situation, including simulation models and a range of classical relational databases, GIS, and on-line data acquisition, a versatile environmental decision support system with real-time characteristics for real-time decision support can be configured. Related concepts and applications of expert systems can be found in Hushon (1990), Diaz (1995), AICE (1995), Sriram (1997), and Jain (1998). The chaining of the action sequence in these systems are predefined directions. But some complex and changeable emergency situations can't be solved by operational chaining of predefined directions; they need indefinite amount model and other knowledge from other intelligent systems parallel operation and analysis.

The EIDSS is not only expert system for risk assessment and management, but also have the function of emergency response, loss evaluation and emergency material allocation. The EIDSS design start with task analysis, which breaks the task into hierarchical subtasks and the maps the relationships between the subtasks. The emergency event management process is decomposed as some basic subtasks such as even simulation, risk assessment, emergency response, loss evaluation and emergency material allocation. The EIDSS is a real-time DSS follows human or a set of task

analysis agents, dynamically defining a sequence of subtasks, solving the event or task at hand. The relationship network is dynamic.

2. THE ARCHITECTURE OF EIDSS

2.1 The framework of the EIDSS

The EIDSS is not just model-based decision support system, which combines the information system, the model base, the knowledge base, the case base and the geographically distributed resources. The body of the EIDSS is the model base, but the system has some server-agents which can provide help and advice based on other bases or systems. The framework of the EIDSS is shown in Figure 1.

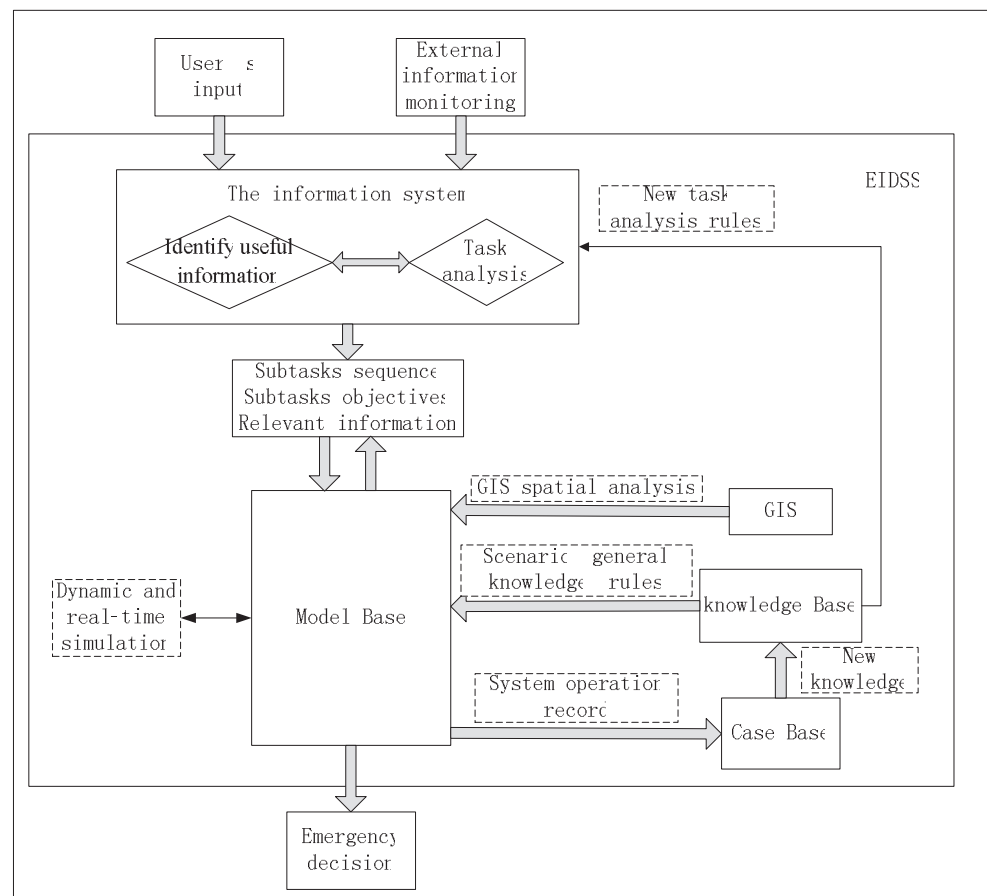


Figure 1: The framework of the EIDSS

The EIDSS is a rule-based DSS which can either be goal driven using backward chaining to test whether some hypothesis is true, or data driven, using forward chaining to draw new conclusions from existing data (e.g., Liebowitz, 1997; Nilsson, 1998). Forward chaining implies that upon assertion of new knowledge all relevant inductive rules are fired exhaustively, effectively making all knowledge about the current state explicit within the state. Forward chaining may be regarded as progress

from a known state (the original knowledge) toward a goal state. Backward chaining systems work from a goal state back to the original state. This means that no rules are fired upon assertion of new knowledge. When an unknown predicate about a known piece of knowledge is detected, all rules relevant to the knowledge in question are fired until the question is answered or until quiescence.

In the EIDSS environment, forward chaining is used for helping the user to turn the task into subtasks sequence in the information system and guiding the user using the model base to achieve task from one subtask to the next subtask based on the new information compiled from other resources including knowledge base, case base and user's inputs. The forward chaining achieve the emergency decision-making according to emergency information. Backward chaining is used for getting new knowledge from the case base including the EIDSS previous operation records for decision-making. The new knowledge can modify the rules of the agent which can judge the implementation status of the task or subtask and improve the intelligence and efficiency of the task agent.

2.2 The Information System

The information system must deal with the immense volume of information coming in from the emergency commanders' dictates and the emergency event monitoring systems. The main function of the information system is a process of learning the users' decision-making tasks and information dependency between subtasks. The functions of the information system are two-fold; (1) to break the decision-making tasks into subtasks, and (2) to identify information dependencies between subtasks. The information system focuses on the following areas: (1) what tasks and subtasks are involved for the decision point, and (2) what information (from other decisions or subtasks in the process) is required, and (3) how information is passed between subtasks.

The subtasks include emergency simulations, risk assessment, emergency response, loss evaluation and emergency material allocation, etc. The actual sequence of tasks and subtasks within a project is depending on its status and dynamic context; the conditional action sequence is defined by a task agent. According to the user's need or task analysis rules, the task agent breaks the decision-making tasks and objectives of tasks into subtasks and objectives of the subtasks. Figure 2 shows the task analysis process of the information system. The objectives of subtask can help the EIDSS choose the appropriate models from the model base or the decisions from other databases. These task analysis rules refer in their condition parts to the users' dynamically evolving need and the results of context subtasks or the new information from the emergency event monitoring systems. So the sequence and the amount of the subtasks are dynamical.

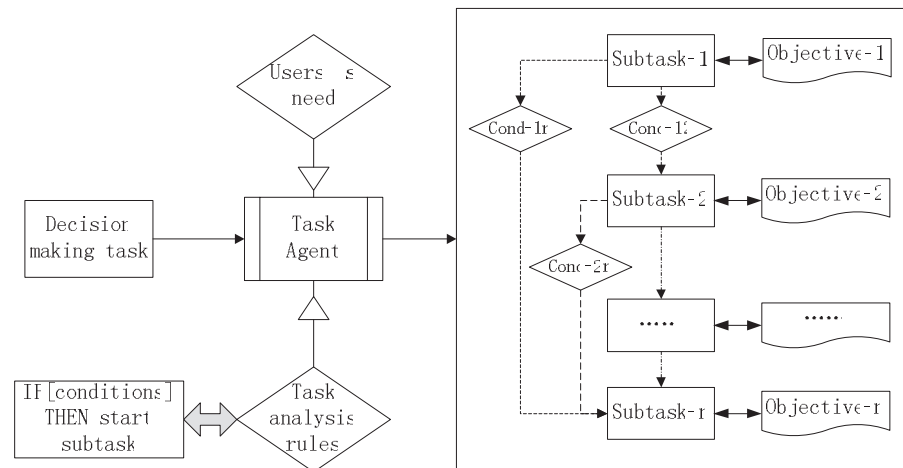


Figure 2: The task analysis process of the information system

2.3 The Model Base

The model base is the main decision-making tool in the EIDSS. Decision-making with model is the basis of intelligent decision-making, can solve most of subtasks in the emergency decision-making process.

Emergency decision-making process of solving the problem with the models has four stages: (1) getting the information which the subtasks need at all stages from the information system; (2) choosing the optimal model or the suitable model at every stage, according to the relevant information of the subtasks, the result of the related models and objectives of the subtasks; (3) running the selected models according to the models arranged in the order, at the same time, transferring the previous model output parameters to the corresponding input parameters of the later models; (4) repeating the three steps in order until complete all the subtasks to get emergency decision making relevant information. The model chain (M1i, M2j, ..., Mnk) which is combined with the optimal model or satisfied model at all the stages is an optimal or satisfied solving model program for the emergency decision-making (QI Changsong, 2007). The framework of the emergency decision-making process and the relationship between the models can come into being a model solving space.

Since the framework for decision-making process with the time passing, the circumstances or the information changing needs dynamic change, but the number of subtasks is limited, the objectives of subtasks is relatively clear, the relationship between the subtasks is clear in a certain time period. So the model solving space of the emergency decision-making process can be formed the models compounding structure network as shown in Figure 2. The models compounding network describes the relationship between the models and the transmission relationship between the parameters in the decision-making process. The information flowing operation Op (subtask(stage), information (or related model), model) in the Figure 3 shows the model need the information (or related model) to use in the subtask (or stage).

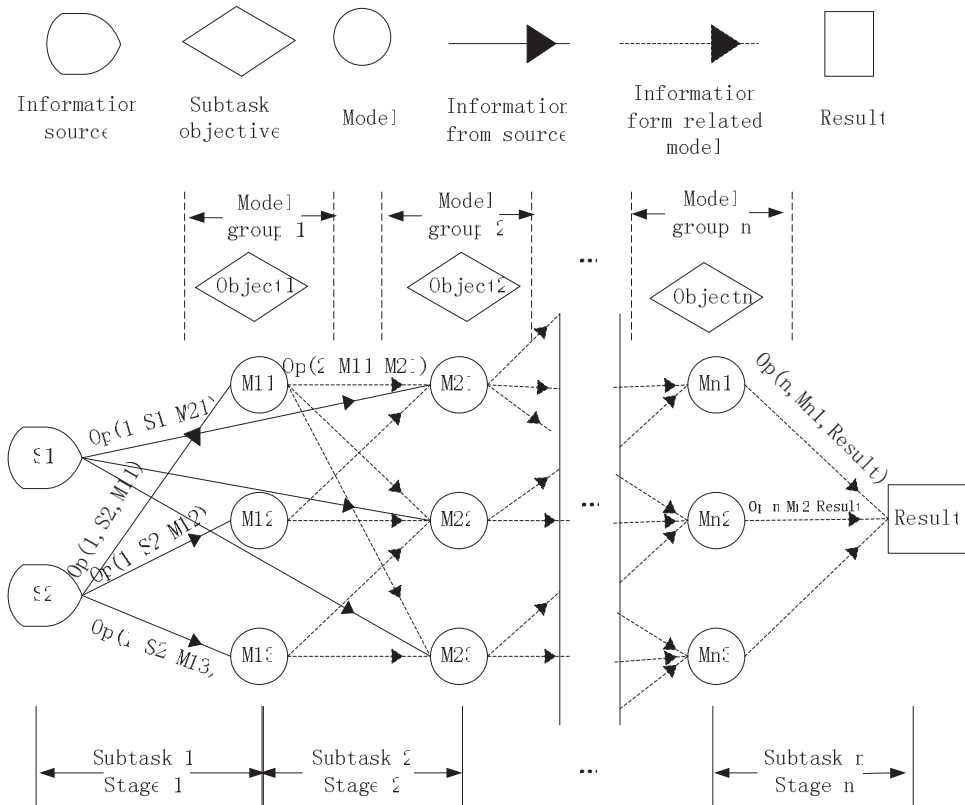


Figure 3: The models compounding structure network

According to the emergency decision-making process, the emergency decision-making using the compounding models can be considered as choosing the suitable model combination framework with emergency information. The information system gives the optimal or suitable subtask sequence or net, and the model base uses corresponding optimization algorithms to choose optimal or satisfied models in accordance with the subtask objectives and relevant information. The emergency information is analyzed by the selected models, the information transfers in the model chain to achieve the best value of benefits or to meet the emergency decision-making requirements. In other words, the optimal solution of model compounding models is corresponding to the best or satisfied path from the initial node to the target node. We can see that getting the optimal solution or a satisfied solution for the emergency decision making is equivalent of search the best or satisfied path from the initial information to the information required by emergency decision-making in the model solving space. As a result, the model solution for the emergency decision-making can be turned into searching the best or satisfied path in the model solving space.

2.4 Other Base and Resources

The system controls the communication with the various actors involved, and it provides guidance and advice based on the rules and several databases, including the embedded GIS for spatial analysis, case base for

operation knowledge or knowledge base for scenario, general knowledge and model selecting rule.

Many models based on the GIS spatial analysis are used to simulation, risk assessment, emergency response, loss evaluation and emergency material allocation. The models read parts of their input from the GIS or the result of GIS spatial analysis to ensure that their parameter sets represent the best current knowledge about an emergency event. The results of the models based on the GIS technology are more actual results than those without GIS.

Backward chaining to provide support for data compilation and estimation has proven very effective for the implementation of a real-time environmental decision support system. For example, the system operation records are accessed in the case base which analyzes the records and compares the calculated results of models with the real results for evaluating the operation and models performance. The analysis results can become new rules or new knowledge for knowledge case which can provide scenario, rules and general knowledge such as hazardous material character.

3. CONCLUSION

The architecture of emergency intelligent decision support system (EIDSS) is presented. The rule-based framework makes it easy to guide the user through complex tasks that involve complex tools. By combining the intelligent model base with information system, GIS, case base and knowledge base, it becomes possible to bring together advanced analytical tools with an easy to use decision support framework for emergency response.

The information system can implement a real-time task analysis follows human or a set of task analysis agents, dynamically defining a sequence of subtasks at hand, and the model base can dynamically choose the suitable model combination framework with emergency information and run the selected models to solve the event or task at hand.

The EIDSS can use dynamic chaining with indefinite amount model and other knowledge from other intelligent systems to parallel operate and analyze for some complex and changeeful emergency events.

The system as a driver for both the sequence of the necessary steps, as well as for the preparation and interpretation of model runs and their results provides a powerful set of tools that can be configured for a broad range of applications.

The EIDSS provides a good emergency solution and dynamic model combination according to different decision-making environment and objects. Quantitative physical model and the method of comprehensive evaluation based on analytic hierarchy process can be used to quantify some decisions. The results are useful to help managers make scientific preparedness plan during emergency response.

ACKNOWLEDGMENT

The authors would like to acknowledge the supports provided by Beijing Municipal Science & Technology Commission (D08050600380801).

REFERENCES

- Nan Tu. (2002), TASKICDA: A methodology for designing multi-agent decision support systems. Ph.D. Thesis, University of Minnesota, 157 pp.
- Fedra, K. (1995), Chemicals in the environment :GIS ,models ,and expert systems, in James Devillers, Ed., *Toxicology Modelling*, 1(1), Carfax Publishing Company, UK, pp.43–55.
- Fedra, K. (1998), Integrated risk assessment and management: overview and state-of-the-art, *Journal of Hazardous Materials*, 61, 5–22.
- Fedra, K. (2000), *Environmental Decision Support Systems: A Conceptual Framework and Application Examples*. Ph.D. Thesis, University of Geneva, 368 pp.
- Hushon, J. (1990), *Expert Systems for Environmental Applications*, ACS Symposium Series ,431, American Chemical Society, Washington, D.C.
- Jain, L.C., Ed., (1998), *Knowledge-Based Intelligent Techniques in Industry*, CRC Press International Series on Computational Intelligence, CRC Press, Boca Raton, FL.
- Liebowitz, J., Ed., (1997), *The Handbook of Applied Expert Systems*, CRC Press, Boca Raton, FL.
- Nilsson, N.J. (1998), *Artificial Intelligence, A New Synthesis*, Morgan Kaufmann, San Francisco.
- Sriram, R.D. (1997), *Intelligent Systems for Engineering: A Knowledge-Based Approach*, Springer Verlag, Heidelberg.
- Tsai, J.J-P. & Weigert, T. (1993), *Knowledge-Based Software Development for Real-Time Distributed Systems*, Series on Software Engineering and Knowledge, Volume 1, World Scientific Pub Co, Hackensack, NJ.
- AICE (1995), *Expert Systems in Process Safety*, American Institute of Chemical Engineers.
- Diaz, A.C. (1995), Condale: a Canadian AI success story, *Canadian Artificial Intelligence*, 36(Winter).
- Kurt Fedra (2002), Lothar Winkelbauer. A Hybrid Expert System, GIS, and Simulation Modelling for Environmental and Technological Risk Management, *Computer-Aided Civil and Infrastructure Engineering* 17, pp.131–146
- QI Changsong (2007), SUN Jigui. Model Net: A Representation of the Static Structure of Modelbase [J]. *International Journal of Pattern Recognition and Artificial Intelligence*, 2007, 21(4): 791-807.

ANALYSIS OF THE EMERGENCY DERIVATION CHAIN CHARACTERISTICS CAUSED BY SNOW DISASTER

CHANGKUN CHEN, YUNFENG SUN and ZHI LI
Disaster Prevention Science and Safety Technology Institute, Central
South University, Changsha Hunan China 410075
Email: cckchen@mail.csu.edu.cn

ABSTRACT

Phenomena of serial derivation crises which caused by snow disaster are described with snow disaster derivation chain (SDDC). Economy damage induced by snow crisis in South China at 2008 is mainly due to its serial derivation crises. Based on the analysis on the evolutive process of snow disaster crises, special categories and features of the SDDC are obtained and the controlling methods are given. Research purpose is to reduce the damage influence of the snow disaster crises, and provide theoretical foundation for controlling them.

1. INTRODUCTION

Snow disaster can bring about series of social and economic problems. Especially, snow disaster crises occurring in South China in 2008 have serious damages to the People's living and society, such as the discontinuance of Beijing-Guangzhou railway line and the traffic paralysis in Beijing-Zhuhai Expressway. According to the official statistics, economic loss reached 200 billion Yuan, 11.8 million hm² of crops area is affected, 354 000 buildings collapsed and 107 people were death in the disaster.

At present, research on the snow disaster is mainly focusing on the following aspects, such as the cause of snow disaster, classification, prediction, numerical simulation, real-time monitoring, assessment and emergency management of snow crises are analyzed [1-3]. However, there are few researches on snow disaster crisis evolvement itself, and the influence of the evolutive characteristics of the snow disaster crisis on the measure establishment for the risk control is ignored [4]. Characteristics of different evolutive chains in the snow disaster are analyzed in order to reduce the damages and realize the risk control.

2. ANALYSIS OF EVOLUTIONARY PROCESS OF SNOW DISASTER CRISES

The evolvement of snow disaster crises is defined as the process of snow disaster crises evolving to the succedent derived disasters. The evolutionary process based on the snow disaster in South China is analyzed as shown in Figure 1.

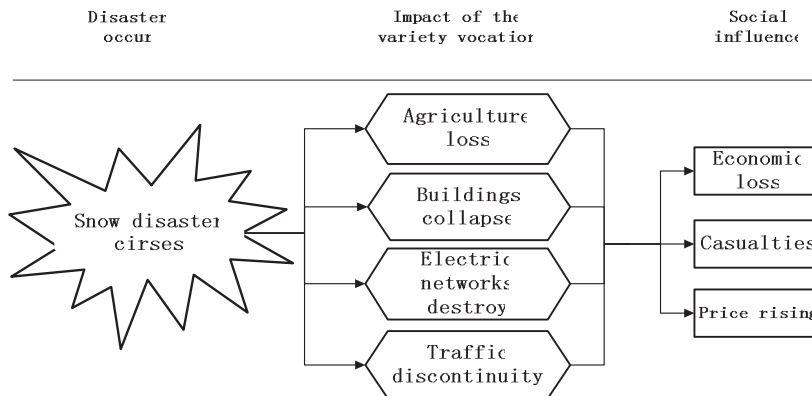


Figure 1: Flow chart of snow disaster crises evolvement

3. ANALYSIS OF CATEGORIES AND FEATURES OF SDDC

SDDC are divided into four special categories in this paper and their features and control methods are proposed further.

Straight chain structure of snow disaster crises

Straight chain structure of the derived snow crisis is given as the relationship of the single causal disaster affair causing the corresponding single derived crisis affair as the example shown in Figure 2.

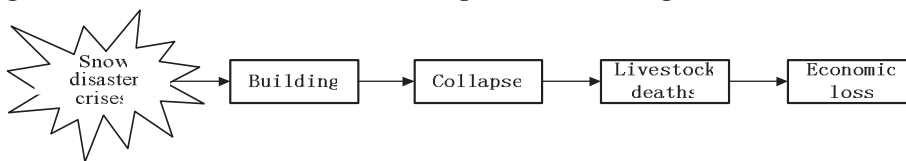


Figure 2: Straight chain structure

The characteristics of straight chain structure are presented as follows: the simplex relationship between the cause and effect of crisis affairs is that one cause results in one corresponding effect which is also the cause of another effect, so the final effect would not occur with the break of one part of the chain. The control on the straight chains can be realized by breaking the earlier part of the cause and effect chain.

Straight divergent chain structure of snow disaster crises

Straight divergent chain structure of the derived snow crisis is expressed as the relationship that the single causal crisis affair results in corresponding several derived disaster affairs as shown in Fig.3.

The characteristics of straight divergent chain structure are proposed as follows: the comparative complicated relationship between the cause and effect of crisis affairs is that one cause results in several corresponding effects which are also the cause of other effects, so these final effects would not happen if only it's corresponding causal crisis affair is controlled.

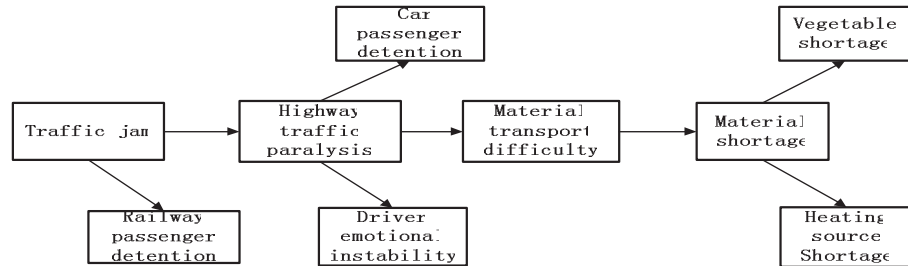


Figure 3: straight divergent chain structure

Self-circulation chain structure of snow disaster crises

The structure of self-circulation chain is defined as the relationship that the single derived crisis affair is induced by corresponding single causal disaster affair, and especially the last effect in the chain can also lead to the first cause affair to form a close cycle crisis chain, which is shown in Fig. 4(a) and Figure 4(b) as examples.

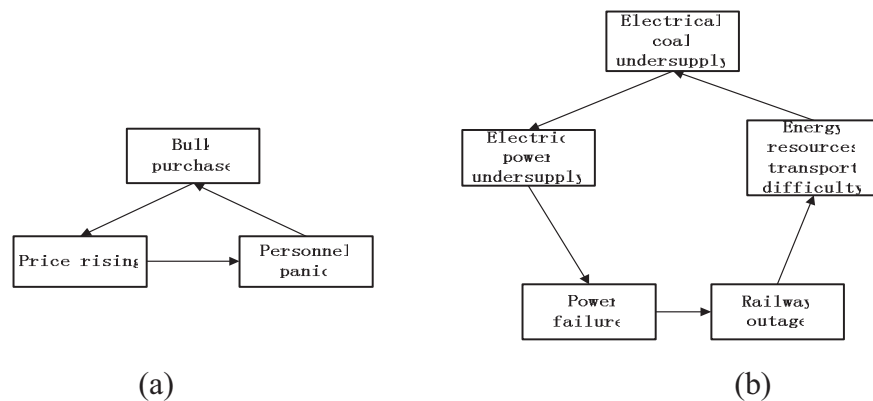


Figure 4: Self-circulation chain structure: (a) price rising Self-circulation chain (b) power failure Self-circulation chain

The characteristics of self-circulation chain structure are given as follows: self-circulation chain of the derived snow crisis is a cricoid structure, so that it would be destroyed if the connection between any cause and effect in the chain is broken.

Concentrative chain structure of snow disaster crises

Concentrative chain structure is described as that the relationship of several causal crisis affairs leading to the same derived disaster affair which is illustrated as shown in Fig.5.

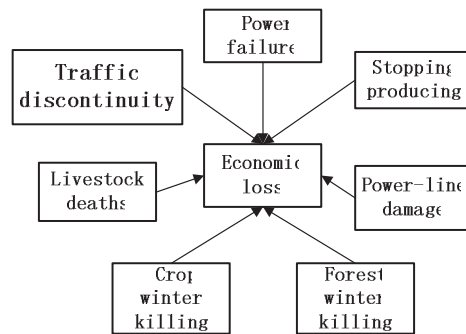


Figure 5: Concentrative chain structure

The characteristics of concentrative chain structure are presented as follows: the complicated relationship between the cause and effect of crisis affairs is that one effect is caused by several corresponding causes which are also the effects of other causes, so the final effect would not happen only when all of its causal affairs are avoided.

4. CONCLUSION

Four categories of SDDC namely straight chain structure, straight divergent chain structure, self-circulation chain structure and concentrative chain structure are analyzed and summarized based on the evolutionary processes of snow disaster crises in 2008. Then the controlling methods are proposed. And the most important emergency measurement for the disaster is to control the key factors of the derived chain and destroy the relation between the causal and result affairs.

REFERENCES

- Stanley A. Changnon and David Changnon., 2005. *Snowstorm catastrophes in the United States*. Environmental Hazards, Vol.6 No.3: 158-166.
- XU Geng-hui., 2005. *Recent Advances and Expection in Studies of Precaution Against Snow Disaster in Pasture*. Bimonthly of XinJiang Meteorology, Vol. 28 No.3: 1-6.
- Gao an-ning, Chen jian, Li yan-lan., 2008. *Assessment and Thinking on the Rare Frozen D isaster in 2008 in Guangxi*. Journal of Catastrophology. Vol.23 No.2: 83-86.
- Chen Chang-kun, Sun yun-feng, Li Zhi., 2008, *Analysis of the Emergency derivation chain caused by ice disaster*. Jouranal of Institute of Disaster-Prevention Science and Technology. Vol.10 No.2: 67-71.

URBAN FIRE RISK MAPPING USING GIS: A CASE STUDY OF YUSHAN TOWN IN KUNSHAN CITY, CHINA

CHENGCHENG GAI, WENGUO WENG and HONGYONG YUAN
Center for Public Safety Research, Department of Engineering Physics,
Tsinghua University, Beijing 100084, China
gaicc07@mails.tsinghua.edu.cn

ABSTRACT

Urban fire is a usual disaster in real life, causes huge live loss, property loss and infrastructure collapse. Urban fire risk assessment model, in order to identify, classify and map fire hazard areas is presented in this paper. This model considers several influence factors in urban fires, including building density, building fire resistance rating, population density, land use, distance from hazardous building, water and fire station. Through GIS spatial analytical procedure, the fire risk ranging from high to low is derived, according to its sensitivity to fire or fire-inducing capability. Spatial analyst is used to combine some single influence factor risk maps to display the total fire risk map. This model is illustrated with a case study of fire risk of Yushan town in Kunshan city. It is suggested that risk mapping is helpful for the urban fire management to minimize urban fire hazard. In addition, advantages and disadvantages of this approach, and the recommendation are discussed.

1. INTRODUCTION

With the development of economy and rapid urbanization process, the city scale is extended rapidly, while the city population increases fast. Preventing and administering urban fire accidents has become one of the significant urban problems for city fire managers. Because of the highly population density and economic value in city, urban fire usually causes more life and property loss than the industrial fire and wildfire.

The development of GIS (Geographic Information System) has provided a powerful tool for managing and solving city safety problems. GIS is a professional computer system for collecting, storing, managing, retrieving, transforming, analyzing, and displaying of spatial data. It can be used for many kinds of purpose in both macro and micro scales. In the public safety field, GIS can make comprehensive analysis using the natural, social and economic spatial data. Especially in the natural disaster area, GIS has been applied in the simulation and early warning system, emergency management system, and disaster damage assessment etc.

Fire risk assessment has three forms: single building, enterprise (eg. Petrochemical Enterprise) and region (eg. forest or city). Region urban fire

assessment is a new research topic, and little research is related to it. It has many problems in urban fire assessment and map of fire hazard.

Each year, urban fire causes tremendous loss of natural resources, human lives and property. A better job of effectively guarding against the risk and reducing the loss is important for both long-term urban fire management planning and strategies. To minimize this threat, the foremost task is to identify urban fire hazards in the study area. Following the identification, a precisely analysis on the potential hazards is made, with reasonable planning and improving. Japan government has carried out the classification of city hazards to show the different risk rate. This method, considering territorial meteorological elements, wood-frame construction of species, communications facilities and fire control safety system, adopts fire engineering methods, statistical techniques and quantitative evaluation algorithm to determine the risk class. Yang Hongrui developed a statistic model of fire risk assessment based on fire losses, population density, buildings density, road density and fire protection force. Using GIS to analyze the urban fire risk, the operation process of fire-zone division is set up by using spatial analysis of ARCVIEW. Yin Haiwei et al. selected main forest fire factors to quantify the forest fire risk with factor-weights union method under GIS. It showed a higher reliability through comparing to the actual fire-affected sites in 1987. Iwan Setiawan et al. implemented a spatially weighted index model to develop the fire hazard assessment model. Fire-causing factors such as land use, road network, slope, aspect and elevation data were considered. It produced a final peat swamp forest fire hazard map, which was validated through the actual fire occurrence map. Emilio Chuvieco et al. made some improvement that topography, meteorological data, fuel models and human-caused risk were mapped and incorporated within a GIS. Three danger maps of probability of ignition, fuel hazard and human risk were generated, and all of them were overlaid in an integrated fire danger map.

The purpose of this study is to develop an urban fire risk assessment model, in order to identify, classify and map fire hazard areas. Such maps will help the Fire Department officials prevent and minimize urban fire activities, and plan city fire protection construction. The risk evaluation results will be revealed on GIS thematic map, which is convenient for large scale study in short time, especially for decision making and management.

2. MATERIALS AND METHODS

2.1 Study Area

The study area is Yushan Town as the seat of Kunshan city government. Kunshan City is a county-level city under the jurisdiction of Suzhou, located in the Yangtze River Delta, between two metropolises, Shanghai and Suzhou. The Yushan Town is chosen for the study since it is representative of a typical and urbanizing town in the Jiangsu province.

Yushan town is a modern and industrially vital town, which has a physical land size of 118 square kilometers and a population of 180,000

people. Because of the significant growth, it is desirable to plan seriously for safety management. (Fig.1)

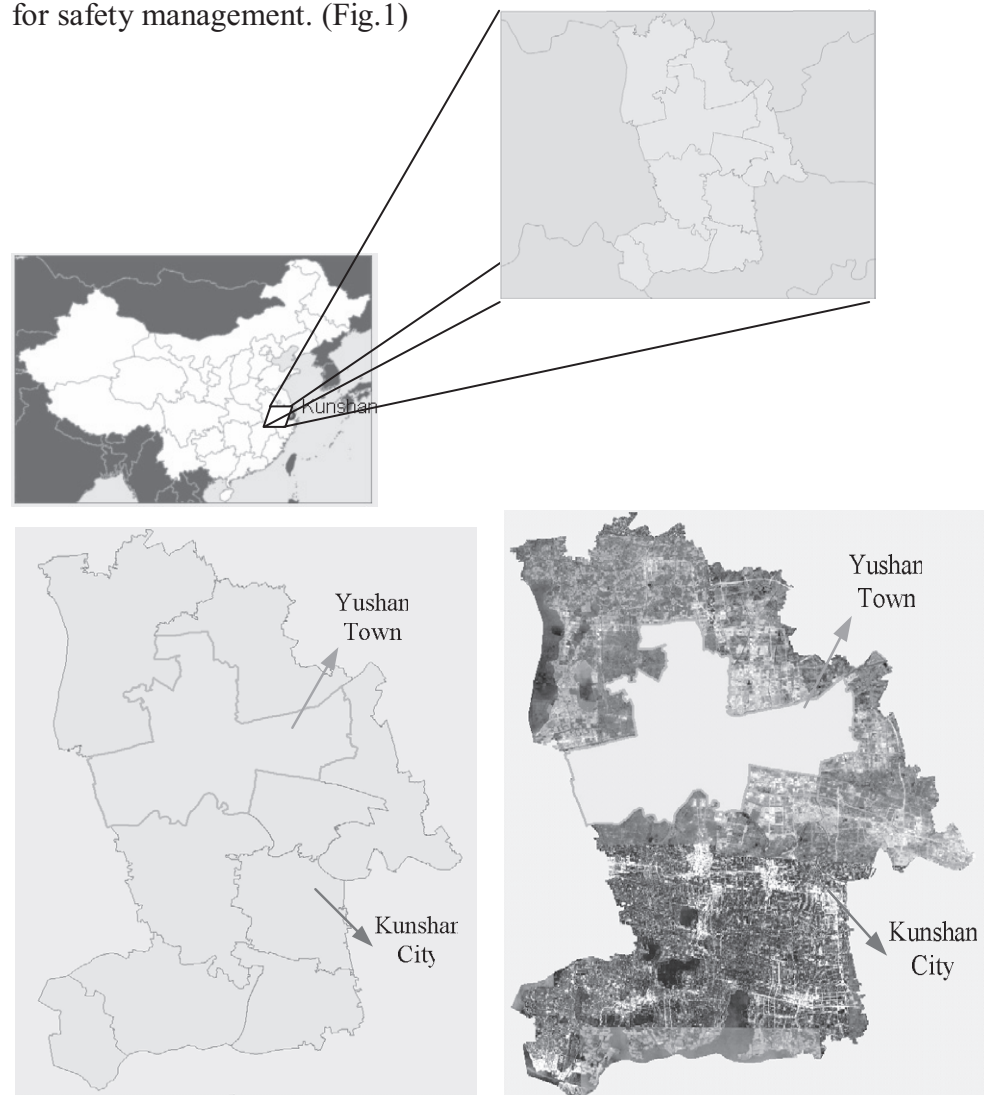


Figure1: Location of the study area and lands at TM image of the kunshan city

2.2 Methods

GIS has powerful abilities of spatial information analysis. Users can acquire new knowledge and information through the observation and experiment of the initial data, so as to make decisions based on it. In a certain area, there would be multiple theme maps to illustrate all kinds of information about it. This data can be vector layer of point, line, surface and raster layer structure.

The process for data collection and preparation in order to integrate the model with GIS is presented in Figure 2.

The main objective of the research is to assess the potential of urban fire hazard. This is to be achieved by correlating information collected in the field. In addition, the selections of variables for spatial analyses are influenced by the availability of data in this area. Hazards differ from place to place due to variations in land use, structural density patterns, population

density and demographic indices. A spatially weighted index model is used to develop the fire hazard model. This model considered the influence of several factors in urban fires. Based on the local conditions, parameters such as building density, building fire resistance rating, population density, land use, distance from hazardous building, water and fire station are taken into consideration.

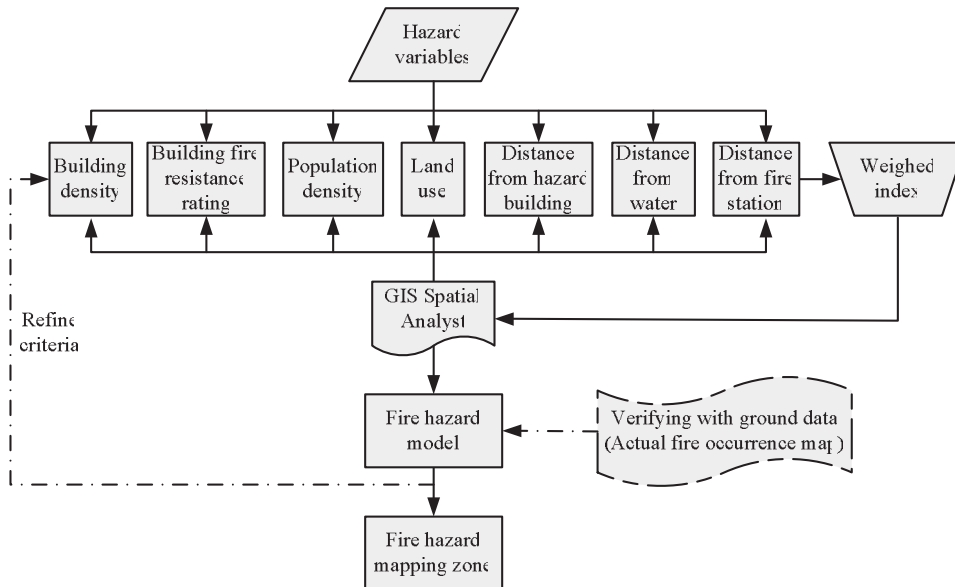


Figure2: Flow chart of urban fire risk methodology

According to the various factors affecting the fire, they are divided into several levels, such as the reunification of five. Each class has different values. The weight to the class of each factor is determined subjectively by the severity observed in the local condition, from 1 (low) to 10 (high). Five categories of urban fire risk ranging from very high to very low are derived automatically.

The building density is classified according to their attribute that has an influence on ignition and spread of building fires. The building fire resistance rating is created according to the combustion property of building materials and components. The materials flammability increases the chance of catching fire and the rate of fire spread. Population density and land use are assigned many classes too. It is usually stated that the greater the population in a locality, the greater the fire risk. A dense commercial region will pose a different level of hazard comparing to a residential or industrial region. Distances from hazardous building, water, and fire station have important influences on urban fire. The risk decreases farther from the hazardous building. However, distances from water and fire station are considered to be an easily accessible existing technology of the fire service. It means that a zone closer to these places is evaluated a lower rating. The weights and classes of the variables assumed are given in the Table 1.

For a certain region, the fire risk is calculated with the data acquired and the weights for each variable based on the local condition. The equation used in GIS to determine the fire hazard model is shown in Equation (1).

$$F_R_V = W1 * B_D + W2 * B_F_R + W3 * P_D + W4 * L_U + W5 * D_H_B + W6 * D_W + W7 * D_F_S \quad (1)$$

Where F_R_V is the numerical index of Fire Risk; B_D is the Value of Building Density; B_F_R is the Value of Building fire resistance rating; P_D is the Value of Population Density; L_U is the Value of Land Use; D_H_B is the Value of Distance from Hazardous Building; D_W is the Value of Distance from Water; D_F_S is the Value of Distance from Fire Station. W_i ($i=1\dots7$) is the weight of the risk index value.

Table1: Classification of fire hazard factors and criteria scores

| Variables | Weights | Classes | Values |
|----------------------------------|---------|--------------------------------------|--------|
| Building Density | 9 | Based on the kernel smoothing in GIS | 5 |
| | | | 4 |
| | | | 3 |
| | | | 2 |
| | | | 1 |
| Building Fire Resistance Rating | 7 | IV | 5 |
| | | III | 4 |
| | | II | 3 |
| | | I | 2 |
| Population Density | 9 | >1200People per Square Kilometer | 5 |
| | | 900-1200People per Square Kilometer | 4 |
| | | 600-900People per Square Kilometer | 3 |
| | | 300-600People per Square Kilometer | 2 |
| | | 0-300 People per Square Kilometer | 1 |
| Land Use | 5 | Commercial region | 5 |
| | | Residential region | 4 |
| | | Industrial region | 3 |
| | | Education & sport region | 2 |
| | | others | 1 |
| Distance from Hazardous Building | 7 | 0-300m | 5 |
| | | 300-600m | 4 |
| | | 600-900m | 3 |
| | | 900-1200m | 2 |
| | | >1200m | 1 |
| Distance from Water | 3 | >200m | 5 |
| | | 150-200m | 4 |
| | | 100-150m | 3 |
| | | 50-100m | 2 |
| | | 0-50m | 1 |
| Distance from Fire Station | 5 | >1200m | 5 |
| | | 900-1200m | 4 |
| | | 600-900m | 3 |
| | | 300-600m | 2 |
| | | 0-300m | 1 |

3. RESULTS AND DISCUSSIONS

With the description in the above section, the final factors adopted for the urban fire risk map are building density, distance from hazardous building, water and fire station considering the actual situation and GIS data of Yushan town in Kunshan city.

3.1 Building Density

Building density is an important influence factor because building fire is one of the most serious forms of urban fire. The larger the spaces between buildings, the greater the chances that the fire can be extinguished. Large building density can result in high fire load, so the fire spread fast. Large crowds of people gather in the buildings. The map of building distribution can represent fire risk to a certain point.

One of the techniques for performing this analysis is kernel density estimation methods (KDE methods) or kernel smoothing, a spatial statistical method that generates a map of density values from the point event data. In the spatial analysis, kernel smoothing creates a smooth map of density values in which the density at each location reflects the concentration of points in the surrounding area. Each point contributes to the density value of that grid cell based on its distance from the center. Nearby points are given more weight in the density calculation than those farther away. The building density calculation of the kernel smoothing is performed using ArcGIS software. Buildings are shown as points in this map, with areas of higher kernel density being shown in darker tones. From the raster image, we can quickly identify the high-density sites. In accordance with reclassifying this input raster, relating classes from 1 to 5 were designated, representing building density based fire risk value, which is shown in Fig. 3 and 4.

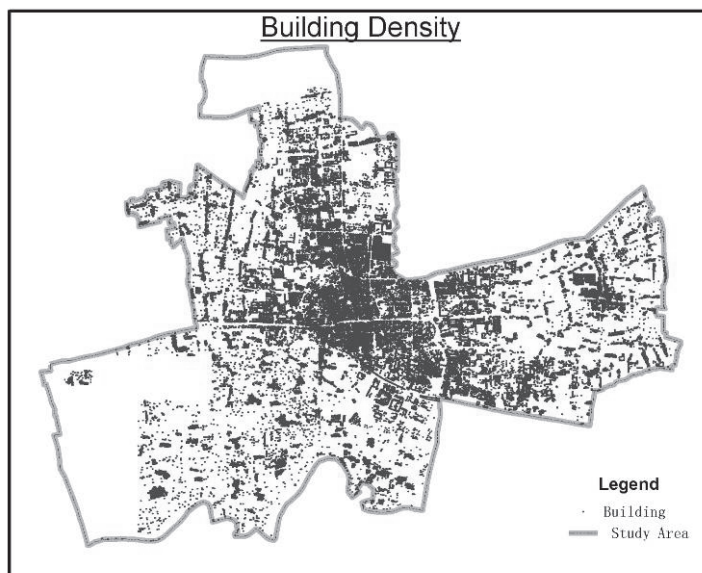


Figure 3: Building density distribution as a factor affecting fire risk

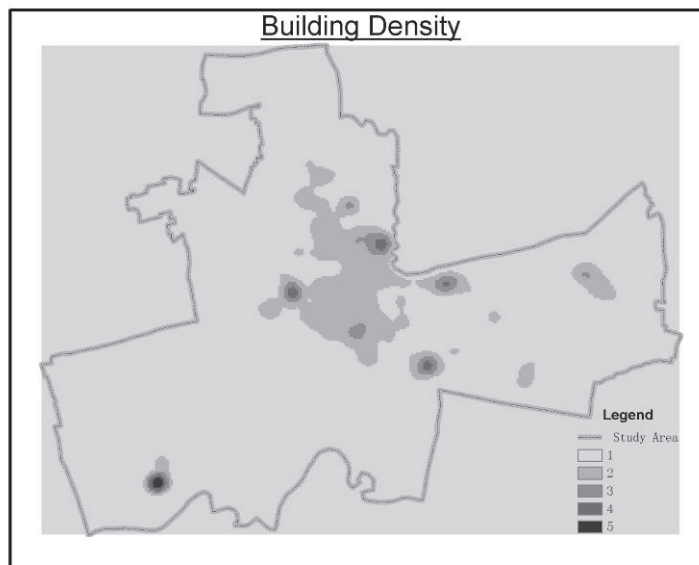


Figure 4: Kernel smoothing building density map

3.2 Distance from Hazardous Building

Distances from hazardous building, water and fire station are produced according to Table 1, and fire risk value of each sub-compartment based on these factors is obtained. In general, cases of urban fire occur more in the areas of hazardous building (such as Gas Station, petrochemical industry, etc.) nearby than in the areas of father away. These areas produce and store inflammable or explosive dangerous goods, which has greatly increased the fire risk level around them.

Euclidean distance is one of the main ways to perform distance analysis in ArcGIS Spatial Analyst. We use the Euclidean distance tool to measure straight-line distance from each cell to the closest source and classify by distance. The distances are measured as the crow flies (Euclidean distance) in the projection units of the raster, such as feet or meters and are computed from cell center to cell center. Distance from hazardous building is mapping according to Table 1. The distances represent different levels of risk, with closer areas being shown in darker tones. Fig. 5 gives the distance distribution from hazardous buildings.

3.3 Distance from Water

It is believed that humans near the water sources can easily put the fire out. The water source, as a fire risk reducing factor, also can be used as a natural barrier to prevent the spread of fire. It is converted into a raster surface and again the Euclidean distance function is used to calculate the distance from each area. Fig. 6 shows the distance distribution from water.

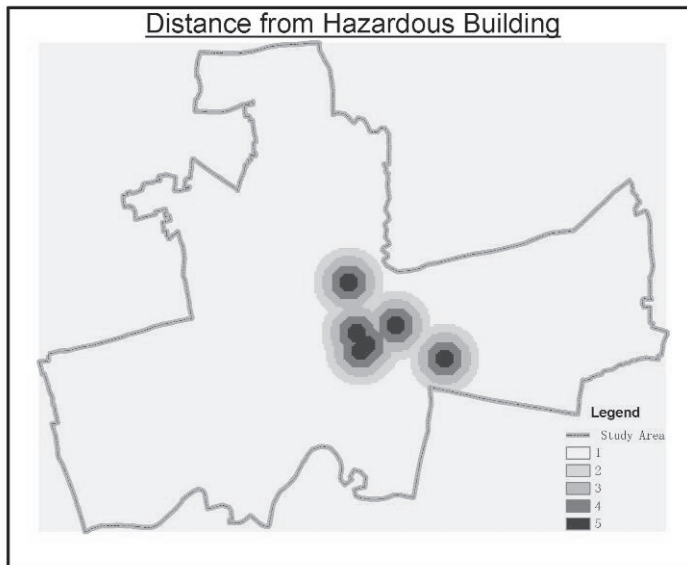


Figure 5: Distance from hazardous building as a factor affecting fire risk

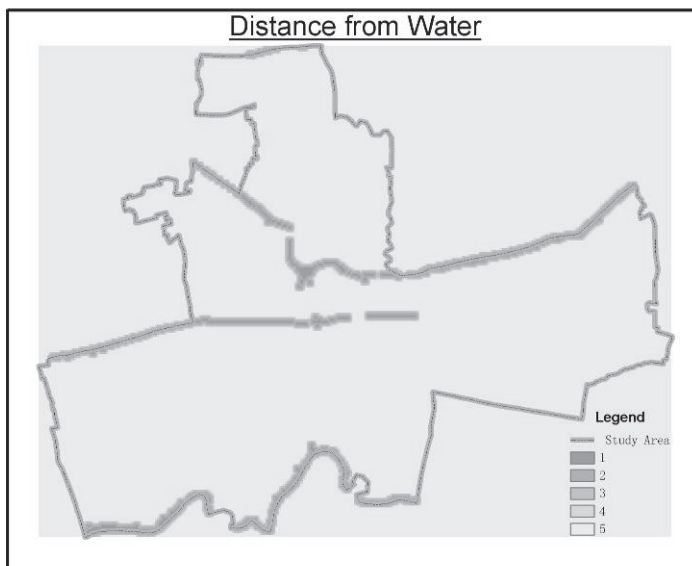


Figure 6: Distance from water as a factor affecting fire risk

3.4 Distance from Fire Station

It is expected that the distance from a grid cell to the nearest area of fire station would influence the Fire size and spread. Fire station is a fundamental force to putting the fire out. The closer to the fire stations, the lesser time the firefighters spent on the way. So it's much safer near the fire station. To simulate this factor area classified as anything other than the fire stations are converted into a raster and then a Euclidean distance function is run on them to determine the distance from these areas. Fig.7 gives the distance distribution from fire station.

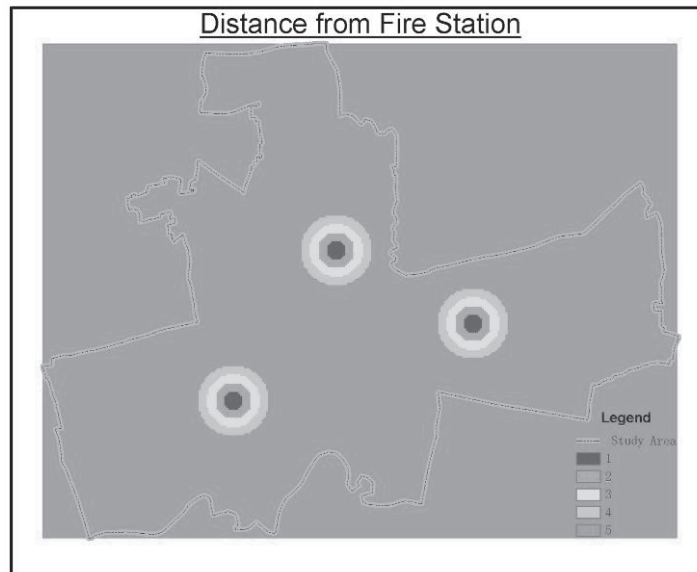


Figure 7: Distance from fire station as a factor affecting fire risk

3.5 Final Map of Fire Risk

Based on Equation (1), F_{R_V} was calculated and classified using ArcGIS software with assigning subjective weights to the classes of all the layers to produce the final map of urban fire risk.

This raster method is better than vector buffers for effective calculation in GIS. The different weighted overlay is calculated by Raster Calculator in ArcGIS Spatial analyst. We input and analyze multiple raster variables from different sources. The final fire risk map is displayed in Fig. 8. This Figure shows that high risk zones mainly distribute in the center of the city, not far off the actual observation. It is also shown that the areas near the fire stations are safe.

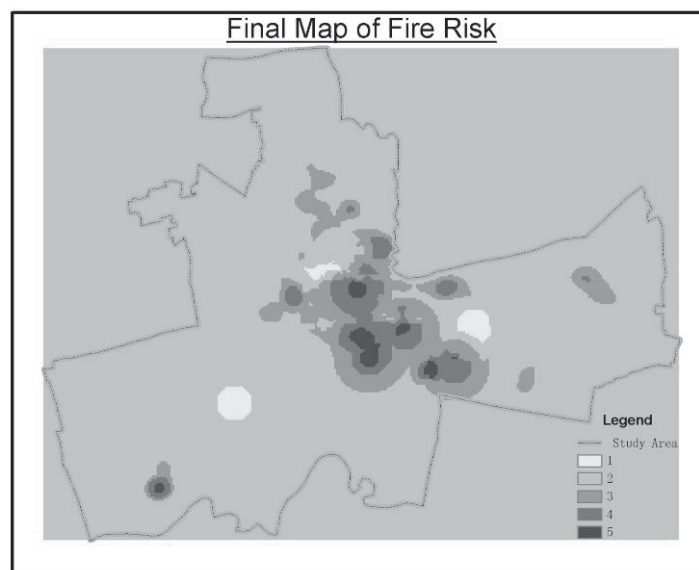


Figure 8: Final map of fire risk in the study area

4. CONCLUSIONS

This spatially weighted index model utilizing GIS Spatial Analyst and multi-criteria analysis is presented to represent the fire risk in the urban area. Yushan town in Kunshan city is chosen to give an example of urban fire risk. In the process of calculation, kernel density estimation methods and Euclidean distance surfaces are created for each component (building density, distance from hazardous building, distance from water and distance from fire station) of the criteria. These four components were used for a subjective way to determine weights, which are then multiplied with the factors and added together.

Future work is to validate the presented model using historical fire data with fire risk map. It can check up the utility of this method, for some feedback correction on the variables. This model can be applied to other cities, by exchanging the variables and the weights with the actual situations. The final urban fire risk map would be helpful to site fire fighting resource and enhance urban safety.

ACKNOWLEDGMENT

The authors would like to acknowledge the supports provided by Beijing Municipal Science & Technology Commission (D08050600380801).

REFERENCES

- DU Xia, ZHANG Xin, LIU Ting-quan, and MA Yu-he, 2004. The current status and applying of city fire risk assessment technology in foreign country. *Fire Science and Technology*. Vol. 23, 137-139. (in Chinese)
- YANG Hong-rui, 2003. Urban fire risk assessment using GIS. *Journal of the Chinese People's Armed Police Force Academy*. Vol. 19, 23-24. (in Chinese)
- YIN Haiwei, KONG Fanhua, LI Xiuzhen, 2005. GIS-based forest fire risk zone mapping in Daxing'an Mountains. *Chinese Journal of Applied Ecology*. Vol. 16, 833-837. (in Chinese)
- XU Dong, DAI Li-min, SHAO Guo-fan, TANG Lei, Wang Hui, 2005. Forest fire risk zone mapping from satellite images and GIS for Baihe Forestry Bureau, Jilin, China. *Journal of Forestry Research*. Vol. 16, 169-174.
- Iwan Setiawan, A.R.Mahmud, S.Mansor, A.R.Mohamed Shariff and A.A.Nuruddin, 2004. GIS-grid-based and multi-criteria analysis for identifying and mapping peat swamp forest fire hazard in Pahang, Malaysia. *Disaster Prevention and Management*. Vol. 13, 379-386.
- EMILIO CHUVIECO and JAVIER SALAS, 1996. Mapping the spatial distribution of forest fire danger using GIS. *International Journal of Geographical Information Systems*. Vol. 10, 333-345.
- S.Bhaskaran and B.Forster, 2005. Development of a Semantic Fire Hazard Categorization Model with Geospatial Information Technologies. *International Journal of Geoinformatics*. Vol. 1, 11-20.

APPLICATION OF FUZZY COMPREHENSIVE ASSESSMENT METHOD TO EVALUATE FULL-SCALE EMERGENCY EXERCISE PLAN

LIGANG DU^{1,2}, SHIFEI SHEN^{1,2} and TINGXIN QIN³

¹Center for Public Safety Research, Tsinghua University, Beijing, China

²Department of Engineering Physics, Tsinghua University, Beijing, China

³China National Institute of Standardization, Beijing, China

ABSTRACT

Conducting emergency exercises can improve emergency response capabilities. Emergency exercise plan plays an important role in the whole process of exercises. This paper introduces the basic concept of emergency exercise and presents an index system and a fuzzy comprehensive assessment method to evaluate the full-scale emergency exercise plan. Compared with traditional subjective judge to the emergency exercise plan, this method enhances the validity and efficiency of assessment result. An example of fire emergency exercise is also evaluated by the method in which the usefulness is validated.

Keywords: *Emergency Exercise; Exercise Plan; Index System; Fuzzy Comprehensive Assessment*

1. INTRODUCTION

In recent years, with the rapid development of economy in China, public safety events have happened more frequently than before. Therefore, it is important to construct a strong emergency response system to protect cities and people away from the damage of public safety events. Conducting emergency exercises can validate procedures and equipments, and also improve emergency response capabilities. In fact, both State Emergency Response Law^[1] and State Emergency Plan^[2] mandate that all the entities, including government, organizations and enterprises, should conduct emergency exercises periodically. The value of conducting disaster exercises is underscored in virtually all discussions of disaster planning^[3].

The emergency exercise plan plays an important role in the whole process of exercises. Through the plan, we can know the purpose, procedures and rules for emergency exercises. If the emergency exercise plan is poorly designed, the emergency exercise probably tends to fail and wastes a lot of money and time. So it is necessary to evaluate the emergency exercise plan before putting emergency exercises into realistic practice. This paper will focus on the evaluation of emergency exercise plan.

2. EMERGENCY EXERCISES

Full-scale exercises simulate a community-wide disaster by testing multiple functions at the same time. It also tests the coordination among these functions. The complexity of full-scale exercises requires thorough planning of the scenario. It also requires coordination among the multiple controllers and evaluators. There is also a need for training the controllers^[4].

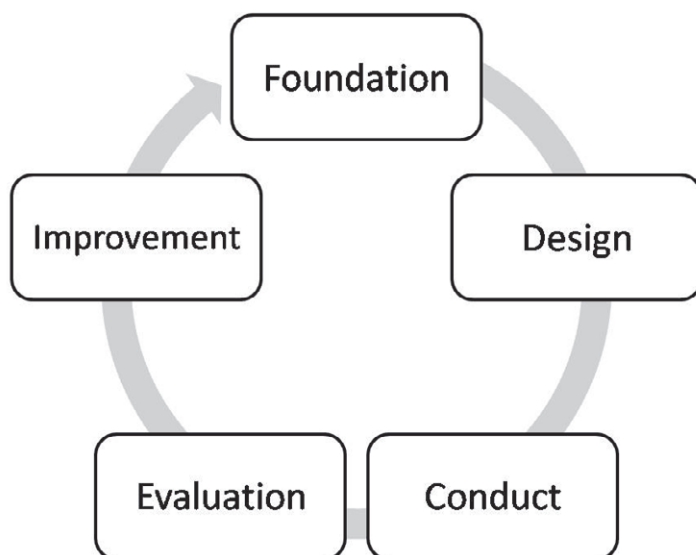


Figure 1: Basic phases of emergency exercises

Figure 1 shows the five basic phases^[5] of an emergency exercise. The first and second phases are the activities prior to the exercise. Organizers should prepare the emergency exercise plan during these two phases, which covers background information, scenarios, responsibilities, resource management and rules.

In the conduct phase, there are five kinds of personnel—controllers, simulators, participants, assessors and spectators^[6]. The basic responsibilities for different people are shown in Table 1.

Table 1: Responsibilities for different people

| Title | Responsibilities |
|-------------|---|
| Controller | Control the progress of the exercise according to the scenarios |
| Simulator | Play the role as some relevant agencies or simulate some accidents like fog and fire |
| Participant | Response to the situation as they are under the real emergency situation |
| Assessor | Collect data from the whole process, evaluate the emergency exercise and write final report |
| Spectator | View the emergency exercise and learn from it (people from other organizations) |

Each kind of people plays an important part in the process of emergency exercise.

Evaluation and improvement are the last two phases in the emergency exercise, which give the final report and suggestions for improving emergency management capability.

The circle in Figure 1 shows that the emergency exercise is a dynamic process. There is no end in the circle and organizations can improve their emergency management capability through the dynamic process.

It will always cost much for a full-scale emergency exercise. Therefore, it is better to be fully prepared for this kind of emergency exercise. The best way to test the sufficiency of an emergency exercise is to evaluate the emergency exercise plan, which contains all of the important information on the emergency exercise. In the next 3 sectors, a fuzzy comprehensive assessment method is introduced and applied to evaluate full-scale emergency exercise plan.

3. INDEX SYSTEM FOR EVALUATING EXERCISE PLAN

As the full-scale emergency exercise plan is systematically organized and designed, it is necessary to develop an index system for evaluating it.

3.1 Index system

The development of an index system is the basis for evaluating exercise plan. Table 2 shows a second layer index system for evaluating full-scale emergency exercise plan. The index system should include five important aspects--background information, scenario design, responsibilities, resource management and rules. There are also three to five detailed indexes under each aspect.

3.2 Weight of index

There are totally five first-layer indexes and twenty-one second-layer indexes. Each title plays a different part in the emergency exercise plan, which means that each index has a different weight in the index system. Since there are too many uncertain factors, it is very difficult to calculate the weight precisely. In this case, Delphi method^[7], a systematic, interactive method which relies on a panel of independent experts, can be used to determine the weight of each index effectively.

The procedure of Delphi method is as follows:

(1) Ask experts (the total number is r) to assign weight to each index and the result is $W_{i1}, W_{i2}, \dots, W_{in}, i = 1, 2, \dots, r$

(2) Calculate the average weight for each index $\bar{W}_k = \frac{1}{r} \sum_{i=1}^r W_{ik}$
 $k = 1, 2, \dots, n$

(3) Calculate the differentiation of each value $\delta_{ik} = \frac{|W_{ik} - \bar{W}_k|}{\bar{W}_k}$
 $i = 1, 2, \dots, r, k = 1, 2, \dots, n$

- (4) Re-evaluate the weight of the index whose differentiation is out of requirement
 - (5) Repeat Steps (1)-(4) until the best weight to each index is gained.
- $$\overline{W}_1, \overline{W}_2, \dots, \overline{W}_n, i = 1, 2, \dots, r$$

Table 2: Index System for Full-scale Emergency Exercise Plan

| First Layer | | Second Layer | |
|-------------|---|--------------|-------------------------------------|
| No. | Title | No. | Sub-title |
| 1 | Background Information(U_1) | 1.1 | Background(U_{11}) |
| | | 1.2 | Purpose(U_{12}) |
| | | 1.3 | Scope(U_{13}) |
| 2 | Scenario Design(U_2) | 2.1 | Master Event List(U_{21}) |
| | | 2.2 | Procedure(U_{22}) |
| | | 2.3 | Map(U_{23}) |
| 3 | Assignments and Responsibilities(U_3) | 3.1 | Controller(U_{31}) |
| | | 3.2 | Simulator(U_{32}) |
| | | 3.3 | Participant(U_{33}) |
| | | 3.4 | Assessor(U_{34}) |
| | | 3.5 | Spectator(U_{35}) |
| 4 | Resource Management(U_4) | 4.1 | Field and House(U_{41}) |
| | | 4.2 | Facilities(U_{42}) |
| | | 4.3 | Communication Equipment(U_{43}) |
| | | 4.4 | Photo & Video Equipment(U_{44}) |
| | | 4.5 | Finance Support(U_{45}) |
| 5 | Rules(U_5) | 5.1 | Site Rules(U_{51}) |
| | | 5.2 | Safety Rules(U_{52}) |
| | | 5.3 | Media(U_{53}) |
| | | 5.4 | Assessment Standard(U_{54}) |
| | | 5.5 | Contact(U_{55}) |

4. APPLICATION OF FUZZY ASSESSMENT METHOD

Fuzzy mathematical assessment is one of the chief methods to quantify a value for a subject which can not be adequately counted or measured^[8]. Fuzzy comprehensive assessment can describe the uncertainty of the indexes.

- (1) Define vectors to represent each index
- $$U = \{U_1, U_2, U_3, U_4, U_5\}$$
- $$U_i = \{U_{i1}, U_{i2}, \dots, U_{in}\}$$

Thus, it is easy to describe the indexes.

(2) Give a weight to every factor $W_U = \{W_1, W_2, W_3, W_4, W_5\}$ according to its importance. The weight hereby is determined by Delphi method in Sector 3.2. The sum of all the weights is 1.0.

(3) Define the comment set (constructed with evaluation vectors) as follows

$V = \{V_1, V_2, V_3, V_4, V_5\}$. On the assumption that every emergency exercise plan can be distinguished into five grades, the final result will also depend on the comment set.

Table 3: Description of comment set

| Item | Description |
|-------|-------------|
| V_1 | Very good |
| V_2 | Good |
| V_3 | Common |
| V_4 | Bad |
| V_5 | Very Bad |

(4) Construct subordinate degree function and fuzzy relationship matrix. There are two kinds of methods to determine subordinate degree. One is a subjective method and the other is an objective method. Subjective method means that some experts' experience can be used to determine the subordinate degree by statistics. Objective method means to use data calculation or set subordinate degree functions. Fuzzy relationship matrix can be written after the subordinate degree is given.

$$R = (R_1, R_2, R_3, R_4, R_5)^T = \begin{bmatrix} R_{11} & R_{12} & R_{13} & R_{14} & R_{15} \\ R_{21} & R_{22} & R_{23} & R_{24} & R_{25} \\ R_{31} & R_{32} & R_{33} & R_{34} & R_{35} \\ R_{41} & R_{42} & R_{43} & R_{44} & R_{45} \\ R_{51} & R_{52} & R_{53} & R_{54} & R_{55} \end{bmatrix}$$

(5) Calculate the final Results. Use proper fuzzy arithmetic operators and then we can get the final assessment results, which can be expressed as follows.

$$F = W_U \circ R = (W_1, W_2, W_3, W_4, W_5) \circ \begin{bmatrix} R_{11} & R_{12} & R_{13} & R_{14} & R_{15} \\ R_{21} & R_{22} & R_{23} & R_{24} & R_{25} \\ R_{31} & R_{32} & R_{33} & R_{34} & R_{35} \\ R_{41} & R_{42} & R_{43} & R_{44} & R_{45} \\ R_{51} & R_{52} & R_{53} & R_{54} & R_{55} \end{bmatrix} = (B_1, B_2, B_3, B_4, B_5)$$

5. CASE STUDY AND DISCUSSION

The index system and method can be applied to a fire emergency exercise plan of a supermarket in a mega city. According to the data from experts, the weight and subordinate degree can be calculated by Delphi method. Table 4 indicates the weight and subordinate degree.

Table 4: Weight and subordinate degree

| U_i | W_i | U_{ij} | W_{ij} | V_1 | V_2 | V_3 | V_4 | V_5 |
|-------|-------|----------|----------|-------|-------|-------|-------|-------|
| U_1 | 0.1 | U_{11} | 0.2 | 0.3 | 0.5 | 0.2 | 0 | 0 |
| | | U_{12} | 0.4 | 0 | 0.1 | 0.3 | 0.4 | 0.2 |
| | | U_{13} | 0.4 | 0.2 | 0.6 | 0.1 | 0.1 | 0 |
| U_2 | 0.3 | U_{21} | 0.3 | 0.1 | 0.2 | 0.6 | 0.1 | 0 |
| | | U_{22} | 0.5 | 0.6 | 0.4 | 0 | 0 | 0 |
| | | U_{23} | 0.2 | 0.5 | 0.4 | 0.1 | 0 | 0 |
| U_3 | 0.2 | U_{31} | 0.3 | 0.7 | 0.2 | 0.1 | 0 | 0 |
| | | U_{32} | 0.2 | 0 | 0 | 0.2 | 0.3 | 0.5 |
| | | U_{33} | 0.2 | 0.8 | 0.2 | 0 | 0 | 0 |
| | | U_{34} | 0.2 | 0 | 0 | 0 | 0.1 | 0.9 |
| | | U_{35} | 0.1 | 0 | 0 | 0.2 | 0.5 | 0.3 |
| U_4 | 0.1 | U_{41} | 0.1 | 0.2 | 0.2 | 0.6 | 0 | 0 |
| | | U_{42} | 0.5 | 0.3 | 0.2 | 0 | 0 | 0 |
| | | U_{43} | 0.2 | 0 | 0.1 | 0.3 | 0.4 | 0.2 |
| | | U_{44} | 0.3 | 0 | 0 | 0.1 | 0.4 | 0.5 |
| | | U_{45} | 0.2 | 0 | 0 | 0.1 | 0.4 | 0.5 |
| U_5 | 0.3 | U_{51} | 0.3 | 0.7 | 0.2 | 0.1 | 0 | 0 |
| | | U_{52} | 0.2 | 0 | 0.1 | 0.3 | 0.5 | 0.1 |
| | | U_{53} | 0.2 | 0.3 | 0.4 | 0.2 | 0 | 0 |
| | | U_{54} | 0.1 | 0 | 0 | 0.3 | 0.4 | 0.2 |
| | | U_{55} | 0.2 | 0.9 | 0.1 | 0 | 0 | 0 |

Use the simple linear model as the fuzzy arithmetic operator. Thus, we can get the conclusion from calculation.

$$F = [0.1 \ 0.3 \ 0.2 \ 0.1 \ 0.3] \circ \begin{bmatrix} 0.1400 & 0.3800 & 0.2000 & 0.2000 & 0.0800 \\ 0.4300 & 0.3400 & 0.2000 & 0.0300 & 0 \\ 0.3700 & 0.1000 & 0.0900 & 0.1300 & 0.3100 \\ 0.1700 & 0.1400 & 0.1700 & 0.2800 & 0.2900 \\ 0.4500 & 0.1800 & 0.1600 & 0.1400 & 0.0400 \end{bmatrix} \\
 = [0.3690 \ 0.2280 \ 0.1630 \ 0.1250 \ 0.1110]$$

The final result indicates the subordinate degree of “Very Good” is 36.90%, which is the largest from the five subordinate degrees. According to the principle of largest subordinate degree, the assessment result of this fire emergency exercise plan of a supermarket in a mega city is very good. The subordinate degree is also shown in Figure 2.

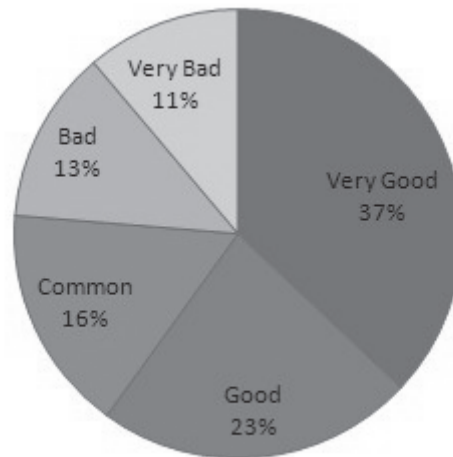


Figure 2: Final Assessment Result

Another way to represent the final result is to assign score to each comment vector. Define the full score as 1.0 and “Very good” equals to 1.0, “Good” to 0.8, “Common” to 0.6, “Bad” to 0.4, “Very Bad” to 0.2. Multiply the subordinate degree and the score. Thus, the final result is

$$F' = [0.3690 \quad 0.2280 \quad 0.1630 \quad 0.1250 \quad 0.1110] \begin{bmatrix} 1.0 \\ 0.8 \\ 0.6 \\ 0.4 \\ 0.2 \end{bmatrix} = 0.7214$$

Although the final result is good, there are still some weaknesses in the emergency exercise plan. The subordinate degrees of V_1 in the first and third row are only 0.14 and 0.17. It means that the background information and the assignment and responsibilities need to be strengthened. Before the real emergency exercise, the two parts need to be re-designed.

6. CONCLUSION

This paper applies fuzzy comprehensive assessment method to evaluate full-scale emergency exercise plan. There are two important parts in the process-construction of index system and application of the fuzzy mathematical method.

The index system is well designed for emergency exercise but only given for reference. It should be adjusted according to the practical

requirement. Compared with traditional subjective judge to the emergency exercise plan, this method enhances the validity and efficiency of assessment result. In the case study, the usefulness of this method is validated. Therefore, this method can be used to evaluate many full-scale emergency exercise plans and help to enhance the effectiveness of emergency exercises.

ACKNOWLEDGEMENT

This research is supported by “11th Five-Year Plan” National Scientific and Technological Supporting Project-“Key Technical Standards Project” (2006BAK04A08)

The background information of the case is provided by the fire department of Shijiazhuang city.

REFERENCES

- Emergency Response Law of People’s Republic of China, 2007
State Emergency Plan for Public Safety Events, 2006
Danny M. Peterson, Ronald W. Perry. The impacts of disaster exercises on participants, *Disaster Prevention and Management*, Volume 8, pp.241-254, 1999
Michael K. Lindell, Carla S. Prater, Ronald W. Perry. *Introduction to Emergency Management*. John Wiley Press, United States, 2007
U.S. Department of Homeland Security, *Homeland Security Exercise and Evaluation Program*, 2007
Deng Yunfeng. Planning and organization of the emergency exercises for serious accidents. *Labor Protection*, 4, 2004
Ye Yicheng, Ke Lihua, Huang Deyu. *Systematic comprehensive assessment technology and application*. Metallurgy industry press, Beijing, 2006
Shang Hongyan, Wang Xuping, Liu Xiaodong. Application of fuzzy assessment method to emergency response capability in hazardous materials transportation, *Second International Conference on Innovative Computing, Information and Control, ICICIC 2007, 2008*, p 4428055

APPLICATION OF NSGA II IN EMERGENCY POINT LAYOUT OPTIMIZATION OF INDUSTRIAL ZONE

DONGXUE LI and MAO LIU
Center for Urban Public Safety Research of Nankai University,
Tianjin, China
Ledon393@163.com

ABSTRACT

Emergency point layout optimization of industrial zone is an important part of industrial area plan, which impacts the overall function of industrial area. On the issue of this problem, a multi-objective and multi-constraint mathematical model is put forward taking all factors affecting into consideration. And the traditional single objective optimization of emergency point layout optimization is converted to a multi-objective optimization problem. The problem is solved by NSGA II, by filtering out so-called dominated solutions, the choice can be restricted to a small number of promising solution candidates. Then a series of Pareto-optimal solutions are produced as a result. The solution sets obtained by NSGA II distribute uniformly and this algorithm has good convergence and robustness, also a reasonable solution could be offered to the decision maker. Combining with emergency point layout optimization of a certain industrial zone and considering the number of emergency point, construction costs and running time, this paper validates the algorithm and the result obtained agrees well with the actual situation.

1. INTRODUCTION

Emergency point layout optimization includes emergency point location and area of responsibility attribution. Emergency point of industrial zone can make first aid as soon as possible when disasters and emergencies occur, which impacts the overall emergency response function of industrial zone. Taking all factors affecting into consideration, emergency point layout optimization is no long a single objective optimization but a multi-objective optimization problem. Investigations on the location of emergency facilities have already a rather long tradition. Yi Wei and Ozdamar Linet [1] put forward a location attribution model for materials distribution and evacuation measures in disaster response activities, they thought the whole plan included offering materials, evacuation and shifting wounded to emergency point. Lili Yang and Bryan F. Jones et al [2] introduced genetic

algorithms (GA) in fire station location and a good effect had been made. Karl F. Doerner et al [3] discussed multi-criteria location planning for public facilities in tsunami-prone coastal areas with NSGA-II [3-6, 8] algorithm, and coverage region, risk and cost was considered at the same time.

The main objectives of this paper are to fully consider the various influencing factors of the given area in the location optimization and to establish an emergency point layout optimization model which is understandable and practical to industrial authorities. The NSGA-II algorithm yields an approximation to the set of Pareto-efficient solutions. As other heuristic approaches, it provides an attractive trade-off between the quality of the solution set approximation and the computation time required to achieve this approximation. The reasons why we decided for NSGAI are that: (i) NSGAI is currently considered as one of the best-performing MOCO (multi-objective combinatorial optimization) meta-heuristics; and (ii) our problem structure, where a feasible solution is given by a vector of integers from a small candidate set, is especially well-suited for a “chromosome” representation of solutions and the application of the classical genetic operations “mutation” and “crossover”.

This paper is organized as follows: Section 2 presents a mathematical model for emergency point layout optimization of industrial zone. NSGAI algorithm is described in section 3. Application of emergency point layout optimization of certain industrial zone with NSGAI is discussed in section 4. Finally, some results and discussions are given in section 5.

2. MATHEMATIC MODEL FOR EMERGENCY POINT LAYOUT OPTIMIZATION

The improvement of system safety needs much input, so a problem of how to achieve emergency point layout optimization is put forward. And the disposal of this issue influences on if limited emergency supply can be used fully and if the due emergency response objective of emergency point can realize. In fact, the process of emergency point layout optimization of industrial zone is a collection of decision-making and the implementation of decision-making under a series of objective constraints. Emergency point layout optimization of industrial zone should follow the principle of people-oriented and taking economical factors into consideration adequately. Firstly the first aid needs must be satisfied, then emergency time, construction cost and service area of emergency points and so on should be taken into account.

According to the fundamentals presented, a multi-objective optimization mathematical model of emergency point is given. At present, the model with constraints is described as follows:

$$\begin{aligned} & \text{Min} (f_1(x), f_2(x), \dots, f_m(x)) \\ & \text{S. t.} \quad \begin{cases} g_i(x) \geq 0, & i = 1, 2, \dots, p \\ h_j(x) = 0, & j = 1, 2, \dots, q \\ x_i^{(L)} \leq x_i \leq x_i^{(U)}, & i = 1, 2, \dots, n \end{cases} \end{aligned}$$

An-variable solution vector x which satisfies all constraints and variable bounds as mentioned above is called a feasible solution. $f_k(x)$ ($k=1,2,\dots,m$) is the k optimization objective; $g_i(x) \geq 0$ is inequality constraint and $h_j(x)=0$ equality constraint; $x_i^{(L)} \leq x_i \leq x_i^{(U)}$ denotes the range bound of x_i , $x=(x_1, x_2, \dots, x_n)$ is the solution vector and x_l ($l=1, 2, \dots, n$) denotes the l independent variable.

On the issue of multi-objective optimization, because of the characteristic of itself, it is by no means an easy task. There are incompatible conflicts between every two objective functions. For one objective function, the solution maybe the best one while for others it will be not good enough. So the optimization of multi-objective is an optimization in some sense. Contrary to the classical approaches, multi-objective optimization procedures aim at finding a finite, representative set of Pareto-optimal solutions in a problem. In this paper, we introduce NSGAI algorithm to solve the function optimization problem. To the point of emergency point layout optimization of industrial zone, the last results we want to obtain are a series of Pareto-optimal solutions, and then according to the actual circles and experts' experience the most rational solution can be made. In addition, if necessary we can endow impact coefficients to different optimization objectives in data processing [3].

3. NSGA

3.1 NSGA description

As the meta-heuristic approach to solve the described problem, we have chosen the Elitist Nondominated Sorting Genetic Algorithm (NSGA II), which was developed by Deb (2002) on the basis of Genetic Algorithm (GA). The NSGAI algorithm yields an approximation to the set of Pareto-efficient solutions. The solution sets obtained by NSGA II distribute uniformly and this algorithm has good convergence and robustness, also a reasonable solution could be offered to the decision maker. As all genetic algorithms, NSGAI is an iterative, population-based search procedure. NSGAI computes a series of so-called generations, where each generation consists of a set of feasible solutions of the optimization problem under consideration. Because of the multi-objective nature of our problem formulation, it is not possible to provide the decision maker with a single "optimal" solution. However, by filtering out so-called dominated solutions, the choice can be restricted to a small number of promising solution

candidates. A specific feature of NSGAI is that each generation is composed of two sub-populations of equal size, so it avoids the loss of excellent individuals. The procedure of NSGAI is similar to GA, the difference is that it has a step of elitist strategy which is the core of the arithmetic, and all this will be discussed in the next section.

3.2 NSGA II procedure

NSGA II procedure for finding a well-distributed and well-converged set of multiple Pareto-optimal solutions in a multi-objective optimization problem is described as follows. Like in GA, NSGA II starts with a population of N_{pop} random solutions. As shown in Fig 1. Initially, a parent population P_0 is generated by randomly assigning values to the genes of M chromosomes. For each of the chromosomes formed in this way, the K objective function values are computed. Then, non-dominated sorting and crowding distance sorting are applied to the population P_0 , and selection, crossover and mutation are also used in order to create an offspring population Q_0 of size M . Image points of a solution set with non-dominated fronts and crowding distance is displayed in Fig 2. Therein, for performing selection, the so-called crowded-comparison operator is applied, which prefers chromosomes with lower nondomination level; for two chromosomes with equal nondomination level, the chromosome with higher crowding distance is preferred. Lastly, the elitist strategy is performed which includes population combination, non-dominated sorting and crowding distance sorting. After the steps described above, we select a new population and the procedure comes to a end. The particular process is described in the next section.

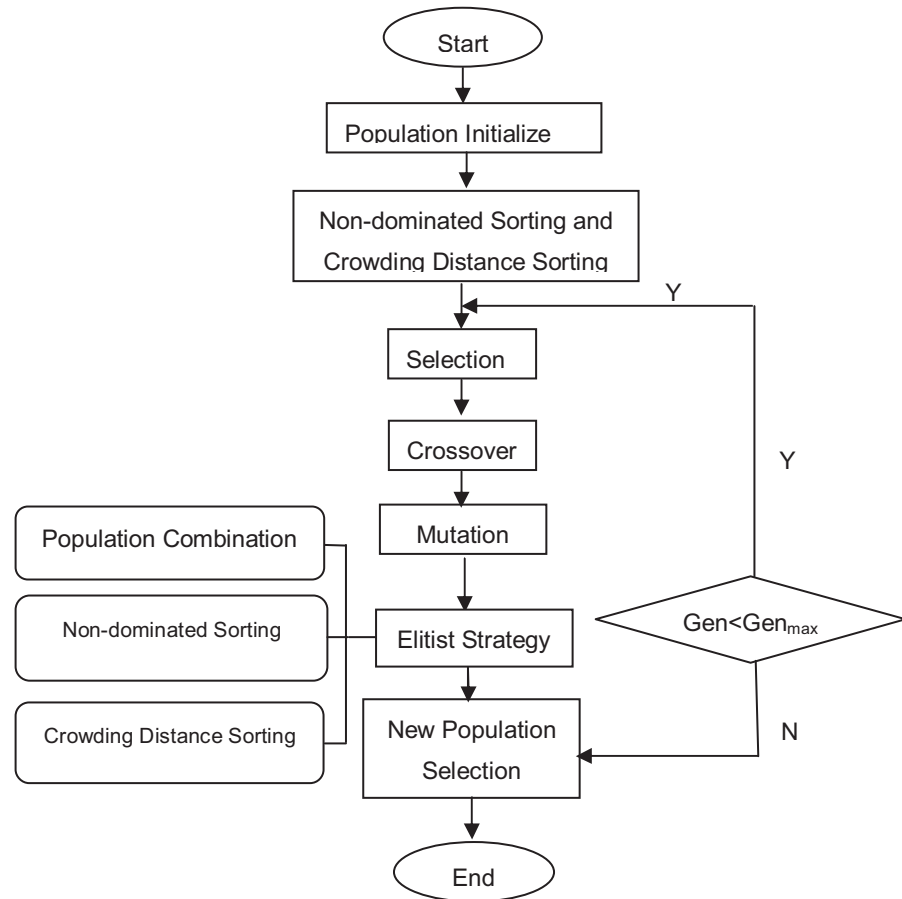


Figure 1: NSGA flow chart

Let us now assume that we have just constructed a generation t consisting of the two sub-populations P_t and Q_t (initially, $t=0$). The parent population P_t and the offspring population Q_t are then combined to a population R_t of size $2M$. Next, this population has to be reduced to a size of M . For this purpose, all solutions of R_t are sorted based on nondomination by fast non-dominated sorting. Once the non-dominated sorting of the set R_N is over, the new population is filled with solutions of different nondominated fronts, one at a time. The filling starts with the best non-dominated front and continues with solutions of the second non-dominated front, followed by the third nondominated front, and so on. The fronts are included into a new population P_{t+1} until for a certain front r , the new population P_{t+1} reaches a size of more than M . The fronts $r+1$, $r+2$, etc are rejected. The solutions of the last front r to be included are sorted using the crowding distance sorting. Those solutions that have the largest crowding distance are assigned to the new population until P_{t+1} reaches a size of M . Fig 3 shows a scheme of NSGAI. To the new population P_{t+1} obtained in this way, selection, crossover and mutation are applied again, which gives a population Q_{t+1} , and the procedure described above is repeated till the

generations reach the largest one or the solutions satisfy convergence conditions.

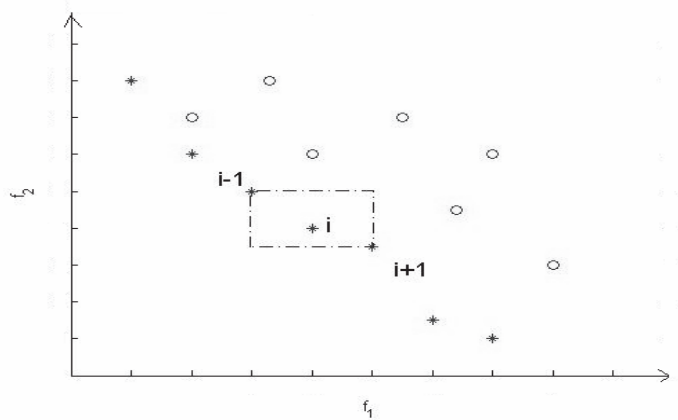


Figure 2: Image points of a solution set with non-dominated fronts and crowding distance

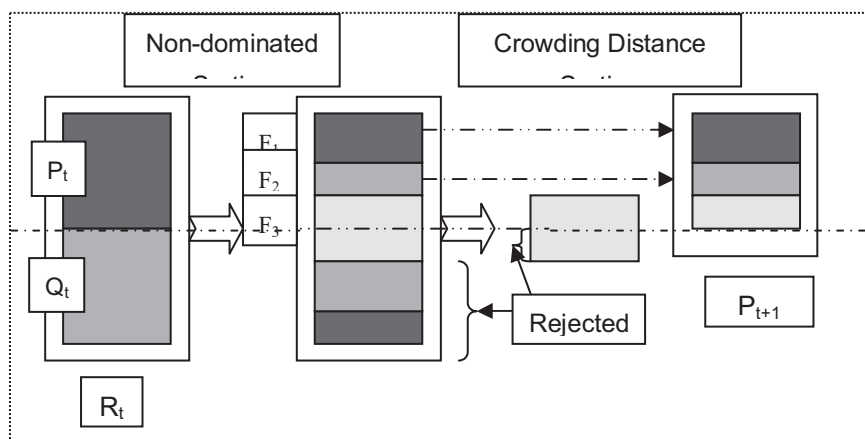


Figure 3: NSGAII scheme, according to Deb (2002)

4. OPTIMIZATION INSTANCE ANALYZING

4.1 Problem description

Emergency point layout optimization of certain industrial zone is illustrated in this part and NSGAII algorithm is demonstrated in the problem solving. There are 6 operating areas in the industrial zone and emergency point can be constructed in any operating area, every point can serve certain area of the industrial zone. The number of emergency point should be least and the cost should be less than 25 millions on the condition of satisfying all servicing area. The running time of every emergency point and operating area should be less than 5 minutes and the overall running time of emergency response is the shortest. What's more, there must be at least one

emergency point in operating area 1, 2, 3 and the same to area 4, 5, 6. The serving area of every emergency point should not be more than 3. The running time of every two operating areas is illustrated in table 1 and the constructing cost of every emergency point in corresponding area is displayed in table 2. Now constitute a best emergency point layout optimization scheme according to these objectives and constraints [9].

Table 1: Run time of every two operating areas (Minutes)

| Operating Area(OA) | OA 1 | OA 2 | OA 3 | OA 4 | OA 5 | OA 6 |
|--------------------|------|------|------|------|------|------|
| OA 1 | 0 | 4 | 4 | 10 | 9 | 7 |
| OA 2 | 4 | 0 | 8 | 11 | 5 | 3 |
| OA 3 | 4 | 8 | 0 | 4 | 5 | 7 |
| OA 4 | 10 | 11 | 4 | 0 | 5 | 8 |
| OA 5 | 9 | 5 | 5 | 5 | 0 | 5 |
| OA 6 | 7 | 3 | 7 | 8 | 5 | 0 |

Table 2: Emergency material storage cost of every operating area

| Operating Area(OA) | OA 1 | OA 2 | OA 3 | OA 4 | OA 5 | OA 6 |
|--------------------|------|------|------|------|------|------|
| Cost (Million) | 11.5 | 12 | 13 | 13 | 11.5 | 11.5 |

4.2 Problem solving

In term of the mathematic model for optimization problem brought forward in part 2 and the known conditions in 4.1, a multi-objective optimization mathematic model is constituted as follows:

$x_i=0$ denotes founding emergency point in industrial zone, or $x_i=0$, x_{ij} gives the running time between operating area i and j . Three objectives show the least emergency points, the lowest cost and the shortest overall running time.

$$Min z_1 = x_1 + x_2 + x_3 + x_4 + x_5 + x_6$$

$$Min z_2 = 11.5x_1 + 12x_2 + 13x_3 + 13x_4 + 11.5x_5 + 11.5x_6$$

$$Min z_3 = \sum_{i=1}^6 x_i \sum_{j=1}^6 x_{ij}$$

$$S.t \begin{cases} x_1 + x_2 + x_3 \geq 1 \\ x_4 + x_5 + x_6 \geq 1 \\ 11.5x_1 + 12x_2 + 13x_3 + 13x_4 + 11.5x_5 + 11.5x_6 \leq 25 \\ x_i = 0 \text{ or } 1 \quad (i = 1, 2, \dots, 6) \end{cases}$$

For the model above, we deal with it using NSGAI. The initial population size is 20 and generation is 100. The crossover and mutation probability is 0.9 and 0.02 respectively. Each optimization procedure is run at least five times from different initial populations to build a confidence on

the obtained optimized solutions. After computing we obtain a series of Pareto-optimal solutions see Table 3.

Table 3: Compare of the six emergency points (EP) location layout

| Sequence number | Pareto-optimal solution | Num of EP(z_1) | Cost of EP(z_2) | Total running time(z_3) |
|-----------------|-------------------------|--------------------|---------------------|-----------------------------|
| 1 | (1, 0, 0, 0, 1, 0) | 2 | 23 | 18 |
| 2 | (0, 1, 0, 0, 1, 0) | 2 | 23.5 | 17 |
| 3 | (0, 0, 1, 0, 0, 1) | 2 | 24.5 | 16 |
| 4 | (0, 0, 1, 0, 1, 0) | 2 | 24.5 | 18 |
| 5 | (0, 1, 1, 0, 0, 0) | 2 | 25 | 16 |
| 6 | (0, 1, 0, 1, 0, 0) | 2 | 25 | 16 |

Owing to the particularity of the problem, the number of emergency point must be integer, so the vector solution is discrete and the number is restricted to 2. From table 3 and fig. 4 and fig. 5 we can see the first three solutions have predominance over others, but we can't come to a conclusion which solution is the best one directly. For example, the first solution gives the least cost but the longest time while the third solution give the shortest time but more cost. If you want to have a middle course, you will select the second one. The characteristic of solutions selecting is no best but better. The decision makers should choose the better solution in term of the actual condition and their experiences.

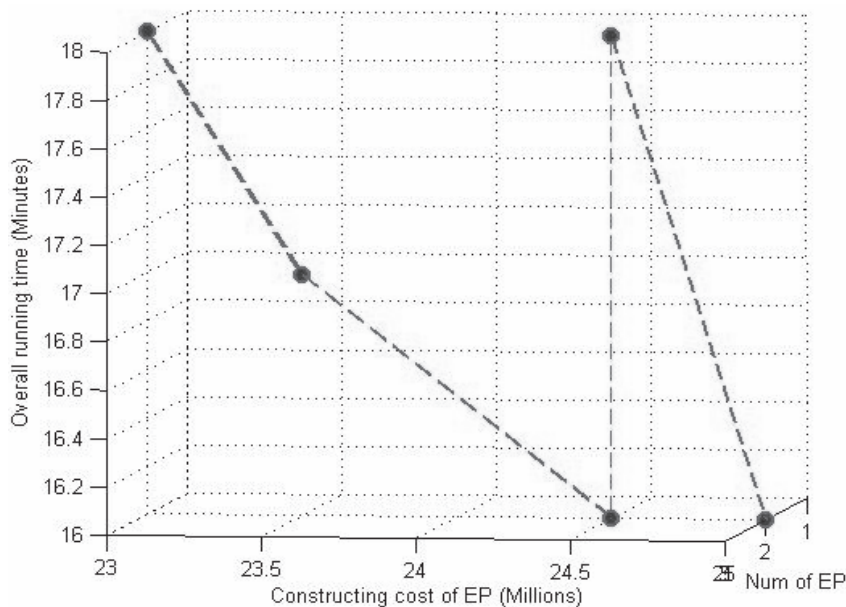


Figure 4: Three-dimension distribution compare of emergency point layout

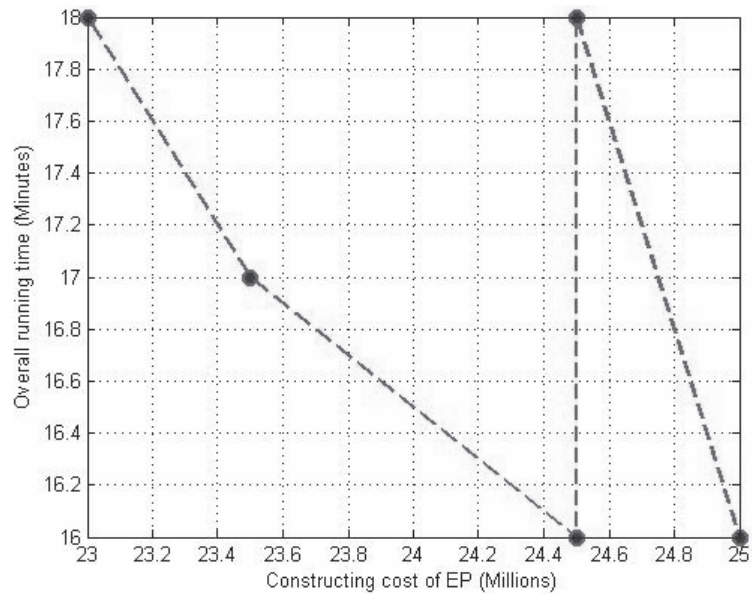


Figure 5: Compare of emergency point layout
(Num of emergency points = 2)

5. CONCLUSION AND DISCUSSION

We have presented a model for multi-objective optimization of emergency point taking more correlative factors into account. The model uses classical optimization criteria from location analysis and a coverage criterion, but it encompasses also a time criterion and a cost criterion. We have used NSGAI as our meta-heuristic multi-objective solution technique. NSGAI is a new method for multi-objective optimization and also it is effective for problem solving. The author introduces the method to safety field for safety layout and emergency response. On the issue of emergency point layout optimization in this paper, we have obtained a series of Pareto-optimal solutions. But the solutions are not final outcome for the problem, a lot more comparing and selecting work should be done. In the course of Pareto-optimal solutions searching, a lot of parameters must be given. And for a more appropriate and reasonable solution, more than one running should be used. After the procedure above, we solve the emergency point optimization successfully.

Alternative techniques both from the GA field and from other meta-heuristic areas should be investigated and compared to the NSGAI approach. This method may be used for exercises and it enables decision makers to verify their decision by comparing it with the output of the model. Also the proposed procedure is capable of solving other kinds of optimization problems. But the model and method have there deficiencies born, there is still a lot of experiments and modification work to be done.

REFERENCE

- Yi Wei, Ozdamar Linet, 2007. A dynamic logistics coordination model for evacuation and support in disaster response activities[J]. *European Journal of Operational Research*, 179 (3), 1177 -1193.
- Lili Yang, Bryan F. Jones, Shuang-Hua Yang, 2007. A fuzzy multi-objective programming for optimization of fire station locations through genetic algorithms[J]. *European Journal of Operational Research* 181, 903–915.
- Karl F. Doerner, 2008. Walter J. Gutjahr, Pamela C. Nolz[J]. Multi-criteria location planning for public facilities in tsunami-prone coastal areas, Springer.
- Kalyanmoy Deb, Amrit Pratap, Sameer Agarwal, et al, 2002. A fast and elitist multi-objective genetic algorithm: NSGA-II[J]. *IEEE Transactions on Evolutionary Computation* 6(2), 182-197.
- Pradyumn Kumar Shukla, Kalyanmoy Deb, 2007. On finding multiple Pareto-optimal solutions using classical and evolutionary generating methods[J]. *European Journal of Operational Research* 181, 1630–1652.
- Kalyanmoy Deb, Kishalay Mitra, Rinku Dewric, 2004. Saptarshi Majumdar[J]. Towards a better understanding of the epoxy-polymerization process using multi-objective evolutionary computation[J]. *Chemical Engineering Science* 59, 4261 – 4277.
- Feng Shigang, Ai Qian, 2007. Application of fast and elitist non-dominated sorting generic algorithm in multi-objective reactive power optimization[J]. *Transactions of China electrotechnical society* 22(12), 146-151.
- Kalyanmoy Deb, Santosh Tiwari, 2008. Omni-optimizer: A generic evolutionary algorithm for single and multi-objective optimization[J]. *European Journal of Operational Research* 185, 1062–1087.
- Xu Jiuping, Yang Chao, Zhang Min, et al, 2004. *Operations research(Second section)*[M]. Beijing: Science Press.

NETWORK PUBLIC OPINION CAUSED BY PUBLIC SAFETY INCIDENTS

KUI ZHENG¹ and XUEMING SHU²

¹State Key Laboratory of Fire Science,
University of Science and Technology, Hefei, China

²Department of Engineering Physics, Centre for Public Safety Research,
Tsinghua University, Beijing, China
zhengkui@mail.ustc.edu.cn

ABSTRACT

When a public safety incident happened, the overflow of the network public opinion leads to psychological panic of public, enhances the perniciousness of disaster, and influences the status of the society stability greatly. In this article, it was advanced of early-warning method of public safety incidents based on network public opinion, and grading warning strategy was also be given. The datamining technology of information processing can be used in automatic collection and statistic analysis with network public opinion during the course of public safety incidents. Topic Detection and Tracking (TDT) technology can be used in massive network information retrieval automatically and news topic tracking of public safety incidents. The application of network public opinion early-warning model is developed on National Public Safety Incidents Emergency Platform of China, which provides scientific support for government's emergency decision-making and policy-making.

1. INTRODUCTION

With the development of society, public safety is becoming a more and more important subject all over the world, especially in China. From the state government to all local governments of China, public safety incidents are causing wide attention. At the beginning of 2006, Stated Emergency Preparatory Schemes of China was published, in which public safety incidents have been divided into four types that is natural disasters, accidents disasters, public health, and social security. It is quite significant to study on science and technologies involved in social safety, which has much relative with the government functions (SHU Xue-ming, 2007).

During the disasters, no matter natural disasters or accidents, people always have tremendous psychological impact in their minds, especially in the circumstances of overflow of rumors. Along with the whole process of disasters, people's political attitudes will change according to government managers and related intermediary of the social.

In the modern society, Internet provides us more free virtual space to express our attitude. Network public opinion can be obtained from masses attitude on Internet during the course of public safety incidents. According to the network public opinion, we can develop an early-warning model of

public safety incidents to support the government's emergency decision-making and policy-making.

2. PUBLIC OPINION AND NETWORK PUBLIC OPIONION

In the narrow sense, public opinion is people's political attitudes towards State Management in certain social space around the happening, development and changes of the intermediary social events (WANG Lai-hua, 2005). Broadly speaking, public opinion is the total of most people's belief, attitudes, views and emotions, etc. according to the phenomena and problems in the society.

With the rapid development of Internet on a global scale, it has been recognized as the "fourth media" after the newspaper, radio and television, and it has been one of the main carriers of public opinion. Network public opinion is the public opinion on the Internet. The main source of network public opinion is News, BBS, Blog, and RSS, etc.

Network public opinion is always global, free, real-time, interactive and anonymous.

3. DATA COLLECTION OF NETWORK PUBLIC OPIONION

In June 2007, there was an earthquake in a city in the south-west China. This earthquake killed two and injured more than 300 people, and affected 180 thousand people. The direct economic losses of the earthquake were 2.5 billion Yuan. Moreover, the Chinese College Entrance Examination was also hold at that time. So, on the Internet, people discussed warmly about whether those candidates at the city can join the examination smoothly or not. When the network public opinion was obtained, government transported large quantities of supplies to the disaster area and adopted a series of measures to insure those students attending the examination. The emergency program was accurate and timely because of the network public opinion.

From the example, we can see that network public opinion plays an important role in public safety incidents emergency management and policy-making. So, according to the network public opinion, an early-warning method of public safety incidents was advanced by our research team.

According to our research, a system structure was given which is shown in figure 1, and the system operation processes is shown in figure 2.

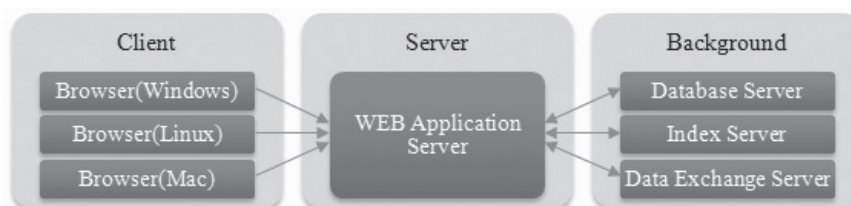


Figure 1: System Structure

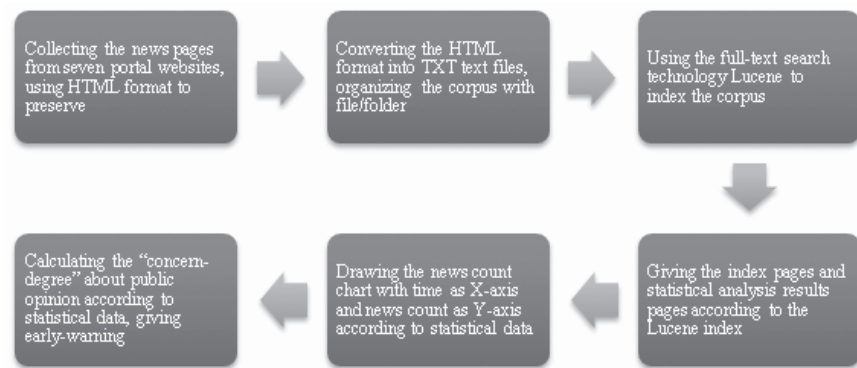


Figure 2: System Operation Processes

It's quite difficult to download all the news pages from the news portal websites (e.g., news.sina.com.cn, news.qq.com, news.sohu.com, people.com.cn, xinhuanet.com, and so on). However, the form of the news pages in some news portal websites is stable for us to parser, and all of them have been downloaded.

Firstly, a tool called "Offline Explorer" was used to download the news pages as shown in figure 3. However, the tool is not so suitable and seems insufficient faced with such a large site, since its main use is to download the whole of a small site.

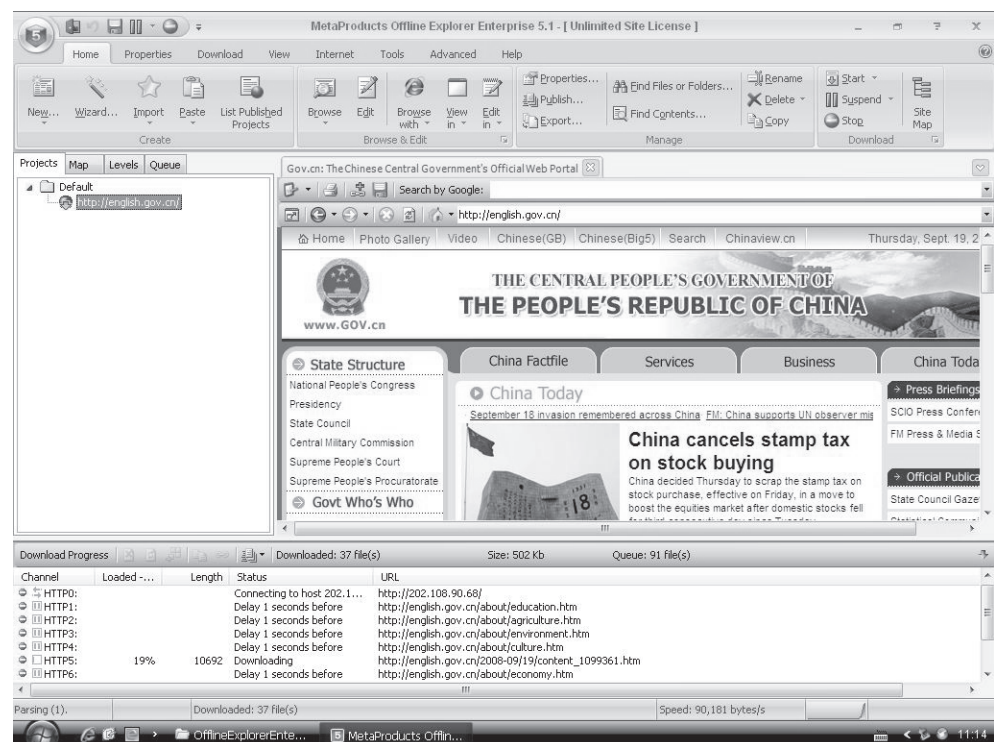


Figure 3: The Interface of Offline Explorer

Then, we found the rules of "news.qq.com", that is the page: "http://news.qq.com/a/20070101" concludes all the hyperlinks of the news pages on Jan 1, 2007. So, another download tool called "Flashget" which is wildly used in China was used to download all the news pages at "news.qq.com" in 2007 as shown in figure 4. ("news.qq.com" is established

by Tencent, Inc. Founded in November, 1998, Tencent, Inc. has grown into China's largest and most used Internet service portal. In its nine-year history, Tencent has been able to maintain steady and fast-paced growth by always putting its users first.)

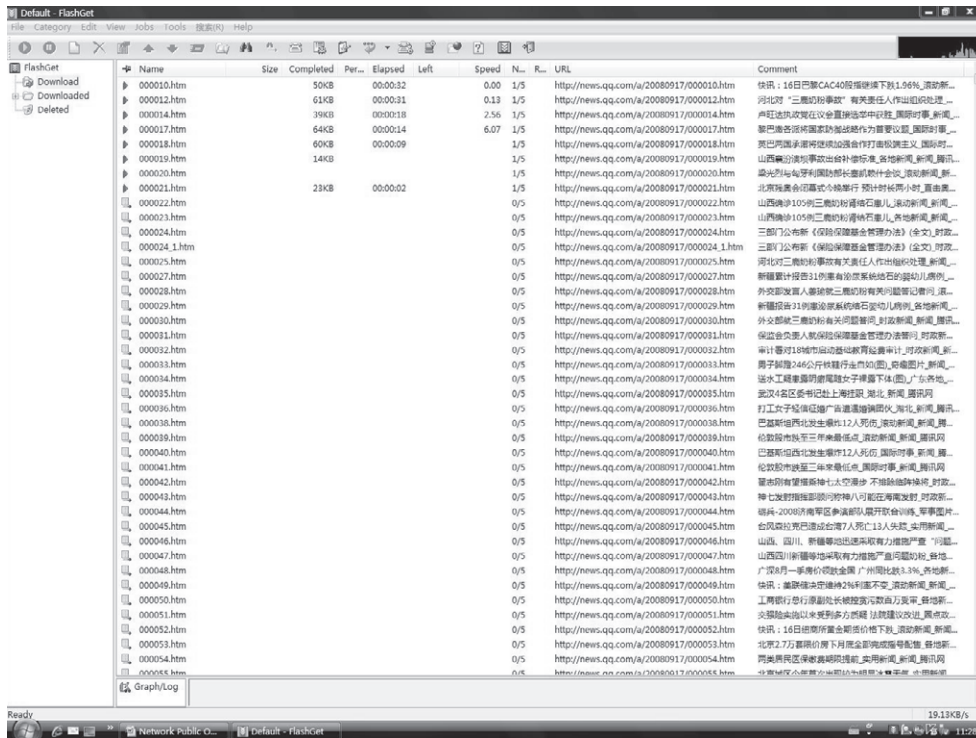


Figure 4: The Interface of Flashget

4. CONTENT ANALYSIS OF NETWORK PUBLIC OPIONION

After all the news pages were downloaded, they were needed to be translated into TXT documents. Another tool called “TextForever” was used to change HTML into TXT. In the process of changing, the redundant information such as advertisement and navigation in the news page was removed, and only the main body of the news page was remained.

When all the news pages have been collected, we need to make index for them. An open source tool kit called “Lucene” was used to do the work.

Lucene is not a complete full-text search application, but a text written by Java indexing engine kits. It can be easily embedded in a variety of applications to address applications in order to achieve the full text indexing / search functions. Lucene is a support which can be viewed as full text indexing database system. Using Lucene to complete a full term for the process of fundamental logic includes two processes. One is that the index of the segmentation text is warehoused; another is that the search results are given based on search conditions. Lucene full-text search process first index, which read a number of documents from the command line, storage the document by path (path field) and content (body Field) two fields, and index the full-text content. The index unit is the document object, and each document object contains a number of field objects.

Once a certain topic was given, the application started to search all the files from the index, and counted the matching files every day during the process of the topic. Then, a chart with time as X-axis and news count as Y-axis was given to help user to decide how the topic had attracted people.

The following chart is a search example. From the chart, we can see the amount of network public opinion change from May to August. Moreover, many peaks in the curve are relative to the effect of government emergency management measures, which give us much information to early-warning of network public opinion.

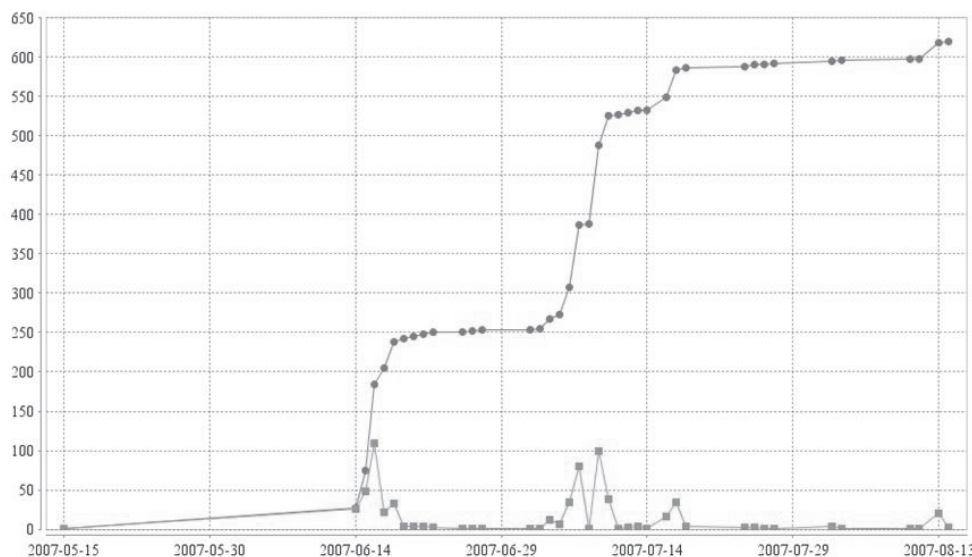


Figure 5: The Chart of Coverage about “Illegal Brick Kiln Affair”

5. EARLY-WARNING MODEL OF NETWORK PUBLIC OPINION

According to the obtained data, a term named “concern-degree” will be used to describe how people concern about the certain incident.

Assuming that a certain moment t , the system has monitored N_t sites reported news about the certain topic;

Order S_i ($i = 1, 2, \dots, N_t$) as the count of news about the certain topic at No.i website up to the certain moment t ;

Order B_j ($i = 1, 2, \dots, S_i$) as the count of page view to No.j news at No.i website up to the certain moment t ;

Order C_j ($i = 1, 2, \dots, S_i$) as the count of comment to No.j news at No.i website up to the certain moment t ;

In addition, four thresholds N_m, S_m, B_m, C_m were given to describe the acceptable maximum of the sites number, the news count, the view count, and the comments count.

Then we can give the following formula:

$$R = \max \left\{ \frac{N_t}{N_m}, \sum_{i=1}^{N_t} \frac{S_i}{S_m}, \sum_{i=1}^{N_t} \sum_{j=1}^{S_i} \frac{B_j}{B_m}, \sum_{i=1}^{N_t} \sum_{j=1}^{S_i} \frac{C_j}{C_m} \right\}$$

When $R \leq 0.2$, we believe that the given topic has been almost no cause for concern;

When $0.2 < R \leq 0.5$, we believe that the given topic has attracted the attention of the people;

When $0.5 < R \leq 1.0$, we believe that the given topic has been cause for considerable attention;

When $R > 1.0$, we believe that the given topic has been cause for strong concern.

6. DISCUSSION AND CONCLUSION

We are living in an open society which has developed means of communication, mobility frequent, and increasingly in-depth building of information. Internet is the supply of advanced culture and an important means of communication, and network public opinion is more closely related to social stability.

The technological means to deal with the Internet information analysis are constantly developed. This study selected a special aspect in the rapid development of network technology process to explore, which designed a system framework targeted mainly for public safety monitoring, and implemented frequency statistic and output of public safety sensitive words.

1. The acquisition of public opinion in the network monitoring system was constructed. The advanced search engine technology was used to achieve a comprehensive network monitoring of public opinion, and data mining based on modern information processing technology was used to monitor and track the topic.

2. The comprehensive application time-and-space-crossed was implemented. The incident link between time and space was analyzed, and the incident occurred at a picture was informed to forecast the development trend of events.

3. The “concern-degree” of public opinion was proposed. The research of calculating method according to people’s concern about public opinion provided a reliable basis for the early-warning of public opinion.

4. An early-warning model of public opinion was established. Forecasting the incident development trend and grading early-warning are provided effective support for the government’s emergency decision-making and policy-making.

REFERENCES

SHU Xue-ming and ZHENG Kui, 2007. Study on Social Stability Model and Forecast Method of Social Safety. The 1st International Conference on Risk Analysis and Crisis Response, Shanghai, China. Sept. 25-26.

JIANG Bo, SHU Xue-ming and SHEN Shi-fei, 2007. Study on Criminal Prediction based on GIS Map of KS City. Joint CIG/ISPRS Conference on Geomatics for Disaster and Risk Management, Toronto,

Canada. May 23-25.

WANG Lai-hua and LIU Yi, 2005. Research on Public Opinion and Sentiment in China. *Journal of Tianjin University (Social Sciences)*. 7(4), 309.

WANG Lai-hua, 2005. Initially on the Changes of Public Sentiment. *Academic Exchange*. 141(12), 155.

http://www.tencent.com.hk/about/about_e.shtml

<http://www.chedong.com/tech/lucene.html>

A NEW KRIGING-BASED FINITE ELEMENT METHOD FOR HIGHLY ACCURATE DYNAMIC ANALYSIS

KANOK-NUKULCHAI WORSAK¹, WICAKSANA CITRA²
and THANH TAM BUI³

¹ Professor, School of Engineering and Technology,
Asian Institute of Technology, Thailand

² Former Graduate Student, School of Engineering and Technology,
Asian Institute of Technology, Thailand

³ Research Engineer, School of Engineering and Technology,
Asian Institute of Technology, Thailand
worsak@ait.ac.th

ABSTRACT

This paper presents dynamic analyses by the finite element methods (FEM) with Kriging shape function (Kriging-based finite element methods). Previous study has shown that application of Kriging-based FEM shows remarkable accuracy for static problem (Plengkhom and Kanok-Nukulchai, 2005). In this study, the application of Kriging-based FEM is enhanced to dynamic problems. One dimensional (Timoshenko beam) and two dimensional (Mindlin plate) dynamic analyses are conducted. Some numerical examples of free and forced vibration are taken to evaluate the accuracy of the method. For each analysis, the accuracy of Kriging-based FEM is compared with the standard FEM. The result shows that Kriging-based FEM shows significant improvement of accuracy compared to the standard FEM especially for two dimensional problems.

1. INTRODUCTION

One drawback of the standard finite element (FEM) is the general limitation of its shape functions due to their construction over the element structure. Meshless method is one of the attempts to overcome this drawback, but it creates another problem. Meshless shape function does not have Kronecker's delta property, so that the essential boundary condition has to be enforced. Based on those two conditions, attempts to investigate a method that combines the advantage of FEM shape function and meshless shape function are conducted. Previous studies (Tongsuk and Kanok-Nukulchai, 2004, Plengkhom and Kanok-Nukulchai, 2005) have found a good method which is called Kriging-based FEM. It is called Kriging-based since Kriging interpolation is used in the formation of FEM shape functions. Their study has shown that Kriging-based FEM has a very good performance and could achieve higher accuracy compared to the standard finite element method for elastostatic problems. More investigation is needed to evaluate the method for more complex problems. In this study,

the use of Kriging-based FEM will be enhanced for dynamic analysis. It includes free vibration and forced vibration of one dimensional Timoshenko beam and two dimensional Mindlin plate problems.

2. KRIGING INTERPOLATION

In the context of shape function, Kriging interpolation can be written in the following form:

$$u_i^h(x) = \sum_i^n N^a(x) u_i^a \tag{1}$$

$$N^a(x) = \sum_j^m p_j(x) A_j^a + \sum_k^n r_k(x) B_k^a \tag{2}$$

Where p_j is vector of polynomial basis, and r_k is the vector of correlation function between nodes in the domain of influence. m is the number of the polynomial basis term and n is the number of nodes in the domain of influence. A and B can be written in the following form

$$\mathbf{A} = (\mathbf{P}^T \mathbf{R}^{-1} \mathbf{P})^{-1} \mathbf{P}^T \mathbf{R}^{-1} \tag{3}$$

$$\mathbf{B} = \mathbf{R}^{-1} (\mathbf{I} - \mathbf{P} \mathbf{A}) \tag{4}$$

Where \mathbf{P} is $n \times m$ matrix that collects values of polynomial basis function at given n set of coupling nodes and \mathbf{R} is the $n \times n$ matrix of correlation functions. Two types of correlation functions will be used in this study; gauss and quartic spline correlation function. Based on the study, it is found that gauss correlation function is better than quartic spline for one dimensional problem, but for two dimensional problems, quartic spline is better than gauss in term of accuracy. Quartic spline correlation function can be written as:

$$R(x_i, x_j) = \begin{cases} 1 - 6d^2 + 8d^3 - 3d^4 & \text{for } d \leq 1 \\ 0 & \text{for } d > 1 \end{cases} \tag{5}$$

While gauss correlation function can be written as:

$$R(x_i, x_j) = e^{-\left(\theta \frac{r_{ij}}{d_{\max}}\right)^2} \tag{6}$$

where $d = \frac{r_{ij}}{d_{\max}} \theta$, r_{ij} is the distance between two points, θ is correlation parameter and d_{\max} is the maximum distance between two points in the domain of influence. Plengkhom (2005) has investigated and proposed that the value of θ has to be set in between two limits to ensure the stability of the method. The bounds are proposed as follows

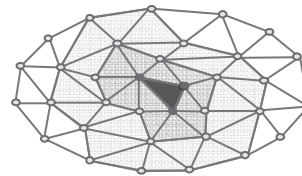
Lower bound:

$$\left| \sum_{i=1}^n N^i - 1 \right| \leq 1 \times 10^{-10+m} , \text{ where } m \text{ is the order of basis function} \quad (7)$$

Upper bound: $\text{Det}(\mathbf{R}) \leq 1 \times 10^{-k}$, where k is the dimension of the problem (8)

The proposed upper and lower bound limits above are the mathematical consideration which guarantees the quality of Kriging interpolation with rational physical meaning. The lower bound will ensure the consistency property of correlation matrix \mathbf{R} since too low θ will allow too much influence of all nodes and decreases the non singularity of correlation matrix \mathbf{R} . The upper bound will ensure the kriging interpolation's quality.

Layered domain of influence concepts will be used in this study, and it can be illustrated in the following figure:



■ One layer ■ Two layers ■ Three layers

Figure 1: Layered domain of influence

3. TIMOSHENKO BEAM

In the Galerkin discretized equation of beams, the unknown variables can be interpolated using Kriging shape function as

$$u(x) = \sum_n \phi^n u^n = \{\phi\} \{u\} \quad (9a)$$

$$\theta(x) = \sum_n \eta^n \theta^n = \{\eta\} \{\theta\} \quad (9b)$$

The global equations for free vibration of Timoshenko beams can be defined as:

$$\begin{bmatrix} [K_u]_1 & [K_\theta]_1 \\ [K_u]_2 & [K_\theta]_2 \end{bmatrix} - \omega^2 \begin{bmatrix} [M_1] & 0 \\ 0 & [M_2] \end{bmatrix} \begin{bmatrix} u \\ \theta \end{bmatrix} = \begin{bmatrix} 0 \\ 0 \end{bmatrix} \quad (10)$$

Where:

$$[K_u]_1 = \int kGA \{\phi_{,x}\}^T \{\phi_{,x}\} dx; \quad [K_u]_2 = - \int kGA \{\eta\}^T \{\phi_{,x}\} dx;$$

$$[K_\theta]_1 = - \int kGA \{\phi_{,x}\}^T \{\eta\} dx \quad [K_\theta]_2 = \int kGA \{\eta\}^T \{\eta\} dx + \int EI \{\eta_{,x}\}^T \{\eta_{,x}\} dx$$

$$[M_1] = \int \rho A \{\phi\}^T \{\phi\} dx; \text{ and } [M_2] = \int \rho I \{\eta\}^T \{\eta\} dx .$$

Moment and shear forces can be expressed as: $M = EI \frac{d\theta}{dx}$ and

$$Q = \frac{dM}{dx} - \rho I \frac{d^2\theta}{dt^2}.$$

4. MINDLIN PLATE

In the Galerkin discretized equation of plates, the unknown variables can be interpolated using Kriging shape function as

$$u(x, y) = \sum_n \phi^n u^n = \{\phi\} \{u\} \tag{11}$$

$$\theta_x(x, y) = \sum_n \eta^n \theta_x^n = \{\eta\} \{\theta_x\} \tag{12}$$

$$\theta_y(x, y) = \sum_n \xi^n \theta_y^n = \{\xi\} \{\theta_y\} \tag{13}$$

The global equations for free vibration of Mindlin plate can be defined as:

$$\begin{bmatrix} [K_u]_1 & [K_{\theta_x}]_1 & [K_{\theta_y}]_1 \\ [K_u]_2 & [K_{\theta_x}]_2 & [K_{\theta_y}]_2 \\ [K_u]_3 & [K_{\theta_x}]_3 & [K_{\theta_y}]_3 \end{bmatrix} - \omega^2 \begin{bmatrix} [M_1] & 0 & 0 \\ 0 & [M_2] & 0 \\ 0 & 0 & [M_3] \end{bmatrix} \begin{bmatrix} u \\ \theta_x \\ \theta_y \end{bmatrix} = \begin{bmatrix} 0 \\ 0 \\ 0 \end{bmatrix} \tag{14}$$

Where:

$$[K_u]_1 = \int D_s \{ \phi_{,x} \}^T \{ \phi_{,x} \} + \{ \phi_{,y} \}^T \{ \phi_{,y} \} dA \quad [K_{\theta_y}]_1 = - \int D_s \{ \phi_{,y} \}^T \{ \xi \} dA$$

$$[K_{\theta_x}]_1 = - \int D_s \{ \phi_{,x} \}^T \{ \eta \} dA \quad [M_1] = \int \rho h \{ \phi \}^T \{ \phi \} dA$$

$$[K_u]_2 = - \int D_s \{ \eta \}^T \{ \phi_{,x} \} dA \quad [M_2] = \int \rho \frac{h^3}{12} \{ \eta \}^T \{ \eta \} dA$$

$$[K_{\theta_x}]_2 = \int D_b \left[\{ \eta_{,x} \}^T \{ \eta_{,x} \} + \frac{1-\nu}{2} \{ \eta_{,y} \}^T \{ \eta_{,y} \} \right] dA + \int D_s \{ \eta \}^T \{ \eta \} dA$$

$$[K_{\theta_y}]_2 = \int D_b \left[\nu \{ \eta_{,x} \}^T \{ \xi_{,y} \} + \frac{1-\nu}{2} \{ \eta_{,y} \}^T \{ \xi_{,x} \} \right] dA$$

$$[K_u]_3 = - \int D_s \{ \xi \}^T \{ \phi_{,y} \} dA \quad [M_3] = \int \rho \frac{h^3}{12} \{ \xi \}^T \{ \xi \} dA$$

$$[K_{\theta_x}]_3 = \int D_b \left[\nu \{ \xi_{,y} \}^T \{ \eta_{,x} \} + \frac{1-\nu}{2} \{ \xi_{,x} \}^T \{ \eta_{,y} \} \right] dA ; \text{ and}$$

$$[K_{\theta_y}]_3 = \int D_b \left[\{ \xi_{,y} \}^T \{ \xi_{,y} \} + \frac{1-\nu}{2} \{ \xi_{,x} \}^T \{ \xi_{,x} \} \right] dA + \int D_s \{ \xi \}^T \{ \xi \} dA$$

Moment and shear forces can be expressed as:

$$M_x = -D_b \left(\frac{d\theta_x}{dx} + \nu \frac{d\theta_y}{dy} \right) \quad Q_x = \frac{dM_x}{dx} + \frac{dM_{xy}}{dy} + \frac{1}{12} \rho h^3 \frac{d^2\theta_x}{dt^2}$$

$$M_y = -D_b \left(\frac{d\theta_y}{dy} + \nu \frac{d\theta_x}{dx} \right) \quad Q_y = \frac{dM_y}{dy} + \frac{dM_{xy}}{dx} + \frac{1}{12} \rho h^3 \frac{d^2\theta_y}{dt^2} ; \text{ and}$$

$$M_{xy} = -D_b \frac{1-\nu}{2} \left(\frac{d\theta_x}{dy} + \frac{d\theta_y}{dx} \right)$$

5. FREE VIBRATION NUMERICAL RESULTS

In this section free vibration analysis of Timoshenko beam and Mindlin plate are conducted. The results are compared among various layered domain of influence and basis function. The comparison of the result with analytical solution (Blevins, 1986) and the percentage error can be seen in table 1 and 2.

Table 1: Non-dimensionalized frequencies of simply supported Timoshenko beam.

| Mode | Analytical solution | Finite Element Quadratic | Kriging | | |
|------|---------------------|--------------------------|-----------------------|-----------------------|-----------------------|
| | | | Quadratic | | Cubic |
| | | | 2 layers | 3 layers | 3 layers |
| 1 | 3.14159 | 3.14160 (0.00035) | 3.14155 (0.00127) | 3.14162 (0.00072) | 3.14161 (0.00056) |
| 2 | 6.28319 | 6.28319 (0.00014) | 6.28301 (0.00279) | 6.28314 (0.00068) | 6.28316 (0.00048) |
| 3 | 9.42478 | 9.42490 (0.00133) | 9.42426 (0.00548) | 9.42461 (0.00182) | 9.42463 (0.00160) |
| 4 | 12.56637 | 12.56703 (0.00521) | 12.56535 (0.00811) | 12.56589 (0.00383) | 12.56594 (0.00339) |
| 5 | 15.70796 | 15.71013 (0.01380) | 15.70650 (0.00932) | 15.70687 (0.0069) | 15.70698 (0.00625) |
| 6 | 18.84956 | 18.85515 (0.02967) | 18.84816 (0.00743) | 18.84734 (0.01177) | 18.84757 (0.01053) |
| 7 | 21.99115 | 22.00344 (0.05589) | 21.99099 (0.00700) | 21.98707 (0.01856) | 21.98748 (0.01668) |
| 8 | 25.13274 | 25.15684 (0.09590) | 25.13615 (0.01356) | 25.12592 (0.02716) | 25.12653 (0.02470) |
| 9 | 28.27433 | 28.31774 (0.15351) | 28.28503 (0.03784) | 28.26350 (0.03832) | 28.26454 (0.03463) |
| 10 | 31.41593 | 31.48907 (0.23283) | 31.43950 (0.07504) | 31.39971 (0.05163) | 31.40136 (0.04638) |

Note: Number in parenthesis shown percentage error compared with analytical solution.

Table 2: Non-dimensionalized frequencies of simply supported Mindlin plate.

| Mode | Analytical solution | Finite Element Quadratic | Kriging | | |
|------|---------------------|--------------------------|-----------------------|-----------------------|-----------------------|
| | | | Quadratic | | Cubic |
| | | | 2 layers | 3 layers | 3 layers |
| 1 | 19.73921 | 20.04758 (1.5622) | 19.73299 (0.0315) | 19.69406 (0.2287) | 19.69632 (0.2173) |
| 2 | 49.34802 | 50.13142 (1.5885) | 49.40224 (0.1099) | 49.27656 (0.1448) | 49.25566 (0.1872) |
| 3 | 49.34802 | 51.49832 (4.3574) | 49.47867 (0.2467) | 49.31202 (0.0730) | 49.25627 (0.1859) |
| 4 | 78.95684 | 83.68565 (5.9891) | 79.16984 (0.2698) | 78.67757 (0.3537) | 78.73953 (0.2752) |
| 5 | 98.69604 | 102.84713 (4.2059) | 99.14665 (0.4566) | 98.75784 (0.0626) | 98.58097 (0.1166) |
| 6 | 98.69604 | 103.35773 (4.7233) | 99.30485 (0.6168) | 98.91075 (0.2175) | 98.60412 (0.0931) |
| 7 | 128.30486 | 134.68374 (4.9717) | 128.74122 (0.3401) | 127.78995 (0.4013) | 127.94091 (0.2837) |

| Mode | Analytical solution | Finite Element | Kriging | | |
|------|---------------------|-----------------------|-----------------------|-----------------------|-----------------------|
| | | | Quadratic | Cubic | |
| | | | 2 layers | 3 layers | 3 layers |
| 8 | 128.30486 | 134.85498 (5.1051) | 129.21011 (0.7055) | 128.04041 (0.2061) | 127.96972 (0.2612) |
| 9 | 167.78327 | 177.39898 (5.7310) | 169.37883 (0.9510) | 168.32892 (0.3253) | 167.95488 (0.1023) |
| 10 | 167.78327 | 178.63902 (6.4701) | 169.81481 (1.2108) | 168.92496 (0.6805) | 168.08670 (0.1808) |

Note: Number in parenthesis shown percentage error compared with analytical solution.

Table 1 showed that while for one dimensional problem, the Kriging-based FEM with 2 and 3 layers perform better than standard FEM. For two dimensional problems, the Kriging-based FEM performs much better than the standard FEM.

6. FORCED VIBRATION NUMERICAL RESULTS

6.1 Timoshenko beam

Forced vibration of a simply supported Timoshenko beams subjected to moving load is tested here. The condition of loading and parameter of loading are as follows: $E = 2 \cdot 10^9 \text{ kg/m}^2$; $h/L = 1/100$; $L = 10 \text{ m}$; $b = 1 \text{ m}$; $M = 240 \text{ kg/m}$; no damping; load $P = 100 \text{ N}$ moving loads with $v = 10 \text{ m/s}$.

The results of the numerical analysis are compared with the analytical solution. The analytical solution to this problem is taken from (Chopra, 2001). The result shows a very accurate result compared to the analytical solution as shown in figure 2. In order to determine the accuracy, the error norm of displacement, moment and shear are calculated at peak for comparison. Error norm can be defined as the integration of error over the whole domain, so that it represents the average error over the whole domain. For thin beams, in order to eliminate the effect of shear locking, reduced integration is implemented in the analysis. The analysis for linear finite element and linear Kriging-based FEM with one layer shows exactly the same result, and it is of interest to be shown in the comparison. Table 3 shows comparison of quadratic FEM and Kriging-based FEM with quadratic and cubic basis function.

Table 3: Percentage error norm of displacement, moment, and shear (%) at $t = 1.105 \text{ s}$

| | FEM | Kriging | |
|--------------|-----------|-----------|----------|
| | Quadratic | Quadratic | Cubic |
| | | 2 layers | 3 layers |
| Displacement | 0.08600 | 0.07950 | 0.08630 |
| Moment | 0.80980 | 0.71930 | 0.64140 |
| Shear | 5.33040 | 5.10930 | 4.17830 |

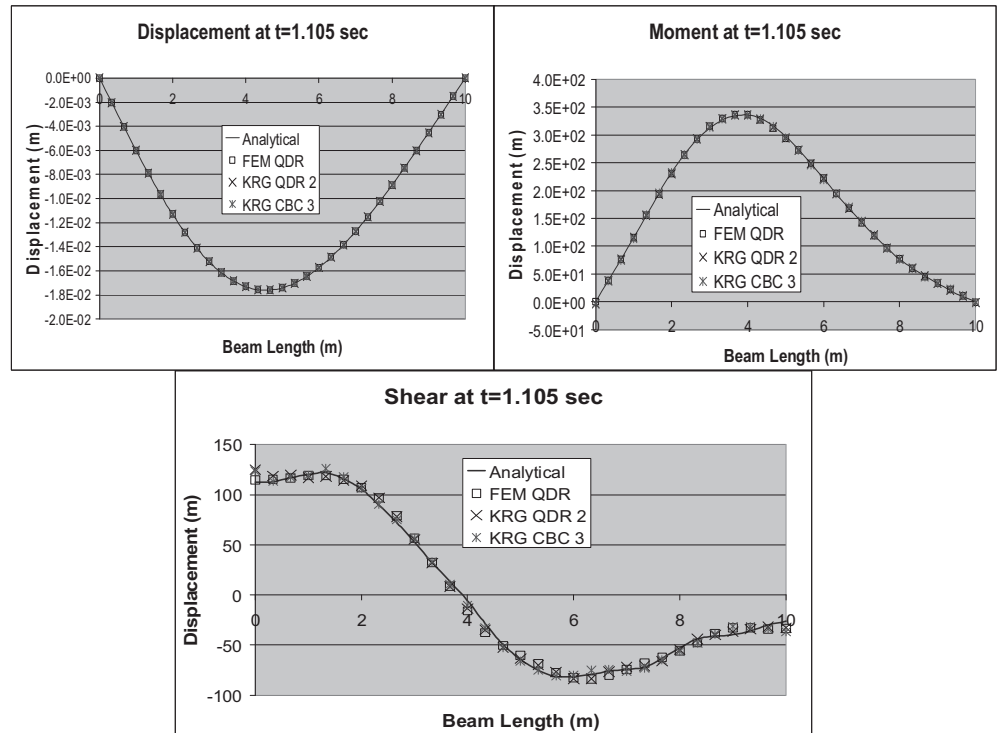


Figure 2: Displacement, Moment, and Shear at $t = 1.05$ sec.

Figure 2 and table 3 above shows that Kriging-based FEM is better than standard FEM especially in term of moment and shear distribution.

6.2 Mindlin plate

The first example problem that will be discussed is the forced vibration analysis of simply supported Mindlin plate subjected to point load at the center of the plate. The loading function and other parameter are defined as follows: $E = 2 \cdot 10^9$ kg/m²; $h = 0.1$ m; $L_x=L_y= 10$ m; $h/L = 1/100$ (thin plate); $M = 240$ kg/m²; no damping; analysis with rectangular element; the loading function triangular pulse force can be seen in figure 3.

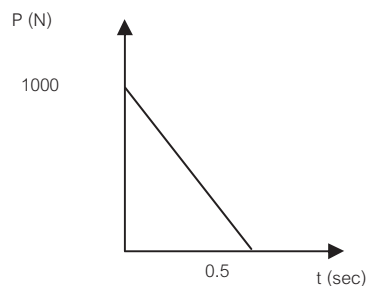


Figure 3: Loading Function

The results of the numerical analysis are compared with the analytical solution (Hinton, 1988). The result of the analysis can be seen in the following figures

Table 4: Percentage error norm of displacement, moment, and shear at $t = 1.55 \text{ sec. (\%)}$

| | FEM | Kriging (25x25 nodes) | | | |
|-----|-----------|-----------------------|----------|----------|----------|
| | Quadratic | Quadratic | | Cubic | |
| | | 2 layers | 3 layers | 3 layers | 4 layers |
| U | 3.0125 | 1.5271 | 0.5386 | 0.4646 | 0.5112 |
| Mx | 17.2050 | 9.0627 | 3.4090 | 2.4573 | 2.7893 |
| My | 17.2050 | 9.0627 | 3.4090 | 2.4573 | 2.7893 |
| Mxy | 8.8236 | 6.2478 | 2.3323 | 3.0538 | 3.0739 |
| Qx | 45.4880 | 23.0620 | 17.4470 | 10.0830 | 10.6410 |
| Qy | 45.4880 | 23.0620 | 17.4470 | 10.0830 | 10.6410 |

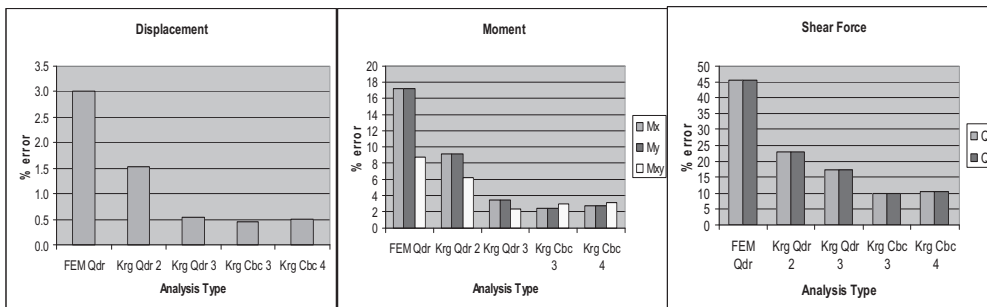


Figure 4: Percentage error norm of displacement, moment, and shear at $t = 1.55 \text{ sec.}$

Table 4 and figures 4 and 5 shown that Kriging-based FEM is more accurate than the standard FEM. Analysis with cubic basis function with three layers of domain of influence is the most accurate one.

The second example problem will discuss about attempts to eliminate shear locking in Kriging-based FEM for Mindlin plate problems. Two methods that will be implemented is the reduced integration method and hybrid plate formulations based on assume strain method (Kwon, 2000). Reduced integration is a well known method which can be simply implemented by using one gauss integration point to integrate the shear stiffness term. Assume strain methods, assumed the variation of the bending and shears strain (usually using polynomial term) within the element. The stiffness matrix for the hybrid plate formulation can be expressed as follows:

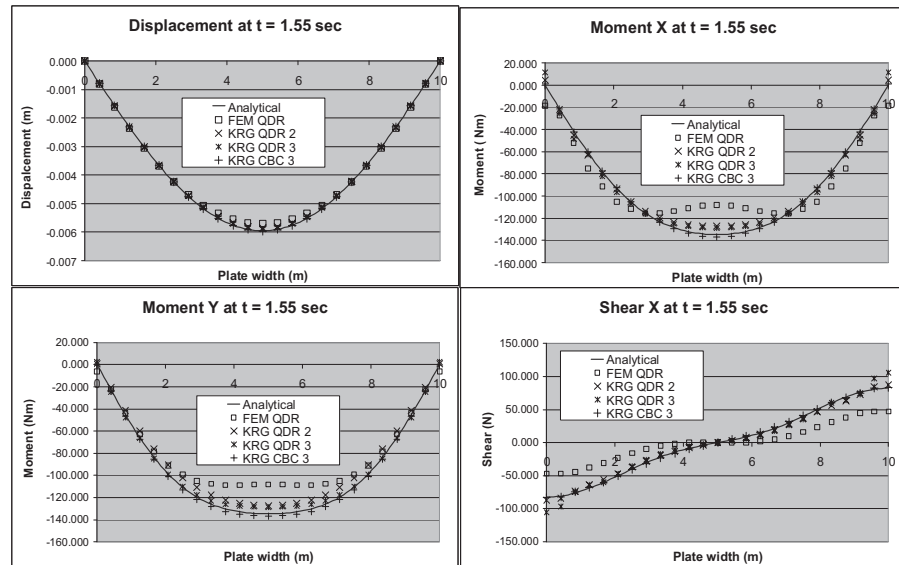


Figure 5: Displacement, moment and shear at middle section at $t=1.55$ sec

$$[K] = [H_b]^T [G_b]^{-T} [H_b] + [H_s]^T [G_s]^{-T} [H_s] \quad (15)$$

Where: $[G_b] = \int_{\Omega} [B_b]^T [D_b] [B_b] d\Omega$

$$[G_s] = \int_{\Omega} [B_s]^T [D_s] [B_s] d\Omega$$

$$[H_b] = \int_{\Omega} [B_b]^T [D_b] L_b [\phi] d\Omega$$

$$[H_s] = \int_{\Omega} [B_s]^T [D_s] L_s [\phi] d\Omega$$

$$L_b [\phi] = \begin{bmatrix} 0 & \frac{\partial \phi}{\partial x} & 0 \\ 0 & 0 & \frac{\partial \phi}{\partial y} \\ 0 & \frac{\partial \phi}{\partial y} & \frac{\partial \phi}{\partial x} \end{bmatrix}$$

$$L_s [\phi] = \begin{bmatrix} \frac{\partial \phi}{\partial x} & -\phi \\ \frac{\partial \phi}{\partial y} & -\phi \end{bmatrix}$$

$$[B_b] = \begin{bmatrix} 1 & 0 & 0 & x & 0 & 0 & y & 0 & 0 \\ 0 & 1 & 0 & 0 & x & 0 & 0 & y & 0 \\ 0 & 0 & 1 & 0 & 0 & x & 0 & 0 & y \end{bmatrix}$$

$$[B_s] = \begin{bmatrix} 1 & 0 \\ 0 & 1 \end{bmatrix}$$

The second example problem is a simply supported rectangular Mindlin plate with point load at center of plate. The loading function and other parameter are defined as follows: $E = 2 \cdot 10^9$ kg/m²; $h = 0.001$ m; $L_x = L_y = 10$ m; $h/L = 1/10000$ (thin plate); no damping; analysis with rectangular element; the loading function sine pulse force can be seen in figure 6.

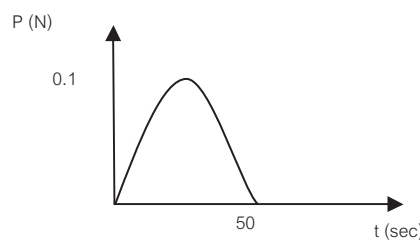


Figure 6: Loading Function

The results of the numerical analysis are compared with the analytical solution (Hinton, 1988). The results shows that without reduced integration or assume strain method, Mindlin plate exhibit shear locking, but both methods can eliminate shear locking for Mindlin plate for rectangular element. The center displacement time history is plotted in figure 7. Figure 7 shows that the analysis without reduced integration vibrates with different frequency (stiffer) compared to the analytical solution (these shows that it exhibit shear locking), while the analysis with reduced integration and assume strain are close to the analytical solution.

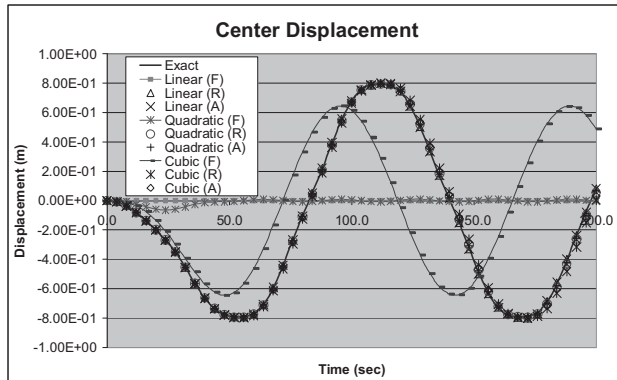


Figure 7: Displacement time histories.

Note: F = Full integration; R = Reduced integration; A = Assume strain

From figure 7, it is quite difficult to determine the most accurate method, since the result is very close to each other. In order to determine the most accurate method, the displacement, moment and shear error norm are calculated at a time step (in this case it is chosen to be at peak center displacement at $t = 54$ sec). The errors are plotted in figure 8.

Figure 8 shows that reduced integration and assume strain method are similar when used with linear basis function. But when higher basis function is implemented, assume strain is more accurate than reduced integration. It can be seen also that reduced integration and assume strain method is only accurate for low basis function, for higher basis function, it became less accurate.

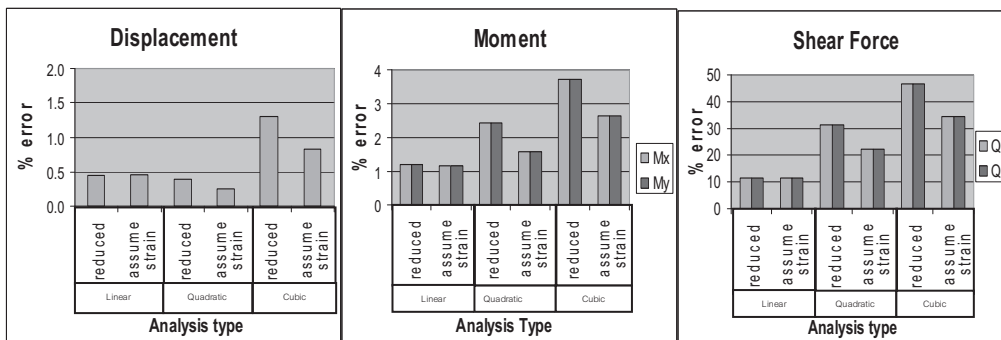


Figure 8: Error norm of displacement, moment and shear at $t = 5.4$ sec.

7. CONCLUSIONS

The use of Kriging-based FEM for dynamic analysis of beam and plate has been presented in the above result. The characteristic and the performance of the methods can be summarized as follows:

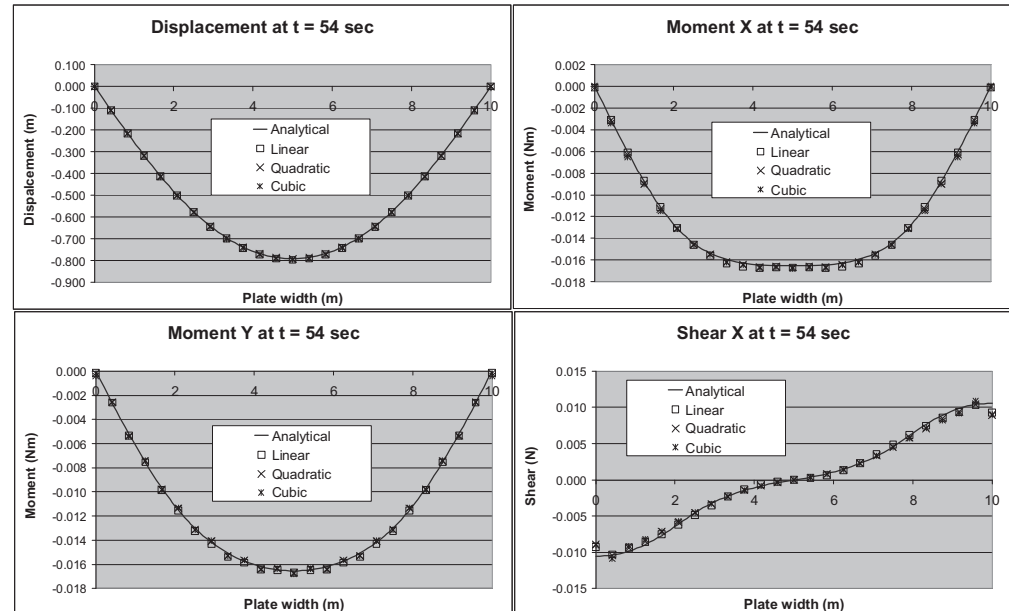


Figure 9: Displacement, moment and shear at middle section at $t = 5.4$ sec. (assume strain method)

1. For dynamic analysis that discussed above, Kriging-based FEM is more accurate than the standard FEM especially for two dimensional (Mindlin plate) problems. The accuracy of Kriging-based FEM can be improved by adopting high basis function and using one additional layer of domain of influence more than the minimum required. From the case analyzed above, it can be seen that cubic basis function with three layer of domain of influence can achieve the most accurate result.
2. High basis function can help reduce the effect of shear locking, but it can not completely eliminate shear locking. Reduced integration and assume strain method can completely eliminate shear locking for Mindlin plate with rectangular element, but both method is only accurate to be used with low basis function (linear and quadratic).

REFERENCES

- Tongsuk, P., and Kanok-Nukulchai, W., 2004, On the Parametric Refinement of Moving Kriging Interpolation for Element Free Galerkin Method, *Computational Mechanics*
- Tongsuk, P., and Kanok-Nukulchai, W., 2004, Further Investigation of Element Free Galerkin Method Using Moving Kriging Interpolation, *International Journal of Computational Methods*, Vol. 1, No. 2, pp. 345-366

- Plengkhom, K. and Kanok-Nukulchai, W., 2005, An Enhancement of Finite Element Method with Moving Kriging Shape Functions, *International Journal of Computational Methods*, Vol. 2, No. 4, pp. 451-475
- Blevins, Robert D., 1986, *Formulas for Natural Frequency and Mode Shape*, Robert E Krieger Publishing Company, Malabar, Florida
- Chopra, Anil K., 2001, *Dynamics of Structures Theory and Application to Earthquake Engineering*, second edition, Prentice-Hall
- Hinton, Ernest, 1988, *Numerical Methods and Software for Dynamic Analysis of Plates and Shells*, first edition, Pineridge Press Swansea U.K.
- Kwon, Young W, Bang, Hyochoong, 2000, *The Finite Element Method Using Matlab*, second edition, CRC Press LLC

ANALYZING THE DEMOGRAPHIC DETERMINANTS OF CRIME IN CHINA

JUN YAN, XUEMING SHU and HONGYONG YUAN
Department of Engineering Physics, Center for Public Safety Research,
Tsinghua University, Beijing, 100084, Peoples Republic of China
j-yan06@mails.tsinghua.edu.cn

ABSTRACT

China is a country with a large population, and population issues has brought some social problems. China's crime rate was gradually upward trend in continuous fluctuations. In the paper, it is to analyze the relationships between demographic determinants and crime in China. Time series data analysis is used, including unemployment rate, urbanization, total population, and the number of population migration. The study use the vector error correction model (VEC) to find the short-run factors that drive annual fluctuations and the long-run factors that determine the level of these crimes. The order of integration of the data was determined using the Augmented Dickey–Fuller (ADF) test. All the indicators were found to be I (1). This article used the JJ (Johansen-Juselius) procedure to test for cointegration. The results show the growth of total crime rate is positively influenced by growth in unemployment, urbanization and total population, and negatively by growth in migration between urban and rural areas in long-run, the level of significance is different.

Keywords: *Crime; Demographic determinants; Cointegration; Vector error correction model*

1. INTRODUCTION

China is a country with a large population. Total population reached 1.31 billion and continued growth with 16 million newborn every year. China has to face a series of social problems at the same time. The registered urban unemployment rate is 4.1 percent in rural areas by the end of 2006. Population migration is another prominent social phenomenon in china. Population migration has promoted the personal exchanges, so more farmers got the opportunity to work in cities and towns, and raised the level of urbanization in Chinese society. Statistical analysis showed the floating population crime has become a great threat to social order. According to statistics, the total crime rate increased from 55.65 cases per 100,000 inhabitants in 1978 to 354 cases per 100,000 inhabitants in 2006, 6.36 times increase, or an average annual growth of 10 percent above (Figure 1).

Researches on the relationship between crime and demographic determinants show the changes of demographic factors effect crime trend. Thirty years ago, Becker (1968), Stigler (1970), Ehrlich (1973), Thaler

(1977), Willis (1983) analyzed the relation of unemployment rate and crime. Most research showed that it is positive correlation between them. Avio and Clark (1976) analyzed that a large percentage of criminal acts by the ages of 15-34 years old male, the two are positively correlated. Fajnzylber, Lederman and Loayza (2002) reported that education level has a negative impact on crime.

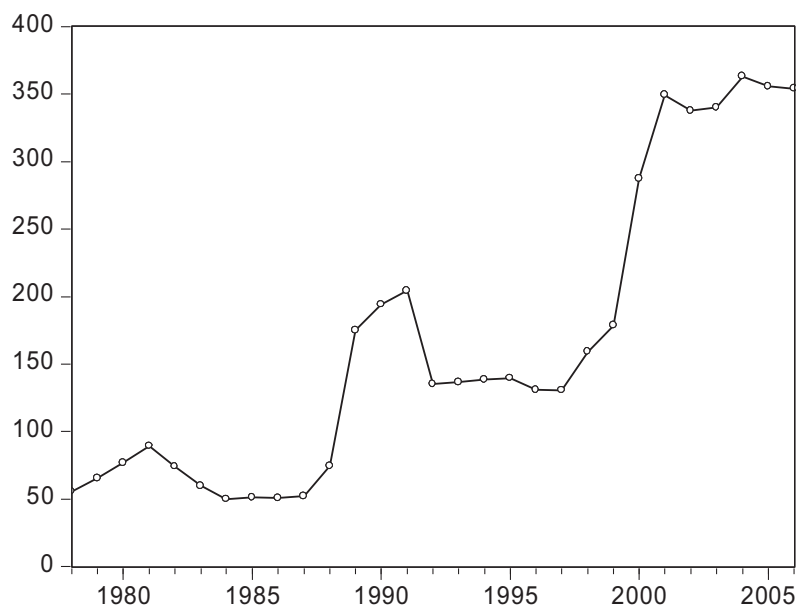


Figure 1: Total crime rate (1978-2006)

In China, Researchers paid attentions to the effect of socio-economic variables on crime. HU (2006) uses a linear regression model and the correlation analysis methods to discuss the impact of macroeconomic factors on crime. He pointed out gap between rich and poor, unemployment, urbanization, increased mobility of the population, the detection rate fell, which lead to China's fast-growing crime. ZHANG (2005) analyzed the social reason of the crime rate growth in the transformation society of china.

Different from previous studies, there are impact of one another between crime and determinants, and variables in the model are endogenous variables. So the vector auto regression (VAR) is used for analyzing the impacts between crime rate and socio-economic and demographic determinants. The rest of the paper is organized as follows. Section II presents the data and pretreatment. Section III introduces the method and the results from the VAR model. Concludes are given in section IV.

2. DATA AND PRETREATMENT

This article uses time series observations to study the demographic determinants of crime over the period between 1978 and 2006. Chinese Government is committed to increasing educational investment, and the people's quality is improved. The total population is used as the proxy for population level. The level of urbanization is measured as the percentage of

the population that lives in urban. The level of urbanization is used as the demographical indicator. Some study show that crime rate is higher in more urban areas, urbanization led to much people and wealth gathered in a small area, then provides an opportunity for crime. Floating population crime accounts for a large part in total crime. So the number of population migration is introduced into the dynamic model. Besides indicators discussed above, model also uses the unemployment rate as the endogenous variables in the model. Most observations used in the model were obtained from China statistical yearbook. The number of population migration for 1978-2006 was produced by the author's calculations, and data from China statistical yearbook. To reduce the impact of heteroscedasticity, all variables are expressed in logarithms (Figure 2). Figure 2 show the variables are strongly trended, the original series is obviously nonstationary.

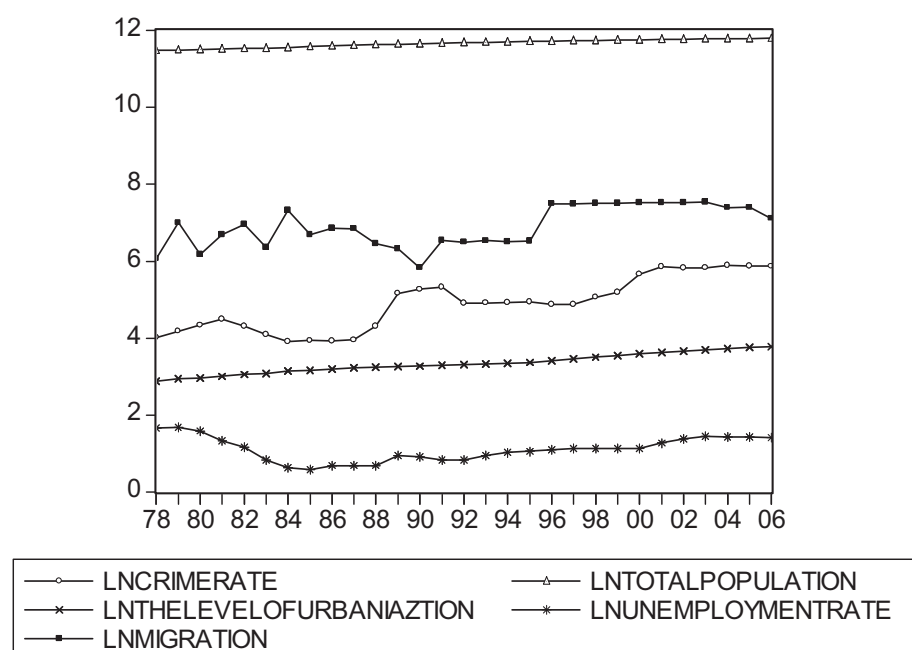


Figure 2: Recorded crime and demographic indicators (1978–2006)

The order of integration of the data was determined using the Augmented Dickey–Fuller (ADF) test, which confirm all the variables were found to be I(1) at the 5 percent significance level. The results of the ADF tests for stationarity are presented (Table 1).

Table 1: ADF test results

| Series | ADF Statistic | t- | Equations form | Prob. |
|--------------------------|---------------|----|---------------------|--------|
| level | | | | |
| lncrime | -1.153685 | | Intercept | 0.6790 |
| lnunemploymentrate | -0.817093 | | None | 0.3530 |
| lnenrolmentrate | -1.924082 | | Intercept and trend | 0.6145 |
| lnmigration | -2.759897 | | Intercept | 0.0770 |
| lnthelevelofurbanization | 1.424932 | | Intercept | 0.9984 |
| first differences | | | | |
| Δlncrime | -3.415591 | | Intercept | 0.0193 |

| Series | ADF t-Statistic | Equations form | Prob. |
|--|-----------------|---------------------|--------|
| $\Delta \ln \text{unemploymentrate}$ | -2.771196 | None | 0.0075 |
| $\Delta \ln \text{enrolmentrate}$ | -7.004600 | Intercept and trend | 0.0000 |
| $\Delta \ln \text{migration}$ | -9.703900 | Intercept | 0.0000 |
| $\Delta \ln \text{thelevelofurbanization}$ | -4.545262 | Intercept | 0.0013 |

3. MODEL

3.1 Cointegration

As discussed above, all time series observations used in the model are nonstationary, and are I (1). The relationship among the variables is possible spurious. Engle and Granger (1987) pointed out that if a stationary linear combination of two or more nonstationary series exists, the nonstationary time series are said to be cointegrated. Cointegrating equation may be interpreted as a long-run equilibrium relationship among the variables. In this article, Johansen method is used to test cointegration among time series. The level data crime rate and the cointegrating equations have linear trends, and lag of the first differenced terms is 1, a long-run equilibrium relationship between demographic determinants and crime is as follows:

$$\begin{aligned}
 \text{Incrimerate} = & 20.78 \ln \text{thelevelofurbanization} - 7.33 \ln \text{migration} \\
 & (4.34589) \qquad (0.69001) \\
 & [-4.78294] \qquad [10.6290] \\
 + & 22.4 \ln \text{totalpopulatioin} + 2.47 \ln \text{unemploymentrate} \\
 & (12.6514) \qquad (0.44394) \\
 & [-1.77099] \qquad [-5.56388] \\
 - & 0.51t - 269.93 + \varepsilon_t \\
 & (0.27878) \\
 & [-1.83781]
 \end{aligned} \tag{1}$$

where ε_t is a stationary series, stand errors and t-statistics are reported in parenthesis and square brackets respectively. Equation implies there is a long-run equilibrium relationship among five variables. Urbanization has a significant positive effect on crime. Its elasticity is equal to 20.78, which means an increase 1 percent of urbanization will heighten 20.78 percent of crime rate. The effect of population migration on crime has been the focus of controversy. Population migration and population floating are two different concepts. Registered permanent residence system is carried out in China. If the registered permanent residence changes, it is called population migration, instead, known as population floating. Higher education, move out for survival and development play an irreplaceable important role in population migration. The increased number of population migration reflects the more job and educational opportunities, so population migration becomes significantly positive for crime. Unemployment is found to be positive relationship with crime. But the unemployment data used in

model is obtained from national bureau of statistics, which refers to the urban unemployment rate, and is not a true reflection of actual levels, so model still underestimated the impact of unemployment on crime. Population has a positive effect, but the impact is weak.

3.2 Vector error correction model

In previous researches based on single equation analysis, crime was defined as endogenous variables, and other variables were exogenous. But criminology theory is not enough to provide a dynamic specification that identifies all of these relationships. In our model, crime and demographic indicators are interrelated, and variables may appear on both sides of equations. The vector auto regression (VAR) is commonly used for forecasting systems of interrelated time series, its mathematical representation is

$$y_t = \Gamma_1 y_{t-1} + \dots + \Gamma_p y_{t-p} + \varepsilon_t \tag{2}$$

where y_t is a k vector of endogenous variables, $\Gamma_1, \dots, \Gamma_p$ are matrices of coefficients to be estimated, and ε_t is a vector of innovations. For example, 2th order VAR (p) has model forms:

$$\begin{pmatrix} y_t \\ x_t \end{pmatrix} = \begin{pmatrix} \Gamma_{11,1} & \Gamma_{12,1} \\ \Gamma_{21,1} & \Gamma_{22,1} \end{pmatrix} \begin{pmatrix} y_{t-1} \\ x_{t-1} \end{pmatrix} + \begin{pmatrix} \Gamma_{11,2} & \Gamma_{12,2} \\ \Gamma_{21,2} & \Gamma_{22,2} \end{pmatrix} \begin{pmatrix} y_{t-2} \\ x_{t-2} \end{pmatrix} + \dots + \begin{pmatrix} \Gamma_{11,p} & \Gamma_{12,p} \\ \Gamma_{21,p} & \Gamma_{22,p} \end{pmatrix} \begin{pmatrix} y_{t-p} \\ x_{t-p} \end{pmatrix} + \begin{pmatrix} \varepsilon_{1t} \\ \varepsilon_{2t} \end{pmatrix} \tag{3}$$

The variables in our model are $I(1)$, and these series are cointegrated, so the vector error correction (VEC) is to be built. VEC model is restricted VAR, which cointegration relations is built into model. The cointegration term, *error correction term*, correct the deviation from long-run equilibrium through a series of partial short-run adjustments. By defining the first differences $\Delta y_t = y_t - y_{t-1}$, equations (2) can be written as the corresponding VEC model is:

$$\Delta y_t = B e c m_{t-1} + A_1 \Delta y_{t-1} + \dots + A_p \Delta y_{t-p} + u_t \tag{4}$$

where A_1, \dots, A_p are matrices of coefficients to be estimated, the first term on the right-hand side is the error-correction, can be got from cointegration equation. B is k vector of associated coefficient, which measure the speed of error correction, should always be negative. By OLS estimator, VEC model for crime and demographic indicators is obtained. The crime dynamic model is detailed (Table 2).

Table 2: Dynamic model for crime and demographic indicators

| |
|--|
| Vector Error Correction Estimates |
| Sample (adjusted): 1980 2006 |
| Included observations: 27 after adjustments |
| Standard errors in () & t-statistics in [] |
| |

| | | | |
|--|------------|----------------|-----------|
| $\Delta \ln \text{crime rate}_t = -0.09 \text{ecm} + 0.18 \Delta \ln \text{crime rate}_{t-1} + 25.5 \Delta \ln \text{the level of urbanization}_{t-1}$ | | | |
| | (0.05885) | (0.19930) | (12.3926) |
| | [-1.42284] | [0.93792] | [2.05863] |
| $- 0.3 \Delta \ln \text{migration}_{t-1} + 19.33 \Delta \ln \text{total population}_{t-1} \quad (5)$ | | | |
| | (0.12840) | (12.9819) | |
| | [-2.46244] | [1.48885] | |
| $+ 0.59 \Delta \ln \text{unemployment rate}_{t-1} - 0.97$ | | | |
| | (0.38642) | (0.51125) | |
| | [1.52730] | [-1.90852] | |
| R-squared | 0.397048 | Log likelihood | 8.238096 |
| Adj. R-squared | 0.216163 | Akaike AIC | -0.09171 |
| Sum sq. resids | 0.858757 | Schwarz SC | 0.244247 |
| S.E. equation | 0.207214 | Mean dependent | 0.062474 |
| F-statistic | 2.195027 | S.D. dependent | 0.234049 |

The model results show the short-run effect between crime and demographic indicators. The coefficient of error correction term is negative, which means the long-run mechanism has a restrain impact on short-run fluctuation, but t-statistics shows it is insignificant. Urbanization is significantly and positively correlated to crime rate. Urbanization has a significant positive impact on crime rate in long-run. Urbanization may lead to the concentration of population density and social wealth in local region, which heighten crime level. Population migration has a small and significantly negative effect for crimes, with a 1 percent point increase in the number of migration being associated with a 0.3 percent reduction in the short run and a 7.33 percent decline in the long run. As discuss above, population migration is due to accept higher education or move out for work mostly. Government should provide more learning and employment opportunities, which will play an important effect on reducing crime. The population growth rate shows a small and insignificant sign both in long-run and short-run. So it is incorrect to say the population growth brings crimes directly. Finally, unemployment is negatively correlated to total crime. Although it is insignificant, it is significant in long-run.

4. CONCLUSION

Quantitative study of crime is rare in China, and most literatures are based on the regression and correlation analysis. But China is in rapid development stage, all kinds of social-economic and demographic indicators and crime statistics data have shown fluctuation in growth trend. Most results from correlation analysis show the positive correlation between crime and other indicators. And the existence of multicollinearity, may result in wrong conclusions about relationships between independent and dependent variables. In this paper the VEC model is built based on the time series data over the period 1978-2006 in China, which focus on the short-run and long-run affections of demographic variables on total crime rate. Our crime model includes some indicators, which reflect population development in Chinese society. The results are shown as follows:

In China, crime rate has a gradually upward trend in continuous fluctuations. Crime trends and demographic factors keep the long-run equilibrium relationship.

China's level of urbanization continue to speed up the pace each year. The concentration of people and wealth has also provided opportunities for crime. Population migration provides more work and education opportunities for people. Crime dynamic equation show the growth of total crime rate is positively influenced by urbanization, and negatively by growth in migration between urban and rural areas significantly in long-run and short-run. And urbanization has a big effect for crimes in magnitude.

Many literatures pointed out that the unemployment rate is a determinant of crime. Our research also finds growth in unemployment appears to be positively and significantly correlated with the crime rate in long-run, but it is insignificant in short-run, and it is small in magnitude. Weaker effect is possible due to the narrow statistical scope of unemployed people.

Although total population has a positive effect on crime rate, it is insignificant both in long-run and short run. So it cannot simply say that population growth will lead to increased crime rate.

The negative coefficient of error correction term means the long-run mechanism has a restrain impact on short-run fluctuation, but t-statistics show it is insignificant.

ACKNOWLEDGEMENTS

I am grateful to Professor YUAN Hongyong and SHU Xueming for their support. The views expressed in this paper are entirely my own and do not represent the views and policies of the Chinese government.

REFERENCES

- Avio, K.L., Clark, C.S., 1976. Property crime in Canada: an econometric study. Canada.
- Becker, G., 1968. Crime and punishment: An economic approach. *Journal of Political Economy*, 76, 169–217.
- Ehrlich, I., 1973. Participation in illegitimate activities: A theoretical and empirical investigation. *Journal of Political Economy*, 81, 521-565.
- Engle, Robert F., and Granger, C. W. J., 1987. Co-integration and Error Correction: Representation, Estimation, and Testing. *Econometrica*, 55, 251–276.
- Fajnzylber, P., Lederman, D., and Loayza, N., 2002. What causes violent crime? *European Economic Review*, 46, 1323-1357.
- Hu Lianhe, Hu Angang, and Xu Shaogang., 2005. A Case Study of the Impact of the Disparity between the Rich and the Poor upon Criminal Offences (in chinese). *Management World*, 2, 34-44
- Stigler, G.J., 1970. The optimum enforcement of laws. *Journal of Political Economy*, 78, 526-536.
- Thaler, R., 1977. An econometric analysis of property crime. *Journal of*

Public Economics, 8, 323-38.

Willis, K.G., 1983, Spatial variations in crime in England and Wales: testing an economic model. *Regional Studies*, 17, 4, 261-72.

Zhang Xiaohu, 2002. The Discussion and Analysis on the Increase of Crime Rate during the Transition Era in View of Social Stratification. *Sociological Research*, 1, 91-106

THE COMPARISON AND SELECTION OF THE RISK ANALYSIS METHODOLOGIES ON THE WHOLE PROCESS OF DANGEROUS CHEMICAL ACCIDENT

CHAO ZHANG^{1,2}, DONGSHAN CAI¹ and YI LIU^{1,2}

1. Department of Engineering Physics Tsinghua University, China

2. Center for Public Safety Research, China

liuyi@tsinghua.edu.cn

ABSTRACT

The dangerous chemical accident, including fire, explosion and leakage incidents, should be paid sufficient attention because of its serious sequence such as human casualty, wealth loss, building damage, water pollution, traffic disruption, people evacuation and so on. The whole process of dangerous chemical refers more than ten factors, which makes its risk analysis complicated. Tens of methodologies have been developed to undertake a risk analysis on dangerous chemical, which includes index estimate methodologies, data analysis methodologies and sequent analysis methodologies. First, this paper develops a series of factors through researching hundreds cases, and then uses three methodologies to analyze the cases, and compare the results. Last, the conclusion is that, the methodology which refers to the dynamics of accident evolution and vulnerability analysis is the best for the risk analysis on the whole process of dangerous chemical accident.

1. INTRODUCTION

The dangerous chemical problem and their diversification have increased as far as the industrial development. Meanwhile, the complication of the modern city makes it possible that the serious damage made by the accidents. The hazard accident behaves as three models, fire, explosion, leakage of gas or liquid, all of them maybe lead to human casualty, wealth loss, building damage, water pollution, traffic disruption and people evacuation. For example, the hazard explosion happened in the Jilin Chemical Plant resulted in people panic and foreign argument except of the above consequence.

The whole process of dangerous chemical accident consists of the happening, development, direct consequence and derived consequence orderly, and many factors, which should be reduced to four classes as the inherent risk of the hazard, the circumstance condition nearby, the derived event factor and the emergency action, can impact the final sequent, complicating the risk analysis.

Scores of methods have been developed to analyze the risk of hazard(Tixier et al., 2002), which deal from three different points of view,

as the index estimation methodology, the case data analysis methodology and the sequent analysis methodology. Each of them includes several methods.

This paper develops a risk factor system firstly, through researching hundreds of cases which happened in China. And then, use one of the three different risk analysis methodologies separately and compare each result to explore the character and applicability. The conclusion is that, we should develop a methodology which based on the dynamics of accident evolvement and vulnerability analysis when we research the risk of the whole process on dangerous chemical.

2. ESTABLISHMENT OF THE RISK FACTOR SYSTEM

The whole process of the dangerous chemical accident consists of several parts orderly, such as the happening, development, evolvement, direct consequence and derived consequence, referring to tens of risk factors, which is summed up for class as inherent risk of the hazard, the circumstance nearby, the derived event factor and the emergency action. We should think of every risk factor if we want to obtain an effective risk analysis result.

The direct reason of the damage made by dangerous chemical accident is the release of the hazard. The impact factors of the energy amount released are the reserves, reactivity, flammability and the toxicity. The last three factors express the severity of the direct damage for the same quality. The four factors are induced into the hazard inherent risk.

The circumstance condition nearby includes the population density, the wealth density, the infrastructure effected (the plant of water, electricity, oil and gas) and the important protection effected (the place where people pay more attention to such as school, gymnasium). The population density and the wealth density impact the human casualty and the wealth loss directly. The infrastructure and the important protection contribute more than other things to the social attention.

The dangerous chemical accident may derive the secondary incidents such as fire, explode, leakage of poison, water pollution and traffic disruption. Therefore, the secondary event factor includes four factors, such as hazard neighborhood, water area function, water area scale and traffic condition.

The risk factor system is established after researching hundreds accident cases, and the structure is expressed by figure 1.

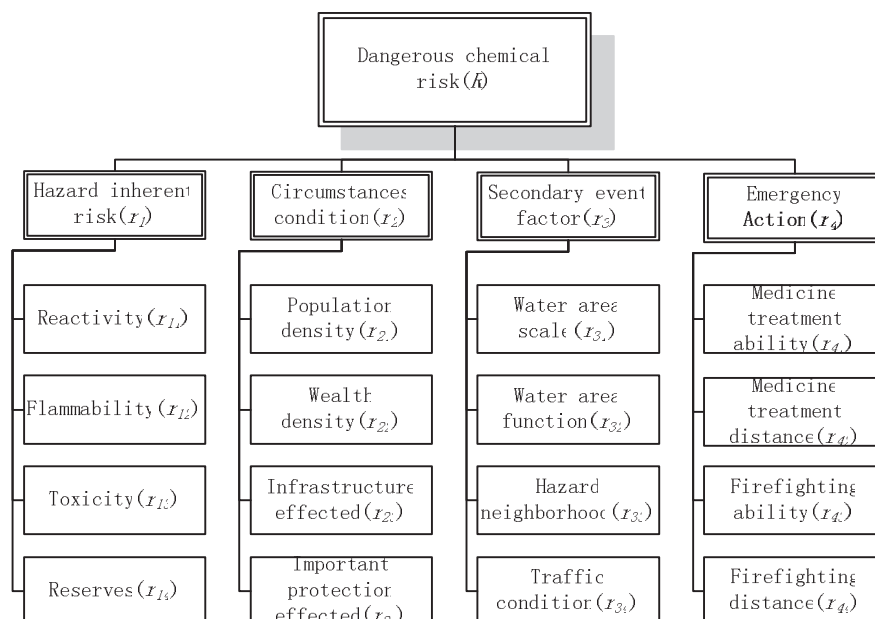


Figure 1: The risk factor system

3. THREE CLASSES OF METHODOLOGIES OF RISK ANALYSIS

Scores of methods have been developed to analyze the risk of hazard. They may be induced into three classes: the index estimation methodology, the case data analysis methodology and the sequent analysis methodology. Each of them includes several methods.

3.1 Index estimation methodology

The index estimation methodology obtains the risk result through the estimation of the risk factors. Each factor has a weight value and an estimation value. The first one expresses the importance of the factor and the second one express the severity with a given practical case. Both of the two kinds of value are quantified by experts with the help of their experience. The product of the weight and estimation expresses the severity of the practical case on the specified risk factor, and the summation of every product expresses the whole risk of the case.

The index estimation methodology is exercisable and easy to study. The one who know the risk factor system, the weight and the estimation criterion of the factors can manage the risk analysis work.

Otherwise, this methodology is more objective than the other two methodologies because of the weight and estimation criterion brought by the experts' experience. This one is carried out when we do not need an accurate risk result.

Some method of the index estimation methodology is enumerated as follows:

- Checklist (Khan and Abbasi, 1998)
- Hazard and Operability HAZOP(Kennedy and Kirwan, 1998)

- safety assessment of major flammable, explosive and toxic hazards(Zongzhi, 1998)
- AHP, the Analysis of Hierarchy Process(Saaty, 1994)
- Fuzzy Comprehensive Evacuation(Moselhi, 1995)

3.2 Case data analysis methodology

The case data analysis methodology obtains the risk result through the mathematical analysis of the practical cases data. All the risk factors are quantified according to the fact. And then the mathematical analysis is performed to investigate the weight of each fact. The estimation of the risk factor is given by the practical data too.

This kind of methodology is more objective than the index estimation methodology as all the data is either the actual one or the calculation result. But we must pay sufficient vigor to collect the practical cases' data. Even if we have obtained the risk analysis result, maybe we did not know the mechanism of the whole process and the relationship between each risk factor and the final result.

Some method of the data analysis methodology is enumerated as follows:

- Artificial Nerve Network(Ung et al., 2006)
- Genetic Algorithms(Varetto, 1998)
- Time Serial Analysis(Wing et al., 2004)
- Rough Set(Pawlak, 2000)
- Bayes Theory(Zellner, 2007)
- Grey Relationship Analysis(Cheng and Wang, 2004)

3.3 Sequent analysis methodology

The sequent analysis methodology obtains the risk result through the simulation of the incident development with the help of the physics formula such as the leakage, diffusion, fire, explosion and poisoning simulation. We can obtain the physic parameter such as the temperature, overpressure, thermal radiation and the poison density of gas or liquid density.

The sequent analysis methodology calculate accurate physic parameter if we have the entire condition parameter s.

Some method of the sequent analysis methodology is enumerated as follows:

- Leakage simulation
- Diffusion simulation
- Fire simulation
- Explosion simulation
- Poisoning simulation

4. THE APPLICATION CASE OF EVERY METHODOLOGY

Three cases are enumerated as the applied example to illuminate the specialty of different methodologies.

4.1 The AHP method of the index estimation methodology(C. Zhang)

First, we collect hundreds of hazardous cases and select 34 of them. Then, the AHP method is used to calculate the total risk.

The criterion system is as Table 1, the weight system is as Table 2, The accident rank by government and risk rank by this study is as Table 3, and the figure presents the final result.

Table 1: The criterion system of the AHP method.

| Level-1 | Level-2 | Level-3 | Comments |
|----------------------------------|-----------------------------------|-------------------------------------|--|
| Inherent risk (r_1) | Category (r_{11}) | Explosion possibility (r_{111}) | High, Medium, Low |
| | | Causticity (r_{112}) | High, Medium, Low |
| | | Toxicity (r_{113}) | High, Medium, Low |
| | Reserves (r_{12}) | | Large size |
| | | | Medium size |
| | | | Small size |
| Accident derivation (r_2) | Water area pollution (r_{21}) | | Mainstream |
| | | | Branch |
| | | | Brooklet |
| | Traffic break (r_{22}) | | Expressway |
| | | | Highway |
| | | | Road |
| Circumjacent condition (r_3) | Economy (r_{31}) | | Shopping centre |
| | | | Industrial park |
| | | | Residential area |
| | | | Village |
| | Population (r_{32}) | | Shopping centre & Industrial park |
| | | | Residential area & Schools |
| Emergency rescue (r_4) | Medical treatment (r_{41}) | | High-level, Medium-level, Normal level |
| | Fire fighting team (r_{42}) | | High-level, Medium-level, Normal level |

Table 2: Weights of criterion system

| $W_1: 0.6205$ | | | $W_2: 0.0569$ | | | $W_3: 0.3226$ | | $W_4: 0.1813$ | |
|-------------------|-------------------|-------------------|------------------|------------------|------------------|------------------|------------------|------------------|------------------|
| $W_{11}: 0.4137$ | | | $W_{12}: 0.2068$ | $W_{21}: 0.0474$ | $W_{22}: 0.0095$ | $W_{31}: 0.0538$ | $W_{32}: 0.2688$ | $W_{41}: 0.0604$ | $W_{42}: 0.1209$ |
| $W_{111}: 0.2356$ | $W_{112}: 0.0403$ | $W_{113}: 0.1378$ | | | | | | | |

Table 3: The accident rank by government and risk rank by this study

| Accident rank (by government) | I | II | III | IV |
|--------------------------------------|-----------|----------|--------|-----------|
| Representative Color (by government) | red | orange | yellow | blue |
| Risk rank (this study) | I | II & III | | IV |
| Risk value (this study) | ≥ 50 | 35~50 | | ≤ 35 |

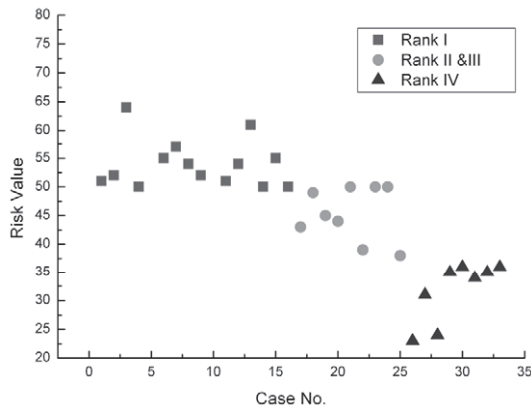


Figure 2: The total risk by the AHP method

4.2 The AHP combines with GRA method of the case data analysis methodology

The whole process of the hazard accident is complicated, and more the ten risk factors should be referred to. Therefore, sixteen factors are selected to obtain the risk through thirteen cases. The risk factor system is presented in figure 1 and Table 4 shows the scores (0 to 100) which are transformed from the actual data as the compare sequence. The main damage brought by the accident, including human casualty and wealth loss, is converted into one factor, the damage index as the reference sequence (represented by letter *t*).

| | 1 | 2 | 3 | 4 | 5 | 6 | 7 | 8 | 9 | 10 | 11 | 12 | 13 |
|----------|-----|-----|-----|-----|-----|-----|-----|-----|----|-----|-----|-----|-----|
| r_{11} | 0 | 100 | 0 | 0 | 0 | 50 | 75 | 0 | 75 | 0 | 0 | 0 | 50 |
| r_{12} | 0 | 100 | 75 | 100 | 75 | 100 | 100 | 0 | 0 | 100 | 0 | 0 | 100 |
| r_{13} | 100 | 0 | 25 | 50 | 50 | 50 | 75 | 100 | 75 | 75 | 75 | 100 | 100 |
| r_{14} | 24 | 20 | 37 | 100 | 15 | 1 | 18 | 10 | 5 | 1 | 2 | 20 | 5 |
| r_{21} | 100 | 16 | 65 | 30 | 4 | 29 | 31 | 31 | 24 | 13 | 7 | 23 | 7 |
| r_{22} | 100 | 3 | 6 | 10 | 1 | 9 | 3 | 6 | 55 | 1 | 2 | 11 | 3 |
| r_{23} | 0 | 0 | 100 | 25 | 0 | 0 | 0 | 0 | 0 | 0 | 0 | 0 | 0 |
| r_{24} | 100 | 25 | 50 | 50 | 25 | 25 | 0 | 75 | 0 | 0 | 0 | 0 | 50 |
| r_{31} | 100 | 0 | 0 | 0 | 0 | 50 | 0 | 0 | 75 | 25 | 50 | 25 | 100 |
| r_{32} | 100 | 0 | 0 | 0 | 0 | 25 | 0 | 0 | 75 | 100 | 100 | 100 | 100 |
| r_{33} | 25 | 0 | 100 | 75 | 0 | 0 | 0 | 0 | 13 | 0 | 0 | 0 | 13 |
| r_{34} | 75 | 25 | 25 | 100 | 100 | 25 | 75 | 50 | 25 | 100 | 75 | 100 | 50 |
| r_{41} | 25 | 50 | 100 | 25 | 25 | 75 | 50 | 75 | 50 | 50 | 75 | 50 | 75 |
| r_{42} | 2 | 99 | 1 | 11 | 4 | 28 | 5 | 5 | 55 | 100 | 20 | 60 | 20 |
| r_{43} | 25 | 75 | 25 | 25 | 100 | 50 | 50 | 75 | 50 | 75 | 75 | 75 | 75 |
| r_{44} | 34 | 49 | 100 | 18 | 24 | 15 | 6 | 5 | 75 | 99 | 62 | 59 | 20 |
| <i>t</i> | 768 | 100 | 3 | 36 | 152 | 377 | 24 | 23 | 11 | 119 | 42 | 176 | 20 |

We use the method which combines the Analytic Hierarchy Process (AHP) and the Grey Relationship Analysis (GRA). First, the GRA is used to get the grey relationship value between the risk factor and the damage index directly as the reference of the risk factors' weight used in AHP. But neither the AHP nor the revised-AHP can't calculate the eigenvalue of the compare matrix and give the weight of the risk factors. We have no choice but to

regard the grey relationship value as the weight. The result is presented by Figure 3.

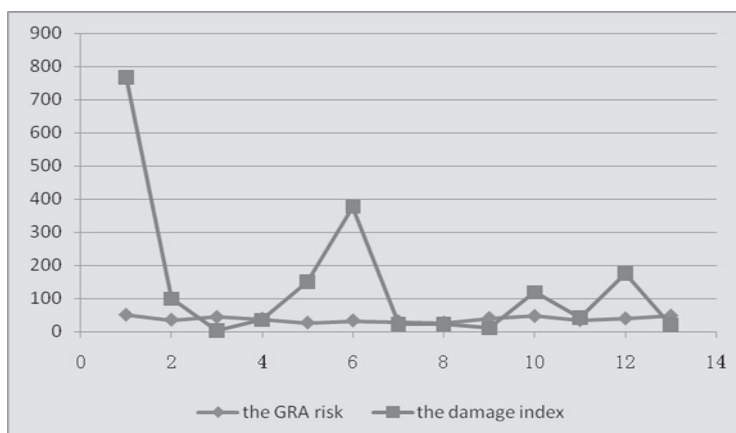


Figure 3: The GRA method result

4.3 The gas leakage simulation of the sequent analysis methodology

The dangerous chemical accident behaves in three forms: fire, explode and leakage. The research about the three incidents is mature and several software has been developed to simulate these accidents. The ALOHA serious software of America is one of the outstanding simulation tool. An appointed leakage case is presented in figure 4(ADMINISTRATION, 2007).

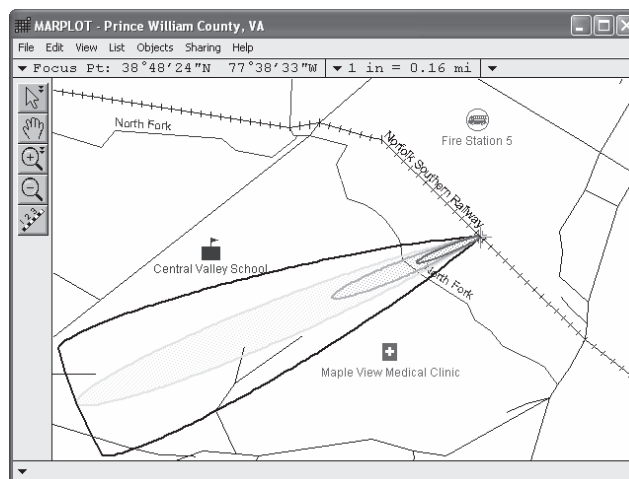


Figure 4: the leakage simulation by ALOHA

5. CONCLUSION

5.1 The selection and comparison of different methodologies

| | Advantage | Disadvantage | Applicability |
|-----------------------------|--------------------------------|--|--|
| The index estimation | Easy to learn Easy to apply | Base on the experts' experience More subjective | Do not need Accurate result Qualitative assessment or risk rank |

| | | | |
|-------------------------------|---|--|---|
| The case data analysis | Base on the actual data More objective | Math knowledge Loss of cases | Conditional enough cases Quantitative assessment |
| The sequent analysis | Mutual technique Accurate dose profile | Less risk factor Hard to refer secondary incident | Main object is the sequent physical parameter |

5.2 A new methodology for the whole process of hazard

As a researcher we should explore every part of the whole process and recognize the principle for each node of the Risk Chain (Figure 5). The Risk Chain is the frame presenting the main sub-course of the hazard accident and including almost every important risk factor.

There are two key techniques of this method, the sequent simulation and the vulnerability analysis. The first one is not difficult because of the mutual research in existence. To solve the second question we can use several methods such as the Probit Function, the Toxic Load and so on(HSE, 2008).

The dynamics of accident evolvment and vulnerability analysis are the main technique of the Risk Chain frame. With the help of some other techniques such as Trigger Condition Analysis and the Risk Classification Model, it's possible to get an accurate result of the whole process on dangerous chemical.

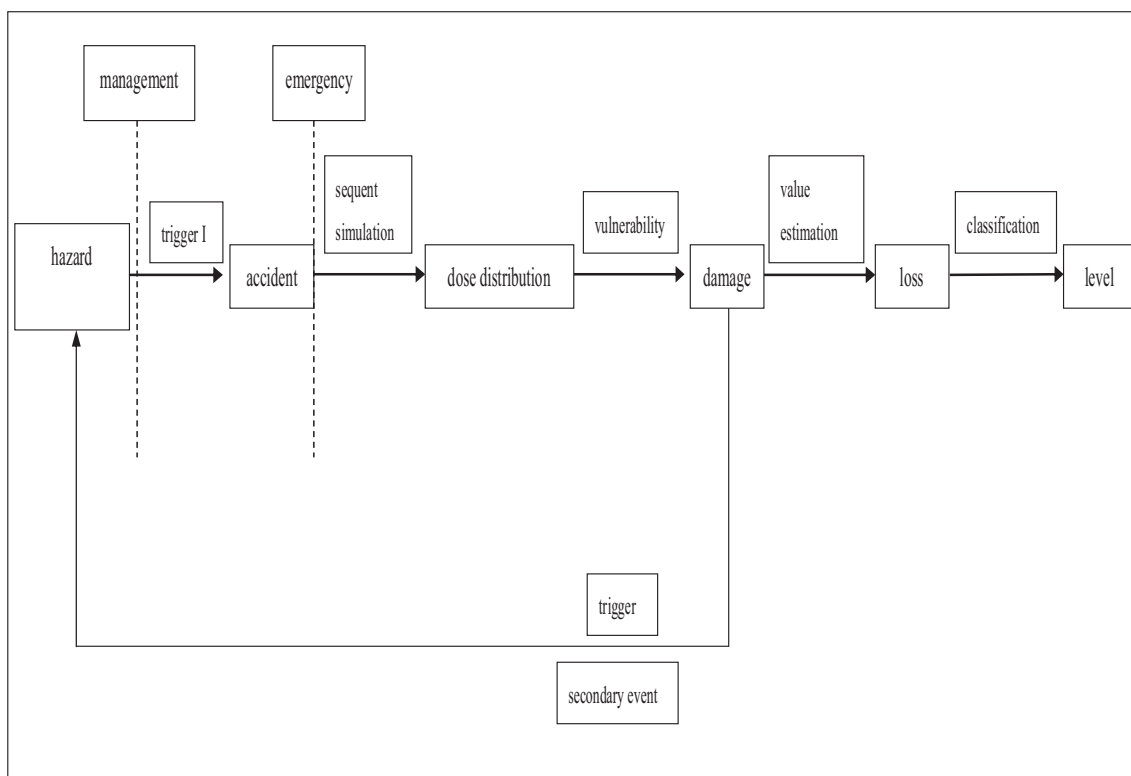


Figure 5: The Risk Chain

REFERENCES

- ADMINISTRATION, U. S. E. P. A. N. O. A. A., 2007, ALOHA USER'S MANUAL.
- C. Zhang, Y. L., S.F. Shen, A New Method on Risk Assessment of Dangerous Chemicals, *Proceedings of the 2nd International ISCRAM CHINA Workshop*.
- Cheng, S. P., and R. Y. Wang, 2004, Analyzing hazard potential of typhoon damage by applying grey analytic hierarchy process, *Natural Hazards*, **33**, 77-103.
- HSE, O. s. o., 2008, Indicative Human Vulnerability to the Hazardous Agents Present Offshore for Application in Risk Assessment of Major Accidents.
- Kennedy, R., and B. Kirwan, 1998, Development of a hazard and operability-based method for identifying safety management vulnerabilities in high risk systems, *Safety Science*, **30**, 249-274.
- Khan, F. I., and S. A. Abbasi, 1998, Techniques and methodologies for risk analysis in chemical process industries, *Journal of Loss Prevention in the Process Industries*, **11**, 261-277.
- Moselhi, O., 1995, Pricing Construction Risk - Fuzzy Set Application, *Journal of Construction Engineering and Management-Asce*, **121**, 163-164.
- Pawlak, Z., 2000, Rough sets and decision analysis, *Infor*, **38**, 132-144.
- Saaty, T. L., 1994, Fundamentals of Decision Making and Priority Theory with the Analytic Hierarchy Process, *RWS Publications, Pittsburgh, PA*, 1-527.
- Tixier, J., G. Dusserre, O. Salvi, and D. Gaston, 2002, Review of 62 risk analysis methodologies of industrial plants, *Journal of Loss Prevention in the Process Industries*, **15**, 291-303.
- Ung, S. T., V. Williams, S. Bonsall, and J. Wang, 2006, Test case based risk predictions using artificial neural network, *Journal of Safety Research*, **37**, 245-260.
- Varetto, F., 1998, Genetic algorithms applications in the analysis of insolvency risk, *Journal of Banking & Finance*, **22**, 1421-1439.
- Wing, A., A. Daffertshofer, and J. Pressing, 2004, Multiple time scales in serial production of force: A tutorial on power spectral analysis of motor variability, *Human Movement Science*, **23**, 569-590.
- Zellner, A., 2007, Generalizing the standard product rule of probability theory and Bayes's Theorem, *Journal of Econometrics*, **138**, 14-23.
- Zongzhi, W., 1998, Safety Assessment and Control of Major Flammable, Explosive and Toxic Hazards, *China Safety Science Journal*, **8**, 5.

REDUCIBILITY OF SEISMIC AND POST-EARTHQUAKE URBAN FIRE HAZARD IN DENSELY INHABITED DISTRICTS BY SIMULTANEOUS SEISMIC & FIRE-RESISTIVE REINFORCEMENT OF LOW-RISE WOODEN BUILDINGS

YUKO KAWAGOE, YUJI HASEMI, M.MURAKAMI,
N.KAWAI, M.YAMADA, N.YASUI,
T.SAKATA, S.KOBATA, and H.KAMIYA,
Waseda University, Tokyo, Japan,
Yuko.kawagoe@akane.waseda.jp

ABSTRACT

Densely inhabited districts (DIDs) with decrepit wooden buildings generated during the industrialization and recovery from the War in Japan are considered today as a nest of significant seismic hazard aggravated by subsequent urban fire. This paper presents an outline of the R & D project to develop retrofit technology to improve seismic and fire-safety performance of existing low rise buildings. The project includes (1) tests of seismic and post-shake fire safety performance of load-bearing walls with proposed reinforcement, (2) feasibility design study of retrofitting existing houses with the proposed method, and (3) quantification of its effectiveness for regional safety through urban fire simulations. The seismic and fire tests were conducted on specimens of wood-frame walls and have revealed capability of simple reinforcement with conventional products to achieve reasonable seismic and fire safety performance. The design studies for retrofitting existing wooden houses suggest possibility to achieve post-shake fire safety ensuring prevention not only of catching fire from adjacent or urban fires but of spreading fire to adjacent buildings with increase of cost not higher than 40% of the single seismic reinforcement. Moreover, the study suggests capability of the proposal method not disturbing the life in the house during the renovation process. The urban fire simulations suggest the equivalency of the proposed method applied to 30% of whole old houses with the single seismic reinforcement on 70% of total houses.

1. INTRODUCTION

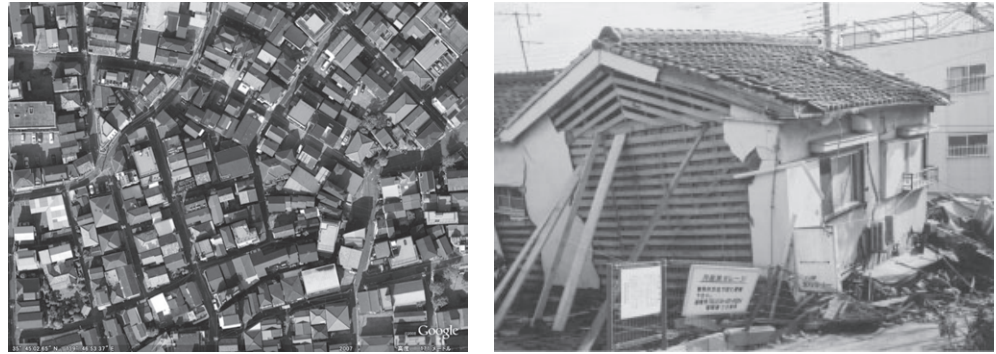
There is general belief that 80km² in total of densely inhabited districts (DIDs) with low-rise wooden buildings in Japan faces potential significant hazard aggravated by urban fire at the event of an earthquake. Most of such districts were generated through the industrial development and the reconstruction of war-ravaged urban areas, and feature dense inhabitation of low rise wood based low-rise buildings with weak protection against

earthquake or fires. After over around half century since their formation, the buildings are generally decrepit, and hollowing-out of local community in such districts can be easily seen; significant decrease of young generations and increase of empty houses are typical such signs. The government recognizes its resolution as an urgent policy issue.

Improvement of regional safety and livability of DIDs has been long based on the overall replacement by high-rise fire resistive buildings, but there is general difficulty for this approach to resolve this problem within reasonable time span because of the necessity of the agreement of all present inhabitants for the redevelopment and the achievement of the feasibility of the project and so on. On the other hand, numbers of local authorities have begun support for the retrofit of existing low-rise housings for the reduction of life hazard due to earthquake. However, anti-seismic reinforcement of wooden houses in DIDs without improvement of fire safety may result in the augmentation of the risk and hazard of post-earthquake fires that could cause fatal damage as widely recognized from the experiences at the Great Kanto Earthquake (1923) and Fukui Earthquake (1948). The Great Hanshin Earthquake (1995) caused over 200 earthquake fires but still got rid of significant conflagrations only because of weak wind. Through experiences with urban earthquakes, it is recognized that fire spread in DIS becomes more significant if wooden houses without fire protection survive from total collapse by earthquake.

This paper presents an outline of the R & D project to develop retrofit technology to improve seismic and fire-safety performance of existing low rise buildings simultaneously. Since the significance of the risk and hazard of conflagrations in a DID is attributed to the fast collapse of the structures of wooden houses resulting in generation of fierce flames and fire brands causing fast ignition on leeward buildings, the project has targeted to develop retrofit technology to make the load-bearing assemblies maintain the mechanical fire safety performance after an earthquake. Common low rise buildings in DIDs are required to have fire protection of external walls against external fires, but the past earthquake disasters have raised significant question to the survivability of such protection from earthquake. Moreover, the risk of conflagration in DIDs is essentially attributed to the survivability of load-bearing assemblies to internal fires is essentially questionable.

The basic idea for the development is to apply fire-rated panel products not to cause out-plane deformation as seismic reinforcement of existing post and beam frames. This could reduce the risk of collapse of the building both at the event of a significant earthquake and at internal or external fires. For this purpose, following studies were conducted. (Assembly level) Shear tests and post-shear fire tests of wall assemblies (Building level) Feasibility study of the application to buildings (District level) Study of the reducibility of conflagrations by the proposed technology



The assembly level studies focus development of seismic reinforcement method that enables to maintain and, if necessary, improve fire resistance required for urban buildings after earthquake. For this purpose, along with seismic and post-shake burn tests of load bearing walls, sustainability of the load bearing walls until the end of a fire was studied to reduce the risk of the collapse of whole structure and spreading fire to surrounding buildings. The building level studies are essentially development of anti-seismic design method of whole building structure to make it possible to maintain the fire safety performance of assemblies supporting vertical load and feasibility study from market acceptability point of view. The district level studies focus the hazard assessment of post-earthquake urban fires. Analysis is made to clarify relation between the strategy and the investment and the post-earthquake fire hazard through parametric studies by numerical simulations of urban fire spread. The contents of the project cover wide range of studies, and this report intends to provide an outline of the research and its outcome.

2. SEISMIC AND POST-EARTHQUAKE FIRE PROTECTIVE PERFORMANCE OF LOAD-BEARING WALLS

Seismic damage to the fire safety performance of building arises generally from the out-of-plane deformation of walls. Such deformation may also cause collapse of the whole structure of wooden buildings. In order to prevent out-of-plane deformation of the cover panel due to seismic effect, gypsum-based panel materials are chosen for the covering. Two designs for external walls and five designs for internal walls are chosen as the specimens. After small scale furnace screening tests, the following tests were conducted on the retrofit designs, namely 5 internal walls and 2 external walls (Table.1) to examine the seismic and post-earthquake fire safety performance of the retrofitted wall panel construction.

- (1) In-plane shear tests
- (2) Fire resistance tests on wall specimens after the shear tests
- (3) Both-sides fire tests of wall assembly with simulated seismic cracks

The specimens include not only newly developed products but conventional gypsum-based panels. It is for the interest in developing such technology in the range of the “grass-root technology”, available throughout the country.



Photo.3 Horizontal test Photo.4 Loaded fire test Photo.5 Both-sides fire test

Both-sides fire tests were conducted on three designs of internal walls, anticipating possibility that fire spread in a dwelling will result in making both sides of internal bearing walls exposed to fire heating. Mechanical fire protective performance of internal load-bearing walls under both-sides heating was examined to seek the capability of wooden houses to prevent collapse and subsequent enormous flaming.

2.1 Test Methods

2.1.1 The horizontal (shear) loading test

Shear tests were conducted to quantify the seismic performance of various design to retrofit load-bearing walls. Two levels of maximum deformation angles were chosen: $1/60\text{rad}$ corresponding to the maximum load [P_{max}] of bearing wall and $1/30\text{rad}$ corresponding to the ultimate load [$P_u=0.8P_{\text{max}}$]. The wall-fulfilment ratio, ultimate load-bearing capacity and other seismic performance indices were obtained. The distortion angle of each specimen was returned to ± 0 radian before the loaded fire resistance test to ensure vertical loading during the fire tests.

2.1.2 The loaded fire resistance test

Furnace temperature was controlled according to the ISO834 Standard Time-Temperature curve. The tests were continued until any clear sign for either fire penetration or collapse of the specimen came out. As a rule, the loading level was determined to 17kN, twice as heavy as the average stress of posts on the first story of two story common wooden buildings. Temperature, axial contraction and deformation of the pillar to the wall surface were measured. The fire protective performance of the specimens was assessed according to the maximum temperatures of back surface (MTB), the maximum axial contraction (MAC) and the maximum rate of axial contraction (MRAC). 30 minutes tolerance was intended because there is wide consensus that burning of live fire load in dwelling would not last over 30 minutes and most of fire regulations for detached houses require 30 minutes fire resistance or shorter.

2.1.3 Both-sides Fire Exposure Tests

Since wall furnaces are not suitable for such tests, a column furnace and wall specimens with narrower width to match the column furnace size were used. Because of the general difficulty to give horizontal loading to such specimen, the seismic damage was simulated by artificial gaps along the joints of the protection layer. Heating was continued until any acceleration of deformation starts on the specimen. The tests were not conducted on the external walls because the external walls are considered as fire separation, and both-sides heating never occur as long as the wall is not penetrated.

2.2 Test results

Summary of the test results are shown in Table 1. All the newly developed external walls and internal walls show reasonable seismic and post-shear fire protective performance, but it is noteworthy that reinforced gypsum board, typical conventional product easily found in market, achieved also comparable performance. The mechanical fire safety performance for both-sides heating are rather higher than the single-side heating, it is because of the symmetrical spread of charring of columns at both-sides heating preventing bending moment in the columns.

Table.1 Test result

| | | deformation angle(rad) | wall-fulfillment ratio | MAC (mm) | MRAC (mm/min) | MTB (°C) | fire- and quake-proof performance (min) | |
|---|--|------------------------|------------------------|----------|---------------|----------|---|----------------------|
| | | | | | | | Loaded fire test | Both-sides fire test |
| inside of outer wall & partition wall | Plaster Boad GB-R (12.5mm) | 1/30 | - | 12 | 5.5 | 228 | 42.25 | 41.0 |
| | | 1/60 | 1.2 | 5 | 0.4 | 222 | 35.25 | |
| | Load-bearing Plaster Board (12.5mm) | 1/30 | - | 4 | 0.5 | 317 | 50.75 | 41.5 |
| | | 1/60 | 2.2 | 2 | 0.2 | 277 | 47.00 | |
| | Plywood (4mm) + Plaster Boad GB-R (12.5mm) | 1/30 | - | 4 | 0.7 | 275 | 28.25 | - |
| | | 1/60 | 1.5 | 1 | 0.2 | 328 | 26.75 | |
| Nonwoven grass fabric Plaster Boad (12.5mm) | 1/30 | - | 12 | 4.6 | 158 | 57.00 | 48.0 | |
| | 1/60 | 2.2 | 4 | 0.5 | 284 | 36.50 | | |
| Cellulose fabric Plaster Boad (12.7mm) | 1/30 | - | 11 | 5.8 | 106 | 46.00 | - | |
| | 1/60 | 3.0 | 13 | 3.5 | 112 | 57.00 | | |
| outer wall | Steel sandwich panel wall (35mm) | 1/30 | - | 4 | 0.4 | 308 | 56.00 | - |
| | ※back side : Plaster Boad GB-R (12.5mm) | 1/60 | 3.6 | 2 | 0.2 | 259 | 55.50 | - |
| | Ceramics Siding Board (24mm) | 1/30 | - | 36 | 19 | 246 | 73.25 | - |
| | ※back side : Plaster Boad GB-R (12.5mm) | 1/60 | 3.3 | 4 | 0.3 | 381 | 55.00 | - |

3. FEASIBILITY STUDY OF RETROFITTING WHOLE BUILDING

In order to study the reality of the research ideas from architectural design point of view, retrofit design was conducted on several actually existing detached houses which had already been retrofitted for single seismic reinforcement. Originally most of the wooden buildings in the DIDs at issue were built until 1970s and generally do not comply with the current seismic requirements. This report delivers only the results on the building shown in Figure.1.

3.1 Targeted Seismic Performance of Wooden Houses

The practical seismic assessment of small wooden buildings in Japan is based on the wall-fulfilment ratio(WFR), which represents the relative seismic capability divided by the anticipated shear load level. It is believed that for WFR less than 0.7, the building may collapse under a strong earthquake, and if it falls in 1.0 – 0.7, the building may still be damaged by strong earthquake. The retrofiting design tries to achieve WFR 1.0. The necessary standard strength of the particular building to be studied is then 35.24kN for the first floor and 18.11kN for the second floor.

3.2 Retrofitting Design

Three levels of reinforcement are considered for this feasibility study, (R-A) simple seismic reinforcement to achieve WFR not less than unity, (R-B) application of the seismic and fire reinforcement tested in this project to achieve WFR around unity, and (R-C) (R-B)+additional bracing to achieve the WFR not less than unity. The contents of the reinforcements are summarized as follows.

R-A : The load-bearing walls on the first floor and all the external walls are reinforced with diagonal braces (2 power metallic materials), and structural plywood panels.

R-B : All the external walls are retrofitted with the steel sandwich panels. The capital and foot of each column is reinforced with metal fittings.

R-C : (R-C) + diagonal braces on the external wall not satisfying the shear resistance condition.

3.3 Results and discussions

Summary of the test results are shown in Table.2. The R-B has resulted in WFR not less than 1.0 for both of the X- and Y- directions, leaving WFR of the shorter wall on X-direction being 0.93. R-C, R-B's improved version has been found to achieve WFR of all the walls larger than unity. The cost analysis has resulted in cost of R-B approximately 30% higher than R-A and little cost difference between R-B and R-C. Use of the ceramic siding board, another tested external retrofiting material, may result in slightly weaker WFR, but will reduce the cost for the easier handling by small builders and the wider availability in the market. Moreover, the study suggests capability of the proposal method not disturbing the life in the house during the renovation process.

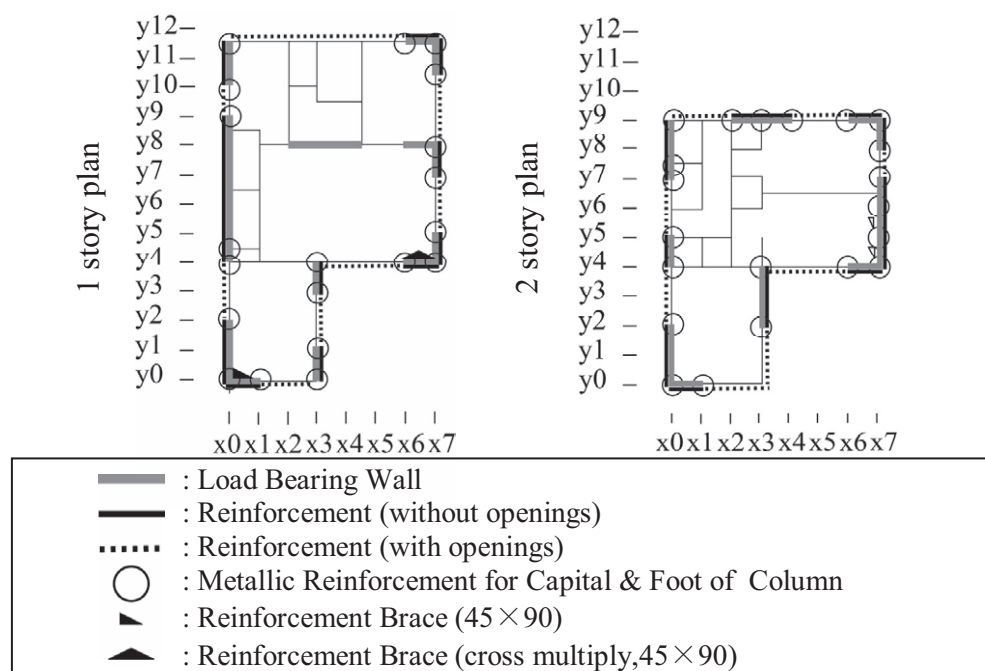


Figure 1: The floor plan and R-C plan

Table.2 result of the earthquake diagnosis

| | estimate (million yen) | one-story | | | | two-story | | | |
|------------|---------------------------|------------------|----------------|------------------|----------------|------------------|----------------|------------------|----------------|
| | | X | | Y | | X | | Y | |
| | | strength (kN) | grade point | strength (kN) | grade point | strength (kN) | grade point | strength (kN) | grade point |
| Non-Repair | - | 26.48 | 0.75 | 35.93 | 1.01 | 13.39 | 0.73 | 22.92 | 1.26 |
| R-A | 2.17 | 65.20 | 1.85 | 53.16 | 1.5 | 21.89 | 1.2 | 23.96 | 1.32 |
| R-B | 2.78 | 32.82 | 0.93 | 56.84 | 1.61 | 23.25 | 1.28 | 62.00 | 3.42 |
| R-C | 2.82 | 36.49 | 1.03 | 59.00 | 1.67 | 23.26 | 1.28 | 62.01 | 3.42 |

4. EFFECTIVENESS OF THE RETROFITTING OF EXISTING BUILDINGS FOR REGIONAL DISASTER REDUCTION

Effectiveness of the reinforcement for the reduction of post-earthquake urban fire hazard is studied through numerical fire spread simulations on an actual DID in the Greater Tokyo Area with the BRI urban fire simulator. BRI urban fire simulator is a physics-based model to calculate time of house-to-house fire spread with building conditions such as fire rating, opening conditions and distance and wind direction and velocity as parameters. Figure.2 is the district for the study, where location and fire rating of each building had been investigated. The fire ratings are based on the Building Standard Law; FP (Fire-Proof construction), QFP (Quasi-Fire-Proof construction), FPA (Fire Protective construction with incombustible cladding), FPB (Mortared Fire Protective construction), NW (Wooden house without fire protection). FPB was the most common for low rise detached and collective housings in urban districts from the 1950s to the 1970's. Most of the DIDs in Japan at issue consist of NW and FPB. Wind direction and velocity were chosen as NE, the most frequent wind direction and 4.0m/s, 33% higher than the annual average respectively.

4.1 Post-earthquake fire safety performance of existing buildings

As seen in Photo-1, earthquake may reduce the fire safety performance of buildings through generation of gaps, cracks in the walls. From the past investigations on the seismic damage to wooden buildings, we make the following assumptions. Fire Protective Construction has been generally applied to small buildings with minor seismic consideration; past investigations suggest significant seismic deformation of such buildings which should lead to the falling of the claddings at the event of a strong earthquake. From this consideration, “FPA” and “FPB” are assumed to lose the fire protection against the external wall after an earthquake.

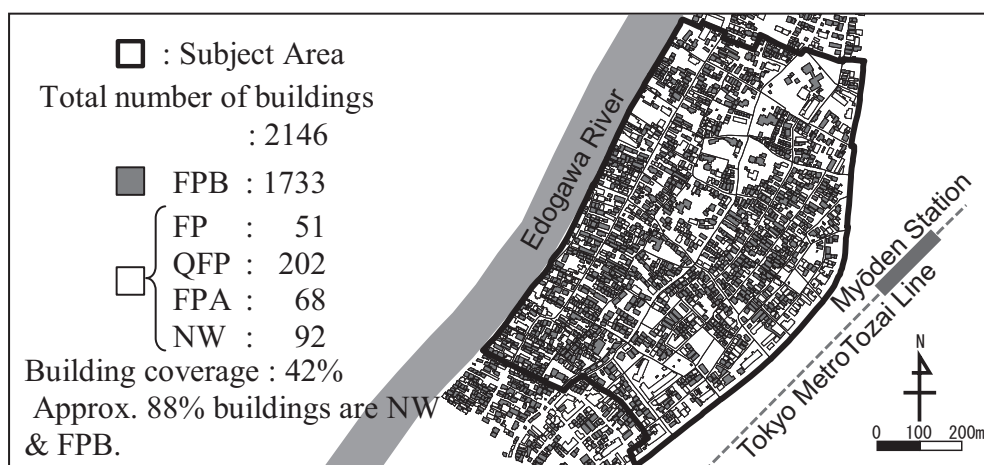


Figure 2: Subject District, distribution and fire rating of buildings

Table 3: Default time to burn down, the openings and roof, external wall (sec)

| | FP | QFP | FPA | FPB |
|--------------------------|-------|-------|-------|-----|
| collapse openings | 1,200 | 1,200 | 600 | 300 |
| burn down the roof | — | 1,800 | 1,200 | 600 |
| burn down the outer wall | — | — | 1,800 | 900 |

On the other hand large scale burn test and wall assembly fire tests on wood-based Quasi-Fireproof Construction have shown only minor reduction of the fire safety performance even after significant shear testing. From this observation, it is assumed that earthquake does not affect the fire safety performance of “QFP” and “FP”. The fire spread simulation was first conducted for the present conditions of the buildings damaged by earthquake (Figure. 3, upper right edge). The simulation suggests that post-earthquake fire outbreak in any of the 70% of the blocks will result in the involvement of over 100 buildings. These blocks with extremely high fire hazard will be referred to as the high-hazard blocks.

4.2 Levels of Reinforcement

Three levels of reinforcements are considered (Table.4): (R-I) simple seismic reinforcement, (R-II) seismic and fire protective reinforcement to maintain the fire protection against external fires and (R-III) reinforcement to maintain fire protection against external fires and prevent collapse of the load-bearing assemblies at the event of post-earthquake fire. R-I essentially

does not improve the fire protection performance of external and other walls, while R-II is to replace the external cladding so that the external wall can prevent fire penetration due to external fires. R-III will further prevent collapse of major load bearing walls until the decay of the fire itself. If these reinforcement is applied to an existing FPB building, it is natural to assume its pre- and post-earthquake fire protective performance as indicated in Table.4.

Table 4: Fireproof performance of reinforced building

| | intended structural member | Assumed for Rating | |
|--------------|--|--------------------|-----------------|
| | | pre-earthquake | post-earthquake |
| Non-Retrofit | — | FPB | NW |
| R-I | whole building structure | FPB | FPB |
| R-II | outside of outer wall | FPA | FPA |
| R-III | both sides of outer wall small building ($< 100\text{m}^2$) | QFP | QFP |
| | All load bearing walls big buildings ($\geq 100\text{m}^2$) | | |

4.3 Strategies to reform DIDs with retrofitted buildings

The effectiveness of the proposed technology for urban safety is studied through fire spread simulations by changing the retrofitted buildings to all buildings ratio (RBR, 30%, 50% and 70% were chosen). However, there is variety of density of NW and FPB buildings in the studied area, and it was thought that making any priority of the retrofitting to weaker parts of the area could improve the efficiency of the urban reform. In order to examine effectiveness of such ideas, following strategies were considered.

1) Random reform(Re-1)

Buildings to be retrofitted are chosen randomly in each block according to the design RBR level.

2) Reform with priority to high-hazard blocks(Re-2)

The high-hazard blocks are given the first priority to retrofit FPB level existing buildings. Improvement of other blocks are made only when the reinforcement of the high-hazard blocks does not satisfy the design RBR level.

4.4 Results of Urban Fire Simulations and Discussions

In order to assess the effectiveness of the levels of reinforcement and the urban reform strategies, number of fire-involved buildings in two hours from fire outbreak is compared (Figure.3). Average number of buildings involved by fire decrease as the RBR level increased, and general effectiveness of R-III reinforcement compared with others is obvious. The simulations suggest that R-III for RBR=30% achieve a similar reduction of burnt houses with R-I for RBR=70%. R-III's achievability of high regional safety by retrofitting rather small number of buildings is noteworthy because retrofitting of existing dwellings generally needs long negotiation with residents. Interesting thing in Figure.3 is that, for R-III, fire hazard is not improved by the increase of RBR, whilst increase of RBR for R-I or R-

II results in the notable reduction of fire hazard. This inconsistency was unexpected, but the effectiveness of R-III reinforcement higher at random reform scenario is attributed to the very high capability of R-III in preventing fire propagation from the retrofitted building. Since urban fire can hardly “penetrate” R-III reinforced building and burn the next building, R-III reinforcement becomes more effective in reducing the spread of urban fire if reinforced buildings are scattered in DID rather than they are concentrated.

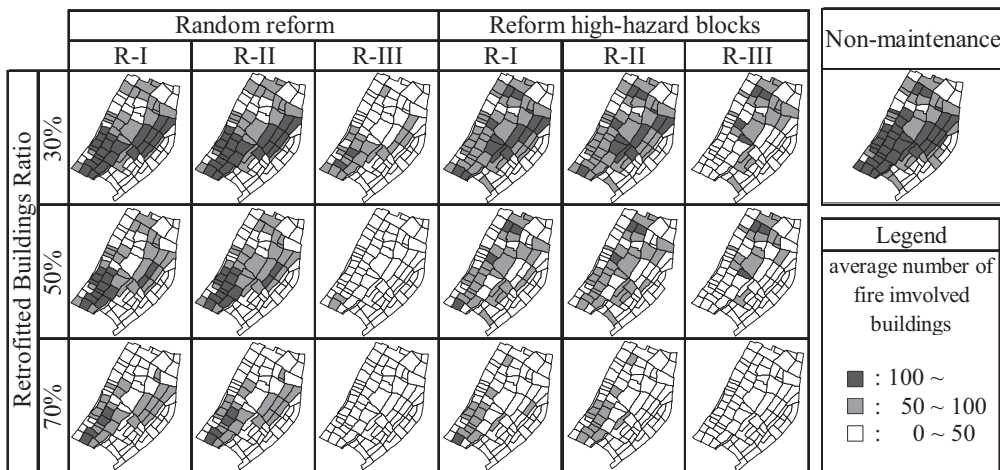


Figure 3: Results of Urban Fire Simulations

5. CONCLUSIONS

In this project, feasibility of the simultaneous seismic and fire resistive reinforcement of small wooden buildings has been studied and the following conclusions can be drawn.

- (1) Reinforcement of wooden post and beam construction by gypsum based panel materials is effective to improve seismic performance and to ensure post-earthquake fire resistive performance. Reinforced gypsum board, a conventional product widely available in the market, is found to be effective.
- (2) Reinforcement of external walls by the tested products of sandwich panel and ceramic siding panel are found to achieve seismic performance enough to support all the seismic shear and sustain the fire resistive performance to prevent fire penetration and collapse of the building.
- (3) The cost analysis has resulted in the cost of the simultaneous seismic and fire-resistive reinforcement approximately 30% higher than the simple seismic reinforcement.
- (4) The urban fire simulations suggest effectiveness to the regional safety of the simultaneous seismic and fire protective reinforcement significantly higher than the simple seismic reinforcement.
- (5) Effectiveness of the simultaneous seismic and fire resistive reinforcement is more significant when it is applied randomly in

DID rather than when any priority for its application is considered e.g. for weaker blocks.

REFERENCES

Science Council of Japan, Recommendation to the Government: Need to Ensure Safety in Giga-cities at the Event of Strong Earthquake, 2005. (*in Japanese*)

Y.Hasemi, Ed.: Development of Retrofit Technology of Wooden Urban Buildings for the Simultaneous Improvement of Seismic and Fire Protective Performances, Construction Technology R & D Fund, MLIT, 2007(*in Japanese*)

T.Iwami, Y.Ohmiya, Y.Hayashi, T.Naruse, S.Takeya, K.Kagiya, E.Itoigawa, T.Kato, K.Shida, A.Hokugo, W.Takahashi, Ed: *Development of Evaluation Technologies for Fire Spreading in Urban Area*

Report of Building Research Institute, No.145, 2006(*in Japanese*)

Y.Hasemi, M.Murakami,N.Kawai, M.Yamada, N.Yasui, S.Oshiumi, Y.Shimizu, S.Kobata, H.Kamiya, T.Sakata, H.Nagamori, Ed: *Seismic and Post-earthquake Fire-resistive Performance of Conventional Post & Beam Wall Retrofitted for The Reduction of Post-earthquake city fire hazard in densely inhabited districts*, AIJ Journal of Technology and Design Vol.14 No.27 2008(*in Japanese*)

Y.Kawagoe, Y.Hasemi, N.Yasui, H.Kamiya, S.Kobata, Ed: *Reducibility of Seismic and Post-earthquake Urban Fire Hazard in Densely Inhabited Districts by Simultaneous Seismic & Fire-resistive Reinforcement of Low-rise Wooden Buildings*, Vol.14, No.28, 2008. (*in Japanese*)

A STUDY FOR PROMOTING COMMUNICATION BETWEEN RESEARCH INSTITUTES AND GENERAL SOCIETY

ABE MARIKO¹ and MEGURO KIMIRO²

¹International Center for Urban Safety Engineering

²Institute of Industrial Science, The University of Tokyo, Japan

abe@risk-mg.iis.u-tokyo.ac.jp

ABSTRACT

The social intelligence sharing and the consensus building are important in the field of the safety of the society. Therefore, the laboratories in this field are requested to send the information that is easily understandable to the general society, and to respond to the voices from the general society moreover. Recently, various communication media exist such as face-to-face conversation and website. In this situation, how the laboratory of disaster mitigation should send and receive the information to/from the general society?

Every year, the largest institute of one university in Japan holds the Open House event for the general public to introduce their latest research and achievements. In this paper, the authors take up the case with one laboratory of urban disaster mitigation engineering in this event, and describe communications between the laboratories and the general society.

1. INTRODUCTION

In the democratic societies, the social intelligence sharing and the consensus building are important especially in the field of the safety of the society. Therefore, the laboratories in this kind of field are requested to send the information easily understandable to the general society, and to respond to the voices from the general society moreover. Recently, various communication media exist such as face-to-face conversation and website. In this situation, the authors are considering about how the laboratory of disaster mitigation should send and receive the information to/from the general society. In this paper, the authors take up the case of the face-to-face communication.

Every year, the largest institute of one university in Tokyo, Japan (B-Institute of A-University) holds the Open House event for the general public to introduce their latest research and achievements. In this paper, the authors take up the case with the laboratory of urban disaster mitigation engineering (C-Laboratory) in this event, and describe communications between the laboratories and the general society.

2. THE RESEARCH FIELD

2.1 B-Institute of A-University

A-University, the oldest Japanese university, known for its long history dating back to 1877, is currently consisted of 10 faculties, 11 institutes, 15 graduate schools, and a number of shared facilities. B-Institute is the largest among these institutes, and now includes 5 research departments, 1 guest chair, 2 endowed chairs, 6 research centers, 3 collaborative research centers, 1 outside experiment station, some shared facilities, and administrative offices. The faculty members of the B-Institute, in addition to pursuing research in their respective fields, play an active role in the graduate school by conducting courses, experiments, exercises, research meetings, and so on, as well as supervising graduate students for their master's and doctoral theses in the divisions of Engineering and Science.

2.2 Communication between B-Institute and the General Society

B-Institute not only tries to educate the postgraduate students but also tries to educate the people of the other positions in the general society such as the engineers of the private organizations. B-Institute is also acknowledged for its keen promotion of international scientific interaction through exchange students and researchers. Moreover, study results have been widely introduced to the general society through the courses, the seminars and other opportunities as shown in table 1.

*Table 1: Communication between B-Institute and the general society
(face to face communications only)*

| Event | Frequency | Contents |
|--|------------|--|
| Open House | 1/year | Open House event for the general public to introduce the latest research and achievements (1954-) |
| The Outside Experiment Station Open House | 1/year | Open House event for the general public to introduce the latest research and achievements (2003-) |
| The IIS Symposium | Irregular | The international symposium for researchers (-2007) |
| Evening Seminars | 2/year | Open course for the general public to introduce the latest research and achievements |
| Friday seminar for high schools students | 20-30/year | Open seminar for high schools students (2004-) |
| B-Institute Academic Lecture Courses | 1-2/year | Open seminar event for the general public to introduce the latest research and achievements |
| Individual open tour for junior high schools and high schools students | Irregular | Individual open tour for junior high schools and high schools students |
| B-Institute Seminar | 3/year | Seminar including experiment and practice |
| B-Institute Special Seminar | 5-8/year | Course that brings a series of lecture of basic knowledge necessary for research and development (1987-) |

| Event | Frequency | Contents |
|---|-----------|--|
| SNG (Scientists for the Next Generation) | --- | Experiences of experiments and classes outside IIS for elementary schools, junior high schools and high schools based on recent research by teachers, staffs, and postgraduate's volunteers (1997-) |
| Tours for junior high school and high school students at Open House | 1/year | Research introduction for Junior high school and high school students at Open House (1997-) |
| Class for junior students outside IIS | Irregular | Through lecture and practice, students will learn that mathematics and science learnt in elementary schools, junior high schools and high schools are related to the research and many other things. |
| UROP (Undergraduate Research Opportunity Program) | 1/year | Research introduction course for 1st or 2nd grade students at the university of Tokyo, where research program is made by students themselves. Know-how of research is learnt through experiencing experiment and fieldwork, etc. (2001-) |

In this research, the authors take up the event of Open House with the case of C-Laboratory of urban disaster mitigation engineering.

2.3 C-Laboratory

C-Laboratory consists of 1 professor, 1 special associate professor, 5 researchers, 2 secretaries, 1 worker, and 18 students (2 doctor course students, 10 master course students and 6 undergraduate) (in August, 2008). Master course first grade students are in the charge of the laboratory events and tasks. The place in the laboratory is located on the south end of the sixth floor of the main building of B-Institute.

At C-Laboratory, researches on developing strategies to minimize damages to society by hazards such as earthquakes are conducted by taking into account both the “hard” and “soft” measures. The biggest lesson from the recent earthquakes in Japan, such as the Southern Hyogo Earthquake (1995), is the fact that without “hard” measures, mitigation of human loss cannot be achieved, and “soft” measures such as the popular “Real-Time Earthquake Disaster Prevention System” aims at quick restoration and revival of social functions. With this lesson in mind, many researches are done in the following themes.

- Investigation, AEM, Masonry
- DEM, Retrofitting
- Evacuation, Tsunami Disaster Mitigation System
- Power Supply
- Disaster Management Manual
- Social System

2.4 Communication between C-laboratory and the General Society

The activities by C-Laboratory in the field of communication with the general society are as follows. The authors show not only the communications outside the laboratory but also the communications inside the laboratory. Because most of the students in C-laboratory will graduate

and begin to work in the general society outside C-Laboratory after the 2-3 years, education to those students inside the laboratory is one of the most important communications with the general society.

Activities by entire C-Laboratory:

- **The Research exhibitions and demonstrations in Open House**
- The Disaster Mitigation Summit (the disaster mitigation lecture by the students from the several universities, for the audiences from the general society, held once a year at the university in Shizuoka, Japan)
- Management of C-laboratory website (members list, introduction of the researches, laboratory events and others)

Activities by the professor:

- Doing research, making theses, and giving presentations at the academic conferences (There are a lot of researches as the project that cooperates with the enterprise, NPO, and the governments.)
- Committee activities related to the disaster mitigations such as the country or local governments, cooperative lifeline companies and others
- Disaster mitigation lectures for the students in two universities
- Disaster mitigation lectures for the general persons outside the university
- Writing or Supervision of the books, picture-story shows, cartoons and others
- Interviewee on TV or radio programs, newspapers and others

Activities by the students:

- Doing research, making theses, and giving presentations at the academic conferences (There are a lot of researches as the project that cooperates with the enterprise, NPO, and the governments.)

In this paper, the authors take up the case of the research exhibitions and the demonstrations in Open House.

3. C-LABORATORY'S ACTIVITIES IN OPEN HOUSE

In this paragraph, the authors show C-Laboratories activities in Open House. The schedule of Open House is shown in Table 2 and Table 3.

Table 2: The whole schedule (2008)

- | |
|---|
| <ul style="list-style-type: none">• <u>24th in April to 22nd May</u>: all students meeting from 10:00-12:00 on every Thursday (study of the researches of C-Laboratory, practice about the panel explanations and demonstrations)• <u>May</u>: making of the new panels• <u>Two days before Open House</u>: set up the panels on the walls of the corridor• <u>The day before Open House</u>: set up the panels, desks, chair, spotlights, power supply codes and others/rehearse of the experiments and the demonstrations• <u>Open House (three days)</u>: panel exhibitions and demonstrations 16:00-17:30 on the final day: remove the panels and others 18:00-20:00 on the final day: the closing party• <u>About one week after Open House</u>: Opening the data to the public and keeping tools and materials• <u>Within several weeks after Open House</u>: Reflection meeting by students, professor and associate professor |
|---|

Table 3: The example of the explanation member's charge schedule (2008)

| 5/29(Thu) (10:00 - 17:00) | | | | | | | | | |
|-----------------------------------|-----------------------|---|---------------------------------|---------------------------------------|-------------------------------|---------------------|---------------------------------|--|--------------------------|
| research field (leader) TME | Introduction (Abe) | Damage Investigation, AEM, Masonry (Fujieda) | DEM, Retrofitting (Ejima) | Evacuation, Tsunami (Yoshinari) | Power Supply (Hanatani) | Manual (Higashi) | Social System (Sorimachi) | Demons- tration etc. (Nomura) | reserve (coordinator) |
| 10:00-12:00 | Kishida | Sakthi | Ejima | Yoshinari | Yoan | Higashi | Nomura | Sorimachi | Abe |
| 12:00-14:00 | Takaishi | Paola | Fujieda | Inoue | Hanatani | Hiruma | Sorimachi | Nomura | |
| 14:00-15:30 | Nomura | MIN ZAW | Ejima | Takaishi | Koh | Hiruma | Inoue | Sakurai | Abe |
| 15:30-17:00 | Hiruma | Tatiana | Sakurai | Yoshinari | Saito | Kishida | Koh | Takaishi | Inoue |

| Numbers of Presentation for Members above | | | | | |
|---|----|----|---|---|--|
| B4 | M1 | M2 | D | R | |
| 6 | 6 | 5 | 3 | 2 | |
| 6 | 6 | 5 | 9 | 3 | |
| 6 | 6 | 6 | | | |
| 6 | 3 | 6 | | | |
| 6 | 6 | 6 | | | |

3.1 The contents of the activities

During Open House, the Students work in their allocated time between 10:00 to 17:00. During 3 days of Open House, the students spend much time in the corridor in front of C-Laboratory's rooms, explaining the panels or doing demonstrations. 5-6 explanation charge times (about 10 hours in total) are allocated to each student, but students are actually working during their free time, helping others.

3.1.1 The Panel exhibition

The explanation of the research by the students, using the panels on the walls, is the main activity of C-Laboratory's Open House. About 100 panels are shown on the walls of the corridor. The size of the panel is 74cm×103.5cm.



Figure 1: Introduction by a student



Figure2: A lot of panels on the wall

3.1.2 The demonstration and the touch-panel system

The students do the demonstrations of the liquefaction and the shaking table, and the explanation of the researches by using the big touch-panel.



Figure3: Demonstration

3.2 Layout

The layout of C-Laboratory exhibition space and explanation member's standing position is shown in figure 5.

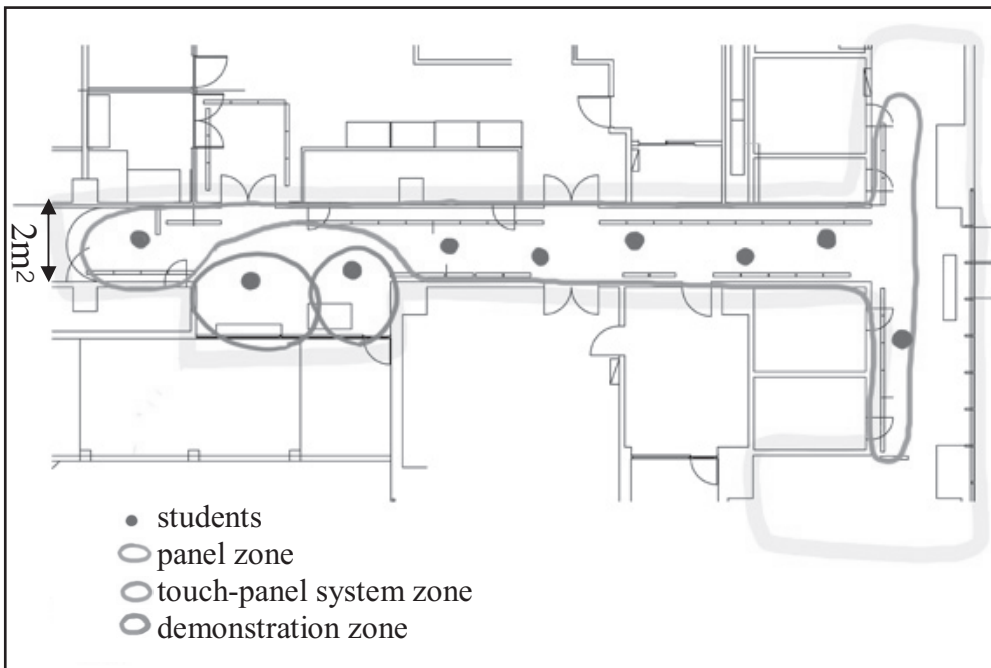


Figure5: Layout of C-Laboratory exhibition and demonstration

3.3 After the exhibition

3.3.1 Opening the data to the public and keeping tools and materials

After Open House, the data of the exhibited research panels are opened on the Web site in the laboratory. After selecting the panels for the daily exhibition on the wall of the corridor in front of C-Laboratory, the students put the panels into the panel-cases and keep in the storage of C-Laboratory. The touch panel system and the experiment kits are also kept at the fixed position. These works are done within one week after Open House.

3.3.2 The meeting for reviewing the activities in Open House

Within several weeks after Open House, the meeting for reviewing the activities in Open House is held. Before the meeting, students gather the data of the questions and comments by the audiences, and the feedback comments such as impressions and lessons by the students (since 2007). The details will be shown in Chapter 4.

4. FEEDBACK ABOUT OPEN HOUSE

The numbers of the questions and comments by the audience in Open House were about 89 in 2007 and about 77 in 2008. (An accurate number of the questions and comments could not be counted, if the student got same questions from two or more audiences, he/she often forgot the number). The numbers of the feedback comments such as impressions, lessons by the students were about 55 in 2007 and about 99 in 2008 (each student submitted more than 2 comments).

4.1 The questions and comments by the audience

- By comparing the questions and comments between 2007 and 2008, the authors found six similar questions. This data shows the effectiveness of referring the past questions and the comments of the past Open House. However, in the several cases in 2008 Open House, some students' response to that kind of questions were not appropriate. This shows the students' lack of studying.
- New students who have only spent 2 months in C-Laboratory must deal with the audience as the "specialist of the disaster mitigation" in Open House". Besides the questions about the research, the students were asked about their principles such as "What is your motivation for doing the research of the disaster mitigation?" Such questions have the good effect for the students to grow as the specialist of the disaster mitigation field.
- Many questions and comments were about the additional effects and the social contribution of the research. These questions and comments both locate the researches in the society. The former can be interpreted "Doesn't the research influence the bad effect to the general society?" and the latter can be interpreted "Is the research useful for the general society?" These questions and comments are very profitable to research. In addition, the audiences from the government or the enterprise sometimes offer the joint research or the joint business.
- Many audiences asked students to give them some advice about their worries on the disaster mitigation. To deal with these questions, the information of the research exhibition at C-Laboratory is not enough. So, the students should introduce the clues to know more detailed information such as the introduction of other laboratories of the suitable research themes for that question.

- Some other questions and comments about the meaning of the words and the method of the experiments were asked.

4.2 Feedback from the students

The feedback comments by the students include succession of the information and know-how, the explanation technique, the layout of the panels and others, the corporation with the other laboratories, and so on. Many of the new students said that it was good opportunity for them to learn the current research topics of the C-Laboratory.

5. CONSIDERATIONS

According to the data mentioned in the chapter 4, Open House can be a good opportunity for C-Laboratory as the chance to get feedback from the general society. On the other hand, in the past Open House, the students did not make full use of the feedback information. This is because the students didn't arrange or analyze the data gathered from questions and comments by the audiences and the feedback comment by the students.

In order to improve this situation, the authors propose the database of Open House as making the environment for further communications between C-Laboratory and the general public in Open House. This database (The Open House Database) is based on the New Style Disaster Manual for Implementation of efficient Disaster Countermeasures (Kondo, Hamada and Meguro; 2001).

In Open House, students are expected to have the basic understanding of the whole research topics of C-Laboratory, and the deeper understanding of the topics of the research which they take charge of the explanation. Especially for the new students, it is necessary to learn these contents in just two months from April to May, but they are busy because of the searching job or the attending the classes, and often cannot gather together. So, the database on the web is effective for each student to prepare for the Open House smoothly. The authors propose the function and use image of the database in figure 6.

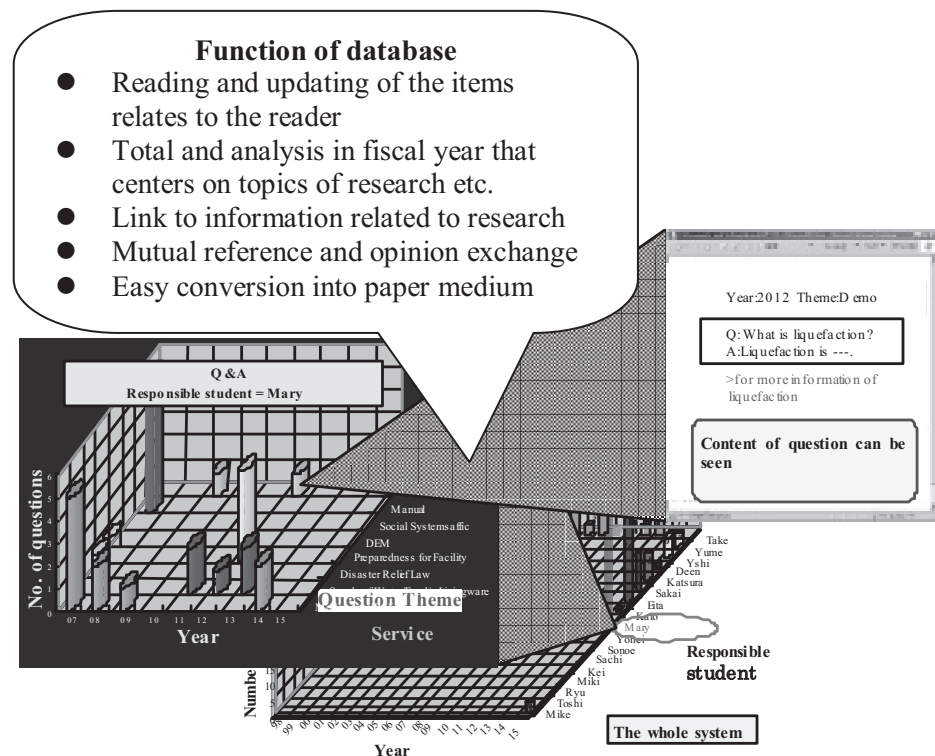


Figure 6: Function and use image of the Open House database

6. CONCLUSIONS

The social intelligence sharing and the consensus building are important in the field of the safety of the society. Therefore, laboratories in this field are requested to send the information easily understandable to the general society, and to respond to the voices from the general society moreover. In this paper, the authors took up the case of the approach and the problems of the research exhibitions by one laboratory of urban disaster mitigation engineering in Open House of the biggest institute in Japan and describe communications between the laboratories, institutes and the general society.

According to the data of the questions and comments by the audiences, and the feedback comments such as impressions, lessons by the students, Open House can be a good opportunity for the laboratory as the chance to communicate with the audiences and get feedback from the general society. On the other hand, in the past Open House, the students did not make full use of that feedback information. This is because the students didn't arrange or analyze the data gathered. In order to improve that situation, the authors propose the database of Open House as making the environment for further communications between the Laboratory and the general public in the Open House.

In the next step of this research, the authors will try to gather more case collections about the communications between the laboratories and the general society, and creating the database useful for the various laboratories, institutes to communicate with the general society.

REFERENCES

Dean, D., 1996. Museum Exhibition. Routledge, London

Kondo, S., Hamada, S. and Meguro, K., 2001. Proposal of New Style Disaster Manual for Implementation of Efficient Disaster Countermeasures. Proceedings of the JSCE Earthquake Engineering Symposium 26:2, 1481-1484.

The University of Tokyo homepage: http://www.u-tokyo.ac.jp/index_e.html

IIS homepage: http://www.iis.u-tokyo.ac.jp/index_e.html

Meguro laboratory homepage: <http://risk-mg.iis.u-tokyo.ac.jp/>

STUDY ON EPIDEMIC SPREADING ON ALTERNATE SOCIAL NETWORKS

SHUNJIANG NI^{1,2} and WENGUO WENG¹

¹Center for Public Safety Research, Department of Engineering Physics, Tsinghua University, Beijing, 100084, P. R. China

²School of Aerospace, Tsinghua University, Beijing, 100084, P. R. China
wgweng@tsinghua.edu.cn

ABSTRACT

In this paper, a model of epidemic spreading on alternate social networks is presented and investigated numerically. The alternate social network consists of a family network and a public network, simulating the human contacts during some time (e.g. nighttime when the human usually stays with family) and another time (e.g. daytime when the human usually stays in the public place such as workplace, school, shopping mall, etc.) respectively. Here the family network is comprised of several sub fully connected networks since there are few persons in a family. While the public network consists of several sub networks which can exhibit small-world properties and scale-free degree distribution, representing various types of local interactions among social groups in modern society. Epidemic spreading occurs alternately on the family network and the public network. Typical relationships characterizing the spreading process such as epidemic curves and ranges, etc. are discussed. The influences of the network topology and the active time span of the sub networks on the epidemic spreading process are investigated. Simulation results show that the spreading process on the alternate social networks is independent of the topologies of the public network, and an oscillation behavior of the epidemic curve is observed.

1. INTRODUCTION

Traditionally, the Susceptible-Infected-Susceptible (SIS) model, the Susceptible-Infected-Removed (SIR) model and their derivatives are the mathematical models for the study of infectious diseases in epidemiology (Hethcote, 2000). However, these analytical models have one serious disadvantage—they do not take into account the patterns or structures of social interactions within population which can be modeled with complex networks. Most of these complex networks share some important topological feature such as small world (SW) properties (Watts and Strogatz, 1998) and scale free (SF) degree distribution (Barabasi and Albert, 1999). And then the dynamics of epidemic spreading in complex network has been extensively studied. Studies show that both the disease characteristics and the topological features of the complex network determine the dynamics of

the spread of disease (Pastor-Satorras and Vespignani, 2001a; Pastor-Satorras and Vespignani, 2001b).

In order to capture the information on social interactions, many complex networks have been used to model the social contacts (Keeling and Eames, 2005). The spreading of a disease on top of structured scale-free networks (Moreno and Vazquez, 2003) and in a population with a hierarchical structure of interpersonal interactions (Grabowski and Kosinski, 2004) has been studied in detail by large scale numerical simulations with the SIR and SIS models. Other efforts to consider more realistic contact patterns are to use the generated network by computer simulations based on the actual census, land-use and population-mobility data (Eubank, Guclu, Kumar, Marathe, Srinivasan, Toroczkai and Wang, 2004; Meyers, Pourbohloul, Newman, Skowronski and Brunham, 2005). But these models only can partially simulate the social interactions due to the fact that the time information of the social interactions is neglected. Thus, some recent efforts to consider the time information are to introduce dynamical network to model the spread of an infectious disease in a population of mobile individuals (Frasca, Buscarino, Rizzo, Fortuna and Boccaletti, 2006) and to adopt the adaptive network that the susceptible are able to avoid contact with the infected by rewiring their network connections (Gross, D'Lima and Blasius, 2006).

However, most of the above studies concern the case of single network which means that all individuals belong to the same social group all the time, which may be true only for certain short time duration. Actually, in modern society, daily human activities are marked by strong habits with little day-to-day variety (Huang, Sun, Hsieh, Chen and Lin, 2005). For instance, students will go to school in mornings, frequently contact with their classmates and teachers, and stay home with their parents after school; adults will go to their workplaces on time and stay there until off duty. Individuals constitute some local interactions among social groups in a certain time, after that, these interactions dismiss and form some different ones. It means that individuals form different networks in different time durations, that is, the networks have its own active time span, during which the epidemic spreading may occur. In this paper we firstly constitute an alternate social network which consists of a family network and a public network to simulate the human contacts during some time (e.g. nighttime when the human usually stays with family) and another time (e.g. daytime when the human usually stays in the public place such as workplace, school, shopping mall, etc.) respectively. Moreover, as mentioned above, the network topology features are crucial for the spreading process of diseases. Unfortunately, most of the network-based epidemic models lead to different epidemic dynamics, which does not accord with practical situation because the epidemic spreading behaviors should be sole on a real society. This

inconsistency implies us to believe that these network models have missed some information on the social interactions. Thus in this paper, we secondly study a susceptible-infected-removed (SIR) model on the presented alternate social networks. Epidemic spreading occurs alternately on the family network and public network according to the network active time span. Through the paradigm of alternate networks, this study tries to find more realistic patterns of social interactions.

2. THE MODEL

The alternate social networks consist of two components: a public network and a family network representing the population structure formed during some time (e.g. nighttime when the human usually stays with family) and another time (e.g. daytime when the human usually stays in the public place such as workplace, school, shopping mall, etc.) respectively (Figure 1). In the current network, a closed finite population of N individuals is considered, which is randomly partitioned into several subgroups whose size are uniformly distributed in the interval $[a, b]$. Individuals in the same subgroup can be represented as a couple of co-workers at the same workplace, a group of students at the same school, and so on for the public network, or just a household for the family network. It is assumed that each subgroup is isolated from others, so only contacts among individuals in the same subgroup are allowed. For example, if Individual i belongs to subgroup A of family network and subgroup B of public network, he will always stay in the Subgroup A during nighttime and the Subgroup B during daytime. In the words of complex networks, these subgroups can be defined as sub networks with certain topology. All sub networks formed during some time (e.g. daytime) are referred to the public network. Similarly, the family network consists of all sub networks (namely households) formed during another time (e.g. nighttime). The main difference between the public network and the family network is the topology. For the public network, all sub networks can be either a set of small-world (SW) networks or a set of scale-free (SF) networks, with the average degree $\langle k \rangle$; while for the family network, all sub networks are fully connected since there are few nodes. The term ‘alternate’ means that disease transmission will be ongoing when the network (public or family) is active, and the infection process will be shifted onto the other network (family or public) as soon as the current network is deactivated.

The construction methods for sub networks of the public network are described as follows. The small-world network is generated using the procedure described in Ref. (Watts and Strogatz, 1998): (i) Start from a one dimensional ring lattice with desired size satisfying the periodic boundary condition and connect each node to its $\langle k \rangle$ neighbors; (ii) Rewire each edge of the lattice with probability p , ignoring the self-connection and duplication of edges. The scale-free network is generated using the algorithm in Ref. (Barabasi and Albert, 1999): (i) Start from an initial network of m fully interconnected nodes. (ii) At each time step, a new node

with m edges that link to m different old nodes. The connection probability of a new node to the already present node i is given by $\Pi(k_i) = k_i / \sum_j k_j$. Finally, a network with an average degree $\langle k \rangle = 2m$ is generated, and the degree distribution follows a power law $p(k) = 2m^2 k^{-3}$.

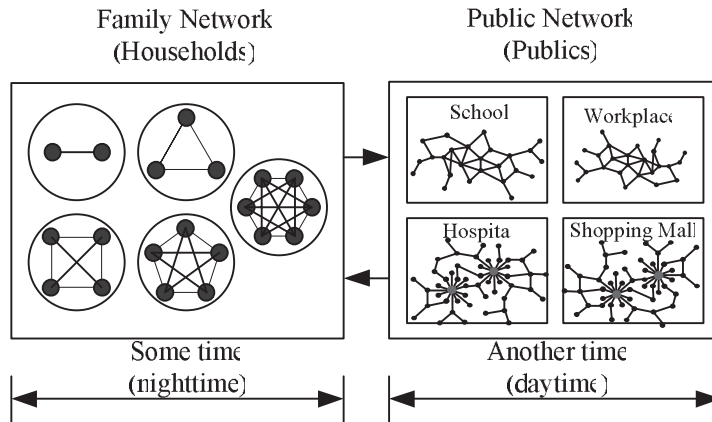


Figure 1: Schema of the alternate social networks. The family network and the public network are formed during some time (e.g. nighttime when the human usually stays with family) and another time (e.g. daytime when the human usually stays in the public place such as workplace, school, shopping mall, etc.), respectively. Dots represent individuals and lines between dots represent contacts between individuals that could potentially lead to disease transmission. Each household in the family network is fully connected, while in the public network each sub network can be a small-world or a scale-free network. For both of the family and the public networks, the size of sub networks is uniformly distributed.

Epidemic spreading is modeled using the SIR mechanism. Each individual on the public network or family network is in one of three permitted states: susceptible (S), infected (I), and recovered (R). Initially, the status of $N - N_0$ individuals is set susceptible with N_0 randomly selected individuals infected. The dynamics of the model are such that at every discrete time step of duration 1 (time unit), every infected individual in the network: (1) infects its nearest neighbors, if susceptible, with probability p_s per neighbor. (2) with probability p_r recovers and can no longer be infected or infect others. This spreading mechanism will be iterated for n time-steps (called as network active time span) on one network (the public or the family), and after that the process will be alternated on the other network (the family or the public) with another n time-steps. This process can be readily iterated in numerical simulations alternately until changes no longer happen.

3. RESULTS

In this section, we present some results from numerical simulations of the model described in Section 2, with a system size N and N_0 randomly selected infected individuals. All the simulation data are collected over 200 independent simulations, each of which corresponds to a different realization of the public network and different initially infected individuals.

For the purpose of comparison and discussion, we also perform simulations of some other networks: 1) The population is modeled by only one network (called the single network hereinafter), the small-world network or the scale-free network, of which the topology and generation algorithms are the same as those for sub networks of the public network. 2) The single public network as well as the family network, referred to one of two components of the alternate social network. We mainly study the influence of three parameters on the epidemic dynamics: the network active time span n , the rewiring probability p of the SW sub network of the public network, and the infective probability p_s .

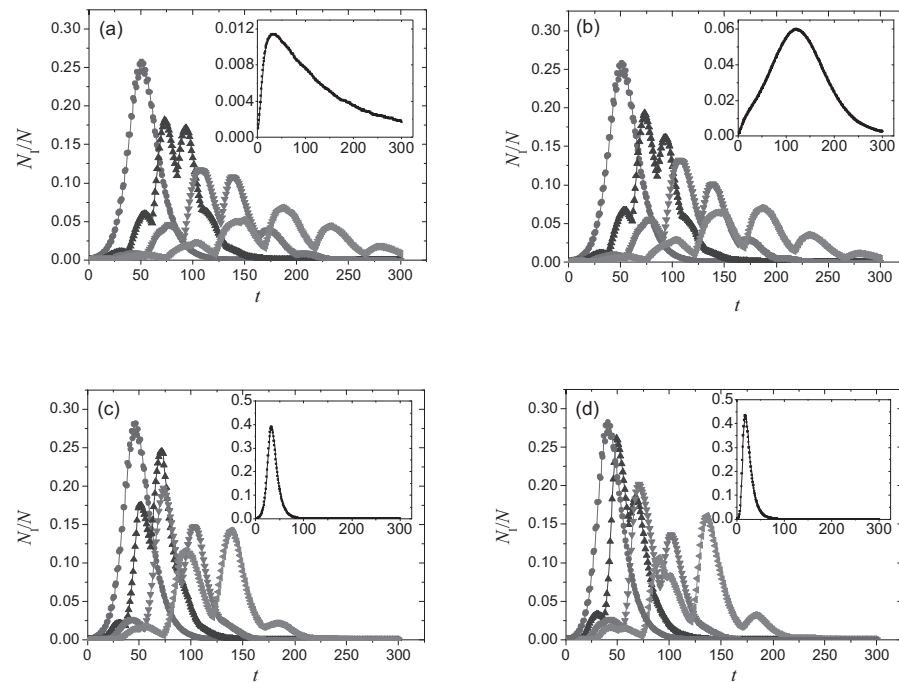


Figure 2: Evolution of the percentage of infected individuals on the alternate social networks for different values of network active time span $n=1$ (circle), $n=12$ (triangle up), $n=18$ (triangle down), and $n=24$ (triangle left). In the inset, the corresponding epidemic curve on the single network, whose topology is the same as that of the public network, is shown. Subfigures (a), (b) and (c) correspond to the sub network of the public network with small-world (SW) topology with a rewiring probability $p=0.001$ (a), 0.01 (b), and 0.3 (c), while subfigure (d) is for the sub networks of the public network with scale-free (SF) topology. The average node-degree for both the SW and SF sub networks is 10, while the sub networks of the family network are fully connected. The size of the sub networks is uniformly distributed in the interval $[50, 150]$ and $[2, 6]$ for the public network and family network, respectively. The other parameters of the model are $N=10^4$, $N_0=10$, $p_s=0.05$, and $p_r=0.1$.

Figure 2 shows the evolution of the percentage of infected individuals on the alternate social networks for different values of n and rewiring probability p . Figure 2 (a), (b) and (c) correspond to SW sub network of the public network while Figure 2 (d) is for SF sub network of the public

network. The corresponding results on the single network whose topology and construction procedure are the same as those of the public network's sub network, are shown in the insets of Figure 2 (a), (b), (c) for SW network and Figure 2 (d) for SF network. For the single network, the infected population increase monotonously and quickly in the initial stage, and then begin to decline monotonously and vanish in the end. The reason is that as the infection spreads the number of susceptible individuals decreases, and after some time, the infection speed will be lower than the recovered speed. Interestingly, it can be seen that the epidemic curves of SIR model on the alternate social networks express an oscillation behavior which cannot be seen in the single network. We investigate the relationship between this unique feature and the parameter n , finding that the oscillation becomes more obviously as n increases (ranges from 1 to 24). This phenomenon implies that the family network and the public network play different roles in the epidemic dynamics, which can be seen in Figure 3. Figure 3 shows the evolution of the percentage of infected individuals on the family network and the public network, and it can be found that the infection on the family network is much more quickly than those on the public networks (the time to reach the peak on the family network is about 6, much less than that on the public network). Moreover, as shown in Figure 4, the infection curves from the family network reach the peak at the same time $t = 6$, regardless of the values of N_0 , and the infected population on the family network has only a small increase before it decreases relative to that on the public network. So it is concluded that the oscillation behavior found on the alternate social networks will not happen when the parameter n is less than the time at which the epidemic curve on the single family network reaches its peak. For example, we examined the behavior of epidemic spreading with several values n around 6, and found that the obvious oscillation behavior did not occur for $n < 6$ (Figure 5). From Figure 5, it is indicated that when $n < 6$ at Figure 5(a) and (c), the curves are almost smooth and there are no obvious oscillation behavior, otherwise when $n > 6$ at Figure 5(b) and (d), it has obvious oscillation behavior.

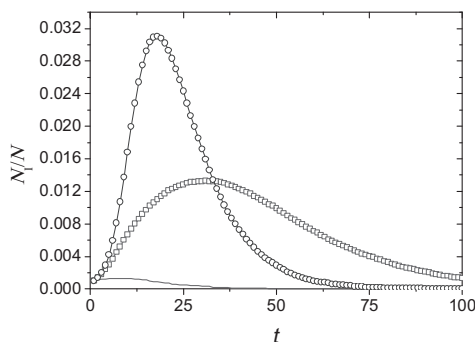


Figure 3: Evolution of the percentage of infected individuals on the family network (line) and the public network (square for SW sub networks with a rewiring probability $p=0.01$ and circle for SF sub networks). The other

parameters of the model are $N=10^4$, $N_0=10$, $p_s=0.05$, $p_r=0.1$, $[a, b]=[2, 6]$ for family network (fully connected) and $[50, 150]$ for public network with $\langle k \rangle = 10$.

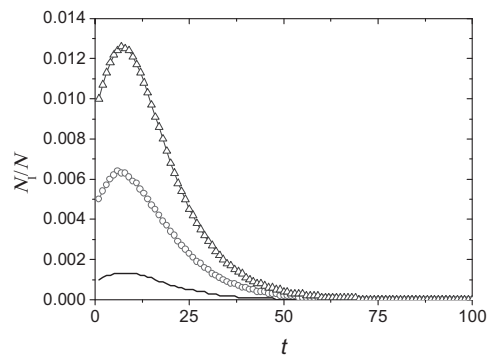


Figure 4: Evolution of the percentage of infected individuals on the family network under different values of $N_0=10$ (line), $N_0=50$ (circle), and $N_0=100$ (triangle up). All curves reach the peak at the same time $t=6$. The other parameters of the model are $N=10^4$, $p_s=0.05$, $p_r=0.1$, $[a, b]=[2, 6]$.

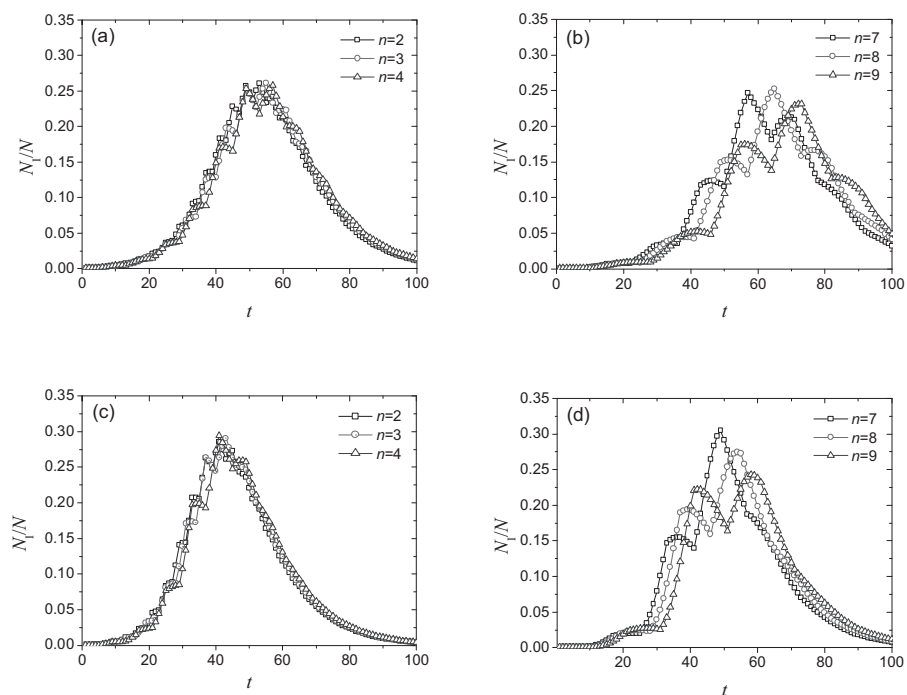


Figure 5: Evolution of the percentage of infected individuals on the alternate social networks for different values of n around 6. The topology of the public network's sub network is SW for (a) and (b), and SF for (c) and (d). Obvious oscillation behavior on both the SW and SF public networks occurs only for $n > 6$. The other parameters of the model are $N=10^4$, $N_0=10$, $p=0.01$, $p_s=0.05$, $p_r=0.1$, $[a, b]=[2, 6]$ for family network (fully connected) and $[50, 150]$ for public network with $\langle k \rangle = 10$.

Another interesting phenomenon is about the influence of the sub network's topology on the epidemic dynamics. In Figure 2, it can be seen that the spreading process on the single SW network (in the inset) is very

sensitive to p , while on the alternate social networks p has very limited impacts on the infection process. Moreover, the spreading processes on the alternate networks with SW sub networks and SF sub networks are very similar.

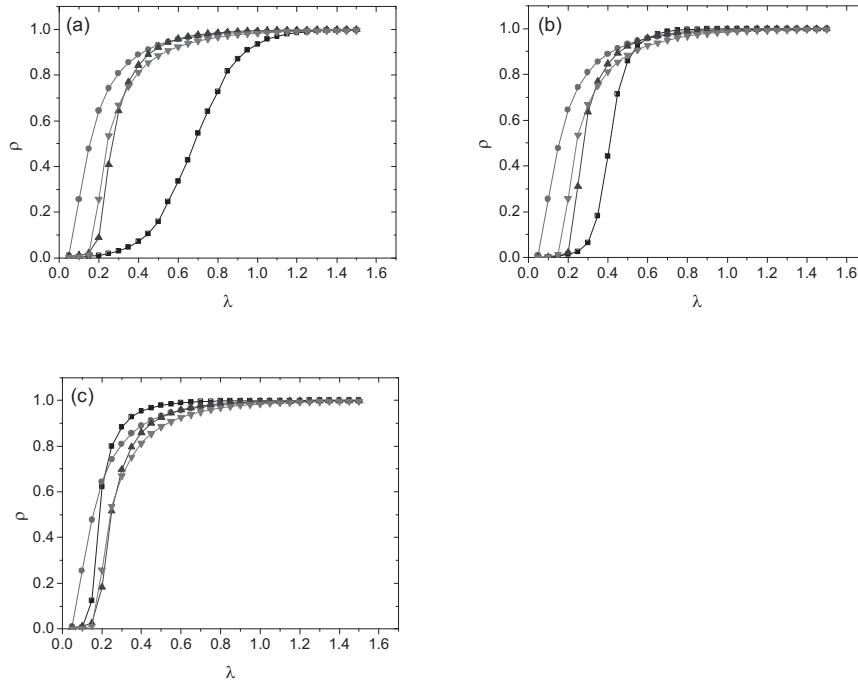


Figure 6: The fraction of ever infected individuals ρ as a function of the parameter $\lambda=p_s/p_r$ with $p_r=0.1$ for different network topologies: single SW network (square), single SF network (circle), alternate social networks with SW sub networks (triangle up), and alternate social networks with SF sub networks (triangle down). For alternate social networks, $n=8$. Subfigures (a), (b) and (c) are for different values of the rewiring probability $p=0.001$ (a), $p=0.01$ (b), and $p=0.3$ (c). The values of other parameters are $N=10^4$, $N_0=10$, $[a, b]=[2, 6]$ for family network (fully connected) and $[50, 150]$ for public network with $\langle k \rangle=10$.

In order to do a further analysis on the phenomenon described above, we examined the evolution of the epidemic size as a function of the infective probability (Figure 6). It can be seen that the epidemic threshold on single SW network varied obviously as the rewiring probability p increases, while on single SF network it almost disappears, which has been pointed out by the previous researchers (Pastor-Satorras and Vespignani 2001b). Surprisingly, the infection spreads on the alternate social networks with SW public network is nearly independent of p , and is almost the same as that on the alternate social networks with SF public network. This indicates that the infection mechanism of SIR has the same epidemic dynamics on the alternate social networks, regardless of the topology of the sub networks. In other words, the epidemic spreading on the presented alternate social network is independent of the topologies of the public network, which accords well with the practical observation. In the true

society, it should have only one epidemic spreading mechanism in spite of the SW and SF characteristics of the society network.

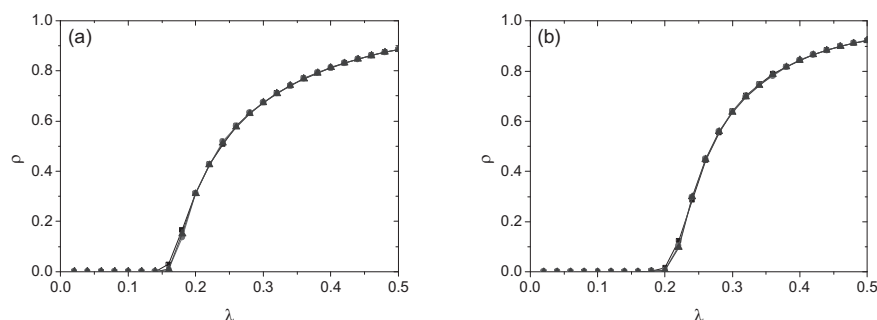


Figure 7: The fraction of ever infected individuals ρ as a function of the parameter $\lambda = p_s/p_r$ with $p_r = 0.1$ on the alternate social networks for different network size: $N = 5000$ (square), 10^4 (circle), and 10^5 (triangle up). Subfigures (a) and (b) correspond to SF sub networks and SW sub networks ($p = 0.001$), respectively. The values of other parameters are $N_0 = 10$, $n = 8$, and $[a, b] = [2, 6]$ for family network and $[50, 150]$ for public network with $\langle k \rangle = 10$.

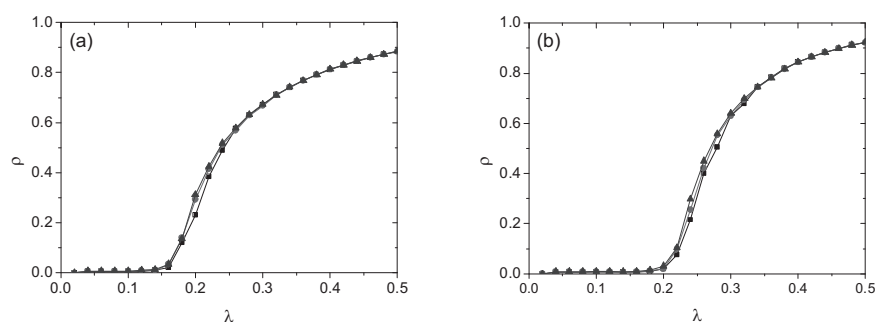


Figure 8: The fraction of ever infected individuals ρ as a function of the parameter $\lambda = p_s/p_r$ with $p_r = 0.1$ on the alternate social networks for different initial infected densities: $N_0 = 1$ (square), 5 (circle), and 10 (triangle up). Subfigures (a) and (b) correspond to the cases of SF sub networks and SW sub networks ($p = 0.001$) respectively. The values of other parameters are $N = 10^4$, $n = 8$, and $[a, b] = [2, 6]$ for family network and $[50, 150]$ for public network with $\langle k \rangle = 10$.

Finally, we studied the dependence of the diagram near the critical point with the system size (Figure 7) and the initial infected density (Figure 8), and found that a non-zero epidemic threshold exists, which is irrelevant with the finite size effect as well as the initial infected density. The results of Figure 7(b) and Figure 8(b) are different from that the epidemic threshold on SF network almost disappears (Pastor-Satorras and Vespignani 2001). It means that although SF networks are measured in real societies, the existence of certain kind of family networks prevents the spreading of the disease across the whole network.

4. CONCLUSIONS

This paper introduces an alternate social network of human interactions to study the dynamics of spread of SIR epidemic. This alternate social network consists of a family network and a public network, on which the spreading process takes place in turn. The alternate social network consists of a family network and a public network, simulating the human contacts during some time (e.g. nighttime when the human usually stays with family) and another time (e.g. daytime when the human usually stays in the public place such as workplace, school, shopping mall, etc.) respectively. And the spreading process takes place in turn on the family network with fully connected topology and public network with SW or SF characteristic. Both the family network and the public network are comprised of several sub networks which are assumed isolated from each other. The 'alternate' means that the spreading process will alternately go on either the family network or the public network when the network is active.

By means of many numerical simulations with the model, it is found that the influence of the topologies of the sub networks of the public network on the epidemic dynamics is very limited. This phenomenon indicates that epidemic spreading mechanism of the alternate social networks model is independent of the topologies of the sub public networks, i.e. SW and SF characteristics. We have also studied the oscillation behavior of the epidemic curves, which is dependent on the network active time span n . By examining the spreading processes on the family network and the public network respectively, it is concluded that the oscillation behavior happens when the network active time span n is more than the time that the spreading curve on the single family network reaches its peak. Besides, we compared the results with those on the single network based on SW and SF networks, and found that the oscillation behavior is unique for the alternate social networks. The influences of the system size and the initial infected density on the critical point were also investigated, and a non-zero epidemic threshold was found, in both of the cases of alternate SF networks and alternate SW networks. This result allows claiming that although SF networks are measured in real societies the existence of the family networks can prevent the spreading of the disease across the whole network.

REFERENCES

- Hethcote, H. W. 2000. The mathematics of infectious diseases. *Siam Review*, **42**(4), 599-653.
- Watts, D. J. and Strogatz, S. H. 1998. Collective dynamics of 'small-world' networks. *Nature*, **393**(6684), 440-442.
- Barabasi, A. L. and Albert, R. 1999. Emergence of scaling in random networks. *Science*, **286**(5439), 509-512.
- Pastor-Satorras, R. and Vespignani, A. 2001a. Epidemic dynamics and endemic states in complex networks. *Physical Review E*, **63**, 066117.
- Pastor-Satorras, R. and Vespignani, A. 2001b. Epidemic spreading in scale-free networks. *Physical Review Letters*, **86**(14), 3200-3203.

- Keeling, M. J. and Eames, K. T. D. 2005. Networks and epidemic models. *Journal of the Royal Society Interface*, **2**(4), 295-307.
- Moreno, Y. and Vazquez, A. 2003. Disease spreading in structured scale-free networks. *European Physical Journal B*, **31**(2), 265-271.
- Grabowski, A. and Kosinski, R. A. 2004. Epidemic spreading in a hierarchical social network. *Physical Review E*, **70**, 031908.
- Eubank, S., Guclu, H., Kumar, V. S. A., Marathe, M. V., Srinivasan, A., Toroczkai, Z. and Wang, N. 2004. Modelling disease outbreaks in realistic urban social networks. *Nature*, **429**(6988), 180-184.
- Meyers, L. A., Pourbohloul, B., Newman, M. E. J., Skowronski, D. M. and Brunham, R. C. 2005. Network theory and SARS: predicting outbreak diversity. *Journal of Theoretical Biology*, **232**(1), 71-81.
- Frasca, M., Buscarino, A., Rizzo, A., Fortuna, L. and Boccaletti, S. 2006. Dynamical network model of infective mobile agents. *Physical Review E*, **74**, 036110.
- Gross, T., D'Lima, C. J. D. and Blasius, B. 2006. Epidemic dynamics on an adaptive network. *Physical Review Letters*, **96**, 208701.
- Huang, C. Y., Sun, C. T., Hsieh, J. L., Chen, Y. M. A. and Lin, H. L. 2005. A novel small-world model: Using social mirror identities for epidemic simulations. *Simulation-Transactions of the Society for Modeling and Simulation International*, **81**(10), 671-699.

APPLICATION OF SOCIAL THEORY TO THE DEVELOPMENT PROCESS OF AN EMERGENCY RETRO-FITTING METHOD

MICHAEL HENRY¹ and YOSHITAKA KATO²

¹Department of Civil Engineering, University of Tokyo, Japan
mwhenry@iis.u-tokyo.ac.jp

²International Center for Urban Safety Engineering
Institute of Industrial Science, University of Tokyo, Japan
katoyosh@iis.u-tokyo.ac.jp

ABSTRACT

Post-disaster retro-fitting and repair operations are necessary in order to prevent further loss of life in the event of after-shocks and to restore infrastructure functionality. However, unpredictable conditions in the wake of a disaster make it difficult to quickly apply these operations due to the short-comings of the conventional retro-fitting methods. New technologies in the concrete industry should attempt to reduce technical demand and cost of retro-fitting operations while increasing adaptability, speed, and worker safety.

A new retro-fitting method utilizing fiber sheets with hydraulic resin is being developed to meet these requirements. The development has, thus far, focused on the general engineering aspects necessary to define the capability of the technology. However, this technology will require the input of not only engineers, but other social groups who will be involved in the utilization of the technology. Sociology of technology was studied in order to understand the technological innovation process and how interaction between social groups produces new technologies. Each social group relevant to the technology has its own perspective on how the technology should be developed. Therefore, to promote a development process which takes into account these different perspectives, the problems and solutions of these social groups should be considered by the innovator during the development process.

1. INTRODUCTION

Japan is constantly at risk from disasters such as earthquakes, and a high level of safety is necessary to ensure that infrastructure survives should a disaster occur. However, existing infrastructure is aging and the economic demand necessary to upkeep it is growing, resulting in a decrease in safety levels and an increase in susceptibility to disaster damage. As the number of weak structures increases, post-disaster retro-fitting and repair operations will also increase. These operations should be speedy and efficient in order to prevent further loss of life. However, conventional retro-fitting methods

are plagued by the need for heavy machinery and intensive operations, which not only make mobilization difficult, but restrict the people who can assist to a small set of trained workers. Retro-fitting methods which reduce the technical demand of the operations, as well as increase adaptability and worker safety, may enhance post-disaster recovery capability.

One such method currently being investigated utilizes fiber sheets with hydraulic resin as a wrapping material around damaged concrete members to increase structural performance. While this method shows promise from an engineering perspective, how to successfully develop and apply this innovation practically is a different problem. A retro-fitting method such as the one proposed will involve a wide range of actors for successful implementation: while engineers are concerned with mechanical performance, government officials may be interested in cost reduction or storage and distribution, and citizens may be concerned about the technical difficulty of application. These are just a few examples of how different social groups may view potential problems related with it.

In order to more fully understand the innovation process, this paper proposes the study of the sociology of technology. This social theory can be used as a means to study how technological development occurs as a negotiation between different social groups. First, the emergency retro-fitting method will be briefly introduced to provide a basic understanding of the work done by the innovators up to this point. Then the social theory background will be explained to show how the interaction between social groups drives the development process. Finally, the social model will be conceptually applied to the development process of the emergency retro-fitting method by considering the relationship between the relevant social groups and their unique problems and solutions.

2. EMERGENCY RETRO-FITTING METHOD

The new retro-fitting method should improve upon conventional methods. Steel plate jacketing requires heavy machinery and large scale operations, which are difficult to mobilize in the wake of a disaster, and full strength cannot be achieved quickly due to the extensive nature of the repair operations. Pre-cast panels come in fixed sizes, so they have little flexibility for the large variety of structural shapes and post-disaster scenarios. Fiber-reinforced plastic (FRP) jacketing is construction intensive, must be applied by a specialist, and requires time before full strength can be achieved.

Considering the short-comings of the conventional retro-fitting methods, the new retro-fitting method should attempt to meet the following criteria: not require the use of heavy equipment; be easily transported by people; utilize simple construction methods without specialized knowledge; achieve necessary performance within several hours; and be applicable without the use of heat or fire. By selecting these requirements, the simplicity and ease of application can be met, as well as improved safety for the workers and faster restoration of structural performance.

Based on these requirements, a repair method utilizing fiber sheets containing hydraulic resin was proposed. This method borrows from the medical industry, where plaster is wrapped around broken limbs in order to

provide strength and protect the bone during healing. Conceptually, the repair method would proceed as in Figure 1: after a structure has been damaged by a disaster, fiber sheets are wrapped around the structure and water sprayed to induce hardening, thus restoring structure performance.

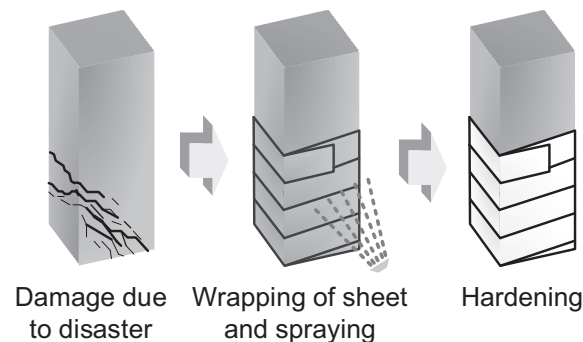


Figure 1: Conceptual application process of the fiber sheet method

Initial development utilized medical plaster as the wrapping material (Fig. 2). However, the strength of the medical plaster in its hardened state could not satisfactorily restore performance (Suzuki et al., 2008). As a result, a new material which combined multi-axial glass fiber sheets with high-strength hydraulic polyurethane resin was created (Fig. 3).

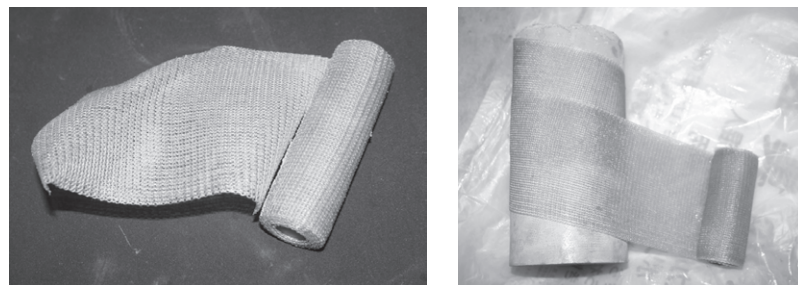


Figure 2: Medical plaster sheet and application

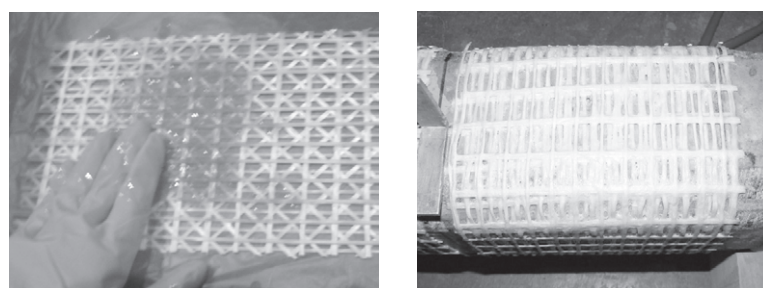


Figure 3: Fiber sheets with resin and application

Testing of the fiber sheets found that the material properties were satisfactory and, furthermore, the effect of retro-fitting can be quickly seen as the resin hardening period is short (Suzuki et al, 2008). The application method is simple, requiring only wrapping and spraying of water, and safe, as no special equipment is necessary. Finally, the material itself is relatively lightweight and easily handled. Therefore, the material meets the initial design criteria chosen based on the short-comings of the existing methods.

3. SOCIOLOGY OF TECHNOLOGY

Concrete technology has its own unique history of innovation and development. This technological development is carried out by human innovators; therefore, in order to understand how and why such development occurs, sociology of technology should be applied.

3.1 Social Construction of Technology

Social Construction of Technology (SCOT) is a theory used by sociologists of technology to explain technological innovations, and generally focuses on how new artifacts are shaped. In SCOT, technological development is driven by the interactions between relevant social groups, rather than other factors such as market demand. These social groups represent different perspectives on the problems related to the innovation process. As a result of these diverse interests, development of the artifact occurs as a negotiation between the social groups. Furthermore, the technology is considered fully developed when it is accepted as such by those who developed it. This section is an overview of Pinch and Bijker (1987); other references will be noted where necessary.

3.2 Formation of artifacts through social groups

A social group may be defined as an organization or group of individuals who all share the same perspective on an artifact. The relevant social groups can therefore be identified as those groups which possess some perspective on the artifact (Fig. 4). After the relevant social groups have been identified, they should then be described, in order to provide an understanding of their characteristics. This allows for a clearer insight into the function of the artifact as seen by each group.

From each social group, problems and solutions can be identified, as shown in Figure 5. Social groups may have different problems, or shared problems may have different solutions, thus leading to conflict in the development process. These problems may lie not only in the technical area, but in other areas as well, such as economic or legal. Furthermore, as the number of solutions is varied, the potential forms for the artifact is also quite large, depending on which problems and solutions are resolved.

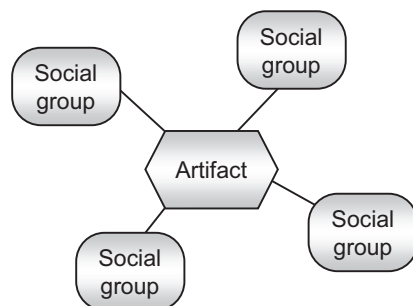


Figure 4: Relationship between artifact and relevant social groups

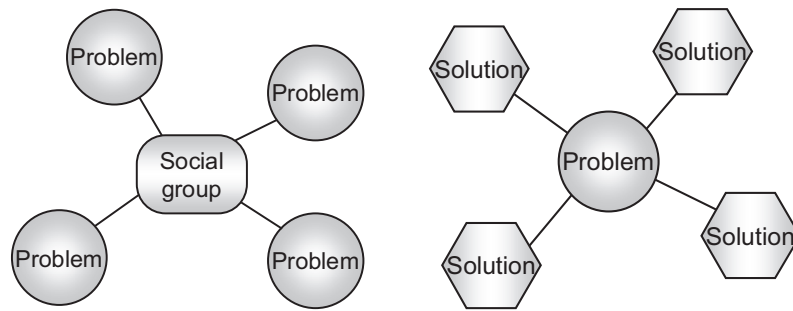


Figure 5: Relationship between a social group and its perceived problems (left) and a problem and its possible solutions (right)

An artifact has reached “closure” when the form of the artifact becomes stable and the problems are solved. However, it is not always necessary to solve all the problems; rather, the social groups just need to believe that the problems are solved. Closure can be achieved in many ways. One is rhetorical closure, which attempts to reach closure by convincing the social groups that the problem is solved by means such as advertising. Another way to achieve closure is by redefining the problem such that the artifact provides a solution to a problem which wasn’t considered before.

3.3 Heterogeneous engineering

If the social groups used for this analysis reach beyond the technical field, then this type of development may be “heterogeneous engineering.” This is a term proposed by John Law, who wrote that, in order to achieve successful innovation, innovators must be more than just engineers or scientists; that they needed to become “heterogeneous engineers” (Law, 1987). Heterogeneous engineers gather not only technical knowledge, but attempt to create networks which contain the people, skills, and artifacts necessary to achieve successful technological development. This network-building derives from Bruno Latour and Michael Callon’s “actor-network theory,” which studies the formation of networks consisting of both human and non-human actors during times of change (Latour, 2005). Successful engineering, as explained by Donald MacKenzie (borrowing from Law), involves building networks which bind together the human and organization with the technological (MacKenzie, 1987).

4. APPLICATION OF SOCIAL THEORY

This type of social analysis is typically performed in a descriptive manner; that is, it is applied retroactively to understand how an innovative process occurred. However, a prescriptive analysis could provide insight into how to guide future development.

4.1 Initial development (engineer’s perspective)

As explained in Section 2, the new retro-fitting method needs to solve several problems associated with the conventional methods. These are the

problems as seen from the perspective of the engineer (or innovator), so the relationship between the artifacts and problems can be drawn as shown in Figure 6. Based on this initial concept, a retro-fitting method utilizing medical plaster would solve these problems (Fig. 7).

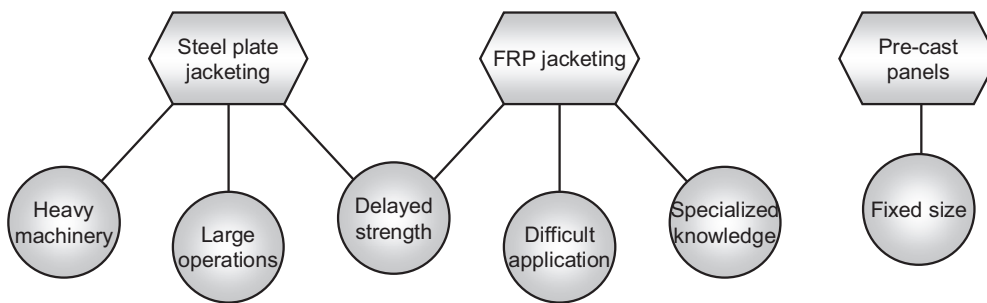


Figure 6: Problems with conventional retro-fitting methods

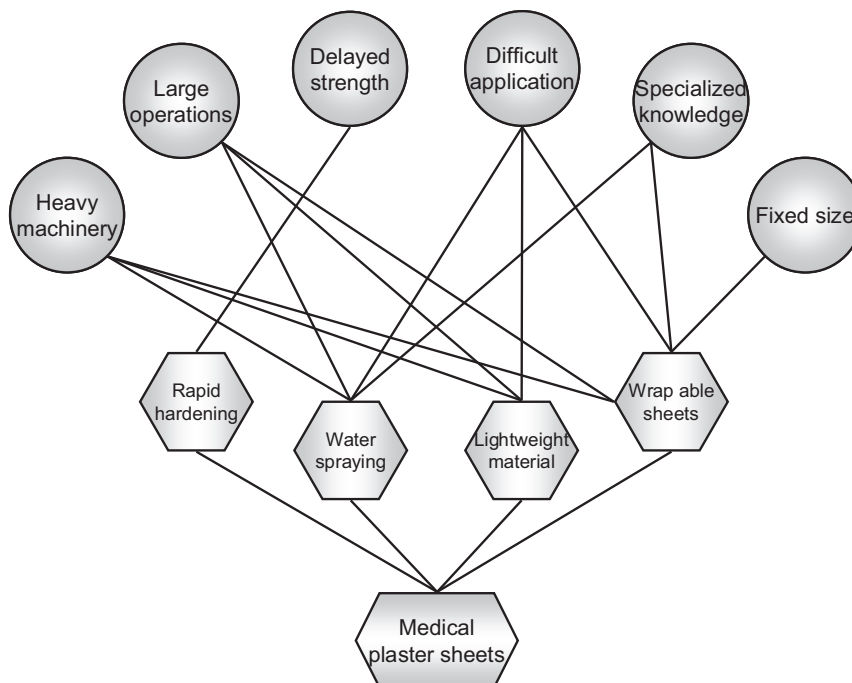


Figure 7: Medical plaster method and its related solutions

However, the medical plaster raised a new problem in the development process – namely, it failed to achieve satisfactory strength performance. Therefore, the glass fiber sheet with hydraulic resin was created in order to solve this problem (Fig. 8). Since the fiber sheets method shared the same characteristics as the medical plaster sheets, with the exception of improved material strength, it solved all the problems of the conventional methods as well.

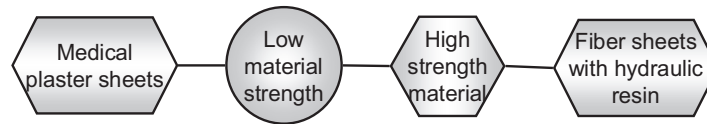


Figure 8: Problem with medical plaster and the fiber sheet solution

Initial development focused entirely on the perspective provided by the engineer. As a result, all problems and solutions have been proposed and solved based on the engineer's perspective, as shown in the preceding descriptive analysis. However, other relevant social groups will necessarily have their unique problems and solutions.

4.2 Future development (other social groups' perspective)

Heterogeneous engineering can promote successful technological innovation due to the integration of non-technical perspectives into the development process. By utilizing the perspective of the non-engineers into the development of the retro-fitting method, the final product will be a result of multiple perspectives. Furthermore, this is an important integration as other social groups will be relevant actors when applying the retro-fitting method in the practical situation.

Beginning with a new retro-fitting method, these social groups may not share the same perspective that engineers do. As explained in the previous section, from the engineering perspective the new artifact should improve upon the conventional methods; the problems with the conventional methods were also identified from the engineering perspective. However, other social groups may hold different problems. A simple, speculative example is given in Figure 9. Here, two additional social groups are introduced: the government official and the volunteer worker. From the perspective of the government official, the cost of the new retrofitting method will determine what solution it can provide. If the new retrofitting method is relatively cheap (a small percentage of the cost of conventional methods), then the government may opt to purchase a large stock of the material and store it for future disaster response. However, if the material is expensive (a high percentage of the cost of conventional methods), then it would be more difficult to purchase and store a large stock. Therefore, the government official might have two solutions: either redevelop the method using cheaper materials in order to reduce the cost, or to utilize the retro-fitting method on existing structures, in which case it would provide a cost-savings relative to the conventional methods. A volunteer worker's perspective is more focused on the interaction between the worker and the method, so ease of application of the retro-fitting method is the problem. Solutions may include minimizing technical skill (make it easy for the worker to perform with little training) or requiring only basic equipment (ease of mobilization and application).

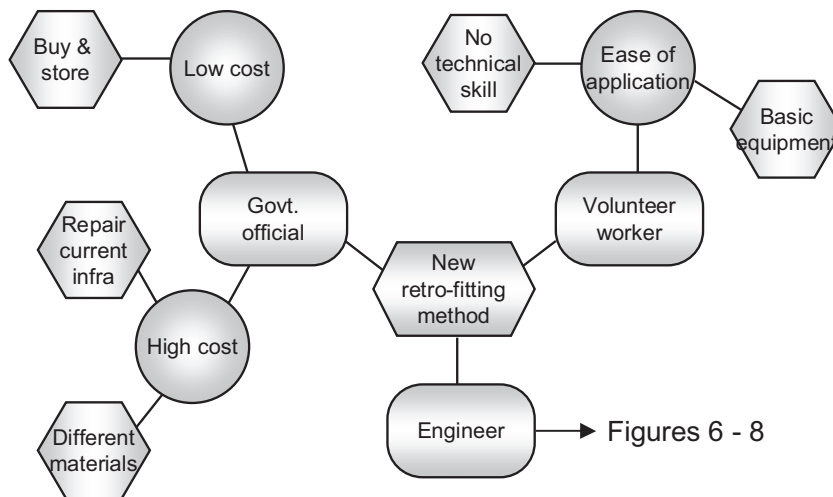


Figure 9: Example of different social groups' perspectives

4.3 Surveying the perspective of other social groups

In Figure 9, only three sample social groups are given, and the problems and solutions of each group are based on speculation. These areas can only be filled in by surveying the social groups to understand their unique problems and solutions. Once this survey has been performed, then a more comprehensive prescriptive analysis can be conducted by utilizing the full range of problems and solutions as provided by the social groups.

5. CONCLUSION

There is no assured path for success in technological development. However, sociologists of technology have found that creating a social network which includes not only technological but also non-technological aspects may help enhance the development process. This “heterogeneous engineering” approach is useful as the development process occurs as a negotiation between the problems and solutions of relevant social groups.

A method for examining the development of technological artifacts was applied to a new emergency retro-fitting method. When applied descriptively to the engineer’s perspective, it was shown how the problems with existing retro-fitting methods could be solved by attributes of the new method. However, the full usefulness of this analysis may be realized when combined with survey information from the perspectives of many different social groups. By plotting the problems and solutions as given by these groups, a path for technological development may be found which utilizes heterogeneous engineering from an early stage, thus increasing the diversity of input used in the development process. Although such survey data was not provided here, a framework was established which may be used, not only for this artifact’s development, but potentially any development process in which the artifact should reflect a wide range of perspectives.

ACKNOWLEDGEMENT

This research was supported by a financial grant from the Japanese Ministry of Land, Infrastructure, Transport, and Tourism (MILT) for the research and development of construction technology.

REFERENCES

- Latour, B. 2005. *Reassembling the Social*, Oxford Press, New York.
- Law, J., 1987. Technology and heterogeneous engineering. *The Social Construction of Technological Systems*, MIT Press, Cambridge.
- MacKenzie, D., 1987. Missile accuracy: a case study in the social pressures of technological change. *The Social Construction of Technological Systems*, MIT Press, Cambridge.
- Pinch, B. and Bijker, W., 1987. The social construction of facts and artifacts. *The Social Construction of Technological Systems*, MIT Press, Cambridge.
- Suzuki, R., Maehara, S., Ito, M., Kato, Y., 2008. Development of safety emergency retrofitting method for damaged structure by disaster – proposing the method and examination the possibility of the method. *University of Tokyo, Institute of Industrial Science Journal*, Vol. 60 No. 3, pp. 28-31. (in Japanese)
- Suzuki, R., Maehara, S., Ito, M., Kato, Y., 2008. Development of safety emergency retrofitting method for damaged structure by disaster – selecting material and effect of material property on repair effects. *University of Tokyo, Institute of Industrial Science Journal*, Vol. 60 No. 3, pp. 32-35. (in Japanese)

ROLE OF FIRE FORCES IN RESCUE AND ITS DEVELOPMENT TRENDS IN FUTURE

JIANFENG YANG^{1,2} and YINGCHUN CHEN²

Center for Public Safety Research , Tsinghua University, China

Hebei Baoding Fire Bureau, China

yjf08@mails.tsinghua.edu.cn

ABSTRACT

With the continuously development of social economy, the national industrialization and urbanization is increasing rapidly. All sorts of different public emergencies and disasters always occurred, while the community emergency rescue mission is getting heavier and heavier. Public security fire forces, as a major professional rescue forces play more and more important role in various rescue. At the same time it is also facing new opportunities and great challenges. This article analyses the feasibility of fire forces rescue in the community firstly. And then according to the influences of different rescue types, models, the disposal principles, difficulties, we try to discuss the development trend of diversification in the future rescue of fire forces and give some suggestions about the expanding ways of fire forces social functions during the emergencies and disasters.

1. INTRODUCTION

With the continuously development of social economy, the national industrialization and urbanization is increasingly rapid. All sorts of different public emergencies and disasters always occurred, while the community emergency rescue mission is getting heavier and heavier. In China, the main force of emergency rescue is the troops and the masses of the people under the leadership of the CPC. Fire forces are the major professional part among them which is equipped with all sorts of rescue equipments. Participating in emergency rescue of fire forces is also the need of social objective development, the need of increasingly disasters and urgent, difficult, dangerous heavy tasks. This article analyses the feasibility of fire forces rescue in the community firstly. And then according to the influences of different rescue types, models, the disposal principles, difficulties, we try to discuss the development trend of diversification in the future rescue of fire forces and give some suggestions about the expanding ways of fire forces social functions during the emergencies and disasters.

2. ANALYSIS OF FEASIBILITY OF FIRE FORCES PARTICIPATING IN EMERGENCY RESCUE

Social emergency rescue includes mainly of dangerous chemicals leaked, road traffic accidents, earthquakes and its secondary disasters, building

collapses, production safety accidents, air crashes, explosions and terrorist incidents etc. And in line with disposal of flood and drought, weather disasters, geological disasters, forest grassland fires and other natural disasters, mining, marine accidents, major environmental pollution, nuclear radiation accidents and public health emergencies, and so urgent, difficult, dangerous and heavy tasks And content. Fire forces participating in emergency rescue is the need of social development, mainly focuses on the following aspects:

2.1 Social Emergency Rescue is the Responsibility of Fire Forces

"Fire Law" clearly provides that: "Apart from completing fire fighting task, the fire forces should also participate in other disaster or accident rescuing work." This is the first time that the tasks clearly defined in law and it is also provides a powerful legal protection for the fire forces to be a leading agency for the implementation of a social rescue.

2.2 Fire Forces' Participating in Emergency Rescue is the Need of Increasing Disasters

In China's rapid economic development and social transformation process, fire forces' participate in the emergency rescuing is the need of increasingly prominent disasters and urgent, difficult, dangerous and heavy tasks development. Based on "Fire Law" relevant regulations, apart from completing fire fighting task, the fire forces should also participate in other disaster or accident rescuing work. For example: Hebei Baoding Fire Detachment accepted 119 alarm for 264 times from January 1st to June 20th in 2008. Among them the real fire fighting is actually only 146 times while there are 118 times that was participating in, such as toxic gas leakage, the tower crane rescue, traffic accidents, building collapse incident, accounting for 44.7% of the total. That is demonstrated that fire forces attend more social rescues more frequently than the fire fighting at present.

2.3 Fire Forces has Advanced Equipment

Emergency rescuing is a complex and dangerous social activity so it must have the necessary modern rescue equipment to complete the task. In recent years, each local fire detachment has been equipped with fire rescue vehicles, cited high car, lighting cars, anti-virus and anti-chemical warfare equipment, and detectors, life-saving, alert, plugging etc. Some detachments also have the special equipment for disposal of anthrax virus and other special disasters of. In addition, fire forces are on duty for 24 hours, so they can keep the effective implementation of social rescue.

2.4 Fire Forces has High-quality Team

Fire forces always maintain the structure of young contingent. In the style of discipline, it is rapid mobility, heroic tenacity and has the courage to dedicate them to the spirit. At the same time the team members have proficiency operational fire theory, rescue and fire fighting theory,

participated in the disposal of various disasters and can adapt to the continuing work of the durability and resistance to resist the interference of outsiders. These provided a powerful guarantee quality for the completion of the increasingly arduous and complicated task of the rescue.

2.5 Fire Forces' Participating in Emergency Rescue is the Need of International Development

Fire forces participate in emergency rescue is the international common practice. Such as fire forces in the United States assume most of the social emergency rescue mission. In the "9.11" incident rescue, fire forces played the most important rescuing role. Japanese "Fire Law" clearly defined that the fire forces should attend the social emergency rescue work and give out detail demand about the team members quality and equipments. In other countries such as France, Britain, Russia, Hong Kong, Singapore, fire forces are also responsible for different rescue and relief missions. Therefore, following the development of the world fire prevention trend, we must strengthen the construction of our country's fire forces social rescue work.

3. THINKING ON STRENGTHEN FIRE FORCES FUNCTION IN SOCIAL EMERGENCY RESCUE

3.1 Strengthen Emergency Rescue Organization and Establish 119 Command Systems

At present, our country's emergency rescue communication systems are all settled in regional. Government, fire bureau, police, traffic, earthquakes and other departments are all independent construction and development. There is not a unity social interaction communications system. Such situation is not suitable for dealing with serious disasters. Present existing emergency rescue departments can not guarantee the operation coordinately. They established their own command center and it is a waste of resources can not have great efficiency. Therefore, the establishment of a uniform social rescue organization and command system is critical and important. According to our country's circumstances, fire forces is the current core rescue forces, so establishing the Fire Services (119) as the main rescue Emergency Response communication system is the most suitable selection. And 119 command systems is formatted for a long time, the masses are all familiar with it. And it has the characteristic of rapid reaction, covering a wide range of different area and command high automation degree. So establishing 119-centered command system is the best choice for integrating current different government resources and finishing rescue tasks with high efficiency.

3.2 Strengthen the Construction of Professional Fire Troops to Meet Special Needs of Disaster Rescue Incidents

The main problems of our country's rescue system are: lack of integration; multiple inputs; function of one kind of rescue forces is single. In the emergency rescue system construction, government plays the main essential role. Development of fire forces is suitable to the needs of public functions of public security rescue and now it is the main force in the emergency rescue systems. While in the construction of fire troops, the professional fire troops are the key one. During the developing of professional fire troops, we must not only consider the need of objective reality but also the possibility of economic strength. In the large and medium-sized cities just like capitals in provinces, cities in the east part of our country, professional Fire Battalion should be established. While in the middle cities we can just do some adjusting and alternate the common fire troop to professional fire troop. In some of the underdevelopment economic cities should establish stronger professional fire defense classes. For example, in Baoding City of Hebei Province, the Fire Battalion established for eight years. And it has successfully disposed and participated in more than 200 poison gas leaking accidents and other special disasters rescue and always play key role in the rescue tasks finishing.

3.3 Scientific Training to Improve Rescue Level

In the current stage, in many places simulated training facilities are not established restrictedly in accordance with the standards because of the economic conditions. Then the special technical training courses can not be carried out. On the other hand, lack of actual combat training system and some unscientific training contents make it difficult to require the actual rescue training aim.

In order to strengthen the scientific fire training, first of all is to strengthen the theoretical study business. And the commanders at all levels need to strengthen the special disasters disposal theories especially dangerous goods and chemical gas properties, technical parameters and disposal of special professional knowledge. Second is to strengthen the training of tactical application. Social rescue training must make the "actual combat" as the center, highlight the technical application and should be targeted. The third is to strengthen scientific and technological training. During social rescue training, it is necessary to pay attention to the training methods' scientific, but also pay attention to the training contents' scientific. The fourth is to strengthen disaster relief plans making.

3.4 Accelerating the Construction of Special Equipments in Professional Fire Troops

Fire forces have been equipped with some special advanced equipment, but there are still a wide gap compared to the actual combat and rescue's needs. One is the equipments number, the other is the rescue equipment's performance is lagged behind the requirements of actual combat.

In the equipment construction we must highlight the idea "first is to save people". So that the governments at all levels should increase the fire rescue equipment construction input according to the "city fire station construction standards", and it should be suited with the economic development and social needs. First, we should enhance the equipments just like life detector, dumping, life-saving campaign and search and rescue dogs, rescue helicopters and so on. And we must pay attention to advanced technology and comprehensive disposal capacity of the new equipment. The third is to strengthen the existing equipment's innovation and excavating their deep potential.

3.5 Strengthen the Cross-linked Capability to Form Social Rescue Joint Forces

Social rescue is a complex system involving all aspects of society departments and units. So we must strengthen the unified organization of all aspects of command and coordination.

The first is the establishment of local command center under the leadership of the government. Secondly, the fire forces should take the initiative to strengthen collaboration and cooperation with local industries, departments and units of other social rescue forces. The third is to strengthen the inter-regional fire rescue operations. Finally, simulation training should be strengthened.

4 Development Trend of Fire Forces Rescue

4.1 Establishing Social Emergency Rescue System and Making Fire Forces as the Public Security Main Forces

During the emergency management planning making, it is necessary to clarify that fire units is the backbone of the team development. Secondly, the fire units is the current implementation of a social emergency forces, it is located throughout the large and medium-sized cities and towns. So we should manage fire, rescue, and ambulance together as soon as possible. Thirdly, strengthen fire forces' comprehension system in organization and management.

4.2 Seeking Diversified Development of Fire Forces and Making Duty Fire Brigade as the Main Forces

Most developed countries have implemented professional fire forces policy, and the implementation applied both in active duty and career fire system. However, there is a huge team of volunteer firemen is the common feature. At this stage, in order to meet the arduous task of emergency relief, the coexistence of active duty, the contract system and volunteer fire system have obvious advantages.

4.3 Integrating Existing Disaster Relief Resources and Letting Fire Forces Playing a Key Role

Integrating different rescue resources and establishing more contacts among them, so they can apply emergency rescue management mechanism well during the wartime. Establishing rapid deployment system for emergency rescue equipment and materials reserves. Integrating social information resources can shorten the rescue time and increase rescue proficiency.

REFERENCES

- Fu Libing, 2006. Study on the Function and Position of national firefighting force in construction of emergency rescue force system. *Science and Technology of West China* 26, 72-76.
- Zhang Yichao, 2005. The conditions and strategy for national firefighting force to be engaged in rescue and aid operations. *Fire Technique and Products Information* 10, 10-13.
- Shi Jianchang, 2005. Study on the development of emergency rescue function of the fire troop. *Fire Science and Technology* 3, 85-86.
- Fang Jiang Yuan, Xu Tong, 2006. The establishment and development of a socialized emergency management system with firefighting force as the main body. *Fire Technique and Products Information* 3 42-44.
- Gu An-yong, Sui Hu-lin, Liu Hai-xia, 2005. Discussion on construction of the national fire and rescue emergency integrated communications system. *Fire Science and Technology* 2, 93-95.

DEVELOPMENT OF EMERGENCY RETROFITTING METHOD USING FIBER SHEETS CONTAINING HYDRAULIC RESIN

MASAMITSU SUZUKI¹, RYO SUZUKI²
MASANORI ITO³ and YOSHITAKA KATO⁴

¹Architecture and Civil Engineering,
Shibaura Institute of Technology, Japan

²East Japan Railway Company, Japan

³Tokyu Construction, Japan

⁴International Center for Urban Safety, IIS, University of Tokyo, Japan
m-suzuki@iis.u-tokyo.ac.jp

ABSTRACT

A new emergency retrofitting method for disaster-damaged structures is proposed utilizing fiber sheets containing hydraulic polyurethane resin. The simplicity, speed, and safety of this repair system make it feasible as a recovery technology. Compressive and bending tests were conducted on damaged specimens repaired utilizing medical gips (plaster cast) applied in different ways. It was found that application is simpler when the sheet edge is not fixed. In addition, performance was improved when the sheet rolls were continuously applied. However, the plaster cast used in medical care was found to not be applicable as a repair material due to low strength. Therefore, a new material composed of glass fiber sheets containing hydraulic polyurethane resin was developed and tested. Compressive and bending tests were conducted on specimens repaired using different resin and sheet types to examine the effect of material properties on repair performance. It was found that, when there is adhesion between the fiber sheet and the specimen, there is a large effect on the repair performance of high strength resins. For the non-adhesion case, resin strength was found to have no effect.

1. INTRODUCTION

In Japan, the importance of aseismic reinforcement in concrete structures was realized after the Hanshin/Awaji great earthquake disaster of 1995. Aseismic reinforcement improves ductility primarily by avoiding the brittle "shear fracture" which occurs in column members. Main transportation and emergency transportation roads in the Tokyo metropolitan area are mostly reinforced by this method; however, there are still many structures which may suffer serious damage due to the scale of the earthquake. In addition, new structures cannot avoid damage, as they are designed to permit some damage during a large-scale earthquake. When structures are damaged by natural disasters, they require emergency retrofitting to ensure safety and functionality. Conventional methods, however, cannot adequately cope with

subsequent aftershocks, and large-scale repair works are time consuming. The purpose of this research is to develop a new retrofitting method which can be applied quickly, easily, and safely in the wake of a natural disaster.

2. CONCEPTUAL METHOD

2.1 Repair material and construction method

The development of an emergency retrofitting method should attempt to satisfy the following requirements: to be applied quickly, easily, and safely. Therefore, the authors proposed a new emergency retrofitting method which provides the repair by wrapping fiber sheets containing hydraulic polyurethane resin around the damaged RC column and spraying with water to begin hardening. This concept is illustrated in Figure 1. The idea of this method borrowed from the application of plaster cast used in medical care, shown in Figure 2. The conventional plaster cast used in medical care combines plaster of Paris and cotton cloth. However, in recent years a product made of fiber sheet containing hydraulic polyurethane resin is becoming the mainstream.

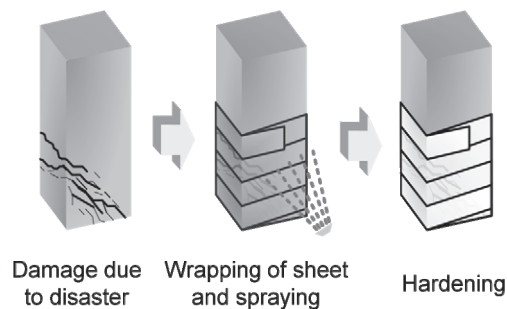


Figure 1: Summary of conceptual method



Figure 2: The plaster cast used in medical care

The hydraulic polyurethane resin can harden in several minutes after coming in contact with water, so the effect of repairs can be seen quickly because time to resinous hardening is short. Safety is high because hardening requires only water application. The fiber sheet is lightweight and can be wrapped around structures of various forms. Large-scale machinery is unnecessary since the only construction is wrapping. As a result the construction is simple and easy, and can be performed quickly. The fiber

sheets have been used for aseismic reinforcement and prevention of cover concrete spalling in tunnels, so it is a reliable material with proven results.

This method utilizes the fiber sheet containing hydraulic resin as a finished product. By utilizing a manufactured product, construction time is reduced compared to conventional methods since it is not necessary to apply an adhesive to the structure or to perform extensive preparations. Also, since the quality of the material, such as resin thickness, is controlled during the manufacturing process, the reliability of the fiber sheets should be high.

2.2 Target structures

Structures which suffer from shear fracture or bending shear fracture are the target structures for this method. In columns which suffer shear fracture, the horizontal stress suddenly falls after the maximum stress. In addition, the column undergoes cyclic horizontal load due to earthquake motion while under axial load so the axial stress falls. Concrete which fractures in shear loses concrete cover and the reinforcing steel buckles, but concrete under bending fracture has higher toughness because the safety factor for bending is higher. In past disasters, structures in which bending fracture was observed were still usable even without emergency repair measures. However, structures which fail in shear need extensive repair. Therefore, this method is applicable to columns which suffer shear fracture or bending shear fracture. The method shall be applied at damage levels which do not reach collapse.

3. TESTING OF MEDICAL PLASTER

The development of the retrofitting method is important for understanding how the different methods of construction and materials have an influence on the effect of repairs. The goals of the initial investigation were to examine the feasibility of the method and to identify construction factors which may affect the repairs. Medical plaster (casting tape) was utilized in these initial experiments. Since casting tape is a medical product, the authors believed it may not be easily transferred to application at the construction site; however, since fiber sheets containing hydraulic resin are already available and in use, the handling was found to be convenient.

3.1 Property of casting tape

The casting tape is knitted from glass fiber in the horizontal and vertical directions, and greatly elongates when tension is applied in the horizontal direction (Fig. 3). When utilizing the casting tape as a repair material, its performance may differ depending on whether the tape was placed in tension before hardening. A tensile test was performed to compare the strength of hardened tape without tension versus that with tension. From the result of this test, the characteristics of the casting tape in tension, as it would be when wrapped around the structure, were found to be satisfactory.

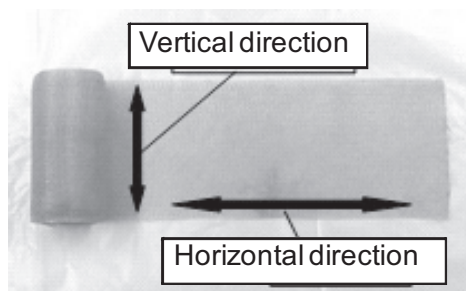


Figure 3: Casting tape

3.2 Experiments utilizing medical plaster

3.2.1 Experimental procedure

The restraining effect in the cross direction using the casting tape was confirmed by compressive toughness test of repaired the cylinder specimens. The shearing repair effect was also confirmed by the bending shear test on repaired the prism specimen. Geometries of cylinder and beam specimens are shown in Figure 4. When performing the experiment, first specimens were given damage by loading. The loading was performed to a maximum load point, and then the specimen was unloaded. Next, the damaged specimens were repaired by wrapping the casting tape. Immediately after wrapping, the specimen was submerged in water and soaked for around 1 minute to harden the polyurethane resin. Specimens were then removed from the water and allowed to harden further for around 20 minutes. Then the ends of the casting tape were fixed by the prescribed method, as explained in the next section. Specimens were loaded again after 1 hour.

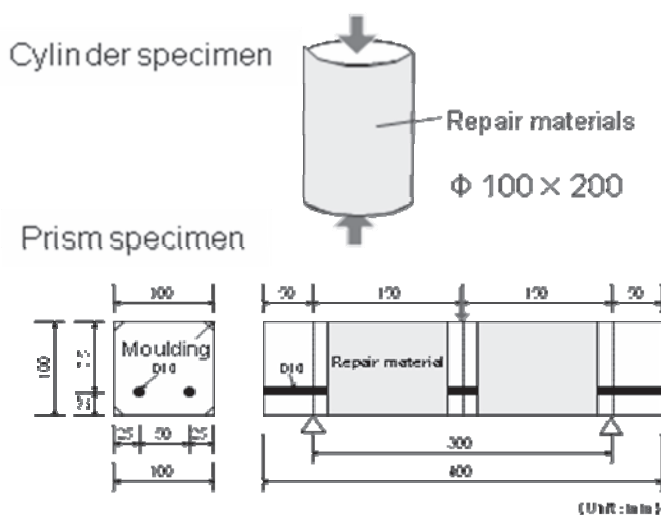


Figure 4: Specimen configuration

3.2.2 Test Result

3.2.2.1 End anchorage

Three methods of end anchorage method were examined: epoxy resin, pp-band, or no anchorage (Fig. 5). Normalized load-displacement behavior

of specimens by different end anchorage is shown in Figure 6. Normalized load is calculated by dividing the repaired specimen load by the maximum load without damage. For epoxy resin and pp-band specimens, the maximum load was slightly higher than the no anchorage case before the second incline (incline after load-displacement relations changed). This indicates that there was a restraining effect from the epoxy resin and pp-band. However, the effect of end anchorage on repair performance was relatively small, as load and displacement at when the sheets broke were almost the same for all three cases. As a result, the no-anchorage method is preferable because it is simple and easy, and provides the same repair effect.

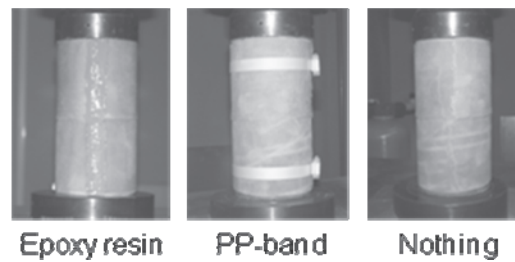


Figure 5: End anchorage

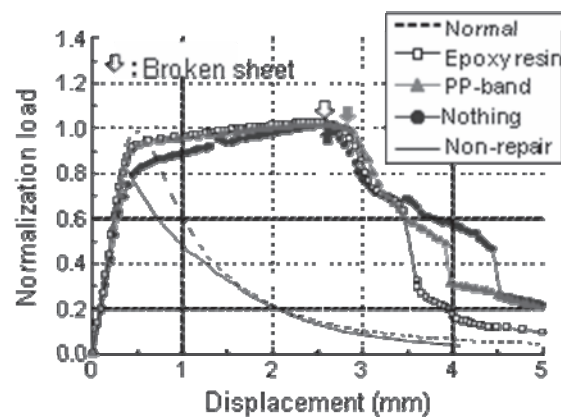


Figure 6: Normalized load-displacement behavior of specimens with different end anchorage

3.2.2.2 Wrapping continuity

Two wrapping methods were examined. Non-continuous wrapping used one sheet per sheet width with no overlap longitudinally. Continuous wrapping used one sheet continuously, with the sheet wrapping at an angle and spiraling upwards (Fig. 7). Normalized load-displacement behavior of specimens with different continuity is shown in Figure 8. From this result, it was found that sheet continuity had an influence on the maximum load before yielding. The continuous-wrapping specimen kept the initial modulus and exceeded the maximum normalized load of the non-repaired specimen – nearly 1.0 versus 0.82, respectively. It was concluded that for continuous wrapping the maximum load rose because there was no gap at the center of the specimen due to the overlap in wrapping.

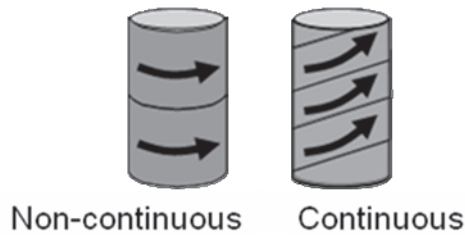


Figure 7: Wrapping continuity

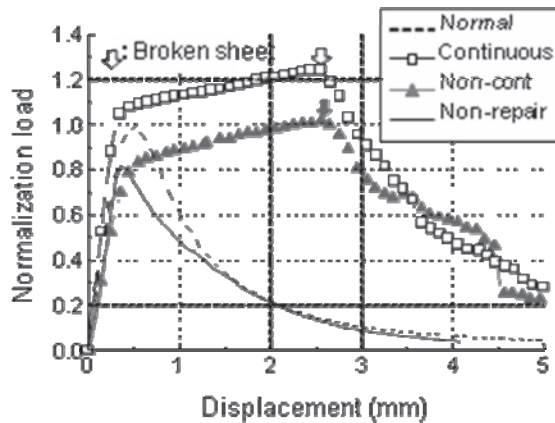


Figure 8: Normalized load-displacement behavior of specimens with different wrapping continuity

3.2.2.3 Concrete adhesion

It was found that adhesion with the concrete influenced the shearing repair effect from the previous test result. However, not all specimens could confirm improved ductility under after repair as the load suddenly fell after exceeding the maximum load. This led to the belief that the strength of the casting tape is not sufficient.

4. DEVELOPING A NEW REPAIR MATERIAL

As a result of the previous experiments, it was found that the casting tape was brittle and inappropriate as a repair material. Glass fiber and hydraulic polyurethane resin were chosen as new repair materials.

4.1 Hydraulic polyurethane resin

Two hydraulic polyurethane resin mixes, resin-A and resin-B, were created by diluting pure resin with water. The reaction of resin and water was observed and resinous strength measured. From the experimental result, resinous strength was confirmed to decrease with increasing dilution. Solutions with 80% resin were found to foam, but in 75% solutions no foaming was observed, so 75% was set as the maximum dilution factor.

Resin-A, mixed at 75%, was called high-strength; resin-B, mixed at 50%, was called low-strength.

4.2 Glass fiber sheet

Glass fiber sheets were composed of glass fibers arranged in different orientations (Fig. 9). Fibers in the 2-axes mesh were arranged at right angles in the longitude-latitude directions. Fibers in the 4-axes mesh were arranged with two axes at right angles in the longitude-latitude direction with two more axes of fibers at forty five-degrees. The mechanical properties of the glass fiber as given by the manufacturer are shown in Table 1.

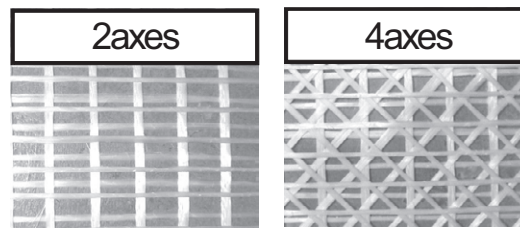


Figure 9: Glass fiber sheet

Table 1: Mechanical properties of glass fiber sheet

| Direction | Tensile strength [N/mm ²] | Failure strain [%] | Modulus of elasticity [N/mm ²] |
|-----------|--|-----------------------|---|
| Horizon | 883 | 2.0 | 4.42×10 ⁴ |
| Vertical | 1274 | 2.0 | 6.73×10 ⁴ |
| Diagonal | 954 | 2.0 | 4.77×10 ⁴ |

4.3 New product development

The new repair material was produced by containing hydraulic polyurethane resin in the glass fiber sheet. Testing of the bond with concrete was conducted with sheet type and resin strength as experimental factors. The results are given in Table 2. The interface detachment fracture energy for design is set at 0.5 N/mm² by the sheet reinforcement guidelines; however, test specimens exhibited higher fracture energy. Therefore, the new repair material has enough adhesion force even if surface treatment is not performed beforehand.

Table 2: Bond test result

| Resin strength | Sheet | Muximum load [kN] | Fracture mode | Interface detachment fracture energy [N/mm] |
|----------------|-------|----------------------|------------------------------|--|
| Low | 2axes | 6.5 | nterface detachment fracture | 0.60 |
| | 4axes | 6.49 | sheet fracture | — |
| High | 2axes | 9.88 | nterface detachment fracture | 1.37 |
| | 4axes | 7.2 | sheet fracture | — |

5. TESTING OF NEW MATERIAL

5.1 Experimental procedure

In order to understand the influence of the new material on repairs, compressive toughness test was performed with repaired cylinder specimens (Fig. 4). In addition, the effect of repair on shear was measured by the bending shear test on repaired prism specimens (Fig. 10). For each test the experimental variables were the resin strength and adhesion. Before repairing, damage was given to the specimens by unloading at 80% of maximum load.

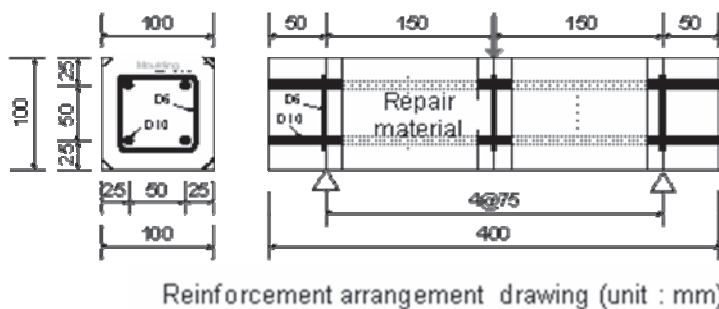


Figure 10: Geometry of shear specimens

5.2 Result

5.2.1 Compressive toughness

From the resin strength results, the resin strength was much smaller than the sheet strength; therefore, it was thought that the influence of the resin strength was small. Comparing the sheet type results, 2-axes sheet had a higher repair effect than 4-axes sheet, so the diagonal fibers did not show a restraining effect. Influence of adhesion on repair was unconfirmed.

5.2.2 Bending toughness

Normalized load-displacement behavior of specimens with different adhesion (4-axes, low-strength) is shown in Figure 11. Adhesion specimens showed higher maximum load than non-adhesion specimens. For non-adhesion specimens, the second incline after the maximum load was less steep. Therefore, the effect of adhesion is not clear when shear repair is necessary to recover ductility behavior. 2-axes specimens had similar results.

Normalized load-displacement behavior of specimens with different resin strength (4-axes) is shown in Figures 12 and 13 for adhesion and non-adhesion, respectively. The influence of resin strength was different depending on the adhesion condition. The largest effect could be seen for the 4-axes and adhesion case. When applying the 4-axes sheet, adhesion along the axis in the diagonal direction ran almost perpendicular to the shear cracks, so the adhesion strength provided a repair effect. For the 4-axes and non-adhesion case, the influence of resin strength was small. The resin strength does not affect the tensile strength in the axial direction, which would explain why no strength effect was seen in this case.

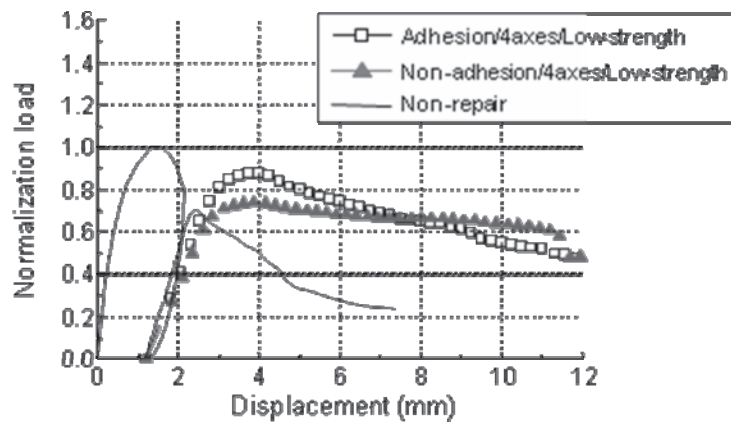


Figure 11: Normalized load-displacement behavior of specimens with different adhesion

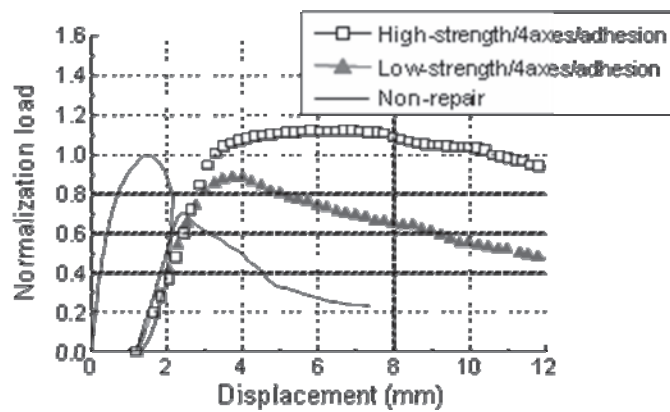


Figure 12: Normalized load-displacement behavior of specimens with different resin strength (adhesion)

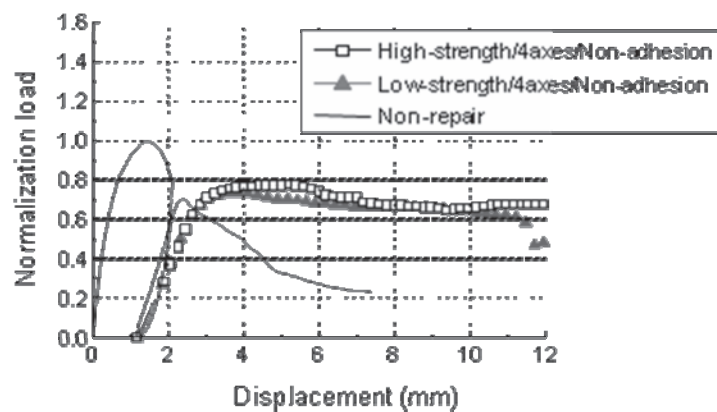


Figure 14: Normalized load-displacement behavior of specimens with different resin strength (non-adhesion)

6. CONCLUSION

A new retrofitting repair method using fiber sheets containing hydraulic resin was proposed. An initial investigation was performed utilizing medical plaster as a wrapping material. However, the mechanical property was not satisfactory for repair application so a new product was developed. This new material was created from glass fibers arranged in sheets and containing hydraulic resin. A retrofitting method utilizing this product would not require large-scale machinery and the only construction operation would be wrapping of the sheet. Therefore the construction is simple and each can be performed quickly. In addition, the effect of repairs can be seen quickly as the time to resin hardening is short. Finally, the safety of this method is high because the hardening process only requires the application of water, so no dangerous methods such as fire are necessary. However, whether adhesion is necessary between the concrete and the sheet is not entirely clear. In the adhesion case, the influence of resin strength on repair effect is large, but in the non-adhesion case the influence of resin strength is small.

ACKNOWLEDGMENT

This research was supported by a financial grant from the Japanese Ministry of Land, Infrastructure, Transport, and Tourism (MILT) for the research and development of construction technology. The authors would also like to thank Mitsui Chemicals Polyurethanes, Inc., Nippon Electric Glass Co., Ltd., and Tokyu Construction Co., Ltd. for their research support and Michael Henry for his help during the composition of this report.

REFERENCES

- JSCE., 2000. Concrete library 101. *The repair and reinforcement guidelines of concrete structure using fiber sheet*, JSCE, Japan.
- Suzuki, R., Maehara, S., Ito, M., Kato, Y., 2008. Development of safety emergency retrofitting method for damaged structure by disaster - proposing the method and examination the possibility of the method. *University of Tokyo, Institute of Industrial Science Journal*, Vol. 60 No. 3, pp. 28-31. (in Japanese)
- Suzuki, R., Maehara, S., Ito, M., Kato, Y., 2008. Development of safety emergency retrofitting method for damaged structure by disaster - selecting material and effect of material property on repair effects. *University of Tokyo, Institute of Industrial Science Journal*, Vol. 60 No. 3, pp. 32-35. (in Japanese)

ASSESSMENT OF EMERGENCY RESPONSE POLICY BASED ON MARKOV PROCESS

YAFEI ZHOU and MAO LIU
Research Center of Urban Public Safety,
Nankai University, Tianjin, 300071, P.R China
zhouyafei@mail.nankai.edu.cn

ABSTRACT

Major accidents can induce many adverse effects, they will not only endanger the health and safety of the population, but also bring bad influence to the environment around. In order to reduce the casualty and property losses caused by the accident, we should mitigate its adverse effects. One of the most important aspects of mitigating the adverse effects caused by the accident is the restriction of the exposure of the population to the ensuing extreme phenomena (e.g. fallout, toxic clouds, thermal radiation, overpressure, fragments etc.). In order to mitigate the adverse effects caused by the accident, emergency response policy (ERP) and corresponding protection action should be established. To maximize its effectiveness, ERP should be evaluated and optimized, while the most important criteria to evaluate the ERP is minimizing the health consequence of the accident.

A discrete state stochastic Markov process was used to simulate the movement of the evacuees in this paper. The study area was divided into nodes with different shape and size, the links that connected the nodes were used to represent the road network in the area. Transition from node-to-node was simulated as a random process where the probability of transition depended on the dynamically changed states of the destination and origin nodes and also on the link between them. Solution of the Markov process provided the expected distribution of the evacuees in the nodes of the area as a function of time. Then, according to the way how extreme phenomena impact individual and the dose-response relationship, the people's health effects (e.g., death, several kinds of injuries etc.) obtained in the evacuation process can be calculated, so that the accident's health consequence can be determined. Finally, different emergency response policies can be evaluated with corresponding health consequence, so that the emergency policy can be optimized.

1. INTRODUCTION

The industrial equipments that use hazardous materials (toxic, flammable, explosive) and nuclear power plant will induce major accidents potentially, this will not only endanger the health and safety of the population, but also have a negative impact on the environment. The protection-action of such

incidents is to stop them occurred and to mitigate their adverse effects after the accidents happened. An important aspect to mitigate adverse effects of the accident is to limit the number of people who exposed to extreme phenomena (such as radioactive fallout, poison gas cloud, thermal radiation, overpressure, debris).

In order to ensure the effectiveness of protective actions, it's necessary to assess the Emergency Response Policy (ERP) according to the degree of various consequences caused by the accident. One of the most important criterions in ERP assessment is to minimize the health consequences of the accident. If protective actions include evacuation, one of the most important factors in estimating the health consequences accurately is to estimate dynamic displacement of the population in risk realistically. The aim here is to simulate the dynamic movement of the crowd, so that the emergency plan can be optimized according to the health consequences (minimum), while the optimization of the evacuation routes in accordance with the minimization of the migration cost will not be discussed in this paper.

Evacuation simulation of emergency situations such as chemical and nuclear accidents, as well as, natural disasters such as hurricanes, floods, volcanoes, earthquakes and forest fires, has been extensively studied and reported. Southworth has conducted a comprehensive review of region evacuation model, summed up that the information of transport structure, the spatial distribution of population, the use of vehicles in emergency situations, the individual response time to emergency circumstances, the choice behavior of evacuation routes and destination, etc. were needed in the simulation of large-scale evacuation of the population. Lee D.Han simulated emergency traffic evacuation around a nuclear power station in Tennessee with VISSIM which is a microscopic traffic simulation system based on time and behaviors. Cova et al. proposed an approach of evacuation paths based on driveways. Church and Sexton studied the influence mode of traffic conditions on evacuation time. Most of the evacuation models are used in the plan formulation stage, some models provide traffic information as a time of function, while others are based on simulation models initially designed for traffic problems.

In this paper, a discrete state stochastic Markov process modified by Paraskevi et al. was used to simulate the movement of the population and calculate spatial and temporal distribution of the population in evacuation, so that the ERP can be evaluated according to health impact of the accident. This paper consists of five sections. Section 2 describes the stochastic Markov model which would be used to simulate spatial and temporal distribution of the population. Section 3 presents the evaluation process of health consequences. Section 4 offers a numerical solution of the Markov model and discusses calculation of the health consequences through a case study. Finally, the section 5 offers a summary and the conclusion of the work.

2. STOCHASTIC EVACUATION MODEL

Basic elements of the model are as follows:

The study area is divided into N sub-regions, which are called grid nodes;

One node represents a geographical area which is artificially determined, the size and shape of the area can be changed according to requirement while not require the same division. That is, a node is not required to correspond to a single structure or function area of the real world, it can represent a region that contains one or more buildings.

The nodes are connected between each other by links. The link can be a road that connects two building blocks. If the node corresponds to more than one building block, then the link represents the capability of connection of two adjacent nodes.

The model introduces the concept of transition probability rate $a_{ij}(t)$, which is the probability rate of an individual transferring from node (i) at time t to node (j) at time $t + \Delta t$. It satisfies the following conditions:

$$\sum_{i,j=1}^N a_{ij}(t) = 0, a_{ii}(t) = -\sum_{\substack{i=1 \\ i \neq j}}^N a_{ij}(t), a_{ij}(t) > 0 (\text{if } i \neq j)$$

The probability $a_{ij}(t)$ depends on the travel time between node (i) and node (j), i.e. the individual prefers to choose destinations that have shorter travel time. Calculation of $a_{ij}(t)$ can be divided into two cases of no congestion and congestion, the processes are as follows respectively:

① With no congestion:

$$a_{ij}(t) = \frac{U}{d_{ij}} (i \neq j) \tag{1}$$

Where,

U- is the average speed of vehicles;

d_{ij} - is the length of the link between node (i) and node (j);

$a_{ij}(t)$ equals to zero if node (i) is not connected to node (j) or if there are constraints.

② With congestion:

$$a_{ij}(t) = \begin{cases} \left(\frac{U}{d_{ij}} \right) [1 - r_i(t)] [1 - r_j(t)] & \text{if } i \neq j \\ -\sum_{\substack{j=1 \\ i \neq j}}^N a_{ij}(t) & \text{if } i = j \end{cases} \tag{2}$$

Function $r_i(t)$ is congestion level of node (i), it can be calculated with the following formulation:

$$r_i(t) = \begin{cases} r_{\max} & \text{if } n_i(t) \geq cM_i \\ r_{\max} \left[1 - \exp \left(\frac{-n_i(t)}{M_i - n_i(t)} \right) \right] & \text{if } n_i(t) < cM_i \end{cases} \tag{3}$$

Where,

$n_i(t)$ – is the number of vehicles participating in the evacuation in node (i) at time t $\{n_i(t) = x_i(t) \cdot n_T\}$;

$x_i(t)$ – is the probability of the individual (or vehicles) appearing in node (i) at time t $\{0 \leq x_i(t) \leq 1\}$;

n_T – is the total number of vehicles participating in the evacuation;

r_{\max} , c – are parameters impacting individual (or vehicles) behavior ($r_{\max} < 1, c < 1$);

M_i – is the maximum capacity of node (i).

This paper aims at solving the crowd evacuation under congestion.

The movement of population is simulated randomly with the stochastic Markov model, selection of next node and link is based on traffic information of the current node and link. The model can be described with the following formulation:

$$\dot{x}(t) = x(t) \cdot A(t) \tag{4}$$

Where,

$x(t)$ – is an $1 \times N$ vector with elements $[x_i(t)]$;

$\dot{x}(t)$ – is an $1 \times N$ vector with elements $\left[\begin{matrix} \dot{x}_i(t) \end{matrix} \right]$;

$A(t)$ – is a $N \times N$ vector with elements $[a_{ij}(t)]$;

$\dot{x}_i(t)$ – is the derivative of $x_i(t)$ with respect to time;

Δt – is time interval.

Eq. (4) can be solved through discretizing the time of transitions as follows:

$$x(n+1) = x(n)P(n) \tag{5}$$

Where,

$x(n)$ – is a $N \times N$ vector with elements $x_i(n)$;

$x_i(n)$ – is the probability that an individual (or vehicles) participating in the evacuation is in node (i) in the interval Δt_n , Δt_n is the interval between time t_n and time $t_n + \Delta t_n \{n = 1, 2, \dots, T\}$;

$P(n)$ – is a $N \times N$ vector with elements $P_{ij}(n)$;

$P_{ij}(n)$ – is the transition probability of an individual from node (i) at time $t_n = n \cdot \Delta t$ to node (j) at time $t_{n+1} = (n+1) \cdot \Delta t$ $\left\{ 0 \leq P_{ij}(n) \leq 1 \text{ and } \sum_{i,j=1}^N P_{ij}(n) = 1 \right\}$;

n – is the current time step $\{n = 1, \dots, T\}$;

T – is the total number of time steps considered $\{T = T_e / \Delta t\}$;

T_e – is the total time considered for the evacuation simulation.

The transition probability $P_{ij}(n)$ can be calculated with the following formulation:

$$P_{ij}(n) = \begin{cases} \frac{a_{ij}(t)}{\sum_{\substack{j=1 \\ i \neq j}}^N a_{ij}(t)} \left[1 - \exp \left(- \sum_{\substack{j=1 \\ i \neq j}}^N a_{ij}(t) \cdot \Delta t \right) \right] & \text{if } i \neq j \\ \exp \left(- \sum_{\substack{j=1 \\ i \neq j}}^N a_{ij}(t) \cdot \Delta t \right) & \text{if } i = j \end{cases} \quad (6)$$

The residual population changing with time in the evacuation region and the total time required to complete the evacuation can be obtained after solving the stochastic Markov model.

3. ASSESSMENT OF HEALTH CONSEQUENCES

One of the most important criteria in ERP assessment is to minimize the consequences caused by the accident. Here the stochastic Markov model was used to evaluate the population distribution that changes with time, so that people’s health consequences can be estimated. In this article, poison gas leakage was selected as an example to assess health consequences of the accident.

An individual’s absorption dose at node (i) in interval $\Delta t_n (t_n < t < t_n + \Delta t_n, n = 1, \dots, T)$ was assumed as a constant, which can be calculated using the non-linear relationship of toxic load and exposure concentration and time. It can be shown as follows:

$$D_i(t_n) = C_i^\alpha \Delta t_n \quad (7)$$

Where,

C_i – is the gas concentration at node (i), which is calculated by use of gas diffusion models;

α – is toxic load index associated with types of gases;

Δt_n – is exposure time.

Absorption dose (D_T) of individual can be calculated through the following two-step:

First, the individual's average absorption dose $[D(t_n)]$ at time $t_n (n=1, \dots, T)$ can be obtained through averaging out all nodes in the study area:

$$D(t_n) = \sum_{i=1}^N x_i(t_n) C_i^\alpha \Delta t_n \tag{8}$$

Where,

$x_i(t_n)$ – is the probability that the individual appears at node (i) at time t_n , that can be calculated with the Markov model described in the second part.

Then the overall average dose received by an individual in the process of the evacuation is:

$$D_T = \sum_{n=1}^T D(t_n) \tag{9}$$

Conditional probability PD of various consequences (such as death, various injuries, etc.) caused by individual's exposure to dose D, can be obtained according to corresponding "probability variable":

$$P_D = \frac{1}{\sqrt{2\pi}} \int_{-\infty}^{Y-5} \exp\left(-\frac{u^2}{2}\right) du \tag{10}$$

In practice, the Eq.(10) can also be transformed from probability variable to percentage with the following equation:

$$P_D = 50 \left[1 + \frac{Y-5}{|Y-5|} \operatorname{erf}\left(\frac{|Y-5|}{\sqrt{2}}\right) \right] \tag{11}$$

Where erf is error function; Y is probability variable, it can be given as follows:

$$Y = k_1 + k_2 \ln(D_T) \tag{12}$$

k_1, k_2 are constants depending on types of accidents.

Let N_0 be the number of people exposed to a dose D. Then, the average expected number of people related to the respective consequence N_c is:

$$N_c = N_0 \cdot P_D \tag{13}$$

By comparing the N_c under various emergency strategies, the ERP can be assessed.

4. CASE STUDY

There is a densely populated area with many large, medium and small enterprises, some of which (such as oil refineries, chemical plants, etc.) use a large number of hazardous substances. To reduce injuries of the accident,

it's necessary to develop emergency response policies (ERP) and take protective actions including evacuation when accidents happened.

The area was divided into 441 discrete nodes with the same size, as shown in Figure 1. Vehicles were assumed to move only in the direction away from the dangerous source. Initial number of vehicles and maximum capacity of each node was distributed according to the regional response operation center. The average evacuees per vehicle was assumed 3, the average speed (U) of evacuation vehicles was 10km/h, c and r_{\max} was 0.8 and 0.9 respectively. Four corners of the study area were selected as evacuation exits, so that the evacuees can stay away from the dangerous source, as can be seen in Figure 1.

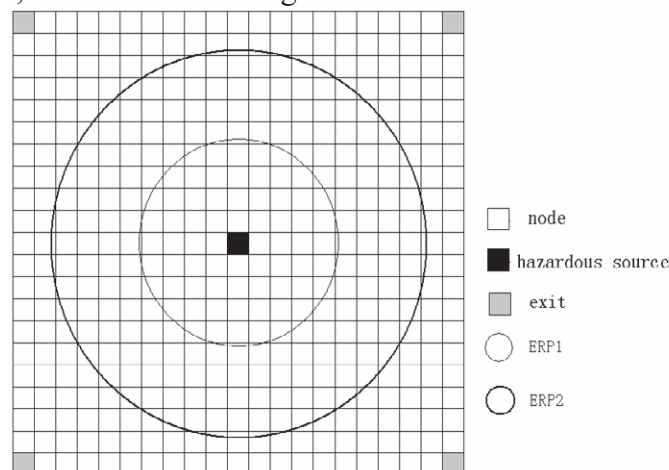


Figure 1: Accident description

The hazardous source in Fig.1 was assumed to have a liquid chlorine tank leak, the leakage amount was 500kg. Two ERPs were considered. Radius of evacuation scope of ERP1 and ERP2 was 1km and 1.9km respectively.

① Calculation of population distribution

On the basis of the Markov model described in the second part, the population changing with time within the region can be calculated with C# programming language. Part of the codes are as follows:

```
using System;
using System.Collections.Generic;
using System.ComponentModel;
using System.Data;
using System.Drawing;
using System.Text;
using System.Windows.Forms;

namespace Evacuation
{
    public partial class EvacuationModel : Form
    {
        //bool debug = true;
        public EvacuationModel()
        {
            InitializeComponent();
        }
    }
}
```

```

        //PC = new PaintCurve(hLines, vLines);
        setTooltips();
    }

    private void button1_Click(object sender, EventArgs e)
    {
        if (InitializeDataFromUI() == false)
        {
            DialogResult result = System.Windows.Forms.MessageBox.Show("Data
invalid!\r\n" +
                "Press OK to use default value\r\n" +
                "Press Cancel to complete the table.",
                "Are you sure", MessageBoxButtons.OKCancel,
                MessageBoxIcon.Exclamation);
            if (result == DialogResult.Cancel)
                return;
            else updateTextBoxes();//更新面板数据
        }
        InitializeVars();//初始化数据
        //PaintCurve(e, hLines, vLines); //画曲线
        Ready = true;
        this.Invalidate();
    }

```

Remaining population within the evacuation region changed as a function of time, as can be seen in Fig.2.

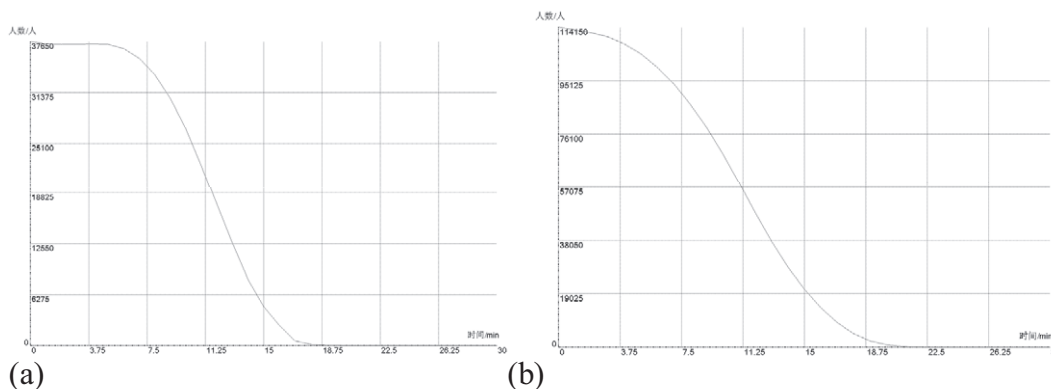


Figure 2: Remaining population in the evacuation region. (a) ERP1, (b) ERP2

Evacuation scope of ERP1 was smaller, people had fewer options during the evacuation, therefore, at the beginning of the evacuation, there would be congestion and evacuation speed was slow. The relatively flat cure in the beginning of Fig.2(a) reflected this problem. With the continuation of evacuation, people moved to nodes having lower level of congestion and the evacuation speed were gradually accelerated.

Evacuation scope of ERP2 was bigger, people had more options during the evacuation, so the probability of congestion can be reduced.

② Assessment of health consequences

To simplify the calculation process, C_i in Eq.(7) was calculated using box model in accordance with the initial concentration of chlorine. It's necessary to use more accurate models (such as CFD model Fluent) to evaluate C_i . Here, α is 2, k_1 is -8.29, and k_2 is 0.92. According to the

Eq.(7) – Eq.(11), with the results of the Markov model, health consequences under different ERPs can be calculated.

Calculation results are as follows:

$$P_{D_1} = 15.02\%, \quad N_{c_1} = 5648$$

$$P_{D_2} = 15.96\%, \quad N_{c_2} = 18218$$

Clear time of ERP1 was shorter, so people's various consequences due to exposure to the chlorine was smaller. However, its evacuation efficiency was lower, especially at the beginning of the evacuation.

ERP2 had a longer clear time, people had a longer time exposed to chlorine and it's more possible to produce a variety of consequences as the cumulative effect. Nevertheless, the evacuation was more efficient, and there was less congestion.

5. CONCLUSIONS

One of the most important factors to assess ERPs is the possible health consequences (death or casualties) under the guidance of that ERP. And that is the guideline of this paper.

Here, we select health consequences (death or injury) as our reference indexes to study the effectiveness of different ERPs, and help decision-makers make correct decisions in an emergency situation. That is, minimization of health consequences is used as determination standard to assess and optimize the ERP.

In real-time command stage after the disaster, if there is enough warning time, the model can be used to help decision-makers to conduct real-time emergency rescue decision-making. The ERP can be adjusted dynamically and real-timely, of course, this can not be separated from the support of site information and transmission technology.

REFERENCES

- Paraskevi S.Georgiadou, Ioannis A.Papazoglou, Chris T.Kiranoudis, Nikolaos C.Markatos. Modeling emergency evacuation for major hazard industrial sites. *Reliability Engineering and System Safety*. 2007.VOL.92:1388-1402.
- Southworth F. *Regional evacuation modeling: a state-of-the-art review*. ORNL/TM-11740. Oak Ridge, Tennessee: Oak Ridge National Laboratory; 1991.
- Cova T J., Johnson J P. Microsimulation of neighborhood evacuations in the urban-wild land interface[J].*Environment and Planning*, 1997.
- Church R L, Ryan M S. *Modeling small area evacuation : can existing transportation infrastructure impede public safety?* 1998:123~131
- Michael H. Triche;Andrew J. Graettinger;Akhilesh Pa. *Emergency Evacuation Modeling Based On Geographical Information System*

Data. University of Alabama Civil and Environmental Engineering Department.

- BUSVINE J R. The toxicity of ethylene oxide to *Calandra oryzae*, *C. granarius*, *Tribolium castaneum*, and *Cimex lectularius*. *Annals of Applied Biology*, 1938, 25:605–632.
- Papazoglou IA, Aneziris O, Bonanos G, Christou M. SOCRATES: a computerized toolkit for quantification of the risk from accidental releases of toxic and/or flammable substances. *Int J Environ Pollut* 1996;6(4-6):500-533.
- M. Markiewicz. *Mathematical modeling of the heavy gas dispersion*. http://manhaz.cyf.gov.pl/manhaz/monography_2006_5/part02/4_M_Markiewicz_Mathematical%20Modelling%20Heavy%20Gas%20Dispersion.pdf
- Keun-Won Lee. A Methodology for Assessing Risk from Released Hydrocarbon in an Enclosed Area. *Journal of Loss Prevention in the Process Industries*. 2002. Vol. 15:11-17

EMERGENCY RESPONSE OF RADIOLOGICAL ATTACKS HAPPENED IN THE CITY

QIYAN ZHENG, LIJUN ZHANG and WEIQI HUANG
Commanding and Engineering Institute of Chemical Defense,
Beijing, China
zhenqy02@mails.tsinghua.edu.cn

ABSTRACT

The scenario that terrorists use radiological diffuse device in crowded location is the most potential mode of the radiological attack in the city, which can achieve the terrorists' intention of disturbing the social order and inducing the public scare. Radiological attacks happened in the city have some characteristics such as the uncertainty of the attacked location and the release source, emergency response and crime investigation usually proceed simultaneously, the attacked spot need recover to normal as soon as possible, etc.. Against these characteristics, emergency response of radiological attack events happened in the city was discussed from three stages: first response, early response and late recovery.

1. INTRODUCTION

In the eve and period of the Beijing Olympic Games, a series of bombings happened in the cities of Yunnan Kunming, Kashgar and Kuqa, Xinjiang in china, these blast events show that China's cities face the reality of the terrorist threat. Terrorist attacks involving radioactive, radiological attacks, is one type of the terrorist threats what China's cites are facing.

Radiological attacks, also known as the nuclear or radioactive attacks(ICRP, 2004), generally include three types(NCRP, 2002; IAEA, 2003):

- 1) Viciously releases radioactive substances with conventional bombs or other means, such as the use of the so-called radiological dispersal device (RDD);
- 2) Attacks on a nuclear facility to arise a nuclear accident;
- 3) Detonate temporary nuclear device (IND), such as the rough nuclear weapons.

Compare the above three types, the use of RDD will be the most impossible mode of the radiological attacks in the city. This is because:

- 1) There are many rigorous security measures and a variety of systems which ensuring it's safety in the nuclear facilities, the attacks on nuclear facilities hardly to be succeed.
- 2) Producing of the IND demands holding the nuclear fissile material in high concentrations, also need high technological level, but most of the terrorist organizations hardly meet these demands.

3) Producing of RDD is relatively easy for terrorists, they can use conventional explosives to diffuse the general radioactive sources (such as medical and industrial sources), or process the sources into the form easy to disperse, so the terrorists can disperse radioactive substances into environment as long as they open the container that radioactive sources in it.

4) If the terrorists use the RDD in a densely populated location, they will result in radioactive contamination of the environment and the person's radiation injury, more importantly, will cause a wide range of social panic most probably because of the fear of radiation hazards.

Because of the most probability of using RDD by terrorists in the radiological attacks in the city, the characteristics are analyzed here for such events as the representative of the urban radiological attack, and discuss the emergency response for these events.

2. CHARACTERISTICS OF RADIOLOGICAL ATTACKS HAPPENED IN THE CITY

Compared with the nuclear and radioactive accidents, radiological attacks happened in the city have some notable characteristics(Zheng, 2006):

1) The time and location are totally random and unpredictable for radiological attacks happened in the city. Such events are likely to occur in some densely populated places, there usually haven't any radioactive materials in these places, so the judgment and response are not prepared for radiological attacks.

2) In the early stage of a radiological attack, the information about the source, such as type, total number and so on, is difficult to be obtained; such information can only be realized through the environmental monitoring, sampling and analysis in the process of emergency response after the attacks.

3) The radioactive substances released in the radiological attack happened in the cities will have complicated diffusion or re-diffusion processes because of the complexity of the urban environment and a large number of people's activities.

4) The victims at the scene of explosion attacks possibly have some physical injury accompanied with radioactive contamination, and the following medical rescue act will likely expand the scope of radioactive contamination.

5) Except the extreme scenario, the irradiation won't result in the immediate death, but may result in serious psychological burden.

6) In order to carry out the crime investigation and evidence preservation, the attack location will be controlled by the police as a crime scene, but crime investigation and evidence preservation are often conflict with the radiation protection.

7) In order to resume normal order of urban life as soon as possible, the radioactive contamination must be cleaned out as quickly as possible.

3. EMERGENCY RESPONSE ABOUT THE RADIOLOGICAL ATTACKS HAPPENED IN THE CITY

According to the characteristics of the radiological attacks happened in the city, the emergency response may be divided three stages: first response, early response and late restoration.

3.1 First responses

For any terrorist incident, the first to reach the spot is often the police officers, firefighters or staffs of emergency medical treatment, their first responses are to evacuate public, insulate the attack scene, fight fire, and treat the injured. The first response stage is the first few hours after the terrorist event's happening.

When the first responders enter the scene, they must first determine the nature of the terrorist event is a conventional terrorist event, or is involved in radioactive, chemical or biological agents. If the event is to identify a radiological attack, the first responders shall immediately request the support of professional personnel on radiation monitoring. And the first responders need pay attention to:

- 1) Evacuate the crowd to the windward direction or the crosswind direction, and control them at a fixed place to prepare for the detection of radioactive contamination and decontamination treatment, but also to avoid radioactive contamination spread to a larger area.

- 2) The demarcation of the isolated area had better be based on the preliminary results of the monitoring; before gaining the monitoring results, the scope of the area is isolated as larger as possible, so that it can contain the spread area with high concentration of radioactive substances, to avoid those unrelated person entering the region and accepting unnecessary exposure, but also to avoid a further spread of radioactive substances because of a large number of personnel actions.

- 3) Before medical first-aid personnel move the wounded, it is necessary to carry out the wounded simple decontamination treatment, such as take off the coat, cleanout exposed skin, etc., to avoid bringing radioactive material into ambulances and hospitals.

The actions of the first responders are crucial for the emergency response of the radiological attacks. If those actions are proper, they can effectively control the exposed crowds and the scope of radioactive pollution, and can greatly limit the consequences of radiation hazards in the most extents. First responders usually do not have the professional background of radiation protection, so it is necessary to conduct the radiation protection training in peacetime, and equip with some rapid radiation measurement equipments. Those equipments will give alarm signals when the radiation level is higher than the natural radiation background. At the same time, the first responders must pay attention to their own protection. For example, to avoid prolonging in the event scene and carry personal dosimeters, real-time monitor the individual dose for no more than the dose limits.

3.2 Early Responses

Early responses are those actions that the professional radiation emergency personnel enter the attack scene and carry out radiation monitoring and personnel decontamination, also include on-site security, fire fighting, medical treatment, crime investigations and other actions. The duration of early response stage is about a few hours to above 10 hours.

When professional radiation emergency personnel enter the scene, the first thing to do is to use monitoring equipment to rapidly detect the radioactive contamination region, and establish the pollution control area. Then they need collect some samples and analyses the concentration and composition of the radioactive nuclides. If there no analysis instruments at the scene, samples must be sent to the laboratory. It's necessary to make a preliminary assessment on the event's scale. In addition, the responders need deal with radioactive detection and decontamination for those crowds evacuated from the attack scene.

Early responders need pay attention to:

1) Equip with the necessary monitoring equipment and wear protective clothing, and continually monitor the individual dose.

2) Be careful in those hot zone formed by the crowd flow, or a spread of radioactive material, mark those regions.

3) For some airproof spaces, such as shopping malls, subway stations, etc., the air-conditioning or ventilation systems must be promptly closed after the evacuation, to prevent the radioactive material spread to the external environment.

4) Collect samples for dust, soil, the surface attachment of objects, vegetation, water, etc., if it is indoors, to collect air samples.

5) Analyze the samples' radionuclide composition as soon as possible, to provide important reference information for the early prevention and treatment. For example, if there is radioactive isotope of iodine, responders shall organize the exposure personnel to take stable iodine as soon as possible, to reduce the inhalation irradiation from radioactive iodine in great extent.

6) The assessment of event' scale should be based on actual monitoring data as much as possible, though some prediction models of accident consequences are available, but their applicability in the small-scale, complex surface of the urban environment still needs to be verified(Chen, 2005; Wei, 2006).

7) After detect and decontaminate those polluted personnel in the evacuated crowds, collect urine or other samples for further examination of interior contamination, to judge whether need medical treatment.

In early response stage, in addition to professional radiation emergency personnel, there are police, fire man, medical personnel, crime investigation officers, etc., they should be provided the necessary protection guidance by radiation emergency responders, and do their work on the premise ensuring compliance with the three principles of radiation protection.

3.3 Late restoration

Late restoration mainly is radioactive clearance of the spot, to restore the environmental level of contaminated area so that people can live there freely. Furthermore, need educate the public with basic knowledge about radioactive, to eliminate their fears about radioactive, and the impact of radiological attacks on the order of the normal city life. The duration of the late recovery stage is about a few days to several months.

In late restoration stage, the decontamination of environment mainly includes sweeping and scouring of the roads, ground and the buildings, clearing away the city's green space. If radiological attack happened in shopping malls, subway stations or other internal space, then the whole internal space need be swept, scrubbed and cleaned, and the indoor air must be filtered. Throughout the decontamination process, continue to carry out radiation monitoring, until the monitoring results show that radiation levels have reached the allowed standards, and then can confirm the completion of decontamination. Radioactive waste, such as the dust from the decontamination, soaked soil by water used for decontamination, should be collect, carry and bury on remote disposal site.

For radiological attacks in the city, there may be a small amount of food being contaminated, which can be disposed as radioactive waste. In general, water pollution will not occur in such events.

In the late stage, the media's education and guidance for public is very important. Government must use all kinds of media to educate the public of the basic knowledge of radioactive, making them have some certain understanding about the health effects of radioactive substances, the enormous difference between radiological attack and the explosion of nuclear weapons, and the effectiveness of emergency actions, dispelling public fear of radiation. In particular, for those affected personnel in spot, through education and guidance of the media, they won't have serious psychological burden.

The late recovery time should be short as much as possible, so as to avoid causing long inconvenience to city life. So the late restoration should collect a lot of manpower and material resources to carry out rapidly, which requires the city to do a good emergency preparedness against radiological attacks in peacetime.

4. Conclusions

There are some notable features for radiological attacks in the city. Against these features, emergency response of radiological attacks in the city is divided into three stages: first response, early response and late restoration, which is based on the response acts, and is different from the early, middle and late stages of nuclear accident or nuclear and radiological terrorism incident(Pan, 2005). The major response acts and the problem needed to pay attention to in the various response stages were discussed. These discussions provide references for developing emergency plans of radiological attacks in the city.

REFERENCES

- ICRP, 2004. *Protecting People Against Radiation Exposure in the Aftermath of A Radiological Attack*. ICRP Publication 96.
- NCRP. USA, 2002. *Management of Terrorist Events Involving Radioactive Material*. Translated by Pan Z Q, Chen Z Z. Atomic publishing company, Beijing. (in Chinese)
- IAEA, 2003. *Method for Developing Arrangements for Response to a Nuclear or Radiological Emergency*. Updating IAEA-TECDOC-953.
- Zheng Q Y, Shi Z Q, Wang X Y, 2006. Some concepts and emergency countermeasures about radiological attack. *Atomic Energy Science and Technology*(Suppl), 204~208. (in Chinese)
- Chen X Q, Pan Z Q, Zhang Y X, Chen J Y, 2005. Forecast Model and Its Design for Early Emergency Response to Nuclear Accidents. *Radiation Protection* 1, 1~10. (in Chinese)
- Wei D, Dong F J, Dong X L, 2006. Prediction of Diffusion Concentration of Radioactive Nuclides during Nuclear Accident. *China Safety Science Journal* 3, 107~113. (in Chinese)
- Pan Z Q (editor in chief), 2005. *Management of Terrorist Events of Nuclear and Radioactive*. Science publishing company, Beijing. (in Chinese)

RESEARCH ON UNIVERSAL MODE OF DESCRIBING AND ORGANIZING EMERGENCY CASES BASED ON CASE-BASED REASONING

QIUYAN ZHONG, YINGJU ZHANG,
XIN YE and JIANGNAN QIU
School of Management , Dalian University of Technology,
Dalian, China, 116024

ABSTRACT

Searching for emergency action schema of the most similar historical emergency case to aid current emergency decision-making is a kind of very convenient and effective method to deal with emergencies. This paper applied Case-Based Reasoning (CBR) to emergency aid decision-making and proposed an universal mode of describing and organizing emergency cases based on three-tier structure to facilitate the retrieval of similar emergency cases. Then the mode was proved to be applicable and helpful for emergency decision-making by the development of CBR prototype system.

1. INTRODUCTION

Recent decades have seen significant increases in the number, scope and complexity of emergencies, which challenges social capability for real-time response. Especially since the 9/11 Terrorist Attacks, SARS and the Sichuan Large Earthquake in China, people pay more and more attention to the timely and efficient response to emergencies. It has been proved that it is a very direct and efficient way to help those commanders who are in the emergent environment to respond rapidly to emergency by searching for the similar cases that have been responded successfully in the past. However, cases that can be used as reference now exist in the form of dispersed and non-structural case texts lacking an universal mode of case description, which leads to great difficulty in searching for similar cases quickly and efficiently. This paper applied case-based reasoning to emergency aid decision-making to facilitate the retrieval of the most similar cases and thus assisting emergency decision-makers in making efficient decision rapidly for the command of emergency.

2. THE ADVANTAGES AND DIFFICULTIES OF APPLYING CASE BASED REASONING(CBR)TO EMERGENCY AID DECISION-MAKING

Case-Based Reasoning (CBR), initiated by Roger Schank(1982), is an important research direction of artificial intelligence in recent years. It has been widely applied into problem solution, law case, medication, diagnoses, computer-aided design and so on. CBR is a method that imitates humanity's ability both for reasoning and cognition mechanism to solve domain problems effectively. It is recognized that people commonly solve problems by remembering how they solved similar problems in the past. It is often more efficient to solve a problem by starting with the solution to a previous similar problem than by generating the entire solution from scratch. According to analysis of the above, it is feasible and necessary to apply CBR to emergency commanding and decision-making by recommending the action schema taken successfully previously to decision-makers, thus assisting them to react immediately to the current damage. Applying CBR to emergency aid decision-making can make full use of expert knowledge and experience that contained in the process of responding to the emergencies in the past, which were called emergency cases. Furthermore, it is because CBR uses cases as carrier rather than knowledge or rules to make use of expert experience, thus avoiding the defects of traditional knowledge inference, such as difficulty in obtaining knowledge and knowledge presentation, etc.

The greatest challenge of successfully applying CBR to emergency aid decision-making is to design universal mode of describing and organizing emergency cases. Although the CBR in emergency aid decision-making has attracted much research interests of academic in domestic and overseas, their attention is kept on the theory level or focused on a certain kind of emergency cases, such as fire disaster, etc. Guo,et al. (2006) applied frame representation to describe emergency cases without explaining the mapping relation between case description and storage mode, lacking further research on the level of application. Wang (1999) pointed that emergency cases consist of many attribute features with hierarchical structure, but when the type of emergency changes, the set of attribute features for a certain type of emergency cases is no longer applicable, thus having certain limitation of his research. The same limitation can be found in the literature 4,etc. This paper proposed an universal mode to describe and store emergency cases based on three-tier structure to avoid the limitation of describing one kind of emergency cases at a time only, which was found in related research. Furthermore, the mapping relation between case description and storage model was displayed. At last, the mode was proved to be applicable by the development of CBR prototype which will facilitate the application of CBR to emergency aid decision-making.

3. THE PROCESS OF EMERGENCY AID DECISION-MAKING BASED ON CBR

The process of emergency aid decision-making based on CBR can be described as follows:

- 1) Input information of current emergency.
- 2) Retrieve the similar case with the current emergency in case base .
- 3) Revise the solutions based on expert knowledge and certain rules stored in knowledge base.
- 4) Output the modified solutions to help decision-makers make an efficient action schema to command current emergency.
- 5) Evaluate the solution and retain the valuable information in case base.

4. THE UNIVERSAL MODE OF EMERGENCY CASE DESCRIPTION

4.1 Characteristic analysis for emergency cases

Proper description and storage mode for emergency cases based on their special characteristics should be designed so that they can be described in the way that computers can recognize. Therefore, characteristics of emergency cases were concluded in the paper as follows:

- 1) Emergency cases are non-structural and non-standard

The available emergency cases now mostly exist in the form of text, which are non-structural, non-standard and have some problems of concept inconsistency. In order to be identified and reasoned by computers, these textual cases should be stored in a standard and universal way.

- 2) Emergency cases cover with very broad domains

According to the Master State Plan for Rapid Response to Public Emergencies promulgated by Chinese State Council, emergency can be divided into four classes, namely, natural disaster\accident\public health and welfare. Every type of emergency consists of several kinds of sub-emergency. For example, typhoon, storm and earthquake all belong to natural disaster. Therefore, the whole attributes of emergency cases involve many domains, which can hardly be described in the same way.

- 3) Most emergency cases consist of several emergency events, each of which was called meta-event in the paper.

For example, an earthquake case itself may consist of rainstorm event, debris flow event and plague event, etc. Furthermore, every meta-event may have several states during the whole evolution process of emergency.

Therefore, present emergency cases were mostly recorded based on state information that evolved from the start to the end.

4.2 Concept Tree building for emergency domain

The problem of concept in emergency cases lacking consistency and standard should first be solved in order to design the universal mode of describing and organizing emergency cases. Therefore, we built up a secondary directory of concept tree for emergency domain under the branch of Engineering Technology referring to Classified Chinese Thesaurus. The concept tree can be displayed as follows: Emergency Management--Emergency, and every concept layer consists of many concepts referring to the Method of Split Facet, proposed by Smith(1983), which classifies things by the form of Thing-Type-Part-Component-Nature-Process-Operation-Instrument. The paper couldn't be able to display the whole branches for the concept tree due to the limited spaces. Based on the analysis above, it can be seen that concept tree is a kind of classification of thesaurus, and its effects on emergency cases can be concluded as follows:

- (1) Classifying the different concept layers in the emergency domain.
- (2) Making concepts in the emergency cases standard and consistent, which will be helpful for describing the emergency cases in a more unified way.
- (3) Building relationship between concepts which can avoid the confusion of concepts.

4.3 Ontology model for emergency

It has been learned that emergency cases cover with very broad domains from the analysis above. Furthermore, the attribute features vary with the type of the emergency cases. Some common features can be concluded when the whole emergency cases were considered to be one system, however. Therefore, ontology model for emergency(OME) was created in the paper. Referring to the generally accepted definition of Ontology that "an ontology is a formal, explicit specification of a shared conceptualisation" (1994). OME was defined as follows: All the description features that contained by every kind of emergency cases and that never vary with the kind of the emergency is called ontology model for emergency. It can be learned by the definition that OME is a base class for emergency cases, which abstracts common elements for emergency domain and

extracts common attribute characteristics for these common elements. Based on sufficient analysis for emergency cases, the paper put forward a set-representation for OEM from the perspective of System Theory.

$$E = \langle X, S, Y \rangle$$

E stands for OEM, X stands for input, with which the external can make effects on the system. X can be sub-divided into inducement input, nature input, social effect input, and artificial control input. S stands for state information, which can represent feature vector for the state, spacial information, resource and related technical parameter, etc. Y stands for output, which means the effects that the system made on the external.

There are many attributes in OEM, such as Event name, Event type, Time and Place of occurrence, etc.

4.4 Meta-event model for emergency

It can be learned from characteristic analysis for emergency cases above that most emergency cases consist of several emergency meta-events. Therefore, it is very necessary to create meta-event model to describe emergency meta-event for the emergency case after its basic information has been described by using emergency ontology model. Inheriting of features in emergency ontology model, meta-event model consists of individual characteristics for a certain kind of emergency event. Every meta-event model describes the individual information of the meta-event in the same way as that in the ontology model, namely input, state and output. For example, the Typhoon meta-event model created in the paper as follows:

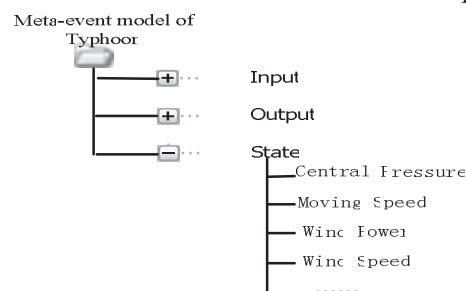


Figure 1: Typhoon meta-event model

It can be seen from the Typhoon meta-event model displayed above that there are many individual features for typhoon, such as the central pressure, moving speed, wind power and wind speed, etc. in the sub-component of State except the common features inherited from OEM.

4.5 Hierarchical representation for emergency cases

An emergency case was organized in the following form of hierarchical representation based on the third attribute characteristic analyzed above in the paper: basic information for the emergency case—meta-event information—state information—attribute information. The hierarchical representation can be described by the following Fig 2.

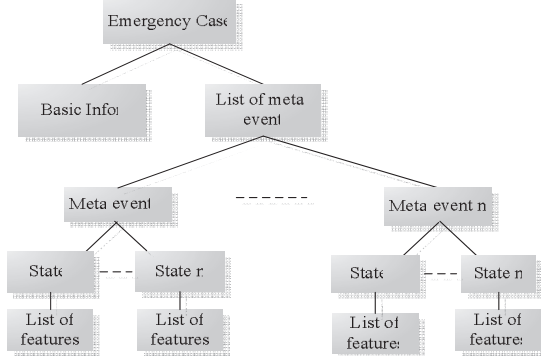


Figure 2: The hierarchical representation of emergency case

4.6 The universal mode of describing and organizing emergency cases

4.6.1 The creation of emergency case base based on relational database

The creation of the case base depends on the form of case representation. Therefore, relational database was applied in the research to store emergency cases because of the hierarchical representation of emergency cases. The advantages of applying relational database here can be concluded as follows: The emergency cases can be organized in a very simple and loose mode when there are not many cases in the case base, but such loose and disorder state of cases should be avoided when the number of cases become larger and larger, such problem can be well solved by the inherent management mechanism of relational database.

4.6.2 An universal mode of describing and organizing emergency cases based on three-tier architecture

An universal mode of describing and organizing emergency cases based on three-tier architecture was designed in the paper, which can be displayed in the following Fig3.

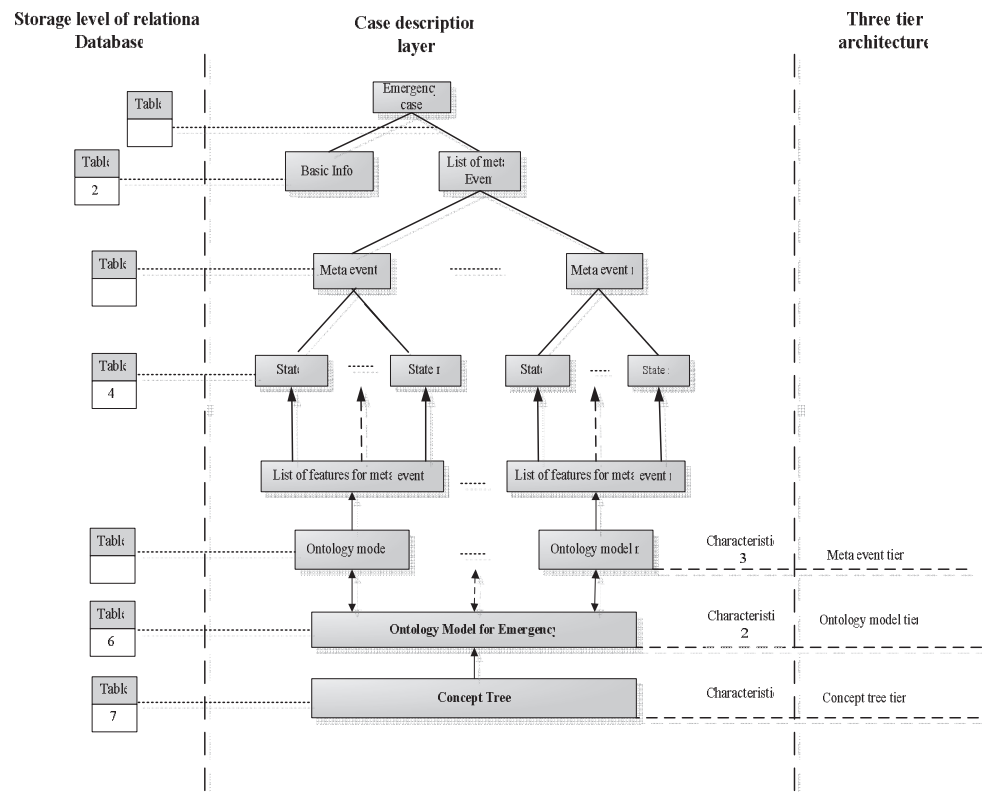


Figure 3: An universal mode of describing and organizing emergency cases based on three-tier architecture

Table 1 is Case—Meta-event Relation Table, which describes the relationship between emergency case and meta-event information contained by it; Table 2 is Basic Case Information Table; Table 3 is Meta-Event Information Table; Table 4 is Meta-Event State Information Table; Table 5 is Meta-Event Model; Table 6 is Ontology Model for Emergency; Table 7 is Concept Tree Table. The above seven database tables that in the storage layer of the relational database connected with each other by some certain association relationship to form the storage schema in relational database for emergency cases. The hierarchical representation for emergency cases was described based on the three-tier architecture, which means concept tree tier, ontology model tier and meta-event model tier. The dashed line in the picture between storage layer of the relational database and case description layer stands for mapping relationship between case description and case storage.

5. COMPUTER REALIZATION

To prove the universal mode of describing and organizing emergency cases based on case-based reasoning discussed in this paper to be applicable, a prototype system for emergency aid decision-making was developed by utilizing Java Script as interface development tool and SQL server2000 as database server. The interface of the prototype system can be displayed by the following Fig 4.

| Interface | | Emergency case representaior | | |
|-----------|--------------------------|------------------------------|-------------------|---------------|
| | | Basic Info | Metz-even | State |
| + | Concept tree Interface | Case 1 | List of metz-even | List of state |
| + | Ontology mode Interface | Case 2 | List of metz-even | List of state |
| + | Metz-even mode Interface | Case 3 | List of metz-even | List of state |
| | | | | |
| | | Case r | List of metz-even | List of state |

Figure 4: The interface for prototype system

There are two parts of information displayed on the interface. Calling module for interface was displayed on the left of the interface, which consisted of concept tree interface, ontology interface and meta-event model interface. The process of describing emergency case information based on CBR is as follows: Calling the proper meta-event model interface according to the type of meta-event contained by the current emergency case which is being described. Then the description will be finished by inputting the basic case information, meta-event information and state information. Every emergency case was displayed in the form of basic case information, meta-event information and state information just as the hierarchical representation that is displayed on the right of the interface. The computer realization of the universal mode of describing and organizing emergency cases designed in the paper laid a solid foundation for the final realization of the Emergency Aid Decision-making Support System based on CBR (EADSSCBR).

6. CONCLUSION

The paper presented an universal mode to describe and organize emergency cases based on CBR to facilitate the retrieval of similar emergency cases. The universal mode will efficiently avoid the limitation of describing one kind of emergency cases at a time only, which was found in related research.

Then the mode was proved to be applicable by the development of CBR prototype which will facilitate the application of CBR to emergency aid decision-making.

REFERENCES

- Roger Schank,1982. *“Dynamic Memory: A Theory of Remindinand Learning in Computers and People,”*Cambridge. Cambridge University press.
- Guo Yongchun,Lu Xinghua,LiuYun,2006.*Research on Emergency Decision Support System based on case base* .Micro-Computer Information. 22 (8) :148-150.
- Wang Jiyu, Wang Jintao,2003.*A Study of Emergency Decision Support System Based on Case-Based Reasoning* .Management Science,16(6):46-51.
- F Ricci, P Avesani, A Perini,1996. *Cases on Fire: Applying CBR to Emergency Management*. New Review of Applied Expert Systems, (6):175-190.
- N.Smith,1983. *Modern linguistics*.Foreign Language Teaching and Study press.
- Pete A, kleinman D L,Pattipati K R,1994.*Structural congruence of tasks and organizations*[C]. In: Proceedings of the Command and Control Research and Decision Aids,NPS,Monterey,CA, 168-175.

COMPARISON OF ESTIMATED AND OBSERVED SEISMIC INTENSITY MAP OF SELECTED EARTHQUAKES

M. A. NOOR¹ and H. KUMAGAI²

¹Bangladesh University of Engineering and Technology,
Dhaka 1000, Bangladesh,

²National Institute for Earth Science and Disaster Prevention,
Tsukuba, Japan
mnoor@ce.buet.ac.bd

ABSTRACT

In this paper, we are interested in studying large historical earthquakes in and around Bangladesh ($M_w > 6.0$) because of the hazards they pose to society. For example, the 1897 Great Assam, India earthquake was felt in most of Bengal and hundreds of people lost their lives. The estimation of earthquake hazards is important for the development of building codes, land use planning and the assessment of property insurance rates. Seismic intensity has been traditionally used worldwide as a method for quantifying the shaking pattern and the extent of damage for earthquakes. The intensity map is more readily interpreted than other maps of ground motion parameters. Our objective here is to convert magnitude to intensity; the first step in the process is to convert magnitude to Peak Ground Acceleration (PGA) and then PGA to intensity. Here we used Kanno et. el. relation to convert Magnitude into PGA and then we used Wald et. el. equation to convert this PGA to intensity. We verify our result with the measured intensity values Off Chuetsu earthquake occurred in Japan on 16 July 2007. We found that our method could predict the measured intensity very well. We then compared the estimated intensity contour map with observed map for four selected historical earthquakes of Bangladesh using above process. Using this method, we can estimate the intensity of any location for a given earthquake. We may use this method to prepare intensity map for future earthquakes in any location and may use this map for land use plan of major cities of Bangladesh, which eventually should contribute to urban safety planning. We also calculated total PGA contributed by the historical earthquakes in this region and found striking similarity between high total PGA contour line and fault line direction.

1. INTRODUCTION

Every day there are about fifty earthquakes worldwide that are strong enough to be felt locally, and every few days an earthquake occurs that is capable of damaging structures. We are interested in studying large earthquakes because of the hazards they pose to society. For example, the 1897 Great Assam, India earthquake was felt in most of Bengal and hundreds of people lost their lives. The estimation of earthquake hazards is

important for the development of building codes, land use planning and the assessment of property insurance rates. Strength of earthquakes (intensity) can be estimated from the maximum amplitude of the “P” wave, which is proportional to seismic energy released in small to moderate earthquakes. In the Richter scale, the assigned magnitude increases by one unit for every tenfold increase in the recorded amplitude.

Seismic intensity has been traditionally used worldwide as a method for quantifying the shaking pattern and the extent of damage for earthquakes. Though derived prior to the advent of today’s modern seismic instrumentation, seismic intensity still provides a useful means of describing information contained in these recordings. Such simplification is helpful for those users who are unfamiliar with instrumental ground motion parameters. That is not to say that instrumentally derived seismic intensity alone is sufficient for loss estimation. In fact, peak velocity and spectral response may provide a more physical basis for such analyses. However, for the majority of users, we expect that the intensity map will be more readily interpreted than other maps of ground motion parameters. Strength of earthquakes can also be measured using the Modified Mercalli Intensity (MMI) scale, which is a qualitative scheme based on extent of damage. Because surface damage is most intense near the epicenter and generally decreases with distance, for any given earthquake this scale may vary widely with geographic location.

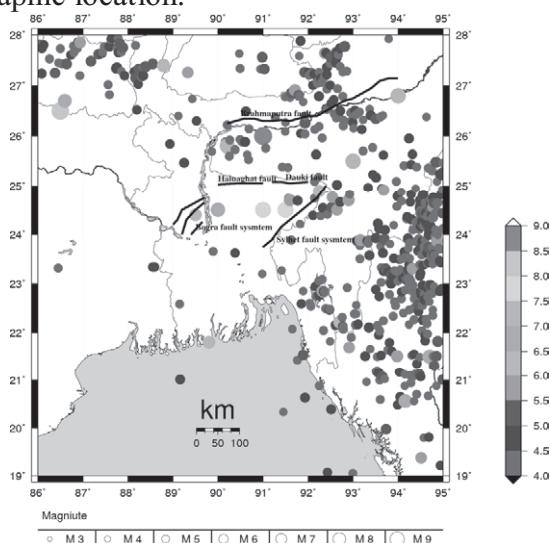


Figure 1: Seismicity of Bangladesh

A seismicity map of earthquakes from -2150BC to 1997AD more than magnitude 4 in Bangladesh and its neighboring region are shown in the Figure 1. In this paper, we studied how to estimate intensity distribution for a region from a known magnitude. We described the procedure of estimating intensity from magnitude at the outset. Using the methodology described in this paper we then estimated the intensity distribution of four historical earthquakes in and around Bangladesh and compared with historical observed data. This study is very important as, if we can estimate the intensity distribution for any earthquake which may occur in future, which will help the policy maker to prepare a land use plan. We verify our result with the measured intensity values of Off Chuetsu earthquake occurred in Japan on 16 July 2007. We found that our method could predict

the measured intensity very well. We also calculate total PGA contributed by the historical earthquakes in this region and found striking similarity between total PGA contour line and fault line direction.

2. EARTHQUAKE INTENSITY ESTIMATION

Magnitude to PGA and PGV

We used Kanno et. al. (2006) relation to convert earthquake magnitude to PGA and PGV. Kanno et. al. (2006) collected all available Japanese seismic waveform data, including those from the many strong-motion observation stations set up by the Japanese government and other organizations, and used them to establish a new database. A large number of high-quality strong-motion records were obtained from these new networks. Based on the new database, they proposed new standard attenuation relations not only for peak values, such as PGA and PGV, but also for 5% damped acceleration response spectra, as a contribution to a future national seismic hazard map of Japan. They assembled the largest possible number of seismic waveforms, obtaining a total of 91,731 records from 4967 events in Japan and 788 records from 12 events in countries other than Japan and selected 11,542 records from 184 events in Japan and 377 records from 10 events elsewhere for regression analysis. Two simple regression models were proposed for shallow (focal depth of 30 km or less) and deep (focal depth of more than 30 km) events.

$$\log \text{pre} = a_1 M_w + b_1 X - \log(X + d_1 \times 10^{e_1 M_w}) + c_1 \pm e_1 \quad (D \leq 30 \text{ km}) \quad (1)$$

$$\log \text{pre} = a_2 M_w + b_2 X - \log(X) + c_2 \pm e_2 \quad (D > 30 \text{ km}) \quad (2)$$

where pre is the predicted PGA (cm/sec²), PGV (cm/sec), or 5% damped response spectral acceleration (cm/sec²), D is the focal depth (km), M_w is the earthquake magnitude, X is the distance from epicenter, and a_1 , b_1 , c_1 , a_2 , b_2 , and c_2 are the regression coefficients. Coefficient $e_1 = 0.5$ was selected for all periods in the present study. e_1 and e_2 are one standard deviation. Determined regression coefficients for the base model in Equations 1 and 2 for PGA, and PGV, are given in Tables 1 and 2.

Table 1: Regression coefficients for shallow event model of PGA and PGV

| Type | A_1 | b_1 | c_1 | d_1 | e_1 |
|------|-------|---------|-------|--------|-------|
| PGA | 0.56 | -0.0031 | 0.26 | 0.0055 | 0.37 |
| PGV | 0.70 | -0.0009 | -1.93 | 0.0022 | 0.32 |

Table 2: Regression coefficients for deep event model of PGA and PGV

| Type | A_2 | B_2 | c_2 | e_2 |
|------|-------|---------|-------|-------|
| PGA | 0.41 | -0.0039 | 1.56 | 0.40 |
| PGV | 0.55 | -0.0032 | -0.57 | 0.36 |

Site effects and regional features (local anomalous seismic intensity) has been considered in their study but we did not consider those in our present study. Using above method attenuation law that has been used in the present study shown in the Figure 2.

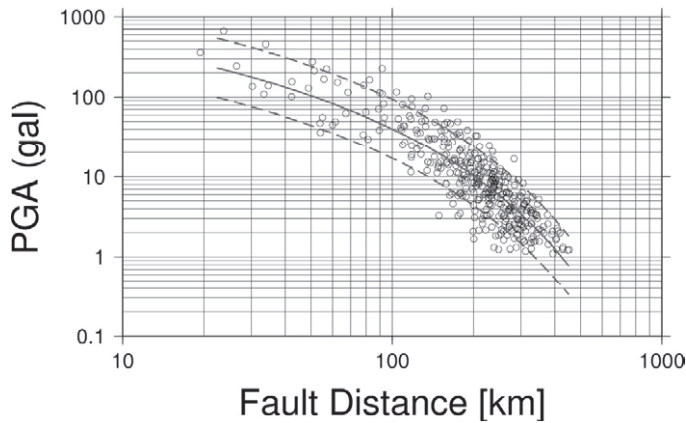


Figure 2: Attenuation curves used in the present study

2.2 Intensity to PGA

Wald et al. (1999) have recently developed regression relationships between Modified Mercalli intensity (MMI) (later revised by Richter, 1955, Wood and Neumann, 1931) and PGA or PGV by comparing the peak ground motions to observed intensities for eight significant California earthquakes. For the limited range of Modified Mercalli intensities $V \leq I_{mm} < VIII$, Wald et. al. (1999) found that for PGA,

$$I_{mm} = 3.66 \log(\text{PGA}) - 1.66 \quad (s=1.08) \quad (3)$$

and PGV within the range $V \leq I_{mm} < IX$,

$$I_{mm} = 3.47 \log(\text{PGV}) + 2.35 \quad (s=0.98) \quad (4)$$

Since we are also interested in estimating intensity at lower values, and our current collection of data from historical earthquakes does not provide constraints for lower intensity, Wald et. el. (1999) has imposed the following relationship between PGA and I_{mm} :

$$I_{mm} = 2.20 \log(\text{PGA}) + 1.00 \quad (5)$$

The corresponding equation for PGV and I_{mm} is:

$$I_{mm} = 2.10 \log(\text{PGV}) + 3.40 \quad (6)$$

Using peak acceleration to estimate low intensities is intuitively consistent with the notion that lower (<VI) intensities are assigned based on felt accounts, and people are more sensitive to ground acceleration than velocity. Higher intensities are defined by the level of damage; the onset of damage at the intensity VI to VII range is usually characterized by brittle-type failures (masonry walls, chimneys, unreinforced masonry, etc.) which are sensitive to higher-frequency accelerations. With more substantial damage (VII and greater), failure begins in more flexible structures, for which peak velocity is more indicative of failure.

2.3 Limitations of earthquake intensity measures

Although important and a successful approach to the early study of earthquake size, intensity has problems, when we expand our study to

earthquakes that are not located near reference structures or earthquakes that occur deep beneath Earth's surface. For a fixed earthquake size, the region of strong shaking can be an indication of the regional geologic structure. One aspect of intensity that is difficult to quantify is the effect of the near-surface geology on the intensity of seismic shaking. We call this effect a site effect because it is local to each site. Several physical parameters can affect shaking intensity. The primary control of the site response is the rock or soil type, and a secondary control structure is the water content.

3. VERIFICATION OF INTENSITY ESTIMATION

In this study, we took a simple approach of directly mapping the historical intensity distribution across Bangladesh. We used MMI intensity scale. We used Equations 1 and 2 for the magnitude-intensity relations. We made no assumptions about earthquake occurrence models. Since these are the results of the past earthquakes, the distributions will be different from the expected intensities from future earthquakes. However, our results should be useful for comparison with the probabilistic intensity maps for seismic hazard. We verified our results using the recent earthquake occurred in Japan on 16 July, 2007. It has detailed measured seismic intensity and PGA contour map.

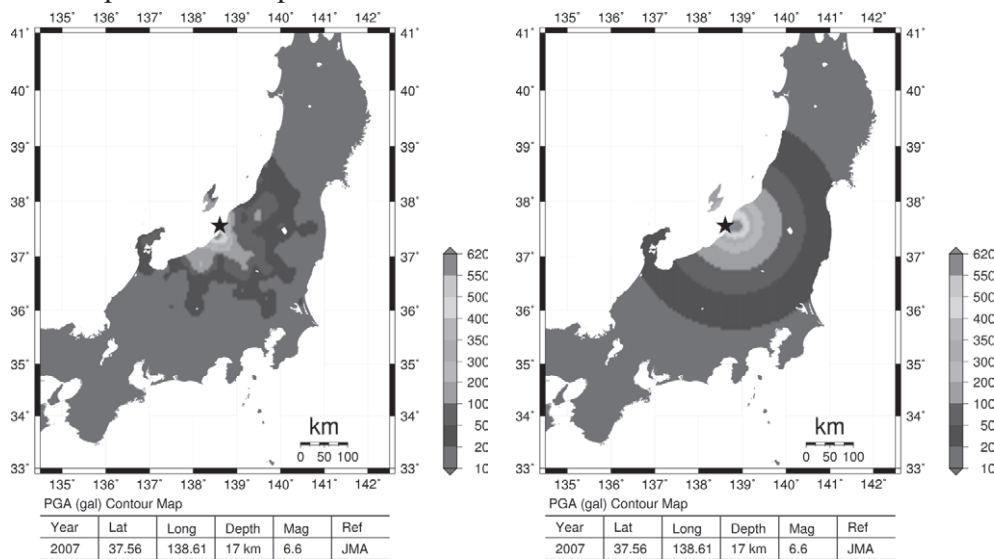
We selected Off Chuetsu earthquake occurred in Japan in 16 July 2007 for verification purpose. We calculated the measured ground intensity from K-net (Japan) strong motion data. This intensity was calculated using the maximum observed ground PGA. We used the relations given in Equations 3 and 5 to convert PGA to MMI. We first plotted these on maps and then compared these with our estimated intensity and PGA contour map using the assumed magnitude-intensity equation and attenuation law of Japan using K-net waveforms.

We at the outset tried to estimate the PGA from the magnitude of the Off Chuetsu earthquake using the relation given in Equation 1, as this a shallow depth (16 km) earthquake. We then compared the measured value (Figure 3(a)) with estimated value (Figure 3(b)). We can see from the figures that there exist good agreement between the estimated value and measured value. We then calculated intensity by using Equations 3 and 5, and shown in Figure 4. These also show very good agreement. These equations may be used in calculating intensity of a location if data is available. This can also be used for land use planning by assuming any future of desired magnitude.

4. COMPARISON BETWEEN ESTIMATED AND OBSERVED SELECTED HISTORICAL EARTHQUAKES OF BANGLADESH

We mapped the recorded seismic intensity for earthquakes in Bangladesh from 1885 to September 2000 using compiled historical records and MMI intensity data. We used a total of four events that had USGS magnitude level of 6 or greater in and around Bangladesh for our intensity and PGA estimation analysis. Figure 5 shows the selected earthquakes on map. Records are given in Table 3. Investigations of seismic intensities from historical earthquakes are useful for characterizing the damaging ground motions that have occurred in the past. We described each historical

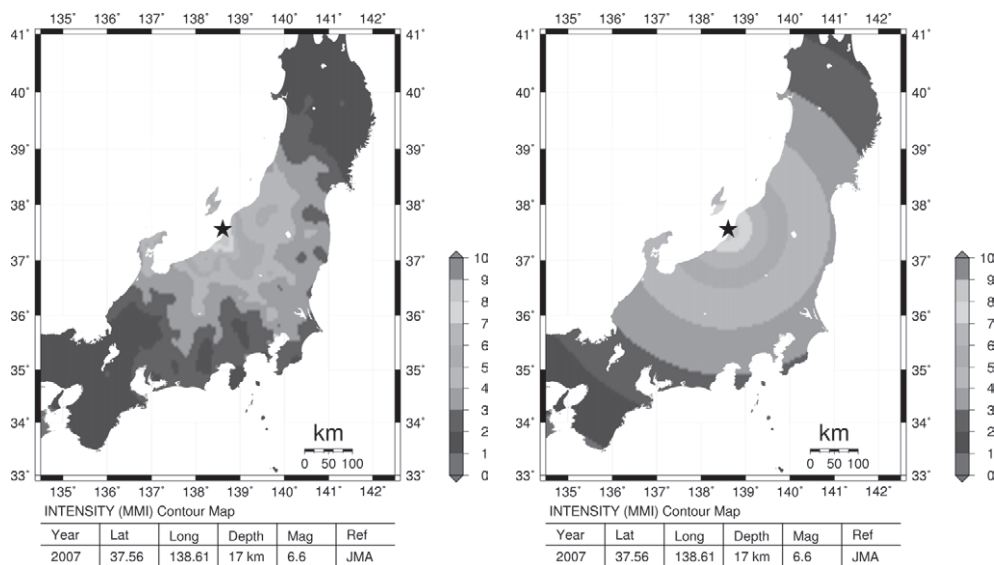
earthquake briefly in the following sections and then presented our results for respective earthquakes.



(a) Measured

(b) Estimated

Figure 3: PGA map of Off Chuetsu earthquake



(a) Measured

(b) Estimated

Figure 4: Intensity map of Off Chuetsu earthquake

Table 3: Selected historical earthquakes (USGS)

| No. | Year | Lat | Long | Mag | Depth | Name |
|-----|--------------|------|------|-----|-------|-----------------------------------|
| 1 | 10 Jan. 1869 | 25.5 | 93.0 | 7.4 | 30 km | Cachar-Manipur (Assam), India |
| 2 | 14 Jul. 1885 | 24.5 | 90.0 | 6.8 | 30 km | Great Bengal (Near Sirajganj) |
| 3 | 12 Jun. 1897 | 26.0 | 91.0 | 8.7 | 60 km | Great Assam, India |
| 4 | 8 Jul. 1918 | 24.5 | 91.0 | 7.6 | 60 km | Srimongal (Srimangal), Bangladesh |

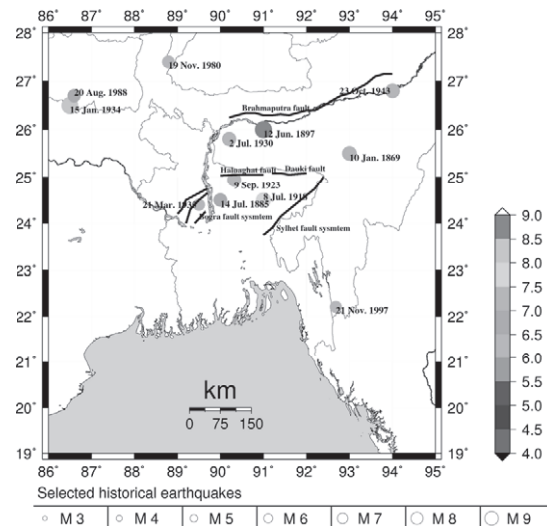


Figure 5: Historical earthquakes in and around Bangladesh

4.1 1869 Earthquake

This $M > 7$ earthquake occurred in the Sylhet region (Silchar) of what is now NE Bangladesh. Although numerous accounts of this earthquake were compiled by the Oldhams (Oldham, 1884) the data are insufficient to estimate a causal fault or a precise magnitude. Estimate magnitude from different sources was found $M_w = 7.39$. The most likely fault to be associated with this earthquake is the eastern extremity of the Dauki fault, as hinted by Austin, 1869 who was undertaking first-order triangulation in the region at the time. Few first hand accounts of the event exist outside the covers of Oldham. We first, for this earthquake, estimated the maximum PGA using the relation given in Equation 1 considering this a shallow event. We then estimated the intensity of the earthquake from given magnitude using the relation given in Equations 3 and 5. Figure 6 and 7 show the estimated and observed (Oldham, 1883) intensity contour map, respectively for this earthquake. We may observe from this figure that the estimated intensity for Dhaka city is 5.

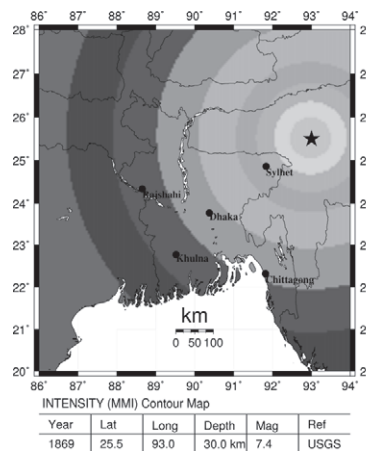


Figure 6: Estimated intensity map for 1869 earthquake

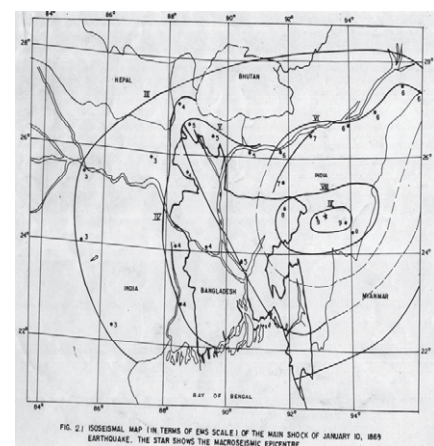


Figure 7: Observed intensity map for 1869 earthquake (Oldham, 1883)

4.2 1885 earthquake

The 1885 Bengal Earthquake, also known as Manikganj Earthquake, is one of the major earthquakes triggered in the historical past. The 1885 Bengal Earthquake with its possible epicenter near Kudalia in Saturaia (Manikganj) and magnitude between 6 and 7 is of great concern for a megacity like Dhaka. The earthquake damage and consequent casualty risk of Dhaka are very high because of its very high population of about 13 million and large percentage of unplanned buildings and structures. The earthquake disaster risk index (EDRI) for Dhaka stands top among the twenty high risk cities in the world (Khan, 2005). Following the same process mentioned earlier we estimated the PGA first then estimated the intensity and compared with observed intensity map (Middlemiss, 1885). The estimated intensity contour map and observed intensity map are given in Figure 8 and Figure 9, respectively. We may observe from the figures that for both estimated and measured cases intensity for Dhaka city is 7.

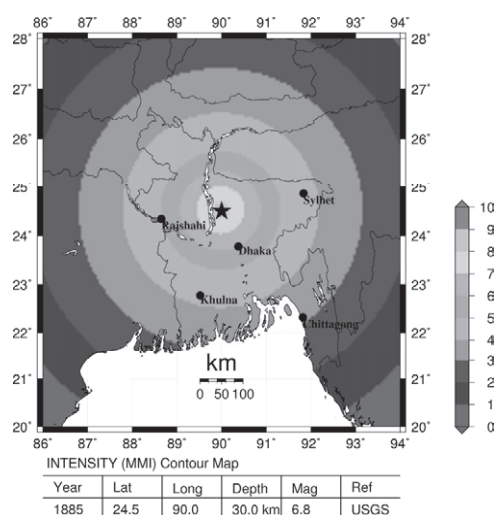


Figure 8: Estimated intensity map for 1885 earthquake

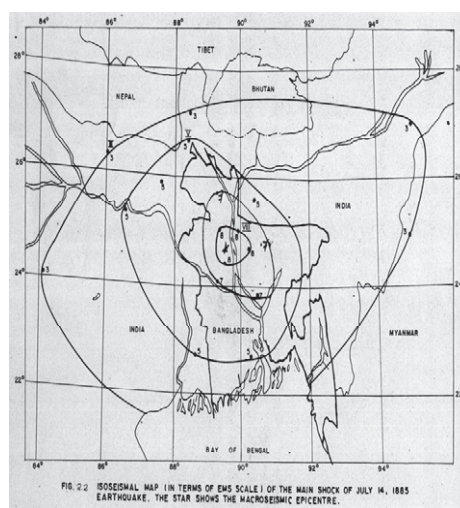


Figure 9: Observed intensity map for 1885 earthquake (Middlemiss, 1885)

4.3 1897 earthquake

The 1897 Shillong earthquake, northeast India is considered to be one of the largest in modern history (Rajendran and Rajendran, 2003). Oldham’s memoir (Oldham, 1899) on this event widely considered as a classic treatise opened new vistas in observational seismology; many questions on the associated faulting mechanisms however remain unresolved. While most previous studies have suggested that the earthquake originated on a gentle north-dipping thrust that is considered to be associated with the Himalayan tectonics, a recent geodetic model by Bilham and England (Bilham and England, 2001) invokes a steep, south-dipping reverse fault, close to the northern topographic edge of the Shillong Plateau. Following the same process described earlier we estimated the PGA first then estimated the intensity. Comparison between estimated intensity contour map and observed intensity map is shown in Figure 10 and Figure 11, respectively.

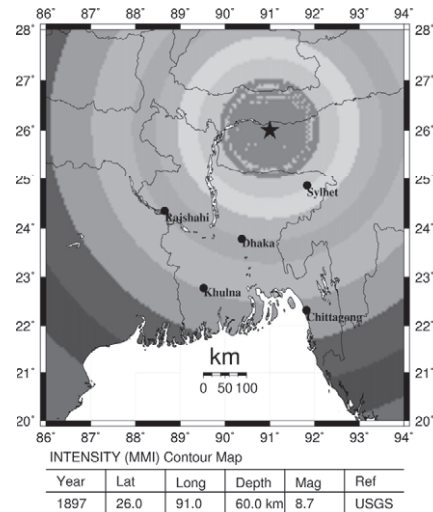


Figure 10: Estimated intensity map of 1897 earthquake

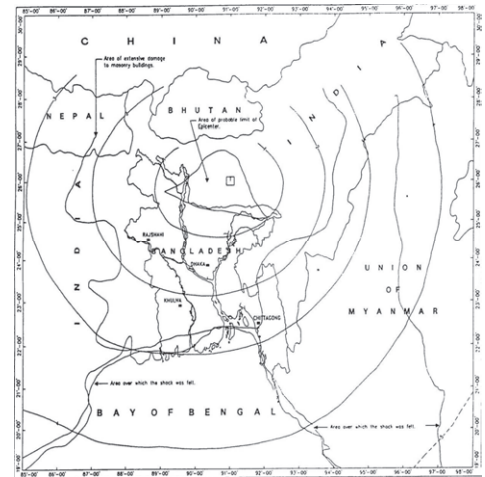


Figure 11: Observed intensity map of 1897 earthquake (Oldham, 1899)

4.4 1918 earthquake

1918 Known as the Srimangal Earthquake, occurred on 18 July with a magnitude of 7.6 and epicenter at Srimangal, Maulvi Bazar. Intense damage occurred in Srimangal, but in Dhaka only minor effects were observed. It devastated a relatively small area in the southern part of the Sylhet district of Bangladesh adjoining northern part of Tripura. This earthquake originated due to rupture along the high angle reverse Sylhet fault where it is intersected by NW trending Mat fault. Its depth of focus was 60 km. Following the same process mentioned earlier we estimated the PGA first then estimated the intensity. The estimated intensity contour map and observed intensity map (Stuart, 1920) for this earthquake are given in Figure 12 and Figure 13, respectively.

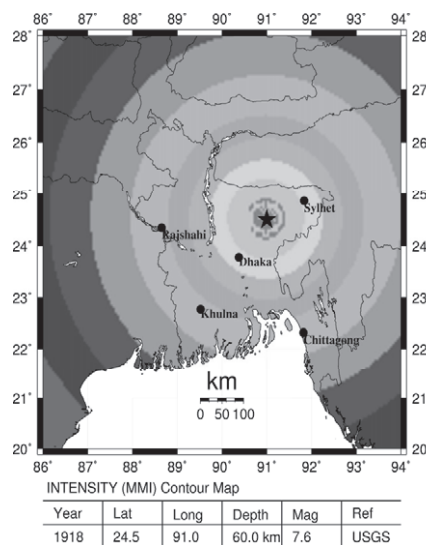


Figure 12: Estimated intensity map of 1918 earthquake

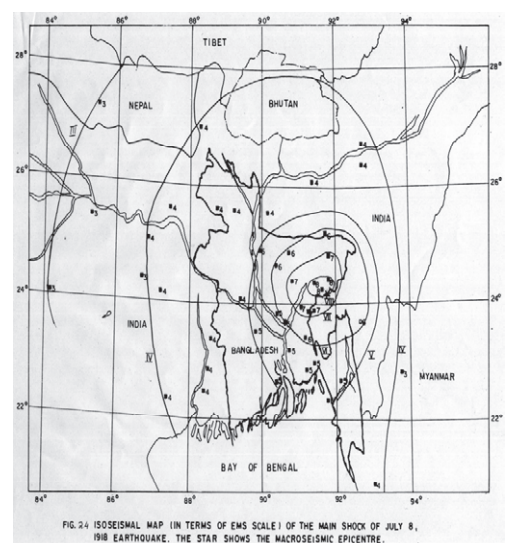


Figure 13: Observed intensity map of 1918 earthquake (Stuart, 1920)

5. TOTAL PGA

We estimated the contribution of all historic earthquakes (except 1897) to the total PGA of this region. We omit two very massive earthquakes as they tend to bias the result. Total PGA plot is shown in Figure 14. If we superpose the fault map of the region then we can see that the estimated total PGA is higher along the major fault directions. This technique may be used to estimate the fault direction if there is no fault data available for any region.

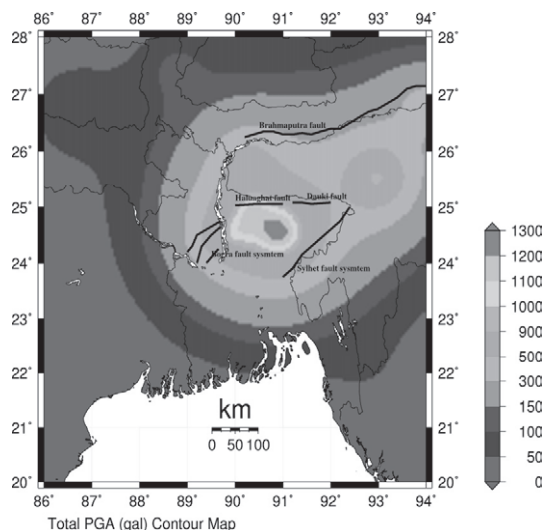


Figure 14: Total PGA map of all selected historical earthquakes

6. CONCLUSION

In this paper, we presented a process to convert Earthquake magnitude to Intensity scale by using Kanno et. el. relation to convert Magnitude into peak ground acceleration and then Wald et. el. equation to convert peak ground acceleration to Intensity. We verified our result using Off Chuetsu earthquake which struck Japan on 16 July, 2007. We found that these two equations could predict the measured intensity very accurately. We used this process, then, to estimate the intensity of four historical earthquakes in and around Bangladesh. These intensity maps were also verified with the observed intensity maps. We found good agreement between the values. These maps can be used by policy makers for land use plan of major cities of Bangladesh. We estimated the contribution of all historic earthquakes (except 1897) to the total PGA of this region. After superposing the fault map of the region then we found that the estimated total PGA is higher along the major fault directions. This technique may be used to estimate the fault direction if there is no fault data available for any region.

REFERENCES

- Austin, G. (1869). Notes from assaloo, north cachar, on the great earthquake of 10 January 1869. *Proc. Asiatic Soc. Bengal*, 15 March 1869:91–99.

- Bilham, R. and England, P. (2001). Plateau pop-up during the great 1897 Assam earthquake. *Nature*, 410:806–809.
- Kanno, T., Narita, A., Morikawa, N., Fujiwara, H., and Fukushima, Y. (2006). A new attenuation relation for strong ground motion in Japan based on recorded data. *Bull. Seis. Soc. Am.*, 96(3):879–897.
- Middlemiss, C. S. (1885). Report on the Bengal earthquake of 14th July, 1885. *Records. Geol. Surv. India. Vol. XVIII*, Part. 4, pp 201-220.
- Oldham, T. (1883). A catalogue of Indian earthquakes from the earliest times to the end of 1869 A.D. *Mem. Geol. Surv. India. Vol. XIX*, Part. 3.
- Oldham, R. D. (1884). Note on the earthquake of 31 December 1881. *Records of the Geological Survey of India*, 17 (2): 47–53.
- Oldham, R.D. (1899). Report on the great earthquake of 12th June, 1897. *Mem. Geol. Surv. of India, Vol. XXIX*, 1-379
- Rajendran, C. and Rajendran, K. (2003). The 1897 shillong earthquake, northeast India: A new perspective on its seismotectonics and earthquake history. *American Geophysical Union*.
- Richter, C. F. (1958). In *Elementary Seismology*, pages 135–149, 650–653. W. H. Freeman and Co., San Francisco, USA.
- Stuart, M. (1920). The Srimangal earthquake of 8th July, 1918, *Mem. Geol. Surv. of India, Vol. XLVI*, Parts 1 and 2.
- Wald, D. J., Quitoriano, V., Heaton, T., and Kanamori, H. (1999b). Relationships between peak ground acceleration, peak ground velocity and modified mercalli intensity in California. *Earthquake Spectra*, 15(3):557–564.
- Wood, H. O. and Neumann, F. (1931). Modified mercalli intensity scale of 1931. *Bull. Seism. Soc. Am.*, 21:277–283.

COLLECTOR COMPARISON OF AIRBORNE SALT ATTACK FOR MARINE INFRASTRUCTURES IN TAIWAN

KAI-LIN HSU and CHAO-SHUN CHANG
Department of Construction Engineering,
National Kaohsiung First University of Science and Technology, Taiwan.
vichsu@ccms.nkfust.edu.tw

ABSTRACT

As known, Taiwan is surrounded by sea. As a result, the corrosion induced by air-borne salt from the sea is unavoidable for the marine infrastructure. In this research, in order to understand the distribution and corrosion influence of air-borne salt in Taiwan, by setting up onsite-exposure tests, i.e. the air-borne salt collector proposed by Public Work Research Institute (PWRI , 1993) in Japan and Japan Industrial Standard(JIS) Z2382 (1998), the corrosion map of air-borne salt in Taiwan will be developed . By analyzing the collected air-borne salt, the effect and availability of the different types of air-borne salt collectors can be compared. Then, the environmental factors such as temperature, rainfall, wind direction, etc. can be correlated with the stochastic distribution of air-borne salt.

Through the collected data up to 18 months, the comparison of the air-borne salt corrosion collectors for southern Taiwan marine infrastructures is illustrated through the analysis given in this paper, which can be used as the design reference for the required service life under various air-borne salt attack environments.

1. INTRODUCTION

At present, RC structures are still the representative construction works at practice. Because the weather in Taiwan is sea-island weather, the RC structures in Taiwan are prone to be attacked by chloride ion. The corrosion of RC structure is hard to be found at its incubation period while it reaches its deterioration period when found. As a result, how to prevent in the design stage or early stage of corrosion is the key to effectively solve the corrosion problem of RC structures.

As known, the potential corrosion of the marine RC structures may resort to the amount of air-borne salt, which strongly depends on the meteorological and geographical features of the location. However, the site data on air-borne salt in Taiwan has been not fully established, this research aims at conducting up-to-18 month experimental program; i.e. site collection and analysis of air-borne salt and meteorological information for the southern Taiwan marine area at more-than-ten locations. Through the

collected data up to 18 months (Lin 2008), the availability of the air-borne salt corrosion map for Taiwan marine infrastructures is illustrated through the analysis given in this paper, which can be used as the design reference for the required service life under various air-borne salt attack environments.

2. SELECTION OF AIR-BORNE SALT (ABS) COLLECTORS AND EXPOSURE LOCATIONS

In order to trap air-borne salt near Taiwan marine area, the ABS collectors suggested by JIS Z2382 and PWRI were adopted due to the similar experience in Japan. The details for both types of ABS collectors are described as follows.

2.1 ABS collector suggested by JIS Z2382

The type of JIS Z2382 ABS collector is composed of 10cm x 10cm gauze clipped in hollow acrylic frame, as shown in Figure1. This apparatus is so simple that the air-borne salt can be easily seized from all the exposure direction only except for the space near the acrylic frames.



Figure 1: Layout of ABS collector suggested by JIS Z2382 .

2.2 ABS collector suggested by PWRI

The type of PWRI ABS collector is composed of 10cm x 10cm vent open in stainless steel box collector, as shown in Figure2. In order to facilitate the flow of air convection, there is another opening with 10cm x 10cm in the opposite side of the vent. In order to compare the effect of both ABS collectors and prevent the effect of different exposure position, these two ABS collectors were integrated into one set as also shown in Figure2 (a), in which the location of the openings of the collectors are set at the same height in spite of the horizontal distance at 10 cm.

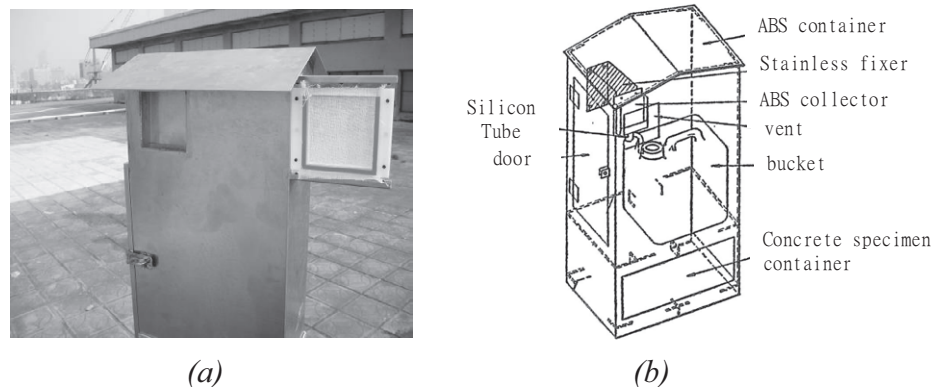


Figure 2: Layout of ABS collector suggested by PWRI.

Table 1: Geographical Information of Exposure Sites.

| No. | Location | Wind-face (direction/degree) | Distance to seashore (m) | height (m) |
|-----|--------------------------|------------------------------|----------------------------|--------------|
| 1 | Port 10 Kaohsiung harbor | west/270 | 1162 | 12 |
| 2 | Port 1 Kaohsiung harbor | west/270 | 431 | 39 |
| 3 | Dalinpu Kaohsiung | north-west/280 | 791 | 13 |
| 4 | Jeguang Kaohsiung | west/270 | 278 | 9 |
| 5 | Nanje Kaohsiung | south/180 | 2553 | 31 |
| 6 | Chedin Kaohsiung | south-west/250 | 169 | 17 |
| 7 | Anpin, Tainan | south-west/220 | 453 | 14 |
| 8 | Annan, Tainan | south-west /200 | 5078 | 8 |
| 9 | Chigu, Tainan | north-west/350 | 150 | 9 |
| 10 | Jianjun, Tainan | north-west /280 | 302 | 30 |
| 11 | Koliao, Tainan | south-west /210 | 150 | 11 |
| 12 | Budai, Chiayi | north/360 | 294 | 11 |

2.3 Exposure Site Selection of ABS collector

In order to trap the air-borne salt information around the southern Taiwan marine area, 12 sites from Chia-yi to Kaohsiung have been selected, the geographical information and location of which are given in Table 1 and Figure3 individually. However, for clarifying the collection effect of PWRI and JIS ABS collectors, 3 set of PWRI ABS collectors and 2 set of JIS ABS collectors were first installed on Port 10 of Kaohsiung harbor (No.1) as well as 2 set of PWRI ABS collectors and 1 set of JIS ABS collector were built up on Port 1 of Kaohsiung harbor (No.2) during 2006.12 and 2007.12. Furthermore, one site meteorological station for collecting on-site weather information was set on Port 1 of Kaohsiung harbor in 2007.07, as illustrated in Figure4. Afterwards, since 2008.01, one set of PWRI ABS collector and one set of JIS ABS collector were added for another 10 sites, which spread from Kaohsiung to Chiayi (i.e. No.3 to No.12), as shown in Figure3. Its is worthwhile for the selection of No.5 and No.8 sites that the distance to the seashore for both sites are larger than 1 km due to the validation

consideration on distance effect for air-borne salt in Taiwan present design specification of RC structure.

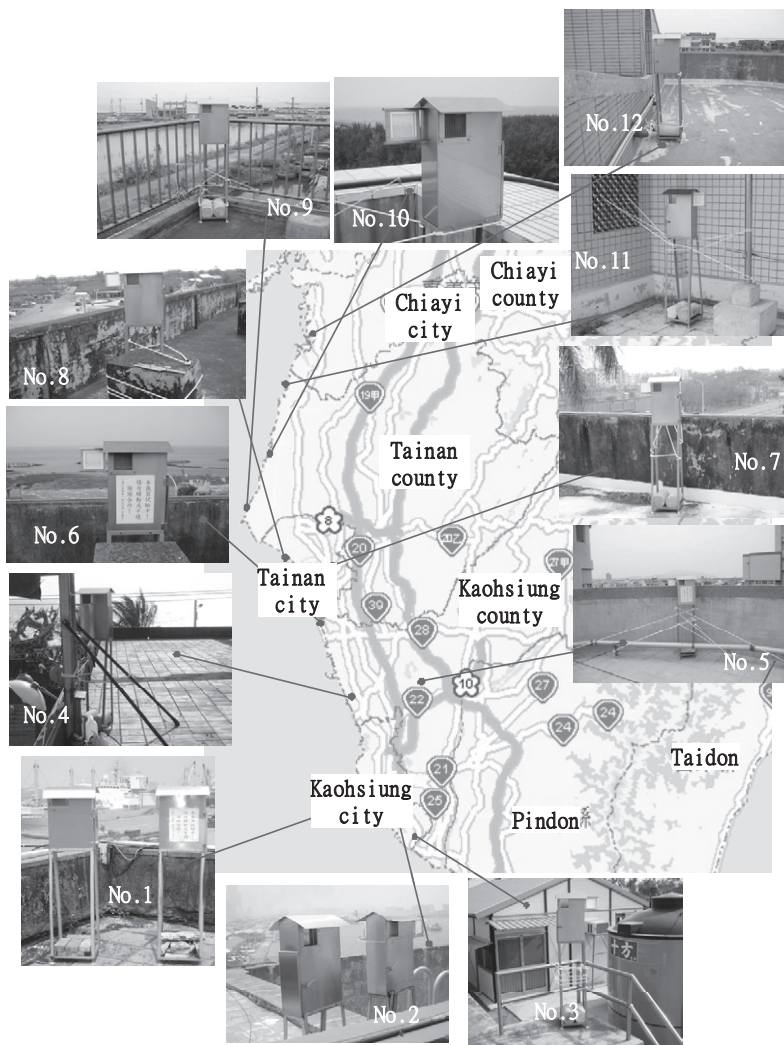
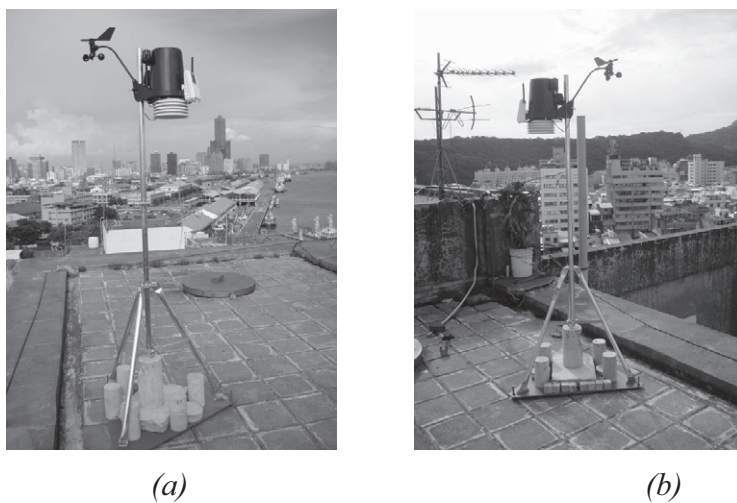


Figure 3: Exposure-Site Locations of ABS collectors.



(a)

(b)

Figure 4: On-site Meteorological Station.

2.4 Analysis of collected chloride

For analyzing the concentration of collected air-borne salt (ABS), automatic titration tester is utilized by titrating 0.01 N AgNO₃ for measuring the weight percentage of collected ABS either from PWRI or from JIS ABS collectors. Then, the concentration of analyzed salt can be converted to the amount of air-borne salt per unit day (mdd, 1mg/dm²/day, 1dm² = 100cm²) as given in Eq.(1).

$$\text{Amount of Air-borne salt (mdd)} = \frac{\text{concentration of ABS (mg/ml)} \times \text{volume of collected solution (ml)}}{\text{collection period (day)} \times \text{collector area (dm}^2\text{)}} \quad (1)$$

3. RESULT AND DISCUSSION

After up-to-18 month on-site collection, the dependency of ABS on distance to seashore, height of ABS collector, weather factor including rainfall, temperature, humidity and wind were investigated first; then, the feasibility of PWRI and JIS ABS collectors was discussed finally.

3.1 Dependency of ABS on distance to seashore

As shown in Figure5, for PWRI ABS collector, when the distance to seashore exceeds 500m, the declination tendency of ABS turns obvious while the collected ABS is close to zero when the distance to seashore is over 1000m. As for JIS ABS collector, the declination tendency of ABS can be observed when the distance to seashore is over 500m while this tendency may be violated for the case that the distance to seashore is up to 5000m. As a result, from the on-site observation, there seems to be accepted that the amount of ABS may decrease with the increase of the distance to seashore. However, this observation may be varied for the different type of ABS collectors.

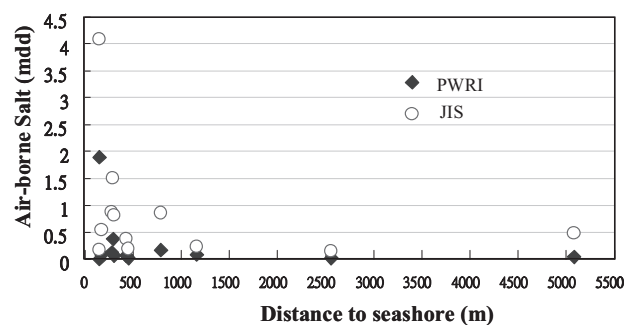


Figure 5: Dependency of Air-borne Salt on Distance to Seashore.

3.2 Dependency of ABS on height of ABS collector

As shown in Figure6, for both types of ABS collector, there seems to be no clear dependency of ABS on height of ABS collector. Although the

largest amount of ABS seems to be found under the height within 15m, there is also some near-zero amount of ABS within height 15m. Frankly speaking, the observation for dependency of ABS on height of ABS collector cannot conclude clearly.

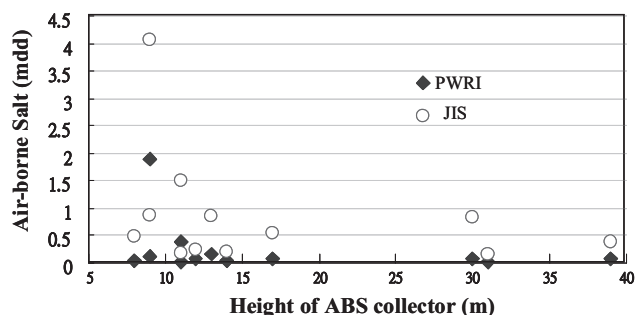


Figure 6: Dependency of Air-borne Salt on Height of ABS Collector.

3.3 Dependency of ABS on weather factors

By recognizing the amount of air-borne salt will be affected by not only the geographical conditions but also the climate conditions, one on-site meteorological station was installed at Port 1 of Kaohsiung Harbor for collecting on-site wind velocity, wind direction, temperature, humidity and rainfall data. Moreover, the weather information at Nanje, Shougan, Jouin, Chenjin, Linyuan, Chaotou, Poje, Shinin, Annan, Kaohsiung, Tainan, Younkan, Shanhua and Jyugin were purchased from Central Weather Bureau of Taiwan. By interpolating all purchased weather information, all weather information at the on-site ABS collectors can be estimated. However, during the sorting of the weather information, it was found that there was high peak of rainfall and wind velocity due to typhoon invasion between 2007.07 and 2007.08. In order to distinguish the influence of the typhoon on air-borne salt, the weather information during 2007.07 and 2007.08 were separated with the weather information during other observation period, which were tabulated in Table 2.

Table 2: Recorded Weather Information and ABS during Typhoon Invasion.

| Location | Collector Type | Exposure Period (Year/month/day) | Air-borne salt (mdd) | temperature (°C) | humidity (%) | Wind velocity (m/s) | Wind-face ratio | rainfall (mm) |
|-----------------------------|----------------|----------------------------------|----------------------|------------------|--------------|---------------------|-----------------|---------------|
| Port 10 of Kaohsiung Harbor | PWRI | 2007.07.26~08.23 | 1.477 | 29.35 | 72.77 | 2.732 | 0.231 | 1966.4 |
| | | 2007.07.26~08.23 | 0.957 | 29.35 | 72.78 | 2.732 | 0.231 | 1966.4 |
| | | 2007.07.26~08.23 | 1.494 | 29.35 | 72.77 | 2.732 | 0.231 | 1966.4 |

| Location | Collector Type | Exposure Period (Year/month/day) | Air-borne salt (mdd) | temperature (°C) | humidity (%) | Wind velocity (m/s) | Wind-face ratio | rainfall (mm) |
|---------------------|----------------|-------------------------------------|-------------------------|---------------------|-----------------|------------------------|-----------------|------------------|
| | JIS | 2007.06.12~07.10 | 0.011 | 30.57 | 66.52 | 2.274 | 0.233 | 72.3 |
| | | 2007.08.07~09.04 | 0.011 | 28.58 | 78.82 | 2.410 | 0.245 | 2115.3 |
| | | 2007.06.26~07.10 | 0.009 | 31.11 | 66.30 | 3.069 | 0.225 | 30.5 |
| | | 2007.08.07~08.21 | 0.007 | 28.27 | 91.02 | 3.368 | 0.241 | 1516.9 |
| Port 1 of Kaohsiung | PWRI | 2007.07.26~08.21 | 1.654 | 28.83 | 78.35 | 2.696 | 0.163 | 1945.6 |
| | | 2007.07.31~08.28 | 3.288 | 28.49 | 80.61 | 2.77 | 0.12 | 1959.6 |
| Harbor | JIS | 2007.08.21~09.04 | 0.009 | 29.08 | 74.09 | 1.688 | 0.185 | 171 |

3.3.1 Rainfall

If excluding the influence of typhoon invasion, the dependency of ABS on the recorded rainfall can be given in Figure7. For PWRI collector, with the increase of rainfall, there is moderate raise of ABS. If the rainfall due to typhoon is included, as shown in Figure8, it is obvious that there is clear dependency of ABS on the rush of rainfall. On the other hand, for JIS collector, with the increase of rainfall, the collected ABS showed the decrease tendency. Especially, when the rainfall is over 300mm, the ABS collected by JIS type is almost close to zero. For such kind of variation, "washout effect" may be a good reason for explaining the huge different of ABS collection; that is to say, for larger rainfall, the recorded ABS should be less due to the washout.

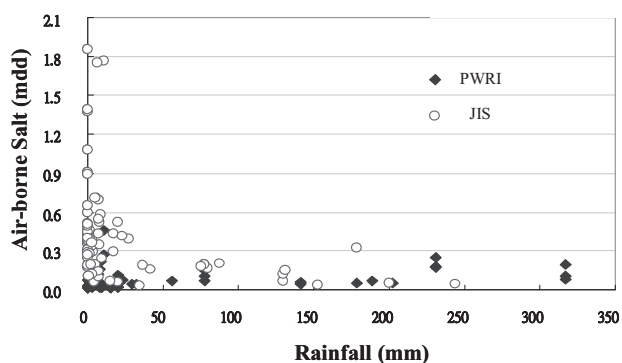


Figure 7: Dependency of Air-borne Salt on Rainfall excluding Typhoon Invasion.

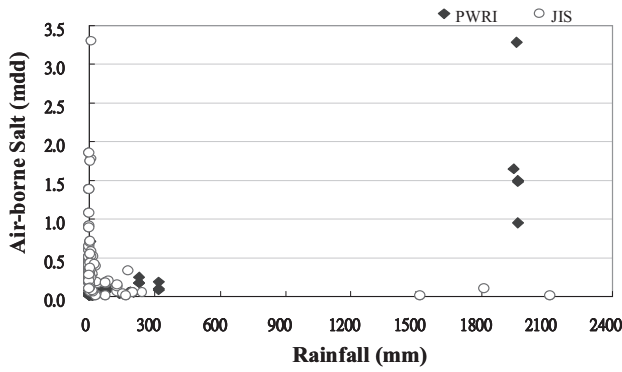


Figure 8: Dependency of Air-borne Salt on Rainfall including Typhoon Invasion.

3.3.2 Temperature

As shown in Figure 9, it seems quite obscure for the dependency of ABS on temperature, either for PWRI type or for JIS type.

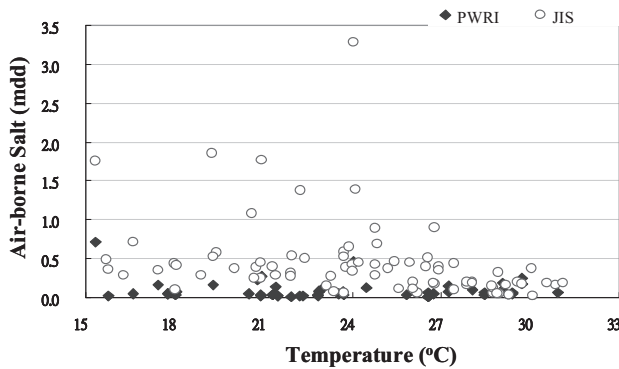


Figure 9: Dependency of Air-borne Salt on Temperature.

3.3.3 Humidity

As shown in Figure 10, it can be found that there is bell-type distribution of ABS along the increase of humidity, either for PWRI type or for JIS type, which means the accumulation of ABS due to humidity on the surface of the collector will grow up to certain limit; then, owing to the weight of ABS and the formation of water drop on the surface of the collector, the fall of water drop will bring down the accumulated ABS.

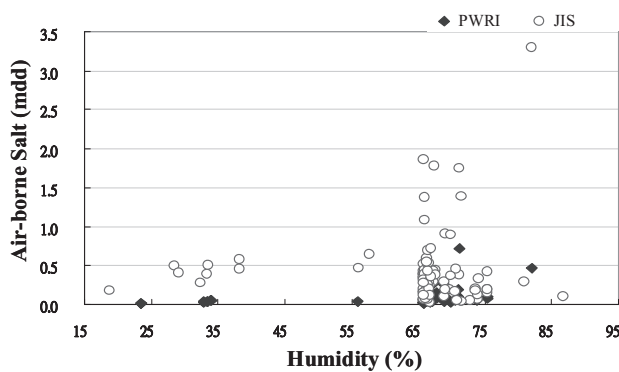


Figure 10: Dependency of Air-borne Salt on Humidity.

3.3.4 Wind

In order to clarify the dependency of ABS on wind, there will be two factors for discussion – one is wind velocity and the other is wind-face ratio. The wind-face ratio is defined as the ratio of wind direction vertical to the surface of the collector per collection period. As shown in Figure 11, it is difficult to judge if there is clear dependency of ABS on wind velocity, either for PWRI type or for JIS type. However, for JIS type, the amount of ABS seems to be generally larger than the amount of ABS from PWRI collector with the increase of wind velocity, which coincides with the observation findings of on-site RC structures.

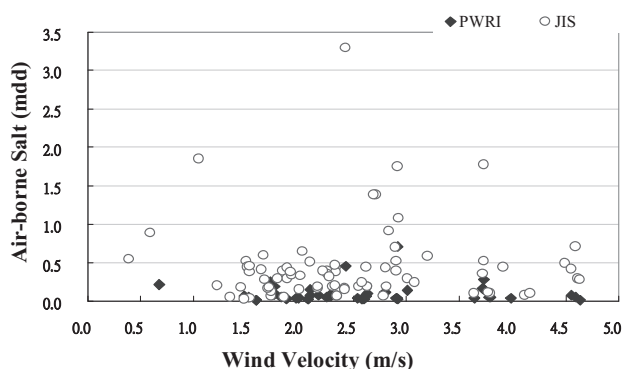


Figure 11: Dependency of Air-borne Salt on Wind Velocity.

As for the wind-face ratio, from Figure 12, it is also hard to find if there is clear dependency of ABS on wind-face ratio. However, for JIS type, the amount of ABS seems to be generally larger than the amount of ABS from PWRI collector with the increase of wind-face ratio, which coincides with the observation findings of on-site RC structures. But, the declination tendency of JIS type collector over wind-face ratio=0.2 reveals that the accumulation of ABS on the surface of JIS type collector has its limit.

3.4 Feasibility of ABS collectors

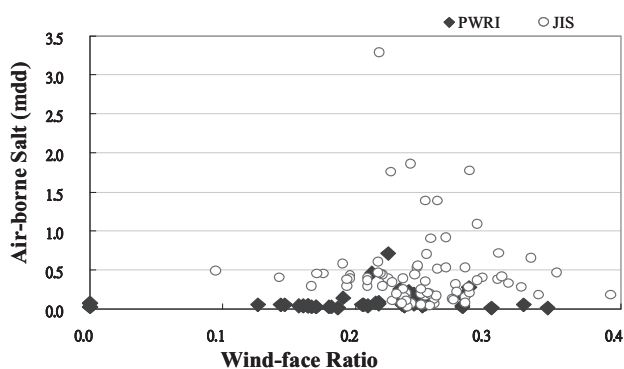


Figure 12: Dependency of Air-borne Salt on Wind-face Ratio.

From all the above discussions, it can be first concluded that the ABS trapped by PWRI collector is found to be lower than the ABS trapped by JIS collector. In addition, from the analysis experience for both type collectors, it is also found that PWRI collector seems to be fit for more-than-30-day exposure test while JIS collector is only valid for less-than-15-day exposure

test. Furthermore, for considering the effect of rainfall and humidity, the recognized "washout effect" seems to be reflected in the result of JIS collection. As for the dependency of collection effect on wind, the finding is no clear difference between PWRI and JIS collectors. By integrating all the comparison effects, although the short collection period is the main drawback for JIS collector, JIS collector has higher priority to PWRI collector on reflecting air-borne salt feature of on-site RC structures.

4. CONCLUSION

Through up-to-18 month exposure test, the collection effect of PWRI and JIS collectors on ABS was compared by means of geographical and weather information. So far, by considering the dependency of ABS on distance to seashore, height of ABS collector, rainfall, temperature, humidity, wind velocity or wind-face ratio, JIS type collector seems to be suitable for reflecting the air-borne salt feature of on-site RC structures although the short collection period of JIS type collector limits its use. As a result, how to combining the advantage of JIS with the improved collection period of JIS is the next research issue on on-site exposure test for air-borne salt.

REFERENCES

- Bridge Sector of Public Work Research Institute, 1993. *National Survey on Air-Borne Salt (IV) – Distribution Characteristics of Air-borne Salt and Wind*, PWRI Publication, No.3175, pp. 1~26. (in Japanese)
- Japan Weathering Test Center, 1998. JIS Z 2382 Measurement of Corrosion Factors from Atmosphere. (in Japanese)
- LIN, Y.Z., 2008. *Performance-based design for anticorrosion of reinforced concretes under air-borne salt attack*, Master Thesis, National Kaohsiung First University of Science and Technology. (in Traditional Chinese)

AN EVALUATION OF POTENTIAL COMMUNITY HILL SLOPE INSTABILITY AROUND METROPOLITAN AREA IN TAIWAN

KUO-HUNG TSENG

Associate Professor, Department of Construction,
National Kaohsiung First University of Science and Technology, Taiwan
bob@ccms.nkfust.edu.tw

ABSTRACT

The purpose of this study is to find the effects of hazardous factors on hill slopes and then to develop a statistical model for the assessment of community hill slope instability around the Kaohsiung metropolitan area in Taiwan. Field investigations on hill slope include failed and non-failed slopes, and their surrounding slope stability measures are conducted for 200 sites. The data is collected from each site for the selected 11 affecting factors including slope gradient, slope aspect, slope height, rock strata, plant coverage, erosion condition, weathering condition, slope drainage, toe cutting, slope seeping and slope maintenance, which are considered the main factors affecting the slope instability. Each affecting factor is quantified by using the dangerous index method. The statistical model was developed based on quantified values of each factor through the discriminate analysis to identify the slope's susceptible instability. The model was verified from the 50 sets of data collected and the results indicated that the accuracy to predict the slope failure is about 72% on the basis of the selected affecting factors. It is believed that the proposal model will provide a guideline for the city environment development in Kaohsiung city government.

1. INTRODUCTION

The development of hillside community is one of the most important land uses in the city of Taiwan. However, these hill slopes are located on the earthquake zone, attacked by the heavy rainfall from storms during each summer and often over-occupied with human activities, causing the hazards of slopes to frequently occur and the safety of community residents is endangered. Therefore development of community on hill slopes around the city has been a major concern for the city government. In recent years Kaohsiung County Council has enthusiastically accelerated the development of industry and commerce which attracts numerous people from adjacent cities to crowd into county. This leads the density of population increased drastically and causes the limited and usable lands of the county are gradually of shortage. A tendency of developing hillsides is consequently getting fast expending. However, the development of hillsides tends to

diversity and complexity, including resorts, community housing, temples, orchards, schools, public facilities, and etc. The hillsides in the Kaohsiung metropolitan area are located within the geological province of the Central Range composed of fracture slates and of the Western Foothills composed of soft rocks such as conglomerate, sandstone, shale and mudstone. Due to the complexity of geological structures, soft rocks appearing on the hillsides, and intense rainfall within a short period, the hillsides in the area innately tend to unfavorable stable. Because of overdevelopment and usage of hillsides and lack of control to geological conditions and hydrogeology, these trigger the several hillside damages occurred in the historic records. These damages of hillsides threaten the prosperous development in the Kaohsiung metropolitan area, safety of community residents and protection of assets. It is therefore that the aim of this study attempts to find the effects of hazardous factors on the community hillsides and to develop a statistical model for the analysis of the potential hazardous hillsides in the Kaohsiung area. The study is subsequently to be as a guideline of planning and design of hillsides stability for the local governments.

2. GEOMORPHOLOGICAL AND GEOLOGICAL SETTING

The community hillsides investigated in the study mainly located at Dashe, Dashu, Yanchao and Chishan of Kaohsiung County as show in Figure1. Dashe is located at central part of Kaohsiung plain, west bordered with Nantzu, north bordered with Yanchao, west bordered with a small group of hill to Dashu, and south bordered with Renwu. Guanginshan of northeastern Dashe appears at the end of Neimen Hill. The slope gradient is about 15°-23° with elevation of 50-100 meters above sea level. The bedrock exposed at Guanginshan is of Nanshihlan sandstone composed of thick-bedded, fine to medium-grained sand stone and muddy sandstone with intercalation of sandstone and shale. The rock belongs to weak and soft and presents a lower resistance to abrasion and erosion. Dashu is located at a hillside south of the Lingkou and west of the Gaobing stream. The highest land is at the border between Dashe and Shengsian, with elevation of 225 meters above the sea level. The northwest side is higher than the southeast side, and the mountain is stretching east to west. The geology is of red soil of Pleistocene and the Nanshihlun sandstone consisted of mainly thick-bedded carbonaceous shales intercalated with thick bed of fine to medium-grained, poorly cemented sandstone. Yanchao is located at central part of the Kaohsiung County, a junction zone between Kaohsiung plain and Neiman Hill. The bedrock exposed is a massive mudstone with age ranging from pliocene to pleistocene. The mudstones are consists of fine and loose cemented particles. It usually suffers severe erosion that easily leads to steep channels and abrupt slopes and looks like a piece of barren land. Because of containing much inorganic salts that there are frost-like crystals which are unfavorable to plant-growth. Rock formations exposed in Chishan include the Shinei formation of the Pliocene, Nanshiken formation of Plocene and Dawo fine sandstone, Nanhua mudstone of Pliocene and Linko conglomerate of Pleistocene. (Wang 1997) Due to the complex and

different rock formation, the sandstone tends to more protuberant than mudstone and forms a ridge. The mudstone suffers easily severe erosion and leads to deep and wide erosive channel. There are major faults exposed in the vicinity of the area, including Chishan fault and Fengshan fault. The Chishan fault is a major high angle reverse fault. It trends in a NE-SW direction in the Kaohsiung-Pingtung area. The Fengshan fault trends in a close north-south direction and is situated between the Fengshan hill and the Pingtung plain. (Sun 1964)

The climate in these areas is tropical with average temperatures ranging from between 18.6 and 28.7 degree Celsius, and average annual rainfall is about 1500mm.

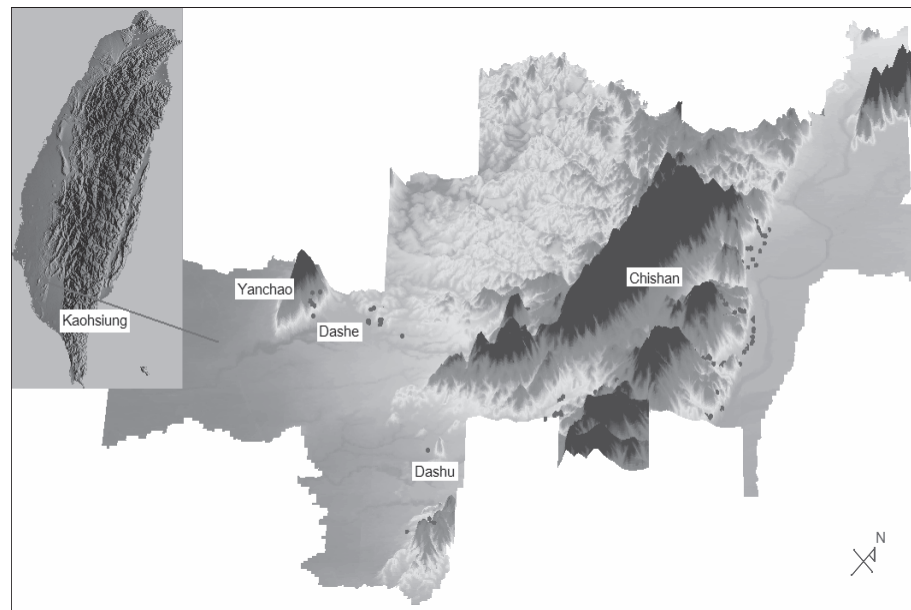


Figure 1 : Locations of sites

3. METHODOLOGY

Several factors may affect the slope instability. In general, it can be classified two major categories, i.e. potential factors and induced factors. Potential factors involve the factors that cause the slope instability from slope itself, such as slope gradient, slope height, and etc. Induced factors involve the factors that cause the slope instability from the external forces such as earthquake, typhoons, rainfall and etc. Induced factors may be associated with time and dynamic conditions such that an analysis of slope stability leads to difficulties. Potential factors are easier to obtain in spatial conditions and are used to perform an assessment of the slope instability. Hence, the data of the potential factors are used to conduct the statistical analysis in this study. A total of 200 sites of community hill slopes, located at Chishan, Yanchao, Dashe, and Dashu of the Kaohsiung County, is investigated. The data of affecting factors includes slope gradient, slope aspect, slope height, erosion condition, plant coverage, weathering condition, toe cutting, slope drainage, slope seeping, and slope maintenance, and distance to fault. The total data sets have been divided into two parts. The

first part containing 150 data sets out of 200 data sets has been used for statistic analysis to develop a model to identify the slope instability. Rest of 50 data sets is used for validation purpose. These data sets can be referred to work by Chen (2007).

3.1 Data collection of influential factors

The data of influential factors considered in hillsides is collected from the field. A total of 12 factors is preliminarily chosen and how to classify is described as follows :

1 . Slope gradient : The slope gradient of each hillside is measured by using a compass placed on the board on the slope. It is divided 5 grades : $<20^\circ$, $21^\circ-30^\circ$, $31^\circ-40^\circ$, $41^\circ-60^\circ$, and $>60^\circ$.

2 . Slope aspect : The slope aspect of each hillside is measured by using a compass and is divided 4 grades : NW, NE, SW, and SE.

3 . Slope height : The slope height is a vertical distance from the point observed to the top of the slope. It is divided 5 grades : $H<5m$, $6m\leq H<10m$, $11m\leq H<15m$, $15m\leq H<20m$, $>20m$

4 . Rock stratum : It is obtained by pointing the coordinates, obtained from GPS at fields, on the geological map. Most of rocks can be classified sandstone, intercalation of sandstone and shale, conglomerates, and mudstone

5 . Plant coverage : It is observed by eyes based on the percentage of area planted and is divided 5 grades : very dense ($>75\%$) , dense ($51\%-75\%$) , medium ($26\%-50\%$) , loose ($11\%-25\%$) and very loose ($\leq 10\%$) .

6 . Erosion condition : It is observed from the trace of washout appeared on the slope and is divided 5 grades : none, slight, medium, severe, and completed erosion.

7 . Weathering condition : It is based on ISRM classification of weathered rocks and is divided 5 grades : none, low, moderate, high, and completed weather.

8 . Slope drainage : It is observed from the drainage structures and drainage conditions at the slope and toe and is divided 5 grades : excellent, good, fair, poor and very poor.

9 . Slope seeping : It is observed whether the groundwater seeps out from the slope and is divided 5 grades: dry, damp, seeping, and flowing .

10 . Toe cutting : It is measured at the field and is divided 5 grades: $H\leq 1m$, $1m<H\leq 3m$, $3m<H\leq 5m$, and $H\geq 5m$.

11 . Slope maintenance : It is observed the conditions of retaining structures or slope protection measures at the toe and slope and is divided 5 grades : excellent, good, fair, poor and very poor.

12 . Distance to fault : The Arc GIS incorporated with digital geological map is used and measures a distance from a location investigated to the adjacent fault. It is divided 5 grades : $<50m$, $51-200m$, $200-500m$, $500-1000m$, and $>1000m$

3.2 Factor ratings

After data of affecting factors for each hill slope is obtained, it is subsequently required to quantify each grade of the factor for a statistical analysis purpose. A method of dangerous index (Jian 1992) is used to rate each grade of the factor. Firstly, a ratio of failure, x_i , is calculated as

$$x_i = \frac{n_i}{N_i} \quad (1)$$

where n_i is the number of failure at the i th grade of factor and N_i is the total number of failure at the i th grade of factor.

Secondly, the failure fraction, S_i , is calculated as

$$S_i = \frac{x_i}{\sum x_i} \quad (2)$$

Finally, the rating, D , of each factor classified is calculated as

$$D_i = \frac{9(S_i - S_{\min})}{(S_{\max} - S_{\min})} + 1 \quad (3)$$

The rating value of D is ranging from 1 to 10. Table 1 shows the results of rating based on the method of dangerous index of 11 affecting factors classified.

3.3 Multiple discriminant analysis

In order to identify the most influential factors on hill slope instability and quantify their relative contribution, a multiple discriminant analysis (Huberty 1994, Kuo 2002) is performed. The data sets are first prepared including 12 factors of 150 failed and non-failed slopes. The principal component discriminant analysis, F test, allowed a preliminary selection of the most significant variables. It is found that 11 factors out of 12 influential factors input, including slope gradient, slope aspect, slope height, rock stratum, erosion condition, weathering degree, plant coverage, slope, toe cutting, slope drainage, slope seeping, and slope maintenance, are statistical significant except the factor of distance to fault. This may reasonably explain that more than 1000 meters of the distance to fault are found in most of hillsides investigated. This factor is naturally little of effects on the hillside stability and is not chosen in the analysis. These 11 factors are subsequently used as input variables for the multiple discriminant analysis. The discriminant functions are then obtained for different conditions of slope instability, including non-failure, slight failure, moderate failure, and severe failure. The coefficients of each discriminant function obtained from analysis are shown in Table 2.

Table 1: Criteria of factor ratings

| Factors | Class | | | | |
|----------------------|-----------|--------------------------------------|--------------|----------|-----------|
| | Ratings | | | | |
| Slope gradient | ≤20° | 21°-30° | 31°-40° | 41°-60° | ≥61° |
| | 1 | 4.302 | 5.937 | 7.349 | 10 |
| Slope aspect | NW | NE | SW | SE | |
| | 1 | 4.499 | 8.2 | 10 | |
| Slope height | 0m-5m | 6m-10m | 11m-15m | 16m-20m | ≥21m |
| | 1 | 2.344 | 4.049 | 10 | 10 |
| Rock stratum | Sandstone | Intercalation of sandstone and shale | conglomerate | Mudstone | |
| | 1 | 5.768 | 6.716 | 10 | |
| Plant coverage | ≥76% | 51%-75% | 50%-26% | 11%-25% | ≤10% |
| | 1 | 2.631 | 3.461 | 7.218 | 10 |
| Erosion condition | none | slight | moderate | severe | completed |
| | 1 | 1.701 | 3.279 | 8.378 | 10 |
| Weathering condition | none | low | moderate | high | completed |
| | 1 | 3.328 | 4.763 | 7.226 | 10 |
| Slope drainage | excellent | good | fair | poor | very poor |
| | 1 | 2.307 | 2.659 | 8.944 | 10 |
| Slope seeping | dry | damp | seeping | flowing | |
| | 1 | 2.069 | 7.232 | 10 | |
| Toe cutting | none | 1m~3m | 4m~6m | 7m~9m | ≥10m |
| | 1 | 3.854 | 4.512 | 6.958 | 10 |
| Slope maintenance | excellent | good | fair | poor | very poor |
| | 1 | 2.265 | 3.389 | 6.062 | 10 |

The accuracy of the discriminant functions can be found in the analysis that 82% of overall 150 hill slopes are successfully classified. Finally, it is worth to know which factor would be the most influential on the slope instability. According to the results of the analysis, the influential factors contributing to slope instability are in order of slope seeping, plant coverage, toe cutting, slope aspect, slope maintenance, erosion condition, slope gradient, weathering condition, slope drainage, rock stratum, and slope height.

Table 2: Discriminant function coefficient for 4 grade of slope failure conditions

| Failure degree \ Factors | Non-failure | Slight Failure | Moderate Failure | Severe Failure |
|--------------------------|-------------|----------------|------------------|----------------|
| Slope gradient | 1.597 | 1.643 | 2.19 | 1.73 |
| Slope aspect | 1.143 | 1.630 | 1.49 | 2.005 |
| Slope height | 0.701 | 1.030 | 0.824 | 1.989 |
| Rock strata | 1.681 | 1.820 | 1.974 | 2.564 |
| Plant coverage | 0.834 | 1.118 | 0.712 | 0.904 |

| Failure degree Factors | Non-failure | Slight Failure | Moderate Failure | Severe Failure |
|---------------------------|-------------|----------------|------------------|----------------|
| Erosion condition | 0.009 | 0.364 | 0.436 | 0.840 |
| Slope drainage | 0.352 | 0.364 | 0.312 | 0.335 |
| Slope seeping | 0.515 | 0.540 | 2.365 | 1.791 |
| Weathering condition | 0.769 | 1.063 | 0.854 | 1.456 |
| Toe cutting | -0.084 | -0.132 | -0.100 | -0.960 |
| Slope maintenance | 0.233 | 0.425 | 0.674 | 0.499 |
| constant | -19.742 | -29.592 | -40.798 | -51.411 |

3.4 Validation of discriminant model

The predicted model developed is verified on the data sets of 50 out of 200 sites investigated. The rating value of each factor for 50 hill slopes is input the presented above 4 discriminant functions, respectively, the classification of slope instability is determined by a maximum value calculated from those functions. The results of analysis show that the accuracy of the presented discriminate model is about 72% on the 50 hill slopes as shown in Figure 2. However, if the grades of slight failure, moderate failure, and severe failure are combined as a failed, it is found the discrimination accuracy is about 81% for non-failed hill slopes and about 66% for failed hill slopes.

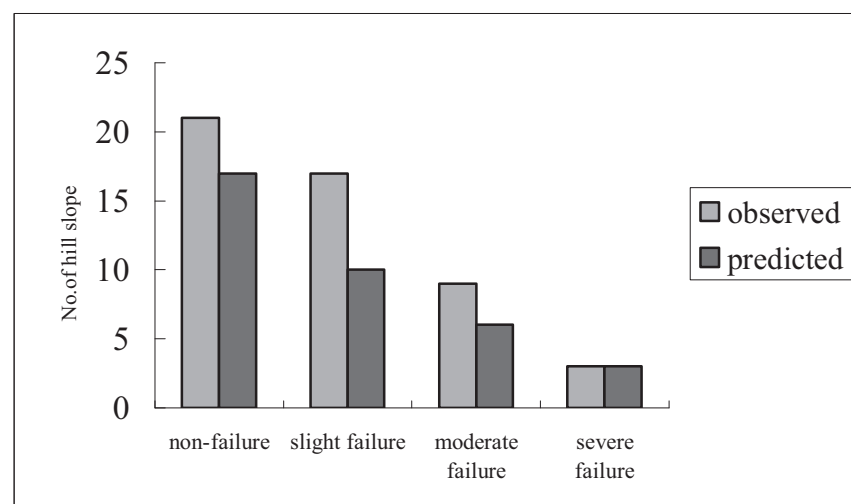


Figure 2 : Comparison between observed and predicted hill slopes

4. CONCLUSIONS

This study is focused on the affecting factors of investigation on the community hillsides at Chishan, Dashu, Dashe, and Yanchao of the Kaohsiung County. The ratings of each affecting factor are evaluated by

using a method of dangerous index. A model developed for the assessment of the hill slope instability is based on a method of discriminate analysis. The data of affecting factors is collected from the field investigation. The affecting factors include the slope gradient, slope aspect, slope height, erosion condition, plant coverage, rock strata, weathering condition, toe cutting, slope drainage, slope seeping, and slope maintenance. Data sets of 150 out of 200 are used to develop an assessment model and the data sets of the rest are used to verify the model developed. The results show that the accuracy of the developed model is about 82% on the training data sets. The model was verified from the 50 data sets and the results indicated that the accuracy to predict the slope failure is about 72%. The influential factors contributing to slope instability are in order of slope seeping, plant coverage, toe cutting, slope aspect, slope maintenance, erosion condition, slope gradient, weathering condition, slope drainage, rock stratum, and slope height.

REFERENCES

- Chan, Y.C., 2007. The Study for Potential failure on Community hill slopes. Thesis of Master of Science, National Kaohsiung First University of Science Technology
- Huberry, C.J., 1994. *Applied Discriminant Analysis*, John Wiley, New York, NY, pp 182-208
- Jian, L.B., 1992. Application of Geographic Information System in the Quantitative Assessment of Hillslope Quantitative Stability. Thesis of Master of Science, National Chung Hsing University. (In Chinese)
- Kuo, R.B., 2002. A Study on Determining Slope Stabilization Methods with Discriminant Analysis. Thesis of Master of Science, National Taiwan University of Science and Technology. (In Chinese)
- Lan, Y.S., 1999. Study on Estimating the Probability of Slope Land slide by Discriminate Analysis. Thesis of Master of Science, National Taiwan University of Science and Technology. (In Chinese)
- Sun, S.C., 1964. Photogeological Study of the Taiwan-Kaohsiung Coastal Plain Area, Taiwan, *Petroleum Geology of Taiwan*, No.3. pp 39-51.
- Wang, S.H., 1997. The Characteristic of the Disasters of Environmental Geology at Chyi-Shan Area, Thesis of Master of Science, National Cheng Kung University. (In Chinese)

INFLUENCE OF INITIAL CURING ON CHLORIDE PENETRATING CHARACTERISTICS IN CONCRETE EXPOSED TO DIFFERENT MARINE ENVIRONMENT

WEN XUE¹, JIANGUO DAI²,
HIROSHI YOKOTA² and WEILING JIN¹

¹College of Civil Engineering and Architecture, Zhejiang University,
Zhejiang 310027, China;

²Port and Airport Research Institute, Japan.
xuewen2006@gmail.com

ABSTRACT

Concrete durability is influenced by both the initial curing condition and the following exposure environment besides the constituents of concrete itself. In this contribution, 15 concrete cylinders were cast and cured in five conditions characterized with different humidity (air-curing and water-curing) and curing durations (1d, 5d and 14d). After curing, all the cylinders were exposed separately under three kinds of marine environment including splash zone, tide zone and immersion zone for 6 months. Then the total chloride contents in concrete were measured using the automated ion-selective electrode method. The apparent chloride diffusion coefficient D_a and surface chloride content C_0 were obtained by fitting the chloride concentration profiles with the Fick's second law. The testing results show that the initial saturated curing has a great impact on reducing the early-stage chloride absorption. Given a specific environment the value of C_0 tends to be low when saturated curing was fully applied at the early age. On the other hand, exposure environment influences not only the accumulation of chloride on the surface but also the value of D_a . A severer cyclic wet-dry environment results in a higher chloride accumulation on the surface layer but a lower D_a value. In conclusion, a refined durability design requires considering the effects of both the initial curing conditions and the following exposure environment. Moreover, the apparent chloride diffusion coefficient D_a and surface chloride content C_0 cannot be treated as two independent design parameters for a certain service environment.

1. INTRODUCTION

Concrete durability is influenced by both the initial curing condition and exposure environment besides the constituents of concrete itself. It was reported that the compressive strength of silica fume concrete cured at 65% RH was lower than that cured at 100% RH (Atis, 2005). The pore structures were improved with the fulfilling of curing so that the permeating

of gas or liquid was blocked (Nasir, 2004). Ramezaniapour (1995) measured the electric flux of concrete cured under same humidity but different durations through ASTM C1202 method and found that long curing duration helped to reduce the electric flux of concrete. Khatib (1999) discussed the positive impact of long duration and high humidity of curing on the concrete permeability through an immersion testing. Jaegermann (1990) deposited the concrete which was cured under different durations to the atmosphere by the seashore of Mediterranean for 3 years, and found that the sufficient initial curing increased the chloride resistance of concrete significantly at the early period of exposure.

The strong relationship between initial curing conditions and the concrete durability performance had been studied, while for the real coastal concrete infrastructures, the durability is affected by the marine environment as well. However, there are few researches discussing about the coupling effects of initial curing condition and exposure environment imposed on the chloride penetrating characteristics in concrete recently.

In this contribution, fifteen concrete cylinders were cast and cured in five conditions characterized by different humidity (air-curing and water-curing) and curing durations (one day, five days and fourteen days). After curing all the cylinders were exposed into three kinds of marine environment including splash zone, tide zone and immersion zone separately for six months. The coupling effect of initial curing condition and following exposure environment on the chloride penetrating characteristics in concrete was discussed.

2. EXPERIMENT

2.1 Materials

Cylinder specimens were cast ($\text{Ø}100\text{mm} \times 200\text{mm}$) in plastic moulds. The materials were produced in Japan. The details of concrete mix and the aggregate properties are displayed in Table1 and Table2.

Table1. Concrete mix (kg/m^3)

| W/C | Cement | Water | Sand | Gravel | Water Reducer | S/(S+G) (%) | Slump (mm) |
|-------|--------|-------|------|--------|---------------|-------------|------------|
| 55.5% | 318 | 176 | 848 | 950 | 3.18 | 47.9 | 18cm |

Note: Max size of gravel=20mm; Max size of sand=5mm.

Table2. Aggregate properties

| | Specific gravity (kg/m^3) | Absorption (%) | Fineness modulus |
|--------|--------------------------------------|----------------|------------------|
| Sand | 2.62 | 1.21 | 2.67 |
| Gravel | 2.69 | 0.34 | 6.46 |

The specimens were kept in an indoor environment with the temperature of 23°C and 75% RH on average for 24hours after casting. Two bottoms of each specimen were sealed with epoxy right after curing was over, and the cylinder surface was to be exposed to the seawater.

2.2 Initial curing conditions

Five different curing conditions were adopted. Details of curing conditions are given as below.

(1) The group of specimens which was exposed into real marine environments right after demoulding was coded as A1.

(2) The group of specimens which was covered by wet burlap and placed in the curing room of constantly 25°C and 50% RH for five days was coded as A5.

(3) One group of specimens were cured in the same condition as A5 for the first five days after demoulding. Then the wet burlap sheet was removed and the concrete was deposited in the same room as A5 for further night days. This group was coded as A14.

(4) Specimens which were cured under fresh water for five days in the same room as A5 and A14 were coded as W5.

(5) Specimens which were cured under fresh water for fourteen days in the same room as W5 were coded as W14.

2.3 Exposure environment

The specimens were exposed in splash zone, tide zone and immersion zone separately for six months. The exposure site adopted in this study was located by the Kurihama Bay, Japan. The temperature and humidity variation of this area during the whole exposure period was recorded (see Figure1).

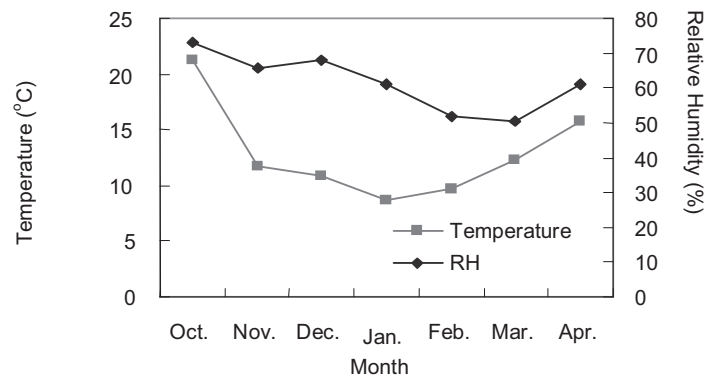


Figure 1: Variation of temperature and RH during the whole exposure period

Tide zone and immersion zone were located in the same pool about 2.5m deep. Seawater from the bay was pumped in and drained out automatically at an interval of six hours (see Figure2). The specimens in the immersion zone were under seawater all the time, and those in the tide zone were subjected to the wet-dry cycle twice a day at the ratio of 1:1. Splash zone was located in the atmosphere by the seaside. The seawater shower in this area was automatically controlled at an interval of eight hours (see Figure3). The wet-dry ratio was 1:2.

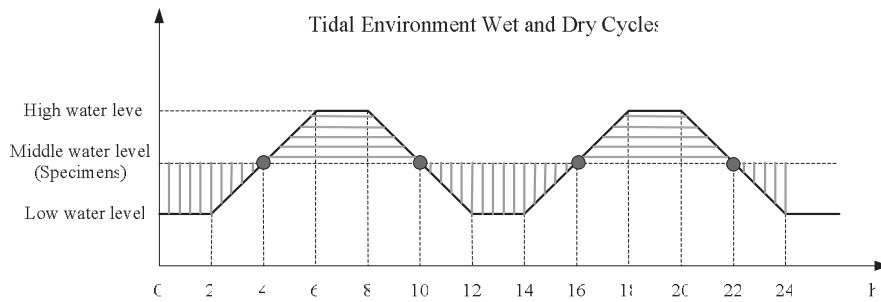


Figure 2: Seawater level variation and specimens' location in Tide and immersion zones

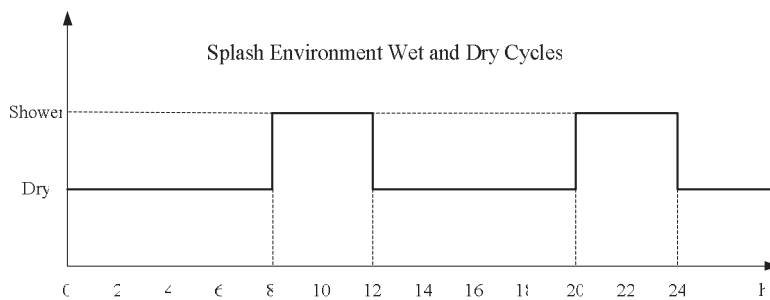


Figure 3: Showering controlled schedule in Splash zone

2.4 Test method

After six months exposure, the two epoxy-sealed bottoms of each cylinder were cut off at the thickness of 30mm and the left cylinder was central sliced into a 10-mm-thick piece along the diameter. The slice was further cut into strips at the depth of 5mm, 10mm, 15mm, 20mm, 30mm, 40mm, and 50mm from the surface. All the samples were dried in the chamber of 40°C and 100%RH for 24h and powdered afterwards. The automated ion-selective electrode method was used to measure the total chloride content of each concrete sample. The apparent chloride diffusion coefficient D_a and surface chloride content C_0 were obtained by fitting the chloride concentration profiles with the Fick's second law (see Equation 1).

$$C(x,t) = C_{0s} \left\{ 1 - \operatorname{erf} \left(\frac{x}{2\sqrt{D_a \cdot t}} \right) \right\} \quad (1)$$

Where, $C(x,t)$ is the chloride concentration at a depth x (mm) at time t (year); C_{0s} is the chloride concentration at the surface which is derived from regression; erf is the error function; D_a is the apparent diffusion coefficient (cm^2/s).

3. TESTING RESULTS

3.1 Chloride concentration profiles

Figure4 illustrates the chloride concentration distribution in each specimen. Using these concentration values the apparent diffusion coefficient and surface chloride content were obtained from Equation 1 (see Table3, Figure5 and Figure6). To compare the amount of chloride penetrating in concrete quantitatively, the values of total chloride content C_t were calculated through computing the area below profiles (see Table3).

In the case of W14, the chloride concentration at each depth was lower than all the other concrete exposed in the same environment, correspondingly the value of C_t was the lowest. Chloride ions cumulated significantly in the surface layer of A1. For the concrete cured under the same condition but exposed in different environments, the value of C_0 in splash zone was the highest while its D_a value was the lowest (see Table3).

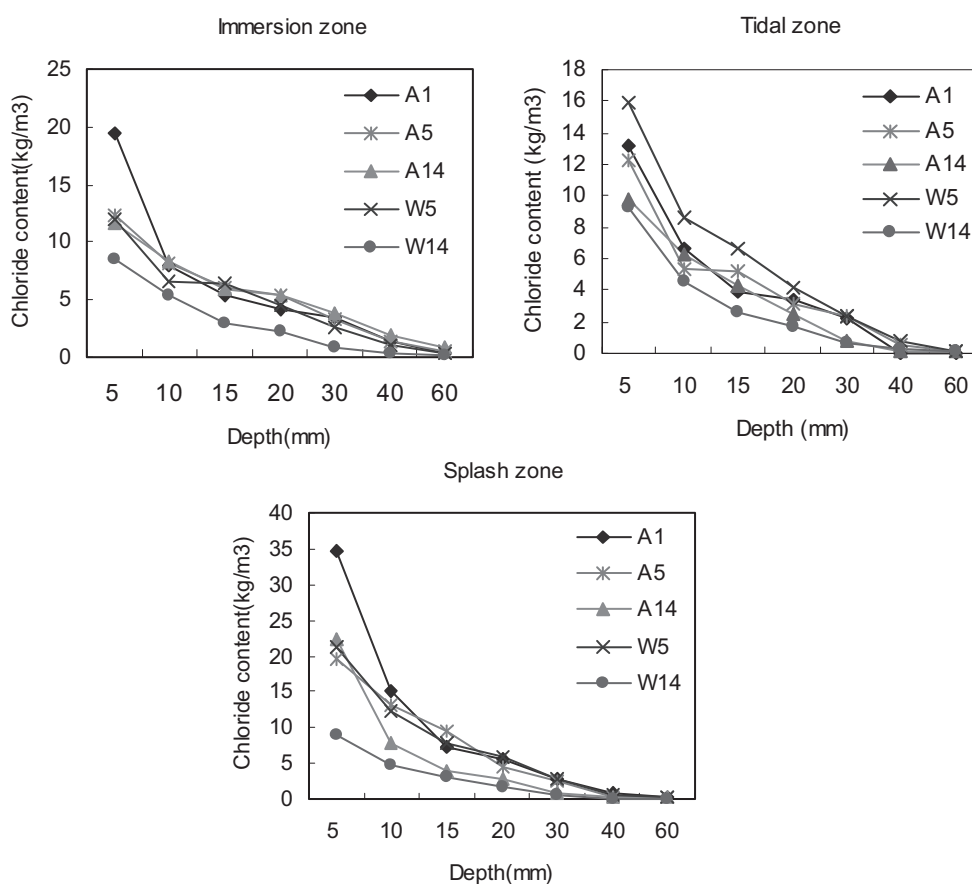


Figure 4: Chloride concentration distribution of concrete

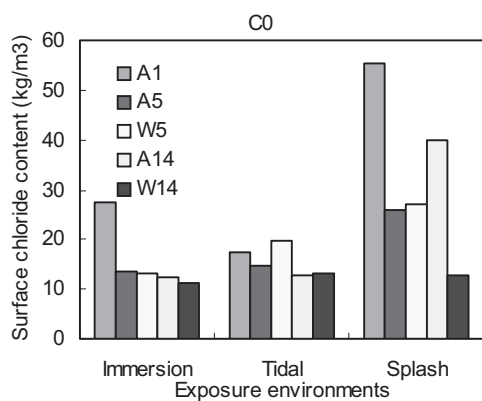


Figure5 : Surface Chloride content

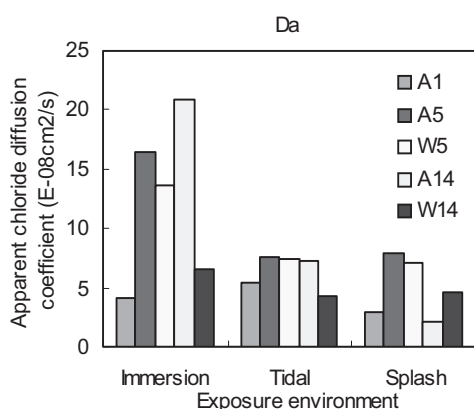


Figure 6 :: Apparent D value

Table3. Surface chloride content and Apparent chloride diffusion coefficient

| Exposure environments | Curing regimes | Curing durations (days) | Specimen codes | C ₀ (kg/m ³) | D _a (E-08 cm ² /s) | C _t (kg/m ³) |
|-----------------------|----------------|-------------------------|----------------|-------------------------------------|--|-------------------------------------|
| Tide zone | Air | 1 | A1 | 19.92 | 7.42 | 52.74 |
| | | 5 | A5 | 14.73 | 7.48 | 39.88 |
| | | 14 | A14 | 12.93 | 7.29 | 30.21 |
| | Water | 5 | W5 | 17.51 | 5.49 | 40.99 |
| | | 14 | W14 | 13.34 | 4.25 | 27.20 |
| Splash zone | Air | 1 | A1 | 55.44 | 3.04 | 102.30 |
| | | 5 | A5 | 25.87 | 7.82 | 60.81 |
| | | 14 | A14 | 39.96 | 2.19 | 62.42 |
| | Water | 5 | W5 | 27.22 | 7.01 | 68.44 |
| | | 14 | W14 | 12.71 | 4.65 | 25.96 |
| Immersion zone | Air | 1 | A1 | 27.55 | 4.14 | 62.09 |
| | | 5 | A5 | 13.70 | 16.40 | 46.21 |
| | | 14 | A14 | 12.58 | 36.60 | 43.35 |
| | Water | 5 | W5 | 13.24 | 13.70 | 42.92 |
| | | 14 | W14 | 11.41 | 6.56 | 27.85 |

Note: C₀ = surface chloride content; D_a = apparent diffusion coefficient and C_t = total chloride ions penetrated into concrete.

3.2 Modified apparent diffusion coefficient

The transferring mechanism of chloride in the concrete surface was complicated (Zhangyi, 2008) and the capillary suction dominates the chloride moving in the surface layer of about 15mm in depth (Nilson, 2003). On the purpose of studying diffusion mechanism only, the first point at the depth of 5mm of each profile was removed and the modified D_a values were calculated from Equation 1 (see Table4, Figure7). The results indicated that modified D_a values of concrete cured under same condition were in the sequence of Immersion> Tide> Splash.

Table4: Modified D_a ($E-08cm^2/s$)

| | Immersion zone | Tide zone | Splash zone |
|-----|----------------|-----------|-------------|
| A1 | 31.40 | 18.40 | 15.20 |
| A5 | 25.20 | 16.40 | 7.75 |
| W5 | 18.60 | 13.70 | 13.90 |
| A14 | 36.60 | 7.77 | 9.64 |
| W14 | 14.00 | 11.80 | 7.97 |

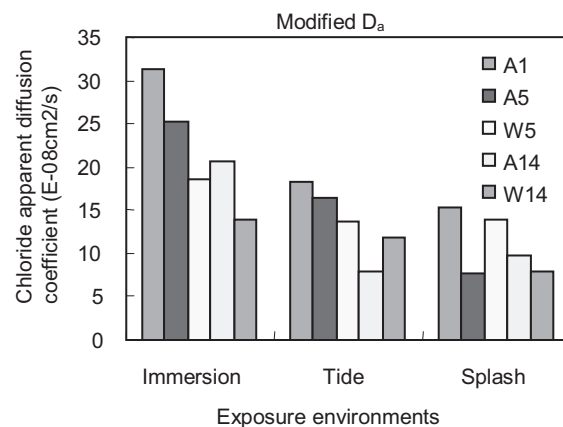


Figure 7: Modified D_a

4. DISCUSSION

It could be understood from the exposure testing data that the surface chloride content C_0 and the apparent diffusion coefficient D_a were influenced by both initial curing conditions and following exposure environments.

4.1 Influence of initial curing conditions

The deduced surface chloride content C_0 obtained from the chloride concentration profiles were shown in Figure6. The most severe chloride

accumulation was found in the surface layer of concrete A1 in each exposure environment and the C_0 value of W14 was the lowest. It's known that during the first three days of hydration, the big pores with the size larger than 2000Å were more than 98% of all the pores and the pore networks were almost connected. With the proceeding of sufficient curing, the pore size and the connectivity of pore network were improved (Yao, 2007). In the case of A1, concrete wasn't cured after demoulding in a normal way. Those big and connected pores resulted in the initial suction of chloride when initially contacting with seawater. The series of A5, W5, A14 and W14 were cured in relatively sufficient ways. Those four groups of concrete could be denser than A1 at the surface layer so that the initial suction effect through big and connected pores was weakened.

Besides the initial chloride suction through big pores in the surface layer, capillary suction was another dominating way of chloride penetrating into concrete. The drier the concrete surface was, the easier the capillary suction occurred and it would continue until the surface layer got saturated (Jin, 2002). In the case of W14, the fourteen days 100% RH curing condition produced the saturated surface layer of the concrete so that the capillary suction was not serious. This situation was found in all of the three exposure environments as well.

The modified apparent diffusion coefficient D_a was reduced significantly with the fulfilling of saturated curing. D_a value of W14 in immersion zone was only half to A1 and was also lower than other series of concrete. The similar sequence of D_a was found in the other two environments. This could be understood that W14 was cured under an almost saturated condition, which helped to form a denser inner micro-structure to prevent the chloride diffusing in concrete, for fourteen days. As a result the value of D_a was lower.

4.2 Influence of exposure environment

Comparing the data of C_0 in Figure6, it could be found that the wet-dry cycle of the exposure environment was another reason for the chloride accumulation in the surface layer. For the concrete cured under the same condition, the initial saturation and the inner structure were almost the same. Therefore, the initial suction effects of the concrete were not in big difference when exposed into different environments. The ratio of wet-dry cycle in splash zone was 1:2 which was severer than the tide zone. During the period without seawater shower, specimens in splash zone were exposed to the atmosphere and suffered from air-drying. The pore water especially in the surface layer vaporized easily so that the pore saturation reduced. Thus, chloride ions were easily sucked into concrete by capillary effect when the seawater shower started again. Suction effect was an irreversible process. The severer the wet-dry cycle was, the worse the chloride accumulation would be.

D_a value was influenced by the wet-dry cycle of the exposure environment significantly as well. The diffusion coefficient of same concrete exposed in different environment was sequenced as Immersion>Tide>Splash (see Figure7). Although the values of C_0 and C_t of the concrete in splash zone were higher than those of other concrete, the D_a

value of this group was the lowest. It could be distributed to the lack of transferring media for chloride diffusion. In the case of splash zone, concrete was air-dried for 2/3 of the whole exposure duration. The evaporation of the pore water reduced the amount of transferring media for chloride diffusion directly. While in tide zone, the wet-dry ratio was 1:1 which was much easier than splash zone was. Furthermore, tide zone was located in the same seawater pool with immersion zone, during the dry period specimens were exposed to a relatively moist environment but weren't subjected to air-drying directly. This circumstance was able to produce a moist inner environment of concrete and helped the chloride to transfer easily. Taking A14 series for instance, for the same diffusing depth between X_1 and X_2 (see Figure 8), the transferred ratio of chloride (C_3/C_2) in the concrete in tide zone was larger than in splash zone (C_2/C_3), which meant chloride diffused relatively easier in tide zone concrete than in splash zone concrete. In the case of immersion zone, the sufficient and stable moisture supply provided sufficient transferring media for chloride diffusing. Therefore, the D_a value of concrete exposed in tide zone could be larger than in splash zone.

Based on the analyzing above, it could be concluded that D_a was an index describing the ability of chloride diffusion in concrete. If chloride moving was promoted by the plenteous of pore water, D_a value was relatively large. Contrarily, D_a value decreased when the transferring media of pore water was insufficient.

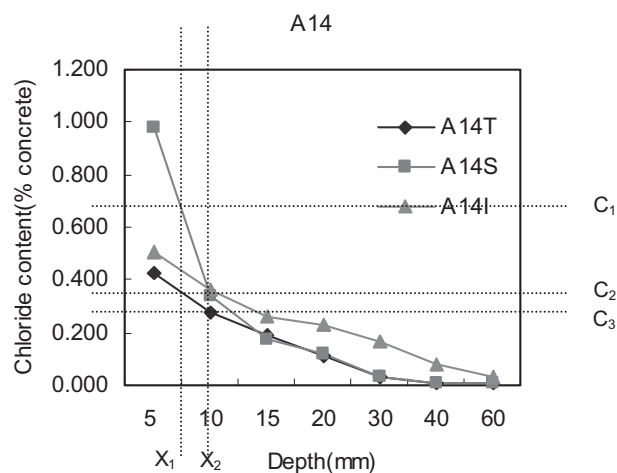


Figure 8: Chloride diffusion ability

5. CONCLUSION

Based on the scope of this study, the following conclusions are made:

1. For the concrete exposed in marine environment, the initial saturated curing has effects on reducing the surface chloride accumulation and preventing chloride diffusing in concrete. These effects are more significant in the splash zone.

2. For the same concrete exposed in those three environments, the sequence of C_0 is Splash zone > Tide zone > Immersion zone; the values of D_a are sequenced as Immersion > Tide > Splash.

3. The severe wet-dry cycle is the other reason for the surface chloride accumulation and causes the reduction of D_a .

4. D_a is the index describing the relative diffusing ability of chloride in concrete. It cannot be used to evaluate the concrete durability state individually.

5. The coupling effect of initial curing condition and following exposure environment should be taken into account in the durability design for concrete structure located in marine environment.

ACKNOWLEDGEMENTS

The authors are very appreciated for the financial support from Chinese Scholarship Council; Joint research project supported by National Science Foundation of China and Japan Science Promotion Society.

REFERENCES

- Atis, C. D., Ozcan, F., 2005. Influence of dry and wet curing conditions on compressive strength of silica fume concrete. *Building and environment* 40,1678-1683.
- Nasir Shafiq, Cabrera, J.G., 2004. Effects of initial curing condition on the fluid transport properties in OPC and Fly ash blended cement concrete. *Cement and concrete composites* 26, 381-387.
- Ramezaniapour, A.A, 1995. Effect of curing on the compressive strength, resistance to chloride ion penetration and porosity of concrete incorporating slag, fly ash or silica fume. *Cement and concrete composites* 17,125-133.
- Khatib, J.M., Mangat, P.S., 1999. Influence of super plasticizer and curing on porosity and pore structure of cement paste. *Cement and concrete composites* 21,431-437.
- Jaegermann, C., 1990. Effect of water-cement ratio and curing on chloride penetration into concrete exposed to Mediterranean Sea climate. *ACI Materials* 84,333-339.
- Zhangyi. Chloride transportation model and the application[D], 2008..Zhejiang University, China.
- Yao, C.J.. Penetration Laws of Chloride Ions in Concrete Infrastructures at Coastal Ports [D]. 2007. Zhejiang University, China.
- Nilson, H., David Darwin, and Charles Dolan., 2003. *McGraw Hill Higher Education: Design of Concrete Structures* [M].
- Jin,W.L.,Zhao,Y.X.,2002. *Science Press: Durability of Concrete Structures* [M].

SEISMIC PERFORMANCE OF WOODEN BUILDINGS IN JAPAN

MIKIO KOSHIHARA

Assoc. Professor, Institute of Industrial Science,
the University of Tokyo, Japan
kos@iis.u-tokyo.ac.jp

ABSTRACT

The Japan has a longstanding heritage of wooden houses. At the same time, Japan is a country beset by earthquakes. Wooden houses in Japan have suffered great damage caused by strong earthquakes. In the 1995 earthquake in Kobe, a great number of detached wooden houses were destroyed. Even in Tokyo, there are today five million wooden houses. Forty percent of the existing wooden houses in Japan, and ninety percent of them built before 1981 have insufficient protection against seismic events. There are useful reinforcement methods for these insufficient wooden houses, but they have not been popularized because of a low sense of imminent crisis about earthquakes. It is important to cultivate the minds of these homeowners about the danger of earthquake so a good housing stock can be protected.

1. INTRODUCTION

Japan has a longstanding heritage of wooden houses. At the same time, Japan is a country beset by earthquakes. Wooden houses in Japan have suffered great damages caused by strong earthquakes. In the 1995 earthquake in Kobe, a great number of wooden houses was destroyed and more than 5,000 human lives were lost. This paper presents an overall survey of wooden houses mainly in Japan, focusing on their seismic performance.

2. CATEGORIES OF WOODEN HOUSES IN JAPAN

2.1 Seismic Elements and Design Method for Wooden Buildings

As shown in Table 1, there are many types of wooden buildings in Japan. They are different in terms of seismic elements and how each seismic design method is applied.

2.2 Traditional Wooden Buildings

The first category, traditional wooden buildings, includes temples, shrines and old folk houses (Figure 1). However, at present very few are newly constructed of wood.

Table 1: Categories of Wooden Buildings and Design Method

| Type of Buildings and Construction | Seismic Design | Seismic Elements | Seismic Design Method |
|------------------------------------|--------------------------|---|---|
| Traditional Wooden Buildings | Shrine, Temple, Pagoda | frame, wall and rocking effect | not applicable or special analysis |
| | Folk House | | |
| Detached Wooden Houses | Conventional | shear wall (bracing or board) | Effective Wall Length Method |
| | Two-by-Four | | |
| | Prefabricated | | special analysis |
| | Moment-Frame system | | |
| Heavy Timber Structure | Ordinary Frame | moment resisting frame, truss, etc. | Working Stress (Allowable Stress) Design Method |
| | Long Span or Space Frame | | |
| High-rise Wooden Building | | moment resisting frame, shear walls, etc. | Performance- Based Design Method |

2.3 Detached Wooden Houses

The second category includes single-family detached wooden houses. Japan has a stock of about 30 million units, and 600 thousand units are newly constructed every year. This category can be divided into four types according to the classification of construction method: conventional construction, two-by-four system, prefabricated houses and moment-frame system.

The conventional construction method was derived from traditional construction methods (Figure 2(1)). The structural system of both methods has posts and beams. Houses of this type account for the largest share (60 percent) among wooden detached houses.

The two-by-four system (Figure 2(2)) was introduced from North America, where its original system is the most common construction method and is called light-frame construction or platform construction. The name "two-by-four" comes from the sectional size of dimension lumber (approximately two inches by four inches). This structural system consists of walls with nailed boards.

There are various systems of prefabricated wooden houses, but the most popular system is a panelized one (Figure 2(3)). Walls, roofs, and floors are made of wood panels with glued boards, and its structural system is based on these panel elements.

Recently some houses have been constructed with a moment-resisting frame. (Figure 2(4))

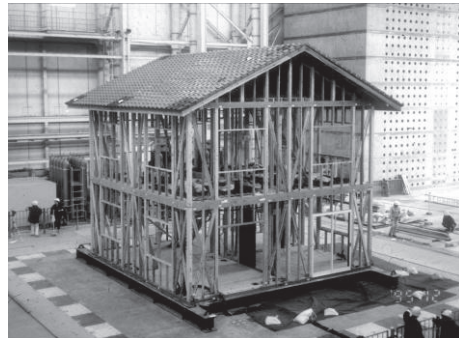


(1) Traditional Wooden Building



(2) Traditional Wooden Houses

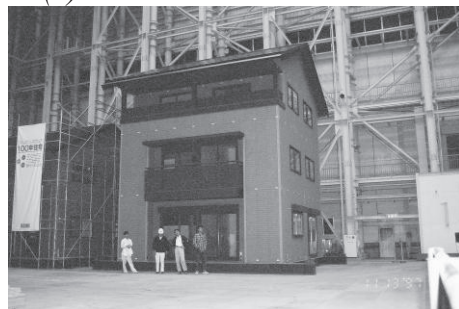
Figure 1: Traditional Wooden Buildings



(1) Conventional construction



(2) Two by four Houses system



(3) Prefabricated Houses



(4) Moment frame system

Figure 2: Detached Wooden Houses



(1) Heavy Timber Structure



(2) 5storied Wooden Building

Figure 3: Heavy Timber Structures

2.4 Heavy Timber Structure

The third category is heavy timber structure, used for example, to build schools, gymnasiums and museums (Figure 3(1)). After around 1960 this type was replaced by steel structure. However, quite a few heavy timber

buildings have been built after around 1980. There are great varieties in the structural system of heavy timber structure. Moment-resisting frames and trusses are widely used for ordinary buildings such as schools, and space frames are often employed for big buildings such as gymnasiums. From 2000 we have been able to build fireproof wooden structures. For example, a new five-story wooden building has been built in Kanazawa (Figure 3 (2)). This building was built by a wooden hybrid system whose elements, columns, and beams are wood-inserted steel bars or steel plates.

3. HISTORIES OF DAMAGES DUE TO EARTHQUAKE

Many earthquakes have occurred in and around Japan, and many typhoons have also besieged her in the past. Some of them resulted in a great amount of damage to wooden buildings, with many human lives lost. Table 2 shows such disastrous earthquakes and typhoons.

The 1981 Nohbi Earthquake, which occurred in the middle of the main island of Japan, was a very big one with estimated magnitude of 8.0 on the Richter scale. Most wooden buildings at the time were built by carpenters using traditional construction methods. After the earthquake, scientific research on the seismic design of buildings was initiated.

Next in intensity was the 1923 Kanto Earthquake that hit Tokyo and the metropolitan area of Japan. The disastrous earthquake caused great damage to buildings as well as loss of human lives. The first regulations on seismic design were introduced into Japanese building law after this earthquake: a seismic coefficient of 0.1 for seismic design was adopted. However, only the following stipulation was added at the time: that some bracings should be installed in wooden buildings. Accordingly, most wooden houses did not have to install such bracings.

The 1948 Fukui Earthquake occurred in a rural district, but many people lost their lives mainly due to the collapse of detached wooden houses. The investigation of the damage showed that the degree of the damage to wooden houses had a strong correlation with the shear wall ratio of the house. The wall ratio is defined as the amount of walls in length in the unit area of the floor. The result was taken into consideration when the new building law was established in 1950.

The Niigata, Tokachi-oki, and Miyagiken-oki earthquakes were big ones that resulted in great damage to buildings, especially reinforced concrete structures. Wooden houses also suffered damage, but the damage was not so serious. It looked as if Japanese wooden houses had finally become strong enough to survive severe earthquakes.

However, such an optimistic view was betrayed by the 1995 Hyogoken-nambu Earthquake, which is also known as the Kobe Earthquake. About 100,000 buildings, including wooden houses, were completely destroyed (Figure 4) and more than 5,000 people were killed. It is estimated that about 80 percent of them lost their lives because of the collapse of wooden houses. Various investigations and researches have been made after the earthquake. Some results were taken into account in the revision process of the building law in 1998. After the Kobe Earthquake, many disastrous earthquakes have occurred.

Table 2: Major disastrous earthquakes in Japan (after Meiji restoration)

| Year | Earthquake and Typhoon | Damage | Casualty |
|------|-------------------------------|---------|----------|
| 1981 | Nohbi Earthquake | 220,000 | 7,273 |
| 1923 | Kanto Earthquake | 254,000 | 142,000 |
| 1934 | Muroto Typhoon | 93,000 | 2,702 |
| 1948 | Fukui Earthquake | 48,000 | 3,769 |
| 1964 | Niigata Earthquake | 9,000 | 26 |
| 1968 | Tokachi-oki Earthquake | 4,000 | 52 |
| 1978 | Miyagiken-oki Earthquake | 7,000 | 28 |
| 1995 | Hyogoken-nambu Earthquake | 240,000 | 6,433 |
| 2004 | Niigataken-chuetsu Earthquake | 17,000 | 65 |



1995 Hyogoken-nambu
Earthquake



2004 Niigataken-chuetsu
Earthquake

Figure 4: Damage to Wooden Houses in Japan

4. SEISMIC DESIGN METHODS FOR WOODEN BUILDINGS

4.1 History of design methods

The provision of seismic design for structures was introduced in Japanese building law for the first time in 1924, right after the great Kanto Earthquake. However, detailed design method for wooden buildings was not introduced until 1950, when the building standards law was established. Since then, the allowable-stress design method is applied to ordinary wooden buildings and the effective wall-length method is applied to detached small wooden houses.

The effective wall-length method is still used today for its simplicity. The numerical values of the coefficient used in this method have changed several times, and the numerical values at present were stated in the revision of the building standards law in 2000. The load-carrying capacity method was introduced in the 1980 revision. However, it had rarely been used for wooden buildings, because the number of large wooden buildings that should be designed by the method was small.

The performance-based design method was introduced into the building standards law in 1998, under the heading of “Calculation of Response and Limit Strength.”

4.2 Effective wall-length method

The effective wall-length method consists of two components: the required ratio of wall length and the resistance factor of shear wall. The required ratio of wall length, p , was determined based on the assumption that the weight of each part (roof, wall, and floor) is the same in typical wooden houses and that the design base shear coefficient is 0.2 according to the minimum requirement in the building standards law. The value of resistance factor of a shear wall, q , was determined based on racking tests. The following relationship should be satisfied in the seismic design of every wooden house.

$$p \times A \leq \Sigma(q \times l) \tag{1}$$

where

p = required ratio of wall length (cm/m², Table 3)

A = area of the floor (m²)

q = resistance factor of each shear wall (Table 4)

l = real length of shear wall (cm)

Table 3: Required Ratio of Wall Length p (cm/m²)

| Roof \ Story | Single Storied | Two storied | | Three storied | | |
|--------------------|----------------|-----------------------|-----------------------|-----------------------|-----------------------|-----------------------|
| | | 1 st story | 2 nd story | 1 st story | 2 nd story | 3 rd story |
| Heavy(Clay tile) | 15 | 33 | 21 | 50 | 39 | 24 |
| Light(Metal plate) | 11 | 29 | 15 | 46 | 34 | 18 |

Table 4: Resistance Factor of Wall q (Examples)

| Type of Wall | | Resistance Factor |
|-----------------------------|----------|-------------------|
| Mud Wall | | 0.5 |
| Bracing | 15×90 mm | 1.0 |
| | 30×90 | 1.5 |
| | 45×90 | 2.0 |
| | 90×90 | 3.0 |
| Plywood $t \geq 12$ mm | | 2.5 |
| OSB $t \geq 12$ mm | | 1.0 |
| Gypsum board $t \geq 12$ mm | | 1.0 |

In the above expression, $p \times A$ corresponds to the earthquake force and $\Sigma(q \times l)$ corresponds to the resistance.

In the revision of the building standards law in 2000 two design techniques were introduced clearly. One is the design technique for the effect of eccentricity and the other is the design technique for the joint of the top and bottom of columns with wall.

In Japan wooden detached houses have been designed not only by structural engineers but also carpenters. This is why the very simple design method of effective wall length is needed.

4.3 Allowable-stress design method

The allowable-stress design method has been used for bigger buildings, such as schools and offices. Recently this method has been used for wooden detached houses, too. There are moment-resisting frames as seismic elements, but these are not estimated in the effective wall-length method. The standard seismic base shear coefficient is 0.2. The stress in the members and joints are checked for long-term and short-term loads.

4.4 Load-carrying capacity method

In the revision of the Building Standard Law in 1980, load-carrying capacity method (the method used to examine the performance against very severe earthquakes) was introduced. The method is based on the approximate relationship between the linear response and the nonlinear response. In any approximation, the energy of linear response and that of nonlinear response are regarded equal. The seismic base-shear coefficient for very severe earthquakes is 1.0. The design seismic base shear coefficient could be decreased according to the ductility of the structure.

4.5 Performance-based design method

The performance-based design method (“Calculation of Response and Limit Strength”) introduced in the recent revision of the Building Standard Law in 1998 is based on the approximate relationship between the linear response and nonlinear response, in which the nonlinear response is replaced by the equivalent linear response. So far, very few wooden buildings have been designed by this method, because it is not yet popular among structural engineers and the data for it are not enough for practical use.

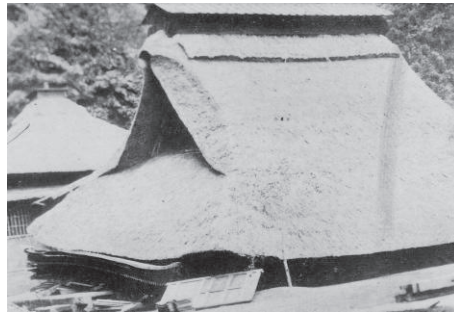
5. SEISMIC CAPACITY EVALUATION

5.1 Revaluation of Traditional Wooden Building

Traditional wooden buildings such as shrines and temples are not engineered structures. Some of them were destroyed by earthquake (Figure5), but many of them have survived severe earthquakes. Some researches are being made on the structural behavior of them by the modern techniques of earthquake engineering.



Kenchoji-temple



Enkakuji-temple

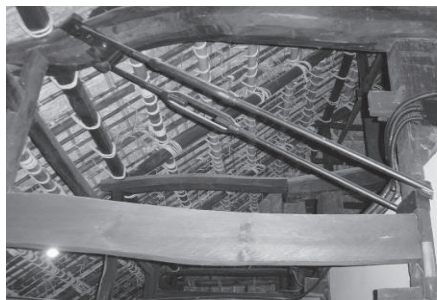
Figure 5: Damage of Traditional Wooden Structure on 1923 Kanto Earthquake

The structure of traditional wooden buildings consists of columns and beams. However, the frame of columns and beams was not structure strong enough to resist horizontal force caused by earthquakes. Therefore, "Nuki" was introduced to reinforce the frame in the medieval age (around 1200 AD). "Nuki" is a horizontal member that penetrates a column and fastened with wedges. "Nuki" still plays a very important role in newly built temples and shrines. Mud walls, rocking effect of columns and "Kumimono" (bracket complex) were considered as seismic elements.

Applying special seismic design method, "Performance Based Design Method", "Working Stress Design Method" and etc., seismic capacity of these traditional wooden buildings were evaluated. Some buildings were reinforced by these design method (Figure 6).



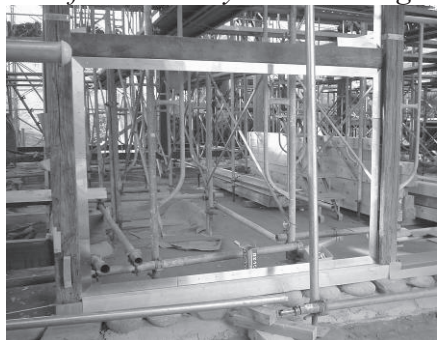
Folk House (Hirai-House)



Reinforcement by steel bracings



Reinforcement of Joints



Reinforcement by Plywood Wall

Figure6: Seismic Reinforcement of Folk House

5.2 Existing Wooden Houses

In Recent Earthquakes, the old small houses damaged very much. On Kobe Earthquake, 80% of deaths in the earthquake were caused by damages of old small houses that built by wood frames or light steel frames. Now, in Japan, there are many houses of old and poor quality. The houses were called existing ineligible houses. It is required to make diagnoses on old houses. As results of diagnoses, the house reinforcement might be recommended. In Japan, many local governments promote the seismic diagnosis and seismic reinforcement. However, many residents don't intend to try requesting diagnosis and reinforcement for his house. Many people are wondering the governmental warning of the great earthquake hit to his house in its life duration. If the possibilities of strong earthquake hits were given in stochastic value, the meaning of value would be vague and unreliable. The residents have attachments on their existing houses. The elderly people will take much effort to settle in the new house. The practice of seismic retrofit would depend on the philosophy of residents. There are many issues in the promotion of the existing house reinforcement. The seismic engineer must present the reliable and economic seismic diagnosis and reinforcement methods for the existing wood houses. But some simplified diagnosis method like "Effective Wall Length Method" is required for carpenters and house builder who diagnose houses.

The other sides, the seismic capacity evaluation of existing wooden house were revised in 2004 and many reinforcement methods are developing. Figure7 shows some methods of the existing house reinforcement.



Wall with Oil Dumper



Steel Bracing



Steel Pole



Dumper

Figure7: Existing House Reinforcement

6. CONCLUSION

To upgrade the seismic performance of wooden buildings, different ways should be taken according to the category of the building; some simplified design method is required for detached wooden small houses and more sophisticated method could be used for traditional wooden buildings. Researches on both aspects should be made.

TRIAL TEST ON THE EVALUATION OF SOIL CEMENTATION GENERATED BY THE FUNCTION OF MICROORGANISM

DAISUKE SUGIMOTO¹ and REIKO KUWANO²

¹Department of Civil Engineering, The University of Tokyo, Japan
motto@iis.u-tokyo.ac.jp

²International Centre for Urban Safety Engineering,
Institute of Industrial Science, The University of Tokyo, Japan
kuwano@iis.u-tokyo.ac.jp

ABSTRACT

A new technique of ground improvement by the microbial function has been recently proposed, in which soil cementation can be generated by introducing calcium, organic matter and microorganism into soil. In this study, a trial test was performed in order to evaluate the degree of soil cementation generated by the microbial function, using Trigger and Accelerometer method (TA method) for the measurement of shear wave velocities transmitted in a specimen.

Notable change in shear wave velocities was observed during the test, implying that the TA method is capable of assessing the degree of cementation developed in soil in the non-destructive manner.

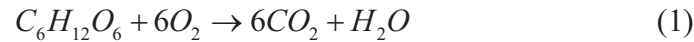
1. INTRODUCTION

Loose sandy soils are vulnerable to earthquakes, as they would be liquefied when they are saturated. When sandy backfill of buried pipe is insufficiently compacted and the buried pipe is broken, some amount of the backfill sand would be flown out of the breakage and surrounding ground would be loosened. Both phenomena can be prevented if some cementation is developed in the soil.

In order to improve soil, chemical agent such as cement or lime is generally added to the soil. Instead, a new environment friendly technique has been recently proposed to improve soil by the function of microbe. Kawasaki et al. (2006) reported that the permeability of sandy soil could be lowered by the generation of calcium carbonate, introducing yeast fungi, organic matters and calcium into soil. Hata et al. (2008) proposed in-situ permeability control using microbial cementation, showing that microbial analysis using molecular techniques is effective for the monitoring and management of the calcium carbonate precipitation process. However, the physical and mechanical properties of cemented soil have not been well understood. In this study, the degree of cementation in sand specimen in triaxial test was evaluated by the change of shear wave velocity measured by Trigger and Accelerometer method.

2. MICROBIAL CEMENTATION

When appropriate nutrition is given to microorganism in soil, they generate carbon dioxide by respiration, which turns to be carbonated ion in the pore water. If calcium ion exists and the pH of the environment is alkaline, the precipitation of calcium carbonate mineral occurs. Following is a reaction when glucose is used as nutrition (Kawasaki et al. 2006).



3. A TRIAL TEST FOR THE EVALUATION OF MICROBIAL CEMENTATION

A trial test was preformed to evaluate the degree of microbial cementation. Dry Toyoura sand was air pluviated in loose state, of which dry density of $1.44g/cm^3$, to prepare triaxial cylindrical specimen of $\phi 50mm$ by $h100mm$. Isotropic confining stress of $30kPa$ was applied, then “bio-grout” percolated into the specimen from the bottom to the top, by giving approximately $1m$ head difference. The flush of bio-grout was terminated after one day from the start of flushing as the flush rate notably diminished. The specimen was then left and monitored for a week. The bio-grout was made from the water taken from a pond, to which source of nutrition and calcium was added. Composition of bio-grout is shown below.

| | |
|-------------------------------------|---------------------------------|
| Tris buffer | 0.1mol/L |
| Sucrose | 0.01mol/L |
| CaCl ₂ 2H ₂ O | 0.01mol/L |
| Microbes | bacteria which inhabit the pond |

Shear wave velocities transmitting through the specimen were measured by Trigger and Accelerometer method, so called TA method, originally proposed by AnhDan et al. (2003). Shear wave of $2kHz$ generated by triggers on a top cap was monitored by two small accelerometers attached to lateral surface of the specimen. Wave velocities were calculated by the difference of wave arrival time and wave travel length. The operation and system of TA method is schematically presented in Figure 1. A photo of the specimen equipped with the sensors is shown in Figure 2.

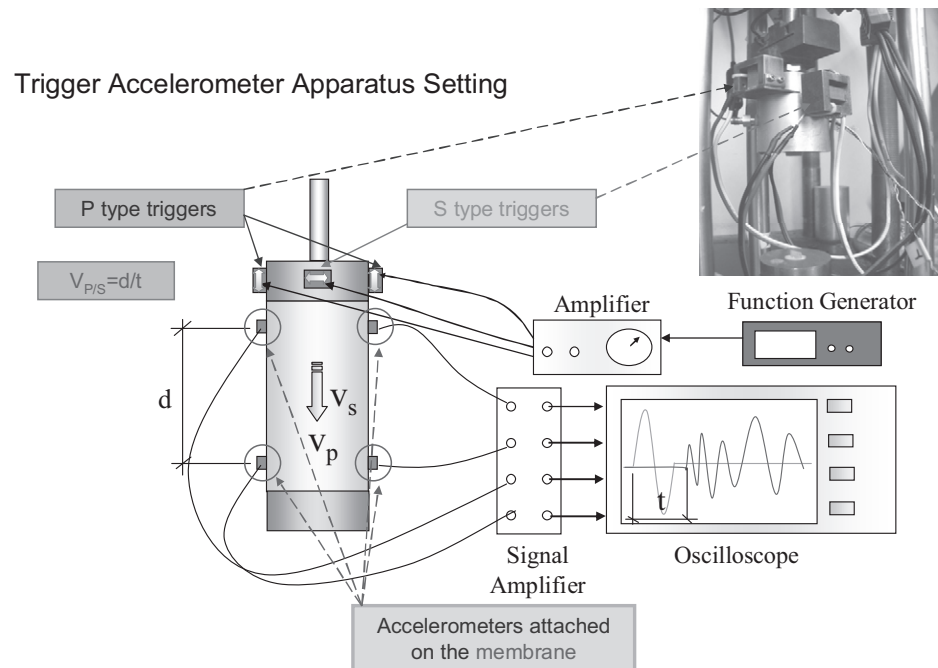


Figure 1: Trigger and Accelerometer method

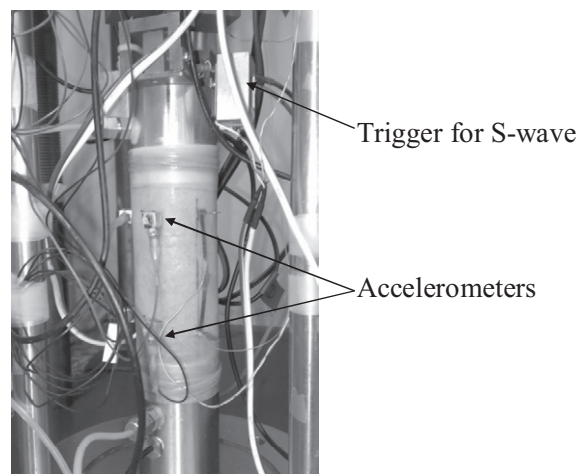


Figure 2: Specimen equipped with sensors for TA method

4. DEVELOPED CEMENTATION AND CHANGE OF SHEAR WAVE VELOCITY

A photo of specimen after the test is shown in Figure 3. Cementation appeared to develop as the specimen could self-stand, but it was significantly non-uniform. Full saturation of the specimen with bio-grout could not be achieved as the flushing was terminated in the course of saturation process due to notable decrease in permeability. It was probably the main cause for the non-uniform development of cementation.



Figure 3: Photo of the specimen after the test

Shear wave velocities, V_s , are plotted against elapsed time in Figure 4. The value of V_s was 212m/s at the start of grout flushing, then showing slight increase and decrease, it became 233m/s after one week. It is indicated that small strain shear stiffness, G , was expected to increase by more than 10%. Although it should be noted that shear stiffness evaluated by wave measurements may contain certain amount of errors, as the velocity increase in this test was measured in an identical specimen under the constant stress condition, it can be thought that the observed velocity increase was due to the development of cementation. Figure 5 indicates that the received waveform after one week showed larger response compared to that after on day. It may be also due to the effects of cementation created between sand grains.

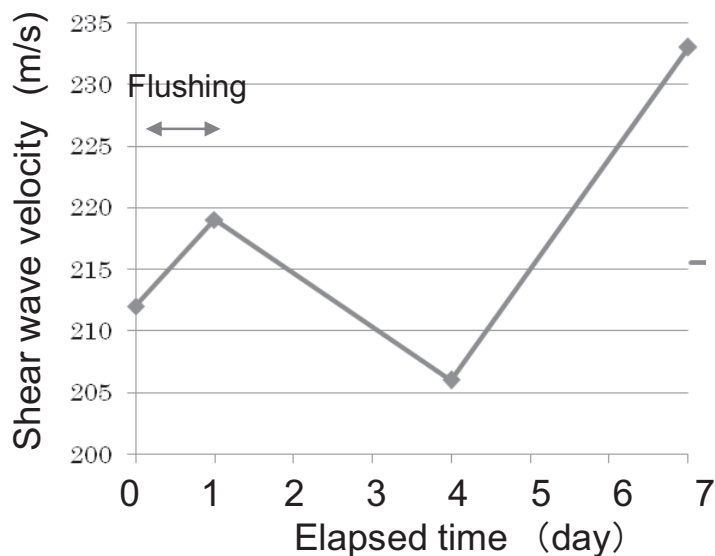
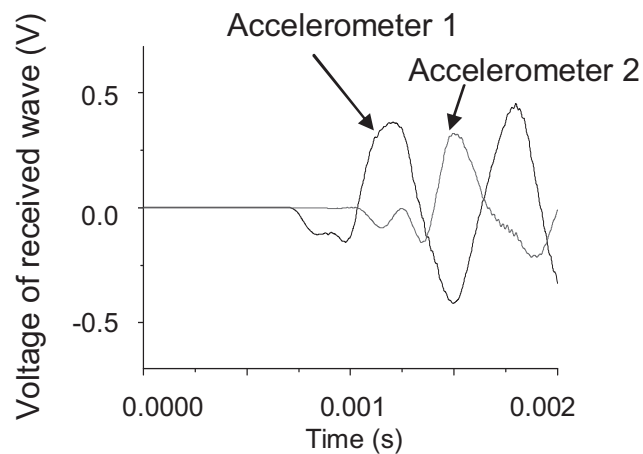
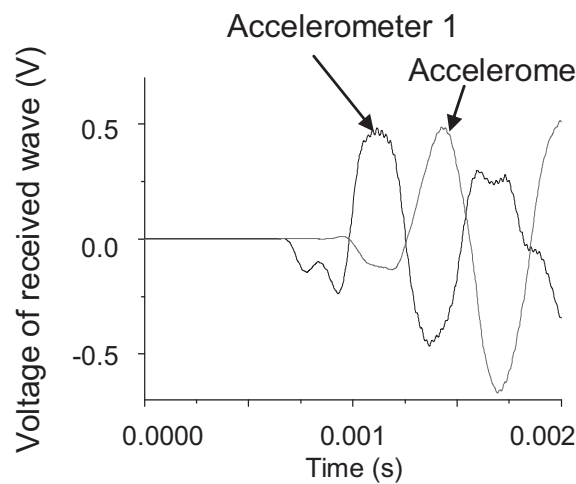


Figure 4: Change of shear wave velocity



(a) after one day



(b) after one week

Figure 5: Received wave forms

5. CONCLUSIONS

A trial test was performed to evaluate the degree of cementation created by the microbial functions. Using microbes naturally inhabited in the pond, some cementation could be generated in a loose sand specimen, although it was not uniform. Shear wave velocities propagating through the specimen increased by approximately 10%, implying the development of cementation in the course of the test. Trigger Accelerometer method can be applicable to assess the progression of cementation in non-destructive manner.

REFERENCES

- Kawasaki, S., Murao, A. Hiroyoshi, N. Tsunekawa, M. and Kaneko, K., 2006. Fundamental study on microbial cementation grout. *Oyo-Chishitsu*, Vol. 47, No.1, 2-12 (in Japanese).
- Hata, T., Kuwano, R. and Abe, H. 2008. Fundamental study of in-situ permeability control technique using microbial function. *Doboku Gakkai Ronbunshuu G, Journal of Japan Society of Civil Engineers*, Vol. 64, No. 2, 168-176.
- AnhDan,LQ, Koseki,J and Sato,T. 2002. Comparison of Young' s moduli of dense sand and gravel measured by dynamic and static methods. *Geotechnical Testing Journal*, Vol.25, No.4, 349-368.

DEVELOPMENT OF HAZARD PREDICTION SYSTEM FOR INTENTIONAL ATTACKS IN URBAN AREAS

RYOHI OHBA¹, SHINSUKE KATO²,
OSAMU UKAI³ and TOMOHISA YAMASHITA⁴
¹Nagasaki R&D Center, Mitsubishi Heavy Industries, Japan
²Institute of Industrial Science, University of Tokyo, Japan
³AdvanceSoft Corp., Japan
⁴National Institute of Advanced Industrial Science and
Technology, Japan
ryohji_ohba@mhi.co.jp

ABSTRACT

A hazard prediction system has been developed for chemical, biological and radiological (CBR) attacks in urban areas with the use of the mesoscale meteorological model, RAMS and its dispersion model HYPACT. The developed simulation system can predict 1) concentration of hazardous gases and 2) the number of casualties based on the population database of Japan.

RAMS is equipped with an optional scheme to simulate airflow around buildings based on the volume fraction of the buildings within each grid cell. However, this scheme requires significant computational time if applied for fine meshes. Accordingly, we have developed a new computational scheme using the RAMS code with a mesh size of a few meters to simulate the effect of a building complex on the dispersion. This scheme requires computational time of as little as a few minutes on a conventional personal computer. The computational scheme first extracts the shapes of the buildings from a digital map database. Then, a set of steady flows is calculated for 16 wind directions using a fine mesh, and the results are saved as a database. Next, the scheme calculates an unsteady flow on a coarse mesh, which is nudged by a linear combination of the relevant data from the 16-wind direction steady airflow database. The nudging is performed at the boundaries of the fine mesh domain using the Least Mean Square Method (LMSM). The dispersion prediction scheme is currently being validated with the use of field and wind tunnel data.

1. INTRODUCTION

In recent years, the likelihood of attacks by chemical, biological and radiological (CBR) agents in mega-cities may be increasing. In Japan, the Japanese cult Aum Shinrikyo carried out Sarin gas attacks in Nagano and Tokyo. The attack in the residential area of Matsumoto City, Nagano

resulted in 7 deaths and 586 injuries. The attack on five subway lines in the Tokyo metropolitan area led to 12 deaths and over 5500 injuries.

The Ministry of Education, Culture, Sports, Science and Technology of Japan (MEXT) commenced a national project for urban safety in 2007. As a part of this project, MEXT assigned a research consortium consisting of the University of Tokyo, the National Institute for Advanced Industrial Science and Technology (AIST), Mitsubishi Heavy Industries (MHI) and AdvanceSoft, Corp. to develop a new hazard prediction and mitigation simulation system for CBR attacks. This simulation system is intended for use by first respondents to attacks such as municipal fire protection and police agencies. Therefore, the system needs to be able to simulate gas diffusion with minimal computational time on a conventional personal computer (PC).

2. SIMULATION SYSTEM

2.1 System description

The developed simulation system, called MEASURES, consists of an airflow database, a dispersion model, and a damage prediction model (Figure 2.1-1). Meteorological data can be loaded onto the system by the user directly or through the Internet. The databases of the airflow, topography, and population are pre-installed on the system. Less than 15 minutes of computational time are required for 12 hours of simulation. The output of simulations such as wind vectors, gas concentration, and casualty counts for every 10 minutes of simulated time are displayed on the screen, and are thus available to the users during and after the simulation.

2.2 Meteorological model

Most meteorological models are available in the public domain as open source codes. Examples of such models are RAMS, WRF, and MM5. To simulate airflow around building complexes with a mesh size of a few meters, the RAMS (Regional Atmospheric Modeling System) code developed by Pielke et al. of Colorado State University (<http://www.atmet.com/>) was modified. First, the two-dimensional turbulence model by Mellor and Yamada (1982) was replaced by a three-dimensional turbulence model as in Trini Castelli (2006) to simulate complex airflow around buildings and terrain. The simulated vertical profiles of wind velocity around a building were compared and verified with the wind tunnel database from Hamburg University (<http://www.mi.uni-hamburg.de/Data-Sets.432.0.html>) (Figure 2.2-1).

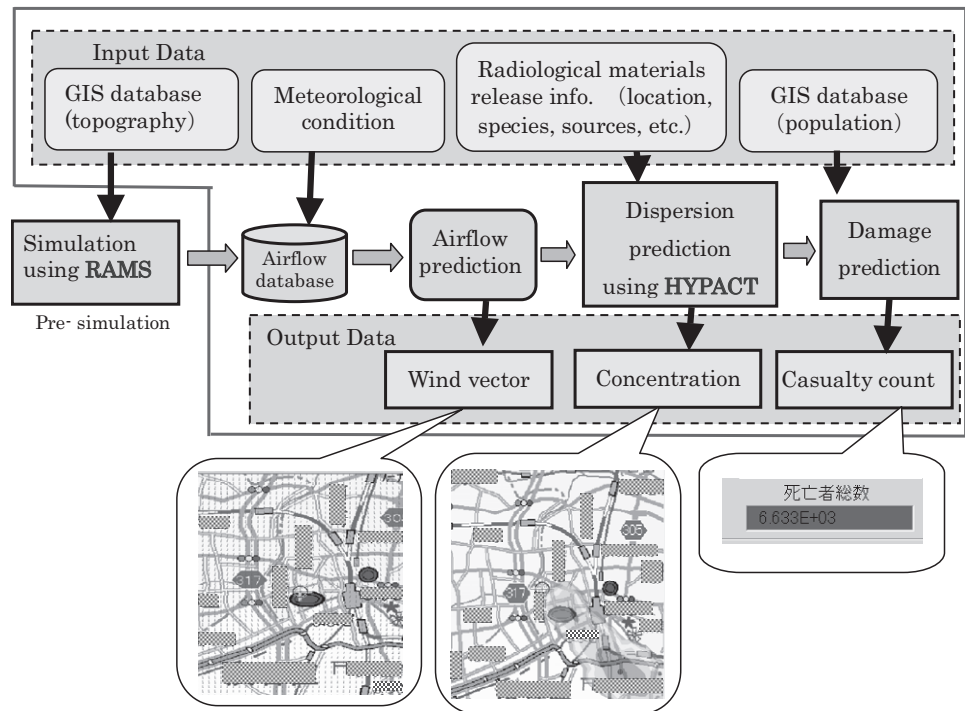


Figure 2.1-1: Structure of the advanced edition of MEASURES

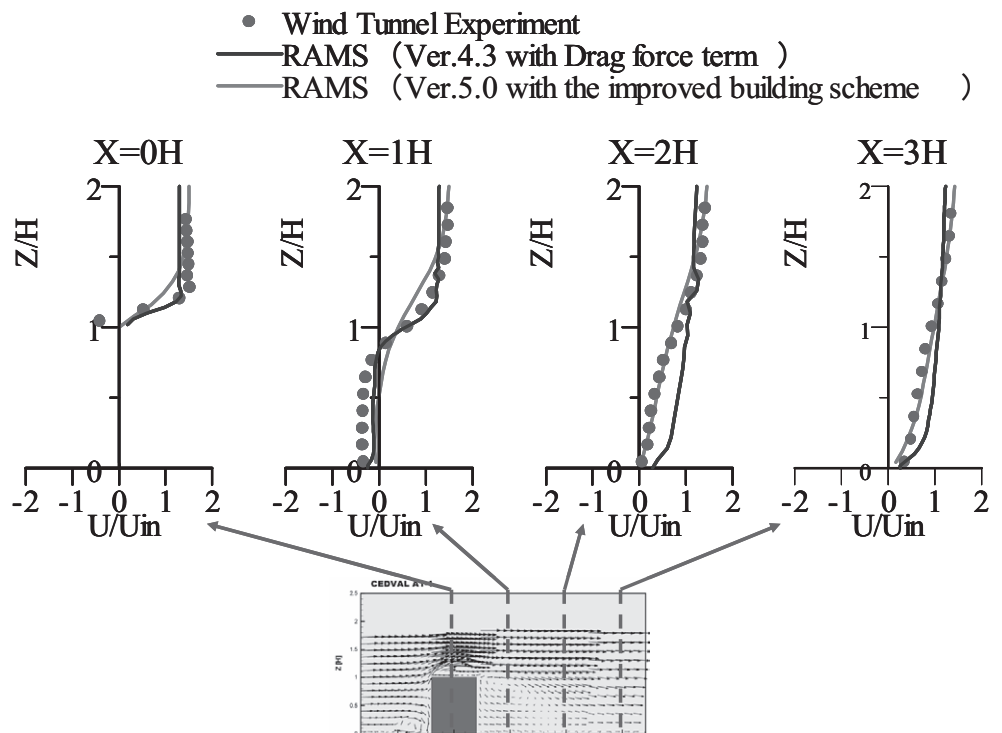


Figure 2.2-1: Comparisons of vertical wind profiles between RAMS simulation and wind tunnel data

Subsequently, the high speed computing scheme, Database Computing System of Air Flow (DCSAF) was developed by MHI (Ohba, 2007). The computing system of DCSAF can be summarized as follows:

1) Steady-state airflow is calculated for a location of interest under various atmospheric conditions: a total of 48 conditions were generated by combining 16 wind directions and 3 atmospheric stabilities.

2) A time series of airflow is generated for the location of interest. In this procedure, the 3-dimensional wind data from the database of 48 atmospheric conditions are interpolated at each time step for the wind direction and the atmospheric stability observed at the location at that time step (Figure 2.2-2).

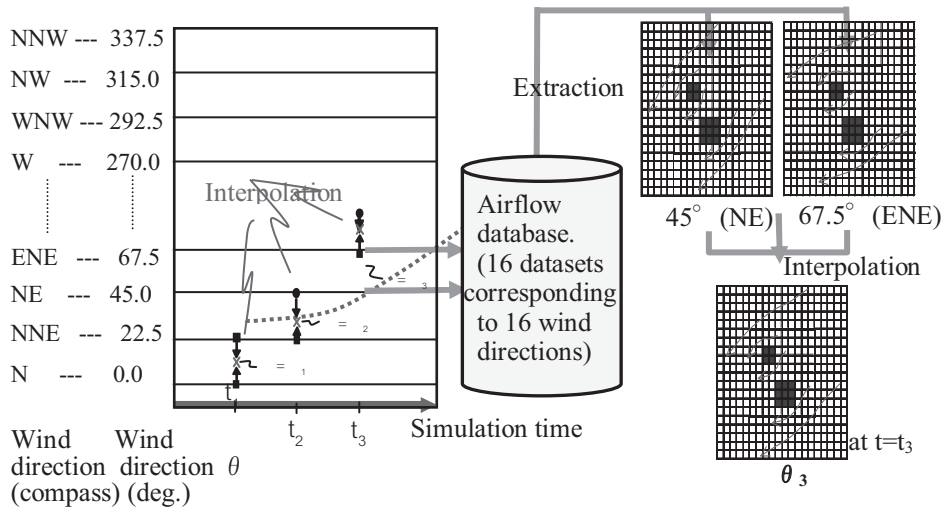


Figure 2.2-2: Simulation of a time-series of unsteady airflow with the interpolation of an airflow database

Because computational time is inversely proportional to the mesh size, simulation with a small mesh size requires significant computational time. However, with the use of DCSAF, the computational time is reduced by a factor of approximately 100 compared to that by a conventional model (Table 2.2-1).

Table 2.2-1: Time required to compute one simulated hour using a PC. Times given are those required to calculate the large-scale grids, the small-scale grids, and the large- and small-scale grids combined, respectively.

| Model | 100 m < | 100 m > | Total |
|---------------|----------|----------|----------|
| Present model | Few min. | Few sec | Few min. |
| Conventional | 10 min. | 200 min. | Few hrs |

2.3 Atmospheric diffusion model

The HYPACT (HYbrid PArticle and Concentration Transport) code is an atmospheric diffusion code that can be coupled to RAMS. This code is based on a Lagrangian particle model that satisfies mass conservation in complex airflow and can adopt the finite difference method at large distances downwind to reduce computational time.

The simulated results of gas concentration were compared and verified with the observational data from Tokai that were collected by the Japan Atomic Energy Research Institute (JAERI) in 1991 and 1992 as shown in Figure 2.3-1(Hayashi,1998). The effect of building complexes on airflow is well simulated by RAMS and HYPACT for wind velocity and turbulence intensity (Figure 2.3-2).

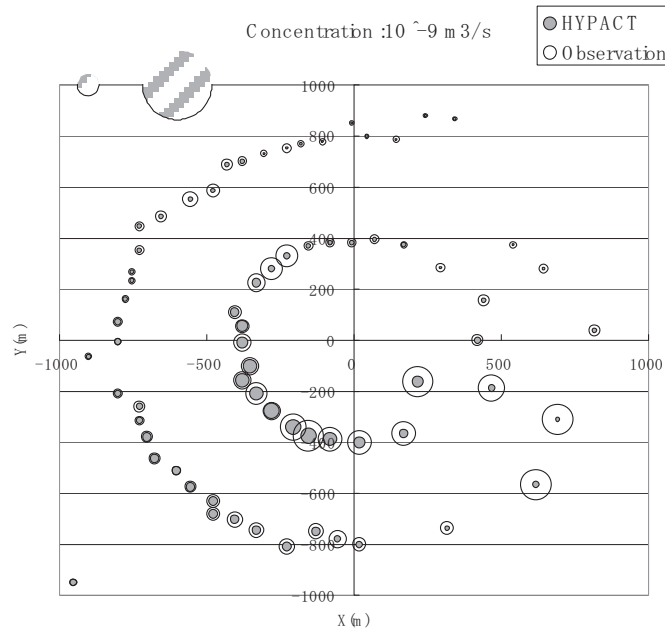


Figure 2.3-1: Comparisons of ground-level concentration at measurement points. The size of the circular symbols indicates the concentration

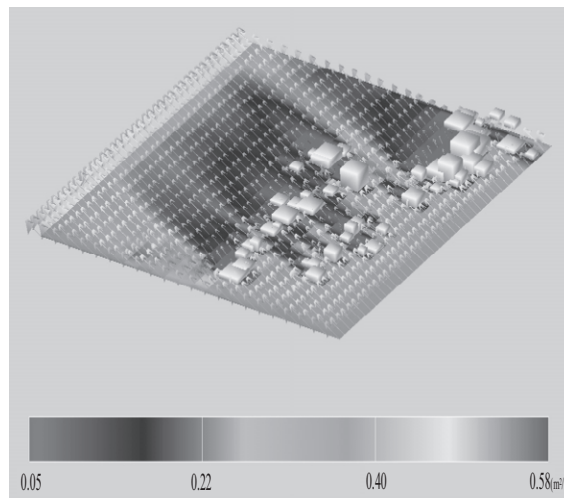


Figure 2.3-2: Simulated wind vectors (arrows) and turbulence intensity (contours) around buildings (white blocks)

3. APPLICATIONS FOR EMERGENCY RESPONSE PLAN

3.1 Overview

The research consortium consisting of the University of Tokyo, the National Institute for Advanced Industrial Science and Technology (AIST), Mitsubishi Heavy Industries (MHI) and AdvanceSoft Corp. is currently in the process of developing a hazard prediction and mitigation simulation system for CBR attacks as assigned by MEXT in 2007. The year-by-year schedule of each sub-theme is shown in Table 3.1-1. A schematic overview of the envisioned completed project is shown in Figure 3.1-1.

Table 3.1-1: Year-by-year schedule of each sub-theme

| Sub theme | 2007 | 2008 | 2009 |
|---|---------------------------------------|---|--|
| 1) Prediction system for atmospheric diffusion (MHI) | High-speed computing system | Validation of the system with field experimental data | Evaluation of total system with emergency response drill by Tokyo metropolis |
| 2) Prediction system for diffusion in enclosed space (Advance-Soft) | Base system, Add sub-models | Make-up and Validation of the system | |
| 3) Verification Test (Tokyo University) | Wind Tunnel Experiment | Full-Scale Experiment | |
| 4) Development of evacuation assist system (AIST) | Development of integrated system | Validation of evacuation assist system | |
| Annual target | Development of fundamental technology | Validation of each technology | Evaluation of total system |

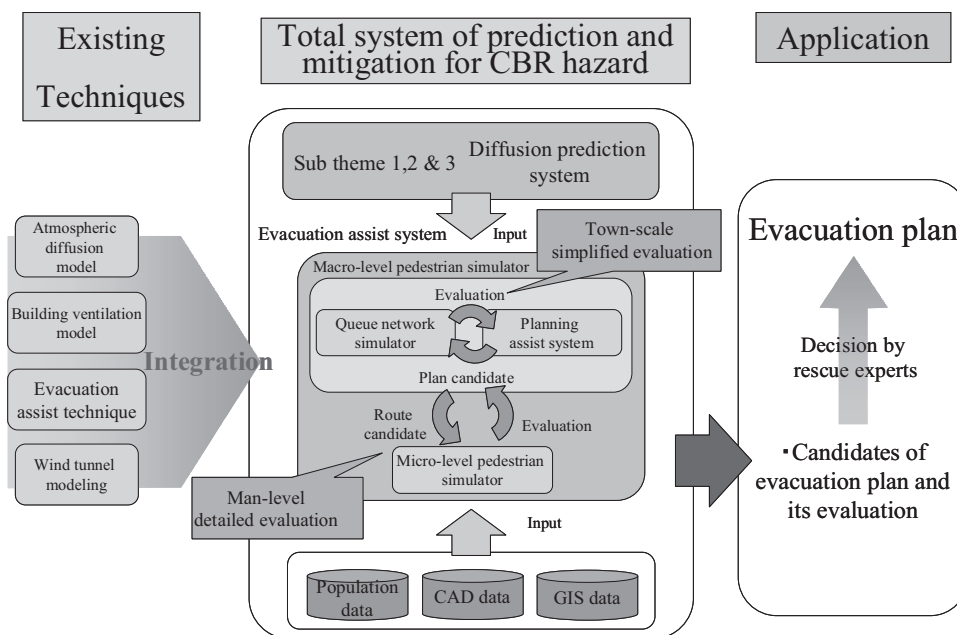


Figure 3.1-1: Schematic overview of the envisioned completed MEXT project for hazard prediction

3.2 Prediction of outdoor gas diffusion

The developed hazard prediction system can display gas concentration and casualties as contour maps.

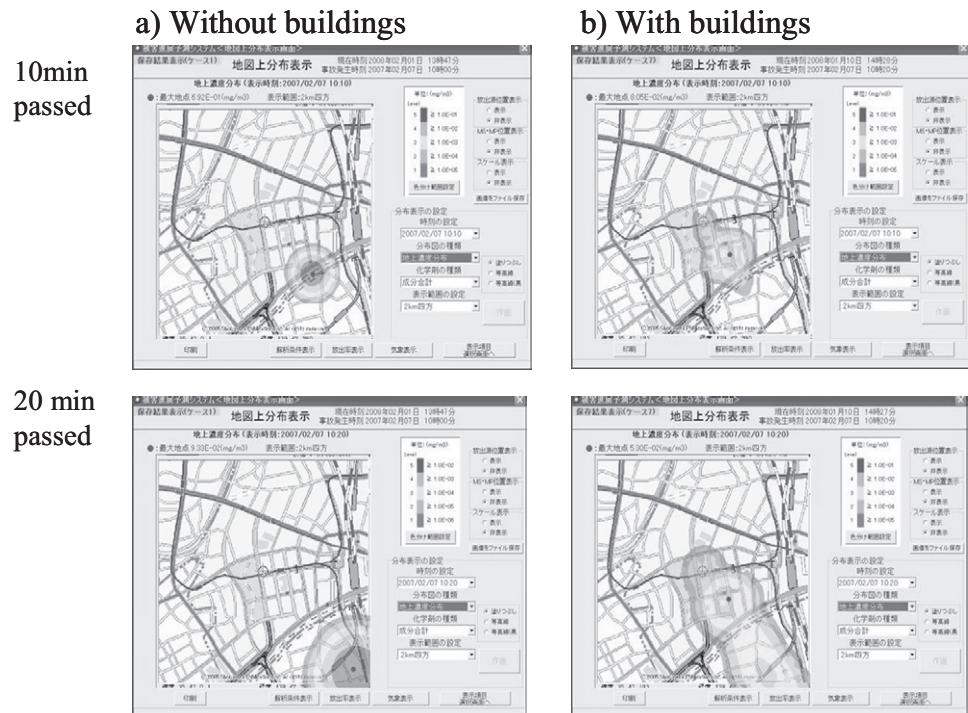


Figure 3.2-2: Comparison of the gas concentration distribution with and without buildings after an instantaneous gas release. Red and blue on the color bars indicate high and low concentrations, respectively.

Figure 3.2-2 indicates the effects of stagnation by building complexes on gas diffusion in an urban area. Based on a Geographical Information System (GIS) database of building shapes, all the buildings are simplified for the numerical simulation as in Figure 3.2-3.

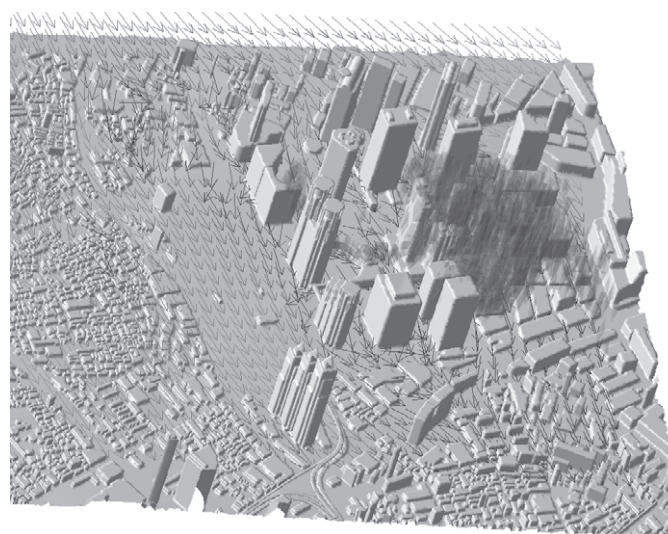


Figure 3.2-3: 3-D view of buildings, extent of diffused gas (green) and wind vectors (blue)

3.3 Prediction system of indoor gas diffusion

AdvanceSoft is developing a practical prediction system for diffusion in enclosed space in the event of a CBR terrorism. This system is based on EVE SAYFA (Enhanced Virtual Environment Simulator for Aimed and Yielded Fatal Accident), which is outcome of the project of “Revolutionary Simulation Software” (RSS) (2005-2008).

The system can be related to airflow control in a space involving complex airflow paths including human activity areas. The structure of EVE SAYFA is shown in Figure 3.3-1.

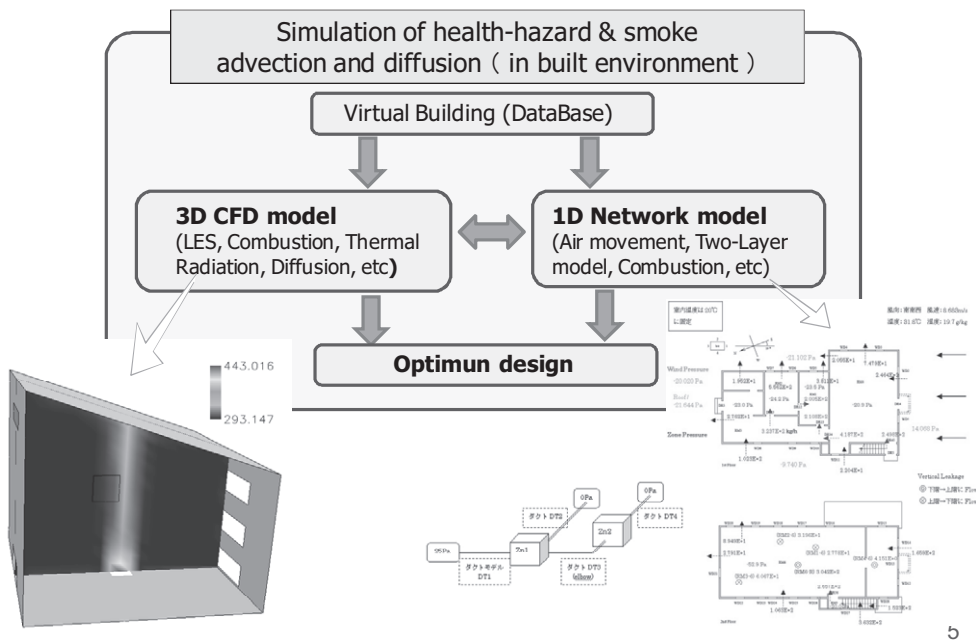


Figure 3.3-1 Structure of EVE SAYFA

We can reduce the total computing time, saving the result of air movement simulation in Database and reusing for diffusion simulation. This procedure is shown in Figure 3.3-2(right).

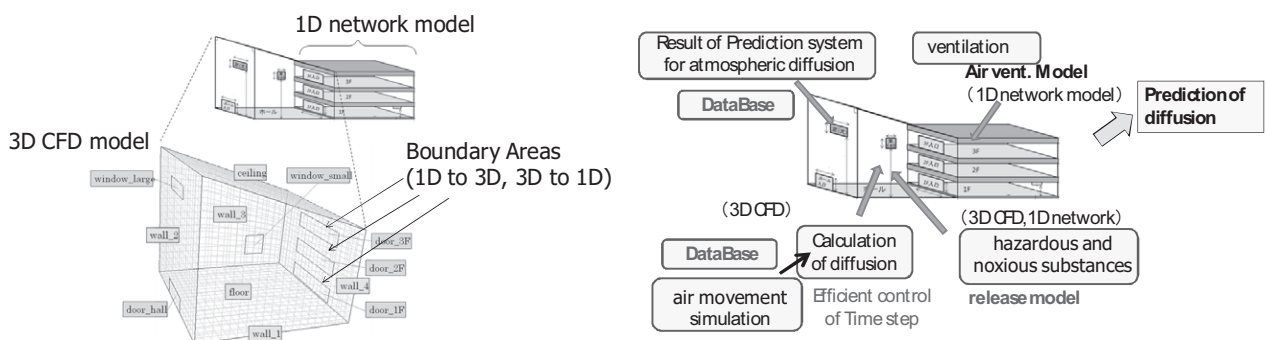


Figure 3.3-2 Combining models(left) and improvement models(right) of EVE SAYFA

3.4 Assistance system of evacuation planning

National Institute of Advanced Industrial Science and Technology (AIST) proposes an assistance system of evacuation planning, for estimation of evacuation from disasters caused by CBR terrorism. These disasters, which are likely to be caused in urban areas, have many characteristics different from natural disasters. These disasters are caused intentionally, which means we must prepare for the worst; there are still few case that CBR terrorism were actually conducted, which means we still know little about what damage will be caused by such terrorism; unlike natural disasters, these disasters are not always harmful to some of the urban infrastructure, which means that they could be utilized for more efficient evacuation.

We have built a network-based pedestrian simulator, shown in Figure 3.4-1, to be used to estimate the damage done by CBR terrorism. Compared to previous grid based and continuous space based simulators which took hours to conduct simulations with less than thousands of evacuees, our network-based simulator are designed to conduct simulations much faster, taking less than few minutes for simulation with ten thousands of evacuees.

Our pedestrian simulator is designed to be used with hazard prediction systems of outdoor and indoor gas diffusion, which calculates how harmful gases spread. Using data provided from hazard prediction systems, our assistance system of evacuation planning can be used to estimate how much damage will be done, for various evacuation scenarios. These results could be used to make and evaluate evacuation plans against CBR terrorism.

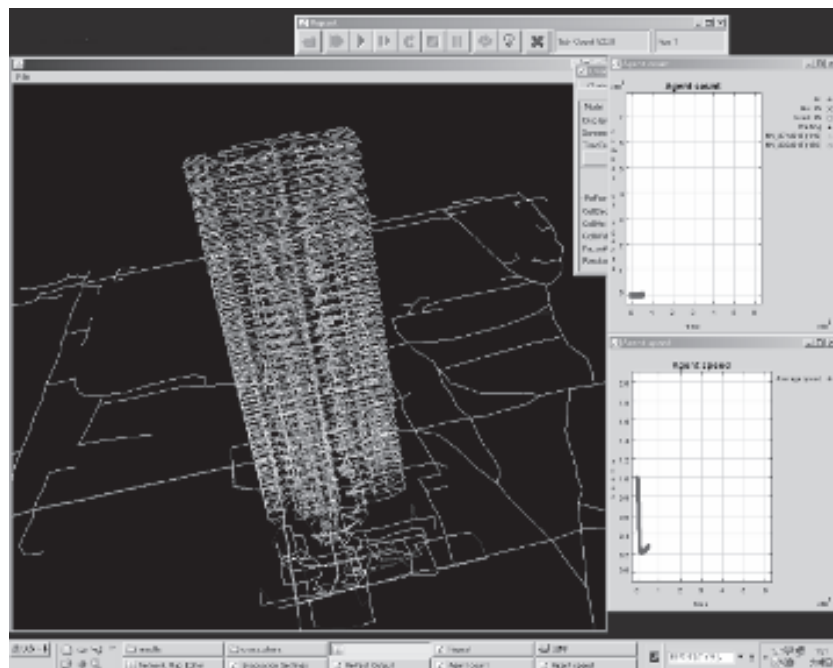


Figure 3.4-1 3D view of our network-based pedestrian simulator

3.5 Application of prediction system

To validate the applicability of the developed hazard prediction system, the system was run for the CBR attack drills that were conducted in Tokyo and Kitakyushu. The main purpose of this system is to assist municipal fire protection and police agencies at the pre-test stage of routinely conducted drills (Table 3.5-1).

Table 3.5-1: Emergency response items
(Reference: U.S. National Research Council report)

| Response items | | Time | Action plan |
|-----------------|--------------------|---------------|--|
| Pre-test | Drill | Routine | Imaginary scenario →round table drill→working drill |
| Actual accident | Emergency response | 0 – 2 hours | Prediction of source terms |
| | Initial stage | 2 – 12 hours | Making a evacuation plan based on real time simulation |
| | Second stage | 12 – 24 hours | Decision making of recovery timing |
| | Recovery action | 1 – few days | Detail reproduction of public hazard |

4. SUMMARY

To summarize, the CBR hazard prediction system can:

- 1) simulate the effect of building complexes on airflow and gas diffusion in urban areas.
- 2) compute unsteady airflow and gas diffusion using a mesh size of a few meters on a conventional PC.

REFERENCES

- Hayashi, T. et al., 1998, Data of long term atmospheric diffusion experiments (autumn, 1991), Japan Atomic Energy Research Institute, JAERI-Data/Code 98-026 (in Japanese).
- Mellor, G. L., and Yamada, T., 1982. Development of a Turbulence Closure Model for Geophysical Fluid Problems. *Reviews of Geophysics and Space Physics* 20, No.4, 851-875.
- National Research Council, Tracking and predicting the atmospheric dispersion of hazardous material releases: Implications for homeland security, National academies press
- Ohba, R., Kouchi, A., and Hara, T., 2007. Hazard Projection System of Intentional Attack in Urban Area, 11th Annual George Mason University, Conference on “Atmospheric Transport and Dispersion Modeling” July 10-12, 2007 (Poster) .
- RAMS/HYPACT technical description, <http://www.atmet.com/>
- Trini Castelli, S., Hara, T., Ohba, R., and Tremback C.J.Y., 2006. Validation studies of turbulence closure schemes for high resolutions in mesoscale meteorological models, *Atmospheric Environment* 40, 2510-2523.

EARTHQUAKE EVACUATION PLAN FOR OLD DHAKA, BANGLADESH

ISRAT JAHAN¹, MD. YOUSUF REJA¹
and MEHEDI AHMED ANSARY²

¹BNUS, BUET, Bangladesh

²Dept. of Civil Engineering, BUET, Bangladesh

sheulyurp@yahoo.com

ABSTRACT

An effective evacuation plan is of utmost importance considering any disaster mitigation measures through reducing loss to a great extent. Evacuation plan for a locality can make them self-dependent in facing a disaster and make them be able to cope with a disaster. In preparing an earthquake evacuation plan the vulnerability of the existing structures along with the prevailing circumstances are studied. A sample-based survey in the selected case study area was done to make the plan efficient. The site selected is in Old Dhaka considered as earthquake vulnerable zone due to high density of population living in a very compact land area with close proximity of buildings including vulnerable structures along narrow local streets. To have an effective evacuation plan, this paper goes through the vulnerability assessment of buildings in the study area 'Ward no. 68' of Old Dhaka using RVS (Rapid Visual Screening) method to picture out whether the building needs detail evaluation or not. Also Turkish Level I and II method are used for more detail evaluation of buildings as proposed evacuation site. Finally, an earthquake evacuation plan for the study area has been prepared considering the relevant criterion. This paper represents the 3D evacuation plan for the study area using GIS software.

1. INTRODUCTION

The Earthquake Risk is prominent in a disaster prone country like Bangladesh. Recently it experienced a record of series of tremor throughout the country indicating Bangladesh with the capital city Dhaka sits on a major earthquake zone. Once a great earthquake occurs, Dhaka will suffer immense losses of life and property due to unplanned city development without maintaining any rules and regulations. Dhaka as the hub of all major activities and major connecting part with outside worlds, any disastrous attack on this city will have very severe long term consequences for the entire country. In Dhaka with a large population of more or less 12 million, the most densely and vulnerable part is Old Dhaka and it is considered as earthquake vulnerable zone due to its high population density, vulnerable structures, low preparedness and others. There is a saying among the earthquake experts: "earthquakes do not kill, what kills is a building that falls, a gas escape or a column". "The human factor changes a natural hazard into a disaster" (Compound). This damage of structure is the main

cause for human injury and death (Choudhury, 1996). It is very important to reduce human vulnerability through prevention as we can't stop any natural disaster but can take pre-cautions in reducing the post effects. In order to reduce the loss due to an earthquake, an effective evacuation plan for specific area is of utmost importance considering any disaster mitigation measures with existing site situations. With the active involvement of the local community an evacuation plan will be more effective. To reduce loss the inhabitants must learn what to do to cope with the disaster. The plan must be publicized to the local community with their doing as per the plan, along with capacity building through training on their activities during evacuation. As such this will reduce the assumed impacts due to any disaster to a minimum.

2. PURPOSE OF THE STUDY

- To prepare an effective evacuation plan considering the prevailing site condition to reduce the loss of lives and properties due to an earthquake.
- Vulnerability assessment of the buildings in the selected area.
- Acknowledge the important public places including open spaces, public buildings like school, religious centers, community centers and others within the community as post-disaster shelters.
- Identify probable evacuation paths to the shelters.
- To promote earthquake awareness including preparedness and mitigation programs within the community.
- Over all, presenting an evacuation proposal for the area.

3. RATIONALE OF THE STUDY

During an earthquake the probability of a large number of building to collapse is absolute in Bangladesh due to the poor construction quality of buildings. Also due to poor fire preparedness in high-rise buildings of Dhaka city, many buildings may catch fire and people may die due to lack of poor evacuation facilities. An effective evacuation plan can reduce loss due to a disaster to a great extend. Evacuation plan for a locality can make them self-dependent in facing a disaster and make them be able to cope with a disaster.

If the people are aware how to cope with the disasters, the losses will be less. The local people with knowledge of evacuation techniques and an evacuation plan for the community can help themselves before the outside help reaches that reduces the effects of disaster to a great extend.

4. STUDY AREA

A highly dense congested area of the older part of Dhaka cit, Ward no. 68, is selected as the study area due to its earthquake vulnerability. The site is

characterized by a large no. of population living in a very compact land area with close proximity of buildings along a very narrow local street. In most cases it is difficult to differentiate the buildings from each other. The prevailing circumstance gives a view of buildings may collapse without any disaster like earthquake. The condition is unthinkable and unimaginable what may happen with an attack of earthquake.

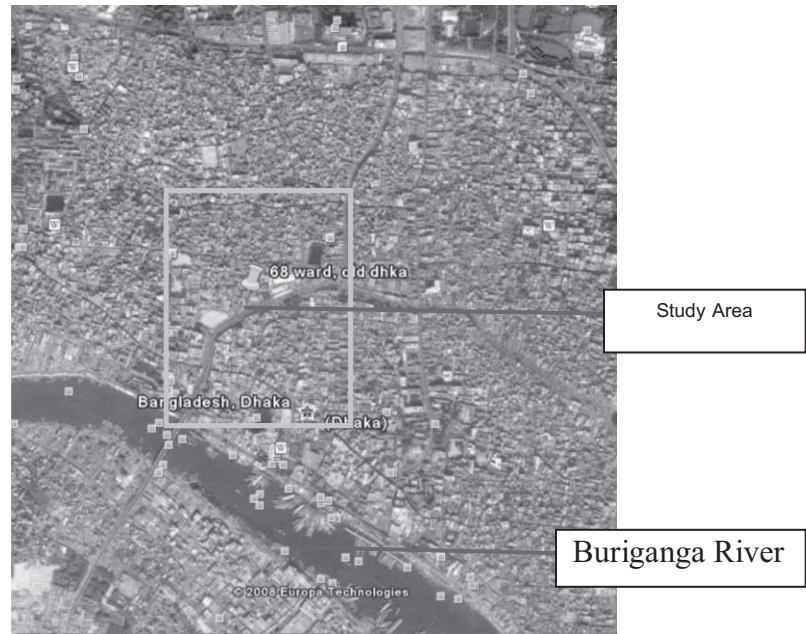


Figure 1: Aerial view of the study area (Ward no. 68, Old Dhaka)



Figure 2: showing boundary line of study area (68 no. Ward)

5. METHODOLOGY

To have an effective plan justified to the respective region, data on vulnerability of the existing buildings in the target area have collected. Besides the prevailing site condition and other criterion relevant to prepare the plan must be studied and analyzed. It is a very difficult and time-consuming task to assess the vulnerability of the existing buildings in any target area. In analyzing the vulnerability of the buildings two different visual screening methods, i.e. FEMA-RVS and Turkish Simple Survey (Level-I & Level-II) Procedure has been used. The Level-I Turkish method is almost similar to the RVS method. The rapid visual screening (RVS) method has been used in this research to assess 1064 buildings and the detail evaluation of the proposed buildings for evacuation is made applying the Turkish Level-2 method. The religious place like mosques, the community centers, educational institutes like schools, colleges and other public places along with the open spaces like park, playground are considered as evacuation sites. Finally after collecting data from field level, A GIS based evacuation plan is generated based on the existing site condition like buildings, road network system, and proposed places for evacuation, etc. by applying different evacuation techniques. Over all a 3D elevation model of the area showing the escaping route with the shortest path directing to evacuation site from each specified group segment is to be prepared.

6. SURVEY FINDINGS

A GIS based base map of the study area has been collected from Dhaka City Corporation Authority. Based on the collected map, there is about 1300 nos. of buildings in the study area excluding the under construction, katcha and semi-pucca structures. And a sample survey on 1064 buildings is done to collect the vulnerability data of the existing buildings that covered 80% of the whole ward area.

6.1 Type of Building Structures

At the first stage of urbanization and city development in our country, the capital city Dhaka flourished from the older part. Only URM (Unreinforced masonry buildings) structures were constructed that's why the no. of URM structures is significant in this area. 69% of the buildings are C3 structures, around 30% are URM and only 1% are C2 structures. The no. of C2 is only a few in this area as there are only some recently constructed 7-8 storied structures with lift facility and shear wall. 3 types of structured buildings were found in the site, the categories are shown in table 1.

Table 1: Type of building structures found in the site

| Building identifier | Photograph | Characteristics and performance |
|--|---|--|
| <p>C3(Moment resisting frame)</p> |  <p>9, P. K. Roy Lane</p> | <ul style="list-style-type: none"> • Usually masonry exposed in exterior. • Concrete columns and beams may be full wall thickness |
| <p>C2(Concrete shear wall buildings)</p> |  <p>20, Islampur Road</p> | <ul style="list-style-type: none"> • Concrete shear wall buildings are usually cast in place. • Shear wall thickness ranges from 6-10 in. • These buildings generally perform better than concrete frame buildings. • Damage commonly observed in taller buildings are caused by vertical discontinuities and irregular configurations. |
| <p>URM (Unreinforced masonry buildings)</p> |  <p>4/2 Rai Ishwar Chandra Road</p> | <ul style="list-style-type: none"> • These buildings often use weak line mortar to bond the masonry unit together. • Unreinforced masonry usually shows header bricks in the wall surface. • The performance of this type of construction is poor due to lack of anchorage of walls to floors and roof, soft mortar and narrow piers between window openings. |

6.2 Building by their Height

It is interesting to notice that the 2 storied buildings are more in number followed by 3 storied buildings in the study area. As old Dhaka is the most ancient part of the capital, the number of URM structure is prominent here which are most commonly of one to two storey. Figure shows the distribution of buildings according to their height.



Figure 3: 3D view showing building height of the study area

6.3 Land Use Pattern

The data collected from field is being analyzed to have an effective plan for the target area. In preliminary stage, the land use distribution pattern of the study area is evaluated based on the sample survey data. It is found that the residential and residential-commercial mixed type land use pattern is predominant there. Figure 4 shows the Land use distribution in the study area (Ward No. 68). Most often the ground floors of most of the residential buildings are being used for commercial purpose.

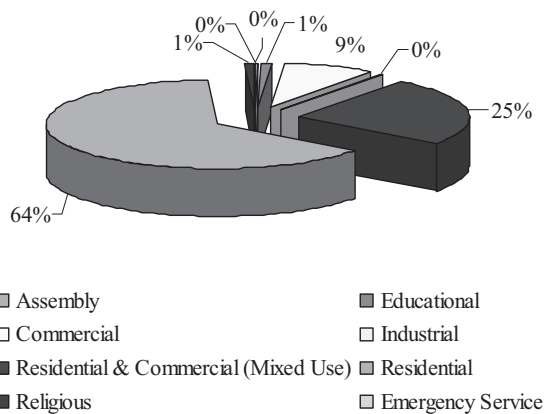


Figure 4: Land Use pattern of the Study Area (based on Sample Survey)

6.4 Vulnerability Assessment of the Existing Buildings

The study area is highly vulnerable to earthquake due to its high density of population and poor structural build up. Figure 5 shows how congested the area is with the figures 6 to 9 to apparently visualize the vulnerability of the area.



Figure 5: Plan showing the organic pattern of Ward 68



Figure 6: Unplanned urbanization- contiguous building character

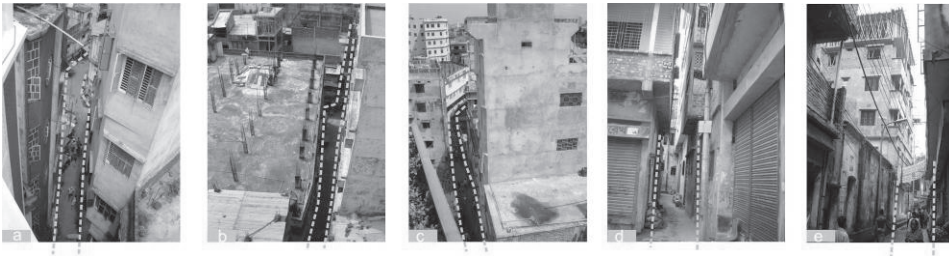


Figure 7: Poor infrastructure---- narrow road width in terms of building height, building density & also population density.

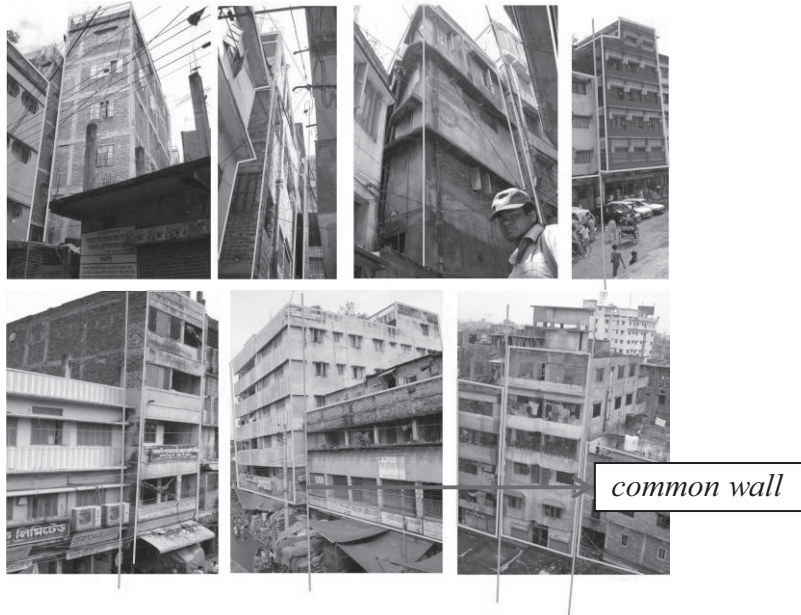


Figure 8: The adjacency of building without any set back, serious Pounding may occur during earthquake

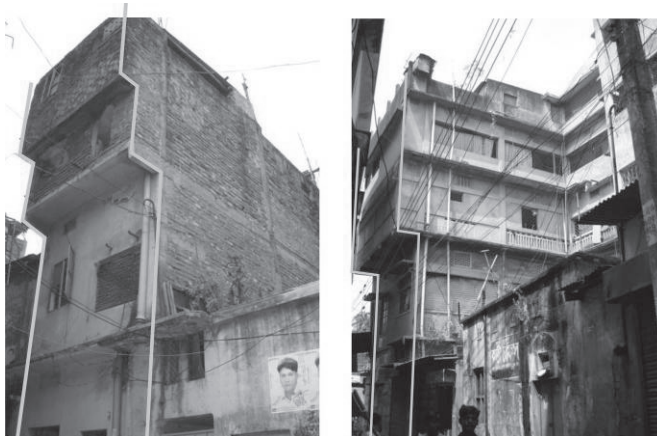


Figure 9: vertical irregularity

The earthquake vulnerability of the buildings is measured using the Rapid Visual Screening (RVS) Method and detail evaluation of the proposed evacuating buildings is made using the Turkish Simple Survey (Level-I & Level-II) method.

The score below which a structure is assumed to require further investigation is termed as “cut-off” score. It is suggested that buildings having an S score less than the “cut-off” score should be investigated by an experienced seismic design professional experienced in seismic design. If the obtained “final score” is greater than the “cut-off” score the building should perform well in a seismic event. A score of 2 is used in this study as a “cut-off” score.

RVS score ‘0’ is given to the buildings that showed negative results, that means the buildings are in emergency need of detail evaluation by any structural engineer and take further actions like retrofitting, etc. based on the result found. The results show that 44% score for buildings was found to touch the cut off value according to FEMA method and all of them require further detailed analysis on vulnerability to determine the level of actual risk.

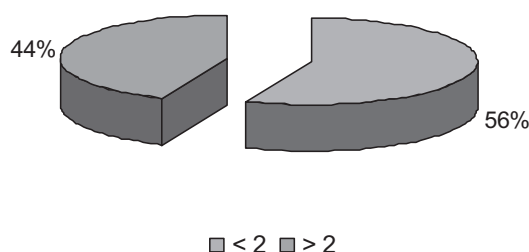


Figure 10: Buildings according to the RVS cut-off Score

A more detail analysis of the proposed evacuation centers has been done in Turkish level-I and level-II method in comparison with the RVS method. It has been found from other studies that the Turkish method is more compatible in the circumstances of our country. A “cut-off” performance score of 50 has been suggested for both survey levels.

Table shows a comparative view of these two methods. It is clear that most of the structures fall below the cut-off score in the RVS method but in Turkish Method, most of them stay above the cut-off score that is, they don’t need further detail analysis.

Table 2: Vulnerability Scores of the proposed evacuation centers

| Name & address | RVS Score | Score in level-I | Score in level-II |
|--|-----------|------------------|-------------------|
| Kamranga Mosque | 0 | 110 | 106 |
| Islampur Jamme Mosque | 0.4 | 65 | 57 |
| Jhabbu Khanam Jamme Mosque | 1.9 | 90 | 100 |
| Shahjada mia Jamme Mosque | 1.7 | 105 | 106 |
| Zindabahar 2 nd Lane Jamme Mosque | 2.4 | 50 | 47 |
| Ahmed Bawyani School | 0 | 75 | 85 |
| Anandomoyee Girls’ High School : St. 01 | 2.2 | 110 | 108 |
| St. 03 | 2.2 | 115 | 120 |
| Babubazar Ghat Jame Mosque | 1.7 | 120 | 125 |
| Haybat Nagar Dewan School | 1.7 | 115 | 113 |
| Jumman Community Center & Ward Commissioner’s Office | 1.7 | 125 | 125 |
| Mahutuli Mosque | 2.2 | 125 | 130 |
| Maulana Mosque | 2.2 | 125 | 130 |

7. PROPOSED EARTHQUAKE EVACUATION PLACES

The religious sites like mosques, the community centers, educational institutes like schools, colleges and other public places along with the open spaces like park, playground are considered as evacuation sites to cover post disaster shelter for earthquake. Most often the schools are considered as the Shelter place from any kind of disaster in this country. So it is an emergency task to make the building itself safe during and after the occurrence of disaster ensuring the safety of its residing people, i.e. the students. Turkish Level-I and Level-II, a more detail analysis of the building is used to assess the structures proposed to be used as evacuation place.

Vulnerability assessment by detailed methods must be conducted for buildings proposed as evacuation centers. Then the vulnerable ones must be retrofitted. The structures adjacent to the open space should be earthquake resistant or retrofitted. The buffer zone for each evacuation center has to be determined depending on its capacity.

The capacity of an evacuation center can be calculated as follows:

$$\text{No. of people} = \text{Size of the space} / \text{area required for each person (0.7 m}^2\text{)}$$

Table 3: Evacuation centers and their capacity

| Name | Area (sft) | Capacity (No. of people) |
|---|------------|--------------------------|
| Babubazar Ghat Jamme Mosque | 3,660 | 457 |
| Shajada Mia Jamme Mosque | 2,163 | 270 |
| Islampur Jamme Mosque | 27,300 | 3412 |
| Jhabbu Khanam Jamme Mosque | 10,500 | 1312 |
| Zindabahr 2 nd Lane Jamme Mosque | 6,440 | 805 |
| Kamranga Jamme Mosque | 3,200 | 400 |
| Zindabahr Playground | 19,000 | 2375 |

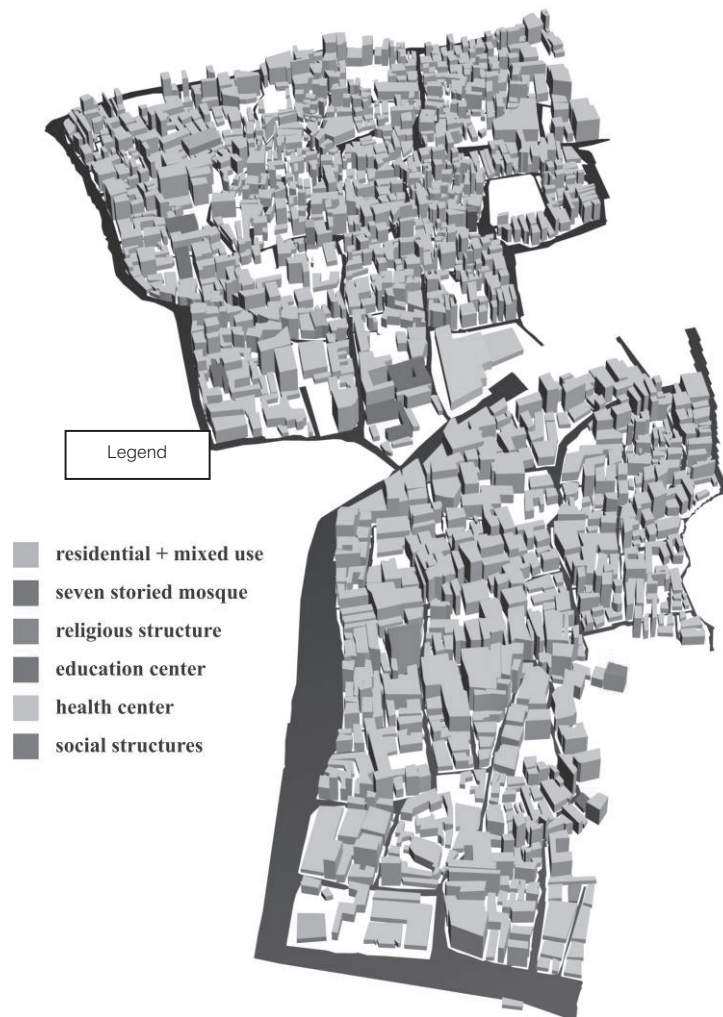


Figure 11: 3d view showing public building in study area

8. EVACUATION PATHS

An evacuation path or emergency exit route for earthquake vulnerable zone is the selected path without any hindrance during the earthquake occurrence and free to go to the evacuation sites. Evacuation path of a particular area will be selected in a way such that it will be the most convenient to use as the exit route for the people experiencing an earthquake. Every evacuation path will be led to a pre-defined safe evacuation center. Length of path should be as small as possible.

An evacuation path should have a minimum width all the way through. In general, the minimum width = Fire truck vehicle width + car width.

If the existing width of the proposed evacuation path is less than the required minimum, then the structures on both sides of the path may have to be reconsidered for reconstruction or destruction or retrofitting to increase the width and ensuring free movement. As these paths should be free from all kind of damage, building adjacent to this road should be earthquake resistant. It should be designed as such that all lifeline facilities beneath the street should be safe after earthquake and least damage will occur.

Roads should be designed in a segmental manner. Thus damaged portion can easily be replaced after disaster and a simple crack can't hamper the whole path during disaster. Again, utility pipes should be innovatively designed through using damper. Boundary walls should be designed as such that it not only ensure privacy and security but also reduce the risk of being collapsed or creating hazards during disaster period.

Road widths at different point have been measured along the evacuation paths. It has been observed that width of road is not the same all the way through. At certain points roads are quite narrow. They must be widen up to at least 20 feet by demolishing the adjacent structures.

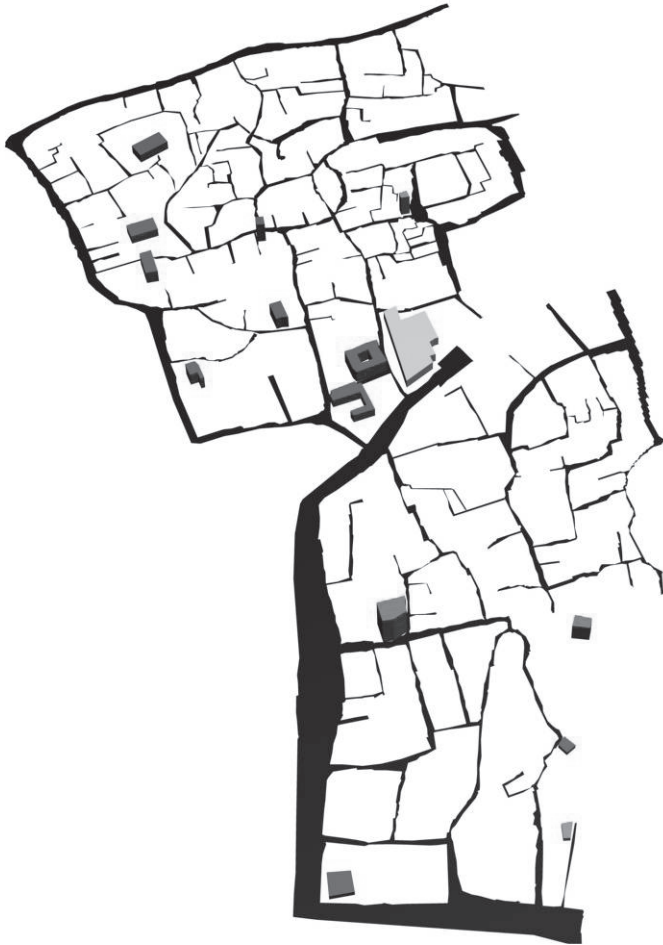


Figure 12: Road layout & public building in Ward no. 68.

9. CONCLUSIONS

This study tries to assess the prevailing condition in old part of Dhaka city and tries to depict the situation what may happen if an earthquake occurs. Both of the methods in building vulnerability assessment have limitations in terms of incorporating the parameters relevant to the design and construction practices in Bangladesh and many countries. Finally this study tries to conclude with some proposals related to Earthquake evacuation that will be effective with respect to concerned area. The proposals are:

- Based on the evacuation proposal presented in this study a large scale evacuation plan for the entire Old Dhaka should be prepared.
- A GIS based evacuation plan needs to be prepared based on the existing site condition like buildings, road network system and proposed places for evacuation etc.
- The whole area must be segregated into different groups according to vulnerability and capacity of evacuation places. Overall, a 3D elevation model of showing the escaping road with the shortest path directing to evacuation site from each specified group segment is to be prepared.
- Launch extensive mass awareness programs for earthquake; the awareness must include city dwellers, government officials, municipality officials, politicians, engineers, architects, designers, builders, medical people etc.
- Develop appropriate training materials for different groups, such as planners, engineers, contractors, masons, bar binders, volunteers, fire fighters, doctors, nurses, first aid providers etc. take training programs at the appropriate levels to impart these trainings.
- Install and operate seismic instruments at suitable locations in the country.
- Develop a comprehensive regional catalogue of all recorded historical earthquakes in Bangladesh and adjacent regions that influence the country's seismic hazards.
- Prepare a regional seismic hazard map of Bangladesh using the existing information and incorporate appropriate building code.
- Develop Bangladeshi scientists including seismologists, engineers, architects, geologists and other technicians through training and higher education programs to achieve leadership in all aspects of earthquake hazard assessment studies.
- Conduct special studies on structural soundness of hospitals, fire fighting centers, schools and university buildings.
- Demonstrate retrofitting and introduce motivation program of retrofitting through municipality leadership (for Dhaka city this may be RAJUK).

REFERENCES

- Ansary, M.A., 2004. *Seismic Loss Estimation of Dhaka for an Earthquake of Intensity VII*. Oriental Geographer, Dhaka University.
- Campo, M. A., nd, 2006. *Study of Awareness of Earthquake Risk in the population of Mendoza*. URL: <http://proventionconsortium.org/files>.
- Choudhury, J.R., 1996. *Design and construction of houses to resist natural hazards*. Workshop on housing and hazards organized by Dept. of Civil Engg, BUET, Dhaka, in association with Earth Resources Centre, University of Exeter, U.K.
- Rahman, M. G. F., 2004. *Seismic Damage Scenerio for Dhaka City*. M.Sc. Engg. Thesis, Department of Civil Engg., BUET, Dhaka.

REMOTE SENSING AND GIS APPROACH FOR TSUNAMI DAMAGE ASSESSMENT –A CASE STUDY

W.N. PREMADASA and D. DMDOK
Department of Earth Resources Engineering, University of Moratuwa,
Sri Lanka
wuditha@gmail.com

ABSTRACT

Tsunami cause widespread damage to the properties as well as human lives in the coast regions. Sri Lanka is a highly vulnerable country for tsunami since Java-Sumatra is a very active subduction zone, where there were several very large earthquakes during the last three years. Current study investigated the potential of remote sensing and GIS in damage detection after a hazardous event. The case study was carried out at Galle, Sri Lanka and the primarily focus was on identification and assessment of damage due to tsunami in 2004. The gravity of damage could not be identified only with the satellite data always therefore GIS data and field observations had to be employed in such situations. A field survey was carried out to identify the damaged areas and to investigate the existing situation at present. There is an extensive need for a proper evacuation plan for the country. An evacuation plan was developed for the Gall city using the road map. Schools and religious places such as temples and mosques near to coastal line were used as gathering places. Using the Contour map of the area, high elevation points were identified as evacuation places. The shortest path to evacuation places from the gathering places were calculated using Arc view Network Analyst Extension. Local authorities can use the proposed evacuation plan and maps to minimise the damage in a possible future tsunami event.

1. INTRODUCTION

Identification and assessment of damage after a natural or man made hazard is essential in various views. It basically helps to assess the magnitude of the damage as well as for rehabilitation and reconstruction activities.

In the view point of Sri Lanka, December 26 2004 tsunami was the worst hazard, which Sri Lankans had to face recently. According To United Nations reports, over 30,000 were dead, 4,000 more were missing, one million were displaced and US\$ 1.5 billion worth property was lost due to the tsunami. Remote sensing and Geographical information systems (GIS) with high resolution data is a useful tool as an immediate means to identify and assess the damage due to a hazard.(Wijetunge, 2006). But only the remotely sensed data cannot give high accuracy identifications since field verifications have to be done along with that. If a possible hazardous

the area. Changes between the satellite images were detected for the original image and band rationed image using change detection algorithm. Damage detection and identification for buildings was also done with visual observation (Figure 2) of the satellite data (Mehdiyev et al, 2005) and the current status was verified using field investigations. Evacuation plan was developed using the road map of the area.

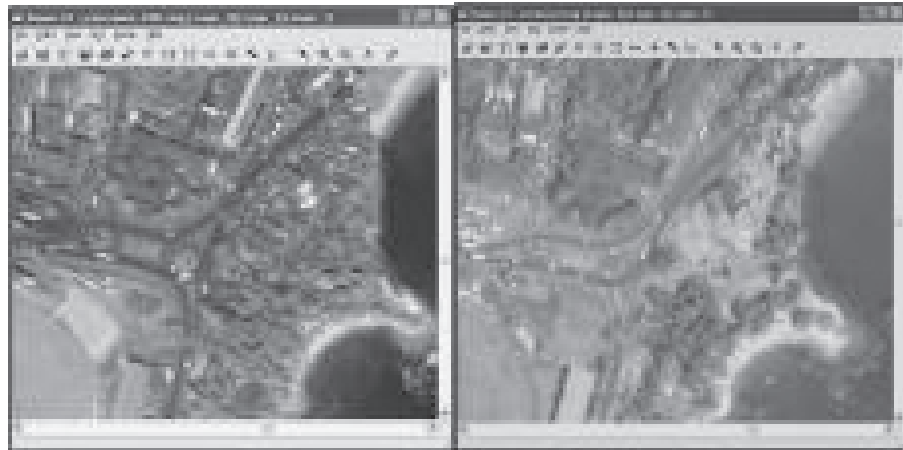


Figure 2: Visual interpretation of satellite data

4. RESULTS AND DISCUSSION

4.1 Damage detection

The damage detection was done with comparison of satellite images using change detection algorithm (Figure 3). Detection of damage is not 100% accurate due to distortion such as noise in the satellite data.

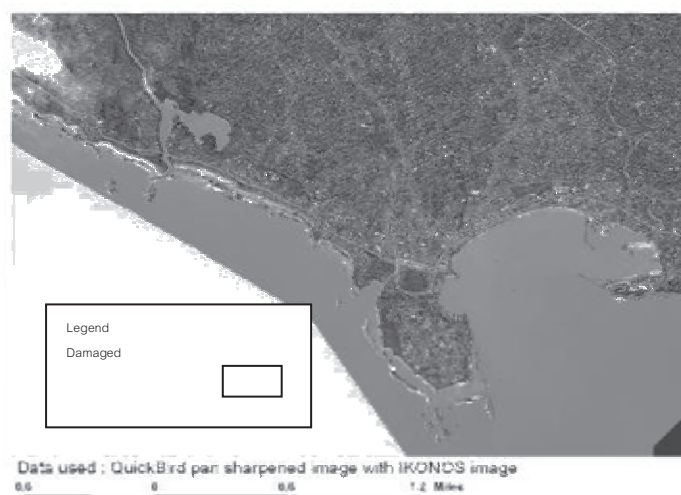


Figure 3: Damage detection using change detection algorithm- Galle

There for visual observation of satellite data was also used to identify the building damage (Figures 4 & 5).

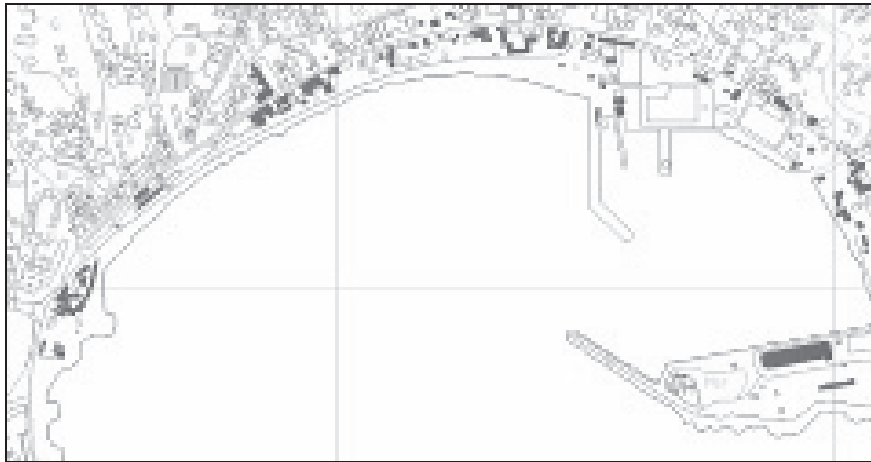


Figure 4: Building damage identified using visual observation of satellite data

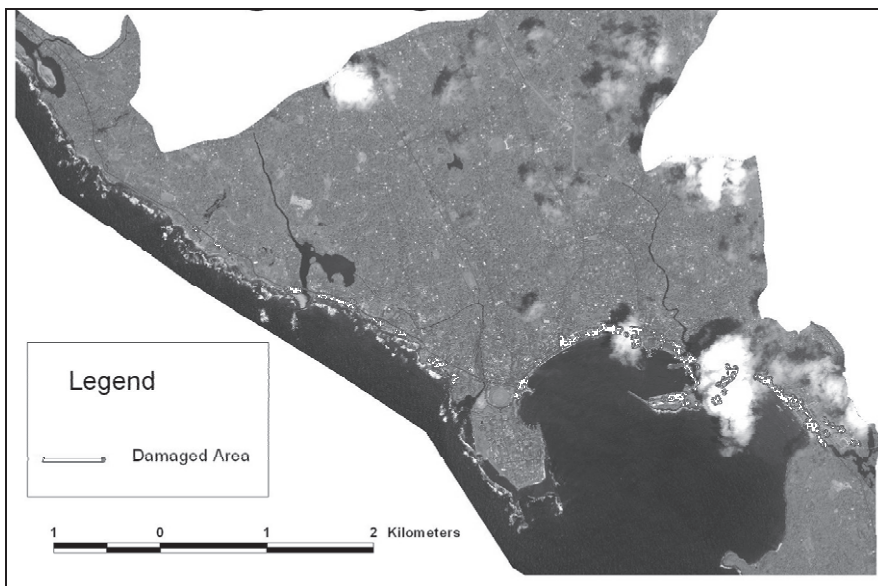


Figure 5: Building damage of Galle MC

Table 1: Total damage in the Study area

| Criteria | Number |
|---|--------|
| Number of Deaths | 774 |
| Number of People missing | 143 |
| Houses Fully Damaged within 100m | 763 |
| Houses with partly damages within 100m | 495 |
| Houses fully damaged out side 100m | 155 |
| Houses with partly damages outside 100m | 652 |
| Number of families affected | 6364 |
| Number of persons affected | 31867 |

4.2 Generation of new buffer zone

The buffer zone imposed by the government is 100m from the coastal line. But comparing with the inundation data we suggest that there should be

alterations to this buffer zone. A new buffer zone (Figure 6) limit was developed using the existing buffer and inundation data.

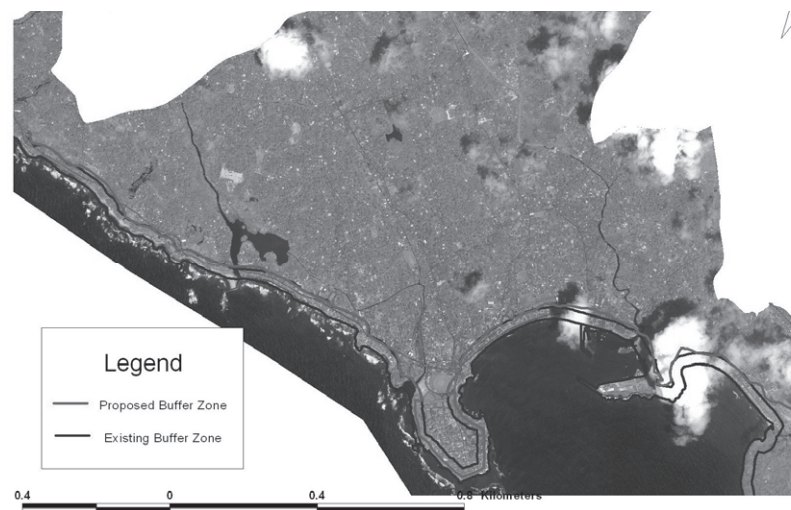


Figure 6: New buffer zone limit of the area

4.3 Evacuation plan for the Galle MC

The inundated area was identified with previous data, and the proposed evacuation plan is based on that data. Present area is mostly a flat land area except a limited numbers of high elevation locations. Using the 3D model (Figure 7) higher elevation locations were selected as evacuation places. People are advised to gather to the gathering places or else use their own vehicles to evacuate to safe places. Shortest path available (Figure 9) was identified using the arc view3.2 network analyst extension. (Turk and Gumusay, 2004)

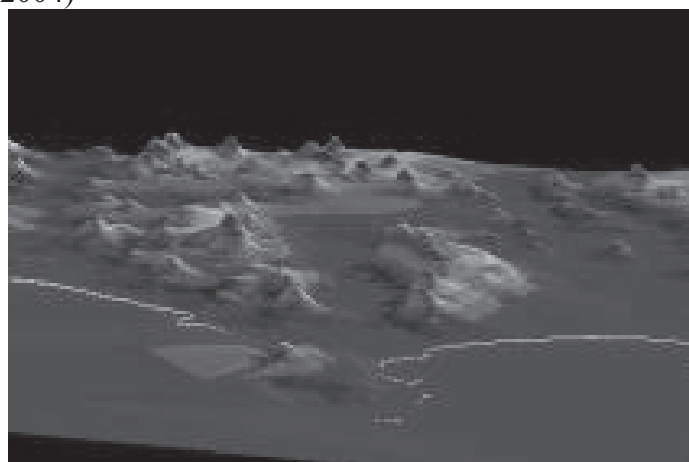


Figure 7: 3D model of the study area

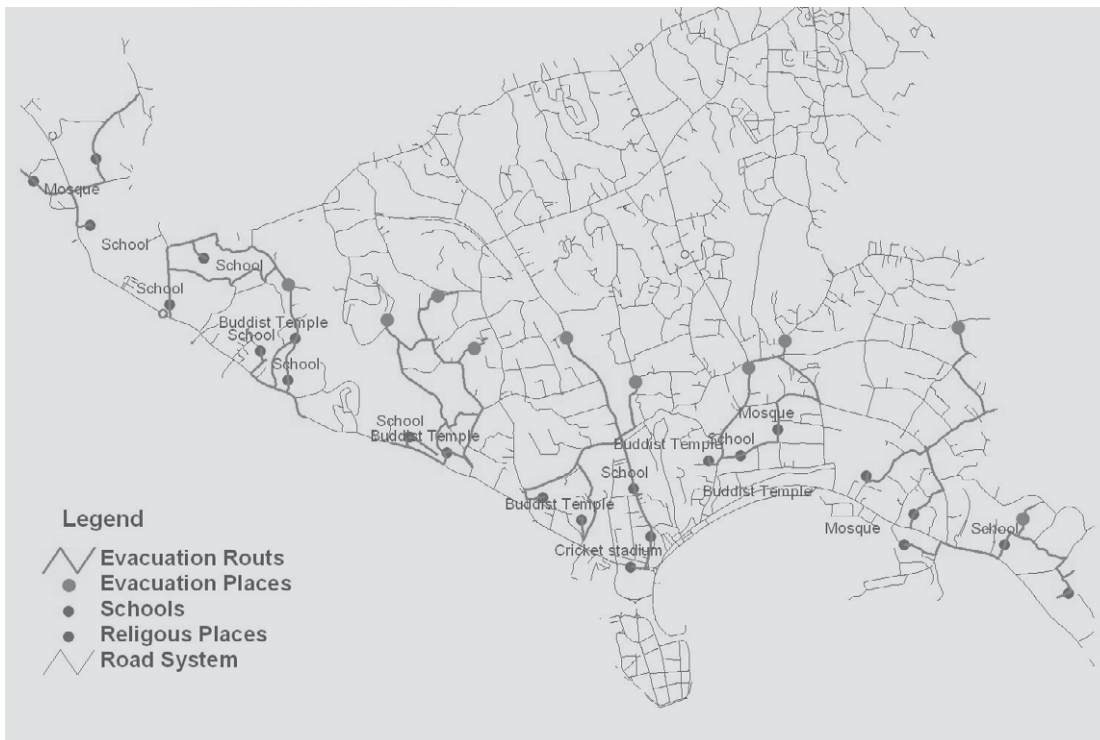


Figure 8: Evacuation plan for Galle MC

5. CONCLUSION

Remote Sensing and GIS is one of most appropriate tools for rapid damage assessment for tsunami affected area for rehabilitation purposes and generation of evacuation plan. Structural damage occurred due to tsunami is very high within the 100m areas. However, significant structural damages have occurred beyond the 100m limit in some areas. Therefore it is recommended to extend the existing 100m buffer zone up to 200m distance from the shore. Network analysis is one of the reliable tools for generate shortest possible path for evacuation from the existing schools and other public places located in the inundated areas.

6. RECOMMENDATIONS

Following recommendations are proposed for future studies.

- Use of Satellite data having Infra Red band so the damage on vegetation could also be detected.
- Use RS and GIS for detecting damages and assessment for other hazards prevalent in the country such as landslides and floods.
- Develop an evacuation plan for the whole country.

ACKNOWLEDGEMENTS

The authors are thankful to Divisional secretariat, Galle-four-gravets Divisional Secretariat division and also Dr. Aththanayake, Geological Survey and Mines Bureau, Sri Lanka for their valuable time spent and for the help in collecting data. We would also like to thank academic and non academic staff of department of Earth Resources Engineering, University of Moratuwa for their support given to complete this research. Our sincere thanks should go to anonymous reviewers for improving the quality of the paper.

REFERENCES

- Mehdiyev Magsud , Kyaw Sann Oo, Jagath Rajapaksha, 2005, Tsunami Disaster Damage Detection and Assessment Using High Resolution Satellite Data, *GIS and GPS – Case study in Sri Lanka, J.ACRS2005*, 5(2).
- T.Turk, M.U.Gumusay,2004, *GIS Design and application for tourism,J. ISPRS*, p. 485
- Janaka J. Wijetunge, 2006, Spatial distribution of Tsunami height and the extent of inundation in Sri Lanka,J. *Science of tsunami hazards*,24(1),pp. 225-239.

A METHOD ON IMPROVING THE ADAPTABILITY OF TIME SERIES MODELS AND ITS APPLICATION IN THE ANALYSIS OF PUBLIC SECURITY

WEI WANG

Department of Mathematics, Information School,
Renmin University of China, Beijing, 100872, P.R.China
wwei@ruc.edu.cn

ABSTRACT

Times series analysis is the method which based on the historical records to build model and then to make statistical inference for the future trends. The emphasis in time series analysis is on studying the dependence among observations at different points in time. The model will be different because of the sample data choice and the estimation method. Owing to the complexity and uncertainty of the real problems, the characteristics of times series will be variant probably in coming periods. So in order to make a proper prediction for future evolution, improving the adaptability of the model is necessary.

This paper proposes the dynamic error regulation method to improve the adaptability of time series models. We first translate the time series model into the form of state space. Then, based on the principle of control theory, we analyse the controllability of the model, and then introduce a dynamic error regulation term into the time-series model to revise the model. In the end of the paper, we will demonstrate the efficiency of this method through some actual case studies.

1. INTRODUCTION

In the study on the problem of social safety, it is often necessary to concern about the changing trend of events number relevant to the safety situation. The evolution of events number is very important to the decision or management about the safety circumstances. Time series analysis is one of the essential tools to the technical analysis of safety problem. In fact, any series of observations ordered along a single dimension, such as time, may be thought of as a time series. The events number of public security is, of course, a time series.

Since Box and Jenkins (1970, 1976) published the seminal book *Time Series Analysis: Forecasting and Control*, a number of books and a vast number of research papers have been published in this area. Time series analysis and its applications have become increasingly important in various fields of research, such as business, economics, engineering, medicine, environ-metrics, social sciences, politics, and so on (Chatfield, 2004, Thoma

and Wilson, 2007, Zhang and Qi, 2003).

The emphasis in time series analysis is on studying the dependence among observations at different points in time. What distinguishes time series analysis from general multivariate analysis is precisely the temporal order imposed on the observations. Many economic variables, such as GNP and its components, price indices, sales, and stock returns are observed over time. So are some variables in public safety, for example, the events number. In addition to being interested in the contemporaneous relationships among such variables, we are often concerned with relationships between their current and past values, i.e., relationships over time. At the same time, time series method can avoid the trouble which encountered in other methods such as regression analysis method in which some necessary factors, for instances, the climate, the consumers' favour etc., cannot be explained very well (Thoma and Wilson, 2007).

Through the analysis of establishing the model by using the general time-series analysis method, we can get the conclusion that the model will be different because of the choice of sampled data and the estimation method. On the other hand, because of the complexity and uncertainty of the real world, the characteristics of time series will change probably in coming periods. Therefore, we need to find some ways to improve the adaptability of the model and to enhance the predictive ability of the model. So improving the adaptability of the model is necessary.

By now, the improvement of time series model has been performed by increasing the order of models, or by choosing the proper forms of fitness functions method. There also have methods such as adaptive method, natural network, etc. (Tang, 2001). There hasn't nearly nothing been done by using the method of feedback to revise the model.

This paper proposes the dynamic error regulation method to improve the adaptability of time series models. We first translate the time-series model into the form of state space. Then, based on the principle of control theory, we consider the controllability of the model, and then introduce a dynamic error regulation term in the model to revise the time-series model. In the end of the paper, we will demonstrate the specific application of this method through some actual case studies. It indicates the efficiency of the method.

2. THE COMMON TIME SERIES MODELS AND THE PROBLEM

In the theory of time series analysis, the fundamental series type is the stationary time series. There have been almost completely results on it. For stationary time series, the common models are the ones such as: auto-regression (AR) model, moving average (MA) model, and the synthetic form of AR and MA, i.e. the ARMA model. For the $ARMA(p, q)$ model, its general form can be described as:

$$X_t - \phi_1 X_{t-1} \cdots - \phi_p X_{t-p} = \alpha_t - \theta_1 \alpha_{t-1} - \theta_2 \alpha_{t-2} - \cdots - \theta_q \alpha_{t-q} \quad (1)$$

where $\phi_1, \phi_2, \dots, \phi_p, \theta_1, \dots, \theta_q$ are $p+q$ weighted coefficients. The definition of the forms and the coefficients can be found in the book of Box, Jenkins and Reinsel (1994) or the book of Zhang and Qi (2003).

For non-stationary time series model, usually, it can be built in three steps. Firstly, by choosing the proper way to preprocess the data, such as taking logarithm, getting the proper order of difference, etc., we can get a stationary time series. Secondly, using the method of stationary time series method, we can get the model for the new stationary series. Thirdly, from the inverse transformation of the first step, we can get the model on the original non-stationary time series. One of such kind of time series models is known as autoregressive integrated moving average (ARIMA) models. This class of models has proved to be useful in representing both stationary and non-stationary time series. An ARIMA model may contain only an autoregressive (AR) term, only a moving average (MA) term, or both. Another important model of non-stationary time series is GARCH model. It is shown that the model has been used widely in the modeling of some complex processes, such as financial process.

An important consideration when modeling time series is the principle of parsimony. That is to say, to representing the systematic structure of the series with as few parameters as possible. Essentially, this means simpler representations of a time series process are more desirable than more complex ones if both are adequate. This principle leads to the use of mixed ARMA models, rather than just pure AR or pure MA models. The principle of parsimony will be further appreciated when the common occurrence of outliers in time series is taken into consideration. While a large number of interesting topics may be presented regarding the building and application of ARIMA models (Engel, Haugh and Pagan, 2005).

As to the problem of prediction, there are many possible ways to forecast a time series. The main emphasis of forecasting techniques presented thus far is on the methods explicitly based on time series models such as ARIMA and transfer function models. Various ad hoc methods, including those using moving averages and weighted smoothing, had been in use long before model-based forecasting methods were widely accepted. With the understanding of their relationships, we can better understand the strength and limitation of traditional forecasting methods, and consider the direction of improvement for forecasting in using such methodology. Some traditional forecasting methods were developed based on statistical theory, while most others were developed mainly based on empirical experiences. These methods share a similar characteristic. That is, the forecasts are based essentially on smoothing (averaging) past values of a time series using some type of weighting scheme. Time series methods are employed assuming that recent periods are the best predictors of the future. Averaging methods are developed based on an average of weighted observations. Smoothing methods are based on averaging past values of a series in a decreasing (exponential) manner (DeJong, Liesenfeld and Richard, 2005).

That is to say, times series analysis is the method that based on the historical records to build model and then make statistical inference for future development. The emphasis in time series analysis is on studying the dependence among observations at different points in time. The model will be different because of the sampled data quality and the estimate method. Because of the complexity and uncertainty of the real world, the characteristics of time series will change probably in coming periods. So improving the adaptability of the model is necessary. Therefore, the paper

will consider the problem to improve the adaptability of time series models. It will also have a great impact on the predictive ability.

3. THE METHOD ON IMPROVING THE ADAPTABILITY OF TIME SERIES MODELS

In this section, we will propose the method of revising time-series models by using the errors between estimation values and real measurements to regulate the model. That is to say, we will use error feedback to revise the adaptability of the models. So, first, we introduce the form of space state on time series model. And then we consider the possibility of using feedback control for the state space model. At last, we give the method for revising the model.

3.1 The state space form of time series models

For the sake of simplicity, we consider only the form of ARMA model, the general form of ARMA can be described as follows.

$$\begin{aligned}
 y(i+n) + p_{n-1}y(i+n-1) + \dots + p_1y(i+1) + p_0y(i) \\
 = q_{n-1}u(i+n-1) + \dots + q_1u(i+1) + q_0u(i)
 \end{aligned} \tag{2}$$

where $y(k)$ is the output, $u(k)$ is the input, p_1, p_2, \dots, p_n and q_1, q_2, \dots, q_n are given constants. In order to get the state space form of time series model (2), we should choose the state variables as follows (Gong, 1988).

$$x_1(i) = y(i) - c_0u(i) \tag{3a}$$

$$\begin{cases}
 x_1(i+1) = x_2(i) + c_1u(i) \\
 \vdots \\
 x_{n-1}(i+1) = x_n(i) + c_{n-1}u(i) \\
 x_n(i+1) = -p_0x_1(i) - \dots - p_{n-1}x_n(i) + c_nu(i)
 \end{cases} \tag{3b}$$

where c_1, c_2, \dots, c_n are coefficients needed to be given.

Replacing the variables (3a) (3b) into (2), and comparing the coefficients of $u(k), u(k+1), \dots, u(k+n)$, we can get the following results about the coefficients.

$$\begin{aligned}
 c_0 &= q_{n-1} \\
 \begin{cases}
 c_1 = q_{n-2} - p_{n-1}c_0 \\
 c_2 = q_{n-3} - p_{n-2}c_0 - p_{n-1}c_1 \\
 \dots\dots\dots \\
 c_n = q_0 - p_0c_0 - p_1c_1 - \dots\dots\dots - p_{n-1}c_{n-1}
 \end{cases}
 \end{aligned} \tag{4}$$

So, we can translate (2) into the following matrix form

$$\begin{bmatrix} x_1(k+1) \\ \vdots \\ x_{n-1}(k+1) \\ x_n(k+1) \end{bmatrix} = \begin{bmatrix} 0 & 1 & & \\ \vdots & & \ddots & \\ 0 & & & 1 \\ -p_0 & -p_1 & \dots & -p_{n-1} \end{bmatrix} \begin{bmatrix} x_1(k) \\ \vdots \\ x_{n-1}(k) \\ x_n(k) \end{bmatrix} + \begin{bmatrix} c_1 \\ \vdots \\ c_{n-1} \\ c_n \end{bmatrix} u(t) \tag{5a}$$

and

$$y(k) = \begin{pmatrix} 1 & 0 & 0 & \dots & 0 & 0 \end{pmatrix} \begin{pmatrix} x_1(k) \\ x_2(k) \\ \vdots \\ 0 \\ 0 \\ x_n(k) \end{pmatrix} + c_0 u(t) \tag{5b}$$

where (5a) is the state space of (2), (5b) is the output equation, c_1, c_2, \dots, c_n can be decided by (4).

3.2 The characteristics of error feedbacks and some related results

From the viewpoint of control theory we know, the characteristics of feedbacks are something like that it can improve the performance the closed-loop system by using the error to regulate the system. That is the reason why we use error feedback to revise the adaptability of the model.

Now, we consider the following general form of linear system

$$X(k+1) = AX(k) + Bu(k) \tag{6}$$

in which $x(0)$ is given.

We hope to choose the control series $\{u(k)\}$ such that, as $k \rightarrow \infty$, the error vector $x(k) - x^*(k)$ will convergence to zero. In such a circumstance, the error of real output and the required output will also convergence to zero. In doing so, here we use the conclusion about pole assignment (Gong, 1988).

Theorem 1: Consider the following linear system

$$X(k+1) = AX(k) + Bu(k) \tag{7}$$

where $X(t) \in R^n$. If there exists a feedback control law which has form of from state to input as follows

$$u(k) = KX(k) + w(k) \tag{8}$$

such that the following closed-loop system

$$X(k+1) = (A + BK)X(k) + Bw(k) \tag{9}$$

has the poles at the given positions of the complex plane, the sufficiency and necessary condition is that the system of (7) is controllability.

3.3 The realization of adaptability of time series models

For a time series model, such as (2), we can always introduce the variable $\varepsilon_t = X_t - X_t^*$, in which X_t^* is the estimated one by using the model (2) and X_t is the observed one. And we can get the error system about ε_t . In such case, we can turn the problem of revising the model into the problem of regulating of error system. That is to say, we should find the regulation way to revise the error system, such that $\varepsilon_t \rightarrow 0$.

For the given model such as (2), we get the following error system

$$\varepsilon_t - \phi_1 \varepsilon_{t-1} \cdots - \phi_p \varepsilon_{t-p} = \alpha_t - \theta_1 \alpha_{t-1} - \theta_2 \alpha_{t-2} - \cdots - \theta_q \alpha_{t-q} \quad (10)$$

Under certain circumstances, we can mend the system in following ways.

Firstly, change the model (10) into model (5), and get the state equation and its output equation like (5a) and (5b).

Secondly, judge the controllability of system (5), that is, the rank of the controllability matrix of $P_c = [B \ AB \ A^2B \ \cdots \ A^{n-2}B \ A^{n-1}B]$ is n or not.

Thirdly, introduce the feedback if the system is controllability. Let $u(k) = KX(k) + w(k)$, where $K = (k_1, k_2, \dots, k_n)$. Calculate the characteristic roots of characteristic equation $p(s) = |sI - (A + BK)| = 0$. And suppose the coefficients of $p(s) = 0$ are equal to the required coefficients of the characteristic equation determined by the given poles, we can get the gains matrix $K = (k_1, k_2, \dots, k_n)$. Then the original system (5) is changed into

$$X(k+1) = (A + BK)X(k) + Bw(k) \quad (11)$$

The new system of (11) is the revised system. And it is stability. That is the model we want.

It is the error regulation that the model has the adaptability, and it can also improve the prediction ability of the model. When the original system (5) is observability, the revised problem can also be solved in the similar way.

4. SOME ACTUAL CASES STUDIES

In this section, we hope to demonstrate the efficiency of the method by providing some of the actual cases studies. We will consider the modelling of time series about the Gross Domestic Product (GDP) by the method given above. The sample data can be found form the main page of the Statistics Bureau of Chinese Government network, and the sample period of GDP is form 1978 to 2006.

4.1 The modelling of the time series

4.1.1 The preprocessing of the sample data

From the scatter diagram of the sample data, we can see that the series on the GDP of per person ($GDPP_t$) has the tendency in the exponential form. Therefore, by taking the logarithm, we can get the new series about the sample data *i.e.* $\ln(GDPP_t)$. From its scatter diagram we know that, $\ln(GDPP_t)$ will increase in linear form. So, here we build the regression model of $\ln(GDPP_t)$ related with time. And then we consider the time-series model on the error (ε_t) of $\ln(GDPP_t) - \ln(GDPP_{t-1})$. In order to compare the method given above with the common time series method, we will leave the data of 2006 for comparison.

4.1.2 The identification of the model

From the graph of the autocorrelative function (ACF) and the partial autocorrelative function (PACF) of ε_t we know that the PACF of ε_t is truncated after $t = 2$. And its autocorrelative function is with certain tailed. Therefore, we choose AR(2) as the model of the series of ε_t .

4.1.3 The parameters estimation of AR(2)

Using the software of E-Views (Gao, 2005), we can get the following estimation results.

Table 1: The estimation results of parameters in AR(2) of ε_t

Dependent Variable: E

Method: Least Squares

Sample(adjusted): 1980 2004

Included observations: 25 after adjusting endpoints

Convergence achieved after 3 iterations

| Variable | Coefficient | Std. Error | t-Statistic | Prob. |
|--------------------|-------------|-----------------------|-------------|-----------|
| AR(1) | 1.573143 | 0.124011 | 12.68549 | 0.0000 |
| AR(2) | -0.795453 | 0.123491 | -6.441375 | 0.0000 |
| R-squared | 0.914576 | Mean dependent var | | -0.005456 |
| Adjusted R-squared | 0.910862 | S.D. dependent var | | 0.132703 |
| S.E. of regression | 0.039620 | Akaike info criterion | | -3.542357 |
| Sum squared resid | 0.036104 | Schwarz criterion | | -3.444847 |
| Log likelihood | 46.27946 | Durbin-Watson stat | | 1.731761 |
| Inverted AR Roots | .79 -.42i | .79+.42i | | |

Therefore, we can get the model of AR(2) as follows.

$$\varepsilon_t = 1.573\varepsilon_{t-1} - 0.795\varepsilon_{t-2} + \nu_t \tag{12}$$

The predict model is the one as follows.

$$GDPP_t = \exp(5.651 + 0.144t + 1.573\varepsilon_{t-1} - 0.795\varepsilon_{t-2} + \omega_t) \tag{13}$$

Based on the calculation we know that the characteristic roots of the characteristic equation of (12) $\phi(B) = 1 - 1.573B + 0.795B^2 = 0$ are all in the unit circle. So the model of (12) is more stationary than the model of AR(2).

4.2 The revision of the model

4.2.1 Getting the state space form

We can translate the form (12) into the following form. From the time series model

$$y(k + 2) - 1.573y(k + 1) + 0.795y(k) = u(k + 2)$$

we let

$$x_1(k) = y(k) - c_0u(k)$$

$$\begin{cases} x_1(k+1) = x_2(k) + c_1 u(k) \\ x_2(k+1) = -0.795 x_1(k) + 1.573 x_2(k) + c_2 u(k) \end{cases}$$

Comparing the coefficients of $u(k)$, we can get the coefficients c .

$$\begin{cases} c_0 = 1 \\ c_1 = 1.573 \\ c_2 = 1.679 \end{cases}$$

Therefore, we can get its state space form as follows.

$$\begin{pmatrix} x_1(k+1) \\ x_2(k+1) \end{pmatrix} = \begin{pmatrix} 0 & 1 \\ -0.795 & 1.573 \end{pmatrix} \begin{pmatrix} x_1(k) \\ x_2(k) \end{pmatrix} + \begin{pmatrix} 1.573 \\ 1.679 \end{pmatrix} u(k) \quad (14a)$$

$$y(k) = (1 \quad 0) \begin{pmatrix} x_1(k) \\ x_2(k) \end{pmatrix} + u(k) \quad (14b)$$

4.2.2 The judgement of controllability

It is easy to get the controllable matrix of (14) as $P_c = (B \quad AB) = \begin{pmatrix} 1.573 & 1.679 \\ 1.679 & 1.39 \end{pmatrix}$. Because $\det(P_c) \neq 0$, P_c is a matrix with full rank. Therefore, the states of model (14) are controllability.

4.2.3 Determining the form of feedback control

From the theory of linear system, we get the feedback in the following form $u(k) = KX(k) + w(k)$, where $K = (k_1 \quad k_2)$, then the state space form is as follows

$$X(k+1) = (A + BK)X(k) + Bw(k) \quad (15)$$

Then the characteristic equation is

$$|\lambda I - (A + BK)| = \begin{vmatrix} \lambda - 1.573 k_1 & -1 - 1.679 k_2 \\ 0.795 - 1.679 k_1 & \lambda - 1.573 - 1.679 k_2 \end{vmatrix} = 0 \quad (16)$$

Suppose the poles are $\lambda_1 = 0, \lambda_2 = 0.795$, then $p(\lambda) = \lambda^2 + 0.795\lambda$. Let the relevant coefficients of the two characteristic equations are equal, we can get $k_1 = 0.573, k_2 = -1$. Let $K = (0.573 \quad -1)$, and instead it into equation (15), we can get the following new system

$$\begin{pmatrix} x_1(k+1) \\ x_2(k+1) \end{pmatrix} = \begin{pmatrix} 0.901 & -0.573 \\ 0.167 & -0.106 \end{pmatrix} \begin{pmatrix} x_1(k) \\ x_2(k) \end{pmatrix} + \begin{pmatrix} 1.573 \\ 1.679 \end{pmatrix} u(k) \quad (17a)$$

$$y(k) = (1 \quad 0) \begin{pmatrix} x_1(k) \\ x_2(k) \end{pmatrix} + u(k) \quad (17b)$$

Because of the poles of matrix $\begin{pmatrix} 0.901 & -0.573 \\ 0.167 & -0.106 \end{pmatrix}$ are $\lambda_1 = 0, \lambda_2 = 0.795$, which are all in an unit circle, then the system is stable.

We can get the new revised model of (14) in the following input and output form

$$y(k+2) - 1.007y(k+1) - 0.263y(k) = w(k+2)$$

Then the revised model of (12) can expressed in the form as follows.

$$\varepsilon_t = 1.007\varepsilon_{t-1} + 0.263\varepsilon_{t-2} + \omega_t \tag{18}$$

Form some calculation we know that the characteristic equation of (18) is $\phi(B) = 1 - 1.007B + 0.263B^2 = 0$, and its roots will be in an unit circle. Then the $AR(2)$ model described by (18) is stable. Therefore, we get the predict equation as follows.

$$GDPP_t = \exp(5.651 + 0.144t + 1.007\varepsilon_{t-1} + 0.263\varepsilon_{t-2} + \omega_t) \tag{19}$$

4.3 The check and predict of model

In order to compare the results before and after the revision, we calculate $\Delta_1 = \varepsilon' - \varepsilon$ and $\Delta_2 = \varepsilon'' - \varepsilon$, the first one is the result of before revision, the second one is the result of after the revision, and the figures are as follows.

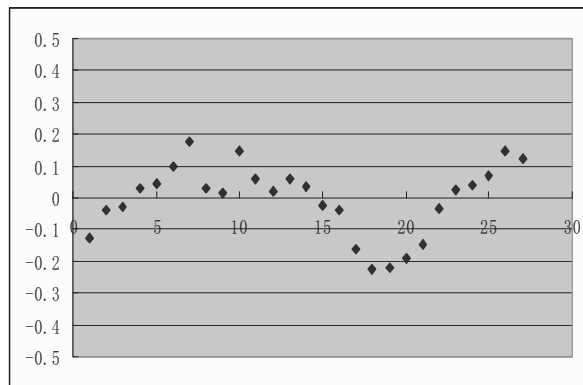


Figure 1: The scatter diagrams of $\Delta_1 = \varepsilon' - \varepsilon$

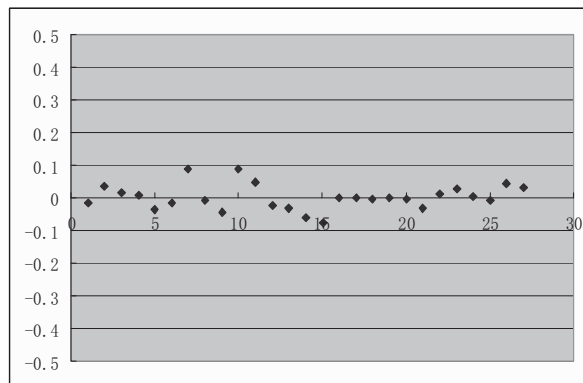


Figure 2: The scatter diagrams of $\Delta_2 = \varepsilon'' - \varepsilon$

From the comparison we know that, the revised model (19) is more precise than the model (13) in simulating the sinuous of ε_t .

Now, we predict the result of 2006' GDPP. Replace the value into the model (13) we can get $GDPP_t = 16789.3$. The error is $4.38\% < 5\%$. And put the value into model (19) we can get $GDPP_t = 16627.14$. The error is $3.38\% < 5\%$. Therefore, the model (19) is better than the model (13). The new model can be more precise to simulate the real sinuous of ε_t .

It should be noted that for the same kind sample data we can use different time series methods for the model. In this example, we use the difference of $\ln(GDPP_t) - \ln(GDPP_{t-1})$ to build the model. We can also build the model by using other time-series methods, and then to revise the models. For other kinds of models, we can still use the method discussed above.

5. CONCLUSION

The adaptability of time-series models is the important aspect for time series analysis. Therefore, to improve the adaptability is one of the important aspects for time series analysis. This paper provides the useful method for such kind of problem by using error feedbacks. For other kinds of time-series models we can also revise the model by using the method above. It needs further consideration when the system is uncontrollable.

Acknowledgement. Here, the author would like to thank Mr. Ou Weiqiang for his contributing on some of the actual case analysis.

REFERENCES

- Chatfield, C., 2004. *The Analysis of Time Series*, Chapman & Hall.
- Box, G. E. P., Jenkins, G. M. and Reinsel, G. C., 1994. *Time Series Analysis: Forecasting and Control*, 3rd Edition, Pearson Education Asia Limited and Posts & Telecommunications Press.
- Thoma, M. A. and Wilson, W. W., 2007. Market adjustments over transportation networks: a time series analysis of grain movements on the mississippi inland waterway system , *Journal of Transport Economics and Policy*, Vol. 41, Part 2, pp. 149–171.
- Tang, X., 2001. Time Series forecasting of quarterly barge grain tonnage on the McClellan-Kerr Arkansas River navigation system, *Journal of the Transportation Research Forum*, 40, 91–108.
- DeJong, D.N., Liesenfeld, R., and Richard, J. F., 2005. A nonlinear forecasting model of GDP growth, *Review of Economics and Statistics* 87: 697-708.
- Engel, J., Haugh, D. and Pagan, A., 2005. Some methods for assessing the need for non-linear models in business cycles, *International Journal of Forecasting* 21: 651-662.
- Zhang Shujing, and Qi Lixin, 2003. *The Concise Course on Time Series Analysis* [M]. Tsinghua University Press, Beijing Jiaotong University Press, Beijing.
- Li Zinai, and Pan Wenqing, 2005. *Metro-economics*, (Second Edition) [M]. Higher Education Press, Beijing.
- Gong De-en, 1988. *The Introduction on Economics Control* [M]. Renmin University of China Press, Beijing.
- Gao Tiemei, 2005. *The Method and Modelling on Metrieconomics Analysis—EViews Applications and Examples* [M]. Tsinghua University Press, Beijing.

RISK ASSESSMENT OF GLOBAL-SCALE NATURAL DISASTER

TAIPING CHANG

Department of Construction Engineering, National Kaohsiung First
University of Science and Technology, Kaohsiung, Taiwan
tpchang@ccms.nkfust.edu.tw

ABSTRACT

Most policy makers adopt the global maps of natural hazard occurrence and risk in the decision-making process. The ranking of countries or regions by relative exposure provides a system for natural hazard mitigation and risk management. However, the calculations underlying global natural hazard risk mapping depend on the availability and quality of geophysical and socio-economic data, which are highly variable from region to region, and may hinder the application of global rankings to regional decision making. In the present study, we summarize a recent integration of natural hazard occurrence, exposure and loss data by the World Bank's "Hotspots" project and describe the advantages and difficulties in such an approach. We also make several suggestions for more highly resolved, regional and sub-national analyses.

1. INTRODUCTION

The decision process based on risk assessment, combined with an appreciation of local circumstances and institutional capacity is absolutely needed for the policy maker (Godschalk et al., 1999). However, it is difficult to make risk comparisons across regions or nations without a systematic approach both to the methodologies of natural hazard risk assessment and the underlying observations of natural hazard occurrence, severity and direct and indirect losses.

Here, we summarize one approach to the development of an evidence base for risk-based decision-making for multiple natural hazards on a global scale. The approach published by Dilley et al., (2005; see also Arnold et al., 2006; hereafter "Hotspots") is being used by several organizations, including the United Nations and The World Bank, to support enhanced risk reduction efforts and disaster risk management. On one hand, the historical completeness, availability and quality of global hazard, vulnerability and loss data make this a difficult task (Dilley et al., 2005). On the other hand, the available global data do make it possible to estimate the relative exposure of populations and economic activity to different natural hazards. Despite "Hotspots" is an advance, but it also signifies specific needs for more research, standardized data procurement and more highly resolved regional and sub-national analyses. The main purpose of this paper is to present a summary of recent work on global-scale natural hazard risks and its role in supporting disaster risk management. We also summarize some of

the deficiencies in the data analyses, and suggest some tactics for making the improvement in disaster risk identification and assessment.

2. ESTIMATION OF MULTI-HAZARD OCCURRENCE AND SEVERITY

One recent study, by The World Bank (the Hotspots study), has combined estimates of multiple natural hazard occurrence with suitable exposure proxies for risk. In particular, it combines hazard occurrence and severity, population and economic data, and loss data to derive relative risk estimates. Therefore, in the present study the summary is achieved based on the Hotspots study only. The Hotspots study estimates global relative risk using proxies based on the geographic distribution of population density and economic productivity sampled on a latitude and longitude grid. The raw data used in this analysis has been coded onto a regular grid of spherical quadrilaterals according to latitude and longitude. The geographic distribution of past occurrence and severity of hazards is calculated for six geophysical and weather-related phenomena (earthquakes, landslides, volcanoes, storms, floods and drought) and sorted into deciles. The individual hazard deciles are added to calculate an aggregate multi-hazard index for different combinations of hazards. After Hotspots and references, Table 1 lists the data used in the hazards.

The difficulty in combining multiple hazards into one multi-hazard index is obvious in the various measures of severity, periods of observation and spatial resolution given in Table 1. Generally these quantities reflect an underlying single-hazard analysis and specialized scientific understanding of the hazard phenomena rather than an attempt to produce a uniform hazard severity index. One approach to multi-hazard indexing is to develop robust measures of the geographic extent and duration of a particular hazard occurrence, thus integrating the severity of the event in space and time so that it can be linked to measures of human impacts.

Table 1: Summary of data sources for hazards discussed in text

Table 1
Summary of data sources for hazards discussed in text (after Table 3.3, Hotspots, pp. 27–29)

| Hazard | Severity measure | Period of observation | Spatial resolution | Source/comments |
|-------------|---|-----------------------|--------------------|---|
| Cyclones | Wind-speed exceedance | 1980–2000 | 30" | UNEP/GRID-Geneva PreView |
| Drought | Smoothed precipitation anomaly | 1980–2000 | 2.5° | IRI Climate Data Library |
| Flood | Large event count | 1985–2003 | 1° | Dartmouth Flood Observatory World Atlas of Large Flood Events |
| Earthquakes | 10% in 50 year ground acceleration exceedance probability | n/a | 1' (sampled) | Global Seismic Hazard Assessment Program (GSHAP) |
| Earthquakes | Large event count (>4.5 Richter magnitude) | 1976–2002 | 2.5' (sampled) | Advanced National Seismic System (ANSS/USGS) Earthquake Catalog |
| Volcanoes | Event count (does not include ash plume) | 1979–2000 | 2.5' (sampled) | UNEP/GRID-Geneva and NGDC |
| Landslides | Computed index | n/a | 30" | Norwegian Geotechnical Institute |

3. ESTIMATION OF MULTI-HAZARD EXPOSURE

The Hotspots study used 20 years of loss data (EM-DAT) compiled by the Centre for Research on the Epidemiology of Disasters (CRED; Sapir and Mission, 1992) and other sources to compute historical loss rate coefficients. These loss rates were then used to compute potential mortality and economic loss using gridded population density and GDP per unit area for 2000, gridded on 2.5'×2.5' cells (roughly 14 km² on average). The absolute economic loss estimates were also normalized by GDP to provide a more appropriate measure of relative impact Table 2 lists the socio-economic data used in the loss calculation.

As done in Hotspots, the calculation of mortality and economic loss from an empirical loss rate analysis at global scales is rough since it neglects more precise estimates of physical fragilities and social vulnerabilities where they exist. Such estimates may be available on regional or urban scales, however, at present, there is no globally uniform assessment of vulnerabilities. The raw gridded socio-economic data is masked so that areas with low population density but high agricultural productivity are included. This mask is shown in Figure 1.

Table 2: Summary of data sources used for mortality and economic loss calculation (after Hotspots, Table 3.4, p.31 corrected)

| Exposure element | Parameter | Period | Spatial resolution | Source/comment |
|------------------|---|----------|--------------------|---|
| Land | Area | 2000 | 2.5' | GPW Version 3 (beta) |
| Population | Density | 2000 | 2.5' | GPW Version 3 (beta) |
| Economy | National/subnational GDP | 2000 | 2.5' | World Bank DECRG based on Sachs et al. (2001) |
| Agriculture | Allocation of national agricultural GDP to agricultural land classification | 2000 | 2.5' | World Bank DECRG based on Sachs et al. (2001) |
| Road density | Length of roads and railroads | ca. 1993 | 2.5' | VMAP(0) |



Figure 1: Depiction of predominant agriculture type, use as activity mask for hazard exposure calculation. Data from FAO/UN. See Hotspots for full reference

4. SUMMARY OF HOTSPOTS MORTALITY AND ECONOMIC LOSS ESTIMATIONS

In Figure 2, the total masked population exposed to the six natural hazards is presented. Table 3 shows the population and land area included in the top three deciles of hazard occurrence and severity. Figure 2 and Table 3 together illustrate the relative level of population exposure for different hazards. As it can be found from Table 3, around 2.3 billion people are exposed to flood hazards, nearly half that number are exposed to drought, and half that again are exposed to cyclones. Geophysical hazards including earthquakes, volcanoes and landslides together account for potential exposed population slightly less than the exposure to cyclones. These comparisons may have implications for the weight given to mitigation and preparedness policies for specific hazards. For example, Figure 3 presents population density as a function of hazard decile for each of the included hazards. High population densities and hazard severity are correlated for volcanoes, cyclones and floods. In Figure 4, the estimated mortality for the six included hazards is presented. The figure actually verifies the traditional knowledge that significant mortality arises in regions exposed to constant flooding and severe storms, especially along eastern continental coastlines. A somehow serious result is the magnitude of drought mortality, especially in sub-Saharan Africa and South Asia.

Similarly, total economic loss is mapped by compiling existing economic loss data against the frequency and severity of hazard occurrence. Hotspots total economic loss is shown in Figure 5.

The total economic loss normalized by gridded economic activity may be a more relevant measure of the importance of hazard mitigation to development, and supplies a general risk proxy for comparing regional exposure. Hotspots economic loss normalized by sub-national GDP is shown in Figure 6

Figures. 4-6 provide quantitative support for the qualitative conclusions that populations near coasts are most exposed to hydro-meteorological hazards while those near mountain belts and active tectonic areas are most exposed to geological hazards. Significant areas of sub-Saharan Africa are exposed to drought. Elsewhere, the most significant exposures to geophysical events occur where population density or economic activity intersect with active tectonic boundaries.

As indicated in Hotspots (Chapter 7), 35 countries have more than 5% of their population living in areas identified as relatively high in mortality risk from three or more hazards. Ninety-six countries have more than 10% of their population in areas at risk from two or more hazards. One hundred and sixty countries have more than one-fourth of their population in areas at relatively high mortality risk from one or more hazards. Many of the areas at higher risk of economic loss from multiple hazards are associated with higher-than-average densities of GDP, that is, there is a relatively high degree of exposure of economically productive areas.

Table 3: Characteristics of high-hazard areas by hazard: top three deciles (after Table 4.1, Hotspots, P.43)

| Hazard | Population (million) | % Total | Land area (million km ²) | % Unmasked |
|------------|----------------------|---------|--------------------------------------|------------|
| Cyclones | 550 | 9.1 | 2.5 | 1.9 |
| Drought | 1100 | 18 | 12.9 | 9.8 |
| Flood | 2300 | 37.7 | 11.5 | 8.8 |
| Earthquake | 328 | 5.4 | 2.9 | 2.2 |
| Volcanoes | 45 | 0.9 | 0.1 | 0.1 |
| Landslides | 66 | 1.1 | 0.8 | 0.6 |



Figure 2: (after Hotspots) Multiple hazard population exposure on 5'' x 5'' grid, showing top 3 deciles (top 30%) of severity for several hazard combinations

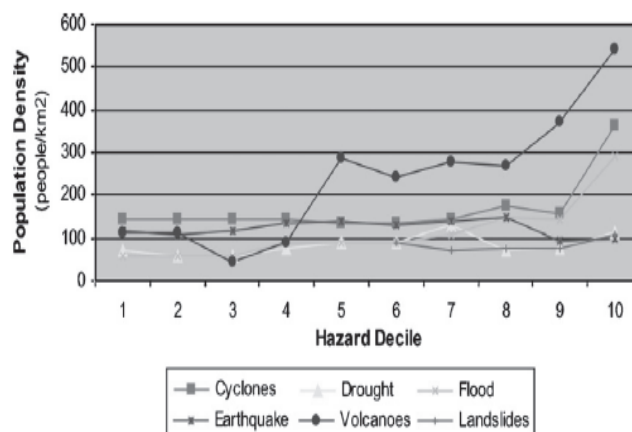


Figure 3: Population density as a function hazard decile (occurrence/severity), showing especially strong correlations between density and volcano, cyclone, and flood severity

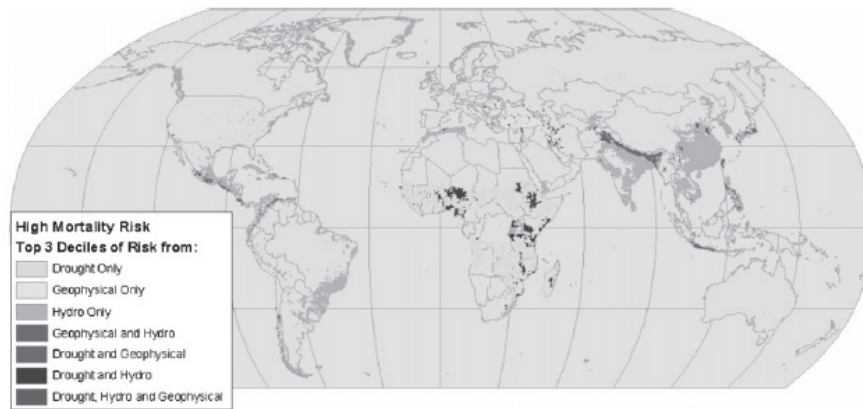


Figure 4: Hotspots mortality calculation for various hazard combinations

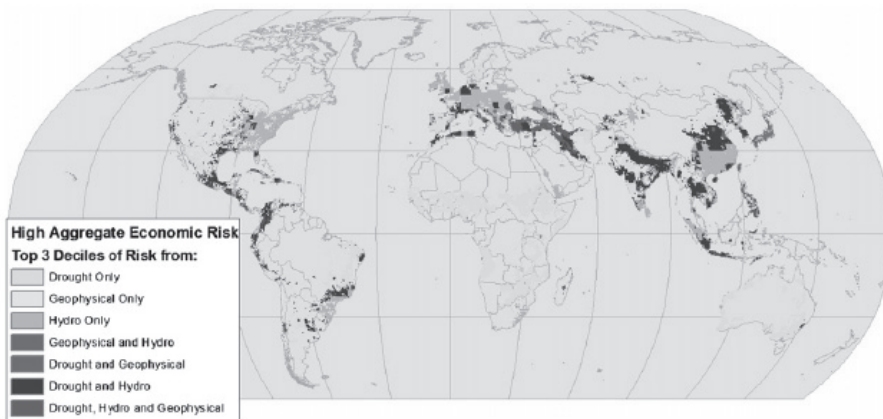


Figure 5: Aggregated economic loss

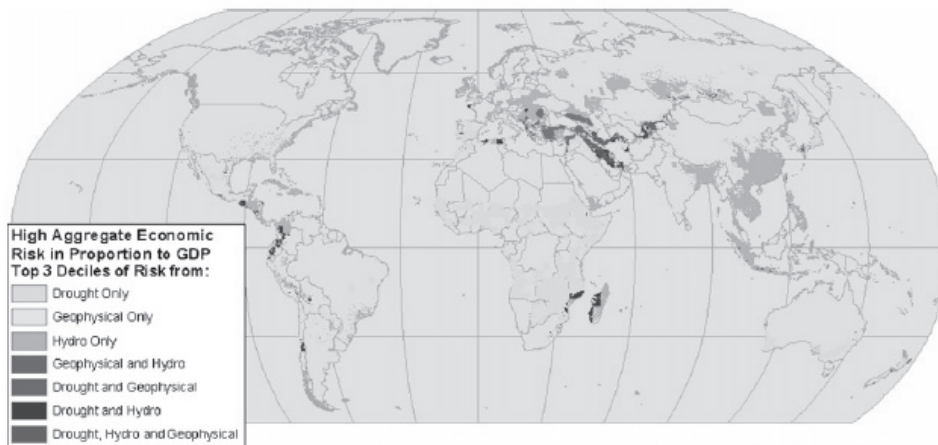


Figure 6: Aggregate economic loss normalized by distributed GDP.

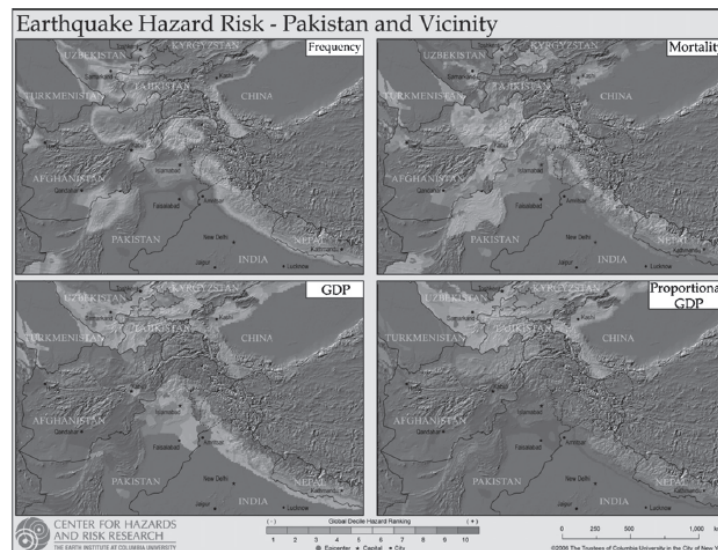


Figure 7: Exposure, mortality, and total GDP and normalized GDP loss for Pakistan and surrounding countries, using the Hotspots data compilation and computed after the 8 October 2005, magnitude = 7.6 earthquake, Epicenter of earthquake shown by red dot.

5. THEMES IN THE GLOBAL ANALYSIS

The global integration of existing and compiled hazard and loss data is valid only insofar as the fundamental data is comprehensive and accurate. Global compilations should have uniform resolution and accuracy, which sometimes forces them to bypass the contributions of more highly resolved or accurate results available for smaller regions, countries or cities.

The occurrence of the Pakistan earthquake in October 2005 illustrates this problem, as well as the need to incorporate more locally accurate scientific understanding of hazard phenomena. Figure 7 depicts the global hazard exposure results for central Asia, calculated using the Hotspots data compilation, along with the epicenter of the earthquake. The globally uniform approach uses the past occurrence of large events as indicators of potential hazard. The global catalogs are reasonably uniform above a certain magnitude level, but are not necessarily the best indicators of potential earthquake activity in a particular location. Earthquakes are a manifestation of dynamic earth processes, which are illuminated by comprehensive regional analysis performed by geologists and seismologists. Often this analysis integrates a refined study of earthquake patterns and mapped geology. In the case of Pakistan, Seeber and Armbruster (1979) performed such an analysis on the patterns of small earthquakes observed on a temporary local deployment of earthquake monitoring instruments. Such data would not necessarily appear on the global catalogs used for the global synthesis. Seeber and Armbruster argued for the potential failure of the fault segment that ultimately ruptured in the catastrophic earthquake in 2005.

It is quite exciting the mortality analysis shown in Figure 7 is a relatively accurate depiction of actual mortality, which suggests that the

mortality “rate” calculation based on historical analysis may accurately represent actual human vulnerability in regions with similar socio-economic parameters. The economic loss predictions are less accurate, which suggests that more attention needs to be given to defining and characterizing the appropriate economic indicators and other social vulnerabilities in such regions.

6. USING THE GLOBAL MAPS

Generally speaking, the hazard mitigation, disaster risk reduction and risk transfer all require overarching approaches customized and implemented at a local level. To do this requires a deep understanding of the vulnerabilities and hazard phenomenology specific to a region, country, city or other location. Global exposure maps cannot provide this level of detail; however, globally consistent analysis can be used to assess the relative importance of hazard exposure on a regional basis, and to identify regions where more detailed analysis is needed.

The primary purpose of global risk maps is to develop a sense of urgency and rational policy making within the global development community. A quantitative, relative ranking of exposure by country, city or regionally allows an informed, evidence-based inclusion of natural hazard exposure risk in country development strategies. This is confirmed by several evidence of inclusion of hazards risk assessment in Country Assistance Strategies and Poverty Reduction Strategy Papers by both The World Bank and the UN.

The global maps provide a consistent baseline assessment of natural hazard exposure, and thus are a starting point for more detailed regional studies. In some countries, the need for national assessments has already been recognized, and more detailed studies have been performed. Elsewhere, detailed regional assessments and the national capacity to perform them do not exist. The global maps provide the logic for initiating new regional studies and compiling existing ones.

7. CONCLUSIONS

The consequence of global hazard and risk mapping efforts should be a renewed emphasis on constructing the scientific and technical capacity to assess, monitor and predict hazard. Hazard assessment must be confirmed in enhanced scientific and technical collaborations, geophysical monitoring and data exchange at national and regional scales, and international communication of scientific results. Needless to say, there must be institutional mechanisms for combining these individual efforts into overall risk assessments and hazard mitigation planning. Generating this capacity is possible, but preserving this capacity is best accomplished by developing the fundamental educational and research institutions and civil institutions in high-risk developing regions.

The global maps should also be adopted to launch regional, country-level and urban multi-hazard risk assessments. The global synthesis

provides only a baseline, which is nevertheless useful for conducting international interest and support in further assessment. The framework of collaborations needed for continuing the global syntheses also is a framework for sharing methodologies, best practices, raw geophysical data and other information needed to design and implement risk reduction tactics.

REFERENCES

- Arnold, M., Chen, R.S., Deichmann, U., Dilley, M., Lerner-Lam, A.L., Pullen, R.E., Trohanis, Z. (Eds.), 2006. *Natural Disaster Hotspots: Case Studies*, Disaster Risk Management Series No. 6. The World Bank Hazard Management Unit, Washington, DC, 184pp.
- Dilley, M., Chen, R.S., Deichmann, U., Lerner-Lam, A.L., Arnold, M., Agwe, J., Buys, P., Kjekstad, O., Lyon, B., Yetman, G., 2005. *Natural Disaster Hotspots: A Global Risk Analysis*, Disaster Risk Management Series, No. 5. The World Bank Hazard Management Unit, Washington, DC, 132pp.
- D.R. Godschalk, T. Beatley, P. Berke, D.J. Brower, E.J. Kaiser, C.C. Bohl and R.M. Goebel, *Natural Hazard Mitigation: Recasting Disaster Policy and Planning*, Island Press, Washington, DC (1999) (575pp.).
- D.G. Sapir and C. Misson, The development of a database on disasters, *Disasters* **16** (1) (1992), pp. 74–80.
- Seeber, L., Armbruster, J., 1979. In: Farah, A., DeJong, K., (Eds.), *Seismicity of the Hazara Arc in Northern Pakistan: Decollement vs. Basement Faulting in Geodynamics of Pakistan*, GSP Quetta, pp. 131–142.
- Skorik, A., Isanuk, M., Lerner-Lam, A., 2004. Time-varying multi-hazard index using empirical methods, *EOS Transactions AGU*, 85(47), Fall Meeting Supplement, Abstract PA23A-1445.
- Schumm, S. A., Mosley, M. P., and Weaver, W. E., 1987. *Experimental geomorphology: the study of small landforms*. John Wiley, New York.

MODEL TESTS ON THE BEHAVIOUR OF FLEXIBLE BURIED PIPE IN SANDY BACKFILL WITH INSUFFICIENT COMPACTION

REIKO KUWANO¹ and DONG HEE KO²

¹International Centre for Urban Safety Engineering,
Institute of Industrial Science, The University of Tokyo, Japan

²Department of Civil Engineering, The University of Tokyo, Japan
kuwano@iis.u-tokyo.ac.jp

ABSTRACT

In order to investigate effects of state of backfill soil on the behavior of buried flexible pipe under cyclic loading, a series of model test was performed in a small sand chamber. Small load cells were installed in the model pipe to obtain the distribution of acting stresses on the pipe.

The acting stress on the crown and the base of the pipe was notably large due to the stress concentration, and a big amount of residual stress on the base was remained after cyclic loading. Cyclic loading seemed to magnify the stress concentration. The horizontal stresses acting on the side of the pipe gradually decreased as the number of applied cyclic loads. Thus, increase in vertical stress and decrease of horizontal support result in softer response and larger deformation of pipe. Those cyclic effects are bigger in the loose ground than dense ground.

1. INTRODUCTION

The design of flexible buried pipes usually demands ensuring good compaction of backfill soil, as it is well known that their behavior is largely governed by the properties of surrounding backfill. However, in practice, it does not seem to be always easy to secure the good compaction, because of the congested and limited surrounding space.

The structural response of flexible buried pipes has been long investigated since the pioneer work by Marston & Anderson (1913), Spanglar (1941) and others. Extensive and systematic studies have been recently carried out by Yoshimura et al. (1997) and Yoshimura & Tohda (1998), based on centrifuge testing. They were summarised as proposed design charts constructed by the elastic FEM analysis in which the relative stiffness of pipe to the surrounding soil was taken into account (Tohda & Yoshimura, 1999).

Most of the previous studies mainly focused on the response of flexible pipe under static loading. The behaviour of flexible pipe subjected to cyclic loading has not been fully understood. In this research,

experimental study has been conducted to examine effects of backfill soil condition on the behaviour of flexible buried pipe under cyclic loading.

2. APPARATUS AND TEST METHOD

A series of model test was conducted applying three stress levels of cyclic loading to the model ground with a buried flexible pipe. A density of backfill soil was varied from loose to dense.

2.1 Model ground

A model ground was constructed in a soil chamber of 46cm wide, 20cm long and 33cm high as schematically shown in Figure 1. Backfill material used was Toyoura sand, uniform fine sand having a mean particle size of 0.16mm. A model pipe was placed on the base layer of which a relative density was 90%. Side and above the pipe were backfilled in the specified density by the multiple sieving air pluviation method. Especially for the dense ground condition, the backfill sand below the spring line of the pipe was well compacted in order to achieve the specified relative density of 90%.

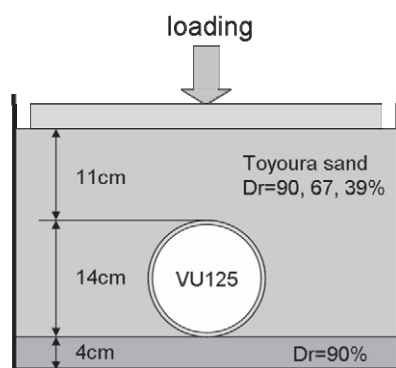


Figure 1: A small soil chamber and model ground

2.2 Model pipe

A PVC pipe (VU125: outer diameter of 140mm and thickness of 4.1mm) was used for a buried model pipe. Small load cells capable of measuring both normal and shear forces were installed in the pipe in order to evaluate acting pressures on the pipe surface at eight locations as shown in Figure 2. Strain gauges were attached in outer and inner surface of pipe in addition to the measurement of vertical and horizontal diameter changes, to obtain the information on the pipe deformation.

A small load cell (LC), which was 52mm long, 5mm wide and 21mm high, can measure both compression/tension and shear forces up to 98N each. A photo of the LC is shown in Figure 3. A loading plate of 10mm by 20mm, made of PVC, was attached to the load cell. The LCs were installed into the pipe using metal attachments stationed at the inner surface of the pipe. The gap between loading plate and the pipe which was 3mm in each

direction in previous study (Kuwano and Miyashita, 2008) has been modified to be twice in this test. In order to avoid sand grains falling through this gap, a membrane with 0.1mm thickness was used to cover the gap as shown in figure 2. It was confirmed that the reading of the LC was not affected by the pipe deformation unless a force was acting on the loading plate of the LC.

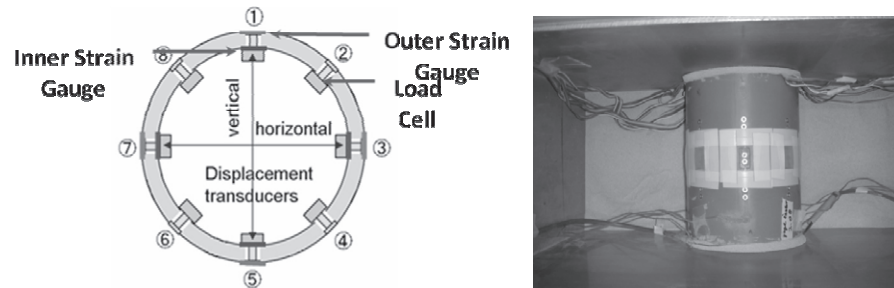


Figure 2: A model pipe

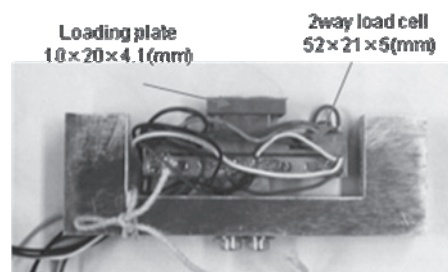


Figure 3: A photo of load cell

2.3 Test method and conditions

Load was applied to the surface of model ground through a rigid plate of 42cm wide, so that the model ground was subjected to one dimensional compression. A vertical pressure of 10kPa was applied first, which was equivalent to overburden soil pressure of approximately 60cm. Then cyclic loading of three stress amplitude levels, 50kPa, 100kPa and 200kPa, was applied. Repeated loads were given 100 times at each stage. All loading/unloading/reloading was made in a displacement control at a rate of ± 0.02 mm/sec. The cyclic stress amplitude of 50kPa was roughly equivalent to the live load used in the road design practice in Japan.

Backfill soil was made in dense and loose state. In one case, only the side of the pipe was backfilled in loose state, below and above the pipe was made in dense state. Test cases and their conditions are summarized in Table 1.

Table 1: Test conditions

| No. | Model ground | Cyclic loading |
|---------|---|---|
| Case L | Dr=39% | 100 times cyclic loading with stress amplitude of 50, 100 and 200kPa, |
| Case D | Dr=90% | |
| Case DL | Base and above the pipe: Dr=90% Side of the pipe: Dr=39% | |

3. TEST RESULTS AND DISCUSSIONS

3.1 Effects of different backfill densities

Relationship between normal stresses acting on the pipe at the LC location of 1, 3, 5 and 7, and displacements of pipe diameter for test case L is shown in Figure 4. Vertical/normal stresses measured at LC1 and LC5 are plotted against a displacement of vertical diameter. Similar values were recorded at LC3 and LC7 as the model was in the symmetric condition and the average of these values is plotted against displacement of horizontal diameter. In Figure 4, relationship between applied pressure and displacement/settlement of the ground surface is also shown. Test results of case D are shown in Figure 5 in the same manner.

Overall deformation of the pipe and the ground was notably larger in case L. Magnitude of stresses recorded at LC1, 5 are similar between case L and D, even though the stress of LC1 in case L is a little bigger than applied pressure due to stress concentration. While the value of stress at horizontal direction (LC3 and LC7) was distinctively small in case D, because ground at side of the pipe was confined.

Stress distributions at the maximum and residual values at each cyclic loading stage are shown in Figures 6 and 7 for case L and D respectively. 1-100max means the maximum value of stress at the 100th cycle of 1st loading stage (50kPa) and 1-residual means that the residual value after the 1st cyclic loading stage (still subjected to 10kPa). The concentration of stress at LC1 appears in the stress distribution as vertically upward stretching oval shape in case L and D. It is also noted that the residual stress at LC5 increased as the cyclic loading progressed and remained with big amounts for both case L and D.

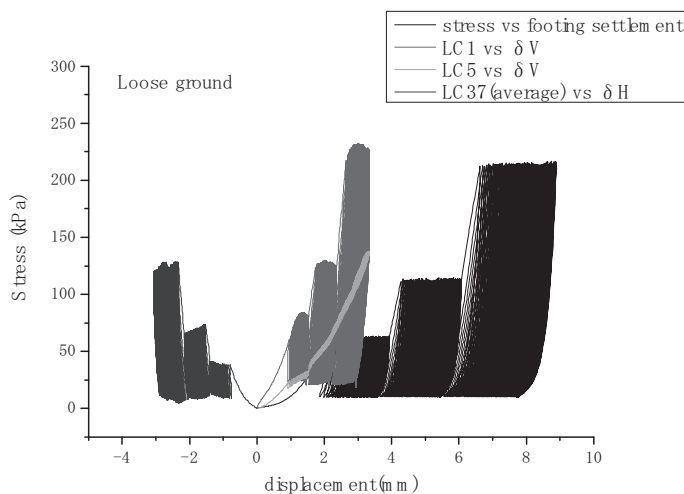


Figure 4: Deformation and stresses acting on the surface of pipe and ground in case L.

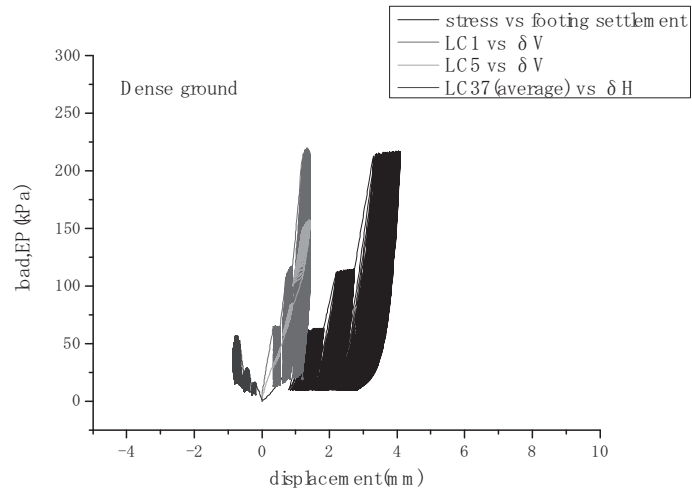


Figure 5: Deformation and stresses acting on the surface of pipe and ground in case D.

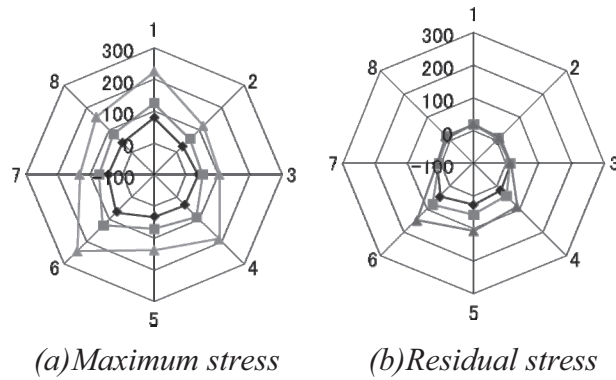


Figure 6: Distribution of normal stresses acting on the pipe surface in case L

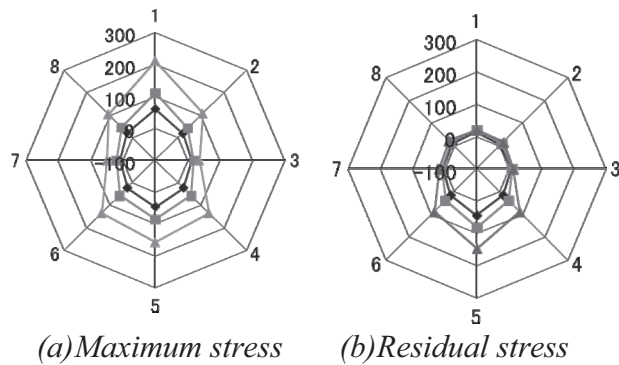


Figure 7: Distribution of normal stresses acting on the pipe surface in case D

3.2 Effects of cyclic loading

In Figures 8 and 9, an average normal stress at LC3 and 7 is plotted against an average normal stress at LC1 and 5 for case L and D, respectively. Normal stresses at LC3 and 7 are in the horizontal direction and those at LC1 and 5 are in the vertical direction. A ratio of horizontal stress and vertical stress indicates a kind of earth pressure (K). In case L, the horizontal and vertical stress ratio is around 0.74. In case D, the ratio is around 0.27. The earth pressure in loose ground is much bigger than dense ground.

The graph moves to right-down direction with increasing of cyclic number. It is implied that normal stresses of the pipe in vertical direction increase with increasing of cyclic number and those in horizontal direction decrease with increasing of cyclic number. The cyclic effect (the amount of the change) is bigger on the loose ground than dense ground.

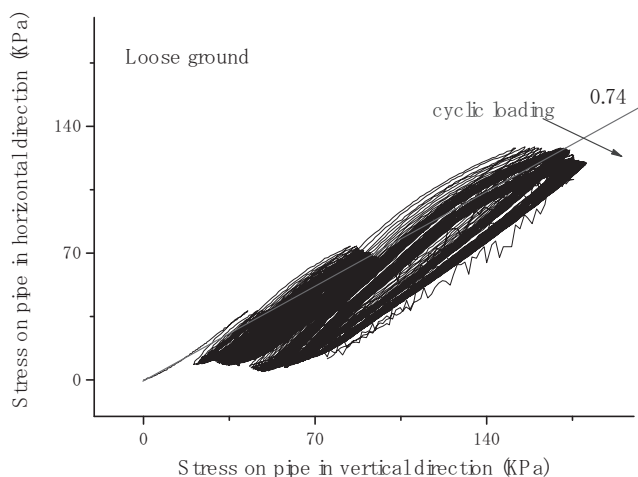


Figure 8: Normal stresses acting on the pipe in the horizontal and vertical directions in case L.

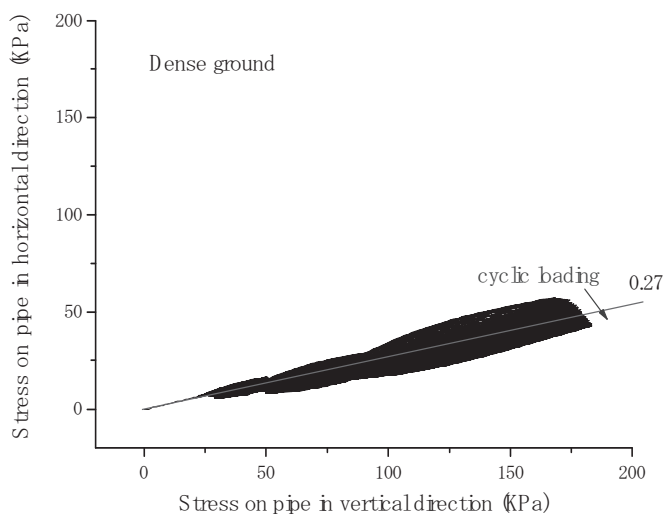


Figure 9: Normal stresses acting on the pipe in the horizontal and vertical directions in case D.

3.3 Behavior in poorly compacted backfill

In the construction site, the compaction of backfill may not be always easy, especially at the vicinity of pipe. In test case DL, considering such a situation, only the side of the pipe was backfilled in a loose state. The base layer and above the pipe are made in a dense state as shown in Figure 10. Stresses and displacement of the pipe and ground in case DL are shown in Figure 11. Trend of acting stresses and resulting deformation was somehow in between case L and D. But, significant stress concentration on the base part of the pipe was observed. The stress distribution acting on the pipe was similar to that in case L, as shown in Figure 12.

Average values of stresses at LC1 and LC5 are plotted against vertical displacements of pipe diameter for all the test cases in Figure 13. The inclination of the plots indicates a kind of stiffness of pipe response, reflecting also lateral confinement of backfill. Case D shows the stiffest pipe response due to the strong support from the lateral backfill soil.

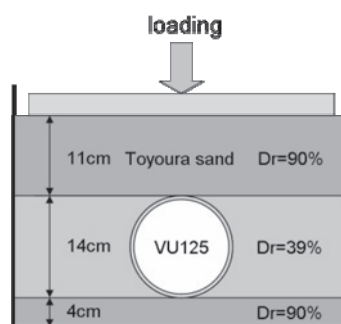


Figure 10: Model ground of poorly compacted backfill around a pipe.

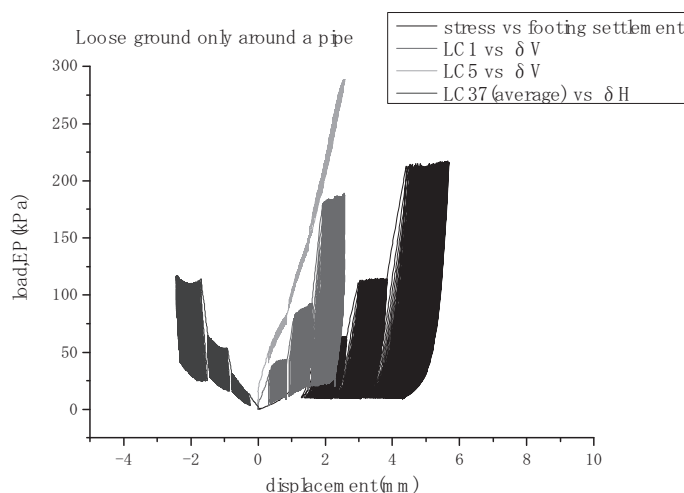


Figure 11: Deformation and stresses acting on the surface of pipe and ground in case DL

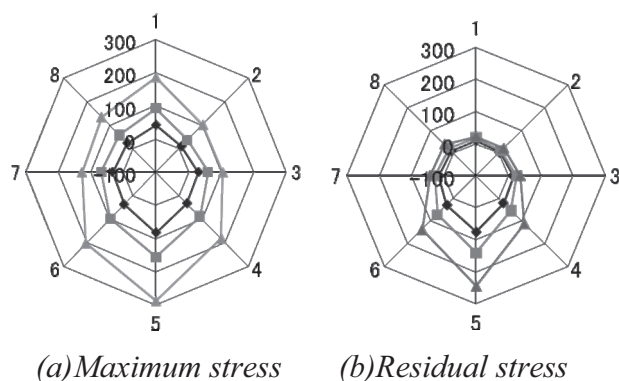


Figure 12: Distribution of normal stresses acting on the pipe surface in case DL

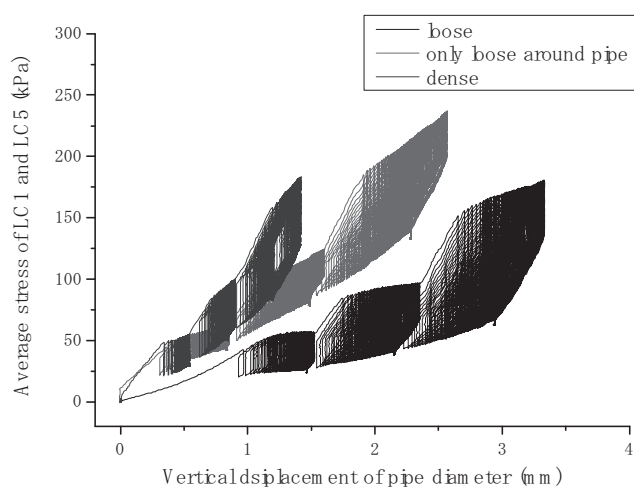


Figure 13: Comparison of stress-deformation relationship of pipe

4. SUMMARY

In order to investigate effects of backfill density state on the behavior of buried flexible pipe under cyclic loading, a series of model test was performed in a small soil chamber. Following conclusions were obtained.

(1) When a flexible pipe was buried in loose backfill soil, overall deformation of the pipe and the ground was notably larger than in dense backfill soil. And, the stress and displacement of the pipe in the horizontal direction were relatively quite small in dense ground due to lateral confinement of backfill. Besides, a big amount of residual stress on the base part of the pipe was shown in all tests.

(2) When a buried pipe was applied by cyclic load, the acting stresses on the crown and base of the pipe are notably large due to the stress concentration. Cyclic loading seemed to magnify the stress concentration. The horizontal stresses acting on the side of the pipe gradually decrease as the number of applied cyclic load. And these cyclic effects are bigger on the loose ground than dense ground.

(3) Considering the condition of construction site, the backfill was made in a loose state only the side of the pipe. The characteristics of stress and strain distribution were similar to those in the loose backfill, while the normal stress on the base part of the pipe was much large and the stress concentration was significant.

REFERENCES

- Marston, A. & Anderson, A.O. 1913. The theory of loads on pipes in ditches and tests of cement and clay drain tile and sewer pipe. Bulletin 31, Iowa Engineering Experiment Station, Iowa State College, Ames, Iowa.
- Spangler, M.G. 1941. The structural design of flexible pipe culverts. Bulletin 153, Iowa Engineering Experiment Station, Iowa State College, Ames, Iowa.
- Tohda, J. & Yoshimura, H. 1999. Proposal of a rational design method for buried flexible pipes. Journal of Japanese Society of Civil Engineers, No.617/3-46, pp.49-63 (in Japanese).
- Yoshimura, H., Tohda, J. & Li, L. 1997. Experimental study on earth pressure and deformation of buried flexible pipes. Journal of Japanese Society of Civil Engineers, No.561/3-38, pp.245-255 (in Japanese).
- Yoshimura, H. & Tohda, J. 1998. FE elastic analysis on mechanical behaviour of buried flexible pipes measured in centrifuge model tests. Journal of Japanese Society of Civil Engineers, No.596/3-43, pp.175-188 (in Japanese).
- Kuwano, R. & Miyashita, T. 2008. Model Tests on Behaviour of Flexible Buried Pipe in Sand with Different Densities, Proceeding of International Geotechnical Conference on Development of Urban Areas and Geotechnical Engineering, St. Petersburg (to appear)

EXPERIMENTAL STUDY ON THE EVALUATION OF LOOSENING SURROUNDING A CAVITY IN SOIL

MARI SATO¹ and REIKO KUWANO²

¹Department of Civil Engineering, The University of Tokyo, Japan

²International Centre for Urban Safety Engineering,
Institute of Industrial Science, The University of Tokyo, Japan
msato@iis.u-tokyo.ac.jp

ABSTRACT

Damaged old sewer pipes are known to often cause void/cavity or loosening in the surrounding soil, which may lead to a cave-in in the road. In this research, in order to understand the mechanism and governing factors of cavity formation/expansion in the ground, a series of model tests simulating flowout of soil through a crack/gap in a buried pipe was conducted.

It was found that a cavity and surrounding loosening in the ground can extend rapidly upward when the ground consists of poorly graded sand, especially when it is fully saturated. Quantitative evaluation was also given to the loosening around a cavity.

1. INTRODUCTION

An old deteriorated sewer pipe, when it is damaged, may eventually cause local subsidence or a cave-in in the road. Recently, the number of pipes which are older than the service life time of 50 years, has been rapidly increasing. Accordingly, incidents of a cave-in are found to be more frequent in urban areas. In spite of the significance, full investigation of the road cave-in is often skipped as the urgent road restoration is usually prioritised. It is difficult to clearly identify the real cause by the fact that eventual cave-in is likely to occur long after the initial formation of a cavity in soil. The congested underground lifeline structures also make it complicated.

Kuwano et al. (2006a) conducted a survey to obtain basic information on how the damaged sewer pipes were related to the collapses of road, which occurred from 2001 to 2003. The survey was performed by sending questionnaires and interviewing local government officers in seven cities where the sewerage system had started more than 30 years ago and the management and maintenance of old sewer pipes are likely to be the concerned issues. It was found that even small gaps or cracks could lead to road cave-in and the rainfall appears to be one of the most important factors, as schematically shown in figure 1. Based on the survey results, Kuwano et al. (2006b) performed a series of model tests to investigate how a cavity initially forms in soil and how it progresses up to the ground surface. In this

paper, the typical process of cavity formation/expansion in sandy soil and the quantitative evaluation for the loosening surrounding the cavity is shown.

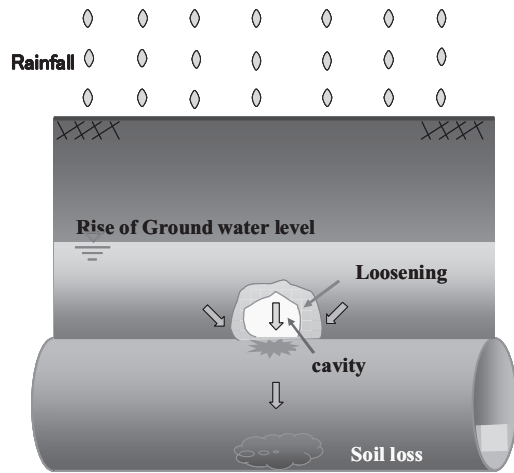


Figure 1: A cavity and loosening formed above the defect of buried pipe

2. TEST APPARATUS AND PROCEDURE

A test apparatus used in this study is shown in Figure 2. Model ground of 300mm wide, 50mm long and 200mm high was made in a small soil chamber having an opening of 5mm in a base plate, through which water was supplied and drained. A cavity was formed above the opening at the base, after the water flow in and out of the opening repeatedly.

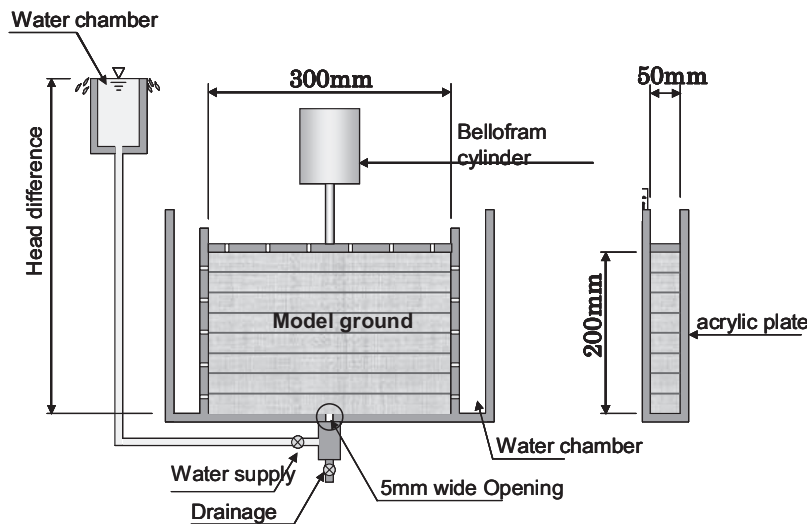


Figure 2: Model test apparatus for generating cavity/loosening in soil

Two sandy materials were used for the model ground. One is Toyoura sand, clean uniform fine sand, and the other is natural sand which contains fines of around 10%. Physical properties and particle size distribution are shown in Table 1 and Figure 3, respectively.

Table 1: Physical properties of model ground materials

| Material | Maximum dry density ρ_{dmax} (g/cm ³) | Minimum dry density ρ_{dmin} (g/cm ³) | Model ground (Dr=80%) | | |
|--------------|--|--|--|-----------------------|-----------------------------------|
| | | | Dry density ρ_d (g/cm ³) | Water content w(%) | Hydraulic conductivity k(cm/s) |
| Toyoura sand | 1.65 | 1.32 | 1.57 | 14.0 | 9.6×10^{-3} |
| Natural Sand | 1.56 | 1.18 | 1.46 | 17.5 | 5.0×10^{-4} |

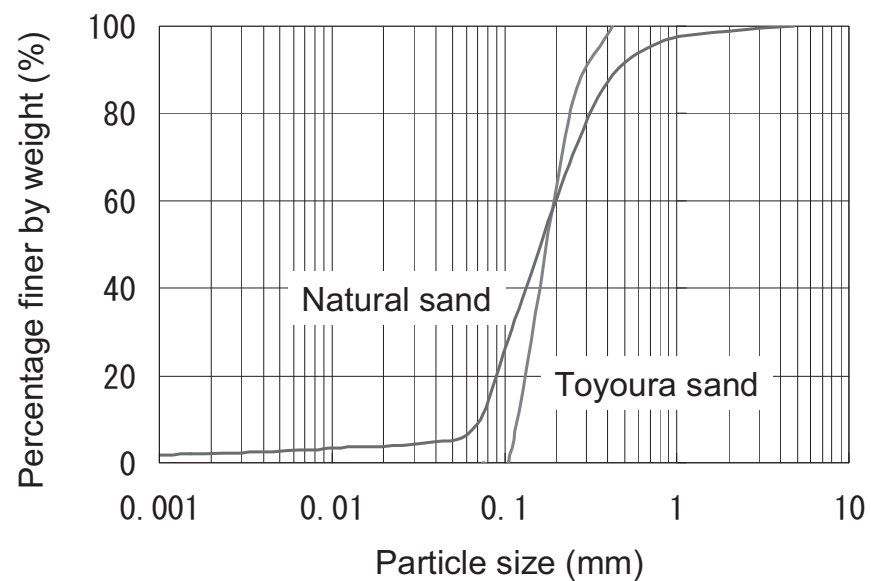


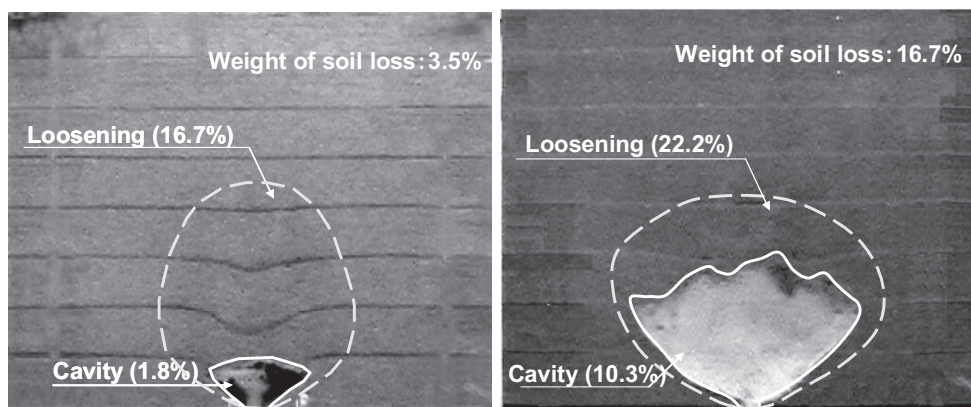
Figure 3: Particle size distribution of tested materials

For the preparation of model ground, soil was placed into the chamber and compacted to relative density of 80% by eight layers. At each layer, colored soil was placed in order to observe the deformation of ground. A load equivalent to an overburden of 80cm was applied on the surface of model ground. Water of approximately 100cc was supplied into the opening with 1m head difference. After pausing 1 minute, the drainage valve was opened to let water and soil flow out. This cycle of water supply/drainage was repeated until the cavity or loosening reached the ground surface.

At each cycle of water supply/drainage, a photograph was taken to observe a cavity and deformation of the model ground. The weight of soil flown out of the opening was also measured.

3. CAVITY AND SURROUNDING LOOSENING

Typical form of cavity and surrounding loosening created in the model ground is shown in Figure 4. A cavity of fan-like shape, having slope at both sides and arching ceiling, was generated above the opening. Area of loosening was evaluated by the ground deformation which was visible by colored sand layers.



(a) Toyoura sand after 3 cycles (b) Natural sand after 13 cycles

Figure 4: Cavity and loosening formed in the model ground

Loosening was developed above and around the cavity in a different manner in Toyoura sand and natural sand. Loosening in Toyoura sand developed largely and rapidly above the cavity compared to that in natural sand.

4. EVALUATION OF LOOSENING

In order to evaluate a cavity and loosening developed in the ground, some indices were proposed as shown in Table 2. Referring to Figure 4a, weight of soil flown out from the chamber up to cycle 3 was 3.5% of initial total weight of soil. On the other hand, cavity area identified by the observation was 1.8% of total soil area. The difference of those, that is 1.7% soil, can be thought to come from estimated loosening area, assuming that the deformation developed in the plain strain condition. Thus, decrease in dry density in estimated loosening area, which is defined to be degree of looseness, can be evaluated to be 11%. Degree of looseness for natural sand was estimated in the same manner, to be 54%.

It can be said that the cavity generated in Toyoura sand accompanies large area of loosening (Ratio of loosening and cavity = 8.3) although the degree of loosening is relatively small (11%), while loosening in natural sand loses nearly half amount of soil (54%) but the loosening area is limited (Ratio of loosening and cavity = 1.2).

Table 2: Indices for evaluation of cavity and loosening in soil

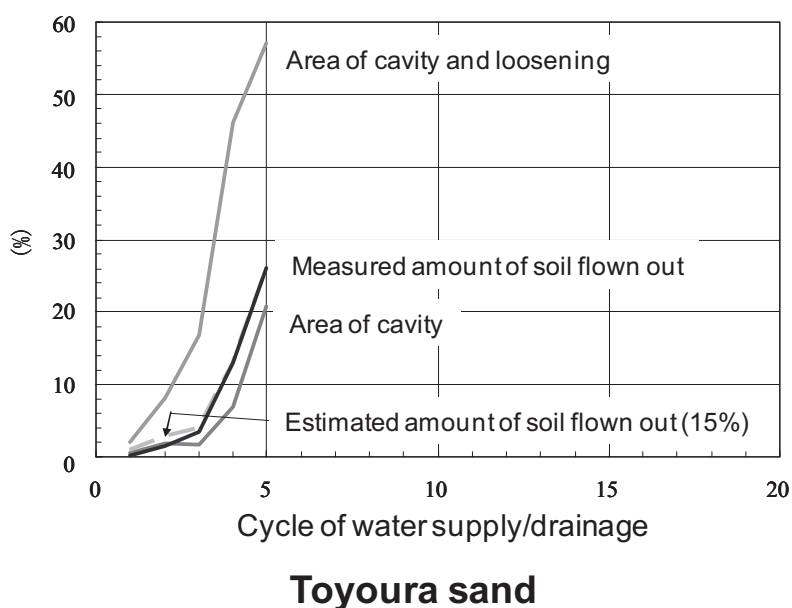
| Index | Definition and description | Value for figure 4 | |
|---------------------------------|---|--|--|
| | | (a) Toyouura sand after 3 cycles | (b) Natural sand after 13 cycles |
| Ratio of soil loss | Dry weight ratio of lost soil in total soil | 3.5% | 16.7% |
| Area of cavity | Ratio of cavity area in total soil area | 1.8% | 10.3% |
| Area of estimated loosening and | Ratio of estimated loosening and cavity area in total soil area | 16.7% | 22.2% |

| Index | Definition and description | Value for figure 4 | |
|-------------------------------|---|---------------------------------------|--|
| | | (a) Toyoura sand after 3 cycles | (b) Natural sand after 13 cycles |
| cavity | | | |
| Area of estimated loosening | Ratio of estimated loosening area in total soil area excluding visible cavity area | 14.9% | 11.9% |
| Ratio of loosening and cavity | Degree of loosening area extension in comparison to cavity area (Area of estimated loosening/ Area of cavity) | 8.3 | 1.2 |
| Degree of looseness | Decrease in dry density in estimated loosening ((Ratio of soil loss – Area of cavity)/Area of estimated loosening) | 11% | 54% |

*Total soil area is 25cm wide, 5cm long and 20cm high

Area of cavity, loosening, and ratio of soil loss are plotted against cycle of water supply/drainage in Figure 5. Cavity and loosening developed rapidly with cycles in Toyoura sand and the loosening reached the ground surface after the 5th cycle. Rate of loosening/cavity development is moderate in natural sand, which sustained until the 13th cycle.

When the degree of loosening is assumed to be 15% for Toyoura sand and 50% for natural sand, ratio of soil loss can be estimated and are plotted in Figure 5 in broken line. It almost matches well to the measured weight of soil loss for all the cycles. The degree of loosening appeared to be consistent in the whole process of cavity and loosening development and to be dependent on soil properties.



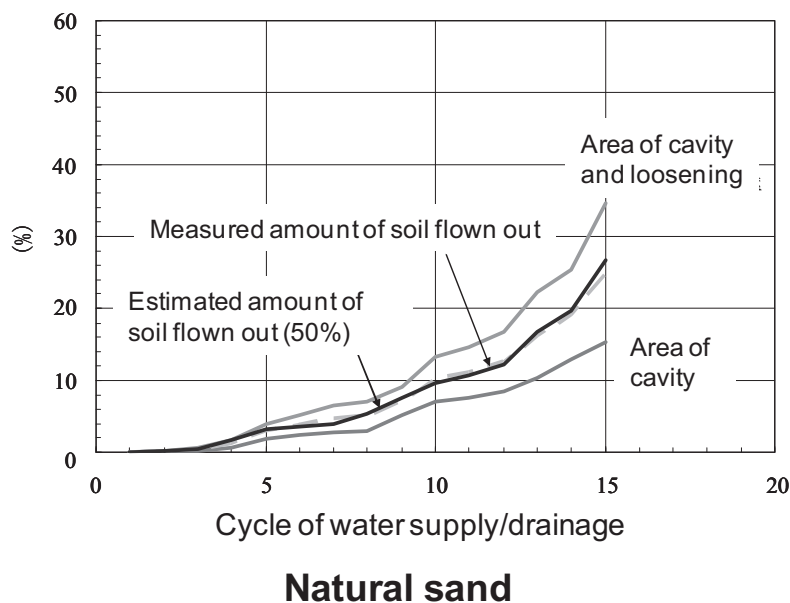


Figure 5: Process of cavity/loosening formation

5. SUMMARY

It was found in the cave-in's survey (Kuwano et al., 2006) that small gap/crack of pipes may cause cave-in's in the road and heavy rainfall was one of the most important factors. Following these facts, a series of model tests was performed, observing outflow of soil through 5mm opening in the bottom of a soil chamber.

It was found in the model tests that cavity and surrounding loosening part in the poorly graded sand can rapidly expand. The loose area transmits vertically rather than horizontally, until it eventually reaches the ground surface. Formation of cavity and loosening can be quantitatively evaluated by the proposed indices. The degree of loosening appeared to be consistent in the whole process of cavity and loosening development and to be dependent on soil properties.

REFERENCES

- Kuwano, R., Yamauchi, K., Horii, T. and Kohashi, H. 2006. *Defects of sewer pipes causing cave-in's in the road*, Proc. of 6th International Symposium on New Technologies for Urban Safety of Mega Cities in Asia, Phuket, November 2006.
- Kuwano, R., Horii, T. and Kohashi, H., 2006. *Evaluation of loose ground surrounding a cavity due to the outflow of soil*, Proc. of 41th annual conference, Japanese Geotechnical Society, Kagoshima, 1785-1786 (in Japanese).

A STUDY ON ESTIMATION OF CROWN PROJECTION AREA FOR WIND PRESSURE ANALYSIS USING LIDAR DATA

TAKAHIRO ENDO, HITOSHI TAGUCHI,
P.J. BARUAH and HARUO SAWADA

International Center for Urban Safety Engineering (ICUS),
Institute of Industrial Science (IIS), the University of Tokyo, Japan
tendo@iis.u-tokyo.ac.jp

ABSTRACT

In order to estimate specific wind pressure of actual forest, an estimation method of tree crown projection area against arbitrary wind direction using LiDAR data is proposed. The method which we propose consists of four procedures: 1) searching of geographical top position of a tree crown, 2) segmentation of point cloud for each tree crown, 3) fitting of 3D approximate curve model to the segmented point cloud, and 4) estimation of crown projection area where arbitrary wind directly hits. Using the methodology tree crown projection area by using LiDAR data could be estimated. The sunny crown length in the edge of forest was longer than that of trees inside forest. Moreover, its projection area against south east direction was largest. For trees standing in the edge of the forests, forest management practices in Japan, recommends a unique crown shape having longer length in southeast side in order to prevent strong wind into the forest. The results of this study corresponded to this recommendations. This research indicates that LiDAR data might be able to estimate actual tree crown projection area against arbitrary wind direction. Additionally, the results indicate that LiDAR measurements not only provides direct measurements of geographical position, but also that of physical parameters.

1. INTRODUCTION

A forest sometimes suffers destructive damage for sudden storm or typhoon (Shidei, 1987). IPCC Fourth Assessment Report points out that climate change is going on. Therefore, in Japan, intensity of storm or typhoon may become stronger and frequency of occurrence of them may increase in the future (MLIT, 2007). On the other hand, mountain area and a steep range of hills form 70 percent of the countries in Japan. Recently, in the upriver district forest needing silviculture is increasing (MLIT, 2007). The reason why frequency of occurrence of fallen trees by strong wind in upriver district becomes high is clear (MLIT, 2007).

In order to reduce the damage of the forest, the important matter is to control the growth of each tree based on its location. In other words, trees

which stand in the edge of forest have to be of unique shape to act as windbreakers to prevent the strong wind invading the inside forest. On the other hand, trees which stand inside the forest sometimes have to be thinned to get suitable height, DBH and crown shape. So, trees inside the forest or in the edge of forest have to be managed for getting suitable crown shapes respectively. Crown shape is a key parameter to find growth condition and wind-resistance. However, to measure actual tree crown shape has been difficult since its shape often can not be measured at the ground in spite of being an important growth indicator.

Previous researches applied equation (1) to independent trees such as road side trees. In this research, crown projection area was calculated by crown width and crown length (Shindei, 1987; Ishikawa, 2005). The reason why this research used crown width and length as crown projection area against wind direction was clear. It was difficult to measure actual crown projection area against wind direction.

$$W=1/2C_D\rho v^2S \quad (1)$$

$$S=lw$$

where W is Wind pressure (kg.s/m^2), C_D is coefficient of resistance of crown, ρ is air density (kg/m^3), v is wind velocity (m/s), S is crown projection area (m^2), l is crown length (m), w is crown width (m)

If an actual tree crown in forest can be measured, risk of trees which are likely to fall by wind pressure may be estimated by equation (1) and suitable silvicultural method can be proposed.

In this context, airborne LiDAR can be of great use. LiDAR technology, one of remote sensing technologies, can directly measure spatial position of target. LiDAR can measure geographical position of target as point cloud by using laser beam, DGPS and IMU. Thus, tree crown can be measured as point cloud by LiDAR.

This study aims to develop an estimation method of tree crown projection area for wind pressure analysis using LiDAR data.

2. MATERIALS

2.1 Field data

Test area is a plantation forest managed by Mitsubishi Paper Mills Co., Ltd. The site is located in the northern part of Honshu Island, Japan (lat. $40^{\circ}39'$ N, long. $141^{\circ}5'$ E). The ground elevation is between 190-240m above sea level. The dominant tree species are Japanese cedar (*Cryptomeria japonica*) and Japanese red pine (*Pinus densiflora*). Mixing rate of cedar and pine in the area is about 75.4% and 24.6% respectively according to field sampling. Thus, the forest is a cedar plantation with randomly mixed pine trees. Southeast edge of this area faces the flat ground. So, southeast wind directly hits this area.

A field survey was conducted in the first week of August 2004. Precise geographic position of every tree top was measured using a GPS (DL4, NovAtel inc.) and a beacon receiver (MBX-3S, CSI Wireless) for

differential GPS positioning. Height of individual trees was acquired with a portable laser measurement device (LaserAe300, MDL). DBH and tree species for all trees were recorded.

2.2 LiDAR data

LiDAR data for the test area was acquired under relatively clear skies. LiDAR data was acquired on 11th and 12th August, 2004 using an airborne laser scanner at a cruising speed of 110 kt and at a height of 1830 meters. Scan rate, pulse rate and scanning width were 39.0 Hz, 46.0 kHz, and 647 meters respectively. Average footprint size was 0.47 meters. The scanner was ALS50, a product of Leica Geosystems, that has horizontal accuracy and vertical accuracy of + 30 cm and + 15 cm respectively. The average density of laser reflection was 14.65 pulses per square meters.

3. METHODOLOGY

3.1 Preprocessing

Digital Elevation Model (DEM) with a mesh size of 1m was created from whole point cloud derived from LiDAR measurement. Digital Canopy Model (DCM) was created by the subtraction of DEM from point cloud. Triangulated irregular network (TIN) was created from DCM for searching geographical top position of tree crown.

3.2 Searching of geographical highest position of a tree crown

The height of arbitrary point and the averaged height of neighborhood points were calculated by using TIN. In this study, neighborhood points were vertices of 3rd triangle since area of 3rd triangle corresponded to size of small tree crowns. If the height of arbitrary point was higher than that of neighborhood points, the arbitrary point was made a candidate point of geographical top position of tree crown. The candidate points were merged by a clustering method which clustered points within 1.2m to a single point. In our site, 1.2m was minimum distance between tree crowns. The merged points became the estimated geographical top position of tree crown.

3.3 Segmentation of each crown area

In order to segment whole point cloud to each tree crown, a constraint-rule was proposed. The rule was that a boundary between adjacent tree crowns might exist between geographical top positions of adjacent crowns and a point with the lowest height might be on boundary. A point with the lowest height was searched on a segment between geographical top positions by using the rule. As a result, there existed several points with the lowest height around a geographical top position. A polygon including a geographical top position was created by the neighborhood points with the lowest height. Point cloud in the polygon was

searched and specific point cloud in each polygon was segmented as point cloud of specific tree crown.

3.4 Fitting of 3D approximate curve model

The point cloud was fitted by the 3D approximated curve model. The methodology adopted was according to Endo et al. (2007). Each 3D crown shape was reconstructed by the specific geographic top position and point cloud.

3.5 Estimation of crown projection area

The specific tree crown projection area was calculated by the estimated 3D crown shape and arbitrary wind direction. In order to estimate the area hit directly by wind, the estimated crown projection area was recalculated based on the geographical location of specific tree and neighborhood trees. The recalculated crown projection area became the specific crown projection area against arbitrary wind direction. In this study, crown projection area against east wind, southeast wind, and south wind was simulated. Generally, it is said that a southeast wind by typhoon is strong.

4. RESULTS AND DISCUSSION

4.1 Accuracy of estimation of geographical top position of tree

Number of trees and its geographical top position were compared with the field data (Figure 1). Number of trees with its correct position was 90 trees per 117 trees (76.9%). 27 trees were not detected. A total of 11 trees corresponding to wrong geographical top position were detected. The results of investigation of DCM around un-detected trees, those trees were not independent trees and were merged with neighborhood tree. So, we considered that un-detected trees were hidden by a neighborhood tree with large crown. On the other hand, we considered that the segmentation procedure in our methodology did not exactly detect actual top geographical position of the trees. In case of searching of a geographical top position of the crown with large width and irregular shape, (for example, the crown may consist of several tree crowns), the crown had several candidate points which spread around a geographical top position. Several geographical top positions might be detected in spite of one geographical top position since the clustering method used the fixed threshold distance. We considered that the clustering method has to be modified to improve accuracy of geographical top position.

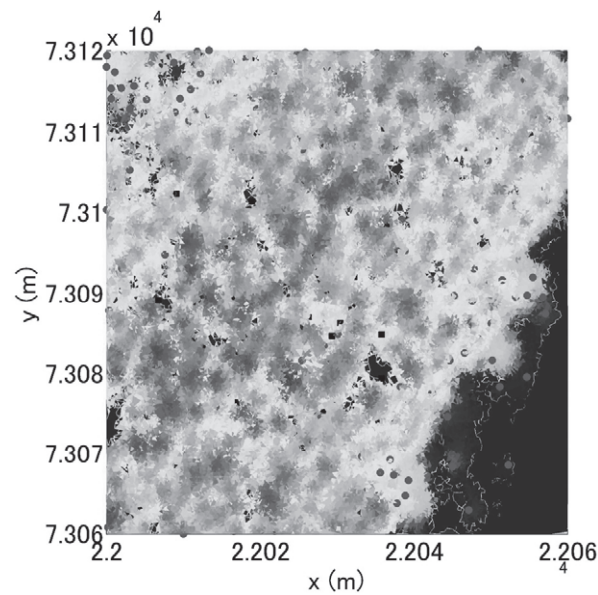


Figure 1: Comparison between the estimated number of trees & geographical top position, and field data. Gray circle stands for the estimated geographical top position. Black square stands for the measured geographical top position.

4.2 Evaluation of each crown area

Figure 2 shows the segmented tree crown with point cloud. Almost all crown areas were segmented well. However, the segmented crown areas were smaller than actual crown areas. As a result of detailed analysis, in case of one large crown with nearby two small crowns, a boundary between two small crowns did not exist between their geographical top positions. Therefore, boundary detecting method has to be improved.

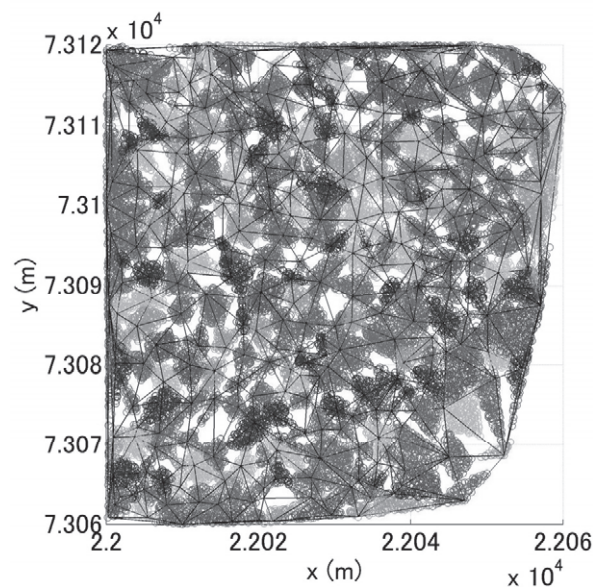


Figure 2: The result of the segmented tree crowns with point cloud.

4.3 Accuracy of 3D approximate curve fitting

The calculated 3D crown shapes are shown in figure 3. The averaged correlation coefficient between the point cloud and the approximated 3D curves was 0.58. The standard deviation was 1.5m. But in case of fitting independence trees, the averaged correlation coefficient became 0.78. The sunny crown length in the edge of forest was longer than that of trees inside forest. This result corresponded to actual crown shape. We found that these trees could prevent the strong wind invading the forest from southeast direction.

From the results of these, we consider that the approximation was successful. The reasons for low value for averaged correlation coefficient were probably due to lower accuracies of detecting geographical top positions and in segmenting crown area. We considered that if accuracies of these procedures are improved, the correlation coefficient becomes higher.

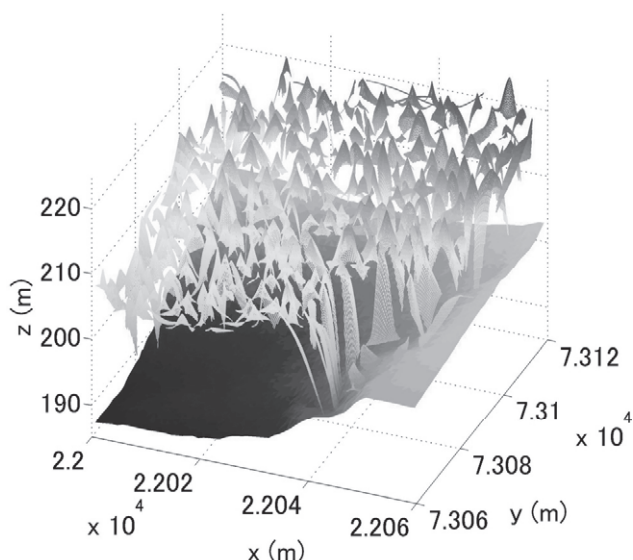


Figure 3: The calculated 3D tree crowns on DEM.

4.4 Crown projection area against three wind direction

In order to analyze relationship between the estimated crown shape and three wind directions, we chose area from the edge of forest (figure 4). Figure 4 shows 3D crown shapes and crown projection area against southeast wind as a sample of results. The relationship between crown projection area and wind direction is shown as figure 5.

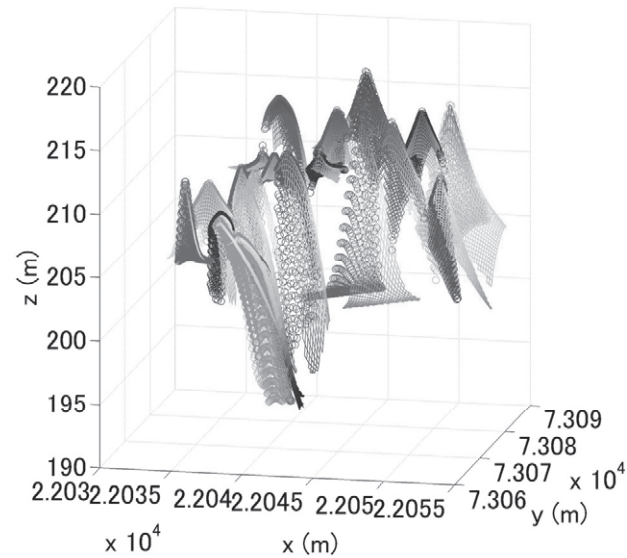


Figure 4: The 3D crown shapes at the edge of the forest, and the result of the simulated crown projection areas against the southeast wind direction.

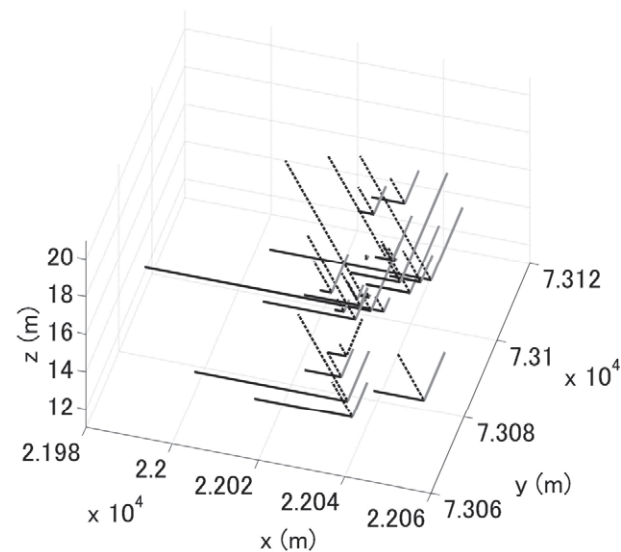


Figure 5: The result of crown projection areas against east, southeast and south wind direction. Black solid line, gray solid line and black dot line represents crown projection area against east, southeast and south wind direction, respectively.

Specific vectors in figure 5 indicate origin point corresponding to a geographical top position, a direction corresponding to a wind direction and a length corresponding to a crown projection area. Each crown projection area against different wind direction was different since its crown shape was different. We compared summation of each crown projection area against three wind directions in this area. Crown projection areas against south, southeast and east wind were 202.25 m^2 , 294.75 m^2 and 265.75 m^2 ,

respectively. Almost all trees in this area had long crown to southeast side. In general, trees in the edge of forest have to serve as windbreakers (Hokkaido Forestry Research Institute, 2006). For effective wind breaking, the crown shape has to possess long crowns towards the open exterior space facing the wind. In our case, exterior space was at the southeast side. These crown shapes and crown projection areas corresponded to the trees with the standard shape recommended by the general treatment method for forestry. We considered that the simulated crown projection area derived from our method was reasonably correct.

5. CONCLUSION

This research proposed the new estimation method of crown projection area against arbitrary wind direction using LiDAR data in order to evaluate wind pressure of the forest. The proposed method consisted of four steps: 1) searching of geographical highest position of tree crown, 2) segmentation of point cloud of tree crown, 3) fitting of 3D approximate curve model to a point cloud, and 4) estimation of a crown projection area which wind hits directly. Since the proposed method is preliminary research, it still needs some improvement. However, the method could estimate actual crown projection area which has been difficult to calculate until now. The results of this study indicate that LiDAR data may become useful tool to evaluate risk of trees which are likely to fall by wind pressure. Additionally, the results indicate that LiDAR measurement not only provide measurements of geographical position, but also that of physical parameters.

ACKNOWLEDGEMENT

I would like to express my gratitude to the MITSUBISHI PAPER MILLS LIMITED which provided us test sites. Furthermore, I would like to thank the Kokusai Kogyo Co., Ltd. which supported data collection.

REFERENCES

- Endo T., Taguchi, H., and Yasuoka, Y., 2007, Development of classification method of road side trees by aerial laser scanner data. *Proceeding of JSPRS*, Nagaoka, Japan, 151-152.
- Ishikawa, H., 2005. Experimental Study on Flow Characteristics of Trees. *Nagare* 24, 483-490.
- Shidei, T., 1987. Forest protection science. *Asakura Publishing Co., Ltd.* Tokyo.
- The Hokkaido Forestry Research Institute;
<http://www.hfri.pref.hokkaido.jp/03kikaku/fuugai/t18higai.pdf>
- The Ministry of Land, Infrastructure, Transport and Tourism;
http://www.mlit.go.jp/kisha/kisha07/05/051129_2_.html

GREEN BUILDINGS: CURRENT STATUS AND PROSPECTS

PRANAB J. BARUAH¹, AKIMASA SUMI¹ and TAKAHIRO ENDO²

¹Integrated Research System for Sustainability Science (IR3S)
The University of Tokyo, 7-3-1 Hongo, Bunkyo-ku, Tokyo 113 8654 Japan
²Institute of Industrial Science (IIS), The University of Tokyo
pjbaruah@ir3s.u-tokyo.ac.jp

ABSTRACT

With global warming becoming mainstream policy issue for governments and businesses alike due to increasing public awareness about environment, buildings are coming under focus for their large carbon emission and use of humongous amount of energy, water and material both during construction and utilization phase. “Greening” of real-estate, which started a decade earlier in several developed countries, is gaining momentum and moving into new frontiers as developed countries are acting towards low-carbon economy and emerging economies are urbanizing rapidly amid sustainability concerns. In this paper, we review current trends in embracing green buildings and how different factors, such as, green-building rating-systems worldwide are shaping the movement in various countries. Based on findings from other studies, we discuss how higher energy costs, greater environmental concern and innovations in technologies (such as in IT) will give positive dynamics to green building market for achieving lesser environmental impact.

1. INTRODUCTION

According to 4th Assessment Report of IPCC (IPCC, 2007), it is ‘very likely’(>90% likelihood) that global warming of about 0.6^oC over the past century is due to anthropogenic increase of green house gases (GHG), mainly CO₂. Since 1970 to 2004, commercial and residential buildings constitute about 8% of the total anthropogenic GHG emissions in CO₂ equivalent (IPCC, 2007). Considering the energy, water and other resources consumed during construction and utilization of the buildings in their entire lifespan, built environment is responsible for about 40% of CO₂ emission, 30% of solid waste generation and about 20% of water effluents. In terms of resources used, about 40% of energy, 20% of water and 10% of land-area are used by the building and construction sector (UNEP-SBCI, 2006). This makes it a key sector and a “key factor for sustainable development” with its immense benefits to the society and at the same time associated negative impacts without appropriate attention (UNEP-SBCI, 2006). Additionally, as numerous studies have found, indoor air quality and energy efficiency in buildings are key factors of health of the inhabitants. Now, with increasing public awareness about environment as a result of globalization and internet, governments and businesses alike are putting increasing focus on the real-estate sector to reduce CO₂ emission for mitigation of climate change. The sector is becoming important from another dimension in

context of successful mitigation of climate change and sustainability - the future of the world is urban, with about 60% of human population (~5 billion) projected to live in cities by 2030 from 50% (~3.2 billion) in 2005 (Deutsche Bank Research, 2008), and mostly in developing countries. Also, “greening” of building sector for green buildings is gaining momentum particularly from the fact that, it presents with several “long hanging fruit” solutions to reduce GHG emissions and increase energy efficiency with minimal or sometimes negative costs.

This review paper discusses the essentials of a green building, green building rating systems around the world, key factors effecting its development along with current and future trends of green building market. Based on currently available studies, a qualitative outlook of the future of green buildings in emerging economies is also presented.

2. WHAT IS GREEN BUILDING

Although the terms “sustainable building” and “green building” are often used interchangeably in activities such as advertisements and speeches, they are fundamentally different. This shows the poor understanding of the concept of sustainability among different stakeholders and highlights the fact how some entities in society are using these terms for “green washing” to profit from increased public interest in environmental issues.

Based on the UN Bruntland Commission Report, which popularized and defined the concept of sustainable development as “*..the development which meets the need of the present without compromising the ability of the future generations to meet their own needs*”, a sustainable building can be defined as the “*...one that can be produced and continue to be produced over the long term without adversely affecting the natural environment necessary to support human activities in the future*”. On the other hand, green building can be stated as the “*..one that uses energy and material more effectively both in production and operation while polluting and damaging natural systems as little as possible*”. (Straube, 2006). Therefore, while a sustainable building has no net impact in environment and co-exists with world’s ecological balance indefinitely, a green building “*focuses on incremental steps to solve known and measurable problems with our current practice*”(Building Science, 2008).

Based on present environmental & sustainability concerns, available technology and knowledge of linkages between different systems on earth (i.e. social, economical, environmental), green building is a step towards a sustainable society by being significantly better than similar, or average, building of same size and type in the same location by reducing the overall impact of the built environment on human health and the natural environment in following areas:

- Landuse
- Material and Resources Efficiency
- Design and Delivery Process
- Social Transformation
- ♦ Water Resources Management
- ♦ Community Development
- ♦ Energy Efficiency
- ♦ Global Ecological Impact
- ♦ Durability
- ♦ Indoor environmental Quality
- ♦ Affordability
- ♦ Transport

3. GREEN BUILDING MOVEMENT

Brief History

Several ancient societies practiced principles of geomancy which has similar attributes to present green buildings. The Chinese used *Fengshui*, which comprises of broad spectrum of theories regarding selection of a location, layout of buildings etc. Indian geomancy principles in *Vastu Shastra* laid out criteria for layout and planning of buildings to influence the peace and prosperity of its inhabitants. Both of these guidelines use principles of astronomy, and incorporate energy and environment in their practices. Ancient Greeks used passive solar heating techniques to build entire cities to receive solar heat in winter (US-EPA, 2008).

Although green building features described above has been incorporated collectively or in isolation through centuries in various parts of the world, modern green building movement started in western developed economies around 1970s out of interests in improving energy efficiency due to oil crisis and environmental movements. In 1990s, the movement gained momentum with the UN Earth Summit, Rio de Janeiro in 1992 passing Agenda 21 for sustainable development, release of UK's and world's first building environment assessment system BREEAM in 1990, US Department of Energy's Energy Star Program in 1992 and formation of US Green Building Council (USGBC) in 1993. Recent years have seen sudden upsurge in interest among buyers, developers, builders and governments across the world (including emerging economies) to build green buildings voluntarily or through mandated programs.

Present status

With global warming becoming a central issue for businesses and governments in recent years, green building movement is gaining momentum in developed economies, notably in USA, EU, and Japan.

According to Martin et al. (2007), green building movement in USA is nearing a tipping point with tremendous growth seen in non-residential market. In 2004, non-residential market accounted for about 2% of the US market (about \$ 3.3 billion), which is growing and forecasted to be about \$10-20 billion in 2010. McGraw-Hill Construction suggests residential green building market to grow to \$19 to \$38 billion by 2010 from \$7.2 billion in 2005. Without any market measure on green building development, growth in certified buildings by building certification systems are quoted often in reports. The report said that, value of newly constructed registered buildings by USGBC's LEED certification system has grown from \$792 million to \$10 billion in 2006. Another summary from USGBC (Green Buildings, 2008), states the annual market for green building in products and services to be \$12 billion. Number of certified homes by US-EPA Energy Star are increasing at rapid rate and value of such homes stands at \$26 billion in 2005. In early 2008, National Association of Home Builders (NAHB) has launched the voluntary NAHB National Green Building Program, which is seen to compete aggressively with LEED rating system.

Though USA does not have national green building policies with mandates, several states are adopting mandates for greener buildings. Notable among them are state of California and Washington D.C. From beginning of 2009, California non-residential buildings would require energy-use reporting, and from beginning of 2010 commercial buildings would have to report on their energy-

use and Energy-Star certification status to potential buyers and leasers (Building Green, Sep.16, 2008). Washington D.C. will require the city buildings to benchmarked annually starting in 2009 with annual benchmarking for private buildings to be done between 2010 and 2013 (Building Green, Sep.1, 2008).

In EU, the Energy Performance of Buildings Directive (EPBD), based on 1993 'SAVE' Directive on energy efficiency, came into effect in January 2006. EPBD provides a common methodology for calculating energy performance and setting energy performance standards of buildings (in both new and existing) in individual member states. It is estimated that, with proper implementation of EPBD, 11% reduction in oil consumption can be achieved in 2020 (EurActive, Sep 15, 2008). However, progress is reported to be slow with only Denmark, Germany and Austria fully complying with the EPBD and other states lagging behind (EurActive, Apr 26, 2008). In EU-wide effort for greener buildings, Germany proposed mandatory energy efficiency labeling for buildings and apartments in April, 2007 (Reuter, Apr 20, 2007). At present, UK does not have a single plan of action on green building. However, variety of policies, regulations, performance standards, guidance documents and voluntary initiatives by numerous organizations are available. UK Building Research Establishment (BRE)'s voluntary rating system BREEAM and USGBC's LEED are increasingly being embraced by businesses.

In Japan, energy efficiency has been a core national policy due to its lack of natural resources and as a strategy for energy security since the oil shock of 1970s. Surprisingly, there is no government policy to promote efficiency exclusively in the building sector where about 25% of total energy is used for space heating and cooling of buildings. Energy consumption in commercial buildings in Japan is about 8% of world energy consumption in such places (European Business Council Japan, Jul 2008). However, under Energy Conservation Law, 1979 (amended 1999), voluntary energy saving labeling programs for home appliances exist and mandatory reporting of energy conservation measures in buildings over 2000 m² floor space were introduced in 2003 and tightened in April 2006. Statistics shows that compliance rate is increasing, from 34 % in 1999 to 74% in commercial buildings, and is likely to increase in future (Hong et al., 2007). In 2004, Japan Sustainable Building Consortium (JSBC) introduced the voluntary CASBEE green building rating system to assess the environmental efficiency of buildings, popularity of which is increasing among government and industry as well as in other Asian countries.

Elsewhere in developing economies, China and India, two emerging giants are slowly but seriously adopting green buildings as their population rapidly urbanize and real-estate sector is growing at a blazing speed. Currently, China's buildings consume about 18% of total energy and projected to reach 40% by 2030 when the urban population reaches 1 billion (Howard et al., 2007). China's Ministry of Construction (MOC) has unveiled "Evaluation Standard for Green Building", which took effect on June 1, 2006 and is similar to USGBC's LEED rating system. Rating systems such as LEED and CASBEE are being increasingly adopted for upcoming projects. For a greener Summer Olympics 2008, China used Tsinghua University's Green Olympic Building Assessment System (GOBAS), which is based on CASBEE.

In India, building energy consumes about 33% of total energy in 2005. Integrate Energy Policy unveiled in 2006 identifies 10 key areas for efficiency improvement, half of which relate to building sector. For Investments above

\$11.6 million, developers need clearances from government before construction in terms of environmental impact assessment. There is no national mandatory green building related program. Recently, there is growing interest in USGBC-LEED rating system promoted by Indian Green Building Council (IGBC). Bureau of Energy Efficiency (BEE) is working on to mandate energy audit of buildings and Ministry of New and Renewable Energy Sources (MNRE) is planning to develop a voluntary green building rating system with an incentive mechanism (Hong et al., 2007).

Factors driving green building movement

Nelson (2007) and Martin et al (2007) cite several factors driving investments in and demand of green buildings in US. However, most of these factors are also working in other parts of the world in varying mix and degrees. According to Martin et al. (2007), several studies have found that, a particular class of tenants are interested and creating demand of green buildings at present. They are referred as *LOHAS customers*, *Creatives* or *True Blue Greens* who are well-educated & wealthier than average, and well-aware of key environmental issues such as climate change.

Next, governments are playing increasingly active role due to realization of the benefits of pursuing green building programs in context of rising energy prices and tackling mitigation of climate change through minimal costs. They are moving forward by formalizing new regulations, raising awareness and through tenancy by setting standards for building it sets for its own occupancy. In countries like China, where government has a strong influencing power on businesses by virtue of the political system will possibly be the biggest driver in setting the movement in the right and faster path.

Third, due to increasing environmental awareness among general public, companies are responding by taking environmental action and being “green”. Moving to green facilities is providing them with greater credibility on their greening commitment to stay ahead of the pack. At the same time, builders and developers are realizing this necessity to green-up to prove their socially responsible character and at the same time retain competitive advantage by moving before being pushed by governments through new regulations. Investors are realizing that “future of building is green” and finding a new socially responsible investing (SRI) opportunity in a lucrative sector. With recent worldwide downturn in conventional real-estate market, green buildings are also getting new investors due to their positive returns and increasing market.

Last but not the least, professional and international organizations like USBGC and UNEP-SBCI are playing an active role by creating awareness of the opportunities, serving necessary professional information, creating quantitative assessment systems and presenting the movement with a business case. Especially, the green building assessment systems are paving ways for both public and corporate policymaking. Also, they are motivating innovation across builders as well as suppliers of materials and by providing summaries of building performance which are helping to create demand through awareness (Cole et al., 2005)

4. GREEN BUILDING ASSESSMENT SYSTEMS

Green building assessment systems provide effective framework for assessment of building environmental performance quantitatively to be presented in terms of indicators which are easy to understand. It can integrate the complex concept of sustainable development effectively into building and construction process. Conventionally, buildings are designed to meet building code requirements. Green building assessment systems go beyond the code to incorporate various elements concerning sustainability to improve overall building performance and minimize life-cycle environmental impact and cost (Gowri, 2004).

Assessment tools developed till date may be classified into two categories. First category is based on a purely criteria based system assigning point values to a selected number of parameters on a scale. BREEAM (UK), LEED (USA) and Green Stars (Australia) are some examples of this category. Second group of tools are based on life cycle assessment (LCA) methodology employing “cradle to grave” assessment approach to the inputs in order to evaluate (mainly) environmental impacts from key outputs. Example of such tools are BEES (USA), Beat (Denmark), ECO QUANTUM (Netherlands), ECO-PRO (Germany), EQUER(France) etc. (Larsson et al., 2001; Hikmat, 2008). Table 1 lists the major green building assessment systems from different countries/organizations.

Most assessment system’s primary focus is on energy efficiency, resource efficiency, indoor air environment, water resources management and sustainable site selection. Among the rating systems in Table 1, those getting wider recognition worldwide are BREEAM, LEED, CASBEE, GreenStar, and GBTool. We discuss in brief the first four rating systems below.

Table 1: Major green building assessment systems.

| Country | Assessment tool |
|-------------|---|
| UK | <ul style="list-style-type: none"> ◆BRE Environmental Assessment Method (BREEAM) ◆Environmental Estimator (ENVEST) |
| USA | <ul style="list-style-type: none"> ◆USGBC Leadership in Energy and Environmental Design (LEED) ◆NAHB National Green Building Standard ◆US-EPA Energy Star for New Homes ◆DOE Building America ◆Building Environment and Economical Sustainability (BEES) |
| Canada | <ul style="list-style-type: none"> ◆Green Building Tool (GB Tool) ◆Green Globes CEE & EEC ◆LEED-Canada ◆BREEAM-Canada |
| Australia | <ul style="list-style-type: none"> ◆Green Star AGBC ◆National Building Environment Rating Scheme (NABERS) |
| Germany | ◆German Ministry of Transport, Construction, and Urban Development (DGNB) Sustainable Building Certificate |
| Netherlands | <ul style="list-style-type: none"> ◆BREEAM-Netherlands ◆Eco Quantum |
| Japan | ◆JSBC Comprehensive Assessment System for Building Environmental Efficiency (CASBEE) |
| Korea | ◆Korea Green Building Label |
| Singapore | ◆Building and Construction Authority (BCA) Green Mark |
| Hong Kong | ◆Hong Kong Building Environment Assessment Method (HK-BEAM) |

| Country | Assessment tool |
|---------|---|
| China | <ul style="list-style-type: none"> ◆ China Green Building Standard ◆ Green Olympic Building Assessment System (GOBAS) |
| India | <ul style="list-style-type: none"> ◆ LEED-India, 2007 ◆ The Energy and Resources Institute GRIHA (TERI-GRIHA) |
| Brazil | <ul style="list-style-type: none"> ◆ LEED-Brazil ◆ AQUA |

BREEAM is the first green building rating tool in the world, developed by Building Research Establishment (BRE) and private sector researchers of UK in 1990. It is a voluntary assessment system. Recently, a tougher version of the system has been released in 2008, emphasizing more on energy efficiency and requiring mandatory credits. The system is recognized by UK building industry and is being adopted in Canada, Australia, India and EU countries.

USGBC developed the voluntary LEED rating system in 1998 with a market-driven strategy to accelerate adoption of green building practices (Bowri, 2004). It was inspired by BREEAM to serve the building community in US. Originally developed for new commercial buildings (LEED-NC), LEED has gone through major update in 2003 and now several versions, such as, LEED for Homes, LEED for Existing Buildings (EB), LEED for Core and Shell (CS), LEED for Commercial Interiors, LEED for School, Healthcare & Retail and LEED for Neighborhood development. According to USGBC, the system will have a major overhaul in early 2009. In the new version, points will be allocated differently and reweighed, and the entire process will be flexible to adapt to changing technology, account for regional differences and encourage innovation. Over the years, LEED has gained immense popularity around the world with the system being adopted in countries like Canada, UK, Brazil, China, India and Middle-East. Green Building (2008) reported that, nearly 4 billion commercial building space is being registered or certified by LEED rating system with projects in 69 countries and 57,400+ accredited professionals. Figure 1 below gives a comparison between LEED-NC and BREEAM 2008 in credit weightage given to different green building features (Greenworkplace, Aug 11, 2008).

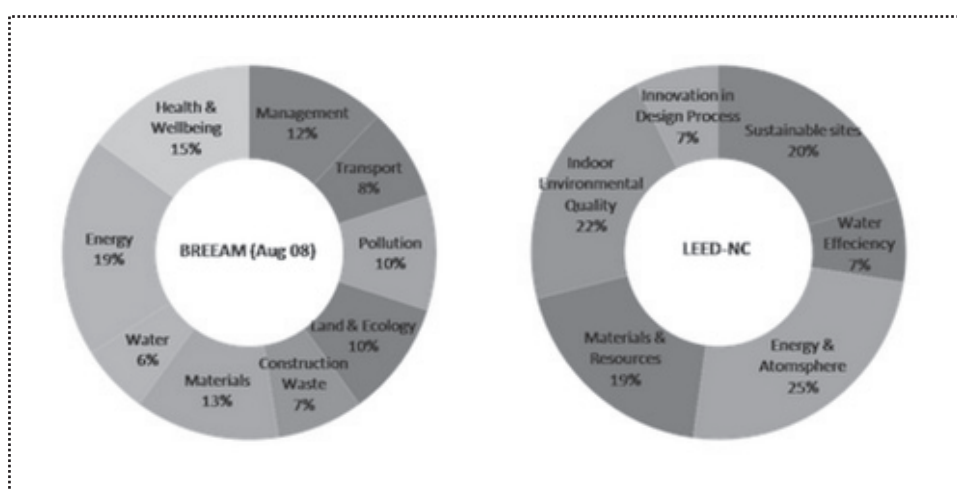


Figure 1: Comparison of LEED-NC and BREEAM 2008 weights (source & copyright: Greenworkplace, Aug 11, 2008)

Japan Green Building Council (JGBC) unveiled the CASBEE rating

system for new construction in 2004. It has four integrated tools on building life-cycle: pre-design tool for owners and planners, design tool for architects and engineers, environmental labeling tool for labeling body and sustainable operation and renovation tool for owners and caretakers. Noteworthy difference with LEED and BREEAM is that it re-categorizes the positive building attributes to a Quality (Q) category and negative attributes as loading (L) category to estimate a Building Environmental Efficiency (BEE) index as Q/L. The concept has gained popularity because it can provide trade-off between environmental loadings and quality of space provided. Based on Q/L value ranking is given to a building's sustainability. Table 2 lists the rating categories available in BREEAM, LEED and CASBEE.

Table 2 : Rating categories in BREEAM, LEED and CASBEE

| BREEAM | LEED | CASBEE |
|-----------|-----------|--------|
| Excellent | Platinum | S |
| Very Good | Gold | A |
| Good | Silver | B+ |
| Pass | Certified | B- |
| | | C |

Despite their positive influence on different stakeholders in the movement, green building assessment tools such as LEED or BREEAM are criticized for their lack of assessment scope post-construction. Critics argue that, these systems award points based on design features pre-construction which may not be constructed properly as designed (such as sealing tightness in windows). Additionally, simulated usage pattern of resources, such as energy or water, during design phase may be drastically different during utilization. Certification not before but after construction, and based on few years of energy & resources utilization data, is often recommended. Others point out the necessity of integrating LCA-based analysis into the systems. Also, caution is advised before using a foreign system in local conditions, as a system developed for a certain country may not produce expected performance when applied in another country due to differences in climatic, economic and cultural conditions. Both LEED and BREEAM are addressing these issues in their latest and coming versions.

5. COSTS AND BENEFITS OF GREEN BUILDINGS

Green buildings are often cited to incur higher cost, which is proved as a misconception by several recent studies. According to Nelson (2007), examination of 33 LEED office and school buildings in 2003 by a consultant firm Capita E Analysis found that, overall cost premium for green buildings to be about 2%, averaging 0.7% for the LEED-certified buildings, 2.1% for the LEED-Silver, 1.8% for the LEED-Gold, and 6.5% for the LEED-Platinum building. The study also found that, cost premiums declined as regional experience in green building increased. Another comprehensive 2005 study by engineering firm Morrison Hersh field reviewed four U.S. studies and estimated construction cost premium required to meet different levels of LEED certification. Their result showed cost premiums averaged only 0.8% for the LEED certified buildings, 3.5% for the LEED-Silver, and 4.5% for the LEED-Gold and jumped to 11.5% for LEED-Platinum buildings. There is increasing

consensus among green building developers that, with careful planning and integrated design of the sustainable concepts, the cost premium can indeed be minimal to non-existent (Nelson, 2007).

The benefits of green building can come from energy and water savings, reduced waste, improved indoor environmental quality, increased comfort/productivity, reduced employee health costs and lower operation and maintenance costs (Kats, 2003). According to USGBC, LEED-certified buildings are 25-30% more energy efficient and more likely to generate renewable energy. Another study by Co Star group in 2008, found that, Energy-star and LEED-certified buildings has higher occupancy rate, higher rental rate and higher sale price per square feet when compared with conventional buildings. For existing buildings, studies have found that payback period for various green retro-fitting should be between 3 to 6 years (Nelson, 2007).

6. FUTURE DIRECTIONS

All trends clearly show that, green building movement worldwide is picking up momentum. Start of various green building programs in key future growth countries such as China, planning of mandated green building program in India, release of newer version of BREEAM system and the coming version of LEED in 2009 are fewer examples to indicate tremendous growth ahead for green buildings as an industry. Many have said year 2007 to be the tipping point for green building construction. By aggressive estimates, annual LEED-NC and CS combined is expected to reach about 200 million square foot from about 30 million square foot in 2006 (Nelson, 2007). Launching of UNEP-SBCI in 2006 and United Nation Framework Convention on Climate Change (UNFCCC)'s decision to prioritize building sector in coming Conference of Parties (COP)-14 in December 2008 in Poland will also accelerate awareness about greener building among different stakeholders. Additionally, increasing emphasis on localized renewable energy generation and current rapid growth of other clean-tech sectors are likely to give boost to the sector. Deployment of innovative, cheap and energy efficient technologies such as Light Emitting Diode (LED) providing clean bright light will likely give great impetus to the movement and will be key to bring the movement successfully to lower income countries. Last but not the least, with proper planning and active participation of relevant stakeholders, potential-laden Information and Communication Technology (ICT) sector can provide added efficiency by its "enabling effect". The recent SMART2020 (2008) report has shown that, through deployment of proper ICT, buildings can significantly save energy consumption and reduce GHG emission to an extent of 15% in 2020. To achieve this potential, the report outlined measures such as, intelligent lighting and HVAC (Heating, Ventilation, Air-conditioning), voltage optimization, installation of ICT-based BMS (Building Management System) and smart grids.

7. CONCLUSION

With importance in immediate action for climate change mitigation, depleting natural resources and increasing energy cost, green buildings are poised to be the

future of building and construction industry. Green buildings are right step towards sustainable low carbon society providing added benefits of health and comfort and achieved at minimal or negative costs to the users. Assessment systems for green building are proving to be useful framework to achieve the intended goals while presenting it with a business case. Coming years are likely to see explosive growth in green building investment across the world with more government mandates and increasing public interest. In coming years, innovative and cost-effective technologies as well as incorporation of existing technologies in smart ways will be the key to increase the energy efficiency and GHG reduction potential of green buildings.

REFERENCES

- Building Green, Sep.1, 2008. *D.C. Requires Building Owners to Report Energy Use*. <http://www.buildinggreen.com/auth/article.cfm/2008/8/28/D-C-Requires-Building-O> captured Sep 19, 2008.
- Building Green, Sep 16, 2008. *Energy Use Reporting Mandated in California*. <http://www.buildinggreen.com/auth/article.cfm/2008/9/16/Energy-Use-Reporting-Ma> captured Sep 19, 2008
- Building Science, 2008. *Towards Sustainability: Green Buildings, Sustainability Objectives. And Building America Whole House Systems Research, Research Report-0801*. Building Science Corporation.
- Cole, R.J., Howard, N., Ikaga, T., and Nibel S., 2005. *Building environmental assessment tools: current and future roles, Unit 4/5*. World Sustainable Building Conference, September 2005, Tokyo.
- Deutsche Bank Research, 2008. *Megacities: Boundless Growth ?*. Editor: Josef Auer, Deutsche Bank Research.
- EurActive, Sep 15, 2008. *Report: Slow progress on greening Europe's buildings*. <http://www.euractiv.com/en/energy-efficiency/report-slow-progress-greening-europe-buildings/article-175348> captured Sep 19, 2008
- EurActive, Apr 26, 2008, *Green Buildings*. <http://www.euractiv.com/en/energy-efficiency/green-buildings/article-163411> captured Sep 19, 2008
- European Business Council Japan, Jul 2008. *Thermal insulation - a key to improved energy efficiency and reduced CO2 emissions in Japan*. <http://www.ebcjp.com/news/EBC%20Thermal%20position%20paper%20July%202008.pdf> captured Sep 19, 2008
- Gowri, K., 2004. Green building rating systems: an overview. *ASHRAE Journal*, November 2004, 56-59.
- Green Buildings, 2008. *Green Building, USGBC and LEED*. Sep 2008, USGBC.
- GreenWorkplace, Aug 11, 2008. *BREEAM - the UK equivalent to LEED - toughens up*. <http://www.thegreenworkplace.com/search?q=BREEAM> captured Sep 19, 2008.
- Hikmat, H., and Ali, S.F.N., 2008. Developing green building assessment tool for developing countries- case of Jordan, Building and Environment, *Building and Environment, In Press*.
- Hong, W., Chiang, M.S., Shapiro, R.A., and Clifford, M.L., 2007. *Building Energy Efficiency : Why Green Buildings Are Key to Asia's Future*. (Edited by: Margarethe, P.L.), Asia Business Council, 320 pp.
- Howard, S., and Wu, C., 2007. *China's clean revolution*. The Climate Group, 34pp
- IPCC, 2007. *Climate Change 2007: Synthesis Report*. Intergovernmental Panel on Climate Change, 57 pp.
- Kats, G.H., 2003. *Green building costs and financial benefits*, Massachusetts Technology Collaborative, 8 pp.

- Larsson, N.K., and Cole, R.J., 2001. Green building challenge: the development of an idea. *Building Science and Information*, 29(5), 336-345.
- Martin, J., Swett, B., and Doug, W., 2007. *Residential green buildings: identifying latent demand and key drivers for sector growth*. Master's Project, Ross School of Business, University of Michigan, April 2007, 93 pp.
- Nelson, A.J., 2007. *The Greening of U.S. Investment Real Estate –Market Fundamentals, Prospects and Opportunities*. RREEF Research, 47 pp.
- Reuter, Apr 20, 2007. *Germany proposes energy efficiency labels for homes*. <http://www.reuters.com/articlePrint?articleId=USL2071423920070420> captured Sep 19, 2008
- SMART 2020, 2008. *Enabling the low carbon economy in the information age*. The Climate Group, 87 pp.
- Straube, J., 2006. Green Building and Sustainability. *Building Science Digest 005*, Buildingscience.com.
- US-EPA, 2008. *Green Buildings*, United States Environmental Protection Agency, <http://www.epa.gov/greenbuilding/pubs/about.htm> captured Sep 19 2008.
- UNEP-SBCI, 2006. Sustainable Buildings & Construction Initiative, 2006 Information Note, United Nations Development Program, 12 pp.

CYCLONE DISASTER RISK OF BANGLADESH

M. A. NOOR¹ and N. AHMED²

¹Bangladesh University of Engineering and Technology, Dhaka 1000, Bangladesh,

²Public Works Department, Dhaka, Bangladesh
¹mnoor@ce.buet.ac.bd

ABSTRACT

Several powerful periodic cyclones during final years of the 1990s and early of 2000 remind us, Bangladesh still remains at high risk of human, economic and social losses in the face of natural disasters. Cyclone research in Bangladesh has been mainly dominated by geographical and technological approaches rather than social or risk perspectives. Probably this is because cyclone mainly considered as physical phenomena. While it is related to physical phenomena, it mostly affects society, community, people, institutions, environment and the overall countries development. Finally, this turns into serious threat to meet the target of MDG's. Although a considerable improvements in recognition, prediction, mitigative measures, and warning systems, the economic losses and casualties due to over population on the costal areas remains high. In order to improve understanding the relationship between development and disaster risk at the global level, UNDP has started development of a Disaster Risk Index (DRI). In this paper, it is argued that less attention has been given to conducting in depth research on disasters, especially from risk perspective. This paper presented different perspective of cyclone risk assessment and established cyclone Disaster Risk Index (DRI) for the local level for Bangladesh. This will help to prepare and plan habitable human settlements at coastal areas.

1. INTRODUCTION

According to Norwegian Institute for Urban and Regional Research (NIBR), Asia is the most disaster-prone continent, with China, Bangladesh, India and Iran on top of the list when measured by absolute number of affected people (Sørensen et al, 2006). Impact of Natural Disasters on GDP of Bangladesh, 1990-2000 is 5.21% (DFID Report, 2005). Among 84 high cyclone prone countries around the world with highly populated coastal areas and deltas, Bangladesh, China, India, the Philippines, and Japan are at risk (UNDP, 2004). Cyclone is a characteristic feature of Bangladesh's physical environment and accepted as a normal hazard of social and economic life of Bangladesh. Historically, cyclone is mentioned as a disaster in this belt in the book Ain-e-Akbari of 16th century. During the last three decades almost all of the coastal areas and offshore islands of Bangladesh faced cyclones.

A DFID scoping study found that poverty alleviation, development and disaster risk reduction (DRR) are highly correlated (DFID report 2005). Inadequate attention to DRR can hinder progress in poverty alleviation and

sustainable development. Most recently to improve understanding the relationship between development and disaster risk at the global level, UNDP has started development of a Disaster Risk Index (DRI) for individual country. In this paper, it is argued that less attention has been given to conducting in depth research on disasters, especially from risk perspective. This paper is an attempt to assess the cyclone risk in different perspective from UNDP and attempted to calculate cyclone Disaster Risk Index (DRI) for local level coastal areas for Bangladesh, rather for whole country.

2. TRENDS IN TROPICAL CYCLONES

The Bay of Bengal is potentially energetic for cyclonic storms due to its favorable atmospheric and oceanic condition. Therefore, the highest incidence of TCs, almost 7% of total number of annual storms, located here. Amongst two storms generate winds of 55 mph or greater (as cited in Bowditch, 1977). Mainly, two cyclonic seasons are in the north Indian Ocean, viz. pre-monsoon (especially May) and post-monsoon (especially October and November). A few cyclones form in transitional monsoon months June and September also. Singh et al (2001) have shown an increased TC frequency during November and May over the north Indian Ocean from 1877 to 1998.

3. IMPACTS OF TROPICAL CYCLONES

Cyclones lead to several social, economic and environmental losses. The overall impact is country's ability to recover from this human and material damage, depends on several factors. The impact of the same cyclone between two countries is different in terms of fatalities, the number of people affected and the damage cost. For example, Hurricane Andrew struck Florida in 1992 with 23 people losing their lives. While a similar tropical wind storm hit Bangladesh in 1991, resulting in 100,000 deaths and the displacement of millions of individuals from widespread flooding (Adger et al, 2005; as cited in DFID, 2005). Whereas the cyclone of 1970 took the lives of 300,000 people but the cyclone of the same intensity of 1991 killed 138,000 people, and the cyclones of 1997 and 1998 resulted in only 111 and 19 deaths respectively, as shown in Table 1.

Table 1: Impact of Cyclones in Bangladesh

| Year | Scale | Deaths | Affected / Displaced | Total Damages (US\$ ' 000s) |
|------|------------------------------------|---------|----------------------|-----------------------------|
| 1970 | Similar to 1991 and 1997 3,648,000 | 300,000 | 3,648,000 | 86,400 |
| 1991 | 235 kmph | 138,000 | 15,438,849 | 1,780,000 |
| 1997 | 250 kmph | 111 | 3,052,738 | Not available |
| 1998 | 150 kmph | 19 | 108,944 | Not available |
| 2007 | 220 kmph | >4,000 | | |

Source: DFID (2005)

Note: The cyclones of 1970, 1991 and 1997 were of the same intensity

Beneficial climatic and soil conditions of cyclone-prone coastal areas of Bangladesh derived several economic activities like agriculture, fisheries and tourism. But the periodic attack of cyclones destructs the infrastructure and destroys livelihoods. In addition to the settlement patterns population growth and increased rural/urban migration act as increasing dynamic pressures to people's exposure to cyclone. Moreover, losses act together with other financial, political, health and environmental issues. Such disaster losses may setback social investments aiming to poverty and hunger, provide access to education, health services, safe housing, drinking water and sanitation, or to protect the environment as well as the economic investments. Thus it retards the 8 targets of MDG's for a sustainable development. Table 22 shows a scenario of the severity. It is imperative to have a method of calculating the impact of cyclones in social and economic life of people.

Table 2 Summarized Table of severe wind storm in Bangladesh from 1904 to 2007

| Types | No. of Events | Killed | Injured | Homeless | Affected | Total Affected |
|--------------|---------------|---------|---------|-----------|------------|----------------|
| Wave / Surge | 2 | 3 | 10 | 12,000 | 0 | 12,010 |
| Wind Storm | 153 | 618,599 | 930,113 | 9,972,568 | 61,999,305 | 72,901,986 |

Source: EM-DAT: The OFDA/CRED International Disaster Database, Created on Feb-10-2008. Events recorded from Nov/1904- Nov/2007

4. VULNERABILITY PATTERNS OF TROPICAL CYCLONES

There are many dimensions of vulnerability. Among these social vulnerability refers to the inability of people, organizations, and societies to withstand adverse impacts from multiple stressors and shocks like natural disasters to which they are exposed.

Mainly people of Bangladesh are vulnerable to disasters for three reasons. Firstly, the important type of vulnerability- poverty. It is an indicator of lack of access to resources, income opportunities and inequitable distribution of power. People of Bangladesh are poor and marginalized; it is difficult for them to access resources such as development loans or land. People here are simply unable to recover their losses due to their miserable poverty. In addition to the economic dimension, there are also other aspects of social positioning such as class, religion, community structure, community decision making processes and political issues that determine poor people's vulnerability. Therefore, poor are economically as well as vulnerable to social, cultural and political capacities to cope with disasters.

Second is vulnerable livelihood of the people. According to DFID (2005), this has three components - livelihood assets (human, social, physical, natural and financial capital), livelihood strategies and livelihood outcomes. This sort of vulnerability arises due to shortage of jobs, low income, declining natural resources, and decreasing profitability of rice

farming. Frequently cyclones adversely affect the livelihoods of people by damaging their means of earning (destruction of the factory, loss of land due to erosion in flooding, destruction of the shop) and/or tools (loss of draught animals, plowing tools, etc) in case of Bangladesh.

Third, patterns of natural resource use are changing, as urban development and commercial quarrying and environmental degradation. Localized and systemic environmental degradation is becoming highly influential as well, lowering the natural resilience to cyclones. Phenomena like El Niño/La Niña, climate change and the potential for rising sea levels, are affecting the patterns and intensity of cyclones.

5. DISASTER RISK APPROACHES

Alexander (1993) identified six schools of thought on natural hazards and disaster studies: the geographical approach, the anthropological approach, the sociological approach, the development studies approach, the disaster medicine approach and the technical approach. Among these approaches two disciplines, geography and sociology, have dominated the field of disaster research since the 1950s and have emphasized the environmental and behavioral aspects of disaster. Unfortunately, only recently researchers turned their attentions to the larger questions of social change related to disaster or the pre-impact conditions in disaster areas as sources of post-impact changes (Oliver-Smith, 1986).

Although both the geographical and sociological approaches have dominated in developed societies, in Bangladesh it mainly followed the geographical approach. Disaster research from sociological approach is done only in rare occasions in Bangladesh (Nasreen, 2004). Probably this is because cyclone mainly considered as Hydro-meteorological event. But though it is related to physical phenomena, it mostly affects society, community, people, institutions, environment and the overall countries development.

Since 1970s, engineers, architects, social scientists, social activists all have been highlighted on the impact of natural hazards. They find that the impacts not only depend on the physical resistance of a structure, but on the capacity of people to absorb the impact and recover from loss or damage. Now it is clear that development processes were not only generating different patterns of vulnerability, but were also changing and increasing patterns of hazard due to events such as impact of global climate change. Finally, disasters are no more viewed as extreme events created entirely by natural forces but as unresolved problems of development (Yodmani, 2000). Thus the focus of interest moved to social and economic vulnerability, with increasing evidence that natural hazards had widely varying impacts on different social groups and on different countries. According to Munich Re during the last four decades economic losses have increased more than ten times per decade. The causal factors of disaster thus shifted from the natural event towards the development processes that generated different levels of vulnerability. Disaster Risk has been presented by Ward, 1999 as follows:

$$\text{Disaster risk} = \frac{\text{Hazard} * \text{Vulnerability}}{\text{Manageability}}$$

Manageability here stands for the degree to which a community can intervene and manage a hazard in order to reduce its potential impact. Manageability is synonymous to Capacity so we can substitute to have the following disaster risk formula:

$$\text{Disaster risk} = \frac{\text{Hazard} * \text{Vulnerability}}{\text{Capacity}}$$

6. DISASTER RISK INDEX

Disaster Risk can be expressed in different ways for example by the number of people killed, percentage killed or percentage killed as compared to the exposed population. Each of these measures has advantages and inconveniences. As per the UNDP report this paper use the first two for DRI for cyclone calculation, and the percentage killed as compared to the exposed population for calculating relative vulnerability. Though exposed populations to cyclone should not be compared without standardization.

UNDP Bureau for Crisis Prevention and Recovery made a global report “Reducing Disaster Risk - A Challenge For Development (2004)” that provides the Disaster Risk Index (DRI), as the first global assessment of disaster risk factors through country-by-country. “It enables the calculation of the average risk of death per country with comparison of human vulnerability and exposure to three critical natural hazards: earthquake, tropical cyclones and flooding. It also identified of development factors that contribute to disaster risk. In the DRI, this relationship is expressed through the concept of physical exposure, referring to the number of people located in areas where hazardous events occur combined with the frequency of hazard events. Physical exposure is not an indicator of vulnerability, but is a condition sine qua non for disaster risk to exist. It also enables the identification of a number of socio-economic and environmental variables that are correlated with risk to death and which may point to causal processes of disaster risk.” In the DRI, countries are indexed for each hazard type according to their degree of physical exposure, their degree of relative vulnerability and their degree of risk which is calculated using following formula

$$R = PhExp * Vul \quad (1)$$

Where, *PhExp* is the physical exposure, i.e. the frequency and severity multiplied by exposed population; *Vulnerability* is the concept that explains why, with a given level of physical exposure, people are more or less at risk. In theory, vulnerability is modified by coping capacity and adaptive capacity.

Two methods are available for calculating physical exposure. First, by multiplying hazard frequency by the population living in each exposed area. The frequencies of hazards were calculated for different strengths of event, and physical exposure was computed as follows,

$$PhExp = \sum F_i * Pop_i \quad (2)$$

Where, $PhExp$ is the physical exposure at national level, F_i is the annual frequency of a specific magnitude event in one spatial unit; Pop_i is the total population living in the spatial unit.

A second method was used when data on the annual frequency of return of a specific magnitude event was not available. In this case (Cyclone), physical exposure was computed by dividing the exposed population by the numbers of years when a particular event had taken place as shown below,

$$PhExp = \sum \frac{Pop_i}{Y_n} \quad (3)$$

Where, Pop_i is the total population living in a particular buffer, the radius of which from the eye varies according to the strength, Y_n is the length of time in years $PhExp$ is the total physical exposure of a country (here used for second level administrative area, namely district), in other words the sum of all physical exposure in this country (here district).

Frequency of cyclone is calculated based on the following formula,

$$E(x) = \lambda = -\ln(1 - P(x \leq 1)) \quad (4)$$

Where, $E(x)$ is the statistical expectation, i.e. the average number of events per year, $P(x)$ is the probability of occurrence.

Here, to obtain physical exposure, a frequency per year was derived for each cell. Cells were divided to follow district borders, and then population was extracted and multiplied by frequency in order to obtain the average yearly physical exposure for each cell (BBS, 2006). For simplicity, cyclones are grouped in one category. Here, equation 2 is used to ascertain physical exposure of population of a particular locality.

7. CYCLONE DRI AND BANGLADESH

DRI help to assess cyclone disaster risk for the individual areas of Bangladesh to find a holistic picture of the country. It calibrated according to the risk of death between 1980 and 2007.

Here, data from 23 coastal districts of Bangladesh were selected for DRI calculation from 1980 to 2007. This is because of the data before this period is not reliable. 191 cyclones in the period of 28 years have been considered. Total population of these coastal areas is 43.7 million. The key steps followed in producing the DRI, according to UNDP report, were:

7.1 Calculation of Physical Exposure

People are more or less vulnerable to cyclone depending on a range of social, economic, cultural, political and physical variables. The risk of death in a natural disaster is a function of physical exposure and vulnerability to cyclone. The DRI calculated for the areas exposed to cyclones and the population living in these areas to arrive at a calculation of physical exposure for each district. This is the average number of people exposed to a hazard event in a given year. Physical exposure varies both according to the number of people as well as to the frequency of cyclone. In the DRI, physical exposure is expressed both in absolute terms (the number of people exposed in a country) and in relative terms (the number exposed per million

people). When more people are killed with respect to the number exposed, the relative vulnerability to the hazard in question is higher. BBS (2006), population data have been used to calculate physical exposure.

7.2 Calculation of Relative Vulnerability

Vulnerability of locality depends on the physical exposure of a spatial unit and no of the death for a particular disaster. Here, for a set of cyclones and for a district relative vulnerability is the total number death in million to the exposed population to those cyclones. Total number of death for each cyclone was taken from EM-DAT database.

7.3 Results and Discussion

Figure 1 reveals that loss of human life from cyclone is tied to development status of a region. Low and medium developed areas have almost similar loss patterns. While, some developed areas are occupying the bottom part of the graph indicating low numbers of fatalities per million. No developed region has recorded more than 200 deaths per million population from 1980-2007.

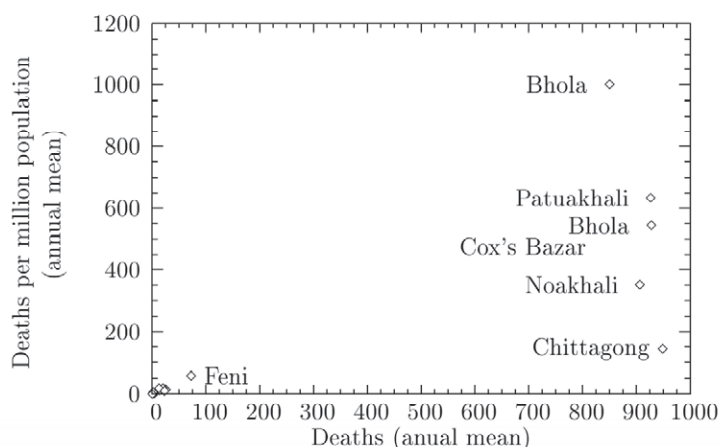


Figure 1: Development status and disaster deaths

This observation reinforces intuitive views about the disaster development relationship. This heightens the inequality especially in rural char areas. Livelihoods there at risk due a range of factors: poverty and asset depletion, environmental degradation, market pressures, isolation and remoteness, the weakness or lack of social services and climate change. Therefore, contemporary patterns of urbanization and rural livelihoods needs to be viewed alongside other critical development pressures.

The size of exposed populations with the number of recorded deaths to cyclones is used as a measure of relative vulnerability as shown in Figure 2. The areas closest to the shoreline of the Bay of Bengal show highest relative vulnerability. The large number of recorded deaths shows that in this case high vulnerability accompanies high physical exposure. Most vulnerable areas can be identified from the figure which is middle of the southern part. It should be noted form the Figure 3 that the highest no average cyclone occurs in south eastern mainly Chittagong area. Though

having highest no of death and highest no of average cyclones per year this are is less vulnerable than other coastal region. Mainly, physical exposure in million populations is very large, and the area is more developed than other areas.

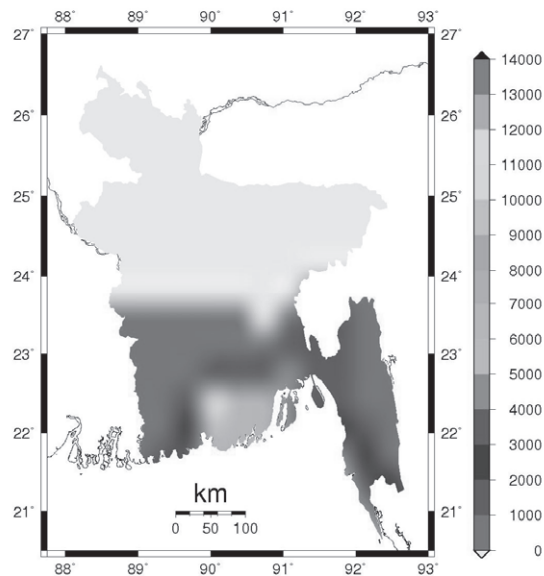


Figure 2: Relative vulnerability at district level for 1980 to 2007 cyclone

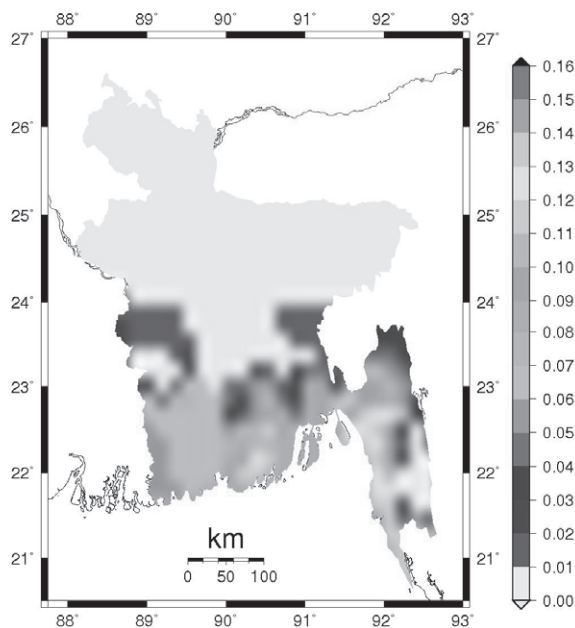


Figure 3: Average storm per year for individual district

The analysis carried out for tropical cyclone risk showed a strong correlation between physical exposure and human development. An area with large, predominantly rural populations and with a low development is most closely associated with cyclone risk. There are a number of reasons for this. Rural housing in many areas are tend to be more vulnerable to high winds, flooding and landslides than urban housing and are generally be

associated with higher mortality. Conversely, the weakness or nonexistence of emergency and rescue services in rural areas and lack of access to disaster preparedness and early warning are all other factors that would help to explain mortality rates. The cyclone preparedness programme in Bangladesh is one of the few success stories. By coupling cyclone shelters and community-based preparedness measures, the programme has managed to dramatically reduce vulnerability from the 1970s to the (still high) levels observed in the 1980-2007 reporting period (Table 1).

8. CONCLUSIONS AND RECOMMENDATIONS

From the above analyses it can be concluded that there is a good relationship between the cyclone risk and development process in Bangladesh. DRI can be a useful tool for this purpose. It has also been established, here, that social, economic and livelihood analysis is vital in calculating DRI. But with out good governance achieving development is very difficult. Changing governance always offers possibilities for the integration of international with national and local action to reduce disaster risk. The increased role played by civil society in poverty alleviation, development and disaster risk reduction highlights the capacity of local actors to organize and confront disaster risk. More positively, meeting the targets of MDG's could result in a substantial reduction of cyclone disaster risk.

Governance is a critical area for innovation and reform in achieving cyclone risk reduction within human development. It is important to identify those governance tools that will be likely to simultaneously benefit disaster risk reduction and human development. This would include a presumption for equality in participation in decision making across genders, religious and ethnic groups and economic classes. It is also important to identify governance reform that might inadvertently contribute to the generating of human vulnerability. Social networks are often in competition with one another and though this is not a bad thing in itself, when disaster or development aid is fed through and strengthens clientelistic networks this can foster corruption and inequality, further entrenching disaster risk. The theme good governance and the analysis of the DRI should contemplate each other.

REFERENCES

- Alexander, D. (1993), *Natural Disasters*. London: UCL Press.
 BBS (2006) Bangladesh Bureau of Statistics, *Statistics Bangladesh*, 2006.
 Bowditch, N., (1977), *The American Practical Navigator*, Vol 1, U.S. Department of Defense
 Briefing Notes, Compiled for the 5th Working Group Meeting of the Asian Urban Disaster Mitigation Program, Cambodia, 23-25 February 2000, Organized by Asian Disaster Preparedness Center, Bangkok, Thailand.
 DFID (2005), *Natural Disaster and Disaster Risk Reduction Measures- A Desk Review of Costs and Benefits*, Report, 8 December, 2005

- Nasreen M. (2004) Disaster Research: Exploring the Sociological Approach to Disaster in Bangladesh e-Journal of Sociology. Vol. 1. No. 2. July, 2004.
- Oliver-Smith, A. (1986), Disaster Context and Causation: An Overview of Changing Perspective in Disaster Research' in Vinson H. Sutlive et al (Eds) Natural Disasters and Cultural Responses. Williamsburg: Department of Anthropology, College of William and Mary.
- Singh, O. P.; Khan, T. M. A. and Rahman, M. S. (2001), Frequency of tropical cyclones increased in the north Indian Ocean? CURRENT SCIENCE, VOL. 80, NO. 4, 25 February 2001.
- Sørensen, J.; Vedeld, T. and Haug, M. (2006), Natural hazards and disasters- Drawing on the international experiences from disaster reduction in developing countries REPORT (16. January 2006), Norwegian Institute for Urban and Regional Research (NIBR).
- UNDP (2004), Reducing Disaster Risk – A challenge for development, a global report. Bureau for Crisis Prevention and Recovery, New York.
- Yodmani S (2000) Paper Presented on “Disaster Risk Management and Vulnerability Reduction: Protecting the Poor” at The Asia and Pacific Forum on Poverty, Organized by the Asian Development Bank.

TRAFFIC FLOW ANALYSIS FOR AN APPROPRIATE EVALUATION OF LOST TIME IN SIGNAL CONTROL

SHINJI TANAKA, TAKESHI ONO and MASAO KUWAHARA
Institute of Industrial Science, The University of Tokyo, Japan
stanaka@iis.u-tokyo.ac.jp

ABSTRACT

An appropriate evaluation of lost time in signal control theory is quite important because it affects the determination of the cycle time. Analyzing observed vehicle trajectory data at different intersections, this study evaluates the all red time focusing on the conflict points and calculates the lost time properly based on the saturation flow rate. As a result, it is revealed that the lost time could be shortened by the method using conflict point analysis and an accurate acquisition of the saturation flow rate is very important for the proper lost time calculation.

1. INTRODUCTION

Lost time in signal control is a period which is not used effectively for incoming traffic flow at an intersection. When we design signal phases, we need to insert yellow signal to stop vehicle flow from one direction and all red (= red for all direction) signal to clear up running vehicles from an intersection before the next signal phase starts and vehicles from a different direction enter the intersection. Here, all red time is not used additional incoming traffic, so it is called as “clearance loss”. At the next signal phase, vehicles can not start at the exact moment of the beginning of green signal but start a little bit later, and the flow rate increases gradually to the saturation flow rate. This period when the capacity is partially used is called as “starting loss”. And, lost time is the summation of these two losses.

To prevent traffic accidents like head-on collision in an intersection, it is very important to secure enough all red time. However at the same time, to set a too long all red time leads to inefficiency and may sometimes cause traffic congestion. Therefore, to evaluate all red time and to set it properly is a very important issue.

Furthermore, in signal control theory, lost time is an important factor to determine the cycle time of the signal. And in congested situation, cycle time influences delay at a signalized intersection. Therefore, an appropriate evaluation of lost time is important in this aspect, too.

In Japan, all red time is determined by the distance between stop lines divided by vehicle running speed. This method is quite simple, but not bad if the last vehicle is a go-straight vehicle. However, vehicles go different directions at an intersection and right-turn vehicle can often be the last one in normal 2-phase signalized intersections. In such a case, this method does

not have valid reasons to calculate all red time. We need a more accurate and reliable method.

In this study, we pick up some intersections whose signal phase ends with right-turn vehicles and make observations. Based on this, we examine the feasibility of a different method to calculate the all red time in such intersections. And after this, we calculate an accurate lost time focusing on the signal phase with right-turn vehicles.

2. THEORITICAL REVIEW

2.1 Method to calculate all red time

There are two major methods to calculate all red time in the world. One is used in Japan and the United States, calculated by the following equation.

$$AR = \frac{W}{V} \quad (1)$$

where, AR : all red time (sec), W : distance between stop lines (m), and V : vehicle running speed (m/s)

The other is used in Germany, which employs an idea of “conflict point”. In this method, all the possible intersecting points (= conflict points) of vehicle trajectories are considered between the target phase and the next phase, and the time difference of the last vehicle and the next first vehicle is calculated as follows.

$$AR = t_r - t_e \quad (2)$$

where, t_r : travel time for the distance “from the stop line to the conflict point plus vehicle length” by the last vehicle (sec), t_e : travel time for the distance “from the stop line to the conflict point” by the next first vehicle (sec)

Figure 1 shows the concept of this method. To avoid a collision in the intersection, Equation (2) is needed.

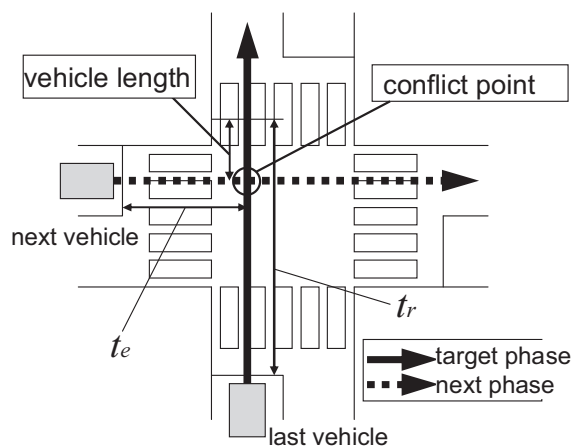


Figure 1: Conflict point by consecutive 2 vehicles

2.2 Method to calculate lost time

In the conventional signal control theory, lost time is calculated by the following equation.

$$L = \sum_j^n (Y_j + AR_j) - n \tag{3}$$

where, L: lost time (sec), Y: yellow time (sec), AR: all red time (sec), n: number of signal phase change

This means that lost time can be calculated just by the summation of yellow and all red time basically. The reason of this idea is that yellow time is used as a part of effective green time and we assume it is approximated almost equal to the starting loss time. Figure 2 shows this idea.

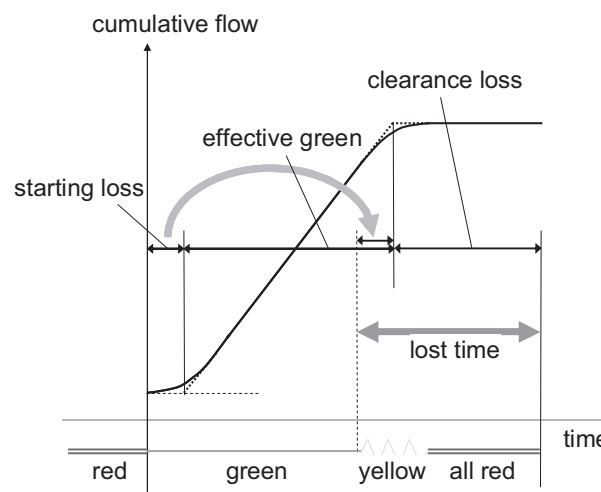


Figure 2: Conventional method to calculate lost time

However, this assumption that starting loss and effectively used yellow is the same is not guaranteed in the actual vehicle movements. And, if we focus on the right-turn vehicle movements at the timing of signal phase change, it can vary depending on the signal phase patterns as shown in Table 1. Here, right-turn vehicles have to make turning during absence of oncoming traffic in “normal green”, but they can do it freely in “exclusive green”. These different vehicle movements should be considered in lost time calculation.

Table 1: Differences of right-turn vehicles by signal phase patterns

| Signal phase pattern | Starting point | Starting timing |
|-----------------------------------|---------------------|----------------------|
| A) normal green only | inside intersection | start of yellow |
| B) normal green + exclusive green | inside intersection | start of right arrow |
| C) exclusive green only | stop line | start of right arrow |

3. FIELD OBSERVATION

To evaluate the validity of the current all red time and lost time based on actual vehicle movement data, we conducted field observation survey using

video camera at three intersections considering different types of right-turn movements. Figure 3 shows an example of the recorded image at the intersection C.



Figure 3: An example of observed intersection

3.1 Intersection A (normal green only)

This intersection has 1 lane (for one side) roads for both directions. The speed limit is 40km/h. Table 2 shows the signal steps of this intersection. Vehicles can make right-turn during step 1 and 4.

Table 2: Signal steps at intersection A

| STEP | 1 | 2 | 3 | 4 | 5 | 6 | 7 | 8 | 9 |
|----------------|----|--------|---------|----|--------|---------|----|--------|---------|
| traffic flow | | yellow | all red | | yellow | all red | | yellow | all red |
| duration (sec) | 23 | 3 | 2 | 30 | 3 | 2 | 21 | 3 | 3 |

cycle length: 90 sec

(solid arrow: vehicle flow, dotted arrow: pedestrian flow)

3.2 Intersection B (normal green + exclusive green)

This intersection has 3 lanes (for one side) road for one direction and 2 lanes (for one side) road for the other. The speed limit is 60 km/h for the former and 40 km/h for the latter. Table 3 shows the signal steps of this intersection. Vehicles can make right-turn during step 1-3 and 4-6.

Table 3 Signal steps at intersection B

| STEP | 1 | 2 | 3 | 4 | 5 | 6 | 7 | 8 | 9 | 10 |
|----------------|----|--------|----|--------|---------|----|--------|----|--------|---------|
| traffic flow | | yellow | | yellow | all red | | yellow | | yellow | all red |
| duration (sec) | 87 | 3 | 10 | 3 | 3 | 35 | 3 | 10 | 3 | 3 |

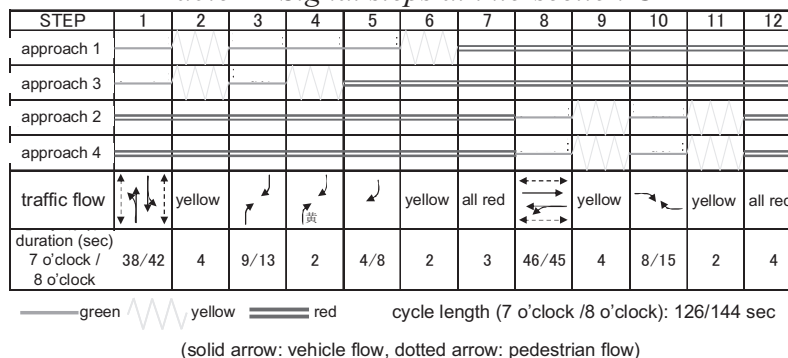
cycle length: 180 sec

(solid arrow: vehicle flow, dotted arrow: pedestrian flow)

3.3 Intersection C (exclusive green only)

This intersection has 5 lanes (for one side) road for one direction and 4 lanes (for one side) road for the other. The speed limit is 60 km/h for the former and 40 km/h for the latter. Table 4 shows the signal steps of this intersection. Vehicles can make right-turn during step 3-5 and 10.

Table 4 Signal steps at intersection C



4. EVALUATION OF ALL RED

4.1 Calculation of all red

All red time in these intersections is set by the conventional Japanese method. Here, we applied conflict point method to calculate all red time based on the observed vehicle movement data. To apply this method, Equation (2) is a little bit modified, that is,

$$AR = t_{r85} - t_{e15} \tag{4}$$

where, t_{r85} : 85 percentile value of travel time for the distance “from the stop line to the conflict point plus vehicle length” by the last vehicle (sec), t_{e15} : 15 percentile value of travel time for the distance “from the stop line to the conflict point” by the next first vehicle (sec)

The reason why we need this modification is, to use actual vehicle movement data, the values of t_r and t_e are not identical but have some distribution among observed samples, therefore we decided to use “safer” values. The result of the calculation is shown in Table 5.

Table 5: All red calculated by different methods

| | | (unit: sec) | |
|----------------|---------|-----------------|-----------------------|
| | | Current setting | Conflict point method |
| intersection A | step 3 | 2 | 3.03 |
| | step 6 | 2 | 7.64 |
| intersection B | step 5 | 3 | 3.29 |
| | step 10 | 3 | 2.16 |
| intersection C | step 7 | 3 | 2.85 |

4.2 Discussion

First, in the intersection A, the result shows that longer all red time are needed. By checking from the recorded video, the last vehicles were right-turn ones for both cases of step 3 and step 6. Their turning movements were interrupted by oncoming vehicles or pedestrians, and it seemed to require longer all red times. We may need further data cleansing or sample investigation to get more reliable result.

As for the intersection B, the calculation result of all red time from the conflict point method becomes almost same or shorter as the current setting. This value was calculated from the case that a right-turn vehicle is the last one of the phase. If we calculate all red using the go-straight vehicle as the last one, the values become 5.07 (sec) and 4.05 (sec) for both cases. It means that all red time can be shortened by the flow direction based conflict point method.

In the intersection C, we calculated all red for step 7 only due to the data limitation. Figure 4 shows the conflict points at this step. There are 7 possible conflict points in this step, but there were very few data for point 6 and an enough margin for point 7, therefore we used point 1 to 5 to calculate the all red time. As a result, we derived a little bit shorter all red time than the current one.

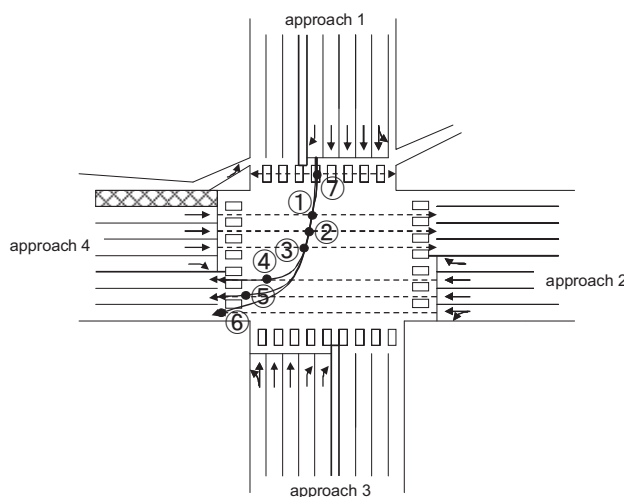


Figure 4: Conflict points at step 7 in intersection C

By the way, we used 85 percentile and 15 percentile value for the calculation to consider safety, but if we use the average value, all red time become 1.21 (sec) in the case of the intersection C. It means that all red time calculation greatly depends on how much we care about safety

5. EVALUATION OF LOST TIME

Using the observed data at the intersection C, we calculated lost time of the phase for right-turn vehicles during step 3 to 5, which is the summation of starting loss and clearance loss. The result is shown in Table 6.

Table 6: Lost time for step 3 - 5 at intersection C

| (unit: sec) | | |
|---------------|----------------|-----------|
| Starting loss | Clearance loss | Lost time |
| -0.40 | 3.27 | 2.87 |

5.1 Starting loss

Starting loss is calculated as follows. First, cycles which include longer time headway than 4 (sec) and less passing vehicles than 6 are eliminated from the analysis so that we can capture saturated flow situations. Then, a regression line is drawn using 2nd to 6th vehicle's passing time, and the starting loss is derived by the difference between the green starting time and the intersecting point of this line to x-axis. The result was a negative value (-0.40 sec), which may be because vehicles were well prepared to start when the green signal began as there was yellow signal just before it.

5.2 Clearance loss

Clearance loss is calculated by the subtraction of the effectively used time from the summation of yellow (2 sec) and all red (3 sec). Here, effectively used time is derived by the average of the passing time of the last vehicle after yellow signal begins, which was 1.73 (sec). Therefore, clearance loss was 3.27 (sec).

5.3 Lost time

Taking the above together, the lost time based on the observed vehicle movement data was 2.87 (sec). This is shorter than the one set by the conventional method (Equation (3)), that is, $2 + 3 - 1 = 4$ (sec). It means that the conventional method may estimate the lost time too much.

6. CONCLUSION

In signal control theory, lost time is a very important factor which affects the efficiency of the signal control and may cause delay in travel. This study showed a possibility to improve the accuracy of the lost time calculation depending on the signal phase patterns using observed vehicle movement data. However, the results shown here are based on a limited number of data and not all flow pattern combinations are covered. For example, the saturation flow rate used in calculating the starting loss is very sensitive to the history of vehicles' passing time. We need further data accumulation and analyses to ensure the reliability of this method.

REFERENCES

Road and Transportation Research Association : *Guidelines for Traffic Signal RiLSA*, 2003

SAFETY ASSESSMENT OF STRUCTURAL CONCRETE WITH DEFECTS AND DAMAGES

KOICHI MAEKAWA and KOHEI NAGAI

Department of Civil Engineering, The University of Tokyo, Japan
maekawa@concrete.t.u-tokyo.ac.jp,
nagai@concrete.t.u-tokyo.ac.jp

ABSTRACT

Coupled analysis of mass transport in concrete and damage mechanics with cracking is presented for structural safety assessment under combined severe loads and environments. Multi-scale modeling of micro-pore formation and moisture transport with solved ions are linked to predict the concrete deformation and steel corrosion. Multi-chemo physical simulation system and nonlinear dynamic mechanics were combined together in time and space domains with mutual data communication. This system was verified under static, dynamic and fatigue loads, and has been applied to safety and serviceability assessment of existing infrastructures subjected to severe damages caused by drying, autogenous shrinkage, steel corrosion and ASR.

1. INTRODUCTION

Life-cycle performance of urban infrastructures are being required and appropriate design methods for both materials and structures are sought in several industrial societies (Baroghel-Bouny 2006). Currently, needs to verify remaining functionality of damaged existing facilities is rising for urban safety. To meet these challenges, keenly expected is a assessment system to deal with structural serviceability and safety under specified loads and ambient conditions.

In this paper, the authors propose an integrated platform of solid mechanics and thermo-hydro dynamics of structural concrete with multi-scales of referential control volume on which chemo-physical events develop with mutual correlation as shown in Figure 1 (Maekawa et al. 2003, 2001, 1999, Asamoto et al. 2006). The space-averaged constitutive model is basically built with regard to cracking in RC elements, and the thermo-hydro state variables are overlaid for multi-scale and multi-chemo mechanical modeling as summarized in Figure 1. Recent application of the multi-scale approach to practical problems is also introduced, and the direction of future development is discussed regarding an integrated knowledge-base of structural concrete.

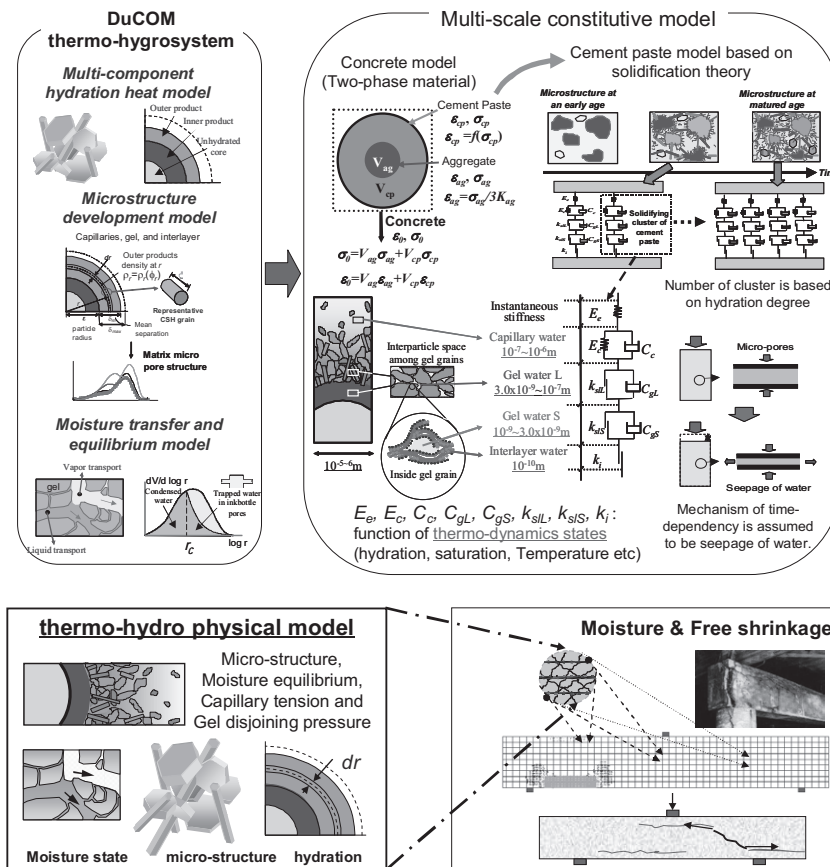


Figure 1: Coupling of thermo-hydro dynamics and damage mechanics for life cycle assessment of structures

2. MULTI-DIRECTIONAL CRACK MECHANICS (meter-scale)

For the largest scale modeling of structural concrete, the smeared crack (Collins and Vecchio 1982) and active crack approach (Maekawa et al. 2001, 2003), which has been applied for seismic analyses, is also applied for multi-directional crack kinematics and its interaction. Meso-scale mechanical states are explicitly included in the form of constitutive models (Figure 2). The stress carrying mechanisms are composed of compression/tension parallel and normal to cracks and shear transfer. By the active crack method, the primary cracking of governing nonlinearity of structural concrete element is identified if some cracks intersect non-orthogonally. Here, path-dependent parameters are renewed only along the active crack in each load step of time.

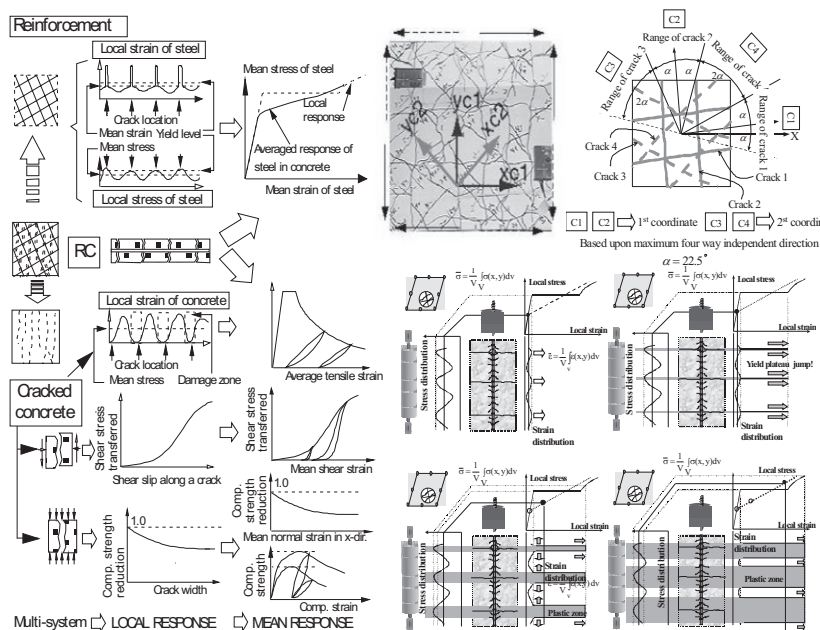


Figure 2: In-plane constitutive model with multi-directional cracking

3. THERMO-HYDRO MODELING (micro-nano meter scale)

Volumetric change caused by temperature and long-term moisture equilibrium in micro-pores are associated with cracking and corresponding structural serviceability, and corrosion of reinforcement has much to do with migration of chemicals through micro-pores. Thus, the coupled system as shown in Figure 3 was proposed (Maekawa et al. 2003, 1999) to simulate the entire thermo-mechanical states of constituent material and structures, and a multi-scale analytical platform named as DuCOM (durability model for concrete) was used. Micro-pore geometry and spaces are idealized by statically formulated pore distribution and internal moisture balance is simultaneously solved with mass conservation requirement. The moisture migration and diffusivity are computed based on the micro-pore size distribution and the space of condensed water channel as shown in Figure 1 and Figure 3.

Chloride ion migration and other chemical reactions such as carbonation and calcium leaching are overlaid on this system (Ishida et al. 2000, Nakarai et al. 2005). The conductivity and diffusion characteristics for mass transport are calculated based upon numerically formed micro-pore structures. The computation of multi-chemo-physical events is carried out by means of the sequential processing with closed-loop predictor-corrector method (Figure 3). Concrete shrinkage associated with microclimate in C-S-H gel and capillary pores is linked with the macroscopic constitutive model with regard to micro-pore and disjoining pressures originated from Van der Waals and Coulomb forces (Figure 1). Micro-corrosion rate is also computed by simulating migration of O₂-CO₂ gas and chloride ion, and the effect of corrosion is integrated in the structural analysis (Toongoenthong et al. 2005). These thermo-dynamic state variables are incorporated into the constitutive modeling and simultaneously solved. Then, we have

approximately 230 simultaneous equations to be solved numerically for chemo-physical and mechanical behaviors of different scales (Ishida et al. 2004, 2000).

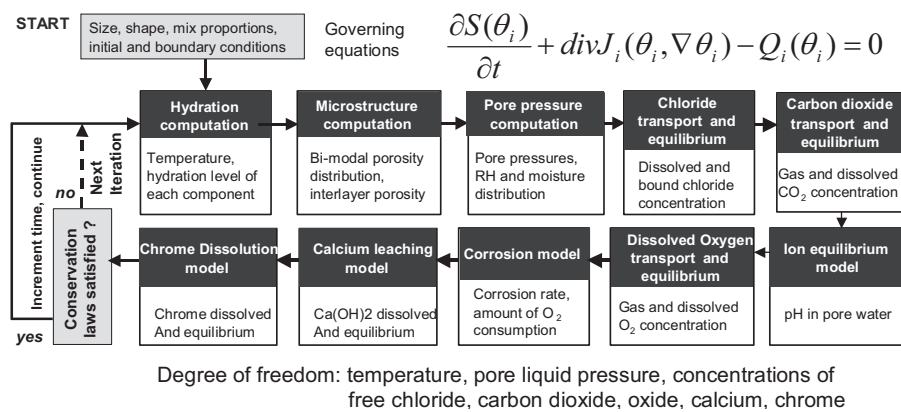


Figure 3: Sequential computation of chemo-physical events

4. DAMAGE MECHANICS WITH CHEMO- PHYSICS AND SAFETY ASSESSMENT OF DAMAGED STRUCTURES

Cracking is influential in mass transport of gases and dissolved ions. These cracks through which ion substances can easily migrate are mutually linked with thermo-hydro dynamic analysis by the hierarchy type of multi-scale modeling as shown in Figure 1. The corroded steel produces volumetric expansion and results in internal self-equilibrated stress, which may lead to additional cracking around reinforcing bars. Figure 4 illustrates the way to amalgamate the damage mechanics and volume expansion of generated corrosion gels. The corrosion gel product formation is considered in the constitutive modeling of reinforcement in the transverse direction. The non-corroded mother steel and the corroded clusters with different mechanical properties are treated as a fictitious aging material of varying volumetric stiffness and expansion according to the magnitude of corrosion. This growing steel is embedded in each finite element similar to smeared crack approach as well.

When the corrosion cracking develops over the beam, shear safety performance differs from the non-damaged reference case (Sato et al. 2003). Figure 5 shows load-displacement relations for RC non-damaged reference and corroded specimens which was submerged into a sodium pond for accelerated corrosion. Here produced was uniformly distributed corrosion along the whole longitudinal steel of 2.1% as the mass loss. Main reinforcing bars were bent up 90 degree inside the anchorage zone, and satisfactory anchorage capacity is expected. The stiffness of the member is much reduced but the capacity is a bit increased. The macroscopic bond loss in the shear span leads to retarded propagation of diagonal shear cracking and may elevate the shear capacity. Computation can capture this property.

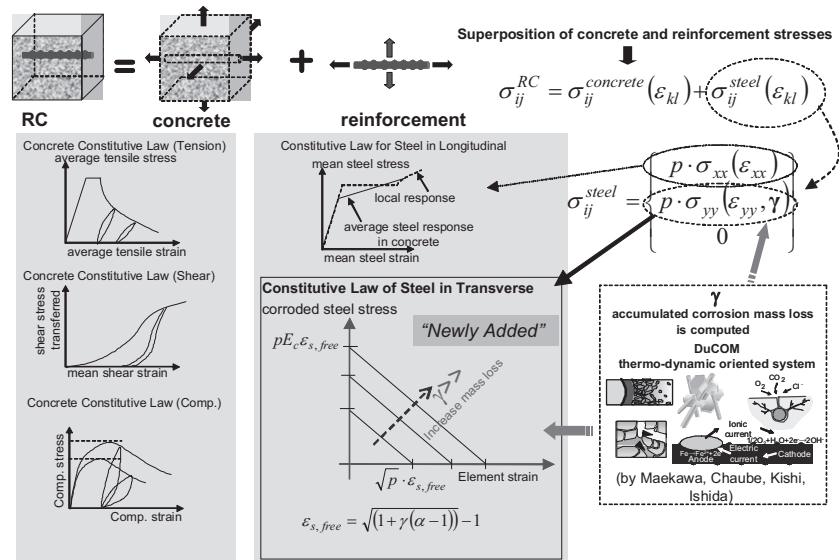


Figure 4: Simulation of corrosion of r/f bars and structural performance assessment

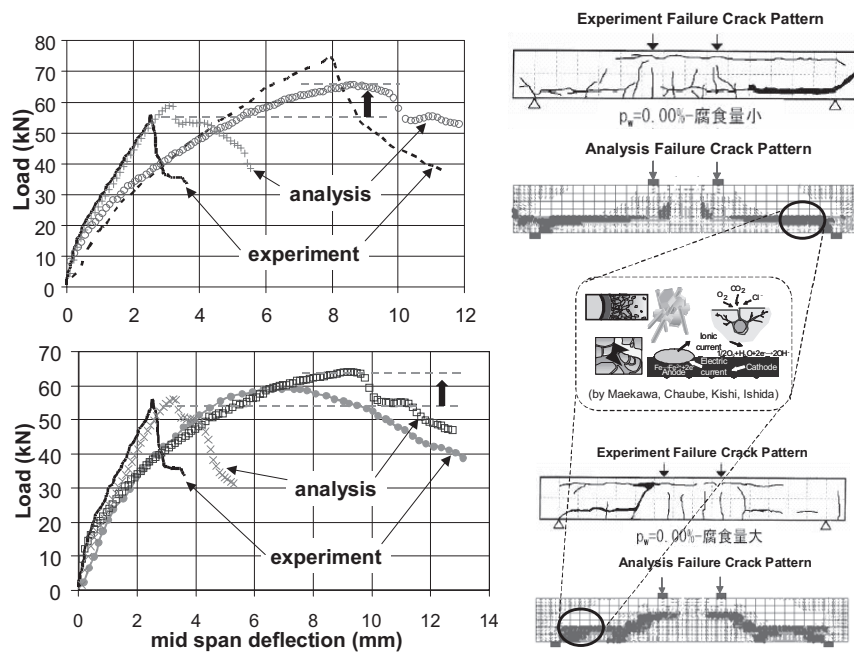


Figure 5: Beam with inherent crack-like defect in the anchorage zone

Figure 6 shows the defect built-in RC members subjected to combined flexure and shear (Chijiwa 2006). This is a mock-up of corrosion cracks, and used for verification of the coupled mechanistic and thermo-dynamic analysis. It can be seen that the quasi-ambient induced damages in the anchorage zone are much severe for structural strength. Unlike the pre-induced damages inside the shear span, a distinct crack slip occurs and the tied arch mechanism is hard to appear if the damage is limited in the narrow anchorage zone. The damage concentrates between the tip of the quasi-ambient induced damages and the loading point, and the diagonal crack width becomes remarkably wide. Larger crack widths with dramatically

rotating axes of principal stresses, which are rare in non-damaged ones but frequent for structural concrete including corrosion cracking, must be considered for structures subjected to combined mechanical and environmental actions (Chijiwa 2006).

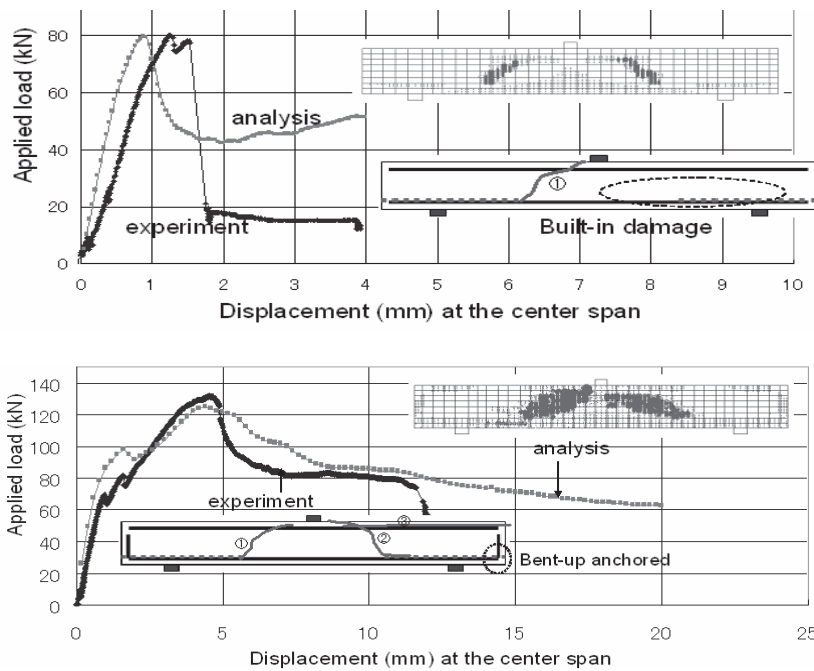


Figure 6: Simulation of partially damaged beam along the main reinforcement

Figure 7 shows the fatigue life simulation of RC members under high cycle shear (Maekawa et al. 2006b). If the pre-corrosion crack develops around the anchorage zone of the web reinforced beam, the fatigue life is tremendously degraded even though the static capacity is almost the same as that of the non-damaged one. On the contrary, the pre-corroded cracking inside the shear span brings much prolonged fatigue life to non-web reinforced members due to the loss of macroscopic bond. The corroded cracks along main reinforcement results in arch-action formed between the supports and the loading point against shear. This fact was also experimentally verified in use of actually damaged RC slabs due to alkali-aggregate reaction.

The coupled analysis can be applied to RC slabs subjected to traveling wheel-type loads as shown in Figure 8 (Maekawa et al. 2006a). Bridge deck slabs are usually utilized under heavy traffic loads with high repetition of traffic passage. Furthermore, moisture and pre-induced cracking by drying and settlement are known to tremendously reduce the fatigue life. The fixed point load produces the punching shear failure of conical planes, but the moving load passages bring about highly anisotropic shear failure which extends to the transverse direction of slabs (Figure 8). As Maeda et al. (1984) and Perdikaris et al. (1988) experimentally clarified, the moving fatigue loads greatly deteriorates the fatigue life (nearly 2-order of repetition). The coupled full 3D analysis can successfully reproduce the shortened fatigue life and failure mode reasonably.

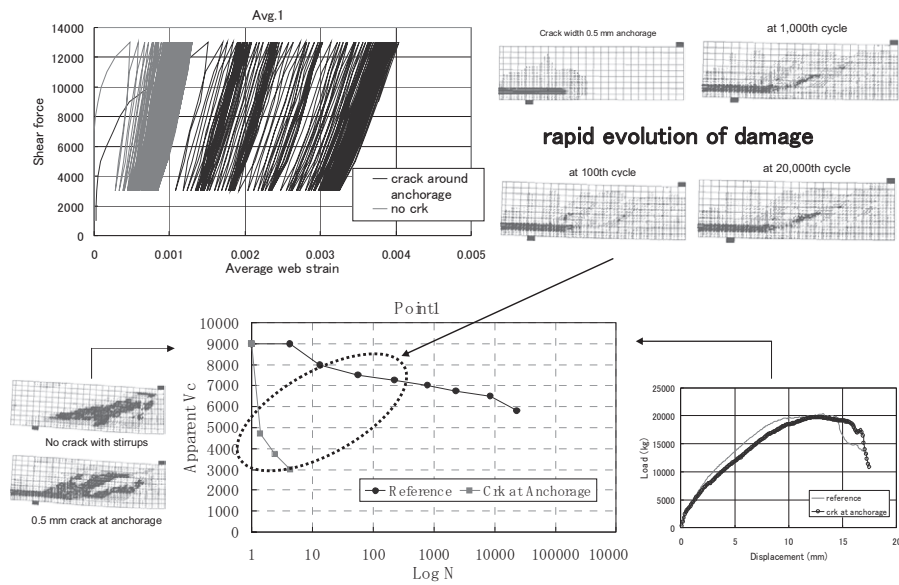


Figure 7: Simulated shear capacity and cracking of corrosion beam under fatigue loads

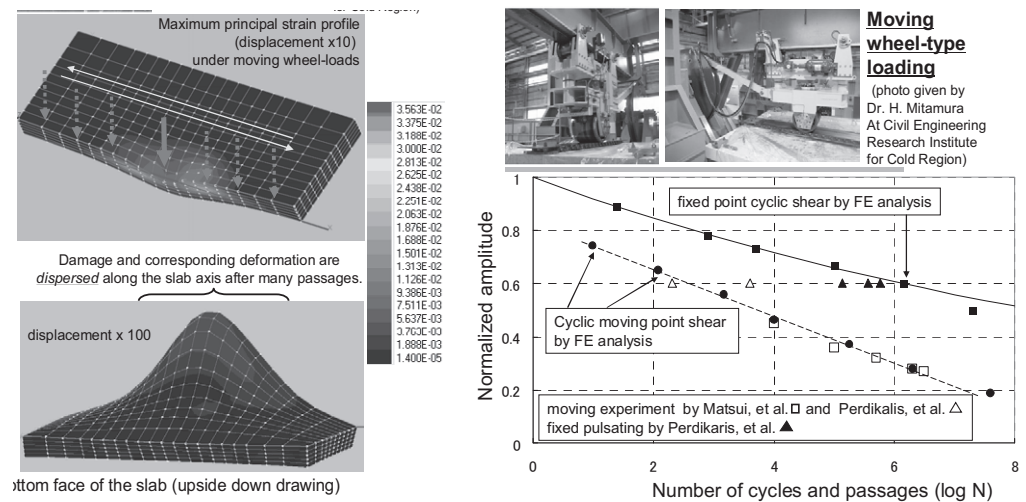


Figure 8: Failure mode of RC slab under traveling wheel-type loads and computed life

Figure 9 is the recent example of application to the practical safety assessment for a 100-years old railway bridge in Tokyo (Sato et al. 2001). Due to uneven settlement of the foundation, some initial damage remains in the form of cracking and arch ribs were strengthened by additional RC arch inside layer in the past. The seismic ground motion was applied to the numerically aged structural concrete and the computed response was used for safety and serviceability assessment in practice. The seismic remaining performance was numerically investigated and the sustainable life with light retrofit was judged.

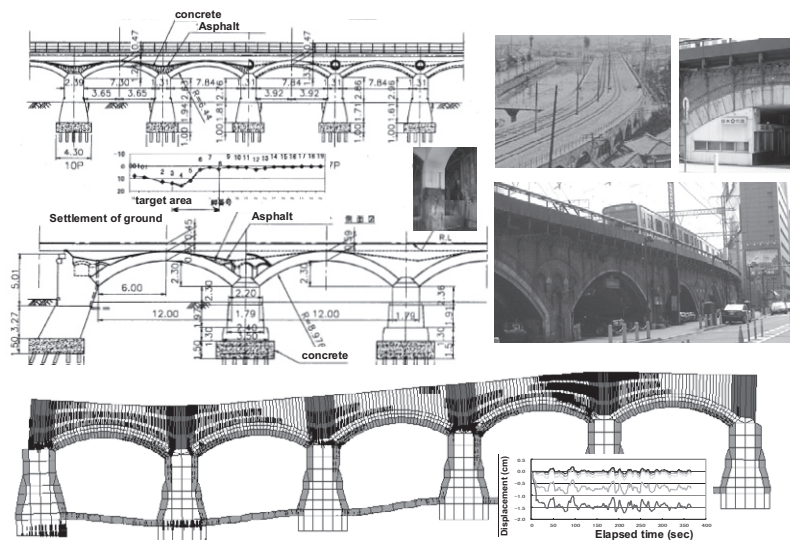


Figure 9: Safety assessment of 100 years-old railway bridges

5. NEW FIBER MATERIALS FOR STRENGTHNING

Fiber Reinforced Cementitious Composite (FRCC) is recently applied widely to surface repair, strengthening and so on (Kunieda et al. 2004). Although its superior performance is investigated under uniaxial loading condition in static, cyclic and fatigue conditions, less attention has been paid to behavior under multi directional cracking condition which may arise when FRCC is used as structural member that exposed to complex stress condition through the service life. An on-going attempt to predict the behavior of cracked FRCC is reported here (Suryanto et al. 2008). High Performance Fiber Reinforce Cementitious Composite (HPFECC), which is categorized as a material that exhibits multiple cracks and strain hardening under tension, is examined experimentally by bending test as shown in Figure 10. Initial-crack was introduced by applying four-point bending test (A-D). The specimen was then cut to readjust the orientation (20, 45, 70, 90 deg) of the pre-cracks (E). Finally, a further bending test was applied (G). The results showed a significant influence of pre-cracks, particularly due to the orientation of the pre-cracks. In most cases (except for the 20 deg case), the degradation of strength was evident, relative to the strength of the no initial damage specimen. The initial-crack also significantly influences the initial stiffness of the specimen. In general, a bi-directional cracking pattern was observed as illustrated in Figure 10. The secondary crack (a subsequent crack formation after the initial-crack) always formed somewhat orthogonal to the initial-crack. The results bring concern that FRCC performance under multi directional cracking should be evaluated fairly for long term maintenance of concrete structure so that incorporation into computational scheme presented in previous sections will be conducted in the near future.

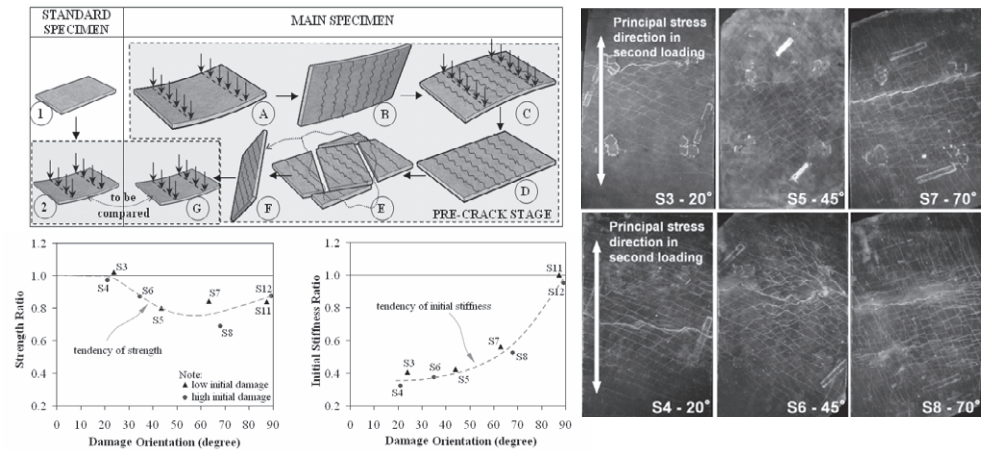


Figure 10: Bending test of HPFRCC with multi directional cracking

6. CONCLUSIONS

Life span simulation system with multi-scale modeling presented in this study predicts performance of structural concrete at arbitrary time during its life, which is expected to contribute the safety assessment of infrastructure.

REFERENCES

- Asamoto, S., Ishida, T., Maekawa, K. 2006. Time-dependent constitutive model of solidifying concrete based on thermodynamic state of moisture in fine pores, *Advanced Concrete Technology*, 4(2), 301-323.
- Baroghel-Bouny, V. 2006. Evaluation and prediction of reinforced concrete durability by means of durability indicators. Part I: new performance-based approach, *Concrete Durability and Service Life Planning*, Proceedings pro046, RILEM, 259-269.
- Chijiwa, N. 2006. Time dependent simulation of reinforced concrete subjected to coupled mechanistic and environmental actions, 6th International PhD Symposium in Civil Engineering, Zurich.
- Collins, M. P. and Vecchio, F. 1982. The response of reinforced concrete to in-plane shear and normal stresses, *University of Toronto*.
- Ishida, T., Maekawa, K., Soltani, M. 2004. Theoretically identified strong coupling of carbonation rate and thermodynamic moisture state in micropores of concrete, *Advanced Concrete Technology*, 2(2), 213-222.
- Ishida, T., Maekawa, K. 2000. An integrated computational system for mass/energy generation, transport and mechanics of materials and structures, *Concrete Library of JSCE*, 36, 129-144.
- Kunieda, M., Rokugo, K. 2006. Recent progress on HPFRCC in Japan *Advanced Concrete Technology*, 4(1), 19-33.
- Maeda, Y. And Matsui, S. 1984. Fatigue of reinforced concrete slabs under trucking wheel load, *Proc. of JCI*, 6, 221-224.

- Maekawa, K., Gebreyouhannes, E., Mishima, T., An, X. 2006a. Three-dimensional fatigue simulation of RC slabs under traveling wheel-type loads, *Advanced Concrete Technology*, 4(2).
- Maekawa, K., Toongoenthong, K., Gebreyouhannes, E., Kishi, K. 2006b. Direct Path-Integral Scheme for Fatigue Simulation of Reinforced Concrete in Shear, *Advanced Concrete Technology*, 4(1), 159-177.
- Maekawa, K., Ishida, K., Kishi, T. 2003. Multi-scale modeling of concrete performance - integrated material and structural mechanics -, *Advanced Concrete Technology*, 1(2), 91-126.
- Maekawa, K., Pimanmas, A., Okamura, H. 2003. *Nonlinear Mechanics of Reinforced Concrete*, Spon Press, London.
- Maekawa, K., Chaube, R. P., Kishi, T. 1999. *Modeling of Concrete Performance*, Spon Press, London.
- Nakarai, K., Ishida, T., Maekawa, K. 2006. Multi-scale physicochemical modeling of soil-cementitious material interaction, *Soils and Foundations*, 46(5).
- Perdikaris, P. C., Beim, S. R. 1988. RC bridge decks under pulsating and moving load, *J. of Structural Engineering*, ASCE, 114(3), 591-607.
- Satoh, Y. et al. 2003. Shear behavior of RC member with corroded shear and longitudinal reinforcing steels, *Proc. of the JCI*, 25(1), 821-826.
- Sogano, T. et al. 2001. Numerical analysis on uneven settlement and seismic performance of Tokyo brick bridges, *Structural Engineering Design*, No.17, JR-East, 96-109.
- Suryanto, B., Nagai, K., Maekawa, K. 2008. A bi-directional cracking test of High Performance Fiber Reinforced Cementitious Composite, *Proc. of the JCI*, 30(2), 279-284.
- Toongoenthong, K., Maekawa, K. 2005. Simulation of coupled corrosive product formation, migration into crack and its propagation in reinforced concrete sections, *Advanced Concrete Technology*, 3(2), 253-265.

OIL SUPPLY CHAIN SECURITY EVALUATION AND COUNTERMEASURES

GUANGYONG XU and QIDONG YONG

Dept. of Oil Application & Management, Logistic Engineering University,
Chongqing 400016, China
Xgy_7728@163.com

ABSTRACT

Paper on the safety of the supply chain, based on systems engineering principles, will focus on analyzing major factors and the establishment of index system and evaluation criteria of the oil supply chain security evaluation and give security measures of oil supply.

1. INTRODUCTION

Oil (refined oil) supply chain refers to the organization and conduct of the supply of fuels and fuel storage, transportation, the addition (or supply), and so on. In the oil supply chain, such as storing, transporting, adding, and so on, we must ensure that the “chain” of security. Otherwise, the supply of fuels would be interrupted. Therefore, the evaluation and ensuring of fuel supply chain security is of great significance.

2. THE MAIN FACTORS IMPACTING OIL SUPPLY CHAIN SECURITY

2.1 Fuels

Oil itself from the risk of their own physical and chemical nature, such as a flammable characteristics encountered fire ignition source could result in fuel combustion; being strong volatile, it would not only result in highly explosive environment and the formation of the environment pollution, but also could easily lead to the loss of oil quality and decreased quality; with strong proliferation, it could easily lead to run, dripping, and leakage, which not only reduces the number but also pollutes the environment, and is easy to cause combustion and explosion accident; easy electrostatic accumulation may occur spark discharge, cause fire and explosion accident; being certain toxic, it is easy to cause acute poisoning and chronic poisoning incidents. It is very dangerous because of these characteristics.

2.2 Personnel

Oil supply is both the target of management and the driving force during supplying. It is likely to be “risk factors” portability or persons stopping risk factors or illegal operations. Therefore, the personnel are the

most complex factor and a key factor affecting safety. The effect primarily lists in the following areas: security consciousness, knowledge level of work style; body function; personal experience.

2.3 Equipment and facilities

Oil equipment and facilities includes the storage, transportation, adding and quality testing equipment and facilities. All activities during oil supply must rely on equipment and facilities and without equipment and facilities, personnel could not complete oil supply task. However, its impact on the safety of oil supply should not be overlooked, which exists mainly in the following areas: the technical specifications of the equipment and facilities; the degree deciding new or old; its own security protection capability of equipment and facilities; whether the equipment and facilities for the security protection are sound, appropriate, useful, convenient in maintenance.

2.4 Management

Management means the various activities when people scientifically organize, command and coordinate according to certain principles in order to achieve the intended target, which can not be achieved only through their personal activities. The purpose of safety management is to coordinate and organize the management factors such as people, fuel, equipment, etc, in the supply environment and to avoid the occurrence of danger. Therefore, whether the oil sectors at all levels establish regulations, whether they implement management organizations, whether they strengthen legal education, whether they define security responsibilities and whether they implement the necessary security measures, organizational measures and technical measures will have an impact on oil security.

2.5 Environment

Environmental factors affecting the safety include the natural environment such as meteorological, geological factors, man-made factors, such as work and living environment and social conditions, such as social, folk, and social factors. Environmental factors not only affect the normal function of the human body to play, but also induce the excitation of insecurity. It is difficult to curb all the great forces of nature. Man-made environment not only will cause staff make errors, but also expose the danger of oil and cause a hidden danger to equipment and facilities, which will affect fuel safety. Social factors are the social atmosphere, the resident social conditions and the mental state of staff, which affected not only the emotional, but also may cause oil, fuel and equipment lost, and even vandalism. The mental state of oil supply personnel will be affected by external staff and values view.

3. THE OIL SUPPLY CHAIN SECURITY EVALUATION

3.1 Comprehensive Assessment System of the oil supply chain security status

Comprehensive Assessment System is created such as the Table 1 according to the above mentioned factors affecting safety.

Human security awareness and responsibility is mainly used to measure cadres and staff safety awareness and compliance (Safety regulations) and law-abiding, and other physical conditions. The status of equipment and facilities is used mainly to value the safety or reliability of the situation. Material conditions are mainly used for evaluation of the risk of unsafe or harmful materials, such as flammable and explosive, spontaneous combusting, toxic, corrosive and so on. The state of the environment is used mainly to judge security of the natural environment and the operating environment. Management and training situation is used mainly to judge the management working conditions of the safety system, safety training, and safety precautions. Accident situation unit is used mainly to value the security responsibility of the leadership and accident hazard.

Table 1: Comprehensive assessment of the security situation

| One indicators (Weight) | two indicators (weight) | grades | | | | | |
|--|--|--------|---|---|---|---|---|
| | | 5 | 4 | 3 | 2 | 1 | 0 |
| Responsibility for the safety awareness | Security awareness (excellent, good, poor, very poor) | | | | | | |
| | Familiarity with the business (familiar with the more familiar, in general, poor, very poor) | | | | | | |
| | Abide by rules and regulations (very good, good, average, poor, poor) | | | | | | |
| | Command or operational errors (no, sometimes, more, more frequent) | | | | | | |
| | Fatigue (no, sometimes, more, more frequent) | | | | | | |
| | Physical quality (good, good, average, poor, poor) | | | | | | |
| Equipment (facilities) situation | Equipment configuration status (excellent, good, poor, very poor) | | | | | | |
| | Strength (excellent, good, poor, very poor) | | | | | | |
| | Aging equipment (excellent, good, medium, aging, very aging) | | | | | | |
| | Safety devices adverse conditions (excellent, good, poor, very poor) | | | | | | |
| | Sound safety facilities (sound and more perfect, in general, does not sound bad) | | | | | | |

| | | | | | | | | | |
|-----------------------------------|---|--|--|--|--|--|--|--|--|
| Materials | dangerous substances or harmful substances(Very small, small, normal, large, large) | | | | | | | | |
| State of the environment | Safety signs (dangerous is the whole point, the majority, and some, on behalf of points, none) | | | | | | | | |
| | Fire (no fire danger point, a fire) | | | | | | | | |
| | Electrostatic (for electrostatic device results: excellent, good, poor, very poor) | | | | | | | | |
| | Lightning (Lightning processing device: excellent, good, poor, very poor) | | | | | | | | |
| | Flooding (flood water excellent, good, poor, very poor) | | | | | | | | |
| Management and training situation | to establish work safety assurance system (very good, good, average, poor, poor) | | | | | | | | |
| | Working to achieve Standardization of safe operation (very good, good, average, poor, poor) | | | | | | | | |
| | Carry out safety technology training (very good, good, average, poor, poor) | | | | | | | | |
| | Risk source identification (very good, good, average, poor, poor) | | | | | | | | |
| | Significant risk source identification results (based on "no, four to one" five classes) | | | | | | | | |
| | plans against major risk sources (excellent, good, poor, no plans) | | | | | | | | |
| Accident situation | three years without incident situation (in the event of an accident, the annual deduction 1) | | | | | | | | |
| | No accidents within the leadership (in the event of an accident, each deduction 1) | | | | | | | | |
| | That the event of an accident situation (without incident, the general, to assess and heavy / large) | | | | | | | | |
| Familiarity with profession | <input type="checkbox"/> very familiar with; <input type="checkbox"/> more familiar; <input type="checkbox"/> general; <input type="checkbox"/> not familiar with <input type="checkbox"/> knowing a little | | | | | | | | |
| Note | Only one ticket can vote down and "0" point indicates in the accident. | | | | | | | | |

Oil supply chain security assessment of the status-fifth of the standard system of using subcontractors points, as shown in table 1. In addition, another grading standard can be used in flammable places, as shown in Table 2.

Table 2 Grading standard in oil warehouse security degree assessment

| sort | falling short of request | Having severe bug | being up to the mustard basically | being up to the mustard |
|--------------------|--------------------------|-------------------|-----------------------------------|-------------------------|
| High fatalness | 0 | 1 | 4 | 8 |
| Moderate fatalness | 0 | 1 | 3 | 5 |
| Low fatalness | 0 | 1 | 2 | 3 |

3.2 Security grading

According to the division above, the calculated results can be divided into the five systems. 5-point means the unit is on firm ground. 4-point means the unit is safe comparatively. 3-point means the unit is on average ground. 2-point means the unit is danger comparatively. 1-point means the unit is deep in danger. 0-point means the accident will occur in the unit at any moment. All above are shown in table 3.

Table 3 State expressed and arithmetic operators of mood

| points mood | 5 | 4 | 3 | 2 | 1 | 0 |
|----------------|-----------|-------------------|---------|---------------------|-----------|----------|
| | V | IV | III | II | I | O |
| ① | excellent | good | medium | poor | Very poor | Accident |
| ② | safe | Safe in general | average | Danger in general | danger | accident |
| ③ | stable | Stable in general | medium | instable in general | instable | accident |
| ④ | excellent | good | medium | poor | Very poor | Accident |

4. COUNTERMEASURES OF GUARANTEEING OIL SUPPLY CHAIN SECURITY

4.1 Establishment of sufficient oil reserves

The so-called oil reserves generally refers to petroleum material accumulation under the relevant law standard, namely the crude oil and the product that have been changed the primitive existence condition, moreover is called as generally for the emergency oil reserves. In a sense, this kind of emergency storage may also be regarded as the sum of social petroleum stock that may momentarily put in the market. At present there are 11 countries or areas in the world that implement this kind of emergency oil reserves by different ways. Oil reserve's basic function may be summarized as: avoiding panic for short of petroleum and maintaining the petroleum security; suppressing the rise in price and adjusting the market supply and demand; Containing supply disruption and participating energy business; Dealing with the thunderbolt and guaranteeing army oil used. Therefore, establishing sufficient oil reserves is the prerequisite that can ensure the oil supply chain security.

4.2 Guaranteeing oil transportation safety

The fuel oils transportation can link oil raises, storage and supplies. It is the key tache in the oil supply chain. Therefore, we must strengthen oil transportation supply effectively. First, we must complete the arduous oil transportation task in the limited time. Once oil transportation supply comes apart, we would encounter a vicious circle that we could not follow step by step just because one step did not follow up. Next, we must achieve the effective oil transportation. Even if oil transport capacity is wonderful, you may complete the transportation task very badly. That is because the quality completing the transportation task is based on the validity of oil supply. In order to carry on oil supply effectively in a short time, operating speed of oil transportation system must speed up. But the enhancement of this kind must take in the suitable place, the appropriate opportunity, and transporting the right amount fuel as a premise. This is the effective oil transportation.

4.3 Enhancement of oil safety control

In order to manage fuel safely, we must set down strict safety control system and the post responsibility, develop the safety and skill training education of the whole staff, carry on security heck, discover hidden danger and carry on analysis, summary and reorganization. Thus we can prevent important targets from catching fire, explosion and potential hazard. Therefore, we must pay attention to unsafe factors in such aspects as management, operation, service maintenance and so on. Thus we can prevent occurrence of safety incident.

ACKNOWLEDGEMENTS

This work was supported by the National Social Science Foundation of China under 07GJY078.

REFERENCES

- YONG Qi-dong, 2005. Study on safety system and safety evaluation for tanker. *Logistics Engineering University Transaction*, vol 2, 12-14
- YONG Qi-dong, 2007. Study on manufacturing accidents and safety evaluation. *Logistics Engineering University Transaction*, vol 8, 13-15

Authors' Index

AUTHORS' INDEX

| | | | |
|----------------------|-----------------------|-------------------------|-----------------------------------|
| A | | H | |
| Aziz, Zeeshan | 145 | Hiroshi, Hayami | 317 |
| Alberty, Chen | 145 | Hong, Chen | 345 |
| Albert P., Plans | 145 | Hui, Zhang | 405 |
| Ahmed, Ansary Mehedi | 233, 239, 365, 657 | Hongyong, Yuan | 427, 439, 487 |
| Akiyuki, Kawasaki | 269, 335 | H., Kumagai | 591 |
| Akimasa, Sumi | 723 | Hiroshi, Yokota | 621 |
| | | Hitoshi, Taguchi | 715 |
| B | | I | |
| Bin, Zhang | 377 | Imtlaz Bnus, Afifa | 233 |
| | | Imtiaz A.B., Afifa | 239 |
| C | | Izumi, Nagatani | 251 |
| Chunlin, Liu | 189, 201 | Itsuki, Noda | 421 |
| Crawford Ra., John | 189 | Israt, Jahan | 657 |
| Cao, Zheng | 297 | | |
| Changkun, Chen | 435 | J | |
| Chengcheng, Gai | 439 | Jae-hyun, Shim | 155 |
| Chao, Zhang | 495 | Jae-hak, Chung | 155 |
| Chao-Shun, Chang | 603 | Jin, Pan | 223 |
| | | Jorgen, Johansson | 259 |
| D | | Jing, Zhang | 279 |
| David, Palermo | 201 | Jianfeng, Li | 377 |
| Dushmanta, Dutta | 287 | Jianghong, Wu | 415 |
| Dongxue, Li | 457 | Jun, Yan | 487 |
| Dongshan, Cai | 495 | Jiangfeng, Yang | 549 |
| Daisuke, Sugimoto | 641 | Jiangnan, Qiu | 581 |
| Dissanayake, Dmdok | 671 | Jianguo, Dao | 621 |
| Dong Hee, Ko | 699 | | |
| | | K | |
| E | | Kimiro, Meguro | 73, 105, 115, 269, 335, 355 |
| Enhua, Wu | 405 | | |
| | | Kaoser A. R | 123 |
| F | | Kazuo, Konagai | 259 |
| Fujio, Koyama | 355 | Kai, Bao | 405 |
| | | Kui, Zheng | 467 |
| G | | Kanok-Nukulchai, Worsak | 475 |
| Golparvar-Fard, Mani | 145 | Kai-Lin, Hsu | 603 |
| Guangyong, Xu | 763 | Kuo-Hung, Tseng | 613 |
| | | Koichi, Maekawa | 753 |
| H | | Koheii, Naga | 753 |
| Hiroshi, Yokota | 135 | | |
| Hong, Huang | 215 | | |
| Haruo, Sawada | 251, 715 | | |
| Hong, Huang | 317, 345 | | |

| | | | |
|----------------------------|------------------|---------------------------|------------------|
| L | | R | |
| Li, Qingshui | 297 | Reiko, Kuwano | 641, 699, 709 |
| Liu, Mao | 297 | Ryohji, Ohba | 647 |
| Lili, Zheng | 405 | Reja M.D., Yousuf | 657 |
| Ligang, Du | 449 | | |
| Lijun, Zhang | 575 | S | |
| | | Sahamitmongkok, Raktipong | 95 |
| M | | S., Takahashi | 135 |
| Masamitsu, Tamura | 19 | Saumil J., Mehta | 145 |
| Mikiko, Ishikawa | 39 | Shinsuke, Kato | 215 |
| M., Iwanami | 135 | Sutra, Dhar Ashutosh | 239 |
| Murshed, Ahmed | 165 | Shifei, Shen | 279 |
| Mahmoud, Bady | 215 | Samuel, Adeloju | 287 |
| Mu, Qing | 297 | Srikantha, Herath | 335 |
| M.V., Khiem | 317 | Sanae, Miyazaki | 355 |
| Miho, Ohara | 355 | Syed Zillur, Rahman | 365 |
| Mao, Liu | 457 | Shunsuke, Soeda | 421 |
| Michael, Henry | 539 | Shifei, Shen | 449 |
| Masamitsu, Suzuki | 555 | Shinsuke, Kato | 647 |
| Masanori, Ito | 555 | Shinji, Tanaka | 745 |
| Mao, Liu | 565 | | |
| Mikio, Koshihara | 631 | T | |
| Mari, Sato | 709 | Tomoya, Shibayama | 11 |
| Masao, Kuwahara | 745 | Taketo, Uomoto | 57 |
| | | Toshibumi, Sakata | 69 |
| N | | T., Matsubashi | 135 |
| Navaratnarajah, Sathiparan | 105 | Takeo, Tadono | 183 |
| Noor M. A. | 123, 591, 735 | Tajima, Yoshimitsu | 259 |
| Naoki, Yahagi | 355 | Tatiana, Torres | 269 |
| N., Ahmed | 735 | Takashi, Tsuchiyu | 345 |
| | | Tomohisa, Yamashita | 421 |
| O | | Tingxin, Qin | 449 |
| Osamu, Ukai | 647 | Thanh Tam, Bui | 475 |
| | | Tomohisa, Yamashita | 647 |
| P | | Taiping, Chang | 689 |
| Paola, Mayorca | 105, 115 | Takahiro, Endo | 715, 723 |
| Peña-Mora, Feniosky | 145 | Takeshi, Ono | 745 |
| Peter, Rogers | 335 | | |
| Pan, Li | 393 | Q | |
| P.J., Baruah | 715, 723 | Quan, Shao | 427 |
| | | Qiyang, Zheng | 575 |
| R | | Qiuyan, Zhong | 581 |
| Richard L, Jaehne | 49 | Qidong, Yong | 763 |
| Rubel, Das | 233 | | |
| Rui, Yang | 279 | | |
| Ryozo, Ooka | 317, 345 | | |
| Raquib, Ahsan | 365 | | |
| Ryo, Suzuki | 555 | | |

W

| | |
|--------------------------|-----------------------|
| Weicheng, Fan | 1 |
| Wenguo, Weng | 1 |
| Waon-ho, Yi | 155 |
| Wataru, Takeuchi | 183 |
| Worakanchana, Kawin | 183 |
| Warnitchai, Pennung | 183 |
| Wendy, Wright | 287 |
| Wenguo, Weng | 393, 415, 427, 439 |
| Wicaksana, Citra | 475 |
| Weiqui, Huang | 575 |
| Wen, Xue | 621 |
| Weiling, Jin | 621 |
| Wuditha Nuwan, Premadasa | 671 |
| Wei, Wang | 679 |

X

| | |
|---------------|----------|
| Xiaoyu, Tang | 223 |
| Xiaohui, Yao | 377 |
| Xiaoqing, Liu | 377 |
| Xuwei, Ji | 393 |
| Xueming, Shu | 467, 487 |
| Xin, Ye | 581 |

Y

| | |
|--------------------|-----------------|
| Yi, Liu | 1 |
| Yoshifumi, Yasuoka | 31 |
| Yoshiaki, Nakano | 85 |
| Yoshitaka, Kato | 95, 539, 555 |
| Yea Saen, Fang | 189 |
| Yoshito, Sawada | 251 |
| Yoichi, Kitsuta | 355 |
| Yutian, Wang | 377 |
| Yunfeng, Sun | 435 |
| Yi, Liu | 495 |
| Yingchun, Chen | 549 |
| Yafei, Zhou | 565 |
| Yingju, Zhang | 581 |

Z

| | |
|---------|-----|
| Zhi, Li | 435 |
|---------|-----|

INTERNATIONAL CENTER FOR URBAN SAFETY ENGINEERING
Institute of Industrial Science, The University of Tokyo
4-6-1 Komaba, Meguro-ku,
Tokyo 153-8505, Japan
<http://icus.iis.u-tokyo.ac.jp>
E-mail: icus@iis.u-tokyo.ac.jp

Tel: (+81-3)5452-6472

Fax: (+81-3)5452-6476